

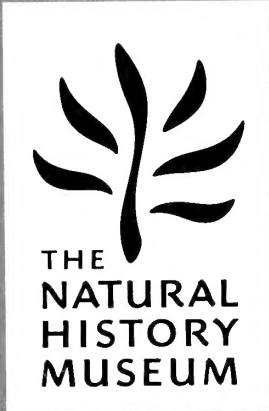


186 A

Bulletin of The Natural History Museum

THE NATURAL
HISTORY MUSEUM
27 JUN 1995
PRESENTED
PALAEONTOLOGY LIBRARY

Geology Series



VOLUME 52 NUMBER 1 27 JUNE 1996

The Bulletin of The Natural History Museum (formerly: Bulletin of the British Museum (Natural History)), instituted in 1949, is issued in four scientific series, Botany, Entomology, Geology (incorporating Mineralogy) and Zoology.

The Geology Series is edited in the Museum's Department of Palaeontology

Keeper of Palaeontology: Dr L.R.M. Cocks

Editor of the Bulletin: Dr M.K. Howarth

Assistant Editor: Mr C. Jones

Papers in the *Bulletin* are primarily the results of research carried out on the unique and ever-growing collections of the Museum, both by the scientific staff and by specialists from elsewhere who make use of the Museum's resources. Many of the papers are works of reference that will remain indispensable for years to come. All papers submitted for publication are subjected to external peer review before acceptance.

A volume contains about 160 pages, made up by two numbers, published in Spring and Autumn. Subscriptions may be placed for one or more of the series on an annual basis. Individual numbers and back numbers can be purchased and a Bulletin catalogue, by series, is available. Orders and enquiries should be sent to:

Intercept Ltd.
P.O. Box 716
Andover
Hampshire SP10 1YG
Telephone: (01264) 334748
Fax: (01264) 334058

Claims for non-receipt of issues of the Bulletin will be met free of charge if received by the Publisher within 6 months for the UK, and 9 months for the rest of the world.

World List abbreviation: *Bull. nat. Hist. Mus. Lond. (Geol.)*

© The Natural History Museum, 1996

ISSN 0968-0462

Geology Series
Vol. 52, No. 1, pp. 1-89

The Natural History Museum
Cromwell Road
London SW7 5BD

Issued 27 June 1996

Typeset by Ann Buchan (Typesetters), Middlesex
Printed in Great Britain at The Alden Press, Oxford

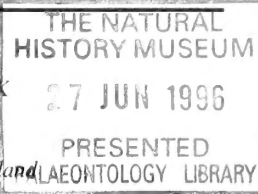
Zirconolite: a review of localities worldwide, and a compilation of its chemical compositions

C.T. WILLIAMS

Department of Mineralogy, The Natural History Museum, Cromwell Road, London SW7 5BD, UK

R. GIERÉ

Mineralogisch-Petrographisches Institut der Universität, Bernoullianum, CH-4056, Basel, Switzerland



SYNOPSIS. A compilation of the chemical data and brief review of the mineral zirconolite, essentially $\text{CaZrTi}_2\text{O}_7$, is presented. A total of 321 chemical analyses, 169 previously unpublished, from 39 of the 46 known terrestrial localities, and covering 10 rock types are tabulated. A brief description of the minerals associated with zirconolite is outlined for each locality. Data from all zirconolite-bearing lunar rocks have also been compiled. The recently published nomenclature scheme for zirconolite is employed throughout.

INTRODUCTION

Zirconolite, although a relatively rare accessory mineral, is found in a wide range of rock types and geological environments. To date, zirconolite has been reported from 46 terrestrial localities and from 13 lunar samples; it has not been reported in meteorites. The chemical composition of natural zirconolite can vary extensively, with the main substitutions involving rare earth elements, actinide elements, niobium and iron. Synthetic zirconolite is a major component in SYNROC, a synthetic polyphase titanate ceramic designed to immobilise high-level radioactive waste.

In this paper, we compile and tabulate all reported chemical data for natural zirconolites, including new, and previously unpublished analyses; we group zirconolites into specific rock types or paragenetic types, and denote those samples that are stored in the collections of the Mineralogy Department, The Natural History Museum, London.

NOMENCLATURE

In the literature, several minerals with stoichiometries close to $\text{CaZrTi}_2\text{O}_7$, but with different crystal structures, have been reported and this has led to confusion in the nomenclature of these minerals. The compound $\text{CaZrTi}_2\text{O}_7$ can exist as three superstructures with monoclinic, orthorhombic and trigonal symmetries (Rossell, 1980), each being a polytype (White, 1984), subsequently redefined as polytypoids (Bayliss *et al.*, 1989). However, the original type material, polymignite (Berzelius, 1824), zirkelite (Hussak & Prior, 1895) and zirconolite (Borodin *et al.*, 1956) are metamict and their structures cannot be unambiguously defined. Further problems in identification and characterisation have arisen, in part because the frequent occurrence of actinide elements in the structure may render the mineral partially or totally metamict, and in part because the often small grain size does not allow for routine crystallographic techniques to be employed. These nomenclature problems have been addressed by Nickel & Mandarino (1987) and most

recently by Bayliss *et al.* (1989), who summarized the crystallographic and chemical characteristics of these minerals, detailed their historical documentation, and rationalized their nomenclature.

Under the Bayliss *et al.* (1989) IMA-approved nomenclature scheme, **zirconolite** is the non-crystalline (metamict) mineral, or the mineral with undetermined polytypoid of $\text{CaZrTi}_2\text{O}_7$; **zirconolite-3O** is the three-layered orthorhombic polytypoid of $\text{CaZrTi}_2\text{O}_7$; **zirconolite-3T** is the three layered trigonal polytypoid of $\text{CaZrTi}_2\text{O}_7$; **zirconolite-2M** is the two-layered monoclinic polytypoid, or aristotype (White, 1984) of $\text{CaZrTi}_2\text{O}_7$; **zirconolite** is polymignite (metamict), and **zirkelite** is the cubic mineral with formula $(\text{Ti}, \text{Ca}, \text{Zr})\text{O}_{2-x}$. Smith & Lumpkin (1993) have subsequently described two additional polytypes which appear to be supercells of the zirconolite-2M and 3T structures (zirconolite-4M and -6T, respectively).

CHEMICAL COMPOSITION

Zirconolite has five cation-acceptor sites, these being Ca in 8-coordination, Zr in 7-coordination, and three distinct Ti sites: Ti(I) and Ti(III) are both 6-coordinate, and Ti(II) is 5-coordinate (Gatehouse *et al.*, 1981; Mazzi & Munno, 1983). In natural (and synthetic) zirconolites, a wide range of cation substitutions can occur (e.g. Ringwood, 1985), ranging in ionic size from 0.051nm (Ti^{4+}) to 0.112nm (Ca^{2+}) – ionic radii data from Shannon (1976) – and charge from 2+ (Mg) to 6+ (W). Predominant substitutions are: the rare earth elements including Y (REE) and actinide (ACT) elements for Ca; Hf for Zr; and Nb, Fe, Ta, Mg and W for Ti. In natural zirconolites the chemical variation is extensive; of the major components, CaO ranges from 1.83 to 16.54%, ZrO_2 from 22.82 to 44.18%, and TiO_2 from 13.56 to 44.91% (Table 1). Up to 79% of the Ca site can be replaced by other cations (e.g. analyses A4, L11, Table 3), and up to 65% of the Ti site (analysis C69, Table 3).

DETAILS

from terrestrial and lunar of their host rock (or analysis numbers, together with references relating both to the first report for that occurrence, and to the sources of the analytical data. Full chemical analyses, where available, are given in Table 3.

Kimberlite. Raber & Haggerty (1979) report zirconolite from three localities in South Africa. All their microprobe analyses are presented in Table 3 (K1 to K3); however, two analyses (K1 and K2) have significantly higher ZrO_2 values than all other zirconolites reported. The number of Zr cations for these analyses, recalculated on the basis of 7 oxygens, exceed the theoretical value by >50% and >100%. It seems probable therefore, that these analytical data are in error, or that the minerals analysed are not zirconolite. Calcirtite has been suggested as a possible alternative mineral for one of these questionable phases (Kogarko *et al.*, 1991). Analyses K1 and K2 are thus omitted from comparative data of zirconolites (such as in Table 1).

Zirconolite described by Raber & Haggerty (1979) is very fine-grained, associated with baddeleyite, \pm zircon, ilmenite, armalcolite and calcite, and is considered to have been formed as a secondary mineral due to infiltration of, and reaction with, a carbonatitic fluid.

Ultrabasic Rocks. Zirconolite has been described from two ultrabasic cumulate complexes – Laouni, Algeria (Lorand & Cottin, 1987) and Rhum, Scotland (Williams, 1978).

At Laouni zirconolite occurs as compositionally homogeneous, discrete grains up to 200 μm in diameter, in plagioclase-rich accumulates. Although baddeleyite also occurs in this intrusion, it is located in cumulates richer in trapped intercumulus liquid. Analyses U1–U2 (Table 3) are from Lorand & Cottin (1987).

In the layered, ultrabasic complex of Rhum zirconolite occurs as a rare, late-stage accessory mineral, associated with apatite, baddeleyite and zircon, predominantly in olivine-rich mesocumulates – i.e. those cumulates with a relatively high proportion of trapped (and fractionated) magma. The microprobe analysis (U3, Table 3) is from Fowler & Williams (1986).

Gabbro Pegmatite. Harding *et al.* (1982, 1984) describe accessory zirconolite (reported as 'zirkelite'), with acicular habit, from a gabbro pegmatite of Tertiary age at St. Kilda, Scotland. The pegmatite consists essentially of ferroaugite, ferroedenite, chlorite, magnetite, Mn-rich ilmenite, quartz and alkali feldspar. Associated with zirconolite are the accessory minerals biotite, epidote, allanite, titanite, apatite and zircon. The pegmatite is considered to have formed from the last residues of basaltic (tholeiitic) liquid from which the major Mg-minerals and feldspars of the Glen Bay Gabbro had previously precipitated.

The zirconolite analysis tabulated here (G1, Table 3) is from Fowler & Williams (1986). Harding *et al.*'s (1982) original analysis totals only 91%, as it excludes many of the heavy REE, Hf and Ta.

Since the ΣREE^{3+} exceeds 50% of the Ca site cations, it is *sensu strictu* a rare earth mineral, and following the Bayliss & Levinson (1988) nomenclature guidelines, this mineral can be classified as **zirconolite-(Y)** [subject to approval from the CNMMN].

Syenite. Zirconolite has been described from four syenite localities.

At Glen Dessarry, Scotland (Fowler & Williams, 1986), zirconolite occurs as an accessory mineral in a rock consisting of aegirine augite, edenitic amphibole, hypersolvus alkali-feldspar, orthoclase, albite and biotite. Zirconolite, typically <10 μm in diameter, is enclosed by alkali feldspar phenocrysts and associated with Fe-Ti oxides, titanite, allanite, apatite and zircon. The microprobe analysis (S1, Table 3) is from Fowler & Williams (1986).

Zirconolite is reported in the alkaline intrusions of the Arbarastakh massif, Aldan, Russia, where segregations of zirconolite occur in [a] '... micaized large-grained pyroxenite...' with accessory apatite and ilmenite (Borodin *et al.*, 1960). In Table 3, analyses S2 (Borodin *et al.*, 1960) and S3 (Gaidukova *et al.*, 1962) are wet chemical determinations on mineral separates; analysis S4 (Wark *et al.*, 1973) is a microprobe analysis of a separate zirconolite grain.

Zirconolite (described as 'polymignite') was reported from the syenite pegmatites of Fredicksvärn, S. Norway by Berzelius (1824), and was a mineral separately analysed by Brögger (1890) using 'classical' wet chemical techniques (S5, Table 3). It also occurs at Langesundsfjord, near Larvik in coarse-grained syenite pegmatites (S6 and S7, Table 3 – previously unpublished microprobe data).

Zirconolite (reported as 'polymignite') was described from a 'sanidinite' at Campi Flegrei, Italy (Mazzi & Munno, 1983). No analysis is included in Table 3, because the total of the reported analysis is low. Material is no longer available for analysis (Munno pers. comm., 1992).

Nepheline Syenite. At Pine Canyon, Utah, USA, zirconolite was found as an accessory mineral associated with hibonite, perovskite and pseudobrookite (Agrell *et al.*, 1986). The rock-forming minerals include corundum, nepheline and Mg-hercynite. Analyses (NS1-NS6, Table 3) are previously unpublished wavelength-dispersive microprobe data (CTW).

At the Elk Massif, Poland, zirconolite and Nb-zirconolite are reported in an association with apatite, fluorite and pyrochlore in agpaitic nepheline syenite pegmatites (Dziedzic, 1984). The major minerals of the pegmatites are microcline, nepheline, aegirine, arfvedsonite, and more rarely eudialyte. No analytical data are given for the zirconolite.

At Chikala, Chilwa Alkaline Province, Malawi, zirconolite occurs also as an accessory mineral, up to 0.3mm in size, in a nepheline syenite (sample number BM1980.P23(1), Platt *et al.*, 1987 – microprobe analyses NS7-NS11, Table 3). The rock-forming minerals are alkali feldspar, nepheline, biotite, apatite and an opaque oxide phase.

At Tchivira, Angola, niobian zirconolite is reported as intimately crystallized with wöhlerite from nepheline syenite rocks of the alkaline complex (Mariano & Roeder, 1989). Analyses NS11 to NS16 are previously unpublished microprobe data of **zirconolite-(Y)** [see above] from Tchivira.

At Pilanesberg, Transvaal, South Africa (Lurie, 1986), zirconolite occurs as an accessory mineral (A.N. Mariano, personal communication, 1993). No analytical data is reported.

At Tre Croci, near Vetralla in the Vico Volcanic complex of the Roman Comagmatic Province, Latium, Italy, crystalline epitaxial zirconolite occurs as an accessory mineral associated with baddeleyite, zircon and rare thorian hellandite in sanidinitic ejectum with nepheline and sodalite (G.C. Parodi, personal communication, 1993). Analyses NS17 to NS21 are previously unpublished microprobe data from this locality.

Carbonatite. Carbonatites, with sixteen reported occurrences of zirconolite, seem to be the most common host rock type for this mineral. In the Kola Peninsula, Russia, zirconolite occurs in four separate carbonatite complexes where detailed descriptions, including studies on crystal morphology and crystal chemistry, is given in Bulakh & Ivanikov (1984).

In the Afrikanda complex, Kola, zirconolite is described from the amphibolitized and fenitized pyroxenites (Borodin *et al.*, 1956). In Table 3 analyses C1–C3 are wet chemical analyses; C1–C2 from Borodin *et al.* (1956) and C3 from Bulakh *et al.* (1960). C4 is a microprobe analysis (Wark *et al.*, 1973).

At Vuoriyarvi, Kola, zirconolite was first described as zirkelite (Bulakh *et al.*, 1960), then '... tentatively described as a niobium variety, niobozirconolite' (Borodin *et al.*, 1960). It is associated with apatite-magnetite rocks (accompanying carbonatites, Zhuravleva *et al.*, 1976), accumulating predominantly in apatite, and was also observed replacing hatchettolite (Kapustin, 1980). Analyses C5–C7 (Table 3) are unpublished wavelength-dispersive microprobe data (CTW) on separate grains (BM1970,39); C8–C11 are wet chemical analyses; C8–C9 from Borodin *et al.* (1960), C8 and C11 quoted in Kapustin (1980); C10 is from Bulakh *et al.* (1960).

Bulakh *et al.* (1960) refer to zirconolite from the Sayan Province, Russia. Analysis C12 (Table 3) is a wet chemical analysis from Bulakh *et al.* (1960).

At Seblyavr, Kola, niobozirconolite was initially identified as zirkelite (Bulakh *et al.*, 1960) and is described as '... the typical mineral of the process of amphibolization-dolomitization confined to carbonatite...' (Kapustin, 1980). The mineral is partly metamict, it has good symmetry habit and displays complicated twinning (Bulakh *et al.*, 1960). Associated minerals are apatite, clinohumite, tetraferriphlogopite, pyrrhotite and richterite. Analysis C13 (Table 3) is a wet chemical analysis from Bulakh *et al.* (1960).

At Kovdor, Kola, zirconolite is associated with zones of carbonatization, Kapustin (1980). C14–C16 (Table 3) are wet chemical analyses: C14–C15 from Kapustin (1980), and C16 from Kukharenko *et al.* (1965). Analyses C17–C34 are unpublished wavelength-dispersive microprobe data (CTW), on chemically-zoned zirconolite grains in a thin section of carbonatite. Associated minerals are baddeleyite and U-Ta-rich pyrochlore (Williams, in press).

At Schryburt Lake, Ontario, Canada, zirconolite occurs intergrown with calzirtite, baddeleyite, and U-rich pyrochlore (Williams & Platt, in preparation). Microprobe analyses (C35–C58, Table 3), show significant variations in $\Sigma \text{REE}_2\text{O}_3$ and Nb_2O_5 . Some of the grains have $\Sigma \text{REE}^{3+} > 50\%$ of the Ca site, and, with Nd as the most abundant REE, this mineral can be classified as **zirconolite-(Nd)**, following Bayliss & Levinson (1988), and subject to approval from the CNMMN.

At Santiago Island, Cape Verde Republic, non-metamict **zirconolite-2M** occasionally up to 2mm in diameter, occurs as an accessory mineral, often associated with pyrochlore, in apatite-rich sōvite, beforsite and glimmerite rocks of the Canafistula carbonatitic plug (Silva, 1979; Silva & Figueiredo, 1980). Analysis C59 (Table 3) is the wavelength-dispersive microprobe analysis from Silva & Figueiredo (1980).

At Phalaborwa, South Africa, zirconolite was first described by Verwoerd (1986) from the carbonatite. Analyses C60–C64 (Table 3) are unpublished wavelength-dispersive microprobe analyses by CTW on sample BM1988,260, kindly provided by Prof. G. Bayer (ETH, Zürich). In this rock, zirconolite is associated with baddeleyite and zircon, the latter mineral probably having crystallized at a later stage. Analyses C65–C66

are unpublished microprobe data (from Bochon University) from Prof. G. Bayer.

At Sokli, Finland, zirconolite (reported as zirkelite) was originally described by Vartiainen (1980) from hydrothermal phoscorites. The crystals have apparently formed '... at the expense of pyrochlore and occur around and as inclusions in pyrochlore ...', and are also found as separate prisms. Analyses C67–C70 (Table 3) are unpublished wavelength-dispersive microprobe data from Dr. I. Hornig-Kjarsgaard (pers. comm., 1992), analysed at the University of Mainz.

At Kaiserstuhl, Germany, zirconolite occurs with calzirtite, baddeleyite, Nb-perovskite and pyrochlore (Keller, 1984). Analyses C71 and C72 are wavelength-dispersive microprobe analyses (Keller, 1984; Sinclair & Eggleton, 1982).

In the Hegau volcanic province, Germany, zirconolite (described as 'Nb-zirconolite') is a typical accessory mineral in the carbonatitic tuffs (Keller *et al.*, 1990). Analyses C73–C88 (Table 3), are unpublished wavelength-dispersive microprobe analyses (CTW) of eight grains from a heavy mineral separate provided by Prof. J. Keller (Freiburg).

At Prairie Lake, Ontario, Canada, niobian zirconolite is reported in association with wöhlerite, pyrochlore, betafite and niobian perovskite (Mariano & Roeder, 1989). A microprobe analysis provided by Dr A.N. Mariano of six major elements is shown in Table 3 (C89).

At the Cummins Range Carbonatite, Kimberley Area, Western Australia, accessory zirconolite occurs in an apatite-amphibolite rock. Qualitative analysis of the zirconolite showed the presence of Ca, Zr, Ti and minor Fe, but with Nb absent (Dr. A.N. Mariano, personal communication, 1993).

At Howard Creek, British Columbia, Canada (Woolley, 1987; p.16), zirconolite is associated with zircon, magnetite and diopside in an apatite calcite carbonatite (Dr. A.N. Mariano, personal communication, 1993). There is no analytical data.

At Catalao, Goias, Brazil (Woolley, 1987; p.179), zirconolite is associated with apatite and phlogopite in a calcite carbonatite (Dr. A.N. Mariano, personal communication, 1993). There is no analytical data.

At Araxá, Minas Gerais, Brazil (Woolley, 1987; p.66), zirconolite occurs as prismatic crystals with anastase in a glimmerite, and also with pyrochlore, baddeleyite and apatite in a calcite carbonatite (Dr. A.N. Mariano, personal communication, 1993). There is no analytical data.

Metasomatic Rocks. Zirconolite has been reported from metasomatic rocks at nine localities, although analyses from only seven of these have been published.

In the Mt. Melbourne Volcanic Field, Victoria Land, Antarctica, zirconolite occurs as isolated grains with a maximum grain diameter of 0.08mm within ultra-potassic veins in a mantle xenolith from a basanite host (Hornig & Wörner, 1991). The major vein-forming minerals are leucite, plagioclase, nepheline, Mg-ilmenite, apatite and titaniferous mica. Analyses M1–M7 (Table 3) are selected from Hornig & Wörner (1991) as being the least 'contaminated' by adjacent silicate minerals.

At the contact between granodiorite with gneisses and marbles in the Bergell aureole, Switzerland/Italy, chemically discontinuously-zoned zirconolite is observed, typically 30–40µm in diameter, associated with allanite and titanite, in a skarn (Gieré, 1986; Williams & Gieré, 1988). The major minerals of the skarn are calcite, spinel, phlogopite and anorthite. The microprobe analyses M8–M22 (Table 3) are unpublished data (CTW) of eleven grains from three discrete zones, the averages of which are published in Williams & Gieré (1988).

In the Oetztal-Stubai complex, Austria, within polymetamorphic metacarbonates, zirconolite and baddeleyite occur in several mineral assemblages consisting of chlorite, ilmenite, apatite, spinel, phlogopite, titanian clinohumite, olivine, calcite, dolomite and diopside (Purtscheller & Tessadri, 1985). Analyses M23-M27 (Table 3) are the wavelength-dispersive microprobe analyses given by Purtscheller & Tessadri (1985).

In the Adamello contact aureole, Italy, compositionally-zoned and corroded zirconolite occurs in two zones within a Ti-rich vein in dolomite marbles at the contact with a tonalite intrusion (Gieré, 1990a). In the phlogopite zone, zirconolite is always found associated with phlogopite and calcite (\pm dolomite), and occasionally with geikelite, rutile and fluorapatite. In the titanian clinohumite zone, zirconolite occurs with titanian clinohumite, spinel, calcite, dolomite, pyrrhotite, geikelite, fluorapatite and minor secondary chlorite. A detailed mineralogical and chemical description is given in Gieré & Williams (1992), and analyses M28-M66 (Table 3) are wavelength-dispersive microprobe analyses from Gieré (1990b).

At Koberg Mine, Bergslagen, Sweden, yttrian zirconolite occurs as anhedral grains, predominantly 20–30 μm in diameter, in an altered phlogopite-rich sample associated with a marble skarn (Zakrzewski *et al.*, 1992). The low analytical totals (analyses M67–M94, Table 3) suggest the zirconolite is hydrated (Zakrzewski *et al.*, 1992).

At the aplitic alkaline syenite complex of Lovozero, Kola, zirconolite (reported as 'zirkelite') has been described in a mineral assemblage including rosenbuschite, from the contact metasomatic rocks of the massif (Semenov *et al.*, 1963). Analyses M95–M96 (Table 3) are the wet chemical data of Semenov *et al.* (1963).

In a dolomitic marble from the Neichi mine, Iwate Prefecture, Japan zirconolite is associated with geikelite and baddeleyite, forsterite and spinel (Kato & Matsubara, 1991). The composition of zirconolite is close to the theoretical composition (analyses M97–M98, Table 3, from Kato & Matsubara (1991)).

At Sør Rondane, Antarctica, Grew *et al.* (1989) report zirconolite (qualitative analysis only, cf. p. 119) from a marble affected by metasomatic processes which had introduced rare metals. Associated minerals include dissakisite-(Ce) (Grew *et al.*, 1991), calcite, dolomite, phlogopite, chlorite, ilmenite–geikelite and spinel.

Rekharskiy & Rekharskaya (1969) discovered zirconolite (reported as zirkelite) intergrown with jordisite and abundant metasomatic pyrite, as veins in zones of altered trachytic to rhyolitic volcanic rocks. Locality details are not reported.

Kinny & Dawson (1992) report the occurrence of zirconolite, as a rare accessory phase associated with zircon and baddeleyite, in a veined and metasomatised harzburgite xenolith from Kimberley, southern Africa. The metasomatism is MARID-related (Kinny & Dawson, 1992) and considered to be associated with kimberlite magma. Analysis M99, Table 3, is the unpublished mean of 6 microprobe analyses (Prof. J.B. Dawson, pers. comm., 1993).

Rubin *et al.* (1993) report zirconolite occurring as inclusions in phlogopite in one sample of a complex skarn from the Ertsberg District of Irian Jaya, Indonesia. No analytical details are given.

Placer Deposit. Zirconolite is reported as millimetre-sized crystals from two placer deposits.

At Jacupiranga, São Paulo, Brazil, zirconolite (named as the

new mineral 'zirkelite'), is found with baddeleyite and perovskite in the heavy mineral fraction from pyroxene sands of '... the decomposed magnetite-pyroxenite of Jacupiranga ...' (Hussak, 1895; Hussak & Prior, 1895; see also Pudovkina *et al.*, 1974). Analyses P1, P2 are unpublished wavelength-dispersive microprobe analyses (CTW) of separate grains (80142). The wet chemical analysis given in Hussak & Prior (1895) is not included here, as the chemical separation techniques employed in the analysis could only provide qualitative data for ZrO_2 and TiO_2 .

In Sri Lanka, zirconolite (reported as 'zirkelite') was observed from two 'gem gravel' localities in the Sabaragamuwa Province: at Walaweduwa in the Bambarabotuwa district, and in southern Sabaragamuwa (Blake & Smith, 1913). Analyses P3, P4 (Table 3) are from Bambarabotuwa, and P5–P7 from Sabaragamuwa; analyses P8, P9 are microprobe data from Lumpkin *et al.* (1986); analysis P10 is an unpublished (CTW) wavelength-dispersive microprobe analysis of several grains (BM1905, 361).

'Other' Rock Types. Sapphirine Granulite: Zirconolite occurs as acicular grains in a mineral assemblage including sapphirine, spinel, enstatite and minor phlogopite from a sapphirine granulite nodule sampled from a xenolith-rich norite wall zone in the Archaean Vestfold Hills, east Antarctica (Harley, 1994). The zirconolite is considered to have been a relatively early crystallising phase during the melt crystallisation history of the entrapped granulite xenolith. Analyses SG1–SG3 (Table 3) are from Harley (1994).

Alnöite: Thin (1 μm) rims of zirconolite (no compositional details given) are reported as overgrowing a baddeleyite crystal from the île Bizard alnöite, Québec, Canada (Heaman & Le Cheminant, 1993). Although the baddeleyite crystals are considered to be mantle-derived xenocrysts, the associated overgrowths, which include perovskite and melilite as well as zirconolite, are considered to have formed after exposure to the alnöite magma.

Lunar. Zirconolite has been observed in several lunar samples, (cf. review by Frondel, 1975). Data from the literature are presented as analyses L1–L13 (Table 3). It occurs in coarse-grained basalts (Apollo 11, 15 and 17), in a feldspathic

Table 1 Range of chemical variation in natural zirconolite

	Terrestrial*		Lunar		
	Maximum	Minimum	Maximum	Minimum	Theoretical composition
CaO	16.54	01.83	10.70	02.63	16.5
REE ₂ O ₃	23.66	0.00	31.98	04.74	
PbO	00.80	00.00	02.19	00.00	
ThO ₂	22.28	00.00	02.34	00.00	
UO ₂	23.98	00.00	01.16	00.00	
ZrO ₂	44.18	22.82	45/40	29.80	36.3
HfO ₂	01.13	00.00	01.34	00.00	
TiO ₂	44.91	13.56	34.60	25.48	47.2
MgO	03.04	00.00	01.15	00.00	
Al ₂ O ₃	03.47	00.00	01.60	00.35	
FeO	10.20	00.00	11.40	04.23	
Fe ₂ O ₃	09.58	01.08	—	—	
Nb ₂ O ₅	27.00	00.19	04.34	00.00	
Ta ₂ O ₅	05.83	00.00	00.40	00.00	
WO ₃	01.44	00.00	—	—	

*Excluding kimberlite analyses K1 and K2 (see text)

ZIRCONOLITE

Table 2 Details of zirconolites from terrestrial and lunar occurrences

Rock type	Sample locality	Country	Analysis number	Reference (Occurrence)	Reference (Analytical data)
Kimberlite	Monastery	South Africa	K1	Raber and Haggerty (1979)	Raber and Haggerty (1979)
Kimberlite	Mothae	South Africa	K2	Raber and Haggerty (1979)	Raber and Haggerty (1979)
Kimberlite	Kimberley	South Africa	K3	Raber and Haggerty (1979)	Raber and Haggerty (1979)
Ultrabasic	Laouni	Algeria	U1-U2	Lorand and Cottin (1987)	Lorand and Cottin (1987)
Ultrabasic	Rhum (+)	Scotland	U3	Williams (1978)	Fowler and Williams (1986)
Gabbro Pegmatite	St. Kilda	Scotland	G1	Harding <i>et al.</i> (1982)	Fowler and Williams (1986)
Syenite	Glen Dessarry	Scotland	S1	Fowler and Williams (1986)	Fowler and Williams (1986)
Syenite	Arbarastakh, Aldan	Russia	S2-S4	Borodin <i>et al.</i> (1960)	Borodin <i>et al.</i> (1960, S2); Gaidukova <i>et al.</i> (1962, S3); Wark <i>et al.</i> (1973, S4)
Syenite	Fredericksvärk (*)	Norway	S5	Berzelius (1824)	Brögger (1890)
Syenite	Langesundsfjord (+)	Norway	S6-S7	Brögger (1890)	CTW (unpubl. data)
Syenite	Campi Flegrei	Italy	-	Mazzi and Munno (1983)	
Nepheline Syenite	Pine Canyon, Utah	U.S.A.	NS1 NS6	Agrell <i>et al.</i> (1986)	CTW (unpubl. data)
Nepheline Syenite	Chilwa Island (+)	Malawi	NS7-NS11	Platt <i>et al.</i> (1987)	Platt <i>et al.</i> (1987)
Nepheline Syenite	Elk Massif	Poland	-	Dziedzic (1984)	No analytical data
Nepheline Syenite	Tchivira	Angola	NS12 NS17	Mariano and Roeder (1989)	CTW (unpubl. data)
Nepheline Syenite	Pilanesberg, Transvaal	South Africa	-	Mariano (pers. comm., 1993)	No analytical data
Nepheline Syenite	Tre Croci, Latium	Italy	NS18-NS22	Parodi (pers. comm., 1993)	CTW (unpubl. data)
Carbonatite	Afrikanda, Kola (***)	Russia	C1 C4	Borodin <i>et al.</i> (1956)	Borodin <i>et al.</i> (1956, C1, C2); Bulakh <i>et al.</i> (1960, C3); Wark <i>et al.</i> (1973, C4)
Carbonatite	Vuoriyarvi, Kola(+)	Russia	C5-C11	Borodin <i>et al.</i> (1960)	CTW (unpubl. data, C5-C7); Borodin <i>et al.</i> (1960, C8, C9); Bulakh <i>et al.</i> (1960, C10); Kapustin (1964, C11)
Carbonatite	Sayan Province	Russia	C12	Gaidukova <i>et al.</i> (1962)	Gaidukova <i>et al.</i> (1962)
Carbonatite	Seblyavr, Kola	Russia	C13	Bulakh <i>et al.</i> (1960)	Bulakh <i>et al.</i> (1960)
Carbonatite	Kodvor, Kola (+)	Russia	C14-C34	Kukharenko <i>et al.</i> (1965)	Kapustin (1980, C14, C15); Kukharenko <i>et al.</i> (1965, C16); CTW (unpubl. data, C17-C34)
Carbonatite	Schryburt Lake (+)	Canada	C35-C58	Williams and Platt (in prep.)	CTW (unpubl. data)
Carbonatite	Santiago Island	Cape Verde Republic	C59	Silva (1979)	Silva and Figueiredo (1980)
Carbonatite	Phalaborwa(+)	South Africa	C60-C66	Verwoerd (1986)	CTW (unpubl. data); G. Bayer (unpubl. data)
Carbonatite	Sokli	Finland	C67 C70	Vartianen (1980)	Hornig-Kjarsgaard (unpubl. data)
Carbonatite	Kaiserstuhl	Germany	C71-C72	Keller (1984)	Keller (1984, C71); Sinclair & Eggleton (1982, C72)
Carbonatite	Hegau	Germany	C73-C88	Keller <i>et al.</i> (1990)	CTW (unpubl. data)
Carbonatite	Prairie Lake, Ontario	Canada	C89	Mariano and Roeder (1989)	Mariano (unpubl. data)
Carbonatite	Howard Creek, B.C.	Canada	C90-C135	Mariano (pers. comm., 1993)	CTW (unpubl. data)
Carbonatite	Cummins Range, Kimberly	W. Australia	-	Mariano (pers. comm., 1993)	No analytical data
Carbonatite	Catalao, Goias	Brazil	C136-C161	Mariano (pers. comm., 1993)	No analytical data
Carbonatite	Araxá, Minas Gerais	Brazil	M1-M7	Mariano (pers. comm., 1993)	CTW (unpubl. data)
Metasomatic	Mt. Melbourne	Antarctica	M8 M22	Hornig and Wörner (1991)	Hornig and Wörner (1991)
Metasomatic	Bergell (+)	Switzerland/Italy	M23-M27	Gieré (1986)	Williams and Gieré (1988)
Metasomatic	Oetzal-Stubai	Austria	M28-M66	Putzscheller and Tessadri (1985)	Putzscheller and Tessadri (1985)
Metasomatic	Adamello (+)	Italy	M67 M94	Gieré (1990a)	Gieré (1990b)
Metasomatic	Koberg, Bergslagen (+)	Sweden	M95-M96	Zakrzewski <i>et al.</i> (1992)	Zakrzewski <i>et al.</i> (1992)
Metasomatic	Lovozero, Kola	Russia	M97-M98	Semenov <i>et al.</i> (1963)	Semenov <i>et al.</i> (1963)
Metasomatic	Neichi, Iwate Prefecture	Japan	-	Kato and Matsubara (1991)	Kato and Matsubara (1991)
Metasomatic	Sør Rondane	Antarctica	-	Grew <i>et al.</i> (1989)	No analytical data
Metasomatic	?	Former USSR	-	Rekharskiy and Rekharskaya (1969)	No analytical data
Metasomatic	Kimberley	South Africa	M99	Kinny and Dawson (1992)	Dawson (unpubl. data)
Metasomatic	Irian Jaya	Indonesia	-	Rubin <i>et al.</i> (1993)	No analytical data
Metamorphic	Vestfold hills	East Antarctica	SG1-SG3	Harley (1994)	Harley (1994)
Alnöite	ile Bizard, Quebec	Canada	-	Heaman and LeCheminant (1993)	No analytical data
Placer (1)	Jacupiranga (***)(+)	Brazil	P1-P2	Hussak (1895); Hussak and Prior (1895)	CTW (unpubl. data) (3)
Placer (2)	Sabaragamuwa Province (+)	Sri Lanka	P3 P10	Blake and Smith (1913)	Blake and Smith (1913, P3 P7); Lumpkin <i>et al.</i> (1986, P8-P9); CTW (unpubl. data, P10)
Lunar	Apollo 11 Landing Site	Moon	L1-L4	Lovering and Wark (1971)	Wark <i>et al.</i> (1973)
Lunar	Apollo 12 Landing Site	Moon	L5	Busche <i>et al.</i> (1972)	Busche <i>et al.</i> (1972)
Lunar	Apollo 14 Landing Site	Moon	L6-L7	Busche <i>et al.</i> (1972)	Busche <i>et al.</i> (1972); Wark <i>et al.</i> (1973)
Lunar	Luna 20 Landing Site	Moon	L8	Roedder and Weiblen (1973)	Roedder & Weiblen (1973)
Lunar	Apollo 15 Landing Site	Moon	L9-L11	Brown <i>et al.</i> (1972)	Brown <i>et al.</i> (1972); Wark <i>et al.</i> (1973)
Lunar	Apollo 16 Landing Site	Moon	-	Lovering and Wark (1974)	No analytical data
Lunar	Apollo 17 Landing Site	Moon	L12-L13	Meyer and Boctor (1974)	Meyer and Boctor (1974)

(*) type POLYMIGNITE

(**) type ZIRCONOLITE

(***) type ZIRKELITE

(+) In BMNH collection

(1) Heavy mineral fraction from pyroxene sand; (2) Heavy mineral fraction from alluvial deposits: two separate localities; (3) Analysis from Hussak & Prior (1895) not included as method used could not adequately distinguish Ti from Zr.

} now all renamed as zirconolite (see Bayliss *et al.*, 1989)

Table 3 Chemical analyses of zirconolites

	K1	K2	K3	U1	U2	U3	G1	S1	S2	S3	S4	S5	S6	S7	NS1	NS2	NS3	NS4	NS5	NS6	NS7
MgO	1.20	0.31	0.49	0.19	0.20	0.35	0.06	0.07	0.53	0.43	0.14	0.16	0.07	0.13	-	-	-	0.48	0.50	0.44	0.42
Al2O3	0.13	0.04	0.23	0.59	0.50	0.31	0.09	0.27	0.23	-	0.10	0.19	0.27	0.19	0.44	<0.05	<0.05	<0.05	<0.05	<0.05	0.43
SiO2	-	-	-	-	-	-	-	-	-	-	-	-	-	-	-	-	-	-	-	-	3.25
Cao	10.11	9.09	11.10	10.67	11.15	10.80	0.25	0.10	0.29	1.18	0.76	0.45	<0.05	<0.05	<0.05	<0.05	<0.05	<0.05	<0.05	<0.05	3.25
TiO2	29.16	16.70	40.48	35.67	35.73	35.76	29.03	4.05	9.05	12.03	11.28	12.61	6.98	12.34	10.05	10.24	10.17	10.21	10.66	10.66	1.83
Cr2O3	1.10	0.06	0.09	0.05	0.05	-	-	-	-	-	-	-	-	-	-	-	-	-	-	-	24.80
MnO	0.11	0.15	0.11	-	0.16	0.15	-	-	-	-	-	-	-	-	-	-	-	-	-	-	-
FeO	6.94	2.38	5.15	4.85	4.87	5.14	8.26	7.70	2.85	4.53	2.30	2.08	7.84	7.93	5.76	5.65	5.62	5.68	5.65	5.46	4.56
Fe2O3	-	-	-	-	-	-	-	-	-	-	-	-	-	-	-	-	-	-	-	-	-
Y2O3	-	-	-	-	-	-	-	-	-	-	-	-	-	-	-	-	-	-	-	-	-
ZrO2	51.12	71.27	41.91	43.58	44.18	37.60	31.33	31.35	35.75	32.32	33.54	29.71	29.83	27.79	35.18	36.19	35.48	35.84	37.29	36.22	37.30
Nb2O5	-	-	-	-	-	-	-	-	-	-	-	-	-	-	-	-	-	-	-	-	-
La2O3	-	-	-	-	-	-	-	-	-	-	-	-	-	-	-	-	-	-	-	-	-
Ca2O3	-	-	-	-	-	-	-	-	-	-	-	-	-	-	-	-	-	-	-	-	-
Pr2O3	-	-	-	-	-	-	-	-	-	-	-	-	-	-	-	-	-	-	-	-	-
Nd2O3	-	-	-	-	-	-	-	-	-	-	-	-	-	-	-	-	-	-	-	-	-
Sm2O3	-	-	-	-	-	-	-	-	-	-	-	-	-	-	-	-	-	-	-	-	-
Eu2O3	-	-	-	-	-	-	-	-	-	-	-	-	-	-	-	-	-	-	-	-	-
Gd2O3	-	-	-	-	-	-	-	-	-	-	-	-	-	-	-	-	-	-	-	-	-
Tb2O3	-	-	-	-	-	-	-	-	-	-	-	-	-	-	-	-	-	-	-	-	-
Dy2O3	-	-	-	-	-	-	-	-	-	-	-	-	-	-	-	-	-	-	-	-	-
Ho2O3	-	-	-	-	-	-	-	-	-	-	-	-	-	-	-	-	-	-	-	-	-
Er2O3	-	-	-	-	-	-	-	-	-	-	-	-	-	-	-	-	-	-	-	-	-
Tm2O3	-	-	-	-	-	-	-	-	-	-	-	-	-	-	-	-	-	-	-	-	-
Yb2O3	-	-	-	-	-	-	-	-	-	-	-	-	-	-	-	-	-	-	-	-	-
Lu2O3	-	-	-	-	-	-	-	-	-	-	-	-	-	-	-	-	-	-	-	-	-
HfO2	-	-	-	-	-	-	-	-	-	-	-	-	-	-	-	-	-	-	-	-	-
Ta2O5	-	-	-	-	-	-	-	-	-	-	-	-	-	-	-	-	-	-	-	-	-
WO3	-	-	-	-	-	-	-	-	-	-	-	-	-	-	-	-	-	-	-	-	-
PhO	-	-	-	-	-	-	-	-	-	-	-	-	-	-	-	-	-	-	-	-	-
ThO2	-	-	-	-	-	-	-	-	-	-	-	-	-	-	-	-	-	-	-	-	-
UO2	-	-	-	-	-	-	-	-	-	-	-	-	-	-	-	-	-	-	-	-	-
(Na,K)2O	-	-	-	-	-	-	-	-	-	-	-	-	-	-	-	-	-	-	-	-	-
H2O	-	-	-	-	-	-	-	-	-	-	-	-	-	-	-	-	-	-	-	-	-
"Others"	-	-	-	-	-	-	-	-	-	-	-	-	-	-	-	-	-	-	-	-	-
TOTAL	99.87	100.00	99.56	99.59	101.28	98.72	99.61	99.26	100.56	100.12	96.85	100.19	98.71	98.17	98.29	98.24	99.20	99.31	99.96	97.64	94.22
cations to 7 oxygens																					
Ca2+	0.667	0.637	0.698	0.690	0.713	0.716	0.295	0.654	0.774	0.789	0.865	0.513	0.871	0.553	0.694	0.686	0.687	0.690	0.713	0.701	0.139
(Y+REE)3+	0.000	0.000	0.000	0.091	0.089	0.163	0.660	0.177	0.074	0.110	0.119	0.361	0.105	0.347	0.202	0.194	0.192	0.192	0.189	0.179	0.398
Pb2+	-	-	-	-	-	-	-	-	-	-	-	-	0.003	0.003	0.067	0.039	0.031	0.029	0.028	0.018	0.016
Th4+	-	-	-	-	-	-	-	-	-	-	-	-	-	-	-	-	-	-	-	-	-
U4+	-	-	-	-	-	-	-	-	-	-	-	-	-	-	-	-	-	-	-	-	-
SUM Ca2+	0.667	0.637	0.698	0.788	0.810	0.965	1.006	0.854	0.949	1.022	0.942	0.981	0.998	0.954	0.931	0.920	0.918	0.926	0.918	0.901	0.685
Zr4+	1.534	2.272	1.199	1.283	1.285	1.134	1.040	1.031	1.046	1.029	1.047	0.993	0.939	0.953	1.106	1.118	1.091	1.102	1.135	1.121	0.945
Hf4+	-	-	-	-	-	-	-	-	-	-	-	-	-	-	-	-	-	-	-	-	-
Si4+	-	-	-	-	-	-	-	-	-	-	-	-	-	-	-	-	-	-	-	-	-
Mg2+	0.110	0.030	0.043	0.017	0.018	0.032	0.006	0.007	0.047	0.042	0.013	0.016	0.007	0.014	-	-	-	-	-	-	0.005
Mn2+	0.006	0.008	0.005	0.008	0.024	0.245	0.470	0.266	0.434	0.143	0.009	0.006	0.077	0.023	0.039	0.005	0.002	0.007	0.002	0.002	0.032
Fa2+	0.357	0.130	0.253	-	-	-	-	-	-	-	-	-	-	-	-	-	-	-	-	-	0.271
Fa3+	-	-	-	-	-	-	-	-	-	-	-	-	-	-	-	-	-	-	-	-	-
Al3+	0.009	0.003	0.016	0.042	0.035	0.023	0.007	0.021	0.158	-	0.008	0.015	0.020	0.016	0.033	0.036	0.037	0.032	0.031	0.031	0.036
C3+	0.054	0.003	0.004	0.002	0.002	-	-	-	-	-	-	-	-	-	-	-	-	-	-	-	-
Nb5+	-	-	-	-	-	-	-	-	-	-	-	-	-	-	-	-	-	-	-	-	-
Ta5+	-	-	-	-	-	-	-	-	-	-	-	-	-	-	-	-	-	-	-	-	-
W6+	-	-	-	-	-	-	-	-	-	-	-	-	-	-	-	-	-	-	-	-	-
SUM Ti4+	1.885	0.996	2.107	1.932	1.916	2.014	2.040	2.153	2.022	1.950	2.025	2.112	1.980	1.980	2.013	2.008	1.973	2.002	2.135	-	-
TOTAL	4.085	3.904	4.004	4.021	4.050	4.042	4.083	4.053	4.000	4.029	3.980	4.045	4.021	4.051	4.041	4.036	4.044	4.045	4.044	4.034	3.773

	NS8	NS9	NS10	NS11	NS12	NS13	NS14	NS15	NS16	NS17	NS18	NS19	NS20	NS21	NS22	C1	C2	C3	C4	C5	C6
MgO	0.18	0.13	0.09	0.11	3.09	3.04	3.53	2.92	3.30	2.95	<0.5	0.08	<0.5	0.05	0.45	0.50	0.10	0.37	0.70	<.05	
Al2O3	0.75	0.89	0.68	0.56	2.97	3.43	2.89	2.94	2.64	0.26	0.19	0.26	0.29	0.25	1.03	1.04	0.76	0.09	<.05	<.05	
SiO2	<.07	<.07	<.07	0.17	0.12	2.02	0.15	0.13	0.17	<.05	0.08	0.07	0.08	0.07	0.05	4.50	4.50	<.05	<.05	<.05	
CaO	7.22	8.08	8.43	10.03	4.08	4.12	3.87	3.64	4.14	7.06	7.24	6.64	9.15	7.53	11.05	10.79	12.01	11.44	11.23	11.50	
TiO2	26.90	27.20	27.80	28.30	32.18	32.30	30.79	32.12	31.77	32.44	24.72	22.35	27.45	26.00	24.57	31.69	29.91	27.50	30.43	15.42	15.01
Cr2O3	-	-	-	-	-	-	-	-	-	-	-	-	-	-	-	-	-	-	-	-	
MnO	0.50	0.28	0.26	0.21	<.05	<.05	<.05	<.05	<.05	<.05	0.98	1.04	0.87	0.75	0.78	0.06	0.13	-	0.55	0.54	
FeO	8.32	7.96	8.47	7.66	1.03	1.00	0.98	0.95	1.05	8.25	8.46	7.55	7.81	8.21	0.36	0.36	2.84	7.41	7.28	-	
Fe2O3	3.83	3.23	3.33	1.84	9.37	9.38	8.85	9.27	9.36	8.14	1.16	0.78	1.66	0.49	1.13	-	-	-	-	-	
Y2O3	27.30	28.80	29.20	29.40	33.09	32.97	32.09	32.82	32.49	31.85	29.30	26.00	31.46	32.27	30.90	32.84	31.17	35.26	32.96	28.91	28.72
Nb2O5	8.10	8.30	8.20	9.60	0.39	0.34	0.52	0.47	0.52	0.47	0.39	0.34	0.26	0.23	0.24	0.28	0.43	0.55	0.53	0.45	0.32
La2O3	0.40	0.53	0.54	0.64	0.26	0.27	0.23	0.24	0.28	0.43	0.56	0.57	1.03	0.83	1.04	-	-	0.32	0.25	0.32	
Ce2O3	1.85	2.54	2.97	3.23	1.91	1.94	1.74	1.66	2.00	2.90	3.62	3.43	7.31	4.46	5.62	6.22	6.00	3.77	2.85	1.41	1.50
Pr2O3	0.43	0.49	0.56	0.47	0.35	0.40	0.37	0.30	0.39	0.55	0.47	0.40	0.40	0.45	0.40	0.45	-	-	0.56	0.31	0.42
Nd2O3	3.97	3.98	4.49	3.96	2.81	2.89	2.57	2.55	2.98	3.88	1.60	1.28	3.79	1.17	2.28	-	-	2.17	1.32	1.23	
Sm2O3	0.79	0.76	0.78	0.61	1.14	1.14	1.07	1.04	1.25	1.29	0.31	0.19	0.65	0.14	0.45	-	-	0.59	0.72	0.38	
Eu2O3	0.30	0.33	0.35	0.31	0.11	0.08	0.07	0.09	0.15	0.13	-	-	-	-	-	-	-	-	0.13	0.23	
Gd2O3	0.86	0.84	0.44	1.62	1.67	1.52	1.55	1.79	1.60	0.20	0.17	0.26	<.15	0.33	-	-	-	-	-	0.22	
Tb2O3	-	-	-	-	-	-	-	-	-	-	-	-	-	-	-	-	-	-	-	-	
Dy2O3	0.99	0.75	0.36	1.95	1.90	1.79	1.92	2.04	1.55	-	-	-	<2	-	-	-	-	0.18	0.38	0.28	
Ho2O3	-	-	-	-	-	-	-	-	-	-	-	-	<2	-	-	-	-	-	-	-	
Er2O3	0.41	0.35	0.40	0.13	0.91	0.89	0.84	0.92	0.91	0.64	-	-	-	-	-	-	-	0.41	0.20	<.16	
Tm2O3	-	-	-	-	-	-	-	-	-	-	-	-	-	-	-	-	-	-	-	-	
Yb2O3	0.49	0.39	0.31	0.22	-	-	-	-	-	-	-	-	-	-	-	-	-	-	-	-	
Lu2O3	-	-	-	-	-	-	-	-	-	-	-	-	-	-	-	-	-	-	-	-	
HfO2	0.43	0.44	0.59	0.81	0.34	0.29	0.33	0.37	0.25	0.44	0.39	0.28	0.88	0.34	0.34	-	-	0.25	0.39	0.47	
Ta2O5	0.69	0.59	0.33	0.70	<.1	<.1	<.1	<.1	<.1	<.1	<.1	<.1	<.1	<.1	<.1	<.1	<.1	-	1.08	1.10	-
WO3	-	-	-	-	-	-	-	-	-	-	-	-	-	-	-	-	-	-	-	-	
PhO	-	-	-	-	-	-	-	-	-	-	-	-	-	-	-	-	-	-	-	-	
ThO2	4.32	1.62	0.89	0.38	0.28	0.23	0.21	0.20	0.23	0.17	<.1	<.1	<.1	<.1	<.1	<.1	<.1	-	0.24	0.31	0.31
UO2	0.96	0.57	0.28	0.13	-	-	-	-	-	-	-	-	-	-	-	-	-	0.57	2.51	3.41	
(Na,K)2O	-	-	-	-	-	-	-	-	-	-	-	-	-	-	-	-	-	8.22	1.75	0.29	
H2O	-	-	-	-	-	-	-	-	-	-	-	-	-	-	-	-	-	3.35	5.66	3.15	
"Others"	-	-	-	-	-	-	-	-	-	-	-	-	-	-	-	-	-	0.06	0.13	-	
TOTAL	99.11	99.07	100.56	100.10	99.48	99.49	98.33	98.34	98.65	98.80	98.62	99.43	98.82	99.69	99.65	101.03	100.32	99.50	97.38	100.30	97.73
cations to 7 oxygens																					
Ca2+ (Y+REE) ³⁺	0.524	0.573	0.589	0.692	0.276	0.279	0.259	0.299	0.250	0.284	0.542	0.565	0.489	0.662	0.558	0.737	0.725	0.797	0.804	0.837	
Pb2+	0.386	0.369	0.391	0.301	0.555	0.559	0.514	0.539	0.578	0.566	0.220	0.190	0.411	0.190	0.296	0.142	0.138	0.092	0.178	0.125	
Th4+	-	-	-	-	0.005	0.004	0.004	0.003	0.004	0.003	0.000	0.000	0.000	0.000	0.000	-	-	-	0.004	0.006	
Li4+	0.015	0.024	0.013	0.006	0.007	0.002	0.008	0.008	0.007	0.007	0.010	0.018	0.018	0.017	0.017	0.017	0.017	0.037	0.032	0.053	
SUM Ca2+	0.992	0.975	0.997	1.000	0.850	0.857	0.792	0.856	0.848	0.867	1.029	1.088	0.982	1.005	0.909	0.024	0.043	0.014	0.015	0.004	
Zr4+	0.903	0.930	0.928	0.923	1.019	1.016	0.979	1.019	1.013	0.993	1.024	0.923	1.055	1.063	1.042	0.997	0.953	1.142	1.044	0.942	
Hf4+	0.008	0.011	0.015	0.006	0.005	0.006	0.007	0.005	0.008	0.008	0.017	0.007	0.007	0.007	0.007	0.005	0.005	0.007	0.014	0.009	
SUM Zr4+	0.911	0.940	0.938	1.025	1.021	0.985	1.026	1.018	1.001	1.032	0.928	1.072	1.069	1.049	0.997	0.953	1.147	1.052	0.957	0.961	
Tl4+	1.328	1.355	1.364	1.370	1.529	1.535	1.448	1.538	1.527	1.560	1.333	1.224	1.419	1.320	1.278	1.484	1.410	1.373	1.487	0.775	
Si4+	-	-	-	-	0.011	0.008	0.126	0.010	0.008	0.006	0.006	0.006	0.006	0.006	0.005	0.004	0.004	0.007	0.007	-	
Mg2+	0.018	0.013	0.009	0.011	0.291	0.286	0.329	0.277	0.315	0.281	0.003	0.009	0.005	-	-	-	-	0.010	0.037	0.071	
Mn2+	0.029	0.016	0.015	0.011	-	-	-	-	-	-	0.060	0.064	0.051	0.043	0.046	0.003	0.003	0.007	0.031	0.031	
F62+	0.472	0.441	0.462	0.412	0.054	0.055	0.052	0.051	0.056	0.495	0.515	0.434	0.441	0.475	-	-	-	0.154	0.414	-	
F33+	-	-	-	-	-	-	-	-	-	-	-	-	-	-	-	-	-	-	-	-	
A13+	0.060	0.070	0.052	0.043	-	-	-	-	-	-	-	-	-	-	-	-	-	-	-	-	
C13+	-	-	-	-	-	-	-	-	-	-	-	-	-	-	-	-	-	-	-	-	
Nb5+	0.248	0.242	0.279	0.011	0.010	0.015	0.014	0.007	0.015	0.107	0.199	0.082	0.163	0.187	0.092	0.081	0.075	0.138	0.745	0.731	
Ta5+	0.013	0.011	0.006	0.012	-	-	-	-	-	-	-	-	-	-	-	-	-	0.020	0.020	-	
W6+	-	-	-	-	-	-	-	-	-	-	-	-	-	-	-	-	-	-	-	-	
SUM Tl4+	2.165	2.150	2.188	2.125	2.122	2.229	2.114	2.137	2.129	2.019	2.042	2.013	1.998	2.014	2.140	1.799	1.951	2.022	2.034	-	
TOTAL	4.066	4.087	4.076	4.000	4.000	4.006	3.996	4.003	3.997	4.080	4.061	4.067	4.073	4.068	3.987	4.019	4.033	3.982	4.011	-	

	C7	C8	C9	C10	C11	C12	C13	C14	C15	C16	C17	C18	C19	C20	C21	C22	C23	C24	C25	C26	C27
MgO	0.36	-	0.36	-	0.70	0.04	0.96	0.70	0.21	0.36	-	0.49	0.39	0.80	0.55	0.74	0.76	0.27	0.39	0.27	0.58
Al2O3	<0.05	-	0.70	-	1.23	-	-	1.23	-	3.47	<0.05	<0.05	<0.05	<0.05	<0.05	<0.05	<0.05	<0.05	<0.05	<0.05	0.72
SiO2	11.36	10.78	11.00	9.59	10.12	10.71	10.22	10.00	9.59	10.12	11.99	12.43	10.82	12.22	10.77	11.47	12.66	12.74	12.30	11.00	
CaO	16.84	22.00	18.19	18.30	16.32	14.08	20.00	18.30	16.32	14.08	18.14	18.95	17.25	17.39	16.54	14.70	23.67	21.05	23.54	18.68	17.00
TiO2	-	-	-	-	-	-	-	-	-	-	-	-	-	-	-	-	-	-	-	-	-
Cr2O3	-	-	-	-	-	-	-	-	-	-	-	-	-	-	-	-	-	-	-	-	-
MnO	0.49	-	0.38	-	2.02	5.56	3.19	5.37	2.02	4.00	7.43	7.54	7.57	7.59	7.77	7.27	6.79	7.31	7.10	7.66	7.66
FeO	7.91	5.16	6.00	5.37	1.11	2.72	3.46	1.08	4.81	2.72	3.46	2.88	-	-	-	-	-	-	-	-	-
Fe2O3	-	1.48	-	-	-	-	-	-	-	-	-	-	-	-	-	-	-	-	-	-	-
Y2O3	0.21	-	-	-	-	-	-	-	-	-	-	-	-	-	-	-	-	-	-	-	-
ZrO2	31.44	22.82	25.00	27.35	28.40	34.39	33.42	27.35	28.40	32.94	30.23	31.19	28.81	29.00	29.27	28.64	30.71	30.53	31.18	30.29	28.84
Nb2O5	21.26	27.00	24.84	16.17	24.40	24.11	11.25	22.47	24.81	19.65	19.45	19.21	19.01	21.15	19.85	20.68	13.97	17.45	14.54	18.25	19.51
La2O3	0.14	-	-	-	-	-	-	-	-	-	-	-	-	-	-	-	-	-	-	-	-
Ce2O3	1.44	3.97	4.00	3.71	2.79	1.40	6.10	3.71	2.79	3.06	1.44	1.64	1.52	1.40	0.97	1.46	1.62	1.42	1.61	1.55	-
Pr2O3	0.25	-	-	-	-	-	-	-	-	-	-	-	-	-	-	-	-	-	-	-	-
Nd2O3	1.49	-	-	-	-	-	-	-	-	-	-	-	-	-	-	-	-	-	-	-	-
Sm2O3	0.33	-	-	-	-	-	-	-	-	-	-	-	-	-	-	-	-	-	-	-	-
Eu2O3	-	-	-	-	-	-	-	-	-	-	-	-	-	-	-	-	-	-	-	-	-
Gd2O3	0.31	-	-	-	-	-	-	-	-	-	-	-	-	-	-	-	-	-	-	-	-
Tb2O3	-	-	-	-	-	-	-	-	-	-	-	-	-	-	-	-	-	-	-	-	-
Dy2O3	<15	-	-	-	-	-	-	-	-	-	-	-	-	-	-	-	-	-	-	-	-
Hf2O3	-	-	-	-	-	-	-	-	-	-	-	-	-	-	-	-	-	-	-	-	-
<16	-	-	-	-	-	-	-	-	-	-	-	-	-	-	-	-	-	-	-	-	-
Tm2O3	-	-	-	-	-	-	-	-	-	-	-	-	-	-	-	-	-	-	-	-	-
Yb2O3	-	-	-	-	-	-	-	-	-	-	-	-	-	-	-	-	-	-	-	-	-
Lu2O3	-	-	-	-	-	-	-	-	-	-	-	-	-	-	-	-	-	-	-	-	-
HO2	0.56	-	0.41	2.00	0.29	0.46	1.50	1.24	0.43	0.46	0.29	0.46	0.43	2.74	2.08	0.56	0.52	0.49	0.48	0.66	0.62
Ta2O5	0.67	-	-	-	-	-	-	-	-	-	-	-	-	-	-	-	0.25	0.25	0.25	0.25	0.43
WO3	-	-	-	-	-	-	-	-	-	-	-	-	-	-	-	-	-	-	-	3.27	1.73
PhO	0.25	-	-	-	-	-	-	-	-	-	-	-	-	-	-	-	-	-	-	-	0.20
ThO2	4.20	2.90	2.72	2.51	2.05	2.73	2.51	2.72	2.51	3.21	2.51	3.20	1.82	2.27	0.89	1.39	6.26	2.48	5.51	2.21	1.36
UO2	<1	-	0.40	1.4	3.20	2.51	0.96	3.20	2.51	1.46	2.27	0.89	0.54	0.13	0.72	0.23	0.28	0.63	0.41	0.56	0.40
(Na,K)2O	-	0.9	2.42	2.48	2.88	2.62	-	3.3	1.13	2.72	-	-	-	-	-	-	-	-	-	-	-
H2O	-	-	0.98	0.98	-	10.64	-	10.64	-	0.41	-	-	-	-	-	-	-	-	-	-	-
"Others"	-	-	-	-	-	-	-	-	-	-	-	-	-	-	-	-	-	-	-	-	-
TOTAL	99.51	99.73	100.68	90.31	99.06	100.41	97.01	99.03	100.06	102.11	98.43	98.66	97.46	98.15	98.11	97.37	97.29	98.08	97.45	98.40	96.69
cations to 7 oxygens																					
Ca2+	0.812	0.755	0.799	0.748	0.748	0.778	0.730	0.727	0.699	0.719	0.860	0.881	0.799	0.879	0.788	0.854	0.895	0.895	0.880	0.814	
(Y+REE)3+	0.104	0.095	0.099	0.099	0.071	0.035	0.149	0.092	0.070	0.074	0.094	0.114	0.101	0.095	0.109	0.060	0.098	0.101	0.094	0.117	0.115
Pt2+	0.004	-	-	-	-	-	-	-	-	-	-	-	-	-	-	0.003	-	-	0.001	0.004	0.004
Tr4+	0.064	0.041	0.045	0.045	0.039	0.032	0.041	0.042	0.039	0.048	0.044	0.044	0.021	0.098	0.038	0.085	0.087	0.033	0.018	0.020	0.017
U4+	-	0.006	0.006	0.049	0.049	0.038	0.014	0.048	0.027	0.010	0.008	0.002	0.011	0.004	0.004	0.009	0.009	0.008	0.006	0.006	0.006
SUM Ca2+	0.985	0.891	0.949	0.892	0.907	0.882	0.935	0.861	0.856	0.868	1.011	1.024	1.004	1.022	0.985	1.006	1.036	1.022	1.018	1.022	1.008
Zr4+	1.023	0.727	0.827	0.971	0.955	1.137	1.086	0.942	1.065	0.987	1.006	0.969	0.949	0.979	0.971	0.988	0.979	0.987	0.986	0.971	-
Hf4+	0.011	-	0.827	0.977	0.965	1.137	1.098	0.911	0.951	1.065	0.998	1.016	0.979	0.958	0.988	0.980	1.000	0.992	1.008	0.980	0.980
SUM Zr4+	1.034	0.727	-	-	-	-	-	-	-	-	-	-	-	-	-	-	-	-	-	-	-
Tl4+	0.845	1.081	0.927	1.002	0.847	0.718	1.003	0.934	0.835	0.741	0.913	0.942	0.894	0.878	0.853	0.768	1.174	1.041	1.160	0.938	0.883
Si4+	-	-	-	-	-	-	-	-	-	-	-	-	-	-	-	-	-	-	-	-	-
Mg2+	0.036	-	-	-	-	-	-	-	-	-	-	-	-	-	-	-	-	-	-	-	-
Mn2+	0.028	-	0.022	-	-	-	-	-	-	-	-	-	-	-	-	-	-	-	-	-	-
Fp2+	0.442	0.282	0.340	0.327	0.117	0.315	0.178	0.305	0.115	0.222	0.139	0.177	0.144	0.416	0.417	0.436	0.426	0.446	0.423	0.375	0.428
Fs3+	-	0.073	0.057	0.149	0.180	0.055	0.241	0.052	0.075	0.056	-	0.271	-	-	-	-	-	-	-	-	-
Al3+	-	-	-	-	0.060	-	0.003	-	-	-	-	-	-	-	-	-	-	-	-	-	-
C3+	-	-	-	-	-	-	-	-	-	-	-	-	-	-	-	-	-	-	-	-	-
Nb5+	0.642	0.798	0.761	0.532	0.761	0.739	0.339	0.689	0.763	0.589	0.574	0.593	0.642	0.616	0.650	0.417	0.519	0.431	0.551	0.609	
Ts5+	0.012	0.007	0.037	0.017	0.023	-	0.027	0.008	0.051	0.037	0.047	0.028	0.033	0.045	0.046	0.094	0.030	0.036	0.030	0.059	0.032
W6+	-	-	-	-	-	-	-	-	-	-	-	-	-	-	-	-	-	-	-	-	-
SUM Tl4+	2.004	2.241	2.144	2.127	1.927	1.901	1.946	2.152	1.977	2.003	2.026	2.012	2.056	2.057	2.051	2.028	2.044	2.039	2.044	2.055	2.055
TOTAL	4.023	3.859	3.920	3.997	3.799	3.921	3.979	3.924	3.784	3.936	4.034	4.052	4.038	4.024	4.014	4.064	4.065	4.067	4.043	-	-

	C28	C29	C30	C31	C32	C33	C34	C35	C36	C37	C38	C39	C40	C41	C42	C43	C44	C45	C46	C47	C48
MgO	0.62	0.30	0.56	0.54	0.60	0.48	0.65	0.59	0.31	0.37	0.33	0.30	0.47	0.22	0.12	0.48	0.32	0.21	0.10	0.19	
Al ₂ O ₃	<0.05	<0.05	<0.05	<0.05	<0.05	<0.05	<0.05	0.19	0.09	<0.05	<0.05	<0.05	<0.05	<0.05	<0.05	<0.05	<0.05	<0.05	<0.05	0.09	
SiO ₂	<0.05	<0.05	<0.05	<0.05	<0.05	<0.05	<0.05	0.27	0.48	0.43	<0.05	<0.05	<0.05	<0.05	<0.05	<0.05	<0.05	<0.05	<0.05	0.07	
CaO	11.20	11.85	11.41	12.12	11.67	12.25	11.12	9.97	9.19	7.77	10.70	10.39	10.68	11.78	5.95	10.49	5.79	6.01	9.11	25.83	
TiO ₂	17.81	22.77	18.12	18.72	16.75	17.18	17.00	18.97	28.12	27.36	23.20	21.07	18.34	22.04	22.52	22.66	19.39	21.25	22.40	23.20	
Cr ₂ O ₃	-	-	-	-	-	-	-	-	-	-	-	-	-	-	-	-	-	-	-	-	
MnO	0.26	0.34	0.20	0.16	0.28	0.20	0.26	0.36	0.20	0.31	0.13	0.34	0.47	0.33	0.21	0.57	0.40	0.44	0.55	0.63	
FeO	7.66	6.79	7.41	7.46	7.39	7.40	7.65	7.06	6.77	6.98	6.98	7.72	6.74	7.37	7.50	8.22	8.03	7.90	7.20	7.48	
Fe ₂ O ₃	-	-	-	-	-	-	-	-	-	-	-	-	-	-	-	-	-	-	-	-	
Y ₂ O ₃	0.27	0.18	0.24	0.31	0.17	0.15	0.30	0.46	1.28	1.40	0.53	0.58	0.56	0.45	0.49	1.18	0.61	0.99	1.26	1.53	
ZrO ₂	29.72	30.72	30.26	31.24	29.07	28.86	29.44	30.67	32.78	32.07	30.51	29.72	30.73	30.68	30.15	28.85	28.87	29.16	28.36	29.10	
Nb ₂ O ₅	20.19	14.47	17.59	18.04	21.21	20.78	20.12	13.36	2.82	3.71	13.10	15.39	13.92	15.48	9.49	17.75	13.56	9.11	9.17	9.91	
La ₂ O ₃	0.30	0.18	0.27	0.40	0.33	0.22	0.37	0.11	0.45	0.60	0.19	0.26	0.32	0.24	0.14	0.53	0.37	0.33	0.53	0.52	
Ce ₂ O ₃	1.58	1.46	1.85	1.62	1.27	1.47	1.76	1.68	5.03	5.75	2.09	2.47	2.15	1.75	2.09	5.53	2.64	3.82	5.27	4.84	
Pr ₂ O ₃	0.34	0.41	0.36	0.48	0.26	0.17	0.23	0.46	1.10	1.08	0.27	0.42	0.38	0.34	0.57	1.31	0.41	0.96	1.25	0.89	
Nd ₂ O ₃	1.45	1.16	1.45	1.49	1.14	1.14	1.75	1.91	4.99	6.15	2.25	2.91	2.03	1.71	2.49	3.22	5.20	7.27	7.71	4.54	
Sm ₂ O ₃	0.34	0.18	0.30	0.40	0.21	0.35	0.23	0.50	1.03	1.17	0.61	0.58	0.43	0.43	0.60	1.96	0.90	1.49	1.90	2.32	
Eu ₂ O ₃	-	-	-	-	-	-	-	-	-	-	-	-	-	-	-	-	-	-	-	-	
Gd ₂ O ₃	0.26	0.35	0.32	0.34	0.30	0.18	0.33	-	-	-	0.91	0.89	0.46	0.53	0.41	0.36	0.40	1.07	0.40	0.82	
Tb ₂ O ₃	-	-	-	-	-	-	-	-	-	-	-	-	-	-	-	-	-	-	-	-	
Dy ₂ O ₃	0.16	<1.15	0.19	<1.15	<1.15	0.20	0.21	0.45	0.49	0.30	0.29	0.19	0.22	0.25	0.72	<1.15	0.52	0.57	0.97	0.56	
Ho ₂ O ₃	-	-	<1.15	<1.15	<1.15	<1.15	<1.15	<1.15	<1.15	<1.15	0.19	<1.15	<1.15	<1.15	<1.15	<1.15	0.15	0.20	0.19	0.22	
Er ₂ O ₃	<1.15	<1.15	<1.15	<1.15	<1.15	<1.15	<1.15	<1.15	<1.15	<1.15	<1.15	<1.15	<1.15	<1.15	<1.15	<1.15	<1.15	<1.15	<1.15	<1.15	
Tm ₂ O ₃	-	-	-	-	-	-	-	-	-	-	-	-	-	-	-	-	-	-	-	-	
Yb ₂ O ₃	-	-	-	-	-	-	-	-	-	-	-	-	-	-	-	-	-	-	-	-	
Lu ₂ O ₃	-	-	-	-	-	-	-	-	-	-	-	-	-	-	-	-	-	-	-	-	
HfO ₂	0.38	0.67	0.72	0.72	0.56	0.55	0.63	0.54	0.57	0.45	0.70	0.75	0.57	0.67	0.67	0.42	0.72	0.65	0.58	0.65	
Ta ₂ O ₅	1.78	2.78	3.99	3.91	1.61	2.80	2.20	0.39	0.29	0.30	<25	0.56	1.04	0.59	0.66	0.32	<25	<25	<25	<25	
WO ₃	<2.25	<2.25	<2.25	<2.25	<2.25	<2.25	<2.25	<2.25	<2.25	<2.25	<2.25	<2.25	<2.25	<2.25	<2.25	<2.25	<2.25	<2.25	<2.25	<2.25	
PbO	0.17	<1	<1	<1	<1	<1	<1	<1	<1	<1	0.45	<1	0.23	<1	0.25	0.37	0.19	<1	<1	<1	<1
Th ₂ O	3.95	2.46	2.85	2.04	4.09	2.26	4.01	6.20	<1	0.12	0.93	2.44	0.64	0.83	1.45	0.76	1.58	1.51	0.54	0.36	
UO ₂	0.14	1.07	0.46	0.24	0.51	0.35	0.35	0.10	0.34	0.20	0.59	0.13	0.24	0.09	0.41	0.03	0.19	0.51	0.45	0.53	
(Na,K)2O	-	-	-	-	-	-	-	-	-	-	-	-	-	-	-	-	-	-	-	-	
H ₂ O	-	-	-	-	-	-	-	-	-	-	-	-	-	-	-	-	-	-	-	-	
"Others"	-	-	-	-	-	-	-	-	-	-	-	-	-	-	-	-	-	-	-	-	
TOTAL	98.58	98.14	98.36	100.42	97.42	97.95	98.51	95.97	97.98	97.83	95.77	97.51	97.64	95.88	98.19	97.06	96.64	97.59	95.72	97.94	
																				98.30	
Cations to 7 oxygens																					
Ca ²⁺	0.807	0.840	0.828	0.856	0.850	0.882	0.808	0.752	0.654	0.565	0.779	0.755	0.776	0.855	0.835	0.452	0.765	0.556	0.445	0.452	
(Y+REE) ³⁺	0.116	0.098	0.122	0.127	0.095	0.094	0.129	0.144	0.377	0.443	0.173	0.205	0.168	0.139	0.175	0.511	0.216	0.363	0.514	0.538	
Pb ²⁺	0.003	-	-	-	-	-	-	-	-	-	-	-	-	-	-	0.005	0.007	0.003	0.002	0.002	
Th ⁴⁺	0.060	0.037	0.044	0.031	0.063	0.035	0.062	0.099	-	-	0.004	0.014	0.038	-	0.013	0.013	0.022	0.024	0.024	0.012	
U ⁴⁺	0.002	0.016	0.004	0.004	0.008	0.008	0.005	0.025	0.025	0.015	0.001	0.005	0.031	0.009	0.032	0.016	0.008	0.009	0.006	0.008	
ΣM ₂ Ca ²⁺	0.989	0.991	0.991	0.999	1.013	1.018	0.975	0.989	1.066	1.073	1.071	1.025	0.985	1.028	1.006	0.972	0.986	1.004	0.998	0.999	
Zr ⁴⁺	0.975	0.991	0.999	1.004	0.964	0.978	0.974	1.053	1.062	1.011	0.983	1.017	1.016	0.972	0.998	0.958	0.983	0.992	0.997	0.987	
Hf ⁴⁺	0.007	0.013	0.014	0.014	0.011	0.011	0.010	0.013	0.011	0.010	0.009	0.014	0.013	0.013	0.013	0.014	0.013	0.012	0.011	0.012	
ΣM ₇ Zr ⁴⁺	1.982	1.004	1.013	1.018	0.975	0.989	0.985	1.066	1.073	1.071	1.025	0.985	1.028	1.006	0.972	0.986	1.004	0.998	0.999	0.999	
Ti ⁴⁺	1.901	1.133	0.923	0.928	0.857	0.868	0.867	1.004	1.455	1.398	1.186	1.075	0.938	1.125	1.120	0.992	1.105	1.208	1.225	1.301	
Si ⁴⁺	-	-	-	-	-	-	-	-	-	-	0.016	0.009	0.007	-	-	-	-	0.002	0.003	-	
Mg ²⁺	0.062	0.030	0.057	0.053	0.081	0.048	0.066	0.062	0.031	0.037	0.033	0.030	0.048	0.027	0.022	0.019	0.033	0.022	0.010	0.005	
Mn ²⁺	0.015	0.019	0.011	0.009	0.016	0.011	0.015	0.021	0.011	0.018	0.007	0.020	0.019	0.012	0.011	0.011	0.010	0.019	0.019	0.003	
Ta ⁵⁺	0.033	0.073	0.070	0.030	0.051	0.041	0.007	0.005	0.006	-	-	-	-	-	-	-	-	-	-	-	
W ⁶⁺	-	-	-	-	-	-	-	-	-	-	-	-	-	-	-	-	-	-	-	-	
ΣM ₁₄	2.055	2.041	2.022	2.009	2.036	2.025	2.040	2.004	2.005	2.026	2.048	1.992	2.000	2.039	2.031	2.091	2.080	2.061	2.071	2.064	
TOTAL	4.027	4.036	4.035	4.045	4.027	4.031	4.030	4.062	4.110	4.091	4.053	4.052	4.011	4.073	4.065	4.023	4.024	4.042	4.024	4.056	

	C49	C50	C51	C52	C53	C54	C55	C56	C57	C58	C59	C60	C61	C62	C63	C64	C65	C66	C67	C68	C69	
Mg0	0.08	0.18	0.28	0.30	0.44	0.28	0.38	0.35	0.27	0.29	0.36	<0.05	<0.05	<0.05	<0.05	<0.05	<0.05	0.15	1.06	1.07	1.13	
Al2O3	<0.05	<0.05	0.09	<0.05	<0.05	0.12	<0.05	0.09	0.14	<0.05	<0.05	<0.05	<0.05	<0.05	<0.05	<0.05	0.13	0.15	0.18	0.03		
SiO2	0.22	0.15	0.23	0.31	0.25	0.19	0.16	0.46	0.17	0.19	0.06	<0.05	<0.05	<0.05	<0.05	<0.05	0.13	0.05	0.03	0.03		
Cao	8.06	6.93	5.84	7.35	10.70	9.78	8.99	8.71	8.00	8.37	12.10	12.36	12.02	11.48	11.31	11.28	12.07	10.32	9.18	9.09		
TiO2	21.68	21.84	20.49	22.90	21.09	23.64	22.28	20.51	22.69	27.24	24.95	36.15	35.39	34.66	34.33	34.45	14.14	14.10	14.40	-		
C12O3	-	-	-	-	-	-	-	-	-	-	-	-	-	-	-	-	-	-	-	-		
MnO	0.36	0.47	0.59	0.32	0.31	0.27	0.25	1.07	0.65	0.33	0.28	0.19	0.21	0.21	0.35	0.26	-	-	-	-		
FeO	7.03	7.46	7.34	7.80	7.87	7.04	7.75	6.56	7.11	6.66	6.53	6.49	6.57	10.20	6.32	-	8.89	7.27	8.56	-		
Fe2O3	-	-	-	-	-	-	-	-	-	-	-	-	-	-	-	-	-	-	-	-		
Y2O3	0.99	1.41	1.06	0.95	0.58	0.51	0.75	0.48	1.10	1.43	0.50	0.32	0.32	0.17	0.36	0.28	-	6.88	6.64	-		
ZrO2	28.10	29.49	28.68	29.50	29.79	30.00	29.54	32.62	30.51	32.42	31.07	35.15	33.71	34.55	31.65	33.67	32.90	32.23	26.17	26.08		
Nb2O5	12.84	10.53	10.97	11.91	16.84	13.21	13.55	13.82	8.78	5.15	12.39	0.19	0.29	0.23	0.38	0.19	0.45	18.50	17.01	16.50		
La2O3	0.32	0.89	0.34	0.28	0.23	0.33	0.19	0.68	0.38	0.15	<0.07	0.13	0.11	<0.07	-	-	-	-	-	-		
Ce2O3	4.00	4.13	6.99	3.78	2.56	2.95	3.24	1.99	5.06	3.50	1.29	0.74	0.91	0.77	-	-	-	-	-	-		
Pr2O3	0.70	1.05	1.60	0.92	0.44	0.66	0.91	1.00	0.84	0.24	<0.14	<0.14	<0.14	<0.14	-	-	-	-	-	1.31		
Nd2O3	5.33	5.91	7.56	5.51	3.22	3.89	4.16	2.04	6.62	4.51	1.26	0.85	1.08	0.61	-	-	-	-	-	-		
Sm2O3	1.43	1.89	1.59	1.46	0.89	0.98	1.43	0.49	1.64	1.15	0.57	0.33	0.36	0.27	0.31	0.26	-	-	-	-		
Eu2O3	-	-	-	-	-	-	-	-	-	-	0.17	-	-	-	-	-	-	-	-	-		
Gd2O3	1.02	1.12	1.04	0.87	0.57	0.59	0.83	0.26	0.99	0.98	0.34	0.32	0.17	0.23	0.33	0.23	-	-	-	-		
Tb2O3	-	-	-	-	-	-	-	-	-	-	-	-	-	-	-	-	-	-	-	-		
Dy2O3	0.58	0.68	0.56	0.61	0.35	0.25	0.30	0.69	0.67	0.57	0.22	0.28	0.21	0.26	0.33	0.15	-	-	-	-		
Ho2O3	-	-	-	-	-	-	-	-	-	-	-	-	-	-	-	-	-	-	-	-		
Er2O3	0.23	0.37	0.26	<1.5	0.28	<1.5	<1.5	<1.5	<1.5	<1.5	0.21	<1.6	<1.6	<1.6	<1.6	<1.6	<1.6	<1.6	<1.6	<1.6		
Tm2O3	-	-	-	-	-	-	-	-	-	-	-	-	-	-	-	-	-	-	-	-		
Yb2O3	<1.8	<1.8	<1.8	<1.8	<1.8	<1.8	<1.8	<1.8	<1.8	<1.8	<1.8	<1.8	<1.8	<1.8	<1.8	<1.8	<1.8	<1.8	<1.8	<1.8		
Lu2O3	-	-	-	-	-	-	-	-	-	-	-	-	-	-	-	-	-	-	-	-		
Hf2O3	0.79	0.59	0.73	0.66	0.76	0.64	0.47	0.60	0.42	0.59	0.42	0.51	0.70	0.85	0.55	0.76	0.32	<2	<2	<2		
Ta2O5	<2.5	0.30	<2.5	<2.5	<2.5	<2.5	<2.5	<2.5	<2.5	<2.5	<2.5	<2.5	<2.5	<2.5	<2.5	<2.5	<2	<2	<2	<2		
WO3	<2.5	<2.5	<2.5	<2.5	<2.5	<2.5	<2.5	<2.5	<2.5	<2.5	<2.5	<2.5	<2.5	<2.5	<2.5	<2.5	<2	<2	<2	<2		
PbO	0.23	0.14	<1	0.14	0.11	0.14	0.14	0.11	0.14	0.11	0.23	<1	0.10	0.10	0.05	0.33	0.68	0.17	0.21	-	-	
ThO2	1.85	1.07	0.13	1.88	0.50	0.55	1.72	3.67	1.73	1.73	1.44	3.46	4.18	4.03	5.58	3.67	4.36	4.85	5.89	7.65	10.80	
UO2	1.14	0.42	0.31	0.46	0.48	0.97	0.24	0.49	0.10	0.25	2.07	1.41	1.44	1.51	1.87	1.68	1.37	1.44	-	-	-	
(Nd,K)2O	-	-	-	-	-	-	-	-	-	-	-	-	-	-	-	-	-	-	-	-		
H2O	-	-	-	-	-	-	-	-	-	-	-	-	-	-	-	-	-	-	-	-		
"Others"	-	-	-	-	-	-	-	-	-	-	-	-	-	-	-	-	-	-	-	-		
TOTAL	96.98	96.49	97.14	98.06	98.31	98.31	96.77	97.28	95.96	96.39	96.77	98.73	98.11	98.46	97.34	98.59	96.99	93.11	95.04	93.73	91.81	95.63

Cations to 7 oxygens																					
Ca2+	0.605	0.525	0.449	0.540	0.761	0.705	0.657	0.643	0.472	0.611	0.846	0.829	0.818	0.792	0.676	0.780	0.783	0.830	0.804	0.739	0.713
(Y+REE)3+	0.375	0.442	0.567	0.366	0.223	0.250	0.299	0.171	0.463	0.341	0.121	0.060	0.070	0.060	0.033	0.056	0.000	0.045	0.052	0.083	0.048
Pb2+	0.004	-	0.003	-	0.029	0.008	0.027	0.058	0.028	0.027	0.021	0.049	0.060	0.060	0.032	0.054	0.004	0.027	0.024	0.020	0.021
Th4+	0.029	0.017	0.002	0.029	0.007	0.015	0.004	0.008	0.004	0.030	0.020	0.020	0.020	0.020	0.027	0.027	0.027	0.027	0.027	0.027	0.180
U4+	0.018	0.007	0.005	0.007	0.015	0.004	0.001	0.961	0.968	0.984	0.1020	0.969	0.975	0.944	0.944	0.966	0.953	0.953	0.953	0.941	-
SUM Ca2+	1.031	0.994	1.023	0.945	1.001	-	-	-	-	-	-	-	-	-	-	-	-	-	-	-	-
Zr4+	0.959	1.017	1.004	0.986	0.965	0.985	0.982	1.095	1.076	0.989	1.073	1.044	1.084	1.084	1.057	1.040	1.009	0.927	0.956	0.955	-
Hf4+	0.016	0.012	0.013	0.014	0.012	0.009	0.013	0.012	0.009	0.013	0.016	0.008	0.009	0.013	0.016	0.014	0.014	0.022	0.016	0.015	-
SUM Zr4+	0.975	1.029	1.019	0.999	0.979	0.981	1.008	1.066	0.989	1.057	1.057	1.099	1.010	1.071	1.062	1.025	0.950	0.972	0.970	-	-
Tl4+	1.141	1.162	1.106	1.181	1.053	1.197	1.142	1.062	1.212	1.395	1.225	1.702	1.691	1.678	1.672	1.729	1.702	1.663	1.773	1.797	1.793
Si4+	0.015	0.011	0.021	0.017	0.013	0.011	0.012	0.013	0.012	0.013	0.004	0.004	0.004	0.002	0.002	0.002	0.002	0.002	0.002	0.002	
Mg2+	0.008	0.019	0.030	0.031	0.044	0.028	0.039	0.036	0.029	0.029	0.035	0.019	0.015	0.010	0.011	0.019	0.014	0.014	0.015	0.015	0.123
Fe2+	0.412	0.441	0.447	0.437	0.396	0.442	0.378	0.422	0.379	0.379	0.340	0.364	0.354	0.354	0.352	0.340	-	0.336	0.321	0.340	0.457
Fe3+	-	-	-	-	-	-	-	-	-	-	-	-	-	-	-	-	-	-	-	-	-
A13+	-	-	-	-	-	-	-	-	-	-	-	-	-	-	-	-	-	-	-	-	-
C3+	-	-	-	-	-	-	-	-	-	-	-	-	-	-	-	-	-	-	-	-	-
Nb5+	0.406	0.337	0.356	0.369	0.506	0.402	0.418	0.430	0.282	0.159	0.386	0.005	0.008	0.007	0.011	0.005	0.005	0.005	0.005	0.005	0.546
Ta5+	0.004	0.006	0.003	0.001	0.003	0.001	0.002	0.004	0.003	-	0.032	-	0.007	0.003	0.006	0.003	0.003	0.003	0.003	0.003	0.116
W6+	0.001	0.005	0.001	0.003	0.001	0.003	0.002	0.004	0.003	-	0.011	-	0.011	0.011	0.011	0.011	0.011	0.011	0.011	0.011	0.116
SUM Ti4+	2.010	2.008	1.988	2.076	2.056	2.068	2.014	2.000	2.001	2.044	2.058	2.054	2.054	2.054	2.054	2.054	2.054	2.054	2.054	2.054	2.120
TOTAL	4.016	4.030	4.020	4.059	4.034	4.047	4.005	4.031	4.074	4.061	4.114	4.097	4.143	4.082	3.984	4.010	4.065	4.009	4.031	-	-

	C70	C71	C72	C73	C74	C75	C76	C77	C78	C79	C80	C81	C82	C83	C84	C85	C86	C87	C88	C89	C90
MgO	0.52	0.85	-	0.30	0.32	0.52	0.48	0.30	0.37	0.45	0.34	0.33	0.32	0.31	0.36	0.35	0.40	0.29	0.31	0.28	-
Al2O3	0.03	-	0.39	0.41	0.19	0.20	0.27	0.28	0.39	0.36	0.34	0.27	0.25	0.29	0.29	0.40	0.40	0.45	<0.05	-	0.08
SiO2	0.18	-	<0.05	<0.05	<0.05	<0.05	<0.05	<0.05	<0.05	<0.05	<0.05	<0.05	<0.05	<0.05	<0.05	<0.05	<0.05	<0.05	<0.05	<0.05	<0.05
CaO	11.16	11.38	12.50	12.57	12.39	12.31	12.33	12.74	12.80	12.05	12.62	12.83	13.11	12.68	12.72	12.53	12.57	12.88	12.65	12.65	10.55
TiO2	19.79	13.56	22.70	28.25	28.39	20.13	20.35	25.20	24.96	27.17	27.40	27.01	28.01	25.47	24.99	24.64	24.59	28.25	29.78	19.13	26.09
Cr2O3	-	-	0.20	0.17	0.14	0.43	0.39	0.26	0.24	0.26	0.23	0.18	0.21	0.21	0.30	0.19	0.32	0.16	0.21	0.40	0.18
MnO	-	0.94	0.20	0.28	0.32	0.18	0.72	0.91	0.88	0.20	0.64	0.54	0.51	0.54	0.64	0.43	0.79	0.98	0.98	0.98	0.98
FeO	8.16	7.41	2.28	6.32	6.18	7.72	7.91	6.88	7.20	6.81	6.51	6.54	6.24	7.01	7.12	6.93	7.09	6.08	7.90	7.89	-
Fe2O3	-	-	5.32	-	-	-	-	-	-	-	-	-	-	-	-	-	-	-	-	-	-
Y2O3	0.46	-	-	0.41	0.34	0.24	0.37	0.35	0.29	0.37	0.35	0.18	0.32	0.33	0.35	0.30	0.30	0.35	0.32	0.32	0.60
ZrO2	27.35	30.51	34.80	37.30	36.33	31.18	31.18	30.43	33.87	35.47	35.19	36.38	35.76	33.75	33.40	33.29	35.89	36.00	30.42	31.77	-
Nb2O5	15.68	22.07	15.70	7.27	7.57	17.34	17.70	12.28	12.36	8.68	9.61	9.43	8.67	11.37	12.08	12.34	12.59	6.99	22.29	8.47	-
La2O3	-	-	-	<1	<1	0.13	0.24	0.15	0.11	<1	0.16	0.14	0.12	0.14	0.13	0.19	<1	0.15	<1	0.18	-
Ce2O3	2.49	0.77	0.90	0.53	0.53	0.95	0.81	0.53	0.65	0.49	0.80	0.43	0.79	0.60	0.72	0.54	0.49	0.49	0.49	0.49	0.39
Pr2O3	-	-	<2	0.43	<2	0.43	<2	0.43	<2	<2	<2	<2	<2	<2	<2	<2	<2	<2	<2	<2	0.24
Nd2O3	-	1.10	-	0.50	0.47	0.80	0.85	0.72	0.56	0.62	0.85	0.74	0.61	0.65	0.64	0.64	0.70	0.55	0.51	1.52	-
Sm2O3	-	0.27	-	<15	0.20	0.25	0.18	0.24	0.16	0.17	0.16	<15	0.17	0.28	0.17	0.26	0.19	<15	-	0.43	-
Eu2O3	-	-	-	-	-	-	-	-	-	-	-	-	-	-	-	-	-	-	-	0.14	-
Gd2O3	-	-	-	-	-	-	-	-	-	-	-	-	-	-	-	-	-	-	-	0.35	-
Tb2O3	-	-	-	-	-	-	-	-	-	-	-	-	-	-	-	-	-	-	-	-	-
Dy2O3	-	-	<18	0.31	0.19	0.24	0.19	0.19	0.19	<18	0.19	<18	<18	<18	<18	0.31	0.20	<18	<18	-	0.19
Ho2O3	-	-	-	-	-	-	-	-	-	-	-	-	-	-	-	-	-	-	-	0.07	-
Er2O3	-	-	-	-	-	-	-	-	-	-	-	-	-	-	-	-	-	-	-	-	-
Tm2O3	-	-	-	-	-	-	-	-	-	-	-	-	-	-	-	-	-	-	-	-	-
Yb2O3	-	-	-	-	-	-	-	-	-	-	-	-	-	-	-	-	-	-	-	-	-
Lu2O3	-	-	-	-	-	-	-	-	-	-	-	-	-	-	-	-	-	-	-	-	-
HfO2	0.40	-	0.27	0.19	0.37	0.35	0.25	0.13	0.26	0.21	0.31	0.30	0.27	0.15	0.45	0.24	0.12	0.12	0.12	0.48	-
Ta2O5	0.21	3.08	-	1.66	1.58	1.79	1.92	1.62	1.77	1.71	1.87	1.75	1.70	1.72	1.83	1.74	1.47	1.52	1.52	2.63	-
WO3	-	-	-	<25	0.30	<25	<25	<25	<25	<25	<25	<25	<25	<25	<25	<25	<25	<25	<25	<25	<1
PbO	-	-	-	<1	<1	<1	<1	<1	<1	<1	<1	<1	<1	<1	<1	<1	<1	<1	<1	<1	<1
ThO2	5.57	5.13	4.10	1.90	1.67	2.53	2.17	1.81	1.67	1.56	1.94	1.62	1.25	1.72	1.96	1.99	2.27	1.62	1.48	6.28	-
UO2	-	1.22	1.40	0.98	0.79	1.40	1.32	0.97	1.06	1.14	0.84	0.97	0.94	0.90	1.08	0.87	1.24	1.07	0.97	1.01	-
(Na,K)2O	-	-	-	-	-	-	-	-	-	-	-	-	-	-	-	-	-	-	-	-	-
H2O	-	-	-	-	-	-	-	-	-	-	-	-	-	-	-	-	-	-	-	-	-
"Others"	-	-	-	-	-	-	-	-	-	-	-	-	-	-	-	-	-	-	-	-	-
TOTAL	92.00	98.29	99.90	97.43	98.38	98.78	99.24	98.88	99.04	97.65	99.39	99.04	98.39	97.87	98.90	98.04	99.32	98.17	98.23	92.79	100.80
cations to 7 oxygens																					
Ca2+	0.847	0.839	0.850	0.861	0.842	0.868	0.864	0.872	0.876	0.827	0.854	0.879	0.887	0.873	0.869	0.862	0.851	0.868	0.911	0.742	-
(Y+REE)3+	0.082	0.053	0.021	0.038	0.054	0.074	0.072	0.054	0.050	0.046	0.052	0.054	0.039	0.053	0.057	0.060	0.061	0.045	0.040	0.000	0.126
Pb2+	-	-	-	-	-	-	-	-	-	-	-	-	-	-	-	-	-	-	-	-	-
Th4+	0.080	0.080	0.059	0.028	0.024	0.038	0.032	0.026	0.024	0.023	0.028	0.023	0.018	0.025	0.029	0.033	0.023	0.021	0.021	0.094	-
U4+	-	0.019	0.020	0.014	0.011	0.020	0.019	0.014	0.016	0.012	0.014	0.013	0.015	0.013	0.018	0.015	0.018	0.014	0.014	0.015	0.976
SUM Ca2+	1.019	0.981	0.950	0.941	0.931	1.000	0.987	0.967	0.968	0.912	0.945	0.970	0.957	0.973	0.974	0.972	0.974	0.955	0.943	0.911	-
Zr4+	0.945	1.024	1.077	1.120	1.124	1.000	0.984	1.061	1.055	1.108	1.084	1.101	1.049	1.054	1.055	1.042	1.106	1.104	0.997	1.017	-
Hf4+	0.008	0.024	1.077	1.125	1.007	1.067	1.060	1.111	1.088	1.099	1.107	1.055	1.059	1.058	1.050	1.111	1.106	0.987	1.026	-	
SUM Zr4+	2.115	2.015	1.920	2.002	2.000	2.058	2.074	2.025	2.004	2.042	2.024	2.007	2.004	2.036	2.042	2.013	2.021	2.111	2.062	-	
TOTAL	4.088	4.031	3.947	4.068	4.058	4.068	4.062	4.059	4.071	4.065	4.058	4.076	4.068	4.071	4.070	4.066	4.065	4.068	4.070	4.020	4.064

	C91	C92	C93	C94	C95	C96	C97	C98	C99	C100	C101	C102	C103	C104	C105	C106	C107	C108	C109	C110	C111
MgO	0.33	0.35	0.32	0.32	0.31	0.33	0.40	0.40	0.47	0.47	0.47	0.47	0.49	0.48	0.46	0.47	0.44	0.45	0.36	0.32	
Al ₂ O ₃	0.08	0.07	0.09	0.08	0.06	0.08	<0.05	<0.05	<0.05	<0.05	<0.05	<0.05	<0.05	<0.05	<0.05	<0.05	<0.05	<0.05	0.05	0.06	
SiO ₂	<0.05	<0.05	<0.05	<0.05	<0.05	<0.05	<0.05	<0.05	<0.05	<0.05	<0.05	<0.05	<0.05	<0.05	<0.05	<0.05	<0.05	<0.05	<0.05	<0.05	
CaO	10.37	10.17	10.33	10.52	10.55	10.00	8.76	9.39	9.15	9.15	8.36	8.29	8.24	8.17	8.09	8.37	8.42	8.43	7.83	9.61	
TiO ₂	25.20	25.13	24.87	24.77	24.43	23.18	23.75	23.91	24.14	24.14	24.27	24.37	24.43	24.55	24.66	24.60	24.41	24.82	25.43	-	
Cr ₂ O ₃	-	-	-	-	-	-	-	-	-	-	-	-	-	-	-	-	-	-	-	-	
MnO	0.17	0.20	0.18	0.17	0.16	0.37	0.98	0.27	0.23	0.22	0.26	0.30	0.30	0.30	0.30	0.30	0.28	0.25	0.26	0.73	0.47
Fe ₂ O ₃	-	-	7.83	7.80	7.86	7.88	7.78	6.87	7.78	7.98	8.00	7.94	7.95	7.94	7.95	7.91	7.85	7.96	7.94	6.63	7.35
Y ₂ O ₃	0.54	0.48	0.48	0.51	0.49	0.57	0.58	0.56	0.50	0.53	0.38	0.37	0.38	0.35	0.35	0.37	0.36	0.38	0.37	0.71	0.54
ZrO ₂	31.61	31.08	31.50	31.28	31.07	30.83	30.82	30.46	29.86	29.89	29.34	28.86	28.86	28.10	28.85	28.84	28.40	28.98	28.79	30.81	31.68
Nb ₂ O ₅	8.50	8.37	8.81	9.39	9.54	8.83	8.58	8.68	8.17	8.06	7.06	6.75	6.91	6.75	6.47	6.61	7.01	6.78	6.98	6.11	7.75
La ₂ O ₃	0.18	0.16	0.15	0.15	0.17	0.18	0.16	0.18	0.16	0.18	0.14	0.08	0.07	0.06	0.06	0.06	0.07	0.09	0.08	0.17	0.16
Ce ₂ O ₃	1.27	1.20	1.18	1.22	1.26	1.33	1.29	1.13	1.08	1.08	0.76	0.71	0.67	0.64	0.71	0.72	0.72	0.72	0.72	1.40	1.18
Pr ₂ O ₃	0.23	0.22	0.24	0.18	0.17	0.23	0.16	0.25	0.20	0.17	0.12	0.10	0.08	0.11	0.09	0.08	0.14	0.15	0.12	0.17	0.13
Nd ₂ O ₃	1.42	1.34	1.29	1.34	1.29	1.34	1.51	1.50	1.47	1.29	1.21	0.94	0.85	0.83	0.78	0.77	0.87	0.83	0.88	1.72	1.32
Sm ₂ O ₃	0.40	0.36	0.37	0.37	0.35	0.42	0.42	0.42	0.35	0.37	0.27	0.26	0.23	0.21	0.24	0.24	0.24	0.23	0.46	0.38	
Eu ₂ O ₃	0.12	0.13	0.11	0.12	0.13	0.13	0.13	0.13	0.13	0.13	0.13	0.08	0.09	0.08	0.09	0.08	0.09	0.08	0.09	0.18	0.14
Gd ₂ O ₃	0.31	0.29	0.28	0.27	0.31	0.35	0.36	0.30	0.30	0.24	0.19	0.20	0.21	0.20	0.18	0.22	0.21	0.21	0.21	0.41	0.32
Tb ₂ O ₃	-	-	-	-	-	-	-	-	-	-	-	-	-	-	-	-	-	-	-	-	
Dy ₂ O ₃	0.17	0.12	0.14	0.14	0.17	0.16	0.15	0.16	0.16	0.12	0.08	0.05	0.05	0.06	0.03	0.07	0.08	0.08	0.08	0.20	0.12
Ho ₂ O ₃	-	-	-	-	-	-	-	-	-	-	-	-	-	-	-	-	-	-	-	-	
Er ₂ O ₃	0.05	0.04	0.05	0.05	0.07	0.06	0.07	0.07	0.08	0.07	0.06	0.06	0.05	0.03	0.05	0.03	0.04	0.04	0.04	0.09	0.05
Tm ₂ O ₃	-	-	-	-	-	-	-	-	-	-	-	-	-	-	-	-	-	-	-	-	
Yb ₂ O ₃	-	-	-	-	-	-	-	-	-	-	-	-	-	-	-	-	-	-	-	-	
Lu ₂ O ₃	-	-	-	-	-	-	-	-	-	-	-	-	-	-	-	-	-	-	-	-	
Ho ₂ O ₃	0.49	0.45	0.49	0.46	0.48	0.47	0.44	0.46	0.43	0.50	0.46	0.45	0.46	0.46	0.45	0.46	0.44	0.49	0.48	0.40	0.40
Ta ₂ O ₅	2.92	2.88	3.02	3.28	3.50	3.71	3.69	3.55	2.91	2.76	2.02	1.77	1.72	1.58	1.55	1.59	1.64	1.56	1.61	2.08	2.58
WO ₃	<1	<1	<1	<1	<1	<1	<1	<1	<1	<1	<1	<1	<1	<1	<1	<1	<1	<1	<1	<1	<1
PbO	<1	<1	<1	<1	<1	<1	<1	<1	<1	<1	<1	<1	<1	<1	<1	<1	<1	<1	<1	<1	<1
Th ₂ O ₃	7.36	8.41	7.88	7.00	7.12	7.68	8.50	9.16	11.21	11.38	15.14	15.70	16.02	16.23	16.32	15.37	15.16	15.46	11.63	8.69	
UO ₂	1.03	0.91	0.84	0.95	0.86	0.83	1.01	1.41	1.49	2.10	2.27	2.36	2.43	2.49	2.42	2.65	2.27	2.42	1.80	1.16	
(Na,K)O ₂	-	-	-	-	-	-	-	-	-	-	-	-	-	-	-	-	-	-	-	-	
H ₂ O	-	-	-	-	-	-	-	-	-	-	-	-	-	-	-	-	-	-	-	-	
"Others"	-	-	-	-	-	-	-	-	-	-	-	-	-	-	-	-	-	-	-	-	
TOTAL	100.88	100.22	100.75	100.89	100.71	100.29	98.11	99.75	100.02	100.11	100.45	99.89	100.50	100.20	100.07	99.63	99.87	99.91	100.09	98.73	99.84
cations to 7 oxygens																					
Ca ²⁺	0.734	0.728	0.734	0.745	0.749	0.718	0.650	0.686	0.672	0.671	0.623	0.622	0.615	0.612	0.607	0.627	0.629	0.630	0.585	0.692	
(+REE) ³⁺	0.116	0.108	0.108	0.105	0.110	0.125	0.127	0.124	0.110	0.106	0.079	0.072	0.070	0.068	0.066	0.073	0.073	0.076	0.074	0.144	
Pb ²⁺	-	-	-	-	-	-	-	-	-	-	-	-	-	-	-	-	-	-	-	-	
Th ₄ ⁺	0.111	0.128	0.119	0.113	0.107	0.117	0.134	0.142	0.175	0.177	0.239	0.250	0.254	0.238	0.260	0.245	0.240	0.242	0.245	0.185	
U ₄ ⁺	0.015	0.013	0.012	0.014	0.013	0.012	0.016	0.016	0.022	0.023	0.032	0.035	0.037	0.038	0.039	0.041	0.035	0.038	0.028	0.017	
SUM Ca ₂₊	0.976	0.977	0.973	0.977	0.978	0.973	0.926	0.968	0.978	0.974	0.975	0.976	0.972	0.982	0.984	0.981	0.987	0.982	0.942	0.951	
Zr ₄ ⁺	1.019	1.013	1.018	1.009	1.003	1.008	1.041	1.013	0.998	0.997	0.994	0.984	0.988	0.983	0.990	0.984	0.986	0.979	1.049	1.038	
Hf ₄ ⁺	0.009	0.009	0.009	0.009	0.009	0.009	0.009	0.009	0.008	0.008	0.010	0.009	0.009	0.009	0.010	0.010	0.010	0.009	0.008	0.008	
SUM Zr ₄₊	1.028	1.021	1.028	1.017	1.012	1.017	1.051	1.021	1.007	1.006	1.004	0.994	0.997	0.992	0.999	0.976	0.984	0.988	1.057	1.045	
T ₄ ⁺	1.267	1.266	1.253	1.237	1.234	1.232	1.208	1.218	1.233	1.245	1.261	1.278	1.271	1.286	1.286	1.291	1.293	1.289	1.280	1.303	1.284
S ₄ ⁺	-	-	-	-	-	-	-	-	-	-	-	-	-	-	-	-	-	-	-	-	
Mg ²⁺	0.032	0.035	0.031	0.031	0.031	0.034	0.034	0.040	0.041	0.049	0.049	0.051	0.050	0.048	0.049	0.048	0.047	0.037	0.032	-	
Mn ²⁺	0.009	0.012	0.010	0.009	0.021	0.058	0.015	0.013	0.015	0.013	0.015	0.015	0.015	0.018	0.018	0.018	0.016	0.015	0.043	0.027	
Fe ²⁺	0.433	0.436	0.433	0.436	0.436	0.436	0.398	0.444	0.457	0.455	0.465	0.463	0.464	0.465	0.465	0.463	0.463	0.464	0.463	0.387	0.413
Fe ³⁺	-	-	-	-	-	-	-	-	-	-	-	-	-	-	-	-	-	-	-	-	
A ₃ ⁺	0.006	0.005	0.007	0.006	0.005	0.006	0.006	0.004	0.006	0.006	0.005	0.005	0.005	0.005	0.005	0.005	0.005	0.005	0.004	0.005	
C ₃ ⁺	0.254	0.253	0.264	0.281	0.286	0.268	0.269	0.253	0.249	0.249	0.222	0.214	0.213	0.205	0.209	0.221	0.224	0.220	0.193	0.235	
Nb ⁵⁺	0.052	0.052	0.054	0.059	0.063	0.068	0.069	0.066	0.054	0.051	0.038	0.034	0.033	0.030	0.030	0.031	0.030	0.031	0.040	0.047	
Ta ₅ ⁺	-	-	-	-	-	-	-	-	-	-	-	-	-	-	-	-	-	-	-	-	
W ₆ ⁺	2.054	2.058	2.052	2.058	2.063	2.062	2.041	2.049	2.058	2.060	2.064	2.061	2.066	2.058	2.061	2.073	2.061	2.059	2.006	2.043	
SUM Ti ₄₊	-	-	-	-	-	-	-	-	-	-	-	-	-	-	-	-	-	-	-	-	
TOTAL	4.059	4.057	4.053	4.053	4.054	4.052	4.052	4.044	4.043	4.038	4.044	4.043	4.032	4.032	4.032	4.030	4.030	4.034	4.036	4.040	

	C112	C113	C114	C115	C116	C117	C118	C119	C120	C121	C122	C123	C124	C125	C126	C127	C128	C129	C130	C131	C132		
MgO	0.31	0.29	0.27	0.31	0.28	0.44	0.46	0.49	0.48	0.44	0.48	0.44	0.35	0.45	0.47	0.46	0.47	0.42	0.47	0.40	0.31		
Al2O3	0.06	0.07	0.07	<0.05	<0.05	<0.05	<0.05	<0.05	<0.05	<0.05	<0.05	<0.05	<0.05	<0.05	<0.05	<0.05	<0.05	<0.05	<0.05	0.06	0.07		
SiO2	<0.05	<0.05	<0.05	<0.05	<0.05	<0.05	<0.05	<0.05	<0.05	<0.05	<0.05	<0.05	<0.05	<0.05	<0.05	<0.05	<0.05	<0.05	<0.05	0.06	0.07		
CaO	10.44	10.43	10.42	10.17	9.85	8.13	7.95	7.87	7.98	8.23	8.00	9.67	9.24	8.67	8.29	8.18	8.25	8.27	8.78	10.47	10.47		
TiO2	25.87	25.69	-	-	-	-	-	-	-	24.06	23.95	24.08	24.61	24.03	24.79	24.96	24.59	24.46	24.27	24.59	24.31	24.24	
Cr2O3	-	-	-	-	-	-	-	-	-	-	-	-	-	-	-	-	-	-	-	-	-	-	
MnO	0.16	0.17	0.13	0.16	0.17	0.28	0.33	0.31	0.32	0.28	0.29	0.18	0.21	0.24	0.28	0.26	0.29	0.29	0.27	0.24	0.17	0.17	
FeO	7.84	7.85	7.81	7.88	7.47	7.89	7.95	7.90	7.95	8.00	7.82	7.87	7.98	7.96	7.88	8.02	7.92	7.91	7.92	7.88	-	-	
Fe2O3	-	-	-	-	-	-	-	-	-	-	-	-	-	-	-	-	-	-	-	-	-	-	
Y2O3	0.52	0.53	0.56	0.47	0.48	0.36	0.37	0.39	0.36	0.34	0.35	0.34	0.39	0.33	0.41	0.35	0.37	0.38	0.35	0.42	0.50	0.50	
ZrO2	31.35	31.51	31.39	31.28	30.16	28.92	28.36	28.44	28.39	28.17	28.39	29.07	30.06	29.22	28.71	28.35	28.34	28.29	28.29	30.94	30.94	30.94	
Nb2O5	8.36	8.60	8.60	8.41	8.69	6.51	6.67	6.77	6.43	6.56	8.26	7.24	6.89	6.75	6.71	6.81	6.62	7.56	9.35	-	-	-	
La2O3	0.17	0.18	0.15	0.16	0.08	0.07	0.06	0.07	0.08	0.06	0.12	0.10	0.10	0.07	0.08	0.08	0.08	0.07	0.11	0.15	0.15	0.15	
Ce2O3	1.23	1.37	1.41	1.20	0.70	0.65	0.64	0.63	0.61	0.93	0.81	0.88	0.71	0.72	0.70	0.69	0.68	0.68	0.68	0.68	0.68	0.68	
Pr2O3	0.20	0.25	0.24	0.21	0.15	0.15	0.15	0.15	0.10	0.14	0.12	0.08	0.14	0.13	0.14	0.16	0.15	0.13	0.08	0.06	0.13	0.22	
Nd2O3	1.38	1.52	1.57	1.34	0.88	0.79	0.83	0.77	0.85	0.92	1.04	0.92	1.03	0.82	0.86	0.80	0.84	0.82	1.02	1.28	-	-	
Sm2O3	0.37	0.43	0.43	0.34	0.24	0.22	0.25	0.23	0.23	0.20	0.25	0.23	0.23	0.24	0.24	0.22	0.24	0.25	0.31	0.35	-	-	
Eu2O3	0.11	0.13	0.12	0.11	0.08	0.07	0.07	0.07	0.09	0.09	0.09	0.08	0.10	0.08	0.08	0.07	0.08	0.09	0.10	0.10	0.10	0.10	
Gd2O3	0.32	0.31	0.28	0.28	0.21	0.20	0.21	0.20	0.20	0.22	0.18	0.25	0.20	0.19	0.20	0.19	0.20	0.22	0.22	0.27	0.28	-	
Tb2O3	-	-	-	-	-	-	-	-	-	-	-	-	-	-	-	-	-	-	-	-	-	-	
Dy2O3	0.19	0.20	0.18	0.16	0.14	0.07	0.06	0.07	0.03	0.04	0.04	0.09	0.06	0.09	0.06	0.06	0.06	0.06	0.06	0.11	0.16	-	
Hf2O3	-	-	-	-	-	-	-	-	-	-	-	-	-	-	-	-	-	-	-	-	-	-	
Er2O3	0.06	0.05	0.07	0.05	0.05	0.04	0.03	0.05	0.05	0.05	0.02	0.03	0.05	0.04	0.03	0.03	0.04	0.05	0.05	0.06	0.06	-	
Tm2O3	-	-	-	-	-	-	-	-	-	-	-	-	-	-	-	-	-	-	-	-	-	-	
Yb2O3	-	-	-	-	-	-	-	-	-	-	-	-	-	-	-	-	-	-	-	-	-	-	
Lu2O3	-	-	-	-	-	-	-	-	-	-	-	-	-	-	-	-	-	-	-	-	-	-	
HfO2	0.39	0.44	0.49	0.50	0.48	0.48	0.50	0.46	0.46	0.47	0.48	0.47	0.47	0.45	0.46	0.45	0.45	0.51	0.49	0.45	0.44	0.44	
Ta2O5	2.78	2.64	2.77	2.95	3.06	1.47	1.57	1.65	1.67	1.41	1.60	2.12	1.92	1.80	1.50	1.46	1.58	1.46	1.59	2.14	3.41	-	
WO3	<1	<1	<1	<1	<1	<1	<1	<1	<1	<1	<1	<1	<1	<1	<1	<1	<1	<1	<1	<1	<1	<1	-
PbO	<1	<1	<1	<1	<1	<1	<1	<1	<1	<1	<1	<1	<1	<1	<1	<1	<1	<1	<1	<1	<1	<1	-
Th2O	7.51	6.34	8.35	7.94	16.37	15.96	16.40	16.59	16.40	15.96	16.53	10.98	12.83	13.75	15.74	15.87	15.87	15.64	15.64	13.15	7.15	-	
UO2	0.95	0.89	1.21	0.90	0.85	2.31	2.58	2.57	2.55	2.64	2.49	2.64	1.54	2.03	2.44	2.50	2.71	2.65	2.57	2.01	0.93	-	
(Na,K)2O	-	-	-	-	-	-	-	-	-	-	-	-	-	-	-	-	-	-	-	-	-	-	
H2O	-	-	-	-	-	-	-	-	-	-	-	-	-	-	-	-	-	-	-	-	-	-	
"Others"	-	-	-	-	-	-	-	-	-	-	-	-	-	-	-	-	-	-	-	-	-	-	
TOTAL	100.57	100.09	100.16	100.32	97.15	99.69	99.45	99.70	99.60	99.93	99.47	99.59	100.09	99.45	99.88	99.82	99.83	99.70	99.07	99.71	100.24	-	
(cations to 7 oxygens)																							
Ca2+	0.739	0.742	0.740	0.728	0.729	0.611	0.602	0.596	0.604	0.616	0.606	0.705	0.677	0.646	0.622	0.613	0.621	0.618	0.625	0.651	0.746		
Y+REE3+	0.113	0.124	0.126	0.109	0.111	0.075	0.070	0.072	0.068	0.072	0.065	0.086	0.075	0.087	0.072	0.073	0.071	0.072	0.071	0.090	0.107		
Pb2+	-	-	-	-	-	-	-	-	-	-	-	-	-	-	-	-	-	-	-	-	-	-	
Th4+	0.113	0.105	0.096	0.127	0.125	0.255	0.263	0.267	0.263	0.249	0.266	0.210	0.217	0.251	0.250	0.254	0.251	0.251	0.207	0.108			
U4+	0.014	0.013	0.018	0.013	0.013	0.036	0.040	0.040	0.040	0.039	0.041	0.023	0.029	0.031	0.038	0.039	0.042	0.041	0.040	0.031	0.014		
SUM Ca2+	0.979	0.984	0.980	0.977	0.977	0.976	0.974	0.976	0.976	0.979	0.984	0.980	0.981	0.982	0.976	0.987	0.985	0.988	0.980	0.980	0.975		
Zr4+	1.011	1.020	1.015	1.016	1.016	0.993	0.977	0.980	0.976	0.994	0.979	0.995	1.002	0.990	0.979	0.982	0.970	0.969	0.973	0.990	1.003		
H4+	0.007	0.008	0.009	0.010	0.009	0.010	0.010	0.010	0.010	0.009	0.010	0.009	0.010	0.009	0.009	0.009	0.010	0.010	0.009	0.008	0.008		
SUM Zr4+	-	-	-	-	-	-	-	-	-	-	-	-	-	-	-	-	-	-	-	-	-	-	
Tl4+	1.286	1.283	1.276	1.256	1.239	1.285	1.279	1.272	1.277	1.293	1.278	1.269	1.283	1.285	1.286	1.281	1.297	1.290	1.263	1.242			
S4+	-	-	-	-	-	-	-	-	-	-	-	-	-	-	-	-	-	-	-	-	-	-	
Mg2+	0.030	0.029	0.027	0.031	0.029	0.046	0.048	0.052	0.051	0.046	0.050	0.036	0.045	0.047	0.049	0.048	0.049	0.044	0.041	0.031			
Mn2+	0.009	0.009	0.007	0.010	0.016	0.020	0.018	0.019	0.017	0.011	0.012	0.014	0.017	0.017	0.016	0.017	0.017	0.016	0.014	0.010			
Fe2+	0.433	0.436	0.431	0.432	0.463	0.470	0.470	0.466	0.473	0.465	0.473	0.445	0.450	0.464	0.466	0.467	0.471	0.465	0.459	0.438			
Fe3+	-	-	-	-	-	-	-	-	-	-	-	-	-	-	-	-	-	-	-	-	-	-	
A3+	0.005	0.005	0.006	0.007	0.005	0.006	0.004	0.004	0.004	0.004	0.004	0.004	0.005	0.005	0.005	0.005	0.005	0.005	0.005	0.005	0.005		
C3+	-	-	-	-	-	-	-	-	-	-	-	-	-	-	-	-	-	-	-	-	-	-	
Cr3+	-	-	-	-	-	-	-	-	-	-	-	-	-	-	-	-	-	-	-	-	-	-	
Nb5+	0.250	0.245	0.258	0.271	0.206	0.213	0.216	0.203	0.210	0.224	0.224	0.216	0.213	0.212	0.216	0.210	0.211	0.211	0.237	0.281			
Ta5+	0.050	0.048	0.050	0.054	0.057	0.028	0.030	0.032	0.031	0.039	0.036	0.034	0.039	0.036	0.034	0.028	0.030	0.028	0.031	0.040	0.062		
W6+	-	-	-	-	-	-	-	-	-	-	-	-	-	-	-	-	-	-	-	-	-	-	
SUM Ti4+	2.064	2.055	2.050	2.045	2.050	2.066	2.062	2.065	2.063	2.059	2.055	2.065	2.064	2.066	2.064	2.071	2.068	2.064	2.058	2.068	-		
TOTAL	4.060	4.067	4.060	4.056	4.047	4.030	4.028	4.026	4.026	4.033	4.031	4.048	4.047	4.046	4.036	4.034	4.033	4.036	4.034	4.035	4.055		

	C133	C134	C135	C136	C137	C138	C139	C140	C141	C142	C143	C144	C145	C146	C147	C148	C149	C150	C151	C152	C153
MgO	0.31	0.30	0.32	0.08	0.11	0.12	0.23	0.33	0.37	0.52	0.33	0.40	0.25	0.10	0.15	0.19	0.32	0.23	0.14	0.21	
Al2O3	0.09	0.07	0.10	0.05	0.06	<0.05	<0.05	<0.05	<0.05	<0.05	<0.05	<0.05	<0.05	<0.05	<0.05	<0.05	<0.05	<0.05	0.08	0.08	
SiO2	<0.05	<0.05	<0.10	0.10	0.09	<0.05	<0.05	<0.05	<0.05	<0.05	<0.05	<0.05	<0.05	<0.05	<0.05	<0.05	<0.05	<0.05	<0.05	<0.05	
CaO	10.56	10.50	10.17	13.50	13.03	13.24	12.96	10.87	9.49	9.81	8.69	10.09	8.90	9.20	10.42	9.85	9.46	8.20	8.81	12.87	
TiO2	24.80	24.81	25.79	37.16	36.00	36.30	35.99	29.16	24.54	23.71	27.14	25.68	28.97	32.93	31.63	30.46	28.52	28.33	32.29	30.69	
Cr2O3	-	-	-	-	-	-	-	-	-	-	-	-	-	-	-	-	-	-	-	-	
MnO	0.15	0.16	0.16	<0.05	0.05	<0.05	0.10	0.15	0.30	0.41	0.29	0.23	0.23	0.07	0.16	0.16	0.25	0.24	0.11	0.15	
FeO	7.87	8.04	4.09	4.59	4.26	4.58	6.72	7.42	7.23	7.43	6.89	7.29	6.89	6.26	6.49	6.83	7.12	7.17	5.31	5.76	
Feo3	-	-	-	-	-	-	-	-	-	-	-	-	-	-	-	-	-	-	-	-	
Y2O3	0.56	0.52	0.54	0.28	0.29	0.36	0.34	0.58	0.65	0.68	0.62	0.55	0.46	0.34	0.37	0.48	0.59	0.57	0.82	0.56	
ZrO2	31.07	30.98	30.83	37.20	36.56	36.58	31.90	29.60	28.54	29.21	28.76	29.53	30.97	32.96	31.80	32.32	30.47	30.30	33.32	33.17	
Nb2O5	9.35	9.14	7.77	1.77	1.92	2.42	2.32	2.17	7.46	11.59	12.34	11.78	9.00	8.39	5.60	2.43	2.81	3.71	4.65	5.24	5.70
La2O3	0.17	0.14	0.17	0.18	0.18	0.20	0.42	0.58	0.51	0.49	0.46	0.46	0.46	0.38	1.00	0.92	0.84	0.77	0.77	0.11	
Ce2O3	1.25	1.19	1.21	1.32	1.59	1.43	1.48	3.25	4.19	3.77	4.26	3.33	4.10	5.66	5.89	5.83	6.20	5.80	1.16	1.28	
Pt2O3	0.25	0.17	0.20	0.25	0.23	0.19	0.61	0.72	0.75	0.79	0.80	0.71	0.86	0.83	0.88	0.80	1.06	0.86	0.23	0.23	
Nd2O3	1.45	1.40	1.40	1.09	1.04	1.04	2.85	3.66	3.29	3.97	2.96	3.65	3.52	3.98	3.63	4.34	4.86	4.19	1.26	1.29	
Sm2O3	0.40	0.39	0.40	0.13	0.20	0.23	0.53	0.69	0.73	0.85	0.62	0.70	0.48	0.33	0.60	0.79	0.62	0.36	0.36	0.36	
Eu2O3	0.13	0.12	0.15	0.06	0.05	0.06	0.21	0.18	0.17	0.15	0.19	0.16	0.08	0.11	0.14	0.22	0.19	0.14	0.10	0.10	
Gd2O3	0.32	0.29	0.32	0.12	0.12	0.16	0.15	0.38	0.46	0.45	0.52	0.46	0.46	0.32	0.13	0.21	0.30	0.43	0.35	0.28	
Tb2O3	-	-	-	-	-	-	-	-	-	-	-	-	-	-	-	-	-	-	-	-	
Dy2O3	0.20	0.15	0.15	0.12	0.13	0.15	0.09	0.20	0.29	0.27	0.33	0.24	0.27	0.23	0.09	0.14	0.19	0.25	0.18	0.28	
Ho2O3	-	-	-	-	-	-	-	-	-	-	-	-	-	-	-	-	-	-	-	-	
Er2O3	0.04	0.05	<0.1	<0.1	<0.1	<0.1	<0.1	<0.1	<0.1	<0.1	<0.1	<0.1	<0.1	<0.1	<0.1	<0.1	<0.1	<0.1	<0.12	<0.1	
Tm2O3	-	-	-	-	-	-	-	-	-	-	-	-	-	-	-	-	-	-	-	-	
Yb2O3	-	-	-	-	-	-	-	-	-	-	-	-	-	-	-	-	-	-	-	-	
Lu2O3	-	-	-	-	-	-	-	-	-	-	-	-	-	-	-	-	-	-	-	-	
Hf2O2	0.43	0.48	0.46	0.70	0.82	0.73	0.78	0.64	0.70	0.65	0.65	0.74	0.66	0.73	0.68	0.70	0.63	0.67	0.77	0.81	
Ta2O5	3.37	2.40	0.25	0.21	0.21	<1	<1	<1	<1	<1	0.38	0.58	0.63	0.49	0.46	0.39	0.39	0.36	0.20	0.41	
WO3	<1	<1	<1	<1	<1	<1	<1	<1	<1	<1	<1	<1	<1	<1	<1	<1	<1	<1	<1	<1	
PbO	<1	<1	<1	<1	<1	<1	<1	<1	<1	<1	<1	<1	<1	<1	<1	<1	<1	<1	<1	<1	
ThO2	6.63	7.20	7.87	0.54	1.06	0.89	0.91	2.09	2.46	2.26	3.33	3.33	4.74	2.82	0.67	1.19	1.83	1.92	2.85	1.10	
UO2	0.78	0.93	1.09	0.12	0.25	0.13	0.29	0.30	0.27	0.36	0.15	0.56	0.48	0.25	0.18	0.05	0.00	0.13	0.18	0.29	
(Na,K)2O	-	-	-	-	-	-	-	-	-	-	-	-	-	-	-	-	-	-	-	-	
H2O	-	-	-	-	-	-	-	-	-	-	-	-	-	-	-	-	-	-	-	-	
"Others"	-	-	-	-	-	-	-	-	-	-	-	-	-	-	-	-	-	-	-	-	
TOTAL	100.38	100.13	99.54	99.09	99.14	98.75	98.85	98.79	99.11	98.54	98.61	98.02	98.13	98.84	98.53	97.51	98.78	97.76	97.92	96.75	
cations to 7 oxygens																					
Ca2+	0.750	0.749	0.729	0.877	0.855	0.869	0.853	0.756	0.679	0.702	0.632	0.720	0.650	0.658	0.720	0.696	0.666	0.595	0.638	0.845	
Y+REE3+	0.119	0.109	0.115	0.077	0.089	0.088	0.086	0.214	0.282	0.258	0.301	0.232	0.280	0.306	0.277	0.298	0.309	0.376	0.336	0.107	
Pb2+	-	-	-	-	-	-	-	-	-	-	-	-	-	-	-	-	-	-	-	-	
Th4+	0.100	0.109	0.120	0.007	0.015	0.012	0.013	0.031	0.037	0.034	0.051	0.051	0.074	0.043	0.010	0.018	0.027	0.030	0.044	0.016	
U4+	0.011	0.014	0.016	0.002	0.003	0.002	0.004	0.004	0.005	0.005	0.002	0.008	0.007	0.004	0.003	0.001	0.001	0.002	0.003	0.008	
SUM Ca2+	0.980	0.981	1.015	1.015	1.113	1.107	1.106	1.120	1.022	0.977	0.975	0.979	0.984	1.011	1.008	1.010	1.012	1.002	1.021	0.989	
Zr4+	1.005	1.006	1.007	1.101	1.093	1.093	1.106	1.010	0.964	0.962	0.966	0.967	0.981	1.004	1.037	1.022	1.035	1.006	0.999	1.035	
H4+	0.008	0.009	0.012	0.014	0.013	0.014	0.012	0.013	0.012	0.013	0.012	0.014	0.013	0.014	0.013	0.013	0.012	0.013	0.014	0.015	
Si4+	-	-	-	-	-	-	-	-	-	-	-	-	-	-	-	-	-	-	-	-	
Mg2+	0.030	0.030	0.031	0.008	0.010	0.010	0.011	0.022	0.032	0.036	0.053	0.033	0.041	0.025	0.010	0.014	0.019	0.032	0.024	0.020	
Min2+	0.008	0.009	0.009	0.000	0.003	0.000	0.005	0.008	0.017	0.017	0.016	0.017	0.013	0.004	0.009	0.015	0.014	0.006	0.008	0.008	
Fe2+	0.436	0.436	0.450	0.208	0.235	0.218	0.235	0.365	0.414	0.404	0.422	0.384	0.416	0.383	0.338	0.358	0.375	0.403	0.405	0.283	
Fe3+	-	-	-	-	-	-	-	-	-	-	-	-	-	-	-	-	-	-	-	-	
Al3+	0.007	0.005	0.008	0.004	0.003	0.003	0.003	-	-	-	-	-	-	-	-	-	-	-	-	-	
Cr3+	-	-	-	-	-	-	-	-	-	-	-	-	-	-	-	-	-	-	-	-	
Nb5+	0.281	0.275	0.235	0.053	0.087	0.084	0.080	0.219	0.350	0.373	0.381	0.271	0.258	0.168	0.071	0.084	0.110	0.142	0.160	0.175	
Ta5+	0.065	0.061	0.044	0.004	0.003	0.004	0.004	0.007	0.011	0.011	0.009	0.008	0.007	0.001	0.003	0.004	0.003	0.007	0.007	0.009	
W6+	-	-	-	-	-	-	-	-	-	-	-	-	-	-	-	-	-	-	-	-	
SUM Ti4+	2.064	2.061	2.076	1.976	1.988	1.978	1.983	2.045	2.072	2.073	2.081	2.073	2.059	2.045	2.028	2.042	2.034	2.059	2.050	2.026	
TOTAL	4.058	4.058	4.071	4.052	4.058	4.055	4.057	4.073	4.051	4.048	4.046	4.064	4.071	4.083	4.080	4.080	4.083	4.070	4.076		

	C154	C155	C156	C157	C158	C159	C160	C161	M1	M2	M3	M4	M5	M6	M7	M8	M9	M10	M11	M12	M13
MgO	0.19	0.15	0.13	0.22	0.15	0.11	0.11	0.16	0.38	0.31	0.29	0.49	0.48	0.50	<.04	0.09	<.04	<.04	<.04	<.04	<.04
Al ₂ O ₃	0.10	0.09	0.08	0.08	0.11	0.10	0.10	0.15	0.53	0.53	0.54	0.58	0.70	0.58	0.72	0.71	0.67	0.80	0.65	0.65	0.54
SiO ₂	0.05	0.10	<.05	0.05	0.24	0.08	<.05	0.15	0.14	0.42	0.27	0.40	0.21	0.44	0.13	0.09	0.13	0.09	0.11	0.07	0.07
CaO	12.38	12.68	12.35	12.13	12.65	12.87	12.72	12.35	12.18	12.53	12.02	13.15	12.95	14.72	13.11	13.52	14.94	14.44	12.93	14.06	14.06
TiO ₂	31.37	31.50	31.34	30.67	32.27	32.60	32.74	31.85	29.91	30.73	30.21	29.78	33.15	34.03	36.85	37.98	38.79	38.24	37.21	39.76	39.76
FeO	-	-	-	-	-	-	-	-	-	-	-	-	-	-	-	-	-	-	-	-	-
MnO	0.07	0.11	0.12	0.15	0.09	0.10	0.05	0.08	0.10	0.53	0.53	0.54	0.58	0.58	0.58	0.58	0.58	0.58	0.58	0.58	0.58
Nb ₂ O ₅	5.62	5.34	5.34	5.81	5.18	5.14	5.16	5.33	6.18	5.85	6.18	6.15	4.93	4.74	3.93	<.05	<.05	<.05	<.05	<.05	<.05
Cr ₂ O ₃	34.84	33.69	33.42	34.10	34.17	33.81	33.84	34.13	32.62	32.08	35.92	32.40	29.73	30.35	28.55	35.26	34.17	34.32	35.77	33.13	33.47
Nb ₂ O ₅	5.34	5.30	5.75	6.15	5.40	4.90	5.28	10.53	9.66	9.39	10.29	8.72	11.08	0.44	0.51	0.45	0.37	1.07	0.34	0.34	0.34
Al ₂ O ₃	0.13	0.11	0.12	0.11	0.13	0.12	0.12	0.12	0.12	0.12	0.12	0.12	0.12	0.12	0.12	0.12	0.12	0.12	0.12	0.12	0.12
Ca ₂ O ₃	1.15	1.07	1.19	1.24	1.13	1.11	1.18	1.24	1.24	1.24	1.24	1.24	1.24	1.24	1.24	1.24	1.24	1.24	1.24	1.24	1.24
Pb ₂ O ₃	0.19	0.20	0.18	0.17	0.23	0.22	0.23	-	-	-	-	-	-	-	-	-	-	-	-	-	-
Na ₂ O ₃	1.14	1.02	1.25	1.14	1.14	1.16	1.19	1.19	-	-	-	-	-	-	-	-	-	-	-	-	-
Si ₂ O ₃	0.32	0.31	0.38	0.35	0.30	0.32	0.35	0.30	-	-	-	-	-	-	-	-	-	-	-	-	-
Eu ₂ O ₃	0.08	0.11	0.12	0.10	0.11	0.13	0.04	0.08	-	-	-	-	-	-	-	-	-	-	-	-	-
Ge ₂ O ₃	0.29	0.23	0.32	0.30	0.29	0.26	0.32	0.28	-	-	-	-	-	-	-	-	-	-	-	-	-
Tb ₂ O ₃	-	-	-	-	-	-	-	-	-	-	-	-	-	-	-	-	-	-	-	-	-
Dy ₂ O ₃	0.21	0.18	0.20	0.20	0.22	0.21	0.23	0.25	-	-	-	-	-	-	-	-	-	-	-	-	-
Hg ₂ O ₃	<.1	<.1	0.10	<.1	<.1	<.1	<.1	<.1	-	-	-	-	-	-	-	-	-	-	-	-	-
Er ₂ O ₃	-	-	-	-	-	-	-	-	-	-	-	-	-	-	-	-	-	-	-	-	-
Sm ₂ O ₃	-	-	-	-	-	-	-	-	-	-	-	-	-	-	-	-	-	-	-	-	-
Eu ₂ O ₃	-	-	-	-	-	-	-	-	-	-	-	-	-	-	-	-	-	-	-	-	-
Ge ₂ O ₃	-	-	-	-	-	-	-	-	-	-	-	-	-	-	-	-	-	-	-	-	-
Ta ₂ O ₅	0.82	0.78	0.79	0.80	0.87	0.73	0.78	0.77	0.49	0.39	0.72	0.45	0.23	0.35	0.34	0.52	0.68	0.32	0.55	1.00	0.65
Hf ₂ O ₅	0.45	0.35	0.41	0.53	0.32	0.43	0.36	0.39	-	-	-	-	-	-	-	-	-	-	-	-	-
WO ₃	<.1	<.1	0.15	<.1	0.15	<.1	0.13	<.1	-	-	-	-	-	-	-	-	-	-	-	-	-
Th ₂ O ₅	0.14	<.1	0.13	<.1	0.13	<.1	0.11	<.1	-	-	-	-	-	-	-	-	-	-	-	-	-
Y ₂ O ₃	1.66	0.98	1.34	1.04	1.34	1.20	0.95	1.13	0.94	1.22	0.61	1.04	0.17	1.47	1.90	1.96	1.25	0.61	2.37	0.60	2.43
Zr ₂ O ₅	-	-	-	-	-	-	-	-	-	-	-	-	-	-	-	-	-	-	-	-	-
Na ₂ K ₂ O	-	-	-	-	-	-	-	-	-	-	-	-	-	-	-	-	-	-	-	-	-
Others*	-	-	-	-	-	-	-	-	-	-	-	-	-	-	-	-	-	-	-	-	-
TOTAL	97.54	95.08	95.64	97.52	96.71	96.17	96.77	96.84	98.05	97.36	98.78	98.04	97.72	97.47	99.07	98.36	100.31	96.76	100.74	101.39	99.71

	M14	M15	M16	M17	M18	M19	M20	M21	M22	M23	M24	M25	M26	M27	M28	M29	M30	M31	M32	M33	M34
MgO	<.04	0.09	<.04	<.04	<.04	0.18	<.04	0.30	0.56	0.63	0.22	0.31	0.93	0.75	0.59	1.21	1.21	0.16	0.14		
Al2O3	0.52	0.62	0.56	0.74	0.72	0.68	0.67	0.62	0.98	1.12	1.14	1.24	1.17	1.39	0.64	0.79	1.28	1.28	1.39		
SiO2	0.16	0.11	<.05	<.05	<.05	<.05	<.05	<.05	0.06	0.10	0.08	<.06	<.06	<.06	<.06	<.06	0.18	0.22			
CaO	15.28	15.21	14.44	11.38	10.59	12.07	7.67	9.53	8.84	13.39	12.24	10.97	13.94	13.78	8.86	9.74	10.68	12.20	12.11	14.05	14.44
TiO2	41.21	41.60	39.97	34.54	32.34	33.62	29.57	30.67	29.62	35.52	25.86	31.12	40.91	42.64	29.43	31.61	33.48	33.21	32.18	39.35	41.59
C12O3	-	-	<.05	<.05	<.05	<.05	0.09	0.09	0.07	0.09	0.01	-	-	-	0.02	-	-	-	-	<.05	
MnO	<.05	-	-	-	-	-	-	-	-	-	-	-	-	-	0.04	0.19	0.13	0.12	0.10	0.07	
FeO	-	-	-	-	-	-	-	-	-	-	-	-	-	-	3.48	2.79	1.96	2.26	1.72	1.01	
Fe2O3	3.16	3.27	3.73	6.32	7.02	5.70	8.40	7.42	7.91	-	-	-	-	-	-	-	-	-	-	-	
Y2O3	0.29	0.42	0.70	3.08	2.92	3.13	6.71	6.91	8.07	2.10	3.08	0.18	0.14	0.22	0.20	0.94	1.19	0.42	0.18		
ZrO2	34.41	35.71	33.97	31.01	30.54	32.14	28.53	30.97	28.10	35.35	34.72	35.15	38.64	35.71	26.85	29.37	30.70	30.28	29.44	33.74	33.80
Nd2O3	0.40	0.30	0.50	1.96	1.59	1.93	1.51	2.03	1.68	5.94	16.47	5.71	1.63	2.49	0.81	0.81	1.98	2.16	0.51	0.43	
La2O3	0.18	0.19	0.17	0.15	0.07	0.10	0.10	<.07	<.07	0.07	0.15	0.15	0.15	0.46	0.21	0.22	1.34	1.18	1.48	1.68	1.77
Ce2O3	0.98	0.94	0.31	0.66	0.99	1.34	0.16	0.33	0.21	0.56	0.15	0.15	0.15	0.46	0.21	0.22	<14	<14	0.38	0.39	<.14
Pr2O3	0.10	<.09	0.21	0.15	0.21	<.09	<.09	<.09	<.09	<.09	-	-	-	-	-	-	0.65	0.71	1.88	2.38	0.94
Sm2O3	<.12	0.28	0.62	0.57	1.20	1.22	1.74	0.42	0.72	0.54	0.04	0.32	0.11	0.21	0.04	0.03	<14	<14	0.52	0.65	<.14
Eu2O3	-	-	-	-	-	-	-	-	-	-	-	-	-	-	-	-	-	-	-	-	
Gd2O3	0.16	<.15	0.51	0.80	0.61	0.61	0.79	0.95	0.96	0.41	-	-	-	0.32	0.06	0.07	<16	<16	0.42	0.48	<.16
Tb2O3	-	-	<.12	0.61	0.68	0.52	1.67	1.36	1.87	0.34	0.31	1.01	0.09	0.09	0.07	<16	<16	0.29	0.45	<.16	<.16
Dy2O3	<.12	<.12	<.12	<.12	<.12	<.12	<.12	<.12	<.12	<.12	<.12	<.12	<.12	<.12	<.12	<.12	<.12	<.12	<.12	<.12	<.12
Hf2O3	0.50	0.57	0.74	0.36	0.78	0.66	0.70	0.47	0.69	0.68	0.71	0.77	0.39	0.37	<24	<24	0.70	0.85	0.40	<.24	
Ta2O5	<.12	<.12	0.19	0.47	0.39	0.34	1.38	0.85	1.37	-	-	-	-	-	<27	<27	<27	<27	<.27	<.27	
WtO3	0.83	0.58	0.74	0.57	0.56	0.96	1.24	0.86	0.76	-	-	-	-	-	0.81	<3	<3	<3	<3	<3	
PbO	<.11	<.11	<.11	<.11	<.11	<.11	<.11	<.11	<.11	<.11	<.11	<.11	<.11	<.11	-	-	-	-	-	-	-
ThO2	0.22	0.21	1.75	1.87	0.88	0.76	1.01	1.20	1.16	0.39	1.65	1.38	0.01	0.21	17.07	13.62	7.49	6.44	4.00	2.73	
UO2	0.14	0.02	0.27	1.88	3.43	0.75	7.18	2.89	3.81	0.02	0.86	0.81	0.07	0.20	5.93	3.87	2.91	2.56	2.58	1.47	0.79
(Na,K)2O	-	-	-	-	-	-	-	-	-	-	-	-	-	-	-	-	-	-	-	-	
H2O	-	-	-	-	-	-	-	-	-	-	-	-	-	-	-	-	-	-	-	-	
"Others"	-	-	-	-	-	-	-	-	-	-	-	-	-	-	-	-	-	-	-	-	
TOTAL	>8.99	160.39	99.23	99.94	98.33	99.54	99.42	97.96	99.56	99.76	101.22	98.78	99.06	99.67	98.90	99.11	99.35	98.58	97.52	100.29	98.96

cations to 7 oxygens

	M14	M15	M16	M17	M18	M19	M20	M21	M22	M23	M24	M25	M26	M27	M28	M29	M30	M31	M32	M33	M34
Ca2+	0.958	0.939	0.917	0.757	0.721	0.807	0.540	0.651	0.624	0.857	0.803	0.734	0.873	0.852	0.680	0.701	0.748	0.847	0.853	0.903	0.915
Y+REE3+	0.052	0.055	0.067	0.211	0.208	0.226	0.363	0.353	0.424	0.098	0.022	0.148	0.018	0.012	0.062	0.058	0.155	0.186	0.078	0.054	
Pb2+	-	0.000	0.001	-	-	-	0.003	0.001	0.001	-	-	-	-	-	-	-	-	-	-	-	-
Th4+	0.003	0.003	0.024	0.026	0.071	0.011	0.015	0.017	0.005	0.023	0.020	0.000	0.003	0.0270	0.231	0.203	0.110	0.098	0.055	0.037	
U4+	0.002	0.000	0.004	0.026	0.048	0.010	0.041	0.058	0.011	0.012	0.011	0.001	0.003	0.042	0.047	0.057	0.150	0.150	0.020	0.010	
SUM Ca2+	1.015	0.997	1.012	1.020	1.048	1.055	1.026	1.063	1.123	0.963	0.860	0.913	0.882	0.869	0.084	0.047	0.057	1.173	1.055	1.016	
Zr4+	1.004	0.982	0.981	0.939	0.946	0.978	0.914	0.963	0.903	1.030	1.037	1.070	1.102	1.005	0.911	0.962	0.979	0.957	0.943	0.987	0.975
Hf4+	0.008	0.008	0.010	0.013	0.007	0.014	0.012	0.013	0.008	0.012	0.012	0.013	0.013	0.006	0.007	0.013	0.016	0.007	0.016	0.007	
SUM Zr4+	0.990	1.012	0.981	0.952	0.983	0.926	0.976	0.912	0.042	0.048	0.082	0.114	0.011	0.918	0.962	0.978	0.970	0.959	0.994	0.975	
Ti4+	1.814	1.803	1.781	1.612	1.546	1.578	1.461	1.471	1.469	1.596	1.191	1.461	1.789	1.850	1.540	1.598	1.647	1.619	1.590	1.775	1.849
Si4+	-	-	-	-	-	-	-	-	-	-	-	-	-	-	-	-	-	-	-	-	-
Mg2+	-	-	-	-	-	-	-	-	-	-	-	-	-	-	-	-	-	-	-	-	-
Mn2+	0.001	-	-	-	-	-	-	-	-	-	-	-	-	-	-	-	-	-	-	-	-
Fe2+	-	-	-	-	-	-	-	-	-	-	-	-	-	-	-	-	-	-	-	-	-
Fe3+	0.139	0.142	0.168	0.295	0.336	0.415	0.356	0.393	-	-	-	-	-	-	-	-	-	-	-	-	-
Al3+	0.036	0.042	0.039	0.054	0.056	0.053	0.050	0.048	0.049	0.089	0.081	0.084	0.055	0.102	0.093	0.107	0.049	0.061	0.091	0.097	
Cr3+	-	-	-	-	-	-	-	-	-	-	-	-	-	-	-	-	-	-	-	-	-
Nb5+	0.011	0.008	0.013	0.055	0.046	0.054	0.045	0.059	0.050	0.160	0.456	0.181	0.043	0.065	0.027	0.025	0.015	0.058	0.064	0.014	0.011
Ta5+	-	-	-	-	-	-	-	-	-	-	-	-	-	-	-	-	-	-	-	-	-
W6+	0.013	0.009	0.011	0.009	0.016	0.021	0.014	0.013	0.004	0.004	0.016	0.008	-	0.002	-	0.014	0.016	0.014	0.014	0.011	
SUM Ti4+	2.023	2.018	2.017	2.031	1.985	1.976	2.017	1.959	1.978	2.017	2.053	2.057	1.979	2.118	2.036	2.005	1.986	1.984	1.985	1.986	2.033
TOTAL	4.028	4.027	4.003	3.996	4.022	3.989	4.013	4.022	3.988	3.988	4.013	4.022	3.986	4.052	3.985	3.986	4.021	4.014	4.038	4.023	

	M35	M36	M37	M38	M39	M40	M41	M42	M43	M44	M45	M46	M47	M48	M49	M50	M51	M52	M53	M54	M55
MgO	0.59	0.81	0.27	1.07	0.07	0.86	0.47	0.22	1.03	0.78	0.49	1.48	0.30	1.34	0.20	2.20	1.22	0.80	1.24	1.98	2.60
Al2O3	1.26	0.85	1.68	0.82	1.37	0.50	0.92	1.37	0.72	1.09	1.35	0.94	0.74	0.81	0.58	0.91	1.33	0.97	0.54	1.32	<.06
SiO2	<.06	0.20	0.18	<.06	0.11	0.40	0.07	0.11	<.06	<.06	<.06	<.06	<.06	<.06	<.06	<.06	<.06	<.06	<.06	<.06	<.06
CaO	10.18	7.94	12.83	9.87	14.49	7.48	13.02	13.58	12.19	13.11	12.24	16.54	10.90	16.10	9.35	8.68	10.48	9.88	9.96	9.25	9.25
TiO2	32.42	28.16	33.13	40.83	30.18	40.15	39.45	31.03	35.02	39.85	33.15	42.94	34.88	44.91	28.75	32.50	33.20	32.25	31.31	28.40	28.40
Cr2O3	-	-	-	-	-	-	-	-	-	-	-	-	-	-	-	-	-	-	-	-	-
MnO	0.17	0.26	<.05	<.05	0.16	0.11	<.05	0.11	0.09	<.05	0.09	<.05	0.14	<.05	0.11	0.09	0.27	0.23	0.19	0.19	0.19
FeO	3.34	4.26	1.74	3.12	0.97	4.58	2.07	1.46	4.64	2.77	1.88	2.68	1.10	2.44	0.72	2.24	3.23	2.74	2.60	2.46	2.51
Fe2O3	-	-	-	-	-	-	-	-	-	-	-	-	-	-	-	-	-	-	-	-	-
Y2O3	0.24	0.17	0.42	1.34	0.45	2.00	0.75	0.32	2.44	0.85	0.45	1.10	0.42	0.96	0.30	0.25	1.83	0.60	0.68	0.37	0.37
ZrO2	27.58	27.63	31.55	28.32	34.59	24.50	28.53	31.66	28.96	31.01	30.66	29.24	31.44	30.18	27.67	30.26	30.71	27.76	27.63	27.63	27.63
Nb2O5	0.79	0.93	0.52	2.35	4.22	3.50	1.60	0.67	3.20	1.60	0.90	2.25	0.91	2.29	0.83	1.78	2.37	1.97	1.38	2.16	1.82
La2O3	0.26	0.15	0.15	0.28	0.21	0.40	<.07	0.16	0.54	0.28	0.20	0.28	<.07	0.26	0.27	0.41	0.36	0.23	<.07	0.07	<.07
Ce2O3	1.21	1.10	1.22	2.40	1.16	3.68	1.12	1.00	3.92	2.01	1.21	1.80	0.70	1.83	0.59	3.82	2.64	2.02	0.90	0.63	0.63
Pt2O3	0.28	<.14	0.40	0.20	0.72	<.14	0.61	0.34	<.14	0.27	<.14	0.34	<.14	0.27	<.14	0.34	<.14	0.63	0.41	0.22	<.14
Nd2O3	1.08	0.52	0.86	2.48	0.88	4.00	1.10	0.54	4.90	2.17	1.05	2.54	0.52	2.21	0.15	0.52	4.09	1.92	1.59	0.70	0.50
Sm2O3	<.14	0.76	0.28	1.08	0.24	<.14	1.47	0.59	0.27	0.80	0.16	0.59	<.14	0.17	1.18	0.32	0.33	0.33	0.17	<.14	<.14
Eu2O3	-	-	-	-	-	-	-	-	-	-	-	-	-	-	-	-	-	-	-	-	-
Gd2O3	<.16	-	-	-	-	-	-	-	-	-	-	-	-	-	-	-	-	-	-	-	-
Tb2O3	-	-	-	-	-	-	-	-	-	-	-	-	-	-	-	-	-	-	-	-	-
Dy2O3	<.16	-	-	-	-	-	-	-	-	-	-	-	-	-	-	-	-	-	-	-	-
Hf2O3	-	-	-	-	-	-	-	-	-	-	-	-	-	-	-	-	-	-	-	-	-
Er2O3	<.17	<.17	0.28	<.17	0.30	<.17	0.33	<.17	0.19	<.17	0.21	<.17	0.18	<.17	0.18	<.17	0.25	<.17	<.17	<.17	<.17
Tm2O3	-	-	-	-	-	-	-	-	-	-	-	-	-	-	-	-	-	-	-	-	-
<.18	<.18	0.20	<.18	0.20	<.18	0.20	<.18	<.18	<.18	<.18	<.18	<.18	<.18	<.18	<.18	<.18	<.18	<.18	<.18	<.18	<.18
Lu2O3	-	-	-	-	-	-	-	-	-	-	-	-	-	-	-	-	-	-	-	-	-
HfO2	<.24	0.49	0.30	1.09	<.24	0.65	1.03	<.24	0.94	0.75	0.25	0.29	0.64	0.88	0.74	0.66	0.83	0.31	<.24	0.53	0.55
Ta2O5	<.27	<.27	<.27	<.27	<.27	<.27	<.27	<.27	<.27	<.27	<.27	<.27	<.27	<.27	<.27	<.27	<.27	<.27	<.27	<.27	<.27
WO3	1.00	0.75	<.3	0.37	<.3	1.02	<.3	1.04	0.43	0.42	<.3	<.3	<.3	<.3	<.3	<.3	<.3	<.3	0.51	0.88	<.3
PbO	-	-	-	-	-	-	-	-	-	-	-	-	-	-	-	-	-	-	-	-	-
ThO2	12.81	15.37	4.81	7.08	1.30	6.32	3.94	3.69	4.44	5.23	5.37	6.36	6.67	6.09	8.47	6.38	7.47	6.26	7.00	6.92	6.92
UO2	6.97	9.20	3.82	2.69	0.78	3.32	2.24	2.26	2.41	2.88	2.64	2.89	1.08	2.52	0.59	14.66	2.48	8.21	13.61	14.04	14.04
(Na,K)2O	-	-	-	-	-	-	-	-	-	-	-	-	-	-	-	-	-	-	-	-	-
H2O	-	-	-	-	-	-	-	-	-	-	-	-	-	-	-	-	-	-	-	-	-
"Others"	-	-	-	-	-	-	-	-	-	-	-	-	-	-	-	-	-	-	-	-	-
TOTAL	100.37	98.79	98.59	99.12	98.32	97.55	97.71	97.53	101.40	101.09	100.18	99.65	98.37	99.92	98.21	98.41	98.02	99.54	99.93	100.05	97.61
Cations to 7 oxygens																					
Ca2+	0.727	0.603	0.848	0.693	0.924	0.552	0.859	0.890	0.519	0.818	0.852	0.841	1.042	0.739	1.001	0.698	0.624	0.731	0.694	0.715	0.679
Y+REE3+	0.081	0.052	0.064	0.228	0.077	0.367	0.088	0.048	0.407	0.171	0.084	0.195	0.047	0.174	0.018	0.041	0.351	0.163	0.133	0.056	0.037
Pb2+	-	-	-	-	-	-	-	-	-	-	-	-	-	-	-	-	-	-	-	-	-
Th4+	0.194	0.248	0.068	0.106	0.098	0.055	0.051	0.066	0.075	0.074	0.093	0.097	0.011	0.134	0.097	0.111	0.083	0.107	0.108	0.108	0.108
U4+	0.103	0.145	0.052	0.039	0.010	0.051	0.031	0.035	0.040	0.036	0.041	0.014	0.035	0.008	0.227	0.037	0.086	0.120	0.203	0.214	0.214
SUM Ca2+	1.106	1.048	1.032	1.066	1.029	1.069	1.033	1.021	1.028	1.046	1.170	1.112	1.037	1.037	1.103	1.110	1.070	1.040	1.081	1.039	1.034
Zr4+	0.886	0.955	0.950	0.904	1.004	0.822	0.856	0.945	0.929	0.947	0.907	0.915	0.902	0.932	0.900	0.940	0.935	0.960	0.982	0.907	0.924
Hf4+	0.010	0.005	0.020	0.004	0.013	0.018	0.016	0.013	0.018	0.016	0.005	0.011	0.016	0.012	0.013	0.016	0.006	0.010	0.011	0.011	0.011
SUM Zr4+	0.886	0.964	0.955	0.925	1.004	0.835	0.875	0.945	0.946	0.960	0.911	0.920	0.913	0.948	0.912	0.953	0.951	0.982	0.917	0.934	0.934
Ti4+	1.625	1.500	1.775	1.632	1.828	1.582	1.859	1.816	1.534	1.649	1.817	1.599	1.899	1.861	1.960	1.641	1.625	1.590	1.578	1.515	1.515
Si4+	-	0.014	0.014	0.025	0.104	0.006	0.088	0.043	0.020	0.101	0.073	0.044	0.141	0.026	0.126	0.017	0.228	0.122	0.078	0.121	0.198
Mg2+	0.059	0.086	0.024	0.016	0.016	0.009	0.004	0.006	0.005	0.005	0.005	0.008	0.014	0.054	0.027	0.006	0.005	0.013	0.011	0.011	0.011
Mn2+	0.024	0.030	0.015	0.070	0.011	0.109	0.045	0.019	0.095	0.045	0.025	0.085	0.024	0.086	0.022	0.056	0.072	0.029	0.041	0.065	0.056
Fe2+	0.186	0.252	0.080	0.171	0.048	0.284	0.104	0.075	0.255	0.145	0.095	0.144	0.054	0.129	0.035	0.130	0.181	0.149	0.143	0.138	0.144
Fe3+	-	-	-	-	-	-	-	-	-	-	-	-	-	-	-	-	-	-	-	-	-
Al3+	0.099	0.071	0.122	0.063	0.098	0.041	0.067	0.099	0.056	0.081	0.097	0.071	0.051	0.073	0.055	0.048	0.072	0.102	0.075	0.043	0.107
Cr3+	-	-	-	-	-	-	-	-	-	-	-	-	-	-	-	-	-	-	-	-	-
Nb5+	-	-	-	-	-	-	-	-	-	-	-	-	-	-	-	-	-	-	-	-	-
Ta5+	-	-	-	-	-	-	-	-	-	-	-	-	-	-	-	-	-	-	-	-	-
Wb+	0.017	0.014	-	0.006	-	0.018	-	0.016	-	0.016	0.007	0.007	-	-	-	-	-	0.009	0.015	-	-
SLM Ti4+	2.019	1.983	2.037	2.046	1.986	2.118	2.125	2.051	2.055	2.005	2.078	2.026	2.062	2.090	1.983	2.093	2.005	1.997	2.039	2.099	2.099
TOTAL	4.021	3.985	4.024	4.036	4.030	4.022	4.032	4.017	4.029	4.088	4.035	4.116	4.080	4.047	4.040	4.039	4.054	4.041	4.020	4.037	4.072

	M56	M57	M58	M59	M60	M61	M62	M63	M64	M65	M66	M67	M68	M69	M70	M71	M72	M73	M74	M75	M76
MgO	1.49	2.37	2.27	1.98	2.28	0.75	2.14	1.98	2.31	2.68	2.22	0.52	0.53	0.37	0.32	0.30	0.34	0.24	0.21	0.32	
Al2O3	0.91	0.86	0.47	0.33	0.43	1.46	0.52	0.63	0.70	0.70	0.80	0.35	0.40	0.38	0.25	0.30	0.21	0.19	0.23	0.26	0.28
SiO2	<0.06	<0.06	<0.06	<0.06	<0.06	<0.06	<0.06	<0.06	<0.06	<0.06	<0.06	<0.06	<0.06	<0.06	<0.06	<0.06	<0.06	<0.06	<0.06	<0.06	
Cao	9.79	9.55	9.33	8.92	9.48	11.86	9.42	9.35	9.07	10.51	7.21	8.33	7.49	7.23	7.37	7.16	7.46	8.98	7.52	7.52	
TiO2	33.50	29.79	29.73	26.39	29.94	35.87	30.31	28.68	29.50	30.66	30.62	26.36	26.33	29.24	28.04	26.72	26.75	26.96	26.58	29.01	27.36
Cr2O3	-	-	-	-	-	-	-	-	-	-	-	-	-	-	-	-	-	-	-	-	-
MnO	0.24	0.24	<0.05	0.20	0.08	<0.05	0.19	0.13	0.14	0.10	0.72	0.78	0.80	0.64	0.83	0.82	0.87	1.10	0.58	0.79	0.79
FeO	2.12	2.29	1.99	4.23	2.34	2.10	1.89	3.21	2.36	2.15	2.22	6.08	6.63	6.26	6.67	7.14	6.90	6.54	5.79	6.54	6.36
Fe2O3	-	-	-	-	-	-	-	-	-	-	-	-	-	-	-	-	-	-	-	-	-
Y2O3	1.13	0.27	0.18	0.08	0.17	0.38	0.18	1.06	0.44	0.28	4.51	3.55	3.76	4.40	4.62	5.28	5.10	4.88	3.22	4.58	
ZrO2	30.90	29.99	29.77	25.96	30.46	32.40	31.85	24.34	27.76	26.65	26.05	28.95	29.23	30.16	29.16	29.33	29.05	29.12	28.92	28.66	
Nb2O5	2.22	1.75	2.20	1.64	1.62	0.74	1.37	2.34	1.85	1.89	1.78	2.77	2.65	2.04	2.73	2.32	3.85	3.52	3.07	2.10	2.76
La2O3	0.23	<0.07	0.07	0.09	0.12	0.34	<0.07	0.09	<0.07	0.12	0.34	0.18	0.08	0.18	0.19	0.13	0.25	0.14	-	-	-
Ce2O3	1.68	0.58	0.59	0.39	0.73	1.98	0.61	1.75	0.81	0.66	1.81	2.45	2.62	2.17	1.63	1.88	1.75	1.70	2.69	1.88	
Pr2O3	0.45	<1.14	<1.14	<1.14	<1.14	0.25	0.18	0.36	<1.14	<1.14	0.19	0.33	0.40	0.52	0.52	0.32	0.39	0.34	0.45	0.29	
Nd2O3	1.93	0.54	0.45	0.21	0.66	1.72	0.97	2.11	0.88	0.60	0.68	3.21	3.20	3.03	3.36	3.09	3.47	3.27	3.31	3.09	
Sm2O3	0.50	0.16	<1.14	<1.14	0.22	0.57	0.26	0.14	0.20	0.24	0.99	1.11	1.13	1.41	1.57	1.29	0.94	1.14	-	-	
Eu2O3	-	-	-	-	-	-	-	-	-	-	-	-	-	-	-	-	-	-	-	-	
Gd2O3	0.39	<1.16	<1.16	<1.16	0.30	<1.16	0.56	0.24	<1.16	0.21	0.49	1.07	1.14	1.22	1.48	1.36	1.43	0.87	1.28		
Tb2O3	-	-	-	-	-	-	-	-	-	-	-	-	-	-	-	-	-	-	-	-	
Dy2O3	0.31	<1.16	<1.16	<1.16	<1.16	<1.16	0.38	0.17	0.16	0.16	1.22	0.85	0.70	0.78	1.02	0.96	0.99	1.03	0.53	0.96	
Ho2O3	-	-	-	-	-	-	-	-	-	-	-	-	-	-	-	-	-	-	-	-	
Er2O3	<1.17	<1.17	<1.17	<1.17	<1.17	<1.17	<1.17	<1.17	<1.17	<1.17	<1.17	<1.17	<1.17	<1.17	0.34	0.36	0.23	0.48	0.37	0.40	0.25
Tm2O3	-	-	-	-	-	-	-	-	-	-	-	-	-	-	-	-	-	-	-	-	
Yb2O3	<1.18	<1.18	<1.18	<1.18	<1.18	<1.18	<1.18	<1.18	<1.18	<1.18	<1.18	<1.18	<1.18	<1.18	0.42	0.16	0.47	0.41	0.42	0.30	0.31
Lu2O3	-	-	-	-	-	-	-	-	-	-	-	-	-	-	-	-	-	-	-	0.42	
HfO2	0.52	0.51	0.59	0.58	0.70	0.39	0.54	0.41	0.48	0.65	0.30	0.52	0.85	0.87	0.98	0.82	0.85	0.89	0.74	1.04	
Ta2O5	<2.27	<2.27	0.41	<2.27	<2.27	<2.27	<2.27	<2.27	<2.27	0.36	0.56	<2.27	0.31	<1.15	<1.15	0.15	0.27	0.32	0.25	0.20	<1.15
WtO3	<3	<3	<3	<3	<3	<3	<3	<3	<3	<3	<3	<3	<3	<3	<3	0.34	0.49	0.58	0.35	0.36	0.37
PbO	-	-	-	-	-	-	-	-	-	-	-	-	-	-	-	0.20	0.21	0.16	0.37	0.18	
ThO2	8.25	8.98	5.96	8.39	4.92	7.04	7.30	8.06	7.62	8.24	1.53	3.05	1.43	1.45	1.86	0.94	0.84	1.46	0.74	1.78	
UO2	5.64	12.26	13.98	23.98	12.14	4.01	11.81	14.66	13.23	15.10	13.16	0.97	1.39	0.78	1.12	1.43	0.59	0.54	0.75	0.37	1.21
(Na,K)2O	-	-	-	-	-	-	-	-	-	-	-	-	-	-	-	-	-	-	-	-	
H2O	-	-	-	-	-	-	-	-	-	-	-	-	-	-	-	-	-	-	-	-	
"Others"	-	-	-	-	-	-	-	-	-	-	-	-	-	-	-	-	-	-	-	-	
TOTAL	100.36	99.41	100.94	101.79	99.55	99.88	98.99	100.96	98.96	100.14	98.78	91.35	93.63	95.17	94.60	94.01	94.64	93.11	92.22	93.48	92.56
cations to 7 oxygens																					
Ca2+	0.674	0.690	0.675	0.679	0.687	0.794	0.679	0.693	0.667	0.727	0.787	0.557	0.564	0.610	0.559	0.549	0.552	0.542	0.572	0.666	0.573
Y+REE3+	0.165	0.041	0.032	0.021	0.043	0.121	0.051	0.182	0.076	0.050	0.063	0.421	0.421	0.378	0.371	0.407	0.411	0.452	0.431	0.351	0.408
Pb2+	-	-	-	-	-	-	-	-	-	-	-	-	-	-	-	0.004	0.003	0.003	0.005	0.004	0.006
Tn4+	0.094	0.127	0.138	0.096	0.128	0.070	0.108	0.115	0.126	0.117	0.128	0.025	0.049	0.022	0.023	0.017	0.017	0.014	0.024	0.012	0.029
U4+	0.081	0.184	0.210	0.379	0.183	0.056	0.177	0.226	0.202	0.228	0.189	0.016	0.022	0.012	0.023	0.017	0.023	0.008	0.012	0.008	0.019
SUM Ca2+	1.013	1.041	1.054	1.178	1.042	1.040	1.215	1.073	1.120	1.157	1.022	1.017	1.010	1.022	1.032	1.012	1.043	1.034	1.035	1.032	1.005
Zr4+	1.620	1.510	1.509	1.410	1.523	1.685	1.534	1.492	1.523	1.554	1.589	1.429	1.409	1.503	1.489	1.425	1.407	1.433	1.431	1.508	1.464
Si4+	-	-	-	-	-	-	-	-	-	-	-	-	-	-	-	-	-	-	-	-	-
Mg2+	0.143	0.238	0.228	0.210	0.230	0.070	0.215	0.204	0.238	0.228	0.225	0.056	0.044	0.047	0.035	0.038	0.038	0.036	0.036	0.022	0.034
Mn2+	0.013	0.014	0.112	0.012	0.005	0.011	0.008	0.011	0.008	0.006	0.006	0.044	0.047	0.035	0.038	0.038	0.038	0.038	0.037	0.037	0.048
Fe2+	0.114	0.129	0.112	0.251	0.110	0.106	0.188	0.135	0.121	0.126	0.367	0.394	0.398	0.423	0.404	0.387	0.347	0.378	0.379	-	-
Fe3+	-	-	-	-	-	-	-	-	-	-	-	-	-	-	-	-	-	-	-	-	-
Al3+	0.069	0.068	0.037	0.028	0.034	0.108	0.041	0.051	0.057	0.056	0.064	0.030	0.034	0.031	0.021	0.025	0.017	0.016	0.019	0.021	0.024
Cr3+	-	-	-	-	-	-	-	-	-	-	-	-	-	-	-	-	-	-	-	-	-
Nb5+	0.065	0.053	0.067	0.053	0.050	0.021	0.042	0.073	0.057	0.058	0.055	0.080	0.085	0.083	0.086	0.074	0.122	0.113	0.089	0.068	-
Ta5+	-	0.008	-	0.016	-	1.974	2.004	1.948	2.033	2.030	2.086	2.051	2.050	2.080	2.069	2.068	2.066	2.068	2.018	2.057	2.082
W6+	-	2.023	2.013	1.961	1.979	-	-	-	-	-	-	-	-	-	-	-	-	-	-	-	-
SUM Ti4+	-	-	-	-	-	-	-	-	-	-	-	-	-	-	-	-	-	-	-	-	-
TOTAL	4.014	4.049	4.006	4.069	4.034	4.039	4.018	4.077	4.042	4.075	4.079	4.101	4.110	4.101	4.090	4.112	4.102	4.093	4.092	4.120	4.102

	M77	M78	M79	M80	M81	M82	M83	M84	M85	M86	M87	M88	M89	M90	M91	M92	M93	M94	M95	M96	M97	
MgO	0.45	0.22	0.17	0.37	0.85	0.28	0.98	1.33	0.95	0.39	0.38	0.32	0.24	0.34	0.19	0.35	0.34	0.20	-	-	0.39	
Al2O3	0.23	0.34	0.17	0.32	0.40	0.19	0.54	0.74	0.57	0.29	0.25	0.27	0.25	0.21	0.19	0.19	0.19	0.10	-	-	1.89	
SiO2	0.58	0.21	0.08	0.16	0.52	0.26	0.86	0.83	0.81	0.23	0.28	0.28	0.12	0.16	0.14	0.37	0.26	0.28	-	-	2.94	
Cao	7.78	8.40	7.70	7.31	8.92	7.81	7.29	7.55	8.20	7.13	7.52	8.14	7.24	7.44	7.64	8.47	7.32	8.75	6.58	8.71	15.83	
TiO2	26.95	28.00	27.24	27.87	26.51	26.47	27.00	27.52	28.18	27.67	27.48	28.38	27.75	27.29	27.35	27.16	27.38	27.51	28.12	33.12	45.72	
Cr2O3	-	-	-	-	-	-	-	-	-	-	-	-	-	-	-	-	-	-	-	-	-	
MnO	0.94	0.84	0.78	0.68	0.64	1.03	0.97	0.59	0.87	0.63	0.85	0.58	0.71	0.75	0.63	2.00	0.88	1.99	-	-	-	
FeO	6.21	5.27	6.64	7.02	7.10	5.17	5.71	7.02	5.77	6.71	6.74	6.58	6.58	6.70	3.63	5.98	3.10	-	1.50	-	-	
Fe2O3	-	-	-	-	-	-	-	-	-	-	-	-	-	-	-	-	-	-	9.58	1.87	1.50	
Y2O3	4.99	3.13	4.97	4.83	5.08	4.49	5.21	4.01	5.02	4.95	4.97	4.18	5.39	5.19	5.18	5.09	5.24	3.28	0.85	-	-	
ZrO2	28.56	30.12	29.13	29.89	28.11	29.18	28.00	29.37	30.23	29.65	29.74	30.06	28.58	28.71	28.84	28.81	28.71	31.04	32.88	36.70	-	
Nb2O5	3.94	2.02	3.71	2.50	2.60	2.44	3.06	2.37	1.83	2.47	3.81	2.80	2.49	3.17	3.72	2.49	2.78	3.12	6.40	4.43	-	
La2O3	0.21	0.32	0.13	0.15	0.12	0.18	0.11	0.17	0.31	0.10	0.20	0.19	0.16	0.13	0.10	0.15	0.11	0.57	-	-	-	
Cr2O3	1.74	2.98	1.74	1.42	1.14	1.77	1.31	2.10	2.10	1.18	1.82	2.11	1.61	1.41	1.63	1.27	1.58	-	3.53	3.53	-	
Pr2O3	0.37	0.61	0.29	0.49	0.41	0.24	0.27	0.35	0.46	0.34	0.47	0.40	0.30	0.42	0.25	0.29	0.36	0.10	0.90	0.73	-	
Nd2O3	3.15	3.18	3.26	2.98	2.67	3.01	2.70	3.13	3.11	2.92	3.39	3.15	2.80	2.89	3.21	2.82	3.22	2.50	3.28	1.77	-	
Sm2O3	1.20	0.91	1.27	1.31	1.21	1.27	1.03	0.97	1.01	1.11	1.10	0.96	1.18	1.08	1.23	1.20	1.32	0.87	1.38	0.37	-	
Eu2O3	-	-	-	-	-	-	-	-	-	-	-	-	-	-	-	-	-	0.28	0.06	-	-	
Gd2O3	1.36	0.94	1.40	1.51	1.53	1.39	1.41	1.16	1.13	1.50	1.37	1.14	1.43	1.41	1.50	1.50	1.44	1.22	1.14	0.27	-	
Tb2O3	-	-	-	-	-	-	-	-	-	-	-	-	-	-	-	-	-	-	-	-	-	
Dy2O3	0.98	0.75	0.92	1.20	1.21	0.92	0.90	0.79	0.76	1.12	0.90	0.94	1.09	1.11	0.97	1.07	1.10	1.08	0.78	0.19	-	
Ho2O3	-	-	-	-	-	-	-	-	-	-	-	-	-	-	-	-	-	-	0.10	0.02	-	
Er2O3	0.43	0.34	0.42	0.60	0.50	0.46	0.46	0.39	0.43	0.43	0.41	0.42	0.50	0.47	0.48	0.55	0.55	0.42	0.44	0.06	-	
Tm2O3	-	-	-	-	-	-	-	-	-	-	-	-	-	-	-	-	-	0.06	0.06	-	-	
Yb2O3	0.40	0.23	0.34	0.35	0.27	0.32	0.30	0.39	0.18	0.45	0.28	0.43	0.55	0.43	0.44	0.55	0.55	0.41	0.20	0.02	-	
Lu2O3	-	-	-	-	-	-	-	-	-	-	-	-	-	-	-	-	-	0.06	-	-	-	
HfO2	0.80	0.90	0.80	0.78	0.77	1.13	0.59	0.69	0.72	0.93	0.80	0.75	1.00	0.78	0.77	0.87	0.70	0.54	-	-	-	
Ta2O5	0.46	0.12	0.20	<15	<15	<15	<15	<15	<15	<15	<15	<15	<15	<15	<15	<15	<15	<15	<15	-	-	-
WO3	0.23	0.51	0.30	0.67	0.42	0.85	0.77	0.14	0.39	0.69	0.67	0.65	0.44	0.26	0.28	0.21	0.25	-	-	-	-	-
PhO	<10	0.27	0.24	0.40	0.80	0.16	0.30	0.21	0.21	0.27	0.17	0.19	0.29	0.21	0.19	0.19	0.22	-	-	-	-	-
ThO2	0.73	1.97	0.66	2.25	2.35	2.39	2.33	1.18	1.39	2.31	1.20	1.56	2.25	2.26	2.23	2.07	1.74	2.19	0.60	0.97	-	
UO2	0.65	0.46	1.49	2.10	1.63	1.87	0.72	1.01	1.58	0.75	0.97	1.89	1.72	0.99	1.89	1.16	2.43	-	-	0.11	-	
(Na,K)2O	-	-	-	-	-	-	-	-	-	-	-	-	-	-	-	-	-	-	1.02	1.87	-	
H2O	-	-	-	-	-	-	-	-	-	-	-	-	-	-	-	-	-	-	0.20	0.20	-	
"Others"	-	-	-	-	-	-	-	-	-	-	-	-	-	-	-	-	-	-	-	-	-	
TOTAL	93.35	93.03	96.56	94.03	92.84	94.95	93.82	94.64	95.12	95.53	95.25	94.41	95.11	93.73	93.33	93.87	92.64	99.62	100.02	100.14	-	
cations to 7 oxygens																						
Ca2+	0.583	0.633	0.582	0.541	0.527	0.601	0.540	0.556	0.601	0.533	0.555	0.600	0.548	0.559	0.576	0.644	0.556	0.666	0.459	0.573	0.959	
Y+REE3+	0.424	0.372	0.426	0.416	0.414	0.410	0.394	0.373	0.373	0.406	0.421	0.386	0.420	0.427	0.434	0.423	0.443	0.394	0.412	0.196	0.000	
Pb2+	-	0.005	0.005	0.007	0.015	0.003	0.006	0.004	0.005	0.003	0.004	0.006	0.008	0.004	0.004	0.004	0.005	0.015	0.004	0.009	-	
Th4+	0.012	0.032	0.012	0.035	0.038	0.039	0.022	0.018	0.022	0.037	0.018	0.024	0.036	0.036	0.033	0.028	0.035	0.030	0.018	0.014	-	
U4+	0.010	0.012	0.007	0.023	0.033	0.026	0.029	0.011	0.015	0.025	0.011	0.015	0.030	0.027	0.015	0.030	0.038	0.018	0.038	0.002	-	
SUM Ca2+	1.029	1.054	1.030	1.022	1.027	1.079	1.005	0.962	1.015	1.006	1.009	1.029	1.040	1.057	1.049	1.134	1.060	1.138	0.880	0.784	0.959	
SUM Zr4+	0.990	1.052	1.018	1.021	0.989	1.046	0.998	1.022	1.028	1.014	1.024	1.005	0.997	1.005	1.015	1.009	1.005	0.986	0.983	0.983	-	
Tl4+	1.417	1.482	1.447	1.416	1.430	1.422	1.449	1.452	1.423	1.469	1.474	1.439	1.423	1.447	1.449	1.470	1.378	1.528	1.944	-	-	
Si4+	0.041	0.015	0.006	0.018	0.038	0.069	0.030	0.059	0.064	0.055	0.064	0.055	0.064	0.068	0.068	0.068	0.068	0.026	0.018	0.180	-	
Mg2+	0.047	0.023	0.009	0.047	0.040	0.039	0.063	0.057	0.034	0.050	0.037	0.050	0.045	0.045	0.042	0.045	0.038	0.120	0.053	0.120	-	
Mn2+	0.056	0.050	0.047	0.045	0.045	0.045	0.045	0.045	0.045	0.043	0.043	0.043	0.043	0.043	0.043	0.043	0.043	0.184	0.184	0.077	-	
Fe2+	0.363	0.310	0.392	0.405	0.422	0.311	0.330	0.403	0.330	0.392	0.330	0.398	0.379	0.388	0.389	0.389	0.215	0.353	-	0.470	0.086	-
Fe3+	-	-	-	-	-	-	-	-	-	-	-	-	-	-	-	-	-	-	-	-	-	
Al3+	0.019	0.028	0.014	0.026	0.034	0.016	0.044	0.060	0.046	0.024	0.020	0.022	0.021	0.017	0.016	0.016	0.008	0.008	0.008	0.137	-	
Ci3+	-	-	-	-	-	-	-	-	-	-	-	-	-	-	-	-	-	-	-	-	-	
Nb3+	0.125	0.064	0.118	0.078	0.083	0.079	0.096	0.074	0.057	0.078	0.119	0.081	0.080	0.100	0.118	0.080	0.089	0.100	0.189	0.123	-	
Ta5+	0.009	0.002	0.004	0.005	0.012	0.008	0.014	0.002	0.007	0.012	0.012	0.012	0.012	0.012	0.012	0.012	0.012	0.005	0.005	0.005	-	
W6+	0.004	0.009	0.005	0.005	0.012	0.007	0.010	0.010	0.010	0.010	0.010	0.010	0.010	0.010	0.010	0.010	0.010	0.005	0.005	0.005	-	
SUM Ti4+	2.081	1.984	2.050	2.057	2.107	1.960	2.101	2.196	2.091	2.052	2.068	2.047	2.054	1.948	2.028	1.928	2.037	2.132	2.041	-	-	
TOTAL	4.100	4.090	4.098	4.101	4.123	4.085	4.094	4.156	4.128	4.086	4.108	4.091	4.101	4.091	4.108	4.099	4.097	4.097	4.091	4.093	3.899	4.012

	M98	P1	P2	P3	P4	P5	P6	P7	P8	P9	P10	SG1	SG2	SG3	L1	L2	L3	L4	L5	L6	
MgO	-	0.71	0.37	2.34	3.04	1.33	1.08	1.96	2.32	2.43	1.89	2.50	2.65	0.36	0.58	0.72	0.65	0.01	0.03		
Al2O3	-	0.12	0.22	-	-	2.26	-	0.67	0.81	0.42	2.50	2.73	2.74	1.60	1.14	1.34	1.07	0.48	0.43		
SiO2	-	16.41	9.80	11.10	6.87	6.78	8.55	9.35	8.18	8.31	8.60	5.47	0.10	0.11	1.90	1.08	0.27	1.74	-	0.25	
CaO	-	21.00	22.30	29.50	30.95	36.26	36.06	34.87	29.00	30.20	21.70	32.50	32.95	32.92	28.30	26.90	34.60	7.31	2.63	3.55	
TiO2	-	45.87	-	-	-	-	-	-	-	-	-	-	-	-	-	-	-	25.48	27.48		
Cr2O3	-	-	-	-	-	-	-	-	-	-	-	-	-	-	-	-	-	-	-		
MnO	-	0.28	0.03	0.26	0.03	-	-	0.07	0.05	0.08	4.97	0.84	0.81	0.88	0.30	0.03	-	0.11	-	0.08	
FeO	-	7.16	7.37	4.07	4.42	4.72	4.65	3.73	-	-	-	-	-	-	-	6.50	5.90	5.95	9.06	7.44	
Fe2O3	0.76	-	-	0.24	1.08	0.40	-	-	-	-	-	-	-	-	-	-	-	-	-	-	
Y2O3	-	31.40	33.20	30.73	32.56	34.19	32.64	35.27	28.30	28.10	28.01	34.34	34.17	34.96	45.40	40.70	40.20	37.21	33.60	32.78	
ZrO2	36.56	-	9.98	11.20	-	-	-	-	-	-	2.61	2.24	2.92	0.14	0.46	0.40	0.63	1.85	2.75	1.62	
Nb2O5	-	0.06	0.04	0.17	2.68	1.40	0.32	0.83	-	-	0.12	0.05	0.38	0.23	0.24	-	-	0.09	0.19	0.29	
La2O3	-	0.74	0.20	0.25	-	-	-	-	-	-	0.28	0.62	2.11	2.45	1.87	1.98	0.48	2.11	1.33	1.64	
Ce2O3	-	1.03	1.19	-	-	-	-	-	-	-	0.11	0.14	0.31	0.58	0.44	-	-	0.07	0.55	0.43	
Pr2O3	-	0.30	0.12	-	-	-	-	-	-	-	0.33	0.42	1.50	3.27	2.69	0.56	3.30	0.63	0.79	3.08	
Nd2O3	-	-	-	-	-	-	-	-	-	-	-	-	0.34	1.37	1.17	1.30	0.22	-	-	0.36	
Sm2O3	-	-	-	-	-	-	-	-	-	-	-	-	-	-	-	-	-	-	1.74	1.08	
Eu2O3	-	-	-	-	-	-	-	-	-	-	-	-	-	-	-	-	-	-	-	-	
Gd2O3	-	0.32	0.43	-	-	-	-	-	-	-	0.24	1.79	1.78	1.78	0.45	1.92	0.42	0.25	2.00	1.45	
Tb2O3	-	-	-	-	-	-	-	-	-	-	-	-	-	-	-	-	-	0.13	0.37	0.42	
Dy2O3	0.17	0.06	-	-	-	-	-	-	-	-	0.30	1.69	1.87	1.70	-	1.61	0.67	0.79	2.64	2.09	
Ho2O3	-	-	-	-	-	-	-	-	-	-	0.20	0.20	<15	0.02	-	-	-	<0.01	0.37	0.38	
Er2O3	-	-	-	-	-	-	-	-	-	-	0.15	0.75	0.88	0.77	-	-	-	0.12	0.19	0.16	
Tm2O3	-	-	-	-	-	-	-	-	-	-	-	-	-	-	-	-	-	-	-	-	
Yb2O3	-	-	-	-	-	-	-	-	-	-	-	-	-	-	-	-	-	0.01	0.01	-	
Lu2O3	-	-	-	-	-	-	-	-	-	-	-	-	-	-	-	-	-	0.54	1.24	-	
HfO2	0.70	0.86	-	-	-	-	-	-	-	-	0.67	0.67	0.69	0.65	0.70	-	-	0.21	0.33	0.44	
Ta2O5	2.75	1.76	-	-	-	-	-	-	-	-	0.20	0.20	-	-	-	-	-	0.72	1.11	0.89	
WO3	-	0.18	0.09	0.38	20.44	18.78	8.33	8.51	0.23	19.50	18.00	22.28	0.61	0.56	0.44	0.83	0.46	0.44	1.19	0.35	0.60
PhO	-	14.00	8.65	0.36	1.08	0.65	4.66	2.08	14.31	1.58	1.90	2.67	0.28	0.52	0.36	-	0.21	0.22	0.30	0.40	0.14
ThO2	-	-	-	-	-	-	-	-	-	-	-	-	-	-	-	-	-	-	-	-	
UO2	-	-	-	-	-	-	-	-	-	-	-	-	-	-	-	-	-	-	-	-	
(Na,K)2O	-	-	-	-	-	-	-	-	-	-	-	-	-	-	-	-	-	-	-	-	
H2O	-	-	-	-	-	-	-	-	-	-	-	-	-	-	-	-	-	-	-	-	
"Others"	-	-	-	-	-	-	-	-	-	-	-	-	-	-	-	-	-	-	-	-	
TOTAL	99.60	102.01	101.40	99.18	98.98	98.36	97.46	98.99	98.27	97.43	97.92	99.89	100.00	100.73	99.21	99.95	100.25	99.81	99.40	99.70	
cations to 7 oxygens																					
Ca2+	1.000	0.719	0.788	0.511	0.490	0.588	0.633	0.567	0.607	0.627	0.444	0.318	0.285	0.309	0.705	0.320	0.558	0.483	0.196	0.259	
Y+REE3+	0.000	0.077	0.094	0.108	0.049	0.008	0.019	0.000	0.030	0.042	0.180	0.551	0.553	0.541	0.130	0.455	0.172	0.200	0.643	0.664	
Pb2+	-	0.003	0.002	0.007	-	-	-	-	-	-	0.008	0.012	-	-	-	0.004	0.008	0.009	0.008	0.004	0.004
Th4+	-	0.218	0.130	0.323	0.288	0.122	0.122	0.029	0.030	0.279	0.384	0.009	0.008	0.006	0.012	0.007	0.006	0.017	0.006	0.009	
U4+	-	0.013	0.005	0.016	0.010	0.087	0.029	0.026	0.024	0.029	0.045	0.004	0.007	0.005	0.003	0.003	0.004	0.006	0.002	0.002	
SUM Ca2+	1.000	1.030	1.019	0.965	0.837	0.784	0.803	0.784	0.972	0.985	1.066	0.882	0.853	0.862	0.847	0.789	0.747	0.713	0.859	0.958	
Zr4+	1.014	1.048	1.073	1.040	1.072	1.071	1.005	1.112	0.942	0.933	1.035	1.062	1.050	1.065	1.361	1.291	1.188	1.119	1.140	1.087	
Hf4+	-	0.014	1.062	1.086	1.040	1.072	1.005	1.112	0.955	0.946	1.050	1.073	1.062	1.077	1.361	1.299	1.193	1.132	1.162	1.105	
SUM Zr4+	1.014	-	-	-	-	-	-	-	-	-	-	-	-	-	-	-	-	-	-	-	
Mn2+	-	0.072	0.037	0.242	0.306	0.127	0.102	0.189	0.236	0.247	0.214	0.236	0.249	0.247	0.033	0.002	-	0.065	0.060	0.001	0.003
F62+	-	0.018	0.015	0.002	-	-	-	-	-	-	-	-	-	-	-	-	-	0.298	0.307	0.527	0.423
F63+	0.033	-	0.410	0.409	0.236	0.249	0.246	0.202	-	-	0.180	0.115	0.315	0.045	0.043	0.046	-	-	-	-	-
Al3+	-	0.010	0.017	-	-	-	-	-	-	-	0.054	0.065	0.038	0.187	0.203	0.202	0.116	0.087	0.098	0.078	0.035
Cr3+	-	-	-	-	-	-	-	-	-	-	-	-	-	-	-	-	0.029	0.023	0.025	0.013	
Nb5+	0.309	0.336	0.032	-	-	-	-	-	-	-	0.081	0.069	0.100	0.004	-	-	0.013	0.017	0.052	0.004	0.013
Ta5+	-	0.051	-	-	-	-	-	-	-	-	0.004	0.004	-	-	-	-	0.012	0.017	0.052	0.004	
W6+	-	1.994	1.950	1.956	2.020	2.126	2.132	2.228	2.087	2.046	1.908	2.027	2.062	2.048	1.838	1.917	2.095	2.151	1.995	1.954	
SUM Ti4+	-	-	-	-	-	-	-	-	-	-	-	-	-	-	-	-	-	-	-	-	
TOTAL	4.008	4.042	4.061	4.026	4.035	3.986	4.037	3.983	3.973	3.980	4.025	3.883	3.978	3.987	4.046	4.006	4.034	3.995	4.015	4.017	

	L7	L8	L9	L10	L11	L12	L13	THEORETICAL
MgO	0.10	1.15	-	<0.01	0.12	-	-	
Al2O3	0.50	0.87	-	0.35	0.46	0.37	0.84	
SiO2	-	0.62	-	0.13	0.10	0.29	0.37	
CaO	3.20	6.15	3.29	3.17	3.21	2.75	2.85	16.54
TiO2	27.10	29.62	26.60	<0.01	27.01	28.70	26.60	47.13
Cr2O3	0.50	0.50	-	-	-	-	-	
MnO	0.30	-	-	-	-	0.13	-	
FeO	11.40	4.23	8.67	7.71	9.00	10.30	9.97	
Fe2O3	-	-	-	-	-	-	-	
Y2O3	10.40	7.70	10.80	7.87	12.80	12.80	12.00	
ZrO2	30.80	30.06	29.80	36.98	29.94	31.50	31.70	36.33
Nb2O5	-	4.34	-	2.34	-	4.25	3.99	
La2O3	0.60	0.08	0.20	0.13	0.27	0.02	-	
Ce2O3	1.90	0.84	1.72	1.23	2.29	1.05	1.11	
Pt2O3	0.70	0.32	1.38	0.40	1.01	0.32	0.26	
Na2O3	3.30	1.04	7.04	2.94	4.79	1.21	2.31	
Sm2O3	1.70	0.55	2.04	1.49	0.65	0.73	1.14	
Eu2O3	0.40	<0.01	0.01	0.12	0.02	-	-	
Gd2O3	2.10	0.33	1.44	1.74	0.95	2.34	1.75	
Tb2O3	0.30	0.24	1.19	0.32	0.46	0.19	0.08	
Dy2O3	0.90	1.59	2.06	2.10	3.19	-	-	
Ho2O3	0.20	0.03	1.27	0.15	1.16	0.95	0.88	
Er2O3	-	1.01	2.11	0.94	1.14	0.90	1.17	
Tm2O3	-	0.20	0.26	<0.01	0.83	0.24	0.3	
Yb2O3	-	1.03	0.46	0.25	0.76	0.50	0.71	
Lu2O3	-	0.36	-	0.26	-	-	-	
HfO2	-	0.86	1.20	1.34	1.03	0.71	0.77	
Ta2O5	-	0.40	-	0.24	-	0.05	0.13	
WO3	-	-	-	-	-	-	-	
PbO	-	2.19	-	0.45	-	-	-	
ThO2	-	2.34	-	0.33	-	-	-	
UO2	-	1.16	-	0.33	-	0.06	0.14	
(Na,K)2O	-	-	-	-	-	-	-	
H2O	-	-	-	-	-	-	-	
"Others"	-	-	-	-	-	-	-	
TOTAL	96.40	99.61	101.54	99.02	101.19	100.36	99.07	100.00
cations to 7 oxygens								
Ca2+	0.239	0.433	0.247	0.233	0.237	0.194	0.205	1.000
Y+REE3+	0.681	0.436	0.910	0.570	0.879	0.635	0.650	0.000
Ph2+	-	0.039	-	0.008	-	-	-	-
Th4+	-	0.035	-	0.005	-	0.001	0.002	-
La4+	-	0.017	-	0.005	-	-	-	-
SUM Ca2+	0.921	0.959	1.157	0.822	1.116	0.829	0.858	1.000
Zr4+	1.048	0.963	1.017	1.239	1.005	1.009	1.039	1.000
Hf4+	-	0.016	0.024	0.026	0.020	0.013	0.015	-
SUM Zr4+	1.048	0.980	1.041	1.265	1.025	1.023	1.054	1.000
Ti4+	1.423	1.464	1.400	1.328	1.398	1.418	1.345	2.000
Si4+	-	0.041	-	0.009	0.007	0.019	0.025	-
Mg2+	0.010	0.113	-	-	0.012	-	-	-
Mn2+	0.018	-	-	-	-	-	-	-
Ft2+	0.666	0.233	0.507	0.443	0.518	0.566	0.560	-
Fe3+	-	0.052	-	0.028	0.037	0.029	0.067	-
Al3+	0.041	-	-	-	-	-	-	-
Ct3+	0.028	-	0.026	-	-	-	-	-
Nb5+	-	0.129	-	0.073	-	0.128	0.121	-
Ta5+	-	0.007	-	0.004	-	0.001	0.002	-
W6+	-	-	-	-	-	-	-	-
SUM Ti4+	2.185	2.064	1.907	1.886	1.972	2.166	2.120	2.000
TOTAL	4.154	4.003	4.105	3.973	4.113	4.018	4.031	4.000

peridotite (Apollo 12), in lithic fragments (Apollo 14, LUNA 20), and in a metamorphosed breccia (Apollo 16). Zirconolite is often associated with baddeleyite as small discrete crystals, no larger than 50 µm in diameter, and is considered to have crystallised at a late stage from interstitial liquids in the lunar basalts (e.g. Busche *et al.*, 1972).

Lunar zirconolites are generally rich in Y and heavy-REE when compared with terrestrial zirconolites (Lovering & Wark, 1974; Kochmasov, 1980; Fowler & Williams, 1986). The majority of the lunar zirconolites have $\Sigma\text{REE}^{3+} > 50\%$ of the Ca site, and with Y being the dominant REE, these may be considered as **zirconolite-(Y)**.

DISCUSSION AND CONCLUSION

Zirconolite occurs as an accessory mineral only, generally less than 0.1 mm in diameter, but from a wide variety of rock types. Its small size and low modal abundance means that it can be easily overlooked using traditional optical microscopy. However, with the increasing accessibility of analytical scanning electron microscopes (usually with a backscatter electron detector attached), zirconolite, even if present at a very low modal abundance, will be readily observed, because its backscatter component is considerably higher than the majority of the rock-forming minerals. It is probable therefore, that the number of zirconolite occurrences will increase significantly in the near future.

It is also evident that zirconolite is often zoned, and/or finely intergrown with other minerals, and early bulk chemical analyses were unable to characterise fully the chemical variability of this mineral. Microprobe analyses, together with a detailed SEM investigation, is therefore essential in any study. It is generally recommended that microprobe analysis is performed using wavelength-dispersive means, because zirconolite can accommodate more than 30 elements at the 0.1 to 1.0 wt.% concentration level (which in energy-dispersive electron microprobe analysis is close to, or below, the detection limit). However, quantitative analysis of sub-micron zones has been successfully undertaken using an energy-dispersive analytical transmission electron microscope (Lumpkin *et al.*, 1994).

As can be seen from the data for natural zirconolite, the range of elements substituting, and the degree of substitution are extensive. The most commonly occurring elements, and therefore the minimum that should be reported in any microprobe analysis of zirconolite are: Mg, Al, Si, Ca, Ti, Mn, Fe, Y, Zr, Nb, Hf, Ta, W, Pb, Th, U and of the REE, La, Ce, Pr, Nd, Sm, Gd.

It should also be noted that Cr and Zn are present in some zirconolites: Cr predominantly from lunar samples, and Zn occasionally from metasomatic samples (e.g. Zakrzewski *et al.*, 1992). H₂O has been reported in wet chemical analyses of separated grains (e.g. Borodin *et al.*, 1960; Bulakh *et al.*, 1960), and has also been inferred from low analytical totals of microprobe data (e.g. Platt *et al.*, 1987; Zakrzewski *et al.*, 1992). Na and K, although also quoted in some wet chemical analyses of separated grains, have not been observed in microprobe analyses. It is probable therefore, that Na and K are *not* present to any significant extent in zirconolite. It is of note also, that Sr and Ba generally do not occur in natural zirconolite, and Pb only rarely does so. These elements might have been expected to substitute more readily for Ca, but it appears that the Ca

structural site does not easily accommodate 2+ cations larger than Ca. The valency state of Fe in zirconolite is unclear: where measured directly on mineral separates, both FeO and Fe₂O₃ are present.

It is evident that zirconolite, although invariably occurring only as an accessory or 'trace' mineral in a range of rock types, is able to accommodate many incompatible elements, such as REE, ACT, Nb, Zr, Hf, Ta to concentration levels whereby it can become a major repository for these elements. As such, it has the potential for playing a significant role in the petrological/geochemical evolution of those rock-types in which it crystallizes. Several studies have provided evidence that zirconolite can reflect changes in the composition of the fluid during its evolutionary history, both in metasomatic systems (Williams & Gieré, 1988; Gieré & Williams, 1992), and in magmatic fractionation processes (Platt *et al.*, 1987).

It is hoped that this review and compilation will prove useful as a comparative database for geologists who discover zirconolite in their samples, and also to material scientists working on various SYNROC projects, in order that they can compare laboratory-based experiments on synthetic zirconolite with studies of the natural forms of zirconolite.

This database is available in a computerised format from CTW. We would be grateful also to receive any additional analytical data and/or material from new occurrences of zirconolite, in order to periodically update this database.

ACKNOWLEDGEMENTS. We are very grateful to Professor G. Bayer (ETH, Zürich) for providing us with zirconolite samples from Phalaborwa, and also for some unpublished data, to Alf Olav Larsen (Porsgrunn, Norway) for samples from Langesundsfjord, to Dr. S.L. Harvey Edinburgh, Scotland for providing information on zirconolite from East Antarctica, to Professor J. Keller (Freiburg, Germany) for permission to analyse zirconolite from Hegau, to Dr I. Hornig-Kjarsgaard (University of Mainz, Germany) for allowing us to include her unpublished data from Sokli, to Professor J.B. Dawson (Edinburgh, Scotland) for unpublished data, to Dr E.S. Grew (University of Maine, USA) for providing material from Sor Rondane, Antarctica, to Dr. A.N. Mariano (Carlisle, Massachusetts, USA) for providing samples and information on several zirconolite localities, and for some unpublished data, to Dr G.C. Parodi (University of Rome, Italy) for samples from Latium, Italy, and to the Kovdor Mining Museum, Kola Peninsula for material from Kovdor. We further wish to thank Drs M. Welch, A.R. Woolley and R.F. Symes and other colleagues at The Natural History Museum, London, also to Professor Andrei Bulakh (University of St. Petersburg) for comments and suggestions which improved the manuscript, and to Greg Lumpkin (ANSTO, Australia) for discussions regarding synthetic zirconolite. This study forms part of a British/Swiss Joint Research Programme, and we gratefully acknowledge funding provided by the Schweizerischer Nationalfonds and the British Council (Grant No. 83BC-033381).

REFERENCES

- Agrell, S.O., Charnley, N.R. & Rowley, P.D. 1986. The occurrence of hibonite, perovskite, zirconolite, pseudobrookites and other minerals in a metamorphosed hydrothermal system at Pine Canyon, Piute County, Utah, USA. Abstract. *Mineralogical Society Bulletin*, 72: 4.
- Bayliss, P. & Levinson, A.A. 1988. A system of nomenclature for rare-earth mineral species: revision and extension. *American Mineralogist*, 73: 422-423.
- Mazzi, F., Munno, R. & White, T.J. 1989. Mineral nomenclature: zirconolite. *Mineralogical Magazine*, 53: 565-569.
- Berzelius, J.J. 1824. Undersökning af några mineralier. *Kungliga Svenska*

- Vetenskapsakademiens Handlanger: 334–358.
- Blake, G.S. & Smith, G.F.H.** 1913. On varieties of zirkelite from Ceylon. *Mineralogical Magazine*, **16**: 309–316.
- Borodin, L.S., Nazarenko, I.I. & Richter, T.L.** 1956. The new mineral zirconolite complex oxide of the AB_2O_5 type. *Doklady Akademii Nauk SSSR* **10**: 845–848 (in Russian).
- , **Bykova, A.B., Kapitonova, T.A. & Pyatenko, Yu. A.** 1960. New data on zirconolite and its niobium variety. *Doklady of the Academy of Sciences, USSR, Earth Science Sections*, **134**: 1022–1024.
- Brögger, W.C.** 1890. Die Mineralien der Syenitpegmatitgänge der Südnorwegischen Augit- und Nephelinsyenite. 46. Polymigmat. *Zeitschrift für Krystalllographie und Mineralogie*, **16**: 387–395.
- Brown, G.M., Emeleus, C.H., Holland, J.G., Peckett, A. & Phillips, R.** 1972. Mineral-chemical variations in Apollo 14 and Apollo 15 basalts and granitic fractions. Proceedings of the Third Lunar Science Conference. *Geochimica et Cosmochimica Acta*, Supplement 3, **1**: 141–157.
- Bulakh, A.G., Ilinskii, G.A. & Kukharenko, A.A.** 1960. Zirkelite from Kola Peninsula deposits. *Zapiski Vsesoyuznogo Mineralogicheskogo Obshchestva*, **89** (3): 261–273 (in Russian).
- & **Ivanikov, V.V.** 1984. *The problems of mineralogy and petrology of carbonatites*. Leningrad University Printing House, Leningrad, 230pp. (in Russian).
- Busche, F.D., Prinz, M., Keil, K. & Kurat, G.** 1972. Lunar zirkelite: a uranium-bearing phase. *Earth and Planetary Science Letters*, **14**: 313–321.
- Dziedzic, A.** 1984 Elk Syenite Intrusion. *Büdety Instytutu Geologicznego*, **347**: 39–47.
- Fowler, M. & Williams, C.T.** 1986. Zirconolite from the Glen Dessary syenite: a comparison with other Scottish localities. *Mineralogical Magazine*, **50**: 326–328.
- Frondel, J.W.** 1975. *Lunar Mineralogy*. Wiley-Interscience, New York, USA, 323pp.
- Gaidukova, V.S., Polupanova, L.I. & Stolyarova, L.K.** 1962. Geological structure and mineralogical-geochemical characteristics of rare-metal carbonatites. *Geologiya Mestorozhdenii Redkikh Elementov*, **17**: 154pp. (in Russian).
- Gatehouse, B.M., Grey, I.E., Hill, R.J. & Rossell, H.J.** 1981. Zirconolite, $\text{CaZr}_x\text{Ti}_{2-x}\text{O}_7$: structure refinements for near end-member compositions with $x=0.85$ and 1.30. *Acta Crystallographica*, **B37**: 306–312.
- Gieré, R.** 1986. Zirconolite, allanite and hoegbomite in a marble skarn from the Bergell contact aureole: implications for mobility of Ti, Zr and REE. *Contributions to Mineralogy and Petrology*, **93**: 459–470.
- 1990a. Hydrothermal mobility of Ti, Zr and REE: examples from the Bergell and Adamello contact aureoles (Italy). *Terra Nova*, **2**: 60–67.
- 1990b. Quantification of element mobility at a tonalite-dolomite contact (Adamello Massif, Provincia di Trento, Italy). PhD thesis no. 9141, ETH Zürich, Switzerland.
- & **Williams, C.T.** 1992. REE-bearing minerals in a Ti-rich vein from the Adamello contact aureole (Italy). *Contributions to Mineralogy and Petrology*, **112**: 83–100.
- Grew, E.S., Asami, M. & Makimoto, H.** 1989. Preliminary petrological studies of the metamorphic rocks of the Eastern Sør Rondane Mountains. *Proceedings of the NIPR Symposium on Antarctic Geosciences*, **3**: 100–127.
- , **Essene, E.J., Peacor, D.R., Su, S.-C. & Asami, M.** 1991. Dissaksite-(Ce), a new member of the epidote group and the Mg analogue of allanite-(Ce), from Antarctica. *American Mineralogist*, **76**: 1990–1997.
- Harding, R.R., Merriman, R.J. & Nancarrow, P.H.A.** 1982. A note on the occurrence of chevkinite, allanite, and zirkelite on St. Kilda, Scotland. *Mineralogical Magazine*, **46**: 445–448.
- , — & — 1984. St. Kilda: an illustrated account of the geology. *British Geological Survey Report*, **16**, No. 7, 46pp.
- Harley, S.L.** 1994. Mg-Al Yttrian zirconolite in a partially melted sapphirine granulite, Vestvold Hills, East Antarctica. *Mineralogical Magazine*, **58**: 259–269.
- Heaman, L.M. & Le Cheminant, A.N.** 1993. Paragenesis and U-Pb systematics of baddeleyite (ZrO_2). *Chemical Geology*, **110**: 95–126.
- Hornig, I. & Wörner, G.** 1991. Zirconolite-bearing ultra-potassic veins in a mantle-xenolith from Mt. Melbourne Volcanic Field, Victoria Land, Antarctica. *Contributions to Mineralogy and Petrology*, **106**: 355–366.
- Hussak, E.** 1895. Mineralogische Notizen aus Brasilein. *Tschermaks Mineralogische und Petrographische Mittheilungen*, **14**: 394–414.
- & **Prior, G.T.** 1895. Lewisite and zirkelite, two new Brazilian minerals. *Mineralogical Magazine*, **11**: 80–88.
- Kapustin, Yu. L.** 1980. *Mineralogy of carbonatites*. Amerind Publishing Company Pvt. Ltd., New Delhi, 259pp. (translated from *Mineralogiya Karbonatitov*, Nauka Publishers, Moscow, 1971).
- Kato, A. & Matsubara, S.** 1991. Geikelite, baddeleyite and zirconolite in dolomitic marble from the Neichi mine, Miyako City, Iwate Prefecture, Japan. *Bulletin of the National Science Museum, Tokyo, Series C*, **17**: 11–20.
- Keller, J.** 1984. Der jungtertiäre Vulkanismus Südwestdeutschlands: Exkursionen im Kaiserstuhl und Hegau. *Fortschritte der Mineralogie*, **62** (2): 2–35.
- , **Brey, G., Lorenz, V. & Sachs, P.** 1990. IAVCEI 1990 Pre-Conference Excursion 2A: *Volcanism and petrology of the Upper Rhinegraben (Urach-Hegau-Kaiserstuhl)*. IAVCEI 1990 Guide, Mainz: 22.
- Kinny, P.D. & Dawson, J.B.** 1992. A mantle metasomatic injection event linked to late Cretaceous kimberlite magmatism. *Nature*, **360**: 726–728.
- Kochemasov, G.G.** 1980. Geochemical features of lunar and terrestrial zirkelite. *Mineralogicheskiy Zhurnal*, **2**: 30–39 (in Russian).
- Kogarko, L.N., Plant, D.A., Henderson, C.M.B. & Kjarsgaard, B.A.** 1991. Na-rich carbonate inclusions in perovskite and calcite from the Guli intrusive Ca-carbonatite, polar Siberia. *Contributions to Mineralogy and Petrology*, **109**: 124–129.
- Kukharenko, A.A., Orlova, M.P., Bulakh, A.G., Bagdasarov, E.A., Rimskaya-Kosakova, O.M., Nefedov, E.I., Ilinskii, G.A., Sergeev, A.S. & Abakumova, N.B.** 1965. *Caledonian complex of alkaline ultrabasic rocks and carbonatites of the Kola Peninsula and North Karelia*. Nedra publishers, Moscow, 772 pp. (in Russian).
- Lord, J.P. & Cottin, J.Y.** 1987. A new natural occurrence of zirconolite ($\text{CaZrTi}_2\text{O}_7$) and baddeleyite (ZrO_2) in basic cumulates: the Laouni layered intrusion (Southern Hoggar, Algeria). *Mineralogical Magazine*, **51**: 671–676.
- Lovering, J.F. & Wark, D.A.** 1971. Uranium-enriched phases in Apollo 11 and Apollo 12 basaltic rocks. Proceedings of the Second Lunar Science Conference. *Geochimica et Cosmochimica Acta*, Supplement 2, **1**: 151–157.
- & — 1974. Rare earth element fractionation in phases crystallizing from lunar late-stage magmatic liquids. Abstract. In: *Lunar Science V*: 463–465. The Lunar Science Institution, Houston, Texas, USA.
- Lumpkin, G.R., Ewing, R.C., Chakoumakos, B.C., Greengor, R.B., Lytle, F.W., Folty, E.M., Clinard, F.W.Jr., Boatner, L.A. & Abraham, M.M.** 1986. Alpha-recoil damage in zirconolite ($\text{CaZrTi}_2\text{O}_7$). *Journal of Materials Research*, **1**: 564–576.
- , **Smith, K.L., Blackford, M.G., Gieré, R. & Williams, C.T.** 1994. Determination of 25 elements in the complex oxide mineral zirconolite by analytical electron microscopy. *Micron*, **25**: 581–587.
- Lurie, J.** 1986. *Mineralization of the Pilanesberg Alkaline Complex*. In: Anhaeusser, C.R. & Maske, S. (eds), *Mineral Deposits of Southern Africa*, **2**: 2215–2228. Geological Society of South Africa, Johannesburg.
- Mariano, A.N. & Roeder, P.L.** 1989. Wöhlerite: chemical composition, cathodoluminescence and environment of crystallization. *Canadian Mineralogist*, **27**: 709–720.
- Mazzi, F. & Munno, R.** 1983. Calciobetafite (new mineral from the pyrochlore group) and related minerals from Campi Flegrei, Italy: crystal structure of polymygite and zirkelite: comparison with pyrochlore and zirconolite. *American Mineralogist*, **68**: 262–276.
- Meyer, O.A.M. & Boctor, N.Z.** 1974. Opaque mineralogy: Apollo 17, rock 75035. Proceedings of the Fifth Lunar Science Conference. *Geochimica et Cosmochimica Acta*, Supplement 5, **1**: 707–716.
- Nickel, E.H. & Mandarino, J.A.** 1987. Procedures involving the IMA Commission on New Minerals and Mineral Names, and guidelines on mineral nomenclature. *Mineralogical Magazine*, **52**: 275–292.
- Platt, G., Wall, F., Williams, C.T. & Woolley, A.R.** 1987. Zirconolite, chevkinit and other rare earth minerals from nepheline syenites and peralkaline granites and syenites of the Chilwa Alkaline Province, Malawi. *Mineralogical Magazine*, **51**: 253–263.
- Pudovkina, R.Z., Dubakina, L.S., Lebedeva, S.I. & Pyatenko, Yu. A.** 1974. Investigation of Brazil zirkelite. *Zapiski Vsesoyuznogo Mineralogicheskogo Obshchestva*, **103** (3): 368–372 (in Russian).
- Purtscheller, F. & Tessardi, R.** 1985. Zirconolite and baddeleyite from metacarbonates of the Oetztal-Stubaï complex (northern Tyrol, Austria). *Mineralogical Magazine*, **49**: 523–529.
- Raber, E. & Haggerty, S.E.** 1979. Zircon-oxide reactions in diamond-bearing kimberlites. In: Boyd, F.R. & Boctor, H.R. (eds), *Kimberlites, Diatremes and Diamonds: their Geology, Petrology and Geochemistry*. Proceedings of the Second International Kimberlite Conference, **1**: 229–240. American Geophysical Union.
- Rekharskiy, V.I. & Rekharskaya, V.M.** 1969. The new zirkelite-jordisite mineral paragenesis. *Doklady of the Academy of Sciences, USSR, Earth Science Sections*, **184**: 144–147.
- Ringwood, A.D.** 1985. Disposal of high-level nuclear wastes: a geological perspective. *Mineralogical Magazine*, **49**: 159–167.
- Roeder, E. & Weiblen, P.W.** 1973. Petrology of some lithic fragments from Luna 20. *Geochimica et Cosmochimica Acta*, **37**: 1031–1052.
- Rossell, H.J.** 1980. Zirconolite – a fluorite-related super structure. *Nature*, **282**: 282–283.
- Rubin, J.N., Henry, C.D. & Price, J.G.** 1993. The mobility of zirconium and other ‘immobile’ elements during hydrothermal alteration. *Chemical Geology*, **110**: 29–47.
- Semenov, I.N., Kochemasov, G.G. & Bykova, A.V.** 1963. Zirkelite and rosenbuschite from contact metasomatic rocks of the Lovozero Massif. *Trudy Instituta Mineralogii Geokhimi i Kristallokhimi Redkikh Elementov Moskva*, **15**: 106–109.

- Shannon, R.D.** 1976. Revised effective ionic radii and systematic studies of interatomic distances in halides and chalcogenides. *Acta Crystallographica*, **A32**: 751–767.
- Silva, L.C.** 1979. Considerações geológicas e estudos preliminares sobre inclusões primárias, fluidas e sólidas, em apatites de rochas carbonáticas e ijolíticas da ilha de Santiago (República de Cabo Verde). *Comunicações dos Servicos Geológicos Portugal, Lisbon*, **64**: 261–268.
- & **Figueiredo, M.O.** 1980. Note on the niobium-rich zirconolite in carbonatitic rocks of Santiago island (Cape Verde Republic). *Garcia de Orta, Série Geologia, Lisbon*, **4**: 1–6.
- Sinclair, W. & Eggleton, R.A.** 1982. Structure refinement of zirkelite from Kaiserstuhl, West Germany. *American Mineralogist*, **67**: 615–620.
- Smith, K.L. & Lumpkin, G.R.** 1993. Structural features of zirconolite, hollandite and perovskite, the major waste-bearing phases in Synroc. In: Bolan, J.N. & FitzGerald, J.D., *Defects and Processes in the Solid State: Geoscience Applications*. The McLaren Volume; Elsevier (in press).
- Vartiainen, H.** 1980. The petrography, mineralogy and petrochemistry of the Sokli carbonatite massif, northern Finland. *Bulletin of the Geological Survey of Finland*, **313**: 126pp.
- Verwoerd, W.J.** 1986. Mineral deposits associated with carbonatites and alkaline rocks. In: Anhaeusser, C.R. & Maske, S. (eds), *Mineral Deposits of Southern Africa*, **2**: 2173–2191. Geological Society of South Africa, Johannesburg.
- Wark, D.A., Reid, A.F., Lovering, J.F. & El Goresy, A.** 1973. Zirconolite (*versus* zirkelite) in lunar rocks. Abstract. In: *Lunar Science IV*, 764–766. The Lunar Science Institution, Houston, Texas, USA.
- White, T.J.** 1984. The microstructure and microchemistry of synthetic zirconolite, zirkelite and related phases. *American Mineralogist*, **69**: 1156–1172.
- Williams, C.T.** 1978. Uranium-enriched minerals in mesostasis areas of the Rhum layered pluton. *Contributions to Mineralogy and Petrology*, **66**: 29–39.
- (in press). The occurrence of niobian zirconolite, pyrochlore and baddeleyite in the Kovdor carbonatite complex, Kola Peninsula, Russia. *Mineralogical Magazine*, **60**.
- & **Gieré, R.** 1988. Metasomatic zonation of REE in zirconolite from a marble skarn at the Bergell contact aureole (Switzerland/Italy). *Schweizerische Mineralogische und Petrographische Mitteilungen*, **68**: 133–140.
- Woolley, A.R.** 1987. *Alkaline Rocks and Carbonatites of the World. Part I, North and South America*. British Museum (Natural History), 216pp.
- Zakrzewski, M.A., Lustenhouwer, W.J., Nugteren, H.J. & Williams, C.T.** 1992. Rare-earth minerals yttrian zirconolite and allanite-(Ce) and associated minerals from Koberg mine, Bergslagen, Sweden. *Mineralogical Magazine*, **56**: 27–35.
- Zhuravleva, L.N., Berezina, L.A. & Gulin, Ye. N.** 1976. Geochemistry of rare and radioactive elements in apatite-magnetite ores in alkali-ultrabasic complexes. *Geochemistry International*, **13**: 147–166.

A review of the stratigraphy of Eastern Paratethys (Oligocene–Holocene)

R.W. JONES

BP Exploration, Uxbridge One, 1 Harefield Rd., Uxbridge, Middlesex, UB8 1PD, U.K.

M.D. SIMMONS

Department of Geology and Petroleum Geology, University of Aberdeen, Meston Building, King's College, Aberdeen, AB9 2UE, U.K.

CONTENTS

Introduction	26
Absolute Chronostratigraphy	26
Micropalaeontological Biostratigraphy and Palaeoenvironmental Interpretation	26
Biostratigraphy	26
Palaeoenvironmental Interpretation	28
<i>Non-Marine Environments</i>	28
<i>Quasi-Marine and Marine Environments</i>	28
Climatostratigraphy	29
Magnetostratigraphy	29
Oxygen Isotope Stratigraphy	29
Sequence Stratigraphy and Palaeogeography	29
Introduction	29
Maykopian	33
Tarkhanian to Konkian	34
Tarkhanian	35
Chokrakian	35
Karaganian	35
Konkian	36
Sarmatian	36
Maeotian	38
Pontian	38
Kimmerian	39
Akhagylian to Khvalynian (Caspian Sea)	40
Akhagylian	40
Apsheronian	42
Bakunian	42
Khazarian, Girkhan and Khvalynian	42
Kuyalnikian to Neoeuxinian (Black Sea)	42
Kuyalnikian	42
Gurian	43
Chaudian	43
Uzunlarian, Karangatian and Neoeuxinian	43
Acknowledgements	43
References	43

SYNOPSIS. All available data pertaining to the regional stratigraphy of Eastern (Ponto-Caspian) Paratethys, much of it in sources not freely available in the west, is reviewed. Particular emphasis is placed on the South Caspian. Where possible, regional datums are calibrated against global standards. An attempt is made to place the regional stratigraphy in a (global) sequence stratigraphic framework for the first time. Palaeogeographic reconstructions are given for selected time-slices.

INTRODUCTION

The Tethyan Ocean began to close in the Eocene as a result of plate collisions along the southern margin of the Eurasian Supercontinent that ultimately gave rise to the formation of the mountain chain extending from the Alps in the west to the Himalayas in the east. The initial response to these plate collisions was the formation of a suite of east–west trending sedimentary basins extending from Austro-Hungary in the west to Central Asia in the east, collectively constituting the intracontinental Paratethyan Sea (Fig. 1). Subsequent tectonic uplift (enhanced by eustatic shallowing) through the Mio-Pliocene led to widespread marginal- to non-marine sedimentation. Ultimate severance of connections to the world's oceans led to the evolution of largely endemic faunas and floras (in particular in Eastern Paratethys, which was more isolated than Central Paratethys). This renders stratigraphic correlation between established Mediterranean and Paratethyan stages extremely difficult. The problem is locally compounded by confusion between chronostratigraphic and lithostratigraphic nomenclature.

In this paper we review all available data, much of it in sources not freely available in the west, on the regional stratigraphy of Eastern Paratethys (Fig. 1). We place particular emphasis on the South Caspian, an area in which the western oil industry is showing a growing interest, and one with which we, through our industrial work and our academic contacts in the Former Soviet Union, are particularly familiar.

We give an indication of the palaeontology of each regional stage. For the sake of brevity and because of their stratigraphic utility, we concentrate on various groups of microfossils, though we acknowledge that macrofossils, especially molluscs, also have stratigraphic value (see, for instance, Ali-Zade (1954), Azizbekov (1972), Ali-Zade *et al.* (1986), (Azerbaijan); Lupov *et al.* (1972) (Turkmenia); Andreev (1981) (Dacic Basin); and Ozsayar (1985) and Taner (1985) (Turkey)). A forthcoming paper (Simmons *et al.* in press) will document in detail the micropalaeontological (including nannopalaeontological and palynological) and macropalaeontological zonation of the

Neogene to Pleistocene sediments of Azerbaijan.

We attempt to place the regional stratigraphy in a global framework by calibrating biostratigraphic and magnetostratigraphic datums against Central Paratethyan and Mediterranean standards, and by suggesting possible calibrations between regional sequence boundaries and flooding surfaces, and the global sequence stratigraphic framework and eustatic sea-level curve of Haq *et al.* (1988).

ABSOLUTE CHRONOSTRATIGRAPHY

Notwithstanding the efforts of such authors as Steininger & Papp (1979), Chumakov *et al.* (1984, 1988, 1992a–b) and Vass (1985), there is no established comprehensive absolute chronostratigraphic time-scale for Eastern Paratethys. Thus, in Eastern Paratethys, absolute chronostratigraphic dating is often only possible by calibration of regional stratigraphic datums against global standards. We have attempted to calibrate regional datums against the Haq *et al.* (1988) timescale, which is the most up-to-date timescale that conveniently integrates bio-, magneto- and sequence-stratigraphic data. The confidence with which this sort of calibration can be made varies considerably with stratigraphic interval (see below).

MICROPALEONTOLOGICAL BIOSTRATIGRAPHY AND PALAEOENVIRONMENTAL INTERPRETATION

Biostratigraphy

Those groups of planktonic organisms traditionally used in the biostratigraphic zonation of the Cenozoic (planktonic foraminifera and calcareous nannoplankton) are restricted in their development in Paratethys because of the isolated

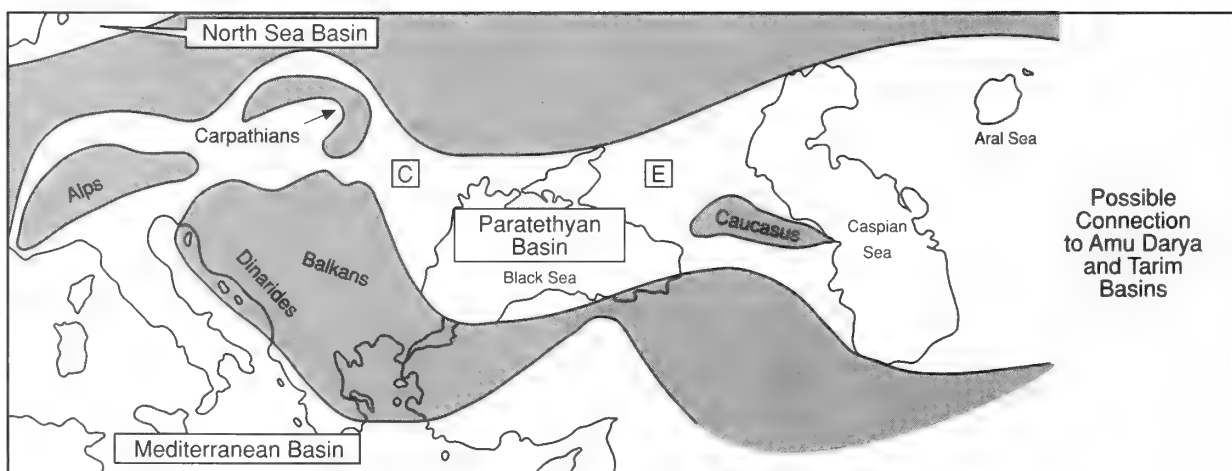


Fig. 1 Geological sketch map of the Paratethyan Basin in the Oligocene. Modified after Steininger & Papp (1979). C = Central Paratethys; E = Eastern Paratethys. Eastern Paratethys can be considered as including the Pontian (Black Sea) Basin and the Caspian Basin. Throughout most of the Miocene, the eastern limit of the Paratethyan Basin was probably the Caspian Basin, but in the Late Pliocene at least it was probably further east once more.

geological evolution of the region. Only locally or periodically (as in the Maykopian, Maeotian and Kuyalnikian/Akchagylian (see section below on sequence stratigraphy)) are they sufficiently well developed to enable ties to global biostratigraphic zonation schemes (Blow (1969) for planktonic foraminifera; Martini (1971) for calcareous nannoplankton).

Biostratigraphic zonation in Eastern Paratethys relies largely on facies-dependent benthonic foraminifera and, especially in the marginal- to non-marine environments of the Mio-Pliocene, benthonic ostracods and terrestrially-derived pollen and spores (see section below on sequence stratigraphy). Important ostracod references include those of Livental (1929), Sveier (1949), Agalarova (1956, 1967), Suzin (1956), Agalarova *et al.* (1961), Mandelstam *et al.* (1962), Faridi (1964), Imnadze (1964,

1974), Sheydayeva-Kuliyeva (1966), Rozyeva (1971), Gramann (1971), Karmishina (1975), Vekua (1975), Krstic (1976), Olteanu (1978), Imnadze & Karmishina (1980), de Deckker (1981), Jiricek (1984), Mamedova (1984, 1985, 1988), Dzhanelidze *et al.* (1985), Aliyulla *et al.* (1985) and Yassini (1986). Important pollen and spore and associated palynomorph references include those of Ramishvili (1969), Dzhabarova (1973, 1978, 1980), Grichuk (1973, 1984), Wall & Dale (1973), Ananova (1974), Shikmus *et al.* (1977), Koreneva & Kartashova (1978), Traverse (1978), Shchekina (1979), Abramova (1982, 1985), Yakhimovich *et al.* (1983), Grichuk *et al.* (1984), Khotinskiy (1984), Mamedov & Rabotina (1984a–b), Shatilova (1984), Ananova *et al.* (1985), Ivanova (1985), Sirenko & Turlo (1986), Bludorova *et al.* (1987), Naidina (1988, 1990a–b,

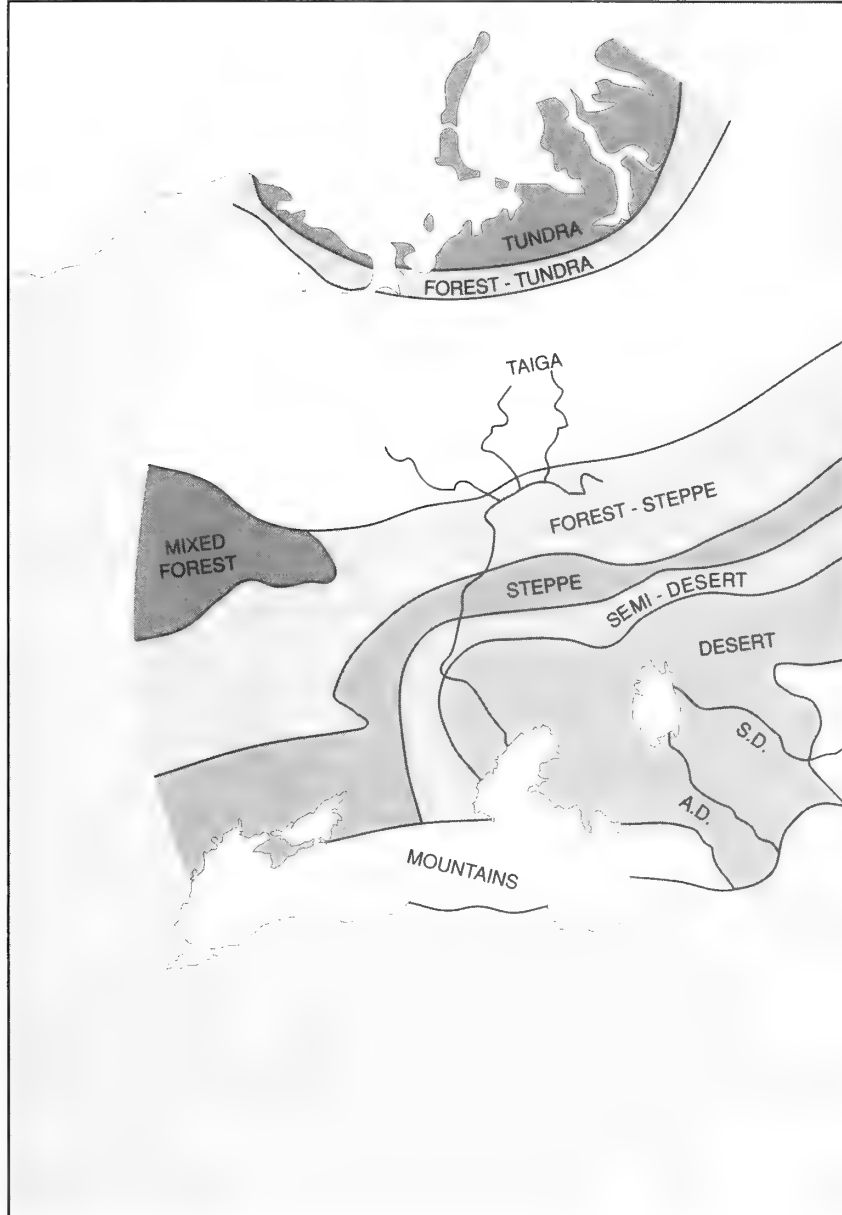


Fig. 2 Vegetation belts in the former Soviet Union. After Knystautas (1987). A.D. = Amu Darya; S.D. = Syr Darya.

1991a-c) and Malaeva & Kulikov (1991).

Other locally stratigraphically useful fossil groups include otoliths (Brzobohaty, 1983), Problematica (*Bolboforma* (Szczecura, 1985; Spiegler & Rögl, 1992)), siliceous microfossils (diatoms (Shishova, 1955; Ushakova & Ushko, 1971; Gasanova, 1965; Rasulov, 1986), radiolarians (Slama, 1983), silicoflagellates (Dumitrica, 1985) and sponge spicules (Riha, 1983)), and, in non-marine environments, vertebrate remains (*Camelopardis*, *Felis*, *Gazella*, *Hippocampe*, *Hyaena*, *Mastodon*, *Mesopithecus*, *Rhinoceros*, etc.) (Kretzoi, 1985; Steininger, Rabeder & Rögl, 1985; Bernor *et al.*, 1987, 1993; Lindsay *et al.*, 1989; Rögl *et al.*, 1993) and charophytes (Rögl *et al.*, 1993).

Ali-Zade *et al.* (1994a, 1994b, 1995, in press), Reynolds *et al.* (in press) and Simmons *et al.* (in press) give further details of the Neogene biostratigraphy of Eastern Azerbaijan.

Palaeoenvironmental Interpretation

Non-Marine Environments. Non-marine environments are characterised by fresh-water ostracods such as *Aglaocypris*, *Candonia*, *Candonella*, *Cyclocypris*, *Cypria*, *Eucypris*, *Ilyocypris*, *Pseudostenocypris* and *Zonocypris*, and terrestrially-derived pollen and spores. Pennate diatoms, fresh-water gastropods and terrestrial vertebrate remains may also be found.

Palaeoclimate can be inferred from the distribution of vegetation types as inferred from pollen and spores. At the present-day, the distribution of vegetation types is determined chiefly by climatic factors (temperature (latitude, altitude), aridity). Thus, for instance, birches characterise the cold 'forest-tundra' of the extreme north, diverse coniferous and deciduous types the 'taiga' of the central area, and grasses and shrubs the arid treeless 'steppe' and semi-desert to the extreme south (Figs 2-3).

Quasi-Marine and Marine Environments. Deposition in oligo- to meso-haline (hereafter 'quasi-marine' (brackish, reduced salinity)) environments prevailed in the Paratethyan Basin (especially in the Caspian) throughout much of its geological evolution because of its restricted connection to the open ocean (see above). However, water depths and sedimentary regimes may have been similar to those of the normal marine realm, and, moreover, deposition under normal or near-normal marine conditions did take place at times (e.g., Maykopian and Akchagylian). Palaeosalinity can be inferred from diatoms (e.g., Ushakova & Ushko, 1971; Schrader, 1979) or from foraminifera and ostracods ranging through to the Recent (see below). Palaeosalinity and/or palaeotemperature curves are presented by Semenenko (1979), Chepalyga (1985) and Demarcq (1985).

Quasi-marine environments in the Black Sea and Caspian Sea are characterised by the benthonic foraminiferal genus *Florilus*, and some species of the genera *Ammobaculites*, *Ammoscalaria*, *Ammonia* and *Elphidium* (salinity tolerance range 1-5 parts per thousand (ppt)), and *Miliammina*, *Haynesina* and *Rosalina* and some species of *Nonion* s.l. and *Quinqueloculina* (1-26ppt) (Macarovici & Cehan-Ionesi, 1962; Tufescu, 1968, 1973; Murray, 1973, 1991; Gheorghian, 1974; Yassini & Ghahreman, 1977; Yanko, 1990b), the ostracod genera *Cyprideis* (2-14ppt), *Maetocythere* (4-14ppt), *Loxoconcha* (5-14ppt), *Bakunella*, *Casiolla* and *Cytherissa* (11-13/14ppt) and *Graviacypris* (12-13ppt) (Gofman, 1966; Yassini, 1986; Boomer, 1993a), and the calcareous nannofossil genus *Emiliania* (11ppt) (Bukry, 1974).

Normal or near-normal marine environments are

characterised by the benthonic foraminiferal genera *Discorbis*, *Textularia*, *Bolivina*, *Bulimina*, *Brizalina*, *Cibicides*, *Gavelinopsis* and *Trifarina* and some species of the genera *Ammonia*, *Nonion* s.l. and *Quinqueloculina* (salinity tolerance range 11-26ppt) (Macarovici & Cehan-Ionesi, 1962; Tufescu, 1968, 1973; Murray, 1973, 1991; Yassini & Ghahreman, 1977; Yanko, 1990b).

CLIMATOSTRATIGRAPHY

Zubakov & Borzenkova (1990) defined a series of climatostratigraphic units called 'climathems' (some conceptual, some stratotypified (and with representative pollen spectra documented)) which they used in the regional correlation of Eastern Paratethys (see also Zubakov, 1993). Of these, 'superclimathems' (SCTs), with an average duration of 200,000 years, are the most useful. SCTs are correlated with half the 370,000-425,000-year cycle of orbital eccentricity, and reflect changes in climate (alternating between 'cryo-' and 'thermo-' meric (cool and warm respectively)).

Zubakov & Borzenkova interpreted pollen spectra dominated by steppe and semi-desert vegetation as being of 'warm' aspect (whereas, in fact, they are more characteristic of aridity than high temperature) and those dominated by forest vegetation as being of 'cool' aspect (whereas they are in fact more characteristic of humidity than of low temperature). In the Caspian, they found the former to characterise regressions and the latter to characterise transgressions, and therefore correlated regressions with 'warm' phases (interglacials) and transgressions with 'cool' phases (glacials) (Fig. 4A). Regression during interglacials is possible if sediment supply and subsidence are in equilibrium but evaporation exceeds precipitation and run-off. Transgression during glacials is possible if sediment supply (reduced by rivers freezing) fails to fill the accommodation space created by subsidence. Note in this context that the level of the Caspian has fallen by some 5m since records were first taken in the 1760's. However, it also appears to have been rising over the last fifty years (currently at a rate of 20cms/year in the South Caspian). Historical records are probably unreliable in a geological context because of the influence of man on the environment. This is particularly true in the case of the Aral Sea, whose level has fallen and whose salinity has risen drastically since the 1960's owing to abstraction of the headwaters of the feeder rivers (the Amu Darya and Syr Darya) to irrigate the cotton fields of Uzbekistan (see, for instance, Boomer, 1993a-b). Incidentally, as a result of this catastrophic ecological change, eleven species of fresh-water ostracod known to have been living in the Aral Sea thirty years ago no longer live there. Only the quasi-marine species *Cyprideis torosa* lives there today.

The evidence for regressions during interglacials and transgressions during glacials appears somewhat equivocal. An equally strong case, and one more in keeping with *a priori* expectation from experience in other parts of the world, can be made for correlating regressions with glacials and transgressions with interglacials (Fig. 4B). One key observation in support of this case is the apparent correlation of the major transgressions not only with warm phases (see, for instance, Skalbdyna, 1985), but also with global transgressions (see, for instance, Haq *et al.*, 1988). Pollen spectra of 'arid' aspect in glacial sediments and of 'humid' aspect in interglacial sediments are explicable in terms of, respectively, contractions and expansions of the forest belt

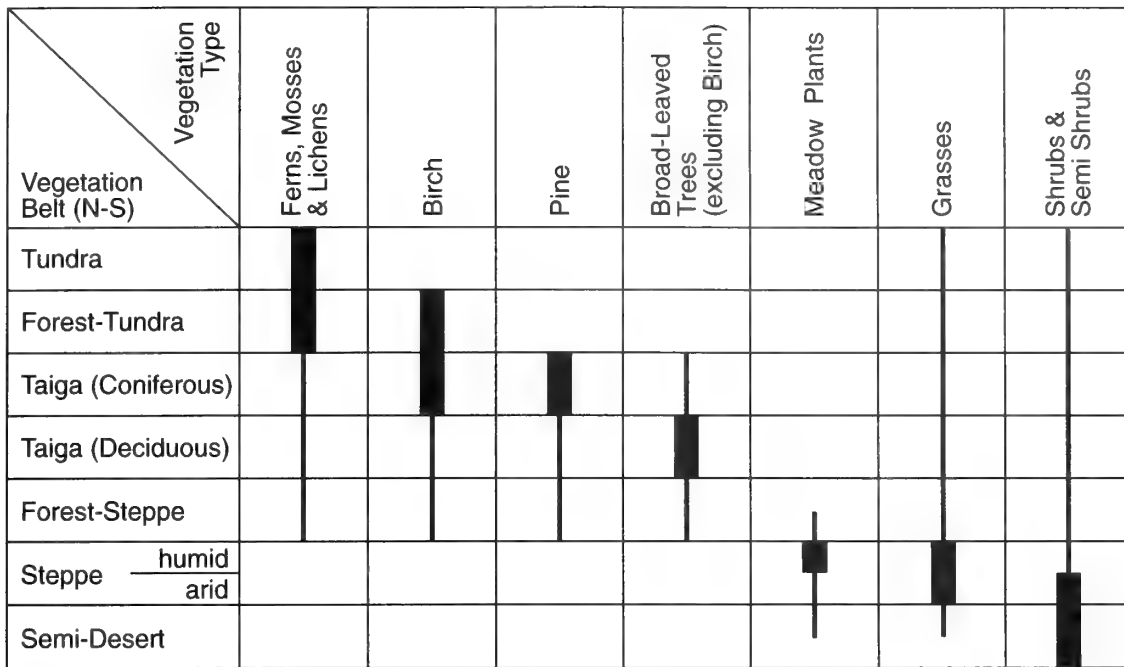


Fig. 3 Distribution of principal vegetation types in relation to vegetation belts. Compiled from various sources. Bar width provides a measure of abundance.

(the former in response to permafrost development). This is also indicated by palaeoclimatic reconstructions for the Late Valdai Glacial and Mikulino Interglacial (Grichuk, 1984; Savina & Khotinskiy, 1984; Velichko, 1984b). An alternative explanation envisages a time lag between the onset of glaciation and the response of vegetation (belts being displaced by up to 2000 km.). Similar disequilibrium phenomena have been described from interstadial complexes in the United Kingdom.

OXYGEN ISOTOPE STRATIGRAPHY

Theoretically, the ages of the Plio-Pleistocene sediments of Eastern Paratethys are resolvable using oxygen isotope stratigraphic techniques. However, in practice, what data there is exists in widely disseminated form and is not particularly useful.

MAGNETOSTRATIGRAPHY

Much magnetostratigraphic data is available from Eastern Paratethys (e.g., Zubakov & Kochegura (1971), Trubikhin (1977), Semenenko (1979), Semenenko & Pevzner (1979), Grishanov *et al.* (1983), Rögl & Steininger (1984), Steininger & Rögl (1984), Chepalyga (1985), Chepalyga *et al.* (1985), Iossofova (1985), Pevzner & Vangengeim (1985a, 1993), Senes (1985), Skalbdyna (1985), Vass (1985), Zubakov & Borzenkova (1990) and Trubikhin *et al.* (1991a–b)). Theoretically, this sort of data ought to enable a correlation between Eastern Paratethys and the rest of the world (which, as noted above, is difficult to do using the available biostratigraphic data). However, in practice the process is complicated by apparently inconsistent definition and usage of magnetostratigraphic units (polarity epochs). It is beyond the scope of this paper to address this problem in any more detail (instead, we simply quote the published magnetostratigraphic (polarity epoch) ranges for the various regional stages). It is nonetheless evident that the potential exists for a refined magnetostratigraphic subdivision of critical intervals using short-lived polarity reversal 'episodes' within the longer-term epochs.

SEQUENCE STRATIGRAPHY AND PALAEOGEOGRAPHY

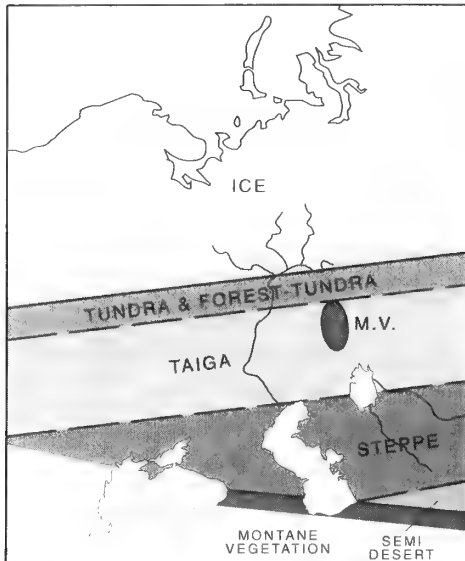
Introduction

No published sequence stratigraphic schemes exist for the Oligocene-Holocene of Paratethys, although relative sea-level changes and associated aspects of sequence stratigraphy are discussed by Rögl & Steininger (1983), Chepalyga (1985, 1991), Demarcq (1985), Krhovsky (1985), Nevesskaya *et al.* (1985), Pogacsas (1985), Pogacsas & Revesz (1985), Skalbdyna (1985), Andalibi (1991), Zubakov & Borzenkova (1990) and Klopovotskaya (1991).

This section attempts to place the regional stratigraphy of Eastern Paratethys in a (global) sequence stratigraphic framework. It is written in the form of a geological history. Stratigraphic (bio-, climato-, magneto- and sequence-stratigraphic) data are summarised on Figs 5–6. Palaeogeographic reconstructions for selected time-slices are given on Figs 7–12. These are based in part on previously published maps (Podobina *et al.*, 1956; Muratov, 1960; Sheydayeva-Kuliyeva, 1966; Ushakova & Ushko, 1971; Senes, 1973; Azizbekova, 1974; Senes & Marinescu, 1974; Luttig &

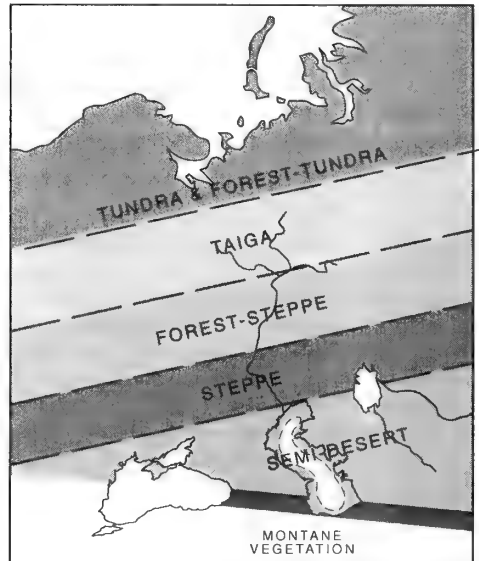
A GLACIAL - TRANSGRESSION

- Rivers frozen. Extensive Permafrost.
- Sediment Supply < Subsidence.
- Expansion of 'Cool' Zone.



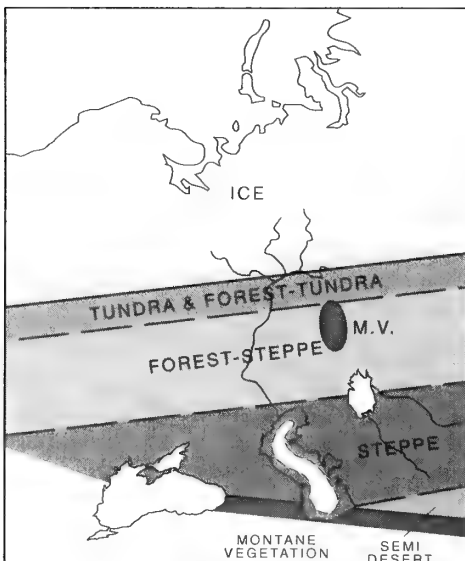
INTERGLACIAL - REGRESSION

- River Systems Reactivated.
- Evaporation > Precipitation / Runoff.
- Expansion of 'Warm' Zone.



B GLACIAL - REGRESSION

- Water locked up in Ice Sheet.
- Pollen Spectra of Arid Aspect.
- Contraction of Forest Zone



INTERGLACIAL - TRANSGRESSION

- Water released from melting Ice Sheet
- Expansion of Forest Zone

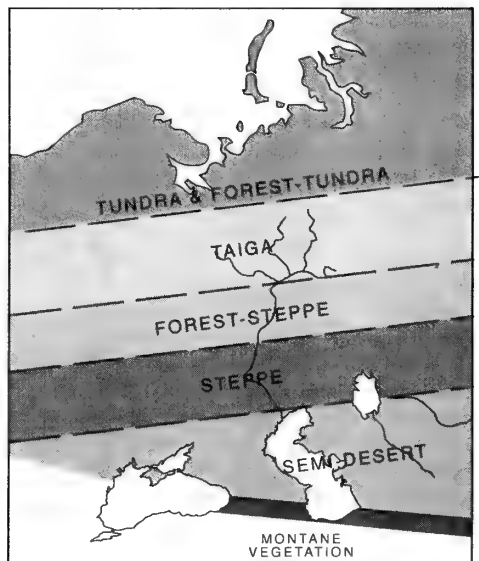


Fig. 4 Response to glaciation – alternative models for the Caspian. A: glacial transgression/interglacial regression. B: glacial regression/interglacial transgression. B better follows the palaeoclimatic reconstruction data given by Grichuk (1984) (see text).

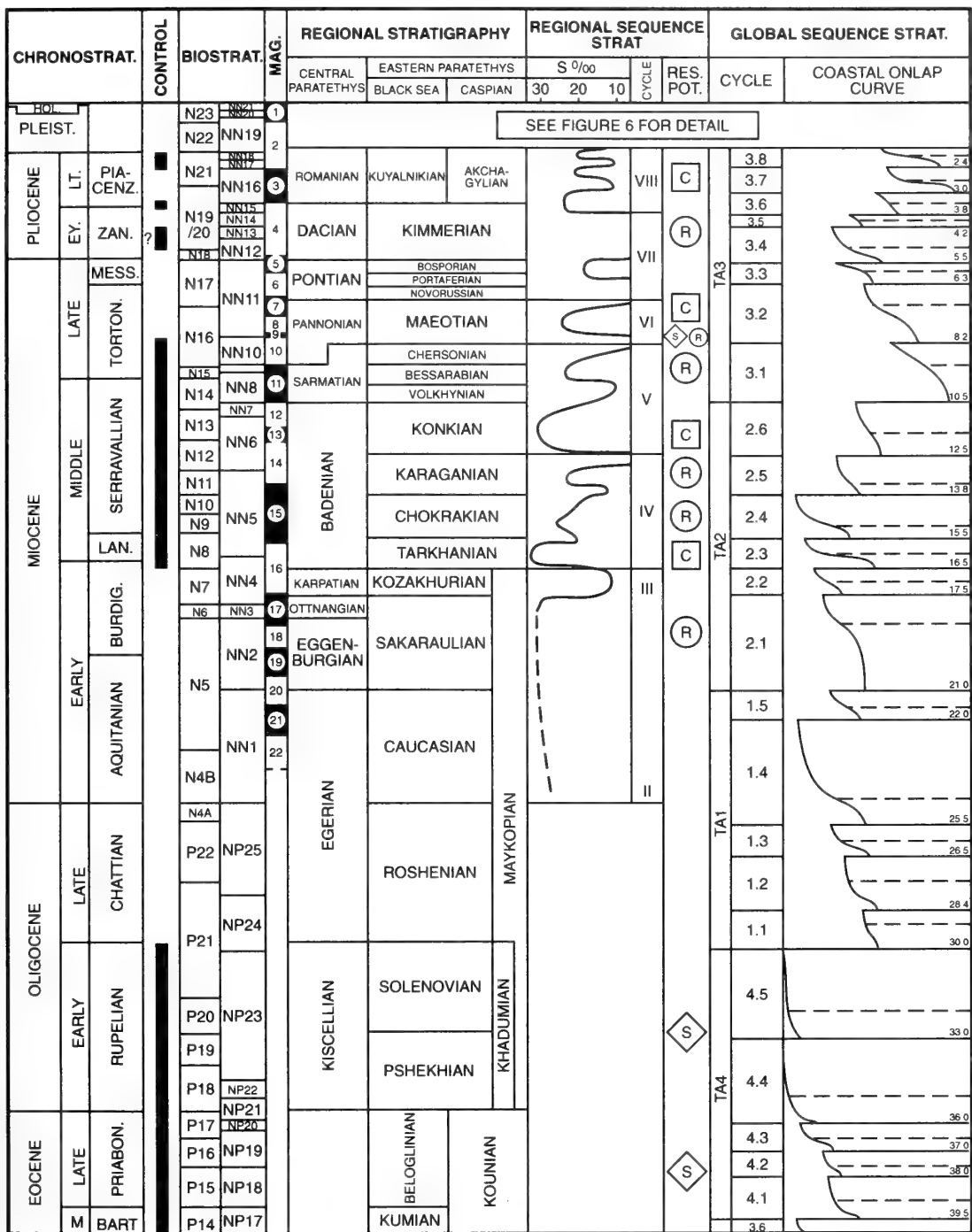


Fig. 5 Stratigraphic summary (Eocene-Holocene). Chronostratigraphy, magnetostratigraphy, global sequence stratigraphy and calibration after Haq *et al.* (1988) (see also chronostratigraphic schemes of Chumakov *et al.*, 1984, 1988, 1992a–b and others). Sequence boundary ages in Ma. Biostratigraphy after Blow (1969) (planktonic foraminifera) (prefixed P and N) and Martini (1971) (calcareous nanoplankton) (prefixed NP and NN). Regional stratigraphy from this paper. Regional sequence stratigraphy modified after Chepalyga (1985). Cycles are regressive (mega) sequences. II–III are equivalent to the ‘Eoparatethyan’, IV to the ‘Mesoparatethyan’ and V–VI to the ‘Neoparatethyan’ of Nevesskaya *et al.* (1985). Curve shows extent of open marine connection (function of sea-level) as inferred from salinity data from palaeontological analyses ($S\text{‰}$ = salinity parts per thousand). Res. pot. = Resource potential (S = source, R = reservoir, C = caprock). The correlation of Eastern Paratethyan sequence stratigraphy with the global coastal onlap curve of Haq *et al.* (1988) is tentative. Where biostratigraphic control constrains the correlation this is indicated.

Steffens, 1976; Steininger, Rögl & Martini, 1976; Hsu, in Ross *et al.*, 1978; Rögl *et al.*, 1978; Steininger & Papp, 1979; Hsu, 1983; Baldi, 1984; Rögl & Steininger, 1983, 1984; Steininger & Rögl, 1984; Voronina & Popov, 1984; Iossofova, 1985; Popescu, 1985; Rusu, 1985; Steininger, Rabeder & Rögl, 1985; Steininger, Rögl & Neveskaya, in Steininger, Senes, Kleeman & Rögl, 1985; Voicu, 1985; Bernor *et al.*, 1987; Neveskaya *et al.*, 1987; Panakhi & Buare Mamadu Lamin, 1987; Veto, 1987; Mamedov, 1989; Olteanu, 1989; Adamia *et al.*, 1990; Dercourt *et al.*, 1990; Tchoumatchenko *et al.*, 1990; Kerimov *et al.*, 1991; Spiegler & Rögl, 1992; Pevzner & Vangengeim, 1993), and in part on previously unpublished maps.

It should be noted that the calibration against the global sequence stratigraphic framework and eustatic sea-level curve of Haq *et al.* (1988) is tentative. Fig. 5 demonstrates where biostratigraphic control exists in order to constrain the calibration. In the absence of such constraint, calibration is made by matching patterns of transgression and regression within a looser stratigraphic framework. The correlation between Eastern Paratethyan and global sequence stratigraphy and eustatic sea-level appears good, with all of the global eustatic sea-level trends finding their expression in Eastern Paratethys. It could be argued that this apparent correlation is entirely fortuitous. However, the stratigraphic signature of the mid-late Cenozoic appears remarkably consistent throughout the world, presumably because at this time it was an 'ice-house' world characterised by over-riding glacio-eustacy (Vail *et al.*, 1991). Indeed, it may be that not only third-order but also higher frequency sea-level oscillations are recognisable in areas characterised by a high sedimentation rate such as Eastern Paratethys (and the Gulf of Mexico (see, for instance, Beard *et al.*, 1982; Lamb *et al.*, 1987; Pacht *et al.*, 1990; Wornardt & Vail, 1990; see also Fig. 6)).

General features of Eastern Paratethyan stratigraphy have been discussed by, among others, Bogdanowicz (1947), Muratov (1960), Subbotina *et al.* (1960), Dzhanelidze (1970), Mamedova (1971, 1987), Stöcklin & Setudehnia (1971, 1972), Azizbekov (1972) (and authors cited therein), Lupov *et al.* (1972), Cicha *et al.* (1975), Jiricek (1975), Ross *et al.* (1978), Nikiforova & Dodonov (1980), Verisharin *et al.* (1982) (and authors cited therein), Alekseyev & Nikiforova (1984), Iossofova (1985), Popov & Voronina (1985), Semenenko & Lulieva (1985), Skaldyna (1985), Volkova *et al.* (1985), Yakhemovich *et al.* (1985), Muratov & Neveskaya (1986), Kereudren & Thibault (1987), Nigarov & Fedorov (1987), Benyamovskoy *et al.* (1988), Steininger *et al.* (1989), Yanko (1990a–b, 1991), Zubakov & Borzenkova (1990), Ghanbari (1991), Ali-Zade *et al.* (1994a, 1994b, 1995, in press), Jones (1996), Reynolds *et al.* (in press) and Simmons *et al.* (in press). Correlations within Eastern Paratethys and between Eastern and Central Paratethys have been discussed by Papp (1969), Chelidze (1973), Rögl, Steininger & Muller (1978), Paramonova *et al.* (1979), Semenenko (1979, 1984), Semenenko & Pevzner (1979), Steininger & Papp (1979), Steininger & Rögl (1979, 1984), Baldi (1980), Semenenko & Lulieva (1982), Rögl & Steininger (1983, 1984), Neveskaya *et al.* (1984, 1985, 1987), Velichko (1984a), Yakhimovich, Bludorova, Zhidovinov *et al.* (1984), Chepalyga *et al.* (1985), Neveskaya & Nosovsky (1985), Nosovsky (1985), Pevzner & Vangengeim (1985), Rögl (1985a), Senes (1985a–b), Senes & Steininger, in Steininger *et al.* (1985), Yakhimovich, Bludorova, Chiguryaeva *et al.* (1985), Zosimovich *et al.* (1985), Yassini (1986), Mekhtiev & Pashaly (1987), Muzylov & Golovina (1987), Steininger *et al.*, in Royden & Horvath (1987), Olteanu (1989), Rögl *et al.* (1991), Fedorov (1994), Markova & Mikhalevskii (1994) and Jones

(1996). A comprehensive bibliography of general stratigraphic references (to 1984) is given by Rögl (1985b).

Petroleum geological aspects have been discussed by, among others, Khain *et al.* (1937), Ismailov & Idrisov (1963), Ali-Zade *et al.* (1966), Shilinski (1967), Ismailov *et al.* (1972), Buryakovskiy (1974, 1993), Alikhanov (1977), Nikishin (1981), Ulmishev & Harrison (1981), Babayan (1984), Panakhi & Buare Mamadu Lamin (1987), Bagir-Zade *et al.* (1988), Akramkhodzhaev *et al.* (1989), Kerimov *et al.* (1991), Kleschev *et al.* (1992), Narimanov (1993) and Reynolds *et al.* (in press). Additional comments on petroleum geology are inserted as appropriate in the succeeding sections.

Maykopian (Figs 7–8)

The Maykopian takes its name from a town in the Caucasus (Likharev, 1958). The term Maykopian refers to essentially argillaceous rocks of Oligocene to Early Miocene age. The Zeivar Formation of Northern Iran and Lower Red Formation (predominantly clastics) of Central Iran (the latter locally contains age-diagnostic lepidocyclinid and nummulitid larger benthonic foraminifera) appear correlative, as does the Qom [Qum] Formation (predominantly carbonates) of Central Iran (which contains numerous age-diagnostic species of alveolinid, lepidocyclinid and miogypsinid larger benthonic foraminifera (Rahaghi, 1973)) (Stöcklin & Setudehnia, 1971, 1972). The Maykopian (in particular the Khadumian) is an important regional source rock (e.g., Veto, 1987). It also constitutes a minor reservoir in the Kobustan-Kura region of the South Caspian (Ali-Zade *et al.*, 1966).

Details of Maykopian stratigraphy have been discussed by Muratov (1960), Ali-Zade (1966), Ali-Zade & Mamedov (1970), Mamedova & Mamedova (1970), Azizbekov (1972), Lupov *et al.* (1972), Khalilov & Mamedova (1973), Bolli & Krasheninnikov (1977), Ali-Zade & Atayeva (1982), Krasheninnikov & Muzylov (1975), Krasheninnikov, Muzylov & Ptukhian (1985), Neveskaya & Nosovsky (1985), Bugrova (1986), Koshkarly (1986, 1993), Krasheninnikov (1986), Krasheninnikov & Ptukhian (1986), Koshkarly & Baldi-Beke (1987), Gasanov & Kyazamov (1988), Nagymarosy (1992) and Koshkarly & Alekperov (1993).

Microbiostratigraphic study of the Maykopian is hindered by massive reworking, reflecting deposition in a foreland basin in front of the emerging Caucasus. Maykopian samples can contain >90% reworked (especially Eocene) microfossils.

The Maykopian has been divided into five sub-stages by various authors (see Fig. 5). In ascending stratigraphic order, these are the Khadumian, Roshenian, Caucasian, Sakaraulian and Kozakhurian. The Khadumian is dated as Early Oligocene on the evidence of planktonic foraminifera and calcareous nannofossils and can therefore be calibrated against global standard biostratigraphic zonation schemes and absolute chronostratigraphic time-scales (see below). In contrast, the Roshenian is dated as Late Oligocene and the Caucasian to Kozakhurian as Early Miocene essentially only on the evidence of benthonic foraminifera (see, for instance, Neveskaya & Nosovsky, 1985).

The youngest sub-stages of the Maykopian appear to be absent in the Dacian Basin in the Western Black Sea region (Steininger *et al.*, in Royden & Horvath, 1987).

Micropalaeontology and Nannopalaeontology. The Khadumian has been dated as Early Oligocene on both planktonic foraminiferal and calcareous nannoplankton evidence. Ali-Zade

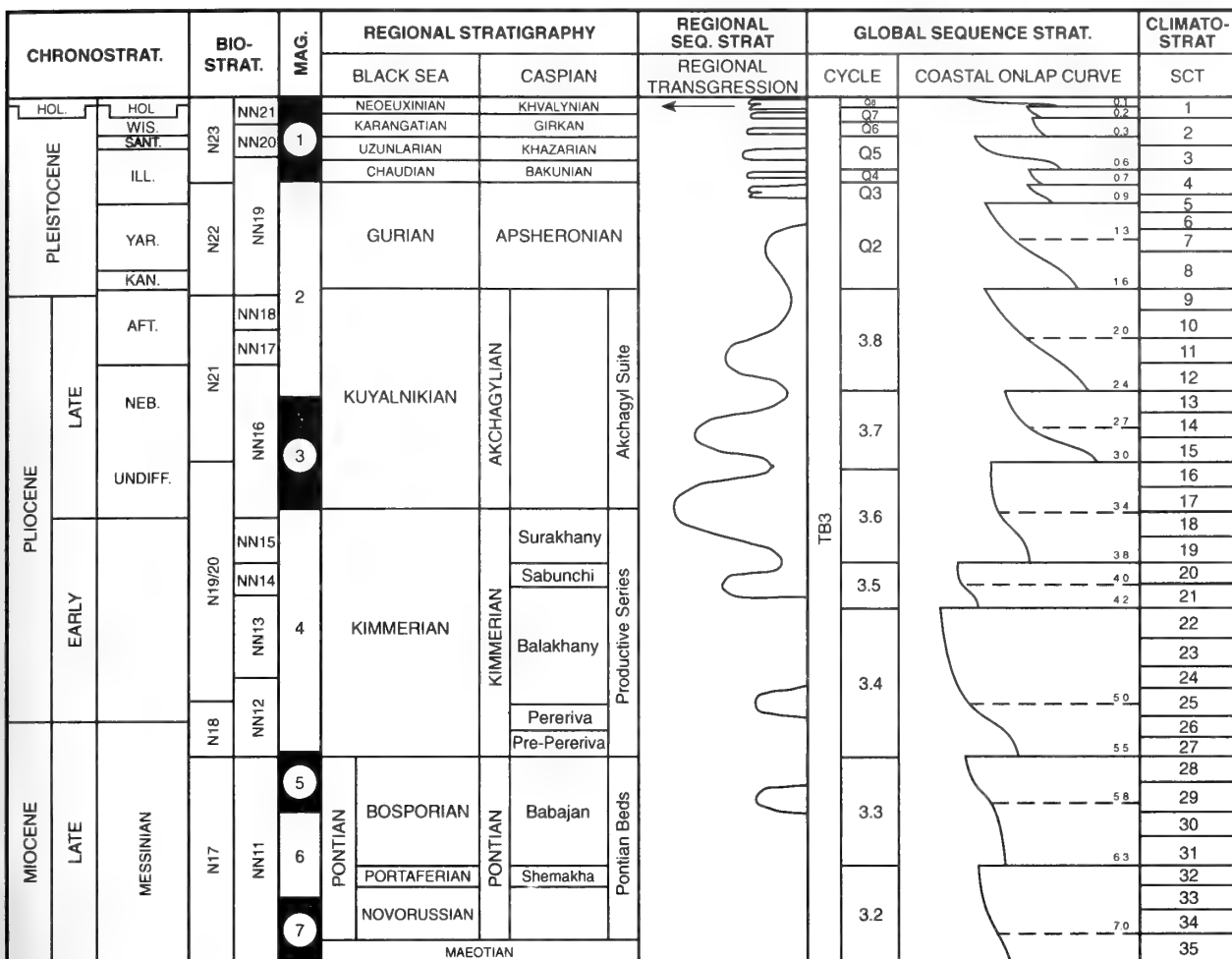


Fig. 6 Stratigraphic summary (Miocene-Holocene). Chronostratigraphy after Beard *et al.* (1982) and Lamb *et al.* (1987) (conceptual Gulf of Mexico deep-water stage nomenclature) (Wis. = Wisconsinian; San. = Sangamonian; Ill. = Illinoian; Yar. = Yarmouthian; Kan. = Kansan; Aft. = Aftonian; Neb. = Nebraskan). Biostratigraphy after Blow (1969) (planktonic foraminifera) (prefixed N) and Martini (1971) (calcareous nanno-plankton) (prefixed NN). Magnetostratigraphic polarity epochs and absolute age values are after Haq *et al.* (1988). Regional stratigraphy from this paper (upper case = chronostratigraphic, lower case = lithostratigraphic units). Regional sequence stratigraphy (transgressions) after Skaldbyna (1985). Global sequence stratigraphy after Haq *et al.* (1988) (third-order cycles TB3.2–TB3.8), and Beard *et al.* (1982) and Lamb *et al.* (1987) (fourth-order cycles Q2–Q8). Sequence boundary and maximum flooding surface ages in Ma. Climatostratigraphy (superclimathems or SCTs) after Zubakov & Borzenkova (1990). The correlation of Eastern Paratethyan sequence stratigraphy with the global coastal onlap curve of Haq *et al.* (1988) is tentative. The extent of biostratigraphic control constraining the correlation is indicated on Fig. 5.

(1966) recorded the planktonic foraminifer *Globigerina officinalis* (Middle Eocene to Oligocene, Zones P14–P22 of Blow, 1969) from the basal ‘*Planorbella* Horizon’ in Azerbaijan. Krasheninnikov (1986) recorded planktonic foraminifera indicative of Early Oligocene (P18) from a stratigraphically similar position (immediately below the ‘Ostracod-Horizon’) in the Kuban-Kuma Interfluvium (North Caucasus). Krasheninnikov *et al.* (1985) recorded *Globigerina tapuriensis* (Oligocene, P18–P20) associated with the larger benthonic foraminifer *Nummulites intermedius* (Early Oligocene) from the Khadumian of Armenia. Later, Krasheninnikov & Ptukhian (1986) recorded *Globigerina sellii* (Oligocene, P19/20 to ‘early’ P22) associated with *Nummulites intermedius* (also Oligocene) and the calcareous nannofossil *Helicosphaera reticulata* (Eocene to Early Oligocene, Zones NP17–NP22 of Martini, 1971) from the Khadumian of Armenia. Koshkarly (1986) recorded the

calcareous nannofossils *Reticulofenestra umbilica* (Eocene to Early Oligocene, NP16–NP22), *Chiasmolithus oamaruensis* (Eocene to Early Oligocene, NP18–NP22), *Isthmolithus recurvus* (Eocene to Early Oligocene, NP19–NP22), *Sphenolithus pseudoradians* (Eocene to Early Oligocene, NP20–NP23) and *Ericsonia subdisticha* (Eocene to Early Oligocene, NP20–NP21) from the Khadumian of Azerbaijan. Later, Koshkarly & Baldi-Beke (1987) recorded *R. umbilica*, *C. oamaruensis*, *I. recurvus* and *S. pseudoradians*, and Koshkarly & Alekperov (1993) *H. reticulata* and *E. subdisticha* from the Early Maykopian of Azerbaijan.

Palynology. Although only non-age-diagnostic palynomorphs were recorded from the Maykopian of the Middle Kura Depression by Dzhabarova (1973), recent observations suggest that some age-diagnostic dinocysts, and pollen and spores do

exist (in the Early, and Middle to Late Maykopian respectively). These will be reported in detail in a future publication. Palynological evidence indicates that the Maykopian is a regressive unit characterised by upwardly-increasing terrestrial input (upwardly-increasing pollen and spore content). Micropalaeontological and sedimentological evidence also indicates shallowing upward.

Tarkhanian to Konkian (Figs 8–10)

These stages have collectively been correlated with the Badenian of Central Paratethys (see, for instance, Steininger *et al.*, in Royden & Horvath, 1987). The Badenian is Middle Miocene (planktonic foraminiferal zones N8–N12 (see, for instance, Papp *et al.*, 1968, Rögl *et al.*, 1978 and Papp & Schmid, 1985); calcareous nannoplankton zones NN5–NN7 (see, for instance, Rögl *et al.*, 1978, Papp & Schmid, 1985 and Meszaros, 1992)). Palynologically, it is locally characterised by mangrove elements (Nagy & Kokay, 1991).

The base of the Badenian (the Moravian sub-stage of Papp *et al.* (1978) (Lagenid Zone)) is defined at the first appearance of the planktonic foraminifer *Praeorbulina* (Zone N8) (Papp *et al.*, 1968). The first appearance of the ancestral form *Globigerinoides bisphericus*, which defines the base of Zone N8 (Blow, 1969), falls within the underlying Karpatian (Cicha *et al.*, 1967). This biostratigraphic control indicates that the base of the Badenian can be correlated with the 16.5 Ma (glacio-eustatic) sea-level low-stand of Haq *et al.* (1988) (Fig. 5).

The middle part of the Badenian (the Wielician sub-stage of Papp *et al.* (1978) (Sandschaler Zone)) is characterised by marginal marine sediments (including evaporites). This

regressive sub-stage can be tentatively calibrated against planktonic foraminiferal Zones N10–N12 or calcareous nannoplankton zones NN5–NN6 (see, for instance, Rögl *et al.* (1978) and Papp & Schmid (1985)). The onset of regressive conditions can be tentatively correlated with the 15.5 Ma (glacio-eustatic) sea-level low-stand of Haq *et al.* (1988) (Fig. 5). The regressive coarse clastics of the Chokrakian and Karaganian in Eastern Paratethys also appear to be associated with this event (though they could be associated with a separate tectonic event). These clastics constitute important reservoirs in the Indol Kuban and Terek Caspian Foredeeps (Ulmishek & Harrison, 1981) and in eastern Azerbaijan (Ali-Zade *et al.*, 1986). Chepalyga (1985) calibrates the Chokrakian and Karaganian against magnetostratigraphic polarity epochs 15–12, while Zubakov & Borzenkova (1990) calibrate them against polarity epochs 16–14.

The top of the Badenian (the Kosovian sub-stage of Papp *et al.* (1978) (Buliminid-Bolivinid Zone)) is defined below the last appearances of *Globorotalia mayeri/siakensis* (N14) and *Globigerina druryi* (N15) (Papp *et al.*, 1978; Papp & Schmid, 1985).

Details of Tarkhanian to Konkian stratigraphy have been discussed by Andrusov (1884), Bogdanowicz (1950a–b, 1965), Shishova (1955), Gasanova (1965), Mamedova (1971), Azizbekov (1972), Lupov *et al.* (1972), Dzhabarov (1973), Cicha *et al.* (1983) and Ali-Zade *et al.* (1986). A monograph of polymorphinid foraminifera of this age from Georgia was published by Dzharelidze (1977).

In eastern Azerbaijan the Karaganian and Konkian, together with the overlying Sarmatian and Maeotian, are collectively referred to as the Diatom Suite (because of the presence of

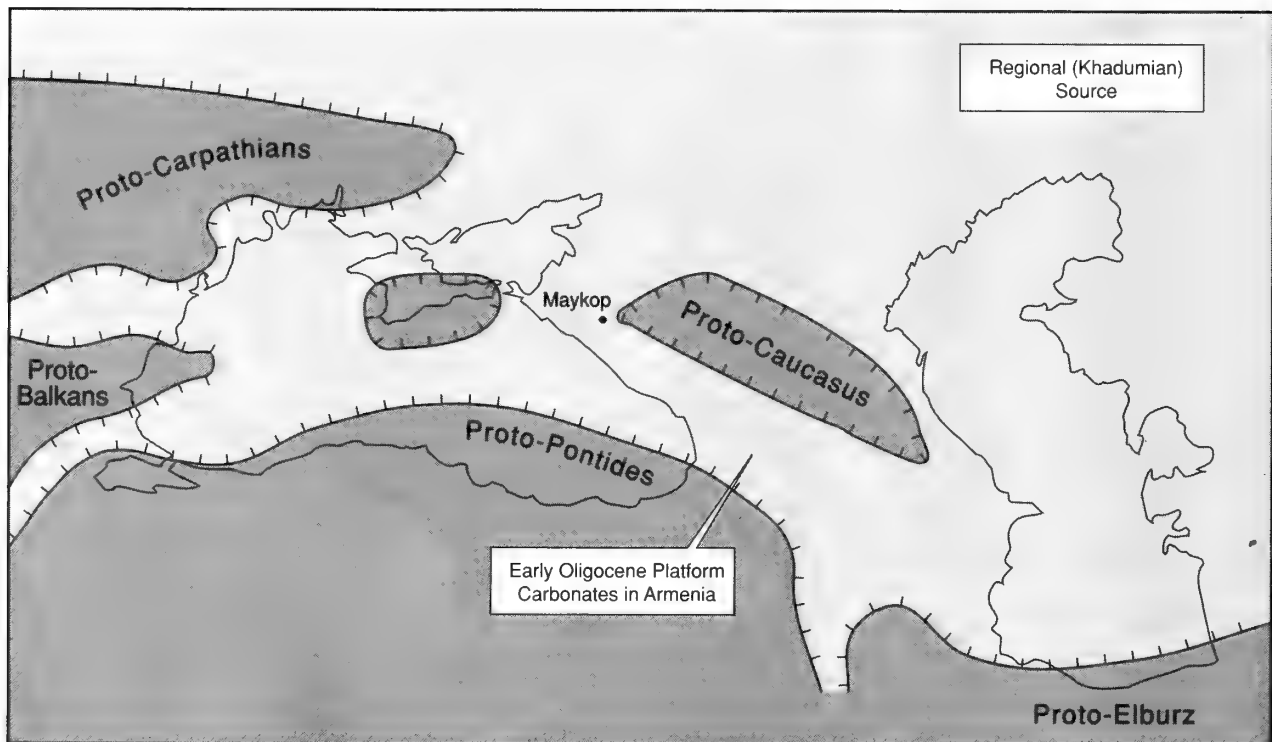


Fig. 7 Palaeogeographic reconstruction, Early Maykopian (Early Oligocene). Solid line indicates relatively well constrained, dashed line poorly constrained shoreline. Ticks on landward side. The location of the Maykopian stratotype is indicated.

diatomaceous limestones). The individual Eastern Paratethyan stages can be recognised within the Diatom Suite on the basis on fish otoliths and benthonic microfossils (particularly molluscs and foraminifera (e.g., Azizbekov, 1972; Ali-Zade *et al.*, 1986) and diatoms (E.Z. Ateava, pers. comm., 1994)). The work of Dzhabarova (1973) suggests that palynology may also be used to recognise the various stages (see notes below).

In eastern Azerbaijan parts of the Diatom Suite are considered to have hydrocarbon source potential.

Tarkhanian (Fig. 8)

The Tarkhanian takes its name from a promontory in the Crimea (Likharev, 1958). The stratotype section yields Middle Miocene (NN5) calcareous nannoplankton (F. Rögl, pers. comm., 1994).

Micropalaeontology. Only non-age-diagnostic quasi-marine, smaller benthonic and rare planktonic foraminifera were recorded by Bogdanowicz (1950a) from the Tarkhanian of Kuban and later by Mamedova (1971) and Azizbekov (1972) from the Tarkhanian of Azerbaijan. These include *Rotalia [Ammonia] ex gr. beccarii* (smaller benthonic), which has a cosmopolitan distribution and probably ranges no older than Middle Miocene (RWJ's unpublished observations), and *Nonion [Florilus] boueanum* (smaller benthonic) and *Globigerina tarchanensis* (planktonic), both of which have also been recorded in the Badenian of Central Paratethys (Papp *et al.*, 1978; Papp & Schmid, 1985).

Chokrakian (Fig. 9)

The Chokrakian takes its name from a lake in the Crimea (Likharev, 1958). It is of Middle Miocene age on regional evidence (see above). Direct biostratigraphic evidence is lacking. The 'Vindobonian Marls' of Northern Iran appear correlative (Stöcklin & Setudehnia, 1971, 1972).

Micropalaeontology. Only non-age-diagnostic, quasi-marine, smaller benthonic foraminifera were recorded by Bogdanowicz (1950b) from the Chokrakian of the western Precaucasus and later by Mamedova (1971) and Azizbekov (1972) from the Chokrakian of Azerbaijan and Popkhadze (1983) for the Chokrakian of western Georgia. These include *Rotalia [Ammonia] ex gr. beccarii* (smaller benthonic), which has a cosmopolitan distribution and probably ranges no older than Middle Miocene (RWJ's unpublished observations), *Nonion [Florilus] boueanum* and *Miliolina [Quinqueloculina] akneriana* spp., both of which have also been recorded in the Badenian of Central Paratethys (Papp & Schmid, 1985), and *Miliolina caucasica*, *Sigmoilina tschokrakensis* and *Tschokrakella longiuscula*, all of which are endemic to Eastern Paratethys. The ostracod, *Leptocythere bardrakensis* was recorded by Popkhadze (1984) from the Chokrakian of western Georgia.

Palynology. Only non-age-diagnostic palynomorphs were recorded by Dzhabarova (1973) from the Chokrakian of the Middle Kura Depression. Pollen spectra are characterised by relatively high incidences of herb and shrub taxa including *Chenopodiaceae* and *Ephedra*. The presence of

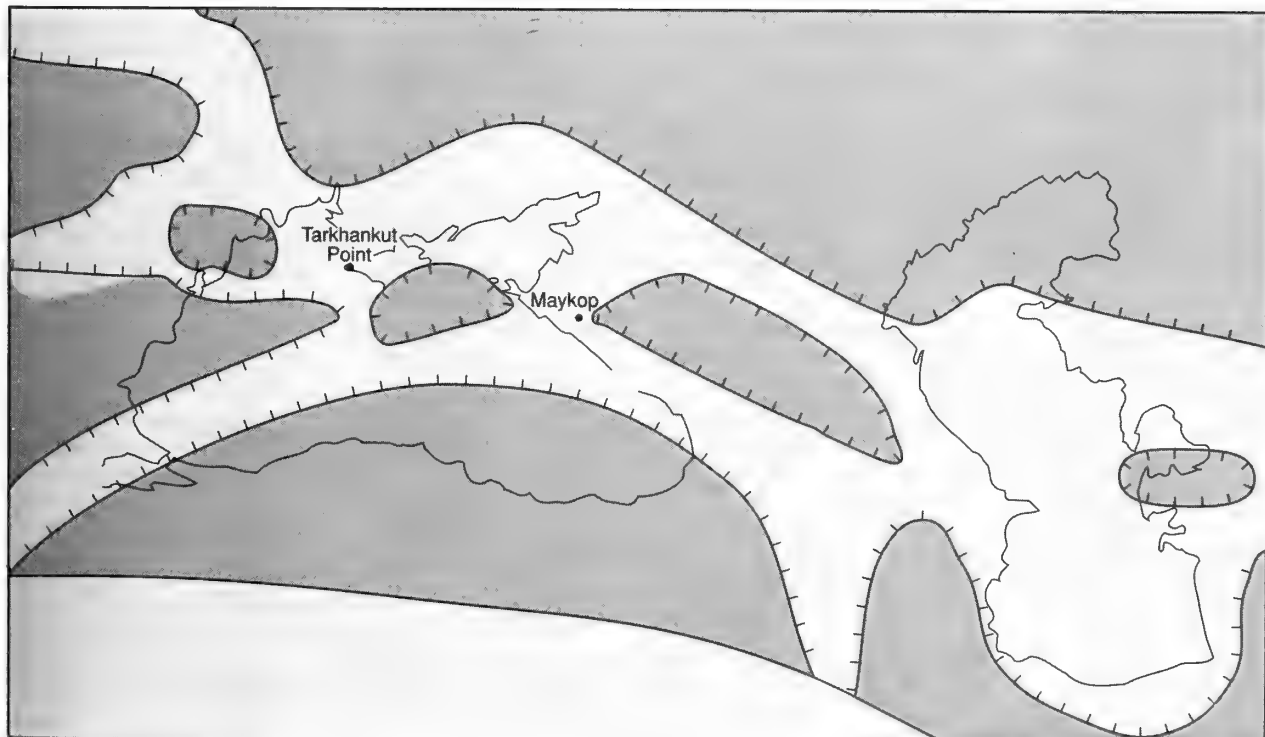


Fig. 8 Palaeogeographic reconstruction, Late Maykopian to Tarkhanian (Late Oligocene to early Middle Miocene). Key as for Fig. 7. The locations of the Maykopian and Tarkhanian stratotypes are indicated.

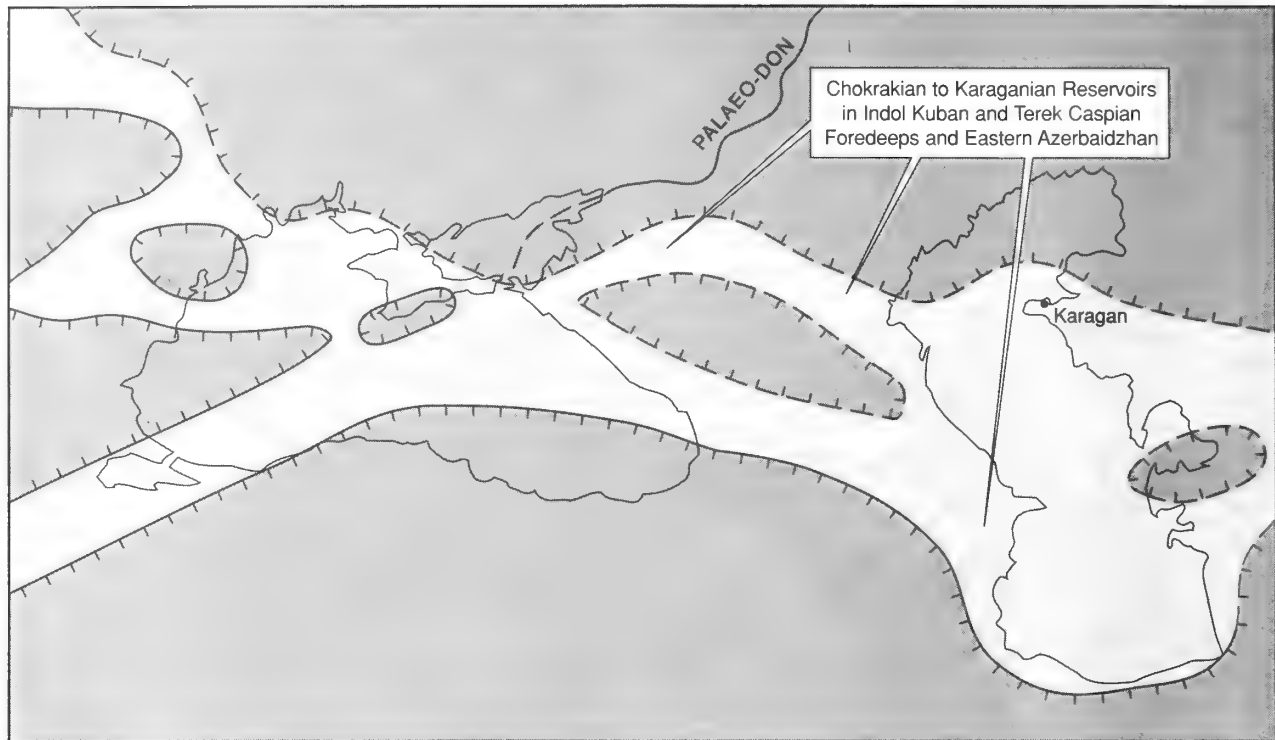


Fig. 9 Palaeogeographic reconstruction, Chokrakian to Karaganian (Middle Miocene). Key as for Fig. 7. The location of the Karaganian stratotype is indicated.

Chenopodiaceae probably indicates the local development of salt-marshes.

Karaganian (Fig. 9)

The Karaganian takes its name from a locality on the Mangyshlak Peninsula in Kazakhstan (Likharev, 1958). It is Middle Miocene on regional evidence (see above). Direct biostratigraphic evidence is lacking. The *Spaniodontella* Beds of Northern Iran appear correlative (Stöcklin & Setudehnia, 1971, 1972).

Micropalaeontology. Only non-age-diagnostic, quasi-marine, smaller benthonic foraminifera were recorded by Mamedova (1971) and Azizbekov (1972) from the Karaganian of Azerbaijan. These include *Nonion bogdanowiczi*. The fish otoliths *Rhombus corius* and *R. corius binagadini* are regarded as index-species for the Karaganian in Azerbaijan (E.Z. Ateava, pers. comm., 1994).

Palynology. Only non-age-diagnostic palynomorphs were recorded by Dzhabarova (1973) from the Karaganian of the Middle Kura Depression. Pollen spectra are characterised by relatively high incidences of tree taxa, which indicates a forested hinterland. The predominance of *Betula* (birch) indicates a climatic regime similar to that of the present-day taiga or forest-tundra.

Konkian (Fig. 10)

The Konkian takes its name from a river in the Ukraine (a tributary of the Dniepr) (Likharev, 1958). It is of Middle

Miocene age on regional evidence (see above). Direct biostratigraphic evidence is lacking. The *Pholas* Beds of Northern Iran appear correlative (Stöcklin & Setudehnia, 1971, 1972).

Micropalaeontology. Only non-age-diagnostic, quasi-marine, smaller benthonic foraminifera were recorded by Bogdanowicz (1965) from the Konkian of the western Precaucasus and by Mamedova (1971) and Azizbekov (1972) from the Konkian of Azerbaijan. These include *Rotalia [Ammonia] ex gr. beccarii* (smaller benthonic), which has a cosmopolitan distribution and probably ranges no older than Middle Miocene (RWJ's unpublished observations), *Articulina gibbosa* and *Miliolina [Quinqueloculina] haidingerii*, both of which have also been recorded in the Badenian of Central Paratethys (Papp & Schmid, 1985), and *Articulina elongata konkensis*, *Bulimina konkensis* and *Elphidium nachischevanicus*, all of which are endemic to Eastern Paratethys. *Bulimina konkensis* and *Elphidium kudakoense*, together with the fish otolith *Trigla konkensis*, are regarded as index-species for the Konkian in Azerbaijan (Podobina *et al.*, 1956; Mamedova, 1971).

Shishova (1955) and Gasanova (1965) recorded the following diatoms from the Konkian of Eastern Azerbaijan: *Actinocyclus ehrenbergi*, *A. rafsi*, *Asterolampra marylandica*, *Cocconeis placentula lineta*, *C. scutellum*, *Coscinodiscus radiatus*, *C. oculus* and *Melosira sulcata*. *Coscinodiscus radiatus* was considered particularly typical.

Palynology. Only non-age-diagnostic palynomorphs were recorded by Dzhabarova (1973) from the Konkian of the Middle Kura Depression. Pollen spectra are characterised by relatively high incidences of tree taxa, which indicates a forested

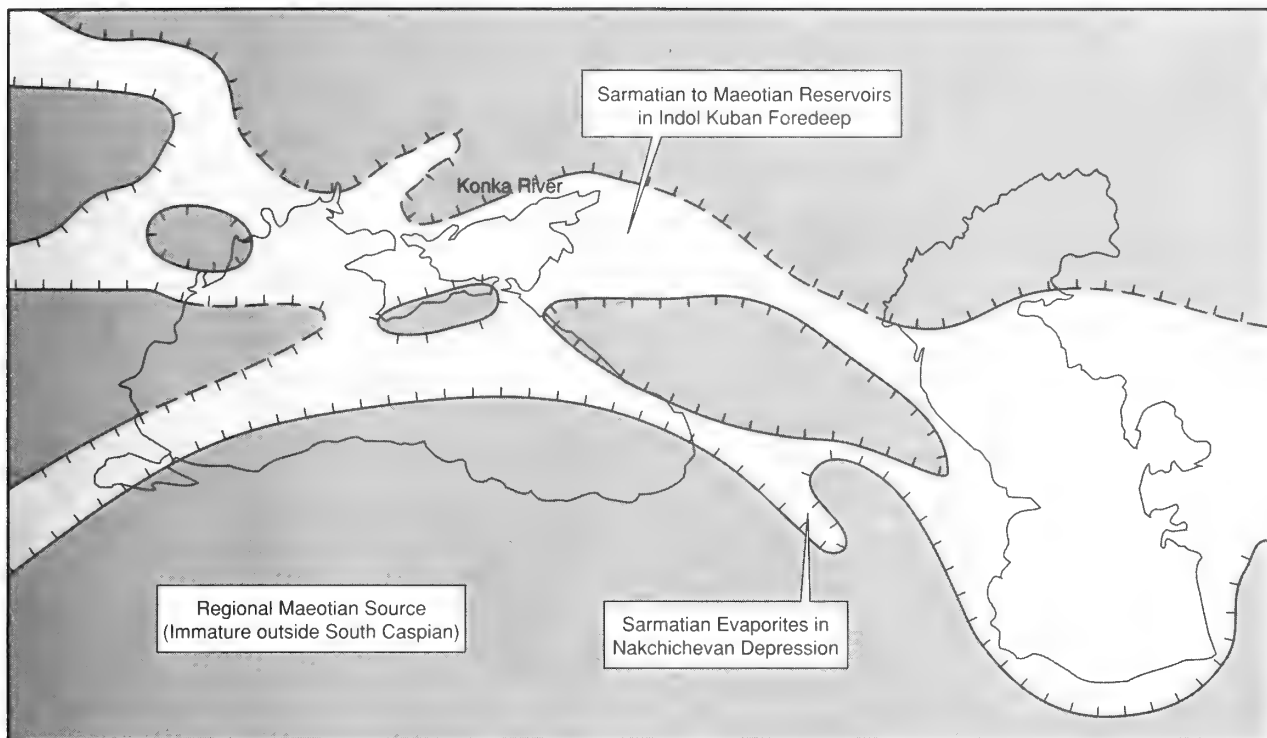


Fig. 10 Palaeogeographic reconstruction, Konkian to Maeotian (late Middle to early Late Miocene). Key as for Fig. 7. The location of the Konkian stratotype is indicated.

hinterland. The predominance of Taxodiaceae (cypresses and swamp-cypresses) indicates a warm-temperate (possibly even subtropical) climatic regime.

Sarmatian (Fig. 10)

The Sarmatian of Eastern Paratethys is probably equivalent to the stratotypical Sarmatian of Central Paratethys (late Middle to early Late Miocene (calcareous nannoplankton zones NN7–NN9) (Meszaros, 1992), planktonic foraminiferal zones N13?–N15), but may also be equivalent to the lower part of the Pannonian (Slavonian) of that area (Late Miocene) (see, for instance, Papp *et al.*, 1974, 1985). Chepalyga (1985) calibrates the Sarmatian of Eastern Paratethys against magnetostratigraphic polarity epochs 10–7, while Zubakov & Borzenkova (1990) calibrate it against epochs 14–9, and Pevzner & Vangengeim (1993) calibrate it against polarity epochs 10–7. The regressive events which characterise the Sarmatian suggest that (within the limits of biostratigraphic control) its base can be correlated with the 10.5 Ma (glacio-eustatic) sea-level low-stand of Haq *et al.* (1988).

The Sarmatian of Eastern Paratethys is characterised by areally restricted regressive marginal marine sediments including coarse clastics, and, in the Nakchichevan Depression, evaporites (though transgressive black shales (with source potential) also occur locally). The 'Sarmatian' of Northern Iran and part of the Upper Red Formation of Central Iran, also characterised by clastics and evaporites, appear correlative (Stöcklin & Setudehnia, 1971, 1972). The Sarmatian of Eastern Paratethys has been divided into three sub-stages, which are, from oldest to youngest, Volkhylian, Bessarabian and

Chersonian. The 'mid' Sarmatian (Bessarabian) represents the culmination of a major regressive phase that began in late Konkian or 'early' Sarmatian (Volkhylian) times (see, for instance, Chepalyga, 1985), and resulted in the first isolation of the South Caspian Basin.

Details of the Sarmatian stratigraphy of Eastern Paratethys have been discussed by Gasanova (1965), Maisuradze (1971), Mamedova (1971, 1987), Azizbekov (1972), Lupov *et al.* (1972), Dzhabarova (1973), Ali-Zade & Aleskerov (1974), Azizbekova (1974), Paramonova *et al.* (1979) and Pevzner & Vangengeim (1993).

Micropalaeontology. Only non-age-diagnostic (and largely endemic), quasi-marine, smaller benthonic foraminifera and ostracods were recorded from the Sarmatian by Podobina *et al.* (1956), Mamedova (1971, 1987), Voroshilova (1971) and Azizbekov (1972) from Azerbaijan, by Azizbekova (1974) from the Nakchichevan Depression, and by Paramonova *et al.* (1979) from various sites in the Ponto-Caspian region. These include rare cosmopolitan species such as *Streblius [Ammonia] beccarii* and *Elphidium macellum* (foraminifera), which probably range no older than Middle Miocene (RWJ's unpublished observations), *Elphidium reginum* (foraminifer) (lower part only), which is also found in the Sarmatian of Central Paratethys (Steininger *et al.*, 1976) and (?reworked) in the Pliocene of the Black Sea (Gheorghian, in Ross *et al.*, 1978), *Nonion* div. spp., *Porosononion* div. spp. and *Quinqueloculina consobrina* (foraminifera) and *Cyprideis littoralis*, *Cythere multistriata*, *Leptocythere stabilis*, *Loxoconcha eichwaldi* and *Xestoleberis lutrae* (ostracods). Podobina *et al.* (1956), Mamedova (1971) and Voroshilova (1971) have indicated that the three subdivisions of

the Sarmatian in Azerbaijan can be recognised on the basis of foraminifera and ostracods.

The alga *Ovulites sarmaticus* and the fish otoliths *Gadidarum minusculus* and *Gobius sarmaticus* are regarded as index-species for the Sarmatian in Azerbaijan (Ateava, personal communication, 1994). The Sarmatian part of the 'Diatom Suite' in Azerbaijan also contains 23 species of diatoms, chiefly *Coscinodiscus*, *Licmophora* and *Navicula* (Gasanova, 1965).

Palynology. Only non-age-diagnostic palynomorphs were recorded from the Sarmatian of the Middle Kura Depression (Azizbekov, 1972; Dzhabarova, 1973). Pollen spectra from the middle (Bessarabian) sub-stage are characterised locally by (as in the 'Cryptomactra-Horizon') relatively high incidences of Pinaceae (pine) pollen and locally (higher in the section) by relatively high incidences of broad-leaved tree pollen (*Alnus* (alder), *Betula* (birch), *Carya* (hickory), *Carpinus* (hornbeam), *Corylus* (hazel), *Juglans* (walnut)) and angiosperm (flowering plant) pollen (Azizbekov, *op. cit.*). Pollen spectra from the upper (Chersonian) sub-stage are also characterised locally by relatively high incidences of broad-leaved tree pollen (*Fagus* (beech), *Quercus* (oak), *Taxodium* (swamp-cypress), *Tilia* (lime) and *Ulmus* (elm)), though locally Polypodiaceae predominate (Azizbekov, *op. cit.*).

Maeotian (Fig. 10)

The Maeotian of Eastern Paratethys is equivalent to the Pannonian (Late Miocene) of Central Paratethys (though possibly only the upper part thereof (Serbian) (see, for instance, Papp *et al.* (1974, 1985) and Pevzner & Vangengeim (1985b)). Rögl (1985a) calibrates it against calcareous nannoplankton Zone NN10. Chepalyga (1985) calibrates it against magnetostratigraphic polarity epochs 6–5, while Zubakov & Borzenkova (1990) calibrate it against polarity epochs 10–7. Krakhmalnaya *et al.* (1993) have recently described a succession at Novaya Emetovka on the Black Sea coast with a good Maeotian mammal fauna which they calibrate against polarity epochs 6 and 5. The Maeotian is represented by a transgressive-regressive cycle. It is locally characterised by black shales (with hydrocarbon source potential). The Maeotian sea was probably characterised by reduced salinity. Similar environmental conditions evidently obtained in the Pannonian of Central Paratethys, where benthonic foraminiferal assemblages are of quasi-marine (brackish water) aspect (*Ammobaculites*, *Ammonmarginulina*, *Miliammina*, *Trochammina*) (Papp *et al.*, 1985).

Details of Maeotian stratigraphy have been discussed by Shishova (1955), Gasanova (1965), Bogdanowicz (1967, 1969, 1974), Mamedova (1971), Voroshilova (1971), Azizbekov (1972), Lupov *et al.* (1972), Popkhadze (1977), Paramonova *et al.* (1979), Ananova *et al.* (1985), Ali-Zade *et al.* (1986), Rasulov (1986), Maisuradze (1988), Naidina (1988) and Ateava (personal communication, 1994).

Micropalaeontology and Nannopalaeontology. Only non-age-diagnostic, quasi-marine, smaller benthonic foraminifera were recorded by Bogdanowicz (1967, 1969) from the Maeotian of the Kuban and Western Precaucasus and by Paramonova *et al.* (1979) from the Maeotian of various sites in the Ponto-Caspian. These include *Elphidium macellum*, which has a cosmopolitan distribution and probably ranges no older than Middle Miocene (RWJ's unpublished observations) and *Nonion* div. spp.

Some stratigraphically and/or palaeoenvironmentally

significant ostracods were recorded by Azizbekov (1972) from Azerbaijan and by Popkhadze *et al.* (1980) from Abkhazia. These include *Leptocythere biplicata*, *L. meotica*, *Loxoconcha meotica*, *L. tamarindus* and *L. viridis* (quasi-marine). *Leptocythere meotica* and *Loxoconcha meotica*, together with the foraminifera *Quinqueloculina sulcensis* (lower part) and *Q. ludwigi* (upper part) and the fish otoliths *Clupea gidjakensis* and *Percidarum sigmalinoides* are regarded as index-species for the Maeotian in Azerbaijan (Podobina *et al.*, 1956; Mamedova, 1971).

Rich diatom floras including *Coscinodiscus gigas*, *C. oclisirides*, *Grammatophora azens*, *Coccineis heteroidea*, *Melosira architecturalis* and *M. sulcata* were recorded by Shishova (1955) from the Maeotian part of the 'Diatom Suite' of the Apsheron Peninsula in Azerbaijan. *Actinocyclus ehrenbergii*, *Cymatosira sovtchenkoi* and *Rhaphoneis maeotica* were recorded by Gasanova (1965). The stenohaline (normal marine) forms *Asterolampha marylanica*, *Coscinodiscus asteromphalus* and *C. lewisanus sensu lato*, the euryhaline (quasi-marine) forms *Actinocyclus ehrenbergii* and *Rhapalodia musculus*, and the freshwater forms *Amphora ovalis* and *Diatoma vulgare* were recorded by Rasulov (1986). *Coscinodiscus lewisanus sensu stricto* is a Middle Miocene species.

A range of diatoms, calcareous nannofossils and ostracods were recorded by Ananova *et al.* (1985) from the Maeotian of the Black Sea. These include *Actinocyclus ehrenbergii*, *Rhaponeis maeotica* and *Thalassiosira maeotica* (diatoms), *Braarudosphaera* spp. (calcareous nannofossil) and *Cyprideis torosa* and *Leptocythere* spp. (ostracods).

Palynology. Only non-age-diagnostic palynomorphs have been recorded from the Maeotian, and only the acritarch *Micrhystridium* sp. was recorded by Ananova *et al.* (1985) from the Maeotian of the Black Sea. Pollen spectra from the Late Maeotian of the Task-Sunzhenskii Region are characterised by relatively high incidences of Asteraceae and Polygonaceae (herbs), *Ephedra* (shrubs) and Gramineae (grasses) (Naidina, 1988). This indicates an open, sparsely forested hinterland and an arid climatic regime similar to that of the present-day steppe or semi-desert. The locally relatively high incidences of Gleicheniaceae (ferns) and Lycopodiaceae (club-mosses) indicate local development of conditions similar to those of the present-day tundra, forest-tundra or mountain belt. The presence of Chenopodiaceae probably indicates local development of salt-marshes.

Pontian

The Pontian takes its name from the ancient name for the Black Sea. It is essentially regressive (though it also includes an overstepping transgressive unit at the base), and is characterised regionally by marginal marine coarse clastics and shallow marine carbonates and locally (Babajan Formation, Bosporian Sub-Stage) by evaporites. Chepalyga (1985) calibrates the Pontian against magnetostratigraphic polarity epoch 4 (Gilbert), while Zubakov & Borzenkova (1990) calibrate it against polarity epochs 6–5. We correlate the Pontian evaporites against those of the stratotypical Messinian, which can be calibrated against magnetostratigraphic polarity epoch 5 (Zubakov & Borzenkova, 1990).

Details of the Pontian stratigraphy of Eastern Paratethys have been discussed by, among others, Sveier (1949), Mandelstam *et al.* (1962), Sheydayeva-Kuliyeva (1966), Agalarova (1967), Vekilov *et al.* (1969), Ramishvili (1969), Rozyeva (1971),

Azizbekov (1972), Lupov *et al.* (1972), Chelidze (1973), Karmishina (1975), Vekua (1975), Krstic (1976), Shchekina (1979), Imnadze & Karmishina (1980), Ali-Zade *et al.* (1986), Sirenko & Turlo (1986) and Yagmurlu & Helvacı (1994).

Micropalaeontology. Only the non-age-diagnostic, quasi-marine, smaller benthonic foraminifer *Elphidium stellatum* was recorded by Imnadze & Karmishina (1980) from the Late Pontian (Bosporian sub-stage) of the Black Sea.

Stratigraphically and/or palaeoenvironmentally significant ostracods recorded by Sheydayeva-Kuliyeva (1966) and Azizbekov (1972) from the Pontian of Azerbaijan (Western Caspian), by Karmishina (1975) from the Northern Precaspian and South-Eastern Kalmyk (Northern Caspian) and Prechernomore (Northern Black Sea), and by Vekua (1975) from Abkhazia (north-eastern Black Sea) include *Bakunella dorsoacuata*, *Caspiolla acronasuta*, *Pontoniella acuminata* and *P. loczyi*. *Bakunella dorsoacuata* and *Caspiolla acronasuta* are quasi-marine species (Yassini, 1986). Species of *Leptocythere*, *Loxoconcha* and *Xestolebris* also occur. It is possible to recognise three ostracod zones in the Pontian of Eastern Azerbaijan (Sheydayeva-Kuliyeva, 1966). It is also possible to recognise three corresponding mollusc zones.

The lower part of the Continental (Cheleken) Series of Northern Iran and the Maragheh Bone Beds of Central Iran can be correlated with the Pontian on vertebrate palaeontological, limited malacological and ostracod evidence (Faridi, 1964; Stöcklin & Setudehnia, 1971, 1972).

Palynology. Only non-age-diagnostic palynomorphs have been recorded from the Pontian. Pollen spectra from the Pontian of Georgia are characterised by relatively high incidences of tropical elements such as *Nypa* (palm) (Ramishvili, 1969). Those

from the Late Pontian (Bosporian sub-stage) of the Ukraine are characterised initially by thermophilic (warm-temperate) and hydrophilic (moisture-loving) elements such as Taxodiaceae (cypresses and swamp-cypresses) and later by arid steppe and semi-desert elements (Shchekina, 1979; Sirenko & Turlo, 1986).

Kimmerian (Fig. 11)

The Kimmerian takes its name from an ancient tribe who lived on the shores of the Black Sea (Likharev, 1958). The Dacian (a stage name sometimes used in the Black Sea region) and the 'Eoakchagylian' (a stage name used in the Caspian Sea region by Zubakov & Borzenkova (1990)) appear synonymous. Semenenko (1979), Pevzner & Vangengeim (1985), Skalbdyna (1985) and Zubakov & Borzenkova (1990) calibrate the Kimmerian against magnetostratigraphic polarity epochs 5–4, while Chepalyga (1985) and Chepalyga *et al.* (1985) calibrate it against polarity epoch 4 (Gilbert). Essentially on the basis of magnetostratigraphic evidence (including the calibration of the underlying Pontian against polarity epoch 5 (see above)), we have tentatively calibrated the major unconformity at the base of the Kimmerian against the 5.5 Ma glacio-eustatic sea-level low-stand of Haq *et al.* (1988) and apparently coincident uplift around and subsidence within the Caspian (leading to a massive sea-level fall (of the order of 1000 m) within the Caspian and the severance of the connection between the Caspian and the Black Sea). Additional unconformities in the Caspian succession cannot be confidently calibrated against any of the third-order glacio-eustatic sea-level low-stands on the Haq *et al.* chart, and may be associated with higher frequency glacio-eustatic low-stands or local tectonic events. Due partly to tectono-eustatic effects (see above), and partly to climatic effects

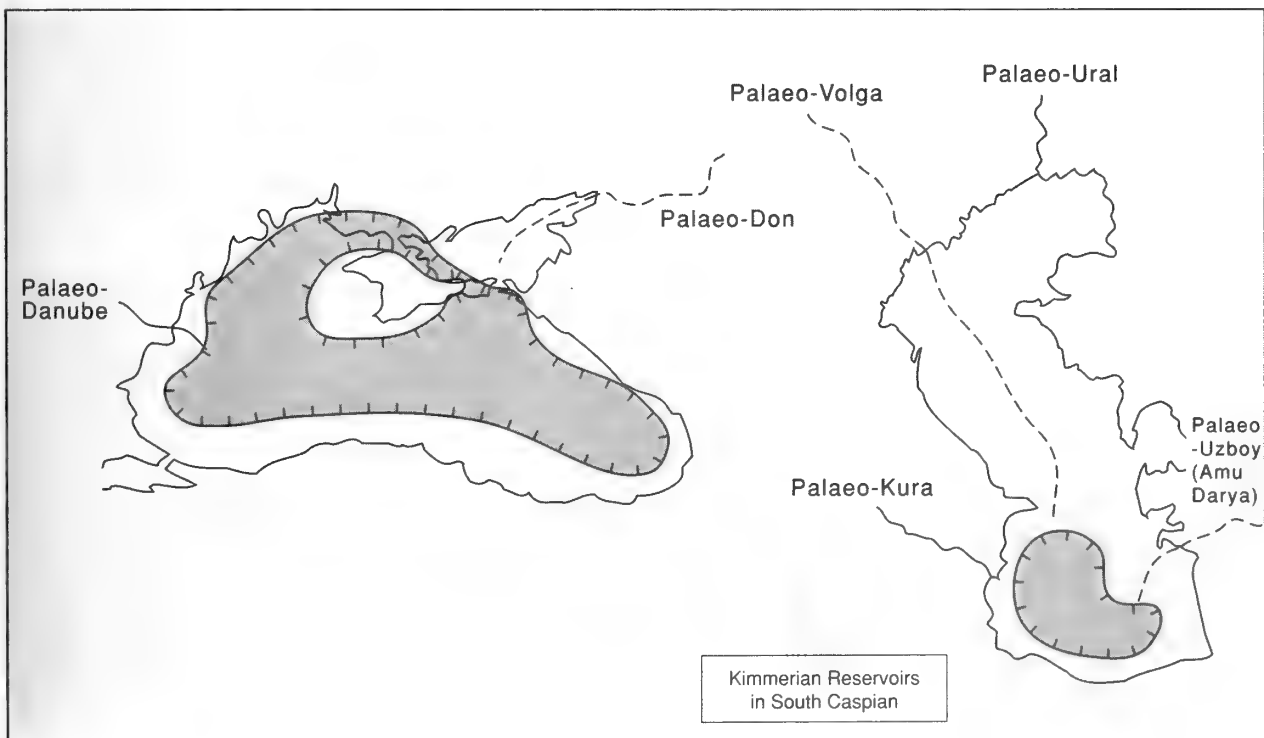


Fig. 11 Palaeogeographic reconstruction, Dacian/Kimmerian (latest Miocene to Pliocene). Key as for Fig. 7.

(an excess of evaporation over precipitation) and a change in the drainage system (with rivers formerly flowing into Paratethys captured by rejuvenated rivers flowing into the Mediterranean, where base-level had fallen considerably during the Messinian salinity crisis (see, for instance, Hsu (1983)), the level and the areal extent of the Caspian 'athalassic lake' were drastically reduced during the Kimmerian. Palaeontological evidence points to a stratigraphically upward reduction in salinity. The basal Kimmerian contains a quasi-marine ostracod fauna (characterised by *Cyprideis littoralis/torosa*) that appears correlative with that of the Messinian 'Lago Mare' facies in the Mediterranean.

In Azerbaijan, the Kimmerian is characterised by several thousand metres (thicknesses of around 4km are typical around the Apsheron Peninsula) of principally Palaeo-Volga-derived, regressive marginal and non-marine coarse clastics comprising the main ('Productivnaya Tolsha' = 'Productive Series') reservoirs in several billion-barrel oil-fields (Khain *et al.*, 1937; Ismailov and Idrisov, 1963; Ismailov *et al.*, 1972; Nikishin, 1981; Babayan, 1984; Kerimov *et al.*, 1991; Narimanov, 1993). The sedimentology of this succession is discussed in detail by Reynolds *et al.* (in press). Constituent lithostratigraphic units include, in ascending stratigraphic order, the Kalin or Kala, Podkirmakina (Pre-Kirmaky Sand (PK)), Kirmakina (Kirmaky Sand (KS)), Nadkirmakina (Post-Kirmaky Sand and Post-Kirmaky Clay (NKP and NKG)), Pereriva, Balakhany, Sabunchi and Surakhany Suites.

Details of Kimmerian stratigraphy have been discussed by, among others, Ali-Zade (1946), Khalilov (1946), Sveier (1949), Agalarova (1956), Mandelstam *et al.* (1962), Rozyeva (1971), Azizbekov (1972), Lupov *et al.* (1972), Ali-Zade (1974), Karmishina (1975), Vekua (1975), Ananova *et al.* (1985), Sirenko & Turlo (1986) and Yassini (1986).

Micropalaeontology Only non-age-diagnostic, quasi-marine, smaller benthonic foraminifera were recorded by Karmishina (1975) from the Kimmerian of Prechernomore (Northern Black Sea). These include *Ammonia beccarii* and *Elphidium incertum*.

Stratigraphically and/or palaeoenvironmentally significant ostracods recorded by Karmishina (1975) and Vekua (1975) from the Kimmerian of Prechernomore (Northern Black Sea) and Abkhazia (North-eastern Black Sea) respectively include *Bakunella doroacuata*, *Caspiocypris labiata*, *Caspiolla acronasuta*, *Cyprideis littoralis/torosa*, *Leptocythere bosqueti*, *Mediocythereis apatoica* and *Pontoniella acuminata*. *Bakunella doroacuata*, *Caspiolla acronasuta* and *Cyprideis torosa* are quasi-marine species (Yassini, 1986). *Caspiocypris labiata* is fresh-water. Ostracods recorded by Karmishina (1975) from the Kimmerian of the Northern Precaspian and South-Eastern Kalmyk (Northern Caspian) include *Candonia angulata*, *C. neglecta*, *C. rostrata*, *Cyclocypris laevis*, *Cypria arma*, *Eucypris naidinae*, *Ilyocypris bradyi*, *I. gibba*, *I. serpulosa* and *Zonocypris membranae*. These are all fresh-water forms.

Microbiostratigraphic study of the Kimmerian 'Productive Series' in Azerbaijan is hindered by massive reworking (Khalilov, 1946; Agalarova, 1956). However, the general pattern of reworking indicates unroofing, which in itself is of some stratigraphic value (with pulses of reworking related to sea-level low-stands). Moreover, the potential exists for biostratigraphic subdivision on the basis of ostracods (see, for instance, Khalilov, 1946; Agalarova, 1956; Azizbekov, 1972). The Kala Suite contains *Cythere [Leptocythere] camellii* and *Paracypris livinalina* (quasi-marine), the Kirmakina Suite *Cythere [Leptocythere] cellula*, *C. [Cyprideis] littoralis/torosa*, *C. olivina*,

C. [Leptocythere] praebacuana, *Hemicythere pontica* and *Loxoconcha diabaroffi* (quasi-marine), the Pereriva Suite *Cyprideis littoralis/torosa* (quasi-marine), the Balakhany Suite *Cythere [Leptocythere] praebacuana*, *Loxoconcha alata*, *L. eichwaldi* and *Xestoleberis lutrae* (quasi-marine), the Sabunchi Suite no *in situ* ostracods, and the Surakhany Suite *Eucypris* (fresh-water) and *Leptocythere* and *Loxoconcha* (quasi-marine).

The Krasnotsvetnaya ('Red-Coloured') Series of Turkmenia can be correlated with the Kimmerian on ostracod evidence (Agalarova, 1956; Lupov *et al.*, 1972). The lowermost part contains *Bakunella*, *Caspiolla*, *Pontoniella* and *Xestoleberis* and is of Pontian aspect, while the uppermost part contains *Leptocythere* and *Limnocythere* and is of Akchagylian aspect.

The upper part of the Continental (Cheleken) Series of Northern Iran can be correlated with the Kimmerian on vertebrate palaeontological, limited malacological and ostracod evidence (Faridi, 1964; Stöcklin & Setudehnia, 1971, 1972). The Lacustrine Fish Beds of Central Iran, locally characterised by volcanic ash bands, can also be tentatively correlated with the Kimmerian (Stöcklin & Setudehnia, *op. cit.*).

Nannopalaeontology. Stratigraphically significant calcareous nannofossils recorded by Zubakov & Borzenkova (1990) from the Kimmerian include *Discoaster quinqueramus* (NN11) (?reworked), *Ceratolithus acutus* ('late' NN12) and *C. rugosus* (NN13–?NN19).

Palynology. Only non-age-diagnostic palynomorphs have been recorded from the Kimmerian. However, at least theoretically, climatostratigraphy ought to have some utility in the stratigraphic subdivision of the 'Productive Series' (with a number of superclimathems discernable on the basis of different pollen spectra). Indeed, the results of preliminary analyses have shown pollen spectra from 'Thermo'-SCT27 in the Ukraine to be characterised by broad-leaved and subtropical forest elements (*Castanea* (chestnut), *Rhus* (rue) and *Taxodiaceae* (cypress and swamp-cypress)) (Sirenko & Turlo, 1986), and those from 'Cryo'-SCT26 and 'Cryo'-SCT24 to be characterised by steppe elements (Ananova *et al.*, 1985; Zubakov & Borzenkova, 1990). 'Thermo'-SCT23 has been shown to be characterised by the quasi-marine acritarch *Sigmalina* (and the quasi-marine diatom *Actinocyclus ehrenbergi*) (Ananova *et al.*, Zubakov & Borzenkova, *opp. cit.*).

Akchagylian to Khvalynian (Caspian Sea) (Fig. 12)

The Akchagylian to Khvalynian of the Caspian Sea appear equivalent to the Kuyalnikian to Neoeuxinian of the Black Sea (Late Pliocene to Holocene). Details of Akchagylian to Khvalynian stratigraphy have been discussed by, among others, Livental (1929), Sveier (1949), Mandelstam *et al.* (1962), Yakhimovich *et al.* (1965, 1984), Dzhabarova (1966), Kuliyeva (1968), Dmitriev *et al.* (1969), Rayevskiy (1969), Sultanov & Sheidayeva-Kuliyeva (1969), Aliyev & Aliyeva (1970), Kopp (1970), Rozyeva (1971), Ushakova & Ushko (1971), Zubakov & Kochegura (1971), Azizbekov (1972), Lupov *et al.* (1972), Ananova (1974), Karmishina (1975), Kaplin (1977), Trubikhin (1977), Fedkovich (1978), Veliyev (1980), Abramova (1982, 1985), Semenenko & Lulieva (1982), Mamedov & Rabotina (1984a), Aliyulla *et al.* (1985), Ivanova (1985), Mamedov & Aleskerov (1985, 1986), Sultanov (1985), Yassini (1986), Aleskerov *et al.* (1987), Bludorova *et al.* (1987), Zhidovinov *et al.* (1987), Naidina (1988), Ali-Zade & Aliyeva (1989), Yanko (1990a–b, 1991), Trubikhin *et al.* (1991) and Mamedova (1993).

Akchagylian (Fig. 12)

The Akchagylian takes its name from a locality near Krasnovodsk on the southern shores of the Gulf of Karabogaz in Western Turkmenia (Likharev, 1958). It appears equivalent to the Kuyalnikian of the Black Sea. Zubakov & Borzenkova (1990) calibrate it against magnetostratigraphic polarity epochs 4 (Gilbert) or 3 (Gauss) to 2 (Matuyama). The Akchagylian is transgressive and is represented by marine shales (constituting an important regional seal in the South Caspian). The transgressions within the Akchagylian temporarily re-established marine connections to the world's oceans. Calcareous nannoplankton data (see below) indicates that they may correspond to the 3.4 Ma, 2.7 Ma and 2.0 Ma maximum flooding surfaces of Haq *et al.* (1988).

Details of Akchagylian stratigraphy have been discussed by, among others, Ali-Zade (1936), Yakhimovich *et al.* (1965, 1983), Dzhabarova (1966), Ali-Zade (1969), Dmitriyev *et al.* (1969), Sultanov & Sheydayeva-Kuliyeva (1969), Aliyev & Aliyeva (1970), Ushakova & Ushko (1971), Zubakov & Kochegura (1971), Azizbekov (1972), Lupov *et al.* (1972), Ananova (1974), Karmishina (1975), Trubikhin (1977), Fedkovich (1978), Sultanov (1979), Semenenko & Lulieva (1982), Mamedov & Rabotina (1984a), Bludorova *et al.* (1987), Zhidovinov *et al.* (1987), Naidina (1988) and Benyamovskoy & Naidina (1990).

Micropalaontology. Only non-age-diagnostic smaller benthonic foraminifera were recorded by Yakhimovich *et al.* (1965), Sultanov & Sheydayeva-Kuliyeva (1969) and Karmishina (1975) from the Akchagylian of the Volga-Urals Region, Azerbaijan, and the Northern Precaspian and South-Eastern Kalmyk (Northern Caspian) respectively. These

include *Ammonia beccarii*, *Bolivina ex gr. advena*, *B. aksaica*, *B. floridana*, *Buccella* sp., *Cassidulina crassa*, *C. oblonga*, *Cassidulinita prima*, *Cibicides lobatulus*, *Discorbis arculus*, *D. multicameratus*, *D. orbicularis*, *D. pliocenicus*, *Elphidium incertum*, *E. kudakoense*, *E. macellum*, *E. subarcticum*, *Nonion aktschagyliticus* and *Quinqueloculina* spp. *Bolivina*, *Cibicides* and *Discorbis* are near-normal marine genera, while the remainder are quasi-marine.

Stratigraphically and/or palaeoenvironmentally significant ostracods recorded by Sultanov & Sheydayeva-Kuliyeva (1969) and Karmishina (1975) from the Akchagylian of Azerbaijan, and the Northern Precaspian and South-Eastern Kalmyk (Northern Caspian) respectively include *Aglaocypris chuzchievae*, *Candonia convexa*, *Ilyocypris gibba* and *Leptocythere verrucosa*. *Aglaocypris*, *Candonia* and *Ilyocypris* are fresh-water forms, while *Leptocythere* is quasi-marine.

In Azerbaijan, the Akchagylian (Akchagyl Suite) contains a diverse marine ostracod and molluscan fauna (Livental, 1929; Ali-Zade, 1954; Sultanov & Sheydayeva-Kuliyeva, 1969). On the Apsheron Peninsula, it can be divided into three units on the basis of ostracods. Freshwater forms (*Candonia*, *Eucypris*, *Ilyocypris*, *Limnocythere*) characterise the lower unit, marine and quasi-marine forms the middle and upper units.

Stratigraphically and/or palaeoenvironmentally significant diatoms recorded by Ushakova & Ushko (1971) from the Akchagylian to Apsheronian of the Krasnovodsk Peninsula in Western Turkmenia include *Actinocyclus chrenbergi* ssp. *ralfsii*, *Campylodiscus noricus*, *C. noricus* ssp. *hibernica*, *Coccineis scutellum*, *Coscinodiscus argus*, *Cymbatopleura elliptica*, *Diploneis bombus*, *D. domblittensis*, *D. fusca* ssp. *pervasta*, *D. rombica*, *Epithemia turgida*, *Grammatophora oceanica*, *Melosira*



Fig. 12 Palaeogeographic reconstruction, Akchagylian/Kuyalnikian (Late Pliocene). Key as for Fig. 7. The location of the Akchagylian stratotype is indicated.

arenaria, *M. scabrosa*, *M. sulcata*, *Navicula lyra* ssp. *elliptica*, *Nitzchia cocconeiformis*, *Rhopalodia parallelia*, *Surirella striatula*, *Terpsinoe musica* and *Triceratum* sp. *Campylodiscus noricus*, *C. noricus* ssp. *hibernica*, *Diploneis domblittensis*, *D. rombica*, *Melosira arenaria*, *M. scabrosa*, *M. sulcata* and *Rhopalodia parallelia* are exclusively fresh-water forms, while the remainder are quasi-marine.

The Akchagyl Beds of Northern Iran can be correlated with the stratotypical Akchagylian on ostracod evidence (Faridi, 1964; Stöcklin & Setudehnia, 1971, 1972). Various volcanics in Central Iran can also be tentatively correlated with the Akchagylian (Stöcklin & Setudehnia, *op. cit.*).

Nannopalaeontology. Stratigraphically significant calcareous nannofoossils recorded by Semenenko & Lulieva (1982) from the Akchagylian include *Discoaster brouweri* (NN8–NN18) (no younger than 1.89 Ma), *D. pentaradiatus* (NN9–NN17) (no younger than 2.33–2.43 Ma) and *Reticulofenestra pseudoumbilica* (NN7–NN15). These are similar to nannoflora found in the Kuyalnikian of the Black Sea region by Semenko & Pevzner (1979), and suggest a link between the two basins at this time.

Palynology. Only non-age-diagnostic palynomorphs have been recorded from the Akchagylian. Pollen spectra from 'Cryo'-SCT14 (and 'Thermo'-SCT15) are characterised by high incidences of *Abies* (fir), indicating a forested hinterland similar to that of the present-day taiga, and a cool, wet climate (Bludorova *et al.*, 1987). Those from 'Thermo'-SCT13 are characterised by *Abies* (fir), *Acer* (maple), *Carpinus* (hornbeam) and *Ulmus* (elm), indicating a warmer climate (Bludorova *et al.*, *op. cit.*). Pollen spectra from 'Cryo'-SCT14 in the Volga-Urals Region are characterised by relatively high incidences of *Lycopodiaceae* (club-mosses), again indicating a cool, wet climate (Yakhimovich *et al.*, 1965, 1983, 1984). Pollen spectra from 'Cryo'-SCTs 12 and 10 are characterised by alternations of *Alnus* (alder), *Betula* (birch) and *Pinus* (pine), indicating a cool, dry climate, and *Tsuga* (hemlock), indicating a warmer, wetter climate (Ananova, 1974; Bludorova *et al.*, 1987). Those from 'Thermo'-SCT11 in the Volga Basin are characterised by relatively high incidences of *Tsuga* (hemlock) (Zhidovinov *et al.*, 1987). Pollen spectra from the undifferentiated Akchagylian of the Tersko-Sunzhenskii Region are characterised by high incidences of broad-leaved tree taxa such as *Fagus* (beech) and *Quercus* (oak), indicating a forested hinterland similar to that of the present-day taiga (Broad-Leaved Forest Zone), and a warm-temperate climatic regime (Naidina, 1988).

Apsheronian

The Apsheronian takes its name from the Apsheron Peninsula in Eastern Azerbaijan (Likharev, 1958). It appears equivalent to the Gurian of the Black Sea (Pleistocene). Zubakov & Borzenkova (1990) calibrate it against magnetostratigraphic polarity epoch 2 (Matuyama). The Apsheronian is essentially regressive in character. Marine connections between the Caspian and the Black Sea were probably only intermittently developed.

Details of Apsheronian stratigraphy have been discussed by Livental (1929), Sultanov (1964), Kuliyeva (1968), Ushakova & Ushko (1971), Azizbekov (1972), Lupov *et al.* (1972), Ali-Zade (1973), Ivanova (1985), Zhidovinov *et al.* (1987) and Mamedova (1988).

Micropalaeontology. Stratigraphically and/or palaeoenviron-

mentally significant ostracods recorded by Kuliyeva (1968) and Mamedova (1984, 1988) from the Apsheronian of the Baku Archipelago in Azerbaijan include *Bakunella dorsoacuata*, *Candonia albicans*, *Caspiocypris lyrata*, *C. rotulata*, *C. sinistrolyrata*, *Caspiolla acronasuta*, *C. gracilis*, *Eucypris membranae*, *Leptocythere andrusovi*, *L. caspia*, *L. fragilis*, *L. multituberculata*, *L. propinqua*, *L. quinquetuberculata*, *L. turquianica*, *L. verrucosa*, *Loxoconcha eichwaldi*, *L. gibboida*, *L. impressa* and *Trachyleberis azerbaijanica*. *Bakunella*, *Caspiolla*, *Leptocythere*, *Loxoconcha* and *Trachyleberis* are quasi-marine forms, while *Candonia*, *Caspiocypris* and *Eucypris* are fresh-water (see, for instance, Yassini, 1986). At least six assemblage zones can be recognised on the basis of ostracods (D.N. Mamedova, pers. comm., 1994). These will be discussed in a forthcoming paper (Mamedova, *in press*) (see also Mamedova, 1988).

Stratigraphically and/or palaeoenvironmentally significant diatoms recorded by Ushakova & Ushko (1971) from the Akchagylian to Apsheronian of the Krasnovodsk Peninsula in Western Turkmenia are listed under 'Akchagylian' above. They include exclusively fresh-water, fresh-water to brackish, and brackish to near-normal marine forms.

The Apsheron Beds of Northern Iran can be correlated with the stratotypical Apsheronian on ostracod evidence (Faridi, 1964; Stöcklin & Setudehnia, 1971, 1972).

Palynology. Only non-age-diagnostic palynomorphs have been recorded from the Apsheronian. Pollen spectra described by Ivanova (1985) from the Apsheronian of Western Turkmenia and by Zhidovinov *et al.* (1987) from the Apsheronian of the Volga Basin are characterised by relatively high incidences of non-tree taxa. This indicates an open, sparsely forested hinterland similar to the present-day steppe or forest-steppe, and a cool-temperate climatic regime.

Bakunian

The Bakunian takes its name from the city of Baku in Eastern Azerbaijan (Likharev, 1958). It appears equivalent to the Chaudian of the Black Sea (Pleistocene). Zubakov & Borzenkova (1990) calibrate it against magnetostratigraphic polarity epochs 2 (Matuyama) to 1 (Brunhes).

Details of the Bakunian stratotype have recently been discussed by Mamedova (1984, 1985, 1993, and *in press*) and Aliyulla *et al.* (1985). Stratigraphically and/or palaeoenvironmentally significant ostracods recorded by Aliyulla *et al.* (*op. cit.*) include *Bakunella dorsoacuata*, *Caspiocypris filona*, *Graviacypris elongata*, *Leptocythere delicata*, *L. lunata*, *L. propinqua*, *Loxoconcha endocarpa*, *Pseudostenocypris asiatica* and *Xestoleberis ementis*. *Bakunella*, *Graviacypris*, *Leptocythere*, *Loxoconcha* and *Xestoleberis* are quasi-marine forms, while *Caspiocypris* and *Pseudostenocypris* are fresh-water (see, for instance, Yassini, 1986). Four assemblage zones can be recognised on the basis of ostracods (Mamedova, *in press*).

The Baku Formation of Northern Iran can be correlated with the stratotypical Bakunian on ostracod evidence (Faridi, 1964; Stöcklin & Setudehnia, 1971, 1972).

Khazarian, Girkan and Khvalynian

The Khazarian takes its name from an ancient tribe who lived in the area between the Don and Volga Rivers, and the Girkan(ian) and Khvalynian take theirs from ancient names for the Caspian

Sea (Likharev, 1958). The Khazarian, Girkan and Khvalynian appear equivalent to the Uzunlarian, Karangatian and Neoeuxinian respectively of the Black Sea (Pleistocene-Holocene). Zubakov & Borzenkova (1990) calibrate the Khazarian, Girkan and Khvalynian against magnetostratigraphic polarity epoch 1 (Brunhes).

Kuyalnikian to Neoeuxinian (Black Sea) (Fig. 12)

The Kuyalnikian to Neoeuxinian of the Black Sea appear equivalent to the Akchagylian to Khvalynian of the Caspian (Late Pliocene to Holocene). Details of Kuyalnikian to Neoeuxinian stratigraphy have been discussed by Wall & Dale (1973), Karmishina (1975), Vekua (1975), Kaplin (1977), Shikmus *et al.* (1977), Schrader (1979), Semenenko & Pevzner (1979), Shatilova (1984), Sirenko & Turlo (1986), Yanko (1990a–b, 1991), Balabanov *et al.* (1991) and Trubikhin *et al.* (1991a–b).

Kuyalnikian (Fig. 12)

The Kuyalnikian takes its name from a locality on the Danube Delta (Likharev, 1958). The Romanian appears synonymous. It appears equivalent to the Akchagylian of the Caspian. Zubakov & Borzenkova (1990) calibrate it against magnetostratigraphic polarity epochs 3 (Gauss) to 2 (Matuyama).

The Kuyalnikian/Akchagylian represents a major transgressive episode when Eastern Paratethys was reconnected with the world oceans (Fig. 12). During this time, marine plankton were introduced into Eastern Paratethys enabling calibration to global datums.

Details of Kuyalnikian stratigraphy have been discussed by Karmishina (1975), Vekua (1975), Semenenko & Pevzner (1979), Shatilova (1984) and Sirenko & Turlo (1986).

Micropalaeontology. Only the non-age-diagnostic, quasi-marine, smaller benthonic foraminifera *Ammonia beccarii* and *Elphidium incertum* were recorded by Karmishina (1975) from the Kuyalnikian of Prechernomore (Northern Black Sea).

Stratigraphically and/or palaeoenvironmentally significant ostracods recorded by Karmishina (1975) and Vekua (1975) from the Kuyalnikian of Prechernomore (Northern Black Sea) and Abkhazia (North-eastern Black Sea) respectively include *Bakunella dorsoacuta*, *Caspiocypris labiata*, *Caspiolla acronasuta*, *Cryptocyprideis bogatschovi*, *Cypria arma*, *Leptocythere andrusovi*, *L. circum sulcata*, *Loxoconcha eichwaldi*, *L. petasa*, *Mediocythereis apatoica* and *Pontoniella acuminata*. *Bakunella dorsoacuta*, *Caspiolla acronasuta* and *Loxoconcha petasa* are quasi-marine species (Yassini, 1986). *Caspiocypris acronasuta* and *Cypria arma* are fresh-water.

Nannopalaeontology. Stratigraphically significant calcareous nannofossils recorded by Semenenko & Pevzner (1979) from the Kuyalnikian include *Discoaster pentaradiatus* (NN9?–NN17) and *Reticulofenestra pseudoumbilica* (NN7?–NN15).

Palynology. Only non-age-diagnostic palynomorphs have been recorded from the Kuyalnikian. Pollen spectra from 'Thermo'-SCT15 are characterised by polydominance (Shatilova, 1984; Sirenko & Turlo, 1986).

Gurian

The Gurian takes its name from an ancient province of what is now Western Georgia (Likharev, 1958). It appears equivalent to

the Apsheronian of the Caspian (Pleistocene). Zubakov & Borzenkova (1990) calibrate it against magnetostratigraphic polarity epoch 2 (Matuyama).

Chaudian

The Chaudian takes its name from a promontory on the Kerch Peninsula (Crimea) (Likharev, 1958). It appears equivalent to the Bakunian of the Caspian (Pleistocene). Zubakov & Borzenkova (1990) calibrate it against magnetostratigraphic polarity epochs 2 (Matuyama) to 1 (Brunhes).

Uzunlarian, Karangatian and Neoeuxinian

The Uzunlarian takes its name from a lake, the Karangatian takes its name from a promontory on the Kerch Peninsula (Crimea), and the Neoeuxinian its name from an ancient name for the Black Sea (Likharev, 1958). The Uzunlarian, Karangatian and Neoeuxinian appear equivalent to the Khazarian, Girkan and Khvalynian respectively of the Caspian (Pleistocene-Holocene). Zubakov & Borzenkova (1990) calibrate the Uzunlarian, Karangatian and Neoeuxinian against magnetostratigraphic polarity epoch 1 (Brunhes).

Details of Uzunlarian, Karangatian and Neoeuxinian stratigraphy have been discussed by Schrader (1979) and Markova & Mikhaleska (1994). Schrader (1979) recorded the palaeoenvironmentally significant diatoms *Actinocyclus divisus*, *A. ochotensis*, *Cymatopleura solea* and *Stephanodiscus astraea* (which indicate a palaeosalinity range of 0.5–3.0 ppt). Markova & Mikhaleska (1994) recorded the ostracods *Amnicythere cymbula*, *Callistocythere alfera*, *C. lopalica*, *C. mediterranea*, *C. quinetuberculata* and *Loxoconcha immodalata* in the stratotypical Uzunlarian.

ACKNOWLEDGEMENTS. We wish to acknowledge our colleagues at the Azerbaijan Academy of Sciences, Baku, in particular Drs Elmira Ateava, Dilara Mamedova and Reyhan Koshkarly, for their assistance in procuring publications, for facilitating fieldwork, and for sharing their extensive knowledge with us. We also wish to acknowledge Dr. Fred Rögl of the Naturhistorisches Museum, Vienna, for his constructive critical review of the manuscript. BP Exploration provided drafting facilities and is thanked for permission to publish.

REFERENCES

- Abramova, T.O. 1982. Cyclicity of spore-pollen spectra in Quaternary deposits of the west coast of the Caspian Sea. In: Kovalev, S.A. *et al.* (editors). *Sea-coasts*: 32–39. Moscow (in Russian).
- 1985. Palynological study of bottom sediments from the Caspian Sea. *Vestnik Moskovskogo Universiteta, Seriya 5 (Geologiya)*. Moscow: 1985 (5): 77–83 (in Russian).
- Adamia, Sh., Lordkipanidze, M., Beridze, M., Kotetischvili, E. & Zutelia, Z. 1990. Paleogeography of the Ukrainian Carpathians, the Crimea and the Caucasus. In: Rakus, M., Dercourt, J. & Nairn, A.E.M. (editors). *Evolution of the Northern Margin of Tethys*. Vol. III: 123–146. Paris.
- Agalarova, D.A. 1956. *Microfauna of the Productive Series and the Red-Coloured Series in Turkmenia*. Ashkhabad: Akademia Nauk Turkmen SSR (in Russian).
- 1967. *Microfauna from Pontian Sediments of Azerbaijan and adjacent regions*. Leningrad ('Nedra') (in Russian).
- Kadirova, Z.K. & Kuliyeva, S.A. 1961. *Ostracoda in the Pliocene and Post-Pliocene deposits of Azerbaijan*. Azerbaijan Scientific Press (in Russian).
- Akramkhodzhaev, A.M., Babadagly, V.A. & Dzhumagulov, A.D. 1989. *Geology and exploration of oil- and gas-bearing ancient deltas*. Rotterdam (A.A. Balkema). English translation.
- Alekseyev, M.N. & Nikiforova, K.V. (editors). 1984. *The boundary between the*

- Neogene and Quaternary Systems in the USSR.* Moscow ('Nauka') (in Russian).
- Aleskerov, B.Dj., Mamedov, A.V., Svitoch, A.A. & Yanina, T.A. 1987. New data on the stratigraphy of the Mishovdag key section in the Pleistocene of Azerbaijan. *Izvestiya Akademii Nauk Azerbaijanskoi SSR, Seriya Nauk o Zemle, Baku.* **1987** (4): 50–57 (in Russian with English abstract).
- Alikhanov, E.N. 1977. *Oil and gas in the Caspian Sea.* Moscow ('Nedra') (in Russian).
- Aliyev, Ad. A. & Aliyeva, L.I. 1970. Subdivision and correlation of Akchagylian deposits in western Azerbaijan. *Izvestiya Akademii Nauk Azerbaijanskoi SSR, Baku.* **26** (2): 56–61 (in Russian).
- Aliyulla, Kh., Vekilov, B.G. & Mamedova, D.N. 1985. On the division of the stratotype section of the Baku Horizon. *Izvestiya Akademii Nauk Azerbaijanskoi SSR, Seriya Nauk o Zemle, Baku.* **1985** (4): 89–93 (in Russian with English abstract).
- Ali-Zade, A.A. 1969. *Akchagylian of Azerbaijan.* Leningrad ('Nedra') (in Russian). — 1973. *Apsheronian of Azerbaijan.* Moscow ('Nedra') (in Russian).
- 1974. The Upper Pliocene in the Caspian Sea region: ideas resulting from recent studies. *Mémoires du Bureau de Recherches Géologiques et Minierès.* **2** (78): 729–731 (in French with English abstract).
- , Akhmedov, G.A., Akhmedov, A.M., Aliev, A.K. & Zeinalov, M.M. 1966. *Geology of the oil and gas fields of Azerbaijan.* Moscow (in Russian).
- & Aleskerov, J.A. 1974. Stages of Sarmatian fauna development and their role in the establishment of biostratigraphic boundaries in Azerbaijan. *Izvestiya Akademii Nauk Azerbaijanskoi SSR, Seriya Nauk o Zemle, Baku.* **1974** (4): 3–8 (in Russian with English abstract).
- Ali-Zade, A.A., Ateava, E.Z., Koshkarly, R.O., Mamedova, D.N., Simmons, M.D. & Jones, R.W. 1994a. The biostratigraphy of the Neogene sediments of Eastern Azerbaijan and the South Caspian Basin. *Biosstratigraphy of Oil and Gas Basins.* St. Petersburg, Abstracts: 7–8. VNIGNI Publication.
- , —, —, — & — In press. The biostratigraphy of the Neogene sediments of Eastern Azerbaijan and the South Caspian Basin. In: Jakovleva, S. (ed.) *Biosstratigraphy of Oil and Gas Basins.* St. Petersburg, Proceedings VNIGNI (in Russian).
- , Gulyev, I.S., Ateava, E.Z., Koshkarly, R.O., Mamedova, D.N., Suleymanova, S.F., Bowman, M.B.J., Brayshaw, A.C., Geehan, G., Henton, J., Jones, R.W., Reynolds, A.D., Simmons, M.D., Varney, T., Samways, G.M., Prenac, P. & Allen, L.O. 1995. Neogene stratigraphy and sedimentology in eastern Azerbaijan: outcrop observations and subsurface implications. *American Association of Petroleum Geologists, Bulletin.* **79:** 1193.
- , Suleymanova, S.F., Bowman, M.B.J., Simmons, M.D., Brayshaw, A. & Reynolds, A.D. 1994b. Outcrop analogue studies and reservoir description, the Neogene Productive Series, Apsheron Peninsula, Eastern Azerbaijan. *Proceedings of the EAPG Meeting.* St. Petersburg, 1994.
- Ali-Zade, K.A. 1936. Fauna of the Akchagylian Beds of Naftalan. *Trudy Azerbaijanskogo Nauchno-Issledovatel'skogo Neftyanogo Instituta,* **32** (in Russian).
- 1946. Analysis of fauna of the Productive Series. *Doklady Akademii Nauk Azerbaijanskoi SSR,* **6:** 3–10 (in Russian).
- 1954. *The Akchagylian Series of Azerbaijan.* Baku (in Russian).
- 1966. The stratigraphy of the Oligocene deposits of Azerbaijan. *Izvestiya Akademii Nauk Azerbaijanskoi SSR, Seriya Nauk o Zemle, Baku.* **1966** (1) (in Russian).
- & Aliyeva, L.I. 1989. New data on the age of the Super-Akchagylian Continental Series of the Naftalan section, Azerbaijan. *Izvestiya Akademii Nauk Azerbaijanskoi SSR, Seriya Nauk o Zemle, Baku.* **1989** (4): 121–122. (in Russian), with English abstract.
- & Atayeva, E.Z. 1982. Composition and stratigraphy of Paleogene-Miocene rocks in western Azerbaijan. *Trudy Instituta Geologii Akademii Nauk Azerbaijanskoi SSR, Baku.* **1982:** 60–69 (in Russian).
- , — et al. 1986. The Miocene of the south-east Caucasus and Lesser Caucasus. Pp. 222–239, in: Muratov, M.V. & Nevesskaya, L.A. *The Neogene System.* 419pp. Moscow (in Russian).
- & Mamedov, T.A. 1970. Stratigraphy of the Paleogene-Neogene boundary in Azerbaijan. *Izvestiya Akademii Nauk Azerbaijanskoi SSR, Seriya Nauk o Zemle, Baku.* **1970** (3–4): 72–80 (in Russian with English abstract).
- Ananova, Ye. N. 1974. *The Neogene pollen deposits of the south of the Russian Plain.* Leningrad (Publishing House of Leningrad University) (in Russian).
- , Volkova, N.S., Zubakov, V.A., Pavlovskaya, V.I. & Remizovsky, V.N. 1985. New data on Taman key section of the Mio-Pliocene Black Sea region. *Doklady Akademii Nauk Soyuz Sotsialisticheskikh Respublik, Leningrad.* **284** (4): 925–928 (in Russian).
- Andalibi, M.J. 1991. Recent changes in Caspian Sea level. *Abstracts, XIII INQUA International Congress, Beijing, China, 1991:* 8.
- Andreescu, I. 1981. Middle Upper Neogene and Early Quaternary chronostratigraphy from the Dacic Basin and correlations with neighbouring areas. *Annales Géologiques des Pays Helléniques hors sér.*, **4:** 129–138.
- Andrusov, N.I. 1884. Geological studies in the Peninsula of Kerch in 1882 and 1883. *Notes Soc. Natur. Novoruss.* **9** (2) (in Russian).
- Azizbekov, Sh. A. (editor). 1972. *Geology of the USSR.* vol XLVII: Azerbaijan SSR. Moscow ('Nedra') (in Russian).
- Azizbekova, I.A. 1974. Facies of Sarmatian deposits of the Nakchichevan Depression. *Izvestiya Akademii Nauk Azerbaijanskoi SSR, Seriya Nauk o Zemle, Baku.* **1974** (2): 10–18 (in Russian with English abstract).
- Babayan, D.A. 1984. Features of the correlation of Pliocene deposits of uplifts of the Livanov Group and the Apsheron Archipelago. *Izvestiya Akademii Nauk Turkmenskoi SSR, Otdelenie Fiziko-Tekhnicheskikh, Khimicheskikh i Geologicheskikh Nauk, Ashkhabad.* **1984** (5) (in Russian).
- Bagir-Zade, F.M., Narimanov, A.A. and Babayev, F.R. 1988. *Geological and geochemical features of the Caspian Sea fields.* Moscow ('Nedra').
- Balabanov, I., Yanko, V.V., Ismaylov, J. & Gey, N. 1991. The Holocene history of the Black Sea Basin. *Abstracts, XIII INQUA International Congress, Beijing, China, 1991:* 15.
- Baldi, T. 1980. The early history of Paratethys. *Bulletin of the Hungarian Geological Society.* **110:** 456–472 (in Hungarian with English summary).
- Baldi, T. 1984. The terminal Eocene and Early Oligocene Events in Hungary and the separation of an anoxic, cold, Paratethys. *Eclogae Geologicae Helvetica.* **77:** 1–28.
- Beard, J.H., Sangree, J.B., & Smith, L.A. 1982. Quaternary chronology, paleoclimate, depositional sequences and eustatic cycles. *American Association of Petroleum Geologists Bulletin.* **66** (2): 158–169.
- Benyamovskoy, V.N., Cheltsov, Yu. G., Musikhin, V.P., Romanyuk, B.N. & Koblova, F.P. 1988. New data on the stratigraphy of the Neogene deposits of the eastern Caspian Depression. *Paleontologicheskii Sbornik, Lvov.* **25:** 91–97 (in Russian).
- & Naidina, O.D. 1990. Faunal and palynological complexes of the Akchagylian of the Ural-Uil interfluve, Eastern Precaspian. *Izvestiya Vuzov Geologiya i Razvedka.* **9:** 20–27 (in Russian).
- Bernor, R.L., Brunet, M., Ginsburg, L., Mein, P., Pickford, M., Rögl, F., Sen, S., Steininger, F. & Thomas, H. 1987. A consideration of some major topics concerning Old World Miocene mammalian chronology, migrations and paleogeography. *Geobios.* **20** (4): 431–439.
- , Mittmann, H.-W. & Rögl, F. 1993. Systematics and chronology of the Gotzendorf 'Hipparium' (Late Miocene, Pannonian F, Vienna Basin). *Annalen des Naturhistorischen Museums Wien.* **95** (A): 101–120.
- Blow, W.H. 1969. Late Middle Eocene to Recent planktonic foraminiferal biostratigraphy. In: Brönnimann, P. & Renz, H.H. (editors), *Proceedings of the First International Conference on Planktonic Microfossils,* Geneva, 1967: 199–412. Leiden.
- Bludorova, Ye. A., Dorofeev, L.I., Nikolaeva, K.A., Sidnev, A.V., Stepanov, L.A., Yasnov, P.G. & Yakhimovich, V.L. 1987. Lower Kama Basin. In: Alekseyev, M.N. & Nikiforova, K.V. (editors), *The boundary between the Neogene and Quaternary Systems in the USSR:* 38–44. Moscow ('Nauka') (in Russian).
- Bogdanowicz, A.K. 1947. Results of the investigations of Miocene foraminifera from the Crimea and Caucasus. *Trudy Vsesoyuznogo Neftyanogo Nauchno-Issledovatel'skogo Geologo-Razvedochnogo Instituta (VNIGRI), Leningrad & Moscow.* **1947:** 5–33 (in Russian).
- 1950a. Stratigraphical subdivision of the Tarkhanian of Kuban on the basis of foraminiferal investigations. *Trudy Vsesoyuznogo Neftyanogo Nauchno-Issledovatel'skogo Geologo-Razvedochnogo Instituta (VNIGRI), Novaya Seriya, Leningrad & Moscow.* **51:** 113–128 (in Russian).
- 1950b. Tschokrakan Foraminifera of the western Precaucasus. *Trudy Vsesoyuznogo Neftyanogo Nauchno-Issledovatel'skogo Geologo-Razvedochnogo Instituta (VNIGRI), Novaya Seriya, Leningrad & Moscow.* **51:** 129–176 (in Russian).
- 1965. New data on Konkian Miliolidae from the western Precaucasus. *Trudy Vsesoyuznogo Neftyanogo Nauchno-Issledovatel'skogo Geologo-Razvedochnogo Instituta (VNIGRI), Paleontologicheskii Sbornik 2, Leningrad & Moscow.* **16:** 34–49 (in Russian).
- 1967. New types of Articuline from the Maeotian of Kuban. *Paleontologicheskii Zhurnal, Moscow.* **1:** 131–132 (in Russian).
- 1969. Maeotian Miliolidae from the western Precaucasus. *Trudy Vsesoyuznogo Neftyanogo Nauchno-Issledovatel'skogo Geologo-Razvedochnogo Instituta (VNIGRI), Leningrad.* **152:** 115–125.
- Bolli, H.M. & Krasnenikov, V.A. 1977. Problems in Paleogene and Neogene correlations based on planktonic foraminifera. *Micropaleontology.* **23** (4): 436–452.
- Boomer, I. 1993a. Palaeoenvironmental indicators from Late Holocene and contemporary Ostracoda of the Aral Sea. *Palaeogeography, Palaeoclimatology, Palaeoecology.* **103:** 141–153.
- 1993b. Sub-fossil Ostracoda and the death of the Aral Sea. *Geology Today (Jan.–Feb. 1993):* 18–22.
- Brzobohaty, R. 1983. *Fish otoliths from the West Carpathian Tertiary and their biostratigraphic significance.* In, Thon, A. (editor), *Miscellanea*

- Micropaleontology*: 247: 266. Hodonin.
- Bugrova, E.M.** 1986. Detail of biostratigraphic division of the Eocene of the Krasnovodsk Peninsula and the Karabogaz'ya region according to foraminifera. In, Krymgol'ts, G. Ya. & Belenkova, V.S. (editors), *Paleontology and Detailed Stratigraphic Correlation*: 41–49. Leningrad ('Nauka') (in Russian).
- Bukry, D.** 1974. Coccoliths as paleosalinity indicators – evidence from the Black Sea. In, Degens, E.T. & Ross, D.A. (editors), *The Black Sea – Geology, Geochemistry and Biology*: 353–363. Tulsa.
- Buryakovskiy, L.A.** 1974. Distribution patterns of oil and gas deposits within the Apsheron Archipelago. *International Geological Review*, **16** (7): 749–758.
- 1993. Outline of general and petroleum geology in Azerbaijan and the South Caspian Basin. *Bulletin of the Houston Geological Society*. February 1993: 16–47.
- Chelidze, A.L.** 1973. Correlation of the Pontian from the Euxinian and Caspian Basins. *Sooobshcheniya Akademii Nauk Gruzinskoi SSR*. Tbilisi, **71** (3): 645–648 (in Russian with English abstract).
- Chepalyga, A.L.** 1985. Climatic and eustatic fluctuations in the Paratethys Basin's history. *Abstracts. VII Congress, Regional Commission on Mediterranean Neogene Stratigraphy (RCMNS)*, Budapest, 1985: 134–136.
- 1991. Pleistocene Black Sea level changes and ecological consequences. *Abstracts. XIII INQUA International Congress*, Beijing, China, 1991: 56.
- , **Korotkevich, E.L.**, **Trubikhin, V.M.** & **Svetlitskaya, T.V.** 1985. Chronology of the Eastern Paratethys regional stages and Hippocrate events according to palaeomagnetic data. *Abstracts. VII Congress, Regional Commission on Mediterranean Neogene Stratigraphy (RCMNS)*, Budapest, 1985: 137–139.
- Chumakov, I.S.**, **Byzova, S.L.** & **Ganzev, S.S.** 1988. Maeotian to Pontian geochronology of Eastern Paratethys. *Doklady Akademii Nauk SSSR*, **303** (1): 178–181 (in Russian).
- , — & — 1992a. *Cenozoic geochronology and correlation of Eastern Paratethys*. Moscow ('Nauka') (in Russian).
- , —, —, **Arias, C.**, **Bigazzi, G.**, **Bonadonna, F.P.**, **Hadler Neto, J.C.** & **Norelli, P.** 1992b. Interlayered fission track dating of volcanic ash levels from Eastern Paratethys: a Mediterranean-Paratethys correlation. *Palaeogeography, Palaeoclimatology, Palaeoecology*, **95**: 287–295.
- , **Ganzev, S.S.**, **Byzova, S.L.**, **Dobrynina, V.Ya.** & **Paramonova, N.P.** 1984. Sarmatian geochronology of Eastern Paratethys. *Doklady Akademii Nauk SSSR*, **276** (5): 1189–1193 (in Russian).
- Cicha, I.**, **Marinescu, F.** & **Senes, J.** 1975. *Correlation du Neogene de la Paratethys Centrale*. Prague.
- , **Senes, J.** & **Tejkal, J.** 1967. *Chronostratigraphie und Neostratotypen Miozan der Zentralen Paratethys. I. Karpatien*. Bratislava.
- , **Zapletalova, I.**, **Molchikova, V.** & **Brozobohaty, R.** 1983. Stratigraphical range of Egean-Burgian-Badenian Foraminifera in West Carpathian Basins. In, Thon, A. (editor), *Miscellanea Micropaleontology*: 99–144. Hodonin.
- de Deckker, P.** 1981. Ostracods of athalassic saline lakes. *Hydrobiologia*, **81**: 131–144.
- Demarcq, J.** 1985. Paleothermic evolution during the Neogene in Mediterranean through the marine megafauna. *Abstracts. VII Congress, Regional Commission on Mediterranean Neogene Stratigraphy (RCMNS)*, Budapest, 1985: 176–178.
- Dercourt, J.**, **Ricou, L.E.**, **Adamia, Sh.**, **Csaszar, G.**, **Funk, H.**, **Lefelf, J.**, **Rakus, M.**, **Sandulescu, M.**, **Tollmann-A.** & **Tchoumachenko, P.** 1990. Anisian to Oligocene paleogeography of the European margin of Tethys (Geneva to Baku). In, Rakus, M., Dercourt, J. & Nairn, A.E.M. (editors), *Evolution of the Northern Margin of Tethys*. Vol. III: 159–190. Paris.
- Dmitriev, A.V.**, **Nazarov, N.O.**, **Nigarov, A.** & **Uzakov, O.** 1969. Studies on the Akchagylian of Turkmenia. *Izvestiya Akademii Nauk Turkmensoi SSR. Seriya Fiziko-Tekhnicheskikh, Khimicheskikh i Geologicheskikh Nauk*. Ashkhabad, 1969 (3): 125–127 (in Russian).
- Dumitrica, P.** 1985. Silicoflagellates – biostratigraphic and paleogeographic markers for Middle Miocene of Central Paratethys. *Abstracts. VII Congress Regional Commission on Mediterranean Neogene Stratigraphy (RCMNS)*, Budapest, 1985: 188–190.
- Dzhabarova, Kh.S.** 1966. The lithostratigraphic and geochemical characteristics of the Akchagylian deposits in the eastern part of the Kura Basin. *Izvestiya Akademii Nauk Azerbajianskoi SSR. Seriya Nauk o Zemle*, 1966 (5): 3–7 (in Russian).
- 1973. Stratigraphic subdivision of Middle Miocene deposits of Middle Kura Depression on palynological data. *Palinologiya Kaynofita*. Moscow, 1973: 173–177 (in Russian with English abstract).
- 1978. Development of Neogene flora of Azerbaijan on the basis of palynological data. *Izvestiya Akademii Nauk Azerbajianskoi SSR. Seriya Nauk o Zemle*, Baku, 1978 (5): 60–65 (in Russian with English abstract).
- 1980. Developmental stages of the Upper Palaeogene and Neogene floras of Azerbaijan according to palynological data. *Proceedings of the Fourth International Palynological Conference*, Lucknow, 1975–1976, **2**: 747–749.
- Dzhanelidze, O.I.** 1970. *Foraminifera of the Lower and Middle Miocene of Georgia*. Tbilisi: 'Metsnerieva' (in Russian).
- 1977. *Polymorphinids of the Miocene of Georgia*. Tbilisi: 'Metsnerieva' (in Russian).
- , **Vekua, M.L.** & **Maizuradze, L.S.** 1985. *Development of Ostracod and Foraminifera Fauna of the Neogene Black Sea/Caspian Sea Zone*. Tbilisi: 'Metsnerieva' (in Russian).
- Faridi, Z.** 1964. Ostracods in the Plio-Pleistocene sediments of Gorgan and Mazanderan (Northern Iran). *Iran Petroleum Institute Bulletin*, **14**: 534–535.
- Fedkovich, Z.N.** 1978. Comparative analysis of complexes of Akchagylian mollusks in the Northern Caspian Depression, the Southern Volga region near Kuibyshev and the Uralian Foredeep near Drenburg, and at the same time in Turkmenia and Azerbaijan. *Voprosy Paleontologii i Stratigrafii Azerbajani*. Baku, 1978: 51–61 (in Russian).
- Fedorov, P.V.** 1994. Some problems concerning the geological history of the Caspian Sea. *Stratigraphy and Geological Correlation*, **2** (2): 71–79.
- Gasanov, T.A.** & **Kyazymov, T.M.** 1988. Paleogene and Neogene sediment accumulation in eastern Lesser Caucasus. *Soviet Geology*, Moscow, **1988** (3): 62–70.
- Gasanova, M.S.** 1965. *Diatomaceous flora of the Middle and Upper Miocene of Kobustan (eastern Azerbaijan)*. First All-Union Palaeontological Council, Novosibirsk (in Russian).
- Ghanbari, E.** 1991. Neogene-Quaternary tectonics in Azerbaijan area (Iran). *Abstracts. XIII INQUA International Congress*, Beijing, China, 1991: 47.
- Gheorghian, M.** 1974. Distribution pattern of benthonic foraminifera on continental shelf of Black Sea off Romanian shore. In, Degens, E.T. & Ross, D.A. (editors), *The Black Sea – geology, geochemistry and biology*: 411–419. Tulsa.
- Gofman, A.A.** 1966. *Ecology of the contemporary and Novocaspian ostracods of the Caspian Sea*. Moscow ('Nauka') (in Russian).
- Gramann, F.** 1971. Brackish or hyperhaline? Notes on paleoecology based on Ostracoda. *Bulletin du Centre de Recherche de Pau*, **5**: 93–99.
- Grichuk, V.P. (editor).** 1973. *Pliocene and Pleistocene palynology*. Moscow ('Nauka') (in Russian).
- 1984. Late Pleistocene vegetation history. In, Velichko, A.A. (editor), *Late Quaternary environments of the Soviet Union*: 155–178. London (Longman) (English translation).
- , **Gurtovaya, Ye. Ye.**, **Zelikson, E.M.** & **Borisova, O.K.** 1984. Methods and results of Late Pleistocene paleoclimatic reconstruction. In, Velichko, A.A. (editor), *Late Quaternary Environments of the Soviet Union*: 251–260. London (Longman) (English translation).
- Grishanov, A.N.**, **Yeremin, V.N.**, **Imnadze, Z.A.**, **Kitovani, T.G.**, **Molotovskiy, E.A.** & **Torozov, R.I.** 1983. Stratigraphy of Upper Pliocene and Lower Pleistocene of Fouri (western Georgia) from paleontology and paleomagnetism. *Byulleten' Komissii po Izucheniiu Chetvertichnogo Perioda*, **52**: 18–28 (in Russian).
- Haq, B.U.**, **Hardenbol, J.** & **Vail, P.R.** 1988. Mesozoic and Cenozoic chronostratigraphy and eustatic cycles. In, Wilgus, C.K. et al. (editors), *Sea-level changes: an integrated approach*: 71–108. Society of Economic Paleontologists and Mineralogists (Special Publication, No. 42).
- Hsu, K.J.** 1983. *The Mediterranean was a desert: a voyage of the Glomar Challenger*. Princeton (University Press).
- Imnadze, Z.A.** 1964. Some data on the ostracods of the Pliocene deposits of western Georgia. *Voprosy Geologii Gruzi*. Acad. Nauk. Gruzinsh SSR. Geol. Inst., XXII Sess., 365–371 (in Russian).
- 1974. Ostracods of the Pliocene of Western Georgia. *Trudy Vsesoyuzny Nauchno-Issledovatel'skii Geologorazvedochnyi Neftyanoi Institut (VNIGNI)*, Leningrad, **152**: 126–133.
- & **Karmishina, G.I.** 1980. Comparison of Pliocene Ostracoda complexes in the northern and eastern Black Sea Region. *Voprosy Stratigrafi*, Leningrad, **5**: 131–148 (in Russian).
- Iossofova, Yu. I.** 1985. The Neogene history of the Palaeo-Don Basin. *Abstracts. VII Congress Regional Commission on Mediterranean Neogene Stratigraphy (RCMNS)*, Budapest, 1985: 271–273.
- Ismailov, K.A.** & **Idrisov, V.G.** 1963. *Oil and gas deposits of the eastern part of the Apsheron Peninsula*. Baku (Inst. Akad. Nauk Azerbajian. SSR).
- , — & **Tagiev, E.A.** 1972. *The Productive Series of the Baku Archipelago*. Baku ('Elm').
- Ivanova, N.G.** 1985. Palynological evaluation of Apsheron deposits of western Turkmenia. In, Grichuk, V.P. & Zaklinskaya, E.D. (editors), *Palynology of the Quaternary Period*: 158–167. Moscow ('Nauka') (in Russian).
- Jiricek, R.** 1975. *Biozonen der Zentralen Paratethys*. Gbely, CSSR (NAFTA).
- 1983. Redefinition of the Oligocene and Neogene Ostracod zonation of the Paratethys. In, Thon, A. (editor) *Miscellanea Micropaleontology*: 195–236. Hodonin.
- Jones, R.W.** 1996. *Micropaleontology in Petroleum Exploration*. Oxford University Press.
- Kaplin, P.A. (editor).** 1977. *Paleogeography and deposits of the Pleistocene of the southern seas of the USSR*. Moscow ('Nauka') (in Russian).
- Karmishina, G.I.** 1975. *Pliocene Ostracoda from the southern (European) USSR*. Saratov (Izd. Saratovskogo Univ.) (in Russian).
- Keraudren, B.** & **Thibault, C.** 1987. On the Plio-Pleistocene formations of the Iranian sector of the Caspian Sea. *Proceedings. International Symposium on*

- Shallow Tethys 2, Wagga Wagga: 141–149 (in French).*
- Kerimov, V.U., Khalilov, E.A. & Mekhtiev, N.U. 1991. The paleogeographic conditions in the formation of the South Caspian Depression in the Pliocene in connection with its gas- and oil-bearing capacity. *Geología Nefti y Gazu*, **10**: 5–8 (in Russian with English abstract).
- Khaïn, V., Apressov, S. & Nirtchink, M. 1937. *Petroleum excursion notes (Azerbaijanian Soviet Socialist Republic)*. Moscow, Leningrad.
- Khalilov, D.M. 1946. Microfauna of the Productive Series of Azerbaijan. *Doklady Akademii Nauk Azerbaijanskoi SSR*, **6**: 11–21 (in Russian).
- & Mamedova, L.D. 1973. Zonal subdivision of Paleogene sediments in Azerbaijan based on foraminifera. *Ocherki po Geologii Azerbaijanskoi SSR, Baku*, **1973**: 218–226 (in Russian).
- Khotinskiy, N.A. 1984. Holocene climatic change. In, Velichko, A.A. (editor), *Late Quaternary Environments of the Soviet Union*: 179–200. London (Longman) (English translation).
- Kleshev, K.A., Shein, V.S. & Clavkin, V.S. 1992. New concepts of geological structure and oil and gas presence in western Turkmenia. *Geologiya Nefti i Gazu*, **5**: 2–6 (in Russian).
- Klopotovskaya, N.B. 1991. The Caucasus at the coldest time of the last glaciation. *Abstracts, XIII INQUA International Congress, Beijing, China, 1991*: 164–165.
- Knystautas, A. 1987. *The natural history of the Soviet Union*. London (Century).
- Kopp, L.M. 1970. Upper Pliocene stratigraphy in the western branches of the Kopet Dag. *Izvestiya Vysshikh Uchebnykh Zavedenii, Geologiya i Razvedka, Moscow*, **6**: 14–20 (in Russian).
- Korenova, E.V. & Kartashova, G.G. 1978. Palynological study of samples from Holes 379A, 380A, Leg 42B. *Initial Reports of the Deep Sea Drilling Project*, **42B**: 951–992.
- Koshkarly, R.O. 1986. Features of nannoplankton distribution in the Paleogene deposits of Azerbaijan. *Izvestiya Akademii Nauk Azerbaijanskoi SSR, Seriya Nauk o Zemle, Baku*, **1986**(1): 107–110 (in Russian with English abstract).
- 1993. Calcareous nannoplankton biostratigraphy of the Palaeogene deposits of Azerbaijan. *Knikhovnicka ZPN*, **14B**(2): 63–68.
- & Alekperov, N. 1993. Biostratigraphy of the Paleogene deposits of Azerbaijan by nannoplankton. *Abstracts, Geological Congress of Turkey, 1993*: 50.
- & Baldi-Beke, M. 1987. Correlation of the Paleogene deposits of Azerbaijan and Hungary by nannoplankton. *Acta Geologica Hungarica*, **30**(3–4): 289–298.
- Krakhmalnaya, T.V., Svetlikskaya, T.V. & Chepalyga, A.L. 1993. New data on stratigraphy, magnetostratigraphy and mammal faunas of the late Miocene locality of Novaya Emetovka (Ukrainia). *Newsletters on Stratigraphy*, **29**: 77–89.
- Krasnenikov, V.A. 1986. The Kuban River sequence (USSR, North Caucasus). In, Pomerol, Ch. & Premoli Silva, I. (editors), *Terminal Eocene Events*: 137–139. Amsterdam (Elsevier).
- & Muzylov, N.G. 1975. Relationship between the zonal scales based on planktonic foraminifera and nannoplankton in Paleogene sections of the north Caucasus. *Voprosy Mikropaleontologii, Moscow*, **1975**: 212–224 (in Russian with English abstract).
- & Ptukhian, A.E. 1985. Stratigraphical subdivision of Paleogene deposits of Armenia by planktonic foraminifers, nannoplankton and nummulites (Pt. I, reference Paleogene sections of Armenia). *Voprosy Mikropaleontologii, Moscow*, **1985**: 130–169 (in Russian with English abstract).
- & Ptukhian, A.E. 1986. Stratigraphical subdivision of Armenian Paleogene deposits by planktonic microfossils and nummulites (regional stratigraphy, zonal scales by planktonic and benthonic microfossils, their correlation). *Voprosy Mikropaleontologii, Moscow*, **1986**: 60–98 (in Russian with English abstract).
- Kretzoi, M. 1985. Sketch of the biochronology of the Late Cenozoic in Central Europe. Pps. 3–20, in Kretzoi, M. & Pecsi, M. (editors): *Problems of the Neogene and Quaternary in the Carpathian Basin*. Budapest (Akademiai Kiado).
- Krhovsky, J. 1985. Central Paratethys ecostratigraphic correlations in relation to the Oligocene sea-level changes. *Abstracts, VII Congress Regional Commission on Mediterranean Neogene Stratigraphy (RCMNS), Budapest, 1985*: 333–335.
- Krstic, N. 1976. Pontian ostracodes in Paretethys and Tethys. *Proceedings, VI Congress Regional Commission on Mediterranean Neogene Stratigraphy (RCMNS), Bratislava, 1975*: 325–330.
- Kuliyeva, S.A. 1968. Stratigraphy of the Apsheron Suite in the Baku Archipelago according to microfaunas. *Doklady Akademii Nauk Azerbaijanskoi SSR, Baku*, **24**(8): 52–54 (in Russian).
- Lamb, J.L., Wornardt, W.W., Huang, T.-C. & Dube, T.E. 1987. Practical application of Pleistocene eustacy in offshore Gulf of Mexico. *Special Publications of the Cushman Foundation for Foraminiferal Research*, **24**: 33–40.
- Likharev, B.K. (Dir.). 1958. U.R.S.S. *Lexique stratigraphique internationale*. Paris, II (1–4).
- Lindsay, E.H., Fahlbusch, V. & Mein, P. 1989. *European Neogene mammal chronology*. Plenum Press.
- Liwalent, V.E. 1929. *Ostracods from the Akchagyl and Apsheronian Beds of the Babazan Section*. Baku (Izd. Rabot Issled. Lab. Po Geol. Neft) (in Russian).
- Lupov, N.P., Semenovich, V.V. & Smirnov, L.N. (editors). 1972. *Geology of the USSR. Vol. XXII: Turkmenian SSR (Geological Description)*. Moscow ('Nedra') (in Russian).
- Luttig, G. & Steffens, P. 1976. *Paleogeographic atlas of Turkey from the Oligocene to the Pleistocene*. Hanover.
- Macarovici, N. & Cehan-Ionesi, B. 1962. Distribution des foraminifères sur la plate-forme continental du nord-ouest de la Mer Noire. *Travaux du Musée Historique Naturelle 'Gr. Antipa'*, Bucharest, **3**: 45–60.
- Maisuradze, P.C. 1971. *Sarmatian Foraminifera of Western Georgia*. Tbilisi, 'Metsnerieva' (in Russian).
- 1988. *Foraminifera of the Maeotian of West Georgia*. Tbilisi; 'Metsnerieva' (in Russian).
- Malava, E.V. & Kulikov, O.A. 1991. Late Pleistocene pollen floras from the dated loess sequence of Kopetdag (Turkmenia). *Abstracts, XIII INQUA International Congress, Beijing, China, 1991*: 229.
- Mamedov, A.V. & Aleskerov, B.D. 1985. Stratigraphy, chronology and paleogeography of the Pleistocene in Azerbaijan and the Caspian regions. *Izvestiya Akademii Nauk Azerbaijanskoi SSR, Seriya Nauk o Zemle, Baku*, **1985**(3): 46–54 (in Russian with English abstract).
- & — 1986. Stratigraphy, chronology and paleogeography of the Pleistocene in Azerbaijan. *Izvestiya Akademii Nauk SSSR, Seriya Geologicheskaya, Leningrad*, **1986**(1): 93–104 (in Russian).
- & Rabotina, Y.N. 1984a. Reconstruction of some climatic elements of the Upper Pliocene in Azerbaijan. *Izvestiya Akademii Nauk Azerbaijanskoi SSR, Seriya Nauk o Zemle, Baku*, **1984**(3): 15–22 (in Russian with English abstract).
- & — 1984b. The vegetation of Azerbaijan in the Early and Middle Pleistocene. *Izvestiya Akademii Nauk Azerbaijanskoi SSR, Seriya Nauk o Zemle, Baku*, **1984**(6): 10–16 (in Russian with English abstract).
- Mamedov, P.Z. 1989. Paleo-deltaic complexes in the north of the South Caspian Depression. *Petroleum Geology*, **25**(9/10): 344–346.
- Mamedova, D.N. 1984. The change of ostracod assemblages at the Apsheron/Baku boundary (materials of the Baku Horizon stratotype). *Izvestiya Akademii Nauk Azerbaijan SSR*, **1984**(2): 127–130 (in Russian, with English abstract).
- 1985. Ostracodes of the type Baku Stage. *Dep. VINITI*, **6**: 1–4 (in Russian).
- 1988. On the study of Ostracoda of the Apsheronian Stage in the Yasamal Valley. *Izvestiya Akademii Nauk Azerbaijan SSR*, **1988**(4): 53–57 (in Russian, with English summary).
- 1993. Ostracodes of the stratotype of Lower Pleistocene in the eastern Caucasus. *Abstracts, Geological Congress of Turkey, 1993*: 49.
- In press. Ostracod biostratigraphy of the Pliocene – Pleistocene sediments of eastern Azerbaijan. In, Simmons, M.D. (ed.) *Recent Developments in Micropalaontology in the Former Soviet Union*. Chapman & Hall.
- Mamedova, L.D. 1971. On the stratigraphy of Miocene deposits of north-eastern Azerbaijan in the light of the study of its microfauna. *Doklady Akademii Nauk Azerbaijan SSR, Baku*, **27**(7): 37–41 (in Russian with English abstract).
- 1987. The sequence of Miocene deposits in the Turzhanchay River valley. *Doklady Akademii Nauk Azerbaijan SSR, Baku*, **43**(6): 79–82 (in Russian with English abstract).
- & Mamedova, N.A. 1970. Paleogene stratigraphy near the village of Gadzhili in the Shemakha region, Azerbaijan. Based on Foraminiferal and Radiolarian Faunas. *Doklady Akademii Nauk Azerbaijan SSR, Baku*, **26**(9): 53–56 (in Russian).
- Mandelstam, M.I., Markova, P., Rozyeva, T.R. & Stepanaitas, N.E. 1962. *Ostracods from Pliocene and Post-Pliocene sediments of Turkmenistan*. Ashkhabad (Izd. Akad. Nauk Turkmen SSR) (in Russian).
- Markova, A.K. & Mikhalevskiy, K.D. 1994. Correlation of Pleistocene marine and continental deposits from the Northwestern Black Sea region. *Stratigraphy and Geological Correlation*, **2**(4): 388–394.
- Martini, E. 1971. Standard Tertiary and Quaternary calcareous nannoplankton zonations. In, Farinacci, A. (editor), *Proceedings of the Second International Conference on Planktonic Microfossils, Rome, 1969*: 739–785. Rome (Edizioni Tecnicoscientia).
- Mekhtiev, Sh.F. & Pashaly, N.V. 1987. Lithology of Middle Pliocene Deposits of the Southern Caspian and their correlation. In, *Lithology and Mineral Resources*: 56–72. Plenum Publishing Corporation.
- Mesaros, N. 1992. Nannoplankton zones in the Miocene deposits of the Transylvanian Basin. *International Nannoplankton Association Newsletter*, **13**(2): 59–60.
- Muratov, M.V. 1960. *A brief summary of the geological structure of the Crimean Peninsula*. Moscow (in Russian).
- & Nevesskaya, P.A. 1986. *Neogene System*. Moscow; Palaeontological Institute (in Russian).
- Murray, J.W. 1973. *Distribution and ecology of living benthic foraminiferids*. London (Heinemann Educational Books).
- 1991. *Ecology and palaeoecology of benthic foraminifera*. London (Longman Scientific & Technical).
- Muzylev, N.G. & Golovina, L.A. 1987. The link of the Eastern Paratethys and the world ocean in the early Middle Miocene. *Izvestiya Akademii Nauk SSSR, Seriya Geologicheskaya*, **12**: 67–73 (in Russian).

REVIEW OF STRATIGRAPHY OF EASTERN PARATETHYS

- Nagy, E. & Kokay, J. 1991. Middle Miocene mangrove vegetation in Hungary. *Acta Geologica Hungarica*, **34** (1/2): 45–52.

Nagy marosy, A. 1992. The response of the calcareous nannoplankton to the Early Oligocene separation of the Paratethys. *International Nannoplankton Association Newsletter*, **13** (2): 62–63.

Naidina, O.D. 1988. Palynological characteristics of Akchagyl deposits of the Tersko-Sunzhenskii petroleum region. *Moscow University Geology Bulletin*, **43** (4): 69–74 (in Russian).

— 1990a. The reconstruction of vegetation and climate of Ciscaucasia in the Akchagyl. *Moscow University Geology Bulletin*, **45** (3): 64–66 (in Russian).

— 1990b. Vegetation and climate changes in the Pliocene of the eastern Precaspian. *Byulleten' Moskovskogo Obshchestva Ispytatelei Prirody. Otdel Geologicheskii*, Moscow, **65** (6): 122–123 (in Russian).

— 1991a. Late Pliocene-Early Quaternary vegetation of the north Caspian area (with reference to palynological records). *Abstracts. XIII INQUA International Congress, Beijing*: 249.

— 1991b. *Palaeogeography of the eastern Precaucasus and the northern Precaspian during the Late Pliocene and the Eopleistocene*. Moscow (State University Dissertation) (in Russian).

— 1991c. Palynological assemblages from the Pliocene of the Precaucasus and Precaspian. *Byulleten' Moskovskogo Obshchestva Ispytatelei Prirody. Otdel Geologicheskii*, Moscow, **66** (1): 130–131 (in Russian).

Narimanov, A.A. 1993. The petroleum systems of the South Caspian Basin. In, Dore (ed.) *Basin Modelling: Advances and Applications*. 599–608. Amsterdam (Elsevier).

Nevezskaya, L.A., Goncharova, I.A., Ilijina, L.B., Paramonova, N.P., Popov, S.V., Bogdanovich, A.K., Gabunia, L.K. & Nosovskiy, M.F. 1984. Stratigraphic chart for the Neogene of the Eastern Paratethyan region. *Sovetskaya Geologiya, Moscow*, **9**: 37–49 (in Russian).

—, —, —, —, —, —, Voronina, A.A., Chepalyga, A.L. & Babak, E.L. 1987. History of Paratethys. *Annales de l'Institut Géologique de Hongrie, Budapest*, **70**: 338–342.

— & Nosovsky, M.F. 1985. Eastern Paratethys. In, Rögl, F. (editor), *Mediterranean and Paratethys Neogene: Report on Activity of the RCMNS Working Groups and Bibliography 1979–1984*: 55–58. Budapest.

— Tikhomirov, V.V. & Fedorov, P.V. 1985. Stratigraphy of Neogene-Quaternary deposits of the Euxinian-Caspian area. *Abstracts. VII Congress Regional Commission on Mediterranean Neogene Stratigraphy (RCMNS)*, Budapest, 1985: 413–415.

— Voronina, A.A., Goncharova, I.A., Ilijina, L.B., Paramonova, M.P., Popov, S.V., Chepalyga, A.L. & Babak, E.V. 1985. History of Paratethys. *Abstracts. VII Congress Regional Commission on Mediterranean Neogene Stratigraphy (RCMNS)*, Budapest, 1985: 416–419.

Nigarov, A.N. & Fedorov, P.V. 1987. Neogene-Quaternary boundary position in western Turkmenia. In, Alekseyev, M.N. & Nikiforova, K.V. (editors), *The boundary between the Neogene and Quaternary Systems in the USSR*: 95–103. Moscow ('Nauka') (in Russian).

Nikiforova, K.V. & Dodonov, A.Y. (editors). 1980. *The Neogene-Quaternary boundary*. Leningrad ('Nauka') (in Russian with some papers in English).

Nikishin, A.V. 1981. Sedimentation rhythms and the composition of Middle Pliocene sections of the southern Caspian region. In, Yudin, G.T. (editor), *Problems in the geology and petroleum- and gas-bearing possibilities of the southern Caspian Basin*: 60–66. Moscow ('Nauka') (in Russian).

Nosovsky, M.F. 1985. Correlation of the USSR South Neogene and Carpathian-Balkan Region. *Abstracts. VII Congress Regional Commission on Mediterranean Neogene Stratigraphy (RCMNS)*, Budapest, 1985: 424–426.

Olteanu, R. 1978. Ostracoda from DSDP Leg 42B. *Initial Reports of the Deep Sea Drilling Project*, **42B**: 1017–1038.

— 1989. The 'Cimpia Moment' (Late Miocene, Romania) and the Pannonian-Pontian boundary defined by ostracods. *Journal of Micropalaeontology*, **82** (2): 239–247.

Ozsayar, T. 1985. The Sarmatian deposits of northern Turkey. *Abstracts. VII Congress Regional Commission on Mediterranean Neogene Stratigraphy (RCMNS)*, Budapest, 434–436.

Pacht, J., Bowen, B., Shaffer, B.L. & Pottorf, W.R. 1990. Sequence stratigraphy of Plio-Pleistocene strata in the offshore Louisiana Gulf Coast: applications to hydrocarbon exploration. In, *Sequence Stratigraphy as an Exploration Tool: Concepts and Practices in the Gulf Coast*: 269–285. Gulf Coast Section, Society of Economic Paleontologists and Mineralogists (Proceedings of the Eleventh Annual Research Conference, Houston).

Panakhi, Sh. A. & Buare Mamadu Lamin. 1987. Problems concerning lithofacial characteristics of Upper Pliocene deposits of the Nizhnekurinsk region in connection with exploration for new oil and gas deposits. *Izvestiya Vysshikh Uchebnykh Zavedenii, Neft i Gaz*, **1987** (4): 14–18 (in Russian).

Papp, A. 1969. Die Koordinierung des Miozäns in der Paratethys. *Verhandlungen der Geologischen Bundesanstalt*, **1969** (1): 2–6.

—, Cicha, I., Senes, A. & Steininger, F. 1978. *Chronostratigraphie und Neostratotypen Miozän der Zentralen Paratethys VI: Badenien*. Budapest.

—, Grill, R., Janoschek, R., Kapounek, J., Kollmann, K. & Turnovsky, K. 1968. Zur Nomenklatur des Neogens in Österreich. *Verhandlungen der Geologischen Bundesanstalt*, **1968**: 9–27.

— Jambor, A. & Steininger, F.F. 1985. *Chronostratigraphie und Neostratotypen Miozän der Zentralen Paratethys. VII: Pannonien*. Budapest.

— Marinescu, F. & Senes, J. 1974. *Chronostratigraphie und Neostratotypen Miozän der Zentralen Paratethys. IV: Sarmatien*. Bratislava.

— & Schmid, M.E. 1985. The fossil foraminifera of the Tertiary Basin of Vienna: revision of the monograph by Alcide d'Orbigny (1846). *Abhandlungen der Geologischen Bundesanstalt*, **37**.

Paramonova, N.P., Ananova, E.N., Andreeva-Grigorovic, A.S., Belokryls, L.S., Gabunia, L.K., Grusinskaya, K.F., Kondkarian, S.O., Karmishina, G.I., Kozireno, T.F., Majusradze, L.S., Movlazade-Ateava, E.Z., Nevezskaya, L.A., Ponomareva, L.D., Roshka, V.N. & Chepalyga, A.L. 1979. Paleontological characteristics of the Sarmatian s.l. and Maeotian of the Ponto-Caspian area and possibilities of correlation to the Sarmatian s.str. and Pannonian of Central Paratethys. *Annales Géologiques des Pays Helléniques*, **1979**: 961–971.

Pevzner, M.A. & Vangengeim, E.A. 1985a. Magnetostratigraphy and correlation of biostratigraphic subdivisions of the Paratethyan and Mediterranean Neogene. *Abstracts. VII Congress Regional Commission on Mediterranean Neogene Stratigraphy (RCMNS)*, Budapest, 1985: 461–462.

— & — 1985b. On understanding of the range and stratigraphic position of the Pannonian. In, Kretzoi, M. & Pesci, M. (editors): *Problems of the Neogene and Quaternary in the Carpathian Basin*: 65–88. Budapest (Akademiai Kiado).

— & — 1993. Magnetostratigraphic age assignments of Middle and Late Sarmatian mammalian localities of the Eastern Paratethys. *Newsletters on Stratigraphy*, **29** (2): 63–75.

Podobina, V.M., Voroshilova, A.G., Ribina, O.I. & Kuzneshova, Z.V. 1956. *Information on microfacies of Middle and Upper Miocene deposits of Azerbaijan*. Azerbaijan Scientific Press (in Russian).

Pogacsas, Gy. 1985. Seismic stratigraphy as a tool for chronostratigraphy: the Pannonian Basin. *Abstracts. VII Congress Regional Commission on Mediterranean Neogene Stratigraphy (RCMNS)*, Budapest, 1985: 465–468.

— & Revesz, I. 1985. Seismic stratigraphy and sedimentological analysis of Neogene delta features in the Pannonian Basin. *Abstracts. VII Congress Regional Commission on Mediterranean Neogene Stratigraphy*, Budapest, 1985: 469–471.

Popescu, Gh. 1985. Microbiostratigraphic correlation of marine Middle Miocene in Central Paratethys. *Abstracts. VIII Regional Commission on Mediterranean Neogene Stratigraphy*, Budapest: 479–480.

Popkhadze, L.I. 1977. *Meotian Microfauna (Foraminifera and Ostracods) from Western Georgia*. Tbilisi. Akad. Nauk. Gruzinski SSR (in Russian).

— 1983 The foraminifera and ostracoda of the Tschokrakan sediments of western Georgia. *Sobschcheniya Acad. Nauk Gruzinski SSR*, **110**: 541–544 (in Russian).

— 1984. A new representative of the genus *Leptocythere* from the Tschokrakan sediments of western Georgia. *Sobschcheniya Acad. Nauk Gruzinski SSR*, **115**: 337–339 (in Russian).

—, Pursteladze, H.N. & Badzoshvili, T.I. 1980. On the Maeotian sediments of Abkhazia. *Sobschcheniya Acad. Nauk Gruzinski SSR*, **98**: 365–368 (in Russian).

Popov, S.V. & Voronina, A.A. 1985. Basins of Eastern Paratethys in Late Oligocene-Early Miocene. *Abstracts. VII Congress Regional Commission on Mediterranean Neogene Stratigraphy*, Budapest, 1985: 481.

Rahaghi, A. 1973. Étude de quelques grands foraminifères de la Formation de Qum (Iran Central). *Revue de Micropaléontologie*, **16** (1): 23–38.

Ramishvili, I. Sh. 1969. *The description of Black Sea flora of western Georgia and their Correlation with present-day flora*. Tbilisi ('Metsniereba') (in Russian).

Rasulov, E.A. 1986. Distribution of diatomaceous flora in the Miocene of Kobustan. *Material from the 5th Interdepartmental Stratigraphic Conference, Baku* (in Russian).

Rayevskiy, M.I. 1969. Paleogeography of the Late Pliocene. Eastern Turkmenia. *Soviet Geology*, **9**: 70–81.

Reynolds, A.D., Simmons, M.D., Henton, J., Varney, T., Hall, S., Bowman, M.B.J., Brayshaw, A.C., Suleymanova, S.F., Ateava, E.Z., Mamedova, D.N., Koshyk, R.O., Ali-Zade, Ak. A. & Guliyev, I.S. In press. Implications of outcrop geology for reservoirs in the Productive Series: Apsheron Peninsula. Azerbaijan. Submitted to *American Association of Petroleum Geologists, Bulletin*.

Riha, J. 1983. Sponge spicules of the Karpatian and Lower Badenian of the Carpathian Foredeep in Moravia, Czechoslovakia. In, Thon, A. (editor), *Miscellanea Micropalaeontologia*: 171–194. Hodonin.

Rögl, F. 1985a. Late Oligocene and Miocene planktonic foraminifera of the Central Paratethys. In, Bolli, H.M., Saunders, J.B. & Perch-Nielsen, K. (editors), *Plankton stratigraphy*: 315–328. Cambridge (University Press).

— (editor). 1985b. *Mediterranean and Paratethys Neogene: report on activity of the RCMNS working groups and bibliography 1979–1984*. Budapest.

—, Bernor, R.L., Dermitsakis, M.D., Müller, C. & Stancheva, M. 1991. On the Pontian correlation in the Aegean (Aegina Island). *Newsletters on Stratigraphy*, **24** (3): 137–158.

- & Steininger, F.F. 1983. Vom Zerfall der Tethys zu Meditarran und Paratethys. *Annalen des Naturhistorischen Museums Wien*, **85/A**: 135–163.
- & — 1984. Neogene Paratethys. Mediterranean and Indo-Pacific seaways. In, Brenchley, P. (editor), *Fossils and Climate*: 171–200. London.
- , — & Müller, C. 1978. Middle Miocene salinity crisis and paleogeography of the Paratethys (middle and eastern Europe). In, Ross, D.A., Nepochnov, Y.P. et al. (editors), *Initial Reports of the Deep Sea Drilling Project*, **42**: 985–990.
- , Zapfe, H., Bernor, R.L., Brzobohaty, R.L., Daxner-Hock, G., Draxler, I., Fejfar, O., Gaudant, J., Herrmann, P., Rabeder, G., Schultz, O. & Zetter, R. 1993. Die Primatefundstelle Götzendorf an der Leitha (Obermiözän des Wiener Beckens, Niederösterreich). *Jahrbuch der Geologischen Bundesanstalt*, **136** (2): 503–526.
- Ross, D.A., Nepochnov, Y.P. et al. (editors). 1978. *Initial Reports of the Deep Sea Drilling Project*, **42**.
- Royden, L.H. & Horvath, F. (editors). 1987. *The Pannonian Basin: a study in basin evaluation*. Tulsa, Oklahoma (American Association of Petroleum Geologists, Memoir No. 45).
- Rozjeva, T.R. 1971. Composition and stratigraphic distribution of the Tertiary ostracodes of Turkmenia. In, Vyalov, O.S. (editor), *Fossil Ostracoda*: 169–178. Jerusalem (Israel Program for Scientific Translation).
- Rusu, A. 1985. Oligocene events in Transylvania and the first separation of Paratethys. *Abstracts, VII Congress Regional Commission on Mediterranean Neogene Stratigraphy, Budapest*, 1985: 502.
- Savina, S.S. & Khotinskiy, N.A. 1984. Holocene paleoclimatic reconstruction based on the zonal method. In, Velichko, A.A. (editor), *Late Quaternary Environments of the Soviet Union*: 287–296. London (Longman) (English translation).
- Schrader, H.-J. 1979. Quaternary paleoclimatology of the Black Sea. *Sedimentary Geology*, **23**: 165–180.
- Semenenko, V.N. 1979. Correlation of Mio-Pliocene of the Eastern Paratethys and Tethys. *Annales Géologiques des Pays Helléniques*, **1979**: 1101–1111.
- 1984. *Stratigraphic correlation of the Upper Miocene and Pliocene of the Eastern Paratethys and Tethys (the Mediterranean)*. Moscow (State University Dissertation) (in Russian).
- & Lulieva, S.A. 1982. The problems of direct correlation in the Upper Miocene and Pliocene of the Eastern Paratethys and Tethys. *Izvestiya Akademii Nauk SSSR, Seriya Geologicheskaya*, **9**: 61–71 (in Russian).
- & — 1985. About the Miocene-Pliocene boundary in Paratethys. *Abstracts, VII Congress Regional Commission on Mediterranean Neogene Stratigraphy (RCMNS), Budapest*, 1985: 507–508.
- & Pevzner, M.A. 1979. Biostratigraphic and paleomagnetic correlation of the Miocene and Pliocene in the Pontic-Caspian region. *Izvestiya Akademii Nauk SSSR, Seriya Geologicheskaya*, **1979** (1): 5–15 (in Russian).
- Senes, J. 1973. Einleitung in Chronostratigraphie und Neostratotypen Miözän der Zentralen Paratethys. *Verlag Slowakischen Akademie Wissenschaftlichen, Bratislava*, **3**: 21–25.
- 1985a. The stratigraphic correlation of the Tethys-Paratethys Neogene. *Abstracts, VII Congress Regional Commission on Mediterranean Neogene Stratigraphy (RCMNS), Budapest*, 1985: 33–42.
- 1985b. Stratigraphic correlation Tethys-Paratethys Neogene: IGCP Project No. 25 (history and aims, organization, results). *Geologicky Zbornik, Bratislava*, **36** (6): 725–746.
- & Marinescu, F. 1974. Cartes paléogeographiques du Neogene de la Paratethys. *Mémoires du Bureau de Recherches Géologiques et Minières*, **88** (2): 767–774.
- Shatilova, I.I. 1984. Late Miocene vegetation of western Georgia. Tbilisi ('Metsniereba') (in Russian).
- Shchekina, N.A. 1979. *The history of flora and vegetation in the south of the European part of the USSR during the Late Miocene-Early Pliocene*. Kiev ('Naukova Dumka') (in Russian).
- Sheydayeva-Kuliyeva, Kh. M. 1966. *Ostracoda in the Pontian layer of Azerbaijan*. Ashkabad (Izd. Akad. Nauk Turkmen SSR) (in Russian).
- Shihlinski, A.S. 1967. *Geology and prospectivity of hydrocarbon deposits of the Pliocene of the Lower Kura Basin*. Baku.
- Shukhman, K.M., Komarov, A.V. & Grakova, I.V. 1977. Stratigraphy of the Upper Quaternary deep-sea sediments in the Black Sea. *Oceanology*, **17** (4): 443–446.
- Shishova, Z.A. 1955. New data from the study of diatomaceous algae in the Miocene of the Apscheron Peninsula. *Doklady Akademii Nauk Azerbajianskoi SSR, Baku*, **11** (6) (in Russian).
- Simmons, M.D., Ali-Zade, Ak.A., Allen, L.O., Atcava, E.Z., Baba-Zade, A.A., Brenac, P., Jones, R.W., Koshkarly, R.O., Mamedova, D.N. & Suleymanova, S.F. In Press. Biostratigraphy of the Neogene Succession in Eastern Azerbaijan. In, Simmons, M.D. (ed.), *Recent Developments in Micropalaeontology in the Former Soviet Union*. Chapman & Hall.
- Sirenko, N.A. & Turlo, S.I. 1986. *Development of the Ukrainian soil and vegetation through the Pliocene and Pleistocene*. Kiev ('Naukova Dumka') (in Russian).
- Skalbdyna, L.N. (editor). 1985. *Geological events in the history of the Pliocene and Pleistocene of southern and northern seas*. Moscow (Akad. Nauk SSSR) (in Russian).
- Slama, P. 1983. Lower Badenian Radiolaria in the Moravian part of the Carpathian Foredeep. In, Thon, A. (editor), *Miscellanea Micropalaentologia*: 145–170. Hodonin.
- Spiegler, D. von & Rögl, F. 1992. *Bolboforma* (Protoptypha, Incertae Sedis) im Oligoziän und Mioziän des Mediterränen und der Zentralen Paratethys. *Annalen des Naturhistorischen Museums Wien*, **94** (A): 59–95.
- Steininger, F.F. & Papp, A. 1979. Current biostratigraphic and radiometric correlations of Late Miocene Central Paratethys stages (Sarmatian s.str., Pannonian s.str. and Pontian) and Mediterranean stages (Tortonian and Messinian) and the Messinian event in the Paratethys. *Newsletters on Stratigraphy*, **8** (2): 100–110.
- , Rabeder, G. & Rögl, F. 1985. Land mammal distribution in the Mediterranean Neogene: a consequence of geokinematic and climatic events. In, Stanley, D.J. & Wezel, F.-C. (editors), *Geological Evolution of the Mediterranean Basin*: 559–571. New York (Springer-Verlag).
- & Rögl, F. 1979. The Paratethys history – a contribution towards the Neogene dynamics of the Alpine orogen (an abstract). *Annales Géologiques des Pays Helléniques*, **1979**: 1153–1165.
- & — 1984. Paleogeography and palinspastic reconstructions of the Neogene of the Mediterranean and Paratethys. In, Dixon, J.E. & Robertson, A.H.F. (editors), *The Geological Evolution of the Eastern Mediterranean*: 659–668. London.
- , Hochuli, P. & Müller, C. 1989. Lignite deposition and marine cycles: the Austrian Tertiary lignite deposits – a case history. *Sitzungsberichten der Österreichischen Akademie der Wissenschaften, Mathematisch-Naturwissenschaftliche Klasse, Abt. I*, **197** (5–10): 309–332.
- , — & Martini, E. 1976. Current Oligocene/Miocene biostratigraphic concept of the Central Paratethys (middle Europe). *Newsletters on Stratigraphy*, **4** (3): 174–202.
- , Senes, J., Kleeman, K. & Rögl, F. (editors). 1985. *Neogene of the Mediterranean Tethys and Paratethys: stratigraphic correlation tables and sediment distribution Maps*. Vienna (University Press).
- Stöcklin, J. & Setudehnia, A.O. 1971. *Stratigraphic Lexicon of Iran (Part I – Central North and East Iran; Part II – Southwest Iran)*. Tehran: Geological Survey of Iran (Report, 18).
- & — 1972. Iran. *Lexique Stratigraphique International*, **III** (9b).
- Subbotina, N.N., Pishchanova, L.S. & Ivanova, L.V. 1960. Stratigraphy of the Oligocene and Miocene deposits of the Pre-Carpathians according to the foraminifera. *Trudy Vsesoyuznogo Neftyanago Nauchno-Issledovatel'skogo Geolo-Razvedochnogo Instituta (VNIGRI)*. Leningrad & Moscow, **153**: 5–146 (in Russian).
- Sultanov, A.D. 1979. *Lithology of Akchagylian deposits of Azerbaijan*. Baku ('Elm') (in Russian).
- & Sheydayeva-Kuliyeva, Kh. M. 1969. On the lithofacial and faunistic characteristics of the Akchagyli deposits of Azerbaijan. *Doklady Akademii Nauk Azerbajianskoi SSR, Baku*, **25** (10): 47–49 (in Russian).
- Sultanov, E.T. 1985. Paleogeography of the Early and Middle Pleistocene in the southeastern Caucasus. *Izvestiya Akademii Nauk Azerbajianskoi SSR, Seriya Nauk o Zemle, Baku*, **1985** (6): 96–102 (in Russian with English abstract).
- Sultanov, K.M. 1964. *The Apsheron Stage in Azerbaijan*. Baku (in Russian).
- Suzin, A.V. 1956. *Ostracods of the Tertiary of the northern Pre-Caucasus*. Moscow (Gost. Ord. Tr. Krasn. Znam. Neft Inst. Gostoptekhizdat) (in Russian).
- Sveier, A.V. 1949. Basic morphology and systematics of Pliocene and Post-Pliocene ostracods. *Trudy Vsesoyuznogo Neftyanago Nauchno-Issledovatel'skogo Geolo-Razvedochnogo Instituta (VNIGRI)*. Novaya Seriya, Leningrad & Moscow, **30**: 1–106 (in Russian).
- Szczechura, J. 1985. *Bolboforma* and similar problematics from the Middle Miocene of Central Paratethys. *Abstracts, VII Congress Regional Commission on Mediterranean Neogene Stratigraphy (RCMNS), Budapest*, 1985: 541.
- Taner, G. 1985. Die Moluskenfauna der Neogenenschichten der Anatolischen Seite von Dardanellen. *Abstracts, VII Congress Regional Commission on Mediterranean Neogene Stratigraphy (RCMNS), Budapest*, 1985: 550–552.
- Tchoumachchenko, P., Cernjavska, S., Goranov, A., Kojuandgieva, E., Nachev, I., Tikolov, T., Ruskova, N., Sapunov, I. & Tronkov, D. 1990. Principal paleogeographic features of Bulgaria. In, Rakus, M., Dercourt, J. & Nairn, A.E.M. (editors), *Evolution of the Northern Margin of Tethys*. Vol. III: 101–121. Paris.
- Traverse, A. 1978. Palynological analysis of DSDP Leg 42B (1975) Cores from the Black Sea. *Initial Reports of the Deep Sea Drilling Project*, **42B**: 993–1015.
- Trubikhin, V.M. 1977. *Paleomagnetism and stratigraphy of Akchagylian deposits of west Turkmenia*. Moscow ('Nauka') (in Russian).
- , Bagin, V.I., Gandler, T.S., Nechaeva, T.B. & Fein, A.G. 1991. Late Holocene of west Turkmenia: paleomagnetism, chronology and climatic events. *Abstracts, XIII INQUA International Congress, Beijing, China*, 1991: 359.
- , Nechaeva, T.B. & Fein, A.G. 1991. Ponto-Caspian Quaternary deposits: stratigraphy, chronology, fine structure of magnetic field. *Abstracts, XIII INQUA International Congress, Beijing, China*, 1991: 359.
- Tufescu, M. 1968. *Ammonia tepida* (Cushman) (Ord. Foraminifera): some features

REVIEW OF STRATIGRAPHY OF EASTERN PARATETHYS



A new protorichthofenioid brachiopod (Productida) from the Upper Carboniferous of the Urals, Russia

C.H.C. BRUNTON

Department of Palaeontology, The Natural History Museum, Cromwell Road, London SW7 5BD

SYNOPSIS. A new genus from the mid Upper Carboniferous of the southern Urals, Russia, is described and interpreted as a surprising, aspinose early form of the Richthofenioida. An undescribed *Protegulifera?* from the Upper Carboniferous of northern Spain and two previously described Permian Russian species are possibly congeneric, but thereafter the stock probably died out. The new genus *Zalvera* contains the new species *Z. sibaica*, specimens from Spain and the two described Permian species.

INTRODUCTION

In 1982 Dr S. S. Lazarev, of the Palaeontological Institute, Moscow, led an expedition to the southern Urals where brachiopods were collected and passed to me for comment and description. The brachiopods include seven taxa which can be assigned to productid families with little difficulty. However, most specimens belong to a distinctive species which initially was difficult to identify, even at phylum level. It now seems clear that these subconical, thin-shelled specimens also belong within the Productida, although they display bizarre characteristics.

Material

The material was all collected from a dense, finely-grained buff-coloured limestone within the Kordailovskaya Formation (probably equivalent to the Verejan Horizon in the Moscow area) dated as late Bashkirian to Lower Moscovian (mid Upper Carboniferous) and occurring at the Sibay stream, on the left bank of the Ural River, 6 km up-stream from Pokrovka, in the southern Urals, Russia. The fragments containing brachiopods amount to about 40 in total, several being multi-parts and counterparts of larger pieces that have been broken down to between 20 and 50 mm in greatest dimension. Some pieces include more than one brachiopod specimen.

From the total of 40 fragments, about half contain the unusual subconical species. Of the rest:

1. Four contain a species reaching about 15 mm in length, with fine spines, densely covering the ventral valve only, but with dorsal valve dimples, and having a low lateral profile. Superficially the species resembles *Stipulina* (Fig. 1).
2. Eleven contain a *Thomasella*-like species, but differ in the absence of rugae over the spinose body region and in having a relatively more strongly ribbed and flanged trail (Figs 2 and 3).
3. Two contain small (*ca.* 7 mm wide) specimens more like *Thomasella* than the above in that they are distinctly rugose up to the start of the flange (Fig. 4a, b).

4. One part and counterpart contains a strongly rugose species (only *ca.* 9 mm wide) resembling a small plicatiferid, but with a widely flanged and ribbed trail (Fig. 5).
5. There are two incomplete specimens of a rugose and less clearly ribbed (reticulate) species with spines near the umbo and on the ventral exterior which resembles *Pectenopproductus proprius* Likharev, a species reported from the Lower Permian of the Caucasus. Muir-Wood & Cooper (1960) were unsure as to whether this genus was a pectinid mollusc, but the presence of spines on these two specimens confirms their affinity with the Productidina (Fig. 7).
6. There is one incomplete ventral exterior, seen also in section, of a deep bodied, small, rounded species apparently lacking rugae or ribs, but with relatively stout spines, which somewhat resembles a Lower Carboniferous leipproductid, such as genus *Magnumbonella* Carter (Fig. 7).
7. Two specimens like the conical shells described below have variably developed radial ribs, starting within 5 mm of the apex and with a low profile. The cone apex seems to have some attachment spines and others are arranged widely on the cone. The species resembles *Planispina armata* (Girty) from the mid Carboniferous of the USA (Fig. 8).
8. There are, in addition, two pieces of a strongly ribbed rhynchonellid and a section through a probable reticulariacean.

These identifiable productids may prove to be new taxa. However, this paper deals only with the more common (ie. in the collection at hand) subconical species. Of these 25 fragments, 21 are of the subconical valve while four include separate parts of what is clearly a different valve and is interpreted as the second valve of the same species.

METHODS

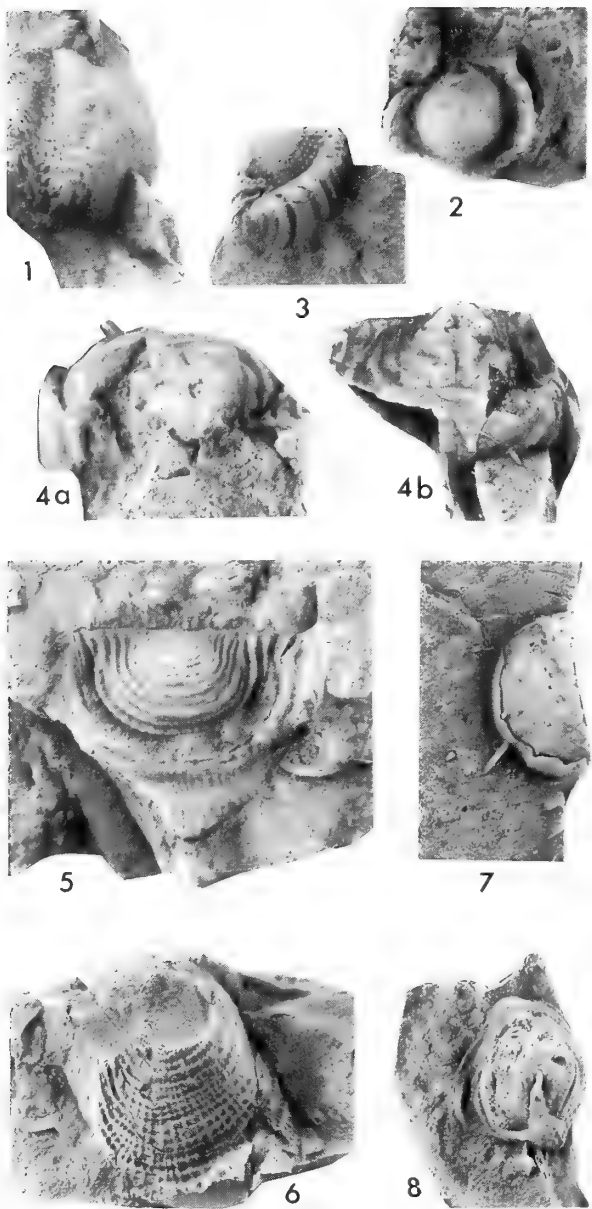


Fig. 1 *Stipulina*-like species, ventral valve exterior, BD9673, $\times 4$.

Figs 2, 3 Two views of a non-rugose *Thomasella*-like species. 2, exfoliated dorsal valve interior and the flanged and geniculated trail, BD9677. 3, oblique view of a complete specimen viewed anterolaterally showing the strongly ribbed trail, BD9676b, $\times 3$.

Fig. 4 Two views of cf. *Thomasella* showing the posterior rugae, flanged trail and ventral spines, BD9673(0), $\times 5$.

Fig. 5 A Plicatiferinid showing the exfoliated dorsal valve interior, BD9674, $\times 4$.

Fig. 6 *Pectenoprodus* ventral valve exterior, BD9675, $\times 2$.

Fig. 7 The incomplete leioproductine ventral valve, BD9688(1), $\times 3$.

Fig. 8 Cf. *Planispina* sp. viewed almost apically, BD9688(0), $\times 1.5$.

The shell material on most specimens is thin, somewhat laminar in appearance and takes the buff colour of the matrix. In order to establish the nature of this shell, slivers from two specimens were studied by qualitative energy dispersive x-ray microanalysis using scanning electron microscopy in the Department of Mineralogy, The Natural History Museum, London. The results show a strong dominance of calcium, with no magnesium or phosphorus present (Fig. 9). The mineralogy indicates dominance of calcium carbonate (lacking magnesium) and the lack of phosphate precludes the presence of apatite. The shell is not calciphosphatic so articulate brachiopods could have been the animals which secreted this shell material.

It seemed unlikely that more material would become available, so it was important to preserve what we had. For this reason only two specimens were sectioned in an attempt to determine what internal structures were present. However, some internal details could also be seen on broken surfaces which cut across specimens while the rock was being broken, as well as on naturally weathered surfaces cutting across the partial interiors of two specimens.

Careful examination of all specimens under a binocular microscope, commonly making drawings using a Wild drawing arm, gradually allowed the recognition of some consistent features on several specimens, which provided a form of orientation. The recognition of the same structures in different views and sections has allowed a general picture of the morphology of these specimens to be built up.

Portions of shell from near the apex and the distal regions of the cone, and from the supposed dorsal valve have been studied uncoated in the environmental chamber of an ISI ABT scanning electron microscope and coated using a S2500 Hitachi machine, both in The Natural History Museum.

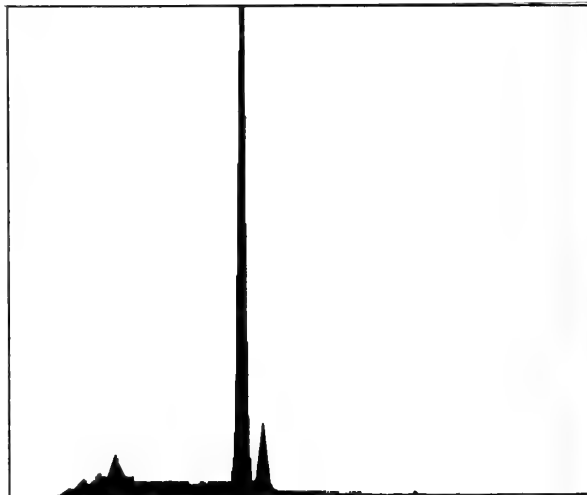


Fig. 9 Plot from qualitative energy dispersive X-Ray microanalysis of non-coated fragments using scanning electron microscopy. The plot displays a major calcium peak (plus a secondary peak to its right), but no phosphorus and only minor amounts of elements with lower atomic weights, to the left.

SYSTEMATIC DESCRIPTIONS

The material described here is housed in the BMNH collections of The Natural History Museum, London. Specimens are uniquely recognised by BD registration numbers.

Order PRODUCTIDA Waagen, 1883

Suborder STROPHALOSIIDINA Schuchert, 1913

DIAGNOSIS. Productida retaining ventral interareas and, commonly, toothed articulation.

Superfamily RICHTHOFENIOIDEA Waagen, 1885

DIAGNOSIS. Ventral valve conical or sphenoidal, dorsal valve recessed below the ventral margins. Normally attached by cicatrix and/or spines.

Family ZALVERIDAE nov.

DIAGNOSIS. Richthofenioids lacking external body spines, with shallow body cavities and short subparallel ventral ridges associated with a near apical chamber involved in the articulation of the valves; marginal ventral valve protective structures absent.

COMMENTS. Currently only the one genus is known. The family differs from the Richthofeniidae most clearly in its lack of external spines and attachment to the substrate. Although *Collumatus* Cooper & Grant, 1969, lacks spines this Permian genus is attached to the substrate by concentric sheets of shell surrounding the base of the ventral valve.

Genus ZALVERA nov.

DIAGNOSIS. Zalveridae retaining small juvenile ventral valve at apex and with strong brachial impressions.

ETYMOLOGY. Anagram of the letters of the name Lazarev.

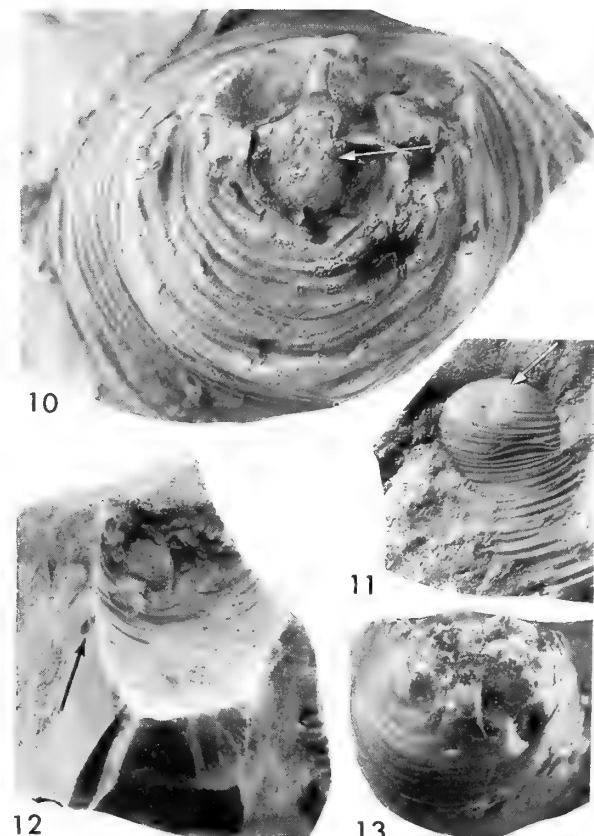
TYPE SPECIES. *Zalvera sibaica* sp. nov.

DISCUSSION. As well as the type species, the genus may usefully accommodate the specimens described by Tschernyshev (1902) as *Teguliferina(?) uralica* and by Likharev, (1932) as *Keyserlingina caucasica*. Unfortunately, little is known of the internal morphology of these species so this assignment is uncertain. Likharev (1931, 1932) specifically noted the absence of internal dorsal valves, wondering if they ever existed. Externally both these species seem to fit better here than in *Prorichthofenia*, which is a true teguliferinine with external spines. In addition, two specimens referred to as *Proteguliferina?* by Winkler Prins in Sanchez de Posada *et al.* (1993) belong in *Zalvera*. See further discussion under the species description.

Zalvera sibaica sp. nov.

Figs 10–24

TYPE SPECIMEN. Holotype, BD9653, from the Kordailovskaya Formation of late Bashkirian to early Moscovian, mid Upper Carboniferous age, 6km up-stream from Pokrovka, Ural River in the southern Urals, Russia (Figs 20a–c).



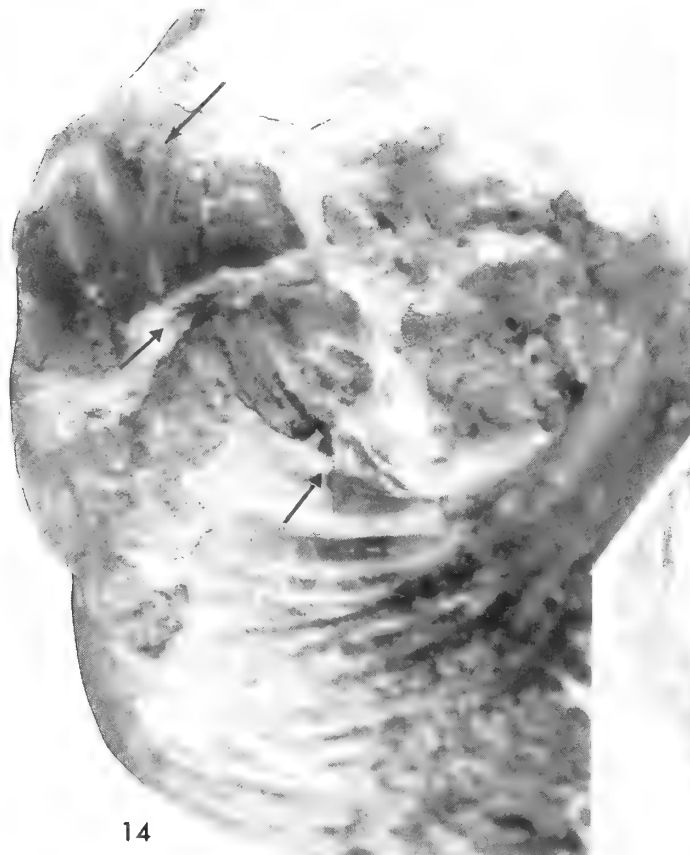
Figs 10–13 *Zalvera sibaica* gen. et sp. nov. from late Bashkirian to early Moscovian rocks in the southern Urals, Russia. **10**, apical view of a slightly crushed specimen including the small regular looking initial growth stages of the ventral valve (arrow). The umbo is to the left. BD9671, $\times 3$. **11**, side view of a specimen showing the inferred subparallel ridges as white lines on the shell (arrow) and rounded apex. BD9669, $\times 1.5$. **12**, part external mould of a specimen viewed towards the apex, in which parts of the subparallel ridges are visible. The rock surface to the left cuts a nodose outgrowth (arrow). BD9661a, $\times 2$. **13**, apical view of a specimen associated with the external mould of figure 12 showing partially exposed subparallel ridges, BD9661b, $\times 2$.

DIAGNOSIS. *Zalvera* with irregular rounded dorsal outline and apex profile, rugae relatively prominent.

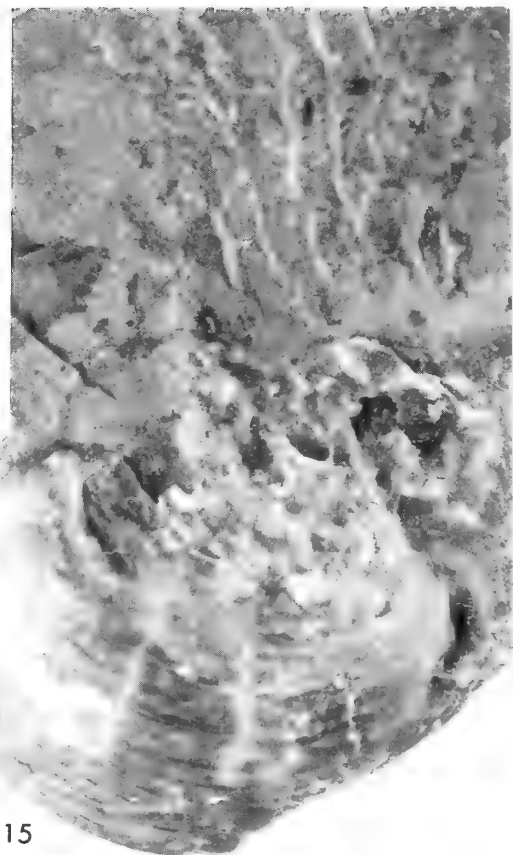
ETYMOLOGY. Species named from the Sibay stream, where the specimens were found.

MATERIAL. All specimens of *Z. sibaica* are from the one locality in the southern Urals (BMNH BD9653 (the holotype), BD9654–9672). A few other fragments occur with specimens of other species.

DESCRIPTION. In one specimen (BD9671) the earliest growth stage of the subconical valve resembles a tiny (*ca.* 5mm diameter) productid valve (Fig. 10). This consists of a subtriangular, gently convex valve exterior, which appears to be covered by closely spaced, but fine spine bases. There is, therefore, a question as to the reliability of this small valve being part of the species. The specimen was cut medially and appears to show continuous shell between the small spinose valve, its thick-shelled gutter-like surround and the remaining



14



15

Figs 14, 15 *Zalvera sibaica* gen. et sp. nov. from late Bashkirian to early Moscovian rocks in the southern Urals, Russia. **14.** oblique apical view of a partially exfoliated specimen showing the fine internal tuberculation on the internal mould (arrow) and positions of the subparallel ridges (arrows), BD9664, $\times 7$. **15.** apical view of a specimen with a xenomorphic apex associated with a bryozoan and showing the subparallel ridge positions, BD9663, $\times 5$.

thin-shelled cone. A small apical spinose valve was also noted by Tschernyshev (1902) in his original description of *Tegulifera*(?) *uralica*. The material has been checked recently by Dr Lazarev (personal communication) who confirmed its presence, so for now it is accepted as part of *Z. sibaica*. Most of the material consists of broken parts of a subconical to subcylindrical structure with a flattened, weakly rounded, 'base' (Fig. 11), extending directly from the initial tiny spinose valve. The cone expanded rapidly to about 15mm in diameter and then expanded gradually to as much as 25mm in diameter. The preserved length is variable, but no specimen exceeds 25mm; some are much more squat in shape. The exteriors are smooth apart from irregularly developed rugae (Fig. 11) and very rare non-hollow, nodose outgrowths on the subcylindrical area (Fig. 12). Growth lines are commonly visible. The shell material is thin except for restricted areas in which there are internal ridges or blunt, rounded endospines. A few specimens display two layers of thin shell in the rugose cone region, each separated by a narrow (less than 1mm) layer of sediment. The place from which the inner, younger, shell layer originated can be found rarely, but indicates that these lamellose layers were growth structures resulting from a mobile mantle epithelium.

On the weakly rounded 'bases', beyond the small initial spinose valve, the shell material appears to be finely pseudopunctate, with small tubercles on internal surfaces (Fig.

14). Breakage and shell exfoliation is common in this area, with the result that complete undamaged exteriors are rare. However, this does allow recognition of some structures from the outside. Most obvious is a pair of plates or ridges (Figs 11, 13), about 2 to 3mm apart distally, diverging slightly from within about 1mm to between 5 and 10mm from the apex, and extending to or beyond the growth stage at which the cone expansion slowed to give a more subcylindrical profile. The presence of drusy crystals between these plates indicates an original cavity in that region. Similar crystals are commonly present apically and externally to these plates in specimens from which the base of the subconical valve appears to have been broken. More complete specimens show signs of shell growth distortion over this basal area; in one example a fenestellid bryozoan is adpressed to the surface (Fig. 15).

The cutting of two relatively complete subconical valves failed to reveal a second valve within the cone, although one specimen has a platform-like 2.8mm extension into the 'internal' space originating about 5mm from the apex. This specimen was cut between the pair of subparallel plates, allowing reference to a position in the shell, and these plates are probably connected, thus forming a chamber. More information about interiors was obtained from broken sections through three specimens, one of which is additionally weathered and displays parts of a flat, thin structure lying near the base of the cone, which can be

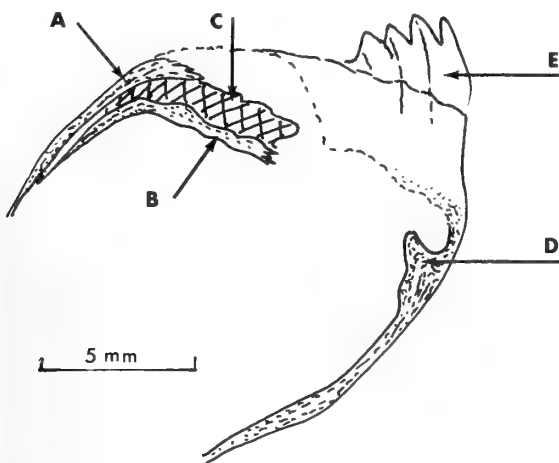


Fig. 16 Drawing of a natural section through a specimen with its apex uppermost and in which part of a dorsal valve is preserved (B). A = ventral valve; C = crystaline cavity infilling; D = part of the ventral valve internal articulatory structure; E = external mould of rugae near the apex. From specimen BD9663(2).

interpreted as a second valve (Fig. 16). The available specimens all display a consistent relationship between the conical valve and internal plate-like structures, indicating that the latter are remnants of a second valve in their positions of articulation, or the support structures for a second valve.

Four different-looking specimens in the collection are taken as being conspecific. These are fragments of nearly complete, oval-shaped valves, 12 to 15mm wide, and are interpreted as interior surfaces, one of which has a counterpart. Their size and general outline would allow them to have fitted into the more apical region of the conical valves. One edge, seemingly parallel to the maximum width, shows a slight median flattening and is taken as being posterior. The most obvious feature is a pair of weak, crescent-shaped ridges (Fig. 17a, b), which bound shallow depressions, follow close to the edges of the valve and originate from posteromedian positions on each side of a low broad median ridge. Surfaces on either side of the crescent-shaped ridges are finely endospinose (Fig. 18). Posteriorly, close to the straighter sector of the margin, is a pair of shallow pits, between which is the posterior end of the wide median ridge. Posteromedianly, a transverse ridge is situated just anterior to the posterior flattened sector. This expands widely anterior to the median ridge, leaving a T-shaped pair of lateral protuberances, 2mm wide (Fig. 19). The lateral and anterior margins of these valves are of thin shell substance, which display growth lines, and seem to be reflexed away from the internal surface, resembling a valve trail.

SHELL STRUCTURE. Scanning electron microscopy of shell sections (Figs 22, 23) and fractured fragments (Fig. 24) show the shell to be composed of somewhat recrystallised laminae, probably originally made up of thin laths. Macroscopic examination revealed rather fine pseudopunctations, especially in the apical regions of the ventral and dorsal valves (Fig. 18), and thus confined mostly to the body region. The conical trail, beyond the body cavity, has fewer internal tubercles (Fig. 22) indicating a reduction in the pseudopunctations.

INTERPRETATION. The scant and poorly preserved characters available indicate a subconical valve, which is interpreted as

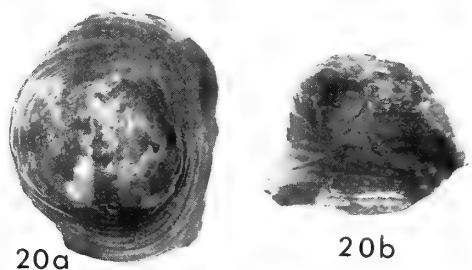
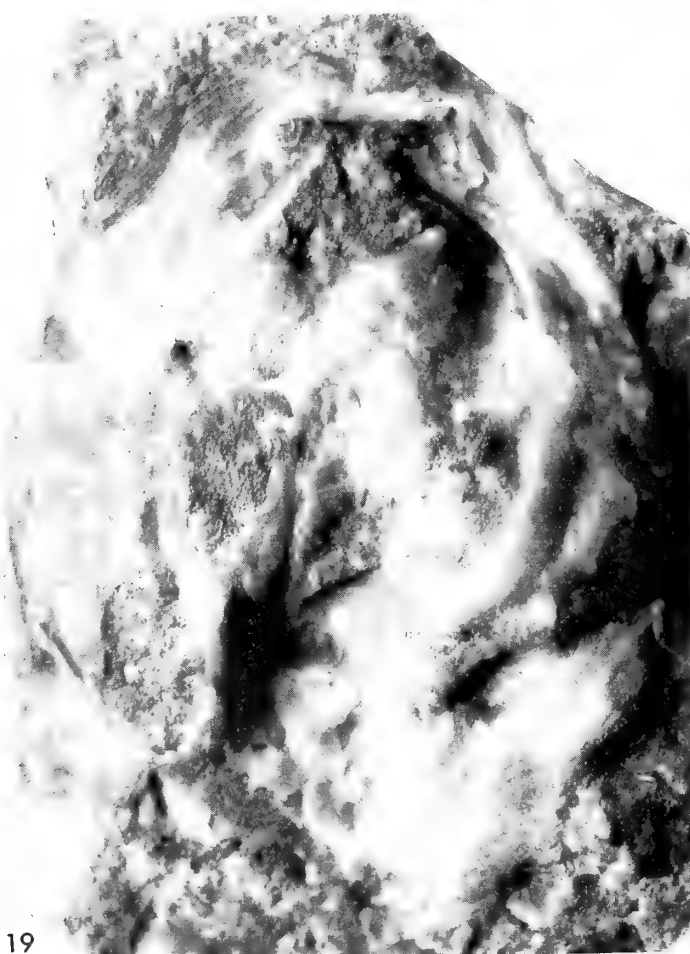
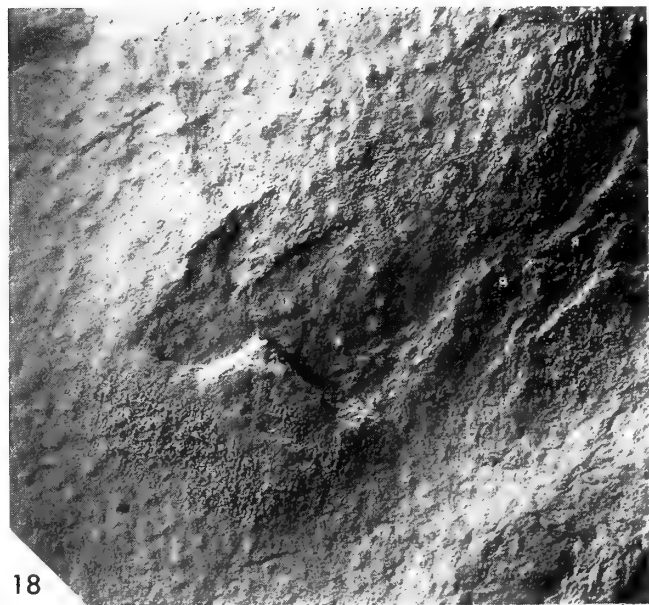
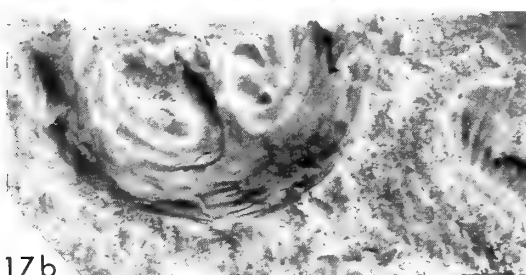
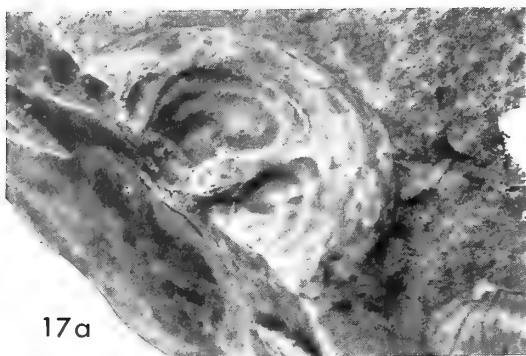
ventral, within which lies a dorsal valve close to the apex of the shell, resulting in a very shallow body cavity. Distal to this was a relatively long subcylindrical skirt of thin shell. The posterior transvere ridge in the dorsal valve articulated with a pair of grooves associated with the subparallel plates in the ventral valve (Fig. 21). Additionally, the dorsal valve bent dorsally around its lateral and anterior margins forming a short trail against the longer internal surface of the ventral valve (Figs 19, 21). There is no direct evidence for the dorsal trail being as long as that of the ventral valve, but it is possible that there was an extremely thin layer of dorsal shell supporting the mantle in this trail region. On the other hand, a long dorsal trail might have hindered the opening of the shell, performed by contraction of diductor muscles attached to the poorly differentiated cardinal process situated between the ventral articular ridges. A short dorsal trail would have left the internal mantle epithelium of the ventral valve open to the sea and vulnerable. Cowan (1970) suggested similar exposed epithelia in lyttonioids, and similarly exposed epithelia occurs in other Productida, including teguliferinids. However, the evidence for this in the present material is insufficient to allow further discussion.

The internal morphology of the few dorsal valves available indicates a standard anatomy in which the lophophore was probably a schizophope, strung from brachial ridges close to the edges of the body cavity (Fig. 17). Dorsal adductor muscles were attached posteromedianly, anterior to the articulation ridge and between the median ridge and posterior ends of the brachial ridges. Diductor muscles were probably attached at a small posteromedian boss, which hardly deserves the term cardinal process.

Externally, the ventral apical region is somewhat distorted on some specimens, which might indicate that initial growth closely followed the substrate. However, the apparent lack of external body spines, which might have been used to fix specimens, and the variable nature of this 'basal' deformation seems to indicate that specimens were not cemented or closely adpressed to a hard substrate, but occurred on, or partially buried in, a relatively soft substrate. Unfortunately, field observations are lacking on both the orientation of specimens in the rock and on the nature of adjacent lithologies. Drusy fillings in body cavity regions could have developed whichever way up the specimens were entombed in the sediment, provided both valves were preserved and the shell was closed. However, the rare specimens showing these features invariably have drusy crystals within the body cavity, not dorsal to the dorsal valve, indicative of an apex down position in life. The rock appears not to include potential hard substrates, other than the fossils themselves, although algae could have caused surfaces to become firm.

Although probably not fixed to a hard substrate, these specimens appear to have resembled richthofenoids lacking adult spines, and lived in areas of soft, fine sediment. If they sat, rather cup-like, with their bases buried in sediment, the ventral trails would have raised the inhalent areas well above the sediment surface. To have achieved this position with only a thin-shelled ventral valve and no anchoring structures indicates that the environment was probably one of quiet water and fine-grained sedimentation.

DISCUSSION. Specimens somewhat resembling this material were described by Tschernyshev (1902) from Lower Permian, Asselian, rocks on the river Yuresan, also in the Urals, Russia, as *Tegulifera* (?) *uralica*. One specimen figured by Tschernyshev (1902, fig. 85, pl. 60, fig. 14) has a small triangular, regular-looking productid valve at its apex like that on *Z. sibaica*



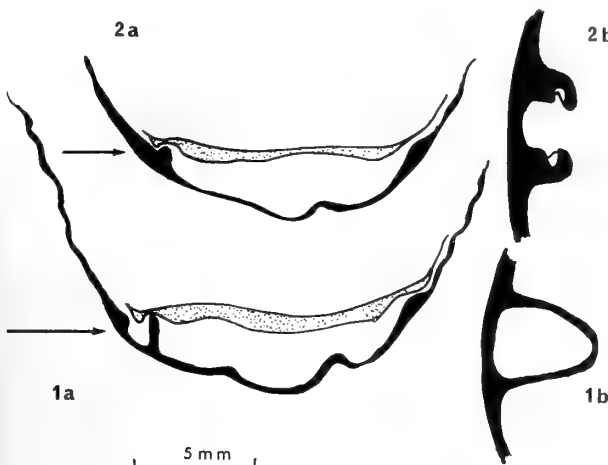


Fig. 21 Reconstruction of the apical area of *Zalvera* in median longitudinal section (1a), between the subparallel ridges, and an apical view of the ventral valve at the arrow position (1b). In 2a the section cuts one of the subparallel ridges in which the articulatory groove is situated (2b). Ventral valve black; dorsal valve stippled.

(BD9671) (Fig. 10). Also, the species seem to be of comparable size and both have similar concentric ornamentation. Dr Lazarev has inspected the Tschernyshev specimen and confirms the similarity.

Another similar-looking species was first described by Likharev in 1931 as *Teguliferina?* (*Chaoella*) *caucasica* and again in 1932 as *Keserlingina caucasica*. It came from Permian rocks in the Caucasus, originally described as *P_{1b}*, but now thought to be of Kazanian, early Upper Permian age. Likharev also recorded related specimens from the Sim river in the southern Urals. Likharev (1932) gives a measure of 9mm for the maximum width, so his specimens are about half the size of the new material. Otherwise the illustrations closely resemble the Carboniferous specimens and one figure (1932, pl. 2, fig. 9b) seems to show similar subparallel marks near the apex. In describing *caucasica* Likharev briefly referred to *uralica*, but other than discussing the apparent small ventral valve at the apex he wrote little to differentiate between the two species.

Thus, somewhat similar specimens to *Z. sibaica* occurred in the Urals at Bashkirian to Moscovian boundary times and again in the Permian. Neither Tschernyshev's *T. uralica* nor Likharev's *K. caucasica* belong in *Teguliferina* or *Keyserlingina*, the latter belonging with the Lyttonioidea on account of its lobate interiors. *Teguliferina* and *Proteguliferina* belong in the Richthofenioidea and are thus more closely related to the new material than is *Keyserlingina*. For instance, *Proteguliferina* displays a weakly concave dorsal valve within a gently convex ventral valve which does not reach the internal margins of the spinose ventral valve. Its ventral marginal epithelium may, therefore, have been exposed.

Girty (1908) described two species, *Tegulifera armata* and *T. kansasensis*, from rocks of late Missourian (mid Kasimovian)

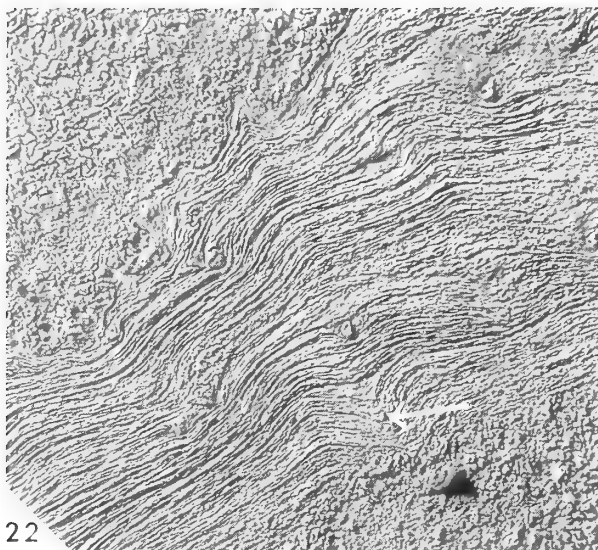
age, from localities in Illinois and Kansas respectively. These species differ in important characters from the new Urals specimens described here. The American specimens are less deeply conical, less rugose, are radially ornamented, and are attached by cementation and external spines, as well as having internal ventral spines. These species were placed by Muir-Wood & Cooper (1960) into *Planispina* Stehli, a genus assigned to the Teguliferininae. The radial ribbing and possible spinose exteriors of two specimens in the Urals collection (Fig. 8) resemble *P. armata* (Girty, 1908, pl. 20, fig. 10).

Sutherland (1989) reported another species, well preserved as silicified specimens, from early Upper Carboniferous (Morrowan [= Bashkirian]) rocks in Oklahoma, USA. This material as yet remains un-named, but is probably closely related to *Teguliferina*, with somewhat similar dorsal valve interiors and similar external rhizoid fixing spines. These Morrowan specimens, therefore, appear to be the earliest known true teguliferinids, and are the earliest known Richthofenioidea.

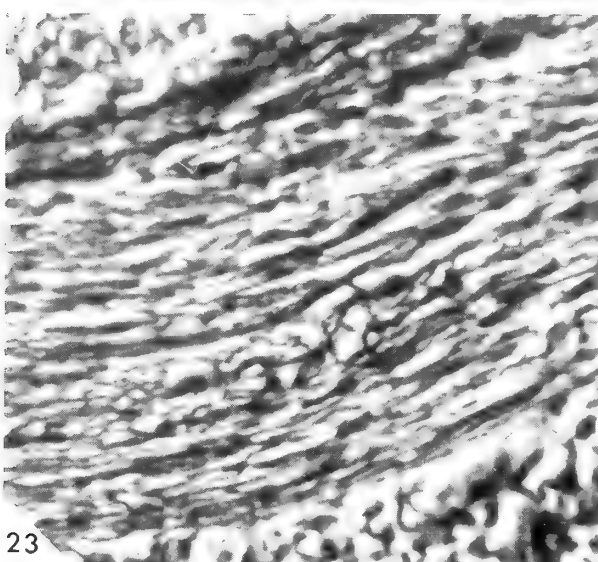
The material from the Urals is of similar age to that described by Sutherland (1989) but is very different in character, resembling more closely the specimens described by Tschernyshev (1902) and Likharev (1931). The brachiopod relationship of the new Urals material is no longer in doubt and the general form of the shell is highly indicative of a richthofenoid relationship. However, other than in the Permian genus *Collumatus* Cooper & Grant, 1969, from Texas, the richthofenoids have external spines to aid the fixing of specimens to hard substrates, commonly within reef environments, while *Z. sibaica* has no such spines. Apart from this difference, the general architecture of the shell fits with that of richthofenoids; a conical ventral valve with a dorsal valve recessed below its margins, the two valves articulating, not by true ventral teeth and dorsal sockets, but by dorsal protuberances fitting into ventral cavities. In detail the Urals specimens differ from the general richthofenoid pattern: they lack external spines, other than perhaps at the earliest stages in ontogeny when ventral valves show signs of fine spines for about 5mm of growth; the body cavity is shallow, with the dorsal valve deeply recessed below the ventral margin; the dorsal valve has internal structures producing relatively thick shelly ridges, the brachial impressions and wide median ridge; the dorsal valve has short, geniculated, thin-shelled margins extending a short distance up the ventral valve interior; the ventral valve interior has a simple posteromedian structure of subparallel plates acting as supports for the dorsal valve; the ventral valve cone interior has sparsely distributed blunt, well rounded, endospines protruding into the space above the dorsal valve exterior; there is no indication of any complete protection for the opening to the subconical valve margins, as in most true richthofenoids.

In a biostratigraphical description of regions in Cantabria, northern Spain, Sanchez de Posada *et al.* (1993) listed '*Proteguliferina?* n. sp.' from 'Kasimovian' rocks. Dr C. F. Winkler Prins has kindly lent me the two specimens from which this reference was made, which he now dates as Moscovian, possibly Podolsky age. They do appear to be congeneric with the new Urals specimens. Specimens (also seen) determined by

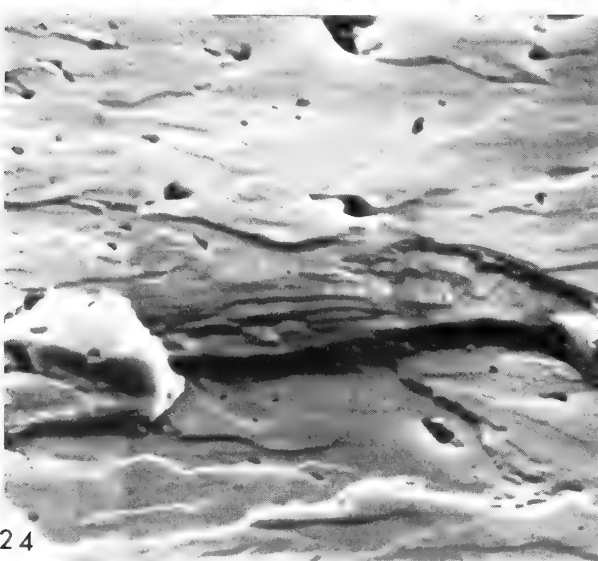
Figs 17–20 *Zalvera sibaica* gen. et sp. nov. from late Bashkirian to early Moscovian rocks in the southern Urals, Russia. **17**, part and counterpart of an incomplete dorsal valve showing probable brachial impressions and the median ridge. The valve margins curve away into the rock in 17a, BD9659, $\times 4$. **18**, scanning electron micrograph showing the finely endospinose surface within the dorsal valve brachial impression, BD9659a, $\times 60$. **19**, a rather elongate, deformed and partly exfoliated dorsal valve interior; posterior is to the top, showing the transverse ridge (exfoliated and arrowed), interpreted as the dorsal articulation structure, and one brachial ridge, on the right, BD9670, $\times 10$. **20**, holotype viewed apically and 'anteriorly' ($\times 1.5$) and obliquely apically ($\times 5$) showing the positions of the subparallel ridges 'posteriorly'. BD9653.



22



23



24

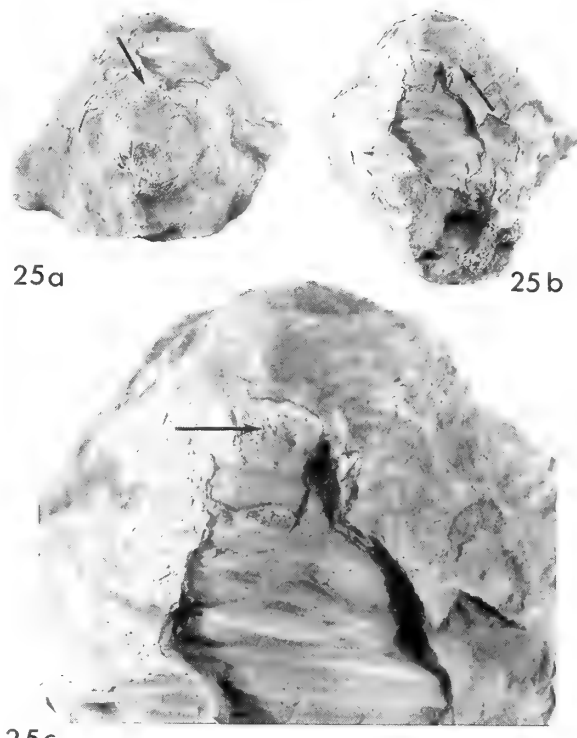


Fig. 25 *Zalvera* sp. from early Upper Moscovian rocks north of Bran-cosera, Palencia, Spain. **25a,b**, apical and lateral views of the specimen ($\times 1$) showing an 'umbonal' region (arrowed). **25c**, an enlargement ($\times 3$) of 25b showing pseudopunctate shell (arrowed) and the layered nature of the valve, each with thin sediment between. National Museum of Natural History, Leiden, WAG 77.

Winkler Prins (personal communication, September 1993) as *Proteguliferina* sp. from Austria are not *Zalvera*, but are more like an early form of the Permian teguliferinid *Acritosia*.

The two Moscovian specimens from northern Spain resemble *Z. sibaica* closely, but appear to differ in having well flattened apices, suggesting closer attachment to the substrate than seen in the specimens from the Urals. Both specimens show signs of the subparallel internal ridges, the apical internal microtuberculation and both have comparable external irregular rugae. These similarities between the Spanish and Russian specimens reinforce the concept of widespread marine faunas in Eurasia during Upper Carboniferous times.

Present evidence, therefore, indicates two almost contemporaneous stocks in the early to mid Upper Carboniferous, one in North America which evolved into the Richthofeniidae, the other in Russia which, although considered as belonging in the Richthofenioidea, was an early 'experimental' stock which lost its spines early in ontogeny and lived on relatively soft substrates, unlike the American forms.

Figs 22–24 *Zalvera sibaica* gen. et sp. nov. from late Bashkirian to early Moscovian rocks in the southern Urals, Russia. **22**, a cut and lightly etched section through a ventral valve just distal to the internal thickening against which the dorsal valve rested. Apex to the top right, exterior to the left. Irregularities in the laminae are oblique sections through pseudopunctae, apparently with taleolae (arrows), BD9669a, $\times 160$. **23**, same section, closer to the apex, $\times 1200$. **24**, a fracture flake of shell from a thickened area of a dorsal valve. Signs of original laths can be seen centrally, BD9670, $\times 5000$.

which were attached and retained spines. While some stratigraphically younger examples of this aspinose stock, in addition to those from northern Spain, may yet be discovered, it seems it did not persist after the Kazanian, when the Caucasian species of Likharev died out. The Permian genus *Collumatus* would appear not to have been derived from this stock, but to be a true richthofenoid which had also lost its spines. A feature of taxonomical importance in the specimens described by Sutherland (1989) from Oklahoma, but not seen in this new material, is the juvenile ventral interarea. A small ventral interarea is also reported in the Teguliferininae (Muir-Wood & Cooper, 1960), which belongs in the Richthofenioidea. It is the presence of interareas in these Carboniferous species that places the Richthofenoidea in the Strophalosiidina, the structure being lost in the more common Permian richthofenoids. In *Zalvera* it seems the earliest growth of the ventral valve was normal for productids, but whether it involved the growth of a juvenile interarea is unknown. If present it might have become incorporated into the later subconical valve growth. In any event, once growth changed, after the initial 4–5 mm, from being a small finely spinose subtriangular valve to a rapidly expanding rounded cone with a spineless exterior, shell growth was holoperipheral. In the North American species there was a short period when the ventral interarea grew before the posterolateral mantle margins grew posteromedianly to continue the style of shell secretion seen for the rest of the valve. This left the juvenile interarea preserved, but with a short suture line posteromedianly where the two mantle margins had grown together and fused, allowing the typical teguliferinid cone to grow. In the Urals material this posterior fusion of the mantles occurred earlier in growth so that no interarea has been preserved. This raises the question as to whether *Zalvera* should be assigned to the Strophalosiidina. The alternative is to consider *Zalvera* within the Productinida as a unique aberrant offshoot showing tendencies towards the morphology of the Richthofenioidea. This seems less likely than placing *Zalvera* in the Richthofenioidea and accepting that the interarea never developed in these unusually-shaped brachiopods. It is hoped that more of this material will become available so as to allow more complete preparation and a better insight into the way in which this strange brachiopod grew.

There is no clear evidence for the origin of the Zalveridae, but it is possible to suggest that the ancestral stock was within the Strophalosiidina. The cone development seems to have been from exaggerated, and posteriorly fused, growth of the ventral

trail. Within strophalosiidines the Aulostegoidea includes many groups with elaborate trails, and as they lack a toothed articulation and have variably developed interareas, they provide possible ancestors for *Zalvera*.

ACKNOWLEDGEMENTS. I thank Dr S. Lazarev, Palaeontological Institute, Moscow, for information about this material and other specimens in Russian collections; Dr Cor Winkler Prins, National Museum of Natural History, Leiden, for the loan of comparable material from Spain and Austria; Dr Patrick Sutherland, University of Oklahoma, for information about his specimens, and Dr R. Cocks for reading and commenting constructively on a draft version of this paper.

REFERENCES

- Cooper, G. A. & Grant, R. E. 1969. New Permian brachiopods from Texas. *Smithsonian Contributions to Paleobiology*, **1**: 1–20.
- Cowen, R. 1970. Analogies between the Recent bivalve *Tridacna* and the fossil brachiopods *Lyttoniacea* and *Richthofeniacea*. *Palaeogeography, Palaeoclimatology and Palaeoecology*, **8**: 329–344.
- Girty, G. H. 1908. On some new and old species of Carboniferous fossils. *Proceedings of the United States National Museum*, Washington, **34**: 281–303, pls 14–21.
- Likharev, B. K. 1931. Über eine problematische Brachiopode aus den unterpermischen Ablagerungen des Nordlichen Kaukasus. *Annuaire des Société Paleontologique de Russie*, Leningrad, **9**: 157–161, figs 1–5.
- 1932. Fauna of the Permian deposits of northern Caucasus, 2 Brachiopoda, Lyttonidae. *Trudy Vsesoyuznogo geologo-razvedchchnogo ob'edineniya NKP* [*Transactions of the Geological Prospecting Service of USSR*], Leningrad & Moscow, **215**: 55–84 (in Russian), 85–111 (in English), 5 pls.
- Muir-Wood, H. M. & Cooper, G. A. 1960. Morphology, classification and life habits of the Productoidea (Brachiopoda). *Memoirs of the Geological Society of America*, New York, **81**: 447 pp., 135 pls.
- Sanchez de Posada, L. C., Martinez Chacon, M. L., Mendez, C. A., Menendez Alvarez, J. R., Truyols, J. & Villa, E. 1993. El Carbonífero de las regiones de Picos de Europa y Mantuo del Ponga (zona Cantábrica, N de España): Fauna y biostratigrafía. *Revista Española de Paleontología*, No. Extraordinario: 87–108.
- Schuchert, C. 1913. Class 2. Brachiopoda, in Zittel, K. A., *Text book of Palaeontology*, I: 355–420. London.
- Sutherland, P. K. 1989. Possible ancestor to the late Carboniferous/early Permian Teguliferinid brachiopods in the Middle Carboniferous of Oklahoma, USA. *XII Congrès International de stratigraphie et de géologie du Carbonifère*, Beijing 1987, *Compte Rendu*, **2**: 355–360, pl. 1.
- Tschernyschev, T. 1902. Die oberkarbonischen Brachiopoden des Ural und des Timan. *Mémoires du Comité géologique*, St Petersburg, **16** (2): 749 pp., 63 pls (in Russian & German).
- Waagen, W. H. 1882–1885. Salt Range Fossils. Pt. 4 (2). Brachiopoda. *Palaeontologia Indica*. *Memoirs of the Geological Survey of India*. Calcutta.



The Upper Cretaceous ammonite *Vascoceras* Choffat, 1898 in north-eastern Nigeria

P.M.P. ZABORSKI

Department of Geology and Mining, University of Jos, P.M.B. 2084, Jos, Nigeria

CONTENTS

Introduction	61
Systematic descriptions	63
Family Acanthoceratidae Grossouvre	63
Subfamily Acanthoceratinae Grossouvre	63
Genus <i>Paravascoceras</i> Furon	63
<i>Paravascoceras cauvini</i> (Chudeau)	63
Genus <i>Pseudovascoceras</i> gen. nov.	67
<i>Pseudovascoceras nigeriense</i> (Woods)	68
Family Vascoceratidae Douvillé	71
Subfamily Vascoceratinae Douvillé	71
Genus <i>Vascoceras</i> Choffat	71
<i>Vascoceras woodsi</i> sp. nov.	72
<i>Vascoceras bullatum</i> Schneegans	76
<i>Vascoceras globosum</i> (Reyment)	76
<i>Vascoceras globosum costatum</i> (Reyment)	78
<i>Vascoceras globosum globosum</i> (Reyment)	79
<i>Vascoceras globosum proprium</i> (Reyment)	80
<i>Vascoceras obscurum</i> Barber	81
<i>Vascoceras harttii</i> (Hyatt)	81
Stratigraphical and phylogenetic discussion	83
Acknowledgements	85
References	86
Appendix	88

SYNOPSIS. Large collections of ammonites that have been referred at one time or another to *Vascoceras* Choffat, can be made under tight stratigraphical control in north-eastern Nigeria. The following forms are present, in order of stratigraphical appearance: *Paravascoceras cauvini* (Chudeau); *Vascoceras woodsi* sp. nov.; *V. bullatum* Schneegans, *V. globosum costatum* (Reyment), *V. globosum globosum* (Reyment) and *Pseudovascoceras nigeriense* (Woods); *V. globosum proprium* (Reyment); *V. obscurum* Barber; and *V. harttii* (Hyatt). Only the last three occur in the Lower Turonian; the remainder are restricted to the Upper Cenomanian, the earliest appearing above the level of the European *Metoicoceras geslinianum* Zone.

Paravascoceras Furon (type species *Vascoceras cauvini* Chudeau) is retained as a separate genus for forms derived from *Nigericeras* Schneegans. *Pseudovascoceras* gen. nov. (type species *Vascoceras nigeriense* Woods) is proposed for ribbed and multituberculated forms thought to have arisen from *Cunningtoniceras* Collignon. *Paravascoceras* and *Pseudovascoceras* are most properly referred to the subfamily Acanthoceratinae since they have an origin separate from that of *Vascoceras*.

Several of the taxa present show a high degree of individual variation. Palaeoecological factors played an important role in their geographical distribution and probably also in their potential for polymorphism. Separate lineages converged on a 'Vascoceras morphology' in north-eastern Nigeria as a response to the particular environmental conditions prevailing there during Late Cenomanian and Early Turonian times.

INTRODUCTION

In Tethyan regions ammonites referred to the genus *Vascoceras* Choffat, 1898, are often present in large numbers in the Upper Cenomanian and Lower Turonian. The upper Benue Trough area in north-eastern Nigeria is a classic region for such faunas.

Its ammonites have been described by Woods (1911), Reyment (1954b), Barber (1957, 1960), Meister (1989), Zaborski (1990a, 1993, 1995) and Courville (1992). Species of *Vascoceras* have been widely employed in biostratigraphical analysis in Nigeria but the taxonomic treatment applied to them has varied widely from author to author. The north-eastern Nigerian faunas are of particular interest since large collections can be made under

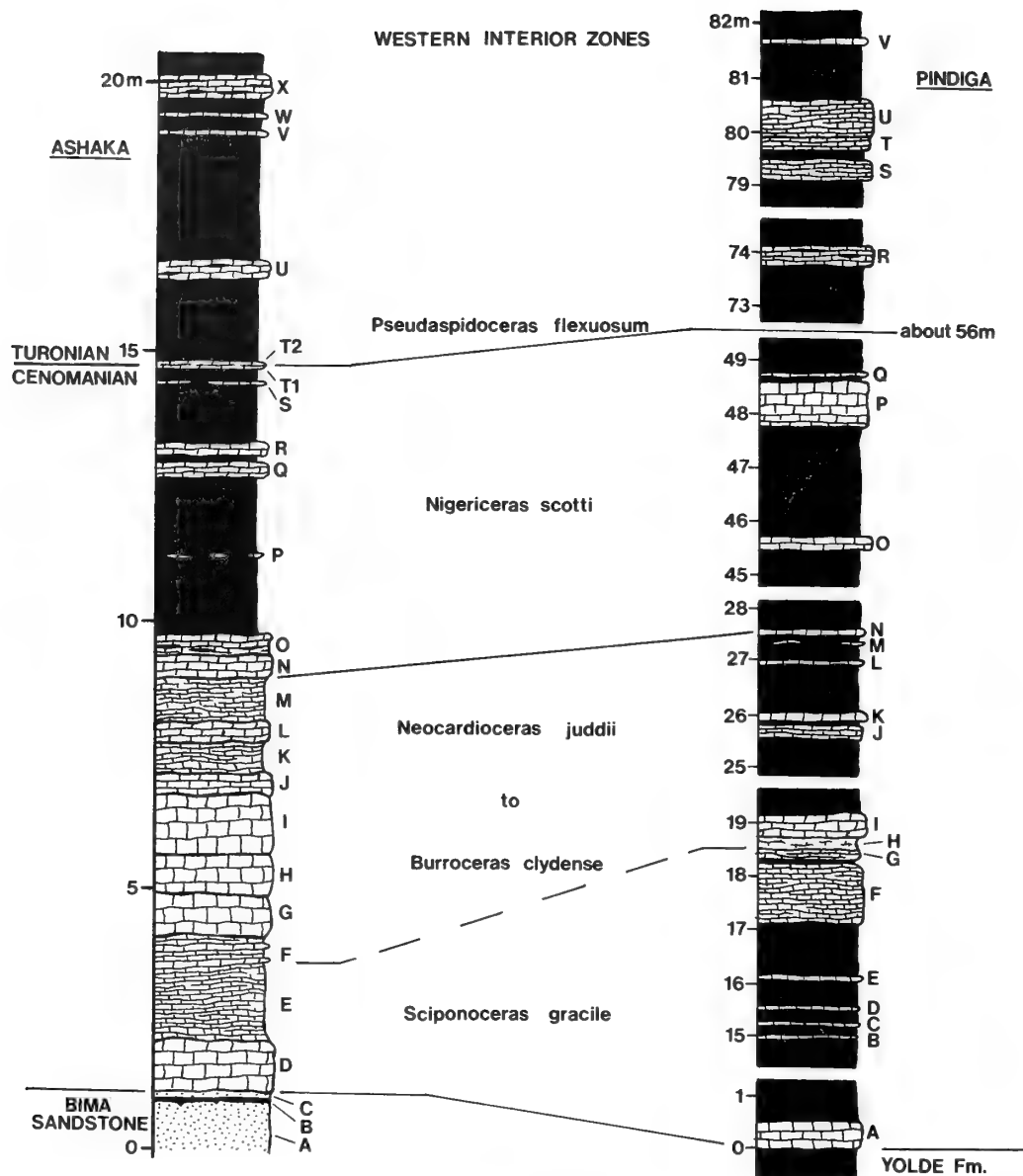


Fig. 1 Stratigraphical sections through the limestone-bearing parts of the Pindiga Formation at Ashaka and Pindiga with letter codes identifying limestone units mentioned in the text. Approximate biostratigraphical correlations with the ammonite biozones of the western interior of the United States (after Cobban *et al.* 1989, Hancock 1991) are also indicated.

tight stratigraphical control, especially at Ashaka quarry. Furthermore, dissection of adults is frequently successful in recovering well-preserved inner whorls which in some cases are invaluable for identification purposes, as well as for analysing ontogenetic development. These attributes have allowed a revised taxonomy to be presented here for the Nigerian faunas.

The family Vascoceratidae as a whole has been discussed by Spath (1925), Furon (1935), Schneegans (1943), Reymont (1954b, 1955, 1956), Barber (1957), Wiedmann (1960), Cooper (1978) and Wright & Kennedy (1981).

From the time of its proposal it has been recognized that the genus *Nigericeras* Schneegans, 1943 is morphologically intermediate between the subfamilies Acanthoceratinae and Vascoceratinae. More recently, a number of additional genera of

intermediate character have been described, a notable feature being the combination of a vascoceratine-type suture pattern with an acanthoceratine-type ornament. Such intermediates include *Microdiphasoceras* Cobban, Hook & Kennedy (1989: 53), *Rubroceras* Cobban, Hook & Kennedy (1989: 54), *Fikaites* Zaborski (1993: 362) and *Pseudovascoceras*, described herein. It is believed here that the family Vascoceratidae is polyphyletic, including homeomorphic derivatives of various acanthoceratine genera. In Nigeria at least the same is true of forms previously referred to the genus *Vascoceras*.

SYSTEMATIC DESCRIPTIONS

Repositories. Unless otherwise stated all the specimens referred to below are housed in the Department of Palaeontology, The Natural History Museum, London, their register numbers being prefixed with the letter C. In addition to those specifically listed, large numbers of *Paravascoceras cauvini*, *Vascoceras woodsi*, *V. bullatum*, *V. globosum costatum*, *V. globosum globosum* and *Pseudovascoceras nigeriense* have also been studied.

Provenance of material. The ammonite-bearing horizons at the two main localities in north-eastern Nigeria, Ashaka and Pindiga, are shown in Fig. 1. A fuller description of these sections and lists of their ammonite faunas were given by Zaborski (1995). The Ashaka section has also been described by Wozny & Kogbe (1983), Popoff *et al.* (1986), Meister (1989) and Courville (1992). The Pindiga section has been described by Barber (1957), Carter *et al.* (1963), Wozny & Kogbe (1983) and Popoff *et al.* (1986). The whereabouts of other ammonite localities mentioned in the text were shown by Zaborski (1990a: fig. 1).

Dimensions (in mm). D, diameter; Wb, whorl breadth; Wh, whorl height; U, umbilical diameter. Figures in parentheses are dimensions as a percentage of the total diameter.

Superfamily ACANTHOCERATAEAE Grossouvre, 1894

Family ACANTHOCERATIDAE Grossouvre, 1894

Subfamily ACANTHOCERATINAE Grossouvre, 1894

Genus **PARAVASCOCERAS** Furon, 1935

(= *Paracanthoceras* Furon, 1935; *Pachyvascoceras* Furon, 1935; *Broggiiceras* Benavides-Cáceres, 1956)

TYPE SPECIES. *Vascoceras cauvini* Chudeau, 1909; by the subsequent designation of Reyment, 1955.

REMARKS. Furon (1935: 60) proposed *Paravascoceras* as a subgenus of *Vascoceras* and it has subsequently been treated as such by, for example, Schneegans (1943), Cooper (1978), Howarth (1985) and Meister *et al.* (1992). Others, for example Reyment (1955), Barber (1957), Wright (1957), Freund & Raab (1969), Schöbel (1975) and Meister (1989), have regarded it as a distinct genus while recently it has been widely listed as a synonym of *Vascoceras* (see, for example, Berthou *et al.* 1985, Kennedy *et al.* 1987, Luger & Gröschke 1989, Cobban *et al.* 1989).

Furon's original diagnosis of *Paravascoceras* specified non-globular forms characterized by a simple suture pattern which was said to distinguish it from *Paracanthoceras* Furon (1935: 59) (type species, by monotypy, *Vascoceras (Paracanthoceras) chevalieri* Furon, 1935). Both these forms show strong ventral ribbing in their later growth stages. Furon included *V. (P.) cauvini*, *V. (P.) cauvini* var. *semiglabra* Furon (1935) and *V. (P.) chudeaui* Furon (1935) in *Paravascoceras*. The last two are here regarded as synonyms of *P. cauvini*. Schneegans (1943: 127–128) showed that sutural differences between *Paravascoceras* and *Paracanthoceras* were insignificant and demonstrated the latter to be a synonym of the former. Indeed, *V. (Paracanthoceras) chevalieri* itself is a synonym of *Paravascoceras cauvini*. Schneegans gave a revised diagnosis of *Paravascoceras* stressing its vascoceratid suture pattern, ovoid to globular whorl section, lack of tubercles and possession of simple ventral ribs or folds in the adult stages. The absence of

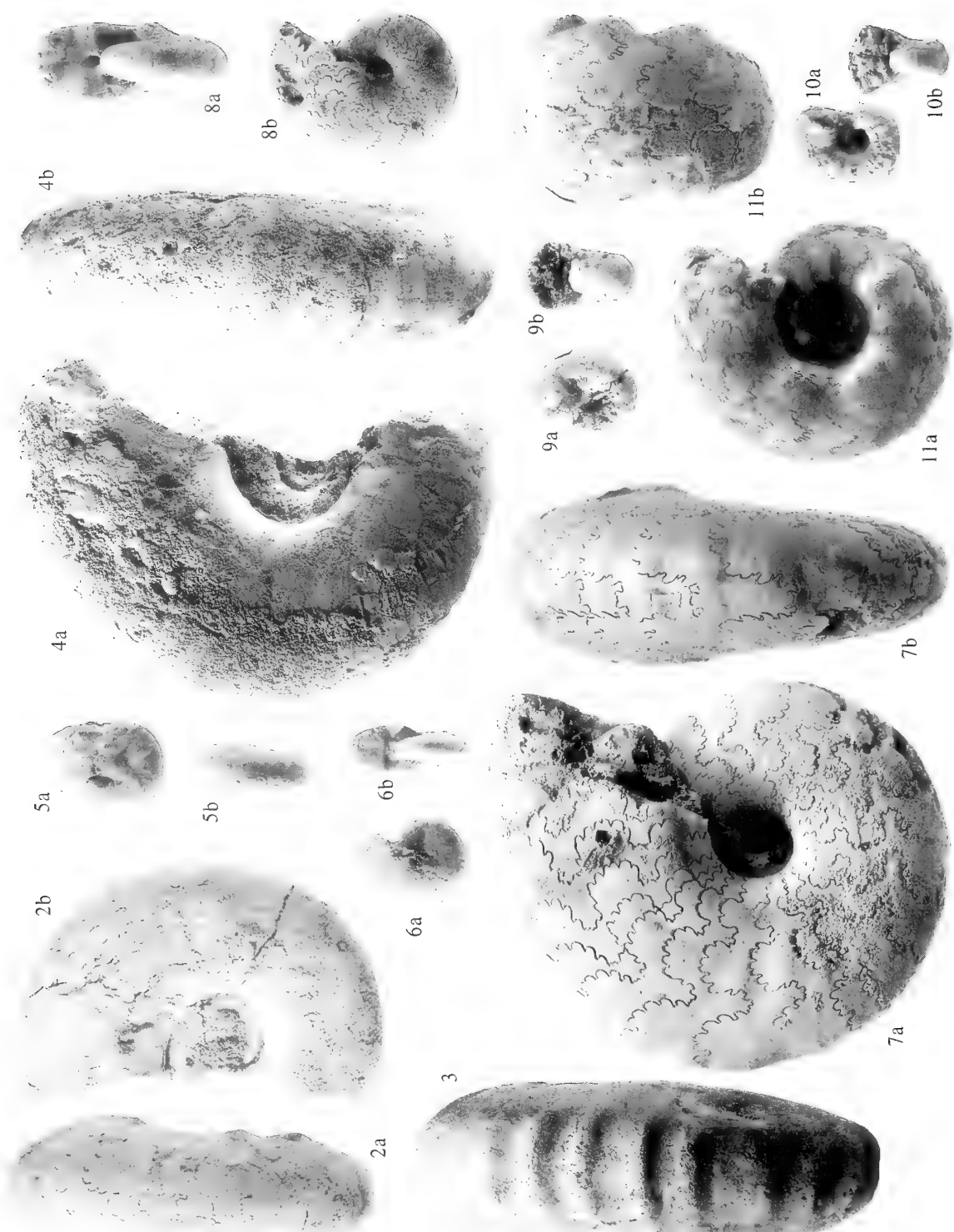
umbilical tubercles has since been cited as a chief distinguishing feature of *Paravascoceras* (see, for example, Freund & Raab 1969, Schöbel 1975, Meister 1989, Meister *et al.* 1992). Berthou *et al.* (1985), however, regarded the presence or absence of umbilical tubercles in *Vascoceras* as an inadequate basis for generic and subgeneric diagnosis, a conclusion accepted by Kennedy *et al.* (1987) and Cobban *et al.* (1989). This view is supported here. There is great inconsistency in this feature even within individual species of *Vascoceras*. Meister *et al.* (1992: 70; see also below) further showed that *P. cauvini* may itself show umbilical tubercles at certain growth stages.

As pointed out by Schneegans (1943: 127), the juvenile stages are often of greater value in taxonomic subdivision of *Vascoceras* than the often highly variable middle and adult whorls. Morphological and stratigraphical evidence from north-eastern Nigeria indicates that *Paravascoceras* was derived from *Nigericeras* (type species *Nigericeras gignouxii* Schneegans, 1943: 119, pl. 5, figs 10–15 = *N. gadeni* (Chudeau); by the subsequent designation of Reyment 1955: 62), an origin separate from that of *Vascoceras* (see below). In recognition of this probability *Paravascoceras* is here treated as a distinct genus. In view of its ornament and suture pattern *Nigericeras* should be included in the subfamily Acanthoceratiniae (see also Kennedy *et al.* 1989, Cobban *et al.* 1989, Kennedy & Wright in press). *Paravascoceras*, therefore, cannot be maintained within the Vascoceratidae but should be transferred to the Acanthoceratiniae also.

There remain problems in providing a reliable and unambiguous morphological diagnosis of *Paravascoceras*. Its members are generally compressed, moderately involute, without umbilical tubercles and with strong regular ribbing on the outer flanks and venter in the later growth stages. The last two features are not, however, consistent while certain rather depressed forms may belong in the genus.

Vascoceras (Pachyvascoceras) Furon (1935: 58) (type species *Vascoceras (Pachyvascoceras) crassus* Furon 1935: 58, pl. 3, figs 2a, b; by the subsequent designation of Reyment 1954b: 257) was proposed on the basis of its globular shape, deep narrow umbilicus and lack of adult ornament. None of these morphological features is sufficient to distinguish *Pachyvascoceras* from *Vascoceras*. Whorl breadth is often particularly variable within individual species of that genus. The phylogenetic affinities of *V. (P.) crassum*, however, may lie with *Paravascoceras* rather than *Vascoceras*. Meister *et al.* (1992) described topotype material which they regarded as variants of *Paravascoceras cauvini* with which they are transitional (see also Schneegans 1943). *Pachyvascoceras* is accordingly treated here as a probable synonym of *Paravascoceras* (see also below under *Vascoceras bullatum* and *V. globosum*).

The genus *Broggiiceras* Benavides-Cáceres (1956: 469–470) was proposed for the Peruvian forms *B. olsoni* Benavides-Cáceres (1956: 471, pl. 55, figs 1–4), the type species, and *B. humboldti* Benavides-Cáceres (1956: 471, pl. 56, figs 3–6). These forms have smooth inner whorls and an adult ornament of strong ventral ribs matching that in *P. cauvini*. *B. olsoni* has whorls a little broader than high. While the opposite condition may prevail on the body-chamber of *B. humboldti*, the two are probably synonyms. In the absence of any significant recorded differences from *Paravascoceras*, *Broggiiceras* is best regarded as a synonym. Schöbel (1975) and Meister *et al.* (1992), indeed, considered both *B. olsoni* and *B. humboldti* as synonyms of *P. cauvini*.



Figs 2–8 *Paravascoceras canvini* (Chudeau). Figs 2–4, Pindiga Formation, unit K, Ashaka. Fig. 2a, b, C.93336, $\times 1$. Fig. 3, C.93337, $\times 1$. Fig. 4a, b, C.93338, $\times 1$. Fig. 5a, b, Pindiga Formation, unit F, Ashaka. C.93556a, $\times 1$. Figs 6, 7, Pindiga Formation, unit O, Ashaka. Fig. 6a, b, C.93313, $\times 1$. Fig. 7a, b, C.93518, $\times 1$. Fig. 8a, b, Pindiga Formation, unit H, Pindiga. C.93540, $\times 1$.

Figs 9–11 *Vascoceras woodsi* sp. nov. Figs 9, 10, Pindiga Formation, Deba Habe. Fig. 9a, b, paratype. C.93596a, $\times 2$. Fig. 10a, b, paratype. C.93596c, $\times 2$. Fig. 11a, b, Pindiga Formation, unit M, Pindiga. Paratype, C.91264, $\times 1$.

- Paravascoceras cauvini** (Chudeau, 1909) Figs 2–8
- 1909 *Vascoceras cauvini* Chudeau: 68, pls 1, 2; pl. 3, figs 1, 2.
- 1921 *Thomasites cauvini* (Chudeau) Chudeau: 463, fig. 1.
- 1933 *Vascoceras cauvini* Chudeau; Furon: 268, pl. 9, fig. 9.
- 1935 *Vascoceras (Paracanthoceras) Chevalieri* Furon: 59, pl. 4, figs 1a, b.
- 1935 *Vascoceras (Paravascoceras) Cauvini* Chudeau Furon: 60, pl. 5, figs 1a, b.
- 1935 *Vascoceras (Paravascoceras) Chudeai* Furon: 61, pl. 4, fig. 2.
- 1935 *Vascoceras (Paravascoceras) Cauvini* Chudeau nov. var. *semiglabra* Furon: 61, pl. 4, fig. 3.
- 1943 *Paravascoceras cauvini* (Chudeau); Schneegans: 128, pl. 4, fig. 2.
- 1943 *Paravascoceras cauvini* var. *evoluta* Schneegans: 130, pl. 8, fig. 2.
- 1943 *Paravascoceras cauvini* var. *inflata* Schneegans: 131.
- 1943 *Paravascoceras chevalieri* Furon Schneegans: 132, pl. 4, fig. 7.
- 1957 *Vascoceras bulbosum* (Reyment) Barber: 19, pl. 6, figs 6, 8; pl. 27, figs 1–6.
- 1957 *Vascoceras depressum* Barber: 19, pl. 6, fig. 5; pl. 27, figs 7–9.
- ?1957 *Paravascoceras aff. cauvini* (Chudeau); Barber: 37, pl. 14, figs 2, 3; pl. 32, figs 8, 9.
- ?1965 *Paravascoceras aff. cauvini* (Chudeau); Collignon: 183.
- 1969 *Paravascoceras cauvini* (Chudeau); Freund & Raab: 20, pl. 3, figs 1–3; text-figs 5a, b.
- 1969 *Paravascoceras tavense* (Faraud) Freund & Raab: 23, pl. 2, fig. 9, text-figs 5e–g.
- 1975 *Paravascoceras cauvini* (Chudeau); Schöbel: 119, pl. 4, fig. 3; pl. 5, figs 1–4.
- ?1981 *Paravascoceras cauvini* (Chudeau); Collignon & Roman (in Amard, Collignon & Roman): 51, pl. 3, fig. 9.
- ?1981 *Paravascoceras chevalieri* (Furon); Collignon & Roman (in Amard, Collignon & Roman): 52, pl. 6, figs 1, 2.
- ?1981 *Nigericeras barcoicense* (Choffat) Collignon & Roman (in Amard, Collignon & Roman): 54, pl. 4, figs 16a, b.
- 1989 *Vascoceras cauvini* Chudeau; Luger & Gröschke: 374, pl. 40, figs 3, 6, 8, 9; pl. 41, figs 1–4; pl. 42, fig. 1; text-figs 6G, H, 8C.
- 1989 *Nigericeras gadeni* (Chudeau) *lamberti* Schneegans; Meister: 10, pl. 3, figs 1–3; text-fig. 6.
- 1989 *Nigericeras jacqueti* Schneegans; Meister: 11, pl. 2, figs 3, 4; pl. 4, fig. 1; text-fig. 7.
- 1989 *Paravascoceras aff. nigeriense?* (Woods) Meister: 16, pl. 5, fig. 3.
- 1990a *Vascoceras cauvini* Chudeau; Zaborski: figs 8, 12–15.
- 1990a *Vascoceras bulbosum* (Reyment); Zaborski: fig. 11.
- 1992 *Vascoceras (Paravascoceras) cauvini* (Chudeau); Meister, Alzouma, Lang & Mathey: 71, pl. 4, fig. 6; pl. 5, fig. 1, pl. 6, fig. 2.
- 1992 *Vascoceras (Paravascoceras) cauvini forme lisse* Meister, Alzouma, Lang & Mathey: 72, pl. 5, fig. 2; pl. 6, figs 1, 3.
- 1992 *Vascoceras (Paravascoceras) cauvini forme comprimée* Meister, Alzouma, Lang & Mathey: 72, pl. 5, fig. 3; pl. 6, fig. 4.
- 1992 *Vascoceras gr. cauvini* Chudeau; Courville: pl. 4, figs 1–3.

MATERIAL AND OCCURRENCE. Thirty-six specimens, C.91304, Pindiga Formation, unit E, Ashaka; C.93556a, b, C.93557–9, C.93932, Pindiga Formation, unit F, Ashaka; C.93336–8, Pindiga Formation, unit K, Ashaka; C.91271–4, C.93304, C.93313, C.93517–8, Pindiga Formation, unit O, Ashaka; C.91278–84, C.93540–2, C.93933, Pindiga Formation, unit H, Pindiga; C.91285–9, C.93539, Pindiga Formation, unit J, Pindiga; C.91312, Pindiga Formation, unit N, Pindiga. The species has a known stratigraphical range from unit E (upper half) to unit O at Ashaka and from unit G to unit N at Pindiga.

DIMENSIONS. See Fig. 12.

REMARKS. In north-eastern Nigeria *Paravascoceras cauvini* includes forms showing whorls slightly to distinctly higher than broad, with rounded to slightly flattened venters and an umbilicus representing 16–29% of the total diameter. The species has a relatively long stratigraphical range here but successive assemblages show some variation.

Material from unit F at Ashaka reaches a maximum diameter of some 100 mm. The adult whorls are smooth or with weak, irregular, crease-like ventral ribbing. The inner whorls, however, may show alternating long and short ribs (Fig. 5). The long ribs arise at umbilical tubercles. All ribs bear vague ventrolateral swellings but there are no siphonal tubercles. Umbilical tubercles or bulges may persist into the middle growth stages. This umbilical ornament is especially pronounced in certain specimens collected from the equivalent horizon (unit H) at Pindiga.

Material from unit K at Ashaka is the oldest found to show the strong ventral adult ribbing which characterizes the species (Fig. 3; Meister 1989: pl. 3, fig. 1).

Material from unit O can be regarded as fully typical of *P. cauvini*. The inner whorls (Fig. 6) are completely smooth. This is usually the case with the middle growth stages also but rare individuals show bullate to clavate umbilical tubercles. Even less frequently there are broad, low, ventrolateral swellings but such features disappear by a diameter of 45 mm. Ventral ribbing is commonly displayed in the later growth stages (see Zaborski 1990a: fig. 14) but this ornament appears at a diameter varying from 60 mm to over 100 mm and is sometimes lacking altogether. Adults reach a maximum diameter of over 160 mm.

In general whorl proportions *P. cauvini* is a very close match for *Nigericeras gadeni* (Chudeau). The middle and adult whorls of the two may be difficult to distinguish unless sutures are visible; *N. gadeni* has square saddles, a narrow L and a distinctly bifid E/L. *P. cauvini* has more rounded and evenly frilled saddles. The material from Ashaka referred to *Nigericeras* by Meister (1989) in fact belongs in *P. cauvini*. The early whorls of *N. gadeni* are distinct, showing a typically acanthoceratine ornament with long and short ribs and seven rows of tubercles (see Schneegans 1943, Zaborski 1990a, Meister *et al.* 1992). Vestiges of a similar ornament, but without siphonal tubercles however, occur in early *P. cauvini* from unit F at Ashaka. The middle whorls of specimens from unit H at Pindiga sometimes show the strong bulge-like umbilical tubercles that are common at the same growth stage in *N. gadeni*. Meister *et al.* (1992: 70) and Courville (1992: 415) have also drawn attention to similarities between the juvenile ornament and in some cases suture pattern of *P. cauvini* and *Nigericeras*.

Nigericeras gadeni characterizes the basal ammonite-bearing beds in north-eastern Nigeria, occurring in unit D at Ashaka and unit A at Pindiga. It therefore predates *P. cauvini*. It is probable that *P. cauvini* is derived from *N. gadeni* by a progressive

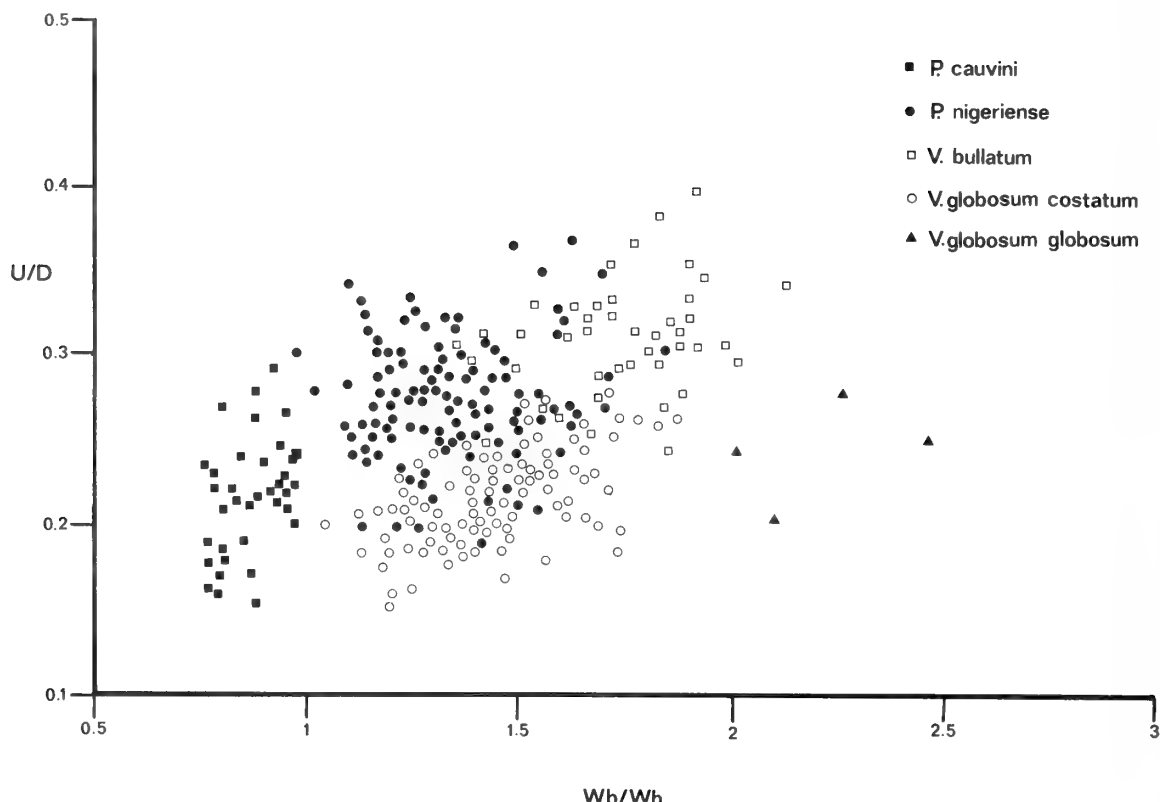


Fig. 12 Shell proportions in *Paravascoceras cauvini* (Chudeau), *Pseudovascoceras nigeriense* (Woods), *Vascoceras bullatum* Schneegans, *V. globosum costatum* (Reyment) and *V. globosum globosum* (Reyment) from unit O at Ashaka. These individuals are the product of collecting carried out over the course of two hours specifically for the purpose of comparing dimensions. This figure also gives a good indication of the relative abundances of the taxa concerned.

loss of juvenile ornamentation (peramorphosis), simplification of suture pattern and development of adult ribbing. Forms from unit F at Ashaka and unit H at Pindiga are transitional in nature.

Schneegans (1943: 119–125) proposed three additional species of *Nigericeras*, *N. gignouxi*, *N. lamberti* and *N. jacqueti* which show an increasingly weaker ornament but which all display the typically acanthoceratine suture pattern of the genus. It may be noted that in north-eastern Nigeria there is a variation in the strength of ornament of *Nigericeras* collected from place to place. Individuals from Teli and from north-east of the Biu Plateau (see Zaborski 1990a: figs 4, 5) have a weak juvenile ornament while those from the Hinna region and from between Kanawa and Wajari (see Zaborski 1990a: figs 6, 7) have stronger ornament. There is, however, no available evidence of this variation having a stratigraphical significance. In Niger, forms of *N. jacqueti* type occur alongside typical *N. gadeni* (Meister *et al.* 1992).

In north-eastern Nigeria *N. gadeni* occurs in the equivalent of the Geslinianum Zone in north-west Europe and the Gracile Zone in the western interior of the United States (Zaborski 1990a). *P. cauvini* ranges through the probable equivalents of the Juddii Zone in north-west Europe and the Clydense to Scotti zones in the western interior (see below). Lewy *et al.* (1984) described *P. cauvini* in association with *Metoicoceras geslinianum* (d'Orbigny) in Israel. Their material, however,

shows broad flank ribbing and umbilical bulges (Lewy *et al.* 1984: fig. 4I) in its middle whorls, features more typical of *Nigericeras* from which it appears to be transitional. Its suture is unknown.

Cooper (1979) and Kennedy & Wright (in press) proposed an origin for *Nigericeras* within *Pseudocalycoceras* Thomel, 1969. The early whorls in *Nigericeras*, however, also resemble the dwarf *Protacanthoceras bunburianum* (Sharpe) (see Wright & Kennedy 1980: 91, figs 29–33, 41–43, 48; 1987: 215, pl. 55, figs 10–16; text-figs 83B, C, 84D–H), a lowest Upper Cenomanian Guerangeri Zone species. *Nigericeras* may be a peramorphic derivative.

The small Nigerian specimens from low in the Pindiga section referred to *Vascoceras bulbosum* (Reyment) and *V. depressum* sp. nov. by Barber (1957) are here regarded as *P. cauvini* as is the material from Ashaka included in *Nigericeras* by Meister (1989).

The *P. cauvini* from Nigeria are compressed forms which fall into a distinct morphological group within the ammonite fauna from unit O at Ashaka (Fig. 12). Individuals from Niger, however, develop a broader whorl section (see Meister *et al.* 1992: pl. 6, fig. 2). These specimens seem to be of the same age as those from unit O at Ashaka. The latter are associated with very large numbers of more inflated ammonites referable to *Vascoceras globosum costatum*, *V. bullatum* and *Pseudovascoceras nigeriense*. These three forms are of markedly

less importance in Niger, if they are present at all. Their possible absence may have allowed populations of *P. cauvini* in Niger to develop a greater range of morphotypes due to lack of competition. Meister *et al.* (1992: 72–76) described a number of additional forms from Niger as *Vascoceras* (*Paravascoceras*) *cauvini forme crassum* (Furon) and *V. (P.) cauvini forme de transition entre forme crassum et V. (P.) proprium* (Reyment). They are further discussed below under *Vascoceras globosum*.

Also of interest in regard to their general whorl proportions are *Paravascoceras rumeaui* Collignon (1957: 122, pl. 16, fig. 2; Freund & Raab 1969: 21, pl. 3, figs 4, 5; text-figs 6c, d; Luger & Gröschke 1989: 380, pl. 41, figs 5, 6; pl. 42, figs 3, 4; text-fig. 8D) from Algeria, Egypt and Israel and *Vascoceras costellatum* Collignon & Roman (*in Amard *et al.* 1981*: 51, pl. 2, figs 6a, b) from Algeria. These species have adult ventral ribbing like that in *P. cauvini* but are more inflated. They may, like the Niger forms, be regional variants of *P. cauvini*. Luger & Gröschke (1989: 375–376) discussed the question of whorl breadth in *P. cauvini* but, unlike Schöbel (1975), regarded *P. rumeaui* as distinct from *P. cauvini*. They further separated individuals with depressed whorls but which were otherwise similar to *P. cauvini* as *Vascoceras cf. cauvini* (Luger & Gröschke 1989: 376, pl. 42, fig. 2; pl. 43, fig. 3; text-figs 6F, 8B).

The *P. cauvini* of Collignon & Roman (*in Amard *et al.* 1981*: 51, pl. 3, fig. 9) have whorls only a little broader than high and probably belong here. Their *Paravascoceras chevalieri* (Furon) (Collignon & Roman *in Amard *et al.* 1981*: 52, pl. 6, figs 1, 2) and *Nigericeras barcoicense* (Choffat) (Collignon & Roman *in Amard *et al.* 1981*: 54, pl. 4, figs 16a, b) are similar to and may be conspecific with *P. cauvini*. The *Paravascoceras aff. chevalieri* of Reyment (1955: 63, pl. 14, figs 1a, b), however, shows three rows of tubercles upon the ventral ribs and more closely resembles early *Thomasites gongilensis* from unit O at Ashaka (see Figs 41–44).

The *Vascoceras* (*Paravascoceras*) *cf. cauvini* from Angola described by Cooper (1978: 130, figs 6C–H, 35–37) is a *Nigericeras*.

Berthou *et al.* (1985: 72) speculated that *Vascoceras barcoicense* Choffat (1898: 67, pl. 17, fig. 1; pl. 22, fig. 5; Berthou *et al.* 1985: 70, pl. 4, figs 1–3) might turn out to be a senior synonym of *P. cauvini*. The strong adult ribbing of the latter species is, however, unknown in *V. barcoicense*. Whorl proportions in the two are similar but nothing is known of the early growth stages in *V. barcoicense*. The species may belong in *Paravascoceras* or alternatively it may be an involute, weakly ornamented variant of *Vascoceras gamai* Choffat, according to Berthou *et al.* (1985: 71).

V. barcoicense exile Cobban, Hook & Kennedy (1989: 47, figs 47, 87Q-S, 89M-GG) from New Mexico resembles *P. cauvini* in whorl proportions but is more involute. Specimens from low in the Pindiga section may be similar in this respect (Fig. 8) but *V. barcoicense exile* has a different juvenile ornament of rather strong ventral ribs. The *V. (V.) cauvini* of Kennedy *et al.* (1989: 82, figs 9G, 20C–G) from Texas are similar to and probably conspecific with *V. barcoicense exile*.

Further involute compressed forms are the *Nigericeras jacqueti involutum* Meister, Alzouma, Lang & Mathey (1992: 68, pl. 4, figs 3–5; text-fig. 14) from Niger. Again, these show similarities with *P. cauvini* from unit H at Pindiga but are consistently more involute. Their suture pattern (Meister *et al.* 1992: fig. 14) is incompletely known but seems to be intermediate between that of *Nigericeras* and *Paravascoceras*. Meister *et al.* (1992) regarded *N. jacqueti involutum* as an offshoot of *N. gadeni* derived through *N. jacqueti jacqueti*. It may be the product of a

local lineage independent of that giving rise to *P. cauvini*.

Genus *PSEUDO-VASCOCERAS* gen. nov.

TYPE SPECIES. *Vascoceras nigeriense* Woods, 1911.

DIAGNOSIS. Moderately evolute to moderately involute, moderately compressed to moderately depressed ammonites. Whorls rounded to subpentagonal. Ornament of umbilical, inner and outer ventrolateral and siphonal tubercles which may be borne upon transverse to concave ribs of varying strength. Additional ventral ribs frequently present. Ornamental elements of highly variable persistence during ontogeny, sometimes extending onto the body-chamber, in other cases confined to the earliest growth stages. Suture line simple with evenly frilled elements; saddles often elongate and rectangular in outline, lateral lobe fairly broad.

REMARKS. Of all the ammonites from north-eastern Nigeria showing ‘vascoceratid’ suture patterns it is the multituberculated forms which have proved most problematical and which have received the most varied taxonomic treatment. This is not surprising given the huge range of morphotypes that are represented within assemblages from the same stratigraphical horizon, at Ashaka unit O. In fact three multituberculated genera are present therein, end members of which are not always easy to differentiate. Forms attributable to *Rubroceras* Cobban, Hook & Kennedy occur as rarities (Zaborski 1993); a larger number of individuals belong in *Fikaites* Zaborski (1993); but the greatest number are here referred to *Pseudovascoceras nigeriense* (Woods).

In his treatment of this last group Barber (1957) assigned them to three genera, *Vascoceras*, *Nigericeras* and *Paramammites* Furon, and no less than seven species. The last two generic determinations can easily be disposed of. The type species of *Paramammites* (by the subsequent designation of Reyment 1954b: 225), *Vascoceras polymorphum* Pervinquière (1907: 336, pl. 21, figs 2, 6; text-fig. 126) (see also Renz 1982: 84–85; Chancellor *et al.*, in press) has a juvenile ornament of varying strength, often with large spinose tubercles, but always lacks siphonal tubercles. The present material has nothing to do with *Paramammites*. Forms with strong adult costae, interrupted ventrally, have often been referred to this genus without knowledge of their ontogenetic development (see also Cobban *et al.* 1989: 51; Zaborski 1990b: 574–575) thus creating a rather confused situation. *Nigericeras* resembles the present material in only one real respect, the presence of seven rows of tubercles. In detail its ornament is more regular and in all genuine members of the genus it is confined to the early whorls (see Schneegans 1943). The suture in *Nigericeras*, although simple, is of a distinctly acanthoceratine pattern, unlike that in the present material and other forms mentioned below also previously referred to *Nigericeras*. Nor can the present material be referred to *Vascoceras*. Its ornament is unlike that in any known species of the genus and quite distinct from that in the type species *V. gamai*.

Cobban *et al.* (1989: 51) pointed out that Barber’s (1957) *Paramammites* needed a new generic name. They suggested that these forms were in part ribbed and tuberculated derivatives of *Vascoceras*. The genus *Pseudovascoceras* is here proposed to include this material, the name alluding to the homeomorphy between smooth members of the type species and true *Vascoceras*. The origin of the genus, however, is thought to lie in

an earlier acanthoceratine genus, probably *Cunningtoniceras* Collignon, 1937 as detailed below.

Nigericeras scotti Cobban (1971: 18, pl. 9, figs 1–4; pl. 18, figs 1–9; text-figs 15–19) from the terminal Cenomanian of the United States western interior may be a *Pseudovascoceras*. It lacks the suture pattern typical of *Nigericeras* but resembles the more strongly ornamented examples of *P. nigeriense*.

The unnamed specimen from Turkestan figured by Kler (1909: pl. 8, figs 3a, b; text-fig. 6) may also be a *Pseudovascoceras*.

The English specimen (C.82287) from the high Cenomanian referred to *Nigericeras cf. gignouxi* Schneegans by Wright & Kennedy (1981: 85, pl. 15, figs 6a, b) is a fragment, the ornament and suture pattern of which cannot be made out clearly. It might be best referred to *Pseudovascoceras*. It occurs alongside *Thomasites gongilensis*. In Nigeria *Thomasites* occurs well above the stratigraphical level of *Nigericeras*, but its earliest members are coeval with *P. nigeriense*.

Pseudovascoceras nigeriense (Woods, 1911)

Figs 14–24, 36, 37

- ?1909 *Vascoceras cauvini* Chudeau: pl. 3, figs 4a, b (only).
- 1911 *Vascoceras nigeriense* Woods: 281, pl. 21, fig. 6; pl. 22, figs 2, 3.
- ?1943 *Vascoceras nigeriense* Woods; Schneegans: 133, pl. 4, fig. 1.
- ?1943 *Paravascoceras cf. barcoicense* (Choffat) Schneegans: 134, pl. 8, fig. 1.
- 1954b *Vascoceras nigeriense* Woods; Reymont: 256.
- ?1955 *Nigericeras ogojaense* Reymont: 62, pl. 13, fig. 6; pl. 14, fig. 3; text-fig. 28.
- 1957 *Vascoceras nigeriense* Woods; Barber: 15, pl. 4, fig. 2; pl. 26, figs 1, 2.
- 1957 *Nigericeras costatum* Barber: 29, pl. 10, figs 3, 4; pl. 11, fig. 3; pl. 30, figs 1–7.
- 1957 *Nigericeras glabrum* Barber: 29, pl. 10, figs 1, 2; pl. 30, fig. 8.
- 1957 *Nigericeras? intermedium* Barber: 31, pl. 11, figs 1, 2; pl. 30, figs 9, 10.
- 1957 *Paramammites tuberculatus* Barber: 31, pl. 12, fig. 1; pl. 13, fig. 2; pl. 31, figs 1–3, 9.
- 1957 *Paramammites raricostatus* Barber: 33, pl. 12, fig. 3; pl. 31, figs 4, 6, 7.
- 1957 *Paramammites inflatus* Barber: 33, pl. 12, fig. 2; pl. 13, fig. 1; pl. 31, figs 5, 8.
- ?1965 *Paramammites laffitei* Collignon: 186, pl. A, fig. 2.
- ?1965 *Paramammites subtuberculatus* Collignon: 187, pl. A, fig. 3.
- 1965 *Vascoceras nigeriense* Woods; Reymont: pl. 2, fig. 2.
- 1965 *Nigericeras costatum* Barber; Reymont: pl. 3, fig. 13.
- ?1965 *Nigericeras ogojaense* Reymont; Reymont: pl. 3, fig. 14.
- 1965 *Paramammites tuberculatus* Barber; Reymont: pl. 3, figs 15a, b.
- 1980 *Nigericeras costatum* Barber; Wright & Kennedy: figs 10a, b.
- 1989 *Paravascoceras nigeriense?* (Woods); Meister: 14, pl. 5, fig. 1; pl. 6, fig. 1; text-fig. 11.
- 1989 *Vascoceras costatum* (Barber) Meister: 23, pl. 10, figs 3, 5; pl. 11, figs 1, 2, 5; text-figs 16a–d.
- 1989 *Vascoceras costatum glabrum* (Barber) Meister: 23, pl. 9, figs 2, 4; pl. 10, fig. 4; text-figs 16e–g.
- 1989 *Vascoceras ellipticum* Barber; Meister: 28, pl. 12, figs 1, 3; text-fig. 18.
- 1989 *Paramammites subconciliatus* (Choffat) Meister: 30, pl.

12, figs 4, 5; pl. 13, figs 1–4; pl. 14, figs 1, 2; pl. 15, figs 1, 4; text-fig. 21.

- 1989 *Paramammites polymorphus* (Pervinquier); Meister: 36, pl. 14, figs 3, 4; text-fig. 24.
- 1990a *Vascoceras nigeriense* Woods; Zaborski: fig. 25.
- 1992 *Vascoceras* sp. gr. *costatum* (Barber) *sensu* Meister, 1989; Courville: pl. 5, fig. 3; pl. 6, figs 2, 3.

LECTOTYPE. Specimen B3237, Sedgwick Museum, Cambridge (see Woods 1911: pl. 22, figs 2, 3); from Kunini, north-eastern Nigeria (selected by Berthou, Chancellor & Lauverjet 1985: 69).

PRESENT MATERIAL AND OCCURRENCE. Sixty-one specimens, C.93305–8, C.93311, C.93315–21, C.93370–93, C.93494a–d, C.93495a–f, C.93496a–d, C.93497–507, Pindiga Formation, unit O, Ashaka.

DIMENSIONS. See Fig. 12.

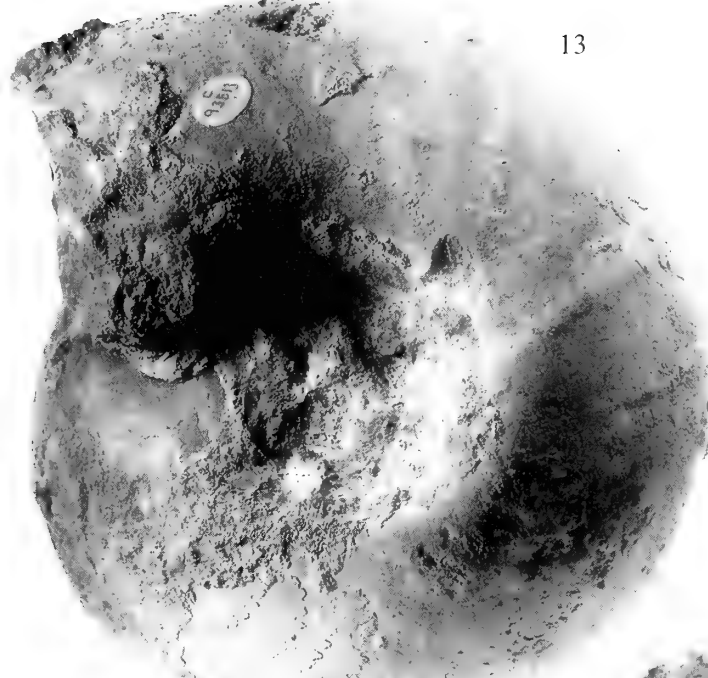
REMARKS. *P. nigeriense* is generally a moderately evolute species having rather compressed to moderately depressed whorls with a rounded to subpentagonal outline. In overall shell proportions it overlaps with both *Vascoceras bullatum* and *V. globosum costatum*; smooth individuals are often especially difficult to distinguish from the last form. The adult diameter varies from about 85 to 120 mm when the body-chamber makes up two-thirds of the final whorl.

It is in its ornamentation that *P. nigeriense* shows its greatest variation, from almost entirely smooth to highly decorated end members. A variation series is shown in Figs 14–24, and there is also abundant figured material in the previous literature (see synonymy list). Dissection of numerous individuals, including those with smooth outer whorls, shows that siphonal tubercles are consistently developed but they may have already disappeared by a diameter of 10 mm. Outer ventrolateral tubercles are also commonly developed while inner ventrolateral and umbilical tubercles may or may not be present. One combination or another of tubercle rows may persist throughout the length of the septate whorls or disappear at any stage in ontogeny. Umbilical tubercles, when present, are the most persistent ornamental features and siphonal tubercles are the least, with the result that numerous individuals show six rows of tubercles in their middle growth stages. Strongly tuberculated forms may in addition display rectiradiate to concave ribs connecting the tubercles. The ribs may branch across the venter while additional ribs with inner and/or outer ventrolateral and siphonal tubercles may be intercalated. Ornamental strength is initiated very early in ontogeny. The ornament of the phragmocone may persist onto the adult body-chamber or this part of the shell may be smooth. Most frequently, however, there are irregularly developed ribs upon the flanks and the venter which vary from strong, broad fold-like structures to fine, dense crease-like features recalling those in adult *Vascoceras woodsi* and *V. bullatum*.

Suture patterns are of a simplified type but the saddles tend to be elongated, especially in strongly ornamented forms. The lateral lobe is fairly wide and often subdivided by a distinct median element.

Meister (1989) separated members of *P. nigeriense* from Ashaka into six taxa, *Paravascoceras nigeriense* (Woods), *Vascoceras ellipticum* Barber, *Paramammites aff. gr. polymorphus* (Pervinquier), *P. subconciliatus* (Choffat), *Vascoceras costatum* (Barber) and *V. costatum glabrum* (Barber). Nevertheless, he showed how the ornamental variation between the last three could easily be interpreted in terms of

13



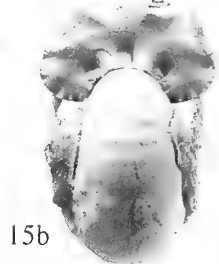
14a



14b



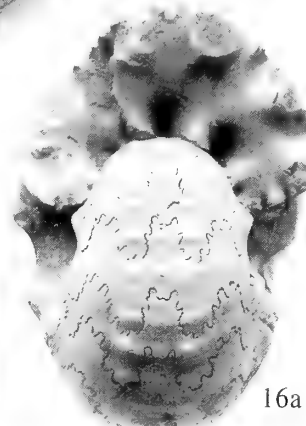
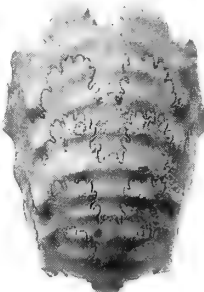
15a



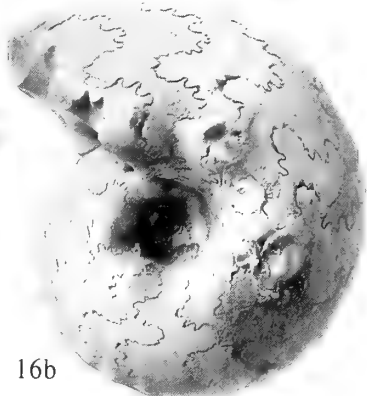
18



17a



16a 16b



17b

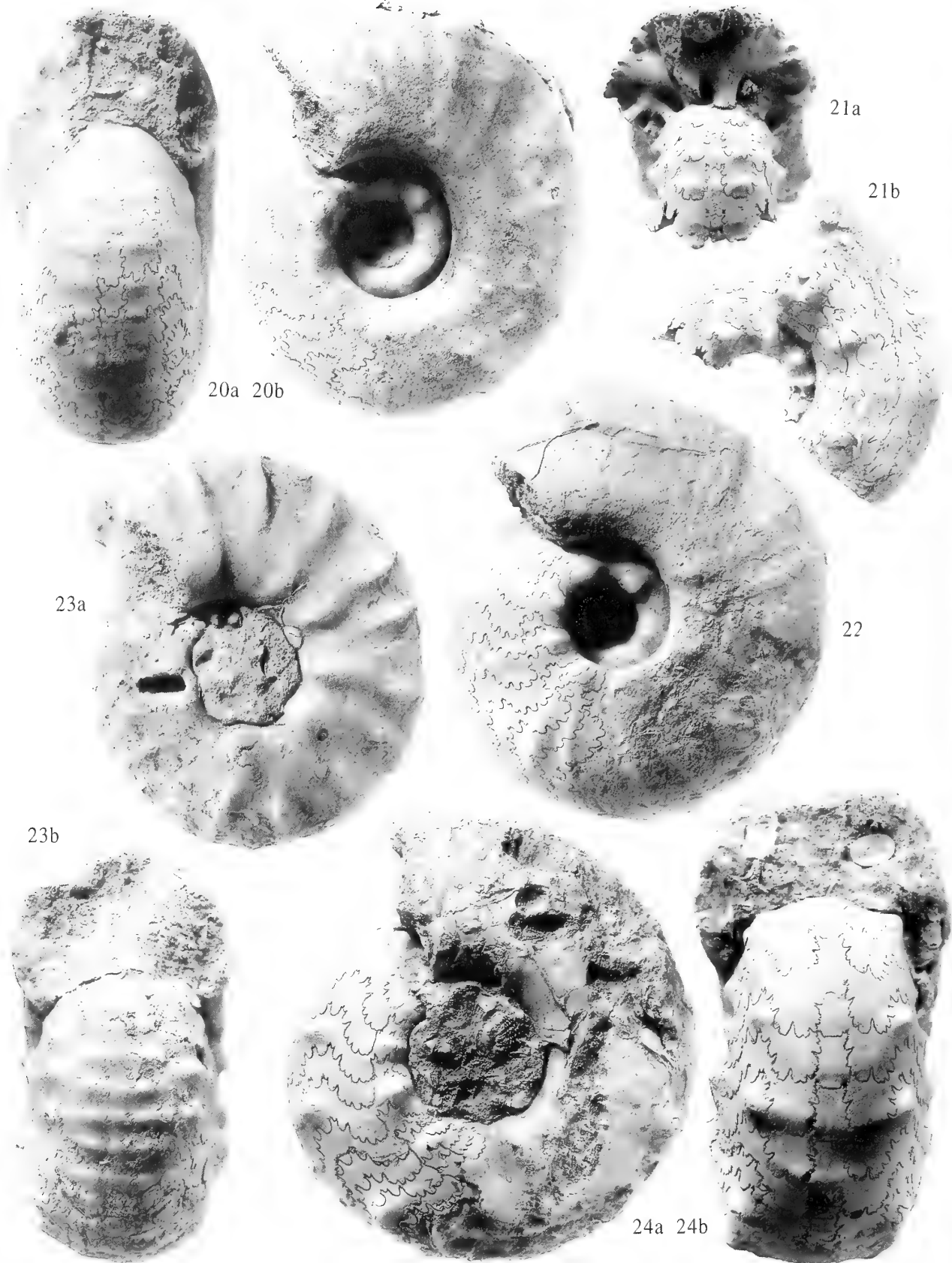


19a 19b



Fig. 13 *Vascoceras bullatum* Schneegans. Pindiga Formation, unit O, Ashaka. C.93513, $\times 1$.

Figs 14–19 *Pseudovascoceras nigeriense* (Woods). Pindiga Formation, unit O, Ashaka. Fig. 14a, b, C.93382, $\times 1$. Fig. 15a, b, C.93383, $\times 1$. Fig. 16a, b, C.93379, $\times 1$. Fig. 17a, b, C.93380, $\times 1$. Fig. 18, C.93321, $\times 1$. Fig. 19a, b, C.93307, $\times 0.75$.



Figs 20–24 *Pseudovascoceras nigeriense* (Woods). Pindiga Formation, unit O, Ashaka. Fig. 20a, b, C.93375, $\times 0.75$. Fig. 21, b, C.93374, $\times 1$. Fig. 22, C.93305, $\times 0.75$. Fig. 23a, b, C.93371, $\times 0.75$. Fig. 24a, b, C.93306, $\times 0.75$.

heterochronic ontogenies (Meister 1989: 34, 36, text-fig. 23). Concerned, however, that the faunas from unit O at Ashaka were condensed and might contain chronologically successive taxa, he refrained from placing them in synonymy. Unit O at Ashaka is the product of a 'slow' rate of sediment accumulation associated with a marine flooding phase. It contains the most diverse marine fauna found at Ashaka including numerous bivalves, gastropods and echinoids as well as a large number of ammonite species (see also Courville 1992: fig. 2). Encrustations of *Plicatula* occur throughout while many of the ammonites show oyster and serpulid overgrowths. There is, however, no significant phosphatization or reworking, and glauconite is rare or absent. There is no reason to believe that this unit represents any greater condensation than several other limestones at Ashaka and elsewhere in north-eastern Nigeria. Phosphatic matter, glauconite and reworked ammonites are common components in the limestone beds of the region, particularly in the upper parts of those interbedded with shales. It is the upper surface of unit O at Ashaka that marks the most significant break in sedimentation, but *P. nigeriense* is found throughout the unit below this level. Both Meister (1989) and Courville (1992) believed they could differentiate between faunas from different levels in unit O (their Niveau 21 and Niveau 22), though their reported successions differ. No significant stratigraphical variation in the nature of the ammonite faunas from this unit has been detected in the present work, apart from the restriction of strongly ornamented *Thomastites* to its upper surface. In the cases of the other ammonites present intraspecific variation is by far the most important factor. No morphometric or ornamental evidence has been obtained which allows objective taxonomic subdivision of *P. nigeriense*. There is a complete intergradation from smooth to strongly ornamented individuals while the latter vary considerably among themselves. In view of these factors all these morphotypes are regarded as conspecific, despite the great differences between end members. Courville (1992: 419–420) came to a similar conclusion and favoured the name *Vascoceras costatum* (Barber) which was used by Meister (1989) for individuals of intermediate ornamental strength. Priority, however, belongs to *Vascoceras nigeriense* Woods, 1911. The lectotype is a smooth end member of the species, as are the individuals referred by Meister (1989) to *Paravascoceras nigeriense?* (Woods) and *Vascoceras ellipticum* Barber.

Smooth examples of *Pseudovascoceras nigeriense* have in the past been compared with *Vascoceras gamai* (Barber 1957: 15; Hancock & Kennedy 1981: 357). Their similarity concerns only the outer whorls, however, and is homeomorphic in nature. Ornamented examples of *P. nigeriense* share similarities with various genera. Meister (1989) referred forms in which the siphonal tubercles disappear early in ontogeny to *Paramammites*, which he regarded as a senior synonym of *Spathites* (*Jeanrogericeras*) Wiedmann, 1960 (type species *Ammonites reveliereanus* Courtiller, 1860). As mentioned above, this material cannot be referred to *Paramammites* or *Jeanrogericeras* as neither shows siphonal tubercles at any growth stage (see Choffat 1898: 64; Pervinquière 1907: 336; Wiedmann 1960: 741; Renz 1982: 84; Berthou *et al.* 1985: 62) and resemblances are superficial only. Some of the present specimens have the appearance of giant *Protacanthoceras proteus* (compare Fig. 23 and Wright & Kennedy 1980: fig. 5). Others with dense, multiple ventral ribbing resemble *Kamerunoceras* Reymont, 1954b (type species *Acanthoceras eschii* Solger, 1904) or *Euomphaloceras* Spath, 1923 (type species *Ammonites euomphalus* Sharpe, 1855), though they lack the typically euomphaloceratine constrictions upon their early

whorls. In its style of ribbing and the generally coarse nature of the tuberculation, the present material most closely resembles *Cunningtoniceras* Collignon, 1937 (type species *Ammonites cunningtoni* Sharpe, 1855). This is mainly a Middle Cenomanian genus (see, for example, Kennedy 1971, Zaborski 1985, Kennedy & Cobban 1990a) but it ranges into the Upper Cenomanian (Wright & Kennedy 1987, Cobban *et al.* 1989, Kennedy & Cobban 1990b). *Pseudovascoceras* may be a descendant of *Cunningtoniceras*. Introduction into north-eastern Nigeria produced peramorphic individuals losing their ornament early in ontogeny and coming to resemble *Vascoceras*. Interestingly there is a morphological overlap between *P. nigeriense* and *Nigericeras ogojaense* Reymont (1955: 62, pl. 13, fig. 6; pl. 14, fig. 3; text-fig. 28); the two are probably conspecific. The latter comes from the southern, oceanward, end of the Benue Trough where smooth individuals are unknown; the holotype (C.47401) and newly collected material (C.93578-61) all show prominent ornament.

Reymont (1979, 1988) has remarked upon the extraordinary polymorphism that may be displayed by vascoceratid species. He believed that in the changeable environment of the Cenomanian-Turonian intracontinental sea in west and Saharan Africa selection would have favoured forms with genetic or phenotypic flexibility. Such taxa would have been capable of responding to environmental fluctuations, each morphotype being best suited to a particular kind of environment. Meister *et al.* (1992) took up this issue in respect of the Niger ammonites. They noted that particular stratigraphical horizons there commonly yield monospecific faunas or assemblages dominated by one species. They speculated that taxa able to occupy niches in the exacting environments prevailing during the Late Cenomanian and Early Turonian faced virtually no competition, the result being a high degree of polymorphism. In unit O at Ashaka a number of ammonite taxa co-exist, largely as a result of introduction of species during a marine flooding episode. While there is some overlap, however, each of the four main taxa described here, *Paravascoceras cauvini*, *Vascoceras bullatum*, *V. globosum costatum* and *Pseudovascoceras nigeriense*, occupies a particular part of the morphological spectrum (Fig. 12). Variation in gross shell proportions to the extent of that suggested by Meister *et al.* (1992) for *P. cauvini* in Niger is not seen in these taxa. On the other hand, within *P. nigeriense* there seems to have been virtually no selection pressure favouring any particular strength of ornamentation. In this respect the polymorphic potential of the species was capable of wide expression. Much the same can be said of *Fikaites varicostatus* Zaborski, the other strongly ornamented form found in some numbers in unit O at Ashaka. This species shows a significant variation in the strength of its ribbing and tuberculation (see Zaborski 1993).

Family VASCOCERATIDAE Douvillé, 1912
 Subfamily VASCOCERATINAE Douvillé, 1912
 Genus *VASCOCERAS* Choffat, 1898

(= *Discovascoceras* Collignon, 1957; *Greenhornoceras* Cobban & Scott, 1972; *Provascoceras* Cooper, 1979)

TYPE SPECIES. *Vascoceras gamai* Choffat, 1898; by the subsequent designation of Roman, 1938.

REMARKS. Choffat (1898: 51–53) had a broad concept of *Vascoceras* as encompassing forms basically united by the

possession of a simple suture pattern. Some of these original members are now referred to *Spathites* Kummel & Decker, 1954. The type species, *V. gamai*, was regarded as part of a group characterized by a wide umbilicus and the possession of a single (umbilical) row of tubercles. Recent discussions of *Vascoceras* have been given by Wright & Kennedy (1981) and Berthou *et al.* (1985). It is commonly suggested that *Paravascoceras*, *Pachyvascoceras*, *Paracanthoceras*, *Broggiiceras*, *Discovascoceras*, *Provascoceras* and, sometimes, *Greenhornoceras* should be regarded as strict synonyms of *Vascoceras* without even subgeneric distinction (see Berthou *et al.* 1985, Kennedy, Wright & Hancock 1987, Luger & Gröschke 1989, Kennedy, Cobban, Hancock & Hook 1989, Cobban *et al.* 1989).

The oldest known species included in *Vascoceras* is the micromorph *Ammonites diartianus* d'Orbigny, the type material of which was redescribed by Kennedy & Juignet (1977). Further examples were subsequently described by Wright & Kennedy (1981: 86, pl. 17, fig. 1; text-figs 29A–F), Förster *et al.* (1983: 133, pl. 3, figs 1–5) and Cobban *et al.* (1989: 47, figs 48, 88TT-AA). *V. diartianum* occurs most frequently in the Geslinianum Zone or equivalents but Kennedy *et al.* (1989: 80) reported examples in New Mexico from equivalents of the underlying Guerangeri Zone. Kennedy & Wright (1985) and Wright & Kennedy (1987) drew attention to the morphological similarity between *V. diartianum* and *Protacanthoceras* of the *P. proteus* Wright & Kennedy group (see Wright & Kennedy 1980: 95, figs 49–51, 57–58; 1987: 216, pl. 55, figs 4, 9, 17, 18, 21–23; text-figs 82B, 83G, M, 84P). They believed the former to have been derived from the latter. Accordingly, *V. diartianum* would constitute the root stock of *Vascoceras* and the above-mentioned suggested synonyms.

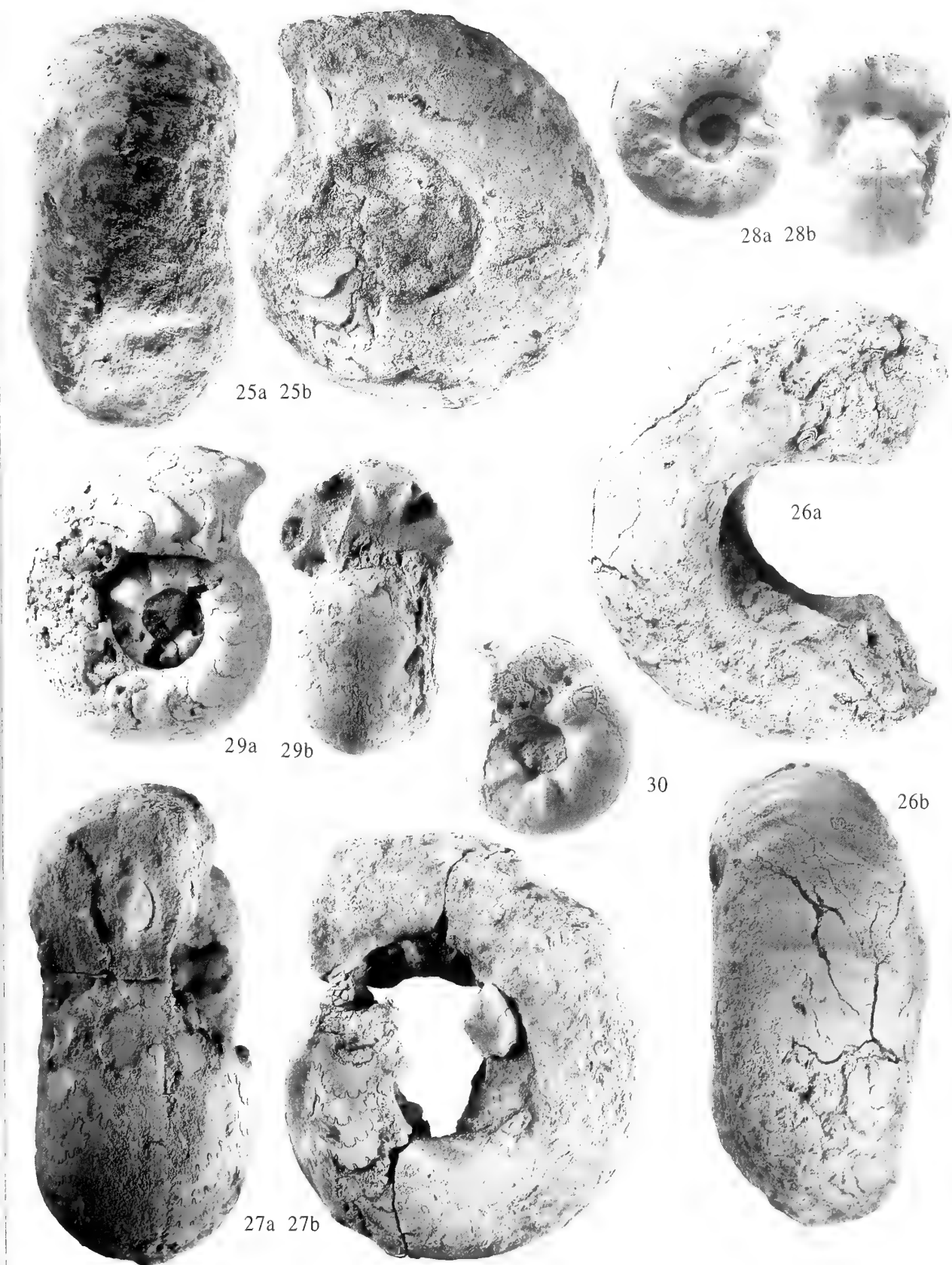
Cooper (1979) was reluctant to admit the Late Cenomanian age of *Vascoceras* and pointed to a number of differences between *Ammonites diartianus* and *V. gamai*, the most significant of which regarded their ornamentation. He proposed the genus *Provascoceras* for *A. diartianus* but regarded the species as ancestral to both *Vascoceras* and *Paravascoceras*. *A. diartianus* is clearly transitional between Acanthoceratinae and Vascoceratidae, retaining the bifid first lateral saddle of the former. Its ornament consists of rounded to twisted to distinctly bullate umbilical tubercles which may envelop practically the whole of the flanks and fine bundled ribbing extending across the venter. Relatively little is known of the inner whorls of topotype material of *V. gamai*. Choffat (1898: pl. 7, figs 3, 4; pl. 8, fig. 4; pl. 10, fig. 2) figured a number of juveniles which show approximately 8 umbilical bullae and 20 coarse, regularly developed major and minor ribs which cross the venter (see also Berthou *et al.* 1985: 67). The umbilical tubercles may be persistent but the ornament generally disappears on the later whorls. A similar juvenile ornament has been described in material referred to *V. gamai* from Egypt (Luger & Gröschke 1989: 378, pl. 40, figs 5, 7) and *V. cf. gamai* from New Mexico (Cobban *et al.* 1989: 45, figs 87W-AA, EE-RR). There are, however, other juveniles from Portugal with rather different ornamentation. *V. silvanense* Choffat (1898: 57, pl. 8, fig. 5; pl. 21, fig. 9) shows massive umbilical bullae but no definite ribbing. Berthou *et al.* (1985: 68) regarded *V. silvanense* as a *nomen dubium* and almost certainly the inner whorls of one or another

of the Portugese species of *Vascoceras*. Another individual (Berthou *et al.* 1985: 68, pl. 3, figs 4, 8, 9) displays about 10 umbilical bullae intermediate in strength between those found in *V. gamai* and *V. silvanense* and about twice as many low ventral ribs mostly arising in pairs from these bullae. Berthou *et al.* (1985: 68) compared this specimen with *V. adonense* Choffat which they regarded as a synonym of *V. gamai*. Its ornament is reminiscent of that in *Ammonites diartianus*. Numerous juvenile whorls of *V. woodsi* are available from north-eastern Nigeria (see below). They show a considerable variation in ornament. Although no comparable variation series is available for the Portugese *Vascoceras*, it is possible that certain *V. gamai* could show an early ornament approaching that in *Ammonites diartianus*. Despite its transitional nature, *A. diartianus* is here regarded as belonging in *Vascoceras* and *Provascoceras* is therefore a synonym.

Discovascoceras Collignon (type species *Vascoceras* (*Discovascoceras*) *tesselitense* Collignon 1957: 125, pl. 1, figs 1a, b; by original designation) was originally proposed by Collignon (1957: 123) as a subgenus of *Vascoceras* but was later raised to the status of a separate genus following an amended diagnosis (Collignon 1965: 179). Its essential characters were given as its triangular whorls, presence of three carinae on the middle whorls, variation in spacing and degree of indentation of the sutures, depth of the umbilicus, egression of the adult whorl and tendency for apertural constriction. Berthou *et al.* (1985: 75) regarded the holotype of *D. tesselitense* as an indeterminate *Vascoceras*, the species as invalid and *Discovascoceras* Collignon, 1957 as a synonym of *Vascoceras*. In view of its ventral carinae they compared the material later described as *D. tesselitense* by Collignon (1965: 181, pl. G, figs 1a, b) with *Pseudotissotia* Peron (see also Hirano 1983: 69–70). They proposed that Collignon's second account be taken as the first valid one of *Pseudotissotia?* *tesselitense*. Collignon's (1965) material, however, shows similarities with Nigerian forms intermediate between *Vascoceras globosum costatum* and *Thomasites* which are described below. Here both the Collignon 1957 and 1965 descriptions are regarded as dealing with *Vascoceras* but the 1965 material could alternatively be assigned to *Thomasites*.

Greenhornoceras Cobban & Scott (type species *Vascoceras* (*Greenhornoceras*) *birchbyi* Cobban & Scott 1972: 85, pl. 22; pl. 23, figs 1–13; pl. 24, figs 1–12; pl. 25; pl. 26, figs 5–8, 11, 12; pl. 27, figs 1–6; text-figs 43–47; by original designation) is amongst the stratigraphically youngest examples of *Vascoceras*. Cobban & Scott (1972: 84–85) distinguished the subgenus *Greenhornoceras* only on the basis of being more involute than *V. (Vascoceras)* and in maintaining a square to rectangular whorl section. Its juvenile ornament of strong, regularly developed long and short ribs gives way to smooth later whorls. There is no compelling reason to regard *Greenhornoceras* as anything other than a strict synonym of *Vascoceras*.

As mentioned above, *Paravascoceras* (= *Paracanthoceras*, *Pachyvascoceras*, *Broggiiceras*) is here regarded as a distinct genus with an origin separate from that of *Vascoceras* and is most properly included in the Acanthoceratinae.



Vascoceras woodsi sp. nov.

Figs 9–11, 25–32

- 1957 *Vascoceras* sp. juv. Barber: 27, pl. 6, figs 2, 4, 7; pl. 27, figs 10–15.
 ?1965 *Vascoceras gamai* Choffat; Collignon: 185, figs 5–7.
 1989 *Plesiovascoceras* aff. gr. *thomi* (Reeside) ou sp. nov. Meister: 11, pl. 4, figs 2, 3, 5; text-fig. 8.
 1989 *Paravascoceras* gr. *evolutum* Schneegans; Meister: 14 (pars), pl. 5, fig. 4 (only); text-fig. 10.
 1990a *Vascoceras* gr. *evolutum* (Schneegans); Zaborski: 7.
 1990a *Vascoceras* sp. Zaborski: figs 9, 10.
 1990a *Vascoceras* sp. juv. Zaborski: figs 16–18, 20, 21.
 1992 *Vascoceras* gr. *thomi* (Reeside) ou *evolutum* (Schneegans); Courville: pl. 5, fig. 1.
 1993 *Vascoceras* sp. nov. aff. *gamai* Choffat; Zaborski: 365.
 1995 *Vascoceras* sp. nov. aff. *gamai* Choffat; Zaborski: 54, 55.

HOLOTYPE. C.93342 (Fig. 27), Pindiga Formation, unit M, Ashaka.

PARATYPES. Thirty-four specimens, C.93339, C.93341, C.93343–4, C.93543, Pindiga Formation, unit M, Ashaka; C.91262–70, Pindiga Formation, unit M, Pindiga; C.91224–5, C.91311, C.91313–4, C.93351, Pindiga Formation, unit N, Pindiga; C.91256–61, C.93355, C.93596a–f, C.93597, Pindiga Formation, Deba Habe.

DIMENSIONS.

	D	Wb	Wh	U
C.93597	94	—	31 (33)	39 (41.5)
C.93351	60	34 (57)	22 (37)	21 (35)
C.91264	53	32 (60)	20 (38)	18 (34)
C.93355	52	31 (60)	18 (35)	20 (38.5)
C.91256	50	29 (58)	20 (40)	17 (34)
C.91263	40	25 (62)	15 (37.5)	13 (32.5)
C.91257	39	24 (61.5)	16 (41)	11 (28)
C.91262	34	20 (59)	13 (38)	10 (29)

DERIVATION OF NAME. After the late H. Woods who first described ammonites from north-eastern Nigeria.

DIAGNOSIS. Evolute *Vascoceras* with whorls broader than high. Middle whorls with rounded or more normally highly bullate umbilical tubercles fusing with inner ventro-lateral bullae to cover the flanks. Adult body-chamber smooth or with umbilical tubercles and/or relatively weak ventral ribbing.

DESCRIPTION. The shell is evolute, the umbilicus widening during growth from about one-third to 40% or more of the overall diameter. The maximum diameter attained is about 120 mm, when the body-chamber makes up two-thirds of the final whorl. In all but the very earliest growth stages the whorls are distinctly broader than high.

Two nuclei are available. In C.93596f the whorls are initially smooth and tubular with a broadly rounded venter. At a diameter of 3 mm broad bullate swellings enveloping the inner half of the flanks appear and give rise to low ribs which cross the

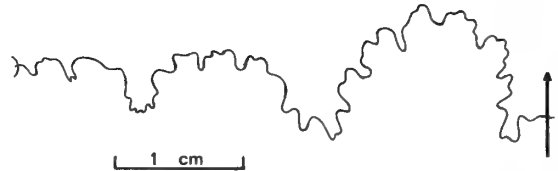


Fig. 31 Suture in *Vascoceras woodsi* sp. nov. Holotype, C.93342. Pindiga Formation, unit M, Ashaka.

venter. The suture shows a direct transition from an entire to an evenly frilled E/L; this saddle is never bifid. In C.93596e about 10 umbilical bullae have developed by a diameter of 6 mm but the venter lacks ribbing.

In the succeeding growth stages (Figs 9, 10) the characteristic ornament consists of 8–10 lateral bullae in each whorl, upon which discrete umbilical and inner ventrolateral swellings can sometimes be made out. Most of the bullae give rise to a narrow rounded rib which crosses the venter and bears outer ventrolateral tubercles. No definite siphonal tubercles can be made out. There may be a single ventral rib bearing only outer ventrolateral tubercles alternating with each major rib. In other specimens no well-developed ribbing exists. In all cases sharply defined ribbing disappears at diameters of 10–15 mm though the lateral bullae persist. At these diameters the venter becomes flattened and the whorls increasingly depressed.

At diameters of 20–60 mm the main ornament consists of 6–8 umbilical tubercles in each whorl which are of variable shape and strength. They are commonly highly bullate but may be rounded, clavate or paired in nature. At first the more bullate types may partially fuse with bullate inner ventrolateral swellings but the latter features quickly fade during growth. Broad, vague fold-like ribs which cross the venter may issue from the umbilical tubercles or the venter may be smooth. Such ribs, however, rarely persist beyond diameters of 40 mm.

Umbilical tubercles may persist onto the adult body-chamber which is frequently compressed. Ventral ribbing may develop here taking the form of irregular closely-spaced plicae at one extreme and moderately strong fairly evenly-spaced ribs at the other.

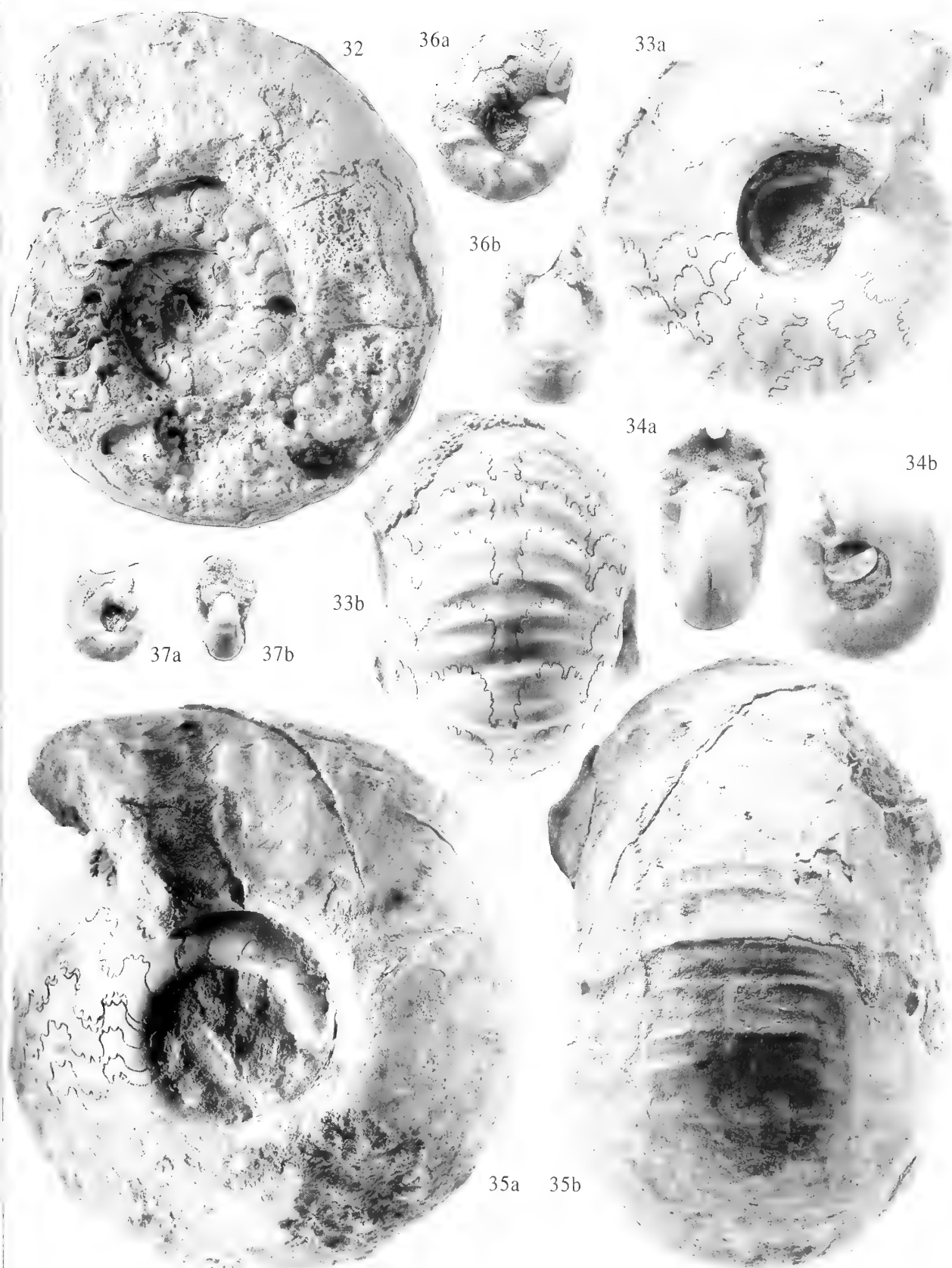
The suture (Fig. 31) is of the typically simple type found in *Vascoceras*.

REMARKS. In a previous account (Zaborski 1990a: 5) doubt was expressed about whether a number of juvenile *Vascoceras* collected from Deba Habe and Pindiga were conspecific. *V. woodsi* has been found at these two localities and at Ashaka. At Pindiga adult specimens are not found, only the middle septate whorls being found in units L, M and N. At Ashaka the species is abundant in units K and, especially, M but the material consists almost entirely of poorly preserved adult body-chambers. At Deba Habe, however, specimens representing all growth stages occur in a 10 cm limestone less than 1 m below the level at which *Vascoceras globosum costatum* and *Pseudovascoceras nigeriense* appear. Occasional juveniles from Ashaka fit comfortably within the morphological range exhibited by the Pindiga and Deba Habe material. There is little doubt that all these specimens are conspecific.

Fig. 32 *Vascoceras woodsi* sp. nov. Pindiga Formation, Deba Habe. Paratype, C.93597, ×1.

Figs 33–35 *Vascoceras bullatum* Schneegans. Pindiga Formation, unit O, Ashaka. Fig. 33a, b, C.93512, ×1. Fig. 34a, b, C.93516a, ×1. Fig. 35a, b, C.93514, ×1.

Figs 36–37 *Pseudovascoceras nigeriense* (Woods). Pindiga Formation, unit O, Ashaka. Fig. 36a, b, C.93499, ×1. Fig. 37a, b, C.93494d, ×1.



Adult *V. woodsi* are closely similar to *V. gamai* Choffat (1898: 54, pl. 7, figs 1–4; pl. 8, fig. 1; pl. 10, fig. 2; pl. 21, figs 1–4; see also Berthou *et al.* 1985 for a revision of the species). The strong regular ribbing of the early whorls in *V. gamai* figured by Choffat (1898: pl. 7, figs 3, 4; pl. 8, fig. 4; pl. 10, fig. 2), however, differs from the ornament at the same stages in *V. woodsi*. It should be noted that certain juvenile specimens from Portugal show similarities with some Nigerian individuals: compare C.91264 (Fig. 11) with *V. silvanense* Choffat (1898: pl. 8, fig. 5), and C.93351 (Fig. 29) with Berthou *et al.* (1985: pl. 3, figs 4, 8, 9). A more complete knowledge of the early whorls in *V. gamai* is necessary for full comparison with *V. woodsi*.

Closer to the Nigerian juveniles is *V. diartianum*, particularly material from Germany which reaches diameters of over 30 mm (see Förster *et al.* 1983). This collection includes individuals with rather rounded umbilical tubercles (Förster *et al.* 1983: pl. 3, fig. 1; compare with Zaborski 1990a: fig. 20) and others with highly bullate umbilical tubercles similar to those common in *V. woodsi* (compare Förster *et al.* 1983: pl. 3, figs 2–5 and C.91263, C.91257, Figs 28, 30 herein). *V. woodsi* is a little younger than *V. diartianum* and derivation from the latter can easily be imagined by peramorphosis and further simplification of suture pattern.

The material from Ashaka described by Meister (1989: 11, pl. 4, figs 2, 3, 5; text-fig. 8) as *Plesiovascoceras* aff. gr. *thomi* (Reeside) belong in *V. woodsi*; *Vascoceras thomi* Reeside (1923) is a synonym of *Fagesia catinus* (Mantell) (see also Wright & Kennedy 1981: 88, 97). Those he referred to *Paravascoceras* gr. *evolutum* Scheegans are partly *V. woodsi* (Meister 1989: pl. 5, fig. 4) and probably partly *Pseudaspidoceras pseudonodosoides* (Choffat) (Meister 1989: pl. 5, fig. 2). *Paravascoceras cauvini* var. *evoluta* Scheegans (1943: 130, pl. 8, fig. 2) is here considered to be a strict synonym of *Paravascoceras cauvini*.

Specimens of *Vascoceras* described by Zaborski (1990a: 5, figs 9, 10) are further examples of *V. woodsi*. They were incorrectly reported as having come from the Gadeni Zone at Pindiga but are from large exotic blocks derived from unit N upstream and not from the immediately adjacent unit A.

Specimens from the Algerian Sahara referred to *V. gamai* by Collignon (1965: 185, figs 5–7) are a very close match for adult *V. woodsi* and may be conspecific. Unfortunately their inner whorls are completely unknown.

Vascoceras bullatum Schneegans, 1943

Figs 13, 33–35

- 1943 *Paravascoceras crassus* (Furon) var. *bullata* Schneegans: 131, pl. 8, figs 3, 4.
- 1989 *Paravascoceras crassum* (Furon); Meister: 18, pl. 6, figs 2, 3; text-fig. 12.
- 1989 *Paravascoceras carteri* (Barber); Meister: 21 (pars), pl. 9, fig. 1 (only).
- 1992 *Vascoceras* gr. *crassum* (Furon) ou *costellatum* Collignon; Courville: pl. 5, fig. 2; pl. 6, fig. 1.

MATERIAL AND OCCURRENCE. Eleven specimens, C.93508–15, C.93516a–c, Pindiga Formation, unit O, Ashaka.

DIMENSIONS. See Fig. 12.

REMARKS. Members of this species are relatively evolute and generally show markedly depressed whorls with a rounded to subtriangular outline. Umbilical bullae may or may not be present. The evenly frilled sutures are characterized by a broad low E/L and a narrow L.

Most individuals are readily recognizable due to the development of regular ribbing on the flanks and venter during their middle ontogenetic stages. The ribs may be coarse and rounded but vary to finer, denser structures in other individuals. Although this ribbing may be developed at diameters of less than 20 mm, some specimens remain smooth throughout ontogeny (see Fig. 13; Meister 1989: pl. 9, fig. 1). Regularly developed ribbing may be a transient feature which disappears or weakens greatly on the later septate whorls. The more involute members of the species overlap in shell proportions with certain *Vascoceras globosum costatum* and *Pseudovascoceras nigeriense* (see Fig. 12) and such individuals may be difficult to differentiate if they lack ribbing.

The juvenile whorls are not distinctive. They are often only moderately depressed and are smooth or ornamented with umbilical bullae alone (Fig. 34).

The adult body-chamber makes up between two-thirds and three-quarters of the final whorl. It may be smooth but generally shows an irregularly developed ornament of coarse, rounded fold-like to denser, sharper, narrow crease-like ribbing on the venter and outer flanks. Meister (1989: 18) pointed out that the body-chamber becomes constricted but the adult aperture itself is flared (Fig. 35). This modification occurs at diameters between 73 mm and 110 mm. There is no clear evidence of size dimorphism, however; other individuals showing a flared aperture do so at diameters of 80, 82, 82, 85, 85, 85, 86, 88, 95, 97, 98, 100 and 104 mm. Cobban & Hook (1983) described a large population sample of *Neptychites cephalotus* (Courtiller) from New Mexico which shows similar adult body-chamber modifications. They too found that adult sizes were highly variable with no discernible bimodal pattern.

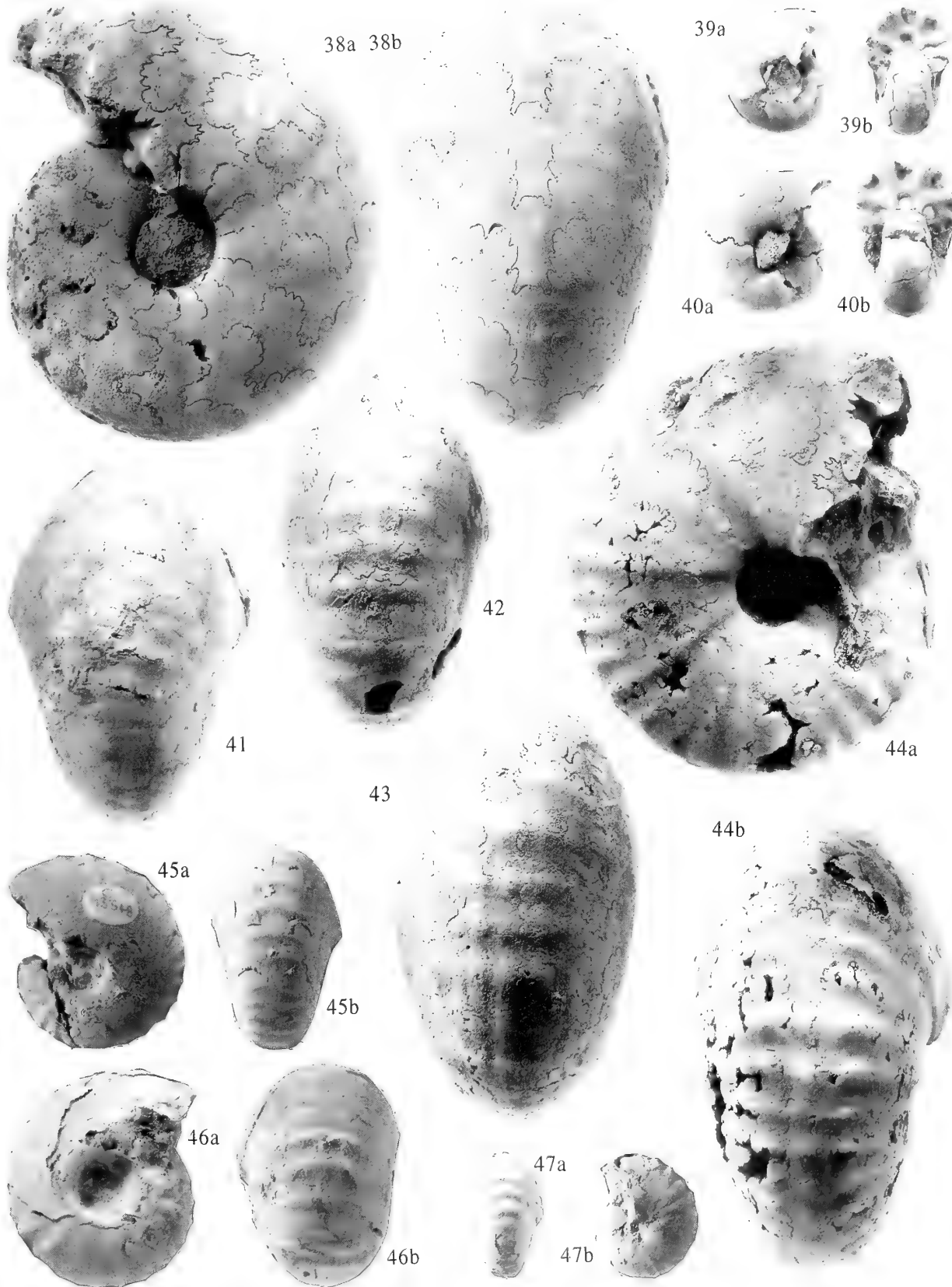
Paravascoceras crassus var. *bullata* Schneegans (1943: 131, pl. 8, figs 3, 4) has depressed whorls and ribbing of a closely similar style to that in the present material. Its umbilicus, representing about 25% of the overall diameter, is narrower than the average in the Nigerian forms described here but in this respect there is an overlap with the more involute individuals (see Fig. 12). Schneegans (1943) regarded his material as a variety of *Vascoceras* (*Pachyvascoceras*) *crassus* Furon (1935: 58, pl. 3, figs 2a, b; text-fig. 17), a slightly less depressed and less evolute form. *V. (P.) crassum* shows only a very weak ornament of fine riblets though its suture pattern is close to that in the present material. As mentioned above, *V. (P.) crassum* may be most properly referred to *Paravascoceras*. In view of the clear similarities between the present material and *Pachyvascoceras crassum* var. *bullatum*, however, the name *Vascoceras bullatum* Schneegans is applied to it. The Nigerian material is distinct from coeval *Paravascoceras cauvini* and is therefore referred to *Vascoceras* rather than *Paravascoceras*, although with some uncertainty.

Paravascoceras costatum multicostatum Barber (1960: 60, pl. 13, fig. 3; pl. 14, figs 1, 2) combines the relatively open umbilicus

Figs 38–40 *Vascoceras globosum costatum* (Reyment). Pindiga Formation, unit O, Ashaka. Fig. 38a, b, C.93527, $\times 1$. Fig. 39a, b, C.93536b, $\times 1$. Fig. 40a, b, C.93536c, $\times 1$.

Figs 41–44 *Thomasites gongilensis* (Woods). Pindiga Formation, unit O, Ashaka. Fig. 41, C.93582, $\times 1$. Fig. 42, C.93579, $\times 1$. Fig. 43, C.93580, $\times 1$. Fig. 44a, b, C.93583, $\times 1$.

Figs 45–47 *Vascoceras globosum proprium* (Reyment). Pindiga Formation, unit T2, Ashaka. Fig. 45a, b, C.93548, $\times 1$. Fig. 46a, b, C.93551, $\times 1$. Fig. 47a, b, C.93547, $\times 1$.



and dense ribbing style of *V. bullatum* with the whorl proportions and suture pattern of *V. globosum costatum*. Material of this kind has not been found in the present study and its precise affinities are uncertain.

Vascoceras rumeaui Collignon (1957) has an ornament of strong ribs similar to that in *V. bullatum* but is less depressed. As discussed above, it may be more closely related to *Paravascoceras cauvini*. *V. durandi* Choffat and the doubtfully distinct *V. kossmati* Choffat (see Berthou *et al.* 1985 for a review) are both depressed, relatively evolute species but lack the marked ribbing and adult apertural modifications seen in *V. bullatum*.

Vascoceras globosum (Reyment, 1954b)

REMARKS. This species was discussed by Kennedy *et al.* (1987: 46). They brought into synonymy a large amount of material described from Nigeria and elsewhere including *Pachyvascoceras globosum* Reyment (1954b) and *Pachyvascoceras proprium* Reyment (1954b) under the name *Vascoceras proprium* (Reyment, 1954b). Barber (1957: 21–27), however, had already treated the above two forms as conspecific and selected *Vascoceras globosum* (Reyment, 1954b) as the species name. *V. globosum* accordingly has priority over *V. proprium* and should replace it. Nigerian specimens assigned to the species are here referred to three subspecies as detailed below.

The *V. globosum* group shows a wide morphological variation and complex phylogenetic relationships. Early members of the group seem to include the ancestors of *Thomasites gongilensis* (Woods). Later members are characterized by rather complex sutures; *V. obscurum* and probably also *Neoptychites* Kossmat were derivatives.

The precise origin of *V. globosum* is obscure. There are no obvious ancestors within the north-eastern Nigerian sections. *V. woodsi* is a possibility but is more evolute and has a stronger, more persistent juvenile ornamentation. *Paravascoceras cauvini* is markedly more compressed while the inner whorls of its later members are entirely smooth, unlike those in *V. globosum costatum*.

Berthou *et al.* (1985: 72) suggested that *Vascoceras* (*Pachyvascoceras*) *crassus* Furon, 1935 was a senior synonym of *Pachyvascoceras costatum* Reyment, 1954b (= *V. globosum costatum*). Meister *et al.* (1992: 72, pl. 7, figs 1, 2, 4, 5) described forms from sections at Tanout Aviation and Birgimari in Niger as *Paravascoceras cauvini* of *V. crassum* type and others transitional from *V. crassum* to *V. proprium* type. The latter group could probably include their *V. gr. ellipticum* Barber (Meister *et al.* 1992: 76, pl. 7, fig. 3; pl. 8, figs 1, 2) from the same sections. These forms are associated with *Paravascoceras cauvini* of typical aspect. Schneegans (1943) also reported passage forms from *P. cauvini* to *V. crassum* in Niger. Meister *et al.* (1992: 74) discussed the possible relationships within the Niger faunas. They remarked that undoubtedly *V. proprium* (= *V. globosum*) had not been found in Niger, and speculated that the horizons with *P. cauvini* contained essentially monospecific ammonite faunas; this species produced a wide range of morphotypes with variable degrees of whorl compression and ornamental strength. According to this interpretation *V. crassum* is a homeomorph of *V. globosum costatum*, the first a member of the *P. cauvini* group, the latter having a separate origin. In support it may be noted that unit O at Ashaka, in which *V. globosum* appears, also contains the abrupt first occurrences of *V. bullatum* and *Pseudovascoceras nigeriense*. The base of unit O is a marine flooding surface suggesting that its fauna is largely an introduced one, the ancestors of which lie

outside north-eastern Nigeria. *Vascoceras* (*Pachyvascoceras*) *crassum* and *V. globosum* are here regarded as distinct from one another; the former, as stated above, is probably best referred to *Paravascoceras*.

Vascoceras globosum costatum (Reyment, 1954b)

Figs 38–40, 50

- 1954b *Pachyvascoceras costatum* Reyment: 257, pl. 3, fig. 6; pl. 4, fig. 3; pl. 5, fig. 2; text-figs 3a, b, 5.
- 1955 *Pachyvascoceras costatum* Reyment; Reyment: 65, pl. 14, figs 2, 4.
- ?1957 *Vascoceras robustum* Barber: 15, pl. 5, fig. 1; pl. 26, figs 5, 6.
- ?1957 *Vascoceras polygonum* Barber: 17, pl. 5, fig. 2; pl. 29, figs 1–3.
- 1957 *Paravascoceras costatum costatum* (Reyment) Barber: 35, pl. 14, fig. 1; pl. 32, figs 1–3.
- 1957 *Paravascoceras costatum quadratum* Barber: 35, pl. 16, fig. 2; pl. 32, figs 10, 11.
- 1957 *Paravascoceras costatum tectiforme* Barber: 37, pl. 14, fig. 4; pl. 15, figs 1, 3; pl. 16, fig. 2; pl. 32, figs 4–7.
- 1965 *Pachyvascoceras costatum* Reyment; Reyment: pl. 3, fig. 17.
- 1976 *Vascoceras robustum* Barber; Offodile & Reyment: 54, figs 23a, b.
- 1976 *Vascoceras ellipticum* Barber; Offodile & Reyment: 55, figs 25a, b.
- 1976 *Paravascoceras costatum* (Reyment); Offodile & Reyment: 55, figs 26a, b.
- 1976 *Paravascoceras tectiforme* Barber; Offodile & Reyment: 55, figs 29a, b.
- 1989 *Paravascoceras tectiforme* Barber; Meister: 21, pl. 7, figs 1, 2; pl. 8, figs 1–5; text-fig. 13.
- 1992 *Vascoceras tectiforme* (Barber) *sensu* Meister; Courville: pl. 7, figs 1, 2.

MATERIAL AND OCCURRENCE. Twenty-six specimens, C.93310, C.93519–34, C.93535a–d, C.93536a–e, Pindiga Formation, unit O, Ashaka.

DIMENSIONS. See Figs 12, 48.

REMARKS. The phragmocone in *V. globosum costatum* reaches a diameter in excess of 130 mm, making it the largest member of the genus known in north-eastern Nigeria. Whorl breadth is slightly to distinctly greater than whorl height while the umbilicus represents 15–28% of the total diameter. In overall shell proportions *V. globosum costatum* overlaps with *V. bullatum* and *Pseudovascoceras nigeriense* and smoother individuals of these two species may be difficult to distinguish from it, especially in their middle growth stages.

At diameters of less than 30 mm (Figs 39, 40) the whorls in *V. globosum costatum* are weakly ornamented. Some forms are virtually smooth, others display umbilical tubercles but most commonly there are weak, broadly rounded ribs, most pronounced ventrally and sometimes with traces of bullate ventrolateral tubercles. The whorls tend to be more compressed in the early than in the later growth stages.

In the middle whorls ornament may be lacking or there may be broad, low ventral ribs. Umbilical tubercles persist in some individuals. In the adult stages irregular fold-like ribs may appear, especially upon the venter. The range of shell shapes and ornamentation is well displayed by the abundant previously described material (see synonymy list).

Suture patterns are of the typically simple type characteristic of *Vascoceras*.

Barber (1957), Meister (1989) and Courville (1992) separated forms of *V. globosum costatum* with subtriangular to triangular whorl sections as *Paravascoceras costatum tectiforme* Barber, *P. tectiforme* Barber and *Vascoceras tectiforme* (Barber). In unit O at Ashaka there is a complete intergradation of forms with rounded and triangular whorl sections. The latter themselves show rounded venters in their early growth stages. This shape variation is attributed no taxonomic significance here.

Of greater interest is the fact that *V. globosum costatum* shows a gradation into *Thomasites* at the same stratigraphical level at Ashaka. A variation series is shown in Figs 41–44, 50. This encompasses more or less smooth forms with ovoid to subtriangular whorls (Figs 41, 50) through forms with weak but definite ventral tubercles and incipient carinae (Figs 42, 43), into strongly ornamented individuals (Fig. 44) occurring in the upper part of the unit and well within the morphological range of *Thomasites gongilensis* (Woods) (see faunas described by Barber 1957, Meister 1989). The *Neptychites cephalotus* (Courtiller) of Meister (1989: 12, pl. 4, fig. 4) and *Thomasites* sp. nov.? of Courville (1992: 420, pl. 10, fig. 4; pl. 12, fig. 1) are further examples of early *Thomasites*. *V. globosum costatum* seems to contain the ancestors of *T. gongilensis*, a species which reaches its acme in unit R at Ashaka where it forms the bulk of the ammonite fauna.

The *Paravascoceras* aff. *chevalieri* (Furon) of Reymont (1955: 53, pl. 14, figs 1a, b) from southern Nigeria also shows three rows of ventral tubercles and resembles the early *Thomasites* from Ashaka. The same can be said of the material of *Discovascoceras tessellitense* described by Collignon (1965: 181, pl. G, figs 1a, b) which shows three ventral carinae, subtriangular whorls and a deep, fairly narrow umbilicus. Hirano (1983) and Berthou *et al.* (1985) compared this material with *Pseudotissotia*, but it appears closer to the Nigerian forms transitional from *Vascoceras* to *Thomasites* described here.

Vascoceras globosum globosum (Reymont, 1954b)

Figs 51, 52

- 1954b *Pachyvascoceras globosum* Reymont: 259, pl. 3, fig. 3; pl. 4, fig. 4; text-figs 3e, 7.
- 1957 *Vascoceras globosum globosum* (Reymont) Barber: 21 (pars).
- 1957 *Vascoceras globosum carteri* Barber: 25, pl. 8, fig. 2; pl. 28, figs 8, 9.
- 1965 *Vascoceras carteri* Barber; Reymont: pl. 3, fig. 12.

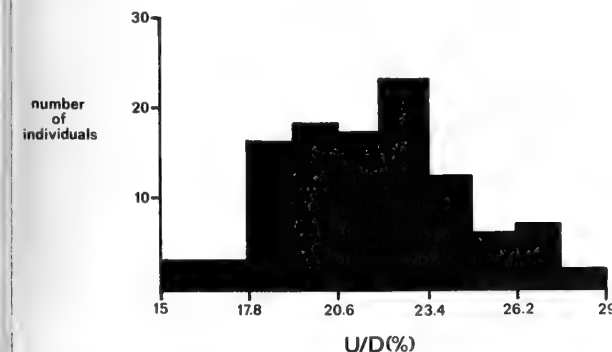


Fig. 48 Shell proportions in *Vascoceras globosum* (Reymont) occurring in unit O at Ashaka. Forms with a high Wb/Wh ratio are here assigned to *V. globosum globosum* (Reymont) (see also Fig. 12).

- 1976 *Paravascoceras carteri* (Barber) Offodile & Reymont: 55, figs 27, 28.
- 1989 *Paravascoceras carteri* (Barber); Meister: 21 (pars), pl. 9, fig. 3 (only); pl. 10, figs 1, 2; text-fig. 14.
- 1992 *Vascoceras tectiforme* (Barber) *sensu* Meister; Courville: pl. 7, fig. 3 (only).
- 1992 *Vascoceras* gr. *globosum* (Reymont) ou *Fagesia* sp. Courville: pl. 8, figs 1, 2.
- ?1992 *Vascoceras* sp. aff. *obscurum* Barber; Courville: pl. 10, fig. 3 (only).

MATERIAL AND OCCURRENCE. Three specimens, C.93544-6, Pindiga Formation, unit R, Ashaka. The form also occurs in unit O at Ashaka and unit O at Pindiga.

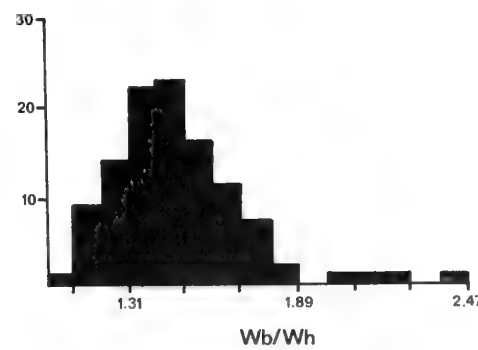
DIMENSIONS. See Figs 12, 48.

REMARKS. *V. globosum globosum* is characterized by its highly depressed whorls which are at least twice as broad as high. Although such forms occur throughout the range of *V. globosum* in north-eastern Nigeria there are morphological and stratigraphical reasons for considering the earlier individuals as a separate subspecies. In unit O at Ashaka highly depressed examples of *V. globosum* are rare but those that occur fall well outside the morphological range of *V. globosum costatum* (see Figs 12, 48). In both unit R at Ashaka and unit O at Pindiga *V. globosum globosum* is the only member of the species that has been found. It is fairly frequent at these levels where the more compressed part of the morphological spectrum is occupied by large numbers of *Thomasites gongilensis*.

The juvenile whorls in *V. globosum globosum* show sharper ribbing than in *V. globosum costatum*. The ribs cross the flank, unlike in *V. globosum proprium* in which they are largely confined to the venter and outer flanks. Specimen C.93544 (Fig. 51) is a very close match for the holotype of *Pachyvascoceras globosum* (C.47408, see Reymont 1954b: pl. 3, fig. 3; pl. 5, fig. 4) which is also a juvenile.

Since details of the inner whorls are useful in identification it is difficult to determine which of the specimens described by Barber (1957: 21) as *V. globosum globosum* should be referred to that subspecies and which are depressed examples of *V. globosum proprium* (see below). His material appears to include both.

The sutures in *V. globosum globosum* are deeply incised; this appears to be a general feature of highly depressed *Vascoceras* which is shared with *V. harttii* (see below). Courville (1992: 421) drew attention to the suture pattern in *V. globosum globosum* and suggested that it may be better referred to *Fagesia* Pervinquier.



This genus, however, as well as being generally more evolute, shows a different ontogeny (see Zaborski 1987: 43 for a discussion). Its juvenile whorls characteristically show strong ribs arising in twos or threes from umbilical tubercles, elements of this ornament persisting to varying stages in later ontogeny. The present material shows an ontogenetic development typical of *Vascoceras* rather than *Fagesia*.

Barber (1957) proposed two species of *Fagesia* from north-eastern Nigeria but pointed out that they were both intermediate with *Vascoceras*. These forms are problematical, being based on a very few specimens of unknown stratigraphical provenance. *F. simplex* Barber (1957: 27, pl. 8, fig. 1; pl. 29, figs 4, 5) has a simple suture and is best regarded as an indeterminate *Vascoceras*. *F. involuta* Barber (1957: 27, pl. 9, fig. 3; pl. 29, figs 6, 7) has a complex suture, narrow umbilicus and highly depressed whorls; the early growth stages are unknown. It may be most closely related to *V. globosum globosum*.

Vascoceras globosum proprium (Reyment, 1954b)

Figs 45–47, 49, 55–57, 63, 64

- 1920 *Vascoceras angermannii* Böse: 217, pl. 16, figs 1, 3 (only); pl. 17, fig. 1.
- 1920 *Neptychites* aff. *cephalotus* (Courtiller); Böse: 221, pl. 18, figs 3, 10, 13.
- 1931 *Thomasites* sp. Adkins: 56, pl. 2, figs 16, 17.
- 1954b *Pachyvascoceras proprium* Reyment: 258, pl. 5, figs 1a, b; text-fig. 3d.
- 1954b *Pachyvascoceras proprium plenum* Reyment: 258, pl. 5, fig. 5; text-figs 3c, 6.
- 1954b *Gomebeoceras?* *bulbosum* Reyment: 263, pl. 4, figs 2a, b;

text-figs 3g, 9.

- ?1957 *Vascoceras ellipticum* Barber: 17 (pars), pl. 6, figs 1a, b; pl. 26, fig. 11 (only).
- 1957 *Vascoceras globosum globosum* (Reyment) Barber: 21 (pars), pl. 7, fig. 1.
- 1957 *Vascoceras globosum plenum* (Reyment) Barber: 23, pl. 7, fig. 2; pl. 9, fig. 2; pl. 28, figs 3–5.
- 1957 *Vascoceras globosum proprium* (Reyment) Barber: 25, pl. 7, fig. 3; pl. 28, figs 6, 7.
- 1957 *Vascoceras globosum compressum* Barber: 25, pl. 7, fig. 4; pl. 9, fig. 1; pl. 28, figs 10, 11.
- 1963 *Pachyvascoceras compressum* (Barber) Powell: 321, pl. 32, figs 2–4, 7; pl. 34, figs 8, 10; text-figs 3b–d, f.
- 1963 *Pachyvascoceras globosum* Reyment; Powell: 321, pl. 34, figs 7, 11; text-fig. 3s.
- 1978 *Paravascoceras carteri* (Barber); Chancellor, Reyment & Tait: 92, figs 15–17.
- 1982 *Paravascoceras carteri* (Barber); Chancellor: 102, figs 35–37.
- 1982 *Paravascoceras compressum* (Powell not Barber); Chancellor: 106, figs 49, 50.
- 1987 *Vascoceras proprium* (Reyment); Kennedy, Wright & Hancock: 46, pl. 4, figs 1–15, 18, 19; pls 5, 6; text-figs 8A–C, 9.
- 1989 *Vascoceras* (*Vascoceras*) *proprium* (Reyment); Kennedy, Cobban, Hancock & Hook: 80, figs 20A, B.
- 1989 *Vascoceras* sp. juv. indet. Meister: pl. 11, fig. 3.
- 1992 *Vascoceras* sp. aff. *obscurum* Barber; Courville: pl. 10, fig. 2 (only).

MATERIAL AND OCCURRENCE. Eleven specimens, C.93365,

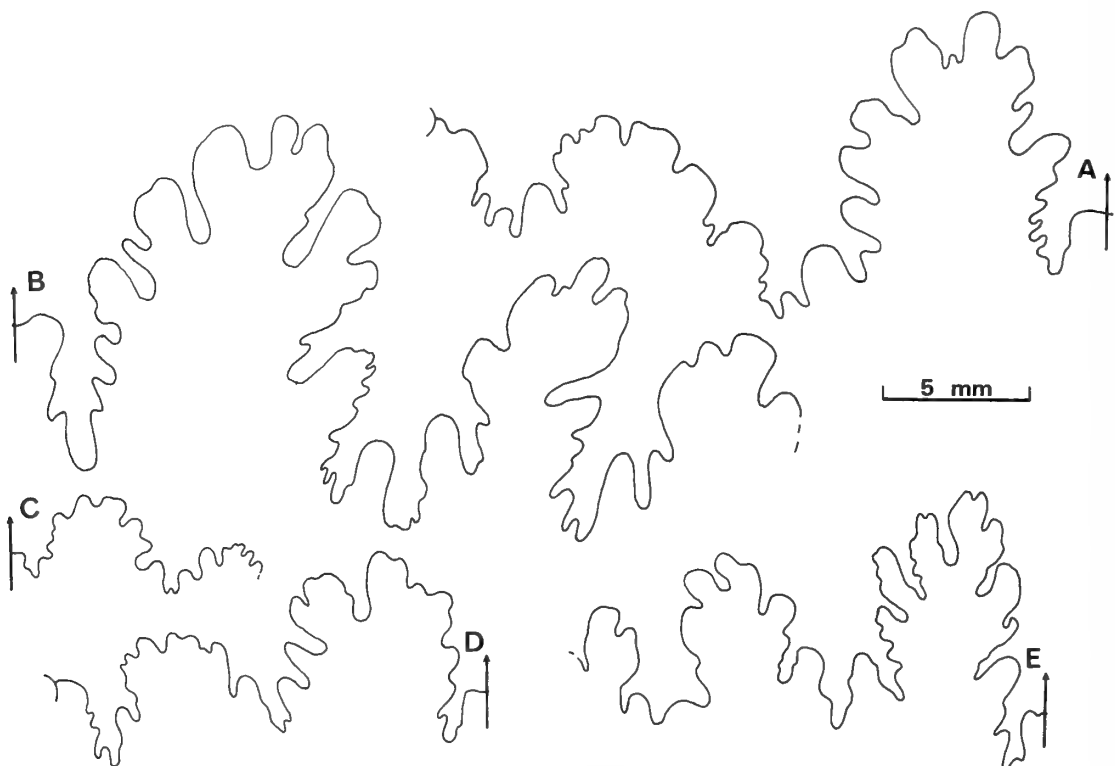


Fig. 49 Sutures in *Vascoceras globosum proprium* (Reyment). A, C.93550 at a diameter of 40 mm. B, C.93906 at a diameter of 54 mm. C, C.93905 at a diameter of 18 mm. D, C.93904 at a diameter of 30 mm. E, C.93549 at a diameter of 38 mm. All specimens from the Pindiga Formation, unit T2, Ashaka.

C.93547-51, C.93904-8, Pindiga Formation, unit T2, Ashaka. The subspecies also occurs in unit T1 at Ashaka.

DIMENSIONS.

	D	Wb	Wh	U
C.93365	64	48 (75)	32 (50)	13 (20)
C.93550	49	45 (92)	21 (43)	—
C.93549	46	30 (65)	21 (46)	—
C.93551	41	34 (83)	21 (51)	10.5 (26)
C.93548	37	23 (62)	17 (46)	6 (16)

REMARKS. *V. globosum proprium* is generally a distinctive form on account of its narrow umbilicus, representing 15–28% of the total diameter, its deeply incised sutures often showing elongate saddles (Fig. 49), and its juvenile ornament of sharp ribbing, almost always confined to the outer flanks and venter. Associated with the juvenile ribs there may be pronounced constrictions which persist until diameters of about 25 mm (Figs 53, 64). Umbilical bullae may or may not be present in the early growth stages. The material from unit T2 at Ashaka varies from moderately compressed (Fig. 45) to highly depressed forms (Fig. 57). The latter resemble the stratigraphically younger *V. globosum globosum*. Their juvenile ribbing style is closer to that in *V. globosum proprium*, however, and they are here treated as end members of that subspecies; similar variants occur in an assemblage of *V. globosum proprium* from Texas (Kennedy *et al.* 1987).

Some individuals have subdued ornamentation. The holotype of *Gomeoceras? bulbosum* Reymont (C.47295, Reymont 1954b: pl. 4, figs 2a, b) is a smooth *V. globosum proprium*.

The holotype of *Vascoceras ellipticum* Barber (C.47679, Barber 1957: pl. 6, figs 1a, b; pl. 26, fig. 11) is probably a further example of *V. globosum proprium*. Other individuals referred to *V. ellipticum* by Barber (C.47680-4) are of uncertain affinities. The example from Dukul (C.47633, Barber 1957: pl. 14, figs 1a, b; pl. 26, figs 3, 4) is an involute abraded specimen difficult to identify with certainty. After dissection many such forms found there at Dukul prove to be *Thomasites gongilensis*.

Courville (1992: 424, pl. 10, fig. 2) reported a specimen of *V. globosum proprium* (his *V. gr. obscurum* Barber) from unit U (his Niveau 32) at Ashaka. The associated fauna described therein, however, is that typical of unit T2 (= upper part of his Niveau 30) at Ashaka. In the present work *V. globosum proprium* has been found only in unit T.

In its complex sutures and constricted inner whorls *V. globosum proprium* resembles *V. venezolanum* Renz (1982: 80, pl. 3, figs 5–11; pl. 24, figs 1–10; pl. 25, figs 1–8; text-fig. 61). The latter, highly variable species, however, generally shows denser, more persistent ribs which cross the flanks, although certain individuals may have subdued ribbing. *V. venezolanum* is known from southern Nigeria (Zaborski 1990b) but from beds containing *Mammites nodosoides* (Schlüter) which are younger than unit T at Ashaka.

Vascoceras obscurum Barber, 1957

Figs 53, 54, 59, 61, 62

- 1957 *Vascoceras obscurum* Barber: 19, pl. 6, figs 3, 9; pl. 27, figs 16–18.
 1989 *Vascoceras obscurum* Barber; Meister: 28, pl. 12, fig. 2; text-fig. 20.

MATERIAL AND OCCURRENCE. Five specimens, C.93552-3, C.93909-10, Pindiga Formation, unit T2, Ashaka; C.93326, Pindiga Formation, unit X, Ashaka.

DIMENSIONS.

	D	Wb	Wh	U
C.93909	64	29 (45)	31 (48)	6 (9)
C.93553	48	24 (50)	26 (54)	4 (8)
C.93326	44	21 (48)	24 (54.5)	4 (9)
C.93552	38	19 (50)	20 (53)	4 (10.5)

REMARKS. *V. obscurum* is a highly involute compressed species with a flattened to tabulate venter in its early stages which becomes rather more rounded during growth. The juvenile whorls bear strong regular ribs, some of which reach the umbilicus but which are mainly confined to the ventral region. The sutures are complex for the genus with fairly elongated highly frilled saddles (Fig. 59).

V. obscurum appears in unit T2 at Ashaka, occurring there alongside *V. globosum proprium*. A similar style of ribbing and complex suture pattern is present in these two forms. *V. obscurum* could be considered as an end member of *V. globosum proprium*. The consistently high degree of involution, the compressed whorls and the flattened venter, however, set *V. obscurum* apart while it has a different stratigraphical range than the latter form, being found in unit X at Ashaka. For these reasons *V. obscurum* is here treated as a discrete species, though it is clearly very closely related to *V. globosum proprium* from which it is probably derived.

The early whorls in *V. obscurum* resemble those in *V. pioti* (Peron & Fourtau) (see Freund & Raab 1969: 28, pl. 4, figs 1–9; text-figs 6d–g). The later growth stages, however, are unknown in the former, precluding comparison with the *Neptychites*-like body-chamber in *V. pioti*.

In what is known of its morphology *V. obscurum* shows a close similarity to *Neptychites*. Pronounced constrictions have not been seen in the available material but are found in the related *V. globosum proprium*. The *V. globosum proprium*-*V. obscurum* lineage may contain the root stock of *Neptychites*.

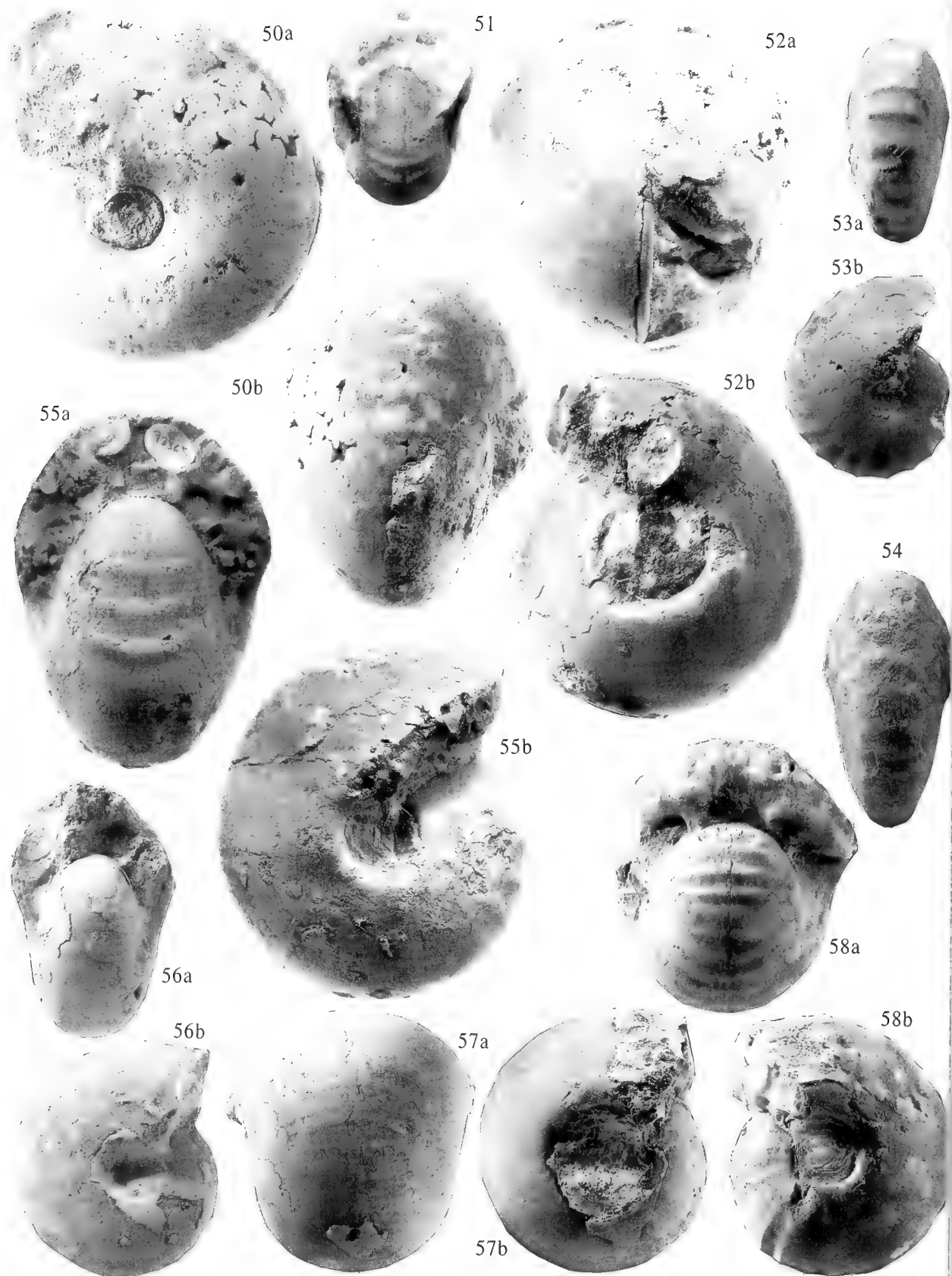
Very similar to *V. obscurum* are the *Neptychites* sp. juv. of Freund & Raab (1969: 47, pl. 8, figs 3–6) from Israel which occur well below the main stratigraphical range of the genus there.

Material from unit O at Ashaka referred to *Neptychites* by Meister (1989: 12, pl. 14, text-fig. 4) is, as mentioned above, an early *Thomasites*. That described by Courville (1992: 421, pl. 12, fig. 2) from unit R as *Neptychites* aff. *cephalotus* (Courtiller) is probably a member of the *V. globosum* group.

Vascoceras harttii (Hyatt, 1870)

Figs 58, 60

- 1870 *Ceratites harttii* Hyatt; 386.
 1875 *Buchiceras hartti* (Hyatt) Hyatt: 370.
 1887 *Ammonites (Buchiceras) harttii* (Hyatt); White: 226, pl. 19, figs 1, 2; pl. 20, fig. 3.
 1903 *Vascoceras hartti* (Hyatt) Hyatt: 103, pl. 14, fig. 16.
 1936 *Vascoceras hartti* (Hyatt); Maury: 247, pl. 22, figs 1, 2.
 1978 *Paravascoceras hartti* (Hyatt) Chancellor, Reymont & Tait: 96, fig. 20.
 1982 *Paravascoceras hartti* (Hyatt); Chancellor: 98, figs 28C, 29–33.
 1985 *Vascoceras (Paravascoceras) harttii* (Hyatt); Howarth:



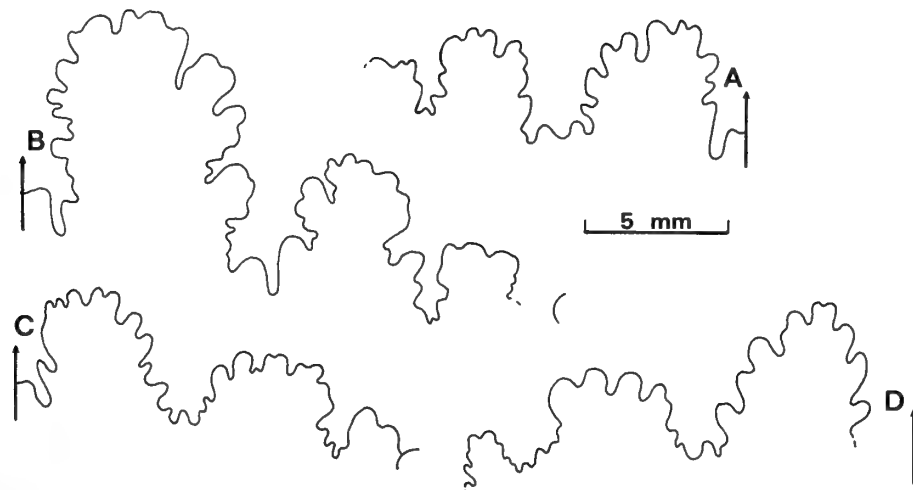


Fig. 59 Sutures in *Vascoceras obscurum* Barber. A, C.93910 at a diameter of 32 mm. B, C.93909 at a diameter of 45 mm. C, C.93552 at a diameter of 30 mm. D, C.93326 at a diameter of 34 mm. All specimens from the Pindiga Formation, unit T2, Ashaka except C.93326 which is from unit X at the same locality.

- ?1989 100, fig. 25 (with synonymy).
Vascoceras hartti (Hyatt); Cobban, Hook & Kennedy: 49, figs 49, 91A-D, G-K.
 1989 *Fagesia superstes* var. *levis* Renz; Meister: 37, pl. 16, fig. 2; text-fig. 26.
 1992 *Vascoceras gr. globosum* (Reyment) ou *Fagesia* sp.; Courville: pl. 9, fig. 1.

MATERIAL AND OCCURRENCE. Two specimens, C.93554-5, Pindiga Formation, unit X, Ashaka.

DIMENSIONS.

	D	Wb	Wh	U
C.93555	79	83 (105)	33 (42)	21 (26.5)
C.93554	49	50 (102)	21 (43)	12 (24.5)

REMARKS. These moderately evolute cadicones show sharp umbilical shoulders, which are undulating in C.93555, and steeply sloping umbilical walls. There are sharply rounded ventral ribs and occasional constrictions in C.93554 (Fig. 58) but they fade by a diameter of 40 mm leaving the internal mould smooth but for transverse growth striae. Neither specimen shows umbilical tubercles.

Kennedy *et al.* (1987: 51) pointed out the difficulty in distinguishing *V. hartti* from globose *V. globosum*. They regarded a more evolute coiling and a steeply sloping umbilical wall as most useful in identifying the former. In these respects the present material is more properly referred to *V. harttii* than the similar *V. globosum globosum*.

In the present work *V. harttii* has been found only in unit X at Ashaka. Meister (1989: 37-38) and Courville (1992: 424) also reported examples from unit U there which they referred to or

compared with *Fagesia superstes* (Kossmat). As with *V. globosum globosum* (see above) these forms have an ontogenetic development characteristic of *Vascoceras* not *Fagesia*. The globose shape and complex suture pattern are not in themselves diagnostic of *Fagesia*.

STRATIGRAPHICAL AND PHYLOGENETIC DISCUSSION

The oldest ammonite-bearing beds in north-eastern Nigeria yield no vascoceratid taxa. They are characterized by *Nigericeras gadeni*, *Metengonoceras dumbli* (Cragin), *Placenticeras (Karamaites) cumminsi* Cragin and *Metoicoceras geslinianum* (d'Orbigny), the last species allowing correlation with the Geslinianum Zone in north-western Europe and the Gracile Zone of the western interior of the United States (see Kennedy 1984, Cobban 1984, Cobban *et al.* 1989). This '*Nigericeras* fauna' is widely recognizable in West and Saharan Africa (see Lefranc 1978, Meister *et al.* 1992).

Paravascoceras cauvini appears in unit E at Ashaka and becomes common in unit F there and in unit H at Pindiga. In the last two horizons it is associated with *Burroceras* sp? (Zaborski 1995). Although not identifiable to species level this material may indicate correlation with the *Burroceras clydense* Zone of New Mexico. *P. cauvini* ranges through units K and M at Ashaka wherein *Vascoceras woodsi* occurs. These units also contain *Pseudaspidoceras pseudonodosoides*, on which basis they can be correlated with the Juddii Zone in the western interior. In south-western New Mexico a gap exists between the Juddii Zone and the basal Turonian Flexuosum Zone (Cobban *et al.* 1989). *Pseudaspidoceras flexuosum* Powell occurs in unit T2 at Ashaka. Units N to T1 at Ashaka belong to the Upper Cenomanian but

Fig. 50 *Vascoceras globosum costatum* (Reyment). Pindiga Formation, unit O, Ashaka. C.93523, $\times 1$.

Figs 51, 52 *Vascoceras globosum globosum* (Reyment). Pindiga Formation, unit R, Ashaka. Fig. 51, C.93544, $\times 1$. Fig. 52a, b, C.93545, $\times 1$.

Figs 53, 54 *Vascoceras obscurum* Barber. Pindiga Formation, unit T2, Ashaka. Fig. 53a, b, C.93552, $\times 1$. Fig. 54, C.93553, $\times 1$.

Figs 55-57 *Vascoceras globosum proprium* (Reyment). Pindiga Formation, unit T2, Ashaka. Fig. 55a, b, C.93365, $\times 1$. Fig. 56a, b, C.93549, $\times 1$. Fig. 57a, b, C.93550, $\times 1$.

Fig. 58 *Vascoceras harttii* (Hyatt). Pindiga Formation, unit X, Ashaka. C.93554, $\times 1$.

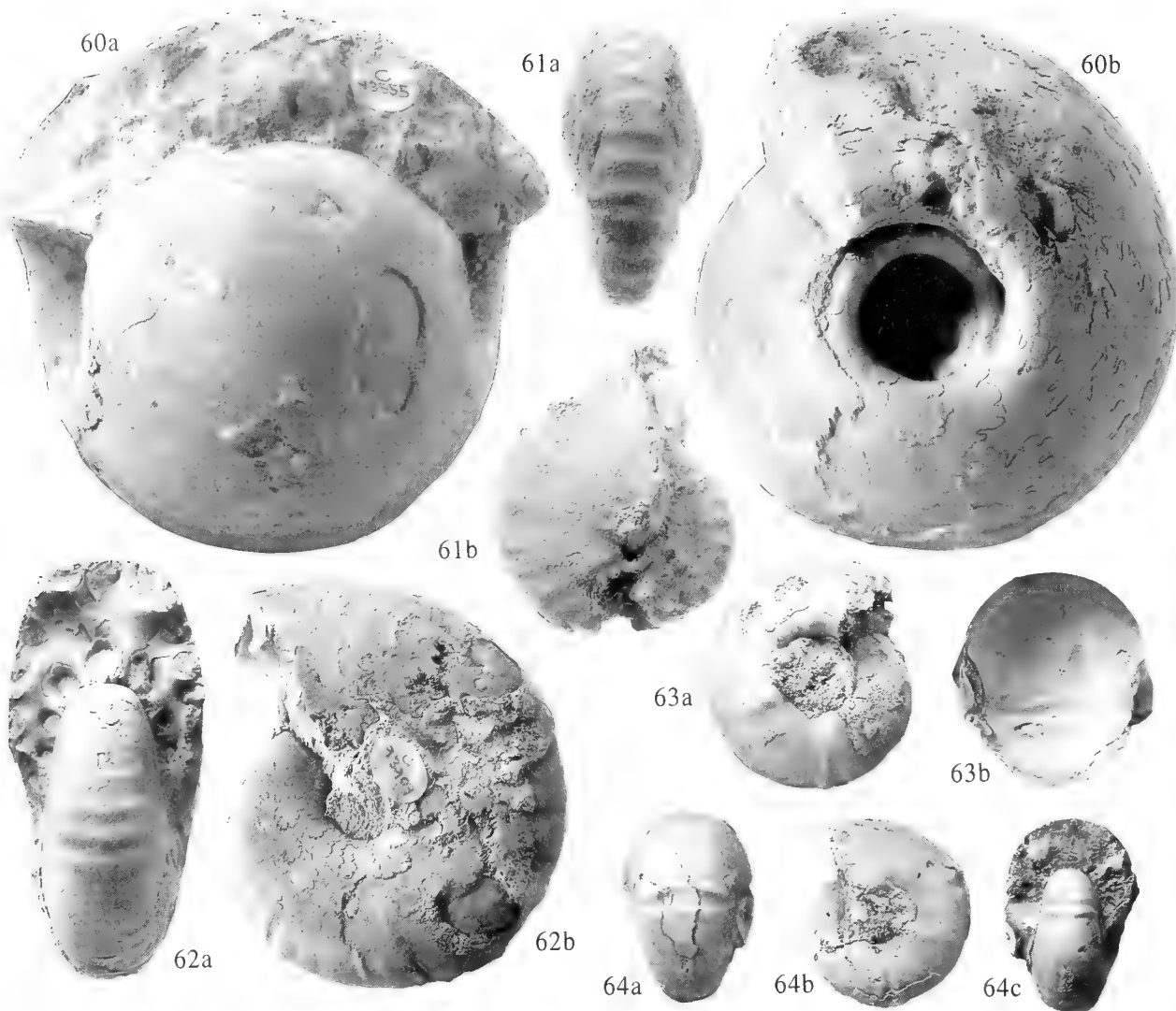


Fig. 60 *Vascoceras harttii* (Hyatt). Pindiga Formation, unit X, Ashaka. C.93555, $\times 1$.

Figs 61, 62 *Vascoceras obscurum* Barber. Fig. 61a, b. Pindiga Formation, unit X, Ashaka. C.93326, $\times 1$. Fig. 62a, b. Pindiga Formation, unit T2, Ashaka. C.93909, $\times 1$.

Figs 63, 64 *Vascoceras globosum proprium* (Reyment). Pindiga Formation, unit T2, Ashaka. Fig. 63a, b. C.93904, $\times 1$. Fig. 64a–c. C.93905, $\times 1$.

lack equivalents in south-western New Mexico. Unit O at Ashaka, which contains the youngest *Paravascoceras cauvini*, *Pseudovascoceras nigeriense*, *Vascoceras bullatum*, *V. globosum costatum* and *V. globosum globosum* is probably at least partially equivalent to beds with *Nigericeras scotti* in south-eastern Colorado.

Unit T2 at Ashaka contains an ammonite assemblage including *Pseudaspidocepheras flexuosum* and *Vascoceras globosum proprium*. These forms occur together in the basal Turonian Flexuosum Zone in west Texas (Kennedy *et al.* 1987), *Thomasites* and *Wrightoceras munieri* (Pervinquière) also being associated in both places. *V. globosum proprium* is further recorded from New Mexico and Hancock (1991) suggested that it may serve as a better marker for the base of the Turonian than *Pseudaspidocepheras flexuosum*. In the Ashaka section, however, it actually appears in unit T1 just below the first occurrence of *P. flexuosum*. A minor discontinuity representing a marine

flooding surface separates units T1 and T2. The fauna of unit T2 seems to have in large part been introduced during this flooding event which may complicate the order of occurrence of these taxa at Ashaka.

Vascoceras obscurum ranges from the basal Turonian unit T2 into unit X at Ashaka. Units U to X at Ashaka, which also represent the known range of *V. harttii*, are of Early Turonian age. They cannot, however, be dated more precisely on the basis of their ammonite faunas which are almost entirely composed of *Pseudotissotia nigeriensis* (Woods) and *Eotissotia simplex* Barber. *V. harttii* has been assigned to the Lower Turonian in Angola (Howarth 1985), Brazil (Bengtson 1983) and Mexico (Chancellor 1982) but material from the Upper Cenomanian of New Mexico has also been referred to the species (Cobban *et al.* 1989: 49, figs 49, 91A–D, G–K).

With the exception of a few taxa 'vascoceratid' ammonites have not proved to be of great value in detailed correlation,

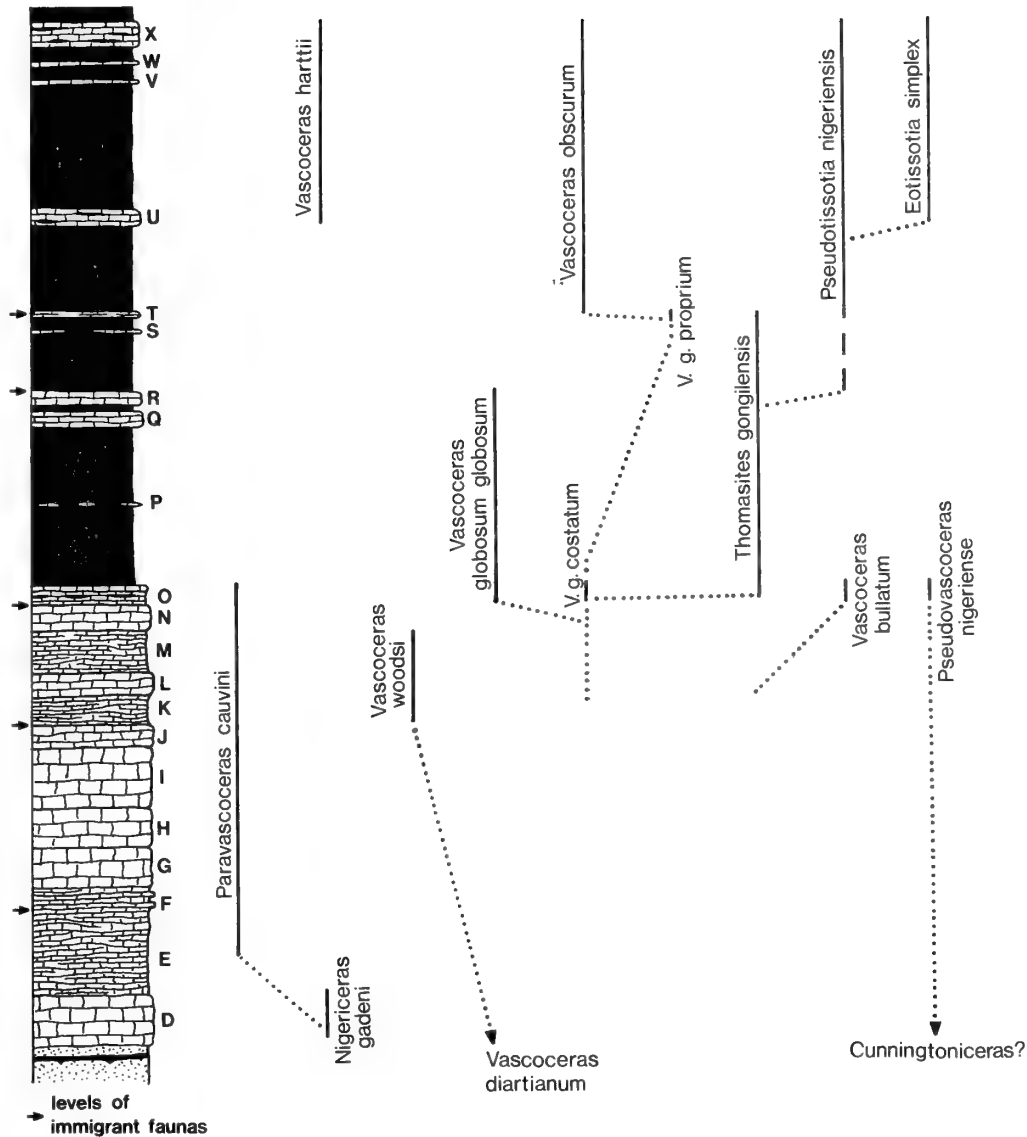


Fig. 65 Stratigraphical ranges in the Ashaka section of taxa mentioned in the text and their suggested phylogenetic relationships.

especially inter-regionally. A number of problems complicate their use including: the variable taxonomic treatment authors have employed; the difficulty of identifying poorly preserved material, especially if the inner whorls are not available; the lack of an exact stratigraphical provenance for many species; and the problem of polymorphism. In regard to the last of these factors Meister (1989) and Meister *et al.* (1992) have made the important point that in certain regions only a portion of the potential morphological range of a species may be expressed on account of palaeoecological factors.

It has long been appreciated that 'vascoceratid' ammonites are predominantly a Tethyan group. Less attention has been paid to the potential palaeoenvironmental influences on their regional distribution. In this regard it is of interest to compare the faunas of north-eastern Nigeria and Niger, the stratigraphical distributions of which are now well understood.

Despite their geographical proximity correlation between these two areas is not as straightforward as might be expected. There is little problem with the horizons of Geslinianum Zone

age; in both places assemblages of *Nigericeras*, *Metoicoceras* and *Metengonoceras* are found. Similarly, in the upper part of the Turonian *Coilopoceras* is present in both areas. There are, however, faunal differences in the intervening sequences. *Vascoceras woodsi* is unknown in Niger. In Nigeria it occurs alongside *Pseudaspidooceras pseudonodosoides* which was compared with *P. tassaraense* Meister, Alzouma, Lang & Mathey (1992) from the Monts Iguelela area of Niger by Zaborski (1995). The two may be of comparable age. *P. tassaraense* occurs alongside *Nigericeras jacqueti involutum*, a form unknown in Nigeria. Slightly lower in the same section there occur large numbers of *Cibolaites(?) africaensis* Meister, Alzouma, Lang & Mathey (1992) which has not been found further to the south. At Tanout Aviation and Birgimari there are horizons dominated by compressed individuals of *Paravascoceras cauvini*. In their ornament or lack of it they match the variation shown by the species in unit O at Ashaka. The Niger faunas, however, include more inflated individuals of *Vascoceras crassum* type. None of the species associated with *P.*

cavini in unit O at Ashaka is found in the described Niger horizons. Higher in the sequence *Thomasites gongilensis*, so abundant in unit R at Ashaka and unit O at Pindiga, and with an overall range from unit O to unit T2 at the former locality, is not found in any of the Niger sections. *Pseudotissotia nigeriensis*, on the other hand, occurs in large numbers at Tanout Aviation but none of the associated taxa in Nigeria accompany it there.

Biostratigraphical comparison between Niger and Nigeria is complicated by the fact that ammonites are restricted to limestone horizons which are, in the main, thin units within dominantly argillaceous sequences. The presence or absence of particular faunas, therefore, may in some cases be related to the occurrence of calcareous beds (see also Meister *et al.* 1992: 91). The possibility of control over ammonite distributions by transgressive pulses of the trans-Saharan sea during the Late Cenomanian and Early Turonian has long been discussed, most recently by Courville *et al.* (1991). Meister *et al.* (1992: 94–95), however, have speculated that local palaeoenvironments were a strong influence on ‘vascoceratid’ distributions, their morphological polymorphism and their consequent evolutionary potential. In support of the latter hypothesis it may be noted that members of evolutionary lineages ‘indigenous’ to north-eastern Nigeria (*Nigericeras*, *Paravascoceras cavini* and *Pseudotissotia nigeriensis*) extend into Niger. Introduced taxa do not. Among these may be mentioned *Burroceras?* from unit F at Ashaka; *Vascoceras woodsi* from units K and M; the greater part of the fauna from unit O including *Pseudaspidooceras footeanum* (Stoliczka), *Fikaites*, *Rubroceras*, *Pseudovascoceras nigeriense* and, probably, *Vascoceras globosum costatum*; *Pseudaspidooceras paganum* from unit R; and *Pseudaspidooceras flexuosum*, *Watinooceras*, *Choffaticeras* and *Wrightoceras munieri* from unit T2. The appearances of these taxa are probably related to transgressive pulses, the influences of which did not fully extend into Niger. As suggested by Meister *et al.* (1992) the absence of these forms and consequent lack of competition may have permitted local intraspecific variants and evolutionary lineages to develop in Niger. Examples would be the inflated variants of *Paravascoceras cavini* and the lineage leading to *Nigericeras jacqueti involutum*. Rather than the overall extent of the trans-Saharan sea as such, more localized influences such as water depth and temperature may have controlled the distribution of taxa. If these factors did apply they would place important constraints on the use of ‘vascoceratid’ species in long distance correlation.

Associated with the above matter is the probability that a number of acanthoceratine taxa independently gave rise to vascoceratid-like forms during Late Cenomanian times. Reyment (1979: 111) suggested that the family Vascoceratidae was polyphyletic, the morphological similarities between its members being due to adaptation to the same kind of epicontinental palaeoenvironments rather than to close phylogenetic affinities. The Late Cenomanian transgression brought several forms into north-eastern Nigeria which show elements of the ‘vascoceratid’ morphology, notably simplified sutures. *Rubroceras* and *Fikaites*, the latter probably derived from *Eucalycceras* Spath, are examples, as is *Pseudovascoceras* which, as mentioned above, may be a descendent of *Cunningtoniceras*. Reyment (1955: 62, text-fig. 27) regarded *Nigericeras* as the root stock of the entire family Vascoceratidae while Cooper (1979) suggested that *Vascoceras diartianum* gave rise to both *Paravascoceras* and the younger *Vascoceras*. It is suggested here that *Paravascoceras* is derived from *Nigericeras* and belongs to a lineage separate to that leading to *Vascoceras*. The earliest *Vascoceras* in north-eastern Nigeria, *V. woodsi*,

appears to be a peramorphic derivative of *V. diartianum*. The immediate origins of *V. bullatum*, *V. globosum* and *V. harttii* are obscure. It may be mentioned, however, that *V. globosum costatum* probably contains the progenitors of *Thomasites gongilensis*. This species in turn gave rise to *Pseudotissotia nigeriensis* in terminal Cenomanian times (see also Barber 1957, Cooper 1979, Meister 1989) from which *Eotissotia simplex* originated as a paedomorph during the Early Turonian (Zaborski 1993). The youngest member of the *V. globosum* group, *V. globosum proprium*, straddles the Cenomanian-Turonian boundary. It gave rise to *V. obscurum* and probably also *Neptychites*. Kennedy & Wright (1979: 681) believed the latter genus to have been derived from *Paravascoceras* but used this name in the sense of *Vascoceras* without umbilical tubercles.

The suggested phylogenetic relationships of forms from north-eastern Nigeria are shown in Fig. 65. Several converging lineages are believed to exist, their frequently homeomorphic similarities being due to colonization of the same palaeoenvironment.

ACKNOWLEDGEMENTS. Thanks are due to Drs M. K. Howarth and H. G. Owen, and Mr. S. Baker for help in many ways. Dr. N. Morris kindly allowed access to a collection of ammonites from Niger. Mr. M. Baku, Quarry Manager, Ashaka Cement Co. kindly allowed easy access to the Ashaka quarry. Photographs were provided by the Natural History Museum (London) Photographic Unit. Dr. W. J. Kennedy kindly made useful suggestions concerning the manuscript.

REFERENCES

- Adkins, W. S. 1931. Some Upper Cretaceous ammonites in western Texas. *Bulletin of the University of Texas Bureau of Economic Geology and Technology*, Austin, **3101**: 35–72, pls 2–5.
- Amard, B., Collignon, M. & Roman, J. 1981. Etude stratigraphique et paléontologique du Crétacé supérieur et Paléocene du Tinrhert-W et Tademait-E (Sahara Algérien). *Documents du Laboratoire de Géologie de la Faculté des Sciences de Lyon*, (H.S.) **6**: 15–173, pls 1–17.
- Barber, W. 1957. Lower Turonian ammonites from north-eastern Nigeria. *Bulletin of the Geological Survey of Nigeria*, Kaduna, **26**: 1–86, pls 1–35.
- 1960. Notes on Upper Cretaceous Ammonoidea from north-eastern Nigeria. *Records of the Geological Survey of Nigeria*, Kaduna, **1957**: 60–67, pls 13–14.
- Benavides-Cáceres, V. E. 1956. Cretaceous system in northern Peru. *Bulletin of the American Museum of Natural History*, New York, **108**: 353–494, pls 31–66.
- Bengtson, P. 1983. The Cenomanian-Coniacian of the Sergipe Basin, Brazil. *Fossils and Strata*, Oslo, **12**: 1–78, 1 map.
- Berthou, P.-Y., Chancellor, G. R. & Lauverjat, J. 1985. Revision of the Cenomanian-Turonian ammonite *Vascoceras Choffat*, 1898 from Portugal. *Comunicações dos Servicos Geológicos de Portugal*, Lisbon, **71**: 55–79, pls 1–6.
- Böse, E. 1920. On a new ammonite fauna of the Lower Turonian of Mexico. *Bulletin of the University of Texas Bureau of Economic Geology and Technology*, Austin, **1856**: 173–252, pls 12–20.
- Carter, J. D., Barber, W., Tait, E. A. & Jones, G. P. 1963. The geology of parts of Adamawa, Bauchi and Bornu provinces in north-eastern Nigeria. *Bulletin of the Geological Survey of Nigeria*, Kaduna, **30**: 1–108, 6 pls., 3 maps.
- Chancellor, G. R. 1982. Cenomanian-Turonian ammonites from Coahuila, Mexico. *Bulletin of the Geological Institution of the University of Uppsala*, (NS) **9**: 77–129.
- , Kennedy, W. J. & Hancock, J. M. In press. Turonian ammonite faunas from central Tunisia. *Special Papers in Palaeontology*, London.
- , Reyment, R. A. & Tait, E. A. 1977. Notes on Lower Turonian ammonites from Loma el Macho, Coahuila, Mexico. *Bulletin of the Geological Institution of the University of Uppsala*, (NS) **7**: 85–101.
- Choffat, P. 1898. Recueil d'études paléontologiques sur la faune crétacique du Portugal. 1. Espèces nouvelles ou peu connus. 2. Les ammonées du Belliasien, des Couches à *Neolobites Vibrayeanus*, du Turonien et du Sénonien. *Memorias da Comissão dos Trabalhos Geológicos de Portugal*, Lisbon, **1898**: 41–86, pls 3–22.

- Chudeau, R.** 1909. Ammonites du Damergou (Sahara meridional). *Bulletin de la Société Géologique de France*, Paris, (4) 9: 67–71, pls 1–3.
- 1921. Ammonites turoniennes du Soudan. *Bulletin du Muséum National d'Histoire Naturelle*, Paris, (2) 6: 463–470, 1 pl.
- Cobban, W. A.** 1971. New and little known ammonites from the Upper Cretaceous (Cenomanian and Turonian) of the western interior of the United States. *Professional Papers of the United States Geological Survey*, Washington, 699: 1–24, pls 1–18.
- 1984. Mid-Cretaceous ammonite zones, Western Interior, United States. *Bulletin of the Geological Society of Denmark*, Copenhagen, 33: 71–89.
- & **Hook, S. C.** 1983. Mid-Cretaceous (Turonian) ammonite fauna from Fence Lake area, west-central New Mexico. *Memoirs of the Institute of Mining Technology, New Mexico State Bureau of Mines and Mineral Resources*, Socorro, 41: 1–50, pls 1–14.
- & **Kennedy, W. J.** 1989. Upper Cretaceous rocks and ammonite faunas of southwestern New Mexico. *Memoirs of the Institute of Mining Technology, New Mexico State Bureau of Mines and Mineral Resources*, Socorro, 45: 1–137.
- & **Scott, G. R.** 1972. Stratigraphy and ammonite fauna of the Graneros Shale and Greenhorn Limestone near Pueblo, Colorado. *Professional Papers of the United States Geological Survey*, Washington, 645: 1–108, pls 1–41.
- Collignon, M.** 1937. Ammonites Cénomaniennes du sud-ouest de Madagascar. *Annales Géologique du Service des Mines de Madagascar*, Tananarive, 8: 29–72, pls 1–11.
- 1957. Céphalopodes néocrétacées du Tinrhert (Fezzan). *Annales de Paléontologie*, Paris, 43: 113–136, pls 16–18.
- 1965. Nouvelles ammonites néocrétacées sahariennes. *Annales de Paléontologie*, Paris, 57: 162–202, pls A–H.
- Cooper, M. R.** 1978. Uppermost Cenomanian-basal Turonian ammonites from Salinas, Angola. *Annals of the South African Museum*, Cape Town, 75: 51–152.
- 1979. Ammonite evolution and its bearing on the Cenomanian-Turonian boundary problem. *Palaontologia Zeitschrift*, Stuttgart, 53: 120–128.
- Courtiller, M. A.** 1860. Description de trois nouvelles espèces d'ammonites du terrain crétacé des environs du Saumur. *Mémoires de la Société d'Agriculture, Sciences et Arts d'Angers*, 3: 246–252, 3 pls.
- Courville, P.** 1992. Les Vascoceratinæ et les Pseudotissotiinae (Ammonitina) d'Ashaka (NE Nigéria); relations avec leur environnement biosédimentaire. *Bulletin des Centres Recherches Exploration-Production Elf Aquitaine*, Boussens, 16: 407–457, pls 1–14.
- , **Meister, C.**, **Lang, J.**, **Mathey, B.** & **Thierry, J.** 1991. Les corrélations en Téthys occidentale et l'hypothèse de la liaison Téthys-Atlantique Sud: intérêt des faunes d'ammonites du Cénomanien supérieur-Turonian moyen basal du Niger et du Nigéria (Afrique de l'ouest). *Compte Rendu de l'Academie des Sciences, Paris*, (2) 313: 1039–1042.
- Douvillé, H.** 1912. Evolution et classification des Pulchelliidés. *Bulletin de la Société géologique de France*, Paris, (4) 11: 285–320.
- Förster, R.**, **Meyer, R.** & **Risch, H.** 1983. Ammoniten und planktonische Foraminiferen aus den Eibrunner Mergeln (Regensburger Kreide, Nordostbayern). *Zitteliana*, Munich, 10: 123–141, pls 1–3.
- Freund, R.** & **Raab, M.** 1969. Lower Turonian ammonites from Israel. *Special Papers in Palaeontology*, London, 4: 1–83, pls 1–10.
- Furon, R.** 1933. Faunes et extension du Crétacé au sud de l'Ahaggar (Cénomanien, Turonien et Sénonien). *Bulletin de la Société géologique de France*, Paris, (5) 3: 259–280, pl. 9.
- 1935. Le Crétacé et le Tertiaire du Sahara soudanais. *Archives du Muséum National d'Histoire Naturelle*, Paris, (6) 13: 1–96, pls 1–7.
- Grossouvre, A.** de 1894. Recherches sur la Craie Supérieure. 2, Paléontologie. Les ammonites de la Craie Supérieure. 264 pp., atlas de 39 pls. *Mémoires pour servir à l'explication de la Carte géologique détaillée de la France*, Paris.
- Hancock, J. M.** 1991. Ammonite scales for the Cretaceous System. *Cretaceous Research*, London, 12: 259–291.
- & **Kennedy, W. J.** 1981. Upper Cretaceous ammonite stratigraphy: some current problems. In, **House, M. R.** & **Senior, J. R.** (eds), *The Ammonoidea*: 531–553. London (Academic Press, for the Systematics Association).
- Hirano, H.** 1983. Revision of two vascoceratid ammonites from the Upper Cretaceous of Nigeria. *Bulletin of Science and Engineering Research Laboratory, Waseda University*, Tokyo, 105: 44–79, pls 1–5.
- Howarth, M. K.** 1985. Cenomanian and Turonian ammonites from the Novo Redondo area, Angola. *Bulletin of the British Museum (Natural History)*, London, (Geology), 39 (2): 73–105.
- Hyatt, A.** 1870. Report on the Cretaceous fossils from Mariom. In, **Hartt, C. F.**, *Geology and physical geography of Brazil*: 385–393. Boston.
- 1875. The Jurassic and Cretaceous ammonites collected in S. America by Prof. James Orton, with an appendix on the Cretaceous ammonites of Prof. Hartt's collection. *Proceedings of the Boston Society of Natural History*, 17: 365–378.
- 1903. Pseudoceratites of the Cretaceous. *Monographs of the United States Geological Survey*, Washington, 44: 351 pp., 47 pls.
- Kennedy, W. J.** 1971. Cenomanian ammonites from southern England. *Special Papers in Palaeontology*, London, 8: 1–133, pls 1–64.
- 1984. Ammonite faunas and the 'standard zones' of the Cenomanian to Maastrichtian stages in their type areas, with some proposals for the definition of the stage boundaries by ammonites. *Bulletin of the Geological Society of Denmark*, Copenhagen, 33: 147–161.
- & **Cobban, W. A.** 1990a. Cenomanian ammonite faunas from the Woodbine Formation and the lower part of the Eagle Ford Group, Texas. *Palaontologia*, London, 33: 75–154, pls 1–17.
- & — 1990b. Cenomanian micromorphic ammonites from the western interior of the USA. *Palaontologia*, London, 33: 379–422, pls 1–7.
- , — & **Hancock, J. M.** & **Hook, S. C.** 1989. Biostratigraphy of the Chispa Summit Formation at its type locality: a Cenomanian through Turonian reference section for Trans-Pecos Texas. *Bulletin of the Geological Institution of the University of Uppsala*, (NS) 15: 39–119.
- & **Juignet, P.** 1977. *Ammonites diartianus* d'Orbigny, 1850, Vascoceratidae du Cénomanien supérieur de Saint-Calais (Sarthe). *Geobios*, Lyon, 10: 583–595, pls 1, 2.
- & **Wright, C. W.** 1979. Vascoceratid ammonites from the type Turonian. *Palaontologia*, London, 22: 665–683, pls 82–86.
- & — 1985. Evolutionary patterns in Late Cretaceous ammonites. *Special Papers in Palaeontology*, London, 33: 131–143.
- & — In press. The affinities of *Nigericeras* Schneegans, 1943 (Cretaceous, Ammonoidea). *Geobios*, Lyon.
- , — & **Hancock, J. M.** 1987. Basal Turonian ammonites from west Texas. *Palaontologia*, London, 30: 27–74, pls 1–10.
- Kler, M. O.** 1909. [Neoceratites of eastern Bukhara]. *Trudy Geologicheskago i Mineralogicheskogo Muzeya*, St. Petersburg, 2 (for 1908): 157–174, pls 6–8. [In Russian].
- Kummel, B.** & **Decker, J. M.** 1954. Lower Turonian ammonites from Texas and Mexico. *Journal of Paleontology*, Tulsa, 28: 310–319, pls 30–33.
- Lefranc, J. P.** 1978. Etat des connaissances actuelles sur les zonations biostratigraphiques du milieu du Crétacé (Albien à Turonian) au Sahara. *Annales du Muséum d'Histoire Naturelle de Nice*, 4 (XIX): 1–19.
- Lewy, Z.**, **Kennedy, W. J.** & **Chancellor, G. R.** 1984. Co-occurrence of *Metoiceras geslinianum* (d'Orbigny) and *Vascoceras cauvini* Chudeau (Cretaceous Ammonoidea) in the southern Negev and its stratigraphic implications. *Newsletters on Stratigraphy*, Leiden, 13: 67–76.
- Luger, P.** & **Gröschke, M.** 1989. Late Cretaceous ammonites from the Wadi Qena area in the Egyptian eastern desert. *Palaontologia*, London, 32: 355–407, pls 38–49.
- Maury, C. J.** 1936. O Cretaceo de Sergipe. *Monografias Servico Geológico e Mineralógico do Brasil*, Rio de Janeiro, 11: 283 pp., 28 pls.
- Meister, C.** 1989. Les ammonites du Crétacé supérieur d'Ashaka (Nigéria). *Bulletin des Centres Recherches Exploration-Production Elf Aquitaine*, Boussens, 13 (supplement): 1–84, pls 1–28.
- , **Alzouma, K.**, **Lang, L.** & **Mathey, B.** 1992. Les ammonites du Niger (Afrique Occidentale) et la transgression transsaharienne au cours du Cénomanien-Turonien. *Geobios*, Lyon, 25: 55–100, pls 1–11.
- Offodile, M. E.** & **Reyment, R. A.** 1976. Stratigraphy of the Keana-Awe area of the middle Benue region of Nigeria. *Bulletin of the Geological Institution of the University of Uppsala*, (NS) 7: 37–66.
- Pervinquier, L.** 1907. *Etudes de paléontologie tunisienne*. 1, Céphalopodes des terrains secondaires. 438 pp., 27 pls. Paris, Carte géol. Tunis.
- Popoff, M.**, **Wiedmann, J.** & **de Klasz, I.** 1986. The Upper Cretaceous Gongila and Pindiga Formations, northern Nigeria: subdivisions, age, stratigraphic correlations and paleogeographic implications. *Elogiae geologicae Helvetiae*, Basel, 79: 343–363.
- Powell, J. D.** 1963. Cenomanian-Turonian (Cretaceous) ammonites from Trans-Pecos, Texas and north-eastern Chihuahua, Mexico. *Journal of Paleontology*, Tulsa, 37: 309–332, pls 31–34.
- Reeside, J. R.** 1923. A new fauna from the Colorado Group of southern Montana. *Professional Papers of the United States Geological Survey*, Washington, 132-B: 25–33, pls 11–21.
- Renz, O.** 1982. *The Cretaceous ammonites of Venezuela*. 132 pp., 40 pls. Basel.
- Reyment, R. A.** 1954a. New Turonian (Cretaceous) ammonite genera from Nigeria. *Colonial Geology and Mineral Resources*, London, 4: 149–164, pls 1–4.
- 1954b. Some new Upper Cretaceous ammonites from Nigeria. *Colonial Geology and Mineral Resources*, London, 4: 248–270, pls 1–5.
- 1955. The Cretaceous Ammonoidea of southern Nigeria and the southern Cameroons. *Bulletin of the Geological Survey of Nigeria*, Kaduna, 25: 1–112, pls 1–25.
- 1956. On the stratigraphy and palaeontology of the Cretaceous of Nigeria and the Cameroons, British West Africa. *Geologiska Föreningens i Stockholm Förhandlingar*, 78: 17–96.
- 1965. *Aspects of the geology of Nigeria*. 145 pp., 18 pls. Ibadan.
- 1979. Variation and ontogeny in *Bauchioceras* and *Gomboceras*. *Bulletin of the Geological Institution of the University of Uppsala*, (NS) 8: 89–111.

- 1988. Does sexual dimorphism occur in Upper Cretaceous ammonites? *Senck. lethaea*, Frankfurt, **69**: 109–119.
- Roman, F.** 1938. *Les ammonites jurassiques et crétacées. Essai de genera*. 554 pp., 53 pls. Paris.
- Schneegans, D.** 1943. Invérités du Crétacé supérieur du Damergou (Territoire du Niger). *Bulletin de la Direction Féderale des Mines et de la Géologie, Afrique Occidentale Française*. Dakar, **7**: 87–150, pls 1–8.
- Schöbel, J.** 1975. Ammoniten der Familie Vascoceratidae aus dem Unterturon des Damergou-Gebietes, République du Niger. *Special Publications of the Palaeontological Institution of the University of Uppsala*, **3**: 1–136, pls 1–6.
- Sharpe, D.** 1855. Description of the fossil remains of Mollusca found in the Chalk of England. I. Cephalopoda: 27–36, pls 11–16. *Monographs of the Palaeontographical Society*, London.
- Solger, F.** 1904. Die Fossilien der Mungokreide in Kamerun und ihre geologische Bedeutung, mit besonderer Berücksichtigung der Ammonitiden. In, Esch, E., Solger, F., Oppenheim, M. & Jäkel, O., *Beiträge zur Geologie von Kamerun*: 83–242, pls 3–5. Stuttgart.
- Spath, L. F.** 1923. Appendix II. On the ammonite horizons of the Gault and contiguous deposits. *Summary of Progress of the Geological Survey of Great Britain*, **1922**: 139–149.
- 1925. On Upper Albian Ammonoidea from Portuguese East Africa. With an appendix on Upper Cretaceous ammonites from Maputoland. *Annals of the Transvaal Museum, Pretoria*, **11**: 179–200, pls 28–37.
- White, C. A.** 1887. Contribuições à paleontologia do Brasil. *Archivos do Museu Nacional Rio de Janeiro*, **7**: 1–273, 28 pls.
- Wiedmann, J.** 1960. Le Crétacé supérieur de l'Espagne et du Portugal et ses céphalopodes. In, Colloque sur le Crétacé supérieur Français (Dijon, 1959). *Compte rendu Congrès des Sociétés Savantes de Paris et des Départements, Section des Sciences, Paris*, **1959**: 709–764, 8 pls.
- Woods, H.** 1911. The palaeontology of the Upper Cretaceous deposits of Northern Nigeria. In, Falconer, J. D., *The geology and geography of Northern Nigeria*: 273–286, pls 19–24. London.
- Wozny, E. & Kogbe, C. A.** 1983. Further evidence of marine Cenomanian, Turonian and Maastrichtian in the Upper Benue Basin of Nigeria (west Africa). *Cretaceous Research*, London, **4**: 95–99.
- Wright, C. W.** 1957. Mollusca 4; Cephalopoda, Ammonoidea. In, Moore, R. C. (ed.), *Treatise on Invertebrate Paleontology*, L: L80–L490. Lawrence, Kansas.
- & **Kennedy, W. J.** 1980. Origin, evolution and systematics of the dwarf acanthoceratid *Protacanthoceras* Spath, 1923 (Cretaceous Ammonoidea). *Bulletin of the British Museum (Natural History)*, London, (Geology), **34** (2): 65–107.
- & — 1981. The Ammonoidea of the Plenus Marls and the Middle Chalk. 148 pp., 32 pls. *Monographs of the Palaeontographical Society*, London.
- & — 1987. The Ammonoidea of the Lower Chalk. 2: 127–218, pls 41–55. *Monographs of the Palaeontographical Society*, London.
- Zaborski, P. M. P.** 1985. Upper Cretaceous ammonites from the Calabar region, south-east Nigeria. *Bulletin of the British Museum (Natural History)*, London, (Geology), **39** (1): 1–72.
- 1987. Lower Turonian (Cretaceous) ammonites from south-east Nigeria. *Bulletin of the British Museum (Natural History)*, London, (Geology), **41** (2): 31–66.
- 1990a. The Cenomanian and Turonian (mid-Cretaceous) ammonite biostratigraphy of north-eastern Nigeria. *Bulletin of the British Museum (Natural History)*, London, (Geology), **46** (1): 1–18.
- 1990b. Some Upper Cretaceous ammonites from southern Nigeria. *Journal of African Earth Science (and the Middle East)*, Oxford, **10**: 565–581.
- 1993. Some new and rare Upper Cretaceous ammonites from north-eastern Nigeria. *Journal of African Earth Science (and the Middle East)*, Oxford, **17**: 359–371.
- 1995. The Upper Cretaceous ammonite *Pseudaspidoceras* Hyatt, 1903 in north-eastern Nigeria. *Bulletin of the British Museum (Natural History)*, London, (Geology), **51**: 53–72, 24 figs.

APPENDIX

A list of previously described material from Nigeria representing taxa discussed herein is given below with revised taxonomic determinations. The page and, where necessary, plate and figure numbers quoted are those in the original publications.

Woods (1911)

281 *Vascoceras nigeriense* sp. nov.

Reyment (1954b)

256 *Vascoceras nigeriense* Woods

257 *Pachyvascoceras costatum* sp. nov.

258 *Pachyvascoceras proprium* sp. nov.

258 *Pachyvascoceras proprium plenum* subsp. nov.

259 *Pachyvascoceras globosum* sp. nov.

263 *Gomeoceras? bulbosum* sp. nov.

Reyment (1955)

63 *Paravascoceras aff. chevalieri* (Furon)

65 *Pachyvascoceras costatum* Reyment

Barber (1957)

15 *Vascoceras nigeriense* Woods

15 *Vascoceras robustum* sp. nov.

17 *Vascoceras polygonum* sp. nov.

17, pl. 4, fig. 1 *Vascoceras ellipticum* sp. nov.

17, pl. 6, fig. 4 *Vascoceras ellipticum* sp. nov.

19 *Vascoceras bulbosum* (Reyment)

19 *Vascoceras depressum* sp. nov.

19 *Vascoceras obscurum* sp. nov.

21 *Vascoceras globosum globosum* (Reyment)

23 *Vascoceras globosum plenum* (Reyment)

25 *Vascoceras globosum proprium* (Reyment)

25 *Vascoceras globosum compressum* subsp. nov.

25 *Vascoceras globosum carteri* subsp. nov.

27 *Vascoceras* sp. juv.

27 *Fagesia simplex* sp. nov.

Revised determination

Pseudovascoceras nigeriense (Woods)

Pseudovascoceras nigeriense (Woods)

Vascoceras globosum costatum (Reyment)

Vascoceras globosum proprium (Reyment)

Vascoceras globosum proprium (Reyment)

Vascoceras globosum globosum (Reyment)

Vascoceras globosum proprium (Reyment)

Thomasites

Vascoceras globosum costatum (Reyment)

Pseudovascoceras nigeriense (Woods)

?*Vascoceras globosum costatum* (Reyment)

?*Vascoceras globosum costatum* (Reyment)

?*Thomasites gongilensis* (Woods)

?*Vascoceras globosum proprium* (Reyment)

Paravascoceras cauvini (Chudeau)

Paravascoceras cauvini (Chudeau)

Vascoceras obscurum (Barber)

Vascoceras globosum globosum (Reyment) (part)

and *V. globosum proprium* (Reyment) (part)

Vascoceras globosum proprium (Reyment)

Vascoceras globosum proprium (Reyment)

Vascoceras globosum proprium (Reyment)

Vascoceras globosum globosum (Reyment)

Vascoceras woodsi sp. nov.

indeterminate *Vascoceras*

- 27 *Fagesia involuta* sp. nov.
 29 *Nigericeras costatum* sp. nov.
 29 *Nigericeras glabrum* sp. nov.
 31 *Nigericeras(?) intermedium* sp. nov.
 31 *Paramammites tuberculatus* sp. nov.
 33 *Paramammites raricostatus* sp. nov.
 33 *Paramammites inflatus* sp. nov.
 35 *Paravascoceras costatum costatum* (Reyment)
 35 *Paravascoceras costatum quadratum* subsp. nov.
 37 *Paravascoceras costatum tectiforme* subsp. nov.
 37 *Paravascoceras aff. cauvini* (Chudeau)
- Meister (1989)**
- 10 *Nigericeras gadieni* (Chudeau) – *lamberti* Schneegans
 11 *Nigericeras jacqueti* Schneegans
 11 *Plesiovascoceras* aff. gr. *thomi* (Reeside) ou sp. nov.
 12 *Neptychites cephalotus* (Courtiller)
 14, pl. 5, fig. 2 *Paravascoceras* gr. *evolutum* Schneegans
 14, pl. 5, fig. 4 *Paravascoceras* gr. *evolutum* Schneegans
 14 *Paravascoceras nigeriensis(?)* (Woods)
 14 *Paravascoceras* aff. *nigeriensis* (?) (Woods)
 18 *Paravascoceras crassum* Furon
 21 *Paravascoceras tectiforme* (Barber)
 21, pl. 9, fig. 1 *Paravascoceras carteri* Barber
 21, pl. 10, figs 1, 2 *Paravascoceras carteri* Barber
 23 *Vascoceras costatum* (Barber)
 23 *Vascoceras costatum* (Barber) *glabrum* (Barber)
 28 *Vascoceras ellipticum* Barber
 28 *Vascoceras silvanense* Choffat
 28 *Vascoceras obscurum* Barber
 30 *Paramammites subconciliatus* (Choffat)
 36, pl. 14, figs 3, 4 *Paramammites polymorphus* (Pervinquieré)
 36, pl. 15, figs 2, 3 *Paramammites* aff. gr. *polymorphus* (Pervinquieré)
 37 *Fagesia superstes* var. *levis* Renz
 Pl. 16, fig. 1 *Thomasites*
- Zaborski (1990a)**
- Figs 8, 12–15 *Vascoceras cauvini* Chudeau
 Figs 9, 10 *Vascoceras* sp.
 Fig. 11 *Vascoceras bulbosum* (Reyment)
 Figs 16–18, 20, 21 *Vascoceras* sp. juv.
 Fig. 25 *Vascoceras nigeriense* Woods
- Courville (1992)**
- Pl. 4, figs 1–3 *Vascoceras* gr. *cauvini* Chudeau
 Pl. 5, fig. 1 *Vascoceras* gr. *thomi* (Reeside) ou *evolutum* (Schneegans)
 Pl. 5, fig. 2 *Vascoceras* gr. *crassum* (Furon) ou *costellatum* Collignon
 Pl. 5, fig. 3; pl. 6, figs 2, 3 *Vascoceras* sp. gr. *costatum* (Barber)
 Pl. 7, figs 1, 2 *Vascoceras tectiforme* (Barber)
 Pl. 7, fig. 3 *Vascoceras tectiforme* (Barber)
 Pl. 8, figs 1, 2 *Vascoceras* gr. *globosum* (Reyment) ou *Fagesia* sp.
 Pl. 9, fig. 1 *Vascoceras* gr. *globosum* (Reyment) ou *Fagesia* sp.
 Pl. 10, fig. 1 *Vascoceras* sp?
 Pl. 10, figs 2, 3 *Vascoceras* sp. aff. *obscurum* Barber
- ?*Vascoceras globosum globosum* (Reyment)
Pseudovascoceras nigeriense (Woods)
Vascoceras globosum costatum (Reyment)
Vascoceras globosum costatum (Reyment)
Vascoceras globosum costatum (Reyment)
?*Paravascoceras cauvini* (Chudeau)
- Paravascoceras cauvini* (Chudeau)
Paravascoceras cauvini (Chudeau)
Vascoceras woodsi sp. nov.
Thomasites
?*Pseudaspidoceras pseudonodosoides* (Choffat)
Vascoceras woodsi sp. nov.
Pseudovascoceras nigeriense (Woods)
Paravascoceras cauvini (Chudeau)
Vascoceras bullatum Schneegans
Vascoceras globosum costatum (Reyment)
Vascoceras bullatum Schneegans
Vascoceras globosum globosum (Reyment)
Pseudovascoceras nigeriense (Woods)
Pseudovascoceras nigeriense (Woods)
Pseudovascoceras nigeriense (Woods)
indeterminate *Vascoceras*
Vascoceras obscurum Barber
Pseudovascoceras nigeriense (Woods)
Pseudovascoceras nigeriense (Woods)
Fikaites varicostatus Zaborski
Vascoceras harttii (Hyatt)
Fikaites varicostatus Zaborski
- Paravascoceras cauvini* (Chudeau)
Vascoceras woodsi sp. nov.
Paravascoceras cauvini (Chudeau)
Vascoceras woodsi sp. nov.
Pseudovascoceras nigeriense (Woods)
- Paravascoceras cauvini* (Chudeau)
Vascoceras woodsi sp. nov.
Vascoceras bullatum Schneegans
Pseudovascoceras nigeriense (Woods)
Vascoceras globosum costatum (Reyment)
Vascoceras globosum globosum (Reyment)
Vascoceras globosum globosum (Reyment)
Vascoceras harttii (Hyatt)
?*Fikaites varicostatus* Zaborski
Vascoceras globosum proprium (Reyment)



Bulletin of The Natural History Museum

Geology Series

Earlier Geology *Bulletins* are still in print. The following can be ordered from Intercept (address on inside front cover). Where the complete backlist is not shown, this may also be obtained from the same address.

Volume 33

- No. 1 An account of the Ordovician rocks of the Shelve Inlier in west Salop and part of north Powys. W.F. Whittard, F.R.S. (Compiled by W.T. Dean). 1979. Pp. 1–69, 38 figs, frontispiece, coloured map, folded, in pocket. £10.00
Map available separately £1.00

No. 2 Miscellanea

- A new, possibly algal, microproblematicum from the Lower Carboniferous of England. G.F. Elliott, 8 Figs.
Acanthopleurella Groom 1902: origin and life-habits of a miniature trilobite. R.A. Fortey & A.W.A. Rushton. 21 figs. Pleistocene bird remains from Torneton Cave and the Brixham Windmill Cave in south Devon. C.J.O. Harrison. 1 fig.

- The succession of *Hyracotherium* (Perissodactyla, Mammalia) in the English early Eocene. J.J. Hooker, 6 figs.
Salenia trisurana sp. nov. (Echinoidea) from the Eocene (London Clay) of Essex, and notes on its phylogeny. D.N. Lewis & R.P.S. Jefferies. 5 figs.

- Tertiary and Cretaceous brachiopods from Seymour, Cockburn and James Ross Islands, Antarctica. E.F. Owen. 33 figs.

- Revision of the rugose coral *Diphyllum concinnum* Lonsdale, 1845, and historical remarks on Murchison's Russian coral collection. B.R. Rosen & R.F. Wise. 3 figs.

- Neuroptera (Insecta) in amber from the Lower Cretaceous of Lebanon. P.E.S. Whalley. 12 figs. 1980. Pp. 71–164. £12.00

- No. 3 The Caradoc faunal associations of the area between Bala and Dinas Mawddwy, north Wales. M.G. Lockley. 1980. Pp. 165–235, 105 figs. £9.00

- No. 4 Fossil insects from the Bembridge Marls, Palaeogene of the Isle of Wight, southern England. E.A. Jarzemowski. 1980. Pp. 237–293, 77 figs. £7.50

- No. 5 The Yorkshire Jurassic fern *Phleopteris braunii* (Goeppert) and its reference to *Matonia* R.Br. T.M. Harris. 1980. Pp. 295–311, 20 figs. £2.75

Volume 34

- No. 1 Relative dating of the fossil hominids of Europe. K.P. Oakley. 1980. Pp. 1–63, 6 figs, 17 tables. £8.00

- No. 2 Origin, evolution and systematics of the dwarf Acanthoceratid *Protacanthoceras* Spath, 1923 (Cretaceous Ammonoidea). C.W. Wright & W.J. Kennedy. 1980. Pp. 65–107, 61 figs. £6.25

- No. 3 Ashgill Brachiopoda from the Glyn Ceiriog District, north Wales. N. Hiller. 1980. Pp. 109–216, 408 figs. £14.75

- No. 4 Miscellanea
Type specimens of some Upper Palaeozoic Athyridide brachiopods. C.H.C. Brunton. 31 figs.

- Two new British Cretaceous Epitonidae (Gastropoda): evidence for evolution of shell morphology. R.J. Cleevley. 14 figs, 1 table.

- Revision of the microproblematicum *Prethiocoprolithus* Elliott, 1962. G.F. Elliott. 4 figs.

- Basiliscus tyrannus* (Murchison) and the glabellar structure of asaphid trilobites. R.A. Fortey. 12 figs.

- A new Lower Ordovician bivalve family, the Thoralidae (? Nuculoidea), interpreted as actinodont deposit feeders. N.J. Morris. 7 figs.

- Cretaceous brachiopods from northern Zululand. E.F. Owen. 13 figs.

- Tupus diluculum* sp. nov. (Protodonata), a giant dragonfly from the Upper Carboniferous of Britain. P.E.S. Whalley. 1 fig.

- Revision of *Plummerita* Brönniman (Foraminifera) and a new Maastrichtian species from Ecuador. J.E. Whittaker. 34 figs. 1980. Pp. 217–297. £11.00

Volume 35

- No. 1 Lower Ordovician Brachiopoda from mid and south-west Wales. M.G. Lockley & A. Williams. 1981. Pp. 1–78, 263 figs, 3 tables. £10.80

- No. 2 The fossil alga *Girvanella* Nicholson & Etheridge. H.M.C. Danielli. 1981. Pp. 79–107, 8 figs, 3 tables. £4.20

- No. 3 Centenary miscellanea
Reassessment of the Ordovician brachiopods from the Budleigh Salterton Pebble Bed, Devon. L.R.M. Cocks & M.G. Lockley. 35 figs.

- Felix Oswald's Turkish Algae. G.F. Elliott. 3 figs.

- J.A. Moy-Thomas and his association with the British Museum (Natural History). P.L. Forey & B.G. Gardiner. 3 figs.

- Burials, bodies and beheadings in Romano-British and Anglo-Saxon cemeteries. M. Harman, T.I. Molleson & J.L. Price. 5 figs, 7 tables, VI appendices.

- The Jurassic irregular echinoid *Nucleolites clunicularis* (Smith). D.N. Lewis & H.G. Owen. 4 figs.

- Phanerotinus cristatus* (Phillips) and the nature of euomphalacean gastropods. N.J. Morris & R.J. Cleevley. 12 figs.

- Agassiz, Darwin, Huxley, and the fossil record of teleost fishes. C. Patterson. 1 fig.

- The Neanderthal problem and the prospects for direct dating of Neanderthal remains. C.B. Stringer & R. Burleigh. 2 figs, 1 table.

- Hippoporidra edax* (Busk 1859) and a revision of some fossil and living *Hippoporidra* (Bryozoa). P.D. Taylor & P.L. Cook. 6 figs. 1981. Pp. 109–252. £20.00

- No. 4 The English Upper Jurassic Plesiosauroida (reptilia) and a review of the phylogeny and classification of the Plesiosauria. D.S. Brown. 1981. Pp. 253–347, 44 figs. £13.00

Volume 36

- No. 1 Middle Cambrian trilobites from the Sosink Formation, Derik-Mardin district, south-eastern Turkey. W.T. Dean. 1982. Pp. 1–41, 68 figs. £5.80

- No. 2 Miscellanea
British Dinantian (Lower Carboniferous) terebratulid brachiopods. C.H.C. Brunton. 20 figs.

- New microfossil records in time and space. G.F. Elliott. 6 figs.

- The Ordovician trilobite *Neseuretus* from Saudi Arabia, and the palaeogeography of the *Neseuretus* fauna related to Gondwanaland in the earlier Ordovician. R.A. Fortey & S.F. Morris. 10 figs.

- Archaeocidaris whatleyensis* sp. nov. (Echinoidea) from the Carboniferous Limestone of Somerset and notes on echinoid phylogeny. D.N. Lewis & P.C. Ensom. 23 figs.

- A possible non-calcified dasycladalean alga from the Carboniferous of England. G.F. Elliott. 1 fig.

- Nanjinoporella*, a new Permian dasyclad (calcareous alga) from Nanjing, China. X. Mu & G.F. Elliott. 6 figs, 1 table.

- Toarcian bryozoans from Belchite in north-east Spain. P.D.

	Taylor & L. Sequeiros. 10 figs, 2 tables. Additional fossil plants from the Drybrook Sandstone, Forest of Dean, Gloucestershire. B.A. Thomas & H.M. Purdy. 14 figs, 1 table.	
	<i>Bintoniella brodiei</i> Handlirsch (Orthoptera) from the Lower Lias of the English Channel, with a review of British bintoniellid fossils. P.E.S. Whalley. 7 figs.	
	<i>Uraloporella</i> Korde from the Lower Carboniferous of South Wales. V.P. Wright. 3 figs. 1982. Pp. 43–155. £19.80	
No. 3	The Ordovician Graptolites of Spitsbergen. R.A. Cooper & R.A. Fortey. 1982. Pp. 157–302, 6 plates, 83 figs, 2 tables. £20.50	
No. 4	Campanian and Maastrichtian sphenodiscid ammonites from southern Nigeria. P.M.P. Zaborski. 1982. Pp. 303–332, 36 figs. £4.00	
Volume 37		
No. 1	Taxonomy of the arthrodire <i>Phlyctaenius</i> from the Lower or Middle Devonian of Campbellton, New Brunswick, Canada. V.T. Young. 1983. Pp. 1–35, 18 figs. £5.00	
No. 2	<i>Ailsacrinus</i> gen. nov., an aberrant millericrinid from the Middle Jurassic of Britain. P.D. Taylor. 1983. Pp. 37–77, 48 figs, 1 table. £5.90	
No. 3	Miscellanea <i>Glossopteris anatolica</i> Sp. nov. from uppermost Permian strata in south-east Turkey. S. Archangelsky & R.H. Wagner. 14 figs. The crocodilian <i>Theriosuchus</i> Owen, 1879 in the Wealden of England. E. Buffetaut. 1 fig. A new conifer species from the Wealden beds of Féron-Glagon, France. H.L. Fisher & J. Watson. 10 figs. Late Permian plants including Charophytes from the Khuff formation of Saudi Arabia. C.R. Hill & A.A. El-Khayal. 18 figs. British Carboniferous Edrioasteroidea (Echinodermata). A.B. Smith. 52 figs. A survey of recent and fossil Cicadas (Insecta, Hemiptera-Homoptera) in Britain. P.E.S. Whalley. 11 figs. The Cephalaspids from the Dittonian section at Cwm Mill, near Abergavenny, Gwent. E.I. White & H.A. Toombs. 20 figs. 1983. Pp. 79–171. £13.50	
No. 4	The relationships of the palaeoniscid fishes, a review based on new specimens of <i>Mimia</i> and <i>Moythomasia</i> from the Upper Devonian of Western Australia. B.G. Gardiner. 1984. Pp. 173–428. 145 figs. 4 plates. 0 565 00967 2. £39.00	
Volume 38		
No. 1	New Tertiary pycnodonts from the Tilemsi valley, Republic of Mali. A.E. Longbottom. 1984. Pp. 1–26. 29 figs. 3 tables. 0 565 07000 2. £3.90	
No. 2	Silicified brachiopods from the Viséan of County Fermanagh, Ireland. (III) Rhynchonellids. Spiriferids and Terebratulids. C.H.C. Brunton. 1984. Pp. 27–130. 213 figs. 0 565 07001 0. £16.20	
No. 3	The Llandovery Series of the Type Area. L.R.M. Cocks. N.H. Woodcock, R.B. Rickards, J.T. Temple & P.D. Lane. 1984. Pp. 131–182. 70 figs. 0 565 07004 5. £7.80	
No. 4	Lower Ordovician Brachiopoda from the Tourmakeady Limestone, Co. Mayo, Ireland. A. Williams & G.B. Curry. 1985. Pp. 183–269. 214 figs. 0 565 07003 7. £14.50	
No. 5	Miscellanea Growth and shell shape in Productacean Brachiopods. C.H.C. Brunton. <i>Palaeosiphonium</i> a problematic Jurassic alga. G.F. Elliott. Upper Ordovician brachiopods and trilobites from the Clashford House Formation, near Herbertstown, Co. Meath, Ireland. D.A.T. Harper, W.I. Mitchell, A.W. Owen & M. Romano. Preliminary description of Lower Devonian Osteostraci	
	from Podolia (Ukrainian S.S.R.). P. Janvier. <i>Hipparium</i> sp. (Equidae, Perissodactyla) from Diavata (Thessaloniki, northern Greece). G.D. Koufos. Preparation and further study of the Singa skull from Sudan. C.B. Stringer, L. Cornish & P. Stuart-Macadam. Carboniferous and Permian species of the cyclostome bryozoan <i>Corynotrypa</i> Bassler, 1911. P.D. Taylor. Redescription of <i>Eurycephalochelys</i> , a trionychid turtle from the Lower Eocene of England. C.A. Walker & R.T.J. Moody. Fossil insects from the Lithographic Limestone of Montsech (late Jurassic-early Cretaceous), Lérida Province, Spain. P.E.S. Whalley & E.A. Jarzemowski. 1985. Pp. 271–412, 162 figs. 0 565 07004 5. £24.00	
Volume 39		
No. 1	Upper Cretaceous ammonites from the Calabar region, south-east Nigeria. P.M.P. Zaborski. 1985. Pp. 1–72. 66 figs. 0 565 07006 1. £11.00	
No. 2	Cenomanian and Turonian ammonites from the Novo Redondo area, Angola. M.K. Howarth. 1985. Pp. 73–105. 33 figs. 0 565 07006 1. £5.60	
No. 3	The systematics and palaeogeography of the Lower Jurassic insects of Dorset, England. P.E.S. Whalley. 1985. Pp. 107–189. 87 figs. 2 tables. 0 565 07008 8. £14.00	
No. 4	Mammals from the Bartonian (middle/late Eocene) of the Hampshire Basin, southern England. J.J. Hooker. 1986. Pp. 191–478. 71 figs. 39 tables. 0 565 07009 6. £49.50	
Volume 40		
No. 1	The Ordovician graptolites of the Shelve District, Shropshire. I. Strachan. 1986. Pp. 1–58. 38 figs. 0 565 07010 X. £9.00	
No. 2	The Cretaceous echinoid <i>Bolechinus</i> , with notes on the phylogeny of the Glyptophyidae and Temnopleuridae. D.N. Lewis. 1986. Pp. 59–90. 11 figs. 7 tables. 0 565 07011 8. £5.60	
No. 3	The trilobite fauna of the Raheen Formation (upper Caradoc), Co. Waterford, Ireland. A.W. Owen, R.P. Tripp & S.F. Morris. 1986. Pp. 91–122. 88 figs. 0 565 07012 6. £5.60	
No. 4	Miscellanea I: Lower Turonian cirripede—Indian coleoid <i>Naezia</i> —Cretaceous—Recent Craniidae—Lectotypes of Girvan trilobites—Brachiopods from Provence—Lower Cretaceous cheiostomes. 1986. Pp. 125–222. 0 565 07013 4. £19.00	
No. 5	Miscellanea II: New material of <i>Kimmerosaurus</i> —Edgehills Sandstone plants—Lithogeochemistry of Mendip rocks— Specimens previously recorded as teuthids—Carboniferous lycopsis <i>Anabathra</i> — <i>Meyenodendron</i> , new Alaskan lepidodendrid. 1986. Pp. 225–297. 0 565 07014 2. £13.00	
Volume 41		
No. 1	The Downtonian ostracoderm <i>Sclerodus</i> Agassiz (Osteostraci: Tremataspidae). P.L. Forey. 1987. Pp. 1–30. 11 figs. 0 565 07015 0. £5.50	
No. 2	Lower Turonian (Cretaceous) ammonites from south-east Nigeria. P.M.P. Zaborski. 1987. Pp. 31–66. 46 figs. 0 565 07016 9. £6.50	
No. 3	The Arenig Series in South Wales: Stratigraphy and Palaeontology. I. The Arenig Series in South Wales. R.A. Fortey & R.M. Owens. II. Appendix. Acritarchs and Chitinozoa from the Arenig Series of South-west Wales. S.G. Molyneux. 1987. Pp. 67–364. 289 figs. 0 565 07017 7. £59.00	
No. 4	Miocene geology and palaeontology of Ad Dabtiyah, Saudi Arabia. Compiled by P.J. Whybrow. 1987. Pp. 365–457. 54 figs. 0 565 07019 3. £18.00	

Volume 42

- No. 1 Cenomanian and Lower Turonian Echinoderms from Wilmington, south-east Devon. A.B. SMith, C.R.C. Paul, A.S. Gale & S.K. Donovan. 1988. 244 pp. 80 figs. 50 pls. 0 565 07018 5. £46.50

Volume 43

- No. 1 A Global Analysis of the Ordovician-Silurian boundary. Edited by L.R.M. Cocks & R.B. Rickards. 1988. 394 pp., figs. 0 565 07020 7. £70.00

Volume 44

- No. 1 Miscellanea: Palaeocene wood from Mali—Chapelcorner fish bed—*Heterotheca* coprolites—Mesozoic Neuroptera and Raphidioptera. 1988. Pp. 1-63. 0 565 07021 5. £12.00
- No. 2 Cenomanian brachiopods from the Lower Chalk of Britain and northern Europe. E.F. Owen. 1988. Pp. 65-175. 0 565 07022 3. £21.00
- No. 3 The ammonite zonal sequence and ammonite taxonomy in the *Douvilleiceras mammillatum* Superzone (Lower Albian) in Europe. H.G. Owen. 1988. Pp. 177-231. 0 565 07023 1. £10.30
- No. 4 Cassiopidae (Cretaceous Mesogastropoda): taxonomy and ecology. R.J. Cleevely & N.J. Morris. 1988. Pp. 233-291. 0 565 07024 X. £11.00

Volume 45

- No. 1 Arenig trilobites—Devonian brachiopods—Triassic demosponges—Larval shells of Jurassic bivalves—Carboniferous marattialean fern—Classification of Plectambonitacea. 1989. Pp. 1-163. 0 565 07025 8. £40.00
- No. 2 A review of the Tertiary non-marine molluscan faunas of the Pebasian and other inland basins of north-western South America. C.P. Nuttall. 1990. Pp. 165-371. 456 figs. 0 565 07026 6. £52.00

Volume 46

- No. 1 Mid-Cretaceous Ammonites of Nigeria—new amphisbaenians from Kenya—English Wealden Equisetales—Faringdon Sponge Gravel Bryozoa. 1990. Pp. 1-152. 0 565 070274. £45.00
- No. 2 Carboniferous pteridosperm frond *Neuropteris heterophylla*—Tertiary Ostracoda from Tanzania. 1991. Pp. 153-270. 0 565 07028 2. £30.00

Volume 47

- No. 1 Neogene crabs from Brunei, Sabah & Sarawak—New pseudosciurids from the English Late Eocene—Upper Palaeozoic Anomalodesmataen Bivalvia. 1991. Pp. 1-100. 0 565 07029 0. £37.50
- No. 2 Mesozoic Chrysalidinidae of the Middle East—Bryozoans from north Wales—*Alveolinella praequoyi* sp. nov. from Papua New Guinea. 1991. Pp. 101-175. 0 565 070304. £37.50

Volume 48

- No. 1 '*Placopsilina*' *cenomana* d'Orbigny from France and England - Revision of Middle Devonian uncinulid brachiopod—Cheilostome bryozoans from Upper Cretaceous, Alberta. 1992. Pp. 1-24. £37.50

- No. 2 Lower Devonian fishes from Saudi Arabia W.K. Parker's collection of foraminifera in the British Museum (Natural History). 1992. Pp. 25-43. £37.50

Volume 49

- No. 1 Barremian—Aptian Praehedbergellidae of the North Sea area: a reconnaissance—Late Llandovery and early Wenlock Stratigraphy and ecology in the Oslo Region, Norway—Catalogue of the type and figured specimens of fossil Asteroidea and Ophiuroidea in The Natural History Museum. 1993. Pp. 1-80. £37.50

- No. 2 Mobility and fixation of a variety of elements, in particular, during the metasomatic development of adinoles at Dinas Head, Cornwall—Productellid and Plicatiferid (Productoid) Brachiopods from the Lower Carboniferous of the Craven Reef Belt, North Yorkshire—The spores of *Leclercqia* and the dispersed spore morphon *Acinosporites lindlarensis* Riegel: a case of gradualistic evolution. 1993. Pp. 81-155. £37.50

Volume 50

- No. 1 Systematics of the meliceritid cyclostome bryozoans; introduction and the genera *Elea*, *Semielea* and *Reptomultelea*. 1994. Pp. 1-104.
- No. 2 The brachiopods of the Duncannon Group (Middle-Upper Ordovician) of southeast Ireland. 1994. Pp. 105-175.

Volume 51

- No. 1 A synopsis of neuropteroid foliage from the Carboniferous and Lower Permian of Europe—The Upper Cretaceous ammonite *Pseudaspidoceras* Hyatt, 1903, in north-eastern Nigeria—The pterodactyloids from the Purbeck Limestone Formation of Dorset. 1995. Pp. 1-88. £37.50

- No. 2 Palaeontology on the Qahlah and Simsima Formations (Cretaceous, Late Campanian-Maastrichtian) of the United Arab Emirates-Oman Border Region—Preface—Late Cretaceous carbonate platform faunas of the United Arab Emirates-Oman border region—Late Campanian-Maastrichtian echinoids from the United Arab Emirates-Oman border region—Maastrichtian ammonites from the United Arab Emirates-Oman border region—Maastrichtian nautiloids from the United Arab Emirates-Oman border region—Maastrichtian Inoceramidae from the United Arab Emirates-Oman border region—Late Campanian-Maastrichtian Bryozoa from the United Arab Emirates-Oman border region—Maastrichtian brachiopods from the United Arab Emirates-Oman border region—Late Campanian-Maastrichtian rudists from the United Arab Emirates-Oman border region. 1995. Pp. 89-305. £37.50

CONTENTS

- 1 **Zirconlite: a review of localities worldwide, and a compilation of its chemical compositions**
C.T. Williams and R. Gieré
- 25 **A review of the stratigraphy of Eastern Paratethys (Oligocene–Holocene)**
R.W. Jones and M.D. Simmons
- 51 **A new protorichthofenoid brachiopod (Productida) from the Upper Carboniferous of the Urals, Russia**
C.H.C. Brunton
- 61 **The Upper Cretaceous ammonite *Vascoceras* Choffat, 1898 in north-eastern Nigeria**
P.M.P. Zaborski

Bulletin of The Natural History Museum

GEOLOGY SERIES

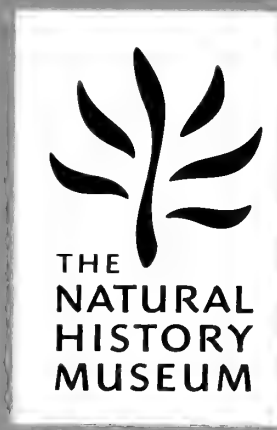
Vol. 52, No. 1, June 1996

S.186 A

0504 0005-0452

Bulletin of The Natural History Museum

Geology Series



VOLUME 52 NUMBER 2 28 NOVEMBER 1996

The *Bulletin of The Natural History Museum* (formerly: *Bulletin of the British Museum (Natural History)*), instituted in 1949, is issued in four scientific series, Botany, Entomology, Geology (incorporating Mineralogy) and Zoology.

The Geology Series is edited in the Museum's Department of Palaeontology

Keeper of Palaeontology: Dr L.R.M. Cocks

Editor of Bulletin: Dr M.K. Howarth

Assistant Editor: Mr C. Jones

Papers in the *Bulletin* are primarily the results of research carried out on the unique and ever-growing collections of the Museum, both by the scientific staff and by specialists from elsewhere who make use of the Museum's resources. Many of the papers are works of reference that will remain indispensable for years to come. All papers submitted for publication are subjected to external peer review for acceptance.

A volume contains about 160 pages, made up by two numbers, published in the Spring and Autumn. Subscriptions may be placed for one or more of the series on an annual basis. Individual numbers and back numbers can be purchased and a *Bulletin* catalogue, by series, is available. Orders and enquiries should be sent to:

Intercept Ltd.
P.O. Box 716
Andover
Hampshire SP10 1YG
Telephone: (01264) 334748
Fax: (01264) 334058

Claims for non-receipt of issues of the *Bulletin* will be met free of charge if received by the Publisher within 6 months for the UK, and 9 months for the rest of the world.

World List abbreviation: *Bull. nat. Hist. Mus. Lond. (Geol.)*

© The Natural History Museum, 1996

ISSN 0968-0462

Geology Series
Vol. 52, No. 2, pp. 91-173

The Natural History Museum
Cromwell Road
London SW7 5BD

Issued 28 November 1996

Typeset by Ann Buchan (Typesetters), Middlesex
Printed in Great Britain by Henry Ling Ltd., at the Dorset Press, Dorchester, Dorset

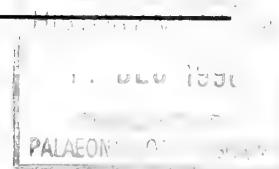
Jurassic bryozoans from Baltów, Holy Cross Mountains, Poland

URSZULA HARA

Panственный Instytut Geologiczny, Rakowiecka 4, 00-975 Warszawa, Poland

PAUL D. TAYLOR

Department of Palaeontology, The Natural History Museum, Cromwell Road, London SW7 5BD



SYNOPSIS. Very few Jurassic bryozoans have been recorded from central or eastern Europe. This paper uses scanning electron microscopy to describe a well-preserved Polish Oxfordian bryozoan fauna consisting of five cyclostome species: *Oncousoecia* sp., *Reptomultisparsa norberti* sp. nov., *Hyporopora baltoensis* sp. nov., *Mecynoecia suprabajocina* sp. nov. and *Apsendesia cristata* Lamouroux, 1821. Most abundant are specimens of *H. baltoensis* with tubular colonies which grew around perished cylindrical substrates. These arboreal colonies may have been epiphytes of algae or alternatively epizoans of sessile animals such as chaetopterid polychaetes, whose organic tubes can be similarly encrusted by bryozoans at the present-day. *H. baltoensis* is compared with other Jurassic species that have colonies with transversely ridged surfaces.

INTRODUCTION

The overwhelming majority of Jurassic bryozoans described in the literature are from western Europe, particularly England, France and Germany (see Walter, 1970). Knowledge of Jurassic bryozoans from elsewhere in the world is extremely limited, therefore, and any faunas from outside western Europe are worthy of attention. This is specially true if, as in the Polish fauna described here, the bryozoans are well-preserved and include new species.

The only previous paper concerning Jurassic bryozoans from Poland is that of Reuss (1867) which described 18 species (not including *Neuropora raristellata* Reuss; *Neuropora* is now regarded as belonging to the 'sclerosponges', see Kazmierczak & Hillmer, 1974) from the Upper Bathonian or Lower Callovian of Balin, near Cracow. Although Reuss's work is in need of revision, the Balin fauna is clearly different from that described here from the Oxfordian of Baltów. A few other species of Upper Jurassic bryozoans have been mentioned from the vicinity of Cmielów and Sobków on the north-western margins of the Holy Cross Mts (Malinowska, 1965; Gugaczewska, 1970).

Our purpose in this short paper is to describe the bryozoan fauna from Baltów, utilizing scanning electron microscopy (SEM), and to compare the species present with established species, especially from the better known, diverse faunas of the western Europe Middle Jurassic.

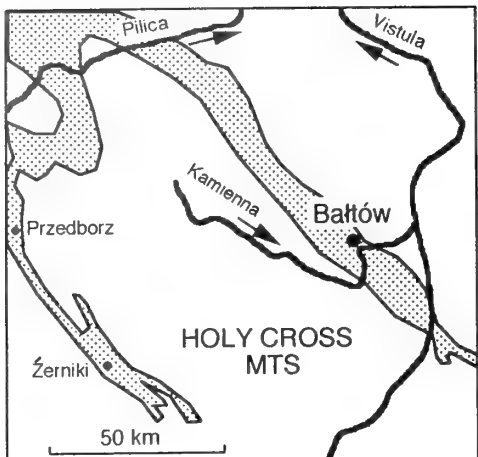
Material and methods. All studied specimens from Poland, which were collected during 1986–88, are deposited in the palaeontological collections of the Geological Museum of the Polish Geological Institute (Panstwowy Instytut Geologiczny) in Warszawa (Muz IG numbers). Comparative material from western Europe is in the collections of The Natural History Museum (BMNH register numbers). Specimens were studied and micrographs prepared using ISI 0A and ABT-55 scanning electron microscopes equipped with environmental chambers for back-scattered electron imaging of coated material (see Taylor, 1986).

LOCALITY AND GEOLOGICAL SETTING

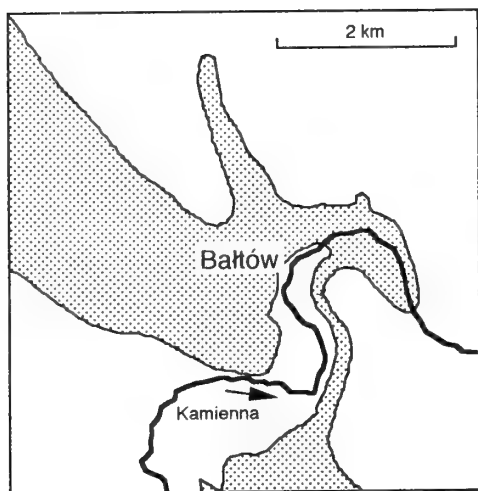
The Upper Jurassic of Baltów yields one of the most abundant and well-preserved cyclostome bryozoan faunas known from Poland. Baltów is situated approximately 15 km north-west of Ostrowiec Świętokrzyski on the north-eastern margin of the Holy Cross Mts (Fig. 1). The bryozoans come from coral-bearing deposits best exposed in the ravined part of the Kamienna River valley at Baltów.

A rich shallow water biota occurs at Baltów (Karczewski, 1960; Liszkowski, 1962, 1976; Roniewicz, 1966, 1968, 1976; Malinowska, 1967; Barczyk 1968, 1969, 1970; Roniewicz & Roniewicz, 1971; Hurcewicz, 1973; Brochwick-Lewinski & Różak, 1976; Maryńska & Kobylinska, 1980, 1984; Gutowski, 1992), including Foraminifera, bivalves, corals, brachiopods, sponges, ammonites, bryozoans, echinoids, crinoids, crabs, serpulid worms, shark teeth and algae (Rhodophycophyta of the genera *Solenopora*, *Parachaetetes* and *Polygonella*). A complex of coral-rich and other limestones is underlain by micritic, platy limestones containing: the bivalves *Gryphaea*, *Isognomon*, *Nanogyra*, *Trigonia* and *Pholadomya*; terebratulid and rhynchonellid brachiopods; ammonites; decapod claws; crinoids; and plant debris. The maximum total thickness reaches 100 metres (see Gutowski, 1992). The coralliferous limestone complex, approximately 15 metres thick, consists of unbedded or indistinctly bedded limestones overlain by bedded limestones (Roniewicz & Roniewicz, 1971). The former vary in thickness from 4 to 10 metres and comprise coral and pelitic limestones. According to Roniewicz & Roniewicz (1971), spaces between the foliaceous and submassive coral colonies are filled by pelitic or chalky limestones with a variable content of organic detritus. The bryozoans described here were collected from these weathered chalky limestones.

Ammonites have not been found in the bryozoan-bearing beds. However, thick-bedded micritic limestones underlying the coralliferous limestone complex contain ammonites of the *Gregoryeras transversarium* Zone, and oncotic limestones overlying the complex contain ammonites of the *Perisphinctes bifurcatus*



A



B

Fig. 1 Location of Baltów. **A**, map of the Holy Cross Mountains with the Upper Jurassic outcrop stippled (based on Roniewicz & Roniewicz, 1971). **B**, map of the Baltów area with the outcrop of the coralliferous limestone complex containing the bryozoan fauna stippled (based on Liszkowski, 1976).

Zone (J. Gutowski pers. comm. to U.H., 1991). Therefore, the bryozoans belong to either the Transversarium or Bifurcatus Zone of the Middle Upper Oxfordian in the Submediterranean ammonite zonal scheme (Cariou *et al.*, 1971; Gutowski, 1992).

SYSTEMATIC DESCRIPTIONS

Order CYCLOSTOMATA Busk, 1852
 Suborder TUBULIPORINA Milne-Edwards, 1838
 Family ONCOUSOECIIDAE Canu, 1918
 Genus *ONCOUSOECIA* Canu, 1918

TYPE SPECIES. *Tubulipora lobulata* Hincks, 1880 (= *Alecto dilatans* Johnston, 1847; see Hayward & Ryland, 1985), Recent.

REMARKS. Species assigned to *Oncousoecia* have encrusting colonies composed of narrow ramifying branches in which the zooids are arranged multiserially. Gonozooids are small to moderately large, and ovoidal or pyriform in shape. They are not pierced by autozooidal apertures.

Oncousoecia sp.

Figs 2–3

MATERIAL. MUZ PIG 1601/II/8.

DESCRIPTION. Single colony comprising two coalescing branches detached from their original substrate.

Autozooids have frontal walls about 0.90–1.00 mm long by 0.25–0.35 mm wide, slightly convex distally but more immersed proximally. Apertures circular, about 0.11–0.15 mm in diameter, with short preserved peristomes tapering markedly distally. Pseudopores large, closely-spaced, often distally pointed. Faint transverse wrinkles on autozooid frontal walls continuous across colony surface.

Two gonozooids present, both asymmetrical as a result of distortion following branch coalescence (Fig. 2). Proximal frontal wall long and indistinguishable from that of an autozooid, raised strongly at its well-marked boundary with the dilated distal part of the frontal wall. Distal frontal wall roughly pyriform in outline, 1.10 mm long by 1.00 mm wide, slightly inflated in height, relatively smooth-surfaced and possessing a higher density of pseudopores than the autozooids. Ooeciopore subterminal (i.e. within the area of the dilated frontal wall), transversely elliptical, 0.07 mm long by 0.15 mm wide, about the same size as an autozooidal aperture. Ooeciostome short, slightly reflexed, bearing very few pseudopores (Fig. 3).

REMARKS. Walter (1970), in his major revision of Jurassic cyclostomes, described five species of *Oncousoecia*. The species from Baltów most closely resembles *O. elegantula* (d'Orbigny, 1850) from the Upper Bajocian of Port-en-Bessin, Normandy, France. However, *O. elegantula* has slightly narrower autozooids, a difference which might be significant given that frontal wall width is one of the more useful morphometric characters for distinguishing between species of Jurassic cyclostomes. In view of the sparse material available from Baltów and the need for SEM study of the type specimens of *O. elegantula* and other Jurassic species of *Oncousoecia*, specific determination of the Baltów specimen is deferred.

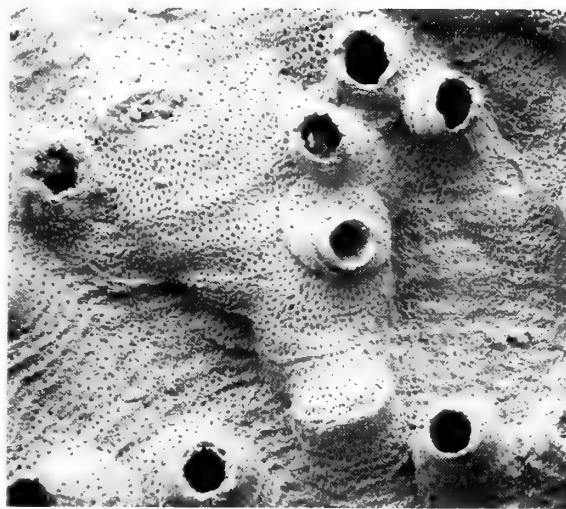
Family MULTISPARSIDAE Bassler, 1935

(= MACROECHIDAE Canu, 1918)

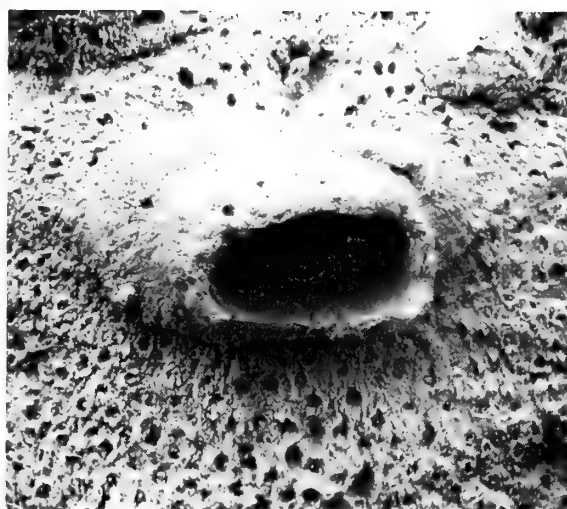
Genus *REPTOMULTISPARSA* d'Orbigny, 1853

TYPE SPECIES. *Diastopora incrassans* d'Orbigny, 1850, Bathonian.

REMARKS. Nomenclatural problems concerning the type species of *Reptomultisparsa*, misidentified when selected by Gregory (1896b), were discussed by Taylor (1984) and resolved by ICZN Opinion 1392 (1986) which designated *Diastopora incrassans* d'Orbigny as the valid type species. An earlier concept of *Reptomultisparsa* encompassing almost all multilamellar tubuliporine species has now been superseded by a concept based on the morphology of the gonozooids, which are longitudinally elongate and have large subterminal ooeciopores (see Taylor and Sequeiros 1982). Some, but not all species of *Reptomultisparsa* are multilamellar.



2



3

Figs 2–3 *Oncousoecia* sp., MUZ PIG 1601/II/8, Oxfordian, Baltów, Poland. Scanning electron micrographs of uncoated specimen. 2, distorted gonozooid and autozooids at coalescence of colony branches, $\times 45$. 3, oooecipore, $\times 167$.

Reptomultisparsa norberti sp. nov.

HOLOTYPE. MUZ PIG 1601/II/1 (Figs 6–7).

DARATYPES. MUZ PIG 1601/II/2 (3 specimens).

NAME. In recognition of the contributions to bryozoology of the Austrian palaeontologist Dr Norbert Vavra.

DESCRIPTION. Colony multiserial, sheet-like, unilamellar, either planar (Fig. 4) or tubular (Fig. 5) in shape. Viewed from the growing edge the colony is thin, generally only one zoid in depth. Early growth stages unknown. Original substrates not preserved.

Autozooids immersed, zooidal boundaries indistinct, frontal walls flat for most of their length though slightly convex distally, about 1.10–1.50 mm long by 0.25–0.35 mm wide. Apertures widely-spaced, circular or a little wider than long, about 0.12 mm in diameter, occasionally closed by terminal diaphragms located at about the level of the frontal wall. Preserved peristomes moderately short, tapering distally. Pseudopores longitudinally elongate, slit-like when unworn (Fig. 8) but elliptical when worn.

Gonozooids apparently infrequent, only a single example having been found (Fig. 6). Distal frontal wall almost flat, longitudinally elongate, 1.50 mm long by 0.65 mm wide. Oooecipore (Fig. 7) ubterminal, larger than an autozooidal aperture, transversely elongate, 0.10 mm long by 0.25 mm wide.

REMARKS. Walter (1970) assigned seven Jurassic species to *Reptomultisparsa*, and Taylor (1980) added one further new species. The autozooids in *R. cobergensis* Walter, 1970, *R. ?margopuncta* Waagen, 1867, *R. cricopora* (Vine, 1881), *R. oolitica* (Vine, 1881) and *R. tumida* Taylor, 1980, have distinctly convex frontal walls, unlike the rather flat frontal walls of *R. norberti*. *Reptomultisparsa incrustans* (d'Orbigny, 1850) differs from *R. norberti* in its much larger gonozooid, as well as its multilamellar colonies invariably encrusting gastropod shells once occupied by hermit crabs (Buge & Fischer, 1970; Taylor, 1994). *Reptomultisparsa ventricosa* (Vine, 1881), a species characteristic of the Aalenian and Bajocian of

Figs 4–8

England, is more similar to *R. norberti* except for its inflated gonozooids with smaller oooecipores, and subcircular pseudopores.

The unilamellar, often tubular colonies of *R. norberti* prompt comparison with *Diastopora*, notably the type species *D. foliacea* Lamouroux, 1821, from the Bathonian of Normandy. There are, however, striking differences in the form of the gonozooid, and in the morphology of the pseudopores as revealed by SEM. In *D. foliacea*, the gonozooid is transversely elongate and has lateral lobes which extend distally of the oooecipore (Walter, 1970, pl. 8, fig. 1), whereas in *R. norberti* it is longitudinally elongate (Fig. 6). Pseudopores in frontal walls of *D. foliacea* zoids are gull-shaped (PDT unpublished), whereas those in *R. norberti* are long and slit-like (Fig. 8). These differences underscore the dual importance in cyclostome identification of specimens with gonozooids and of detailed SEM studies of pseudopore morphology. Without access to these two characters it is often difficult to make confident species determinations.

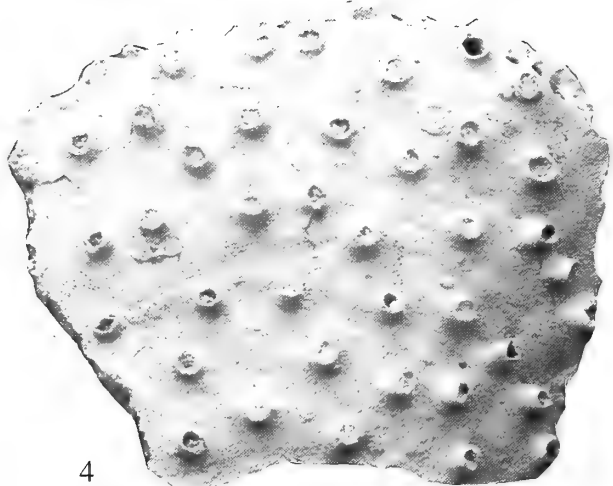
Family PLAGIOECHIIDAE Canu, 1918

(= DIASTOPORIDAE Gregory, 1899)

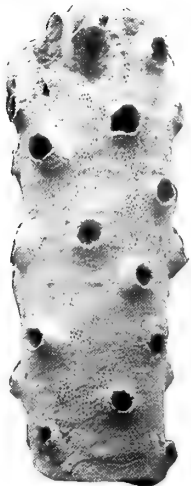
Genus *HYPOROSOPORA* Canu & Bassler, 1929

TYPE SPECIES. *Hyporosopora typica* Canu & Bassler, 1929, Bathonian.

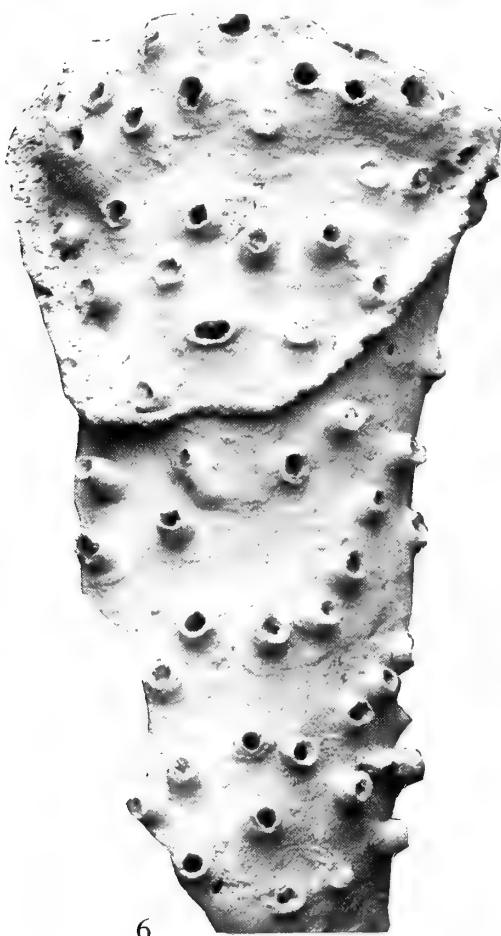
REMARKS. Although *Hyporosopora* was considered to be a junior synonym of *Plagioecia* Canu, 1918, by Walter (1970), differences exist between the two genera in the morphology of their gonozooids. Colonies of the extant type species of *Plagioecia*, *Berenicea patina* Lamouroux, 1816, have gonozooids with exceedingly broad, arcuate frontal walls which are profusely pierced by autozooidal apertures (see Hayward & Ryland, 1985). *Hyporosopora* gonozooids are considerably smaller, typically subtriangular in outline, and are not pierced by autozooidal apertures (see Taylor & Sequieros, 1982).



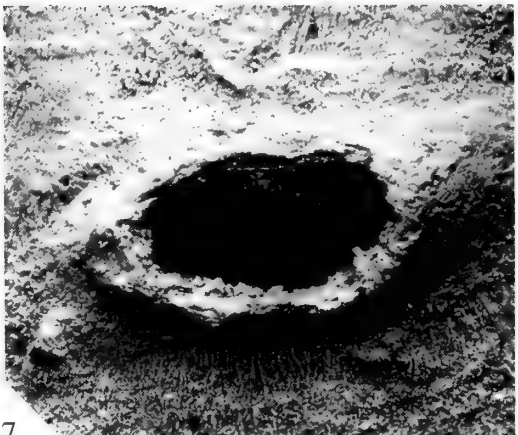
4



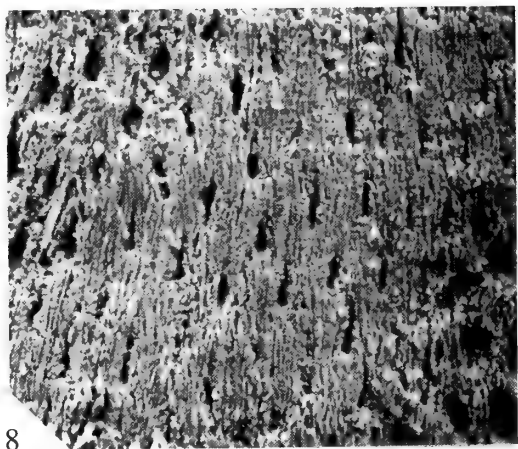
5



6

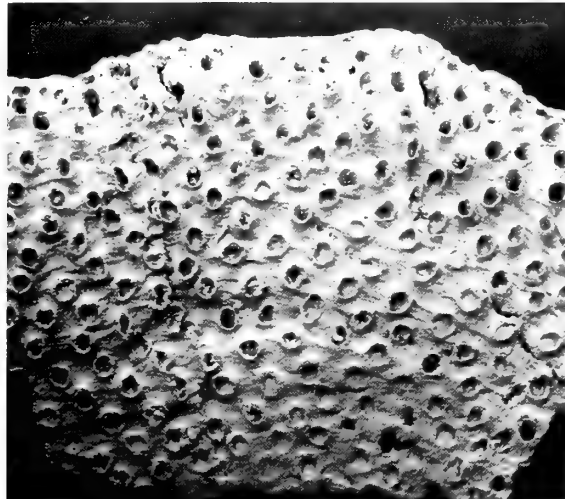


7



8

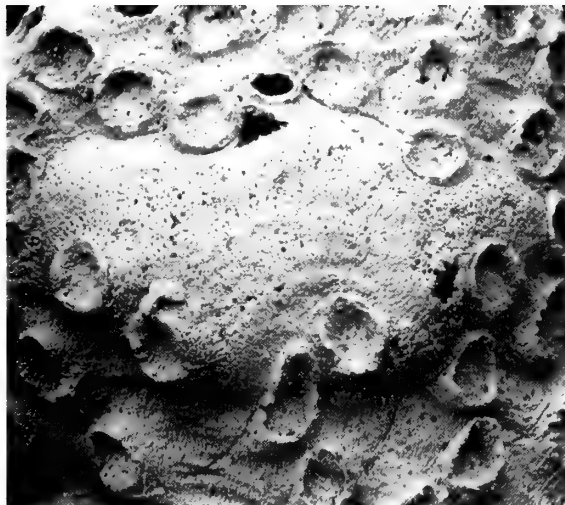
Figs 4–8 *Reptomultisparsa norberti* sp. nov., Oxfordian, Baltów, Poland. Scanning electron micrographs of uncoated specimens. 4, MUZ PIG 1601/II/2 (2), paratype, lamellar colony, $\times 14$. 5, MUZ PIG 1601/II/2 (1), paratype, tubular colony, $\times 21$. 6–7, MUZ PIG 1601/II/1, holotype; 6, autozooids and gonozooids of the fertile colony (ooecipore just above calcite vein), $\times 15$; 7, detail of ooecipore, $\times 138$. 8, MUZ PIG 1601/II/2 (1), paratype, slit-like pseudopores on autozooidal frontal wall, $\times 360$.



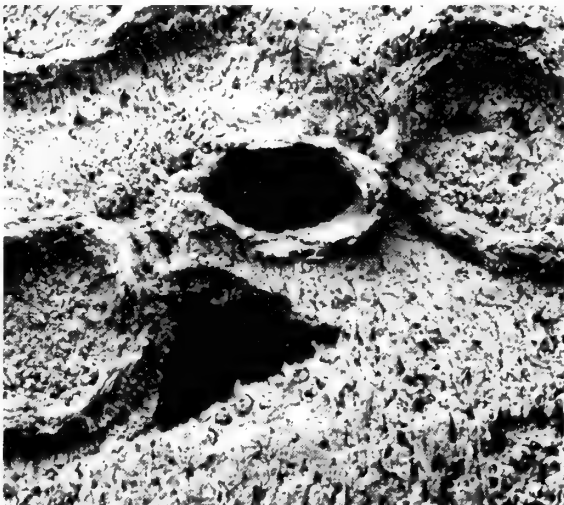
9



10



11



12

Figs 9–12 *Hyporosopora baltvensis* sp. nov., Oxfordian, Baltów, Poland. Scanning electron micrographs of uncoated specimens. **9–10**, MUZ PIG 1601/II/13; **9**, lamellar colony, $\times 18$; **10**, transverse ridges and autozooids, some with terminal diaphragms, $\times 64$. **11–12**, MUZ PIG 1601/II/3, holotype; **11**, gonozooid, $\times 65$; **12**, oocciopore (triangular hole beneath is a breakage in the gonozooid frontal wall), $\times 225$.

Hyporosopora baltvensis sp. nov.

HOLOTYPE. MUZ PIG 1601/II/3 (Figs 11–12).

PARATYPES. MUZ PIG 1601/II/4 and 5, 13–18.

NAME. After Baltów, the type locality.

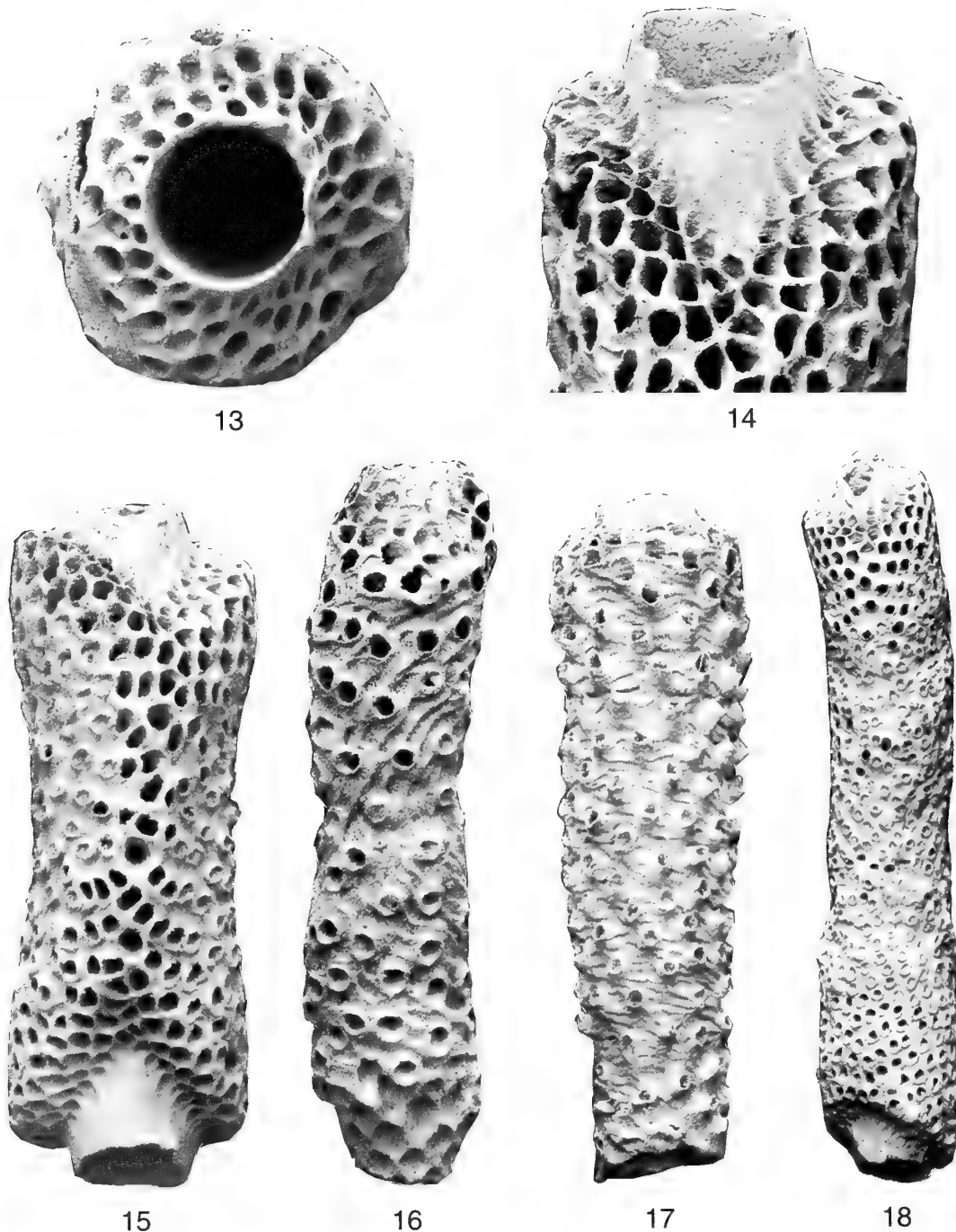
DESCRIPTION. Colony multiserial, sheet-like, bereniciform, commonly unilamellar but occasionally multilamellar, either planar (Fig. 9) or tubular (Figs 13–18) in shape. Tubular colonies possess a distinct suture formed by coalescence of lobes of the growing edge on opposite sides of the colony (Fig. 15). Distal fringe of basal lamina protrudes beyond budding zone at growing edge (Fig. 14) where two or three generations of zooidal buds, some with mural pustules, are visible. Colony surface ornamented by discontinuous transverse ridges, irregularly-spaced 0.02–0.08 mm apart, of low profile and sometimes indistinct, deflected proximally where they

Figs 9–18

meet apertures (Fig. 10); ridges absent over dilated frontal walls of gonozooids (Fig. 11). Original substrates of encrustation not preserved.

Autozooids (Fig. 10) small, immersed, their frontal walls without well-defined boundaries, short, 0.25–0.50 mm in length by 0.11–0.17 mm in width. Apertures small, usually longitudinally elongate but sometimes transversely elongate or circular (especially near the edge of colonies), 0.08–0.17 mm long by 0.06–0.14 mm wide, arranged roughly in quincunx, closely-spaced and often crowded close to the colony perimeter where they are larger in diameter. Terminal diaphragms sporadic in distribution, positioned level with or a little beneath the frontal wall (Fig. 10), and also observed occluding immature buds at the growing edge (Fig. 13). Preserved peristomes moderately long, tapering distally. Pseudopores approximately circular in shape, widely spaced, absent on transverse ridges.

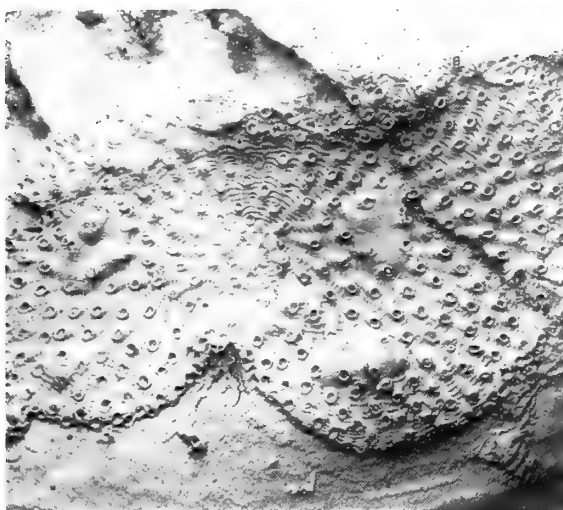
Gonozooids (Fig. 11) subcircular to subtriangular in outline, wider than long, averaging 0.60 mm in length by 0.90 mm in width,



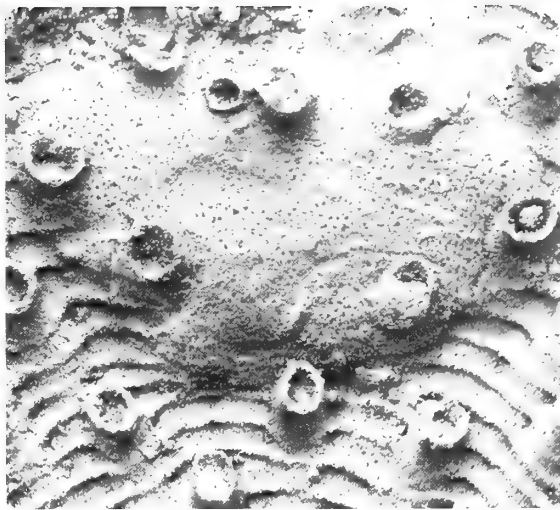
Figs 13–18 *Hyporosopora baltoviensis* sp. nov., Oxfordian, Baltów, Poland. Scanning electron micrographs of uncoated, tubular specimens. **13**, MUZ PIG 1601/II/14, end view showing hollow cavity originally occupied by a cylindrical substrate, $\times 50$. **14–15**, MUZ PIG 1601/II/15; **14**, wide distal fringe of basal lamina, $\times 38$; **15**, side view showing suture formed by anastomosis of opposite colony edges, $\times 23$. **16**, MUZ PIG 1601/II/16, $\times 28$. **17**, MUZ PIG 1601/II/17, $\times 20$. **18**, MUZ PIG 1601/II/18, $\times 12$.

inflated in height, lacking transverse ridges, indented by marginal autozooidal apertures. Floor of gonozooid pustulose, corrugated distally by the convexities of the underlying autozooids. Ooeciopore (Fig. 12) terminal, situated just beyond the inflated part of the gonozooid, small, transversely elongate, averaging 0.06 mm long by 0.09 mm wide, subcircular when the ooecistome is preserved.

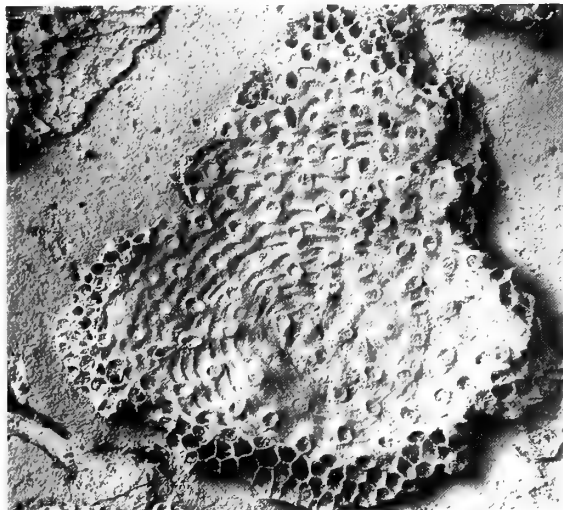
REMARKS. The main distinguishing feature of this new species is the presence of transverse ridges crossing the colony surface. Transversely ridged colonies also occur in four other Jurassic species: *Plagioecia rugosa* (d'Orbigny, 1853) from the Kimmeridgian of La Rochelle (France) (Figs 21–22), *Hyporosopora portlandica* (Gregory 1896a) from the Portlandian of southern England (revised by Taylor



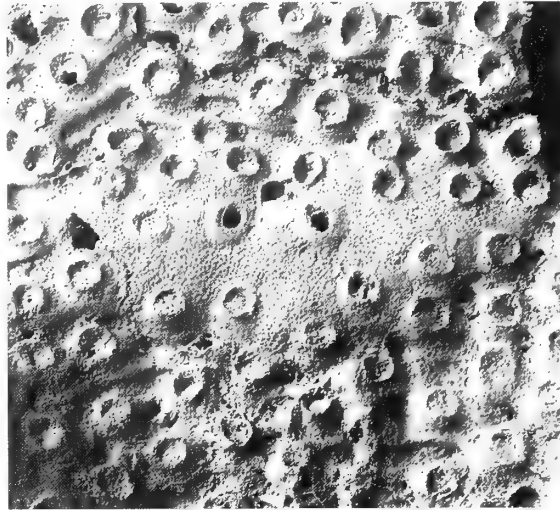
19



20



21



22

Figs 19–22 Jurassic bereniciform cyclostomes with transversely-ridged colonies similar to *Hyporosopora baltoviensis* sp. nov. **19–20.** *Hyporosopora enstonensis* (Pitt & Thomas, 1969), BMNH D51451, holotype, Bathonian, Hampen Marly Beds, Enstone, Oxfordshire, England; **19**, $\times 13$; **20**, gonozooid, $\times 80$. **21–22.** *Plagioecia rugosa* (d'Orbigny, 1853), BMNH BZ51, Lower Kimmeridgian, St Jean des Sables, near La Rochelle, Charente Maritime, France; **21**, small colony with prominent transverse ridges, $\times 14$; **22**, gonozooid in a larger colony encrusting the same substrate, $\times 30$.

1981), *H. enstonensis* (Pitt & Thomas, 1969) from the Bathonian of Oxfordshire (Figs 19–20), and *Mesenteripora undulata* (Michelin, 1845) from the Bathonian of Normandy (revised by Walter, 1970). A few post-Jurassic cyclostomes also possess transversely ridged colonies (e.g. *Plagioecia plicata* (Canu) from the Eocene of France, see Buge, 1979a; *Berenicea undata* Canu & Bassler, 1920 from Eocene of the USA), but this morphology seems to be proportionally less common than in the Jurassic.

Compared with *Hyporosopora baltoviensis*, the gonozooid in *Plagioecia rugosa* is broader and is penetrated by autozooidal apertures (Fig. 22). In other respects, however, the two species are very similar, although the transverse ridges tend to be more strongly developed in *P. rugosa* (Fig. 21). Walter (1970: 218) considered *P. rugosa* to be a junior synonym of *Cellepora orbiculata* Goldfuss, 1826 from the Oxfordian of Streitburg in Germany. The syntypes (Universität Bonn, Goldfuss Collection 104) of *C. orbiculata* have

been studied but are poorly-preserved, lack diagnostic gonozooids, and probably represent more than one species. *C. orbiculata* is probably better discarded.

Hyporosopora portlandica has narrower gonozooids than *H. baltoviensis*, and autozooidal apertures which are more widely-spaced and frequently transversely elongate. Multilamellar growth, rarely seen in *H. baltoviensis*, is very common in *H. portlandica*, resulting from either spiral overgrowth or eruptive budding of subcolonies onto the colony surface. (Note that the considerable discrepancy in autozooidal size between the holotype of *H. portlandica* and many other specimens previously assigned to this species, for example by Taylor (1981), suggests that more than one species may be present).

Gonozooid morphology is similar in *H. enstonensis* and *H. baltoviensis*, but the former species has smaller autozooids and more prominent transverse ridges (Figs 19–20). *M. undulata* has consid-

erably larger autozooids, and some colonies apparently develop erect growth (Walter, 1970, pl. 10, figs 3–8).

In view of the paucity of potential characters for grouping Jurassic bereniciform cyclostome species into genera, consideration must be given to the possibility of using the presence of transverse ridges as a generic character. All of the transversely ridged species seem to be closely-related and are classified within the Family Plagioeciidae. However, they are currently distributed between two or three different genera. Practical problems are associated with the recognition of transverse ridges because, although the ridges are sharp and clearly-defined in some species (e.g. *H. enstonensis*), in others (e.g. *H. baltovensis*) they are gradational with irregular growth checks of the sort which can be found in a wide range of bereniciform cyclostomes. A more complete analysis of character distributions is recommended before any attempt is made to group transversely-ridged species into one genus.

Genus *MECYNOECIA* Canu, 1918

TYPE SPECIES. *Entalophora proboscidea* Milne-Edwards, 1838, Recent.

REMARKS. Although Canu (1918) named *E. proboscidea* Milne-Edwards, 1838, as the type species of *Mecynoecia*, Canu & Bassler (1922: 11) attempted to change the type species to *Pustulopora delicatula* Busk, 1875, stating: 'The widespread and abundant species *Entalophora proboscidea* Milne-Edwards, 1838, was cited as the type of the genus by Canu in 1918, but we have changed the genotype for the reason that several species with different kinds of ovicells are undoubtedly included under this name and it is perhaps impossible at present to determine which one Milne-Edwards described'. This amendment is inadmissible under the International Rules of Zoological Nomenclature and therefore *E. proboscidea* stands as the valid type species of *Mecynoecia* (see also discussion in Buge 1979b; Walter 1987).

The probable type specimen of *E. proboscidea* (Museum Nationale d'Histoire Naturelle, Paris, Risso Collection 5110) has been examined by PDT. Although its colony-form corresponds with the general usage of *Mecynoecia* (e.g. by Harmelin 1976), the specimen lacks gonozooids, thus making precise characterization difficult, a problem considered beyond the scope of the current paper which accepts the generic concept as customarily applied.

Mecynoecia suprabajocina sp. nov. Figs 23–26, 28

HOLOTYPE. MUZ PIG 1601/II/11 (Figs 23–25).

PARATYPES. MUZ PIG 1601/II/9 and 10.

NAME. Indicating its similarity with *M. bajocina* (d'Orbigny, 1850) and the higher stratigraphical occurrence.

DESCRIPTION. Colony erect, branches cylindrical (vinculariform) and narrow (Fig. 23), 1.0–1.2 mm in diameter, ramifying dichotomously. Growth tips low cones in profile, with a radial, spoke-like arrangement of interzooidal walls, visible when viewed from above (Fig. 28). Zooidal budding apparently centred on branch axis. Pseudopores densely-packed and subcircular, absent from broad bands at the zooidal boundaries (Fig. 24).

Autozooids with elongate frontal walls, about 1.0 mm long by 0.21–0.30 mm wide, slightly convex distally but sunken beneath the level of the zooidal boundary wall proximally. Apertures widely-spaced, circular or a little longitudinally elongate, about 0.12–0.14 mm in diameter, sometimes closed by a terminal diaphragm

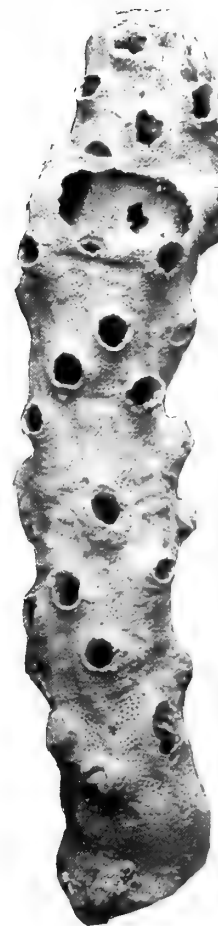
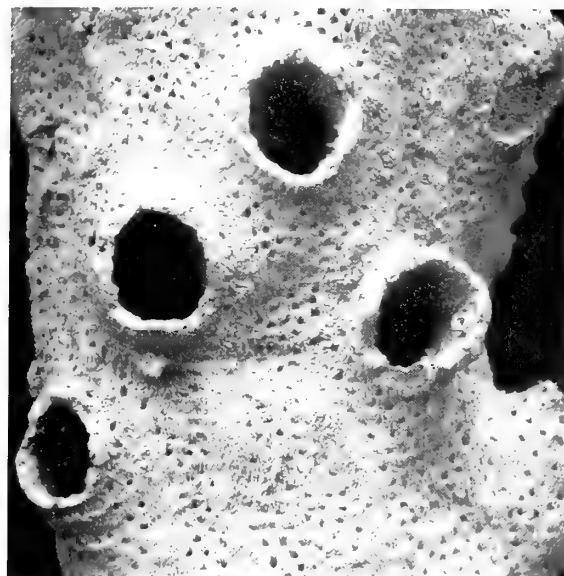


Fig. 23 *Mecynoecia suprabajocina* sp. nov., MUZ PIG 1601/II/11, holotype. Oxfordian, Baltów, Poland. Scanning electron micrographs of uncoated branch with a broken gonozoid close to the distal end, $\times 21$.

located either atop a short peristome or inclined and positioned proximally to the peristomial rim.

Gonozooids (Fig. 26) with globular distal dilated frontal wall, subcircular or transversely elliptical in outline and well inflated. Ooecipore (Fig. 26) located terminally, more or less semicircular, distal edge markedly convex relative to the almost straight proximal edge, wider than long, about 0.10 by 0.17 mm. Preserved ooecistomes short.

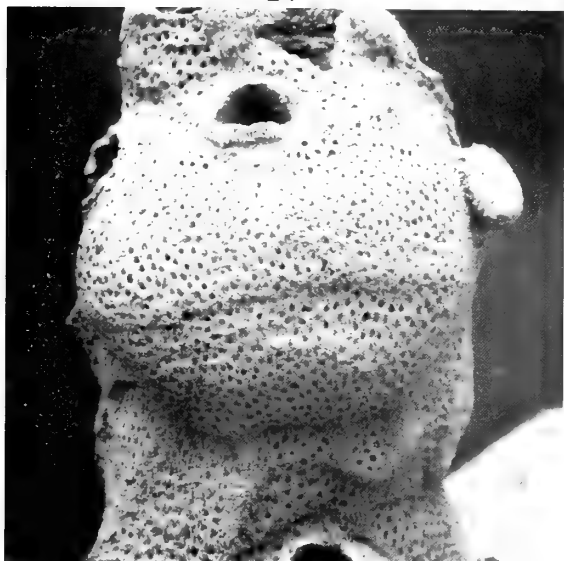
REMARKS. This new species resembles *Mecynoecia bajocina* from the Upper Bajocian White Sponge Oolite of the Port-en-Bessin area of Normandy, and the contemporaneous Microzoa Beds (a facies of the Burton Limestone) of Shipton Gorge, Dorset. However, it differs from *M. bajocina* in the structure of the ooecipore which is almost semicircular (Fig. 25) compared to the ooecipore of *M. bajocina* which is very strongly compressed medially (Fig. 27). In addition, the zooidal boundary areas devoid of pseudopores are substantially wider in *M. suprabajocina* than in *M. bajocina*. Genetic studies of living ctenostome and cheilostome bryozoans have shown clearly that subtle morphological differences signify different species (e.g. Thorpe & Ryland, 1979; Jackson & Cheetham, 1990). Although comparable studies have yet to be made on Recent cyclostomes, it is considered reasonable to favour the taxonomic splitting of cyclostomes on the basis of small but consistent differences in skeletal morphology (e.g. McKinney & Jackson, 1989).



24



25



26



27

Figs 24–27 Jurassic *Mecynoecia*; scanning electron micrographs of uncoated specimens. **24–26.** *Mecynoecia suprabajocina* sp. nov., Oxfordian, Baltów, Poland; **24–25.** MUZ PIG 1601/II/11, holotype; **24**, autozooids with broad areas devoid of pseudopores at zooidal boundaries, $\times 85$; **25**, ooeciopore, $\times 200$; **26**, MUZ PIG 1601/II/10, paratype, gonozoid with intact frontal wall, $\times 65$. **27.** *Mecynoecia bajocina* (d'Orbigny, 1850), BMNH D59492, Upper Bajocian, Shipton Gorge, Dorset, England, gonozoid with typically compressed ooeciopore, $\times 55$.

Family THEONOIDAE Busk, 1859
Genus *APSENDESIA* Lamouroux, 1821

TYPE SPECIES. *Apsendesia cristata* Lamouroux, 1821, Bathonian, Normandy.

REMARKS. Only two species of this genus are recognized: the Jurassic type species and *A. neocomiensis* d'Orbigny from the Hauterivian.

Apsendesia cristata Lamouroux, 1821

Figs 29–32

- 1821 *Pelagia clypeata* Lamouroux: 78, pl. 79, figs 5–7.
- 1821 *Apsendesia cristata* Lamouroux: 82, pl. 80, figs 12–14.
- 1854 *Apsendesia cristata* Lamouroux; Haime: 201, pl. 7, fig. 6 a–k.
- 1854 *Apsendesia clypeata* (Lamouroux); Haime: 202, pl. 7, fig. 7 a–d.
- 1896c *Apsendesia cristata* Lamouroux; Gregory: 167, pl. 9, figs 4–5.

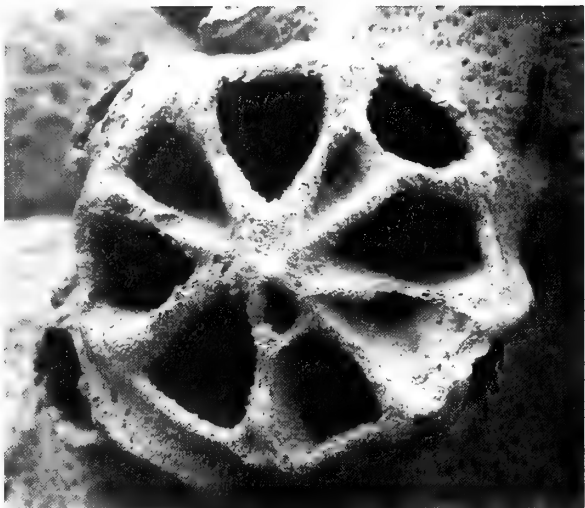


Fig. 28 *Mecynoecia suprabajocina* sp. nov., MUZ PIG 1601/11/9. Oxfordian, Baltów, Poland. Scanning electron micrograph of branch growing tip showing spoke-like arrangement of zoocial walls, $\times 85$.

- 1953 *Apsendesia cristata* Lamouroux; Bassler: 56, fig. 23,4.
 ?1967 *Apsendesia cristata* Lamouroux; Walter: 46, pl. 10, figs 1-2.
 1970 *Apsendesia cristata* Lamouroux; Walter: 202, pl. 20, figs 6-11.

MATERIAL. MUZ PIG 1601/II/6-7.

DESCRIPTION. Colony erect, fungiform, a narrow stalk, about 0.8 mm long, supporting an expanded, cup-shaped head, subcircular in plan view and averaging 4 mm in diameter (Figs 29-30). Autozooids grouped into fascicles which open around the circumference of the head and increase in number through bifurcation. Frontal side of head marked radially by ridge-like fascicles and convex frontal walls of autozooids. Underside of head an exterior wall with pseudopores and concentric growth lines, sometimes giving rise to downward-growing processes or struts each composed of about 3-6 zooids (Fig. 31).

Autozooids long, lacking frontal walls and with polygonal apertures when situated in the centres of a fascicle, but possessing pseudoporous frontal walls and apertures with a curved external edge when situated at the border of a fascicle. Apertures about 0.15 mm in diameter.

Gonozooids not observed in specimens from Baltów (see below).

REMARKS. This is one of the most distinctive of all Jurassic bryozoan species. At Baltów only small colonies, resembling specimens from the French Bathonian described as *Pelagia clypeata* by Lamouroux (1821), have been found. Large colonies depart from a simple cup-shape and become complexly corrugated, like the specimens described as *Apsendesia cristata* by Lamouroux (1821).

The finding of *A. cristata* at Baltów in the Oxfordian extends its range upward from the Lower Callovian (Walter, 1970: 204). An apparent occurrence in the Upper Bajocian of Shipton Gorge (Walter, 1967) is questionable: specimens from Shipton Gorge are extremely small, consisting of little more than a stalk and lacking the characteristic head and fascicles.

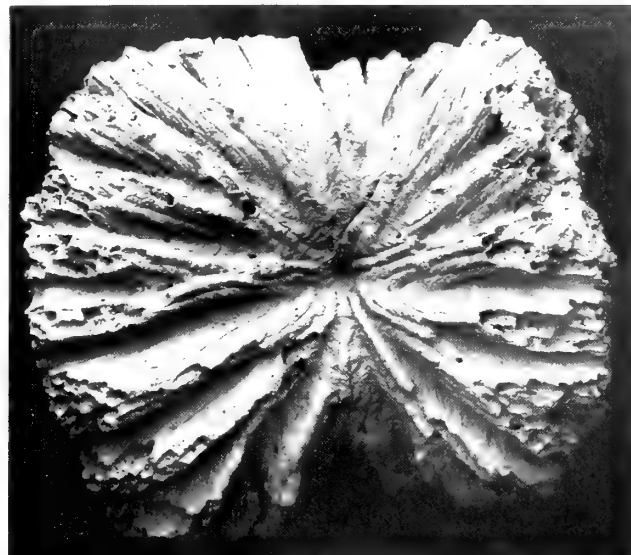
The peculiar gonozooid of *A. cristata*, not found in specimens from Baltów, is illustrated here using SEM for the first time (Fig. 32). It develops within a cleft in a fascicle and has a small ooeciopore

situated in the centre of a bulbous frontal wall. Another unusual feature of *A. cristata* are the processes which may develop from the undersides of colonies (Fig. 31). These are multizoidal, originate at the growing edge (i.e. not by resorption of the exterior wall in more proximal sites), and may extend down to the substratum to form secondary supports for the colony. Voigt (1993) has described similar structures from a variety of other cyclostomes and cheilostomes.

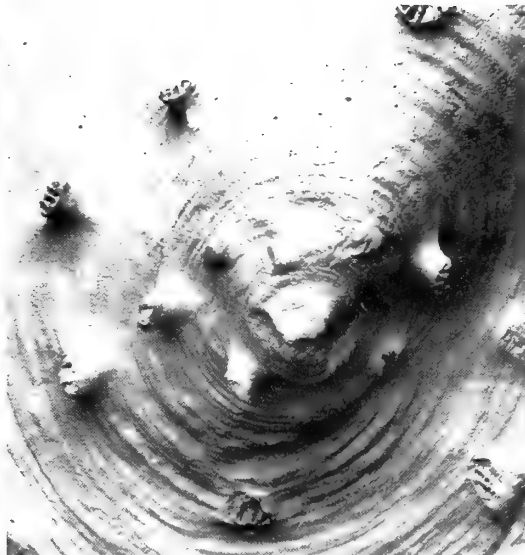
PALAEOECOLOGY

The Baltów bryozoan fauna consists entirely of small, delicate colonies; there is a total absence of the larger, more robust cyclostomes, notably cerioporines, which characterize many other Jurassic bryofaunas. In this respect, the fauna resembles that found in the Upper Bajocian of Shipton Gorge (Walford, 1889, 1894; Walter, 1967), although known species diversity at Shipton Gorge is considerably greater (*ca* 19 spp., vs. 5 spp. at Baltów). Other similarities between the two faunas include the abundance of bereniciform colonies with narrow axial canals, and the shared presence of closely-related species of *Mecynoecia* (and possibly also *Apsendesia cristata*, but see note above). Walter (1967) interpreted Shipton Gorge as a low energy, shallow water environment in which many of the bryozoans grew attached to thin algal filaments. A similar environmental interpretation probably also applies to Baltów, as suggested by the bryozoans (see Maryanska & Koblinska, 1980, 1984), corals (see Roniewicz & Roniewicz, 1971) and brachiopods (e.g. Barczyk, 1968, 1969, 1970). The presence of calcareous algae certainly implies deposition within the photic zone.

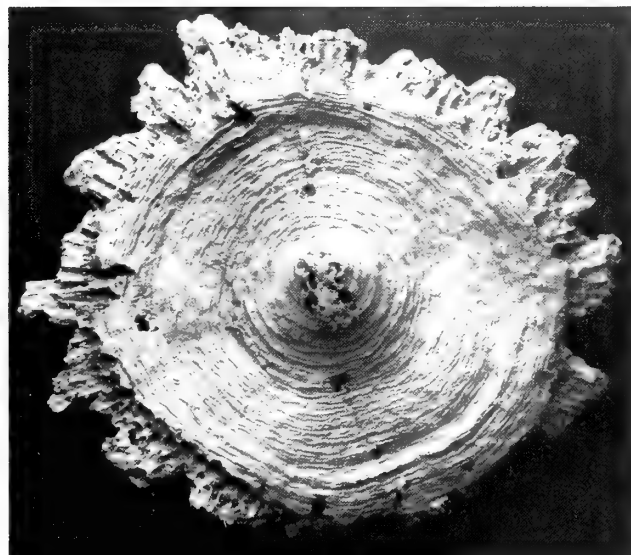
Most specimens of *H. baltvensis* from Baltów have tubular colonies with narrow axial canals (Figs 13-18). This colony-form is not, however, a specific character of *H. baltvensis* as some colonies are flat (Fig. 9). The presence of axial canals is clearly a result of encrustation of cylindrical substrates which were soft bodied and did not fossilize. Indeed, axial canals identical in size to those of *H. baltvensis* can be found in sponges from Baltów, which presumably lived attached to the same substrates as the bryozoans. Occasionally, the axial canals bifurcate, indicating that the organisms concerned had Y-shaped branches. Unfortunately, no informative bioimmurations of the surface details of the perished substrates are present on the basal laminae of the bryozoans. Therefore, the identity of the substrate is equivocal. Recent bryozoans can grow around a variety of cylindrical substrates of both plant and animal origin. For example, Alvarez (1992: fig. 15) illustrated small colonies of the Recent cyclostome *Disporella* sp. growing around un-named cylindrical substrates and leaving axial canals very similar to those found in the Baltów specimens. Bone & James (1993: fig. 7b) figured several different species of bryozoans attached to the cylindrical stems of sea-grasses from shallow water environments of the Lapepede Shelf, southern Australia. Larger diameter axial canals result from growth of the cheilostome *Schizoporella floridana* around rhizomes of seagrass (see McKinney & Jackson 1989: fig. 7.12). Among living animals, the polychaete *Phyllochaetopterus socialis* living at depths beneath the photic zone on the Otago Shelf of New Zealand constructs long horny tubes about 1 mm in diameter. These tubes are fouled by a diversity of bryozoans, including encrusting cheilostomes and cyclostomes, as well as erect colonies of the cyclostomes *Telopora* and *Hornera* (P.D.T. unpublished). Colonies wrap around the circumference of the polychaete tubes. Tube decay would leave an axial canal in the centre of the colony. Some of the tubes divide, possibly as a result of asexual fission of the worms.



29



31



30



32

Figs 29–32 *Apsendesia cristata* Lamouroux, 1821. Scanning electron micrographs of uncoated specimens. **29–30**, Oxfordian, Baltów, Poland; **29**, MUZ PIG 1601/II/6, colony upper surface, $\times 15$; **30**, MUZ PIG 1601/II/7, colony underside, $\times 15$. **31–32**, BMNH D2327 (1), Bathonian, Rerville, Normandy, France; **31**, struts on the underside of a colony, $\times 15$; **32**, gonozooid between fascicles of autozooidal apertures, $\times 35$.

Therefore, caution should be exercised when inferring that fossil bryozoans with axial tubes grew attached to plants and therefore indicate palaeoenvironments within the photic zone.

ACKNOWLEDGEMENTS. The British Council is thanked for providing U.H. with the opportunity to visit and work at the NHM in London.

REFERENCES

- Álvarez, J. A. 1992. Sobre algunas especies de la familia Lichenoporidae Smitt. 1866 (Bryozoa, Cyclostomida) en la región Atlántico-Mediterránea. Parte I: género *Disporella* Gray, 1848. *Cahiers de Biologie Marine*, Roscoff, **33**: 201–243.
- Barczyk, W. 1968. On some representatives of the genus *Craniscus* Dall (Brachiopoda) from Upper Jurassic of Baltów (Border of the Holy Cross Mountains in Poland). *Prace Muzeum Ziemi*, Warszawa, **12**: 177–185.
- 1969. Upper Jurassic terbratulids from the Mesozoic Border of the Holy Cross Mountains in Poland. *Prace Muzeum Ziemi*, Warszawa, **14**: 1–75.
- 1970. Some representatives of the family Thecididae (Brachiopoda) from the Upper Jurassic of Poland. *Acta Geologica Polonica*, Warszawa, **20**: 647–655.
- Bassler, R. S. 1935. Bryozoa. In Quenstedt, W. (ed.), *Fossilium Catalogus*, **1**: Animalia, Part 67, 229 pp. 's-Gravenhage.
- 1953. Bryozoa. In Moore, R. C. (ed.), *Treatise on Invertebrate Paleontology*, Part G, xiv + 253 pp. New York & Lawrence.
- Bone, Y. & James, N. P. 1993. Bryozoans as carbonate sediment producers on the cool-water Lacepede Shelf, southern Australia. *Sedimentary Geology*, Amsterdam, **86**: 247–271.
- Brochwicz-Lewinski, W. & Różak, Z. 1976. Oxfordian idoceratids (Ammonoidea) and their relation to *Perisphinctes* proper. *Acta Palaeontologica Polonica*, Warszawa, **21**: 373–390.

- Buge, E.** 1979a. Découverte du gonozoïde et position systématique de '*Reticulipora plicata*' Canu de l'Éocène du Bassin de Paris (Bryozoa Cyclostomata). *Annales de Paléontologie, Invertébrés*, Paris, **65**: 43–51.
- 1979b. Bryozoaires cyclostomes. *Résultats Scientifiques des Campagnes de la Calypso*, Paris, **11**: 207–252.
- & Fischer, J.-C. 1970. *Atractoscoecia incrustans* (d'Orbigny) (Bryozoa Cyclostomata) espèce bathonienne symbiotique d'un Pagure. *Bulletin de la Société Géologique de France*, Paris, (7) **12**: 126–133.
- Busk, G.** 1852. An account of the Polyzoa, and serularian zoophytes, the Louisiade Archipelago, &c. In MacGillivray, J., *Narrative of the voyage of H.M.S. Rattlesnake, commanded by the late Captain Owen Stanley ... 1846–1850*. **1**: 342–402. London.
- 1859. A monograph of the fossil Polyzoa of the Crag. *Palaeontographical Society Monograph*, London, xiv + 136 pp., 22 pls.
- 1875. *Catalogue of marine Polyzoa in the collection of the British Museum. Part III. Cyclostomata*. 41 pp., 14 pls. London.
- Canu, F.** 1918. Les ovicelles des Bryozoaires Cyclostomes. Etudes sur quelques familles nouvelles et anciennes. *Bulletin de la Société Géologique de France*, Paris, (4) **16**: 324–335.
- & Bassler, R. S. 1920. North American Early Tertiary Bryozoa. *Bulletin of the United States National Museum*, Washington, **106**: 1–879, 162 pls.
- & — 1922. Studies on the cyclostomatous Bryozoa. *Proceedings of the United States National Museum*, Washington, **61** (22): 1–160, 28 pls.
- & — 1929. Etudes sur les ovicelles des bryozoaires jurassiques. *Bulletin de la Société Linnéenne de Normandie*, Caen, (8) **2**: 113–131.
- Cariou, J. H. Enay, R. & Tintant, H.** 1971. Oxfordien. *Compte Rendu Sommaire des Séances de la Société Géologique de France*, Paris, **6**: 18–21.
- Goldfuss, G. A.** 1826–33. *Petrefacta Germaniae*. Teil 1. 76 pp. Dusseldorf.
- Gregory, J. W.** 1896a. A revision of the British Jurassic Bryozoa. Part III. The genus *Berenicea*. *Annals and Magazine of Natural History*, London, (6) **17**: 41–49.
- 1896b. A revision of the British Jurassic Bryozoa. Part IV. The genera *Reptomultisparsa* and *Diastopora*. *Annals and Magazine of Natural History*, London, (6) **17**: 151–155.
- 1896c. Catalogue of the fossil Bryozoa in the Department of Geology, British Museum (Natural History). The Jurassic Bryozoa. 239 pp., 11 pls. London.
- 1899. Catalogue of the fossil Bryozoa in the Department of Geology, British Museum (Natural History). The Cretaceous Bryozoa. Volume 1. 457 pp., 17 pls. London.
- Gutowski, J.** 1992. Górný oksford i kimeryd polnocno-wschodniego obrzeżenia Górz Świętokrzyskich. 187 pp. Warszawa [unpublished Ph. D. thesis].
- Haime, J.** 1854. Description des Bryozoaires fossiles de la formation jurassique. *Mémoires de la Société Géologique de France*, Paris, (2) **5** (2): 157–218, pls 6–11.
- Harmelin, J.-G.** 1976. Le sous-ordre des Tubuliporida (Bryozoa Cyclostomata) en Méditerranée. *Mémoires de l'Institut Océanographique*, Monaco, **10**: 1–326.
- Hayward, P. J. & Ryland, J. S.** 1985. Cyclostome bryozoans. *Synopses of the British Fauna (New Series)*, London, **34**: 1–147.
- Hincks, T.** 1880. *A history of the British marine Polyzoa*. Volume 1, 601 pp. Volume 2, 83 pls. London.
- Hurcewicz, H.** 1973. Calcispongia from the Jurassic of Poland. *Acta Palaeontologica Polonica*, Warszawa, **20**: 223–291.
- International Commission on Zoological Nomenclature.** 1986. Opinion 1392. *Reptomultisparsa* d'Orbigny, 1853 (Bryozoa, Cyclostomata): type species designated. *Bulletin of Zoological Nomenclature*, London, **43**: 140–141.
- Jackson, J. B. C. & Cheetham, A. H.** 1990. Evolutionary significance of morphospecies: a test with cheilostome Bryozoa. *Science*, New York, **248**: 579–583.
- Johnston, G.** 1847. *A history of British zoophytes*. 2nd edition. xvi + 488 pp., 74 pls. London.
- Karczewski, L.** 1960. Slimaki astartu i kimeredu północno-wschodniego obrzeżenia Górz Świętokrzyskich. *Prace Instytutu Geologicznego*, Warszawa, **32**: 1–68.
- Kazmierczak, J. & Hillmer, G.** 1974. Sclerosponge nature of the Lower Hauerian 'bryozoan' *Neopora pustulosa* (Roemer, 1839) from western Germany. *Acta Palaeontologica Polonica*, Warszawa, **19**: 443–453.
- Lamouroux, J.** 1816. *Histoire des Polypiers Coralligènes flexibles, vulgairement nommés Zoophytes*. Ixxiv + 560 pp., 19 pls. Caen.
- 1821. *Exposition méthodique des genres de l'ordre des Polypiers*. 115 pp., 84 pls. Paris.
- Liszkowski, J.** 1962. Stratigraphy of raurackich w okolicach Baltowa. *Przegląd Geologiczny*, Warszawa, **12**: 655–657.
- 1976. Problem IB – Rozwój litofacyjny i paleogeograficzny jury górnnej północno-wschodniej części mezozoicznego obrzeżenia Górz Świętokrzyskich. *Materiały konferencji terenowych*. Przewodnik XLVIII Zjazdu PTG Starachowice, Warszawa: 113–120.
- McKinney, F. K. & Jackson, J. B. C.** 1989. *Bryozoan evolution*. 238 pp. London.
- Malinowska, L.** 1965. Bioherma gabkowa newizu w okolicy Cmielowa. *Biuletyn Instytutu Geologicznego*, Warszawa, **192**: 57–96.
- 1967. Biostratygrafia dolnego i środkowego oksfordu obrzeżenia Górz Świętokrzyskich. *Biuletyn Instytutu Geologicznego*, Warszawa, **209**: 53–93.
- Maryanska, T. & Kobylinska, D.** 1980. Bryozoa. In: *Budowa geologiczna Polski. Atlas skałkamielosci przewodniczących i charakterystycznych*. 3. *Mezozoik-Jura*: 371–372. Warszawa.
- & — 1984. Bryozoa. In: *Budowa geologiczna Polski. Atlas skałkamielosci przewodniczących i charakterystycznych*. 3. *Mezozoik-Kreda*: 338–340. Warszawa.
- Michelin, H.** 1841–48. *Iconographie Zoophytologique. Description par localités et terrains des polypiers fossiles de France et pays environnants*. viii + 348 pp., 79 pls. Paris.
- Milne-Edwards, H.** 1838. Mémoire sur les Crises, les Hornières et plusieurs autres Polypes vivants ou fossiles dont l'organisation est analogue à celle des Tubulopores. *Annales des Sciences Naturelles*, Paris, (2) **9**: 193–238.
- Orbigny, A. d'** 1850. *Prodrome de paléontologie stratigraphique universelle des animaux Mollusques et rayonnés*. **1**, 394 pp. Paris.
- 1851–4. *Paléontologie Francaise. Terrains Crétacés*, **5**, *Bryozaires*. 1192 pp. Paris.
- Pitt, L. J. & Thomas, H. D.** 1969. The Polyzoa of some British Jurassic clays. *Bulletin of the British Museum (Natural History. (Geology Series))*, London, **18**: 29–38.
- Pugaczewska, H.** 1970. Traces of the activity of bottom organisms on the shells of the Jurassic ostraciform pelecypods of Poland. *Acta Palaeontologica Polonica*, Warszawa, **15**: 425–440.
- Reuss, A. E.** 1867. Die Bryozoen, Anthozoen und Spongiaren des braunen Jura von Balin bei Krakau. *Denkschriften der k. Akademie der Wissenschaften, Wien, (Mathematisch-Naturwissenschaftliche Klasse)*, **27** (1): 1–26, pls I–IV.
- Roniewicz, E.** 1966. Les Madréporaires du Jurassique supérieur de la bordure des monts de Sainte-Croix, Pologne. *Acta Palaeontologica Polonica*, Warszawa, **11**: 157–256.
- 1968. *Actinariaeopsis*, un nouveau genre de Madréporaire Jurassique de Pologne. *Acta Palaeontologica Polonica*, Warszawa, **13**: 305–308.
- 1976. Baltów – litologia i ekologia rafy koralowej i koralowo-glonowej oksfordu środkowego: profil na Zarzeczu. In Liszkowski, J., Problem IB – Rozwój litofacyjny i paleogeograficzny jury górnzej północno-wschodniej części mezozoicznego obrzeżenia Górz Świętokrzyskich. *Materiały konferencji terenowych. Przewodnik XLVIII Zjazdu PTG Starachowice*, Warszawa: 121–127.
- & Roniewicz, P. 1971. Upper Jurassic coral assemblages of the Central Polish Uplands. *Acta Geologica Polonica*, Warszawa, **21**: 399–423.
- Taylor, P. D.** 1980. Two new Jurassic Bryozoa from southern England. *Palaeontology*, London, **23**: 699–706.
- 1981. Bryozoa from the Jurassic Portland Beds of England. *Palaeontology*, London, **24**: 863–875.
- 1984. *Reptomultisparsa* d'Orbigny, 1853 (Bryozoa, Cyclostomata): request for the designation of a type species. *Z.N. (S.)* 2400. *Bulletin of Zoological Nomenclature*, London, **41**: 77–79.
- 1986. Scanning electron microscopy of uncoated fossils. *Palaeontology*, London, **29**: 685–690.
- 1994. Evolutionary palaeoecology of symbioses between bryozoans and hermit crabs. *Historical Biology*, **9**: 157–205.
- & Sequeiros, L. 1982. Toarcian bryozoans from Belchite in north-east Spain. *Bulletin of the British Museum (Natural History. (Geology Series))*, London, **36**: 117–129.
- Thorpe, J. P. & Ryland, J. S.** 1979. Cryptic speciation detected by biochemical genetics in three ecologically important intertidal bryozoans. *Estuarine and Coastal Marine Science*, London, **8**: 395–398.
- Vine, G. R.** 1881. Further notes on the Family Diastoporidae Busk. Species from the Lias and Oolite. *Quarterly Journal of the Geological Society*, London, **37**: 381–390.
- Voigt, E.** 1993. Stütz-, Anker- und Haftorgane bei rezenten und fossilen Bryozoen (Cyclostomata und Cheilostomata). *Verhandlungen des Naturwissenschaftlichen Vereins in Hamburg*, (N.F.) 33 [for 1992]: 121–130.
- Waagen, W.** 1867. Über die zone des *Ammonites sowerbyii*. *Geognostisch-paläontologische Beiträge von Dr. E. W. Benecke*, Munich, **1**: 507–668, pls xxi–xxxiv.
- Walford, E. A.** 1889. On some Bryozoa from the Inferior Oolite of Shipton Gorge, Dorset. Part I. *Quarterly Journal of the Geological Society*, London, **45**: 561–574.
- 1894. On some Bryozoa from the Inferior Oolite of Shipton Gorge, Dorset. Part II. *Quarterly Journal of the Geological Society*, London, **50**: 72–78.
- Walter, B.** 1967. Révision de la faune de Bryozaires du Bajocien supérieur de Shipton Gorge (Dorset, Grande-Bretagne). *Travaux des Laboratoires de Géologie de la Faculté des Sciences de Lyon*, Lyon, (n.s.) **14**: 43–52.
- 1970. Les Bryozaires Jurassiques en France. *Documents des Laboratoires de Géologie de la Faculté des Sciences de Lyon*, Lyon, **35** (for 1969): 1–328.
- 1987. Les Bryozaires Cyclostomes Neocomiens de forme 'Entalophora' et 'Spiropora'. *Revue de Paléobiologie*, Geneva, **6**: 29–53.

A new deep-water spatangoid echinoid from the Cretaceous of British Columbia, Canada

ANDREW B. SMITH

Department of Palaeontology, The Natural History Museum, Cromwell Road, London SW7 5BD, U.K.

ALAN McGUGAN

1157 Rolmar CR RR 2, Cobble Hill, Vancouver Island, British Columbia, V0R 1L0, Canada.

SYNOPSIS. A new species of spatangoid echinoid, *Plesiaster vancouverensis*, is described from continental slope debris flow deposits of latest Santonian to early Campanian age on Vancouver Island, British Columbia.

INTRODUCTION

The fossil record of echinoids is overwhelmingly dominated by species of the continental shelf. Although some of these lived in relatively deep water settings, such as the faunas of the North-West European Upper Chalk facies (Smith & Wright 1989, 1990, 1993), or the shelf marginal faunas of Spain (Neraudeau & Floquet 1991) or Tunisia (Zhabib-Turki 1989), records of continental slope and basin faunas remain extremely rare. Bather (1934) described the holasteroid *Chelonechinus* from the Miocene deep-water Suva Formation of Java, and more recently a diverse bathyal echinoid fauna has been discovered in the early Miocene Morozaki Group of Japan (Mizuno 1991) and the Middle Miocene Tatsukuroiso Mudstone of NE Honshu, Japan (Kikuchi & Nikaido 1985). Pliocene deposits of California have also yielded what appear to be bathyal echinoids (Woodring 1938). Here we describe a new spatangoid from late Cretaceous outer shelf to upper continental slope deposits of western Canada.

The new species described here comes from a single horizon within the Upper Cretaceous Nanaimo Group. The Nanaimo Group represents a major sedimentary sequence within the Georgia Basin of south-western British Columbia and was deposited in a fore-arc basin along the western margin of the Canadian continental margin (England 1989). Depositional environments represented within this group range from alluvial to continental slope facies, with the echinoids coming from within a series of debris flows interpreted as upper continental slope facies.

The echinoid horizon was discovered in May 1993 by Dr A. McGugan and Dr. T. England during reconnaissance of the French Creek area. The echinoids were found in a stream section adjoining Fildegarde Farm on French Creek, ca. 1 km upstream from Highway 1 bridge at Coombs, which crosses French Creek approximately seven km due south of Qualicum Beach, Vancouver Island, British Columbia (Fig. 1). The succession at this locality begins with ca. 6 m of bedded shales, siltstones and mudstones of the Haslam Formation (= lower part of the Trent River Formation of England, 1989; Fig. 2). These are overlain by a chaotic conglomeratic debris flow (McGugan, 1992). The matrix is a silty mudstone and included pebbles are a mixture of undated meta-volcanics, argillites, Cretaceous calcareous concretions (some with plant remains), sandstone and siltstone clasts, and many clasts of bedded shale, some up to 4 m in length and showing plastic deformation and slump-roll-type leading edges. The fauna of these beds include foraminifera, ammonites and inoceramid and other bivalves.

The echinoids, all of which belong to the same species, came from

a single bedding plane near the top of the bedded shale series. They are preserved in life orientation and some at least retain associated spines. These echinoids were thus not transported, but lived and died within the environment of deposition represented by the shales. Since the bedded shales are overlain by debris flows, the environment of deposition is taken to be upper continental slope.

The dating of the echinoid level is based on the benthic foraminifera, which are indicative of the *Inoceramus (Sphenoceramus) schmidti* Zone, latest Santonian to Lower Campanian. The associated macrofauna also support a late Santonian – early Campanian age. A molluscan fauna (Table 1) is associated with the echinoids and in the beds immediately overlying, and has been identified by Dr. J.W. Haggart (Geological Survey of Canada, Vancouver). This includes *I. (S.) schmidti*, which is known to range from the latest Santonian to early Campanian in British Columbia and Northern California (Haggart, 1984).

Table 1. Fossil molluscs found in association with *Plesiaster vancouverensis* sp. nov. in the Haslam Formation of French Creek, Vancouver Island. Identifications by J.W. Haggart (Canadian Geological Survey, Vancouver).

Bivalves:

Inoceramus (Sphenoceramus) schmidti Michael
I. ex. gr. subundatus Meek
Acila (Truncacila) demessa Finlay

Ammonite:

Canadoceras yokoyamai (Jimbo)

SYSTEMATIC DESCRIPTION

Class ECHINOIDEA Leske, 1778

Order SPATANGOIDA Claus, 1876

Family MICRASTERIDAE Lambert, 1920

Genus *PLESIASTER* Pomel, 1883

TYPE SPECIES. *Micraster peini* Coquand, 1862.

OTHER SPECIES INCLUDED. *P. cotteaui* Gauthier.

OCCURRENCE. Late Coniacian to early Campanian of North Africa and North America.

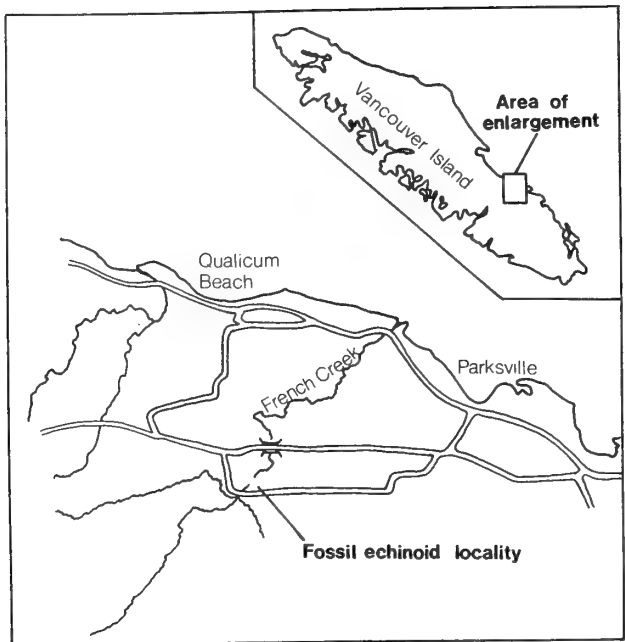


Fig. 1. Map showing the location of the echinoid bed, with insert showing its position on the island of Vancouver.

***Plesiaster vancouverensis* sp. nov. Text-figs 3–5**

TYPES. Holotype, BMNH EE 5078 (Figs 3A, 4A, 4B, 5A); paratypes, BMNH EE5076 (Fig. 3C), EE5077, EE5079–83 (Figs 3B, 3D, 3E, 4C–F, 5B).

OCCURRENCE. Shales towards the top of the Haslam Formation (= lower part of the Trent River Formation), *I. (S.) schmidti* Zone, uppermost Santonian to lowermost Campanian, exposed in river bank of French Creek behind Hildegard Farm, ca. 1 km upstream from the highway 4 bridge over French Creek at Coombs, and 7 km due south of Qualicum Beach, south-eastern Vancouver Island, British Columbia, Canada.

DIAGNOSIS. A species of *Plesiaster* with a well-developed peripetalous fasciole around the posterior part of the test, a broad and strongly petaloid anterior ambulacrum, and with lateral and posterior petals broad and open, extending most of the distance to the

ambitus. The contact between the labral plate and sternal plates is strongly offset towards the left-hand side.

DESCRIPTION. All tests are crushed so accurate dimensions cannot be given. The largest and best-preserved specimen is approximately 63 mm in length and 58 mm in width. Test height and shape in profile are unknown, but the test appears to have been relatively low and gently domed. The test is oviform in outline with the posterior slightly truncated. The widest point on the test lies a little behind the anterior petals at approximately mid-length.

The apical disc is ethmophract with all four genital plates similar in size and each bearing a gonopore (Fig. 3B). The posterior genital plates are not separated by the madreporite. The apical disc lies anterior of centre, 39% of test length from the anterior border.

All five ambulacra are strongly petaloid adapically. Petals are broad and sunken and remain open distally. The anterior petal extends 80% of the distance to the ambitus. It shallows and more or less disappears towards the ambitus so that the anterior is hardly notched. There are ca. 45 pore-pairs in a column at 63 mm test length. The pore-pairs are conjugate, with individual pores widely separated (Fig. 3A). The perradial zone is smooth and approximately as broad as a single pore-zone (Fig. 5B). The lateral petals extend 90% of the distance to the ambitus and are strongly petaloid, tapering slightly towards the ambitus. They diverge from one another at an angle of 135°. There are ca. 55 pore-pairs in a column at 63 mm test length. Individual pores are strongly elongate and conjugate, with successive pore-pairs separated by single rows of miliary tubercles. The posterior petals are similar, but extend only 75% of the distance to the ambitus. They diverge from one another at an angle of 50°. Pores below the petals are single. Around the peristome there are three to five enlarged phyllode pores.

Interambulacra are slightly raised adapically but do not form sharp keels. They remain biserial to the apex. On the oral surface the primibasal plates in interambulacra 1 and 4 are occluded from the peristome border by proximal ambulacral plates (Fig. 3B). The labral plate is elongate and narrow, more than twice as long as broad. The sternal plates are clearly differentiated, but unequal in size; that towards ambulacrum I being smaller and either just in contact with the labral plate (Fig. 3E) or separated from it (Fig. 3D).

The peristome is small and D-shaped; the labral plate does not project over the mouth and there is no distinct lip. The front of the peristome lies 19% of the test length from the anterior border. The periproct is crushed in all specimens. It lies on the posterior surface and is probably hidden in both apical and oral views.

Stage	Zone and Subzone		Formation
Maastrichtian			Gabriola
			Spray
			Geoffrey
			Northumberland
Campanian	<i>Pachydiscus suciaensis</i>	<i>Nostoceras hornbyense</i>	De Courcy
		<i>Metaplatcenticeras cf. pacificum</i>	Cedar District
		<i>Hoplitoplacenticeras vancouverense</i>	Extension Protection
		<i>Inoceramus schmidti</i>	*
	<i>Bostrychoceras elongatum</i>	<i>Pachydiscus haradai</i>	Haslam
Santonian		<i>Inoceramus naumanni</i>	Comox

Fig. 2. Stratigraphic column for the Upper Cretaceous Nanaimo Group showing the level of the echinoid bed (*) (taken from Muller & Jeletzky 1970, and England 1989).

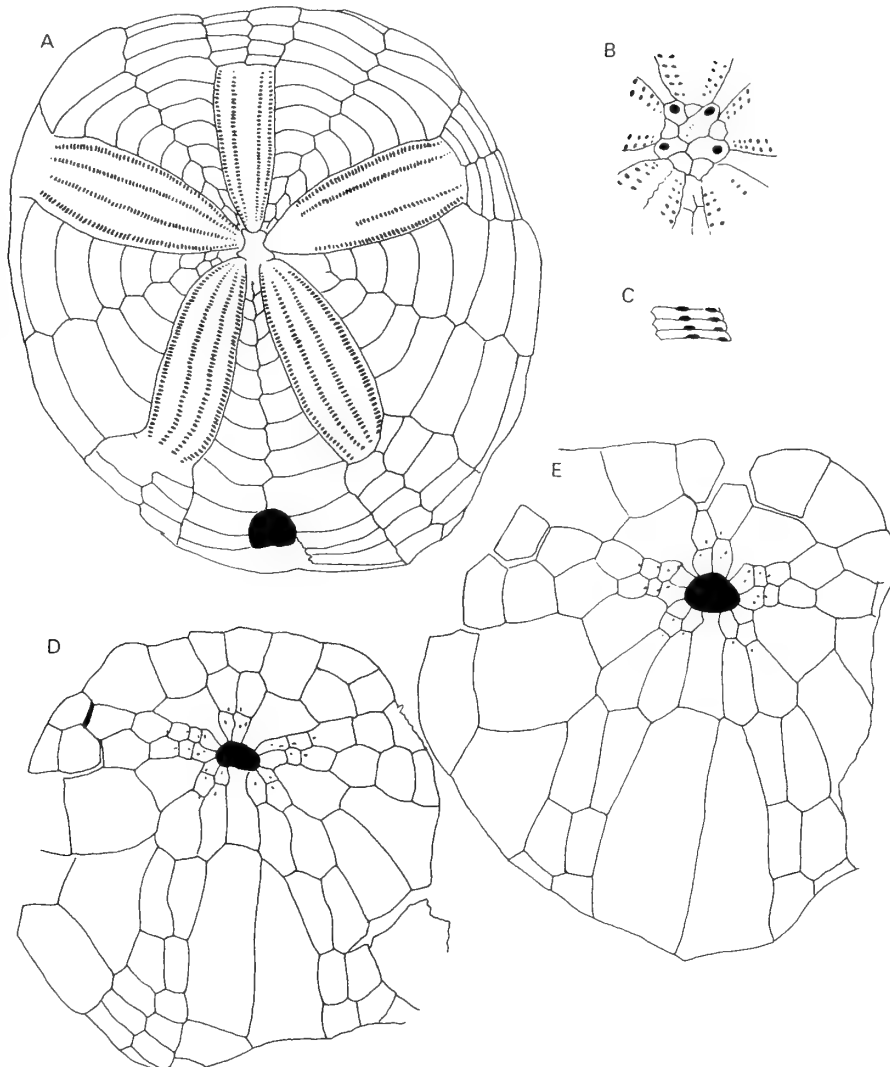


Fig. 3. Camera lucida drawings of *Plesiaster vancouverensis* sp. nov. uppermost Santonian; Lower Campanian, *I (S.) schmidtii* Zone, French Creek, Vancouver Island, British Columbia. A, BMNH EE5078; B, BMNH EE5083; C, BMNH EE5076, D, BMNH EE5079; E, BMNH EE5081.

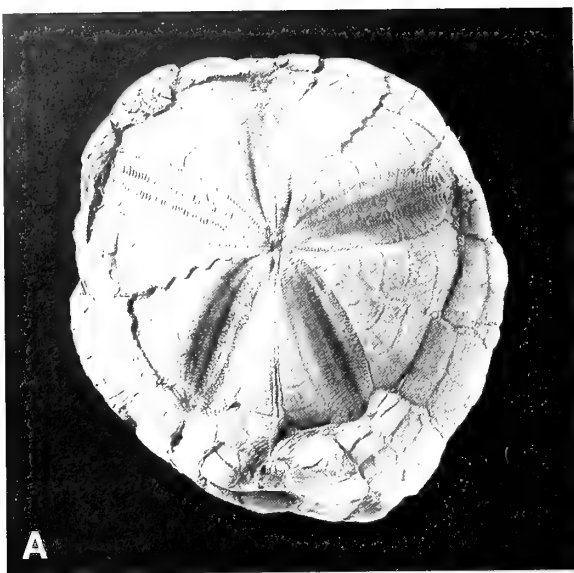
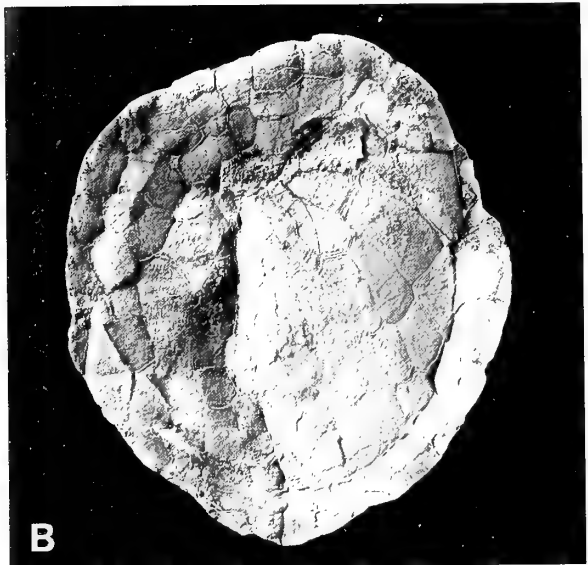
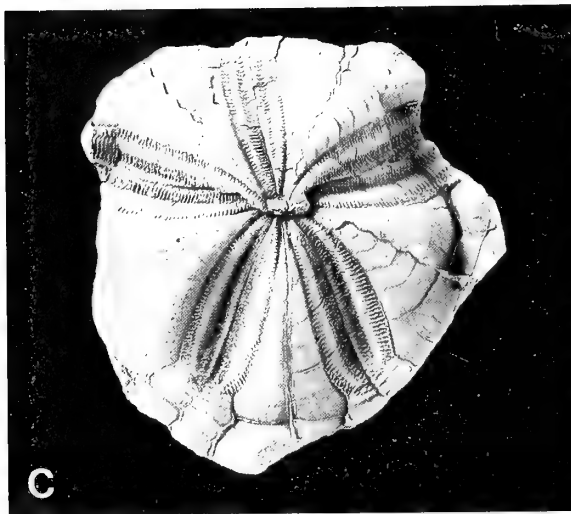
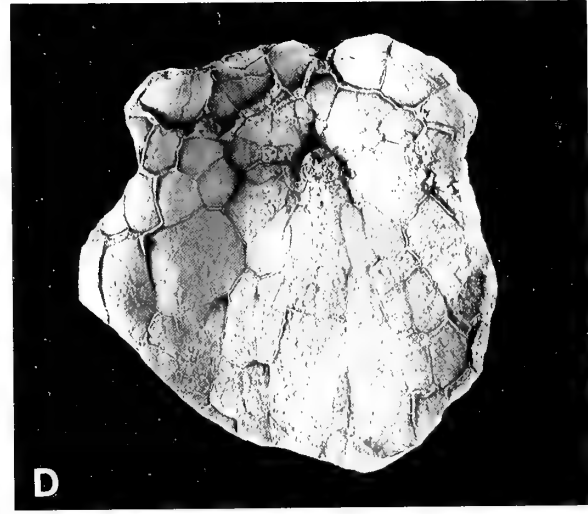
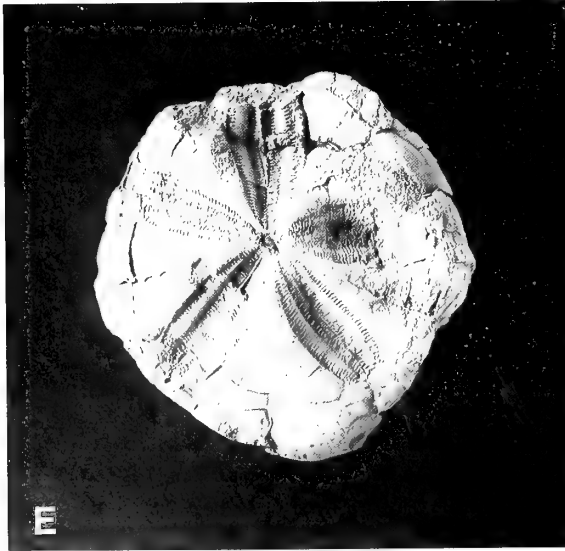
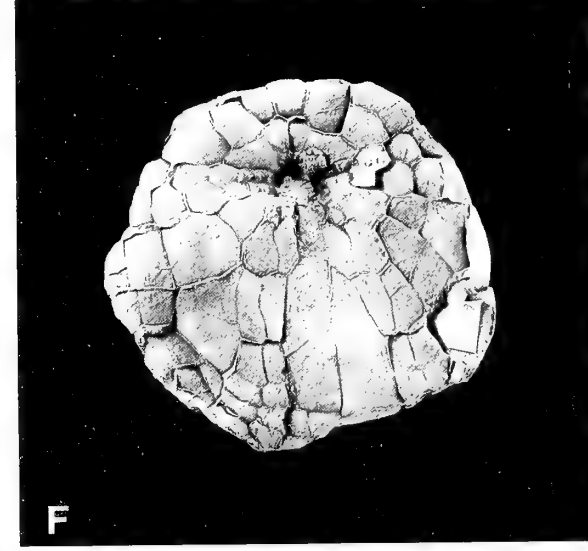
Tuberculation is relatively coarse on the aboral surface, with scattered primary tubercles (crenulate and perforate) up to 0.6 mm diameter set amongst a fine granulation of miliary tuberculation (Fig. 5B). A well-developed peripetalous fasciole, with up to 12 rows of densely spaced (hexagonally packed) miliary tubercles, is developed around at least the posterior of the test. It runs immediately beneath the ends of the petals and is indented in the postero-lateral interambulacra. Unfortunately, most specimens are preserved as internal moulds so it is impossible to tell whether the fasciole continues around the anterior of the test. It is also impossible to tell whether there was a subanal fasciole present.

Some specimens have scattered primary spines preserved flattened against the test surface.

REMARKS. The new species is placed in the genus *Plesiaster* on account of its peripetalous fasciole and petaloid anterior ambulacrum. Only a few spatangoid genera have petaloid anterior ambulacra, namely *Douvillaster* Lambert, 1917, *Plesiaster* Pomel 1883, *Heterolampas* Cotteau 1862, *Isomicraster* Lambert 1901 and *Barnumia*

Cooke 1953. Neither *Douvillaster* nor *Isomicraster* have fascioles and thus differ significantly from the Canadian species. *Barnumia* can also be dismissed from consideration since its fasciole is not peripetalous but lateral, extending around the ambitus and well-separated from the base of the petals. The type species of *Heterolampas*, *H. maresi* Cotteau, has a narrow but continuous peripetalous fasciole and petaloid ambulacra. However, it differs significantly from the Canadian species in its labral and apical disc structure. The apical disc of *H. maresi*, though ethmophract, is composed of an enlarged madreporite plate which occupies the centre of the disc and separates the posterior two genital plates. Its labral plate is large and broadly triangular, firmly abutting both sternal plates. Finally, the peristome of *H. maresi* lies considerably further back from the anterior than that of the new species.

Plesiaster Pomel, 1883, was established for *Micraster*-like forms with a partial peripetalous fasciole developed at the base of the petals. Zhagib-Turki (1987) has given a recent analyses of the North African species and concluded that *Plesiaster* should be placed in synonymy with *Micraster*. However, the differentiation of

**A****B****C****D****E****F**

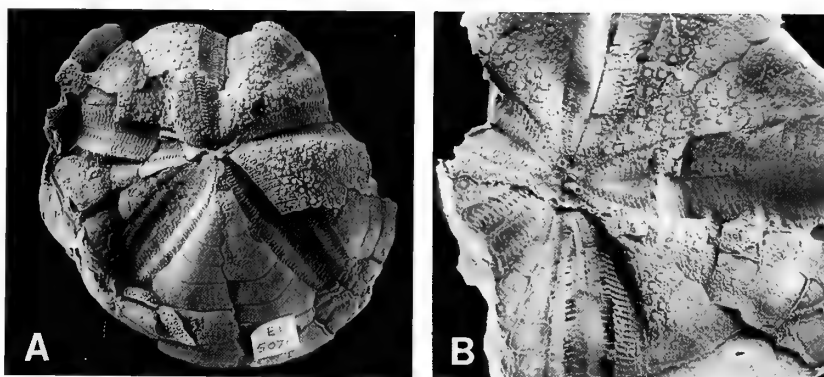


Fig. 5. *Plesiaster vancouverensis* sp. nov. **A**, BMNH EE5076, adapical view of test showing tuberculation style, $\times 1$. **B**, BMNH EE5083, latex cast of external mould showing apical disc and tuberculation style, $\times 2$.

a partial peripetalous fasciole represents an apomorphy for the genus and the distinction is maintained here. The European species that have been assigned to this genus in the past, *P. bucardium* Goldfuss, *P. corarium* Schlüter, *P. parvistella* Schlüter, and *P. minor* Schlüter (e.g. Ernst 1972), differ significantly from the North African type, *P. peini* Coquand. The European species all have short petals, non-petaloid anterior ambulacra, and complete peripetalous and subanal fascioles. They are placed in the genus *Diplodetus* Schlüter 1900. The two North African species, *P. peini* and *P. cotteau* have much longer petals and incomplete fascioles.

The Canadian species comes close to '*Micraster*' *americanus* Stephenson in form, but differs from that species in having a much more strongly petaloid anterior ambulacrum. In *M. americanus* the pores in the anterior ambulacrum are small and separated by a raised interporal granule, whereas those pores in *P. vancouverensis* are conjugate and widely separated from one another in each pair. Furthermore, the petals of *P. vancouverensis* are larger, more open and extend closer to the ambitus than they do in *M. americanus*.

P. vancouverensis differs from the North African species of *Plesiaster* in having a well-developed peripetalous fasciole around the posterior of the test. *P. peini* and *P. cotteau* both have very impersistent fascioles that are really only present at the base of the petals and do not form a continuous band around the posterior.

REFERENCES

- Sather, F.A. 1934. *Chelonechinus* n.g., a Neogene urchinid. *Bulletin of the Geological Society of America*, **45**: 799–876.
- Cooke, W.B. 1953. American Upper Cretaceous Echinoidea. *United States Geological Survey Professional Paper*, **254-A**: 44pp. 16 pls.
- England, T.D.J. 1989. Lithostratigraphy of the Nanaimo Group, Georgia Basin, southwestern British Columbia. *Geological Survey of Canada Paper*, **89-1E**: 197–206.
- Ernst, G. 1972. Grundfragen der Stammesgeschichte bei irregulären Echiniden der nordwesteuropäischen Oberkreide. *Geologisches Jahrbuch*, **A4**: 63–175.
- Haggart, J.W. 1984. Upper Cretaceous (Santonian-Campanian) ammonite and inoceramid biostratigraphy of the Chico Formation, California. *Cretaceous Research*, **5**: 225–241.
- Kikuchi, Y. & Nikaido, A. 1985. The first occurrence of abyssal echinoid *Pourtalesia* from the Middle Miocene Tatsukuroiso Mudstone in Ibaraki Prefecture, northeastern Honshu, Japan. *Annual Report of the Institute of Geosciences, the University of Tsukuba*, **11**: 32–34.
- McGugan, A. 1992. Cretaceous submarine debris flow outcrops. *Geological Society of America Today*, **2**: 57 only.
- Mizuno, Y. 1991. Fossil echinoderms from the early Miocene Morozaki Group in the Chita peninsula, central Japan. In Yanagisawa, T., Yasumasu, I., Oguro, C., Suzuki, N. & Motokawa, T. (eds), *Biology of Echinodermata: Proceedings of the seventh international echinoderm conference, Atami/9–14 September, 1990*, p. 582 only. A.A. Balkema, Rotterdam.
- Muller, J.E. & Jeletzky, J.A. 1970. Geology of the Upper Cretaceous Nanaimo Group, Vancouver Island and Gulf Islands, British Columbia. *Geological Survey of Canada Paper*, **69-25**: 1–77.
- Neraudeau, D. & Floquet, M. 1991. Les échinides Hemicasteridae: marqueurs écologiques de la plate-forme castillane et navarro-cantabre (Espagne) au Crétacé supérieur. *Palaeogeography, Palaeoclimatology, Palaeoecology*, **88**: 265–281.
- Pomel, A. 1883. *Classification méthodique et genera des échinides vivants et fossiles*. Alger, Paris, 120 pp.
- Smith, A.B. & Wright, C.W. 1989. British Cretaceous echinoids. Part 1, General introduction and Cidaroida. *Monographs of the Palaeontographical Society, London*: 1–101, pls 1–32 (publication number 578, part of volume 141 for 1987).
- & — 1990. British Cretaceous echinoids. Part 2, Echinothurioida, Diadematoida and Stirodonta (1, Calycina). *Monographs of the Palaeontographical Society, London*: 101–198, pls 33–72 (publication number 583, part of volume 143 for 1990).
- & — 1993. British Cretaceous echinoids. Part 3, Stirodonta, part 2 (Hemicidaroida, Arbacioida and Phymosomatoida, part 1). *Monographs of the Palaeontographical Society, London*: 199–267, pls 73–92 (publication number 593, part of volume 146 for 1993).
- Woodring, W.P. 1938. Lower Pliocene Mollusks and echinoids from the Los Angeles Basin, California. *United States Geological Survey Professional Paper*, **190**: 1–65, pls 1–9.
- Zhabib-Turki, D. 1987. Les Echinides du Crétacé de Tunisie. Paléontologie générale: systématique, paléocologie, paléobiogéographie. Unpublished Ph. D. Thesis, Faculté des Sciences de Tunis. 613 pp. 25 pls.
- 1989. Les échinides indicateurs des paléoenvironnements: un exemple dans le Crétacé de Tunisie. *Annales de Paléontologie*, **75**: 63–81.

Fig. 4. *Plesiaster vancouverensis* sp. nov. uppermost Santonian; Lower Campanian, *I. (S.) schmidti* Zone, French Creek, Vancouver Island, British Columbia. **A, B**, BMNH EE5078 (internal mould), holotype: **A**, apical view; **B**, oral view. **C, D**, BMNH EE5081 (internal mould), paratype: **C**, apical view; **D**, oral view. **E, F**, BMNH EE5079 (internal mould), paratype: **E**, apical view; **F**, oral view. All $\times 1$.



The cranial anatomy of *Rhomaleosaurus thorntoni* Andrews (Reptilia, Plesiosauria)

ARTHUR R. I. CRUICKSHANK

Earth Sciences Section, Leicestershire Museums, The Rowans, College Street, Leicester LE2 0JJ; and Department of Geology, University of Leicester, University Road, Leicester LE1 7RH

SYNOPSIS. The skull and lower jaw of *Rhomaleosaurus thorntoni* Andrews, 1922, from the Upper Lias of Northamptonshire, are figured for the first time. New information shows that the external nares are in a perfectly normal position, just in front of the orbits. There is little difference between *R. thorntoni*, *R. zetlandicus* and *R. cramptoni*, the type species of the genus. As they can be considered to be conspecific, *Rhomaleosaurus zetlandicus* (Phillips, in Anon, 1854) has priority. *R. zetlandicus* is of more robust construction than the Rhaetian/Hettangian species *R. megacephalus* (Stutchbury, 1846), with, among other differences, teeth having fewer striae and the internal nares of a different construction.

INTRODUCTION

The species *Rhomaleosaurus thorntoni* was proposed by C. W. Andrews in 1922 for a pliosaroid plesiosaur (Brown 1981) from the Toarcian (Upper Liassic) of Kingsthorpe, Northamptonshire. The type specimen (BMNH R4853) comprises a partial skull, partial mandible and much of the postcranial skeleton, but lacks the limbs. Andrews (1922) described the skull and postcranial remains of the specimen in some detail, but illustrated only the sacral vertebrae and the limb girdles. No illustration of the skull and jaw material exists and it is the purpose of this paper to remedy this omission as part of a series of papers to improve knowledge of the Liassic plesiosaurs (Taylor 1992a, b; Taylor & Cruickshank 1993a; Cruickshank, 1994a, b). Andrews discussed the characters of his new species, comparing them most closely with those of *R. cramptoni* (Carte & Baily 1863) (NMING F8785). As will be shown below, however, the differences he enumerated between *R. thorntoni* and *R. cramptoni* cannot now be sustained; in addition, many of the characters of *R. thorntoni* are to be found in *R. zetlandicus* (Phillips, in Anon, 1854) (Taylor 1992a) (YORYM G503).

SYSTEMATIC PALAEONTOLOGY

Class REPTILIA

Subclass SAUROPTERYGIA Owen, 1860

Order PLEIOSAURIA de Blainville, 1835

Superfamily PLIOSAUROIDEA (Seeley, 1874) Welles, 1943

Family PLIOSAURIDAE Seeley, 1874

Genus RHOMALEOSAURUS Seeley, 1874

TYPE SPECIES. *Plesiosaurus cramptoni* Carte & Baily, 1863

Rhomaleosaurus zetlandicus (Phillips, in Anon, 1854)

Figs 1–6

1854 *Plesiosaurus zetlandicus* Phillips, in Anon: 19.

1863 *Plesiosaurus cramptoni* Carte & Baily: 160.

1874 *Rhomaleosaurus cramptoni* (Carte & Baily) Seeley: 448.

1922 *Rhomaleosaurus thorntoni* Andrews: 413.

1992 *Rhomaleosaurus zetlandicus* (Anon, in Phillips, 1854); Taylor: 52.

DIAGNOSIS. A *Rhomaleosaurus* with a more robust and relatively shorter and wider skull, and a steeper profile of the lower jaw symphysis when compared with *Rhomaleosaurus megacephalus* (Stutchbury). Tooth ornament coarse, with widely-spaced ridges and reducing in number towards the tip, triangular in section. Palatal foramina and internal nares lie in the same groove, as opposed to the condition in *R. megacephalus*. The length-width ratio of the snout is 1:1 as opposed to 1.25:1 for *R. megacephalus*.

The specimen described here is BMNH R4853. Andrews (1922: 413) did not formally diagnose *R. thorntoni*, except by distinguishing it from *R. cramptoni* in several characters. Andrews (1922: 414) also gave an opinion that *Plesiosaurus megacephalus* Stutchbury, 1846 belonged to the genus *Rhomaleosaurus*, but gave no reasons (see Taylor & Cruickshank (1989) and Cruickshank (1994a) for discussion).

Plesiosaurus cramptoni (NMING F8785) is the type species of the genus *Rhomaleosaurus* Seeley, 1874, and comes from Alum

INSTITUTIONAL ABBREVIATIONS

BMNH	Palaeontology Collections, The Natural History Museum, Cromwell Road, London SW7 5BD (formerly the British Museum (Natural History))
EICS	Leicestershire Museums, Arts and Records Service, The Rowans, College Street, Leicester LE2 0JJ
MANCH	The Manchester Museum, Oxford Street, Manchester M13 9PL
NMING	National Museum of Ireland, Kilare Street, Dublin 2, Eire
VM	Whitby Museum, Whitby Literary and Philosophical Society, Pannet Park, Whitby, Yorkshire YO21 1RE
YORYM	Yorkshire Museum, Museum Gardens, York YO1 2DR.

Shales at Kettle Ness on the north Yorkshire coast (Benton & Taylor 1984) of Toarcian (Bifrons Zone) age. Other English species that have been referred to this genus include *Plesiosaurus megacephalus* Stutchbury, 1846 and *P. propinquus* Phillips, 1854. Only *R. megacephalus* is represented so far by more than one specimen, and it alone seems to be from the Lower Liassic (Rhaetian/Hettangian) (Cruickshank 1994a). *Plesiosaurus propinquus* differs from other species in having a marked boss on the hind end of the inner surface of the lower jaw, just in front of the glenoid and in place of the dorso-median trough (Taylor 1992a, b), and thus its position within *Rhomaleosaurus* must be reconsidered.

Table 1 Abbreviations used on Figs 1–6.

aiv	anterior interpterygoid vacuity	lgr	lateral groove
carina	carina on crown of tooth	mto	mature tooth
co	coronoid	mx	maxilla
cr	crown	no	notch
d	dentary	orb	orbit
dep	depression	pal	palatine
dmfo	dorsomedian foramen	palv	primary alveolus
ec	ectopterygoid	pmx	premaxilla
en	external naris	po	postorbital
fac	facial processes of the premaxillae	pt	pterygoid
fan	fan-shaped area	ptb	pterygoid boss
fo	foramina	ri	ridged ornament on crown of tooth
gr	groove	rto	replacement tooth
in	internal naris	salv	secondary alveolus
info	foramina associated with internal naris	sof	suborbital fenestra
j	jugal	sp	splenial
		sym	symphysis
		v	vomer
		1	position of first tooth

Oblique lining represents broken or sectioned bone or tooth.

Mechanical stipple represents matrix or crushed bone.

DESCRIPTION. *Skull* (Figs 1, 2). The skull and lower jaw have recently been cleaned and conserved, and they alone will be dealt with here. Only the anterior portion of the skull was collected; the clean break surface runs obliquely from a position in front of the left orbit, through the left external naris, to the front edge of the right orbit, and thence through the postorbital bar. Some bone has been lost from the tip of the premaxillae. The right cheek bar is attached to the snout and runs as far as the end of the maxilla. Attached to the cheek bar is a portion of the palate, comprising the right ectopterygoid and a small part of the pterygoid. The base of the postorbital rests on the posterior end of the jugal. Apart from the obvious break, the skull has been damaged by post-mortem effects which have compressed the bone dorso-ventrally and caused the facial processes of the premaxillae to be shortened, so that the midline of the snout has a step, with the posterior part of the premaxillae, as preserved, being pushed under the anterior part and offset to the right. The maxillae may, in addition, have been squeezed together under the facial processes of the premaxillae. All this disruption has obscured the right external naris. In front of, and lateral to, the position of the hidden right external naris, is a deep depression bottomed with crushed bone and an associated wide groove running to the premaxillary edge. The right jugal is partly visible, and is a narrow bone running under the orbit and ending below the postorbital. However, as the bone is heavily pyritized and crushed, and the sutures much closed up, the prefrontal and lacrimal cannot be distinguished. Similarly the detailed structure of the postorbital – jugal area is obscured. There is no reason to believe that this latter region is any different from that described in *R. megacephalus* (Cruickshank

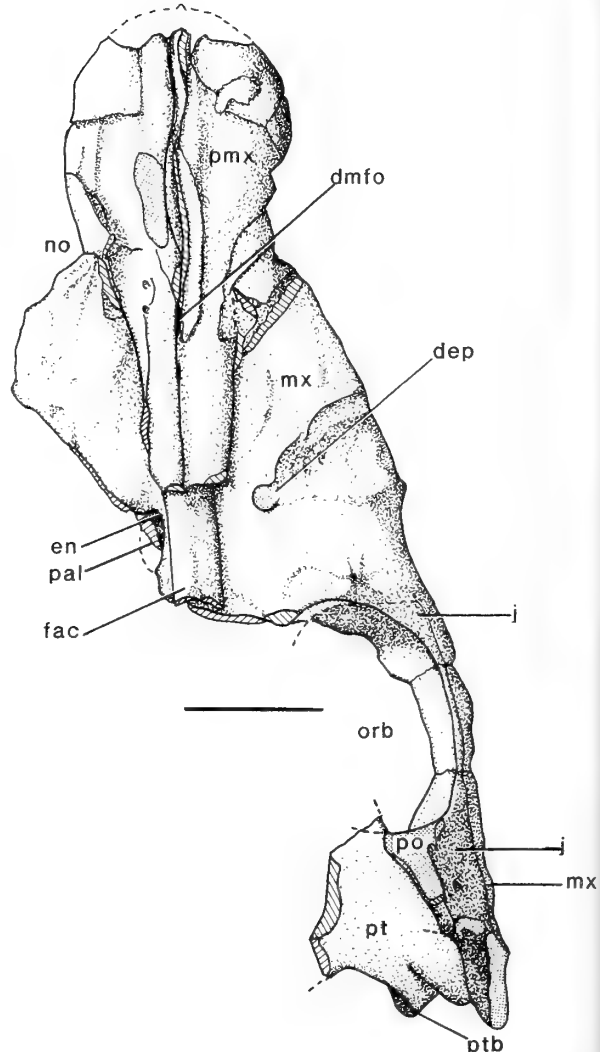


Fig. 1 *Rhomaleosaurus thorntoni* Andrews; dorsal view of the skull; scale bar = 100mm. For abbreviations on this and the other figures, see Table 1.

1994a), or indeed the Kimmeridgian species *Pliosaurus brachyspondylus* (Taylor & Cruickshank 1993b).

The anterior palatal surface shows much less damage. A very few fully erupted (mature) teeth are still in their sockets, but several replacement teeth are present, both in primary and secondary alveoli. The anteriormost edge of the anterior interpterygoid vacuity is visible, as is the lateral part of the outline of the right suborbital fenestra. The tooth sockets towards the rear of the maxilla become very indistinct and an accurate count is not possible, but at least 24 tooth positions can be identified, comprising five in each premaxilla plus 19 or 20 in the right maxilla.

Sutures between the individual bones of the palate cannot readily be distinguished except the premaxillae and maxillae. The vomers are substantial bones, forming a midline bar on the palate. Anteriorly they terminate in a horseshoe-shaped structure with several associated foramina. The vomers widen posteriorly, and are here flanked by grooves which run to the internal nares from fan-shaped areas just behind, and internal to, each diastema, opposite the notches where the premaxillae meet the maxillae. These fan-shaped areas are

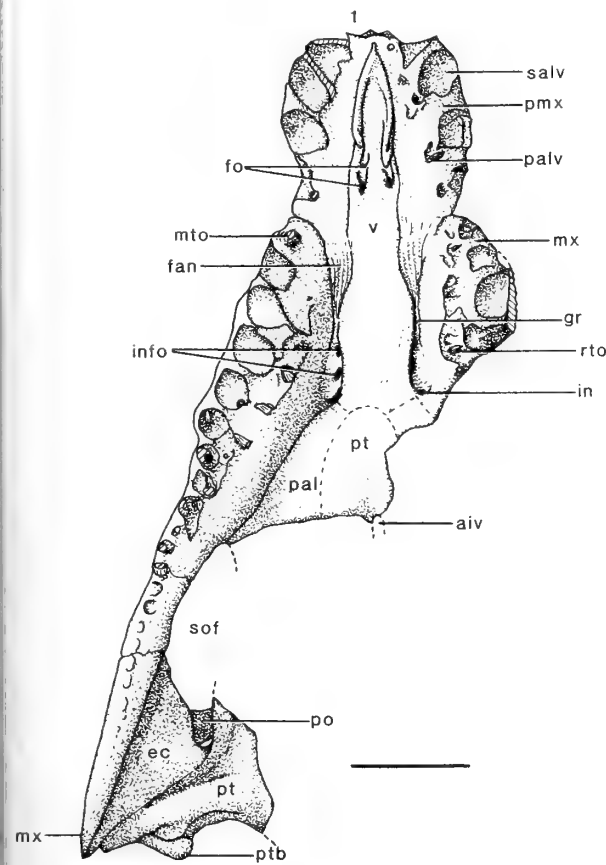


Fig. 2 *Rhomaleosaurus thorntoni* Andrews; ventral view of the skull; scale bar = 100 mm.

covered in a radiating set of shallow grooves, suggesting that they helped anchor the buccal lining.

These features of the internal narial region are different from those of *Pliosaurus brachyspondylus* and *R. megacephalus*, where the structure is more fully known (Cruickshank *et al.* 1991; Taylor & Cruickshank 1993b). In *P. brachyspondylus*, the internal nares lie at the end of grooves in the roof of the mouth, with two prominent oramina lying on the medial faces of the depression in front of each internal naris, all equally spaced. This is markedly different from *R. megacephalus*, where the internal nares lie at the ends of grooves, medial to, and parallel with, supplementary grooves which end in oramina. In neither of these species is there a fan-shaped area medial to the diastema, nor the extra foramina lying within the limits of the internal narial excavation, as illustrated here. As in all plesiosaurs which I have examined, the internal nares lie anterior to the external nares, inviting the explanation that the narial system acted as a hydrodynamically driven olfactory system, and was not used for respiration (Cruickshank *et al.* 1991). The internal nares in *R. zetlandicus* and *R. cramptoni* are not visible, being obscured by the rami of the lower jaw (Taylor 1992b), or matrix.

The badly disrupted posterior palatal elements show that there was a prominent pterygoid boss in exactly the same position as in *R. zetlandicus* (Taylor 1992a; b), and an ectopterygoid lying between the jugal and pterygoid.

Mandible (Figs 3, 4). Parts of the lower jaw preserved include an almost complete right ramus as far back as the end of the dentary, the symphysis and the left ramus to just behind the symphysis, plus a

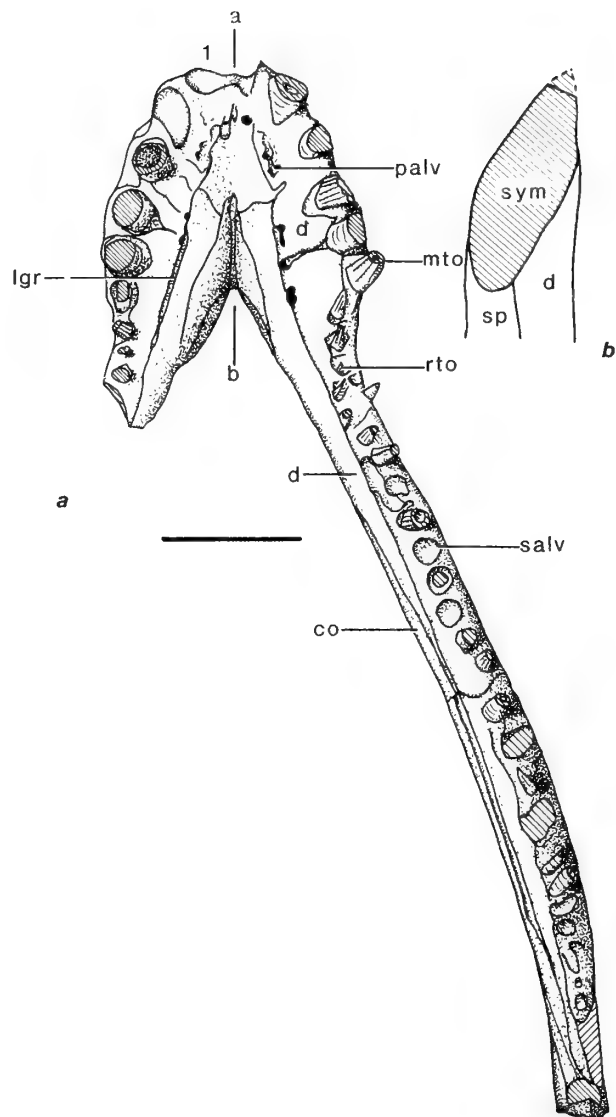


Fig. 3 *Rhomaleosaurus thorntoni* Andrews; lower jaw; 3a, dorsal view; 3b, section through symphysis on line a-b; scale bar = 100 mm.

portion of the middle of the left ramus and the left articular region (not illustrated). These portions of the lower jaw correspond almost exactly to the remains of the skull and no doubt represent what was saved during collection, from what must have been an almost complete cranium.

The symphysis occupies five tooth positions and a further 26 tooth positions can be counted in the right dentary. The general obscurity of sutures makes it difficult to identify individual bones, but as far as can be seen, the structure of this lower jaw is the same as that of *R. zetlandicus* (Taylor 1992b). There are both mature and replacement teeth present in the lower jaw, with their associated primary and secondary alveoli.

On the portion of the left jaw ramus containing the glenoid fossa, there is a large dorso-median trough on the prearticular and articular (Taylor 1992b: fig 7; Cruickshank 1994a: fig 7), which may be one of the determining characters of the genus *Rhomaleosaurus* (Taylor 1992a; Cruickshank 1994a).

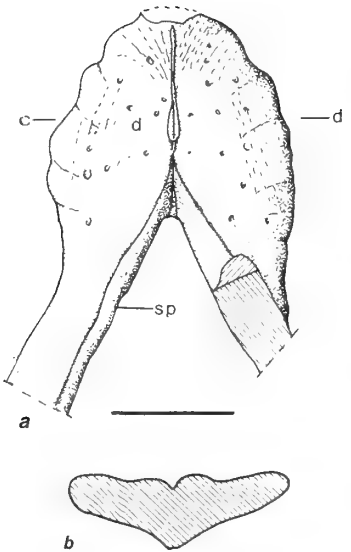


Fig. 4 *Rhomaleosaurus thorntoni* Andrews; symphysis of lower jaw; **4a**, ventral view; **4b**, section through symphysis on line *c-d*; scale bar = 100 mm.

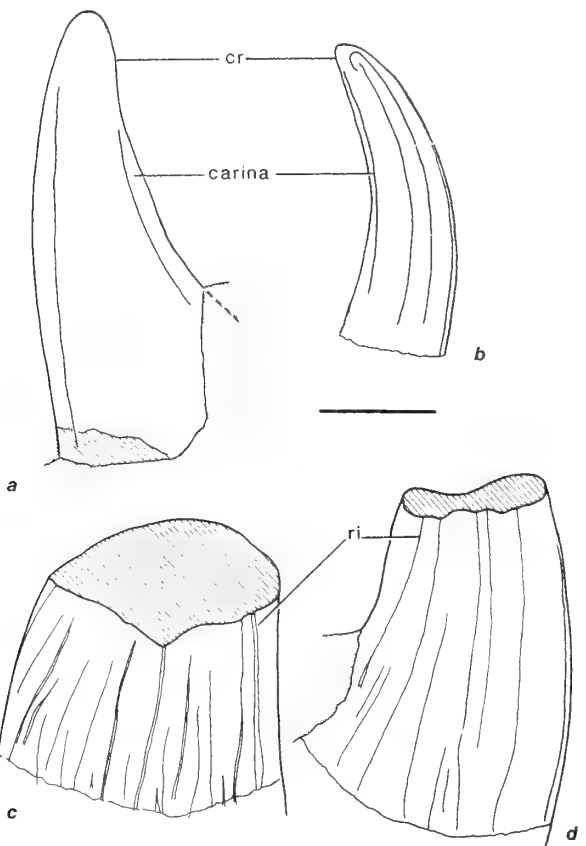


Fig. 5 *Rhomaleosaurus thorntoni* Andrews; teeth; **5a**, replacement tooth crown, position 9, right maxilla; **5b**, replacement tooth crown, position 24, right dentary; **5c**, mature tooth, position 12, right dentary; **5d**, mature tooth, position 8, right dentary; teeth are oriented with crowns towards top; drawn with an Abbé drawing apparatus on a Wild M3 stereomicroscope; scale bar = 5 mm.

Dentition (Fig. 5). The dentition is that of a powerful predator, with a rosette of interlocking, procumbent teeth in the premaxilla and lower jaw symphysis, followed by tooth-rows which, after two small median teeth, have large caniniforms in the upper jaw overlapping somewhat smaller teeth in the lower jaw. The tooth adjacent to the midline in both the upper and lower dentitions is much smaller than the more mesial teeth. In the lower jaw there is a marked reduction in size of teeth immediately behind the fifth position, which continues in a regular manner to the end of the tooth row on the dentary. In the upper jaw the fifth tooth position is very small, and is followed behind the diastema by another small tooth. Tooth positions seven, eight, nine and ten are very much larger caniniforms. Thereafter there is an even more marked reduction in tooth size, when compared with the lower dentition, until the sockets become difficult to distinguish. This arrangement is very similar to that of *R. zetlandicus* (Taylor 1992b), allowing for the incompleteness of that specimen.

It is possible to amplify the description of the individual teeth offered by Taylor (1992b), for *R. zetlandicus*. Those illustrated come from the 9th position on the right maxilla, showing the buccal surface (Fig. 5a); lying across the root of the 23rd tooth on the right ramus of the lower jaw (Fig. 5b); the 12th position of the right ramus of the lower jaw (Fig. 5c); and the 8th position of the right ramus of the lower jaw (Fig. 5d). Figs 5a and 5b are replacement teeth, whereas Figs 5c and 5d are erupted, mature teeth.

The crowns are covered in a coarse ornament, which reduces in number of ridges towards the tooth-tip, but which all seem to have carinae on mesial and distal surfaces. The ornament on these teeth is identical with those illustrated by Taylor (1992b: fig. 9), but quite different from the tooth illustrated by Cruickshank (1994a: fig. 10) for *R. megacephalus*, where the ornament is much finer and more closely spaced. The ridges are triangular in section, and some start slightly below the crown-root boundary.

DISCUSSION

Andrews (1922: 413) compared *R. thorntoni* with *R. cramptoni*, regretting that the shoulder girdle of the latter was not visible and that he could not therefore use it for comparative taxonomic purposes. The skull and vertebral column of each species seemed to be much the same, but he drew attention to the following differences between them. Firstly, he thought that the external nasal openings were much further in front of the eyes in *R. thorntoni* than in *R. cramptoni*. Secondly, he recognized differences in the platforms of their cervical neural arches: in *R. thorntoni* these are nearly horizontal, but in *R. cramptoni* they are strongly inclined. Thirdly, he pointed out that the humerus in *R. thorntoni* was relatively larger, with a more expanded distal end.

Neither of the external nasal openings are very obvious in *R. thorntoni*: that on the right side is obscured by the displaced facial processes of the premaxillae, and that on the left is only partly preserved and probably invisible before the skull was recently cleaned properly. However, there is the depression some distance in front of the right orbit which could have been mistaken for an external nares prior to full cleaning of the specimen, and this would agree with Andrews' identification of an unusually anteriorly placed external nasal opening. This depression is floored with crushed bone, and does not penetrate onto the underside of the dermal bone of the snout. Restoration of the snout region (Fig. 6c) using information now available, shows the external nares to be situated in normal position relative to the orbits.

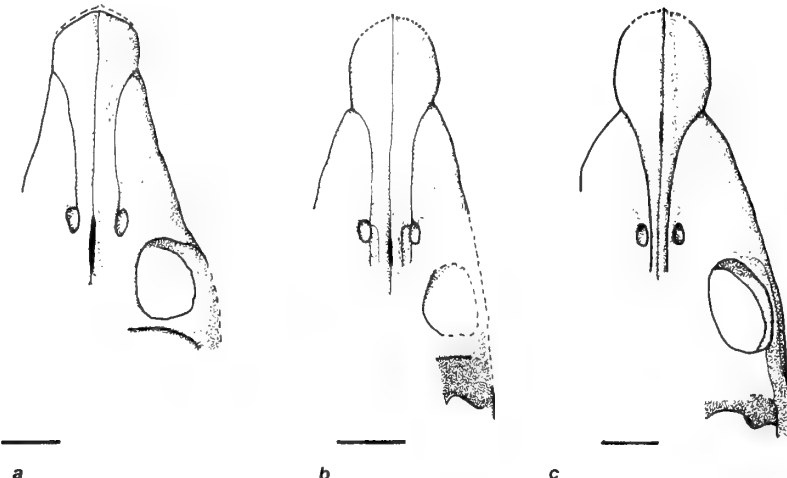


Fig. 6 Outline reconstructions of the anterior portion of skulls; **6a**, *Rhomaleosaurus cramptoni* (Carte & Baily, 1863), from a photograph of the type NMING F8785; **6b**, *Rhomaleosaurus zetlandicus* (Phillips, in Anon, 1854), after Taylor 1992b; **6c**, *Rhomaleosaurus thorntoni* Andrews, 1922; scale bars = 100 mm.

The differences in orientation of the zygapophyses in the cervical vertebrae of Plesiosauria depend on their relative position in the neck. In general the zygapophyses of the anterior cervical vertebrae are horizontally oriented, becoming inclined after the first ten or so. For instance in MANCH LL8004, a specimen of *Macropelta longirostris* (Blake) (Broadhurst & Duffy 1971), there are about 32 cervical vertebrae, of which the first ten have horizontal zygapophyses, while the remainder have zygapophyses angled at about 45° to the horizontal. Liassic plesiosaurs in general seem to have between 28 and 32 cervical vertebrae. Even in the posteriormost cervicals, the rib articulations are placed close to the lower rim of the centra (Taylor & Cruickshank 1993a), and therefore could still appear to be from a more anterior position. Therefore, it is not always obvious from which part of the neck any single vertebra might come, and hence to draw conclusions about zygapophyseal orientation is premature.

The question of the characters of the humeri may well depend on the state of preservation of each. The skull and skeleton of *R. cramptoni* are very much less damaged than those of *R. thorntoni*, and it seems unwise to make strict taxonomic statements on this character without knowing more about individual variation within the genus *Rhomaleosaurus*.

Therefore, the principal points of difference between the two species can be interpreted as being due to either their relative state of preservation, their size, or to an unreliable character, as in the case of the neck vertebrae. On the basis of the foregoing discussion, both *R. cramptoni* and *R. thorntoni* are seen to belong to the same species. In addition they come from approximately the same horizon, in the Toarcian stage of the Liassic (Lower Jurassic) of England.

One other similar pliosauroid is known from the Yorkshire (Eng-and) Toarcian, *R. zetlandicus* (Phillips, in Anon, 1854) (Taylor 1992a). Reconstructions of part of the skulls of *R. thorntoni*, *R. zetlandicus* and *R. cramptoni* are shown for comparison (Figs 6a–c). The relevant differences lie in the overall size of each and in the apparent width of the postorbital bar; in *R. thorntoni* it is relatively wider than in *R. zetlandicus* and *R. cramptoni*, but as all specimens are variously damaged in that area, no firm conclusions can be reached on this character. All specimens have the same short, broad snout, which contrasts with the more slender, relatively longer snout

of the Hettangian *R. megacephalus* (LEICS G221.1851) (Cruickshank 1994a). The Toarcian specimens have similar dentition, possessing sparsely ridged teeth, which also contrasts with those of *R. megacephalus*.

Taking all three Toarcian species together (Fig. 6), it is probable that they represent only size variants of the same species. They are conspecific and should be referred to the single species *Rhomaleosaurus zetlandicus* (Phillips, in Anon, 1854), which has date priority.

In Fig. 6, which compares that part of the skull preserved in R4853 with the other two types, it will be noted that the premaxillaries of R4853 are apparently narrower than those of the other two specimens. The reconstruction was effected using the most conservative measurements, and perhaps this is reflected in a false narrowing of the premaxillary facial processes. It is not likely that, for instance, any conclusions can be drawn from such a reconstruction concerning growth rates, or sexual dimorphism.

SUMMARY AND CONCLUSIONS

- 1 The skull of the type specimen of *Rhomaleosaurus thorntoni* Andrews, 1922, from the Toarcian of Northamptonshire, is illustrated for the first time. Additional information concerning details of its external nares, and reassessment of other characters discussed in the original description, make it difficult to sustain its supposed differences from *R. cramptoni* (Carte & Baily, 1863) from the Toarcian of Yorkshire.
- 2 Comparisons with the type of *R. zetlandicus* (Phillips, in Anon, 1854), also from the Toarcian of Yorkshire, indicate that *R. thorntoni* is merely a larger specimen of *R. zetlandicus*.
- 3 Since all three specimens are shown here to belong to the same species, the correct name for it is *Rhomaleosaurus zetlandicus* (Phillips, in Anon, 1854).
- 4 *Rhomaleosaurus zetlandicus* was the top predator in the Upper Lias of England. *R. megacephalus* from the Rhaetian or Hettangian (Lower Lias) has a longer, more slender snout, and different dentition.

ACKNOWLEDGEMENTS. The type of *Rhomaleosaurus thorntoni* was cleaned at the Natural History Museum, London, under the direction of Dr Angela Milner, at the request of Dr Michael Taylor. I am grateful to Dr Milner for the loan of this specimen, and for access to the mounted cast of the type of *R. cramptoni* (BMNH R34) in the Natural History Museum, and to Dr Taylor for discussion and access to his collection of reference slides. Mr John Martin, Keeper of Earth Sciences, and the Director of the Leicestershire Museums Service provided facilities for the work to be undertaken. The assistance of Mrs Anne Montgomery of the Geology Department, University of Leicester is gratefully acknowledged. Mr Nigel Monaghan (NMING) cheerfully supplied photographs of the type of *R. cramptoni*. John Martin, David Brown, Angela Milner and Michael Taylor read drafts of the manuscript, to its great improvement. The work was done during the tenure of a Leverhulme Fellowship awarded to Dr M A Taylor.

REFERENCES

- Andrews, C. W.** 1922. Notes on the skeleton of a large plesiosaur (*Rhomaleosaurus thorntoni* sp.n) from the Upper Lias of Northamptonshire. *Annals and Magazine of Natural History*, **9**, 10: 407–415.
- Anon** 1854. Report of the Council of the Yorkshire Philosophical Society. *Annual Report of the Yorkshire Philosophical Society for 1853*: **7**, **8**.
- Benton, M. J. & Taylor, M.A.** 1984. Marine reptiles from the Upper Lias (Lower Toarcian, Lower Jurassic) of the Yorkshire coast. *Proceedings of the Yorkshire Geological Society*, **44**: 399–429.
- Broadhurst, F. M. & Duffy, L.** 1971. A plesiosaur in the Geology Department, University of Manchester. *Museums Journal*, **70**: 30–31.
- Brown, D. S.** 1981. The English Upper Jurassic Plesiosauroidea (Reptilia) and a review of the phylogeny and classification of the Plesiosauria. *Bulletin of the British Museum (Natural History), (Geology Series)*, **35**: 253–347.
- Carte, A. & Baily, W. H.** 1863. Description of a new species of *Plesiosaurus* from the Lias, near Whitby, Yorkshire. *Journal of the Royal Dublin Society*, **4**: 160–170.
- Cruickshank, A. R. I.** 1994a. Cranial anatomy of the Lower Jurassic pliosaur *Rhomaleosaurus megacephalus* (Stutchbury) (Reptilia; Plesiosauria). *Philosophical Transactions of the Royal Society of London, (B)* **343**: 247–260.
- 1994b. A juvenile plesiosaur (Plesiosauria: Reptilia) from the Lower Lias (Hettangian: Lower Jurassic) of Lyme Regis, England: a plesauroid–plesiosauroid intermediate? *Zoological Journal of the Linnean Society of London*, **112**: 151–178.
- Small, P. G. & Taylor, M. A.** 1991. Dorsal nostrils and hydrodynamically driven underwater olfaction. *Nature, London*, **352**: 62–64.
- Phillips, J.** 1854. On a new *Plesiosaurus* in the York Museum. *Annual Report of the British Association for the Advancement of Science for 1853*, 54.
- Stutchbury, S.** 1846. Description of a new species of *Plesiosaurus* in the Museum of the Bristol Institution. *Quarterly Journal of the Geological Society of London*, **2**: 411–417.
- Taylor, M. A.** 1992a. Taxonomy and taphonomy of *Rhomaleosaurus zetlandicus* (Plesiosauria: Reptilia) from the Toarcian (Lower Jurassic) of the Yorkshire coast. *Proceedings of the Yorkshire Geological Society*, **49**: 49–55.
- 1992b. Functional anatomy of the head of the large aquatic predator *Rhomaleosaurus zetlandicus* (Plesiosauria: Reptilia) from the Toarcian (Lower Jurassic) of Yorkshire. *Philosophical Transactions of the Royal Society of London, (B)* **335**: 247–280.
- & **Cruickshank, A. R. I.** 1989. The Barrow Kipper, '*Plesiosaurus' megacephalus*' (Plesiosauria: Reptilia) from the Lower Lias (Lower Jurassic) of Barrow upon Soar, Leicestershire. *Transactions of the Leicester Literary & Philosophical Society*, **83**: 20–24.
- & — 1993a. A plesiosaurian reptile from the Linksfield erratic (Rhaetian: Upper Triassic) of Morayshire. *Scottish Journal of Geology*, **29**: 191–196.
- & — 1993b. Cranial anatomy and functional morphology of *Pliosaurus brachyspondylus* (Reptilia; Plesiosauria) from the Upper Jurassic of Westbury, Wiltshire. *Philosophical Transactions of the Royal Society of London, (B)* **341**: 399–418.

The first known femur of *Hylaeosaurus armatus* and re-identification of ornithopod material in The Natural History Museum, London

PAUL M. BARRETT

Department of Earth Sciences, University of Cambridge, Downing Street, Cambridge CB2 3EQ

SYNOPSIS. The first known femur of the British Lower Cretaceous ornithopod dinosaur *Hylaeosaurus armatus* Mantell, 1833 is described. The status of *Campitosaurus valdensis* (Lydekker, 1889) is reviewed, and it is suggested that it might be senior synonym of *Valdosaurus canaliculatus* (Galton 1975).

INTRODUCTION

The purpose of this brief paper is to report and describe the first recognised femur of the nodosaurid ankylosaur *Hylaeosaurus armatus* Mantell 1833, and to clarify the taxonomic position of several ornithopod specimens. The status of *Campitosaurus valdensis* (Lydekker 1889) is also reviewed and it is provisionally placed in synonymy with *Valdosaurus canaliculatus* (Galton 1975). Unless otherwise stated, all of the specimens described are of Wealden (Lower Cretaceous) age and are from the Isle of Wight, England. They belong to the Fox Collection housed in the Department of Palaeontology, The Natural History Museum, London (NHM; register numbers prefixed BMNH in this paper).

SYSTEMATIC PALAEONTOLOGY

DINOSAURIA Owen 1841

ORNITHISCHIA Seeley 1887

THYREOPHORA Nopsca 1915, *sensu* Sereno 1986

ANKYLOSAURIA Osborn 1923

Family NODOSAURIDAE Marsh 1890

Genus **HYLAEOSAURUS** Mantell 1833a

TYPE AND ONLY SPECIES. *Hylaeosaurus armatus* Mantell 1833b; Lower Cretaceous (Upper Valanginian), East and West Sussex, southern England.

***Hylaeosaurus armatus* Mantell 1833**

Fig. 1

1833b *Hylaeosaurus armatus* Mantell: 328.

HOLOTYPE. BMNH R3775, the anterior part of a skeleton embedded in a block of matrix.

HORIZON AND LOCALITY. Hastings Beds (Lower Wealden), Upper Valanginian, Lower Cretaceous (Rawson *et al.* 1978). Tilgate Forest, Cuckfield, West Sussex, England.

REFERRED MATERIAL. As listed by Pereda-Suberbiola (1993) and BMNH R604k (now registered as BMNH R12555), the distal portion of a right femur.

DESCRIPTION AND COMPARISON. The distal portion of a large right femur (Fig. 1a), BMNH R604k (Dawson Collection), from the Wealden, near Hastings, East Sussex, may represent the first recognised femur of *Hylaeosaurus armatus*.

This specimen was originally identified as *Iguanodon* sp.¹ but was later referred to as a large individual of *Hypsilophodon foxii* (Huxley) by Molnar & Galton (1986). However, the femur is much more massive than that of *H. foxii*, and the absence of a marked anterior intercondylar groove suggests that it is not referable to *Iguanodon*. The absence of ridges running up the femoral shaft from the condyles supports the view that R604k is not referable to either of these genera. There is a marked posterior intercondylar groove and the lateral and medial condyles extend equal distances posteriorly from the femoral shaft. The lateral condyle is much more massive than the medial one, and there is a distinct 'step' between the medial condyle and the medial extremity of the femur (Fig. 1b). The femur bears a strong resemblance to that of the Oxfordian nodosaur *Cryptodraco eumerus* (Galton 1983) which also displays a 'step' between the medial condyle and the medial border of the femur. BMNH R604k can be distinguished from the femora of the other known Wealden nodosaur *Polacanthus foxii* (BMNH R175) by a number of features. For example, *Polacanthus* shows no 'step' medial to the medial condyle, and the medial condyle is more massive in *Polacanthus* than in BMNH R604k. It seems unlikely, therefore, that BMNH R604k is referable to *Polacanthus*. It is suggested that BMNH R604k is not ornithopod as previously supposed but thyreophoran, and the locality and the horizon from which the specimen was recovered suggests that it is referable to *Hylaeosaurus*. The relatively small size of the femur (only 83mm across the distal end) suggests that it belonged to a juvenile (W. Blows, pers. comm.). Unfortunately, due to the fragmentary nature of the specimen, this assignment can only be tentative. Nonetheless, the femur provides valuable information on the alleged synonymy of *Hylaeosaurus* and *Polacanthus* (Coombs 1971, Blows 1987, Coombs & Maryanska 1990, Pereda-Suberbiola 1991, 1993).

Coombs (1971) and Coombs & Maryanska (1990) suggested that

¹Lydekker (1888) listed a number of specimens as BMNH R604a–e. These registered numbers include a number of theropod, ornithopod and ankylosaur remains, all of which come from the Wadhurst Clay near Hastings and are part of the Dawson Collection. The femur in question is labelled BMNH R604k. There is no record of this number in either Lydekker (1888) or in the accessions catalogues of the Natural History Museum (S. Chapman pers. comm.). The specimen label identified the femur as *Iguanodon* sp. from the Wadhurst Clay near Hastings.



1a



1b

Fig. 1 *Hylaeosaurus armatus* Mantell. Right femur, distal end; BMNH R12555; **1a**, posterior view, $\times 0.7$; **1b**, distal view (note the 'step' medial to the medial condyle), $\times 0.8$.

Polacanthus is a junior synonym of *Hylaeosaurus*. However, these authors claimed that no homologous elements are present in the holotype material of *Hylaeosaurus* and *Polacanthus* so the proposed synonymy was based largely on the similar geographical and stratigraphical distributions of these genera. In contrast, Blows (1987) suggested that the two genera are stratigraphically distinct, with *Hylaeosaurus* originating from the Hastings Beds (Valanginian) of East Sussex, whilst *Polacanthus* remains have been recovered from the Wessex Formation (Barremian) in the Isle of Wight. He also suggested that the arrangement of the dermal armour differs between the two genera.

Recently it has been proposed that the North American nodosaur *Hoplitosaurus* is a junior synonym of *Polacanthus* (Pereira-Suberbiola 1991, 1993). A specific separation, based on femoral characters, is retained to distinguish the British form (*P. foxii*) from the North American form (*P. marshi* Lucas, 1901). If these two genera are genuinely synonymous then a number of elements referred to *P. (=Hoplitosaurus) marshi* that were previously unknown in the holotype of *P. foxii* (e.g. humerus and scapula) can be used for comparison with *Hylaeosaurus*. Comparisons of the pectoral girdle, forelimb, hindlimb and dermal armour led Pereira-Suberbiola (1991, 1993) to the conclusion that *Hylaeosaurus* and *Polacanthus* were distinct genera.

If BMNH R604k does belong to *Hylaeosaurus*, this would provide another point of comparison between these two genera. The

characters listed above suggest that *Polacanthus* and *Hylaeosaurus* can be distinguished on femoral characters, adding weight to the arguments of Blows (1987) and Pereira-Suberbiola (1993). This specimen has been re-registered as BMNH R12555 in order to avoid confusion with other specimens allotted to BMNH R604, which contains a variety of other specimens from the same locality including *Iguanodon* remains (Lydekker 1888).

ORNITHOPODA Marsh 1881
Family **DRYOSAURIDAE** Milner & Norman 1984
Genus **VALDOSAURUS** Galton 1977

TYPE SPECIES. *Dryosaurus canaliculatus* Galton 1975; Lower Cretaceous (Valanginian-Barremian), West Sussex and Isle of Wight, southern England.

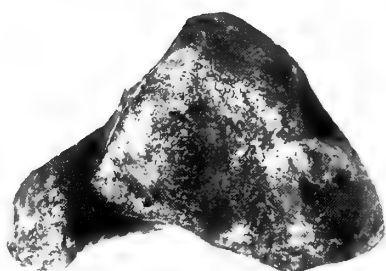
Valdosaurus canaliculatus (Galton 1975)

- 1975 *Dryosaurus? canaliculatus* Galton: 747.
1977 *Valdosaurus canaliculatus* (Galton); Galton: 231.
1982 *Valdosaurus canaliculatus* (Galton); Galton & Taquet: 147.

Fig. 2



2a



2b

Fig. 2 *Valdosaurus canaliculatus* (Galton). Left femur, proximal end, BMNH R12440; note the deep cleft and wide separation between the lesser and greater trochanters. **2a**, postero-medial view; **2b**, proximal view; $\times 1$.

HOLOTYPE. BMNH R184 and BMNH R185, associated left and right femora.

HORIZON AND LOCALITY. Hastings Beds, Upper Valanginian, Lower Cretaceous (Rawson *et al.* 1978). Tilgate Forest, Cuckfield, West Sussex, England. Wealden Shales, Barremian, Lower Cretaceous (Rawson *et al.* 1978), Isle of Wight, England.

REFERRED MATERIAL. Specimens listed by Galton (1975), Galton & Taquet (1982), BMNH R167 an incomplete left femur (see below) and BMNH R170 (now registered as BMNH R12440) the proximal portion of a right femur (see below).

DESCRIPTION AND COMPARISON

Lydekker (1888) referred a number of unassociated limb bone fragments (BMNH R170) to *Hypsilophodon foxii* (Huxley). Galton (1975) noted that two of the femoral fragments within BMNH R170 differed significantly from the majority of femora attributed to this genus. In *H. foxii* the distal end of the femur has a moderate posterior intercondylar groove and lacks an appreciable anterior intercondylar groove. Proximally, the lesser trochanter is separated from the greater trochanter by a narrow cleft (Galton 1974). Galton (1975) showed that the two specimens in question possess a distinct anterior intercondylar groove and he referred these specimens (now registered as BMNH R8420 and BMNH R8421) to *Valdosaurus* (=*Dryosaurus*) *canaliculatus*, a dryosaur from the Wealden of the Isle of Wight (Galton 1977, Galton & Taquet 1982). Examination of the specimens remaining within BMNH R170 has yielded a proximal femoral fragment (Fig. 2a) in which the lesser trochanter is separated from the greater trochanter by a deep cleft (Fig. 2b). This feature is characteristic of the Dryosauridae (*sensu* Sues & Norman 1990) and the locality and horizon from which the specimen comes suggests that it is referable to *Valdosaurus canaliculatus*, BMNH R12440. Several limb bone fragments attributable to *H. foxii* remain as BMNH R170.

Galton (1975) suggested that a small right tibia (BMNH R124), previously listed as *Iguanodon* sp. (Lydekker 1888) was also referable to *H. foxii*. However, the form of the proximal end of BMNH R124 appears to be more similar to that of *Iguanodon* than to that of *H. foxii*. In *Iguanodon* the cnemial crest is longer than in *H. foxii*. In addition, the cnemial crest of *Iguanodon* swings laterally near its anterior margin (see Fig. 3). On the basis of these characters BMNH R124 is referred to *I. cf. atherfieldensis* Hooley. The small size of the specimen suggests that it belonged to a juvenile.

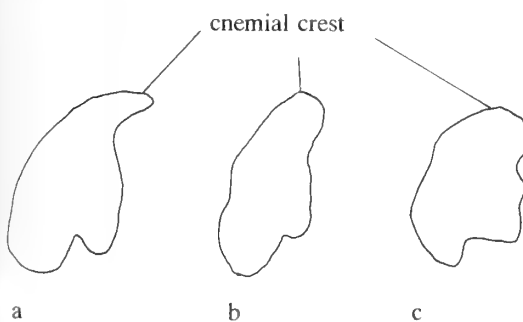


Fig. 3 Proximal right tibiae; 3a, b, *Iguanodon atherfieldensis* Hooley, 1924; 3a, after Norman 1986, 3b, BMNH R124; 3c, *Hypsilophodon foxii* (Huxley), after Galton 1974; anterior is towards the top; drawings not to scale.

ON THE STATUS OF *CAMPTOSAURUS VALDENSIS* (Lydekker, 1889)

The femur BMNH R167 (Fig. 4) has proved something of an enigma. Lydekker (1888) listed it as *H. foxii*, but suggested that it may represent a distinct species of *Hypsilophodon* due to its greater size. Later, Lydekker (1889) suggested that BMNH R167 shared a number of similarities with the femur of his new species *Camptosaurus leedsi*, and he designated BMNH R167 the holotype of another new species, *Camptosaurus vallensis*. However, Gilmore (1909) noted several differences between *C. vallensis* and the North American *Camptosaurus dispar* Marsh, 1879 (the type species of the genus). For example, the fourth trochanter of *C. dispar* is situated on the distal half of the femoral shaft, whilst in *C. vallensis* the fourth trochanter is more proximally placed. Galton (1974) suggested that this and several other features indicated that BMNH R167 was not referable to *Camptosaurus*, but was in fact a large specimen of *H. foxii*. The use of *C. leedsi* as a representative specimen for *Camptosaurus* was also in error. Galton (1980) showed that the holotype of *C. leedsi* (a femur, BMNH R1993) differs from North American *Camptosaurus* in lacking a deep anterior intercondylar groove and by having a proximally placed fourth trochanter. Due to these and other features, Galton (1980) made *Camptosaurus leedsi* the type species of a new genus *Callovosaurus*, which is now regarded as *Camptosauridae nomen dubium* (Norman & Weishampel 1990). Placing *Camptosaurus vallensis* is difficult as the areas that provide most of the features used in distinguishing between ornithopod femora, the form of the distal end and the shape and position of the lesser trochanter, are either missing or badly damaged. Sues & Norman (1990), in their recent review of the Hypsilophodontidae, regard BMNH R167 as *Hypsilophodontidae nomen dubium*. It is suggested here that *Camptosaurus vallensis*

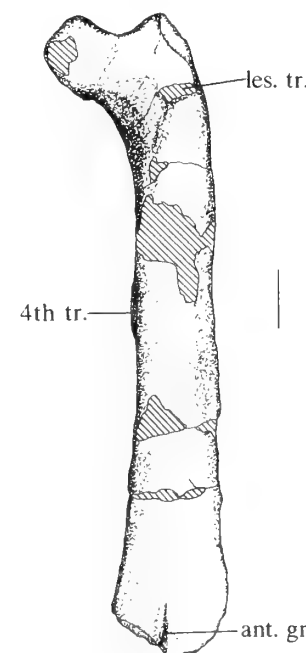


Fig. 4 *Camptosaurus vallensis* (Lydekker, 1889). BMNH R167, anterior view, showing the anterior intercondylar groove; abbreviations: ant.gr. = anterior intercondylar groove, les.tr. = position of lesser trochanter, 4th tr. = fourth trochanter; scale bar = 20 mm.

(Lydekker, 1889) may be a senior synonym of the dryosaur *Valdosaurus canaliculatus* (Galton, 1975), as the beginnings of a marked intercondylar groove can be seen on the anterior face of the distal end of the femoral shaft (*contra* Galton 1974). This assignment is tentative as many diagnostic features are lacking on the specimen.

ACKNOWLEDGEMENTS. My sincere thanks to Dr. Angela Milner and Sandra Chapman of the Natural History Museum, London for their continual help throughout the course of this work. Dr. Milner read several earlier drafts of this paper and made many useful comments. Dr. David Norman and Mr. William Blows provided useful discussion and an anonymous reviewer made constructive comments on a draft of this paper. Photographs were provided by the Photographic Unit of the Natural History Museum. Much needed artistic and photographic advice was provided by Hilary Alberti and Dudley Simmons. This paper results from work undertaken during a Natural History Museum vacation studentship, and was written during the tenure of a NERC studentship (GT4/93/128/G) at the University of Cambridge (Department of Earth Sciences).

REFERENCES

- Blows, W.T.** 1987. The armoured dinosaur *Polacanthus foxxii* from the Lower Cretaceous of the Isle of Wight. *Palaeontology*, **30** (3): 557–580.
- Coombs, W.P.** 1971. The Ankylosauria. Ph.D. thesis (unpublished), University of Columbia, 487pp.
- & **Maryanska, T.** 1990. Ankylosauria. In Weishampel, D.B., Dodson, P. & Osmolska, H. (Eds.) *The Dinosauria*. University of California Press, Berkeley: 456–483.
- Galton, P.M.** 1974. The ornithischian dinosaur *Hypsilophodon* from the Wealden of the Isle of Wight. *Bulletin of the British Museum (Natural History), Geology*, **25**: 1–152.
- 1975. English hypsilophodontid dinosaurs (Reptilia; Ornithischia). *Palaeontology*, **18**: 741–752.
- 1977. The ornithopod dinosaur *Dryosaurus* and a Laurasia – Gondwanaland connection in the Upper Jurassic. *Nature*, **268**: 230–232.
- 1980. European Jurassic ornithopod dinosaurs of the families Hypsilophodontidae and Camptosauridae. *Neues Jahrbuch für Geologie und Paläontologie. Stuttgart. Abhandlungen*, **160**: 73–95.
- 1983. Armoured dinosaurs (Ornithischia; Ankylosauria) from the Middle and Upper Jurassic of Europe. *Palaeontographica A*, **182**: 1–25.
- & **Taquet, P.** 1982. *Valdosaurus*, a hypsilophodontid dinosaur from the Lower Cretaceous of Europe and Africa. *Geobios*, **15**: 147–159.
- Gilmore, C.W.** 1909. Osteology of the Jurassic reptile *Camptosaurus*, with a revision of the species of the genus, and a description of two new species. *Proceedings of the United States National Museum*, **36**: 197–332.
- Lydekker, R.** 1888. *Catalogue of the Fossil Reptilia and Amphibia in the British Museum: Part I*. British Museum (Natural History), London. 309pp.
- 1889. On the remains and affinities of five genera of Mesozoic reptiles. *Quarterly Journal of the Geological Society of London*, **45**: 41–59.
- Mantell, G.A.** 1833a. Observations on the remains of the *Iguanodon*, and other fossil reptiles, of the strata of Tilgate Forest in Sussex. *Proceedings of the Geological Society of London*, **1**: 410–411
- 1833b. *The Geology of the South-East of England*. Longman, London. xix + 376pp.
- Molnar, R.E. & Galton, P.M.** 1986. Hypsilophodontid dinosaurs from Lightning Ridge, New South Wales, Australia. *Geobios*, **19**: 231–239.
- Norman, D.B.** 1986. On the anatomy of *Iguanodon atherfieldensis* (Ornithischia; Ornithopoda). *Bulletin de l'Institut Royal des Sciences naturelles de Belgique: Sciences de la Terre*, **56**: 281–372.
- & **Weishampel, D.B.** 1990. Iguanodontidae and related ornithopods. In Weishampel, D.B., Dodson, P. & Osmolska, H. (Eds.) *The Dinosauria*. University of California Press, Berkeley: 510–533.
- Pereda-Suberbiola, J.** 1991. Nouvelle évidence d'une connexion terrestre entre Europe et Amérique du Nord au Crétace inférieur: *Hoplitosaurus*, synonyme de *Polacanthus* (Ornithischia: Ankylosauria). *Comptes Rendus de l'Académie de Sciences de Paris (Series 2)*, **313**: 971–976.
- 1993. *Hylaeosaurus*, *Polacanthus*, and the systematics and stratigraphy of Wealden armoured dinosaurs. *Geological Magazine*, **130**: 767–781.
- Rawson, P.F., Curry, D., Dilley, F.C., Hancock, J.M., Kennedy, W.J., Neale, J.W., Wood, C.J. & Worsam, B.C.** 1978. A correlation of Cretaceous rocks in the British Isles. *Geological Society of London, Special Report*, **9**: 1–70.
- Sues, H-D. & Norman, D.B.** 1990. Hypsilophodontidae, *Tenontosaurus*, Dryosauridae. In Weishampel, D.B., Dodson, P. & Osmolska, H. (Eds.) *The Dinosauria*. University of California Press, Berkeley: 498–509.

Bryozoa from the Lower Carboniferous (Viséan) of County Fermanagh, Ireland

PATRICK N. WYSE JACKSON

Department of Geology, Trinity College, Dublin 2, Ireland

CONTENTS

Introduction	120
Previous work	120
Material	120
Systematic Palaeontology	122
Order CRYPTOSTOMATA	122
Genus <i>Hexites</i> Shulga-Nesterenko, 1955	122
<i>Hexites paradoxus</i> sp. nov.	123
Genus <i>Nematopora</i> Ulrich, 1888a	124
<i>Nematopora hibernica</i> sp. nov.	124
Genus <i>Pseudonematopora</i> Balakin, 1974	125
<i>Pseudonematopora planatus</i> sp. nov.	126
Genus <i>Rhabdomeson</i> Young & Young, 1874	128
<i>Rhabdomeson progracile</i> Wyse Jackson & Bancroft, 1995	128
<i>Rhabdomeson rhombiferum</i> (Phillips, 1836)	128
Genus <i>Rhombopora</i> Meek, 1872	129
<i>Rhombopora cylindrica</i> sp. nov.	129
<i>Rhombopora hexagona</i> sp. nov.	132
Genus <i>Streblotrypa</i> (Ulrich MS.) Vine, 1884	135
<i>Streblotrypa (S.) pectinata</i> Owen, 1966	136
Genus <i>Clausotrypa</i> Bassler, 1929	137
<i>Clausotrypa ramosa</i> (Owen, 1973) comb. nov.	137
Order FENESTRATA	139
Genus <i>Baculopora</i> Wyse Jackson, 1988	139
<i>Baculopora megastoma</i> (M'Coy, 1844)	139
Genus <i>Diplopatoria</i> Nickles & Bassler, 1900	140
<i>Diplopatoria marginalis</i> (Young & Young, 1875)	140
<i>Diplopatoria tenella</i> Wyse Jackson, 1988	141
Genus <i>Ichthyorachis</i> M'Coy, 1844	142
<i>Ichthyorachis newenhami</i> M'Coy, 1844	142
Genus <i>Thamniscus</i> King, 1849	143
<i>Thamniscus colei</i> Wyse Jackson, 1988	143
Genus <i>Rhombocladia</i> Rogers, 1900	143
<i>Rhombocladia dichotoma</i> (M'Coy, 1844) comb. nov.	144
Order TREPOSTOMATA	146
Genus <i>Leioclema</i> Ulrich, 1882	146
<i>Leioclema indentata</i> sp. nov.	146
Genus <i>Dyscritella</i> Girty, 1911	148
<i>Dyscritella miliaria</i> (Nicholson 1881)	148
Genus <i>Tabulipora</i> Young, 1883a	150
<i>Tabulipora urii</i> (Fleming, 1828)	150
<i>Tabulipora howsii</i> (Nicholson, 1881)	151
<i>Tabulipora minima</i> Lee, 1912	153
Genus <i>Stenophragmidium</i> Bassler, 1952	154
<i>Stenophragmidium</i> sp.	155
Order CYSTOPORATA	155
Genus <i>Fistulipora</i> M'Coy, 1849	155
<i>Fistulipora incrassata</i> (Phillips, 1836)	155
Genus <i>Sulcoretepora</i> d'Orbigny, 1849	157
<i>Sulcoretepora parallela</i> (Phillips, 1836)	158
Genus <i>Goniocladia</i> Etheridge, 1876	159
<i>Goniocladia cellulifera</i> (Etheridge, 1873)	159
Palaeoecology of the County Fermanagh bryozoan fauna	162

Comparison with other Asbian faunas	164
Patterns of bryozoan zoaria replacement by silica	164
Key to the identification of some Carboniferous Bryozoa	165
Acknowledgements	168
References	168

SYNOPSIS. A systematic appraisal of the partially silicified Lower Carboniferous bryozoan fauna of County Fermanagh has demonstrated a rich and diverse bryozoan fauna of which the fenestrate portion has been largely described earlier by other authors. This paper describes the remaining cryptostome, trepostome, and cystoporate elements of the fauna, as well as a few previously ignored fenestrate taxa.

24 species are described (9 cryptostome species; 6 fenestrate species; 6 trepostome species; and 3 cystoporate species) of which 6 are new species and 2 new combinations. The new species are the arthrostylid cryptostomes *Hexites paradoxus*, *Nematopora hibernica*, and *Pseudonematopora planatus*, the rhomboporid cryptostomes *Rhombopora cylindrica*, and *Rhombopora hexagona*, and the trepostome *Leioclema indentata*. The new combinations are *Clausotrypa ramosa* (Owen), and *Rhombocladia dichotoma* (M'Coy). For completeness brief descriptions are given of the following taxa, which have been described more fully elsewhere: *Rhabdomeson progracile* Wyse Jackson & Bancroft, *Baculopora megastoma* (M'Coy), *Diploporaria tenella* Wyse Jackson, *Thamniscus colei* Wyse Jackson, and *Fistulipora incrustans* (Phillips, 1836).

The genus *Leioclema* and the species *Streblytyna pectinata* Owen, *Diploporaria marginalis* (Young & Young), *Dyscritella miliaria* (Nicholson), *Tabulipora howsii* (Nicholson), and *Tabulipora minima* Lee are reported from Ireland for the first time. The following genera are reported from the British Isles for the first time: *Hexites*, *Pseudonematopora* and *Clausotrypa*. Lectotypes are designated for *Diploporaria marginalis* (Young & Young), *Ichthyorachis newenhami* M'Coy, *Rhombocladia dichotoma* (M'Coy), *Dyscritella miliaria* (Nicholson), *Tabulipora howsii* (Nicholson), and *Tabulipora minima* Lee. Nomenclature problems for several species have been clarified. A tabular and dichotomous key is given for the complete fauna (including taxa described earlier by other authors). Patterns of silicification show that replacement of calcified bryozoan zoaria by silica was delayed.

INTRODUCTION

Bryozoans comprise a significant component of Lower Carboniferous faunal assemblages in Ireland. However, they are often fragmentary in nature which has made them difficult to study. Nevertheless, Lower Carboniferous bryozoans have been the subject of research since the mid-1800s when M'Coy (1844) described many species. In the last thirty years recent studies (Miller 1961a, 1961b, 1962a, 1962b, 1963, Owen 1973, Tavener-Smith 1973, Olaloye 1974, Bancroft 1985, 1986b, Bancroft & Wyse Jackson 1995, Wyse Jackson 1988, Wyse Jackson & Bancroft 1995a) have resulted in the description of new taxa, the redescription of previously described taxa, and give detailed quantitative and statistical analysis of these taxa. While these studies have increased the biostratigraphical value of Carboniferous bryozoans from Ireland, there is still considerable work to be carried out to assess faunas of particular Brigantian stages.

This present study adds to the taxonomic diversity of bryozoans described from Ireland, and shows some similarities at generic level, to Lower Carboniferous faunas of the Russian Platform. This paper describes 24 bryozoan species of Lower Carboniferous (Viséan, Asbian) age from County Fermanagh, Ireland. An unusual nodular trepostome and a species of the cystoporate genus *Goniocladia*, that exhibits atypical branching patterns will be described elsewhere.

PREVIOUS WORK

The largely silicified fauna from County Fermanagh, dominated by bryozoans and brachiopods, has been the subject of several papers: Tavener-Smith (1965a) erected the genus *Ptilofenestella*, described a species of *Minilya* (1965b, 1981), noted the occurrence of ovicells in *Fenestella* (1966), described a new species of *Polypora* (1971), and monographed 32 species from eight genera of which three were new (1973). Olaloye (1974) examined the acanthocladiid element, describing nine species of *Penniretepora*, five being new. Three new fenestrate taxa that were discovered in the Carrick Lough fauna

during the present study have been described elsewhere (Wyse Jackson 1988), and two species of the cryptostome genus *Rhabdomeson* and the cystoporate taxon *Fistulipora incrustans* (Phillips, 1836) are described more fully by Wyse Jackson & Bancroft (1995a), and Bancroft & Wyse Jackson (1995).

MATERIAL

The bryozoans described in this study were collected at two localities, Carrick Lough and Sillees River (Fig. 1) from thin beds of pale grey and muddy limestones that have been assigned to the upper part of the Glencar Limestone (Brunton & Mason 1979, George *et al.* 1976) (Fig. 2). Nearly 50 kg of rock from Carrick Lough containing both silicified and calcified bryozoan zoaria was processed, and additionally many thousands of unsorted etched silicified specimens (from the Brunton and Tavener-Smith collections in the Natural History Museum) and a small number of limestone blocks (from the Mason collection in the Ulster Museum) were examined. A small number of silicified specimens extracted from limestone collected from drift deposits close to Lough Gara, County Roscommon were also included in this study.

Silicified bryozoan colonies were acid-etched from the surrounding limestones. Calcified bryozoan zoaria were extracted from the muddy limestone using the surfactant 'Quaternary O'. Specimens were then sorted by taxon and stored in cavity slides. Thin section and acetate peels were produced to examine the internal features of the bryozoans.

Type and other material from the Griffith Collection in the National Museum of Ireland, the Owen Collections in the Manchester (prefix LL) and Ulster Museums, the Vine Collection in the National Museum of Wales, Cardiff (prefix NMW), the Nicholson Collection in Aberdeen University (prefix AUGD), the National Museum of Scotland, Edinburgh (prefix RSM), the Whidborne and Porter Collections in the Sedgwick Museum, Cambridge (prefix SMC), and the Phillips Collection in the British Geological Survey, Keyworth (prefix BSG) was referred to for comparison with the

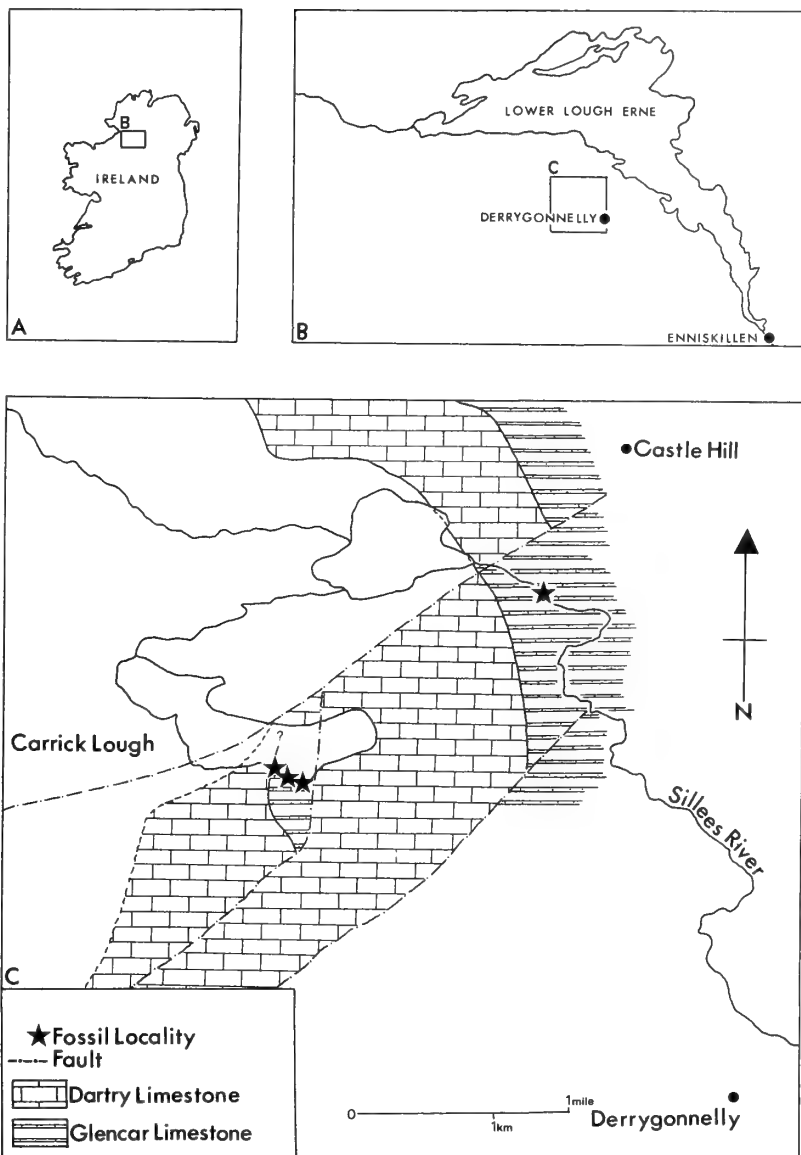


Fig. 1 Location map showing the collecting localities at Carrick Lough and Sillees River, County Fermanagh, Ireland.

study material. A number of taxa from these collections have been assigned and redescribed in the light of taxonomic work carried out on the County Fermanagh fauna.

Specimens have been deposited in a number of museums. The largest collection is lodged in the Natural History Museum, London (prefix BMNH PD). A voucher collection which includes some paratype material has been lodged in the Geological Museum, Trinity College Dublin (prefix TCD.). In addition some paratypes of a number of fenestrates (see Wyse Jackson 1988) have been deposited in the National Museum of Ireland (prefix NMING:F) and the Ulster Museum (prefix BELUM K).

Morphometric measurements for every taxon were taken on at least 12 specimens, if available, and up to ten measurements were made on each parameter on each specimen, using a Leitz binocular microscope fitted with a linear graticule at magnifications of be-

tween $\times 40$ and $\times 100$. The mean, standard deviation, and intracolonial and intercolonial coefficients of variation were computed and are tabulated within the description of each taxon. Abbreviations used in these tables are: CV = Coefficient of Variation; CVw = Intra (within) Colonial Variation; CVb = Inter (between) Colonial Variation; NM = Number of measurements; Mn = Minimum value recorded; Mx = Maximum value recorded; x = Mean value; N = Number of specimens measured; explanations for other abbreviations used are given in Figs 3, 18, 42, 59 and 84.

The measurement scheme for cryptostomes is modified from Newton (1971) (Figs 3, 18); for fenestrates from Tavener-Smith (1973) (Fig. 42); for trepostomes from Boardman (1960) and Cuffey (1967) (Fig. 59); and for cystoporates from Warner & Cuffey (1973) (Fig. 84).

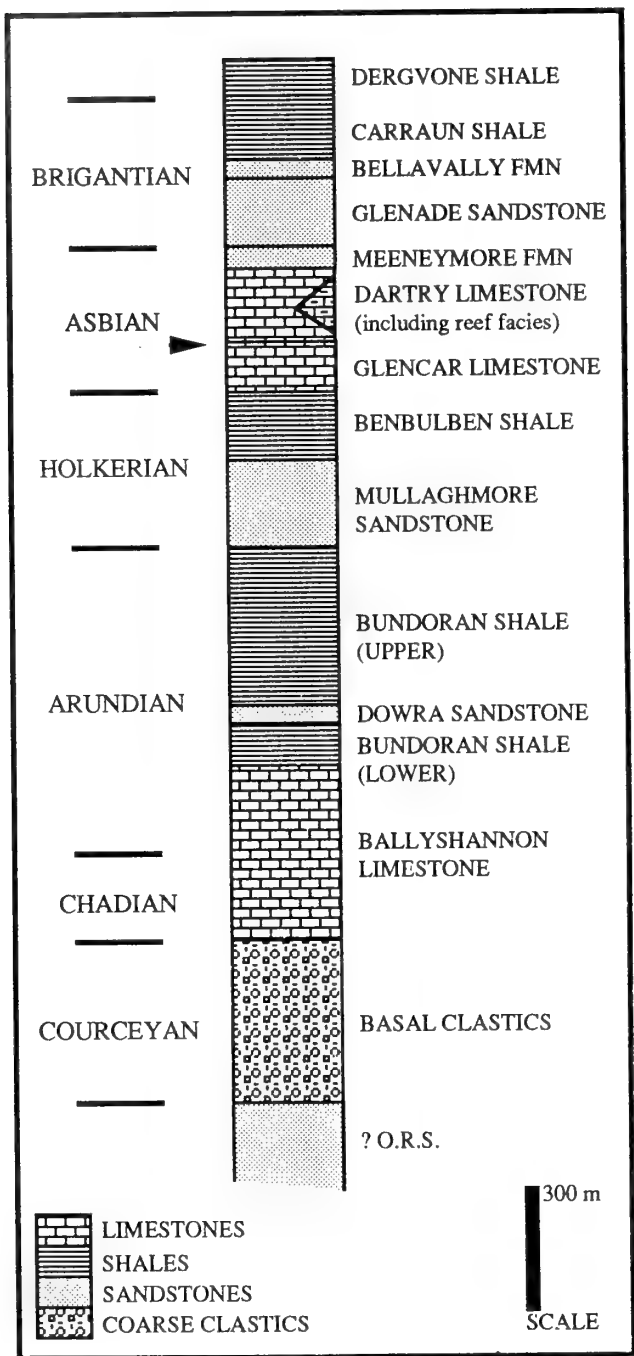


Fig. 2 Stratigraphical succession in west County Fermanagh. Bryozoan horizon at the top of the Glencar Limestone arrowed.

SYSTEMATIC PALAEONTOLOGY

During the course of this study three cases of misidentification of taxa in earlier described collections came to light. All cases have a bearing on the systematics of the Asbian bryozoan fauna described below. The first two cases of misidentification were those of

M'Coy (1844) who identified two Lower Carboniferous bryozoans as being conspecific with two Devonian taxa (*Millepora gracilis* and *Millepora similis*) described three years earlier by Phillips (1841). The Carboniferous taxa have been redescribed and named, below and elsewhere (Wyse Jackson & Bancroft, 1995a) as *Rhombopora cylindrica* sp. nov. and *Rhabdomeson progracile* respectively. *Millepora gracilis* as originally described by Phillips (1841) contains specimens herein considered to belong to two genera – *Rhabdomeson* and *Rhombopora*. The third case of misidentification is that of Owen (1966). *Rhombopora radialis* Owen, 1966 is synonymised with *Pseudonematopora turkestanica* (Nikiforova, 1948). More detailed discussion of the contrasting taxa is given in the discussion section of *Pseudonematopora planatus* sp. nov. and *Rhombopora cylindrica* sp. nov., and in Wyse Jackson & Bancroft (1995a).

For completeness brief descriptions are given of the following taxa which have been described more fully elsewhere: *Rhabdomeson progracile* Wyse Jackson & Bancroft 1995, *Rhabdomeson rhombiferum* (Phillips, 1841), *Baculopora megastoma* (M'Coy, 1844), *Diplopatoria tenella* Wyse Jackson, 1988, *Thamniscus colei* Wyse Jackson, 1988, and *Fistulipora incrassata* (Phillips, 1836).

Phylum BRYOZOA Ehrenberg, 1831
 Class STENOLAEMATA Borg, 1926
 Order CRYPTOSTOMATA Vine, 1884a
 Suborder RHABDOMESINA Astrova & Morozova, 1956
 Family ARTHROSTYLIDAE Ulrich, 1882
 Genus **HEXITES** Shulga-Nesterenko, 1955

TYPE SPECIES. *Hexites triangularis* Shulga-Nesterenko, 1955 by monotypy from the Lower Carboniferous of Chekhurskiv in the Russian Platform.

EMENDED DIAGNOSIS. Arthrostylid with dendroid, erect zoaria composed of small delicate branches, with polygonal cross-sections. Perpendicular lateral branches occasionally developed. Jointing unknown. Autozoocial apertures oval to elliptical in shape, arranged in five to eight longitudinal rows and separated by a distinct ridge. Autozoocial chambers triangular to sub-triangular in cross-section. Zooecia seven to ten times longer than wide, diverging at a low angle with slightly inflated bases and sublinear chambers. Hemisepta and diaphragms not present. Small acanthostyles frequently developed on ridges.

DISCUSSION. The genus *Hexites* Shulga-Nesterenko 1955 was erected for distinctive small dendroid six-sided arthrostylids. Later, Dunaeva (1974: 93) included the eight-sided variety *Hexites quadrangularis*. The taxon from County Fermanagh described here has very similar morphological features to that of *Hexites triangularis* but differs from it in that as many as eight longitudinal rows may be developed. It might be acceptable to erect a new genus to incorporate *H. quadrangularis* and the Irish form but is probably taxonomically unnecessary; rather the diagnosis of *Hexites* has been emended here to include all three taxa.

STRATIGRAPHICAL RANGE. Lower Carboniferous (Viséan).

DISTRIBUTION. Only known from Ireland and the CIS (former Soviet Union).

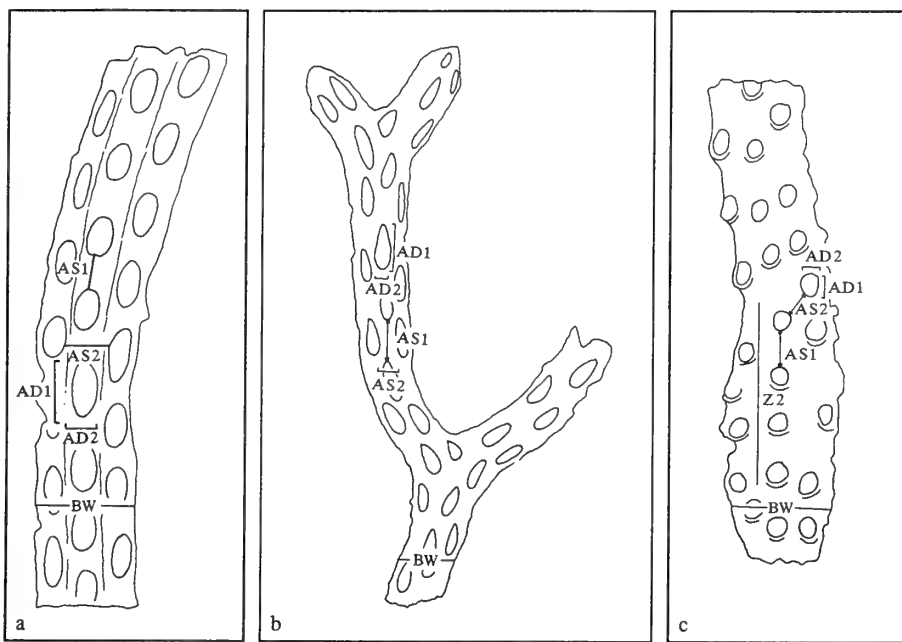


Fig. 3 Measurements taken on arthrostylid cryptostomes in this study. **a**, *Hexites paradoxus* sp. nov.; **b**, *Nematopora hibernica* sp. nov.; **c**, *Pseudonematopora planatus* sp. nov. BW = Branch diameter; AD1 = Autozoecia apertural diameter measured parallel to growth direction; AD2 = Autozoecia apertural diameter measured perpendicular to growth direction; AS1 = Autozoecia apertural spacing measured parallel to growth direction; AS2 = Autozoecia apertural spacing measured perpendicular to growth direction; AR = Number of longitudinal apertural rows around zoarium; Z2 = Number of autozoecial apertures contained within a 2mm line measured parallel to growth direction.

Hexites paradoxus sp. nov.

Figs 3a, 4–5, 8

HOLOTYPE. BMNH PD9410; Upper part of the Glencar Limestone (Viséan, Asbian), Carrick Lough, County Fermanagh.

PARATYPES. BMNH PD9411-9429; TCD.34012-34014, 34125, 4127, 34164, 34167, 42593c, all from the same locality and horizon as the holotype. TCD.42514-42515, Upper part of the Glencar Limestone (Viséan, Asbian), Sillees River, County Fermanagh.

DERIVATION OF TRIVIAL NAME. This *Hexites* species has between five and eight rows of autozoecial apertures, unlike the type species which has six, so therefore is a paradox.

DIAGNOSIS. *Hexites* with a delicate dendroid zoarium. Branches are straight to gently curved with a polygonal to sub-polygonal cross-section. Lateral branches diverge nearly perpendicular to the main stem and are infrequently developed. Autozoecia developed in five to eight longitudinal rows around the complete branch. The reverse surface is seen only as a very thin groove. Autozoecial apertures are small, oval to elliptical in shape. Apertural rows are divided by sharp distinct longitudinal ridges. Stylets developed on edges and occasionally between successive autozoecial apertures.

DESCRIPTION. Colonies are small, delicate, and dendroid. Branches are straight and of constant diameter along their length. Branch cross-sections are polygonal to rarely sub-polygonal. Lateral branches of a similar diameter diverge at unknown intervals perpendicular to the main branch. There is a very slight increase in branch width at ramifications. The largest fragment examined measured 9.8 mm in length.

Autozoecia are developed in five to eight longitudinal rows around most of the branch. In some specimens the reverse surface is

represented by a thin groove (Fig. 5). Autozoecia arise from a thin central axis and diverge from it at a low angle. Chamber bases are slightly inflated. Chambers are sublinear in shape, 0.60 to 0.71 mm in length and at least ten times as long as wide. In cross-section they are triangular to polygonal in shape. The vestibule, which shallows distally, is orientated at an angle of between 45° and 60° to the zoarial surface. The distal wall is thin with slight thickening of the proximal frontal wall. Hemisepta and diaphragms are not present.

Autozoecial apertures (0.28 × 0.14 mm) occur in longitudinal rows that are separated by a sharp to rounded ridge 0.08 mm wide. They are oval to elliptical in shape, and occasionally narrow distally. They are regularly spaced one diameter apart within rows and one to two diameters apart between rows. Autozoecial aperture size is marginally greater and apertural spacing slightly less in those rows closest to the groove on the reverse of branches.

One to two rows of small short acanthostyles 0.02 mm wide occur on the crest of ridges. Interapertural areas may be smooth or be decorated with up to twelve acanthostyles in three rows.

Table 1 Measurements of *Hexites paradoxus* (in mm). N=18.

	NM	x	Mn	Mx	CVw	CVb
BW	136	0.59	0.37	0.72	3.73	8.43
AD1	152	0.28	0.20	0.43	10.55	7.00
AD2	157	0.14	0.08	0.22	10.88	6.64
AS1	142	0.22	0.09	0.42	14.08	4.78
AS2	158	0.26	0.13	0.40	14.81	7.31

DISCUSSION. *Hexites* is easily recognised by the arrangement of autozoecia in well-developed longitudinal rows, with strong interapertural ridges.

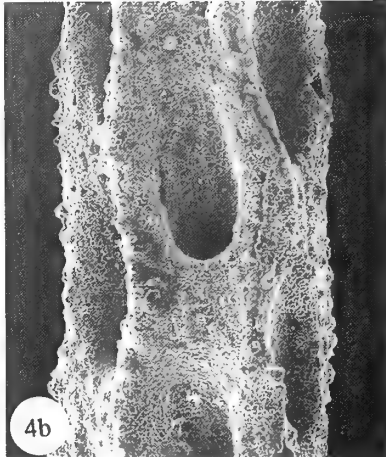
Table 2 Quantitative comparison between Carboniferous *Hexites* species (dimensions in mm).

	AR	BW	AD1	AD2	AS1	AS2
<i>H. paradoxus</i> sp. nov.	5–8	0.37–0.72	0.20–0.43	0.08–0.22	0.09–0.42	0.13–0.40
<i>H. triangularis</i> Shulga-Nesterenko, 1955	6	0.18–0.38	0.17	0.08	—	—
<i>H. quadrangularis</i> Dunaeva, 1974	8	0.52	0.16	0.12	0.18	0.15

Data from original sources.



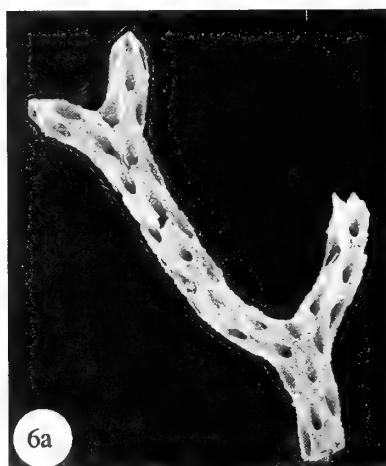
4a



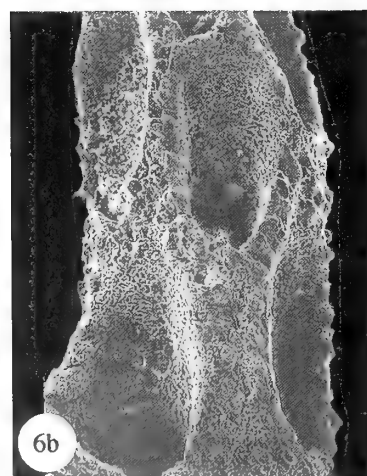
4b



5



6a



6b



7

Genus *NEMATOPORA* Ulrich, 1888a

H. paradoxus is only the third *Hexites* species to be described and first outside of the CIS (former Soviet Union). It differs from the type species *H. triangularis* Shulga-Nesterenko 1955 in having a larger branch width, a variable number of autozoocia rows (five to eight and not the consistent six of the latter), no peristomes, and acanthostyles in interapertural areas. It bears a close resemblance to *H. quadrangularis* Dunaeva 1974, which has 8 rows of autozoocia. However, *H. paradoxus* shows some morphological differences: branches are often thicker, autozoocia apertures are larger, elliptical to oval in shape, and are spaced considerably further apart. On the basis of these morphological differences *H. paradoxus* is erected as a new species (Table 2).

STRATIGRAPHICAL RANGE. Lower Carboniferous (Viséan–Asbian).

DISTRIBUTION. Carrick Lough and Sillees River, County Fermanagh, Ireland.

TYPE SPECIES. *Trematopora minuta* Hall, 1876 by original designation, from the middle Silurian of Waldron, Indiana, U.S.A.

REVISED DIAGNOSIS. Arthrostyrid with delicate, erect, dichotomously branching zoarium. Branches straight, circular to sub-circular in cross-section. Autozoocia arranged in four to ten longitudinal rows, either completely around branches or concentrated on one side of branch. Interapertural areas smooth with acanthostyles developed along ridges. Autozoocia apertures are oval to rhombic, dorsally flared.

STRATIGRAPHICAL RANGE. Middle Ordovician–Lower Permian.

DISTRIBUTION. British Isles, Europe, North America, the CIS (former Soviet Union), Asia.

Nematopora hibernica sp. nov. Figs 3b, 6–7, 9

HOLOTYPE. BMNH PD9430; Upper part of the Glencar Limestone (Viséan, Asbian), Carrick Lough, County Fermanagh.

Figs 4–5 *Hexites paradoxus* sp. nov. Upper part of the Glencar Limestone (Viséan, Asbian), Carrick Lough, County Fermanagh. 4, BMNH PD9410 (**holotype**); 4a, colony fragment comprising a thin slender octagonal to circular-shaped branch; autozoocia are arranged in distinct longitudinal rows divided by strong flexuous ridges, and their apertures are oval in shape, $\times 30$; 4b, detail of 4a showing autozoocia apertures and intervening ridges showing the disposition of small stylets on the crest of ridges, $\times 150$. 5, BMNH PD9414 (paratype), reverse surface showing longitudinal groove, $\times 12$.

Figs 6, 7 *Nematopora hibernica* sp. nov. Upper part of the Glencar Limestone (Viséan, Asbian), Carrick Lough, County Fermanagh. 6, BMNH PD9430 (**holotype**); 6a, small colony fragment showing bifurcation of branches, and regular arrangement of autozoocia apertures in offset rows on obverse surface, $\times 20$; 6b, detail showing distal growing tip of branch and pyriform autozoocia apertures separated by thin interapertural walls patterned by a single row of small stylets, $\times 120$. 7, BMNH PD9442 (paratype), reverse surface showing longitudinal rows of small nodes, $\times 14$.

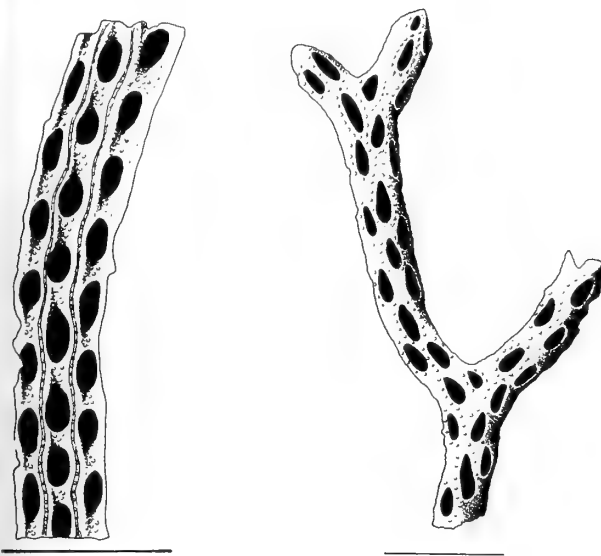


Fig. 8 *Hexites paradoxus* sp. nov. Line drawing of external features of BMNH PD9410; scale bar = 1 mm.

Fig. 9 *Nematopora hibernica* sp. nov. Line drawing of external features of BMNH PD9430; scale bar = 1 mm.

PARATYPES. BMNH PD9431-9449; TCD.34015-34017; BELUM K3145-3146; all from the same locality and horizon as the holotype.

DERIVATION OF TRIVIAL NAME. From the Latin *hibernica* meaning Ireland.

Table 3 Measurements of *Nematopora hibernica* (in mm). N=19.

NM	x	Mn	Mx	CVw	CVb
3W	176	0.59	0.41	0.76	7.99
AD1	176	0.33	0.21	0.44	8.63
AD2	172	0.12	0.08	0.20	10.34
AS1	165	0.27	0.11	0.52	22.04
AS2	170	0.12	0.08	0.21	17.54
					8.29

DIAGNOSIS. *Nematopora* with delicate dendroid zoarium. Branches dichotomise irregularly, are straight in outline and subcircular in cross-section. Autozoocia are developed in four to five longitudinal rows on one surface only. Autozoocia are oval and surrounded by small acanthostyles. Reverse surface barren, with four to five longitudinal rows of faint pustules.

DESCRIPTION. Colonies are small, delicate, erect with irregularly dichotomising branches. The largest fragment examined measures

Table 4 Quantitative comparison between Carboniferous species of *Nematopora* (in mm).

	AR	BW	AD1	AD2	AS1	AS2
<i>J. hibernica</i> sp. nov.	5	0.41-0.76	0.21-0.44	0.08-0.20	0.11-0.52	0.08-0.21
<i>J. afghana</i> Termier & Termier, 1971	-	0.6-1.5	-	-	-	-
<i>J. donbassica</i> Dunaeva, 1961	-	0.89-1.20	0.24-0.32	0.12-0.14	0.29-0.36	0.12
<i>J. kusbasensis</i> Trizna, 1958	10	0.96-1.00	0.18-0.22	0.08-0.12	-	-
<i>J. ivanovi</i> Shulga-Nesterenko, 1955	-	0.70-0.90	0.40-0.45	0.15	-	-
<i>J. parvula</i> Shulga-Nesterenko, 1955	-	0.25-0.30	0.30-0.35	0.07-0.10	-	-
<i>J. tulensis</i> Morozova, 1955	-	0.30-0.40	0.20-0.22	0.10	-	-
<i>J. sp. indet.</i> Sakagami, 1962	8-10	1.00-1.10	0.24	0.13-0.16	-	-

Data from original sources.

16.4mm in length. Branches are straight (range of diameter from 0.41mm to 0.76mm), sub-circular in cross-section. Branch width increases slightly prior to bifurcation. Interapertural areas may bear one to two rows of small acanthostyles which surround autozoocia apertures. The reverse surface is barren, either smooth or with small acanthostyles occurring in four longitudinal rows (Fig. 7).

Autozoocia are arranged quincuncially in four to five longitudinal rows, irregularly spaced within and between rows.

Autozoocia apertures are oval to elliptical in shape, often narrower distally. Vestibules are steep-sided and shallow distally.

DISCUSSION. From the study area only 22 fragments of *Nematopora hibernica* were found. All are hollow silicified fragments in which only the surface has been replaced, and consequently details of internal morphology are unknown.

Externally *Nematopora* is very distinctive. The rhombic shape of the autozoocia apertures, and the abundance of acanthostyles resembles that of *Rhabdomeson rhombiferum* (Phillips), but unlike the latter autozoocia apertures do not occur all the way around the branch.

N. hibernica is only the second species of *Nematopora* to be described from the British Isles *Nematopora hexagona* having been described from the Silurian (Wenlock) of Shropshire (Owen, 1962). Only 27 species of *Nematopora* have been described worldwide throughout its stratigraphic range (Goryunova 1985). Of these only seven, found in the U.S.S.R., Afghanistan, and Japan, occur in the Carboniferous: *N. afghana* Termier & Termier, 1971; *N. donbassica*, Dunaeva, 1961; *N. kusbasensis* Trizna, 1958; *N. ivanovi* Shulga-Nesterenko, 1955; *N. parvula* Shulga-Nesterenko, 1955; *N. tulensis* Morozova, 1955; and *N. sp. indet.* Sakagami, 1962.

STRATIGRAPHICAL RANGE. Lower Carboniferous (Asbian).

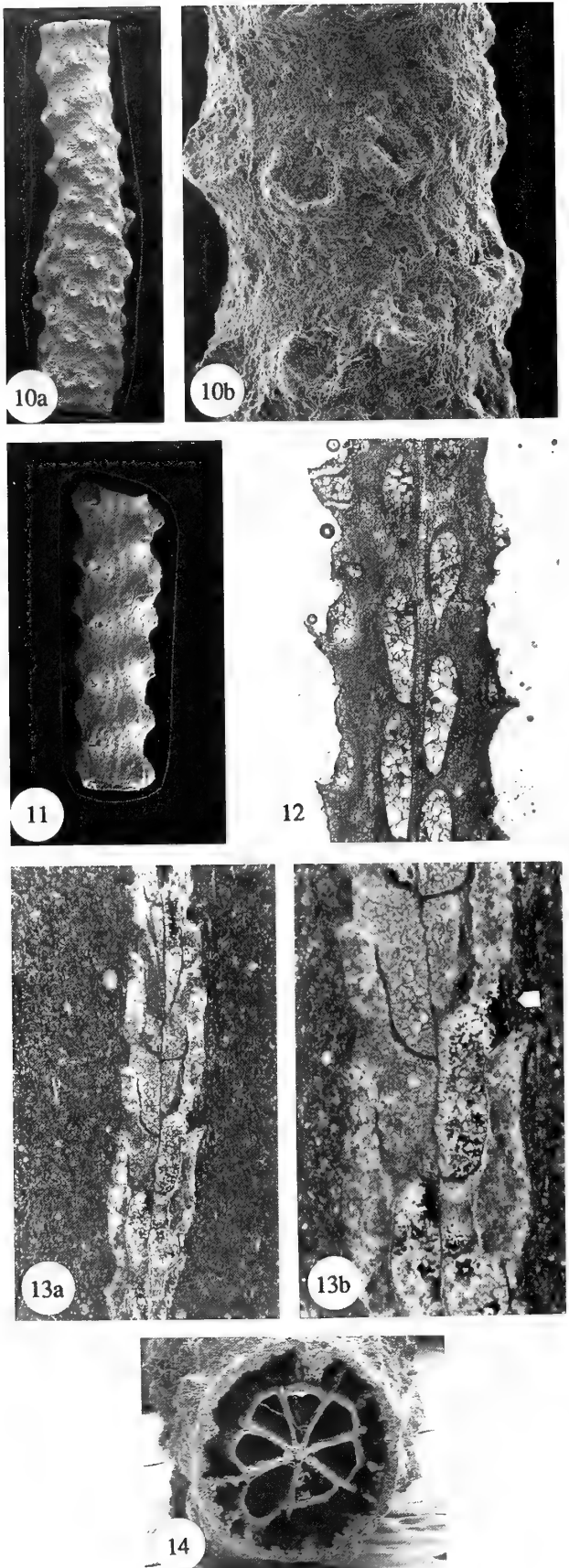
DISTRIBUTION. Carrick Lough, County Fermanagh, Ireland.

Genus *PSEUDONEMATOPORA* Balakin, 1974

TYPE SPECIES. *Nematopora?* *turkestanica* Nikiforova, 1948 by original designation from the Lower Carboniferous of the CIS (former Soviet Union).

EMENDED DIAGNOSIS. Arthrostylid with slender dendroid zoarium, with occasional dichotomising branches. Branches are of constant width and are circular to semicircular in cross-section. Autozoocia occur in 6 to 16 longitudinal rows, and are budded in an annular manner. Autozoocia apertures are circular to oval in shape, with proximal peristomes. Autozoocia originate from a central axis. Skeletal cysts may be present in the exozone. Terminal diaphragms developed in some species. Acanthostyles are absent.

STRATIGRAPHICAL RANGE. Lower Carboniferous (lower Tournaisian-lower Viséan).



DISTRIBUTION. Ireland, England, Belgium, and the CIS (former Soviet Union).

Pseudonematopora planatus sp. nov. Figs 3c, 10–15

HOLOTYPE. BMNH PD9450; Upper part of the Glencar Limestone (Viséan, Asbian), Carrick Lough, County Fermanagh.

PARATYPES. BMNH PD9451-9472, 9741; TCD.34018-34025, 34137, 34160, 34161, 42561, 42607; BELUM K2222; all from same locality and horizon as above. TCD.42516-42519, Upper part of the Glencar Limestone (Viséan, Asbian), Sillees River, County Fermanagh

DERIVATION OF TRIVIAL NAME. From the Latin *planus* meaning plain and unornamented.

DIAGNOSIS. *Pseudonematopora* with slender dendroid zoaria. Branches dichotomise infrequently and at a high angle. They are circular to sub-circular in cross-section and are a constant width throughout their length. Autozoocelial apertures occur in 6 to 8 longitudinal rows. They are circular in shape and have an arcuate, proximally located, peristomial rim. A faint longitudinal ridge occurs in the smooth interapertural area. Autozoocelial budding is annular from a central axis. Chambers diverge at a low angle in the endozone before bending in the exozone to become orientated at an angle of 60° to 70° to the zoarial surface. Zooecial walls are thin in the endozone and do not thicken in the exozone. Terminal dia-phragms may be developed. Skeletal cysts are lacking.

DESCRIPTION. Colonies are small, delicate and have irregularly dichotomising straight branches, which are circular in cross-section and undulatory in outline. The largest fragment examined is 13.2 mm in length. On no specimen were two dichotomies seen.

Autozoocelia occur in 6 to 8 longitudinal rows around the circumference of the zoarium except for a thin barren area on the reverse. They are budded from a distinct central axis in an annular pattern. Zooecial chambers diverge from the median wall at an angle of 10° to 15° in the endozone. The exozone is reached when the chamber bend fairly abruptly through 60° to 70°. The living chambers are orientated nearly perpendicular to the zoarial surface. The complete chamber is nearly four times as long as it is wide. Interzoocelial walls are very thin in the endozone but thicken considerably in the exozone. Basal diaphragms are not developed and the zooecia chambers are simple tubular structures.

Interapertural areas are smooth with a single faint longitudina-

Figs 10–14 *Pseudonematopora planatus* sp. nov. Upper part of the Glencar Limestone (Viséan, Asbian), Carrick Lough, County Fermanagh: 10, BMNH PD9450 (**holotype**); 10a, colony fragment showing cylindrical branch shape, with circular autozoocelial apertures developed in irregular longitudinal rows; apertures surrounded by proximal peristomes that extend beyond the branch margin giving an uneven outline, $\times 12$; 10b, detail of 10a showing the smooth interapertural areas, $\times 80$. 11, BMNH PD9452 (paratype), reverse surface showing longitudinal sinuous series of small nodes, $\times 12$. 12, BMNH PD9470 (paratype), tangential section showing the central axial region with a row of autozoocelial either side of it, and the marginal protrusion of the proximal peristomes, $\times 35$. 13, BMNH PD9471 (paratype); 13a, longitudinal section showing thin axial region from which are budded autozoocelial chambers and the thickened exozone, $\times 20$; 13b, detail of 13a showing brown bodies in autozoocelial chambers trapped behind a thin linear terminal diaphragm (arrowed), $\times 35$. 14, BMNH PD9452 (paratype), transverse section showing radial arrangement of seven autozoocelial chambers around the central axis, $\times 35$.



Fig. 15 *Pseudonematopora planatus* sp. nov. Line drawing of external features of BMNH PD9450; scale bar = 1 mm.

ridge developed between adjacent autozoecial rows. On the reverse surface the interapertural areas are slightly wider than those on the obverse surface. A strong ridge may be developed there.

Autozoecial apertures are small and circular. The apertures of the autozoecia adjacent to the reverse surface are divergent from it (Fig. 11) and are marginally larger than those in other rows on the obverse surface. Peristomes, situated proximally, are commonly developed around apertures. Thin terminal diaphragms close off some autozoecial apertures, behind which small circular brown bodies are found in chambers (Fig. 13b). These brown bodies, which are similar in morphology to those reported by Morrison & Anstey (1979) in some Ordovician trepostomes, represent the degenerated remains of the polypide soft tissues.

Table 5 Measurements of *Pseudonematopora planatus* (in mm). N=13.

NM	x	Mn	Mx	CVw	CVb
BW	130	0.80	0.61	1.20	7.80
AD1	130	0.18	0.10	0.26	10.84
AD2	130	0.13	0.10	0.23	14.74
AS1	130	0.39	0.24	0.63	15.32
AS2	130	0.18	0.10	0.41	26.97
Z	130	3.6	3	5	11.31
AR	13	7.5	6	8	—
					13.50
					12.89

DISCUSSION. *Pseudonematopora* is reported from outside the CIS (former Soviet Union) for the first time. In the County Fermanagh fauna *P. planatus* is quite common. Only three other species have previously been recorded, all from Lower Carboniferous strata: *P. etchorensis* Gorjunova, 1985, the type species *P. turkestanica*

(Nikiforova, 1948) [Balakin, 1974], and *P. balakini* Gorjunova, 1988. *P. planatus* differs from these three species in a number of respects. Zoarial width is narrower in *P. turkestanica* and the number of autozoecial rows is less. More importantly the autozoecial apertures in *P. planatus* are at least half the size as those of the other three species. Skeletal cysts are absent in *P. planatus* but may be developed in the other species. Terminal diaphragms have been reported from both *P. turkestanica* (Owen, 1966) and *P. balakini* (Gorjunova, 1988), and are present in *P. planatus*.

Balakin (1974) noted that variation in zoarial width and fluctuation in the number of autozoecial rows in *P. turkestanica* are both large. *P. planatus* does not show such variation. Coefficients of variation for all measured parameters are low (Table 5). Variation within colonies is greater than variation between colonies in all features except zoarial width (ZW) and the number of autozoecia in a 2mm line (Z2). In these two cases variation within and between colonies is virtually identical.

Rhombopora radialis Owen, 1966 is herein considered to be conspecific with *Pseudonematopora turkestanica* (Nikiforova, 1948). Comparison of Owen's type material (LL.2984 holotype; LL.2985-2989 paratypes; Upper Viséan; Treak Cliff, Castleton, Derbyshire) with illustrations of *Pseudonematopora turkestanica* from the former Soviet Union (Balakin 1974) shows these taxa to have a similar morphology. *Pseudonematopora* is characterised by autozoecia budded from a central axis in an annular fashion, with short chambers and terminal diaphragms often developed, circular apertures with proximal peristomes, and a lack of acanthostyles and metapores. Conversely, *Rhombopora* zoaria are dendroid, with long autozoecia containing hemisepta, and with oval zooecial apertures, many acanthostyles, and occasionally metapores.

Pseudonematopora is a very distinct genus with a straight, occasionally branching zoarium, autozoecia budded from a central axis, apertures with proximal peristomes, and occasional terminal diaphragms. Externally the taxon resembles the cystoporate *Cheilotrypa* Ulrich 1884. However, internal structures and budding patterns in the two are quite different: in *Cheilotrypa* diaphragms are present and autozoecia are budded from a central hollow axial tube (Utgard 1983).

Nematopora has been regarded as ancestral to *Pseudonematopora* (Balakin 1974) because the two taxa display a similar colony shape, autozoecial chamber shape, aperture size and shape, and budding pattern. However, in a computer-based phenetic study on the Rhabdomesina using cluster analysis of 44 features, Blake & Snyder (1987) suggested that *Pseudonematopora* was more closely related to *Osburnostylus* (88% similarity) than to *Nematopora* (78% similarity). Externally, however, *Osburnostylus* with rapid thickening of the zoarium at the level of the autozoecia apertures appears more different from *Pseudonematopora* than is *Nematopora*. Resolution of this phylogenetic problem may be achieved through finds of *Pseudonematopora*, extending its range, both geological and geographical, and by more work on Palaeozoic bryozoans.

STRATIGRAPHICAL RANGE. Lower Carboniferous (Viséan, Asbian).

DISTRIBUTION. Carrick Lough and Sillees River, County Fermanagh, Ireland.

Table 6 Quantitative comparison between *Pseudonematopora* species (dimensions in mm).

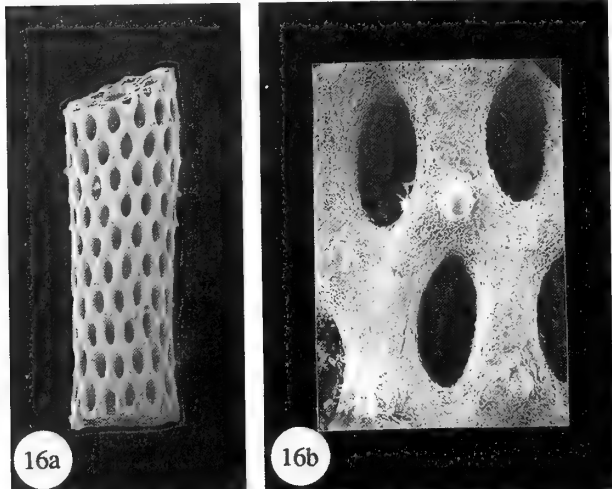
	BW	AR	AD1	AD2	AS1	AS2	Z2
<i>planatus</i> sp. nov.	0.61–1.20	6–8	0.10–0.26	0.10–0.23	0.24–0.63	0.10–0.41	3–5
<i>balakini</i> Gorjunova, 1988	0.88–1.10	—	0.35–0.45	0.22–0.26	—	—	4
<i>etchorensis</i>	0.72–1.08	—	0.33–0.36	0.15–0.19	0.33–0.36	0.20–0.25	3.5
<i>turkestanica</i> (Nikiforova, 1948)	0.80–2.80	8–16	0.25–0.37	0.17–0.22	0.25–0.37	0.15–0.25	3–4

Data from original sources.

Family RHABDOMESIDAE Vine, 1884a
 Genus *Rhabdomeson* Young & Young, 1874

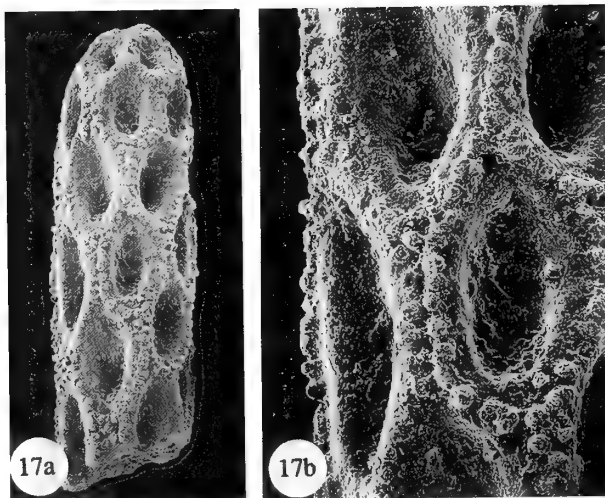
TYPE SPECIES. *Millepora gracilis* Phillips, 1841, by monotypy, from the Devonian of north Devon, England (for discussion relating to the problems with this type species see Wyse Jackson & Bancroft 1995a, 1995b).

Rhabdomeson progracile Wyse Jackson & Bancroft, 1995
 Fig. 16



16a

16b



17a

17b

Fig. 16 *Rhabdomeson progracile* Wyse Jackson & Bancroft 1995. Upper part of the Glencar Limestone (Viséan, Asbian), Carrick Lough, County Fermanagh; BMNH PD9473 (paratype); **16a**, typical zoarial fragment showing cylindrical shape of branch, with the spiral arrangement of autozoocia in curved interlocking rows; autozoocial apertures are oval to elliptical in shape; one large acanthostyle is placed distally of apertures, $\times 25$; **16b**, detail of 16a, $\times 130$.

Fig. 17 *Rhabdomeson rhombiferum* (Phillips, 1836). Upper part of the Glencar Limestone (Viséan, Asbian), Carrick Lough, County Fermanagh; BMNH PD9485; **17a**, growing tip of branch showing cylindrical colony form; autozoocia are arranged in longitudinal and obliquely intersecting rows; apertures are oval in shape, and narrow slightly distally; short blunt stylets surround each autozoocial aperture, $\times 50$; **17b**, detail of 17a showing autozoocial aperture surrounded by stylets, $\times 130$.

MATERIAL. BMNH PD9473-9484, TCD.34026-34028, BELUM K3095, Upper part of the Glencar Limestone (Viséan, Asbian), Carrick Lough, County Fermanagh, Ireland. TCD.42520, Upper part of the Glencar Limestone (Viséan, Asbian), Sillees River, County Fermanagh.

DESCRIPTION. Zoaria are dendroid, with cylindrical branches ranging in diameter from 0.61 to 1.07mm. There may be some increase in branch diameter prior to, or subsequent to, lateral branch development. Bifurcation is rare. The longest zoarial fragment examined measures 8.1mm in length.

Autozoocia are budded from a straight hollow cylindrical axis 0.14 to 0.29mm in diameter, in an annular or spiral pattern. In thin section autozoocial chambers are triangular to pentagonal in shape when seen in transverse section. Vestibules are orientated at a high angle to the zoarial surface. Acanthostyles arise as rods of granular calcite in the lower portions of the exozone. Interchamber endozonal walls are 0.1mm in width and are composed of an inner granular layer surrounded by a fine laminated skeleton.

Autozoocial apertures are pyriform to oval in shape, and moderate to small in size. They are crowded or arranged in quincunx in 14 to 18 longitudinal rows around the branch. Interapertural spacing is greatest longitudinally where apertures are spaced one diameter apart and up to 5 in a 2mm line. Transversely adjacent apertures are spaced less than one diameter apart. Autozoocial apertural dimensions and spacing are approximately constant in each branch fragment. However, some considerable differences are found between zoarial fragments.

A large acanthostyle, up to 0.12mm in height, is always found distal to autozoocial apertures. Rare zoaria bear only this single acanthostyle (Fig. 16b); more frequently one or two smaller acanthostyles lie proximal to the first in a longitudinal line between adjacent autozoocial apertures. Acanthostyles are usually abraded, and appear as faint protruberances on the zoarial surface.

DISCUSSION. A complete systematic description of *R. progracile* is given in Wyse Jackson & Bancroft (1995a).

Rhabdomeson rhombiferum (Phillips, 1836)

Fig. 17

MATERIAL. BMNH PD9485-9506; TCD.34029-34036, 42591b, 42593a, 42595; BELUM K3045, Upper part of the Glencar Limestone (Viséan, Asbian), Carrick Lough, County Fermanagh, Ireland; TCD.42521-42524, Upper part of the Glencar Limestone (Viséan, Asbian), Sillees River, County Fermanagh.

DESCRIPTION. The dendroid zoarium is composed of irregularly bifurcating delicate branches, with a polygonal or circular cross-section, that range in diameter from 0.41 to 0.86mm. Branch width remains approximately constant along their entire lengths. Branching either by bifurcation or development of lateral branches at a high angle of between 68° and 90° from parent branch. There is no increase in branch diameter prior to or subsequent to branch development. In no specimen was there more than one bifurcation or lateral branch observed.

Autozoocial apertures are moderate to large in size, pyriform to oval or ellipsoidal in shape, and are arranged in quincunx in eight to eleven longitudinal rows around branches.

Apertural size, shape and spacing is very variable around the branch. A distinct barren area 0.25mm in width, with four longitudinal rows of small acanthostyles, is found on some branches and can be regarded as delineating the branch reverse surface. In all zoaria the autozoocial apertures are long, thin, and oval in shape on the reverse surface. Towards the obverse surface apertures become

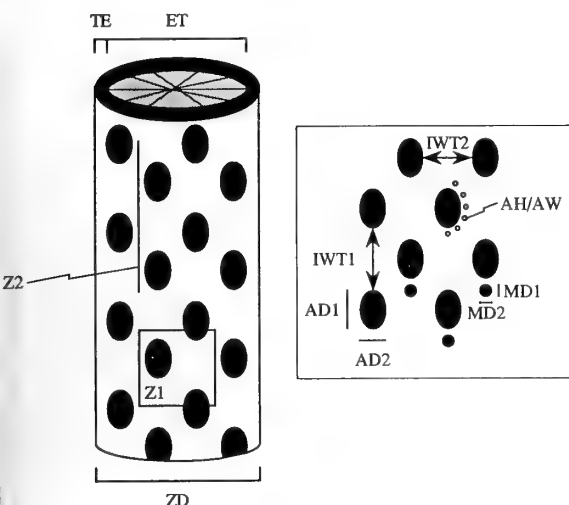


Fig. 18 Measurements taken on rhomboporid and hyphasmoporid cryptostomes in this study: ZD = Width of zoarium measured perpendicular to growth direction; MD = Metapore diameter; MD1 = Metapore diameter measured parallel to growth direction; MD2 = Metapore diameter measured perpendicular to growth direction; AH = Acanthostyle height from base to tip; AW = Acanthostyle width measured at its base; AD1 = Autozoocia apertural diameter measured parallel to growth direction; AD2 = Autozoocia apertural diameter measured perpendicular to growth direction; IWT1 = Autozoocia apertural spacing measured parallel to growth direction; IWT2 = Autozoocia apertural spacing measured perpendicular to growth direction. Z1 = Number of autozoocial apertures contained in 1mm^2 ; Z2 = Number of autozoocial apertures contained within a 2mm line measured parallel to growth direction; AR = Number of autozoocial apertural rows measured around zoarium; ET = Endozone thickness; TE = Exozone thickness.

increasingly pyriform and equidimensional. This variation in apertural size is reflected in apertural spacing; these two parameters (apertural size and apertural spacing) are inversely proportional to each other. Immediately after branching, elongate autozoocia apertures developed around the complete circumference of the daughter branch. Differentiation of apertural dimensions occurs distally within two or three generations along the branch.

Interapertural walls are gently sinuous or occasionally straight and may be raised to produce a ridge between apertural rows. One or two rows of small short acanthostyles (0.02–0.04 mm in diameter) are developed along this ridge. When two rows are present they are separated by a distinct furrow.

Autozoocia apertures are surrounded by 24 to 30 acanthostyles, in various patterns. Commonly they flank only lateral margins and up to six acanthostyles may occur proximal to apertures. Less frequently acanthostyles are arranged in a rhombic pattern, with only one acanthostyle proximal to apertures.

DISCUSSION. A complete systematic description of *Rhabdomesos lombiferum* is given in Wyse Jackson & Bancroft (1995a), as well as a discussion of budding, branching and other features in rhabdomesoniids.

Family RHOMBOPORIDAE Simpson, 1895 Genus **RHOMBOPORA** Meek, 1872

TYPE SPECIES. *Rhombopora lepidodendroides* Meek, 1872 by

original designation, from the Upper Carboniferous of Nebraska City, Nebraska, U.S.A.

Rhombopora cylindrica sp. nov.

Figs 19–25

- non 1841 *Millepora similis* Phillips: 21, fig. 32.
 non 1843 *Millepora similis* Phillips; Morris: 42.
 1844 *Millepora similis* Phillips; M'Coy: 196.
 non 1854 *Ceriopora similis* (Phillips); Morris: 121.
 1854b *Millepora similis* Phillips; M'Coy: 104.
 1862 *Millepora similis* Phillips; Griffith: 196.
 1871 *Ceriopora similis* (Phillips); Young & Armstrong: 33.
 1876 *Ceriopora similis* (Phillips); Armstrong, Young & Robertson: 46.
 1877 *Ceriopora similis* (Phillips); Young & Robertson: 175.
 1881 *Ceriopora similis* (Phillips); Vine: 338.
 1885 *Rhombopora similis?* (Phillips); Vine: 93 pro parte.
 non 1887 *Rhombopora persimilis* Ulrich; Vine: 226, pl. 1, fig. 6.
 1887 *Rhombopora similis* (Phillips); Vine: 226, pl. 1, fig. 7.
 1889 *Rhombopora similis* (Phillips); Vine: 198.
 1987 *Rhombopora similis* (Phillips); Bancroft: 196.

HOLOTYPE. BMNH PD9507; Upper part of the Glencar Limestone, Lower Carboniferous (Viséan, Asbian); Carrick Lough, County Fermanagh.

PARATYPES. BMNH PD9508–9534, 9576, upper part of the Glencar Limestone, Lower Carboniferous (Viséan, Asbian); Carrick Lough, County Fermanagh; Tavener-Smith and Wyse Jackson Collections. BMNH D294 (2 zoaria in a cavity slide of five), D295, Lower Carboniferous, Gayton Boring, Northamptonshire, England; Vine Collection. BMNH D303 (thin section of several zoarial fragments), Shales; Lower Carboniferous; Argyleshire, Scotland; Vine Collection. TCD.28317, 28369, Nant-y-Gamar buildup, Llandudno Pier Dolomite Formation (Viséan, Asbian), near Llandudno, north Wales. TCD.34037–34044, 34122, 34126, 34128, 34165, 42592a, b; BELUM K2175, Upper part of the Glencar Limestone, Lower Carboniferous (Viséan, Asbian); Carrick Lough, County Fermanagh; Wyse Jackson Collection. TCD.41515, Shales above Main Limestone, Pendleian, Upper Carboniferous, Hurst, near Richmond, Yorkshire, U.K. [NZ044 023], Bancroft Collection. TCD.42525–42528, Upper part of the Glencar Limestone (Viséan, Asbian), Sillees River, County Fermanagh, Wyse Jackson Collection.

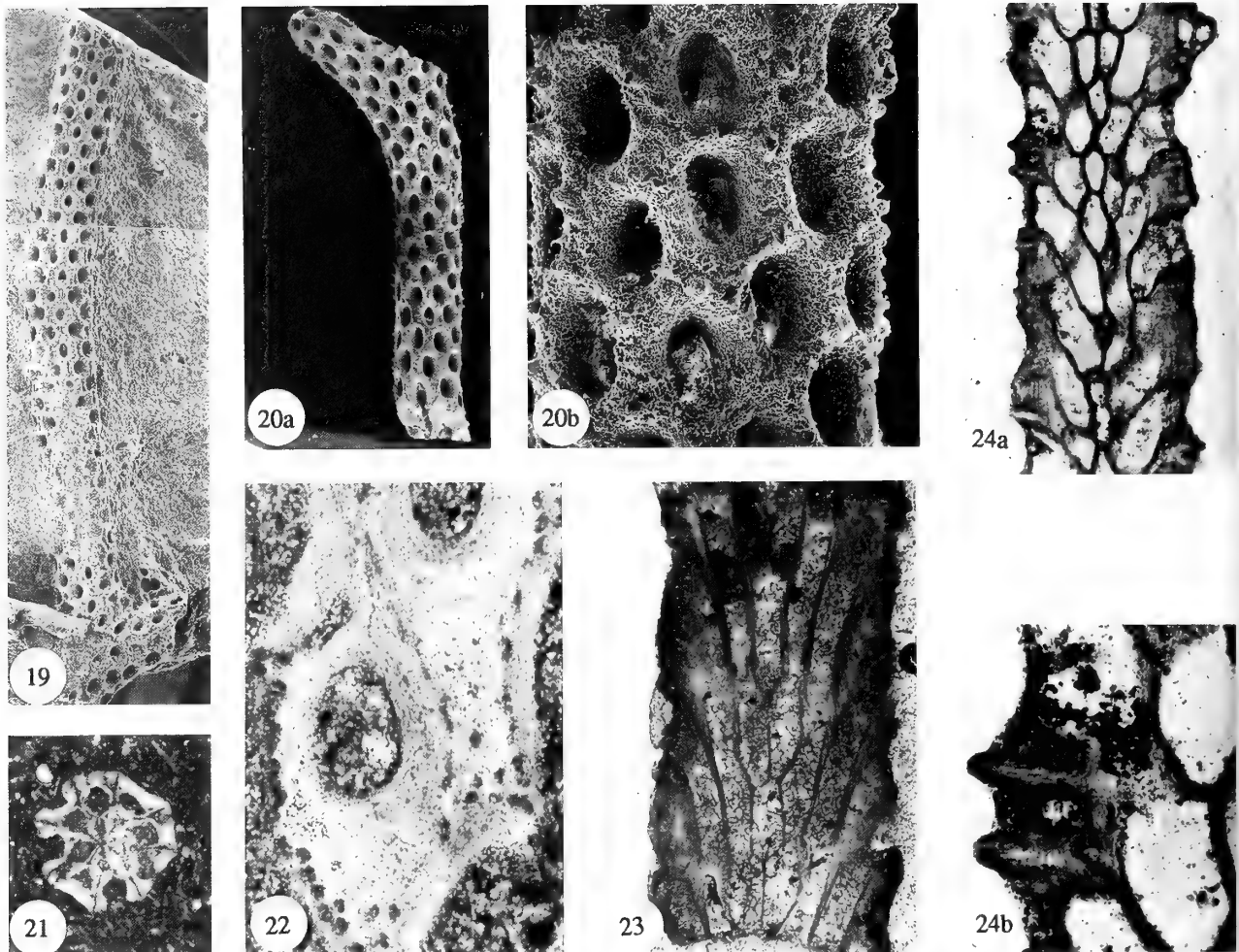
DERIVATION OF NAME. From the cylindrical nature of zoarial branches.

DIAGNOSIS. *Rhombopora* with zoaria comprised of irregularly dividing, thin, cylindrical branches. Autozoocia are budded in a spiral manner from a central linear axis. The exozone region is thin. Autozoocia apertures are oval in shape, moderate to large in size and arranged in quincunx in longitudinal rows around branches. Metapores are rare and occur proximal to autozoocia apertures. Stylets are common and structurally varied: characteristically one to two acanthostyles may be situated at junctions of interapertural walls, and many small heterostyles occur in interapertural areas.

DESCRIPTION. Colonies are composed of delicate, thin bifurcating branches. The largest fragment examined measures 16.2 mm in length.

Branches range in diameter from 0.54 to 1.15 mm and retain a constant width along their length except prior to lateral branch development when a 25% increase in diameter occurs. Bifurcation is infrequent and irregular; lateral ramifications deviate at high angles of between 75° and 87° .

Autozoocia are budded from a straight to undulatory central axis



Figs 19–24 *Rhombopora cylindrica* sp. nov.; 19–23, Upper part of the Glencar Limestone (Viséan, Asbian), Carrick Lough, County Fermanagh; 19, BMNH PD9509 (paratype), colony form showing long straight branches, with interconnected longitudinal and oblique rows of autozoocia, $\times 20$; 20, BMNH PD9507 (holotype); 20a, zoarial fragment with distal growing tip, showing regular arrangement of autozoocial apertures around branch; large acanthostyles are situated at the proximal and distal ends of apertures with smaller heterostyles developed on surrounding walls, $\times 20$; 20b, detail of 20a showing autozoocial apertures and acanthostyles on interapertural walls, $\times 10$; 21, BMNH PD9534 (paratype), transverse section showing radial budding pattern of autozoocia and the differentiation of endozone and exozone; 22, BMNH PD9532 (paratype), tangential section showing oval-shaped autozoocia and heterostyles (C-type stylets) developed on interapertural walls, $\times 100$; 23, BMNH PD9531, (paratype), longitudinal section showing autozoocial chamber shape and the thickened exozonal walls, $\times 40$; 24: Shales above Main Limestone, Pendleian, Upper Carboniferous, Hurst, near Richmond, Yorkshire, U.K. TCD.41515; 24a, longitudinal section, $\times 25$; 24b, detail of 24a showing morphology of acanthostyles, $\times 80$.

at low angles of 10° to 25° and chambers are eight times as long as their maximum width. The chamber bends through 30° to 40° at the endozone/exozone boundary and vestibules are orientated at an angle of 45° to the zoarial surface. In cross-section chambers are rhombic, pentagonal or subcircular in shape. Chamber walls are thin (0.01–0.03 mm), compound (a very thin granular core covered by laminated skeleton) in the endozone and thicker, with a predominantly laminated skeleton, in the narrow exozone region. The exozone varies in width between 0.1 and 0.2 mm and is approximately one fifth the width of branches. Thin terminal diaphragms may be present.

Autozoocial apertures are large to moderate in size, oval to circular in shape, regularly spaced approximately one diameter apart, and spirally arranged in quincunx in 10 to 16 longitudinal

rows around branches. 3 to 6 apertures occur longitudinally and 8 to 10 diagonally along a 2 mm line. Autozoocial apertural size is constant on a zoarium except at branch nodes. The first autozoocial apertures on new branches are long and thin, particularly on the reverse surface of branches. Uniformity of size is regained 4 to 5 apertures along branches. Metapores are rare. They are small (0.01–0.13 × 0.02–0.10 mm), irregular in shape and one or occasionally two are found proximal of autozoocial apertures, with others sparsely distributed elsewhere on interapertural walls. They are usually developed close to branch divisions and zoarial thickening. They originate within the exozone.

Stylets are numerous and structurally varied. They occur in one or two rows, between autozoocial apertures. One or rarely two acanthostyles (up to 0.07 mm wide) occur at autozoocial apices or



Fig. 25 *Rhombopora cylindrica*: sp. nov. Line drawing of external features of BMNH PD9507; scale bar = 1 mm.

some but not all zoaria. 20 to 24 heterostyles (0.01–0.03mm wide) in one or two rows flank autozoocial apertures on all zoaria. A longitudinal groove frequently occurs between heterostyle rows which probably marks the position of the zoocial boundary. Acanthostyles have a thick granular core and develop from the base of the exozone. Heterostyles have a thinner granular core and grow from within the exozone. Skeletal lamellae are bent around acanthostyles.

Table 7 Measurements of *Rhombopora cylindrica* (in mm). N=23.

NM	x	Mn	Mx	CVw	CVb
ZD	187	0.76	0.54	1.15	4.40
Z1	4	8.75	8	10	10.94
Z2	155	4.26	3	6	9.56
AD1	219	0.19	0.10	0.35	12.22
AD2	219	0.11	0.07	0.18	12.18
WT1	219	0.25	0.12	0.55	18.87
WT2	219	0.15	0.09	0.32	24.78
ID1	21	0.04	0.01	0.13	32.17
ID2	21	0.04	0.02	0.10*	24.85
AH	34	0.04	0.01	0.10	27.86
AW	63	0.02	0.01	0.07	20.64
E	18	0.15	0.10	0.20	13.53
					5.66

DISCUSSION. *Rhombopora cylindrica* is quite distinctive and may easily be distinguished by the presence of oval-circular autozoocial pertures, a central axis, a thin exozone, and structurally varied canthostyles.

Coefficients of variation for both zoarial (ZW) and zooecial AD1, AD2, IWT1, and IWT2) parameters within colonies are low. CVw values for metapore diameter (MD1 and MD2) as well as canthostyle height (AH) and width (AW) are large. They are due to the space-filling function of metapores, abrasion of acanthostyles, and poor replacement by silica of small skeletal elements. This is reflected by examining autozoocial aperture dimensions which were more varied in silicified specimens than in calcified specimens. Coefficients of variation between colonies are all extremely low.

Millepora similis was first described by Phillips (1841) as a supposed coral from the Devonian of south-west England. Phillips

collected specimens from two localities: Cannington Park, north Devon, and Hope, near Torquay, south Devon. M'Coy (1844) noted *Millepora similis* from the Lower Carboniferous of Ireland (the Courceyan of St. Doulagh's, County Dublin and the Courceyan/Chadian of Gort, County Galway). This identification was the first of many that confused two distinct taxa of Devonian and Carboniferous age. It is unfortunate that of the two slabs labelled *Millepora similis* from the Griffith Collection (NMMG F7081, 7082) examined by M'Coy neither contains specimens referable to either taxa; but it is evident that M'Coy described a taxon that is different from the Devonian *Millepora similis* of Phillips (M'Coy, 1844: 196).

Subsequently Morris (1854) classified *Millepora* as a zoophyte and transferred *M. similis* into the genus *Ceriopora*, considered then to be a coral, but now known to be a cyclostome bryozoan.

Later still, Young & Robertson (1877) described some Carboniferous bryozoans from the Carboniferous of Scotland, which they regarded as being conspecific with *Ceriopora similis*. Vine (1881) followed this description but later (1885) deciding that the former generic assignment was incorrect, placed all Carboniferous material, as well as Phillips' Devonian taxon, into the newly erected genus *Rhombopora* Meek, 1872.

Rhombopora similis (Phillips, 1841) *sensu* Vine 1885 has only been found in strata of Carboniferous age. It is clear that M'Coy (1844) misassigned a new undescribed Lower Carboniferous bryozoan and that this mistake was compounded and reinforced in later descriptions of Lower Carboniferous material.

Phillips' figured and only extant *Millepora similis* specimen (GSM 7110, ?Hope's Nose Limestone, Middle Devonian (Eifelian), Hope, near Torquay, Devon, England) has been examined. It is a poorly preserved specimen which displays both rhomboporid and ptilodictyid affinities. The zoarium is composed of dendroid, moderately delicate, flattened lense-shaped straight bifurcating branches 1.35–1.80mm in diameter. Autozoocial apertures are developed in eight to ten longitudinal rows. Autozoocial apertures are moderately large, 0.28×0.13mm, distinctly rhombic in shape, and closely packed less than one diameter apart. Interapertural walls are thin and appear to be smooth. A single proximal acanthostyle may be associated with autozoocial apertures. These features contrast with the cylindrical branches and oval to circular-shaped autozoocial apertures developed in *R. cylindrica*.

Vine's figured material (BMNH D294-5: Vine 1887, pl.1, figs 7–8) in the collections of the Natural History Museum, London, and some Vine material in National Museum of Wales, Cardiff has been examined, and all specimens are correctly assigned to the genus *Rhombopora*. They are not conspecific with Phillips' Devonian taxon.

The Carboniferous material represents a new taxon which is described and named here as *Rhombopora cylindrica*. A new epithet is required; *similis* of M'Coy cannot be used on account of original misapplication of the name through misidentification (Article 49 – Code of Zoological Nomenclature, 1985).

A holotype for *Rhombopora cylindrica* sp. nov. is designated from the Lower Carboniferous of Carrick Lough, County Fermanagh, Ireland.

STRATIGRAPHICAL RANGE. Carboniferous (Asbian–Pendleian). The range of *Rhombopora cylindrica* has been increased downwards into the Asbian by its discovery in County Fermanagh and Nant-y-Gamar, north Wales, where the taxon is quite uncommon.

DISTRIBUTION. Carrick Lough and Sillees River, County Fermanagh and Nant-y-Gamar, north Wales. Previously recorded and described (see discussion) from the Brigantian of the Midland Valley of Scotland (Young & Armstrong 1871, Young & Robertson 1877)

and the Arnsbergian of Northamptonshire (Vine 1887) and Lancashire (Vine 1885), and the Pendleian of Yorkshire (Bancroft 1984, Vine 1881).

Rhombopora hexagona sp. nov.

Figs 26–31

HOLOTYPE. BMNH PD9535, Upper part of the Glencar Limestone (Viséan, Asbian), Carrick Lough, County Fermanagh.

PARATYPES. BMNH PD9536-9564; TCD.34045-34048, 34121, 34154, 34170, 42591a, 42592c, 42602a; BELUM K2186, from the same locality and horizon as above; TCD.25687, near base of *Michelinia* Beds, Hook Head Formation (Courceyan), Locality 8 (of Dresser 1960), Lyraun Cove, Hook Head, County Wexford; TCD.25884, *Michelinia* Beds, Hook Head Formation (Courceyan), Locality 15 (of Dresser 1960), Brecaun Church, Hook Head, County Wexford; TCD.25885, *Michelinia* Beds, Hook Head Formation (Courceyan), Locality 40 (of Dresser 1960), Patrick's Bay, Hook Head, County Wexford; TCD.25886, *Linoprotuctus* Beds, Hook Head Formation (Courceyan), Locality 92 (of Dresser 1960), Hook Head, County Wexford.

DERIVATION OF TRIVIAL NAME. From the hexagonal pattern of heterostyles disposed around autozoocial apertures.

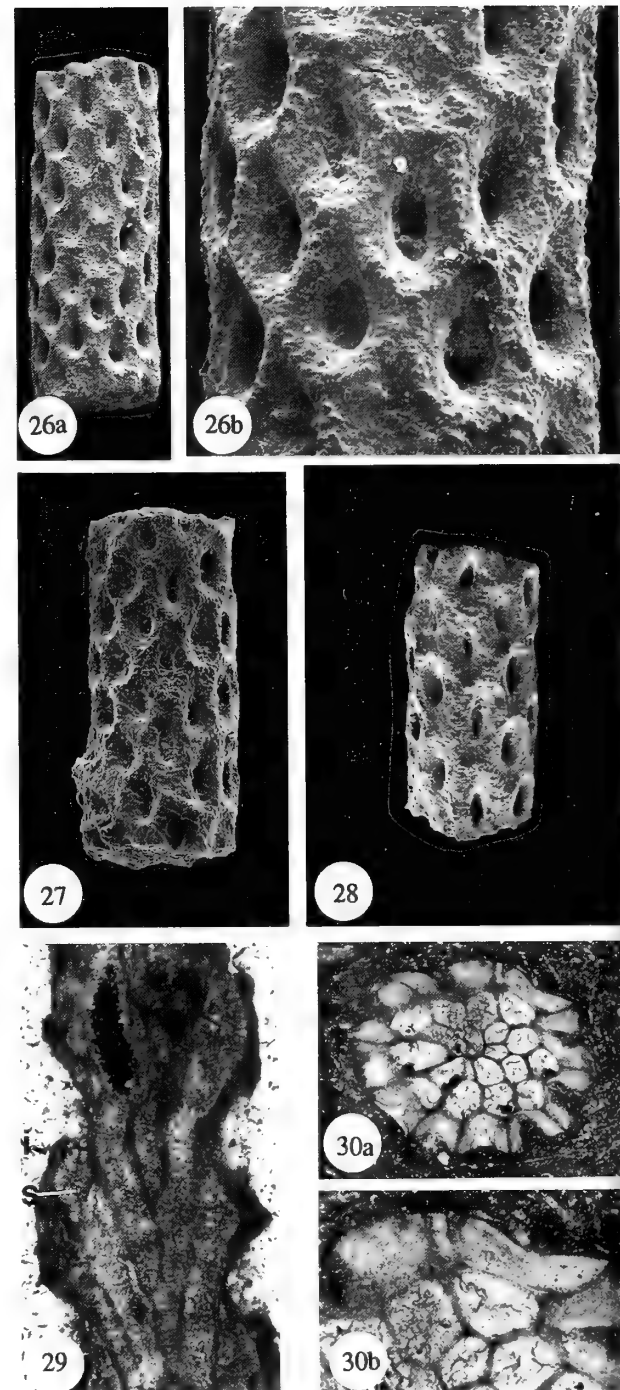
DIAGNOSIS. *Rhombopora* with thin dichotomising cylindrical branches. Autozoocialia are budded from a central linear axis in a spiral manner. Hemisepta are common: a robust inferior hemiseptum is present at the base of the vestibule while a thin superior hemiseptum is found on distal chamber walls high in the endozone. Diaphragms are absent. Autozoocial apertures are oval in shape, vary in size around branches, and are arranged in intersecting oblique and longitudinal rows around the zoarium. Small heterostyles are arranged on ridges between autozoocial chambers in an interlocking hexagonal pattern.

DESCRIPTION. Zoaria are composed of thin cylindrical dichotomising branches that form delicate erect dendroid colonies. No complete colonies were observed: the largest fragment measured 3.38 mm in length.

Branching is infrequent and irregular with either dichotomous bifurcation or lateral perpendicular ramification, producing secondary branches which are slightly narrower than those from which they were derived. All branches retain a constant width along their length.

Autozoocialia deviate from a central axis in a spiral fashion at low angles of 18° to 27°. Chambers are sub-linear in shape, five to six times long as wide, with a slightly attenuated zoocial base. Chambers bend marginally at the exozone and vestibules are orientated at low angles of between 25° and 40° to the zoarial surface. Chamber walls are thin (0.01 mm) in the endozone, with a compound structure of a granular centre surrounded by thin skeletal laminae. The exozone is very thin (0.03–0.15 mm). In cross-section chambers are polygonal in shape.

Autozoocial apertures are large to moderate in size, oval in shape, and arranged in 9 to 15 longitudinally and diagonally intersecting rows around branches. The angle of this intersection varies from 45° to 75°. Long, narrow autozoocial apertures occur on reverse surfaces, while more equidimensional apertures are found towards and on obverse surfaces. Interapertural spacing is inversely proportional to apertural size (see Tables 9 and 12, and Figs 26a and 28). Autozoocial apertures are surrounded by as many as 40 small, blunt, circular heterostyles (0.01 mm in diameter) which arise from the base of, or from within the exozone. They are arranged in single, or occasionally several (particularly on reverse surfaces), rows along the crests of otherwise smooth interapertural walls, or occasionally



Figs 26–30 *Rhombopora hexagona* sp. nov. Upper part of the Glencar Limestone (Viséan, Asbian), Carrick Lough, County Fermanagh; 26, BMNH PD9535 (**holotype**); 26a, colony form, $\times 25$; 26b, detail of 26a showing oval autozoocial apertures and disposition of heterostyles in a hexagonal pattern on interapertural walls, $\times 75$; 27, BMNH PD9536 (paratype), colony fragment, $\times 40$; 28, BMNH PD9537 (paratype), view of 'reverse' surface showing long, thin autozoocial apertures, $\times 25$; 29, BMNH PD9560 (paratype), longitudinal section showing autozoocial chambers with thin superior (labelled 's') and thick inferior (labelled 'i') hemisepta, $\times 35$; 30, BMNH PD9563 (paratype); 30a, transverse section showing circular branch outline, zoocia budded from a central axial area, with thin walls in the endozone and thicker walls in the exozone, $\times 35$; 30b, detail of 30a showing heterostyles on interapertural walls, $\times 75$.

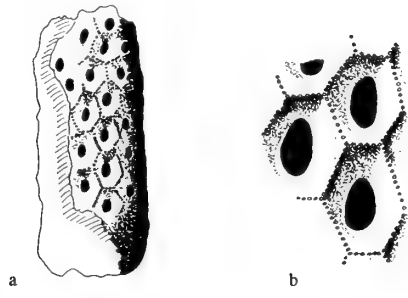


Fig. 31 *Rhombopora hexagona* sp. nov. Line drawings of external features; **a**, colony form; scale bar = 1 mm; **b**, autozoocial apertures surrounded by heterostyles in hexagonal arrangement, scale bar = 0.1 mm.

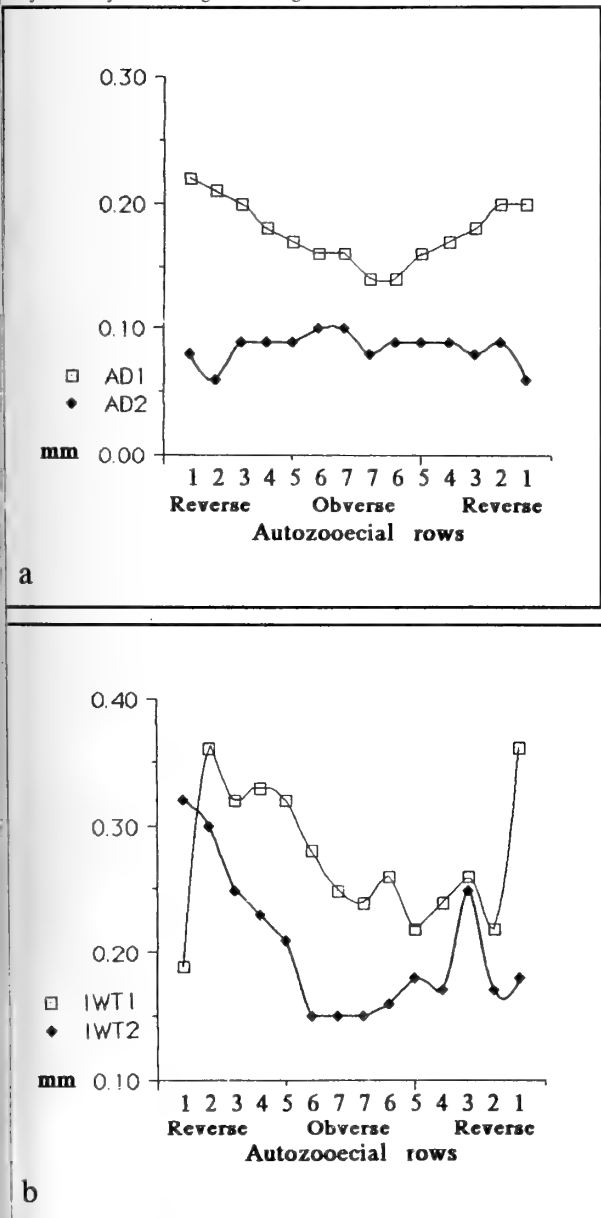


Fig. 32 *Rhombopora hexagona* sp. nov. Graphs of mean values of aperture size and spacing; **a**, apertural size; **b**, apertural spacing. (For explanation of AD1, AD2, IWT1 and IWT2 see Fig. 18).

in an interlocking hexagonal to pentagonal pattern. These hexagons range in size from $0.66 \times 0.25\text{mm}$ to $0.23 \times 0.20\text{mm}$, with the greatest dimensions occurring on reverse surfaces. Autozoocial apertures are generally situated distally within these areas.

Hemisepta are common and are of two types. A prominent superior hemiseptum occurs within the endozone four-fifths along the chamber on distal walls (Fig. 29). They are thin, short (0.04–0.06mm) and have a similar skeletal structure to chamber walls. At the exozone the proximal chamber walls bend through 30° and thicken rapidly to form robust inferior hemisepta 0.13 long by 0.04mm thick. These have a sharp pointed distal extremity and bend marginally into the vestibules. They are composed of laminated skeleton in which lamellae are orientated parallel to the zoarial surface.

Table 8 Measurements of *Rhombopora hexagona* (in mm). N=19.

	NM	x	Mn	Mx	CVw	CVb
ZD	135	0.63	0.48	0.92	4.62	7.71
Z2	25	5.23	4	6	9.93	7.75
AD1	145	0.16	0.10	0.26	20.94	8.32
AD2	146	0.09	0.04	0.18	15.57	5.13
IWT1	139	0.26	0.12	0.66	30.34	3.74
IWT2	136	0.17	0.07	0.39	27.71	4.37
AH	14	0.01	0.01	0.01	50.00	—
AW	31	0.01	0.01	0.02	16.04	—
ET	21	0.43	0.32	0.50	5.72	8.75
TE	42	0.08	0.03	0.15	17.37	2.96

DISCUSSION. *Rhombopora hexagona* is only the second species of the taxon, after *R. cylindrica*, to be recorded from Carboniferous strata of the British Isles and has previously been noted from Courceyan strata of Hook Head, County Wexford (Dresser 1960 MS). A previously recorded species *R. radialis* Owen, 1966 from the Viséan of Derbyshire is regarded as being an arthrostyloid rather than a rhomboporid and is reassigned to the genus *Pseudonematopora*.

Rhombopora hexagona is easily recognised externally from its cylindrical branches on which autozoocial apertures of varying dimensions (which is unusual) are surrounded by a hexagonal pattern of small heterostyles, and internally by the possession of two hemisepta of different sizes and a thin exozone.

The relationship between autozoocial apertural diameter and apertural spacing is illustrated graphically in Fig. 32. Where apertures are long (high AD1) and thin (low AD2) longitudinal autozoocial spacing is moderate (low-high IWT1), and autozoocial spacing between adjacent rows is great (high IWT2). Where apertures are short and fat (low AD1 values; high AD2 values), autozoocial spacing tends to be moderate and narrow (moderate IWT1 values; low IWT2 values). There is an inverse correlation between autozoocial apertural diameters AD1 and AD2 (Fig. 32a) and a moderately positive correlation between autozoocial apertural spacing IWT1 and IWT2 (Fig. 32b). In one specimen (C on Tables 9–12) where 14 autozoocial rows, as against the mean of 10, are developed, these correlations are not good.

Dimensions of 56 other Carboniferous *Rhombopora* taxa are tabulated below. *R. hexagona* differs sufficiently from them, both morphologically and dimensionally, to justify its erection as a new species. It most closely resembles *R. attenuata* Ulrich 1890, in which two acanthostyle types are present, and *R. gracilis* Ulrich 1890, in which acanthostyles are developed at interapertural wall junctions only, but differs in acanthostyle development as well as in the size and spacing of autozoocial apertures.

STRATIGRAPHICAL RANGE. Lower Carboniferous (Courceyan–Asbian).

Table 9 Measurements of autozoocelial aperture length (**AD1**) of *Rhombopora hexagona* around the zoarium from reverse to obverse surface (in mm). N=9 (A-I).

Reverse				Obverse					Reverse					
ROW	1	2	3	4	5	6	7	7	6	5	4	3	2	1
A	—	—	0.17	0.15	0.15	0.13	0.15	0.15	0.14	0.13	0.18	0.18	—	—
B	—	—	0.13	0.21	0.17	0.13	0.16	0.13	0.11	0.12	0.10	0.17	—	—
C	0.22	0.18	0.19	0.18	0.16	0.13	0.13	0.12	0.12	0.13	0.13	0.17	0.20	0.20
D	—	—	0.23	0.13	0.23	0.17	0.15	0.13	0.13	0.14	0.15	0.22	—	—
E	—	—	0.19	0.23	0.17	0.17	0.20	0.10	0.10	0.14	0.14	0.16	—	—
F	—	—	—	0.17	0.12	0.18	0.22	0.20	0.16	0.21	0.22	—	—	—
G	—	—	—	0.18	0.19	0.25	0.18	0.20	0.22	0.30	0.22	—	—	—
H	—	—	0.25	—	0.21	0.20	0.18	0.16	0.14	0.15	0.18	—	—	—
I	—	0.24	0.26	0.23	0.17	0.16	0.12	0.14	0.17	0.15	0.21	0.20	—	—
x	0.22	0.21	0.20	0.18	0.17	0.16	0.14	0.14	0.16	0.17	0.18	0.20	0.20	0.20

Table 10 Measurements of autozoocelial aperture width (**AD2**) of *Rhombopora hexagona* around the zoarium from reverse to obverse surface (in mm). N=9 (A-I).

Reverse				Obverse					Reverse					
ROW	1	2	3	4	5	6	7	7	6	5	4	3	2	1
A	—	—	0.08	0.07	0.08	0.08	0.09	0.08	0.08	0.07	0.09	0.07	—	—
B	—	—	0.09	0.07	0.12	0.10	0.10	0.07	0.08	0.08	0.07	0.06	—	—
C	0.08	0.08	0.10	0.06	0.09	0.10	0.10	0.08	0.10	0.09	0.09	0.08	0.09	0.06
D	—	—	0.12	0.08	0.09	0.12	0.18	0.08	0.08	0.09	0.08	0.12	—	—
E	—	—	0.09	0.08	0.07	0.07	0.06	0.07	0.08	0.06	0.07	0.07	—	—
F	—	—	—	0.16	0.13	0.14	0.14	0.11	0.11	0.13	0.13	—	—	—
G	—	—	—	0.11	0.11	0.10	0.11	0.10	0.09	0.12	0.15	0.13	—	—
H	—	—	—	0.12	0.10	0.12	0.11	0.11	0.10	0.10	0.10	—	—	—
I	—	0.04	0.06	0.08	0.07	0.09	0.08	0.08	0.09	0.09	0.11	0.08	0.07	—
x	0.08	0.06	0.09	0.09	0.09	0.10	0.10	0.08	0.09	0.09	0.09	0.08	0.09	0.06

Table 11 Measurements of interapertural wall thickness (**IWT1**) of *Rhombopora hexagona* around the zoarium from reverse to obverse surface (in mm). N=9 (A-I).

Reverse				Obverse					Reverse					
ROW	1	2	3	4	5	6	7	7	6	5	4	3	2	1
A	—	—	0.19	0.18	0.35	0.31	0.13	0.15	0.20	0.18	0.18	0.21	—	—
B	—	—	0.42	0.29	0.54	0.28	0.25	0.23	0.35	0.30	0.26	0.30	—	—
C	0.19	0.22	0.20	0.17	0.24	0.25	0.28	0.26	0.30	0.22	0.20	0.20	0.22	0.36
D	—	—	—	0.21	0.13	0.21	0.12	0.16	0.13	0.15	—	—	—	—
E	—	—	0.24	0.26	0.21	0.23	0.34	0.15	0.16	0.16	0.35	0.32	—	—
F	—	—	—	0.43	0.35	0.32	0.18	0.23	0.13	0.12	0.14	—	—	—
G	—	—	0.64	0.48	0.30	0.37	0.34	0.37	0.39	0.24	0.28	—	—	—
H	—	—	—	0.52	0.40	0.37	0.34	0.30	0.33	0.32	0.16	—	—	—
I	—	0.51	0.24	0.43	0.40	0.24	0.30	0.33	0.35	0.36	0.40	0.30	—	—
x	0.19	0.36	0.32	0.33	0.32	0.28	0.25	0.24	0.26	0.22	0.24	0.26	0.22	0.36

Table 12 Measurements of interapertural wall thickness (**IWT2**) of *Rhombopora hexagona* around the zoarium from reverse to obverse surface (in mm). N=9 (A-I).

Reverse				Obverse					Reverse					
ROW	1	2	3	4	5	6	7	7	6	5	4	3	2	1
A	—	—	0.24	0.23	0.18	0.17	0.16	0.21	0.22	0.22	0.13	0.26	—	—
B	—	—	0.17	0.31	0.39	0.17	0.20	0.21	0.17	0.23	0.22	0.29	—	—
C	0.32	0.35	0.30	0.21	0.29	0.15	0.13	0.11	0.12	0.13	0.13	0.18	0.17	0.18
D	—	—	—	0.17	0.10	0.21	0.22	0.20	0.23	0.19	—	—	—	—
E	—	—	0.32	0.24	0.25	0.23	0.25	0.23	0.23	0.25	0.26	0.29	—	—
F	—	—	—	0.36	0.17	0.13	0.16	0.13	0.15	0.23	0.18	—	—	—
G	—	—	0.25	0.25	0.14	0.13	0.07	0.06	0.12	0.18	0.23	—	—	—
H	—	—	—	0.13	—	0.10	0.10	0.08	0.09	0.07	0.11	—	—	—
I	—	0.26	—	0.20	0.17	0.12	0.12	0.12	0.13	0.17	0.13	0.25	—	—
x	0.32	0.30	0.25	0.23	0.21	0.15	0.15	0.15	0.16	0.18	0.17	0.25	0.17	0.18

Table 13 Quantitative comparison of *Rhombopora cylindrica* sp. nov. and *Rhombopora hexagona* sp. nov. with some other Carboniferous *Rhombopora* species (dimensions in mm).

	AR	ZD	Z2	AD1	AD2
<i>R. cylindrica</i> sp. nov.	10–16	0.50–1.10	4	0.10–0.35	0.07–0.18
<i>R. hexagona</i> sp. nov.	9–15	0.40–0.90	5	0.10–0.26	0.04–0.18
* <i>R. bifurcata</i> Campbell, 1961	—	1.00–1.60	—	0.20–0.23	0.10–0.13
<i>R. nova</i> Ceretti, 1963	—	1.08–1.25	3	0.38	0.16–0.20
<i>R. multipora</i> Foerste, 1887	20	1.40	7	0.15	0.09
<i>R. prompta</i> Gorjunova, 1988	—	2.52–0.27	—	0.30	0.20–0.22
<i>R. johnsvilleensis</i> Harlton, 1933	—	0.60–0.80	5	0.19	0.10
<i>R. nitidula</i> Harlton, 1933	6	0.4	5	0.29	0.10
<i>R. millepunctata</i> McFarlan, 1942	—	0.6	—	0.14	0.06
* <i>R. lepidodendroides</i> Meek, 1872	—	1.00–3.60	4	0.16–0.29	0.09–0.21
<i>R. ampla</i> Moore, 1929	—	1.00	—	0.31	0.17
<i>R. communis</i> Moore, 1929	—	1.00	3	0.28	0.14
<i>R. constans</i> Moore, 1929	17	1.00	—	0.29	0.14
<i>R. cortica</i> Moore, 1929	—	1.80–2.70	4	0.28–0.29	0.16–0.17
<i>R. fovata</i> Moore, 1929	—	1.00–1.15	—	0.37	0.29
<i>R. munda</i> Moore, 1929	26	1.25	3	0.33	0.18
<i>R. muralis</i> Moore, 1929	—	1.00	—	0.28–0.34	0.20–0.25
<i>R. pilula</i> Moore, 1929	17	1.50–1.70	4	0.43	0.26
* <i>R. tersiensis</i> Nekhoroshev, 1926	—	1.50–2.40	5	0.16–0.25	0.08–0.15
<i>R. binodata</i> Trizna, 1958	—	1.69–2.00	4	0.50	0.4
<i>R. floriformis</i> Trizna, 1958	—	1.60–1.70	7	0.50	0.45
<i>R. insinuata</i> Trizna, 1958	—	1.20–1.40	6	0.35	0.30
<i>R. novitia</i> Trizna, 1958	—	1.15–1.30	5	0.30	0.25
<i>R. perpera</i> Trizna, 1958	—	2.00	3	0.60	0.50
<i>R. sarcinulata</i> Trizna, 1958	—	1.60	5	0.14–0.15	0.08
<i>R. simplex</i> Trizna, 1958	—	1.10–1.50	6	0.15	0.13
<i>R. charasensis</i> Sakagami, 1972	—	2.50–3.80	5	0.19–0.26	0.12–0.18
<i>R. murthyi</i> Sakagami, 1972	—	1.7	4	0.21–0.3	0.10–0.14
<i>R. diaphragmata</i> Shulga-Nesterenko, 1955	—	2.00–3.00	5	—	—
<i>R. riasanensis</i> Shulga-Nesterenko, 1955	—	0.8	4	—	—
<i>R. variaxis</i> Shulga-Nesterenko, 1955	—	2.00–2.50	5	0.25	0.15
* <i>R. armata</i> Ulrich, 1884	—	1.00–1.10	—	—	—
<i>R. crassa</i> Ulrich, 1884	—	2.50–4.50	5	—	—
<i>R. elegantula</i> Ulrich, 1884	—	2.50	4	—	—
<i>R. pulchella</i> Ulrich, 1884	—	0.88	4	—	—
<i>R. incrassata</i> Ulrich, 1888b	—	1.00–1.10	6	0.35	0.30
<i>R. ohioensis</i> Ulrich, 1888b	—	1.00–1.30	—	0.11–0.25	0.07–0.13
<i>R. angustata</i> Ulrich, 1890	6?	0.40–0.50	4	0.17	0.08
<i>R. ?asperula</i> Ulrich, 1890	—	1.00–1.60	—	—	—
<i>R. attenuata</i> Ulrich, 1890	—	0.70–1.00	6	0.15	0.10
<i>R. decipiens</i> Ulrich, 1890	—	1.50–3.00	11	0.15	0.10
<i>R. dichotoma</i> Ulrich, 1890	—	3.00	4	0.12	0.12
<i>R. exigua</i> Ulrich, 1890	—	0.60–0.80	—	0.11	—
<i>R. gracilis</i> Ulrich, 1890	—	1.30	7	0.10	—
<i>R. minor</i> Ulrich, 1890	—	0.50–0.90	—	0.12	—
<i>R. nicklesi</i> Ulrich, 1890	—	0.40–0.90	—	0.17	—
<i>R. simulatrix</i> Ulrich, 1890	—	1.00–2.10	6	0.12	—
<i>R. ?spiralis</i> Ulrich, 1890	—	1.50–2.00	5	0.21	—
<i>R. tabulata</i> Ulrich, 1890	—	1.00–1.50	5	0.18	0.12
<i>R. tenuirama</i> Ulrich, 1890	10	0.40–0.50	5	0.11	0.08
<i>R. transversalis</i> Ulrich, 1890	—	2.50–4.00	5	0.12	—
<i>R. varians</i> Ulrich, 1890	—	2.00–4.00	7	0.12–0.13	—
<i>R. pseudonovita</i> Yang & Lu, 1962	—	1.10–1.70	6	0.12–0.20	0.07–0.11
<i>R. staffordotaxiformis</i> Yang <i>et al.</i> , 1988	—	1.14–1.53	4	0.16–0.21	0.07–0.10

Dimensions condensed from primary sources except where indicated:

*: Sabattini, 1972; *: Huffman, 1970; #: Sakagami, 1972; \$: Ulrich, 1890; †: Lu, 1989.

DISTRIBUTION. Carrick Lough, County Fermanagh, and Hook Head, County Wexford.

TYPES. Duncan (1949) has discussed the problem of Vine's lost material and the implications for the type specimens. She designated a suite of specimens collected by Ulrich in North America (USNM 43311) as (neo)types. Indeed, she should have only designated one neotype. Hageman (1993) has designated one of Ulrich's syntypes (USNM 114392) as the neotype.

DISCUSSION. Confusion has existed over the authorship and the concept of the type species of the genus. J.M. Nickles of the U.S. Geological Survey sent specimens of a bryozoan from the Carbon-

Family HYPHASMOPORIDAE Vine, 1885 Genus *STREBLOTRYPA* (Ulrich MS.) Vine 1884b

TYPE SPECIES. *Streblotrypa nicklesi* (Ulrich MS.) Vine, 1884b, by nonotypy, from the Lower Carboniferous of Hurst, Yorkshire, England and Illinois, U.S.A.

iferous of Kaskasia, Illinois to Vine and Ulrich in 1883. Ulrich, in an 1884 manuscript, named them *Streblytrypa nicklesi* and this description subsequently appeared in print (Ulrich 1890: 667). However, before the appearance of Ulrich's paper, Vine (1884b: 391) published a description of the American specimens together with some specimens from Yorkshire and named them as *S. nicklesi*, stating that this was the name used by Ulrich in his manuscript which as such 'had no validity'. Yet in his subsequent papers Vine (1885, 1889) credits the genus and species, which he consistently names as *nicklesi*, to Ulrich. As was clear later Ulrich had in fact named the taxon *S. nicklesi*, and Hageman (1993) has corrected Vine's error and quotes Ulrich's spelling as the correct name of the type species, and credits Ulrich in Vine as the author. *S. minuta*, described as a new variety by Vine in 1885, was later considered by him to be a variety of *S. 'nicklesi'* (Vine, 1889).

Unfortunately, Vine's original specimens are lost, and it is possible that the American and English forms are not conspecific. Therefore, what is now in question is the original concept of the species and the validity of Hageman's designation of the neotype: should the concept be based upon the American specimens (as is generally agreed (Blake 1983)) or on the now missing British specimen? If it is shown that the original material belonged to two separate taxa then perhaps either the American or British material needs renaming. New collecting is needed at Vine's original locality at Hurst, north Yorkshire, which may yield specimens of *Streblytrypa*, so that comparison with the American material can be made.

Subgenus STREBLYTRYPA (STREBLYTRYPA) (Ulrich MS.)
Vine 1884b

DISCUSSION. Blake (1983: 590) recognized two subgenera in *Streblytrypa*: *S. (Streblytrypa)* and *S. (Streblascopora)* Bassler, 1952. This differentiation is based on the number of axial zooecia contained in the endozone, the location of metapores between autozoocelial apertures, and the presence or absence of hemisepta. Species of *S. (Streblascopora)* display a distinct axial area with more than 10 axial zooecia. Metapores are frequently found beyond the lateral margins of autozoocelia, and hemisepta are rare or absent. The opposite holds for *S. (Streblytrypa)*.

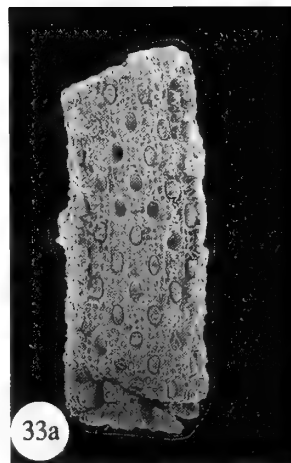
***Streblytrypa (S.) pectinata* Owen, 1966** Figs 33–36

v1966 *Streblytrypa pectinata* Owen: 144, pl.10, figs A–C.

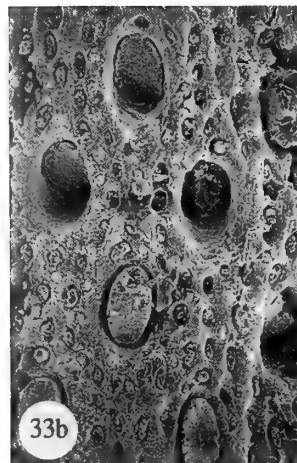
MATERIAL. BMNH PD9565-9579; TCD.34049, 34124, 34129, 34130, 34140; BELUM K3239, Upper part of the Glencar Limestone (Viséan, Asbian), Carrick Lough, County Fermanagh. TCD.42529-42530, Upper part of the Glencar Limestone (Viséan, Asbian), Sillees River, County Fermanagh.

DESCRIPTION. Zoarium ramosa and composed of cylindrical branches 0.67 to 1.04mm in diameter with a circular cross-section.

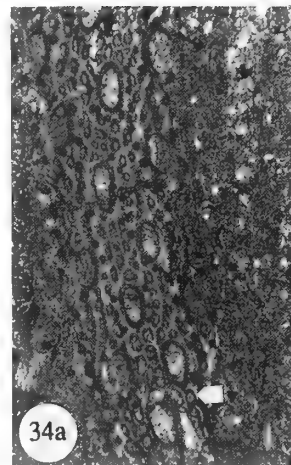
Figs 33–35 *Streblytrypa pectinata* Owen, 1966: Upper part of the Glencar Limestone (Viséan, Asbian), Carrick Lough, County Fermanagh. 33, BMNH PD9565: 33a, zoarial fragment showing dendroid colony form, oval-shaped autozoocelial apertures arranged in longitudinal rows, with three to four rows of metapores developed between, $\times 35$; 33b, detail of 33a, $\times 150$. 34, BMNH PD9578: 34a, tangential section showing autozoocelial apertures surrounded by small metapores (arrowed), $\times 100$; 34b, detail of 34a, $\times 100$. 35, BMNH PD9579: 35a, longitudinal section showing thin exozone pierced by acanthostyles, $\times 30$; 35b, detail of 35a showing acanthostyles in exozonal wall – the calcite rods clearly deflect the skeletal laminae of the outer wall, $\times 100$.



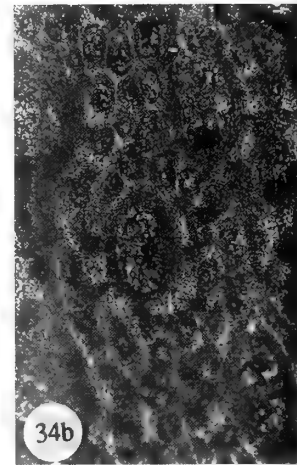
33a



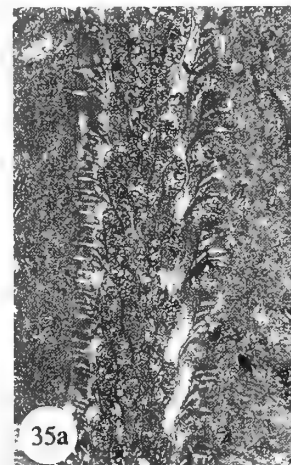
33b



34a



34b



35a



35b

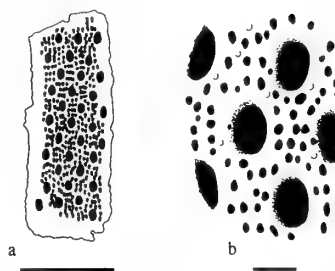


Fig. 36 Line drawing of external features of *Streblytropa pectinata*

Owen, 1966 (BMNH PD9565); **a**, colony form, scale bar = 1 mm; **b**, detail of autozoocoeial apertures surrounded by metapores, scale bar = 0.1 mm.

No complete colonies were observed; the largest fragment examined measured 10.2 mm in length. Branches bifurcate at irregular intervals, and lateral ramifications diverge at a high angle of between 83° and 90°. Branches retain a constant width between ramifications and there is only a slight increase just prior to and after branching.

Autozoocoeial apertures are moderate in size (0.08–0.19 by 0.05–0.10 mm), oval in shape, evenly spaced 2 to 2.5 diameters apart, and occur in 12 to 20 longitudinal rows around the entire branch. Within any one zoarial fragment apertures are of approximately constant dimension. Small oval to occasionally circular-shaped metapores are abundant; twelve to twenty occur in 3 to 4 longitudinal rows between the distal and proximal extremities of adjacent autozoocoeial apertures, and beyond the lateral margins either a single or double row of metapores is present. In cross-section metapores have a thin neck and flare towards the endozone. They are approximately 0.09 mm deep; only a small proportion of metapores penetrate to the base of the exozone.

Autozoocoeia are budded from an axial region in which axial zoocoeia are not present. Chambers are initially recumbent in the endozone and diverge from the branch axis at a low angle of less than 25°. At the exozone they bend through 65° to become orientated nearly perpendicular to the zoarial surface. From this surface the proximal wall of the vestibule slopes at a moderate angle, while the distal wall is perpendicular (Fig. 35a). In cross-section chambers are pentagonal and slightly inflated laterally. Chamber walls in the endozone are thin (0.01 mm) and composed of a granular core covered with very thin laminated layers. The walls thicken rapidly distrozooidally (up to 0.4 mm) in the exozone; much of this expansion is due to metapore development.

Acanthostyles are small (0.02–0.05 mm in diameter) and blunt and are randomly distributed in interapertural areas where they lie at the proximal end of metapores. Acanthostyles arise at the endozone/exozone boundary, thicken slightly laterally and have solid cores composed of granular skeleton, around which is bent laminated skeleton. They form dark granular circles on the zoarial surface.

Table 14 Measurements of *Streblytropa pectinata* in mm. N=13.

MN	x	Mn	Mx	CV	wCVb
D	95	0.87	0.67	1.04	8.75
2	33	6.08	6	7	1.48
D1	114	0.11	0.08	0.19	11.05
D2	113	0.07	0.05	0.10	13.90
S	193	0.34	0.30	0.51	6.50
ID	76	0.02	0.01	0.05	26.25
T	24	0.56	0.41	0.80	10.06
E	32	0.13	0.08	0.22	16.49
H	16	0.03	0.02	0.06	17.15
T	45	0.02	0.02	0.05	18.86
					3.51

DISCUSSION. *Streblytropa pectinata* is very rare in the Lower Carboniferous of the British Isles. From the limestones of County Fermanagh less than 20 zoarial fragments and a small number of specimens in section were found.

The presence of metapores, small acanthostyles, and a thin exozone make this bryozoan very distinctive. Only three other species of *Streblytropa* have been described from strata of Carboniferous age in the British Isles: *Streblytropa cortacea* (Owen 1966), *Streblytropaminuta* (Vine 1889), and *Streblytropa nicklesi* (Ulrich in Vine 1884b). *S. pectinata* differs from *S. cortacea* which possesses a thick exozone and few metapores; *S. minuta*, in which sharp longitudinal ridges and a small number (6 to 8) of metapores are developed; and *S. nicklesi*, which has 9 to 15 metapores and 12 longitudinal rows of autozoocoeial apertures.

STRATIGRAPHICAL RANGE. Lower Carboniferous (Asbian).

DISTRIBUTION. Apart from the occurrences at Carrick Lough and Sillees River, County Fermanagh *Streblytropa pectinata* has previously only been recorded from Castleton, Derbyshire (the type locality).

Genus *CLAUSOTRYPA* Bassler, 1929

TYPE SPECIES. *Clausotrypa separata* Bassler, 1929 by original designation from the Permian of Timor.

DISCUSSION. The taxon has both trepostome and cryptostome features. Of the former the long autozoocoeial chambers, moderately thick exozone, many acanthostyles particularly associated with autozoocoeial apertures. The dendroid zoarial form, arrangement of autozoocoeial apertures and the presence of metapores strongly suggest cryptostome affinities. I consider *Clausotrypa* to have stronger cryptostome than trepostome affinities.

Bassler (1929) assigned the genus to the Order Cryptostomata, family Rhabdomesidae. Many Soviet authors have placed it in the suborder Rhabdomesina Astrova & Morozova, 1956 (Romantchuk 1970, Morozova 1970, 1981), while others assign the genus to the suborder Streblotrypina Gorjunova, 1985 (Gorjunova 1985). Blake (1983: 592) does not consider *Clausotrypa* to be a rhabdomesid, while Gorjunova (1985) does. Blake & Snyder (1987) show, based on a cluster analysis of 44 characters, that *Clausotrypa* is rather unusual. It does not easily fall into any familial grouping.

Recognising the obvious need for fuller taxonomic and comparative studies the genus is tentatively placed here in the family Hyphasmoporidae, Vine 1885.

Clausotrypa ramosa (Owen, 1973) comb. nov. Figs 37–41

v1973 *Sulcoretepora? ramosa* Owen: 304, pl. 9a–c.

HOLOTYPE. The holotype of *Sulcoretepora? ramosa* Owen, 1973 is represented by a zoarial fragment and three thin sections cut from it, collected from shales below the Rossmore Mudstone (upper Viséan), Tullaghoge, County Tyrone, in the collections of the Ulster Museum (BELUM K1830).

MATERIAL. BMNH PD9577; 9627–9637; 9730–9739; TCD.34067–34078, 34136, 34163, Upper part of the Glencar Limestone (Viséan, Asbian), Carrick Lough, County Fermanagh. TCD.42513, 42531–42534, Upper part of the Glencar Limestone (Viséan, Asbian), Sillees River, County Fermanagh.

DIAGNOSIS. *Clausotrypa* forming semi-robust erect cylindrical dichotomising zoaria. Autozoocoeia more frequent on one side of branch than the other. Metapores, closed to the surface, are developed in interapertural areas. Autozoocoeial apertures are circular, moderate in size, widely spaced, and are surrounded by six to eight

acanthostyles. Strong undulating ridges and short acanthostyles are common in interapertural areas.

DESCRIPTION. Zoaria form dendroid expansions of unknown maximum height and are composed of cylindrical dichotomising or bifurcating branches 0.46 mm to 1.12 mm in diameter.

Autozoocia are arranged in poorly defined longitudinal rows and are developed throughout the zoarium. They are budded from a central undulating axis in an annular or irregular pattern. Autozoocia chambers have a sub-linear shape, are eight times as long as wide, and diverge distally from the axis at low angles of between 10° and 20°. They bend slightly at the exozone and vestibules are orientated at a high angle to the zoarial surface. In cross-section chambers are sub-rounded in shape. Endozonal walls are thin, undulatory, and retain a constant width along their length. Chamber walls are thickened in the exozone to a maximum width of 0.52 mm. The exozone averages 0.07 mm in width and is approximately one sixth of the branch diameter on either margin.

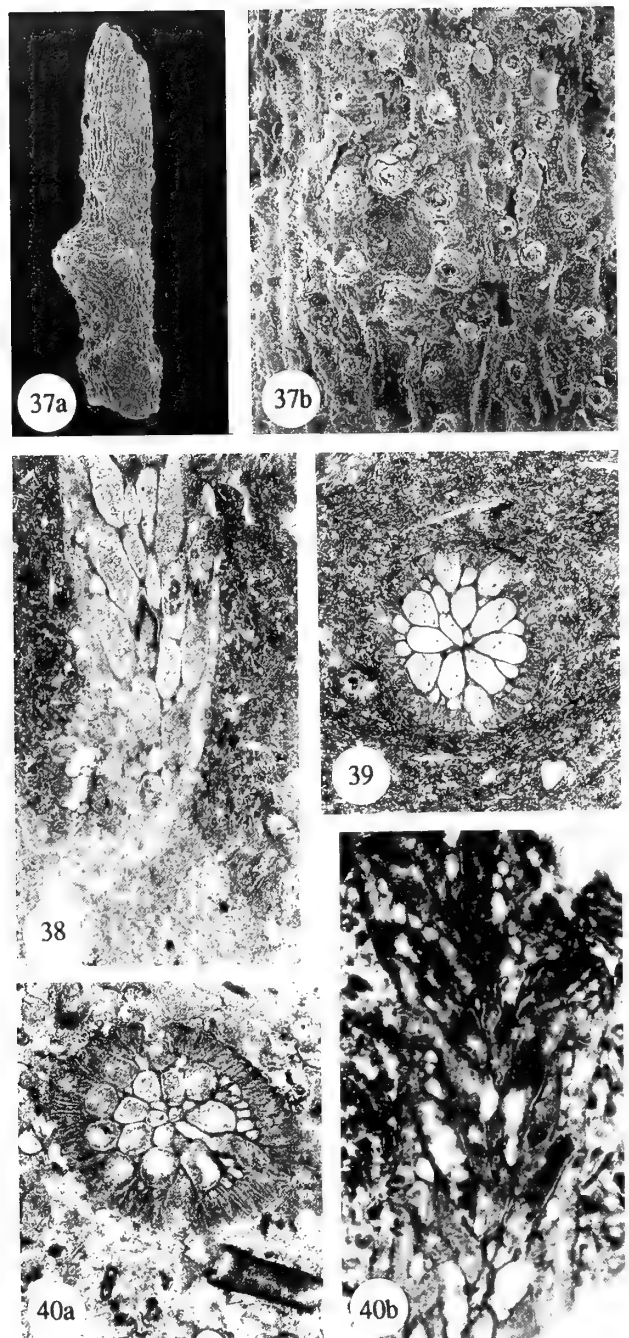
Metapores are developed at the top of the endozone and the base of the exozone. They are small, circular to oval structures, usually closed at the zoarial surface. One or two are disposed between autozoocia.

Autozoocia apertures are moderate in size, oval in shape, widely spaced approximately four to five diameters apart, and are arranged in longitudinal rows around branches. On most zoaria apertures are more abundant on one side of branches than on the other.

Acanthostyles are common. Six to ten surround autozoocia apertures, often resembling a peristome, and they also occur randomly and widely scattered in interapertural areas. They develop from the base of the exozone only. Strong longitudinal ridges also decorate interapertural areas.

DISCUSSION. *Clausotrypa ramosa* was first described as *Sulcoretepora? ramosa* by Owen (1973: 305). He suggested that the taxon is either a sulcoreteporid or a rhabdomesoniid depending on which of the two characters, the presence of mesozoocia ('mesopores' of Owen), or the ramoso zoarial form, is considered to be of stronger generic importance. He assigned the taxon to the former, but ignored the diagnostic features of the genus *Sulcoretepora*, namely the bifoliate zoarial habit and the arrangement of autozoocia in longitudinal rows, budded from a plicated median carina.

Several *Clausotrypa* species have been previously described. Of



Figs 37–40 *Clausotrypa ramosa* (Owen, 1973) comb. nov.; 37–39:

Upper part of the Glencar Limestone (Viséan, Asbian), Carrick Lough, County Fermanagh. 37, BMNH PD9627; 37a, dendroid zoarium showing aborted lateral branch development, oval-shaped autozoocia apertures arranged in crude longitudinal rows, with striated ridged interapertural areas, $\times 25$; 37b, detail of 37a, showing oval-shaped autozoocia aperture surrounded by seven large acanthostyles. Acanthostyles are also developed in interapertural areas, $\times 200$. 38, BMNH PD9636, longitudinal section showing sublinear autozoocia chambers, budded from a poorly defined axis. Circular metapores are present at the endozone/exozone boundary, $\times 25$. 39, BMNH PD9637, transverse section showing pyriform autozoocia chamber cross-sections, circular/polygonal metapores, and acanthostyles in exozone, $\times 25$. 40, Limestone and Shales below Rossmore Mudstone (Upper Viséan), Tullaghoge, County Tyrone; Owen Collection. BELUM K.1830 (lectotype); 40a, transverse section showing pyriform autozoocia chamber cross-sections, and circular/polygonal metapores (figured as *Sulcoretepora ramosa* by Owen, 1973, pl. 9c, $\times 25$); 40b, longitudinal section showing autozoocia chambers budded from an irregular axis, and small circular/polygonal metapores developed at the base of the thin exozone region (figured as *Sulcoretepora ramosa* by Owen, 1973, pl. 9b, $\times 25$).

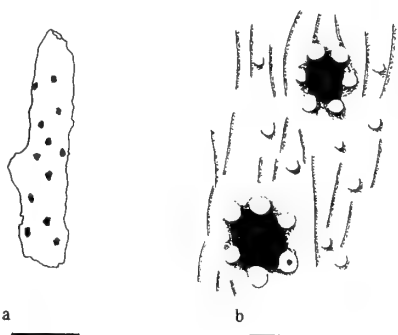


Fig. 41 *Clausotrypa ramosa* (Owen, 1973) comb. nov. Line drawing of external features of BMNH PD9627; **a**, colony form, scale bar = 1 mm; **b**, detail of autozoocia apertures; scale bar = 0.1 mm.

Table 15 Measurements on *Clausotrypa ramosa* (in mm). N=17.

	MN	x	Mn	Mx	CV	wCVb
ZD	102	0.73	0.46	1.12	7.56	5.97
AD1	107	0.11	0.06	0.16	13.06	9.68
AD2	106	0.08	0.05	0.14	14.87	7.67
IWT1	57	0.53	0.28	0.85	12.85	4.14
IWT2	64	0.25	0.15	0.42	17.38	4.38
Z2	13	3.4	2	5	16.05	3.9
ET	6	0.42	0.31	0.52	10.60	4.34
TE	10	0.07	0.03	0.17	14.54	1.33

these only one, *C. limpida* Gorjunova, 1988, is from the Carboniferous, while all the rest occur in Permian strata. Comparison of *C.*

ramosa with these species shows it to be distinct from them all (see Table 16). It is morphologically most similar to *C. monticula* (Eichwald, 1860) but differs significantly by having thicker branches and larger autozoocia apertures. Bassler (1929) regards *Rhombopora?* *spiralis* Ulrich 1890 from the Carboniferous of Kentucky as belonging to *Clausotrypa*. However, after examination of the original description and figures I consider the taxon to be correctly identified by Ulrich.

STRATIGRAPHICAL RANGE. Lower Carboniferous (Asbian).

DISTRIBUTION. Carrick Lough and Sillees River, County Fermanagh and Tullaghoge, County Tyrone, Ireland.

Order **FENESTRATA** Elias & Condra, 1957
Family **ACANTHOCLADIIDAE** Zittel, 1880
Genus **BACULOPORA** Wyse Jackson, 1988

TYPE SPECIES. *Vincularia megastoma* M'Coy, 1844 by original designation, from the Lower Carboniferous (Viséan, Brigantian) of Killymeal, Dungannon, County Tyrone, Ireland.

***Baculopora megastoma* (M'Coy, 1844)**

Fig. 43

MATERIAL. BMNH PD8109-PD8127, TCD.29284-29303, TCD.34124, 34131, 34156, 34162; NMI: F19501-F19520; BELUM K3137, K3436, K12088-K12107, Upper part of the Glencar Limestone, Viséan (Asbian), Carrick Lough, County Fermanagh. BMNH PD8128-PD8132; TCD.42535-42538, Upper part of the Glencar Limestone (Viséan, Asbian), Sillees River, County Fermanagh.

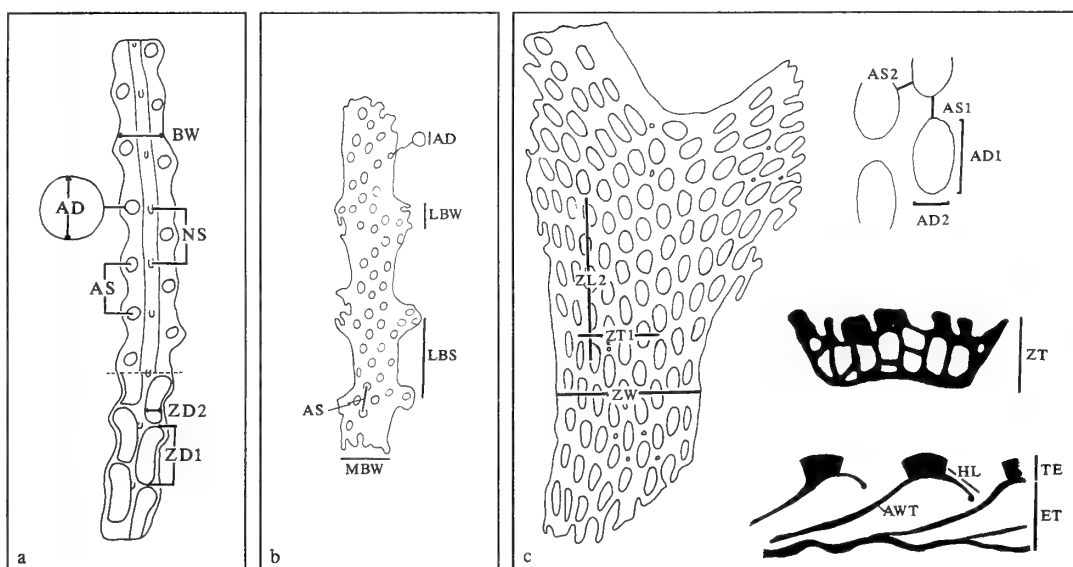


Fig. 42 Measurements taken on fenestrae in this study. **a**, *Diploporella tenella*; **b**, *Ichthyorachis newenhami*; **c**, *Rhombocladia dichotoma*. AD = Autozoocia apertural diameter; AD1 = Autozoocia apertural diameter measured parallel to growth direction; AD2 = Autozoocia apertural diameter measured perpendicular to growth direction; AR = Number of longitudinal autozoocia apertural rows; AS = Autozoocia apertural spacing: minimum distance between two adjacent autozoocia apertures, measured from their centres; AS1 = Autozoocia apertural spacing measured parallel to growth direction; AS2 = Autozoocia apertural spacing measured perpendicular to growth direction; BW = Branch width; ET = Endozone thickness; HL = Hemiseptum length; LBW = Lateral branch width measured perpendicular to growth direction; LBS = Spacing between the centres of two successive lateral branches; MBW = Main branch width measured perpendicular to growth direction; NS = Nodal spacing: distance between two adjacent carinal nodes; TE = Exozone thickness; ZD1 = Length of autozoocia chamber; ZD2 = Width of autozoocia chamber; ZL2 = Number of autozoocia apertures contained in a 2mm line drawn parallel to growth direction; ZT = Zoarial thickness; ZT1 = Number of autozoocia apertures contained in a 1mm line drawn perpendicular to growth direction; ZW = Zoarial width.

Table 16 Comparison of *Clausotrypa* species (dimensions in mm).

	ZD	AD1	AD2	IWT1	IWT2
<i>C. ramosa</i> (Owen, 1973) comb. nov.	0.46–1.12	0.06–0.16	0.05–0.14	0.28–0.85	0.15–0.42
<i>C. limpida</i> Gorjunova, 1988	0.6–0.9	0.25	0.13	—	—
<i>C. clara</i> Krutchinina, 1986	2.5–3.0	0.4–0.5	0.2–0.25	0.2	0.12
<i>C. conferata</i> Bassler, 1929	2.8	0.32	0.25	0.2	0.1–0.15
<i>C. costata</i> Romantchuk, 1981	4.2–4.3	0.21	0.16–0.2	0.3–0.6	0.43–0.64
<i>C. exillis</i> Sakagami, 1961	1.3–1.4	0.1–0.13	—	—	—
<i>C. minor</i> Bassler, 1929	1.3	0.2–0.25	0.15–0.20	1.0	0.3
<i>C. monstruosa</i> Morozova, 1970	4.0–4.5	0.16–0.2	—	—	—
<i>C. monticola</i> (Eichwald, 1860)	1.0–2.5	0.17–0.2	0.12–0.14	—	—
<i>C. petaloidea</i> Romantchuk, 1970	4.8–5.0	0.24–0.25	—	—	—
<i>C. separata</i> Bassler, 1929	0.15–2.6	0.3	0.17	0.4	0.3
<i>C. spinosa</i> Fritz, 1932	1.0–1.5	0.26–0.27	0.13–0.14	0.35	0.3

Data from original sources.

DESCRIPTION. Colonies consist of very slender branches that divide at irregularly spaced intervals, with branches bifurcating at low angles, and with lateral ramifications also occurring. Branches are straight or gently flexuous, and are circular in cross-section. No complete colonies have been discovered, and the largest fragment examined was 1.53mm in length. Bifurcations and lateral branches appear to be widely spaced, as two laterals have not been observed on the same colony. Distal branches are thinner than proximal branches, with a range in diameter from 0.26mm to 0.36mm observed in one colony fragment. Branch width decreases slightly after bifurcation but soon increases to equal the width of the preceding link. Lateral branches are thinner than main branches. The obverse surface bears faint undulating striae, occasionally with rows of small circular stylets (weathering to small pits) along the crests of striae.

Autozoocial apertures are regularly arranged in quincunx, in four to seven longitudinal rows. They are small, circular, lack peristomes and are evenly spaced along the length of the branch. Some apertures are surrounded by six small pustules, giving them a stellate appearance. The reverse surface is smooth or faintly striated. Autozoocial chambers are rectangular in profile with pentagonal bases.

Internally the skeletal arrangement is tripartite; a primary granular layer is surrounded by an inner laminated layer lining zoocial chambers, and an outer laminated layer. Small stylets composed of granular skeleton penetrate through the outer laminated skeleton where they appear as pustules or weathered pits.

DISCUSSION. A complete systematic description of the genus *Baculopora* and the species *B. megastoma* is given in Wyse Jackson (1988).

Genus *DIPLOPORARIA* Nickles & Bassler, 1900

TYPE SPECIES. *Glauconeome (Diplopora) marginalis* Young & Young, 1875, by original designation from the Upper Limestone Shales (Lower Carboniferous) of the British Isles (cited localities: Hairmyres, East Kilbride; Beghill, near Hamilton; Gillfoot, near Carlisle; Hook Head, County Wexford).

***Diploporaria marginalis* (Young & Young, 1875)**
Figs 44, 49

- 1875 *Glauconeome (Diplopora) marginalis* Young & Young: 326, pl.3, figs 14–21.
 1877 *Glauconeome (Diplopora) marginalis* Young & Young; Vine, fig. 207.
 1881 *Glauconeome (Diplopora) marginalis* Young & Young; Vine: 333.

1885	<i>Diplopora marginalis</i> Young & Young; Vine: 83.
1900	<i>Diploporaria marginalis</i> (Young & Young); Nickles & Bassler: 233.
1953	<i>Diploporaria marginalis</i> (Young & Young); Bassler: G127, figs 87–6a, 6b.
1975	<i>Diploporaria marginalis</i> (Young & Young); Graham: 9, pl. 4, figs 6, 6a, 6b.
1987	<i>Diploporaria marginalis</i> (Young & Young); Bancroft: 196.
1991	<i>Diploporaria marginalis</i> (Young & Young); Billing: 41.

LECTOTYPE. Graham (1975) designated a lectotype but cited a cavity slide that contained several zoaria. Consequently Bancroft (1984-ms) designated specimen number 14 in cavity slide HM D144 (Hunterian Museum) as lectotype. This designation is formalised herein.

MATERIAL. Three zoarial fragments, BMNH PD9580; TCD.34050-34051, Upper part of the Glencar Limestone (Viséan, Asbian), Carrick Lough, County Fermanagh.

DESCRIPTION. Zoaria are small non-pinnate expansions, composed of delicate straight branches 0.21 to 0.34 mm in diameter with sub-circular cross-sections. Lateral branches were not developed in the specimen examined.

Autozoocia are arranged in two longitudinal rows along the length of the branch. Autozoocial apertures are small (0.07–0.09 mm in diameter), circular, and are surrounded by a complete peristome. They are regularly spaced two to two and a half diameters apart either side of a median carina. The lateral margin and up to half the apertural diameter protrudes beyond the margin of the branch. This produces a sharp serrated branch outline.

A faint median carina carries regularly spaced oval to circular nodes 0.02 mm in diameter. Two equally faint longitudinal ridges lie either side of the median carina inside the inner margins of autozoocial apertures. Interapertural areas are smooth. The reverse surface is gently rounded and smooth. Internal features were not seen.

Table 17 Measurements of *Diploporaria marginalis* (in mm). N=1.

	NM	x	Mn	Mx	CVw	CVb
BW	10	0.27	0.21	0.34	4.40	—
AD	10	0.08	0.07	0.09	10.52	—
AS	11	0.29	0.28	0.33	28.85	—
NS	6	0.30	0.28	0.32	22.69	—

DISCUSSION. *Diploporaria marginalis* is very rare in the Asbian of County Fermanagh. In the present study only three zoarial frag-

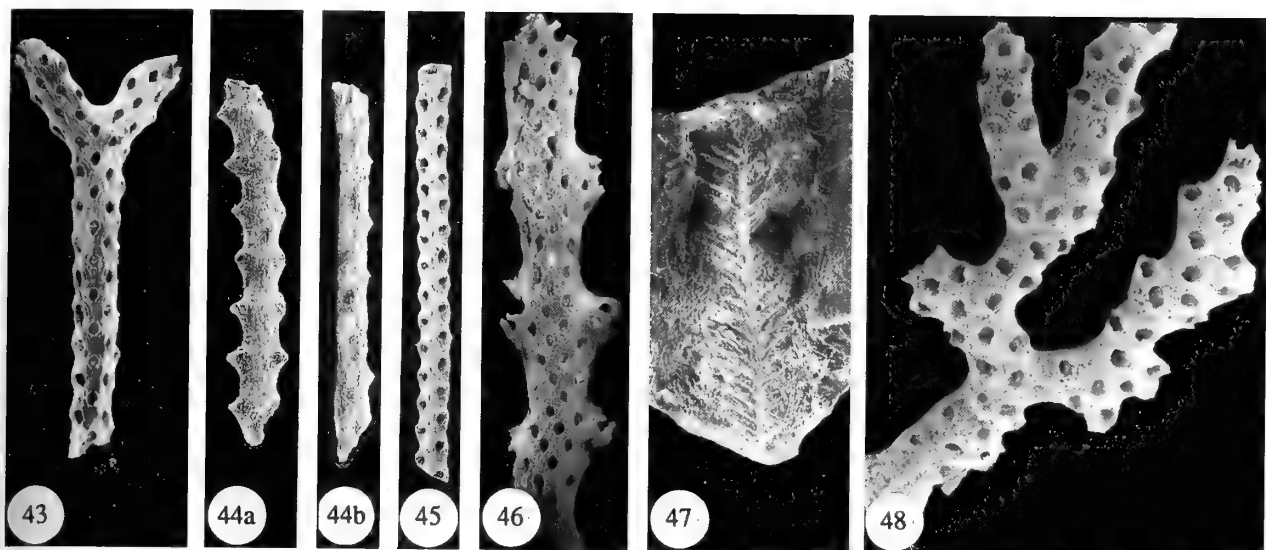


Fig. 43 *Baculopora megastoma* (M'Coy, 1844); Upper part of the Glencar Limestone (Viséan, Asbian), Carrick Lough, County Fermanagh. BMNH PD8109, obverse surface detail with five longitudinal rows of autozoocia and bifurcation of zoarium, $\times 22$.

Fig. 44 *Diploporaria marginalis* (Young & Young, 1875); Upper part of the Glencar Limestone (Viséan, Asbian), Carrick Lough, County Fermanagh. BMNH PD9580; **44a**, obverse surface of branch fragment showing disposition of autozoocia in two longitudinal rows, one either side of a strong median carina. The carina consists of adjacent longitudinal ridges, the central one of which bears distinct nodes. Autozoocial apertures are circular and their edges protrude far beyond the branch margin, $\times 40$; **44b**, lateral view showing elevated carinal nodes, $\times 40$.

Fig. 45 *Diploporaria tenella* Wyse Jackson, 1988; Upper part of the Glencar Limestone (Viséan, Asbian), Carrick Lough, County Fermanagh. BMNH PD8138 (**holotype**), obverse surface detail of a slender zoarium with one row of autozoocia developed either side of a central carinal ridge, $\times 25$.

Figs 46–47 *Ichthyorachis newenhami* M'Coy, 1844; **46**, Upper part of the Glencar Limestone (Viséan, Asbian), Carrick Lough, County Fermanagh. BMNH PD9581, obverse surface showing a strong mainstem and broken lateral branches. Four longitudinal rows of autozoocia are developed on the former, fewer rows on the latter. Autozoocial apertures are small and circular in shape, $\times 20$. **47**, Carboniferous Limestone (Dinantian), Kilmallock, County Limerick. NMING:F6044 (**lectotype**), large colony fragment consisting of a straight mainstem with straight lateral branches diverging at moderate angles. Preservation of the specimen is poor and autozoocia of the mainstem are not seen; some lateral branches carry four autozoocia rows. Figured by M'Coy, 1844, pl. 29, fig. 8, $\times 0.8$.

Fig. 48 *Thamniscus colei* Wyse Jackson, 1988; Upper part of the Glencar Limestone (Viséan, Asbian), Carrick Lough, County Fermanagh. BMNH PD8959 (**holotype**), obverse surface detail showing circular bifurcating branches, autozoocia developed in three to four irregular rows, and circular apertures surrounded by complete peristomes, $\times 20$.

ments were recovered. *D. marginalis* is a distinct species which can easily be recognised from its delicate zoarium with strongly serrated margins caused by autozoocial apertures that project laterally.

It was first described as a *Glauconeum* species by Young & Young 1875. They noted the presence of small orifices proximal to autozoocial apertures which were divided from them by a thin septum. Abrasion of this septum produced a pyriform aperture. Such apertures and 'orifices' have not been observed by subsequent workers. They probably result from the abrasion of the zoarial surface and the revealing of the superior hemiseptum (Ulrich 1890, Bancroft 1984).

Vine (1881, 1885) added nothing to the original description of the species. He refers to a more robust form found in Scotland. However, as he does not illustrate these forms, and as his specimens are lost it is impossible to substantiate these records.

While the two species of *Diploporaria* found in the British Isles (*D. marginalis* and *D. tenella*) show morphological similarities there are a number of important differences between them. The autozoocial apertures in *D. marginalis* possess a prominent outer peristomial rim which extends markedly beyond branch margins giving branches a strongly serrated outline. In *D. tenella* peristomial rims are absent and autozoocial apertures hardly protrude beyond the branch margins giving them a smooth sinuous outline. Apertures are generally spaced further apart in *D. tenella*. Carinal nodes in *D.*

tenella are more evenly and closely spaced than in *D. marginalis*.

STRATIGRAPHICAL RANGE. Lower Carboniferous (Asbian-Brigantian). The range has been extended downwards into the Asbian for the first time.

DISTRIBUTION. This is the first record of this species outside Great Britain where it is common in the Midland Valley of Scotland and rarer in Yorkshire and Lancashire. It is very rare in County Fermanagh.

Diploporaria tenella Wyse Jackson, 1988. Figs 42a, 45

MATERIAL. BMNH PD8138–PD8149, PD8950–8958, TCD.29303–29313, TCD.34132; NMI:F19521–F19530, BELUM K12108–K12117, Upper part of the Glencar Limestone, Viséan (Asbian), Carrick Lough, County Fermanagh. TCD.42539–42542, Upper part of the Glencar Limestone (Viséan, Asbian), Sillees River, County Fermanagh.

DESCRIPTION. Colonies are very small and branches dichotomise irregularly. The largest fragment examined measured 5.9 mm in length. Branches are slender, gently flexuous, and have a sub-circular cross-section. Lateral branches diverge at angles of between 70° to 80° from the main stem and slight flaring of lateral branch bases accompanies their development. Branch surfaces are smooth

to faintly pustulose. A narrow but prominent median carina is developed on the mainstem and lateral branches, and distinct nodes are regularly spaced on the carina at distances equal to the interapertural spacing.

Autozoocial apertures are small, circular, and lack peristomial rims. They are regularly spaced (about twice their diameter apart) and are usually alternately arranged in two longitudinal rows on either side of the median carina, but may occasionally be paired across the carina. The outer margins of autozoocial apertures protrude slightly beyond the lateral margin of branches, producing a gently sinuous branch outline. Internally the chambers are pentagonal in transverse section and longitudinally rectangular. Hemisepta are not developed.

DISCUSSION. A complete systematic description of *D. tenella* is given in Wyse Jackson, 1988.

Genus *ICHTHYORACHIS* M'Coy, 1844

TYPE SPECIES. *Ichthyorachis newenhami* M'Coy, 1844, by monotypy, from the Lower Carboniferous (Viséan, Chadian?) of Killmallock, County Limerick, Ireland.

M'COY'S ORIGINAL DIAGNOSIS. 'Coral plumose, composed of a straight, central stem or midrib, having on either side a row of short, simple branches or pinnae, all in the same plane; obverse both of the midrib and lateral branches rounded, without keel, and each bearing several rows of small, prominent, oval pores, arranged in quincunx; reverse rounded, smooth or finely striated.'

EMENDED DIAGNOSIS. Acanthocladid with pinnate zoarium composed of a mainstem and regularly-spaced, co-planar lateral branches which diverge from the mainstem at a high angle. Dissepiments are absent. Branches are circular to sub-circular in cross-section. Interapertural areas and the branch reverse surface are smooth or faintly striated. Autozoocia are arranged in 4 to 6 longitudinal rows on the mainstem, and in 3 to 4 rows on lateral branches. Autozoocial apertures are small, circular to oval in shape, regularly-spaced, and occur on the obverse surface only.

STRATIGRAPHICAL RANGE. Lower Devonian-Lower Carboniferous.

DISTRIBUTION. British Isles, Europe, United States.

Ichthyorachis newenhami M'Coy, 1844

Figs 42b, 46-47, 51

- v1844 *Ichthyorachis newenhami* M'Coy: 205, pl.29, fig.8.
- 1854b *Ichthyorachis newenhami* M'Coy; M'Coy: 104.
- 1857 *Ichthyorachis newenhami* M'Coy; Jukes: 454.
- 1862 *Ichthyorachis* [sic] *newenhami* M'Coy; M'Coy, pl.29, fig.8.
- 1883 *Ichthyorachis* sp. Vine: 171.
- 1884a *Ichthyorachis newenhami* M'Coy; Vine: 196.
- 1886 *Ichthyorachis* [sic] *nevenhami* [sic] M'Coy; Hoernes: 230, fig. 233.
- 1953 *Ichthyorachis newenhami* M'Coy; Bassler: G128, fig. 88 (3a-c).
- 1966v *Penniretepora triserialis* Owen: 141, pl.9, figs A-C pro parte.

LECTOTYPE. Herein designated NMING:F6044; Killmallock, County Limerick (Viséan, Chadian?); C.B. Newenham Collection; figured M'Coy 1844, pl.29, fig.8. This is the only extant specimen of *Ichthyorachis* from the collection on which M'Coy based his de-

scription. Newenham also collected specimens from County Cork (M'Coy 1844: 206).

MATERIAL. BMNH PD9581-9590, TCD.34052, Upper part of the Glencar Limestone (Viséan, Asbian), Carrick Lough, County Fermanagh.

M'COY'S ORIGINAL DIAGNOSIS. 'Stem and lateral branches with five rows of oval, prominent pores, closely arranged in quincunx; reverse flattened, slightly convex, divided by a deep groove along the middle; obsoletely striated longitudinally; lateral branches half the thickness of the midrib, space between them equal to the diameter of the midrib.'

EMENDED DIAGNOSIS. *Ichthyorachis* with small delicate pinnate zoaria. Two sets of straight lateral branches diverge from either side of a thin, straight central main stem at a high angle. Lateral branches are regularly spaced and may be offset from each other either side of the main stem, but more frequently occur paired. Branches are circular to subcircular in cross-section. The obverse surface is smooth and rounded, with faint longitudinal striae in interapertural areas. The reverse surface is barren, rounded or slightly flattened, smooth, longitudinally striated, or with a central groove occurring down the centre. Autozoocia are arranged in longitudinal rows on branches with 4 to 5 on the main stem and 3 to 4 on laterals.

Autozoocial apertures are small, circular to oval in shape, lack peristomes, and are regularly arranged in quincunx.

DESCRIPTION. Zoaria form small pinnate expansions, consisting of a main stem and lateral branches. The largest fragment in the County Fermanagh assemblage examined is 17.3 mm in length (the lectotype, which was collected in County Limerick, is larger, and measures 53 mm in length (Fig. 47)). The main stem is thin, straight or gently flexuous, and circular in cross-section. A small increase in main stem diameter precedes lateral branch development. Lateral branches lie in the same plane as the mainstem, and branch from it at angles of between 50° and 60°. They are regularly spaced, about 2 diameters apart, and usually paired either side of the main stem. Occasionally they are marginally offset. Lateral branches are thinner than the mainstem with a straight or undulatory margin, and circular cross-section. The longest lateral branch observed is only 1 mm in length: most are broken at their bases. The obverse surface is rounded and faint longitudinal striae are developed along its length. The reverse surface is also rounded, and may bear indistinct longitudinal ridges or be smooth.

Autozoocia are arranged regularly in 4 to 5 longitudinal rows on the main stem, and 3 to 4 rows on the lateral branches. Autozoocial apertures are small, circular, and constantly spaced about 2 diameters apart. Apertural spacing becomes fractionally closer towards the branch node.

Details of internal features are unknown as only silicified fragments have been recovered from Carrick Lough.

Table 18 Measurements of *Ichthyorachis newenhami* (in mm). N=10.

	NM	x	Mn	Mx	CVw	CV
MBW	45	0.70	0.55	0.87	5.52	8.3
LBW	23	0.57	0.50	0.70	8.15	11.1
LBS	27	1.40	1.05	1.75	8.46	11.1
AD	111	0.13	0.10	0.20	9.10	7.7
AS	113	0.36	0.22	0.45	12.46	14.1

DISCUSSION. Although only 10 colonies of *Ichthyorachis newenhami* were measured it was found that they showed very lit-

morphological variation. Main stem width, lateral branch width, lateral branch spacing, and autozoocelial apertural diameter all display low coefficients of variation, both within and between colonies. A slightly larger variation occurs in autozoocelial apertural spacing. *Ichthyorachis newenhami* is a distinctive but uncommon fenestrate form found in the Carboniferous of the British Isles. It has previously been reported only from Counties Cork and Limerick (M'Coy 1844), Hook Head in County Wexford (Courceyan) (Dresser 1960), and Castleton in Derbyshire (Vine 1883, 1884a).

Examination of some of the type specimens of *Penniretepora triserialis* Owen, 1966 from the Upper Viséan of Treak Cliff, Castleton, Derbyshire (holotype: LL.2978; paratype: LL.2980) shows that autozoocelia are arranged in three rows on mainstems and in two rows on lateral branches. This arrangement is characteristic of *Ichthyorachis*, and conceptually cannot be attributed to *Penniretepora*. The gross size of the specimens shows them to lie within the range exhibited by *I. newenhami*. The remaining type material of *P. triserialis* (paratypes: LL.2979, LL.2981-2983), also from the Upper Viséan of Treak Cliff, Castleton, Derbyshire, has been examined and the 'third row of autozoocelia' on mainstems are found to be the cores of braided carinal nodes. These specimens belong to an indeterminate *Penniretepora* species and *P. triserialis* Owen, 1966 is herein regarded as a species inquirenda.

Lower Devonian species of *Ichthyorachis* are also known. *I. nereis* occurs in the Helderbergian of New York (Hall 1874), and *Ichtyorachis* [sic] sp. has been found in the Emsian of France (Rondeau 1890, Bigey 1973).

King (1849, 1850) referred *Ichthyorachis* to his genera *Acanthocladia* and *Thamniscus* owing to the similarities of the branching pattern with the former, and autozoocelial arrangement with the latter. Comparison of the three taxa shows King's reasoning to be incorrect. *Ichthyorachis* is very distinct from the other two taxa. Branches in both *Acanthocladia* and *Thamniscus* are more robust and irregular than in *Ichthyorachis*, and distinct peristomial rims are developed around autozoocelial apertures in *Thamniscus*.

Ichthyorachis does, however, resemble *Baculopora* Wyse Jackson 1988 in the development of 4 or more rows of autozoocelia on branches. However, the two taxa are generically distinct in that *Ichthyorachis* bears regular lateral branches on both sides of the main stem and *Baculopora* does not.

STRATIGRAPHICAL RANGE. Lower Carboniferous (Courceyan-Asbian).

DISTRIBUTION. British Isles.

Family FENESTELLIDAE King, 1850 Genus *THAMNISCUS* King, 1849

TYPE SPECIES. *Keratophytes dubius* Schlotheim, 1820 by original designation from the Permian of Germany.

Thamniscus colei Wyse Jackson, 1988

Fig. 48

MATERIAL. BMNH PD8960-8982; TCD.29314-29323, CD.34152, 42606b; NMI:F19531-F19540; BELUM K2154, 2157, K2166, K2223, K12118-K12127, Upper part of the Glencar limestone, Viséan (Asbian), Carrick Lough, County Fermanagh. BMNH PD8959, 8983-8985; TCD.42543-42546, Upper part of the Glencar Limestone (Viséan, Asbian), Sillees River, County Fermanagh.

DESCRIPTION. The zoarium is small and develops from a flared basal holdfast to an open basket 7mm wide. The heavily calcified

holdfast is barren of apertures, whereas apertures open on the outer side of the basket. Branches are very robust (1.40 mm maximum width), circular in cross-section and bifurcate at irregular intervals at a high angle. Branches maintain a constant width along their length, and there is no increase in branch width prior to or following bifurcation. Branch surfaces are smooth. Autozoocelial apertures are arranged in two to five sub-linear rows in an irregular pattern on the obverse branch surface. The outer peristomial rims of the lateral rows of apertures protrude slightly beyond normal branch margins giving them an undulatory appearance. Autozoocelial apertures are circular, large and are surrounded by prominent thin peristomes. Autozoocelial chambers are elongate, circular in cross-section, and narrow proximally.

DISCUSSION. A complete systematic description of *T. colei* is given in Wyse Jackson, 1988.

Suborder PHYLOPORININA Lavrentjeva, 1979 Family CHAINODICTYONIDAE Nickles & Bassler, 1900 Genus *RHOMBOCLADIA* Rogers, 1900

TYPE SPECIES. *Rhombocladia delicatula* Rogers, 1900 by original designation from the Upper Carboniferous of Kansas, U.S.A.

REVISED DIAGNOSIS. Chainodictyonid with unilaminar, ramosc zoarium, with dichotomous branches which are oval to elliptical in cross-section. Autozoocelia are arranged in 4 to 12 longitudinal rows on obverse surfaces only. Superior hemisepta well developed; basal diaphragms rare. Autozoocelial apertures oval. Reverse surface covered with thin semi-circular ridges.

STRATIGRAPHICAL RANGE. Lower Carboniferous-Lower Permian.

DISTRIBUTION. British Isles, Europe, North America, the CIS (former Soviet Union), China.

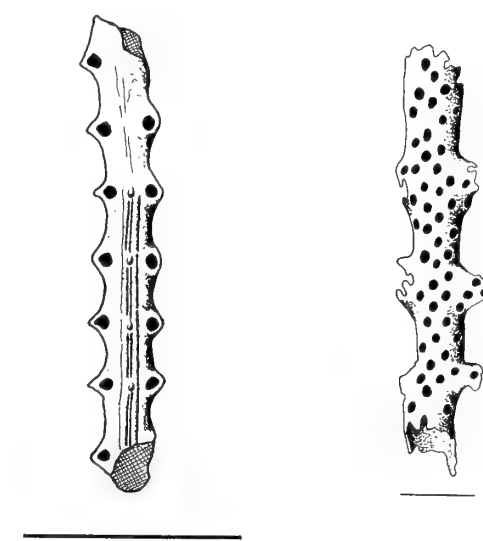
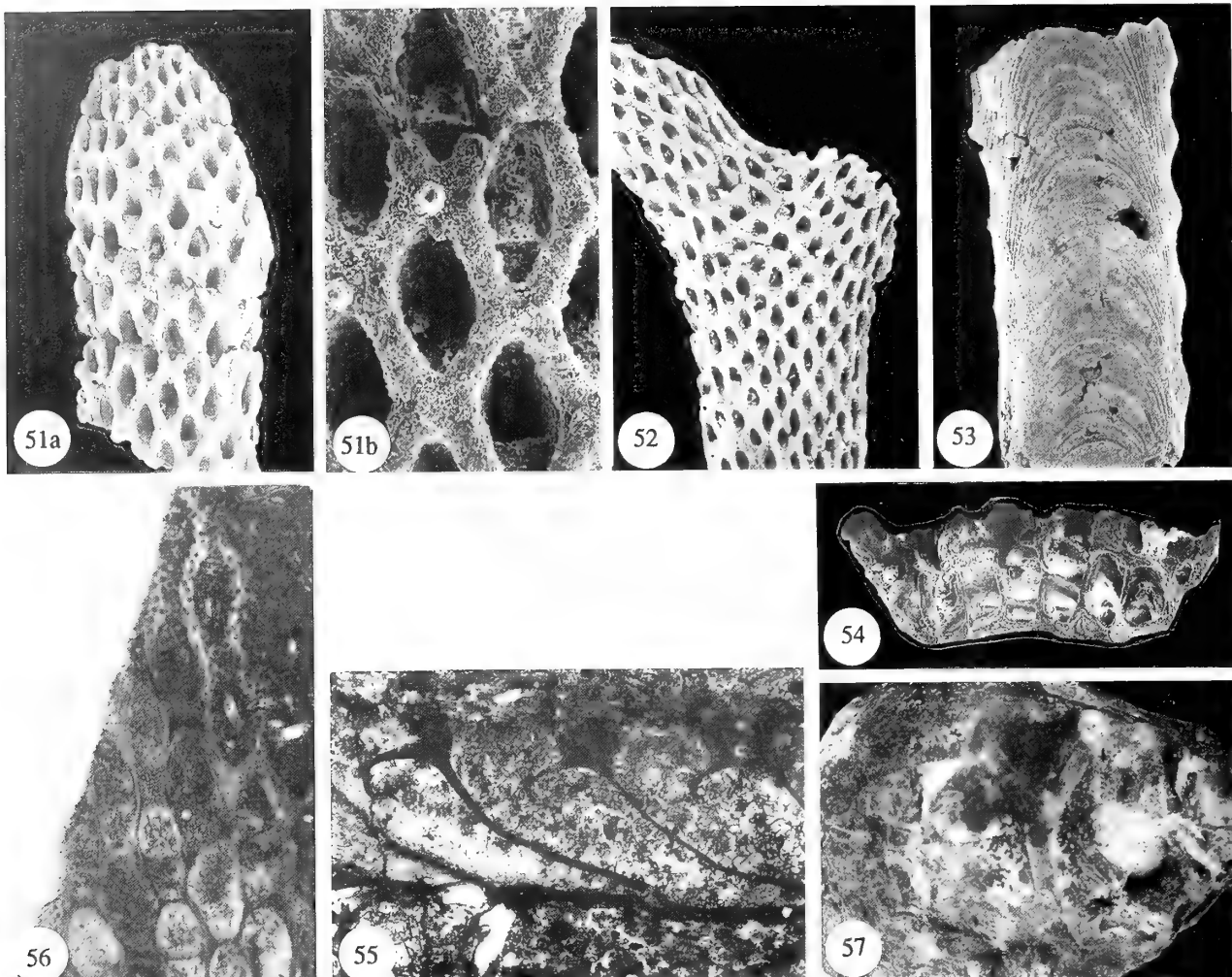


Fig. 49 *Diploporella marginalis* (Young & Young, 1875a). Line drawing of external features of BMNH PD9580; scale bar = 1 mm.

Fig. 50 *Ichthyorachis newenhami* M'Coy, 1844. Line drawing of external features of BMNH PD9581; scale bar = 1 mm.



Figs 51–57 *Rhombocladia dichotoma* (M'Coy, 1844) comb. nov.; **51–56**, Upper part of the Glencar Limestone (Viséan, Asbian), Carrick Lough, County Fermanagh; **51**, BMNH PD9591; **51a**, obverse surface details of a growing tip; autozoocia are arranged in eight longitudinal and obliquely intersecting rows; autozoocelial apertures are rhombic in shape, $\times 40$; **51b**, detail of autozoocelial apertures together with that of the hemiseptum developed from proximal walls; note the position of a single acanthostyle distal of autozoocia, $\times 150$; **52**, BMNH PD9592, obverse surface of a branch with 11–12 rows of autozoocia, $\times 20$; **53**, BMNH PD9593, reverse surface detail showing characteristic semi-circular pattern of basal laminae, $\times 40$; **54**, BMNH PD9593, broken zoarial fragment showing typical cross-section shape of branches, $\times 80$; **55**, BMNH PD9618, longitudinal section showing autozoocelial chamber shape, thin chamber walls, and long hemisepta, $\times 50$; **56**, BMNH PD9614, shallow tangential section showing longitudinal arrangement of autozoocia, with cross-cut hemisepta, and heterostyles developed on interapertural walls, $\times 40$; **57**, NMIG F6030, (lectotype). Carboniferous Limestone, Dinantian (Viséan); locality uncertain; Griffith Collection, reverse surface of branched zoarium showing characteristic semi-circular pattern of basal laminae, and longitudinal lines where autozoocelial walls meet basal wall; figured by M'Coy, 1844, pl. 27, fig. 15 as *Vincularia dichotoma*; $\times 2$.

Rhombocladia dichotoma (M'Coy, 1844) comb. nov.

Figs 42c, 51–58

- v 1844 *Vincularia dichotoma* M'Coy: 198, pl. 27, fig. 15.
non 1850 *Vincularia dichotoma* d'Orbigny, p. 195, pl. 682, figs 7–9.
 1854b *Vincularia dichotoma* M'Coy; M'Coy: 104.
 1857 *Vincularia dichotoma* M'Coy; Jukes: 454.
 1862 *Vincularia dichotoma* M'Coy; Griffith: 198, 235.

LECTOTYPE. NMIG:F7058, here designated; Black Lion, near Enniskillen, County Cavan (Viséan, Asbian); Griffith Collection.

PARALECTOTYPES. NMIG:F6030, here designated; no locality given (?Viséan); Griffith Collection; figured M'Coy 1844, pl. 27,

fig. 15. NMIG:F7056-F7057, F7059-F7060; Black Lion, near Enniskillen, County Cavan (Viséan, Asbian); Griffith Collection; NMIG:F7061; Millicent, Clane, County Kildare (Viséan, Chadian); Griffith Collection. NMIG:F7486-F7489; Kildare, County Kildare (Viséan); Griffith Collection. SMC:E5188; Howth, County Dublin (Courceyan/Chadian, Dinantian); Griffith Collection; SMC:E5189/a–b; Killymeal, Dungannon, County Tyrone (Viséan, Brigantian); Griffith Collection. SMC:E5190; Kildare, County Kildare (Viséan); Griffith Collection.

MATERIAL. BMNH D2564; ?Ireland (?Carboniferous); Shrubsole Collection. BMNH PD9591-9620; TCD.34053-34064, 3415, 34164, 34167, 42563a, b, 42565-42567, 42594, 42604c, 42606, 42609; BELUM K2159, Upper part of the Glencar Limeston

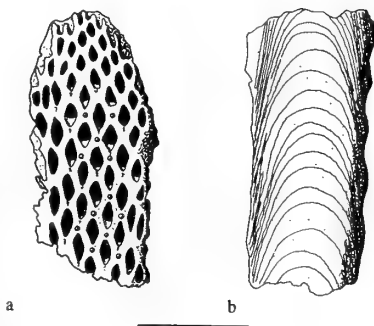


Fig. 58 *Rhombocladia dichotoma* (M'Coy, 1844) comb. nov. Line drawing of external features; **a**, obverse surface (BMNH PD9591); **b**, reverse surface (BMNH PD9593); scale bar = 1 mm.

(Viséan, Asbian), Carrick Lough, County Fermanagh. TCD.42547-42549, Upper part of the Glencar Limestone (Viséan, Asbian), Sillees River, County Fermanagh.

M'Coy's original diagnosis. 'Dichotomous; obverse rounded, with about six equal, parallel, slender, longitudinal ridges, in the concave furrows, between which are five rows of oval, prominent cells, the marginal furrow on each side free of cells; reverse flat, with numerous, semicircular, scale-like wrinkles, and about six longitudinal striae.'

EMENDED DIAGNOSIS. *Rhombocladia* with a ramoso zoarium of dichotomising branches oval to elliptical in cross-section. Seven to twelve longitudinal rows of autozoocial apertures open onto the obverse surface. A single superior hemisepum is developed on the proximal side of apertures and basal diaphragms are rare. Interapertural areas smooth, or with small pustules. Autozoocial apertures oval to rhombic in shape; a single large acanthostyle occurs proximally at each autozoocial aperture. Reverse surface barren, with parallel semi-circular ridges along the length of branches.

DESCRIPTION. Zoaria are ramoso with dichotomously dividing flattened branches. In cross-section branches are oval to elliptical in shape, and convex frontally. The largest fragment examined measures 30.4mm in length.

Autozoocial apertures open on the obverse surface only, and are arranged into 7 to 12 longitudinal rows. The number of rows along a branch is usually stable until a bifurcation point is reached, where the shape and size of apertures becomes variable and the regularity of their organization is lost. Uniformity returns distally beyond bifurcations. Narrow, barren marginal zones on the obverse surface are common in most zoaria. Autozoocial apertures are commonly oval to rhombic, rarely an acute hexagonal shape. Oval apertures are most common along branch margins, with rhombic shapes predominating towards the branch centre.

Interapertural walls are thin and smoothly rounded. They are smooth or bear faint pustules, and a single large acanthostyle, up to 0.18mm in length and 0.03–0.08mm in width, is situated proximally of each aperture. In most zoaria the large acanthostyles have been braded down to the zoarial surface and are evident only as small areas of coarser skeleton.

The reverse surface, formed by the colony basal wall, is undulatory, very thin (0.1mm), and bears thin, parallel, semicircular lines along the entire length of branches (apparently marking former positions of the growing tips of branches). Where the basal wall is braded a series of up to 10 longitudinal rows, representing the proximal portions of autozoocial chamber walls, is visible.

Autozoocial chambers originate on the basal wall and distally

Table 19 Measurements of *Rhombocladia dichotoma* (in mm). N=18.

	NM	x	Mn	Mx	CVw	CVb
ZW	71	1.79	0.80	3.13	7.95	4.39
ZT	23	0.47	0.30	0.56	8.16	8.97
AR	41	10	7	12	6.66	8.60
ZL2	134	4.89	4	7	7.26	8.19
ZT1	97	3.87	3	6	10.72	8.89
AD1	160	0.27	0.19	0.42	9.14	6.97
AD2	160	0.12	0.08	0.18	11.73	6.64
AS1	160	0.09	0.07	0.32	19.81	4.50
AS2	160	0.07	0.04	0.13	14.13	4.63
AW	87	0.04	0.03	0.08	15.26	4.13
AH	21	0.12	0.02	0.18	17.29	0.65
HL	6	0.15	0.10	0.19	9.82	2.53
ET	9	0.33	0.30	0.38	6.01	15.79
TE	8	0.13	0.09	0.17	10.86	3.81
AWT	7	0.01	0.01	0.02	16.67	9.19

curve upwards at a low angle. At the junction of the endozone and exozone the chamber bends abruptly upwards. Here a prominent superior hemisepum (average length 0.15mm) is developed, and is a little reflexed distally. Large acanthostyles originate at the base of the exozone. Endozonal walls are thin (0.01mm). Diaphragms are thin and are found only in the basal areas of the endozone.

DISCUSSION. M'Coy (1844) described and figured *Vincularia dichotoma* from the Carboniferous of Ireland. On the basis of M'Coy's types and conspecific specimens from the Viséan of County Fermanagh, this species is here reassigned to the genus *Rhombocladia* Rogers, 1900. Of the eleven specimens examined by M'Coy and still in existence, none show the obverse surface. M'Coy must therefore have had additional specimens available which are presumed lost. The lateral margin of specimen NMING:F7058 is slightly worn and shows some detail of internal structure, enabling it to be compared to material from Carrick Lough, examined in the present study. All the material is conspecific and NMING:F7058 is here selected as the lectotype for the species *Rhombocladia dichotoma*.

In many cases early workers assigned cylindrical Bryozoa to the genus *Vincularia* which is in fact a cheilostome genus. 16 species of *Rhombocladia* have been previously described. Of these 13 occur in the Carboniferous and have been recorded from the United States (McKinney 1972, Rogers 1900), the CIS (former Soviet Union) (Dunaeva 1961, Gorjunova 1988, Shulga-Nesterenko 1955), the Carnian Alps (Ceretti 1963, 1964), and China (Lu 1989). Three species have been recorded from the Permian: *R. aktashensis* from the CIS (former Soviet Union) (Lavrentjeva 1985) and *R. minor* and *R. spinulifera* from Western Australia (Crockford 1944).

Table 20 shows morphological measurements for all species of *Rhombocladia*. *R. dichotoma* differs significantly from all species except *R. delicatula* Rogers which has a similar zoarial thickness, and number of autozoocial rows. However, in *R. delicatula* prominent superior hemisepa are not present as they are in *R. dichotoma*.

Rhombocladia dichotoma displays the greatest zoarial width of any of the taxa (maximum observed value = 3.13 mm) and the largest number of autozoocial rows. Apertural diameters within the genus are relatively constant. This explains the large width of branches observed in *R. dichotoma*.

Zoarial thickness in all species is similar, with the exception of *R. aktashensis* whose branches are sub-circular in cross-section. The ratio of zoarial width to zoarial thickness in Carboniferous species is approximately 3:1, compared to 3:2 for the Permian species.

McKinney (1972: 60) postulated an erect growth habit for *Rhombocladia* on the basis of the occurrence of a species of *Hederella* encrusting the reverse surface. This interpretation is questionable,

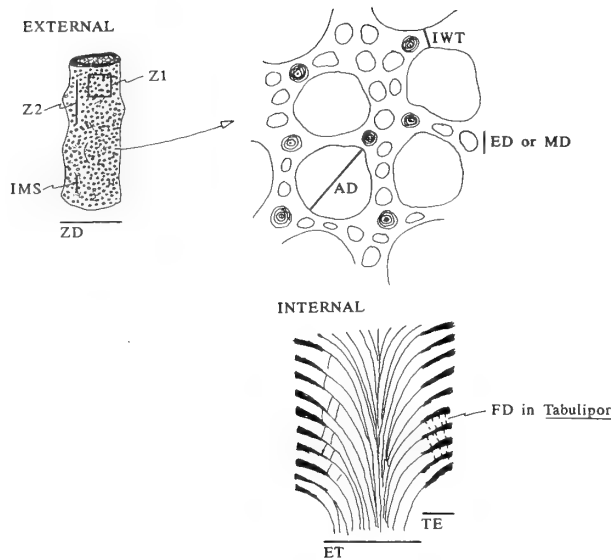


Fig. 59 Measurements taken on trepostomes in this study: ZD = Zoarial diameter measured perpendicular to growth direction; IMS = Internomiticule spacing; AD = Autozooecia apertural diameter: maximum value seen in aperture; IWT = Interzoocial wall thickness; ED = Exilazooecia apertural diameter: maximum value seen in aperture; MD = Mesozooecial apertural diameter: maximum value seen in aperture; Z1 = Number of complete autozoocial apertures enclosed in 1mm^2 ; Z2 = Number of complete autozoocial apertures measured along a 2 mm line; AR = Axial ratio: this measures the ratio of the exozone to the zoarial diameter [AR = $2(\text{TE})/\text{ZD}$; the method employed follows that of Boardman (1960: 21) rather than that of Cuffey (1967: 31) who multiplied the ratio by 100, which makes the obtained values unnecessarily large]; ET = Endozone thickness; TE = Exozone thickness; FD = Diameter of ring septum foramen.

and *Hederella* may have grown over a dead skeleton of *Rhombocladia* lying face downwards on the sea-bed. *Rhombocladia* may have had an encrusting habit as some Carrick Lough specimens show that the zoarium grew around and engulfed some adjacent pinnate bryozoan colonies. The perpendicular attitude of these pinnate colonies, which grew erect, relative to colonies of *Rhombocladia*, suggests that *Rhombocladia* grew horizontally on or just above the sea-bed.

Table 20 Quantitative measurements for all described species of *Rhombocladia* (in mm).

	ZW	ZT	AR	AD1	AD2	AS	HL
<i>R. dichotoma</i> (McCoy, 1844)	1.79	0.47	7–12	0.27	0.12	0.07–0.14	0.15
<i>R. aktashensis</i> Laurentjeva, 1985	1.50–1.80	1.00–1.1	6–8	0.22–0.24	0.12	0.10–0.15	0.03
<i>R. borissiaki</i> Shulga-Nest., 1955	1.00–1.35	0.45–0.50	7–8	0.26–0.34	0.12–0.14	—	0.03–0.05
<i>R. carnica</i> Ceretti, 1964	0.60	—	—	0.30	0.13	0.09–0.10	—
<i>R. coronata</i> Shulga-Nest., 1955	1.10	0.45	6–8	0.19–0.20	0.08–0.15	0.20–0.27	—
<i>R. delicatula</i> Rogers, 1900	1.50	0.52	10	0.26	0.15	0.10	—
<i>R. johnsoni</i> Ceretti, 1964	1.07	0.50	7	0.20	0.21	0.09	—
<i>R. kasimovensis</i> Shulga-N., 1955	0.80–1.20	0.45–0.70	5–7	0.15–0.22	0.08–0.12	—	—
<i>R. minor</i> Crockford, 1944	0.46–0.57	—	2–3	0.24–0.29	0.10–0.15	—	—
<i>R. multispinosa</i> McKinney, 1972	1.4	<1.00	9	0.30–0.42	0.12–0.19	—	—
<i>R. ninae</i> Shulga-Nest., 1955	1.70–2.30	0.70–0.80	8–9	0.20–0.22	0.10–0.12	0.22–0.28	0.02
<i>R. orientalis</i> Lu, 1989	—	0.30–0.50	—	0.22	0.16–0.18	—	—
<i>R. punctata</i> Dunaeva, 1961	1.00–1.08	0.48	—	0.24–0.27	0.12	—	—
<i>R. ramosa</i> Gorjunova, 1988	1.10–1.32	0.86–0.88	6–7	0.18–0.22	—	—	—
<i>R. septata</i> Shulga-Nesterenko, 1955	1.25	0.45–0.52	7	0.27–0.32	0.12–0.14	0.15–0.20	0.09
<i>R. spinulifera</i> Crockford, 1944	0.70–0.95	—	4–6	0.19–0.24	0.16	—	—
<i>R. tenuata</i> Shulga-Nesterenko, 1955	0.80	0.50	7	0.18–0.20	0.10–0.12	—	—

Data from original sources.

STRATIGRAPHICAL RANGE. Lower Carboniferous (Tournasian [Courceyan]–Viséan [Brigantian]).

DISTRIBUTION. British Isles (Counties Cavan, Fermanagh, Kil-dare, and Tyrone, Ireland; Mill Gill, North Yorkshire, England).

Order TREPOSTOMATA Ulrich, 1882
Suborder HALLOPOROIDEA Astrova, 1965
Family HETEROTRYPIDAE Ulrich, 1890
Genus *LEIOCLEMA* Ulrich, 1882

TYPE SPECIES. *Callopora punctata* Hall, 1858, by original designation from the Lower Carboniferous of Iowa, U.S.A.

Leioclema indentata sp.nov.

Figs 60–62

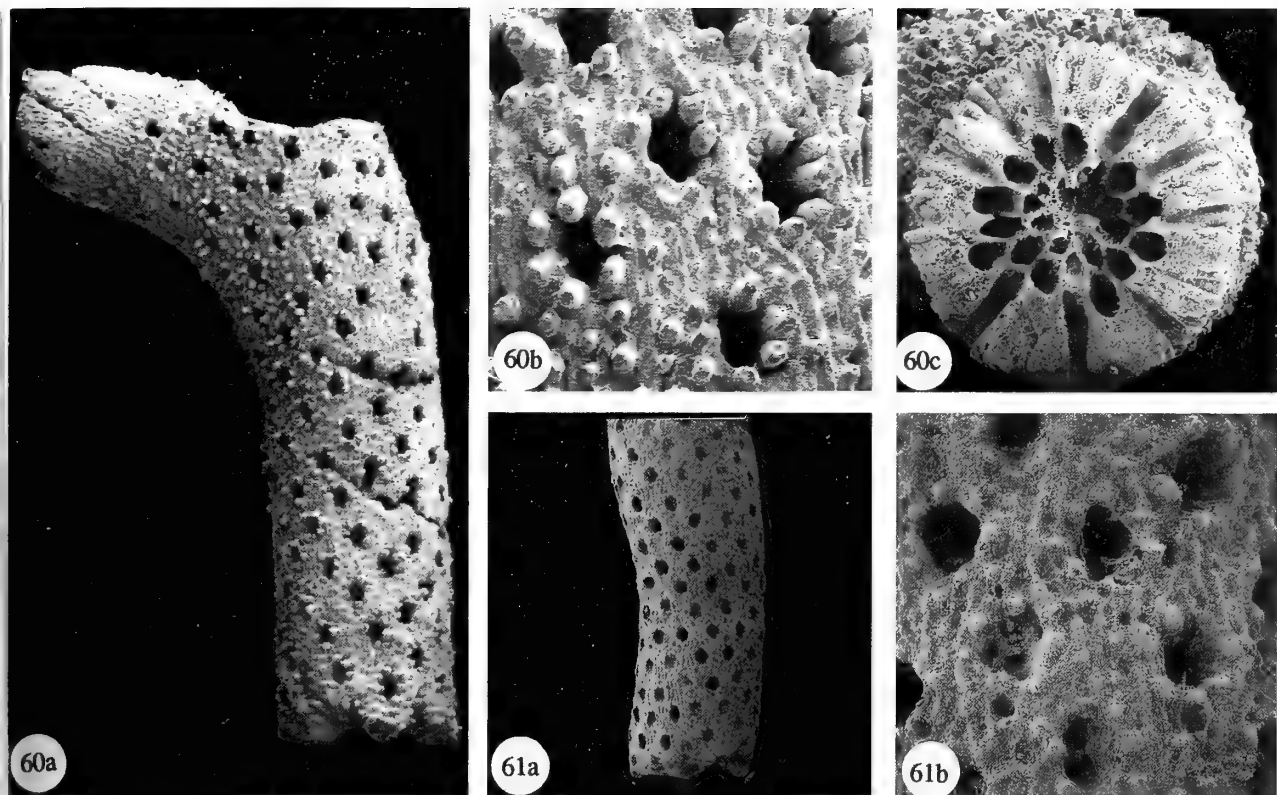
HOLOTYPE. BMNH PD9621, Upper part of the Glencar Limestone (Viséan, Asbian), Carrick Lough, County Fermanagh.

PARATYPES. BMNH PD9564, 9622–9626; TCD.34065–34066, 34123, Upper part of the Glencar Limestone (Viséan, Asbian), Carrick Lough, County Fermanagh. TCD.42550, Upper part of the Glencar Limestone (Viséan, Asbian), Sillees River, County Fermanagh. TCD.28152, Base of reef, Lower Carboniferous (Viséan Asbian), Shanvaus Cross, County Leitrim, G.D. Sevastopulo Collection.

DERIVATION OF TRIVIAL NAME. From the indentation of the autozoocial apertures by acanthostyles.

DIAGNOSIS. *Leioclema* forming ramose erect cylindrical, irregularly dichotomising zoaria. Zoocial walls considerably thickened in exozone. Diaphragms present at zoocial bend. Mesozooecia common between chambers in exozone, closed to the surface. Autozoocial apertures indented by several large acanthostyles.

DESCRIPTION. Zoaria are robust, composed of straight, cylindrical branches 1.15 to 2.13 mm in diameter. Branches are circular in cross-section and bifurcate at irregular intervals. There is a slight increase in branch diameter prior to division; subsequent branches are slightly narrower. The largest fragment examined measures 24 mm long.



Figs 60, 61 *Leio clema indentata* sp. nov.; **60**, Upper part of the Glencar Limestone (Viséan, Asbian), Carrick Lough, County Fermanagh; BMNH PD9621 (holotype); **60a**, rame colony with circular autozoocelial apertures arranged in crude longitudinal rows, surrounded by large acanthostyles, with ridged interapertural areas, $\times 15$; **60b**, detail of 60a, showing oval-shaped autozoocelial apertures surrounded by six to eight large acanthostyles; smaller acanthostyles are developed in interapertural areas, $\times 85$; **60c**, cross-sectional view showing central axial region of thin walled autozoocelial chambers and very thick exozone region, $\times 30$; **61**, base of reef, Lower Carboniferous (Viséan, Asbian), Shanvaus Cross, County Leitrim, TCD.28152; **61a**, rame colony., $\times 20$; **61b**, detail of 61a showing small circular mesozoocelial apertures between autozoocelial apertures, $\times 100$.

Autozoocelia are developed throughout the zoarium. The exact shape of the zooecial chambers is unknown. It appears that the chambers diverge from the centre of the branch at a low angle of 25° to 30° . Zooecia bend through 50° at the endozone/exozone boundary so that vestibules are orientated perpendicular to the zoarial surface. Chamber walls are thin (0.01 – 0.02 mm) in the endozone and thicken rapidly at the exozone which reaches a maximum thickness of 1.10 mm. Thin diaphragms are common at the base of the vestibule. In cross-section chambers are circular, pentagonal or polygonal in shape.

Mesozoocelia are common in the exozone, where they are disposed in three to five irregular rows between autozoocelial chambers, but are not present in the endozone. They are circular, polygonal or irregular in shape, 0.03 to 0.11 mm in diameter, thin walled, hollow, and closed to the surface. No internal diaphragms were observed, perhaps due to the nature of the preservation.

Autozoocelial apertures are oval in shape, moderately large 0.12 to 0.20 mm in diameter, and fairly regularly spaced one to two diameters apart. They are arranged in 16 to 20 poorly defined longitudinal rows. Each aperture is surrounded by six to seven large acanthostyles (0.05 to 0.08 mm in width and up to 0.1 mm in length), which indent the aperture margin.

Smaller randomly orientated acanthostyles, and thin wavy longitudinal grooves are found in interapertural areas which are slightly

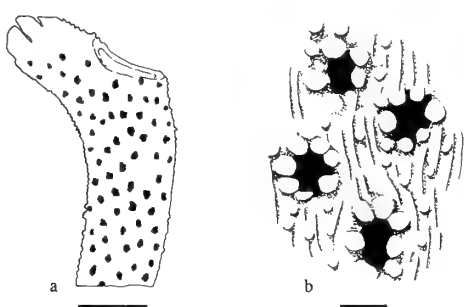


Fig. 62 *Leio clema indentata* sp. nov. Line drawing of external features of BMNH PD9621; **a**, colony form, scale bar = 1 mm; **b**, Detail of surface features, scale bar = 0.1 mm.

Table 21 Measurements of *Leio clema indentata* (in mm). N=6.

	NM	x	Mn	Mx	CVw	CVb
ZD	61	1.66	1.15	2.13	6.92	7.38
AD	60	0.15	0.12	0.20	9.40	9.88
IWT	60	0.18	0.06	0.26	17.33	9.22
Z1	60	6.23	4	8	10.48	11.11
Z2	60	3.60	3	5	13.48	9.11
ET	9	0.84	0.68	1.10	2.69	5.17
TE	18	0.38	0.28	0.51	8.89	6.68

Table 22 Quantitative comparison of *Leioclema indentata* with other Carboniferous *Leioclema* species (dimensions in mm).

	ZD	AD	IWT	Z2	ET	TE
<i>L. indentata</i> sp. nov.	1.15–2.18	0.12–0.20	0.06–0.26	4–8	0.68–1.10	0.28–0.51
<i>L. porosum</i> Crockford, 1947	20	0.2–0.25	0.08	—	—	—
<i>L. shumaradi</i> Girty, 1908	3.5	0.15–0.20	0.20	—	—	—
<i>L. punctatum</i> (Hall, 1858)	2.00–5.00	0.15–0.20	—	5–6	—	—
<i>L. pushmatahensis</i> Harlton, 1933	0.73–1.02	—	—	—	—	—
<i>L. avonense</i> Lee, 1912	22.00	—	—	6	—	—
? <i>L. hirsutum</i> Moore, 1929	1.00–1.40	0.16–0.20	0.1	—	0.9	0.40–0.45
<i>L. tubulosa</i> Nekhoroshev, 1956	3.00–5.00	0.13–0.17	—	5.5–6.5	—	—
<i>L. bifolifera</i> Nikiforova, 1927	4.0	0.20–0.25	0.1	—	1.2	0.8
? <i>L. kobayashii</i> Sakagami, 1962	2.60–3.60	0.21–0.29	0.32–0.40	—	—	—
? <i>L. uzuraense</i> Sakagami, 1964	—	0.16–0.22	—	10	—	—
<i>L. cassis</i> Trizna, 1958	1.80	0.18–0.20	—	10	—	—
<i>L. echinata</i> Trizna, 1958	1.60	0.16–0.18	—	7–10	—	—
<i>L. podunskense</i> Trizna, 1958	2.20–3.20	0.15–0.18	—	5–7	—	—
<i>L. rojkiensis</i> Trizna, 1958	2.00	0.20–0.22	—	6–7	—	—
<i>L. semetra</i> Trizna, 1958	2.75–3.00	0.14–0.16	—	11–12	—	—
<i>L. textila</i> Trizna, 1958	0.80–0.90	0.10–0.16	—	6	—	—
<i>L. clara</i> Trizna, 1962	3.30	0.16–0.20	—	8–9	—	—
<i>L. gracillimum</i> Ulrich, 1888b	1.00–1.50	0.10–0.15	—	8–9	—	—
<i>Larameum</i> Ulrich, 1890	Adnate 1.00	0.2	—	9–10	—	—
<i>L. foliatum</i> Ulrich, 1890	Adnate 1.00–1.50	0.2	—	6	—	—
<i>L. subglobosum</i> Ulrich, 1890	—	0.15–0.20	—	8–9	—	—
<i>L. washsmuthi</i> Ulrich, 1890	Adnate <1.00	0.2	—	6	—	—

Data from original sources.

elevated above the autozoocial apertures. Monticules are not developed.

DISCUSSION. *Leioclema indentata* is very rare in the Viséan of County Fermanagh. Only ten zoarial fragments were found; all of these are silicified and consequently internal structures are not well known. However, some fine skeletal features such as autozoocial diaphragms are preserved, and are seen in broken fragments.

L. indentata can easily be recognised by the indentation of the autozoocial apertures by six to seven large acanthostyles, and from surface ornamentation. Coefficients of variation for measured parameters are all low, including that for interapertural wall thickness (IWT).

25 other *Leioclema* species have been described from the Carboniferous (McKinney 1973, Astrova 1978, and herein), of which only *L. avonense* Lee, 1912, from the Avon area, and *Leioclema* sp. from North Wales (Bancroft, Somerville & Strank, 1988), occur in the British Isles. All are compared with *L. indentata* in Table 22 above. *L. avonense* is unusual in that the zoarium is very thick, exozone walls are not thickened, and that mesozoocia are few. Thus, its taxonomic position is debateable, and may only be resolved by examining Lee's original material.

L. indentata has a gross morphology similar to the North American species *L. gracillimum* Ulrich, 1888b. However, apertural spacing and acanthostyle diameter are considerably less in the latter.

STRATIGRAPHICAL RANGE. Lower Carboniferous (Viséan, Asbian).

DISTRIBUTION. Counties Fermanagh and Leitrim, Ireland.

Suborder AMPLEXOPORINA Astrova, 1965
Family DYSCRITELLIDAE Dunaeva and Morozova, 1967
Genus **DYSCRITELLA** Girty, 1911

TYPE SPECIES. *Dycretella robusta* Girty, 1911, by original designation from the Lower Carboniferous of Arkansas, U.S.A.

***Dycretella miliaria* (Nicholson, 1881)**

Figs 63–66

- v1881 *Monticulipora tumida* var. *miliaria* Nicholson: 123, pl.3, fig.2.
 1884c *Monticulipora tumida* var. *miliaria* Nicholson; Vine: 101.
 1912 *Dycretella miliaria* (Nicholson); Lee: 178, pl.16, figs 9,10.
 1950 *Dycretella miliaria* (Nicholson); Termier & Termier, p.15, pl.55, figs 4–6, 9, pl.60, fig.7, pl.65, figs 7–9.
 1987 *Dycretella miliaria* (Nicholson); Bancroft: 196.

LECTOTYPE. Herein designated AUGD 10135a, Carboniferous shales; Redesdale, Northumberland, England; Nicholson Collection.

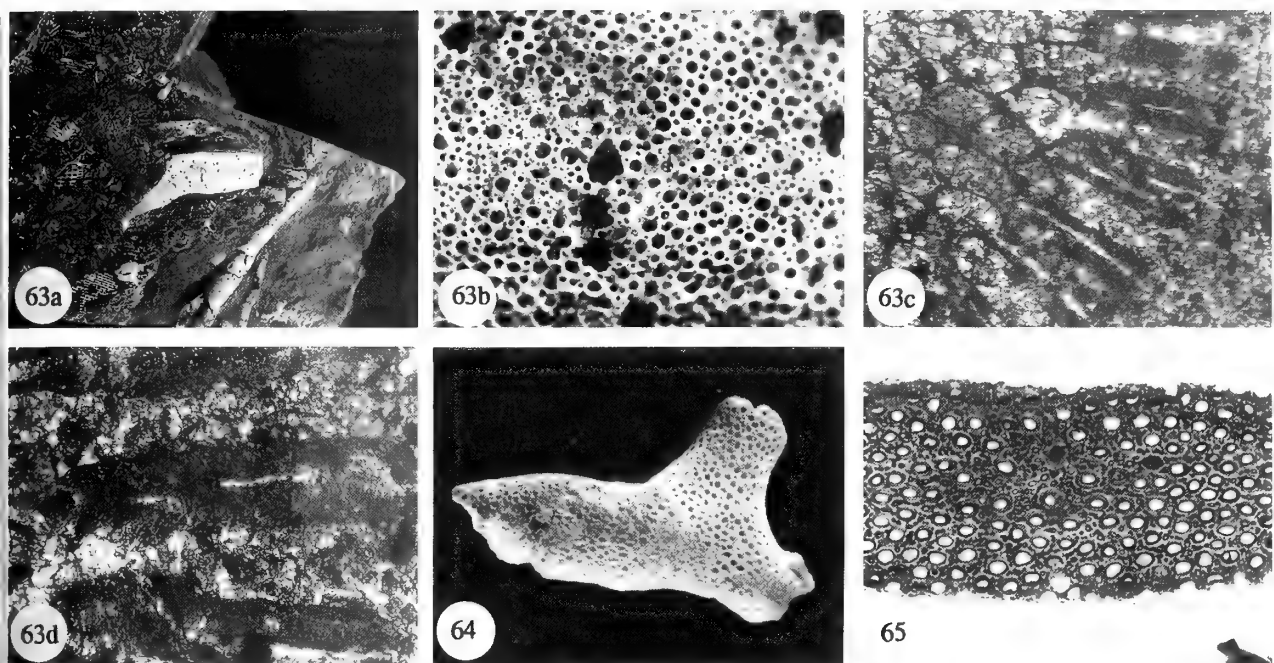
PARALECTOTYPES. Herein designated AUGD 10135b (2 specimens in cavity slide); Carboniferous shales; Redesdale, Northumberland, England; Nicholson Collection. RSM 1967.66.384, RSM 1967.66.387; Carboniferous shales; Redesdale, Northumberland, England; Nicholson Collection.

MATERIAL. BELUM K3442, K3608 Upper part of the Glencar Limestone (Viséan, Asbian), Sillees River, County Fermanagh.

DIAGNOSIS. *Dycretella* with robust dendroid zoarium and irregularly dichotomising branches. Autozoocia are developed throughout the zoarium. Zoocial walls are thin in the endozone but are thick and of constant width in the exozone. Basal diaphragms are rare and indistinct. Autozoocial apertures are circular and of moderate size. Interapertural areas are of variable width, and exilazooecia are abundant. Maculae are quite common. Prominent, large acanthostyles occur at interzoocial intersections interspersed with smaller acanthostyles between.

DESCRIPTION. The dendroid zoarium is robust, the longest fragment examined attaining a length of 30.6mm. Bifurcation is rare but where it occurs no increase in branch width accompanies it.

Autozoocia originate in the endozone by interzoocial budding. From the endozone they diverge at a low angle, but in the exozone they turn through 80° to lie perpendicular to the zoarial surface. In the endozone zoocial walls are thin and undulatory. Walls thicker



Figs 63–65 *Dyscritella miliaria* (Nicholson, 1881); **63**, Upper part of the Glencar Limestone (Viséan, Asbian), Sillees River, County Fermanagh; BELUM K3442; **63a**, large zoarial fragments showing ramose growth-form and large circular autozoocoeial apertures surrounded by irregularly-placed exilazooecia, $\times 1$; **63b**, detail of 63a, $\times 15$; **63c**, cross-section showing autozoocoeial chambers with thickened exozonal walls, $\times 50$; **63d**, detail of 63c, showing exilazooecium developed in exozone between adjacent autozoocoeial apertures, $\times 20$; **64–65**, Carboniferous shales (probably Redesdale Ironstone Shale (Asbian), Lower Limestone Group), Redesdale, Northumberland; **64**, AUGD.10135a (lectotype), ramose branching zoarial fragment with crowded arrangement of autozoocoeial apertures surrounded by much smaller circular or irregularly-shaped exilazooecial apertures, $\times 5$; **65**, GSM 1967.66.384 (paralectotype), tangential section showing oval autozoocoeial apertures surrounded by numerous exilazooecia, $\times 15$.

rapidly at the endozone/exozone boundary, and wall thickness remains constant (mean thickness 0.07mm) throughout most of the exozone. Thin basal diaphragms are infrequently developed in the endozone, whereas very thin diaphragms are occasionally developed in the exozone.

Autozoocoeial apertures are of moderate size, circular in shape, and are closely packed, approximately their own diameter apart.

Interapertural areas are irregular in width. Exilazooecia are very abundant between autozoocoeia and vary greatly in shape and size. They are usually circular to oval, but in interapertural angles small pentagonal forms occur (0.02–0.1mm in diameter). Frequently, one or two exilazooecia are located between autozoocoeia. Exilazooecia originate within the exozone where they form short, narrow tubes. Maculae, 0.4mm in diameter, occur occasionally and comprise clusters of exilazooecia.

Acanthostyles are abundant in interapertural walls. Relatively large acanthostyles (mean diameter 0.03mm) persist at interapertural angles around autozoocoeia while smaller acanthostyles (mean

diameter 0.01mm) are developed in a line on interapertural walls between both autozoocoeia and exilazooecia.

DISCUSSION. This is the first reported occurrence of the trepostome *Dyscritella miliaria* from the Carboniferous of Ireland. The abundance of exilazooecia ('interstitial tubuli' of Nicholson, 1881) makes the taxon very distinctive. It was first described, as *Monticulipora tumida* var. *miliaria*, from the Lower Carboniferous of England (Nicholson 1881). Subsequent specimens from the Midland Valley of Scotland were discovered in the Young Collection at the Hunterian Museum (Bancroft 1984). *D. miliaria* also occurs at Llangollen, North Wales, in strata of Asbian age (A.J. Bancroft, *pers. comm.*, April 1988).

Dyscritella miliaria is rare in the Lower Carboniferous of the

Table 23 Measurements of *Dyscritella miliaria* (in mm). N=5.

NM	x	Mn	Mx	CVw	CVb
D	19	4.59	3.17	6.15	9.65
I	21	16.06	9	22	28.53
Z	25	8.35	7	10	147.80
A	30	0.12	0.09	0.22	12.08
WT	30	0.08	0.03	0.28	38.77
D	30	0.04	0.02	0.10	31.90
T	9	2.64	1.91	3.52	13.47
E	18	0.97	0.57	1.38	8.00
R	9	0.57	0.50	0.70	12.96

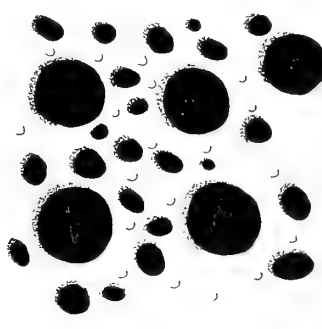


Fig. 66 *Dyscritella miliaria* (Nicholson, 1881). Line drawing of external features of BELUM K3442; scale bar = 0.1 mm.

British Isles. In the large bryozoan sample examined in this study only 4 specimens were found.

In his original description Nicholson failed to notice basal dia-phragms in the endozone. Lee (1912) redescribed the earlier material in which he found ill-defined 'tabulae' (basal diaphragms). Consequently, he correctly placed the specimens in the genus *Dyscritella* and elevated *miliaria* from variety to specific rank.

Coefficient of variation values in Table 23 illustrate a number of features. Zoarial width (ZW) and autozoocial aperture diameter (AD) do not vary greatly either within or between colonies. The within-colony ranges of exilazooacial diameter (ED), autozoocial spacing (AS), and the number of autozoocia in an area of 1mm (Z1) are all large. However, between-colony CVs for these parameters are small because all colonies are of a similar size. There is little within-colony variation, but large between-colony variation in the number of autozoocia in a 2mm line (Z2). This large CV value may be a sampling error arising from the small sample size.

STRATIGRAPHICAL RANGE. Lower Carboniferous (Asbian-?Brigantian).

DISTRIBUTION. Ireland, northern England, North Wales, Midland Valley of Scotland, Morocco.

Family STENOPORIDAE Waagen & Wentzel, 1886

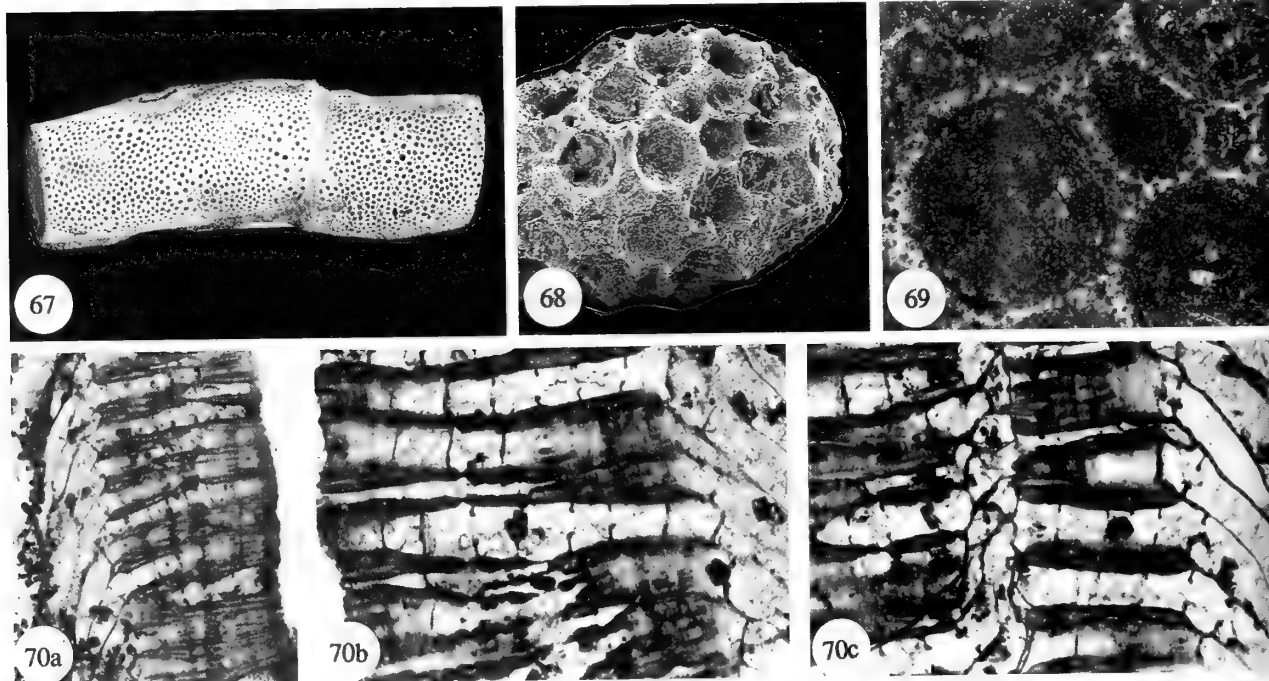
Genus *TABULIPORA* Young, 1883a

TYPE SPECIES. *Cellepora urii* Fleming, 1828 by monotypy from the Lower Carboniferous of East Kilbride, Scotland.

Tabulipora urii (Fleming, 1828)

Figs 67–70, 71a

- 1828 *Cellepora urii* Fleming: 532.
- v1883a *Tabulipora urii* (Fleming); Young: 154.
- v1883b *Tabulipora urii* Young; Young: 264.
- v1883 *Tabulipora urii* Young [sic]; Nicholson: 295.
- 1884b *Tabulipora urii* Young [sic]; Vine: 380, pl. 20, figs 3a–b, 4.
- 1912 *Tabulipora urei* Young [sic]; Lee: 150.
- 1912 *Tabulipora scotica* Lee: 162, pl. 14, figs 4a–d, pl. 15, figs 12, 13, 17, 18.
- 1935 *Tabulipora scotica* Lee; Anderson & Lamont: 216, fig. 6.13.
- 1953 *Tabulipora scotica* Lee; Bassler: G105, fig. 70 – 1a, 1b.
- 1961 *Tabulipora scotica* Lee; Wilson: 91.
- 1969 *Tabulipora scotica* Lee; Owen: 262, pl. 22, figs d–e.
- 1970 *Tabulipora urii* (Fleming); Gautier: 19, pl. 7, fig. 1; pl. 8, figs 1–2.
- 1973 *Tabulipora scotica*? Lee; Owen: 302.
- 1977 *Tabulipora urii* (Fleming); McKinney: 313, pl. 1, fig. 3.
- non v 1986 *Tabulipora scotica* Lee: Kora & Jux: 91, figs 3, g1–4.
- 1987 *Tabulipora urii* (Fleming); Bancroft: 196.



Figs 67–70 *Tabulipora urii* (Fleming, 1828); Upper part of the Glencar Limestone (Viséan, Asbian), Sillees River, County Fermanagh: **67**, BELUM K15200, ramose colony fragment; autozoocia with circular to oval shaped apertures arranged over the whole surface, except on monticules; mesozooecia are developed between autozoocia, $\times 3$; **68**, BMNH PD9638, small encrusting colony on ?echinoid spine, consisting of one layer of autozoocia with circular apertures with polygonal-shaped mesozooecia situated between, $\times 40$; **69**, BMNH PD9472, shallow tangential section showing autozoocial and mesozooocial apertures, and interapertural walls with large acanthostyles at junctions and smaller stylets in between, $\times 35$; **70**, BELUM K15207; **70a**, longitudinal section through thin-walled endozonal area and thickened exozone region; the initial portions of autozoocial chambers lie at a high angle to the zoarial surface, but bend at the exozone and become nearly perpendicular to it, $\times 12$; **70b**, longitudinal section showing exozone and autozoocial chambers; ring septae develop at the top of the endozone with eight per autozoocium; septal necks are inflated and deflected interiorly, $\times 20$; **70c**, longitudinal section showing exozone and autozoocial chambers, and zone of regeneration where the endozone is characteristically thin, $\times 20$.

1988 *Tabulipora urii* (Fleming); Yang, Hu & Xia: 69, pl. 22, figs 5–8.

MATERIAL. BM(NH) PD9472, 9638–9642, 9704; TCD.34079, 42593b, 42604b, Upper part of the Glencar Limestone (Viséan, Asbian), Carrick Lough, County Fermanagh; BELUM K15200–15208, Upper part of the Glencar Limestone (Viséan, Asbian), Sillees River, County Fermanagh.

DESCRIPTION. Zoaria are erect, ramose expansions of bifurcating cylindrical branches reaching 8.20mm in diameter.

Autozoocial chambers are budded interzoocially from the branch centres. Chambers diverge from the centre of branches at a low but constant angle of 30° in the endozone. They bend abruptly at the exozone; vestibules are orientated at angles of between 70° and 80° to the zoarial surface. Autozoocial chambers are ten to twelve times longer than wide. Chamber walls are very thin (0.01mm) in the endozone, but thicken considerably (to 0.05mm) in the exozone, where in some specimens as many as five monilae may occur. They are pear to oval-shaped thickenings of the chamber wall, and may be separated by lengths of thin chamber wall. Skeletal laminae within the wall are deflected away from the zoarial surface from a central dark zone at autozoocial boundaries. In cross section and deep tangential section chambers are polygonal in shape. Ring septa are developed in autozoocial chambers towards the top of the endozone and throughout the exozone. A solitary or pair of thin, widely spaced endozonal ring septa contrast with up to seven thicker and more closely spaced ring septae developed in the exozone. Foramen are circular or oval in shape and are placed either centrally or slightly laterally. The central walls of ring septa constitute a thickened ring that is bent posteriorly. Autozoocial apertures are large, circular to oval in shape, and closely spaced at less than one diameter apart. They are irregularly arranged over the zoarial surface. They are

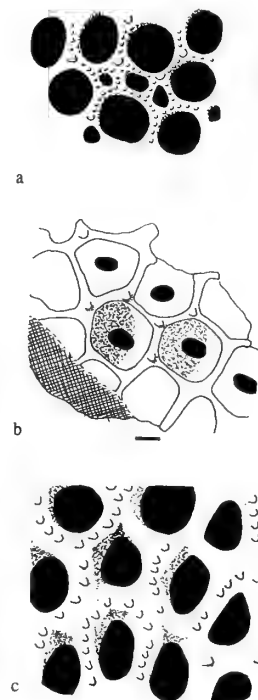


Fig. 71 Line drawing of external features of the *Tabulipora* species described in this study. a, *Tabulipora urii* (Fleming, 1828) (BELUM K15200); b, *Tabulipora howsii* (Nicholson, 1881) (BMNH PD9644); c, *Tabulipora minima* Lee, 1912 (BMNH PD9650); scale bar = 0.1 mm.

poorly developed on monticles where they are marginally larger. The long axes of oval shaped apertures radiate out from monticles and maculae. Interapertural walls are thin. Exilazooecia are very common, and are disposed in one or two rows between autozoocial apertures, or in radiating maculate clusters of up to forty individuals. They are small, thin walled, and circular to polygonal in shape.

Stylets are common and structurally variable, and developed on the thin interapertural walls. Large acanthostyles, 0.04mm in diameter, are found at interapertural junctions. These have a distinctive dark grey core developed from the base of the exozone. Smaller heterostyles (0.01–0.02mm in diameter) are found in one or two rows between acanthostyles. They arise from within the exozone.

Table 24 Measurements of *Tabulipora urii* (in mm). N=8.

	NM	x	Mn	Mx	CVw	CVb
ZD	69	5.59	3.79	8.20	3.84	5.34
Z1	80	10	7	14	11.99	10.48
Z2	80	5.85	4	7	10.73	10.48
AD	80	0.19	0.11	0.29	15.55	9.71
IWT	80	0.11	0.06	0.17	18.08	13.33
ED	80	0.07	0.05	0.14	22.98	6.95
ET	17	1.77	0.70	2.76	5.99	2.17
TE	33	0.97	0.47	1.98	12.51	2.17
IMS	8	4.72	4.10	5.94	17.47	11.32

DISCUSSION. *Tabulipora urii* was first described and figured by Ure (1793) as *Millepore* from the Carboniferous of Kilbride, West Scotland. Subsequently, Fleming (1828) cited Ure's material as the type species of his species *Cellepora urii*. This species was later described by Young (1883a) who noted ring septa in the autozoocial chambers and on the strength of this erected the subgenus *Tabulipora*. *Cellepora urii* is the type species of *Tabulipora* by monotypy.

Lee (1912) revised the British Trepostomata. He examined Young's material and erected a new species, *Tabulipora scotica*, designating it as the type species of *Tabulipora*. He demoted *T. urii* (misspelt 'urei') because he felt that Young had not really proposed it as a new specific name, and because his material contained several species, none of which had been figured. Gautier (1970) stated that *T. urii* is the type species by monotypy, and thus *T. scotica* is invalid. *T. scotica* is regarded as a junior synonym of *T. urii* (Bancroft 1984: 372).

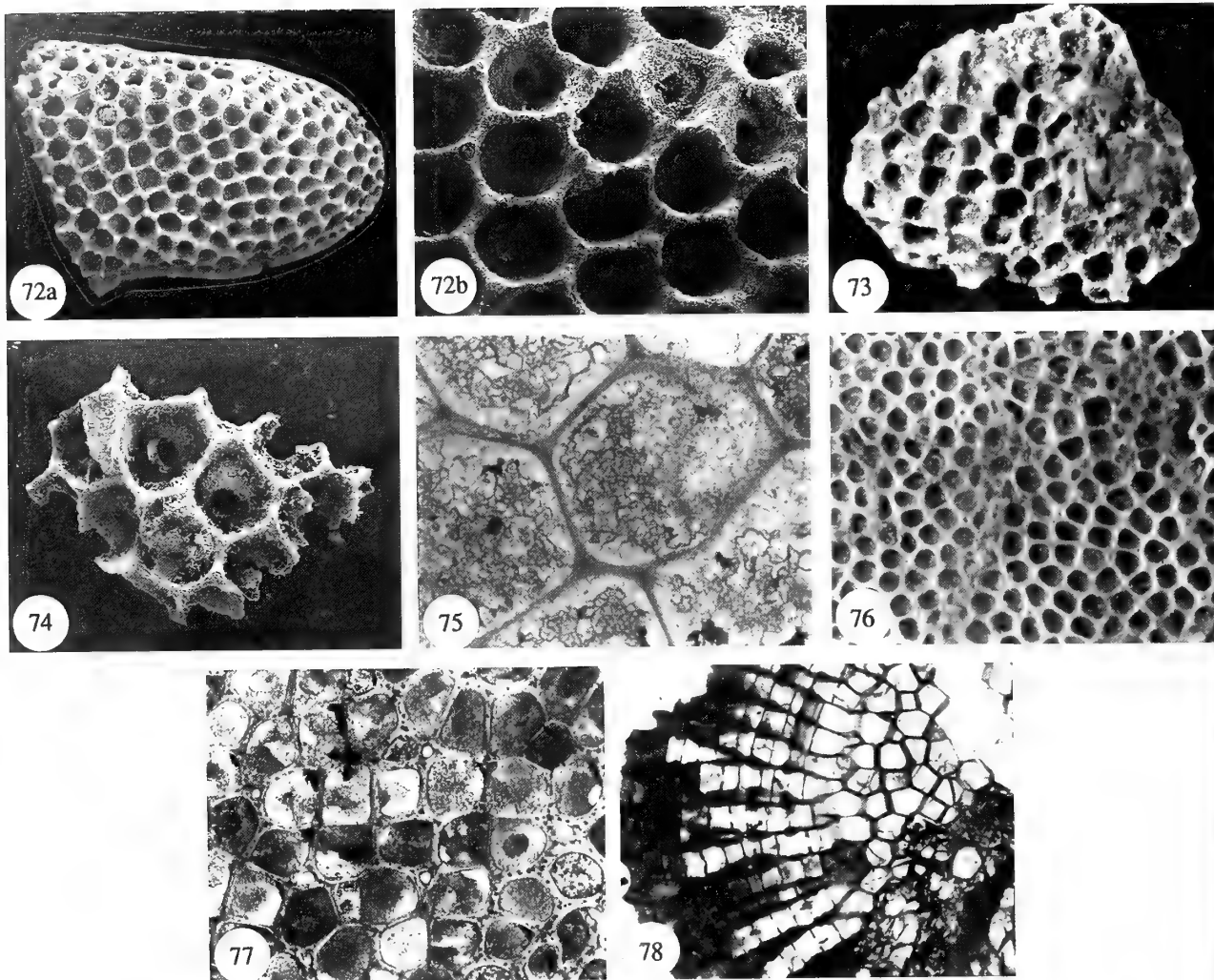
The figured specimens of *T. scotica* described from Egypt (Kora & Jux, 1986) have been examined. Up to nine hemiphragmas are developed in chambers indicating that the specimens are referable to the genus *Stenophragmidium*.

STRATIGRAPHICAL RANGE. Lower Carboniferous (Tournaisian–Brigantian).

DISTRIBUTION. County Fermanagh, Midland Valley of Scotland, ?China.

Tabulipora howsii (Nicholson, 1881) Figs 71b, 72–78

- v1881 *Stenopora howsii* Nicholson: 83, fig. 12.
- v1883 *Stenopora howsii* Nicholson; Nicholson: 285, pl. 10, figs 1–10, text-figs 1a–c.
- 1886 *Stenopora howsii* Nicholson; Nicholson & Etheridge jun.: 177.
- v1889 *Stenopora howsii* Nicholson; Nicholson & Lydekker: 356, fig. 232.
- 1891 *Stenopora howsii* Nicholson; Etheridge jun.: 48.
- 1912 *Tabulipora howsei* [sic] (Nicholson); Lee: 166, pl. 14, figs 9a–c; pl. 15, figs 22–24.



Figs 72–78 *Tabulipora howsii* (Nicholson, 1881); **72–75**, Upper part of the Glencar Limestone (Viséan, Asbian), Carrick Lough, County Fermanagh; **72**, BMNH PD9643; **72a**, adnate zoarium showing regular arrangement of autozoocia with circular apertures, $\times 12$; **72b**, detail of 72a, showing circular autozoocial apertures with ring septa and circular-oval foramen, and acanthostyles positioned on interapertural wall junctions, $\times 40$; **73**, BMNH PD9645, adnate zoarium, $\times 20$; **74**, BMNH PD9644, as 72a, including ring septa with circular-oval foramen, $\times 50$; **75**, BMNH PD9561, longitudinal section showing thin autozoocial chamber walls with acanthostyles developed on interapertural wall junctions, $\times 100$; **76–78**, probably Redesdale Ironstone shale (Asbian), Lower Limestone Group, Redesdale, Northumberland; **76**, AUGD.10134a (paratype), detail of zoarial surface, $\times 20$; **77**, AUGD.10134b (lectotype), shallow tangential section showing arrangement of polygonal autozoocial chambers, centrally placed circular to oval foramen in some autozoocial chambers, rare exilazoocia, and stylelets of two sizes on thin interapertural walls – acanthostyles at wall junctions and heterostyles in between, $\times 40$; **78**, AUGD.10134c (paratype), transverse section through branch showing inner endozone with thin-walled polygonal autozoocial chambers, and outer exozone with moniliform walls and 7–8 ring septa developed per chamber, $\times 20$.

- 1913 *Tabulipora howsei* [sic] (Nicholson); Wright *et al.*: 72.
 1925 *Tabulipora howsei* [sic] (Nicholson) var. nov. Smyth: 150.
 1987 *Tabulipora howsii* (Nicholson); Bancroft: 196.
 1991 *Tabulipora cf. howsei* [sic] (Nicholson); Billing: 41.

LECTOTYPE. Herein designated AUGD 10134b (fig. 12a of Nicholson 1881).

PARALECTOTYPES. Herein designated AUGD 10134, 10134a, and 10134c (fig. 12b of Nicholson 1881). AUGD 10132 and 10141 may be part of the original Nicholson material and so may also be paratypes (Benton & Trewin 1978, Benton 1979).

MATERIAL. BMNH PD9561, 9643-9649, 9653, 9722-9729; TCD.34080-34087, 34121, 34158, 34164, 42564; BELUM K2177.

K3234, Upper part of the Glencar Limestone (Viséan, Asbian), Carrick Lough, County Fermanagh. TCD.42551-42554, Upper part of the Glencar Limestone (Viséan, Asbian), Sillees River, County Fermanagh.

DESCRIPTION. Only small encrusting zoaria were examined; no solid branches were recovered.

Adnate zoaria are thin, up to 1.30 mm thick, and form small circular expansions up to 6.2 mm in diameter. They encrust fenestrate bryozoans, and crinoidal material. Sheets are only one autozoocial chamber high; young autozoocia do not encrust older autozoocia (as in *Fistulipora incrassata*).

Autozoocia are budded from a thin basal wall 0.02–0.03 mm thick and diverge distally in the narrow endozone. At the exozone

they bend slightly and vestibules are orientated perpendicular to the zoarial surface. Chamber walls are only 0.01–0.02mm thick in the endozone, but are considerably thicker, ranging from 0.15–0.18mm, in the exozone. These endozonal walls are straight, and rarely moniliform.

Ring septa are developed within the exozone where generally three to four are found. (A greater number have been reported from solid ramose zoaria where the exozone is thicker (Lee 1912, Bancroft 1984)). The inner margins of the ring septa are unthickened, thin and not deflected posteriorly. Foramen are 0.08 to 0.12mm in diameter, centrally placed, and circular to occasionally reniform in shape.

Autozoocial apertures are large, and polygonal to infrequently circular in shape and are very closely spaced at less than one diameter apart. Exilazooecia are small, with circular apertures. They are uncommon, and usually occur as isolated individuals between autozoocenia at interapertural angles.

Interapertural walls are very thin and angular or rounded with styles developed along their crests. Large acanthostyles are found at interzoocial junctions, while as many as 20 smaller heterostyles may occur between them, around autozoocenia. Acanthostyles reach 0.05mm in thickness and 0.09mm in length.

Table 25 Measurements of *Tabulipora howsii* (in mm). N=14.

NM	x	Mn	Mx	CVw	CVb
MTZ	41	0.45	0.24	1.30	9.10
Z1	72	9	6	11	8.24
Z2	74	6.41	5	8	7.74
AD	130	0.27	0.20	0.35	9.16
IWT	126	0.03	0.01	0.08	24.2
FD	35	0.09	0.06	0.12	11.19
ED	4	0.09	0.05	0.13	—
					2.67

MTZ = Maximum thickness of adnate zoarium from basal wall to external surface.

DISCUSSION. *Tabulipora howsii* is easily recognised by its thick ramose zoaria which may reach a diameter of 20mm, its moniliform exozonal wall, the presence of numerous ring septa, and from the often polygonal to angular autozoocial apertures.

However, no ramose specimens were found; this is unusual as they have previously been recorded in large numbers (Lee 1912, Bancroft 1984). Adnate colonies of *T. howsii* have been reported from Scotland (Bancroft 1984) but these have not been examined in the present study.

The number of exilazooecia may vary greatly from zoaria to zoaria. In the County Fermanagh specimens exilazooecia are generally few in number. However, Bancroft (1984: 376) describes them as common, occurring as either scattered individuals or in maculae, in ramose zoaria from the Midland Valley of Scotland, which suggests that the Fermanagh specimens were young individuals which had not developed ramose branches characteristic of older colonies.

Smyth (1925: 150) noted a variety of the taxon from the Asbian of north Wales, and stated that it conformed in every aspect with Lee's diagnosis except in two features: 30 not 40 autozoocial apertures were contained in a 1cm line, and the foramen were oval not uniform. Within the Scottish and County Fermanagh *T. howsii* populations there is variation in these characters and they are not considered herein to merit varietal status. Examination of Smyth's material (TCD.R11a-g, TCD.21545a, b) shows it to lie within the variation range of *T. howsii* as given by Bancroft (1984).

STRATIGRAPHICAL RANGE. Lower Carboniferous (Asbian–Brigantian).

DISTRIBUTION. Rare, but recorded from Counties Fermanagh and Donegal (Wright *et al.* 1913), the Midland Valley of Scotland, northern England, and North Wales.

***Tabulipora minima* Lee, 1912**

Figs 71c, 79

1912 *Tabulipora minima* Lee: 164, pl.15, fig.21.

1987 *Tabulipora minima* Lee; Bancroft: 196.

LECTOTYPE. Herein designated GAGM 01-53 BYC (longitudinal section in thin section, figured by Lee, 1912).

MATERIAL. Three zoarial fragments, BMNH PD9650, BELUM K2182. Upper part of the Glencar Limestone (Viséan, Asbian), Carrick Lough, County Fermanagh; K3474 Upper part of the Glencar Limestone (Viséan, Asbian), Sillees River, County Fermanagh.

DESCRIPTION. Zoaria are erect, ramose, and composed of moderately robust sub-circular branches. Only two zoaria were examined; the larger measures 14.7mm in length. The nature of branch division is not known.

Autozoocenia are budded from within the endozone. Autozoocial chambers are long, reaching a maximum length of 4.3mm in length. They diverge at low angles of less than 25° in the endozone, and hardly bend posteriorly at the exozone.

Endozonal walls are very thin, undulating or straight. The majority of the autozoocial tube is contained within the endozonal area. Consequently the axial ratio is high. The exozone is only 0.11–0.21mm wide, where chamber walls are of regular thickness. Three to occasionally four ring septa are found per autozoocium. They are thin, with a central circular foramen, and are found towards the top of the endozone and within the exozone.

Autozoocial apertures are large, oval to circular in shape and closely spaced at less than one diameter apart. Interapertural walls are thin and smooth.

Exilazooecia are small, and range in diameter from 0.06 to 0.13mm. They are circular to oval in shape and occur as scattered individuals or in small clusters between autozoocenia.

Styles are of one structural type only. Between 12 and 15 large acanthostyles 0.06mm in diameter surround autozoocial apertures. They are arranged on interapertural walls, with one consistently positioned at interapertural junctions.

Table 26 Measurements of *Tabulipora minima* (in mm). N=2.

NM	x	Mn	Mx	CVw	CVb
ZD	11	2.57	1.80	3.36	4.16
Z1	16	12.95	10	16	11.75
Z2	16	4.71	4	5	9.83
AD	20	0.23	0.15	0.30	13.43
IWT	19	0.08	0.05	0.12	22.92
ED	7	0.09	0.06	0.13	19.52
ET	5	1.99	1.38	2.58	1.46
TE	12	0.17	0.11	0.21	13.33
					8.24

DISCUSSION. *Tabulipora minima* is easily recognised by its moderately robust and often flattened branches, by the presence of a very thin exozone, and by the occurrence of a small number of ring septa in each autozoocium.

It is rare in the British Isles. Only Lee (1912) and Bancroft (1984) have previously recorded it. At Carrick Lough three specimens were recovered. Although one of these was silicified a considerable amount of internal detail, including ring septa, is preserved.

STRATIGRAPHICAL RANGE. Carboniferous (Viséan–Arnsbergian).

DISTRIBUTION. Only recorded from County Fermanagh, Yorkshire, and the Midland Valley of Scotland.

Genus *STENOPHRAGMIDIUM* Bassler, 1952

TYPE SPECIES. *Stenophragma lobatum* Munro, 1912, by original designation from the Lower Carboniferous of Ravenstonedale, Cumbria (formerly Westmoreland), England.

REVISED DIAGNOSIS. Stenoporid with encrusting, rarely ramose zoaria. Encrusting zoaria commonly form flat adnate colonies or hollow erect dichotomising expansions on which monticules are regularly developed.

Autozoocoeial chambers have thickened walls in the exozone, where they are of uniform width or occasionally moniliform. Autozoocoeial chambers diverge distally at a low angle in the thin endozone, becoming perpendicular to the zoarial surface in the wider exozone. Up to five hemiphragms are developed on proximal walls, at the top of the endozone and in the exozone, where they extend halfway across chambers. Autozoocoeial apertures are of moderate size, circular to oval in shape, and closely spaced. Exilazooecia are rare.

Large acanthostyles may be situated at zoocoeial wall junctions, and heterostyles may be disposed between them.

DISCUSSION. This genus, which is restricted to the Carboniferous, was first described from Northern England (Munro 1912). To date nineteen species have been reported; four species have been described from the Carboniferous of the British Isles. The British species are *Stenophragmidium grandyense* (Munro 1912), *S. lobatum* (Munro 1912) [the type species], *S. incrustans* Owen 1973 and *S. ramosum* Owen 1969. To these, five *Tabulipora* species of Lee (1912) may be added, as well as *Tabulipora serrata* Smyth, 1922 (from the Lower Carboniferous (Brigantian) of Ballycastle, County Antrim). They possess 'tabulae' which 'extend only partly, leaving an untabulated space, ... always situated on the distal side ...' (Lee 1912: 171). The 'tabulae' are clearly hemiphragms. Examination and revision of Lee's and Smyth's material may reveal that their six species are referable to *Stenophragmidium*.

STRATIGRAPHICAL RANGE. Lower–Upper Carboniferous

DISTRIBUTION. British Isles, Belgium, the CIS (former Soviet Union), North America, Asia.

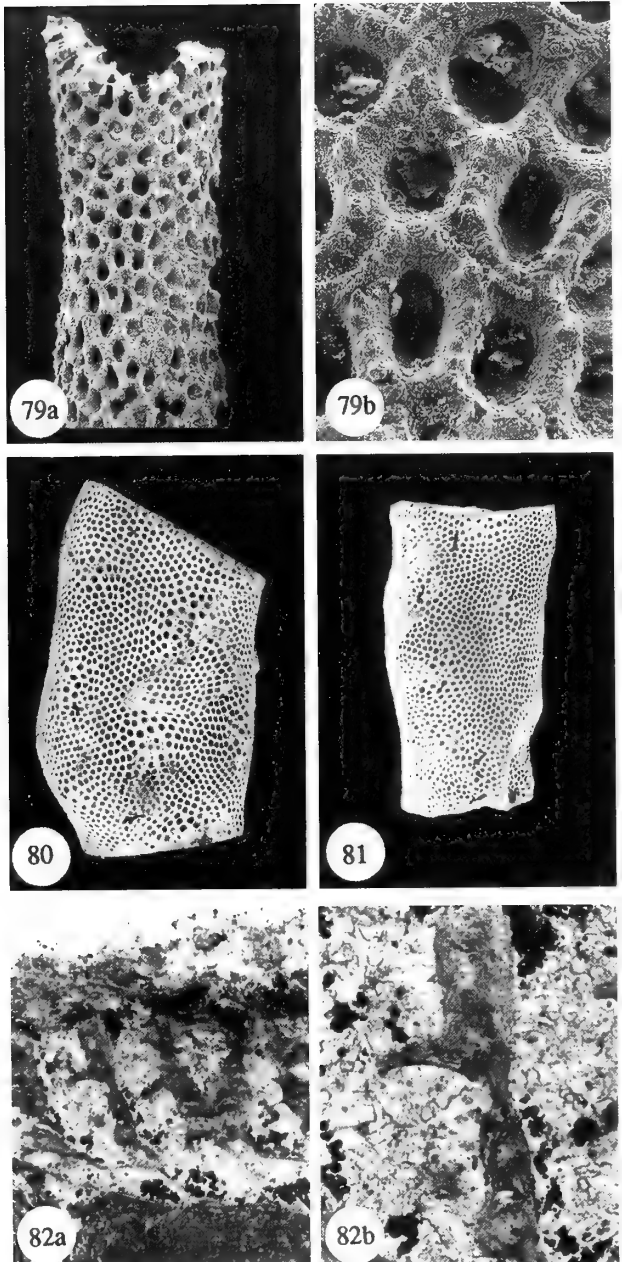


Fig. 79 *Tabulipora minima* Lee, 1912; Upper part of the Glencar Limestone (Viséan, Asbian), Carrick Lough, County Fermanagh;

BMNH PD9650: 79a, portion of ramose colony showing arrangement of autozoocoeia with oval apertures, $\times 20$; 79b, detail of 79a, showing oval autozoocoeial apertures divided by thick interapertural walls on which are developed large acanthostyles, $\times 100$.

Figs 80–82 *Stenophragmidium* sp. Upper part of the Glencar Limestone (Viséan, Asbian), Sillees River, County Fermanagh: 80, BELUM K15209, ramose hollow zoarial fragment, with regular disposition of monticules and autozoocoeia; small exilazooecial apertures are found between autozoocoeia, particularly on monticules; autozoocoeia adjacent to monticules are larger than those in inter-monticular areas, $\times 3$; 81, BELUM K15210, zoarial fragment, details as for 80, $\times 2.5$; 82, BELUM K15214: 82a, longitudinal section through colony showing thin undulatory basal wall, low angle of divergence of autozoocoeia in endozone, increasing in exozone region; chamber walls thin in endozone, thicken rapidly in exozone; a single hemiphragm is situated on proximal chamber walls, bends inwards, and seals half the vestibule, $\times 25$; 82b, detail of 82a, $\times 75$.

Stenophragmidium sp.

Figs 80–83

MATERIAL. BELUM K3436, K15209-K15215 (5 zoarial fragments and 2 longitudinal sections), Upper part of the Glencar Limestone (Viséan, Asbian), Sillees River, County Fermanagh.

DESCRIPTION. Zoaria consist of large erect hollow expansions up to 11.17 mm in width, or thin encrusting adnate sheets 0.28–0.30 mm thick. Autozoocia are budded from a very thin undulating basal wall. Autozoocia chambers are recumbent in the thin endozonal region (0.15 mm) and straight in the wider exozone (0.28 mm). The vestibule lies at a high angle of 80° to 85° to the zoarial surface, and is moderately wide (0.19–0.20 mm).

Autozoocia walls are 0.03–0.04 mm thick in the endozone, but expand rapidly in the exozone to between 0.15 and 0.18 mm. They are usually of constant width, occasionally undulatory, and rarely moniliform. Walls consist of a well defined central hyaline zone (0.02 mm wide) in which laminae are orientated parallel to the growth direction. Thin lateral laminae are derived from this central zone and bend sharply proximally. This is typical leiolemid-type wall structure (after Boardman 1960).

Up to three hemiphrags are developed within and at the base of the exozone, where they arise from proximal walls. They are thin, often straight and occasionally bend slightly proximally. They are short (0.04–0.07 mm in length), usually extend less than half-way into chambers, and have rounded bulbous tips.

Autozoocia apertures are polygonal or irregular in shape, occasionally circular and are closely spaced at less than one diameter apart. Apertures decrease in diameter away from monticules. Interapertural walls are rounded and moderately thick, with as many as 16 stylets occurring along their crests.

Large acanthostyles (0.05–0.07 mm) are usually found at autozoocia wall junctions, with smaller stylets (0.02–0.03 mm) between. Exilazooecia are rare; they are small, with circular to angular apertures. They occur as isolated individuals between autozoocia, or infrequently in groups of 10 to 12 in monticule-centred maculae which are widely spaced at up to 5.53 mm apart.

DISCUSSION. This taxon is known from 14 specimens from which details of both external and internal structure are known. It does not resemble previously described British species, but may be synonymous with *Tabulipora crassimuralis* Lee, 1912. The genus needs revision, which will be undertaken at a future date and until then I prefer to leave this taxon unassigned to any species.

The hollow portions of the zoaria examined all had a posthumous

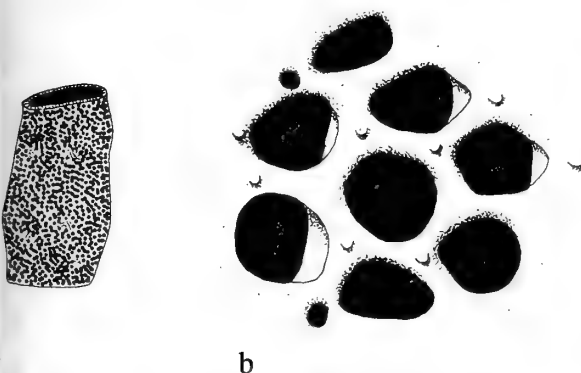


Fig. 83 *Stenophragmidium* sp. Line drawing of external features of BELUM K15209; a, Portion of hollow ramos colony, scale bar = 1 mm; b, detail of autozoocia and exilazooecia and disposition of acanthostyles, scale bar = 0.1 mm.

Table 27 Measurements of *Stenophragmidium* sp. (in mm). N=6.

	NM	x	Mn	Mx	CVw	CVb
ZD	39	7.92	4.81	11.17	11.28	4.38
Z1	60	7.73	5	10	12.08	13.44
Z2	60	5.5	4	8	13.39	6.16
AD	60	0.24	0.15	0.32	10.75	10.84
IWT	60	0.07	0.04	0.12	20.86	7.96
ED	60	0.08	0.06	0.15	21.26	7.55
ET	4	0.64	0.25	1.07	10.60	1.22
TE	4	1.64	0.90	2.76	16.76	1.68
IMS	6	4.45	3.38	5.53	18.34	14.30

infill of micritic mud which was also found in autozoocia chambers. Zoaria possibly encrusted soft algal branches which have now disappeared, or may simply have been hollow.

STRATIGRAPHICAL RANGE. Lower Carboniferous (Viséan, Asbian).

DISTRIBUTION. Ireland, North Wales.

Order CYSTOPORATA Astrova, 1964
Suborder FISTULIPORINA Astrova, 1964
Family FISTULIPORIDAE Ulrich, 1882
Genus *Fistulipora* M'Coy, 1849

TYPE SPECIES. *Fistulipora minor* M'Coy, 1849 by subsequent designation (Milne-Edwards & Haime 1850: lix) from the Lower Carboniferous of the British Isles.

Fistulipora incrassans (Phillips, 1836)

Figs 84a, 85–88, 105

A complete systematic description, full synonymy and discussion of the type specimens is given in Bancroft & Wyse Jackson (1995).

MATERIAL. BMNH PD9651-9676, 9740; TCD.34088-34103, 34138-34139, 34146, 34157, 34159, 34166, 42590, 42610; BELUM K2151, K2153, K2193, Upper part of the Glencar Limestone (Viséan, Asbian), Carrick Lough, County Fermanagh. TCD.42511, Upper part of the Glencar Limestone (Viséan, Asbian), Sillees River, County Fermanagh.

DESCRIPTION. Zoaria form thin unilaminate button-like discs up to 1.3 cm in diameter; encrusting unilaminate or multilaminate sheets up to 1.58 mm thick, or small chaetetiform nodular expansions 30 mm wide by 17 mm high. Colonies often encrust crinoid stems, fenestellid Bryozoa, and occasionally brachiopod valves.

Autozoocia are budded from a very thin basal wall (0.015–0.025 mm thick). They are often initially slightly recumbent, but subsequently become erect and orientated at 80° to 90° to the zoarial surface. Autozoocia are straight, tubular and thin walled. Thin diaphragms are commonly developed at the base of chambers and are less common and irregularly dispersed throughout the remaining portions of chambers. Autozoocia are arranged in straight to curved rows which produce an offset pattern on the zoarial surface. Autozoocia apertures are large (0.17 mm to 0.40 mm); usually circular to oval, occasionally D-shaped, rarely sub-polygonal in shape and spaced 1–2.5 diameters apart. Lunaria are indistinct and not consistently present. They are small – only one fifth the circumference of apertures, crescent-shaped, marginally elevated above the zoarial surface, and discretely indent apertures (by as much as 0.04 mm). Lunaria are found on the proximal sides of autozoocia closest to monticules. In a few zoaria lunaria completely encircle autozoocia apertures, forming low peristome-like collars. Rarely,

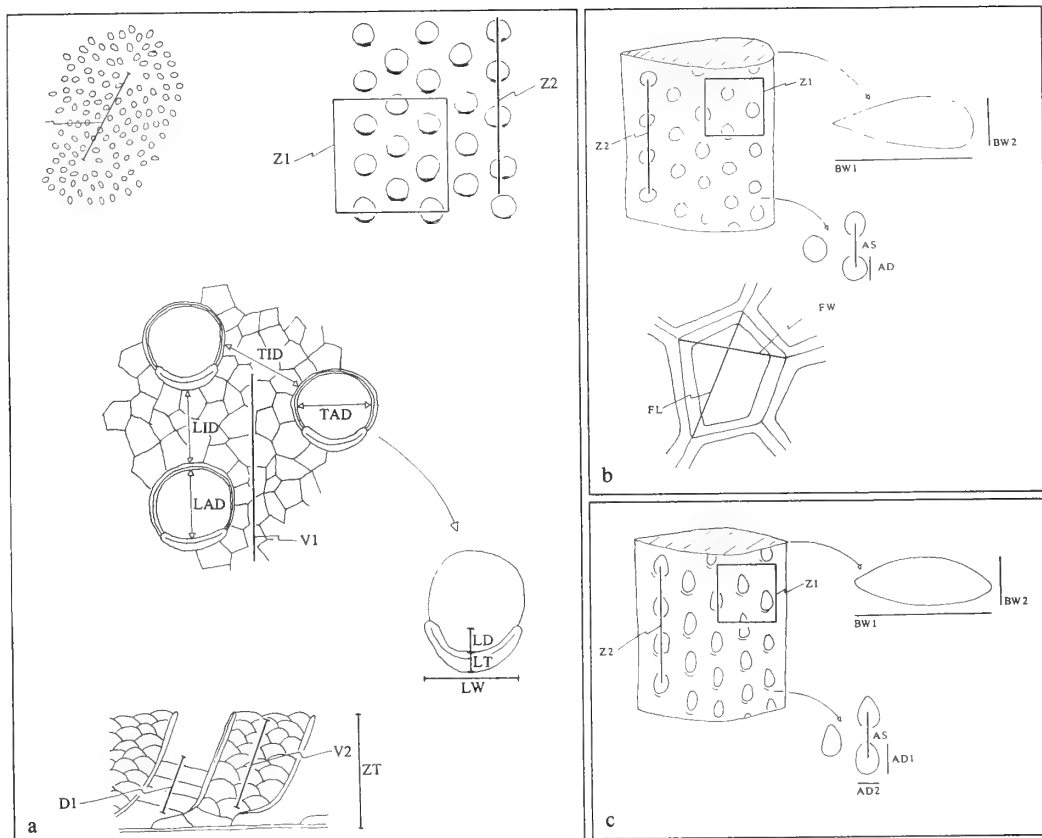


Fig. 84 Measurements taken on cystoporates in this study; **a**, *Fistulipora incrustans* (Phillips, 1836); **b**, *Sulcoretepora parallela* (Phillips, 1836); **c**, *Goniocladia cellulifera* (Etheridge, 1873b); ZT = Zoarial thickness from basal wall to upper zoarial surface; BW1 = Branch width measured parallel to median wall; BW2 = Branch width measured perpendicular to median wall; MS = Distance between adjacent monticule measured from centre to centre; V1 = Number of vesicles contained along a 1mm line; FL = Fenestrule length; FW = Fenestrule width; AD1 = Autozoocia apertural diameter measured parallel to growth direction; AD2 = Autozoocia apertural diameter measured perpendicular to growth direction; AS = Autozoocia apertural spacing; minimum distance between two adjacent autozoocia apertures, measured from their centres; LAD = Autozoocia apertural length measured from lunaria to opposite side; TAD = Autozoocia apertural width measured perpendicular to LAD; LID = Autozoocia apertural spacing in same longitudinal row; TID = Autozoocia apertural spacing between adjacent rows; Z1 = Number of complete autozoocia apertures contained in 1 mm²; Z2 = Number of complete autozoocia apertures contained in a 2mm line; LW = Lunarium width; LT = Lunarium thickness; LD = Lunarium depth; V2 = Number of vesicles seen in transverse section contained along a 1mm line; DI = Number of diaphragms contained within 1mm.

large hood- or cowl-like lunaria are developed. These are 0.1 mm high and cover approximately half the aperture. They are similar to those illustrated by Warner & Cuffey (1973) in *F. incrustans* Moore and *F. carbonaria*.

Monticules are regularly arranged between 2 and 5 mm apart and are conspicuously elevated above the general surface of zoaria. Small maculae (*sensu* Anstey 1981) are found at the apex of each monticule. Autozoocia develop in intersecting semi-circular rows away from monticules.

Vesicles are arranged in 3 to 4 vertical stacks between autozoocia, with 5–8 contained within 1 mm per stack. They are small, rectangular, polygonal or inverted cup-like structures. They become increasingly thinner towards the zoarial surface. Between ten and fifteen vesicles are found in each vertical stack.

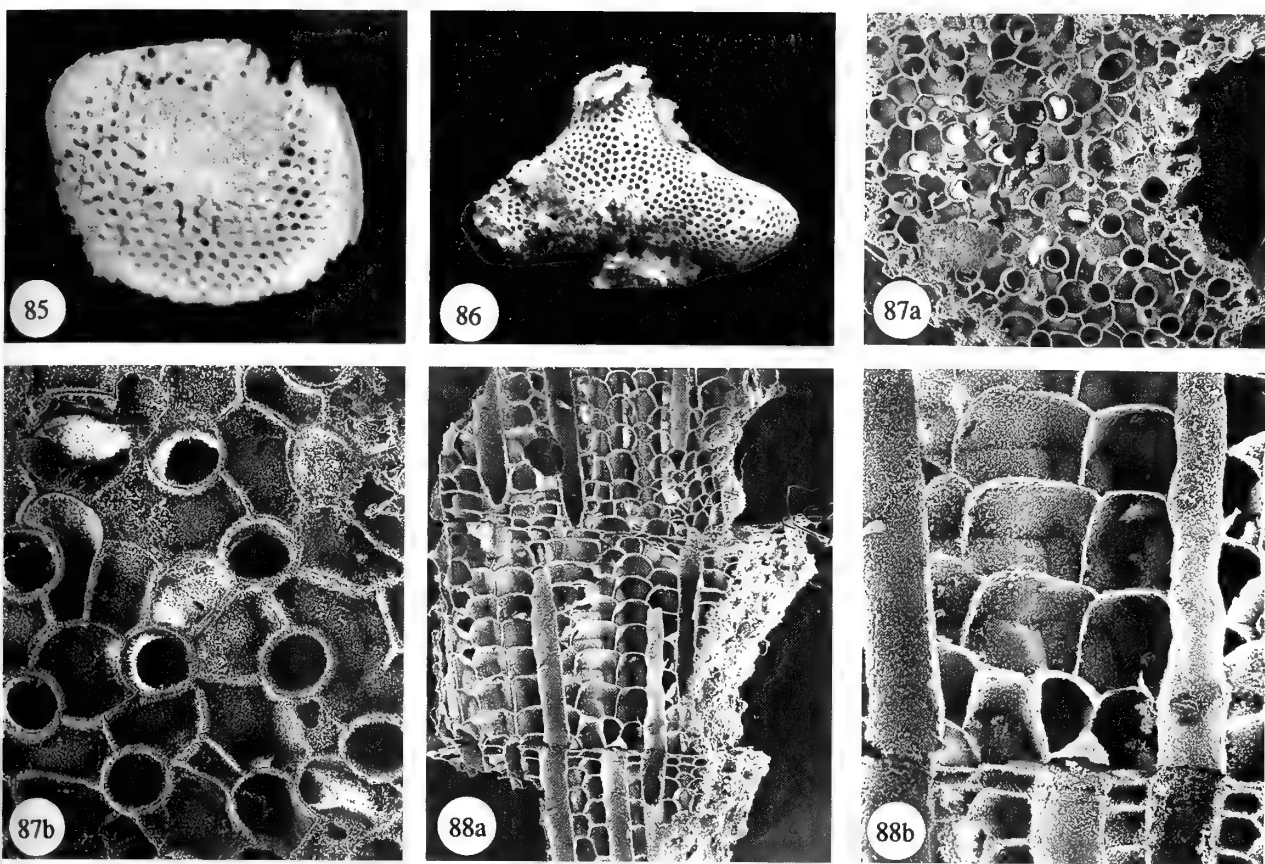
In some large colonies five to six encrusting cycles have been seen (this is not unusual – many more such multilaminate sheets have been observed in massive colonies from other localities).

DISCUSSION. *Fistulipora incrustans* is easily recognised by its encrusting habit, its large circular autozoocia apertures, its stacked

interzoocia vesicular tissue, and by the regular monticular arrangement.

Table 28 Measurements of *Fistulipora incrustans* (in mm). N=15.

	NM	x	Mn	Mx	CVw	CV
ZT	41	0.67	0.20	1.58	18.10	1.6
AD	119	0.27	0.18	0.40	10.73	6.6
LAD	20	0.24	0.20	0.32	10.10	11.3
TAD	20	0.30	0.17	0.36	15.74	17.3
AS	115	0.28	0.10	0.55	23.64	4.1
LID	20	0.41	0.22	0.66	22.42	2.3
TID	20	0.27	0.20	0.45	14.59	4.1
Z1	117	3.5	2	6	16.88	6
Z2	109	3.9	3	6	11.75	7
V1	16	4.6	3	6	16.04	5
V2	20	5.4	3	8	16.60	6
MS	8	2.88	0.63	4.92	12.21	1
LW	18	0.20	0.17	0.23	7.84	20
LD	12	0.01	30.0	10.02	29.25	3
LT	12	0.03	0.02	0.07	23.12	3



Figs 85–88 *Fistulipora incrustans* (Phillips, 1836); Upper part of the Glencar Limestone (Viséan, Asbian), Carrick Lough, County Fermanagh; **85**, BMNH PD9651, small dome-shaped adnate zoarium (encrusting *Baculopora megastoma* fragment) showing regular arrangement of autozoocia in curved intersecting rows; lunaria are situated on the upper edges of apertures, $\times 10$; **86**, BMNH PD9652, chaetetiform colony showing monticular arrangement, $\times 3.5$; **87**, BMNH PD9676; **87a**, transverse view of circular autozoocia separated by vesicular tissue, $\times 20$; **87b**, detail of 87a, $\times 60$; **88**, BMNH PD9675; **88a**, longitudinal section showing three growth increments, simple tubular autozoocia, and vesicular tissue comprising box-like vesicles with domed upper surfaces, $\times 20$; **88b**, detail of 88a, $\times 60$.

It is the only species of *Fistulipora* described from the British Isles. Several previously reported taxa are considered synonymous with it. These are *Fistulipora minor* M'Coy, 1849 (see Owen 1969), and *Berenicea megastoma* M'Coy, 1844, which Young (1882) considered to be an immature *F. incrustans* colony (Bancroft & Wyse Jackson 1995).

F. excelsa Ulrich, 1884, has a similar form and morphometric measurements to *F. incrustans* (Phillips, 1836) and might be synonymous. *F. incrustans* Moore (1929) (a secondary homonym) from Texas has significantly larger elliptical to oval-shaped autozoocia apertures, which are surrounded by complete peristomes, and is not conspecific. On the other hand, the specimens described as *F. incrustans* Moore by Warner & Cuffey (1973) from the Lower Permian of Kansas are similar in most respects, and are probably conspecific with *F. incrustans* (Phillips, 1836).

Some morphological variation is seen both within and between colonies although this is not as considerable as the variation recorded by Warner & Cuffey (1973). They measured parameters in which high variation would be expected (eg. lunaria width and stypore dimensions). In this study a smaller number of parameters were measured: these are associated with the autozoocia (eg. apertural chamber width and spacing) and variation in them is

thought to be indicative of minor environmental changes (Farmer & Rowell 1973).

STRATIGRAPHICAL RANGE. Lower Carboniferous (Courceyan)–Lower Permian.

DISTRIBUTION. *Fistulipora incrustans* is a common species with a wide geographical range. It is frequent in the Lower Carboniferous of the British Isles, and has been recorded from the CIS (former Soviet Union), and North America.

Family CYSTODICTYONIDAE Ulrich, 1884
Genus SULCORETEPORA d'Orbigny, 1849

TYPE SPECIES. *Flustra? parallela* Phillips, 1836 by original designation from the Lower Carboniferous of Whitewell, Yorkshire, England.

REVISED DIAGNOSIS. Cystodictyonid with erect zoaria composed of dichotomising bifoliate branches, elliptical to oval in cross-section. Branches retain a constant width along their length. Autozoocia are budded from a straight or zig-zag median wall

which is composed of a dark central granular skeleton surrounded by laminated skeleton. Autozoocia are arranged in longitudinal rows. Zooecial chambers are long and narrow in the endozone and bend sharply in the exozone. In tangential section, chambers are rectangular in shape. Vesicles are found in the outer endozone and inner exozone, where they occur as irregular to circular cavities. They become less abundant towards the zoarial margin. Indistinct lunaria are found on the proximal edge of the large oval-shaped autozoocia apertures. Interapertural areas are smooth with a single longitudinal ridge developed between adjacent autozoocia rows.

DISCUSSION. Taxonomically *Sulcoretepora* has presented many problems and prompted much argument. At ordinal level it was first regarded as a cryptostome (Vine 1884a), and this view was maintained until recently (Cuffey 1973). It is now recognised as a cystoporate (Morozova 1970, Utgaard 1983). At generic level *Sulcoretepora* was first described by d'Orbigny (1849), who designated Phillip's species *Flustra? parallela* as type species. Subsequently, Ulrich (1882) erected the genus *Cystodictya* (type species, *C. ocellata* from the Mississippian of Somerset, Kentucky, U.S.A.) and placed *Sulcoretepora* in synonymy with it on account of the shared presence of a median wall. Many authors have followed this opinion (eg. Young 1887, Vine 1888). Close examination of the two genera shows that there is a difference in the shape and nature of the median wall. It is always straight in *Cystodictya*, but is undulatory or sharply folded in *Sulcoretepora*. *Mstainia* Shulga-Nesterenko, 1955, has a plicated median wall and is regarded a junior subjective synonym of *Sulcoretepora* (Elias 1964).

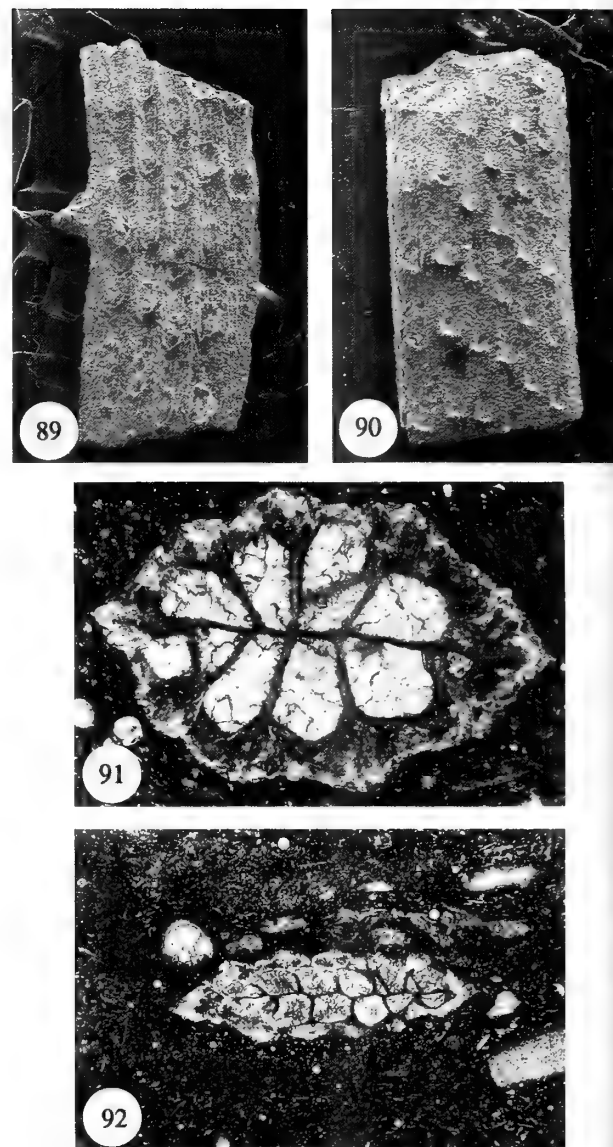
STRATIGRAPHICAL RANGE. Devonian–Permian.

DISTRIBUTION. British Isles, Europe, the CIS (former Soviet Union), United States, Asia.

Sulcoretepora parallela (Phillips, 1836) Figs 84b, 89–93

- 1836 *Flustra? parallela* Phillips: 200, pl.1, figs 47, 48.
- 1843 *Flustra? parallela* Phillips; Morris: 37.
- v1844 *Vincularia parallela* (Phillips); M'Coy: 198, pl. 27, fig. 14.
- 1849 *Sulcoretepora parallela* (d'Orbigny); d'Orbigny: 152.
- 1854 *Sulcoretepora parallela* (d'Orbigny); Morris: 105.
- 1862 *Vincularia parallela* (Phillips); Griffith: 227.
- 1877 *Sulcoretepora parallela* (Phillips); Vine: 273.
- 1880c *Ptilodictya? parallela* (Phillips); Vine: 508.
- 1884a *Arcanopora parallela* (Phillips); Vine: 204.
- 1885 *Cystodictya parallela* (Phillips); Vine: 95.
- 1887 *Cystodictya parallela* (Phillips); Young: 461.
- 1888 *Cystodictya parallela* (Phillips); Vine: 74.
- 1953 *Sulcoretepora parallela* (Phillips); Bassler: 142, fig. 103.
- 1964 *Sulcoretepora parallela* (Phillips); Elias: 380, pl. 5, figs 3–6.
- 1969 *Sulcoretepora parallela* (Phillips); Owen: 265, pl. 23, figs E–F.
- 1983 *Sulcoretepora parallela* (Phillips); Utgaard: 429, fig. 210, 1a–f.
- 1986a *Sulcoretepora parallela* (Phillips); Bancroft: 23.
- 1987 *Sulcoretepora parallela* (Phillips); Bancroft: 196.
- 1991 *Sulcoretepora parallela* (Phillips); Billing: 41.

MATERIAL. BMNH PD9563, 9619, 9677–9700; TCD.34104–34111, 34138, 34142, 34146, 34148–34153, 34157–34158, 34172, 42596, 42600b, 42605; BELUM K2158. Upper part of the Glencar Limestone (Viséan, Asbian), Carrick Lough, County Fermanagh.



Figs 89–92 *Sulcoretepora parallela* (Phillips, 1836); Upper part of the Glencar Limestone (Viséan, Asbian), Carrick Lough, County Fermanagh: **89**, BMNH PD9677, branch fragment showing arrangement of autozoocia in longitudinal rows separated by longitudinal ridges, $\times 15$; **90**, BMNH PD9678, as 89; lunaria are more pronounced proximally of autozoocia apertures; the size and spacing of autozoocia apertures increases in rows from left to right, $\times 15$; **91**, BMNH PD9619, transverse section showing scalloped branch margins, atypical straight median wall, and elongate polygonal autozoocia chambers with rounded lateral margins, $\times 50$; **92**, BMNH PD9563, transverse section with more typical plicated median wall, $\times 20$.

TCD.42555–42558. Upper part of the Glencar Limestone (Viséan, Asbian), Sillees River, County Fermanagh.

DESCRIPTION. Zoaria form quite large expansions of dorsoventrally flattened branches that are elliptical or oval in cross-section. Bifurcation of branches is more common than the development of lateral branches, which are thinner than the main branch. The largest fragment measured is 38.8mm in length and no lateral branches

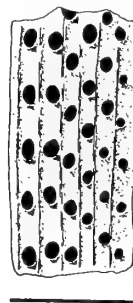


Fig. 93 *Sulcoretepora parallela* (Phillips, 1836). Line drawing of external features of BMNH PD9678; scale bar = 1 mm.

were developed. Mature branches are usually of constant width along their length, but a small amount of thinning distally can occur. The ratio of branch thickness (BW2) to branch width (BW1) ranges from 1:4 to 1:2.

Autozoocia are arranged in 4 to 6 longitudinal rows on the lateral sides of branches. The number of longitudinal rows remains constant along the length of a branch. Autozoocia are of medium to large size and circular to oval in shape. A thin proximal lunarium is present around each autozoocia aperture. Apertures are spaced two and a half to three diameters apart. This spacing increases slightly in the rows adjacent to the median ridge. Here three autozoocia generally occur in a 2mm line, while four occur in the same length in rows away from the median ridge. Between adjacent rows of autozoocia a strong narrow longitudinal ridge is developed. A smaller, fainter ridge is often found either side of the main ridge. This second ridge is found between the distal and proximal ends of two autozoocia in the same row. The interapertural areas are smooth except for the longitudinal ridges.

Branches are internally divided by a thin plicated median wall, from either side of which are budded autozoocia. The median wall is composed of pale laminated skeletal material.

Autozoocia chambers are elongate, narrow, and bend distally in the endozone region. The exozone is extremely thin, being about one sixth the thickness of the branch. Autozoocia chamber walls are thin and straight. In shallow tangential section chambers are tear-shaped and narrower proximally. Deeper sectioning shows the chambers to have a rectangular shape. In cross-section chambers are hexagonal to pentagonal in outline.

Small vesicles, 0.03 mm in diameter, are commonly found between autozoocia and the branch margin. They are most frequently developed in the outer endozone and inner exozone. They are thin-walled, circular to irregular in shape, and may be infilled with stereom in the exozone.

Table 29 Measurements of *Sulcoretepora parallela* (in mm). N=21.

NM	x	Mn	Mx	CVw	CVb
BW1	172	1.02	0.68	1.43	4.39
BW2	38	0.49	0.31	0.75	7.92
Z1	63	—	6	8	8.46
Z2	170	—	3	4	11.57
AD1	200	0.19	0.11	0.29	9.90
AD2	201	0.12	0.08	0.20	11.49
AS	201	0.56	0.38	0.82	11.72

DISCUSSION. *Sulcoretepora parallela* is unmistakable in appearance due to its strap-like branches with a regular arrangement of

autozoocia apertures which are divided by longitudinal ridges. This bryozoan displays very little variation either within or between colonies in a population. Computed coefficients of variation for branch width (BW1), branch thickness (BW2), and autozoocia apertural diameter (AD1 and AD2) are all very low. The values for the other parameters, those that are a measure of autozoocia spacing (Z1, Z2, and AS), are higher, but are still regarded as low when compared with other bryozoan taxa.

Sulcoretepora parallela has a wide distribution in the Carboniferous of the British Isles. It is common in the Carrick Lough/Sillees River assemblage.

Three other species of *Sulcoretepora* have been described from the Carboniferous of the British Isles: *S. ramosa* Owen 1973, *S. raricosta* (M'Coy, 1844), and *S. robertsoni* (Young & Young, 1877). *S. ramosa* is not a sulcoreteporid but is a hyphasmoporid cryptostome. Branches are circular and not bifoliate, it lacks a median wall and lunaria, and acanthostyles are common. It occurs in County Fermanagh and is redescribed herein as *Clausotrypa ramosa* (Owen, 1973).

The other species of *Sulcoretepora* differ from *S. parallela* in a number of respects. *S. raricosta* has autozoocia of similar dimensions to those in *S. parallela* but has more autozoocia developed on one side of the branch than the other. Branches of *S. robertsoni* are nearly circular in cross-section, autozoocia apertures are larger, and interapertural areas are pitted and more ornate (Young & Young 1877).

STRATIGRAPHICAL RANGE. Carboniferous (Holkerian–Pendleian).

DISTRIBUTION. British Isles.

Family GONIOCLADIIDAE Waagen & Pichl, 1885
Genus GONIOCLADIA Etheridge, 1876

TYPE SPECIES. *Carinella cellulifera* Etheridge, 1873, by original designation from the Lower Carboniferous of Carlisle, Scotland.

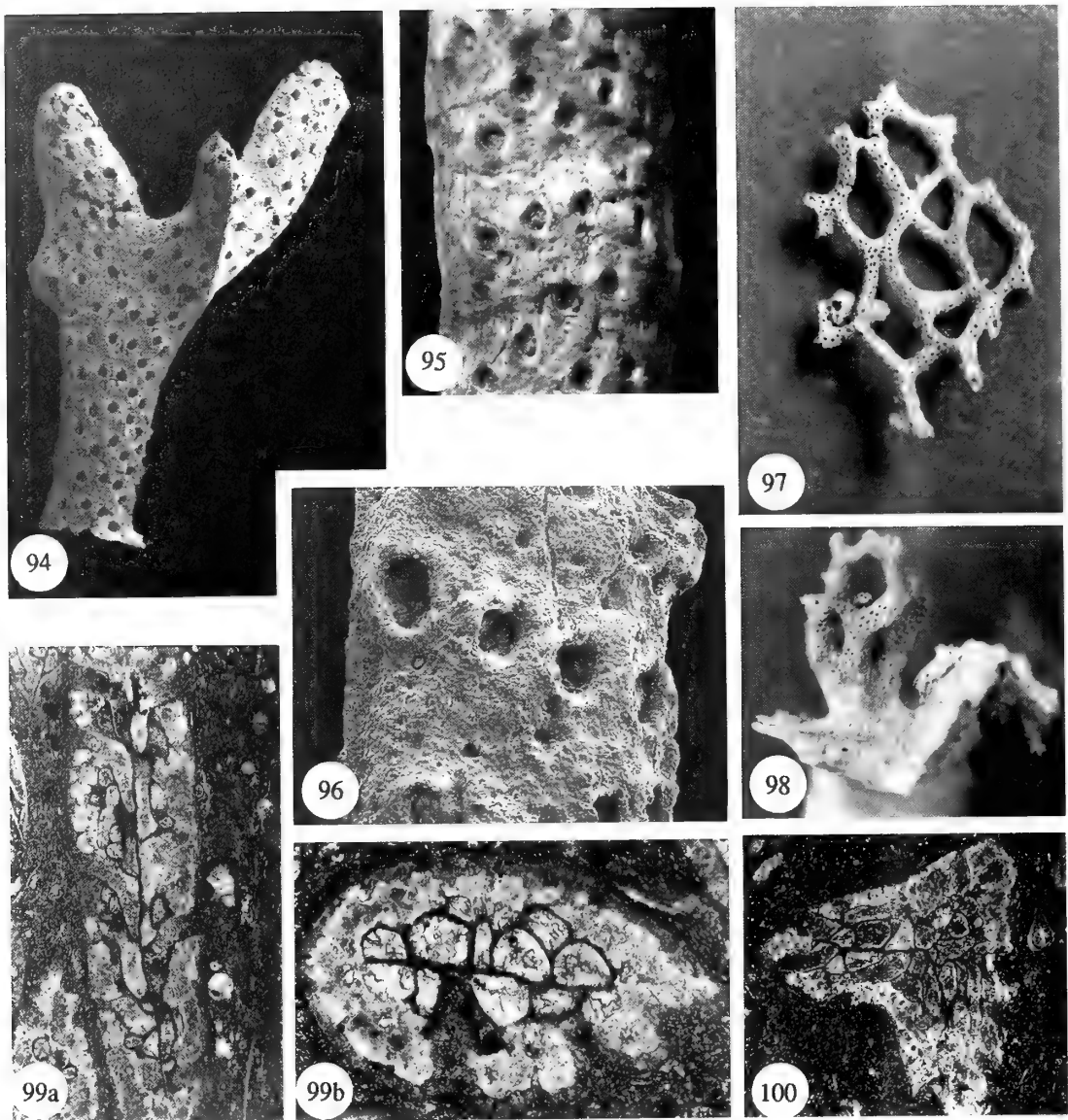
Goniocladia cellulifera (Etheridge, 1873)

Figs 84c, 94–102

- 1873a *Carinella cellulifera* Etheridge: 433.
- 1873b *Carinella cellulifera* Etheridge; Etheridge: 101.
- 1876 *Goniocladia cellulifera* (Etheridge); Etheridge: 522.
- 1880b *Goniocladia cellulifera* (Etheridge); Vine: 81.
- 1880c *Goniocladia cellulifera* (Etheridge); Vine: 507.
- 1885 *Goniocladia cellulifera* (Etheridge); Waagen & Pichl: 804.
- 1887 *Goniocladia cellulifera* (Etheridge); Young: 463.
- 1888 *Goniocladia cellulifera* (Etheridge); Vine: 77.
- 1888 *Goniocladia cellulifera* (Etheridge) var. *robusta* Vine: 78.
- 1953 *Goniocladia cellulifera* (Etheridge); Bassler: 89, fig. 54.
- 1983 *Goniocladia cellulifera* (Etheridge); Utgaard: 434, figs 213, 1a–h.
- 1986a *Goniocladia cellulifera* (Etheridge); Bancroft: 23.
- 1987 *Goniocladia cellulifera* (Etheridge); Bancroft: 196.

MATERIAL. BMNH PD9563, 9701, 9703–9721; TCD.34112–34120, 34135, 34146–34147, 34150–34154, 34157, 42589, 42600a, 42602b, 42604a, 42606c; BELUM K2162–5, K12003, Upper part of the Glencar Limestone (Viséan, Asbian), Carrick Lough, County Fermanagh. TCD.42512, Upper part of the Glencar Limestone (Viséan, Asbian), Sillees River, County Fermanagh.

EMENDED DIAGNOSIS. *Goniocladia* with large reticulate or occasionally adnate zoaria composed of bifoliate straight to gently curved branches. Branches anastomose at regular intervals to form



Figs 94–100 *Goniocladia cellulifera* (Etheridge, 1873b); Upper part of the Glencar Limestone (Viséan, Asbian), Carrick Lough, County Fermanagh: **94**, BMNH PD9719, colony fragment with typical branching pattern at a triple point, $\times 9$; **95**, BMNH PD9704, laterally flattened branch with sharp median ridge on left and rounded carinal ridge on right; autozoocia are arranged in longitudinal rows with circular apertures; lunaria are indistinct; cystopores open to the surface and are seen as small circular ‘pits’ in interapertural areas, $\times 50$; **96**, BMNH PD9718, close-up of branch with circular autozoocial apertures and small cystopore-openings, $\times 45$; **97**, BELUM K2164, portion of reticulate colony. Branches divided perpendicular to the plane of the median wall; they coalesce to form large open rhombic, polygonal to irregularly-shaped fenestrules, $\times 6$; **98**, BELUM K2163, robust holdfast of colony with portion of branch reticulation, $\times 6$; **99**, BMNH PD9721; **99a**, longitudinal section. Autozoocia diverge from a planar thin median wall at low angles; chambers are separated by vesicular tissue which consists of irregular to spherical vesicles, $\times 20$; **99b**, transverse section; the carinal ridge is on the left hand side while the sharper median ridge forms a sharp keel on the right. Autozoocia are polygonal, squat, and the median wall is straight, $\times 40$; **100**, BMNH PD9563, transverse section through a triple point reflected by the division of the median wall, $\times 20$.

large pentagonal or polygonal fenestrules. In cross-section branches are pyriform. They are bisected by a compound median wall which protrudes as a faint carina on the rounded barren surface and as a strong keel on the obverse surface.

Autozoocia are large, circular and arranged in quincunx in four to seven longitudinal rows either side of the median wall, from which they are budded. Low indistinct lunaria are frequently developed around autozoocial apertures. Interapertural areas are smooth.

Autozoocial chambers are narrow, recumbent, and closely packed in the endozone. They diverge away from adjacent chambers in the exozone, and vestibules are orientated at a high angle to the zoarial surface. Autozoocial chamber walls are thin. Basal diaphragms are rare.

DESCRIPTION. Zoaria form large planar reticulate colonies of unknown maximum dimensions. The largest reticular fragment

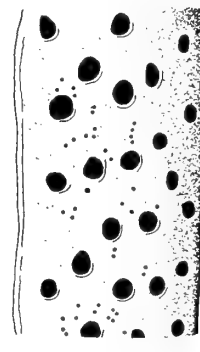


Fig. 101 *Goniocladia cellulifera* (Etheridge, 1873b). Line drawing of external features of BMNH PD9704; scale bar = 1 mm.

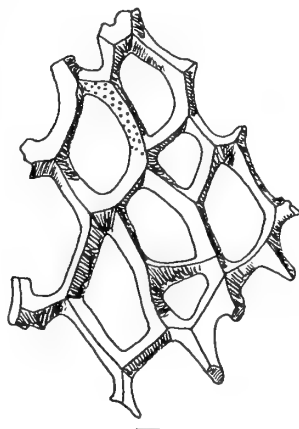


Fig. 102 *Goniocladia cellulifera* (Etheridge, 1873b). Line drawing of portion of a reticulate colony of BELUM K2164; scale bar = 1 mm.

examined measured 19 × 12 mm. Branches are bifoliate, laterally flattened, straight, and maintain a constant width along their length except prior to division when a small increase in width occurs. Branches divide, at angles of 30° to 70°, at short regular intervals. Coalescing of branches produces a regular pattern of pentagonal, hexagonal, or polygonal fenestrules up to 4.9 mm long by 3.4 mm wide. Branch division frequently produces three branches 60° apart. Dissipiments are absent.

Branch cross-sections are narrow with a pyriform to rhombic outline. The barren reverse surface is well rounded with a faint to distinct longitudinal carina while the celluliferous frontal surface is divided by a strong narrow angular median keel. These ridges are the external manifestations of the internal median wall.

Autozoocial apertures are arranged in quincunx in four to seven longitudinal rows, either side of the median ridge. Autozoocial apertures are large, circular to rarely oval in shape. Proximal lunaria are developed around most apertures. The size and thickness of the lunaria decreases towards the median keel. Interapertural areas are smooth and featureless. Autozoocial apertures are regularly spaced within longitudinal rows. Interapertural spacing decreases towards the median keel from five to two diameters apart (Table 31 and Fig. 03).

Colonies arise from stout holdfasts up to 13 mm in width. Initial colony growth is encrusting where autozoocial apertures are large, circular in shape and closely spaced. From this adnate portion three to six erect branches arise, which either remain isolated as erect eschariform colonies or anastomose to form reticulate colonies.

Internally branches are divided by a thin, straight compound median wall. It is composed of a dark coarse central layer surrounded by a thin pale laminated layer. Autozoocia are budded from this wall. In the endozone autozoocial chambers are long, narrow, recumbent, and the thin chamber walls are shared. In transverse section they are semi-circular to pentagonal in shape. Autozoocial chambers curve distally from the median wall at angles of between 60° and 20°, and they diverge away from each other so that in the exozone they are isolated. The thickness of the exozone is greatest at the widest portion of the branch, where vestibules are oriented at a high angle to the zoarial surface, and decreases in the autozoocial rows towards the median keel, where vestibules lie at a low angle to the zoarial surface.

Small hemispherical vesicles 0.01 to 0.03 mm in diameter are commonly found between autozoocial chambers. They are thin-walled, irregularly shaped and may be infilled with stereom in the endozone.

Table 30 Measurements of *Goniocladia cellulifera* in mm. N=18.

	NM	x	Mn	Mx	CVw	CVb
BW1	137	1.47	0.83	2.30	7.38	5.00
BW2	44	0.69	0.33	0.98	9.03	6.21
Z1	62	6.30	4	9	13.06	12.01
Z2	161	3.90	2	6	15.17	9.41
AD	180	0.12	0.10	0.20	11.73	10.28
AS	178	0.57	0.32	1.12	24.90	7.35
FL	7	4.91	3.69	6.56	21.30	-1
FW	7	3.40	2.56	4.40	17.89	-

Table 31 Differences in apertural spacing in longitudinal rows in *Goniocladia cellulifera* (in mm).

	Carinal ridge ----- >Median keel (barren surface) (obverse surface)						
	1	2	3	4	5	6	7
NM	13	13	13	12	12	10	5
Mn	0.73	0.52	0.43	0.42	0.39	0.33	0.47
Mx	1.12	1.04	1.00	1.02	1.00	0.73	0.75
x	0.86	0.71	0.64	0.61	0.59	0.55	0.53

DISCUSSION. *Goniocladia cellulifera* is quite common in the Lower Carboniferous of the British Isles, where it has been described from the Midland Valley of Scotland, Cumbria, Northumberland, and Yorkshire. It is very distinct with an unusual laterally flattened branch bearing a number of rows of autozoocial apertures and a sharp median ridge.

It was first described as *Carinella cellulifera* by Etheridge (1873a), but he later realised that that generic name was pre-occupied by a nemertean worm, and so proposed the name *Goniocladia* (Etheridge 1876). He suggested (Etheridge 1873a, 1873b), on the evidence of external features, that *Goniocladia* was an intermediate between *Polypora* M'Coy and *Fenestella* Lonsdale. While *Goniocladia* does possess a median keel (as in *Fenestella*) and has more than two rows of autozoocial apertures (as in *Polypora*), internally it resembles neither. In *Goniocladia* the zoarium is divided into two by a straight

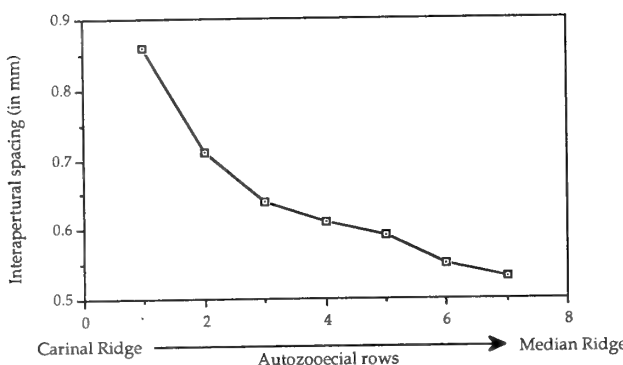


Fig. 103 *Goniocladia cellulifera* (Etheridge, 1873b). Graph of apertural spacing.

vertical median wall from which autozoocia are budded; *Fenestella* and *Polypora* have no such median wall. Autozoocia in these two genera are budded from a basal wall.

STRATIGRAPHICAL RANGE. Lower Carboniferous.

DISTRIBUTION. British Isles.

PALAEOECOLOGY OF THE COUNTY FERMANAGH BRYOZOAN FAUNA

The silicified Viséan fauna found towards the top of the Glencar Limestone has proved to be very diverse. It has been the subject of a number of research papers: the bryozoan element of the fauna has been systematically described by Bancroft & Wyse Jackson (1995), Olaloye (1974), Tavener-Smith (1965a, 1965b, 1971, 1973), Wyse Jackson (1988) and Wyse Jackson & Bancroft (1995a); the brachiopods by Brunton (1966a, 1966b, 1968, 1984); and the sponges by Reid (1970). These workers have recorded a large number of taxa (Tables 32 and 33). Other palaeontological work includes that of Gardiner & Mason (1974) who reported the occurrence of palaeoniscid fish from strata just overlying the Glencar Limestone, at a nearby locality west of Carrick Lough.

The fauna in County Fermanagh is essentially a bryozoan-brachiopod assemblage with rare taxa of other groups, such as trilobites, gastropods, bivalves, sponges and corals. This community is similar to that developed on the slopes of Asbian reefs of the Cracoe area, Yorkshire (Mundy 1978). Brunton (1987) tabulated the diverse and abundant fauna from Carrick Lough and Sillees River (Table 33). The number of bryozoan species described has been increased in this paper, and Bryozoa are now the largest element (numerically by species) in the community. The bryozoan fauna is dominated by fenestellids, which in turn are dominated by fenestellids. However, the delicate cryptostomes are also quite common (Table 32).

During this study one blastoid species and one ostracod species not recorded by Brunton (1987) have been found. Three specimens of the blastoid *Monoschizoblastus rofei* (TCD.9605), common in Asbian strata (Waters & Sevastopulo 1984a, 1984b), and one specimen of the ostracod *Polytylites* (TCD.9606) complete with both left and right valves were found.

Table 32 List of bryozoans from the Lower Carboniferous (Viséan, Asbian) of Carrick Lough and Sillees River (Bancroft & Wyse Jackson 1995; Olaloye 1974; Tavener-Smith 1965a, 1965b, 1971, 1973; Wyse Jackson 1988 and herein; Wyse Jackson & Bancroft 1995a).

Order CRYPTOSTOMATA (9)*

- **Hexites paradoxus* sp. nov.
- **Nematopora hibernica* sp. nov.
- **Pseudonematopora planatus* sp. nov.
- **Rhabdomeson progracile* Wyse Jackson & Bancroft
- **R. rhombiferum* (Phillips)
- **Rhombopora cylindrica* sp. nov.
- **R. hexagona* sp. nov.
- **Streblotrypa pectinata* Owen
- **Claustrotrypa ramosa* (Owen) comb. nov.

Order TREPOSTOMATA (7)

- **Leioclema indentata* sp. nov.
- **Dyscritella miliaria* (Nicholson)
- **Tabulipora urii* (Fleming)
- **T. howsii* (Nicholson)
- **T. minima* Lee
- **Stenophragmidium* sp.
- †*Nodular trepostome*

Order CYSTOPORATA (4)

- **Fistulipora incrassans* (Phillips)
- **Goniocladia cellulifera* (Etheridge, jun.)
- **Goniocladia* sp.
- **Sulcoretepora parallela* (Phillips)

Order FENESTRATA (49)

- **Baculopora megastoma* (M'Coy)
- **Diploporella marginalis* Young & Young
- **D. tenella* Wyse Jackson
- **Ichthyorachis newenhami* M'Coy
- **Thamniscus colei* Wyse Jackson
- **Rhombocladia dichotoma* (M'Coy) comb. nov.
- Penniretepora pluma* (Phillips)
- P. gracilis* (M'Coy)
- P. frondiformis* Olaloye
- P. normalis* Olaloye
- P. cucullea* Olaloye
- P. cf. flexicarinata* Young & Young
- P. sinuosa* (Hall)
- P. elegantula* (Etheridge, jun.)
- P. rotunda* Olaloye
- P. tortuosa* Olaloye
- Fenestella frutex* M'Coy
- F. ivanovi* Shulga-Nesterenko
- F. multispinosa* Ulrich
- F. modesta* Ulrich
- F. hemispherica* M'Coy
- F. parallela* Hall
- F. rufis* Ulrich *multinodososa* Tavener-Smith
- F. plebeia* M'Coy
- F. cf. arthritica* (Phillips)
- F. praemagna* Shulga-Nesterenko
- F. fanata* Whidborne *carrickensis* Tavener-Smith
- F. cf. spinacrisata* Moore
- F. cf. funicula* Ulrich
- F. cf. filistriata* Ulrich
- F. subspeciosa* Shulga-Nesterenko
- F. pseudovirgosa* Nikiforova
- F. cf. albida* Hall
- F. oblongata* Koenig
- F. cf. delicatula* Ulrich
- F. polyporata* (Phillips)
- F. irregularis* Nekhoroshev
- Hemitrypa hibernica* M'Coy
- Levifrenestella undecimalis* Shulga-Nesterenko
- Miniya plummerae* (Moore)
- M. binodata* (Condra)
- M. oculata* (M'Coy)
- Polypora dendroides* M'Coy
- P. verrucosa* M'Coy
- P. stenostoma* Tavener-Smith
- Ptilofenestella carrickensis* Tavener-Smith
- Ptiloporella varicosa* (M'Coy)
- Ptyloporella pluma* M'Coy *parva* Tavener-Smith
- Septopora hibernica* Tavener-Smith

* Described in this study; † to be described elsewhere.

Table 33 Abundance and diversity of the fauna at Carrick Lough and Sillees River.

Element	Number of genera*	Number of species*
Bryozoans	30	69
Brachiopods	47	56
Arthropods		
Trilobites	6	7
Ostracods	1	1
Echinoderms		
Crinoids	2+	2+
Blastoids	1	1
Molluscs		
Gastropods	4	4/5
Bivalves	2	?2
Sponges	?	?10
Corals	3	?4
Annelids	1	1

*Modified from Brunton (1987)

Although the fauna from County Fermanagh is very well-known, its palaeoecology has been a matter of some debate. The succession at Carrick Lough consists of thin alternating beds of dark argillaceous muddy limestones and paler grey to yellowish bioclastic limestones, while at Sillees River the fauna was etched from biomicritic limestones. The lithology of the bryozoan-bearing strata is that of a distal reef or off-reef deeper water facies.

Extensive reef development occurred in the Asbian of north west Ireland (George *et al.* 1976); one such reef lay just south of the

collecting localities which are in proximal reef or off-reef facies (Tavener-Smith 1973).

Bryozoans favour clean sediment-free water in which suitable substrates are available (Schopf 1969, Cuffey 1970). The depositional environment at Carrick Lough and Sillees River did not favour extensive bryozoan colonisation because the water was too muddy, as was the substrate. *Fistulipora incrassata* and *Tabulipora howsii* colonised substrates such as brachiopod shells, spines and other bryozoans. They developed small button-like zoaria, which were size-controlled because the adjacent muddy sediment could not be extensively encrusted by bryozoans. Similar evidence for the soft nature of the substrate is suggested by brachiopod attachment styles. The 56 brachiopod species discussed by Brunton (1987) are more or less equally divided into those that are pedicle supported, quasi-infaunal, and spine supported. Only 3 species were found to be permanently cemented, probably to other brachiopod shells. It is suggested that bryozoans found permanent points of attachment to small shelly substrates from which erect or adnate colonies developed, and that they were not attached directly to any lithic substrate.

Bryozoans are abundant at Carrick Lough and Sillees River, and calcified, decalcified and silicified zoaria have been obtained. Silicification seems to have occurred in the pale limestones and not in the argillaceous and muddy limestones. It is impossible to quantify the abundance of bryozoan colonies in pure numerical values. This is due to the very fragmented nature of the zoaria. Almost without exception all colonies are broken or disarticulated but not heavily abraded nor shredded into fine hash. Bryozoan colonies are found lying on bedding planes and are stacked one upon another.

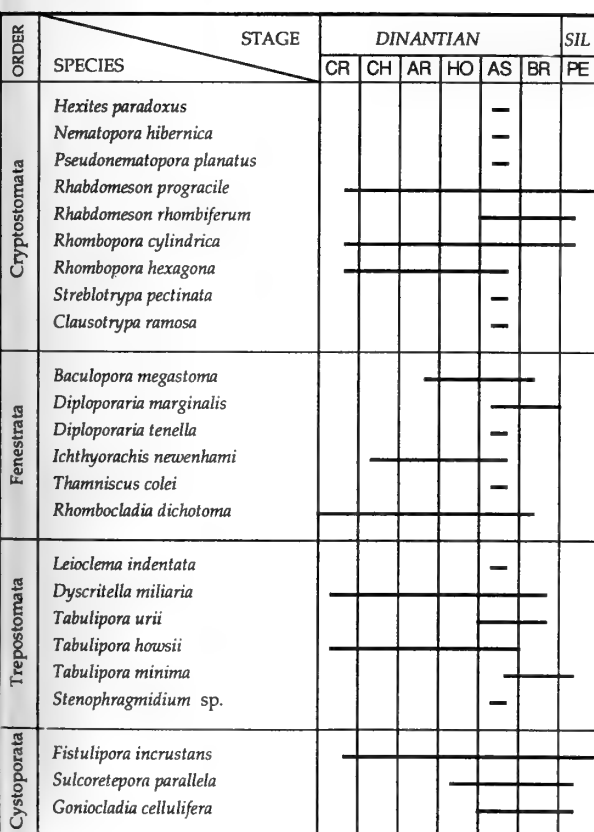
The fauna comprised bryozoans of four of the five stenolaemate orders (cyclostomes were absent), with a numerical and taxonomic weighting towards the fenestellates. The cryptostome taxa all formed small delicate erect expansions and were quite abundant. In contrast, while the trepostomes are taxonomically moderately diverse they occurred in small numbers. The cystoporates which comprised three taxa were reasonably abundant.

The bryozoan community was dominated by large erect planar and conical fenestrate zoaria, which exploited the seawater up to 20 cm above the substrate. Between *Fenestella* s.l. zoaria grew the smaller fenestellids such as *Baculopora*, *Diploporella*, *Ichthyorachis*, *Penniretepora* and *Thamniscus*, as well as the delicate cryptostomes, two *Tabulipora* species and the cystoporates *Sulcoretepora* and *Goniocladia*. Colonising the sea floor were *Rhombocladia*, *Tabulipora*, *Stenophragmidium* and *Fistulipora*. In addition *Stenophragmidium* grew epiphytically on a soft cylindrically shaped substrate (possibly algae), and *Tabulipora* and *Fistulipora* encrusted brachiopod spines and crinoid ossicles.

Few holdfasts were recovered from this fauna, which is in keeping with other fenestrate-rich faunas (F.K. McKinney pers. comm.). Of those that were found, the majority belong to the cystoporates *Goniocladia cellulifera* and *Sulcoretepora parallela*, with a single holdfast of *Thamniscus colei* being present in the sample.

The attitude and prevalence of fenestellid fronds on bedding planes, the limited abrasion, and lack of holdfasts indicates that the fauna has been translocated. This movement has taken place downslope off reef slopes into deeper water. However, the movement distance cannot have been great as fragments display little abrasion of fine surface skeletal detail, such as carinal nodes and the superstructure of *Hemimyrsina hibernica*.

If, as Brunton (1987) postulates, the Carrick Lough and Sillees River fauna is an *in situ* assemblage then bryozoans preserved in growth position would be expected. As outlined above they are not thus preserved. Tavener-Smith (1973) considers that the Carrick Lough fauna is an accumulated assemblage, that is it has not been



Abbreviations: SIL: Silesian; CR: Courceyan; CH: Chadian; AR: Arundian; HO: Holkerian; AS: Asbian; BR: Brigantian; PE: Pendleian.

Fig. 104 Range chart of bryozoans described in this study.

fossilized *in situ*. From the sedimentological and bryozoan evidence this latter interpretation is preferred. However, the possibility that the fauna represents an *in situ* brachipod community into which bryozoans have been washed from adjacent reef slopes cannot be excluded.

COMPARISON WITH OTHER ASBIAN FAUNAS.

Asbian faunas in the British Isles have received little attention, and many species recorded from County Fermanagh have not been recorded elsewhere. Bancroft (1984) and Wyse Jackson, Bancroft & Somerville (1991) document the faunas of several sites in Britain:

Ashfell Road Cutting, Cumbria [1 cryptostome species / 7-8 fenestrate species / several trepostome species / 2 cystoporate species].

Odin Fissure, Treak Cliff, Derbyshire [1/8/1/1].

Penruddock, Cumbria [1/12/several/2].

Redesdale, Northumberland [1/11/3/1].

Nant-y-Gamar, near Great Ormes Head, north Wales [1/3/5/1].

This fauna is somewhat unusual as it is trepostome-dominated.

Carrick Lough and Sillees River, County Fermanagh [9/49/7/4].

These faunas are generally dominated by fenestrates and fenestellids in particular, with taxa of other bryozoan orders, particularly cryptostomes, being conspicuous by their scarcity or apparent absence. This may be due to poor preservation, which makes identification of delicate cryptostome species difficult.

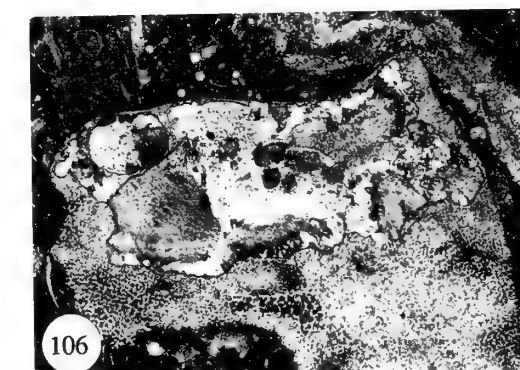
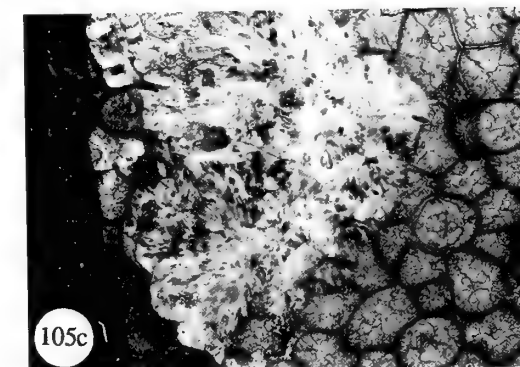
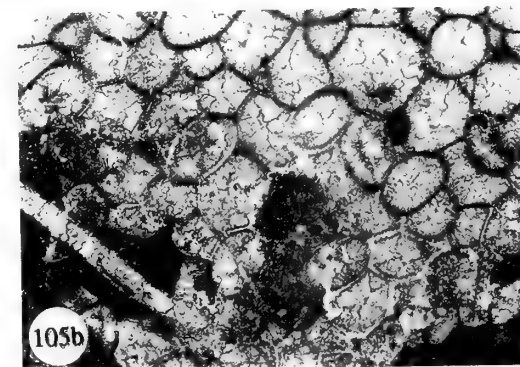
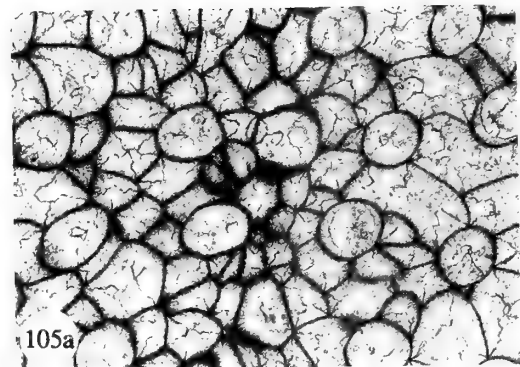
The fauna in County Fermanagh encompasses all species reported from the above localities with the exception of five: *Fenestella matheri*, *Septopora cestriensis*, *Batostomella* sp., an undescribed species of *Leioclema*, and *Stenodiscus tumida*. *Fenestella plebeia* is common to all six localities; *Fistulipora incrustans* and *Hemitrypa hibernica* occur in five while *Fenestella bicellulata* occurs in three.

The importance of the Fermanagh fauna lies in its rich taxonomic diversity and reasonable fossil preservation which will allow for future comparison with other Asbian faunas. Such investigations may reveal that the British and Irish faunas are more diverse than hitherto appreciated.

PATTERNS OF BRYOZOAN ZOARIA REPLACEMENT BY SILICA

Replacement of calcified bryozoan zoaria by silica has allowed for easy extraction from their carbonate matrix by acid digestion. The large number of specimens obtained in this way allows for detailed

Figs 105, 106 Patterns of silica replacement in bryozoan zoaria from the upper part of the Glencar Limestone (Viséan, Asbian), Carrick Lough, County Fermanagh, as illustrated by examples of *Fistulipora incrustans* colonies: **105**, BMNH PD9740; **105a**, euhedral and sub-hedral microquartz replacement of calcite autozoocelial skeletal structure, producing a thin exterior rim that is usually fuzzy in appearance; megaquartz crystals infill the autozoocelial chambers, $\times 25$; **105b**, grading of euhedral and sub-hedral microquartz rim into spherulitic chalcedony which replaces the remainder of the skeleton (Pattern 2), $\times 25$; **105c**, total replacement of skeletal walls and autozoocelial chamber megaquartz infill by pervasive chalcedony and obliteration of original skeletal structure, $\times 25$; **106**, BMNH PD9741, replacement of crinoid ossicle stereom by radial spherulitic chalcedony; typical Pattern 2 to 3 replacement, $\times 25$.



quantitative taxonomic, ontogenetic and palaeoecological studies. However, it has been argued that the silicification process is selective and does not necessarily preserve all elements of a fauna (Whittington & Evitt 1954), and secondly, that preservation is poor and only retains the external features of the skeleton (Cooper & Grant 1972–1975, Tavener-Smith 1973, Taylor & Curry 1985).

Both calcified and silicified bryozoan fragments are found at Carrick Lough and Sillees River, and comparison of both fractions indicates that more taxa are represented silicified than calcified. This probably reflects the ease by which silicified specimens are retrieved. Some authors report excellent preservation by silica of invertebrate skeletal microstructure (Brunton 1976, Holdaway & Clayton 1982), and of plant vessels (Stein 1982), while Schmitt & Boyd (1981) noted that relict ultrastructure is commonly observed in megaquartz crystals. There is no doubt that the process of silicification can produce both excellent and poor preservation. Schmitt & Boyd (1981) noted that the quality of preservation is related to the timing of replacement: poor preservation is due to delayed replacement, whereas excellently preserved fine detail is produced by immediate replacement of the calcite skeleton by silica. They sub-divided silica patterns into five major types, of which patterns 1 to 4 represent delayed replacement and pattern 5 immediate replacement.

A number of randomly orientated thin sections were cut from silicified blocks collected from Carrick Lough. In general bryozoan autozoocelial chambers are infilled with megaquartz, whereas the skeleton is replaced by a mixture of spherulitic chalcedony which is radial in appearance, tiny sub-hedral to euhedral microquartz crystals (<20µm), and occasionally some megaquartz.

Silicification may occur in discrete steps, which will produce different silica styles. Initially the calcite bryozoan zoarium is quite faithfully replaced by euhedral and sub-hedral microquartz crystals, producing a thin exterior rim that is usually fuzzy in appearance (Fig. 105a). As the intensity of silicification increases autozoocelial and vesicular chamber walls are totally replaced by spherulitic chalcedony (Pattern 2 of Schmitt & Boyd 1981) (Fig. 105b). Finally, chalcedony pervades both the walls and the megaquartz crystals that infilled autozoocelial chambers obliterating all original skeletal structure (Fig. 105c). Overgrowing this ubiquitous chalcedony are found small rhombic dolomite crystals. In some zoaria silicification has not been totally pervasive. Where this occurs the outer laminated skeleton (eg. in *Fenestella* s.l.) is replaced, with the inner granular tissue left unaltered.

These silica patterns indicate that replacement of the bryozoan colonies in County Fermanagh was delayed. In many cases replacement is incomplete: colonies may be lightly silicified on their outer surfaces and not silicified internally, or else portions of branches may be silicified and others not. In these situations colonies are very delicate and easily fragmented. Rarely are zoaria completely silicified. However, where this has occurred, considerable skeletal detail is retained, which allows for reasonable taxonomic determinations and morphological descriptions. In these cases the silica style is that of Pattern 2.

there are a large number of species in a genus (as with *Fenestella* s.l.) the latter has been used. In some cases several routes through the key will lead to the same taxon. No attempt has been made to designate the various *Fenestella* species to the genera erected by Morozova (1974).

The key to *Fenestella* s.l. species and other fenestrate taxa is based on the findings of Bancroft (1984), Olaloye (1974), and Tavener-Smith (1965a, 1965b, 1971, 1973). No attempt has been made to check their taxonomic determinations.

Key

- 1 Autozoocelia developed on obverse surface only, tripartite skeleton developed 2
Autozoocelia developed throughout zoarium 26
- 2 Zoaria reticulate 3
Zoaria small pinnate or non-pinnate expansions 12
Zoaria basket or cup-shaped 25
- 3 2 rows of autozoocelia on branches 4
More than two rows of autozoocelia developed 11
- 4 Branches all the same size 5
Branches of two sizes: a few primary and many secondary
Ptiloporella varicosa
- 5 Median carina present 6
Median carina absent
Levifrenestella undecimalis
- 6 Obverse surface protected by a honeycomb-like superstructure
Hemitrypa hibernica
Obverse surface not covered by a superstructure 7
- 7 Carinal nodes arranged in a straight line *Fenestella* s.l. (go to Table 34)
Carinal nodes in two offset zigzag rows 8
- 8 Fenestrules quadrate, hourglass-shaped, serving four autozoocelial apertures 9
Fenestrules elongate, serving 8 autozoocelial apertures 10
- 9 Peristomes large, median carina well developed, reverse surface often nodulose
Minilya plummerae
Peristomes slight, median carina weak, reverse surface smooth to marginally striated
Minilya nodulosa
- 10 Branch margins slightly indented by autozoocelial apertures, median carina weak, one carinal node situated at branch/dissepiment junction
Minilya binodata
Branch margins straight, median carina moderate, arrangement of carinal nodes somewhat irregular
Minilya oculata
- 11 3 rows of autozoocelia, keyhole-shaped apertures
Polypora stenostomata
4–5 rows of autozoocelia, oval apertures, fenestrules oval 2.50mm long
Polypora dendroides
4 rows of autozoocelia, peristomes around apertures, fenestrules elongate 3.30–4.70mm long
Polypora verrucosa
- 12 Zoarium pinnate 13
Zoarium non-pinnate 21
- 13 Lateral branches lack dissepiments 14
Lateral branches connected with dissepiments
Ptyloporella pluma parva
Lateral branches coalesce
Septopora hibernica
- 14 2 rows of autozoocelia on branches 15
More than two rows of autozoocelia
Ichthyorachis newenhami
- 15 1 autozoocelial aperture between lateral branches 16
2 autozoocelial apertures between lateral branches 18
>5 autozoocelial apertures between lateral branches
Penniretepora tortuosa

KEY TO THE IDENTIFICATION OF SOME LOWER CARBONIFEROUS BRYOZOA

In total 29 genera, containing 68 species have been described from the Viséan of County Fermanagh. This key is an aid to their identification. It has been necessary to construct the key in two styles: a multi-element dichotomous-trichotomous portion and a tabular portion. Where possible taxa are keyed out in the former, but where

- 16 Lateral branches straight 17
 Lateral branches sinuous (margins broken by protruding autozoocelial apertures) *Penniretepora gracilis*
- 17 Median carina strong, straight *Penniretepora frondiformis*
 Median carina weak, straight *Penniretepora normalis*
 Median carina consists of 3 sinuous pustulose ridges *Penniretepora flexicarinata*
- 18 Main stem straight 19
 Main stem sinuous *Penniretepora elegantula*
- 19 Lateral branches straight 20
 Lateral branches sinuous *Penniretepora cucullea*
- 20 Peristomes, horseshoe-shaped, developed on distal side of autozoocelial apertures *Penniretepora pluma*
 Peristomes absent *Penniretepora sinuosa*
- 21 2 rows of autozoocelia on branches 22
 More than two rows of autozoocelia on branches 23
- 22 Lateral margins of branches serrated *Diplopatoria marginalis*
 Lateral margins flexuous or smooth *Diplopatoria tenella*
- 23 Branches delicate, flexuous, oval/circular apertures
 *Baculopora megastoma*
 Branches robust, apertures with peristomes 24
- 24 Complete peristomes surround apertures *Thamniscus colei*
 Proximal peristomes only *Thamniscus rankin*
- 25 Branches connected by dissepiments *Ptilofenestella carrickensis*
 Branches bear no dissepiments *Thamniscus colei*
- 26 Zoaria ramosae or encrusting, with polymorphic zoocelia, distinct endozonal and exozonal differentiation 27
 Zoaria possess cystopores 32
 Zoaria dendroid with zoocelia budded from central axis 34
- 27 Mesozoocelia developed 28
 Exilazooecia developed 29
- 28 Zoaria ramosae with thick exozone and autozoocelia heavily indented by acanthostyles *Leioclema indentata*
- 29 Exilazooecia common with many disposed between autozoocelia
 *Dyscritella miliaria*
 Exilazooecia relatively rare 30
- 30 Ring septa developed 31
 Hemiphragma developed *Stenophragmidium* sp
- 31 Zoaria ramosae, autozoocelial apertures circular, ring septa tips slightly thickened, deflected proximally, exilazooecia in clusters *Tabulipora urii*
- Zoaria thin adnate sheets, autozoocelial apertures polygonal, ring septa planar/thin, exilazooecia rare *Tabulipora howsii*
 Zoaria robust, exozone thin, autozoocelial apertures oval, exilazooecia rare *Tabulipora minima*
- 32 Zoaria encrusting, adnate, with well developed rectangular (vesicles) cystopores between tubular autozoocelia *Fistulipora crustans*
 Branches bifoliate with spherical cystopores 33
- 33 Branches strap-like, zoaria budded from a plicated median wall, autozoocelial apertures with proximal lunaria
 *Sulcoretepora parallela*
 Branches sub-rounded, with a distinct keel and carina, autozoocelia budded from a straight median wall *Goniocladia cellulifera*
- 34 Branches articulated, very slender (01–25mm), circular or polygonal in cross-section, hemisepta absent 35
 Branches not articulated, cylindrical (05–60mm), hemisepta usually present in pairs 37
- 35 Autozoocelial apertures present on all branch surfaces 36
 Autozoocelial apertures absent from a distinct reverse surface
 *Nematopora hibernica*
- 36 Branch cross-section polygonal, autozoocelia budded in annular fashion, autozoocelial apertures oval, separated from each other by longitudinal ridges *Hexites paradoxus*
 Branch cross-section circular, autozoocelial budding radial, autozoocelial apertures circular, with proximal peristomes
 *Pseudonematopora planatus*
- 37 Metapores very common, arranged in linear rows in interapertural areas *Streblotrypa pectinata*
 Metapores irregularly disposed in interapertural areas
 *Clausotrypa ramosa*
 Metapores either absent or only 1 per autozoocium 38
- 38 Central axial cylinder present 39
 Axial cylinder not present 40
- 39 Autozoocelial apertures oval, of constant dimensions, with a large acanthostyle situated proximally, smaller styles may be present
 *Rhabdomeson progracile*
 Autozoocelial apertures pyriform, distally flared, of varying dimensions, over 20 small styles developed around apertures
 *Rhabdomeson rhombiferum*
- 40 Autozoocelial apertures circular, of constant size, with acanthostyles and heterostyles disposed in a circle around them, a single metapore may be situated proximal to autozoocelia *Rhombopora cylindrica*
 Autozoocelial apertures circular to oval, of varying size around zoarium with heterostyles arranged in a hexagonal pattern
 *Rhombopora hexagona*

Table 34 Tabular key for the identification of *Fenestella* species from the Viséan of County Fermanagh and from other localities in the British Isles [* = not recorded from Carrick Lough by Tavener-Smith (1973)].

CHARACTER SPECIES \	1	2	3	4	5	6	7	8	9	10	11	12	13	14	15	16	17	18
<i>Fenestella bicellulata</i> *	A	A	A	A	A	B	A	F	A	A	A	C	A	A	C	B	B	D
<i>Fenestella ivanovi</i>	A	B	A	A	B	A	A	C	B	A	A	C	B	A	C	B	A	A
<i>Fenestella frutex</i>	A	B	A	F	B	A	A	B	B	A	A	A	A	A	C	A	B	A
<i>Fenestella multispinosa</i>	A	B	A	A	B	B	A	E	C	A	A	C	B	A	C	A	B	A
<i>Fenestella tuberculo-carinata</i> *	A	B	B	A	B	B	A	G	A	A	A	B	A	C	D	B	A	A
<i>Fenestella plebeia</i>	A	C	B	C	B	A	A	B	A	A	A	A	B	A	D	B	B	A
<i>Fenestella papilliata</i> *	A	C	B	G	C	B	A	G	C	A	?	C	A	C	C	B	A	B
<i>Fenestella morrisii</i> *	A	C	?	E	?	B	C	A	A	A	?	?	?	?	?	A	B	?
<i>Fenestella polyporata</i>	B	D	D	I	D	B	A	F	A	A	A	C	C	A	C	A	B	C
<i>Fenestella quadridecimalis</i> *	B	E	D	I	C	B	B	G	C	A	C	B	D	A	A	B	B	B
<i>Fenestella modesta</i>	A	B	B	B	B	A	A	B	C	A	C	D	A	A	C	B	B	A
<i>Fenestella hemispherica</i>	A	B	B	B	B	B	?	F	A	A	B	C	D	B	B	B	A	B
<i>Fenestella parallela</i>	A	B	B	B	B	B	?	B	C	B	C	D	B	D	A	A	B	A
<i>Fenestella rufis multinodosa</i>	A	B	B	B	B	B	A	G	A	B	C	D	E	A	D	B	A	A
<i>Fenestella cf. arthritica</i>	C	C	C	C	C	B	A	F	A	A	A	A	C	C	C	B	B	B
<i>Fenestella praemagna</i>	C	C	B	H	C	B	B	F	C	A	A	A	C	C	C	B	A	B
<i>Fenesiella fanata carrickensis</i>	A	C	C	B	C	B	A	G	A	C	C	C	C	B	B	A	A	B
<i>Fenestella cf. spinacrista</i>	A	C	C	G	B	B	A	B	A	A	A	C	B	A	C	B	B	B
<i>Fenestella cf. filistrata</i>	D	C	C	D	B	B	A	G	C	C	C	D	E	A	C	A	A	A
<i>Fenestella cf. funicula</i>	A	C	C	C	C	B	A	E	A	A	A	A	C	A	D	B	B	A
<i>Fenestella subspeciosa</i>	B	C	B	G	C	B	B	E	C	B	B	C	E	B	D	B	B	A
<i>Fenestella cf. albida</i>	B	C	C	D	C	B	B	F	B	A	A	D	E	C	C	B	A	B
<i>Fenestella oblongata</i>	B	D	C	E	C	B	A	B	A	C	C	A	D	A	B	B	B	D
<i>Fenestella cf. deliculata</i>	A	D	C	E	B	B	A	E	A	A	A	D	C	A	D	B	A	B
<i>Fenestella irregularis</i>	B	E	D	I	C	B	A	B	A	B	C	C	E	C	C	B	B	A
<i>Fenestella pseudovirgosa</i>	B	C	D	H	C	B	A	F	A	A	A	A	D	A	A	B	B	C

Explanation of characters used in Table 34:

- Branch shape:
A, Straight; B, Sinuous; C, Irregular; D, Partly straight partly sinuous
- Fenestrule length:
A, < 0.5 mm; B, 0.5–1.0 mm; C, 1.0–2.0 mm; D, 2.0–3.0 mm; E, > 3.0 mm
- Fenestrule width:
A, < 0.5 mm; B, 0.5–0.75 mm; C, 0.75–1.0 mm; D, > 1.0 mm
- Number of autozoococial apertures per fenestrule:
A, 2; B, 3; C, 4; D, 5; E, 5–8; F, 2–3; G, 3–4; H, 4–5; I, > 8
- Interapertural distance:
A, < 0.2 mm; B, 0.2–0.3 mm; C, > 0.3 mm
- Zooecial aperture/branch/dissepiment relationship:
A, Aperture occurs at branch/dissepiment junction; B, Apertures situated anywhere along branch length

- Zoarial appearance:
A, Rigid; B, Lax; C, High angle cone
- Fenestrule shape:
A, Square; B, Rectangular; C, Hour-glass; E, Various; F, Elongate-rectangular; G, Elongate-oval
- Fenestrule edges:
A, Straight; B, Indented (by peristomes), C, Slightly undulating
- Carina:
A, Distinct; B, Indistinct; C, Absent
- Inclination of branch sides from carina:
A, Steep; B, moderate; C, Gentle
- Carinal nodes:
A, Large; B, Moderate; C, Small; D, Poorly developed
- Spacing of carinal nodes:
A. Regular – close < 0.25 mm; B, Regular – moderate 0.25–0.50 mm;

- C, Regular – wide 0.50 – 1.00 mm; D, Regular – very wide > 1.00 mm;
E, Irregular
14. Dissepiment depression on obverse surface:
A, Well; B, Moderate; C, Slight; D, None (flush with branch surface – indicative of *Fenestella parallela*)
 15. Dissepiment depression on reverse surface:
A, Well; B, Moderate; C, Slight; D, None (flush with branch surface)
 16. Incipient 3rd row of zooecial chambers developed before bifurcation:
A, Present; B, Absent
 17. Extra zooecial chamber in angle of bifurcation:
A, Present; B, Absent
 18. Rib(s) on dissepiment obverse surface:
A, Present; B, Absent; C, Present (extending to meet carina); D, Occasionally present

ACKNOWLEDGEMENTS. I thank Professor C.H. Holland and Dr George Sevastopulo who supervised the Ph.D. study of which this formed a part. This paper benefitted considerably from a review by Dr F.K. McKinney for which I thank him. I am grateful for the advice of Drs A.J. Bancroft, P.D. Taylor, I.P. Morozova, F.K. McKinney, C.J. Buttler, and all the other bryozoologists who sent me copies of their work. A.J. Bancroft is thanked for permission to examine and figure some of his material from the Upper Carboniferous of Yorkshire. Mr Bill Baird (National Museums of Scotland), Mr Gaynor Boon (Sheffield City Museum), Mr Philip Doughty, Mr John Wilson and Dr Andrew Jeram (Ulster Museum), Mr Stephen Howe and Mr Tom Sharpe (National Museum of Wales), Dr H.C. Ivimey Cook (formerly of the British Geological Survey), Mr Nigel Monaghan (National Museum of Ireland), Dr John Nudds (Manchester Museum), the late Dr David Price (Sedgwick Museum), Dr Ian Rolfe and Dr Neil Clark (Hunterian Museum), Dr Paul Taylor (Natural History Museum, London) and Dr Nigel Trewin (Aberdeen University) all kindly lent material in their care. I am grateful for the help of Mr Jeremy Smith and Dr Phillip Tubbs of the I.C.Z.N. and the late Professor David Webb (TCD) in answering some of my nomenclatural questions. I thank Garry and Bassia Bannister of Dublin who translated some Russian and Ukrainian texts for me at very short notice and in a very short time, also Ide ní Thuama (Royal Irish Academy) and Dr John Moore who located some Soviet and Australian papers for me. This work was carried out while in receipt of grants from Trinity Trust (Dublin) and the Irish Geological Association which are gratefully acknowledged. I am particularly grateful to Paul Taylor for his long-standing encouragement, and I thank my wife Vanessa and my family, especially my brother Michael, for their tolerance and support.

REFERENCES

- Anderson, J.G.C. & Lamont, A.** 1935. The geology of the Glasgow district from its quarries. *Quarry Managers' Journal*, **18**: 212–17, 277–82.
- Anstey, R.L.** 1981. Zoid orientation structures and water flow patterns in Paleozoic bryozoan colonies. *Lethaia*, **14**: 287–302.
- Armstrong, J., Young, J. & Robertson, D.** 1876. Catalogue of the Western Scottish Fossils. Blackie & Son, Glasgow. xxiii + 164pp.
- Astrova, G.G.** 1964. A new order of Paleozoic Bryozoa. *Paleontologicheskii Zhurnal*, **2**: 22–31.
- 1965. The morphology, evolution, and system of the Ordovician and Silurian Bryozoa. *Trudy Paleontologicheskogo Instituta*, **106**: 1–431.
- 1978. The History of Development, System, and Phylogeny of the Bryozoa. Order Trepostomata. *Trudy Paleontologicheskogo Instituta*, **169**: 1–240.
- & Morozova, I.P. 1956. Systematics of Bryozoa of the order Cryptostomata. *Doklady Akademii Nauk SSSR*, (n.s.) **110**: 661–664.
- Balakin, G.V.** 1974. *Pseudonematopora*, a new Early Carboniferous bryozoan genus. *Palaeontologicheskii Zhurnal*, **4**: 130–132. [Translation: *Paleontological Journal*, **8**: 557–559].
- Bancroft, A.J.** 1984. *Studies in Carboniferous Bryozoa*. Unpublished Ph.D. thesis, University of Durham.
- 1985. The Carboniferous fenestrate bryozoan *Ptylopora pluma* M'Coy. *Irish Journal of Earth Sciences*, **7**: 35–45.
- 1986a. The Carboniferous cystoporate bryozoan *Eridopora macrostoma* Ulrich from the north of England. *Proceedings of the Yorkshire Geological Society*, **46**: 23–28.
- 1986b. The Carboniferous fenestrate bryozoan *Hemitrypa hibernica* M'Coy. *Irish Journal of Earth Sciences*, **7**: 111–124.
- 1987. Biostratigraphical Potential of Carboniferous Bryozoa. *Courier Forschungsinstitut Senckenberg*, **98**: 193–97.
- , Somerville, I.D. & Strank, A.R.E. 1988. A bryozoan buildup from the Lower Carboniferous of North Wales. *Lethaia*, **21**: 51–65.
- & Wyse Jackson, P.N. 1995. Revision of the Carboniferous cystoporate bryozoan *Fistulipora incrassata* (Phillips, 1836) with remarks on the type species of *Fistulipora* M'Coy, 1849. *Geological Journal*, **30**: 129–143.
- Bassler, R.S.** 1929. The Permian Bryozoa of Timor. *Paläontologie von Timor*, **16** (28): 36–89.
- 1952. Taxonomic Notes on genera of fossil and recent Bryozoa. *Journal of the Washington Academy of Science*, **42**: 381–85.
- 1953. Bryozoa. In, Moore, R.C. (ed.) *Treatise on Invertebrate Paleontology*, part G. Geological Society of America and University of Kansas Press. xiii + 253pp.
- Benton, M.J.** 1979. H.A. Nicholson (1844–1899), invertebrate palaeontologist: bibliography and catalogue of his type and figured material. *Royal Scottish Museum Information Series, Geology*, **7**: vii + 94pp. Edinburgh.
- & Trewin, N.H. 1978. H.A. Nicholson Catalogue of type and figured material in the Palaeontological Collections, University of Aberdeen, with notes on the H.A. Nicholson Collection. *Publications of the Department of Geology and Mineralogy Aberdeen*, **2**: 1–28.
- Bigey, F.** 1973. Devonian Bryozoa from the Southeastern Armorican Massif, Western France. In, Larwood, G.P. (ed.), *Living and Fossil Bryozoa*: 375–383. Academic Press, London.
- Billing, I.** 1991. Bryozoan growth on brachiopod spines in the Carboniferous of England. In, Bigey, F.P. (ed.), *Bryozoaires actuels et fossiles: Bryozoa living and fossil*. *Bulletin de la Société des Sciences Naturelles de l'Ouest de la France, Mémoire*, (HS) **1**: 39–47.
- Blake, D.B.** 1983. Systematic Descriptions for the Suborder Rhabdomesina. In, Robison, R.A. (ed.), *Treatise on Invertebrate Paleontology*; (Part G), *Bryozoa – Revised*, **1**: 550–592.
- & Snyder, E.M. 1987. Phenetic and cladistic analysis of the Rhabdomesina (Bryozoa) and similar taxa: A Preliminary Study. In, Ross, J.R.P. (ed.), *Bryozoa: Present and Past*: 33–40. Western Washington University.
- Boardman, R.S.** 1960. Trepostomatus Bryozoa of the Hamilton Group of New York State. *United States Geological Survey Professional Paper*, **340**: iv + 87pp.
- Borg, F.** 1926. Studies on Recent cyclostomatous Bryozoa. *Zoologiska Bidrag från Uppsala*, **10**: 181–507.
- Brunton, C.H.C.** 1966a. Silicified productids from the Viséan of County Fermanagh. *Bulletin of the British Museum (Natural History), Geology*, **12**: 173–243.
- 1966b. Predation and shell damage in a Viséan brachiopod fauna. *Palaeontology*, **9**: 355–359.
- 1968. Silicified brachiopods from the Viséan of County Fermanagh (II). *Bulletin of the British Museum (Natural History), Geology*, **16**: 1–70.
- 1976. Micro-ornamentation of some spiriferide brachiopods. *Palaeontology*, **19**: 767–71.
- 1984. Silicified brachiopods from the Viséan of County Fermanagh, Ireland (III). Rhynchonellids, spiriferids and terebratulids. *Bulletin of the British Museum (Natural History), Geology*, **38**: 27–130.
- 1987. The palaeoecology of brachiopods, and other faunas, of Lower Carboniferous (Asbian) limestones in west Fermanagh. *Irish Journal of Earth Sciences*, **8**: 97–112.
- & Mason, T.H. 1979. Palaeoenvironments and correlations of the Carboniferous rocks in west Fermanagh. *Bulletin of the British Museum (Natural History), Geology*, **32**: 91–108.
- Campbell, K.S.W.** 1961. Carboniferous fossils from the Kutting rocks of New South Wales. *Palaeontology*, **4**: 428–474.
- Ceretti, E.** 1963. Bizioi Carboniferi della Carnia. *Giornale di Geologia*, **30**: 255–340.
- 1964. Su Alcuni Bizioi Criptostomi delle Alpi Carniche. *Giornale di Geologia*, **32**: 175–193.
- Cooper, G.R. & Grant, R.E.** 1972–1975. Permian Brachiopods of West Texas. Parts I–III. *Smithsonian Contributions to Paleobiology*, **14**: 1–231 (1972); **15**: 233–79 (1974); **19**: 795–1921 (1975).
- Crockford, J.** 1944. Bryozoa from the Permian of Western Australia. *Proceedings of the Linnean Society of New South Wales*, **69**: 139–175.
- 1947. Bryozoa from the Lower Carboniferous of New South Wales and Queensland. *Proceedings of the Linnean Society of New South Wales*, **72**: 1–48.
- Cuffey, R.J.** 1967. Bryozoan *Tabulipora carbonaria* in the Wreford Megacyclothem (Lower Permian) of Kansas. *Kansas University Paleontological Contributions Bryozoa – Article 1*: 1–96.
- 1970. Bryozoan-environment interrelationships – An overview of bryozoan paleoecology and ecology. *Earth and Mineral Sciences*, **39**: 41–45, 48.
- 1973. An improved classification, based upon numerical-taxonomic analyses, for the higher taxa of entoproct and ectoproct bryozoans. In, Larwood, G. P. (editor) *Living and Fossil Bryozoa*: 549–564. Academic Press, London.

- Dresser, A.M. 1960. *The Polyzoa of the Lower Carboniferous of Hook Head, County Wexford and Malahide, County Dublin*. Unpublished University of Dublin M.Sc. thesis.
- Dunaeva, N.N. 1961. Upper Carboniferous Bryozoans of the West Donets Basin *Izdatie Akademii Nauk Ukrainskoj SSR*: 1–142.
- 1974. Bryozoans of the C₁e zone of the Donbass Region. *Sbornik Vykopnoi fauny ta flora Ukrainskoj*, **2**: 80–97.
- & Morozova, I.P. 1967. Evolutionary features and systematics of some late Paleozoic Trepustomata. *Paleontogicheskii Zhurnal*, 1967: 86–94.
- Duncan, H. 1949. Paleontology – Genotypes of some Paleozoic Bryozoa. *Journal of the Washington Academy of Sciences*, **39**: 122–136.
- Ehrenberg, C.J. 1831. *Symbolae physicae, seu icones et descriptiones mammalium, avium, insectorum et animalium evertebratorum ... Pars Zoologica. 4. Animalia evertebrata exclusis insectis. Decus Primula*, Berlin.
- Eichwald, C.E. 1860. *Letharia Rossica, ou Paléontologie de la Russie: ancienne période*, **1**: 355–518. E. Schweizerbart (Stuttgart).
- Elias, M.K. 1964. Stratigraphy and Paleoecology of some Carboniferous Bryozoans. *Compte Rendu Cinquième Congrès International de Stratigraphie et de Géologie du Carbonifère*, **1**: 375–381.
- & Condra, G.E. 1957. *Fenestella* from the Permian of West Texas. *Geological Society of America Memoir*, **70**: 1–158.
- Etheridge, R. jun. 1873a. Description of *Carinella*, a New Genus of Carboniferous Polyzoa. *Geological Magazine*, **10**: 433–434.
- 1873b. Explanation of sheet 23 – Lanarkshire central. *Memoirs of the Geological Survey Scotland*: 101–103.
- 1876. Carboniferous and Post-Tertiary Polyzoa. *Geological Magazine*, (2) **3**: 522–523.
- 1891. A monograph of the Carboniferous and Permo-Carboniferous invertebrates of New South Wales, Part 1, Coelenterata. *New South Wales Geological Survey Memoirs Palaeontology*, **5**: 1–65.
- Farmer, J.D. & Rowell, A.J. 1973. Variation in the bryozoan *Fistulipora decora* (Moore and Dudley) from the Beil Limestone of Kansas. In, Boardman, R.S., Cheetham, A.H. & Oliver, W.A. (eds.), *Animal Colonies*: 377–394. Dowden, Hutchinson and Ross, Stroudsburg.
- Fleming, J. 1828. *A History of British Animals*. Bell and Bradfute, Edinburgh. xxiii + 565pp.
- Foerste, A.F. 1887. Flint Range Bryozoa. *Bulletin Scientific Laboratories Denison University*, **11**: 71–88.
- Fritz, M.A. 1932. Permian Bryozoa from Vancouver Island. *Transactions of the Royal Society of Canada*, (3) **26**: 93–109.
- Gardiner, B.G. & Mason, T.B. 1974. On the occurrence of the palaeoniscid fish *Eloichthys serratus* in the Viséan of Fermanagh, with a note on the Enniskillen and Egerton collections. *Proceedings of the Royal Irish Academy*, **73B**: 31–36.
- Gautier, T.G. 1970. Interpretive morphology and taxonomy of the bryozoan genus *Tabulipora*. *University of Kansas Paleontological Contributions*, **48**: 1–21.
- George, T.N., Johnson, G.A.L., Mitchell, M., Prentice, J.E., Ramsbottom, W.H.C., Sevastopulo, G.D. & Wilson, R.B. 1976. A correlation of the Dinantian rocks in the British Isles. *Geological Society of London, Special Report*, **7**: 87.
- Girty, G.H. 1908. The Guadalupian fauna. *Professional Paper United States Geological Survey*, **58**: 1–624.
- 1911. New genera and species of Carboniferous fossils from the Fayetteville shale of Arkansas. *New York Academy of Science Annals*, **20**: 189–238.
- Gorjunova, R.V. 1985. The morphology, classification and phylogeny of the bryozoans (Order Rhabdomesida). *Akademii Nauk CCCP*, **208**: 152.
- 1988. New Carboniferous bryozoans of the Gobi Altai. *Trudy Sovmestnaya Sovetski-Mongol'skaya Paleontogicheskaya Ekspeditsiya*, **33**: 10–29.
- Graham, D.K. 1975. A review of Scottish Carboniferous acanthocladiid Bryozoa. *Bulletin of the Geological Survey Great Britain*, **49**: 1–21.
- Griffith, R. 1862. Localities of Irish Carboniferous Fossils. In, M'Coy, F., *A Synopsis of the Characters of the Carboniferous Limestone Fossils of Ireland*; 2nd Edition: 209–271. Williams & Norgate, London.
- Hageman, S.J. 1993. Effects of non-normality on studies of morphologic variation of a rhabdomesine bryozoan, *Streblytropa prisca* (Gabb & Horn). *The University of Kansas Paleontological Contributions*, (NS) **4**: 13.
- Hall, J. 1858. *Geological Survey of Iowa – Paleontology*: 651–653.
- 1874. Descriptions of Bryozoa and Corals of the Lower Helderberg Group. *New York State Museum Natural History 26th Annual Report*, 93–115.
- 1876. The fauna of the Niagara group in central Indiana. *New York State Museum Natural History 28th Annual Report*: 1–32.
- Harlton, B.H. 1933. Micropaleontology of the Pennsylvanian Johns Valley Shale of the Ouachita Mountains, Oklahoma, and its relationship to the Mississippian Caney Shale. *Journal of Paleontology*, **7**: 3–29.
- Hoernes, R. 1886. *Manuel de Paléontologie*. Savy, Paris. xvi + 741pp.
- Holdaway, H.K. & Clayton, C.J. 1982. Preservation of shell microstructure in silicified brachiopods from the Upper Cretaceous Wilmington Sands of Devon. *Geological Magazine*, **119**: 371–382.
- Huffman, S.F. 1970. The Ectoproct (Bryozoan) *Rhomnopora lepidodendroides* Meek, Late Pennsylvanian (Virgilian), Nebraska. *Journal of Paleontology*, **44**: 673–679.
- Jukes, J.B. 1857. *The Student's Manual of Geology*. A. & C. Black, Edinburgh. 607pp.
- King, W. 1849. On some families and genera of corals. *Annals and Magazine of Natural History*, **2**: 338–90.
- 1850. The Permian fossils of England. *Monographs of the Palaeontographical Society of London*. 258pp.
- Kora, M. & Jux, U. 1986. On the early Carboniferous macrofauna from the Um Bogma Formation, Sinai. *Neues Jahrbuch Geologie Paläontologie*, **1986**: 85–98.
- Krutchinina, O.N. 1986. *Clausotrypa clara* sp. nov. In, Morozova, I.P. & Krutchinina, O.N., *Permian Bryozoa of the Arctic region: western sector*. Akademii Nauk CCCP, 'Nauka', Moscow. 143pp.
- Lavrentjeva, V.D. 1979. Phylloporinina, a new suborder of Paleozoic Bryozoa. *Paleontogicheskii Zhurnal*, **1979** (1): 59–68. [Translation: *Paleontological Journal*, **13**: 56–64.]
- 1985. Bryozoan Suborder Phylloporinina. *Akademii Nauk CCCP*, **214**: 1–101.
- Lee, G.W. 1912. The British Carboniferous Trepustomata. *Memoirs of the Geological Survey of Great Britain: Palaeontology*, **1**: 135–195.
- Lu Linhuang 1989. Bryozoans from Chouiniugou Formation of late Early Carboniferous on the northern slope of Mt. Qilian. *Palaeontologia Cathayana*, **4**: 327–433.
- M'Coy, F. 1844. *A Synopsis of the Characters of the Carboniferous Limestone Fossils of Ireland*. Dublin University Press. 207pp.
- 1849. On some new genera and species of Palaeozoic Corals and Foraminifera. *Annals and Magazine of Natural History*, (2) **3**: 119–136.
- 1851a–1855a. *A systematic description of the British Palaeozoic fossils in the Geological Museum of the University of Cambridge*. In, Sedgwick, A. & M'Coy, F., *A Synopsis of the Classification of the British Palaeozoic Rocks*. J.W. Parker, London. 611pp. [pp. 1–184, 1851; pp. 185–406, 1852; pp. 407–611, 1855.]
- 1854b. *Contributions to British Palaeontology*. Macmillan, Cambridge. viii + 272pp.
- 1862. *A Synopsis of the Characters of the Carboniferous Limestone Fossils of Ireland*. (2nd ed.) Williams and Norgate, London. viii + 274pp.
- McFarlan, A.C. 1942. Chester Bryozoa of Illinois and western Kentucky. *Journal of Paleontology*, **16**: 437–458.
- McKinney, F.K. 1972. Nonfenestrate Ectoprocta (Bryozoa) of the Bangor Limestone (Chester) of Alabama. *Bulletin of the Geological Survey of Alabama*, **98**: 1–144.
- 1973. Bibliography and Catalogue (1900–1969) of the Trepustomata (Phylum Ectoprocta). *Southeastern Geology Special Publication*, **4**: 145pp.
- 1977. Autozoocial budding patterns in dendroid Paleozoic bryozoans. *Journal of Paleontology*, **51**: 303–329.
- Meek, F.B. 1872. Report on the paleontology of eastern Nebraska. In, Hayden, F.V., *Final Report of the United States Geological Survey of Nebraska and portions of the adjacent territories*: 81–239. U.S. Government Printing Office, Washington.
- Milne-Edwards, H. & Haime, J. 1850–1854. A Monograph of the British Fossil Corals. Parts 1–5. *Monographs of the Palaeontographical Society of London*. Ixxxi + 322pp. [Part 1, pp. i–lxxxv, 1–72, 1850; Part 2, pp. 72–146, 1851; Part 3, pp. 147–210, 1852; Part 4, pp. 211–244, 1853; Part 5, pp. 245–322, 1854.]
- Miller, T.G. 1961a. Type specimens of the genus *Fenestella* from the Carboniferous of Great Britain. *Palaeontology*, **4**: 221–242.
- 1961b. New Irish Tournaisian Fenestellids. *Geological Magazine*, **98**: 493–500.
- 1962a. North American species of *Fenestella* from the Carboniferous of Great Britain. *Journal of Paleontology*, **36**: 120–125.
- 1962b. On *Hemimyria hibernica* M'Coy. *Geological Magazine*, **99**: 313–321.
- 1963. The bryozoan genus *Polypora* M'Coy. *Palaeontology*, **6**: 161–171.
- Moore, R.C. 1929. A Bryozoan Faunule from the Upper Graham Formation, Pennsylvania, of North Central Texas. *Journal of Paleontology*, **3**: 1–27, 121–156.
- Morozova, I.P. 1955. Carboniferous Bryozoans of the Don Moyen (central) region. *Trudy paleontologicheskogo Instituta*, **58**: 1–98.
- 1970. Late Permian Bryozoa. *Akademii Nauk SSSR*, **122**: 314pp.
- 1974. Revision of the bryozoan genus *Fenestella*. *Paleontogicheskii Zhurnal*, **1974** (2): 54–67. [Translation: *Paleontological Journal*, **8**: 167–180.]
- 1981. Carboniferous Bryozoa of North Eastern USSR. *Akademii Nauk SSSR*, **188**: 1–119.
- Morris, J. 1843. *A Catalogue of British Fossils comprising all the Genera and Species hitherto described; with references to their geological distribution and to the localities in which they have been found*. John Van Voorst, London. x + 222pp.
- 1854. *A Catalogue of British Fossils*. Published privately for the author. London. 372pp.
- Morrison, S.J. & Anstey, R.L. 1979. Ultrastructure and composition of brown bodies in some Ordovician trepostome bryozoans. *Journal of Paleontology*, **53**: 943–949.
- Mundy, D.J.C. 1978. Lower and middle Asbian reef slopes. In, McKerrow, W.S. *The ecology of fossils: an illustrated guide*: 184–193. Gerald Duckworth, London.
- Munro, M. 1912. Description of some new forms of Trepostomatous Bryozoa from the Lower Carboniferous Rocks of the North-Western Province. *Quarterly Journal of the Geological Society of London*, **68**: 574–579.
- Nekhoroshev, V.P. 1926. Early Carboniferous Bryozoa from the Kuznets Basin. *Izvestiya Geologicheskogo komiteta*, **43**: 1237–1290.
- 1956. Lower Carboniferous Bryozoa of the Altai and Siberia. *Trudy Vsesojuzny Nauchno-Issledovatel'skoy Geologorazvedochnoy Institut*, **13**: 1–419.
- Newton, G.B. 1971. Rhabdomesid bryozoans of the Wreford Megacyclothem

- (Wolfcampian, Permian) of Nebraska, Kansas and Oklahoma. *Kansas University Paleontological Contributions*, **56**: 1–71.
- Nicholson, H.A.** 1881. *On the Structure and Affinities of the Genus Monticulipora and its sub-genera with critical descriptions of illustrative species*. Blackwood, Edinburgh and London. 240pp.
- 1883. Contributions to micro-palaeontology – On *Stenopora Howsii* Nich., with notes on *Monticulipora? tumida* Phill., and remarks on *Tabulipora Urii* Young. *Annals and Magazine of Natural History*, **12**: 285–297.
- & Etheridge, R. jun. 1886. On the Tasmanian and Australian species of the genus *Stenopora*, Lonsdale. *Annals and Magazine of Natural History*, (5) **17**: 173–187.
- & Lydekker, R. 1889. *A Manual of Palaeontology for the use of Students*. 3rd Edition. Blackwood, Edinburgh and London. 1624pp.
- Nickles, J.M. & Bassler, R.S.** 1900. A Synopsis of American Fossil Bryozoa including bibliography and synonymy. *United States Geological Survey Bulletin* **173**: 1–663.
- Nikiforova, A.I.** 1927. Materials for the understanding of Lower Carboniferous Bryozoa of the Donets Basin. *Izvestija Geologiceskogo komiteta*, **46**: 245–268.
- 1948. Lower Carboniferous Bryozoa of Karatau. Nizhnekamennogol'nye mshanki Karatau. *Akademii Nauk Kazahskoj CCP, Alma Ata*. 53pp.
- Olaloye, F.** 1974. Some *Penniretepora* (Bryozoa) from the Viséan of County Fermanagh with a revision of the generic name. *Proceedings of the Royal Irish Academy*, **74B**: 471–506.
- Orbigny, A. d'** 1849. Description de quelques genres nouveaux de Mollusques Bryozoaires. *Revue et Magasin de Zoologie*, (2) **1**: 499–504.
- 1850–1852. *Prodrome de paléontologie stratigraphique, universelle des animaux mollusques et rayonnés*. Masson, Paris. xxxxpp.
- Owen, D.E.** 1962. Ludlovian Bryozoa from the Ludlow district. *Palaeontology*, **5**: 195–212.
- 1966. New Carboniferous Polyzoa from Derbyshire. *Geological Journal*, **5**: 135–148.
- 1969. Lower Carboniferous Bryozoa from Scotland. *Geological Journal*, **6**: 257–266.
- 1973. Carboniferous Bryozoa from County Tyrone. *Geological Journal*, **8**: 297–306.
- Phillips, J.** 1836. *Illustrations of the geology of Yorkshire. Part 2: The Mountain Limestone District*. John Murray, London. xx + 253pp.
- 1841. Figures and description of the Palaeozoic fossils of Cornwall, Devon, and West Somerset. Longman, Brown, Green, & Longmans. xx + 231pp.
- Reid, R.E.H.** 1970. Tetracons and demosponge phylogeny. *Symposium Zoological Society London*, **5**: 63–89.
- Rogers, A.F.** 1900. New Bryozoa from the Coal Measures of Kansas and Missouri. *Kansas University Quarterly*, **9**: 1–12.
- Romanchuk, T.V.** 1970. *Clausotrypa petaloidea* sp. nov. In, Morozova, I.P., Late Permian Bryozoa. *Akademii Nauk SSSR*, **122**: 158.
- 1981. New Permian trepostomida, rhabdomesida of the Khabarovsk region. *Paleonticheskii Zhurnal*, **1981**: 53–64. [Translation: *Paleontological Journal*, **15**: 53–66].
- Rondeau, E.** 1890. Etude sur le terrain dévonien aux environs d'Angers. *Mémoires Societie Naturale Agricultural Science Arts Angers*, **4**: 155–191.
- Sabattini, N.** 1972. Los Fenestellidae, Acanthocladidae y Rhabdomesidae (Bryozoa, Cryptostomata) del Paleozoico Superior de San Juan y Chubut, Argentina. Universidad Nacional de la Plata. *Revista del Museo de la Plata*, (NS) **6**, *Paleontologia*, **42**: 257–377.
- Sakagami, S.** 1961. Japanese Permian Bryozoa. *Palaeontological Society of Japan Special Paper*, **7**: 1–58.
- 1962. Lower Carboniferous Bryozoa from the Hikoroichi Series, Japan. *Transactions and Proceedings of the Palaeontological Society of Japan*, (NS) **46**: 227–242.
- 1964. Bryozoa of Akiyoshi. Part 2. Lower Carboniferous Bryozoa from the Uzura Quarry. *Transactions and Proceedings of the Palaeontological Society of Japan*, (NS) **56**: 295–308.
- 1972. Carboniferous Bryozoa from Bukit Charas, near Kuantan, Pahang, Malaya. In, Kobayashi, T. & Toriyama, R. (eds.), *Geology and Palaeontology of Southeast Asia*, **10**: 35–62.
- Schlotheim, E.F. von** 1820. *Die Petrefactenkunde auf ihrem jetzigen Standpunkte durch die Beschreibung seiner Sammlung versteinelter und fossiler Überreste des Thier- und Pflanzenreichs der Vorwelt erläutert von E.F. von Schlotheim*. Part 1. Gotha.
- Schmitt, J.G. & Boyd, D.W.** 1981. Patterns of silicification in Permian pelecypods and brachiopods. *Journal of Sedimentary Petrology*, **51**: 1297–1308.
- Schopf, T.J.M.** 1969. Paleoecology of Ectoprocts (Bryozoans). *Journal of Paleontology*, **43**: 234–244.
- Shulga-Nesterenko, M.I.** 1955. Carboniferous bryozoans of the Russian Platform. *Akademii Nauk CCCP*, **57**: 1–207.
- Simpson, G.B.** 1895. A Handbook of the Genera of North American Paleozoic Bryozoa; with an introduction upon the structure of living species. *New York State Geology 14th Annual Report*: 403–669.
- Smyth, L.B.** 1922. On some new species from the Lower Carboniferous of Ballycastle, County Antrim. *Geological Magazine*, **59**: 21–24.
- 1925. A contribution to the geology of Great Orme's Head. *Proceedings of the Royal Irish Academy*, **18**: 141–164.
- Stein, C.L.** 1982. Silica recrystallization in petrified wood. *Journal of Sedimentary Petrology*, **52**: 1277–1282.
- Tavener-Smith, R.** 1965a. A new fenestellid bryozoan from the Lower Carboniferous of County Fermanagh. *Palaeontology*, **8**: 478–491.
- 1965b. A revision of *Retepora nodulosa* Phillips, 1836. *Geological Magazine*, **102**: 135–142.
- 1966. Ovicells in fenestrate cryptostomes of Viséan age. *Journal of Paleontology*, **40**: 190–198.
- 1971. *Polypora stenostoma*: a Carboniferous bryozoan with cheilostomatous features. *Palaeontology*, **14**: 178–187.
- 1973. Fenestrate bryozoa from the Viséan of County Fermanagh, Ireland. *Bulletin of the British Museum (Natural History)*, *Geology*, **23**: 389–493.
- 1981. The neotype of *Retepora nodulosa* Phillips, 1836. *Geological Magazine*, **118**: 565.
- Taylor, P.D. & Curry, G.B.** 1985. The earliest known fenestrate bryozoan, with a short review of Lower Ordovician Bryozoa. *Palaeontology*, **28**: 147–158.
- Termier, G. & Termier, H.** 1950. Paleontologie Marocaine, II. Invertébrés de L'ère Primaire, pt. 2, Bryozaires et Brachiopodes. *Maroc Service Géologie Notes et Mémoires*, **77**: 1–253.
- & — 1971. Bryozaires du Paléozoïque supérieur de l'Afghanistan. *Documents des laboratoires de Géologie de la faculté des sciences de Lyon*, **47**: 1–52.
- Trizna, V.B.** 1958. Early Carboniferous bryozoans of the Kuznetsk Basin. *Trudy Vsesojuzny nauchno-Issledovatel'skij geologo-razvedochny Instituta*, **122**: 1–436.
- 1962. Carboniferous bryozoans. In, Khalpin, L.L., *Paleozoic biostratigraphy of Sayano-Altaiskoi*. *Trudy Sibiran nauchno-Issledovatel'skij geologo-geofiziki Mineralnogo Syr'ya*, **21**: 55–61, 124–143.
- Ulrich, E.O.** 1882. American Paleozoic Bryozoa. *Journal of the Cincinnati Society of Natural History*, **5**: 121–175.
- 1884. American Paleozoic Bryozoa (continued). *Journal of the Cincinnati Society of Natural History*, **7**: 24–51.
- 1888a. On *Sceptropora* a new genus of Bryozoa, with remarks on *Helopora Hall*, and other genera of that type. *American Geology*, **1**: 228–234.
- 1888b. A list of the Bryozoa of the Waverly Group in Ohio; with descriptions of new species. *Bulletin Scientific Laboratories Denison University*, **4**: 63–96.
- 1890. Paleozoic Bryozoa. *Bulletin of the Geological Survey of Illinois*, **8**: 283–688.
- Utgård, J.** 1983. Paleobiology and Taxonomy of the Order Cystoporata. In, Robison, R.A. (ed.), *Treatise on Invertebrate Paleontology. (Part G) Bryozoa – Revised 1*: 327–439. Geological Society of America and University of Kansas Press.
- Vine, G.R.** 1877. Chapters on Carboniferous Polyzoa. *Hardwicke's Science Gossip* **13**: 108–110, 152–156, 220–222, 271–274.
- 1880a. A Review of the Family Diastoporidae for the purpose of Classification. *Quarterly Journal of the Geological Society of London*, **36**: 356–361.
- 1880b. Report of the Committee appointed for the purpose of reporting on the Carboniferous Polyzoa. *Report of the British Association for the Advancement of Science 1880*: 76–87.
- 1880c. On the Carboniferous Polyzoa. *Geological Magazine*, (2) **7**: 501–512.
- 1881. Notes on the Carboniferous Polyzoa of North Yorkshire. *Proceedings of the Yorkshire Geological and Polytechnic Society*, **7**: 329–341.
- 1883. Notes on the Carboniferous Polyzoa of West Yorkshire and Derbyshire – (an attempt to identify Phillip's species). *Proceedings of the Yorkshire Geological and Polytechnic Society*, **8**: 161–174.
- 1884a. Fourth report of the committee, consisting of Dr. H.C. Sorby and Mr. G.R. Vine, appointed for the purpose of reporting on fossil Bryozoa. *Report of the British Association for the Advancement of Science (Southport, 1883)*: 161–209.
- 1884b. Further notes on new species, and other Yorkshire Carboniferous Polyzoa described by Prof. John Phillips. *Proceedings of the Yorkshire Geological and Polytechnic Society*, **8**: 377–393.
- 1884c. Micro-palaearontology of the Northern Carboniferous shales. III, The Ostracoda, Monticulipora, and Miscellaneous Forms: Redesdale Shales, Northumbrian berland. *The Naturalist*, (NS) **10** (113): 97–103.
- 1885. Notes on the Yoredale Polyzoa of North Lancashire. *Proceedings of the Yorkshire Geological and Polytechnic Society*, **9**: 70–98.
- 1887. Notes on the Polyzoa and other organisms from the Gayton Boring Northamptonshire. *Journal of the Northamptonshire Natural History Society and Field Club*, **4**: 255–266.
- 1888. A Monograph of Yorkshire Carboniferous and Permian Polyzoa. Part 1. *Proceedings of the Yorkshire Geological and Polytechnic Society*, **11**: 68–85.
- 1889. A Monograph of Yorkshire Carboniferous and Permian Polyzoa. Part 2. *Proceedings of the Yorkshire Geological and Polytechnic Society*, **11**: 184–200.
- Waagen, W. & Pichl, J.** 1885. Salt Range Fossils. *Palaeontologica Indica*, Series 1, **1**: 771–834.
- & Wentzel, J. 1886. Salt Range Fossils. *Palaeontologica Indica*, Series 13, **835**: 924.
- Warner, D.J. & Cuffey, R.J.** 1973. Fistuliporacean bryozoans of the Wreford Megacyclothem (Lower Permian) of Kansas. *University Kansas Paleontological Contributions*, **65**: 1–24.
- Waters, J.A. & Sevastopulo, G.D.** 1984a. The paleobiogeography of Irish and British

- Lower Carboniferous blastoids. In, Keegan, B.F. & O'Connor, B.D.S. (eds.), *Echinodermata*: 141–147. Balkema, Rotterdam.
- & — 1984b. The stratigraphical distribution and palaeoecology of Irish Lower Carboniferous blastoids. *Irish Journal of Earth Sciences*, **6**: 137–154.
- Whittington, H.B. & Evitt, W.R.** 1954. Silicified Middle Ordovician trilobites. *Geological Society of America Memoir*, **59**: 1–137.
- Wilson, R.B.** 1961. Palaeontology of the Archerbeck borehole, Canonbie, Dumfries-shire. *Bulletin of the Geological Survey of Great Britain*, **18**: 90–106.
- Wright, W.B., Carruthers, R.G., Lee, G.W. & Thomas, I.** 1913. On the Lower Carboniferous succession at Bundoran in South Donegal. *Proceedings of the Geologists' Association*, **24**: 70–77.
- Wyse Jackson, P.N.** 1988. New fenestrate Bryozoa from the Lower Carboniferous of County Fermanagh. *Irish Journal of Earth Sciences*, **9**: 197–208.
- , **Bancroft, A.J. & Somerville, I.D.** 1991. Bryozoan zonation in a trepostome-dominated buildup from the Lower Carboniferous of North Wales. In, Bigey, F.P. (ed.), *Bryozoaires actuels et fossiles: Bryozoa living and fossil*. *Bulletin de la Société des Sciences Naturelles de l'Ouest de la France: Mémoire*, (HS) **1**: 551–559.
- & — 1995a. Generic revision of the cryptostome bryozoan *Rhabdomeson* Young & Young, 1874 with descriptions of two species from the Lower Carboniferous of the British Isles. *Journal of Paleontology*, **69**: 28–45.
- & — 1995b. *Rhabdomeson* Young & Young, 1874 (Bryozoa): proposed designation of *Rhabdomeson progracile* Wyse Jackson & Bancroft, 1995 as the type species. *Bulletin of Zoological Nomenclature*.
- Yang Jingzhi & Lu Linhuang** 1962. Palaeozoic Bryozoa of Mt. Qilianshan. *Memoirs of the Geology of Mt. Qilianshan*, **4**: 1–114 [In Chinese].
- , **Hu Zhaoxuh & Xia Fengsheng** 1988. Bryozoans from Late Devonian and Early Carboniferous of Central Hunan. *Palaeontologica Sinica*, **173** (23): 1–197 [In Chinese and English].
- Young, J.** 1882. On the Identity of *Ceramopora (Berenicea) megastoma*, M'Coy, with *Fistulipora minor*, M'Coy. *Annals and Magazine of Natural History*, (5) **10**: 427–431.
- 1883a. On Ure's 'Millepore'. *Tabulipora (Cellepora) Urii*, Flem. *Annals and Magazine of Natural History*, (5) **12**: 154–158.
- 1883b. Notes on Ure's 'Millepore'. *Tabulipora Urii*, J. Young (*Cellepora Urii*, Flem.). *Transactions of the Geological Society of Glasgow*, **7**: 264–272.
- 1887. Note on a new family of the Polyzoa Cystodictyonidae (E.O. Ulrich) – with notice of three Carboniferous species. *Transactions of the Edinburgh Geological Society*, **5**: 461–466.
- & **Armstrong, J.** 1871. *On the Carboniferous fossils of the West of Scotland*. Glasgow, 103pp.
- & **Robertson, D.** 1877. Note on the Polyzoa of the Hairmyres Limestone Shale, East Kilbride. *Transactions of the Geological Society of Glasgow*, **5**: 173–175.
- Young, J. & Young, J.** 1874. On a new Genus of Carboniferous Polyzoa. *Annals and Magazine of Natural History*, (4) **13**: 335–339.
- & — 1875. New species of *Glauconome* from Carboniferous Limestone strata of the West of Scotland. *Proceedings of the Natural History Society of Glasgow*, **2**: 325–335.
- & — 1877. On a new species of *Sulcoretepora*. *Proceedings of the Natural History Society of Glasgow*, **3**: 166–168.
- Zittel, K.** 1880. *Handbuch der Paleontologie; Band 1, Bryozoa*: 573–641. München und Leipzig.

CORRIGENDA

Corrections to: Jones, R.W. & Simmons, M.D. 1996. A review of the stratigraphy of Eastern Paratethys (Oligocene-Holocene). *Bull. nat. Hist. Mus. Lond. (Geol.)* **52** (1): 25–49.

1. In Fig. 11 (p. 39) the density of the shading of the land and sea areas has been reversed, due to an error. The figure should show a large area of land (with dark shading) containing the two smaller areas of sea (with pale shading) that cover most of the present-day Black Sea and the southern part of the Caspian Sea.
2. In Figs 7, 8, 10–12 (pp. 34–41) some of the ticks are wrongly shown on the seaward (pale) side of the lines rather than the landward (dark) side.



Bulletin of The Natural History Museum Geology Series

Earlier Geology *Bulletins* are still in print. The following can be ordered from Intercept (address on inside front cover). Where the complete backlist is not shown, this may also be obtained from the same address.

Volume 42

- No. 1 Cenomanian and Lower Turonian Echinoderms from Wilmington, south-east Devon. A.B. SMith, C.R.C. Paul, A.S. Gale & S.K. Donovan. 1988. 244 pp. 80 figs. 50 pls. 0 565 07018 5. £46.50

Volume 43

- No. 1 A Global Analysis of the Ordovician-Silurian boundary. Edited by L.R.M. Cocks & R.B. Rickards. 1988. 394 pp., figs. 0 565 07020 7. £70.00

Volume 44

- No. 1 Miscellanea: Palaeocene wood from Mali—Chapelcorner fish bed—*Heterotheca* coprolites—Mesozoic Neuroptera and Raphidioptera. 1988. Pp. 1–63. 0 565 07021 5. £12.00

- No. 2 Cenomanian brachiopods from the Lower Chalk of Britain and northern Europe. E.F. Owen. 1988. Pp. 65–175. 0565 07022 3. £21.00

- No. 3 The ammonite zonal sequence and ammonite taxonomy in the *Douvilleiceras mammillatum* Superzone (Lower Albian) in Europe. H.G. Owen. 1988. Pp. 177–231. 0 565 07023 1. £10.30

- No. 4 Cassiopidae (Cretaceous Mesogastropoda): taxonomy and ecology. R.J. Cleevely & N.J. Morris. 1988. Pp. 233–291. 0565 07024 X. £11.00

Volume 45

- No. 1 Arenig trilobites—Devonian brachiopods—Triassic demosponges—Larval shells of Jurassic bivalves—Carboniferous marattialean fern—Classification of Plectambonitacea. 1989. Pp. 1–163. 0 565 07025 8. £40.00

- No. 2 A review of the Tertiary non-marine molluscan faunas of the Pebesian and other inland basins of north-western South America. C.P. Nuttall. 1990. Pp. 165–371. 456 figs. 0 565 07026 6. £52.00

Volume 46

- No. 1 Mid-Cretaceous Ammonites of Nigeria—new amphisbaenians from Kenya—English Wealden Equisetales—Faringdon Sponge Gravel Bryozoa. 1990. Pp. 1–152. 0 565 07027 4. £45.00

- No. 2 Carboniferous pteridosperm frond *Neuropteris heterophylla*—Tertiary Ostracoda from Tanzania. 1991. Pp. 153–270. 0565 07028 2. £30.00

Volume 47

- No. 1 Neogene crabs from Brunei, Sabah & Sarawak—New pseudosciurids from the English Late Eocene—Upper Palaeozoic Anomalodesmata Bivalvia. 1991. Pp. 1–100. 0 565 07029 0. £37.50

- No. 2 Mesozoic Chrysalidinidae of the Middle East—Bryozoans from north Wales—*Alveolinella paequovi* sp. nov. from Papua New Guinea. 1991. Pp. 101–175. 0 565 070304. £37.50

Volume 48

- No. 1 '*Placopsilina*' *cenomana* d'Orbigny from France and England—Revision of Middle Devonian uncinulid brachiopod—Cheilostome bryozoans from Upper Cretaceous Alberta. 1992. Pp. 1–24. £37.50

No. 2

- Lower Devonian fishes from Saudi Arabia—W.K. Parker's collection of foraminifera in the British Museum (Natural History). 1992. Pp. 25–43. £37.50

Volume 49

- No. 1 Barremian—Aptian Praehedbergellidae of the North Sea area: a reconnaissance—Late Llandovery and early Wenlock Stratigraphy and ecology in the Oslo Region, Norway—Catalogue of the type and figured specimens of fossil Asteroidea and Ophiuroidea in The Natural History Museum. 1993. Pp. 1–80. £37.50

No. 2

- Mobility and fixation of a variety of elements, in particular, during the metasomatic development of adinoles at Dinas Head, Cornwall—Productellid and Plicatiferid (Productoid) Brachiopods from the Lower Carboniferous of the Craven Reef Belt, North Yorkshire—The spores of *Leclercqia* and the dispersed spore morphon *Acinosporites lindlarensis* Riegel: a case of gradualistic evolution. 1993. Pp. 81–155. £37.50

Volume 50

- No. 1 Systematics of the meliceritid cyclostome bryozoans: introduction and the genera *Elea*, *Semielea* and *Reptomultelea*. 1994. Pp. 1–104.

No. 2

- The brachiopods of the Duncannon Group (Middle-Upper Ordovician) of southeast Ireland. 1994. Pp. 105–175.

Volume 51

- No. 1 A synopsis of neuropteroid foliage from the Carboniferous and Lower Permian of Europe—The Upper Cretaceous ammonite *Pseudaspidoceras* Hyatt, 1903, in north-eastern Nigeria—The pterodactyloids from the Purbeck Limestone Formation of Dorset. 1995. Pp. 1–88. £37.50

No. 2

- Palaeontology on the Qahlah and Simsima Formations (Cretaceous, Late Campanian-Maastrichtian) of the United Arab Emirates-Oman Border Region—Preface—Late Cretaceous carbonate platform faunas of the United Arab Emirates-Oman border region—Late Campanian-Maastrichtian echinoids from the United Arab Emirates-Oman border region—Maastrichtian ammonites from the United Arab Emirates-Oman border region—Maastrichtian nautiloids from the United Arab Emirates-Oman border region—Maastrichtian Inoceramidae from the United Arab Emirates-Oman border region—Late Campanian-Maastrichtian Bryozoa from the United Arab Emirates-Oman border region—Maastrichtian brachiopods from the United Arab Emirates-Oman border region—Late Campanian-Maastrichtian rudists from the United Arab Emirates-Oman border region. 1995. Pp. 89–305. £37.50

Volume 52

- No. 1 Zirconlite: a review of localities worldwide, and a compilation of its chemical compositions—A review of the stratigraphy of Eastern Paratethys (Oligocene-Holocene)—A new protorichthofenoid brachiopod (Productida) from the Upper Carboniferous of the Urals, Russia—The Upper Cretaceous ammonite *Vascoceras* Choffat, 1898 in north-eastern Nigeria. 1996. Pp. 1–89. £37.50

CONTENTS

- 91 Jurassic bryozoans from Baltów, Holy Cross Mountains, Poland
U. Hara and P.D. Taylor
- 103 A new deep-water spatangoid echinoid from the Cretaceous of British Columbia, Canada
A.B. Smith and A. McGugan
- 109 The cranial anatomy of *Rhomaleosaurus thorntoni* Andrews (Reptilia, Plesiosauria)
A.R.I. Cruickshank
- 115 The first known femur of *Hylaeosaurus armatus* and re-identification of ornithopod material
in The Natural History Museum, London
P.M. Barrett
- 119 Bryozoa from the Lower Carboniferous (Viséan) of County Fermanagh, Ireland
P.N. Wyse Jackson
- 173 Corrigenda

Bulletin of The Natural History Museum

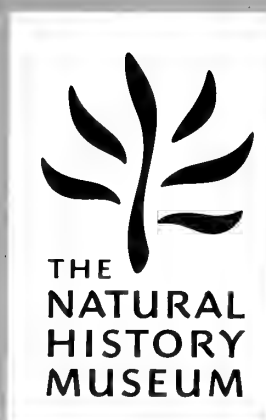
GEOLOGY SERIES

Vol. 52, No. 2, November 1996

Bulletin of The Natural History Museum

THE NATURAL
HISTORY MUSEUM
21 AUG 1997
PRESENTED
PALAEONTOLOGY LIBRARY

Geology Series



VOLUME 53 NUMBER 1 26 JUNE 1997

The *Bulletin* of The Natural History Museum (formerly: *Bulletin of the British Museum (Natural History)*), instituted in 1949, is issued in four scientific series, Botany, Entomology, Geology (incorporating Mineralogy) and Zoology.

The Geology Series is edited in the Museum's Department of Palaeontology

Keeper of Palaeontology: Dr L.R.M. Cocks

Editor of Bulletin: Dr M.K. Howarth

Assistant Editor: Mr C. Jones

Papers in the *Bulletin* are primarily the results of research carried out on the unique and ever-growing collections of the Museum, both by the scientific staff and by specialists from elsewhere who make use of the Museum's resources. Many of the papers are works of reference that will remain indispensable for years to come. All papers submitted for publication are subjected to external peer review for acceptance.

A volume contains about 160 pages, made up by two numbers, published in the Spring and Autumn. Subscriptions may be placed for one or more of the series on an annual basis. Individual numbers and back numbers can be purchased and a *Bulletin* catalogue, by series, is available. Orders and enquiries should be sent to:

Intercept Ltd.
P.O. Box 716
Andover
Hampshire SP10 1YG
Telephone: (01264) 334748
Fax: (01264) 334058

Claims for non-receipt of issues of the *Bulletin* will be met free of charge if received by the Publisher within 6 months for the UK, and 9 months for the rest of the world.

World List abbreviation: *Bull. nat. Hist. Mus. Lond.* (Geol.)

© The Natural History Museum, 1997

ISSN 0968-0462

The Natural History Museum
Cromwell Road
London SW7 5BD

Geology Series
Vol. 53, No. 1, pp. 1-78

Issued 26 June 1997

Typeset by Ann Buchan (Type setters), Middlesex
Printed in Great Britain by Henry Ling Ltd, at the Dorset Press, Dorchester, Dorset

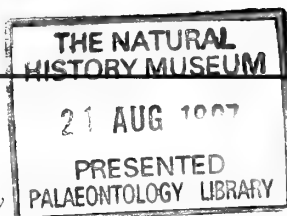
The status of '*Plesictis*' *croizeti*, '*Plesictis*' *gracilis* and '*Lutra*' *minor*: synonyms of the early Miocene viverrid *Herpestides antiquus* (Mammalia, Carnivora)

MIECZYSŁAW WOLSAN

Instytut Paleobiologii PAN, ul. Twarda 51/55, 00–818 Warszawa, Poland

MICHAEL MORLO

Forschungsinstitut Senckenberg, Senckenbergenallee 25, 60325 Frankfurt am Main, Germany



SYNOPSIS. The reputed musteloid carnivorans '*Plesictis*' *croizeti* Pomel, 1847, '*Plesictis*' *gracilis* Pomel, 1853, and '*Lutra*' *minor* Lydekker, 1885 are recognized as junior subjective synonyms of the European early Miocene (Agenian) viverrid carnivoran *Herpestides antiquus* (de Blainville, 1842). The name '*Plesictis*' *gracilis* is a junior objective synonym of '*Plesictis*' *croizeti*, whose type locality is identified as Langy, of Agenian age, central France. The type locality of '*Lutra*' *minor* is Mainz-Mombach, of Agenian age, western Germany. The taxonomic histories of '*Plesictis*' *croizeti*, '*Plesictis*' *gracilis*, and '*Lutra*' *minor* are reviewed, synonomies are provided, and the holotypes described and figured.

INTRODUCTION

The name-bearing types of the reputed musteloid carnivorans '*Plesictis*' *croizeti* Pomel, 1847, '*Plesictis*' *gracilis* Pomel, 1853, and '*Lutra*' *minor* Lydekker, 1885 constitute a part of the unique collections of The Natural History Museum, London. The specimens have not previously been adequately described, and only the holotype of '*Plesictis*' *croizeti* Pomel, 1847 has been figured. The taxonomic histories of the specific names given to them are highly confused.

The present paper provides comprehensive descriptions of the holotypes of '*Plesictis*' *croizeti*, '*Plesictis*' *gracilis*, and '*Lutra*' *minor*, and also reports the complicated taxonomic histories of these names, with evidence that they are all junior synonyms of the European early Miocene viverrid carnivoran *Herpestides antiquus* (de Blainville, 1842).

The following abbreviations are used in this paper: BMNH and NHM, Department of Palaeontology, The Natural History Museum formerly British Museum (Natural History), London; ICZN, International Code of Zoological Nomenclature (The International Commission on Zoological Nomenclature 1985); NMB, Natural History Museum, Basle; SMF, Department of Palaeozoology, The Senckenberg Research Institute and Museum, Frankfurt am Main.

PLESICTIS CROIZETI AND '*PLESICTIS*' *GRACILIS*

HISTORICAL STATUS. Pomel (1847) introduced the specific name '*Plesictis Croizeti*' to designate the partial mandible illustrated in fig. of his pl. 4. Although neither description nor definition accompanied that name, it has nevertheless been made available by indication in accordance with Article 12 (b, 7) of the ICZN. Pomel's fig. 4 of pl. 4, as well as its reproductions published in Bronn & Roemer (1856: I. 60, fig. 14b), Pictet (1857: pl. 4, fig. 8), and Viret (1929: text-fig. 3), represent the reversed mirror image of the original that is stored

in the NHM under register number 26702. As noted in the old vertebrate register at the NHM, this name-bearing type of '*Plesictis*' *croizeti* was purchased by the British Museum (Natural History) in June 1851 from 'M. Pomel' (M.J. Pomel according to Lydekker 1885: xiii).

In 1853 (reprinted in 1854) Pomel proposed the new name '*Plesictis gracilis*' for the partial mandible figured by him in 1847 under the name '*Plesictis Croizeti*', and he incorrectly applied the latter name to a skull of a mustelid carnivoran. Because both specific names were based on the same type specimen, they are objective synonyms according to Article 61 (c, iv) of the ICZN. The senior synonym, '*Plesictis*' *croizeti* Pomel, 1847, is the valid name of the taxon in accordance with the Principle of Priority (Article 23 of the ICZN).

The taxonomic status of '*Plesictis*' *croizeti* (= '*Plesictis*' *gracilis*) was further complicated by Filhol (1879a–b) who considered '*Plesictis*' *croizeti* and '*Plesictis*' *gracilis* to be distinct varieties of '*Plesictis robusta*' Pomel, 1853, which is indeed a synonym of the musteloid carnivoran '*Amphictis antiqua*' Pomel, 1853. Although the type specimen of both '*Plesictis*' *croizeti* and '*Plesictis*' *gracilis* had already been figured or briefly described in Pomel (1847, 1853, 1854), Gervais (1852b, 1859), Bronn (1856), Bronn & Roemer (1856) and Pictet (1857), and the British Museum had been explicitly indicated by Gervais (1852b, 1859) as the institution where the holotype had been kept, Filhol (1879a–b) was, nevertheless, apparently unaware of its existence. At any rate, he made no mention of this specimen. Instead, he assigned a mustelid skull to '*Plesictis*' *croizeti* and two musteloid partial mandibles to '*Plesictis*' *gracilis*, believing that the characters of one of those mandibles, illustrated in fig. 5 of his pl. 22, corresponded to those of the holotype of '*Plesictis*' *gracilis* (his p. 128: 'J'ai trouvé dans la collection du musée de Lyon un maxillaire inférieur possédant des caractères correspondants à ceux que M. Pomel avait fait connaître comme devant servir à faire distinguer spécifiquement le *Plesictis gracilis*'). In addition, in his quotations of Pomel's (1853, 1854) descriptions of '*Plesictis*' *croizeti* and '*Plesictis*' *lemanensis* Pomel, 1853, Filhol (1879a–b) mistakenly reversed the two descriptions, giving Pomel's

The mandibular foramen lies a little below the level of the alveolar border of the body, about 4.5 mm above the ventral border of the ramus and about 13 mm behind the alveolus for M_2 . The foramen faces posteriad and somewhat laterodorsad.

P_3 and P_4 are double-rooted, with the posterior root being larger than the anterior one. The base of the crown bears cingula anterobuccally and posteriorly on both teeth. The cingula are stronger on P_4 ; much of the posterior cingulum of P_3 has been broken away. The posterior cingulum of P_3 is much better developed than the anterior one, which was also true for P_3 , judging from the preserved base of its crown. The posterior cingular region of the base of the P_4 crown is little deflected lingual.

The crown base of both P_3 and P_4 bears three projections arranged one behind the other anteroposteriorly to form a blade compressed buccolingually. The blade slightly curves lingual on the most anterior of the projections, the anterior accessory cusp, in both the premolars and on the most posterior projection, the posterior accessory cusp, in P_4 . The middle cusp, the protoconid, culminates slightly anterior to the half of the tooth length and is distinctly largest, whereas the anterior accessory cusp is smallest. The anterior and posterior accessory cusps are stronger and larger relative to the protoconid on P_4 than they are on P_3 . The cusps are divided by prominent V-shaped notches on P_4 . In both teeth, the tips of the anterior and posterior accessory cusps are noticeably worn away exposing the dentine. Wear has also broken through the enamel at the tip of the protoconid on P_4 , but over a very small area only.

The crown of M_1 is supported by two strong roots. There is no cingulum on the talonid, but there are two cingula running along the buccal base of the trigonid from the anterior end of the paraconid to the most anterior portion of the protoconid buccally and to that of the metaconid lingually. The buccal cingulum is very strong, whereas the lingual one is poorly developed.

The trigonid is notably arched buccad, making its lingual contour concave when viewed occlusally. The carnassial blade comprises the buccal ridge of the paraconid and the anterior ridge of the protoconid, which are divided by a deep, slit-shaped carnassial notch. The carnassial blade is rather deeply worn exposing dentine. The shearing surface on the buccal side of the paraconid and protoconid is considerably worn. Viewed from the occlusal surface, the carnassial edge of the paraconid abruptly turns anteriorly into a long, trenchant lingual ridge descending towards the metaconid from which it is set off by a valley. The carnassial edge of the protoconid curves posteriorly at an obtuse angle to continue into a sharp, partly damaged ridge that descends obliquely until it meets the metaconid. The anterior and lingual ridges of the protoconid delimit the lingual wall of this cusp, which flanks posterobuccally a deep, spacious valley that sets the protoconid off from the paraconid and metaconid. In addition to the anterior and lingual ridges, the protoconid exhibits a very short ridge, which is mostly worn away, on the base of its posterior wall. This short ridge ascends occlusolingual from the anterior end of the anterior edge of the hypoconid. There is an extensive wear facet on the posterior surface of the protoconid.

The metaconid is stout, well detached from the protoconid, and proportionally short anteroposteriorly. In lingual view, it resembles an isosceles triangle with its anterior and posterior profiles being slightly convex. In posterior view, the lingual contour of the metaconid is also slightly convex. A small part of the metaconid projects posteriorly beyond the protoconid so that its posterior edge is visible in buccal view. The slopes of the metaconid are angulated anteriorly, buccally, and posteriorly into ridges of which the buccal ridge is most trenchant or sharpened and the posterior one is most rounded or blunt. The anterior ridge descends towards the lingual ridge of the paraconid, from which it is separated by a valley. The buccal ridge is

united with the lingual ridge of the protoconid at a prominent, V-shaped notch. The posterior ridge meets the lingual wall of the talonid. The occlusal part of the posterior surface of the metaconid is worn.

Viewed occlusally, the posterior wall of the trigonid is almost straight, while the buccal and lingual contours of the crown are concave at the area where the trigonid meets the talonid. The buccal concavity is much better marked than the lingual one.

The talonid is deeply basined. Its buccal wall consists of an anteroposteriorly elongate hypoconid, which is the largest cusp on the talonid. The hypoconid is buccolingually wider and has its outer surface more inclined than is the case for the lingual wall of the talonid, making the talonid basin appear to be shifted lingual in occlusal view. Although wear has breached the enamel along the hypoconid, it is evident that the tip of this cusp was originally situated within the posterior half of the cusp length. The hypoconid is detached from the posterior wall of the talonid by a distinct V-shaped notch that is continued into an occlusobasal groove on the outer surface of the talonid.

The posterior wall of the talonid is lower than the buccal and lingual walls. It is somewhat worn occlusally and produced into three low, poorly differentiated elevations.

The lingual wall of the talonid forms two projections separated from each other by a notch. The anterior of these projections, the entoconulid, is small, whereas the posterior one, the entoconid, is much larger, being the second largest cusp on the talonid. The tips of both the cusps are worn, exposing dentine facets.

TYPE LOCALITY. Although Pomel (1847) did not indicate the place of collection of the name-bearing type of '*Plesictis' croizeti*' explicitly, it is obvious from the contents of his article that the specimen had been excavated from Tertiary deposits in the region of Vaumas and Saint-Gérand-le-Puy (Allier, France). Several years later, Pomel (1853: 97, 1854: 61) expressly attributed that fossil to the Tertiary sediments of Langy ('Terrain tertiaire à Langy'), which is a village situated about 3 km west of Saint-Gérand-le-Puy and some 25 km southwest of Vaumas. Most subsequent authors listed the locality as 'Saint-Gérand-le-Puy'. It deserves to be noted, however, that the name Saint-Gérand-le-Puy has generally been applied in the literature to encompass various fossil sites discovered in several quarries in the region of the village Saint-Gérand-le-Puy, including the locality Langy as well (Cheneval, 1983).

The only published statements about the type locality of '*Plesictis' croizeti*' that were significantly different were those of Gervais (1859) and Dawkins (1880a-b). According to the former author, the holotype of '*Plesictis' croizeti*' was found in calcareous marls of Miocene age in the environs of Issoire in the department of Puy-de-Dôme (his p. 250: 'Fossile dans les marnes calcaires de l'étage miocène aux environs d'Issoire (Puy-de-Dôme)'). Dawkins in his statements (1880a: 386, 'Issoire, Volvic (Puy-de-Dôme)'; 1880b: 505, 'Issoire, Volvic, Puy-de-dome [sic]') simply quoted Gervais (1859). However, neither Gervais nor Dawkins presented any supporting evidence for their assertions.

Gervais's (1859) referral of the holotype of '*Plesictis' croizeti*' to the locality Issoire is rather intriguing since that author was apparently familiar with Pomel's (1847, 1854) papers as indicated by their citations in his work, and since he studied that fossil during his visit to the British Museum (Natural History) shortly after it had been acquired by that institution, which is evident from footnote 2 on p. 11 in Gervais (1852b). In addition, one of the two labels on the type specimen of '*Plesictis' croizeti*', which lies in its box and refers it to '*Herpestes croizeti*' (the only other label on the fossil is its registration number), identifies the holotype as coming from the 'Upper

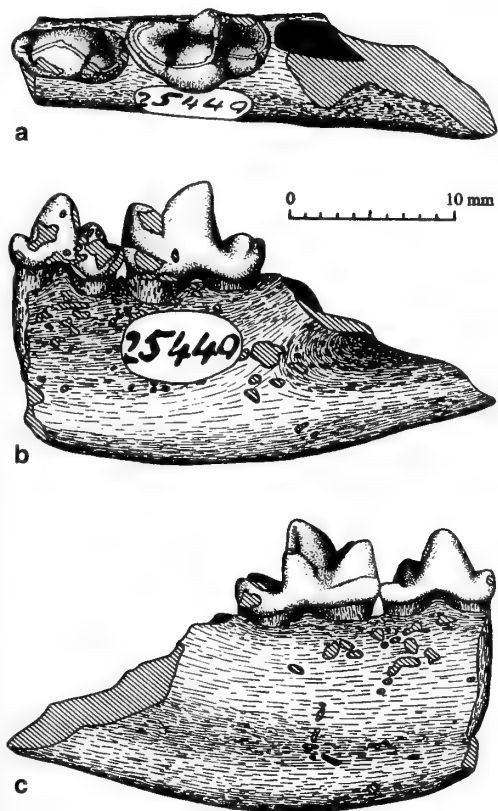


Fig. 2 The holotype of '*Lutra*' *minor* Lydekker, 1885 (BMNH 25449), a partial left dentary with P_4 and M_1 ; **a**, dorsal view; **b**, lateral view; **c**, medial view.

Oligocene' of 'Issoire, Puy-de-Dome [sic], France'. It is thus essentially consistent with Gervais's (1859) statement. There is no evidence, however, to support claim that just this label accompanied the holotype when it was examined by Gervais, or that the data included in it corresponded to those of any original but now lost label known to that worker. On the contrary, it seems to be more probable that the person who wrote the present label simply followed Gervais (1859), especially as both the old vertebrate register at NHM (which recorded Allier' as the locality of the holotype) and Lydekker (1885: 185) (who described it as 'the Lower Miocene of St. Gérand-le-Puy (Allier') support Pomel's (1853, 1854) statement that Langy was the place where the type specimen of '*Plesictis*' *croizeti* was collected.

In conclusion, the correct name of the type locality of '*Plesictis*' *croizeti* Pomel, 1847 is Langy in the department of Allier, central France. The accurate placement of this fossil site is vague. Its age corresponds to the Agenian, early Early Miocene, as indicated by the exclusively Agenian occurrence of many taxa (e.g. *Herpestides antiquus*) attributed by Pomel (1853, 1854) to Langy.

LUTRA' MINOR

AXONOMIC HISTORY. Lydekker (1885: 195) applied the specific name *Lutra minor* to a '[f]ragment of the right ramus of the mandible, containing the last premolar and the carnassial; from the Lower Miocene of Mombach, near Mayence', purchased in '1850' by the British Museum (Natural History). He referred that specimen to

register number 25440. However, as seen from the vertebrate registers at NHM, the number 25440 has never been allocated. Instead, the old vertebrate register records under number 2544g, a '[f]ragment of lower jaw of *S[tephanodon]. minor*' with '2 molars *in situ*' from 'Mayence', purchased in 'Aug[ust]. 1850' from 'M. Becker'. The specimen BMNH 25449 is accompanied by two labels. One of them, which is glued to the fossil, displays its register number in which the '9' is of blurred appearance (see Fig. 2a–b), which may have been the reason for Lydekker's mistake. The other label, lying in the specimen's box, reads as follows: 'Fragmentary mandibular ramus[;]*Potamotherium minor*, Meyer sp.[;]*Formⁿ* Lower Miocene[;]*Loc^y* Mombach, near Mayence[;]*Purch^h* 1850[;]*Cat. 1*, p. 149[;]*Brit. Mus. Geol. Dept.* 25449.' The reference to p. 149 in the first part of Lydekker's catalogue (1885) is an error, of course, because this page is actually devoid of any mention of this fossil; instead, the name of the ursoid carnivore *Cephalogale minor* Filhol, 1879a is quoted there. Another inconsistency between Lydekker's (1885) account of '*Lutra*' *minor* and the data available on BMNH 25449 is that the latter represents the left branch of the mandible, and not the right one as indicated by that author. Otherwise, BMNH 25449 fits Lydekker's description exactly. Moreover, there is no other fossil in the collections of The Natural History Museum in London, which could represent Lydekker's specimen. Accordingly, we conclude that BMNH 25449 must be the specimen referred by Lydekker (1885) to *Lutra minor*.

Lydekker (1885) treated the name *Lutra minor* as a new combination for *Stephanodon minor*, deemed by him to be erected by Hermann von Meyer. However, Lydekker (1885: 195, footnote 1) 'ha[d] been unable to find a reference to this species'. The old vertebrate register at NHM refers the specific name *Stephanodon minor* to specimen 25449, but without any relation to von Meyer's name. Instead, this German palaeontologist is cited in the register in connection with number 25448 ('*Stephanodon monbachensis* [sic] V. Meyer') attributed to the holotype of *Stephanodon mombachensis* von Meyer, 1847, which is indeed a junior synonym of the arctoid carnivoran *Potamotherium valletoni* (Geoffroy Saint-Hilaire, 1833). According to the register, that fossil and three others catalogued under numbers 25450–25452 were purchased in August 1850 from M. Becker as coming from 'Mayence', exactly as specimen 25449. In all likelihood, all these fossils had been studied by von Meyer before they were conveyed to the British Museum. It is thus just possible that H. von Meyer gave the name *Stephanodon minor* to specimen 25449. At any rate, it is very probable that a label stating this name accompanied the specimen originally and was known to Lydekker. Its existence was explicitly stated by Pohle (1920: 17; 'Das Stück war von v. Meyer mit dem Namen etikettiert worden'), who, however, provided no evidence to support his statement. Regardless of this, even if von Meyer was really responsible for the name *Stephanodon minor*, as declared by Lydekker (1885) and followed by Trouessart (1885, 1897, 1904), Schlosser (1888), Pohle (1920), and Haupt (1935), he has not satisfied the criteria of availability of that name and therefore cannot be considered its author according to Article 50 (a) of the ICBN. Instead, Lydekker (1885), who satisfied these criteria through both publishing the name of this taxon and stating in footnote 1 on his p. 195 that 'this species [...] may be only a smaller form of [*Lutra valletoni*]', is the author of the name whose correct original spelling is *Lutra minor*.

The name-bearing type of '*Lutra minor*' has never been figured or adequately described in the literature. The only published information relating to its size and morphological characteristics is that of Lydekker (1885: 195, footnote 1) that '*Lutra*' *minor* 'may be only a smaller form of' *Potamotherium valletoni*. The subsequent authors confined themselves to following this assumption. Trouessart (1885,

1897, 1904) held '*Lutra*' *minor* to be a subspecies of *Potamotherium valletoni* while Pohle (1920), Haupt (1935), and Savage (1957) simply placed it in the synonymy of that species. Schlosser (1888: 123) expressly denied the specific status of '*Lutra*' *minor* ('Ebenso ist auch *Stephanodon minor* H. v. Meyer auf keinen Fall als besondere Art zu betrachten'), including it in *Potamotherium valletoni*, but later (1890) he quoted it as a separate species of *Potamotherium*.

The synonymy list of '*Lutra*' *minor* Lydekker, 1885 includes the following names:

- 1885 *Lutra minor* [or] [*Lutra*] *minor* Lydekker: xxi, 195, 266.
 1885 *Stephanodon minor*; Lydekker: 195, 267.
 1885 [*Lutra valletoni*] *minor*; Trouessart: 47.
 1888 *Stephanodon minor*; Schlosser: 123.
 1890 [*Potamotherium*] *minor*; Schlosser: 82.
 1897 [*Potamotherium Valletoni*] *minor*; Trouessart: 281.
 1904 [*Potamotherium valletoni*] *minor*; Trouessart: 212.
 1920 *Stephanodon minor* [or] [*Stephanodon*] *minor*; Pohle: 16–17, 223.
 1935 *Stephanodon minor*; Haupt: 38.
 1957 *Potamotherium minor*; Savage: 155.

DESCRIPTION OF THE HOLOTYPE. The holotype, by monotypy, of '*Lutra*' *minor* Lydekker, 1885 is BMNH 25449, a fragment of a left dentary with partially eroded P_4 and M_1 (Fig. 2, Tables 1–3). The side-walls of the preserved fragment of body in the holotype dentary are convex in cross-section, excepting the ventral part of the medial wall where the surface of the dentary bone is somewhat depressed along the ventral border. The alveoli for P_4 – M_2 are arranged one behind the other and closely spaced. P_4 and M_1 slightly overlap each other and have pairs of alveoli. Only the anterior part of the M_2 alveolus is preserved; judging from this preservation, the alveolus was single and anteroposteriorly elongated. The masseteric fossa extends anteriorly to the level of the alveolus for M_2 .

The morphological patterns of P_4 and M_1 are congruent with those of the corresponding teeth in the type specimen of '*Plesictis*' *croizeti*, with the exception of the following differences concerning M_1 : in the holotype of '*Lutra*' *minor* the lingual ridge of the paraconid is shorter; the lingual contour of the metaconid is slightly concave; the metaconid is somewhat deflected posteriad, making its posterior contour slightly concave when viewed from the lingual side; there is no crest on the anterior face of the metaconid, so that the anterior slope of this cusp is widely rounded and blunt; and, finally, no elevation could be detected on the posterior wall of the talonid. The crowns of P_4 and M_1 are generally less worn in the holotype of '*Lutra*' *minor* than those of the type specimen of '*Plesictis*' *croizeti*.

TYPE LOCALITY. The old vertebrate register at NHM reports the holotype of '*Lutra*' *minor* as having been collected in 'Mayence' (=Mainz). Lydekker (1885: 195) described it as coming 'from the Lower Miocene of Mombach, near Mayence' (now Mainz-Mombach), perhaps on the basis of an original, but now missing, specimen label. Lydekker's attribution is consistent with that on the label accompanying the holotype at present. Schlosser (1890), who knew both Lydekker's (1885) catalogue and H. von Meyer's unpublished drawings of carnivoran remains from Mainz-Weisenau (as seen from Schlosser 1887: 4, 6), referred '*Lutra*' *minor* (his *Potamotherium minor*) to 'Mainz (Weissenau)' (=Mainz-Weisenau). No evidence exists, however, to suggest that Schlosser's assignment concerned specimen(s) other than the holotype and, moreover, none of the copies of von Meyer's drawings preserved in NMB represents the type specimen of '*Lutra*' *minor*. Consequently, we conclude that Schlosser's *Potamotherium minor* pertained to the holotype of '*Lutra*' *minor*, and hence its referral to the locality Mainz-Weisenau resulted from confusion.

Table 1 Mandible measurements (in mm) of the holotype of '*Plesictis*' *croizeti* Pomel, 1847 and '*Plesictis*' *gracilis* Pomel, 1853 (BMNH 26702), and the holotype of '*Lutra*' *minor* Lydekker, 1885 (BMNH 25449).

	BMNH 26702	BMNH 25449
Distance between posterior-most points of C_1 and M_2 alveolar rims	31.9	—
Greatest distance between alveolar rims for M_1 and M_2	11.6	—
Length of P_1 alveolus (greatest diameter of P_1 alveolar rim)	2.0e	—
Width of P_1 alveolus (least diameter of P_1 alveolar rim)	1.0	—
Length of P_2 alveoli (greatest distance between rims of anterior and posterior alveoli for P_2)	4.6	—
Width of P_2 alveoli (least distance from line connecting lingual-most points of P_2 alveolar rims to buccal-most point of these rims)	2.2	—
Length of P_3 alveoli (greatest distance between rims of anterior and posterior alveoli for P_3)	6.0	—
Length of P_4 alveoli (greatest distance between rims of anterior and posterior alveoli for P_4)	7.3	6.6e
Length of M_1 alveoli (greatest distance between rims of anterior and posterior alveoli for M_1)	8.6	8.5
Length of M_2 alveolus (greatest diameter of M_2 alveolar rim)	2.6e	—
Width of M_2 alveolus (least diameter of M_2 alveolar rim)	2.2	—
Greatest horizontal distance between lateral and medial walls of dentary below M_1 , perpendicular to long axis of dentary	5.6	5.8
Least distance from alveolar border of dentary between P_3 and P_4 to its ventral border, measured on medial side	9.3	—
Least distance from alveolar border of dentary between M_1 and M_2 to its ventral border, measured on medial side	10.5	11.7

'e' indicates an estimated value.

Table 2 Measurements (in mm) of premolar teeth in the holotype of '*Plesictis*' *croizeti* Pomel, 1847 and '*Plesictis*' *gracilis* Pomel, 1853 (BMNH 26702), and the holotype of '*Lutra*' *minor* Lydekker, 1885 (BMNH 25449).

	BMNH 26702	BMNH 25449
Length of P_3 (from anterior-most to posterior-most points of crown)	6.2	—
Width of P_3 (greatest distance between buccal and lingual borders of crown perpendicular to antero-posterior length of tooth)	2.8+	—
Height of P_3 (least distance from occlusal-most point of tooth to basal margin of crown, measured on buccal side)	3.8	—
Length of P_4 (from anterior-most to posterior-most points of crown)	7.2	7.1
Width of P_4 (greatest distance between buccal and lingual borders of crown perpendicular to antero-posterior length of tooth)	3.3	3.4
Height of P_4 (least distance from occlusal-most point of tooth to basal margin of crown, measured on buccal side)	4.1	4.2e

'+' indicates a minimum measurement on an incomplete structure, 'e' indicates an estimated value.

Table 3 Measurements (in mm) of M_1 in the holotype of '*Plesictis*' *croizeti* Pomel, 1847 and '*Plesictis*' *gracilis* Pomel, 1853 (BMNH 26702), and the holotype of '*Lutra*' *minor* Lydekker, 1885 (BMNH 25449).

	BMNH 26702	BMNH 25449
Length (from anterior-most to posterior-most points of crown)	8.7	8.8
Width (least distance from buccal-most point of crown to line joining lingual-most points of paraconid wing and talonid)	4.6	4.7
Trigonid length (least distance from anterior-most point of crown to line connecting notch between protoconid and hypoconid with notch posterior to metaconid)	5.9	6.2
Least distance between buccal and lingual borders of crown across carnassial notch	3.8	3.7
Talonid length (least distance from posterior-most point of crown to line connecting notch between protoconid and hypoconid with notch posterior to metaconid)	2.8	2.6
Talonid width (greatest distance between buccal and lingual borders of talonid perpendicular to antero-posterior length of tooth)	3.7	3.7
Paraconid height (least distance from occlusal-most point of paraconid to basal margin of crown, measured on lingual side)	3.7+	3.8+
Protoconid height (least distance from occlusal-most point of protoconid to basal margin of crown, measured on buccal side)	5.1+	5.6
Metaconid height (least distance from occlusal-most point of metaconid to basal margin of crown, measured on lingual side)	3.7	3.6+
Hypoconid height (least distance from occlusal-most point of hypoconid to basal margin of crown, measured on buccal side)	2.3+	2.5
Entoconid height (least distance from occlusal-most point of entoconid to basal margin of crown, measured on lingual side)	1.9+	2.0+

+ indicates a minimum measurement on an incomplete structure.

To summarize, the correct name of the type locality of '*Lutra*' *minor* Lydekker, 1885 is Mainz-Mombach in Rhineland-Palatinate, western Germany. The exact location of this fossil site is uncertain at present. Tobien (1980) assigned the fossil fauna from Mainz-Mombach (his Mombach) to the *Hydrobia* beds of late Agenian age, early Early Miocene.

CONSPECIFICITY WITH HERPESTIDES ANTIQUUS

During their taxonomic history, '*Plesictis*' *croizeti*, '*Plesictis*' *gracilis*, and '*Lutra*' *minor* have been referred to various arctoid caniform genera, including the mustelids *Plesictis* Pomel, 1846, *Lutra* Brünich, 1771, and *Mustela* Linnaeus, 1758 (for '*Plesictis*' *croizeti*; e.g. Gervais 1852b: 12), the amphictiid musteloid *Amphictis* Pomel, 1853 (for '*Plesictis*' *gracilis*; Viret 1929), and the arctoid *otamotherium* Geoffroy Saint-Hilaire, 1833 (= *Stephanodon* von Meyer, 1847; for '*Lutra*' *minor*). However, the fact that they really belong to none of those genera needs no elaboration. Their name-bearing types differ from the characteristics of these genera in most aspects of their morphology, and more importantly, '*Plesictis*' *croizeti* (= '*Plesictis*' *gracilis*) and '*Lutra*' *minor* do not belong even to the broader Caniformia Kretzoi, 1943, which is evidenced below.

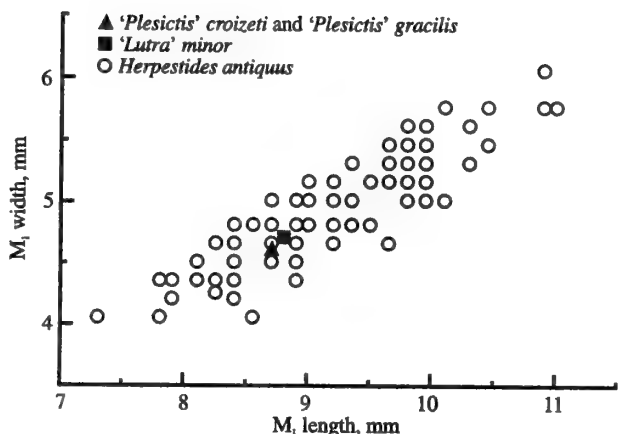


Fig. 3 A diagram of length versus width of M_1 , showing the distribution of individuals in a sample of *Herpestides antiquus* from the Agenian locality Montaigu-le-Blin in France (collection of NMB), compared to that of the holotypes of '*Plesictis*' *croizeti*, '*Plesictis*' *gracilis*, and '*Lutra*' *minor*.

As seen from the descriptions, illustrations (Figs 1–2), and measurements (Tables 1–3) presented in this paper, the holotype of '*Plesictis*' *croizeti* and '*Plesictis*' *gracilis* and that of '*Lutra*' *minor* differ only insignificantly from each other, plainly justifying the conclusion that they represent the same species. The available morphological features of that species unanimously point to its affiliation with the viverrid feliform *Herpestides* de Beaumont, 1967, known from the lower part (Agenian) of the European Lower Miocene. According to de Beaumont (1967), that genus included the single, extensively variable species *Herpestides antiquus* (de Blainville, 1842). A comparison of the holotypes of '*Plesictis*' *croizeti* (and '*Plesictis*' *gracilis*) and '*Lutra*' *minor* with the corresponding portions of dentary and lower dentition of *Herpestides antiquus* from the French locality Montaigu-le-Blin, stored in NMB, revealed that both the morphological traits and size of the holotypes are well within the variability range observed in *Herpestides antiquus* (Fig. 3).

To conclude, on the evidence presented above we consider the name-bearing types of '*Plesictis*' *croizeti* Pomel, 1847, '*Plesictis*' *gracilis* Pomel, 1853, and '*Lutra*' *minor* Lydekker, 1885 to represent the species *Herpestides antiquus* (de Blainville, 1842). Accordingly, we synonymize the first three names with the last one that is the valid name of the species in conformity with the Principle of Priority.

ACKNOWLEDGEMENTS. Our sincere thanks go to J.J. Hooker (NHM) and B. Engesser, P. Jung, C. Mödden, and F. Wiedenmayer (NMB) for their aid and generous hospitality during our research at those institutions. This study was supported by the State Committee for Scientific Research (KBN) grant 6 P204 051 05, the Swiss National Science Foundation, the Alexander von Humboldt Foundation, and the German Research Association (DFG) grant Ro 143/12-1.

REFERENCES

- Anonymous 1839. Marte fossile. *L'Écho du Monde Savant*, 5: 42–43.
- 1849. A. Pomel: Note über die im Allier-Dept. entdeckten fossilen Thiere. *Neues Jahrbuch für Mineralogie, Geognosie, Geologie und Petrefakten-Kunde*, 1849: 872–874.
- Bate, D.M.A. 1903. On an extinct species of Genet (*Genetta plesictoides*, sp. n.) from

- the Pleistocene of Cyprus. *Proceedings of the General Meetings for Scientific Business of the Zoological Society of London*, **1903** (2): 121–124.
- Beaumont, G. de** 1967. Observations sur les Herpestinae (Viverridae, Carnivora) de l'Oligocène supérieur avec quelques remarques sur des Hyaenidae du Néogène. Première partie. *Archives des Sciences*, **20**: 79–107.
- 1976. Remarques préliminaires sur le genre *Amphictis* Pomel (Carnivore). *Bulletin de la Société Vaudoise des Sciences Naturelles*, **73**: 171–180.
- Blainville, H.M.D. de** 1842. Des Viverras. In H.M.D. de Blainville, *Ostéographie ou description iconographique comparée du squelette et du système dentaire des Mammifères récents et fossiles pour servir de base à la zoologie et à la géologie*, **2** (1839–1864): 1–100. J. B. Baillièvre et Fils, Paris.
- Bonis, L.** de 1973. Contribution à l'étude des Mammifères de l'Aquitaniens de l'Agenais. Rongeurs-Carnivores-Périssodactyles. *Mémoires du Muséum National d'Histoire Naturelle. Nouvelle Série, Série C*, **28**: 1–192.
- Bronn, H.G.** 1856. Fünfte Periode. Molassen-Gebirge. In H.G. Bronn & F. Roemer, *H. G. Bronn's Lethaea geognostica oder Abbildung und Beschreibung der für die Gebirgs-Formationen bezeichnendsten Versteinerungen. Dritte stark vermehrte Auflage*, **3** (1853–1856, 6): I–VIII + 1–1130. E. Schweizerbart'sche Verlagsbuchhandlung und Druckerei, Stuttgart.
- & **Roemer, F.** 1856. *Atlas zu H. G. Bronn's Lethaea geognostica oder Abbildung und Beschreibung der für die Gebirgs-Formationen bezeichnendsten Versteinerungen. Dritte stark vermehrte Auflage*. E. Schweizerbart'sche Verlagsbuchhandlung und Druckerei, Stuttgart, 1850–1856. 123 pp.
- Brujin, H. de, Daams, R., Daxner-Höck, G., Fahrlbusch, V., Ginsburg, L., Mein, P. & Morales, J.** 1992. Report of the RCMNS working group on fossil mammals. Reisensburg 1990. *Newsletters on Stratigraphy*, **26**: 65–118.
- Brunich, M.T.** 1771. *Zoologiae fundamenta*. Copenhagen. 254 pp.
- Cheneval, J.** 1983. Les gisements de Saint-Gérand-le-Puy: 150 ans de paléontologie (1833–1983). *Revue Scientifique du Bourbonnais et du Centre de la France*, **1983**: 98–107.
- Cintract, R.** 1951. Catalogue des échantillons types et figurés des collections de paléontologie du Muséum National d'Histoire Naturelle. Mammifères. I. (Multituberculés, Marsupiaux, Primates, Tillodontes, Carnivores et Condylarthres). *Bulletin du Muséum National d'Histoire Naturelle, Série 2*, **22** (Suppl. 1): 1–58.
- Dawkins, W.B.** 1880a. The classification of the Tertiary period by means of the Mammalia. *The Quarterly Journal of the Geological Society*, **36**: 379–405.
- 1880b. *Early man in Britain and his place in the Tertiary period*. Macmillan and Co., London. xxiv + 537 pp.
- Dehm, R.** 1950. Die Raubtiere aus dem Mittel-Miocän (Burdigalium) von Wintershof-West bei Eichstätt in Bayern. *Abhandlungen der Bayerischen Akademie der Wissenschaften, Mathematisch-Naturwissenschaftliche Klasse, Neue Folge*, **58**: 1–141.
- Depéret, C.** 1887. Recherches sur la succession des faunes de Vertébrés miocènes de la vallée du Rhône. *Archives du Muséum d'Histoire Naturelle de Lyon*, **4**: 45–313.
- & **Douxami, H.** 1902. Les Vertébrés oligocènes de Pyrémont-Challonges (Savoie). *Mémoires de la Société Paléontologique Suisse*, **29**: I–VI + 1–91.
- Filhol, H.** 1877a. Recherches sur les phosphorites du Quercy. Étude des fossiles qu'on y rencontre et spécialement des Mammifères. Seconde partie. *Bibliothèque de l'École des Hautes Études, Section des Sciences Naturelles*, **16** (1): 1–338.
- 1877b. Recherches sur les phosphorites du Quercy. Étude des fossiles qu'on y rencontre et spécialement des Mammifères. *Annales des Sciences Géologiques*, **8** (1): 1–340.
- 1877c. Recherches sur les phosphorites du Quercy. Étude des fossiles qu'on y rencontre et spécialement des Mammifères. G. Masson, Paris. 561 pp.
- 1877d. Recherches sur les phosphorites du Quercy. *Thèses Présentées à la Faculté des Sciences de Paris pour Obtenir le Grade de Docteur ès Sciences Naturelles, Série A*, **26**: 1–561.
- 1879a. Étude des Mammifères fossiles de Saint-Gérand le Puy (Allier). (Première partie). *Bibliothèque de l'École des Hautes Études, Section des Sciences Naturelles*, **19** (1): 1–252.
- 1879b. Étude des Mammifères fossiles de Saint-Gérand le Puy (Allier). *Annales des Sciences Géologiques*, **10** (3): 1–253.
- 1880. Étude des Mammifères fossiles de Saint-Gérand le Puy (Allier). (Deuxième partie). *Bibliothèque de l'École des Hautes Études, Section des Sciences Naturelles*, **20** (1): 1–86.
- 1881a. Étude des Mammifères fossiles de Saint-Gérand le Puy (Allier). Seconde partie. *Annales des Sciences Géologiques*, **11** (1): 1–86.
- 1881b. Étude sur les Mammifères fossiles de Ronzon (Haute-Loire). *Bibliothèque de l'École des Hautes Études, Section des Sciences Naturelles*, **24** (4): 1–270.
- 1882. Étude des Mammifères fossiles de Ronzon (Haute-Loire). *Annales des Sciences Géologiques*, **12** (3): 1–271.
- 1883. Notes sur quelques mammifères fossiles de l'époque miocène. *Archives du Muséum d'Histoire Naturelle de Lyon*, **3**: 1–97.
- 1889. Note sur les caractères de la base du crâne des *Plesictis*. *Bulletin de la Société Philomathique de Paris, Série 8*, **1** (1888–1889): 106–108.
- Gaillard, C.** 1899. Mammifères miocènes nouveaux ou peu connus de la Grive-Saint-Alban (Isère). *Archives du Muséum d'Histoire Naturelle de Lyon*, **7** (2): 1–79.
- Geoffroy Saint-Hilaire, [É.]** 1833. Palaeontographie. Considérations sur des ossements fossiles la plupart inconnus, trouvés et observés dans les bassins de l'Auvergne; accompagnées de notes ou sont exposés, les rapports et les différences des deux zoologies, celle des époques antédiluviennes et celle du monde actuel. *Revue Encyclopédique*, **59**: 76–95.
- Gervais, P.** 1852a. *Zoologie et paléontologie françaises (animaux vertébrés) ou nouvelles recherches sur les animaux vivants et fossiles de la France*, **1** (1848–1852): I–VIII + 1–271. Arthur Bertrand, Paris.
- 1852b. Zoologie et paléontologie françaises. Planches XXVI, XXVII et XXVIII. Carnivores fossiles. In *P. Gervais, Zoologie et paléontologie françaises (animaux vertébrés) ou nouvelles recherches sur les animaux vivants et fossiles de la France*, **2** (1848–1852): 1–14. Arthur Bertrand, Paris.
- 1859. *Zoologie et paléontologie françaises. Nouvelles recherches sur les animaux vertébrés dont on trouve les ossements enfouis dans le sol de la France et sur leur comparaison avec les espèces propres aux autres régions du globe. Deuxième édition*. Arthur Bertrand, Paris. VIII + 544 pp.
- Giraud, J.** 1902a. Études géologiques sur la Limagne (Auvergne). *Bulletin des Services de la Carte Géologique de la France et des Topographies Souterraines*, **13** (1901–1902, 87): 1–410.
- 1902b. Études géologiques sur la Limagne (Auvergne). *Thèses Présentées à la Faculté des Sciences de Paris pour Obtenir le Grade de Docteur ès Sciences Naturelles, Série A*, **418**: I–II + 1–410.
- Haupt, O.** 1935. Andere Wirbeltiere des Neozoikums. In *W. Salomon-Calvi (ed.), Oberreinischer Fossilienkatalog*, **9**: 1–103. Verlag von Gebrüder Borntraeger, Berlin.
- Helbing, H.** 1928. Carnivores des oberen Stampien. *Abhandlungen der Schweizerischen Paläontologischen Gesellschaft*, **47** (4): 1–83.
- Kinkel, F. & Boettger, O.** 1903. Geologisch-paläontologische Sammlung. *Bericht der Senckenbergischen Naturforschenden Gesellschaft in Frankfurt am Main*, **1903** (1): 82–101.
- Kretzoi, M.** 1943. *Kochictis centennii n. g. n. sp., ein altertümlicher Creodont aus dem Oberoligozän Siebenbürgens*. *Földani Közlöny*, **73**: 180–195.
- Linnaeus, C.** 1758. *Systema naturae per regna tria naturae, secundum classes ordines, genera, species, cum characteribus, differentiis, synonymis, locis. Editio decima, reformata*, **1**: 1–824. Laurentius Salvius, Stockholm.
- Lydekker, R.** 1885. *Catalogue of the fossil Mammalia in the British Museum (Natural History). Part I. Containing the orders Primates, Chiroptera, Insectivora, Carnivora, and Rodentia*. British Museum (Natural History), London. xxx + 268 pp.
- Mein, P.** 1990. Updating of MN zones. In *E. H. Lindsay, V. Fahrlbusch & P. Mein (eds), European Neogene mammal chronology. NATO ASI Series, Series A*, **180**: 73–90. Plenum Press, New York.
- Meyer, H. von** 1847. [Untitled letter dated from] Frankfurt a. M., 4. Januar 1847. *Neues Jahrbuch für Mineralogie, Geognosie, Geologie und Petrefakten-Kunde*, **1847**: 181–196.
- Pictet, E.-J.** 1853. *Traité de paléontologie ou histoire naturelle des animaux fossiles considérés dans leurs rapports zoologiques et géologiques. Seconde édition*, **1**: I–XIV + 1–584. J.-B. Baillièvre, Paris.
- 1857. *Traité de paléontologie ou histoire naturelle des animaux fossiles considérés dans leurs rapports zoologiques et géologiques. Atlas de 110 planches*. J.-B. Baillièvre, Paris, 1853–1857. 77 pp.
- Pohle, H.** 1920. Die Unterfamilie der Lutrinae. (Eine systematisch-tiergeographische Studie an dem Material der Berliner Museen). *Archiv für Naturgeschichte, Abteilung A*, **85** (1919, 9): 1–247.
- Pomel, A.** 1846. Mémoire pour servir à la géologie paléontologique des terrains tertiaires du département de l'Allier. *Bulletin de la Société Géologique de France, Série 2*, **3** (1845–1846): 353–373.
- 1847. Note sur des animaux fossiles découverts dans le département de l'Allier. *Bulletin de la Société Géologique de France, Série 2*, **4** (1846–1847): 378–385.
- 1853. Catalogue des vertébrés fossiles (suite). *Annales Scientifiques, Littéraires et Industrielles de l'Auvergne*, **26**: 81–229.
- 1854. Catalogue méthodique et descriptif des vertébrés fossiles découverts dans le bassin hydrographique supérieur de la Loire, et surtout dans la vallée de son affluent principal, l'Allier. J.-B. Baillièvre, Paris. 193 pp.
- Redlich, K.A.** 1898. Eine Wirbelthierfauna aus dem Tertiär von Leoben. *Sitzungsberichte der Kaiserlichen Akademie der Wissenschaften, Mathematisch-Naturwissenschaftliche Classe, Abtheilung I*, **107**: 444–460.
- Roger, O.** 1887. Verzeichniss der bisher bekannten fossilen Säugetiere. *Bericht des Naturwissenschaftlichen Vereins für Schwaben und Neuburg in Augsburg*, **29**: 1–162.
- 1896. Verzeichniss der bisher bekannten fossilen Säugetiere. *Bericht des Naturwissenschaftlichen Vereins für Schwaben und Neuburg in Augsburg*, **32**: 1–272.
- Savage, R.J.G.** 1957. The anatomy of *Potamotherium*, an Oligocene lutrine. *Proceedings of the Zoological Society of London*, **129**: 151–244.
- Schlosser, M.** 1887. Die Affen, Lemuren, Chiropteren, Insectivoren, Marsupialier, Creodonten und Carnivoren des europäischen Tertiärs und deren Beziehungen zu ihren lebenden und fossilen aussereuropäischen Verwandten. *Beiträge zur Paläontologie Österreich-Ungarns und des Orients*, **6** (1888): 1–224.
- 1888. Die Affen, Lemuren, Chiropteren, Insectivoren, Marsupialier, Creodonten und Carnivoren des europäischen Tertiärs und deren Beziehungen zu ihren lebenden

- und fossilen aussereuropäischfn [sic] Verwandten. II. Theil. *Beiträge zur Paläontologie Österreich-Ungarns und des Orients*, 7 (1889): 1–164.
- 1890. Die Affen, Lemuren, Chiropteren, Insectivoren, Marsupialier, Creodonten und Carnivoren des europäischen Tertiärs und deren Beziehungen zu ihren lebenden und fossilen aussereuropäischen Verwandten. III. Theil. *Beiträge zur Paläontologie Österreich-Ungarns und des Orients*, 8 (1891): 1–106.
- Sherborn, C.D.** 1925. *Index animalium sive index nominum quae ab A. D. MDCCCLVIII generibus et speciebus animalium imposita sunt. Sectio secunda a kalendis Ianuariis, MDCCCI usque ad finem Decembris, MDCCCL; part VII: 1453–1771*. British Museum (Natural History), London.
- Teilhard de Chardin, P.** 1915. Les Carnassiers des Phosphorites du Quercy. *Annales de Paléontologie*, 9 (1914–1915): 101–191.
- The International Commission on Zoological Nomenclature 1985. *International code of zoological nomenclature. Third edition*. International Trust for Zoological Nomenclature, London; University of California Press, Berkeley. xx + 338 pp.
- Tobien, H.** 1980. Taxonomic status of some Cenozoic mammalian local faunas from the Mainz Basin. *Mainzer Geowissenschaftliche Mitteilungen*, 9: 203–235.
- Trouessart, E.-L.** 1885. Catalogue des Mammifères vivants et fossiles (Carnivores). *Bulletin de la Société d'Études Scientifiques d'Angers*, 14 (1884, Suppl.): 1–108.
- 1897. *Catalogus mammalium tam viventium quam fossilium. Nova editio (prima completa). Fasciculus II. Carnivora, Pinnipedia, Rodentia I. (Protogomorpha et Sciuromorphida)*, pp. 219–452. R. Friedländer & Sohn, Berlin.
- 1904. *Catalogus mammalium tam viventium quam fossilium. Quinquennale supplementum, anno 1904. Fasciculus I. Primates, Prosimiae, Chiroptera, Insectivora, Carnivora, Pinnipedia*. R. Friedländer & Sohn, Berlin. IV + 288 pp.
- Villalta Comella, J.F. de & Crusafont Párró, M.** 1944. Nuevos Carnívoros del Vindoboniense de la cuenca del Vallés-Panadés. *Notas y Comunicaciones del Instituto Geológico y Minero de España*, 13: 55–88.
- Viret, J.** 1929. Les faunes de Mammifères de l'Oligocène supérieur de la Limagne bourbonnaise. *Annales de l'Université de Lyon, Nouvelle Série, I. Sciences, Médecine*, 47: I–VIII + 1–328.
- Wenz, W.** 1921. *Das Mainzer Becken und seine Randgebiete. Eine Einführung in die Geologie des Gebietes zwischen Hunsrück, Taunus, Vogelsberg, Spessart und Odenwald*. Verlag von Willy Ehrig, Heidelberg. 351 pp.
- Wolsan, M.** 1993. Phylogeny and classification of early European Mustelida (Mammalia: Carnivora). *Acta Theriologica*, 38: 345–384.



Baryonyx walkeri, a fish-eating dinosaur from the Wealden of Surrey

ALAN J. CHARIG AND ANGELA C. MILNER

Department of Palaeontology, Natural History Museum, Cromwell Road, London SW7 5BD

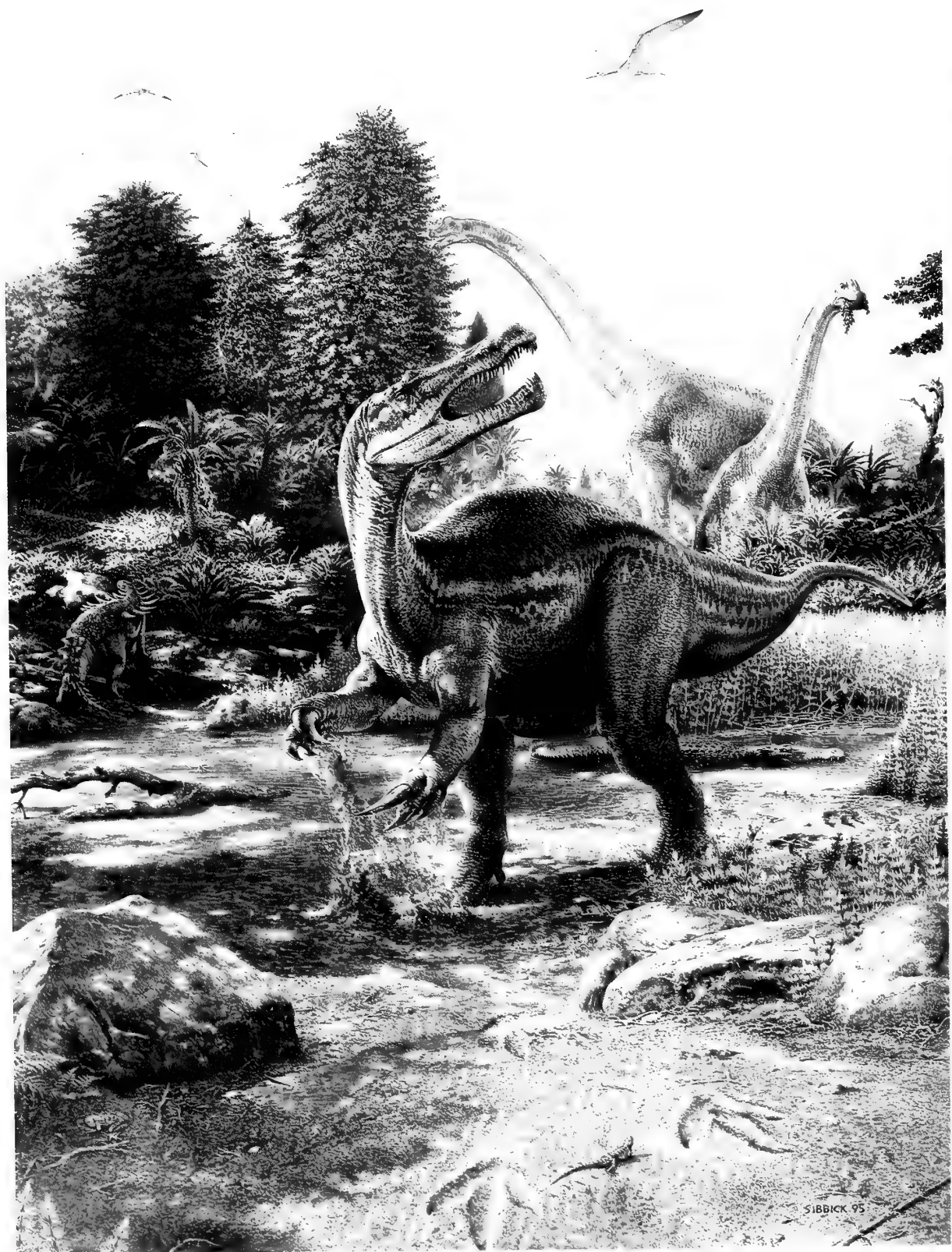
CONTENTS

Synopsis	11
Introduction	13
Systematic description	13
Formal systematics	13
Skull	14
Lower jaw	23
Dentition	28
Vertebral column	30
Ribs	41
Chevrons (haemopophyses)	41
Sternum	42
Pectoral girdle	42
Fore-limb	43
Pelvic girdle	47
Hind-limb	51
Other material referred to the same genus	54
Phylogenetic relationships and systematic position	54
Palaeoecology	60
Functional morphology and mode of life	60
Taphonomy	63
Acknowledgements	64
References	65
Appendix A. Abbreviations used in the illustrations	67
Appendix B. List of contents of each block	67
Appendix C. List of characters and data-matrix, modified from Holtz, 1994a	68

SYNOPSIS. The well-preserved skeleton of a large theropod dinosaur, *Baryonyx walkeri* Charig & Milner, 1986, from the Wealden (Barremian, Lower Cretaceous) of Surrey, is described in detail. It is a large theropod with some resemblance to *Megalosaurus* or *Allosaurus*, but is sufficiently different to merit its earlier designation as the type of the new family Baryonychidae. Its distinguishing characters include: the premaxillary extension of its snout into a spatulate rostrum, a unique increase in the number of the dentary teeth (which are more than twice as numerous per unit length of jaw as the opposing maxillary teeth), an unusually robust fore-limb, and at least one pair of huge manual talons. Lack of fusion between the components of both skull and vertebrae suggests that this 10 metre long animal was immature.

Few other specimens might be referred to *Baryonyx*: a maxilla fragment of *B. walkeri* is recorded from the Barremian of Spain; two snout fragments from the Aptian of Niger, which are virtually identical to the conjoined premaxillae of *Baryonyx*; two isolated tooth crowns, one from the Hauterivian of East Sussex, and one from Surrey; and seven from the Barremian of the Isle of Wight are compared to the genus. On the evidence of jaws and teeth only, the families Baryonychidae and Spinosauridae (*Spinosaurus*, *Angaturama*, and perhaps *Irritator*) are placed in the superfamily Spinocephaloidea. An investigation of the wider affinities of *Baryonyx*, based on a modified version of Holtz's 1994a data-matrix on the Theropoda, suggests that the Spinocephaloidea is a basal member of the Tetanurae and sister-group to the whole of the Neotetanurae (i.e. the Coelurosauria *sensu* Gauthier plus a variable collection of 'allosauroids'), with *Megalosaurus* and *Torvosaurus* as progressively more distant outgroups.

The associated fossil fauna is dominated by *Iguanodon* and many insects, which lived in the vicinity of a sub-tropical delta. *Baryonyx* was terrestrial, a fish-eater, probably a scavenger, and possibly an active predator of small to medium-sized land animals. It made greater use of its fore-limbs and talons in attack and defence than its jaws and teeth, which were used mainly for seizing fish and entrails. The taphonomy of the holotype suggests that the animal is unlikely to have been transported from elsewhere and probably died where found. Its skeletal remains lay in sediments that were mostly submerged in shallow water but exposed to the air for brief periods; the bones were trampled and broken before fossilization.



Frontispiece *Baryonyx walkeri*, holotype, BMNH R9951; restoration of a living animal in the Wealden landscape. Painted by John Sibbick.

INTRODUCTION

Discovery

The discovery of *Baryonyx* was a major event in the history of British dinosaur palaeontology (Milner & Croucher 1987). Extant faunas of large terrestrial vertebrates invariably include only a small proportion of carnivores, these being at the apex of the food pyramid, and fossil faunas were probably no different. Dinosaur discovery in England goes back more than 300 years (Plot 1677) and includes several finds of a few bones or teeth of carnivores. Until 1983, however, the only significant find of a carnivorous dinosaur had been the partial skeleton of *Eustreptospondylus oxoniensis* (originally placed in the genus *Megalosaurus*), found in Oxfordshire in 1871 and now in the Oxford University Museum. Since the discovery of *Baryonyx*, the partial skeleton of an allosauroid has been described from the Wessex Formation (Wealden) of the Isle of Wight (Hutt, Martill & Barker 1996).

Details of the discovery of *Baryonyx* were published by Milner & Croucher (1987). The enlarged ungual phalanx, the famous 'Claw' (originally missing the tip), a second smaller, less complete ungual phalanx and an incomplete haemapophysis, were found on 7 January 1983 by Mr William J. Walker at the Ockley Brick Company's claypit near Ockley, Surrey, and a week later he found the missing tip of the claw. After examining this material at the British Museum Natural History, we visited the site on 7 February and found large ark-brown bones from the pelvis and hind-limb, lying just beneath the surface of the clay. The physical conditions in the claypit prevented us from collecting the skeleton until the period 25 May to 0 June 1983, when a team of eight from the Department of Palaeontology and a number of volunteers excavated two tonnes of matrix containing bone.

All the remains were found within an oval excavation measuring approximately 5 metres by 2 metres (Fig. 49). Most were encased in nodules of sideritic siltstone, which had been deposited around the bones, but some lay unprotected in soft clay. The skeleton was largely disarticulated and the elements gently scattered, but most of them were still lying approximately in their skeletal position, with the animal's skull at one end and its tail at the other. Some nodules were lifted untreated, some were encased in plaster of Paris and others in expanded polyurethane foam.

Preparation

Preparation of the material was especially difficult because of the hardness of the siltstone matrix, made more intractable by the presence of siderite. A few pieces were subjected experimentally to chemical treatment with thioglycollic acid (which dissolves iron but has little or no action on siltstone and other non-ferrous rocks), but it had practically no effect, so most of the matrix had to be removed by mechanical methods. Some field cocoons, the bulk of the rock and the underlying clay were removed rapidly with an industrial shot blaster, a Vacu-Blast Nova 150PB, using plastic shot as the abrasive; as far as is known (R. Croucher and W. Lindsay, pers. comms) this is the first recorded instance of the use of such equipment for preparing fossils. Rock was also removed with hand tools and with tools powered by compressed air, including diamond-tipped circular saws and chisels. For more delicate work close to the bone surface, finely pointed engravers were used under binocular microscopes. Other details of the laboratory work on *Baryonyx* were described by Milner & Croucher (1987).

SYSTEMATIC DESCRIPTION

Suborder THEROPODA Marsh, 1881

Superfamily SPINOSAUROIDEA Stromer, 1915

Family BARYONYCHIDAE Charig & Milner, 1986

TYPE-GENUS. *Baryonyx* Charig & Milner, 1986.

DERIVATION OF NAME. From Greek βαρύς, heavy; οὐνξ, claw.

DIAGNOSIS. As for genus *Baryonyx*.

Genus BARYONYX Charig & Milner, 1986

TYPE-GENUS. *B. walkeri* Charig & Milner, 1986; Early Cretaceous, Surrey, England.

DIAGNOSIS. Monotypic genus, as for species *B. walkeri*.

Baryonyx walkeri Charig & Milner, 1986

DERIVATION OF NAME. For Mr William J. Walker, who discovered the original claw-bone.

HOLOTYPE. Natural History Museum, London: Department of Palaeontology, BMNH R9951.

MATERIAL. The holotype alone; consisting of conjoined premaxillae, conjoined vomers, anterior part of left maxilla, conjoined nasals, left lacrimal, left prefrontal, left postorbital, anterior end of braincase (right frontal, right parietal, right orbitosphenoid, right laterosphenoid), posterior end of braincase together with occiput (both prootics, both opisthotics, basisphenoid, supraoccipital, both exoccipitals, basioccipital), left jugal, both quadrates; both dentaries, both splenials, right surangular, both angulars, right coronoid; some upper teeth *in situ* and many isolated teeth of unknown position in the jaws; axis and 4 further cervical vertebrae, 12 dorsals, 3 or 4 basal caudals, 3 more distal caudals; one axial rib, three other cervical ribs, many dorsal ribs, abdominal ribs, 5 haemapophyses, sternum; both scapulae, both coracoids; both humeri, left radius, left ulna, left pollex with huge ungual, left digit II (complete) or digit III₍₂₋₄₎, other isolated phalanges of both sides; right ilium, both pubes, left ischium; proximal end of left femur and distal end of right, right fibula, right calcaneum, metatarsal fragments, 1 pedal ungual.

LOCALITY. Smokejack's Brickworks (Ockley Building Products Limited, formerly Ockley Brick Company Limited), Wallis Wood, Ockley, near Dorking, Surrey, England. A little below the top of the south-east face, nearest to the works buildings. National Grid reference TQ 113373.

HORIZON. Lower Cretaceous, Wealden Series, Upper Weald Clay; zone of *Cypridea clavata*, near the base of the Barremian; about 7 m below the base of BGS Bed 5c (See Ross & Cook 1995).

DIAGNOSIS. Prenarial region of snout extended into extremely narrow rostrum with spatulate, horizontal expansion at end ('terminal rosette'); snout slightly downturned in lateral view, jaws with sigmoidal margins. Long, low external nares far back on side of

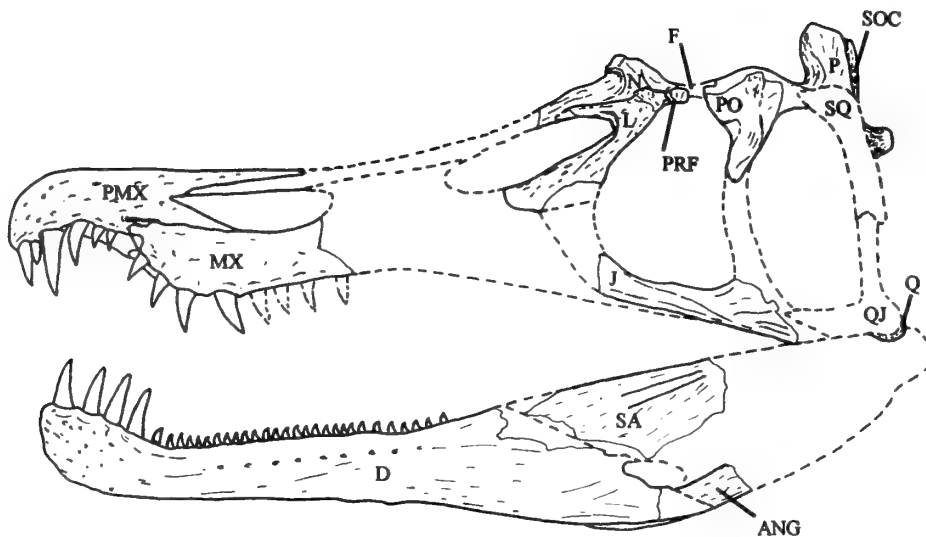


Fig. 1 *Baryonyx walkeri*, holotype, BMNH R9951; reconstruction of skull, from left side. $\times 0.135$.

snout. Complex articulation of premaxilla and maxilla unfused above subrostral notch. Small median knob at posterior end of conjoined nasals, cruciform in dorsal view, with anterior limb of cross drawn forwards into low thin median crest. Occiput deep, with paroccipital processes directed horizontally outwards. Basipterygoid processes descend far below basioccipital, diverging laterally only slightly. Anterior end of dentary upturned in lateral view. 6/7 premaxillary teeth; only 8 maxillary teeth preserved, but probably about 15; 32 dentary teeth, generally smaller than those in the upper jaw, more than twice as numerous per unit length of jaw. Prominent bony wall on lingual side of all teeth. Tooth crowns flattened only slightly labio-lingually, lightly fluted on lingual side; anterior and posterior carinae finely serrated (about 7 denticles per millimetre). Tooth roots exceptionally long and slender. Axis small, with well developed hypophene. Cervical vertebrae with flat zygapophyses and well developed epiphyses; ends of centra not offset, no upward curve to neck; neurocentral sutures unfused; neural spines generally short, but those of basal caudals expanded into large flattened plates. Cervical ribs short, crocodiloid, slight overlap. Humerus relatively well developed; both ends broadly expanded but flattened, offset 35° against each other; shaft massive, almost straight. Radius stout, a little less than half as long as humerus. Ulna also stout, somewhat longer than radius, with powerful olecranon. Exceptionally large manual ungual phalanx, not laterally compressed, probably from digit I. Pubic foot not expanded. Ischium with obturator flange proximally continuous with anterior margin.

Skull

GENERAL DESCRIPTION (Fig. 1). Despite the limited amount of material available, several interesting observations may be made on the skull. It appears to have been long, at least in its anterior portion. Whereas in other theropods the extreme anterior end of the premaxilla gives rise to the steeply ascending nasal process, forming the anterior margin of the external naris, in *Baryonyx* there is no trace of such a process, and the anterior 170 mm of the conjoined premaxillae form a long low rostrum with a smoothly rounded dorsal surface. Even behind this rostrum there is no ascending process, the

confluent external nares appearing merely as an extensive opening lying well back from the tip of the rostrum and passing horizontally from one side of the snout to the other. The first 130 mm of the rostrum are expanded laterally into a spatulate 'rosette', not unlike that found in modern gavials; the first 70 mm of its lower margin are turned down in lateral view. Behind the 'rosette' the rostrum is remarkably narrow from side to side as seen in dorsal view.

The maxilla fits on to the hind part of the ventral margin of the premaxilla by a complex articulation. The resulting effect is that the line of the upper tooth row, passing backwards from the front of the snout, first rises a little and then, at the junction of the two elements, curves strongly downwards and finally flattens out to run horizontally along the ventral margin of the maxilla. The net effect of this sigmoid curvature is that the front of the rostrum is elevated above the level of the maxillary tooth row, not depressed beneath it. This elevation is reflected in the shape of the upper margin of the dentary, the front 140 mm of which slope strongly upwards towards its anterior end. Nevertheless, in the region of the 5th to 6th premaxillary teeth, the gap between the upper and lower jaws seems to have been much wider than elsewhere and may be termed the subrostral notch.

Other noteworthy general features of the skull are:

1. The deep, narrow shape of the occiput, especially deep below the condyle, the basipterygoid processes greatly lengthened.
2. The great length of the dentary, its dentigerous part very shallow with well-marked Meckelian groove on the medial surface.
3. The presence of a prominent bony wall on the lingual side of each tooth row.
4. The exceptionally high tooth count (6 premaxillary teeth on the left side and 7 on the right, as contrasted with a more usual count of 5, and 32 dentary, as contrasted with the usual 16 or so). The only other theropods known with more teeth per unit length of lower jaw than in the corresponding length of upper jaw are *Troodon* (Osmólska & Barsbold 1990) and *Pelecanimimus* (Pérez-Moreno *et al.* 1994), and even there the disparity is far less extreme.
5. The much closer packing of the teeth in the dentary than in the opposing part of the maxilla; as a corollary of this the dentary teeth must have been generally smaller (it should be noted,

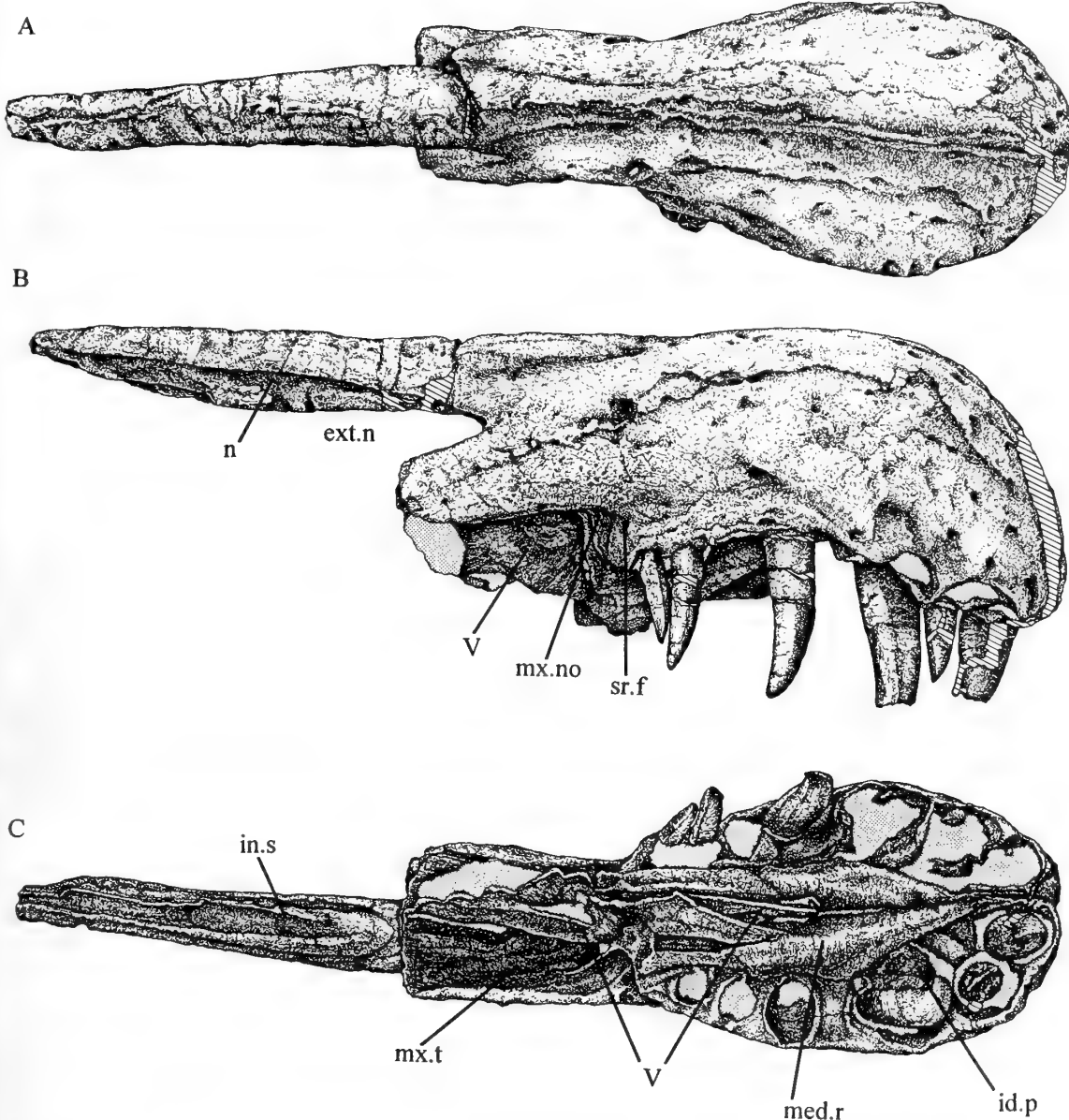


Fig. 2 *Baryonyx walkeri*, holotype, BMNH R9951; snout. A, conjoined premaxillae in dorsal view; B, same, right lateral; C, premaxillae in palatal view, showing also vomers. $\times 0.5$.

however, that our knowledge of the maxillary dentition is restricted to the first 7 teeth).

The extremely fragile, laminar nature of the post-dentary bones in the lower jaw.

The lack of co-ossification between the elements, except in the midline and in the braincase.

The last character suggests that R9951, despite its great size, was juvenile, from which we might deduce that the fully mature animal was probably much larger still. The possibility that a member of the plesiosauridae (see p. 55) might attain a truly vast size is confirmed by Stromer's illustrations (1915) of the dentary of *Spinosaurus aegyptiacus*, an element twice the linear size of that of *Baryonyx*.

REMAXILLA (Fig. 2). Both premaxillae are preserved, firmly

sutured together; the median suture between them is clearly visible on the dorsal surface, though it fades out towards the rear. Both elements are complete anteriorly but broken off behind. The premaxillae (as preserved) are not fused to any other elements; each, however, has (or had) a complex articulation with the maxilla.

The snout is unlike that of most other known dinosaurs, in which an ascending process rises from the very front of the conjoined premaxillae and forms the rounded anterior border of the external nares. Here, by contrast, the snout is long and low; the equivalent process originates 172 mm behind the tip of the snout and is directed almost horizontally backwards. Thus the heavy, robust snout formed by the conjoined premaxillae is seen in lateral view to bifurcate posteriorly into two rami on each side, a short one below (the main body of the premaxilla) and a longer one above (the

'ascending process'); the external naris between them terminates anteriorly in an acute angle. In palatal or dorsal view the snout appears extremely narrow from side to side, and there is a 'waist' between the anterior, dentigerous portion expanded horizontally into a 'terminal rosette' (Charig & Milner 1990) and the two rami, lower and upper, behind.

The lower ramus is broken off transversely not far behind the anterior corner of each external naris, but its full extent on each side of the snout is demonstrated by clear indications of its overlap onto the laterodorsal surface of the left maxilla, indications which suggest that that too was tapered to a point. The dorsal surface of this ramus, forming the floor of the nasal cavity, slopes steeply downward on either side (i.e. it is merely a posterior extension of the side of the snout), but between these slopes is a deep sagittal V-shaped groove.

The upper ramus tapers to a thin spike which presumably met the nasals; it has a smooth outer (i.e. dorsal) surface, but internally (i.e. ventrally), where it borders the nasal cavity, it bears on each side two longitudinal ridges, a low lateral ridge and a stronger medial ridge. Together these produce a shallow lateral groove on each side and a deeper median groove, in the bottom of which the latter suture between the paired premaxillae may still be traced intermittently. These ridges would somehow have supported the internasal septum and associated soft tissues, and the lateral grooves doubtless served for articulation with a forwardly projecting prong from the nasal on each side.

In lateral view the ventral, dentigerous margin of the premaxilla is distinctly downturned, both anteriorly towards the tip and posteriorly towards the articulation for the maxilla; it is smoothly concave between. There is extensive pitting on the outside of the snout, especially towards the tip, which doubtless served for the exit of blood vessels and nerves; a row of nutritive foramina lies just above the bases of the teeth.

In ventral view the terminal rosette has an elongated spatulate shape, around the edge of which lie six dental alveoli on the left side and seven on the right. In these thirteen alveoli only six teeth remain in place, four of them complete to the tip. The first four alveoli on each side are large; nos. 2 and 3 are the largest; nos. 5 to 7 decrease in size progressively. Interdental plates are present, each interrupted by a narrow gap which is rather more posterior than anterior in position.

When the premaxilla is seen in palatal view, the area between the tooth rows on either side appears to be fully occupied by a pair of narrow, transversely rounded 'elements', sutured together in the midline and broken off short just behind the level of the last premaxillary tooth. Each tapers anteriorly to a combined point which abuts against the rear end of a median groove between the medial walls of the first alveolus on each side. Towards the rear each 'element' expands ventrally. From the anterior apex a strongly interdigitating median suture between the two sides pursues a sinuous course backwards for some 30 mm; farther back the interdigitations cease and the two sides are separated by a narrow, elongated, median gap, on either side of which the 'elements' curve out laterally away from each other and then, more posteriorly, almost rejoin. In the region of the anterior half of the median gap their ventral surface is somewhat rugose, suggesting the possible presence in life of a horny pad in the roof of the mouth.

These, however, are not separate elements (despite their close resemblance to vomers) but seem to be integral parts of the premaxilla; they form a pair of stout ridges that support the adjacent tooth rows, lying lateral to them. Posteriorly from the level of the 4th tooth they expand into two vertical flanges, roughly triangular in shape and extending ventrally to an apex just behind the level of the last

(7th) alveolus and then descending again to terminate just behind the subrostral notch.

At the posterior end of the premaxillary tooth row, just below the anterior end of the ventral margin of the lower ramus, is a deep notch which received a rectangular peg-like process on the anterior end of the maxilla. Just in front of this notch lies the subrostral foramen, while just above the notch, in the outer surface of the premaxilla, lie three well-defined pits. A vertical bony buttress separates the notch in front from the anterior end of the deep U-shaped trough behind.

VOMER (Fig. 2C). The ventral (i.e. palatal) surface of the conjoined two lower rami of the premaxilla bears what appears to be a very deep median septum; this divides the concavity of the premaxillary trough into a pair of broad, U-shaped, ventrally facing troughs, each of which received the dorsal edge of the front maxilla. We interpret this as the extreme anterior portion of the paired vomers, fused together to form an extremely slender, vertical lamina which lies in the midline and is clasped between the vertical flanges of the premaxilla (described above). It extends forwards as far as the level of the alveoli for the 4th premaxillary tooth on each side. The central part of this lamina is attached to the roof of the anterior part of the premaxillary trough (though the suture is partly obliterated); anteriorly and posteriorly there is a gap between the dorsal edge of the lamina and the roof of the (inverted) trough. The extreme anterior end of the conjoined vomers tapers to a point and appears to project downwards from the roof of the mouth, in the midline between the premaxillae, an unlikely position that suggests postmortem displacement.

MAXILLA (Fig. 3). All that is preserved is the anterior part of the left maxilla, broken off through the 8th maxillary alveolus. Seen in lateral view, both its upper and lower margins are smooth curves, concave above, and with the lower (dentigerous) margin continuing without interruption around the anterior end; the two margins approach each other posteriorly so that the whole element, though broad from top to bottom in front, narrows appreciably towards the posterior break. Just below the anterodorsal corner the rectangular peg (referred to above under Premaxilla) projects forwards; the maxillary tooth row begins immediately below it and then curves smoothly in a posteroventral direction; when premaxilla and maxilla are placed together in natural articulation there is a small gap of about 20 mm between the last premaxillary tooth and the first maxillary. In *Dilophosaurus* (Welles 1984) this gap in the tooth row is some 40 mm, in an animal which is only about two-thirds the size of the *Baryonyx* holotype. The maxilla extends anteriorly beneath the external naris but is separated from it by the ventral ramus of the premaxilla, so that its most anterior extremity lies some 45 mm farther forward than does the anterior corner of the external naris (in this it contrasts with the condition in *Dilophosaurus*, where there is very little overlap between the two elements and where the most anterior point of the maxilla lies more or less beneath the middle of the naris). Just behind the rectangular peg the medial surface of the maxilla bears a shallow channel running in an anteroventral direction, forming the lateral margin of the external portion of the subrostral canal.

Along the dorsal margin of the lateral face is the long, slightly rugose articular surface for the lower ramus of the premaxilla; it tapers to a point 135 mm behind the front tip of the maxilla and a little way below its dorsal margin. Behind and medial to this, the dorsal margin is smoothly rounded and forms the posterior part of the ventral border of the external naris. The lower margin of the medial face of the maxilla is formed by a stout rounded ridge, lying immediately medial to the tooth row; running above this throughout its length is the articulating surface for the palatine, the antero-

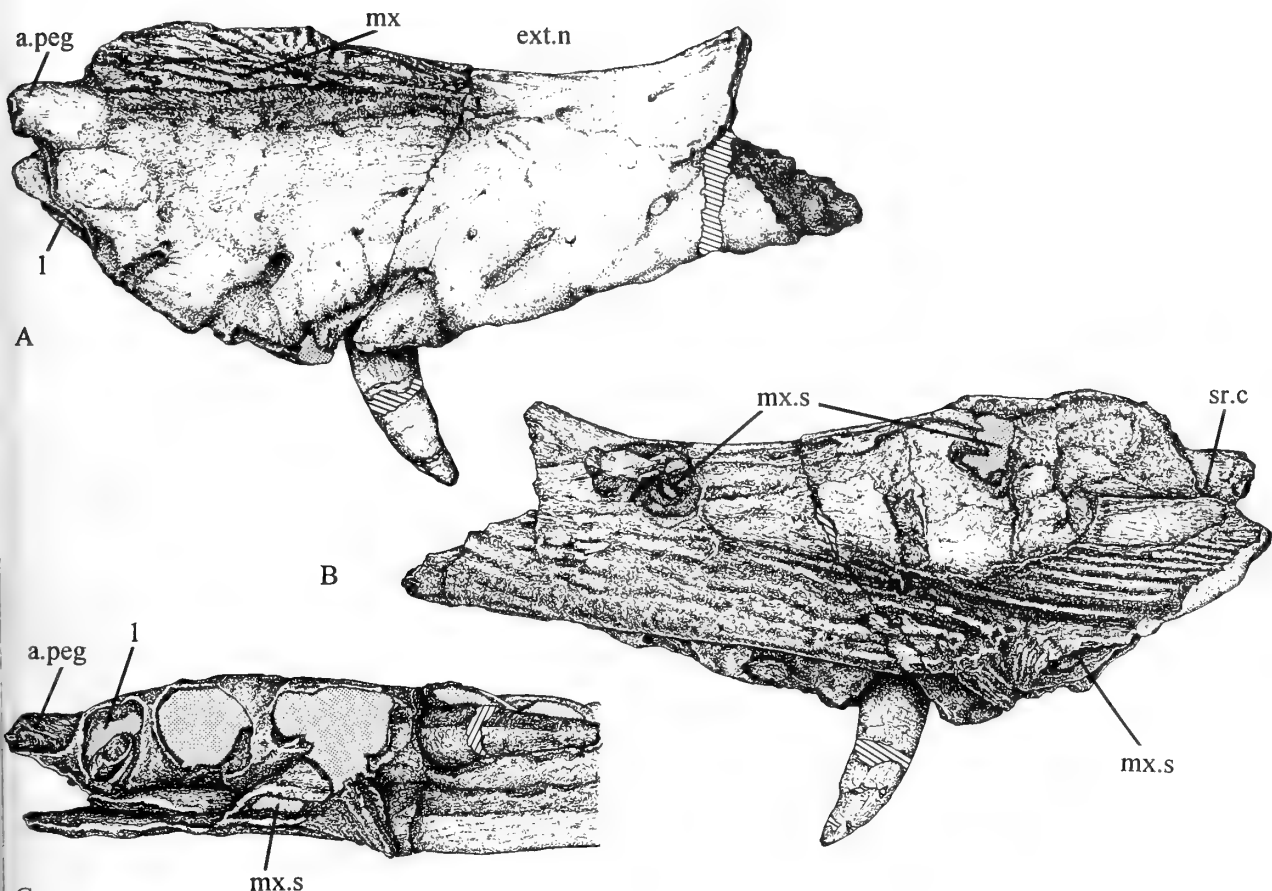


Fig. 3 *Baryonyx walkeri*, holotype, BMNH R9951; left maxilla. A, lateral view; B, medial; C, anteroventral. $\times 0.5$.

portion bearing four prominent longitudinal ridges. Just below the dorsal margin of the medial face lie two large, deep fossae, one above the septum between the 3rd and 4th alveoli and the other above the 6th alveolus. Comparison with other theropod skulls suggests that these may have housed maxillary sinuses.

The most anterior part of the medial face is in fact an anteriorly directed flange (on to the lower half of which run the longitudinal ridges already mentioned). The anterior tip of this flange articulates with a notch on the lateral surface of the anterior process of the palatine (q.v.). The anterodorsal border of the flange forms the medial wall of the internal portion of the subnarial canal.

Seen from below, the anterior/ventral surface of the maxilla is of more or less uniform width. The lateral half of this is occupied by the dental alveoli; the medial half consists posteriorly of the stout rounded ridge referred to above, tapering forwards slightly; anterior to the level of the 4th maxillary tooth this ridge tapers further into the thin medial flange and a less prominent shelf on the inner wall of the large immediately bordering the medial walls of the alveoli. Also on the medial wall of the flange, behind the shelf, a bony wall surrounds what may well be another maxillary sinus.

On the anterior surface of the rectangular peg is a vertical depression, behind which is the first maxillary alveolus. Altogether there are seven alveoli in the preserved portion of the maxilla; the first four are almost contiguous, separated from each other by only a thick bony wall, but from no. 4 backwards they are more widely spaced. Alveoli nos. 2, 3 and 4 are the largest; nos. 1, 5 and 6 are smaller, no.

7 smaller still. The alveoli are subcircular; no. 4 contains a completely erupted, slightly worn tooth, no. 1 contains only the base of a smaller, broken-off tooth only partly erupted, and no. 6 shows the tip of a newly erupting crown.

We suggested (Charig & Milner 1986, 1990) that there was a mobile articulation on each side between the premaxilla in front and the maxilla behind. We now believe that that suggestion was probably wrong. The anterior end of the maxilla can be fitted neatly into the inverted trough formed laterally by the premaxilla and, medially, by the thin sagittal lamina which appears to be an anterior prolongation of the paired vomers; the rectangular peg on the maxilla then locks into the notch on the premaxilla (Charig & Milner 1986, fig. 1; 1990, fig. 9.2). This complex articulation between premaxilla and maxilla would not permit any movement between those elements, for which, in any case, there is no obvious functional requirement.

NASAL (Fig. 4). The paired nasals are fused together into a single element, although it is possible to detect intermittent traces of the median suture. Three fragments were recovered: the major, posterior, fragment (Fig. 4) was found lodged against the left lacrimal. As preserved, the posterior fragment in dorsal view resembles an arrowhead: it is a narrow triangle, with its apex directed forwards, and from the base (hind end) of this triangle a stubby median process – the ‘shaft’ of the ‘arrowhead’ – projects farther posteriorly and must have articulated with the frontals.

The dorsal (external) surface of the conjoined nasals is raised in

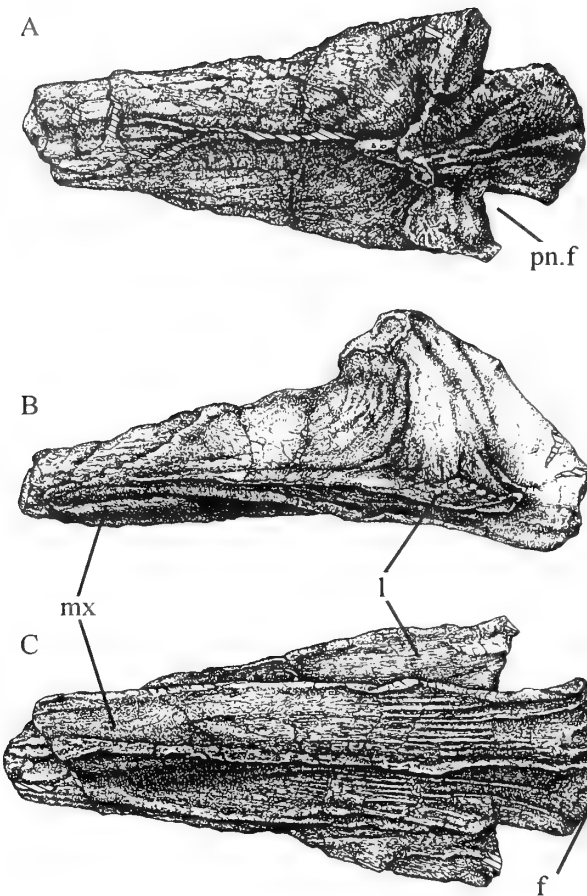


Fig. 4 *Baryonyx walkeri*, holotype, BMNH R9951; posterior part of conjoined nasals. A, dorsal view; B, left lateral; C, ventral. $\times 0.5$.

the midline into a sagittal crest which begins a short way behind the anterior end of the fragment as preserved and continues to its hinder extremity. This is crossed, just anterior to the base of the triangle, by a much lower, rounded transverse ridge; where the two intersect they rise to a tall, prominent peak at the centre of a cruciform excrescence. The anterior part of this sagittal crest is narrow and sharp.

The ventral (internal) surface of the nasals is relatively flat. Paired shallow parasagittal channels, separated by a low median ridge, run the whole length of the fragment and are delimited laterally by sharp ridges running parallel to the mid-line. The parasagittal channels are fairly smooth anteriorly, but more posteriorly bear a series of parallel longitudinal ridges which indicate a firm sutural connexion. The anterior region must have articulated with the ascending process of the maxilla, and the posterior part with an underlying, forwardly projecting process of the frontal; the most posterior part of this surface curves round dorsally so that it faces posteroventrally rather than directly downwards. The lateral extremities are wing-like triangular flat surfaces, the undersides of the lateral portions of the 'arrowhead'. At the extreme posterior end of each lateral 'wing' a very short parasagittal ridge divides the ventral surface into two; the area lateral to this ridge, and, farther forward, the entire width of the surface together form the articulation for the dorsal ramus of the lacrimal. The posterior termination of the lateral wing of the nasal abuts against the anterior face of the dorsal protuberance of the lacrimal (see below). Between the back of the 'arrowhead' and its

'shaft' there lies, on either side, an embayment which must have been part of the margin of a small but distinct fenestra between the nasal, the lacrimal and the prefrontal and frontal. The only theropod we know of that has a fenestra in this position is *Syntarsus* (Raath 1977), for which fenestra Raath proposed the name nasal fenestra¹ although we suggest postnasal fenestra as a more appropriate alternative.

The two more anterior fragments, found in a nearby block (30, Fig. 49) are parallel-sided and triangular in cross-section, the apices being a continuation of the narrow, sharp sagittal crest, little taller than the height at the anterior end of the large fragment. The parasagittal ridge and paired channels continue along the ventral surfaces in line with those on the larger posterior fragment. None of the three fragments join but they indicate that the total length of the nasal was more than 280 mm. Neither fragment shows any trace of a premaxillary articulation at the anterior end.

LACRIMAL (Fig. 5). Only the left lacrimal is preserved. It consists of two rami meeting posteriorly at an angle of about 35°, which encloses the posterodorsal corner of the antorbital fenestra and is considerably more acute than the same angle in other theropods. The nasal (dorsal) ramus is 60 mm long, slender, and tapers to a point; the jugal (ventral) ramus is more than twice as long (155 mm) and stouter.

The dorsal edge of the nasal ramus articulated with the more lateral part of the underside of the nasal bone. The ramus bears a short, horizontal, medially directed lip which underlies the posterior end of its articulation with the nasal. A second, more pronounced lip lies beneath the first one, so that a long narrow groove, some 3 mm wide, is enclosed between the two.

The jugal ramus of the lacrimal projects anteroventrally; its thickened, rounded anterodorsal margin is complete, but its distal half appears to be drawn out posteroventrally into a thinner flange (maximum width as preserved 45 mm), the central part of which is broken off. Its medial surface bears a strong ridge running its entire length and parallel to its dorsal margin. A second ridge is present on the posterodorsal half only, running just below the first ridge and parallel to it, thereby enclosing a deep narrow groove. This groove, continuous with the groove on the nasal ramus, might be supposed to have enclosed the two rami of a V-shaped prefrontal like that found in such theropods as *Allosaurus* (Madsen 1976) and *Sinraptor* (Currie & Zhao 1993). However, the prefrontal is quite different in *Baryonyx*, small and compact without rami, and could not have articulated with these grooves. The distal end of the jugal ramus of the lacrimal articulated with the main body of the maxilla and, more posteriorly, with the jugal itself.

In the axil of the two rami, on their lateral side, is the deep lacrimal vacuity. Towards the base of this vacuity is the external lacrimal foramen, the outer opening of the lacrimal duct; the internal opening sits in a small pit on the posteroventral surface of the jugal ramus some 40 mm below the posterior termination of the bone. Farther down the same surface are two deep pits, probably foramina, one below the other. These may be the equivalent of the single posterior lateral foramen in *Allosaurus* (Madsen 1976: 20) and

¹The literature is somewhat confused with regard to the position of this fenestra. It is unfortunate that, at present, Raath's dissertation of 1977 is not available to us. Colben gave a dorsal view of the skull of *Syntarsus rhodesiensis* (1989, fig. 42B: 'adapted from Raath 1977') which shows the nasal fenestra bordered by nasal, lacrimal and prefrontal but he did not mention the fenestra in his text. However, Rowe (1989: 129) wrote 'At the junction between nasal, prefrontal and frontal [no mention of lacrimal] is a diamond shaped opening, termed the nasal fenestra by Raath (1977)', that lies just above and rostral [i.e. anterior] to the orbit. This structure is known only in the two species of *Syntarsus*. All this was confirmed by Rowe & Gauthier (1990) and by figs 1C and II of Rowe's (1989) paper.

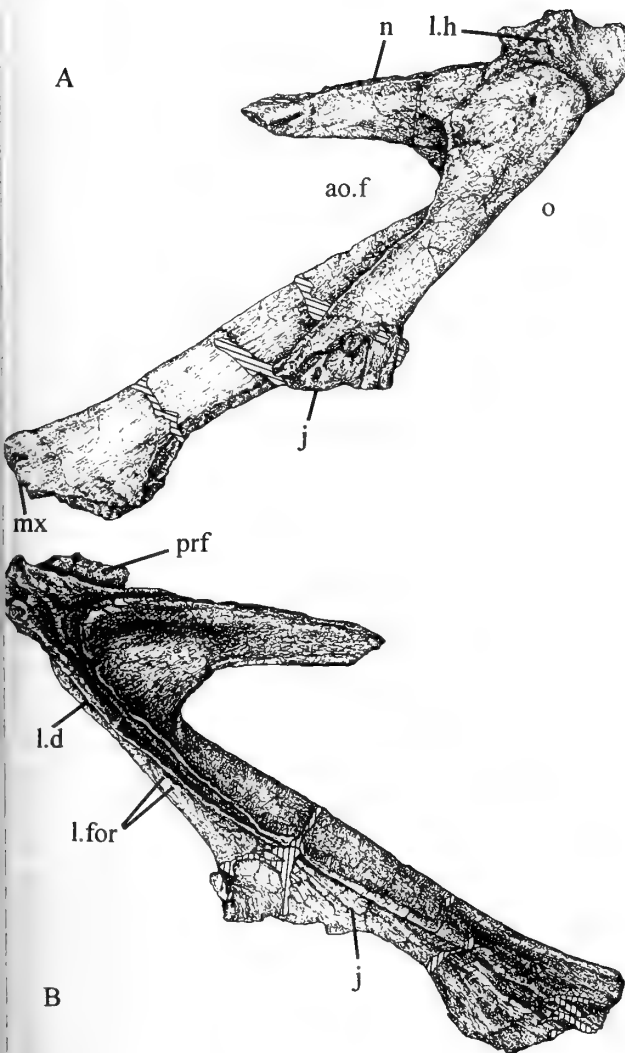


Fig. 5 *Baryonyx walkeri*, holotype, BMNH R9951; left lacrimal. A, lateral view; B, medial view. $\times 0.5$.

Torvosaurus (Britt 1991: 19); another opening on the lateral surface probably connected with one or both of these. At the posterior corner of the lacrimal is a rugose articulation for the prefrontal. Just anterior to the articulation and separate from it, is a dorsal rugose excrescence, about 5 mm high, semicircular in shape, measuring some 20 mm anteroposteriorly and 12 mm across. This may represent the base of a horn core; a similar structure is found in many other theropods, e.g. *Allosaurus*.

PREFRONTAL (Fig. 6). The small, compact and apparently complete left prefrontal proved difficult to identify. It does not have the characteristic V-shape of the typical theropod prefrontal with its two longated rami (as in, for example *Allosaurus* or *Sinraptor*), nor does either of its rugose articulating surfaces fit convincingly against that of the lacrimal. However, we could not envisage it as any other bone from any other part of the skeleton, and, more persuasively, it was discovered in close association with the nasals and lacrimal in block 2A (Fig. 49; Appendix B). Those two elements had been displaced only a little from their proper relative positions, and the prefrontal was lying, as it should, against the posterior end of the lacrimal.

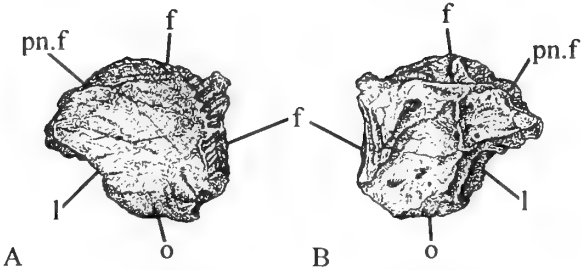


Fig. 6 *Baryonyx walkeri*, holotype, BMNH R9951; left prefrontal. A, dorsal view; B, ventral. $\times 0.5$.

The prefrontal is a thick nubbin of bone, flattened dorsoventrally, with a smooth, slightly concave dorsal surface; seen from above it is roughly isodiametric but of irregular outline. The ventral surface, by contrast, is highly sculptured into ridges and valleys. Anterolaterally the thick margin forms a large, highly rugose facet, which presumably articulated with the posterior end of the lacrimal (although, as stated above, the fit is far from precise). Behind this is a short smooth section of the margin, facing laterally, which would have formed part of the anterodorsal section of the orbital rim.

The posterior part of the margin of the prefrontal forms another articulating facet, only slightly rugose and deeper laterally than medially, which would have abutted against that portion of the frontal that extended laterally between the prefrontal in front and the postorbital behind to reach the orbital rim. The medial surface of the prefrontal is more complex. Dorsally is a deep V-shaped groove, wide anteriorly, tapering posteriorly to an apex, and divided within into two portions by a weak oblique ridge; the anterior portion formed the posterior margin of the postnasal fenestra, the posterior portion articulated with the anterolateral portion of the main body of the frontal. The ventral surface is remarkable only for four parallel ridges running transversely across the finished bone near its posterior margin and for a steep little peak, directed ventrally, at the ventral termination of the lacrimal facet.

POSTORBITAL (Fig. 7). The left postorbital as preserved lacks only its most dorsal portion. As seen in lateral view, it has essentially the shape of a thick lower-case 'y', with the stem of the 'y' (the jugal process) descending posteroventrally and then curving round so that its ventralmost portion is directed steeply downwards. Except dorsally, the margins of the postorbital in lateral or medial view are very thin, almost blade-like.

The anterior half of the lateral surface, curving round medially to form the posterodorsal surface of the orbit, is smooth and convexly swollen throughout its height (i.e., both in its broad dorsal portion and in its narrowing ventral portion). Above the orbit it is weakly rugose, but less so than in *Allosaurus* or *Torvosaurus* (Britt 1991). The posterior half of the lateral surface is weakly concave and leads towards a posteriorly directed flange; the dorsal portion of this flange is broken off but would have articulated with the squamosal, the ventral portion forms part of the anterior border of the lower temporal fenestra. The jugal process is short and square-ended (shorter than the corresponding structures in *Allosaurus* and *Torvosaurus*), and of more or less uniform width. The thick dorsal end of the postorbital is broken off but would have led to a massive facet, directed medially; the greater part of this articulated with the frontal, but a relatively small part articulated at its posterior end with the parietal.

The medial surface is much flatter and, though smooth, is faintly roughened all over. The jugal process bears a distinct vertical

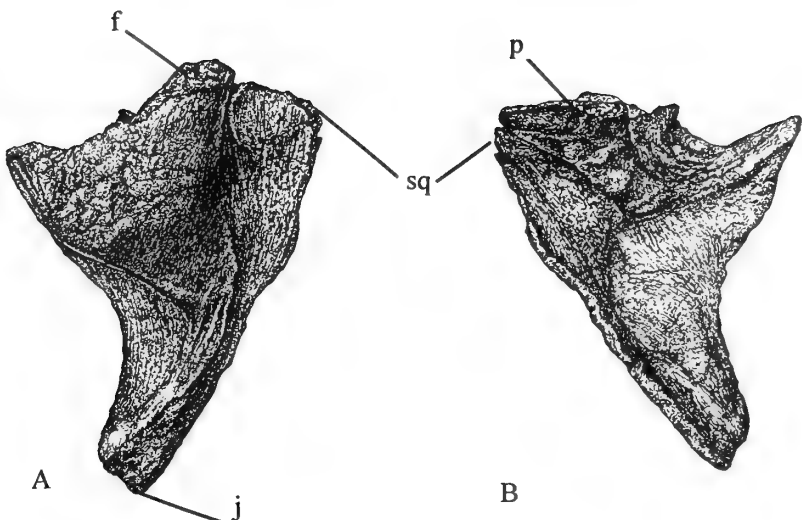


Fig. 7 *Baryonyx walkeri*, holotype, BMNH R9951; left postorbital. A, lateral view; B, medial. $\times 0.5$.

groove, running parallel to its posterior margin. From its posterodorsal region a large process projects mediad, like a flat-topped shelf supported strongly from below by a stout, rounded buttress; this presumably underlay the parietal. Anterior to this a weak concavity faces dorsomedially.

FRONTAL, pariETAL, AND ANTERIOR END OF BRAINCASE (LATEROSPHENOID, ORBITOSPHENOID) (Fig. 8). A stout plate of bone, very thick and with a smooth surface, and sheared off medially just to the right of the midline, comprises the greater part of the right frontal. It is continuous posteriorly with part of the parietal; a fairly straight line across the bone surface, more or less at right angles to the sagittal plane, may well be the suture between them. The parietal, behind that somewhat dubious suture, extends posteriorly and curves dorsally to form a steep transverse crest, thin from front to back; this crest, some 70 mm high, becomes thinner dorsally and ends in a flat top. The weakly concave ventral surface of the frontal is the ceiling of the posterior part of the orbit. The parietal and frontal together

extend laterally to end in a large and extremely rugose facet for articulation with the postorbital; the parietal forms only the most posterior part of this facet, about one-sixth of its entire length. Along the anterior half of this facet the dorsal surface of the frontal (and presumably of the postorbital too) is raised into a conspicuous protuberance. Anteriorly, the frontal may have contacted the prefrontal, but we cannot be sure of this. Ventrolateral to the frontal (and therefore ventral to the parietal) lies the laterosphenoid.

The laterosphenoid forms the wall of the anterior part of the braincase, thick dorsally but tapering ventrally; in posterior view it is seen in section, behind which a gap separates its broken surface from the anterior face of the prootic (with which it once articulated). Its shape, as preserved, is roughly tetrahedral. In lateral view it appears equilaterally triangular, with one apex directed forwards so that it just reaches the back end of the facet for the postorbital; dorsally it fuses with the parietal, and at its posteroventral corner its surface is extended outwards into a short shelf running more or less parallel with its lower margin. In ventral view it is again triangular, but this time it forms a narrow isosceles triangle with the acute angle directed posteriorly; this surface is part of the internal wall of the orbit. The base of the triangle, at the anterior end, fuses with the frontal, and the anteromedial corner curves round medially to border a large notch which may have served for the emergence of cranial nerves III (oculomotor) and IV (trochlear). Medial to this notch lies a thin, eroded, subtriangular plate of bone, which, according to its general shape and topographical relations, could well be the orbitosphenoid; but it is too poorly preserved to be described properly.

Ventral to the frontal and medial to the laterosphenoid (though separated from the latter by a wide cavity) lies a confused mass of bone and matrix, the identity of which is not clear. As it is, quite fortuitously, almost symmetrical with the right-hand wall of the braincase, it gives the impression that it might be the left-hand wall preserved mostly as a natural mould in matrix: but it cannot be because it lies entirely to the right of the sagittal plane.

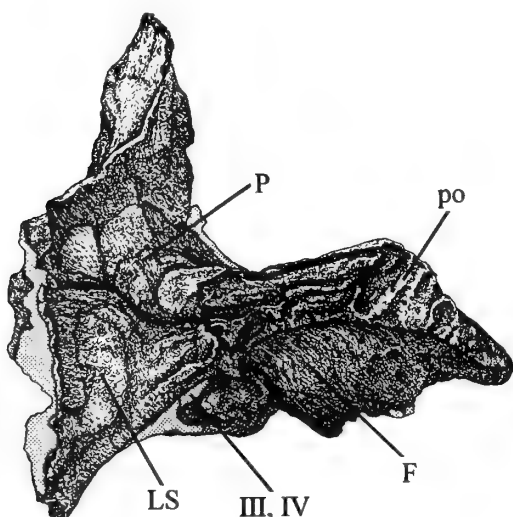


Fig. 8 *Baryonyx walkeri*, holotype, BMNH R9951; right frontal and anterior end of braincase, in lateral view. $\times 0.5$.

POSTERIOR END OF BRAINCASE (WITH OTIC ELEMENTS) AND OCCIPIT (WITH BASISPHENOID) (Fig. 9). The supraoccipital, both prootics, opisthotics and exoccipitals (the latter two elements of the left side detached as a separate fragment), and basisphenoid and basioccipital are preserved. They are described from the posterior forwards

The foramen magnum is semicircular, with a more or less straight lower border and a curved upper border. The lower border lies immediately above the robust, backwardly projecting occipital condyle. Most of the backwardly directed, articulating face of the condyle is formed by the basioccipital; the exoccipitals make only a comparatively minor contribution to this face, namely the dorsolateral corners, each of which is demarcated from the basioccipital by a straight suture running obliquely. (This suture has separated on the left-hand side.) The dorsal surface of the occipital condyle between the exoccipital sutures on either side is also formed by the basioccipital, which bears a shallow longitudinal depression in the midline; this means that the condyle, seen from behind, has a roughly heart-shaped appearance.

A vertical apron of bone, also part of the basioccipital, extends ventrally from beneath the condyle; it is of uniform width, as wide as the condyle itself, and terminates below in a broad median tongue with a shorter, much narrower lappet on either side. The basisphenoid projects even farther ventrally; this has parallel sides for some distance and then terminates in a pair of processes, the basipterygoid processes of the basisphenoid, which splay out ventrolaterally. The lower margin of the basisphenoid, between the splayed processes, forms a smooth concave curve. The posterior surface of the basisphenoid, below the median tongue of the basioccipital, is deeply furrowed in the midline; the furrow becomes broader and shallower ventrally and peters out altogether before reaching the ventral margin.

On either side of the foramen magnum/occipital condyle complex lies a horizontally directed lateral wing, the paroccipital process. This is more or less triangular in transverse section, with one face directed posteriorly, another face dorsally and a little anteriorly, and a third anteroventrally. Its medial part is formed by the exoccipital and its more lateral part by the opisthotic; in most dinosaurs those two elements are fused together indistinguishably, but in this specimen an ill-defined suture still demarcates the exoccipital as a slender triangle with its apex directed laterally. The opisthotic extends also ventrally, lateral to the whole length of the basioccipital. At about mid-height of the occipital condyle, on the suture between the exoccipital and the opisthotic and a short distance lateral from the basioccipital, lies a fairly large foramen which is divided in its depth into two separate canals. Recent Crocodylia possess several foramina in the same general region, one of which, with exactly the same topographical relationships as the foramen in *Baryonyx*, is likewise divided into two and is unequivocally the vagus foramen; we therefore give that same identity to the 'double' foramen of *Baryonyx*. Iordansky (1973: 226) observed that in the crocodilian foramen vagi 'The medial canal extends to the cerebral cavity and is traversed by the IXth and Xth nerves; the lateral canal extends to the middle ear cavity and contains the Ramus communicans (N. sympathetic) connecting the VIIth and IXth nerves.' [actually Xth and XIth; see Romer 1956: 66]. In *Baryonyx* the external aperture of the smaller canal is dorsomedial in relation to its larger, ventrolateral neighbour. There are two internal apertures within the cavity of the brain stem, just anterior to the foramen magnum; the lower one, lying at the junction of the floor and wall of the cavity, connects with the larger, ventrolateral external foramen, while the upper one, lying behind and a little above its partner, probably connects with the smaller, dorsomedial external foramen. Whether these two are precisely homologous to their crocodilian counterparts is open to question. Meanwhile the dorsomedial part of the anteroventral face of the paroccipital process is overlapped by the prootic (q.v.) below and the supraoccipital (q.v.) above.

The left paroccipital process, i.e. exoccipital plus opisthotic, is present but has been cleanly detached from the rest of the skull. It

lacks the ventral extension and has been distorted to some degree. However, laterally it is more complete than the paroccipital process of the right side, and therefore gives a better indication of the true shape and extent of this structure, of which about 25 mm is missing on the right side (see also Charig & Milner 1986, fig. 2; 1990, fig. 9.4).

The dorsal part of the occiput is contributed by the supraoccipital, which forms (a) the central region of the dorsal margin of the foramen magnum, between the medially directed arms of the opisthotics; (b) the central part of the back end of the skull roof; and (c) arising from the latter, a prominent stout process which, though essentially projecting dorsally, is also inclined a little forwards at its upper end. This process, somewhat compressed antero-posteriorly and is rectangular in shape when viewed from front or rear; its dorsal surface is broadly crescentic. On its posterior surface, on either side of its base, is the external aperture of a canal that has its other end in the upper part of the internal wall of the braincase and presumably served for the passage of a large blood vessel. The basal part of the anterior side of the supraoccipital process, together with the dorsal part of the underlying prootics, forms on each side a strongly furrowed surface which must have sutured with the parietal.

The prootic on either side is a solid, chunky element, forming the wall and floor of this posterior part of the braincase; each meets its fellow along the midline of the floor. A row of foramina for the passage of the cranial nerves runs along the angle between the wall and the floor, effectively dividing the internal and external surfaces of the prootic into an upper part and a lower part (see below, next paragraph). Anteriorly each prootic bears furrowed surfaces for articulation with the laterosphenoid and, more dorsally, with the parietal. Between those articulating surfaces, below the floor of the braincase, is the posterior part of the pituitary fossa; it appears here as two deep median concavities (a smaller above and a larger below, with a saddle between) which penetrate horizontally backwards into the substance of the bone. The posterior wall of the pituitary fossa is the dorsum sellae. On either side of the top of the upper concavity is a large foramen, through which the VIth (abducent) cranial nerve is presumed to have passed forward from the floor of the braincase into the pituitary fossa (see Romer 1956: 67) and thence continued in the same direction to emerge laterally into the orbit (see Osborn 1912: 17).

Externally the upper part of the prootic is applied to the anterior surface of the opisthotic, extending about half-way along the length of the paroccipital process. Its lower margin is a smooth, slightly concave curve, separated from the opisthotic behind by a deep furrow which terminates medially in the fenestra ovalis. Just anteromedial to the latter is a foramen for the VIIth cranial nerve and, farther forward still, a large open notch for the emergence of the Vth. Ventral to these nerve exits the lower part of the prootic forms a large plate-like posterolateral process which is applied to the anterolateral face of the basisphenoid.

On the left side, the opisthotic has become detached from the rest of the braincase; this exposes the cavity of the otic capsule, contained within the body of the prootic. Inside this capsule are two small foramina, both of which lead through into the endocranial cavity to emerge posterior to the large foramen for the passage of the Vth nerve. One of these could well be the duct for the passage of the VIIIth cranial (auditory or acoustic) nerve. These ducts and foramina serve for the passage, not only of blood vessels and lymph ducts, but also of pneumatic openings.

The whole of the ventral portion of this occipital fragment, seen in anterior view, is formed from the basisphenoid with its splayed, downwardly projecting basipterygoid processes. As stated above, the more dorsal part of the basisphenoid is hidden by the postero-

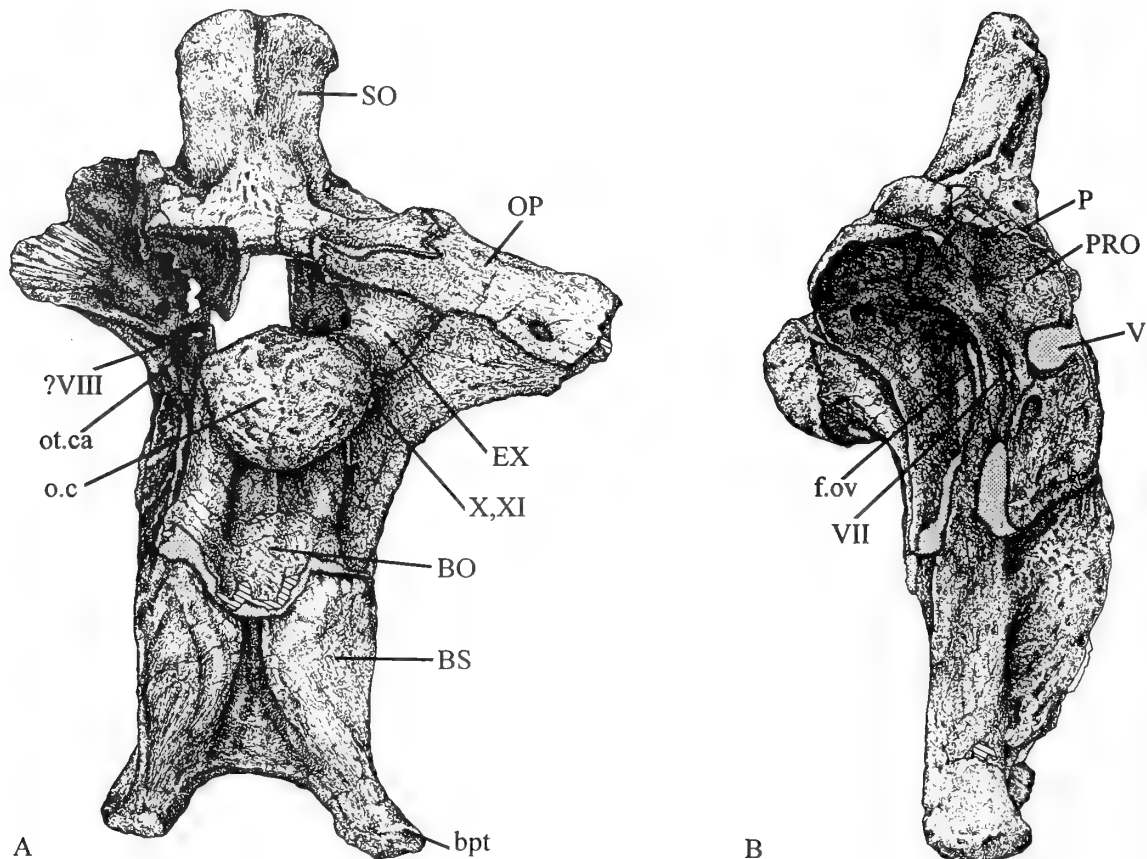


Fig. 9 *Baryonyx walkeri*, holotype, BMNH R9951; occiput and posterior part of braincase, lacking detached left opisthotic. **A**, posterior view; **B**, right lateral. $\times 0.5$.

lateral processes of the prootics. In the midline of the anterior surface is an extremely prominent, ridge-like septum which divides ventrally (like an inverted Y) into a pair of ridges, each leading down towards the basipterygoid process of its side; between the two ridges is a deep cavity. On either side the flat surface of the basisphenoid slopes posterolaterally so that the whole resembles a pitched roof. At the dorsomedial corner of each flat surface, just beneath the postero-lateral process of the prootic, is a moderately deep hollow.

JUGAL (Fig. 10). The left jugal is represented by an elongate portion from the centre of the element, lacking what was probably a significant length at either end. In lateral view the lower margin appears almost straight, while the upper margin forms a smooth, shallow, concave curve that is the wide ventral border of the orbit; thus the element is beginning to widen towards the break at either end, the posterior widening being much the larger of the two. The lower margin is generally rounded, the upper margin sharper. The central part of the bone, directly beneath the centre of the orbit, is fairly robust; the ends of the fragment, however, become rapidly thinner towards the breaks (forwards, backwards and upwards).

The lateral surface is more or less smooth except for a weak ridge running diagonally across the suborbital bar, from the upper margin of the bar beneath the front of the orbit to the lower margin of the bar at about the level of the back of the orbit.

The medial surface, by contrast, is distinguished by a series of features. The lower margin is wrapped around to form a strong,

dorsomedially directed flange; this flange is especially well developed beneath the ascending process, and it passes anteriorly and a little ventrally, becoming weaker as it does so, to merge into the lower margin itself beneath the orbit. Beneath the orbit, too, it is flattened, ridged and grooved parallel to its own length to form an articulation that presumably met the ectopterygoid. Posterior to this, where the flange is developed much more strongly, it encloses a deep trough between the main body of the jugal and itself.

The dorsal margin of the suborbital bar is narrowly rounded in front, forms a sharp raised ridge beneath the centre of the orbit, and posteriorly develops a second, slightly lower ridge more or less parallel with the edge of the orbit. Between the two subparallel ridges is a shallow trough. The lower ridge also forms the upper border of the deep trough enclosed by the ventral flange, the trough being at its narrowest at this point. The flange, and therefore the trough which it helps to enclose, taper away to disappear entirely just in front of the break at the hind end. The ventral margin, at this hind end of the bone as preserved, bears a narrow, medially directed shelf which doubtless formed part of the articulation for an anteriorly directed process of the quadratejugal.

The missing anterodorsal corner of the jugal presumably articulated with the maxilla and the posterodorsal corner with the postorbital.

QUADRATUM (Fig. 11). Both quadrates are preserved complete, each with a broad transverse articulation for the lower jaw at its ventral

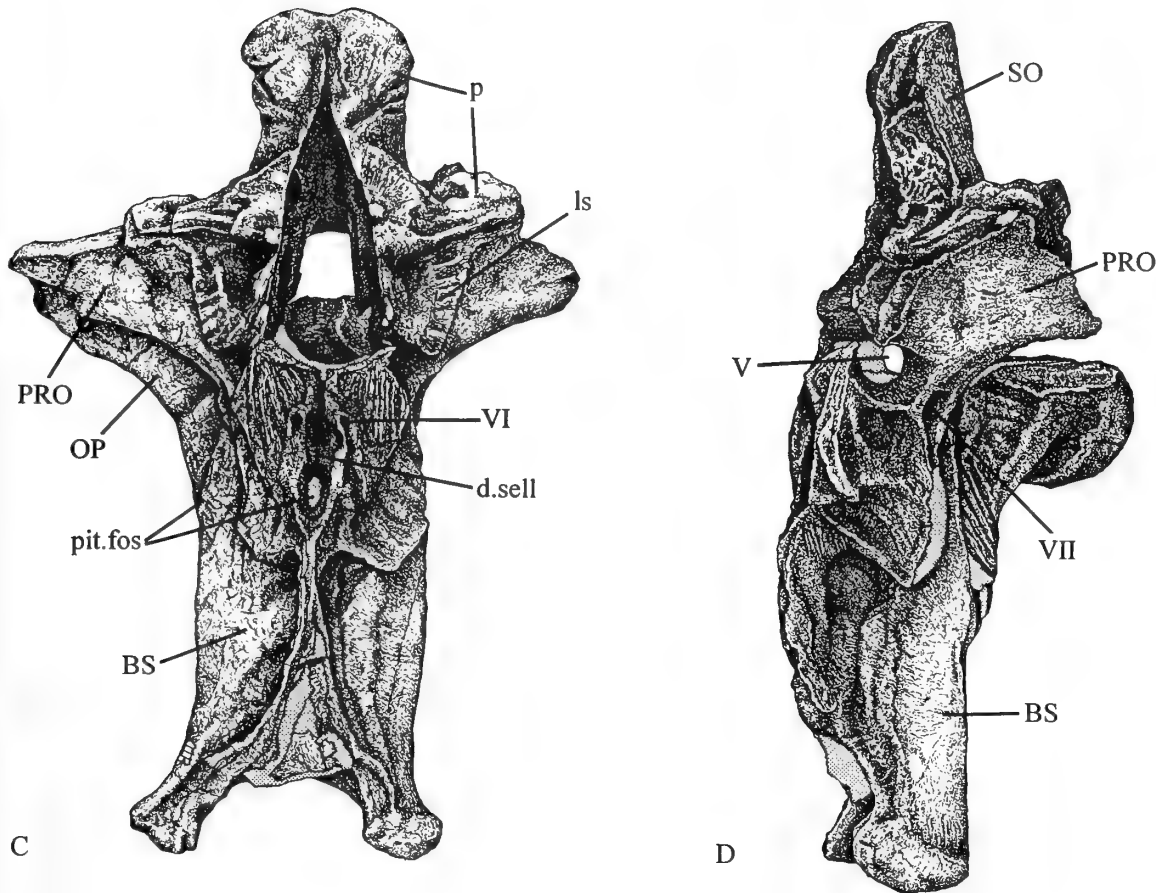


Fig. 9 cont *Baryonyx walkeri*, holotype, BMNH R9951; occiput and posterior part of braincase, lacking detached left opisthotic. **C**, anterior view; **D**, lateral. $\times 0.5$.

end. Viewed posteriorly, the quadrate tapers rapidly upwards from the lower jaw articulation into a narrow shaft that swings a little anterolaterally and then dorsally. It terminates in an expanded knob-like head that fitted into the underside of the squamosal; on the lateral side of the head is a small, distinct, slightly concave facet. The lateral surface of the broad basal part of the quadrate forms a large, rugose, kidney-shaped concavity which provided an immovable sutural attachment for the quadratojugal. Higher up the shaft is a laterally directed ridge, its outer end forming a narrow sutural surface, also for the quadratojugal. Between these two quadratojugal attachments lay a large, elongated quadrate foramen delimited medially by the quadrate and laterally by the quadratojugal. This foramen is much larger than the equivalent foramen of *Allosaurus*, which is almost entirely enclosed by the quadrate.

The entire anterior side of the quadrate is extended forwards into a wide pterygoid flange; the medial side of the lower half of this flange was presumably applied to the lateral face of the pterygoid. In *Allosaurus* this flange is directed obliquely towards the midline. The broad quadrate condyle, extending transversely mediad from the quadratojugal facet, is characterized by a screw-like sigmoid swelling; this is anterior in position on the medial side but curves round below the condyle to a posterior position on the lateral side. This surface, which articulated with the lower jaw, is much wider mediadly than laterally.

Lower jaw (Fig. 12)

Parts of both rami are preserved, including:

Left side: dentary (virtually complete); splenial (fragmentary); angular (partial).

Right side: dentary (a section of the dentigerous bar containing eight alveoli, probably nos. 18–25); splenial (complete); surangular (fragmentary); angular (partial); coronoid (complete).

DENTARY (Figs 13, 14). Of all the elements in the mandible, the left dentary is the best preserved. It was found broken into two: an anterior portion containing the first 26 tooth alveoli and a posterior portion containing the last 6. The broken ends had remained in contact with each other, but the two parts had undergone a relative dislocation to produce a divergence of about 45° from the straight line. Nevertheless, their two ends can be fitted together without the interpolation of any significant missing portion. There were therefore 32 teeth in each complete dentary, 64 in the entire lower jaw.

The anterior two-thirds of the dentary (apart from the terminal expansion) is essentially elongated from front to back and flattened from side to side. Its labial and lingual sides are flat and parallel; the dorsal and ventral margins are nearly parallel, but they do converge a little anteriorly. The dentigerous dorsal surface is also flat and demarcated from the labial and lingual surfaces on either side by a

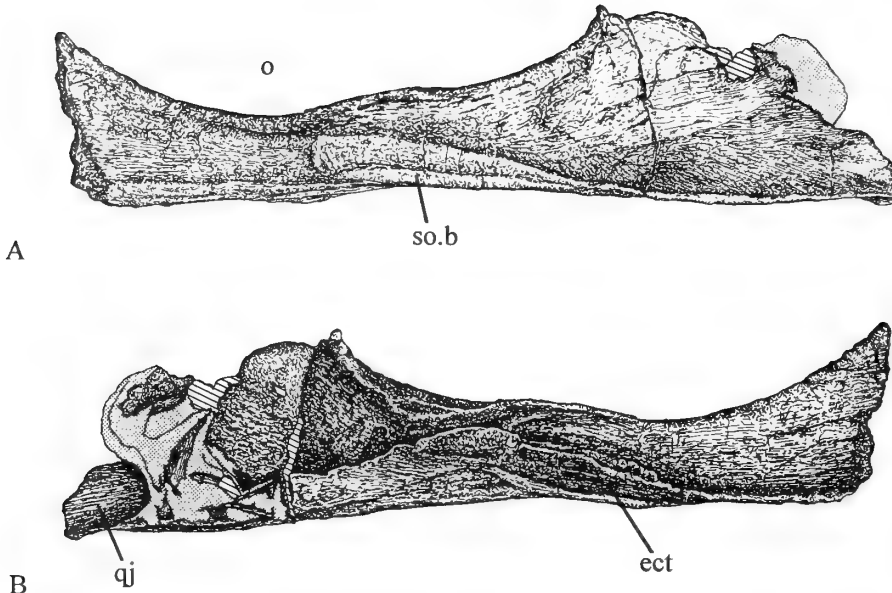


Fig. 10 *Baryonyx walkeri*, holotype, BMNH R9951; left jugal. A, lateral view; B, medial. $\times 0.5$.

right angled corner. The ventral margin is rounded so that it would appear U-shaped in transverse section. Viewed from either side, the dorsal margin is bent significantly upwards as it approaches the anterior end: at about the level of the 9th tooth alveolus it is angled upwards through some 25° and then runs in a more or less straight line to the anterodorsal corner of the bone, i.e. to the region of the 1st tooth. Forwards of the level of the 9th alveolus the dentary starts to expand both vertically and laterally (thereby creating the enlarged 'terminal rosette').

The ventral margin, at the extreme anterior end, passes smoothly into the anterior margin. This region is where the two rami, left and right, joined at the mandibular symphysis. The symphyseal surface,

however, is marked by only a very few short parallel striations on the lingual side of the dentary, suggesting that the symphysis must have been effected through connective tissue only, retaining some mobility between the two jaw rami.

The posterior third of the dentary is altogether much thinner than the anterior part; it has a broader, blade-like appearance, expanded vertically, with the dorsal and ventral margins diverging widely posteriorly. Indeed, the Meckelian groove on its lingual surface widens backwards to the extent that it disappears into a broad, flat surface occupying the entire height of the bone between the dorsal and ventral rims. The labial surface is flat and featureless.

The dorsal and ventral margins of this posterior dentary 'blade'

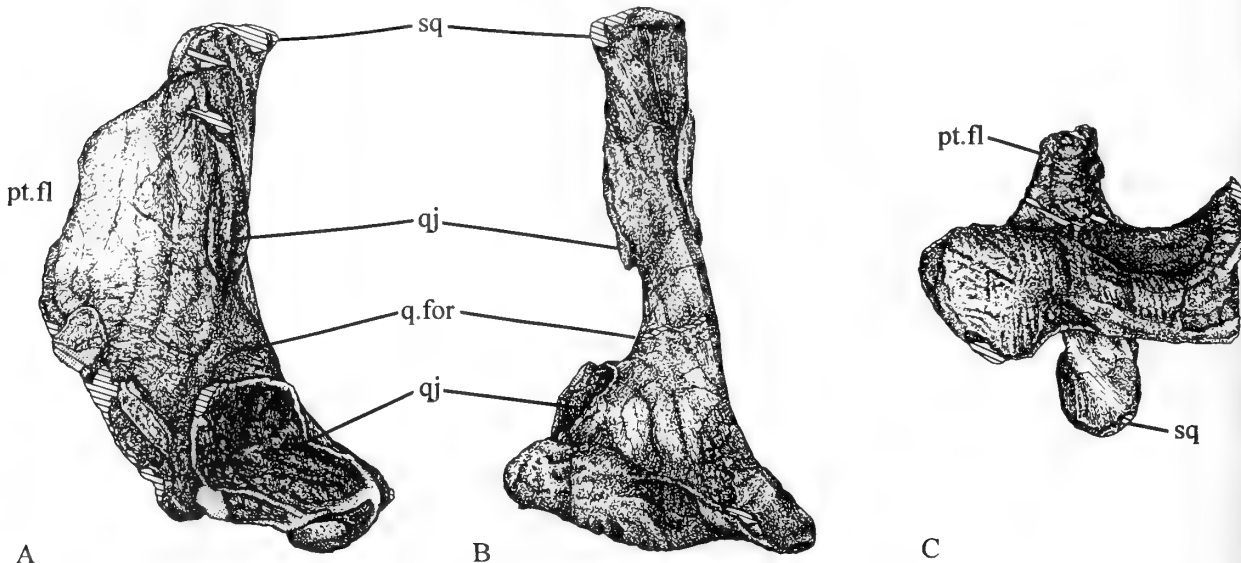


Fig. 11 *Baryonyx walkeri*, holotype, BMNH R9951; left quadrate. A, lateral view; B, posterior; C, ventral. $\times 0.5$.

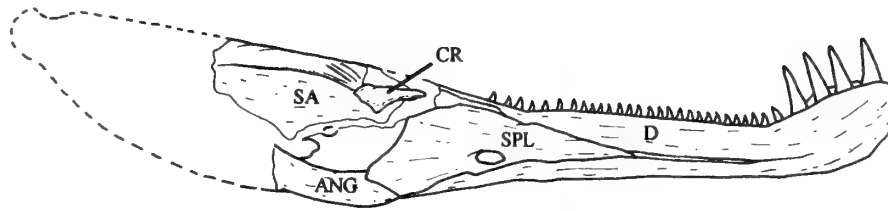


Fig. 12 *Baryonyx walkeri*, holotype, BMNH R9951; partial reconstruction of lower jaw, in medial (lingual) aspect. $\times 0.135$.

are much narrower than are the margins of the stout anterior part of the dentary, but they are still somewhat thickened anteriorly, being backward continuations of the lips of the ever-widening Meckelian groove and continuing to curl round towards each other as distinct overhangs. The dorsal overhang forms a slot for the surangular. As the blade widens posteriorly its ventral lip, which forms a slot for the angular, diminishes and eventually disappears altogether; the form of this fragile posterior end of the dentary is indicated only by an outline that has, in places, been badly damaged and eroded. The ventral margin is nevertheless preserved intact and forms a smooth, slightly convex curve. Its extreme tip (as preserved) is probably not far short of what was once the posterior end of the complete dentary. From that end the dorsal margin of the dentary ascended anterodorsally to the widest point and then descended again forwards, but this part is extremely thin and, as preserved, has an irregularly broken edge. However, at two places on this broken edge there are small lengths of smooth-edged bone of a curved outline, recessed from the general level of the surface, which are doubtless parts of the margins of dentary fenestrae.

In dorsal view the lingual margin of the dentary forms a smooth, gently concave curve, somewhat more marked in front of the 9th alveolus than behind it. The labial margin, by contrast, curves outwards markedly to accommodate the roots of the greatly enlarged first 5 teeth; this swelling produces the mandibular portion of the terminal rosette'.

The Meckelian groove runs lengthwise along the lingual surface of the fragment, at a little below mid-height. It has a strongly overhanging dorsal lip and a fairly well-marked ventral lip, the gap between them being 16 mm; the base of the groove is a smooth channel. Anteriorly the groove becomes shallower and narrower, its lips become less pronounced, and it peters out anteriorly some 60 mm behind the symphysis and beneath the wall separating the 4th and 5th alveoli. Posteriorly, from the 19th alveolus backwards, the lips of the Meckelian groove are themselves grooved and facetted for articulation with the splenial. Indeed, the major part of the lingual surface of the posterior end of the dentary, tapering forwards into the Meckelian groove, served as a slot for the splenial.

The labial surface of the dentary bears a number of foramina, which doubtless served for the passage of blood vessels and/or nerves. There are about 25 scattered over the expanded area at the anterior end, with a much smaller number farther back. There is also a linear series of mental foramina running parallel to the dorsal margin of the bone, lying in a shallow groove at approximately the level of the bases of the alveoli. These do not, however, bear a fixed numerical relationship to the alveoli, being significantly fewer than the latter. They served for the passage of branches of the inferior lveolar nerve and also, presumably, blood vessels. The last foramen of this linear series happens to be on the anterior end of the posterior segment; behind this the shallow groove continues all the way to the posterior end of the dentary as preserved.

The dorsal border of the lingual surface of the dentigerous region of the dentary is, for most of its length, of approximately the same height as the dorsal border of the labial wall and as the interdental plates. The interdental plates are, therefore, barely exposed in lingual view, unlike the usual theropod condition (e.g. *Allosaurus*).

The alveoli themselves vary in form, from squarish/circular in occlusal view (2nd) to egg-shaped (3rd) to a rectangle twice as broad as long (9th). They vary also in size (see 'Dentition'). They are immediately adjacent to each other so that they are separated by no more than a thin interalveolar wall. The lingual wall of the row of alveoli, i.e. the row of interdental plates, is separated from the dorsal rim of the lingual surface of the dentary by a deep paradental groove (the 'nutrient groove' of Osborn 1912). However, each alveolus communicates with the nutrient groove by means of a slot in its interdental plate, with a foramen at its base. For most of the tooth row these slots are narrow and situated posterolingually (see Fig. 14), but, in the case of the larger anterior teeth nos. 1–5, they are much wider and more anterior in position.

SPLENIAL (Fig. 15). The right splenial is preserved complete save for the fragile dorsal margin and posterior end. The left splenial, by contrast, is very incomplete, the only part of its true margin remaining being a small piece of its posterodorsal corner.

The splenial is a thin, narrow, subtriangular sheet of bone, its apex directed anteriorly, which was slotted into the Meckelian groove on the lingual surface of the dentary. The medial (or lingual) surface of the splenial is distinctly convex dorsoventrally, the convexity being more marked in the posterior half of the bone. The lateral (or labial) surface, facing the dentary, is correspondingly concave. Midway along the length of the element, just above its ventral border, is the moderately large splenial fenestra (= the anterior mylohyoid foramen of Currie & Zhao 1993 and the splenial foramen of Madsen 1976, the latter labelled Meckelian canal in his Plate 9), elongated in an anteroposterior direction. This fenestra is completely surrounded by bone in *Baryonyx* and *Sinraptor* but is in a marginal position in *Allosaurus*; in *Ceratosaurus* it is only small, and in *Coelophysis* and *Dilophosaurus* it is absent altogether.

The medial surface bears a sharp ridge just above its ventral margin, which, by virtue of its overhanging nature, produces a ventral-facing groove that received the dorsally directed, wrapped-around lower margin of the Meckelian groove on the dentary. Anterior to the splenial fenestra this splenial groove is well developed; beneath the splenial fenestra it is very shallow, forming nothing more than a faint lip; behind the fenestra the groove is again distinctly present, but it is narrower and shallower than in the anterior region and posteriorly it fades out altogether into a flat, narrow, ventral margin to the bone.

The dorsal margin of the splenial rises to a 'dorsal process'. Anterior to that the edge of the bone, although a little crushed, is almost straight. Posterior to the dorsal process, the dorsal margin of

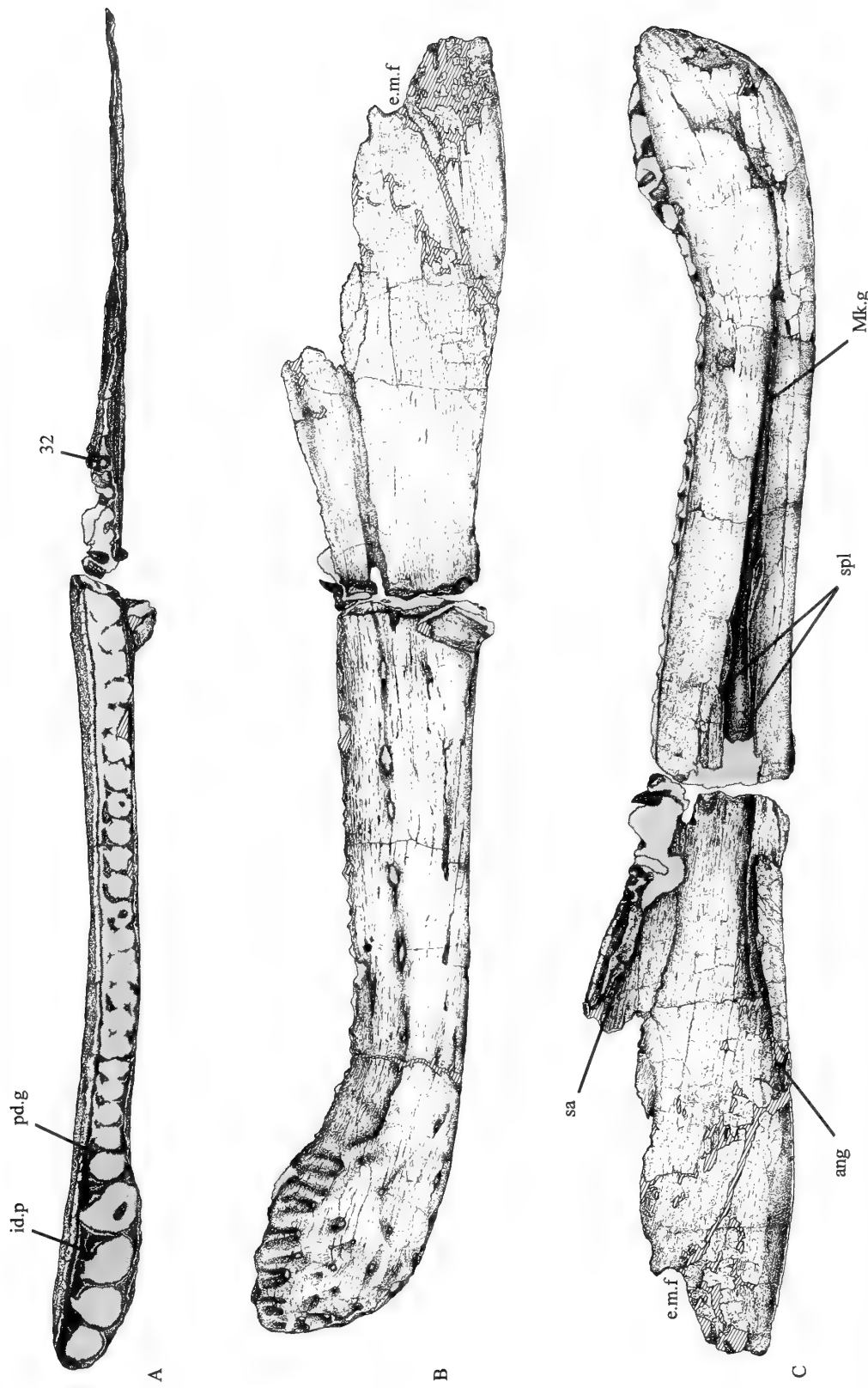


Fig. 13 *Baryonyx walkeri*, holotype, BMNH R9951; left dentary, A, dorsal (occlusal) view; B, lateral (labial); C, medial (lingual). $\times 0.33$.

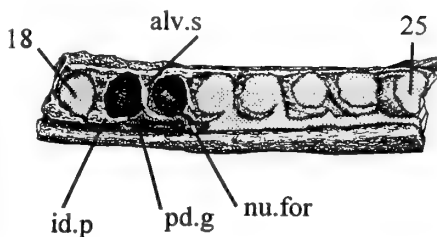


Fig. 14 *Baryonyx walkeri*, holotype, BMNH R9951; part of right dentary, in dorsal (occlusal) view. $\times 0.5$.

the splenial is preserved complete and forms a smooth concave curve, extending posteroventrally and then posteriorly; this, presumably, formed the anteroventral border of the internal mandibular fenestra. The posterior end of the splenial which articulated with the angular is missing.

The anterior tip of the splenial is a flattened tongue that bears strong longitudinal striations on its lateral face. The ventral margin of the latter, just posterior to the splenial fenestra, forms a shelf, which would have received the anterior end of the angular.

SURANGULAR (Fig. 16). Only a large fragment of the right surangular is preserved. This is the central part of the stout upper border of the bone, which itself constitutes the upper border of the posterior half of the mandible as a whole. It consists essentially of a vertical plate, thin and irregularly broken below, which at its upper border is greatly thickened and folded over medially as a brow-like

bar overhanging the deep concavity of the adductor fossa. The bar itself is flattened above into a dorsomedially facing surface, divided by a low central ridge into two shallow parallel channels. This dorsomedial bar narrows posteriorly towards its presumed articulation with the articular, the upper surface loses its twin channels to become smooth and rounded, and the concavity beneath it becomes shallower and disappears just before the posterior break.

A prominent ridge arises in the middle of the lateral surface of the fragment as preserved and runs horizontally backwards, rapidly becoming extremely robust. It terminates at the break but presumably continued backwards as a buttress to the jaw articulation.

ANGULAR (Figs 17A, B). The central portions of both elements are preserved. The right, however, is less complete at either end and adds nothing to description of the left.

The entire angular appears to have been a somewhat boomerang-shaped element, flattened and bow-like and with a pronounced angle in its convex lower border. This lower border is thick and rounded, while the concave upper border is much sharper. The fragment is fairly broad dorsoventrally, but thin and fragile medio laterally. Its anterior end thins anteriorly and is directed a little upwards as well as forwards; its margin appears to be almost complete. The central region, where the blade is narrowest, has a very distinct, weakly concave upper border, which formed the lower margin of the external mandibular fenestra. The posterior end is broken off at right angles to the margins, but the preserved portion clearly indicates that it was both thickening and widening towards the rear.

The medial surface is flat and featureless. The lateral surface, which was applied to other post-dentary elements, is also flat. Posteriorly the thick rounded ventral border is produced laterally

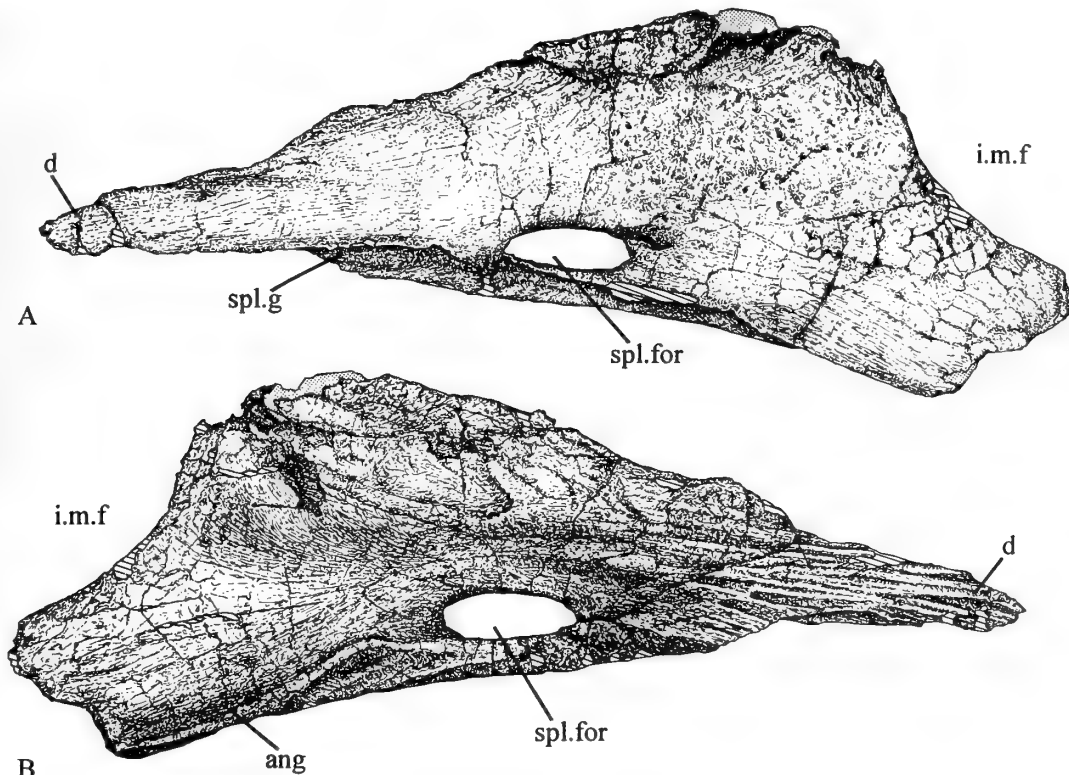


Fig. 15 *Baryonyx walkeri*, holotype, BMNH R9951; right splenial. A, medial (lingual) view; B, lateral (labial). $\times 0.5$.

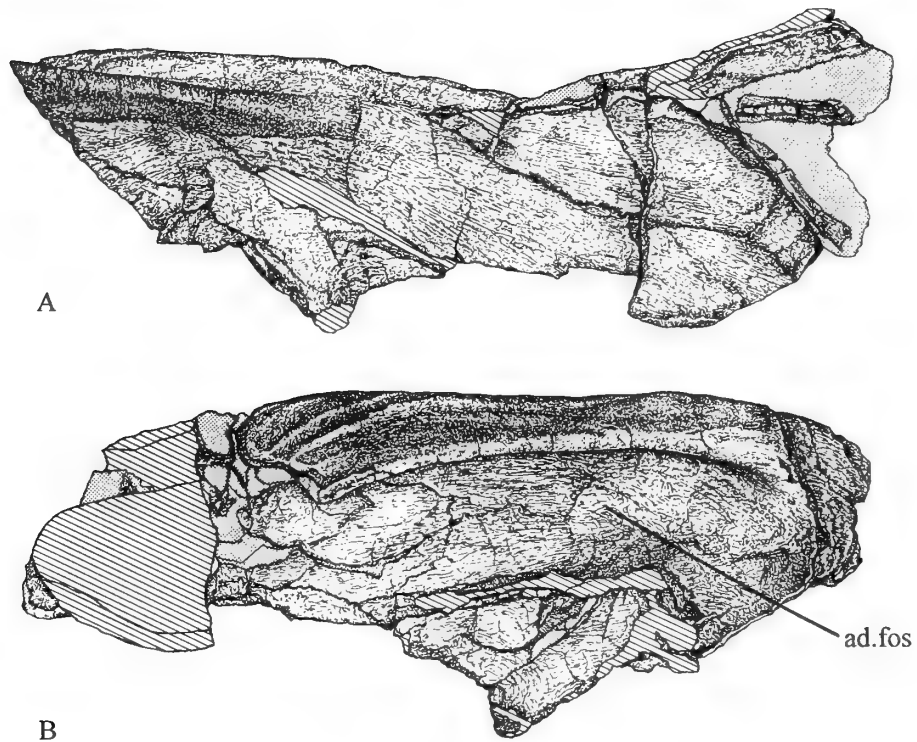


Fig. 16 *Baryonyx walkeri*, holotype, BMNH R9951; right surangular fragment. **A**, lateral (labial) view; **B**, medial (lingual). $\times 0.5$.

into a longitudinal flange with a deep ridged groove above it, presumably for articulation with the prearticular. Farther forwards, however, in the region of the angle in the ventral margin, this flange-and-groove becomes transformed into a simple rounded ridge with an elongated shallow depression between it and the angle; still farther forwards the ventral margin becomes much narrower.

The lateral surface of the angular, at the posterior end of the fragment as preserved and just beneath its dorsal margin (i.e. the lower border of the external mandibular fenestra) is depressed below the general level of the surface. The edge of this depression, demarcating it from the general level, runs more or less parallel to the lower margin of the bone in a gentle curve; the depressed area is therefore much thinner than the rest of the blade.

CORONOID (Figs 17C, D). A small, roughly triangular bone, seemingly complete, is presumed to be the right coronoid. The dorsal edge is the longest; the weakly concave posteroventral edge is slightly shorter; the undulating anteroventral edge is the shortest of the three. Both lateral and medial surfaces are generally flat. A broad, laterally facing facet for the prearticular runs along the anteroventral edge. Two somewhat similar facets for the surangular run along the posterior two-thirds of the dorsal edge, with a narrow ridge between them; one faces obliquely laterally and the other, rather narrower, obliquely medially. The concave posteroventral edge is the anterodorsal margin of the adductor fossa.

Dentition (Figs 18, 19)

Most of the teeth preserved are in isolation; a few remain in the premaxilla and maxilla, but none (except for a few tiny replacing teeth) remains in the dentary. They have a general theropod appearance, being simple recurved cones, somewhat flattened labiolingually,

with serrated mesial and distal carinae. At the same time, however, they show a number of characteristic peculiarities:

1. They have very long roots, tapering significantly towards the apex, so that each tooth as a whole is unusually long and slender. This character creates the false impression that the isolated teeth of *Baryonyx* are less recurved than those of most other carnivorous archosaurs. However, the larger tooth crowns are slightly less recurved than the smaller ones.
2. They show only slight labiolingual flattening, much less than in the more blade-like teeth of nearly all other theropods.
3. The carinae are strongly developed, forming, along both mesial and distal edges of the tooth, a distinct ridge with its surface demarcated from the general surface of the crown by a more or less straight line. The carinae run the full length of the crown.
4. Both mesial and distal carinae bear extremely fine denticles, approximately 7 to the millimetre; the only other theropods with comparable denticle count are *Saurornithoides*, with 7–8 per mm (Sues 1978), and *Ricardoestesia*, with about 5 per mm (Currie *et al.* 1990). The denticles (Fig. 19) are tall, narrow and sub-parallel-sided, with flat or slightly fluted tops (probably due to wear) and relatively uniform in size, irrespective of the size of the tooth. This condition differs markedly from that shown by theropods in general, where the basal length of the tooth denticles increases with increasing tooth size in linear fashion (Farlow *et al.* 1991). *Spinosaurus* (Stromer 1915), *Angaturama* (Kellner & Campos 1996) and *Irritator* (Martill *et al.* 1996) lack serrations altogether.
5. The lingual surfaces of the crowns are longitudinally fluted (i.e. they bear about 6–8 ridges).
6. The enamel on both surfaces has a finely granular appearance.

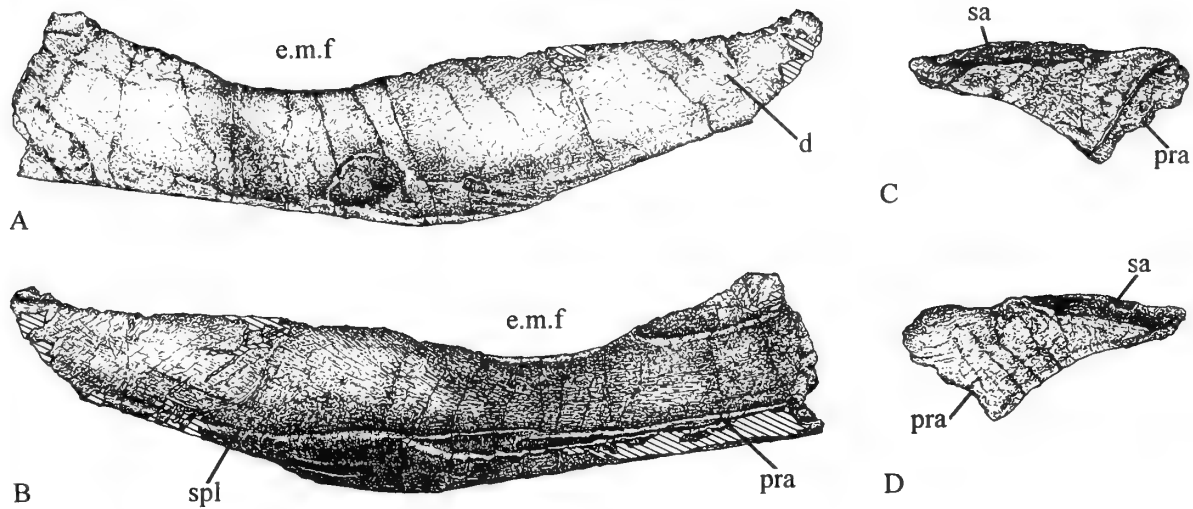


Fig. 17 *Baryonyx walkeri*, holotype, BMNH R9951. **A-B**, anterior part of left angular; **C-D**, right coronoid. **A**, lateral (labial) view; **B**, medial (lingual); **C**, lateral (labial); **D**, medial (lingual). $\times 0.5$.

The only differences between the several teeth preserved are those of size and degree of recurvature. Naturally the size of the actual teeth as preserved varies according to the degree of development of each, but apart from that there is a constant difference between the

sizes of the alveoli, more noticeable in the upper jaw than in the lower. In the premaxilla teeth nos 2 and 3 are the largest, 1 and 4 somewhat smaller, while 5, 6 and 7 form a decreasing series; the largest have twice the diameter of the smallest. In the maxilla the

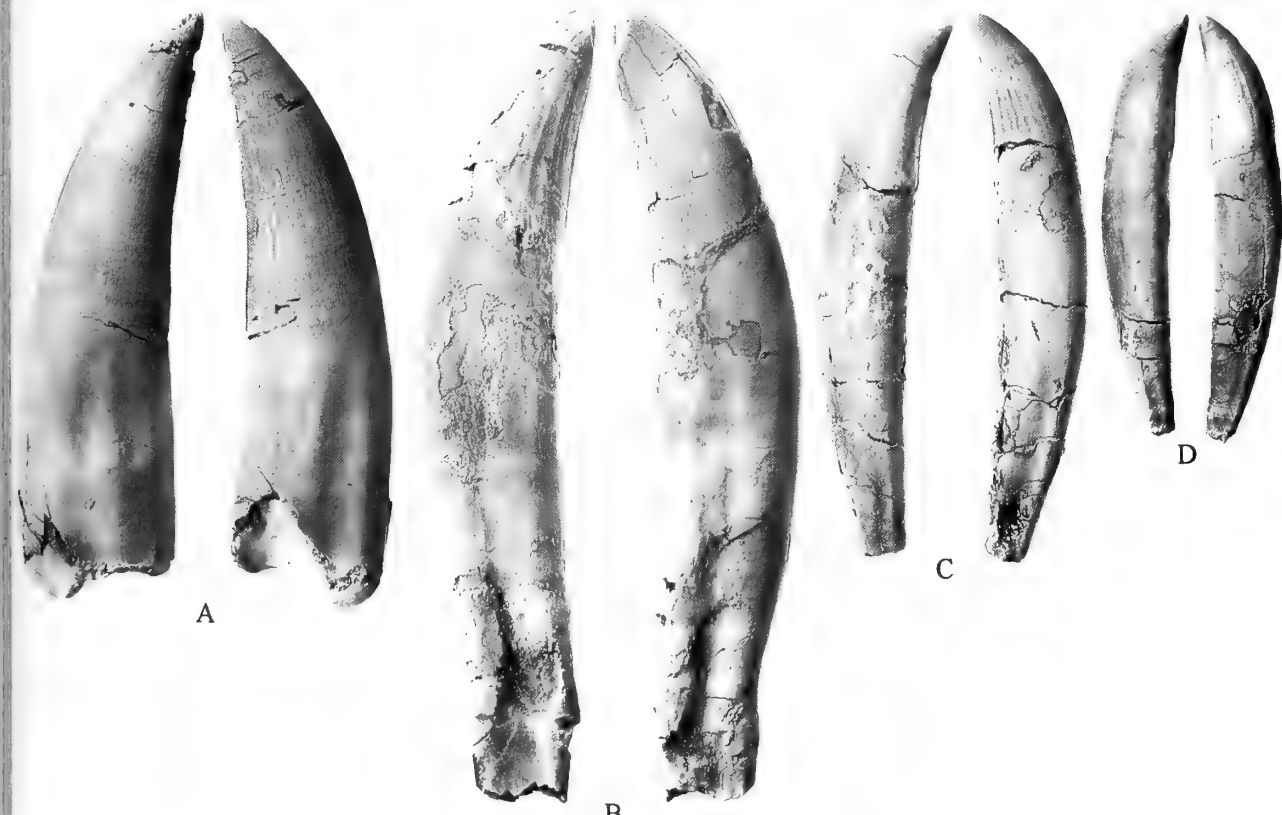


Fig. 18 *Baryonyx walkeri*, holotype, BMNH R9951; isolated teeth. **A**, left upper or right lower symphysial crown in (left) labial and (right) lingual views; **B**, right upper premaxillary or maxillary tooth in (left) lingual and (right) labial views; **C**, left maxillary or right dentary tooth in (left) labial and (right) lingual views; **D**, left dentary tooth in (left) labial and (right) lingual views. Natural size.

**A****B**

Fig. 19 *Baryonyx walkeri*, holotype, BMNH R9951; scanning electron micrographs of tooth crown in Fig. 18C. **A**, denticles on the mesial carina and the granular texture of the enamel, $\times 30$; **B**, higher magnification of four denticles from the centre of row in **A**, $\times 150$.

largest of those in the preserved portion (bearing only the first 7–8 alveoli) is no. 3, from which they diminish fairly regularly in both directions. In the dentary, by contrast, the size of the alveoli is generally much more regular, nos 5–26 forming a straight series of almost uniform diameter; 1–4, however, are appreciably larger, producing a slight swelling corresponding in position to the spatula-

late tip of the upper jaw but much less marked; 27–32 diminish regularly.

Vertebral column

CERVICAL REGION (Figs 20, 21). Five cervical vertebrae are preserved fairly complete, including the axis. Also preserved are the atlantal pleurocentrum (odontoid), the right atlantal neurapophysis, the axial intercentrum, and one cervical rib. The vertebrae were not found in articulation, so they are ordered according to the various morphological trends that they display. If it be assumed that the total cervical count was the usual theropod number, nine, then the vertebrae preserved, in addition to the axis (Ce2), are likely to be Ce3, Ce5, Ce6 and Ce8. Their most important dimensions, together with those of the dorsal vertebrae, are given in Table 1 below.

Table 1 Dimensions of the cervical, dorsal and proximal caudal vertebrae (all measurements are in mm)

	A	B	C	D	E	G	H	I	J	K	L	M
Ce2 (axis)	50	68	53	52	73	—	—	—	—	—	—	—
Ce3	55e	45	70	65	81	126	90	101	—	—	—	—
Ce5	61	39	80	58idc	74	178	115	117	—	—	—	—
Ce6	67e	44e	84	65	95	179	111	110	—	—	—	—
Ce8	84e	62	95	66e	120	204	99	98	—	—	—	—
D1	75e	80	90	80	91	tbd	—	123	87	16	50	27
D2	103	85	100	78	108	109	115	110	100	14	44	25
D3	85e	65	102	77	92	98	83	119	107	12	39	29
D4	80	65	88	87	90	—	—	—	—	—	—	—
D5	83	72	98	82	92	109	62	62	96	28	62	21
D6	88	73	90e	88	88	117	62	61	134	41	nfr	18
D7	—	—	—	—	—	129	70	63	140	48	nfr	20
D8	82e	74	70	84e	93	—	—	—	—	—	—	—
D10	—	—	—	—	—	140	66	—	—	—	—	—
D11	80	81	tbd	tbd	105	161	73	61	197	80	nfr	18
D13	88	96	100	98e	108	—	—	—	—	—	—	—
D14	104e	96	114	94e	110	184	69	68	201i	86	nfr	19
	A	B	C	D	E	F						
CaA	97	111	111	110	134	33						
CaB	91	99	92	107e	144	32						
CaC	114	112	—	—	140	—						

A, transverse diameter of anterior face of centrum; B, vertical diameter of anterior face of centrum; C, transverse diameter of posterior face of centrum; D, vertical diameter of posterior face of centrum; E, length of centrum below, rim to rim; F, transverse width of centrum at narrowest point (i.e. 'waist') (for proximal caudals only); G, length of neural arch (front of prezygapophysis to back of postzygapophysis; mean of both sides where both are available); H, total width across prezygapophyses; I, total width across postzygapophyses; J, height of neural spine (measured from roof of neural canal at anterior end); K, length of neural spine parallel to body axis (measured from point of divergence of postzygapophyses); L, length of neural spine plus rugosities; M, thickness of neural spine (measured at point of divergence of postzygapophyses); e, estimated; i, incomplete; idc, ignoring deep concavity in upper margin; nfr, no further rugosities; tbd, too badly damaged.

The cervical vertebrae themselves have the following general characters:

The neck as a whole tapers from the back towards the front. The centrum of each vertebra is significantly shorter than those behind it. The transverse diameter of the deeply concave posterior face of each vertebra is likewise significantly less than it is in the vertebra following, but the vertical diameters (except in the axis) remain more or less constant. Thus, while the posterior face of the axial centrum is an almost perfect circle, those of the succeeding verte-

brae become progressively more elongate transversely (See Table I, p. 30.) This progressive diminution of the vertebrae in a forward direction culminates in a remarkably small axis, its length being only 7.8% of the estimated length of the skull (comparable figures for *Allosaurus*, *Ceratosaurus*, *Coelophysis*, *Deinonychus* and *Dilophosaurus* are 13.6%, 9.8%, 15.7%, 10.8% and 10.6%). Each centrum is constricted in its middle so that it has a waisted or 'hour-glass' shape, but in fact there is no deepening of the floor of the neural canal within each vertebra like that found in some other archosaurs, e.g. '*Mandasuchus*' (Charig MS 1956). The centra are strongly opisthocoelous, the concavity of each posterior face articulating with a great ball-like convexity on the anterior face of the next centrum behind. There are no ventral keels on the centra. However, a faint ventral ridge is present on the posterior half of the axial centrum and on Ce8; the latter occurrence suggests that the undersides of the unknown Ce7 and Ce9 may have been similarly ridged.

Models were made of the missing cervical vertebrae (namely Ce4, Ce7 and Ce9), their dimensions and characters being estimated as intermediate between the actual vertebrae before and behind in the series as ordered by us. When all eight vertebrae (Ce2-Ce9), actual or modelled, were lined up in what we judged to be reasonable natural articulation between the opposing faces of the centra and between the relatively huge zygapophyses, then the neck was more or less straight; there was no sigmoidal curvature of the neck such as is found in many other archosaurs. More precisely, the two faces of each centrum lie parallel to each other; they are not at an angle to each other as in *Allosaurus*, *Ceratosaurus*, *Deinonychus* and many other archosaurs, in which the necks must have curved strongly upwards.

A large parapophysis projects laterally from an anteroventral position on the side of the centrum (except on the axis, see below) and retains that position throughout the series. The distance between the paired parapophysial facets, seen from below, increases as we pass backwards down the neck. This widening is due to the increasing diameter of the centra and affords useful confirmation of the correctness of our ordering. Immediately posterodorsal to the parapophysis lies a pleurocoel, the size of which increases backwards down the series; the left and right pleurocoels of each centrum appear not to communicate with each other across the midline. In Ce3 each side has two adjacent pleurocoels, separated by a septum.

Although in some instances the centrum and neural arch appear to be firmly sutured together, this is not always the case. In Ce5 the two elements were preserved adjacent but separate; they were somewhat distorted, and had to be taken apart in the laboratory and re-set. In Ce8 the centrum and neural arch were preserved completely separate in the same block. In the other vertebrae the line of the neurocentral suture is clearly visible. It runs more or less straight and horizontal and lies about one-third of the way up the sides of the neural canal. The diapophysis is on the side of the anterior half of the neural arch, directly above the parapophysis and the pleurocoel (in contrast to *Allosaurus*). It is flattened dorsoventrally, projects ventro-laterally and scarcely varies through the series. There are no laminae radiating from the diapophysis connecting it with the zygapophyses, which (as already stated) are remarkably large. The postzygapophyses do not diverge more widely from the midline and from each other than do the prezygapophyses.

The neural spines are low, transversely thin, inclined very slightly backwards, and without spine tables. In Ce5-Ce8 the anterior edge of the neural spine bifurcates ventrally into two ridges that diverge towards the left and right prezygapophyses respectively. The posterior edge bifurcates similarly into two ridges that likewise run down

towards the epiphyses. In both cases, just below the point of bifurcation and between the ridges, a massive, rugose, bony protuberance is developed in the midline, projecting respectively anteriorly and posteriorly, and clearly distinct from the neural spine itself. These projections, which doubtless served for the attachment of interspinous ligaments, vary considerably in size and form (see Fig. 20). Epiphyses are massively developed, but by contrast, there are no hypopophyses (except in the axis) or hynpantra.

The first two cervical vertebrae, the atlas and axis, differ greatly from the typical members of the series that follow them and must be described individually. The atlantal pleurocentrum forms the odontoid peg that protrudes from the front of the axis. Although it was found firmly attached to the dorsal third of the anterior face of the axial pleurocentrum, it is evident that it is not fused thereto; indeed, on the right-hand side it is somewhat displaced from its natural position. It is of fairly typical form: a hemispherical protruding peg with a flattish semicircular dorsal surface, convexly rounded in front, below, and on either side. Posteriorly these lower surfaces flare out like a collar to form a crescentic articulating surface for the (missing) atlantal intercentrum. At the base of the anterior surface is a small median depression which may well be the notochordal pit. The atlantal intercentrum is missing entirely. It may be presumed that it fitted into the middle third of the anterior face of the axial pleurocentrum.

The right atlantal neurapophysis (the right half of the neural arch of the atlas vertebra) appears in dorsolateral view as a large, roughly trapezoidal, plate-like element that arises dorsally by the shorter of its two parallel sides from what might best be described as a footplate below. It widens dorsomedially towards the longer parallel side, which is virtually straight, but at the same time it curves round more horizontally so that it would have approached the left element in the midline to form a roof over the most anterior part of the neural canal. It also becomes much thinner as it approaches its medial margin, which is so thin as to be almost blade-like. The anterolateral part of the smooth external (dorsolateral) surface is strongly convex in all directions. The internal (ventromedial) surface, which is correspondingly concave and almost as smooth, bears a distinct facet close to its posteroventral edge which articulated with the axial prezygapophysis. The anteroventral margin is concave in profile, smooth, and thickly rounded; it forms the rim of the anterior opening of the neural canal, from which the spinal cord passed forwards into the foramen magnum. The posteroventral margin is thin dorsally but somewhat thicker ventrally.

The base of this trapezium is expanded in two directions into what we have referred to above as a 'footplate': a medial process that extends towards the (missing) atlantal intercentrum, and a lateral process that forms a triangular wing when viewed from above or below. Neither of these processes has been perfectly preserved, both being a little eroded towards their ends. To the best of our knowledge no such lateral process has been reported in any other theropod.

The axial intercentrum is represented by the usual crescentic wedge. Allowing for some distortion, its posterior face fits fairly well into the ventral third of the anterior face of the axial pleurocentrum. Its anterodorsal face, which must have articulated with the missing atlantal intercentrum, is extended forwards into a protuberant lip. Between these two faces, beneath the lip, is the ventral surface, slightly concave from front to rear; on either side it curves upwards and becomes narrower.

The axis itself, with the odontoid attached to its anterior face, is almost perfectly preserved. It is very small compared to the presumed size of the skull. It shows strong opisthocoely (like the other cervicals), and its anterior face possesses a pair of facets, situated ventrolaterally, which articulated with the axial intercentrum. There

is one pair of pleurocoels, again as in the other cervicals. The parapophyses, though present, do not project laterally, and the diapophyses are reduced to small pyramidal tubercles. The neural spine possesses the hatchet-like shape typical of many reptilian axes; the epiphyses are very prominent, and a distinct hypophene is present.

According to Madsen (1976: 32), in *Allosaurus* the distance from the prezygapophyses to the postzygapophyses, relative to the width, is greater in the anterior cervicals, subequal in the mid-cervicals, and less in the posterior cervicals. In *Baryonyx*, the exact opposite obtains (see Table 1, p. 30).

Madsen also noted (*loc. cit.*) that in *Allosaurus* the epiphyses are long in the anterior part of the series but decrease progressively backwards to only a small ridge in Ce9. The same applies to *Sinraptor* (Currie & Zhao 1993: 2056). In *Baryonyx* the epiphyses are well-developed throughout the series; the longest of all are in Ce8, but those (though still well-developed) are less robust than the epiphyses of the more anterior vertebrae.

DORSAL REGION (Figs 22–26). The material available contains all or part of at least twelve dorsal vertebrae: seven preserved fairly complete, three centra lacking a neural arch (but one with a prezygapophysis and diapophysis) and two neural arches lacking a centrum. Like the cervicals, they were not found in articulation and have been ordered on their various morphological trends. If we assume that the total dorsal count was the usual theropod number, fourteen (making twenty-three presacrals altogether), then the vertebrae preserved seem to be: D1, D2, D3, D4 (centrum, left prezygapophysis and diapophysis only), D5, D6, D7 (neural arch diameter only), D8 (centrum only), [D9 missing entirely], D10 (neural arch only), D11, [D12 missing entirely], D13 (centrum only), D14. Additionally, there are other vertebral fragments that we cannot assign to any particular vertebra.

The lengths of the centra (see Table 1) are best measured ventrally, rim to rim. Even so, distortion and damage make it difficult to measure accurately, and some values (denoted with an 'e') are nothing more than reasonable estimates based on the information available. The first eight centra, except for D2 and the missing D7, are of a remarkably constant length, all being in the range 88–93 mm. They are a little longer than the anterior cervicals (73–81 mm), about the same as the mid-cervical Ce6 (95 mm), and appreciably shorter than the posterior cervical Ce8 (120 mm). D2, however, is anomalous in that it too is significantly longer (108 mm). The last four dorsal centra, except for the missing D12, are also longer (105–110 mm).

The lengths of the neural arches, measured from the anterior tip of the prezygapophysis to the posterior tip of the postzygapophysis, are likewise variable. They vary too in respect of the proportion of each to the length of the corresponding centrum. In the cervical vertebrae the neural arches are much longer than the centra so that the zygapophyses, anterior and posterior, project far beyond their centra; in the most anterior dorsals, by contrast, they are scarcely any longer at all. However, from about D5 backwards they gradually increase in length until in the last dorsal (D14) they are 67% longer than the centra. It is interesting to speculate as to the functional significance of these great differences.

Nevertheless, certain general characteristics of the dorsal vertebrae may be discerned. The diameters of the centra are, in general, more constant than the lengths referred to above, but they do display a few individual variations, summarized as follows:

Anterior face, transverse diameters 80–88 mm, varying irregularly, except for D1 75 mm (e) (estimate), D2 103 mm, D14 104 mm (e); vertical diameters, 65–81 mm, increasing steadily from D3 to

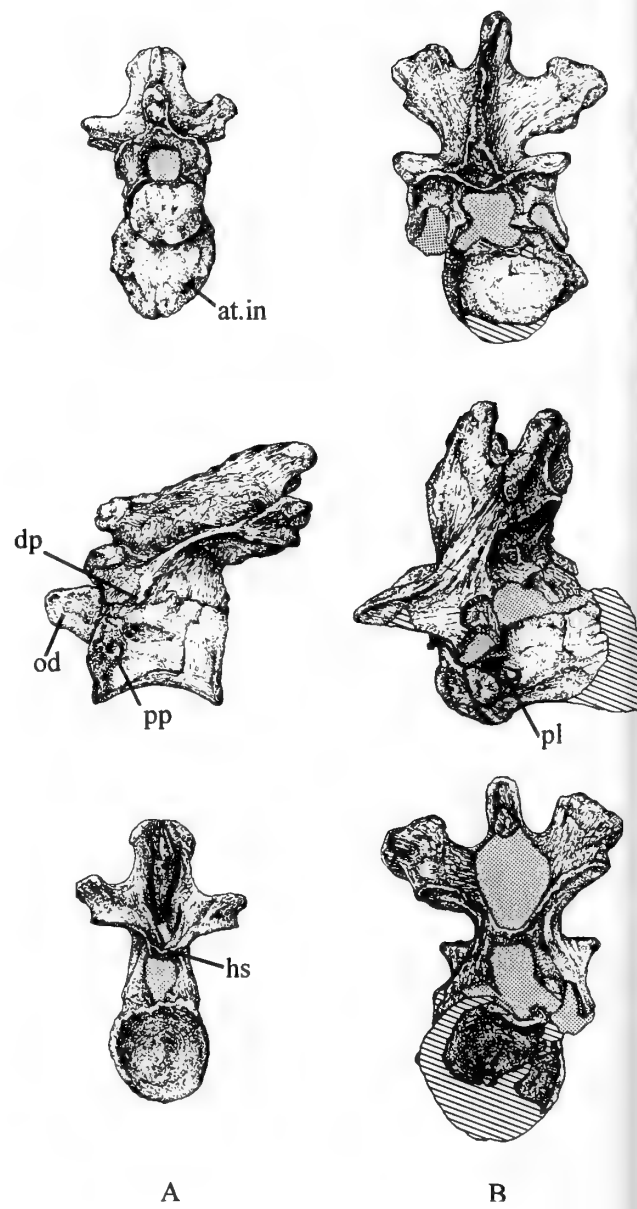


Fig. 20 *Baryonyx walkeri*, holotype, BMNH R9951; cervical vertebrae in (from top downwards) anterior, left lateral, and posterior views. A, axis; B, Ce3. $\times 0.25$.

D11, except for [D1 80 mm, D2 85 mm], D13 96 mm, D14 96 mm. Posterior face, transverse diameters, 88–102 mm, varying irregularly, except for D8 70 mm, D14 114 mm; vertical diameters 77–88 mm, varying irregularly, except for D13 98 mm (e), D14 96 mm (e).

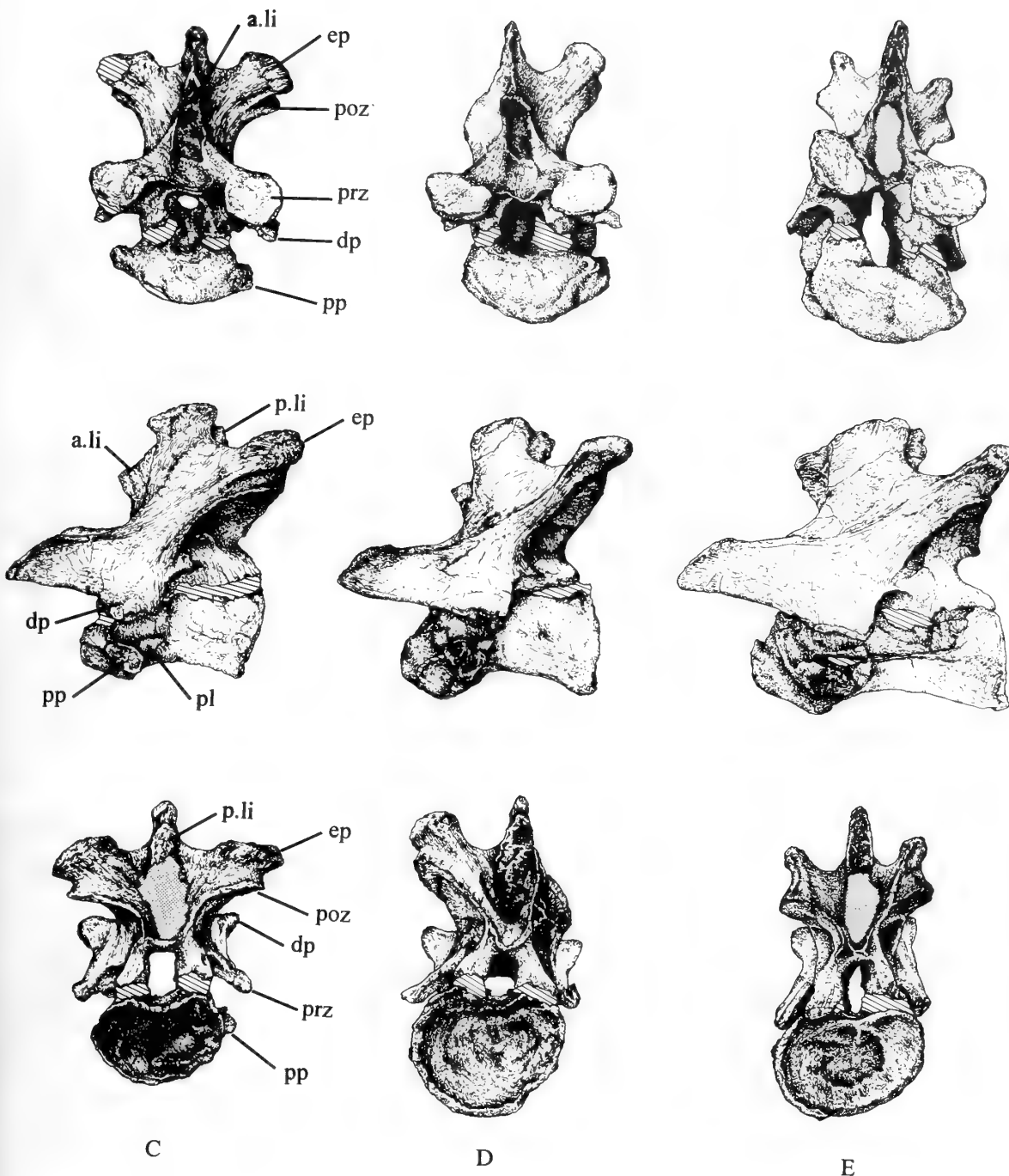


Fig. 20 cont *Baryonyx walkeri*, holotype, BMNH R9951; cervical vertebrae in (from top downwards) anterior, left lateral, and posterior views. **C**, Ce5; **D**, Ce6; **E**, Ce8. $\times 0.25$.

From these figures we may draw the following general conclusions:

- With a few exceptions, the transverse diameters of both faces are greater than the corresponding vertical diameters. Thus the faces are not truly circular but transversely elongate ovals.
- With a few exceptions, the dimensions of the posterior faces are

greater than the corresponding dimensions of the anterior faces with which they articulate (i.e. of the vertebra immediately behind). Individually, however, there seems to be very little or no correlation between the two.

3. There is a tendency for the first two dorsal centra (D1, D2) and the last two (D13, D14) to be stouter than the others. This may be

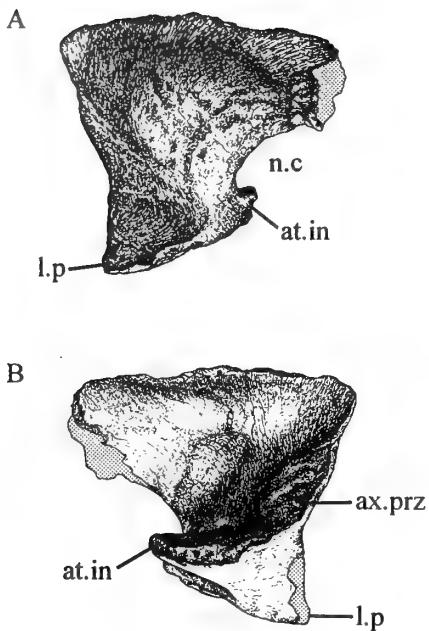


Fig. 21 *Baryonyx walkeri*, holotype, BMNH R9951; right neurapophysis. **A**, lateral view; **B**, medial. $\times 0.5$.

correlated with their being positioned in the body directly above the limbs, D1 and D2 in the shoulder region and D13 and D14 immediately in front of the sacrum.

The degree of curvature of the faces of the centra decreases steadily from front to back of the dorsal series. Thus the anterior face is strongly convex (effectively ball-like) in D1-D3, moderately convex in D4, almost flat in D5, completely flat in D6, and slightly concave (where known) in D8-D14. The posterior face is very deeply concave in D1-D5, moderately concave in D6, very slightly concave in D8 and D11, and then (reversing the trend a little) slightly concave again in D13 and D14. Incidentally, these observations provoke a question: why are D4 and D5 so strongly opisthocoelous, when the anterior faces of D5 and D6 – with which, of course, they respectively articulate – are, by contrast, almost flat and completely flat respectively?

The tendency to develop a ventral keel beneath the centrum increases rapidly in the anterior part of the dorsal series, reaching its maximum in D4 and D5, but thereafter tailing off posteriorly. D1 bears only a modest ridge, best developed at the anterior end. D2 has a distinct keel, running the whole length of the centrum; D3 is much the same, but the keel is slightly better developed; D4 and D5 continue the trend, with the keel becoming somewhat deeper. In D6 and D8, however, the whole centrum has become ‘waisted’, the keel has disappeared but there is still a sharp ridge. D11 is very similar, except that the median ridge is very faint; in D13 it is quite distinct again; and D14 is deeply waisted but its ridge has disappeared altogether.

It is perhaps remarkable that, whereas the faces of the centra of the cervical vertebrae of *Baryonyx* are not ‘offset’ at all, those of the dorsal vertebrae – especially the first six – lie not perpendicular to the axis of the centrum but at an oblique angle thereto. This ‘obliquity’ is very pronounced in D1-D3, diminishes progressively in D4 and D5, and becomes more prominent again in D6. It is also present, albeit to only a minor degree, in D8 and D14, but it is entirely absent

in D11 and D13. This phenomenon is generally considered to indicate curvature of the vertebral column. However, the angle of inclination of an articulating face of a centrum, considered alone, does not indicate this; what would produce a curvature of the vertebral column (i.e. angulation between two adjacent vertebrae) would be a *difference* between the two faces of a centrum, or between two faces that articulate with each other in their respective angles of inclination.

As in most archosaurs, the position of the parapophyses varies greatly along the dorsal series; as we pass posteriorly down the series they migrate upwards and backwards, moving from the centrum (D1-D4) to the neural arch (D11-D14). In the intermediate vertebrae (D5-D10) the parapophysis lies across the neurocentral suture and is therefore formed in part by the centrum and in part by the neural arch. In more detail, the position of the parapophysis is as follows:

- D1 low on centrum, at anteroventral corner
- D2 still low, but a little higher
- D3 almost at mid-centrum level
- D4 anterodorsal at top of centrum, almost reaching neuro-central suture
- D5, D6 only top quarter of parapophysial facet has moved on to neural arch
- D7 parapophysial facet exactly half-way across neurocentral suture
- D8, D10,
- D11 parapophysial facet still partly on centrum
- D13 functionally, completely on neural arch
- D14 wholly on neural arch

In many other archosaurs the parapophysis continues to migrate posteriorly as we pass backwards down the dorsal series, so that, in the posterior dorsals, it eventually comes to lie on the anterior edge of the transverse process itself. This does not happen in *Baryonyx*, where, even in the last dorsal (D14), the parapophysis remains distinct from, and anterior to, the transverse process.

Like the cervicals, the dorsal centra are equipped with pleurocoels, but these peter out posteriorly. In D1 there is a double pleurocoel, just posterodorsal to the parapophysis. In D2 and D3 there is a single pleurocoel in the same position; in D2 it is longer and slit-like, perhaps because of crushing. In D4 and D5 the pleurocoel lies directly behind the parapophysis; it is an oval opening in D4 and smaller in D5. In D6 there is a deep hollow in the same position, but, since it does not connect with the cavity of the bone, it cannot be a true pleurocoel. In D8 there is a longer, shallower cavity; this has virtually disappeared in D11 and has gone altogether in D13 and D14.

The transverse processes are flat-topped. Each has a sharp anterior edge that swings round to form the anterior horizontal lamina (nomenclature of Britt 1993), a ridge continuous with the lateral edge of the prezygapophysis. A similar ridge, the posterior horizontal lamina, likewise unites the posterior edge of the transverse process with the postzygapophysis. Beneath the transverse process lie two thin but powerful supporting buttresses, one (the anterior infradiapophysial lamina) running anteroventrally towards the parapophysis and the other (the posterior infradiapophysial lamina) towards the posterodorsal corner of the centrum. These two laminae, together with the anterior and posterior edges of the transverse process, enclose three deep triangular cavities (the infraprezygapophysial fossa, infradiapophysial fossa, and infrapostzygapophysial fossa respectively). In the more posterior vertebrae of the series the infradiapophysial fossa contains supplementary buttresses of much weaker construction (one each in D10[?] and D14 but three in D11).

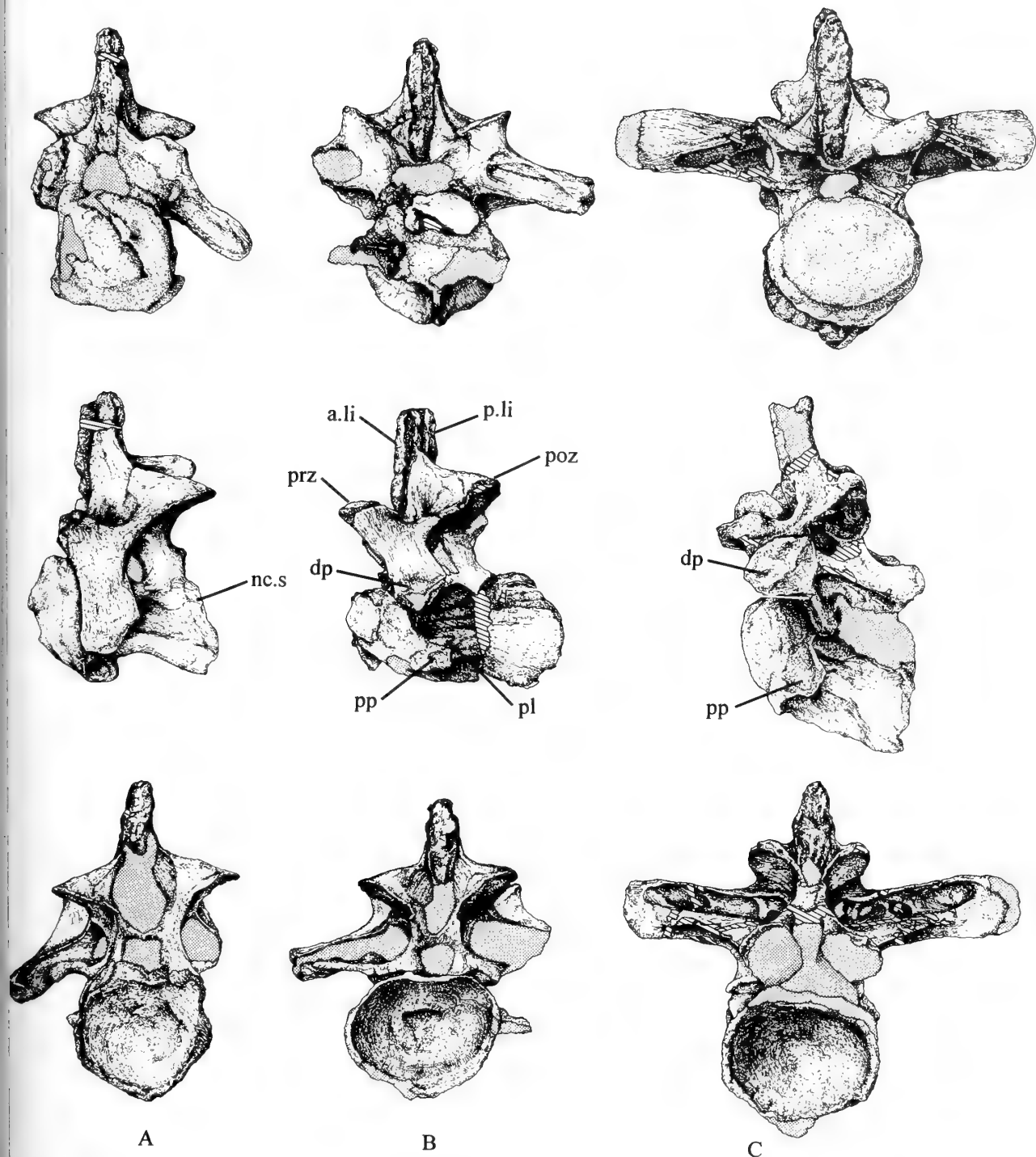


fig. 22 *Baryonyx walkeri*, holotype, BMNH R9951; anterior dorsal vertebrae in (from top downwards) anterior, left lateral, and posterior views. **A**, D1; **B**, D2; **C**, D3. $\times 0.25$.

The lateral projection of the transverse processes from the sides of the neural arch is also directed differently in different parts of the dorsal series. Thus in D1 and D2 they project slightly downwards, in D3 horizontally, in D5 strongly upwards, in D6 a little less steeply upwards, in D7 less steeply still, in D11 very steeply upwards again,

and in D14 less steeply again (much as in D7). In all cases, however, the transverse processes – seen from above – are more or less perpendicular to the body axis; they are angled neither anterolaterally nor posterolaterally.

In the most anterior members of the dorsal series the pre-

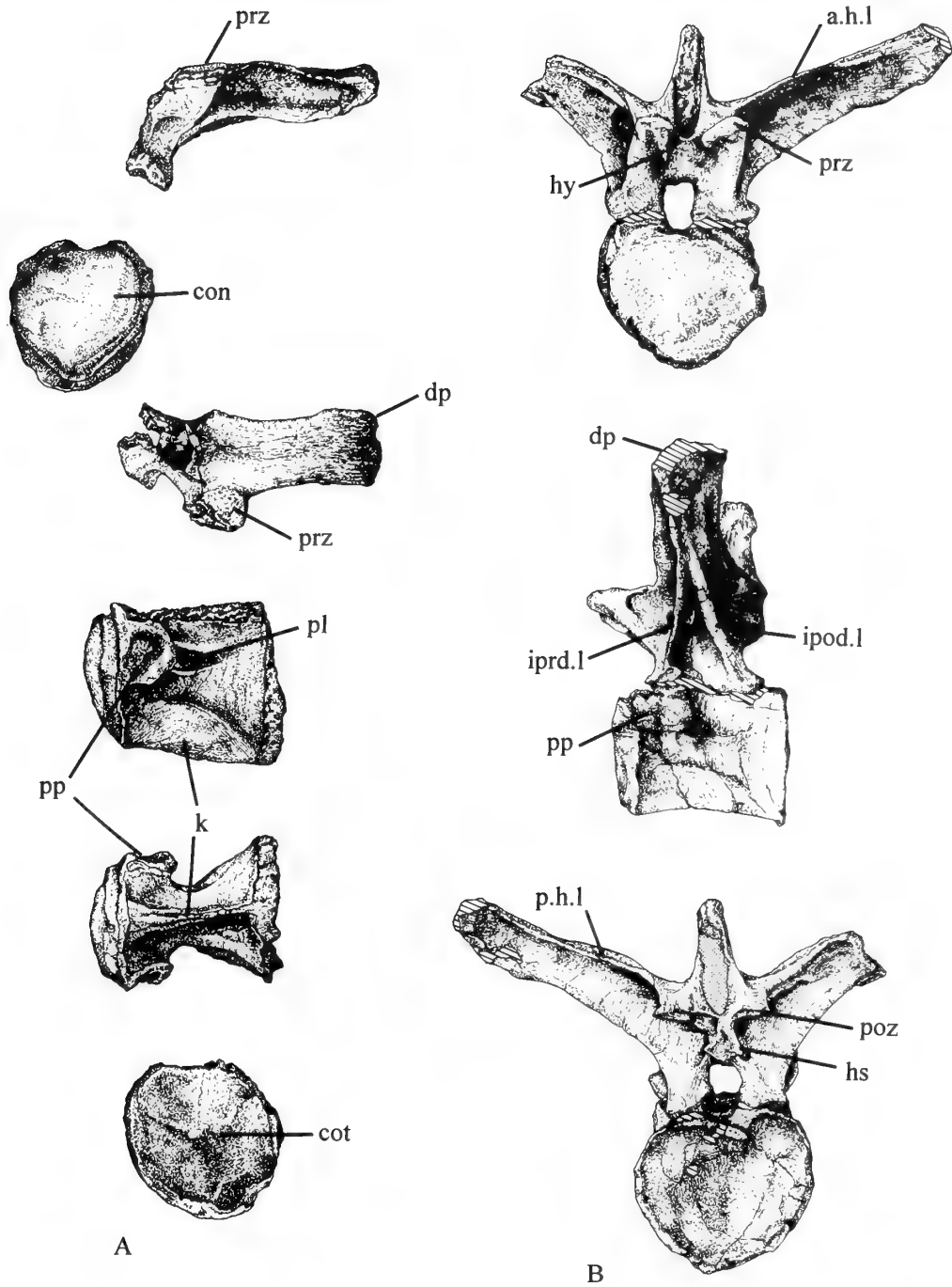


Fig. 23 *Baryonyx walkeri*, holotype, BMNH R9951; 4th and 5th dorsal vertebrae. **A**, D4 (from top downwards) centrum and left transverse process in anterior view; left transverse process in dorsal view; centrum in left lateral, ventral and posterior views. **B**, D5 in (from top downwards) anterior, left lateral, and posterior views. $\times 0.25$.

zygapophysis projects directly from the anterior edge of the dorsal surface of the transverse process. The condition in D1 cannot be seen, the relevant part of the vertebra having been broken off, but it is very noticeable in D2 and progressively less so in D3 and D4. In D5 the prezygapophysis has its own separate peduncle.

The distance (if any) between the posterior edge of the transverse process and the postzygapophysis, along the posterior horizontal

lamina, is yet another highly variable parameter. It is, however, impossible to quantify numerically because all the relevant surfaces and edges are rounded, so that there are no fixed reference points from which to take measurements. In D1-D3 there is a considerable (though diminishing) distance between these two structures. In D5-D7 the rear edge of the transverse process (viewed from the side) joins the postzygapophysis approximately at its middle. In D11 it

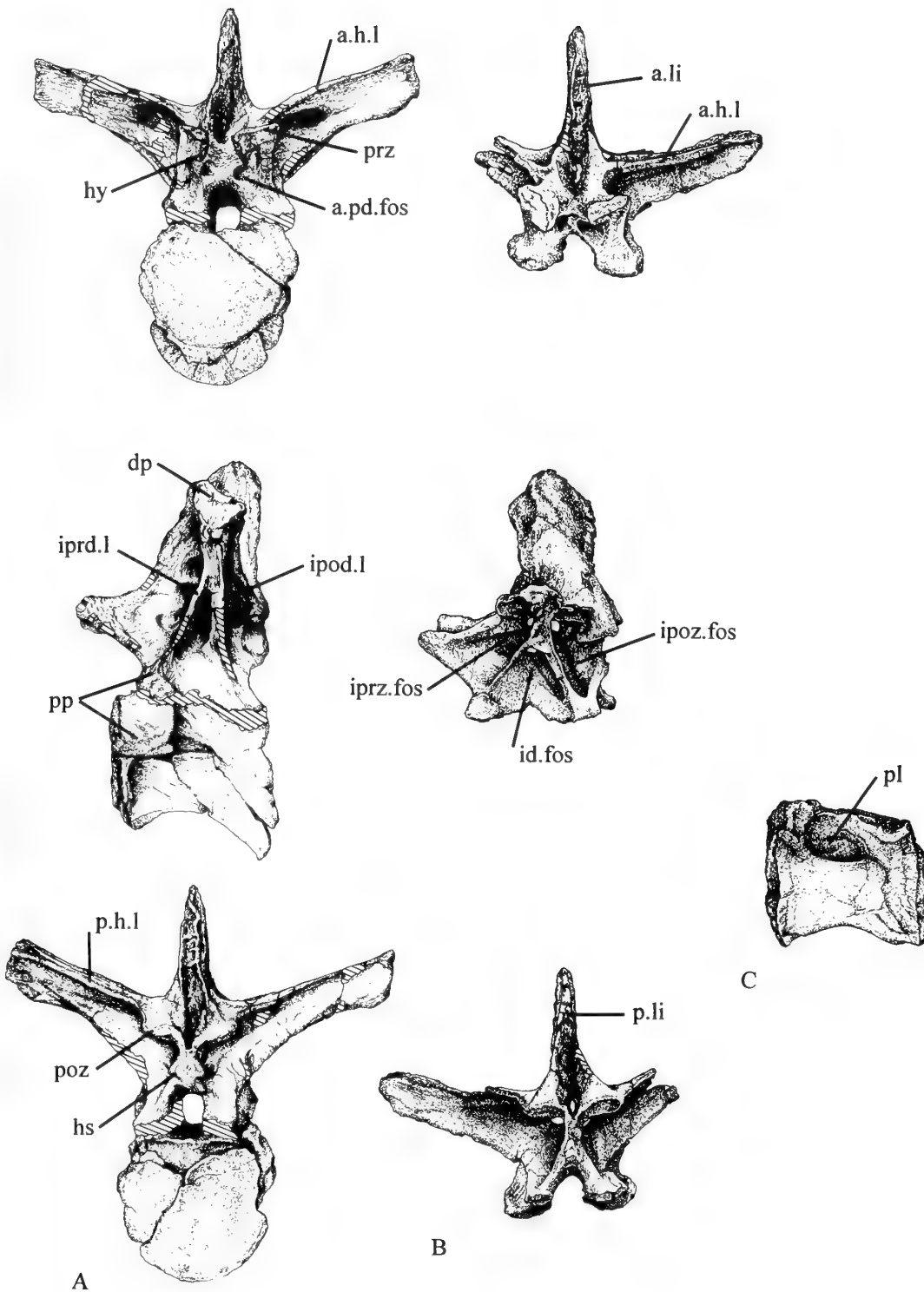


Fig. 24 *Baryonyx walkeri*, holotype, BMNH R9951; 6th-8th dorsal vertebrae. **A**, D6 in (from top downwards) anterior, left lateral, and posterior views; **B**, D7 neural arch and spine in (from top downwards) anterior, left lateral, and posterior views; **C**, D8 centrum in left lateral view. $\times 0.25$.

joins a little way forward of the mid-point, and in D14 it ends just in front of the postzygapophysis.

Baryonyx, like many other large dinosaurs, reduced its weight by developing fenestrations in its neural arches as well as pleurocoels in

its centra. These fenestrations occur in places where the mechanical stresses on the vertebra are not sufficiently great to require complete ossification of the skeletal structure. Essentially, these locations are around the base of the transverse process. Thus, at the proximal end

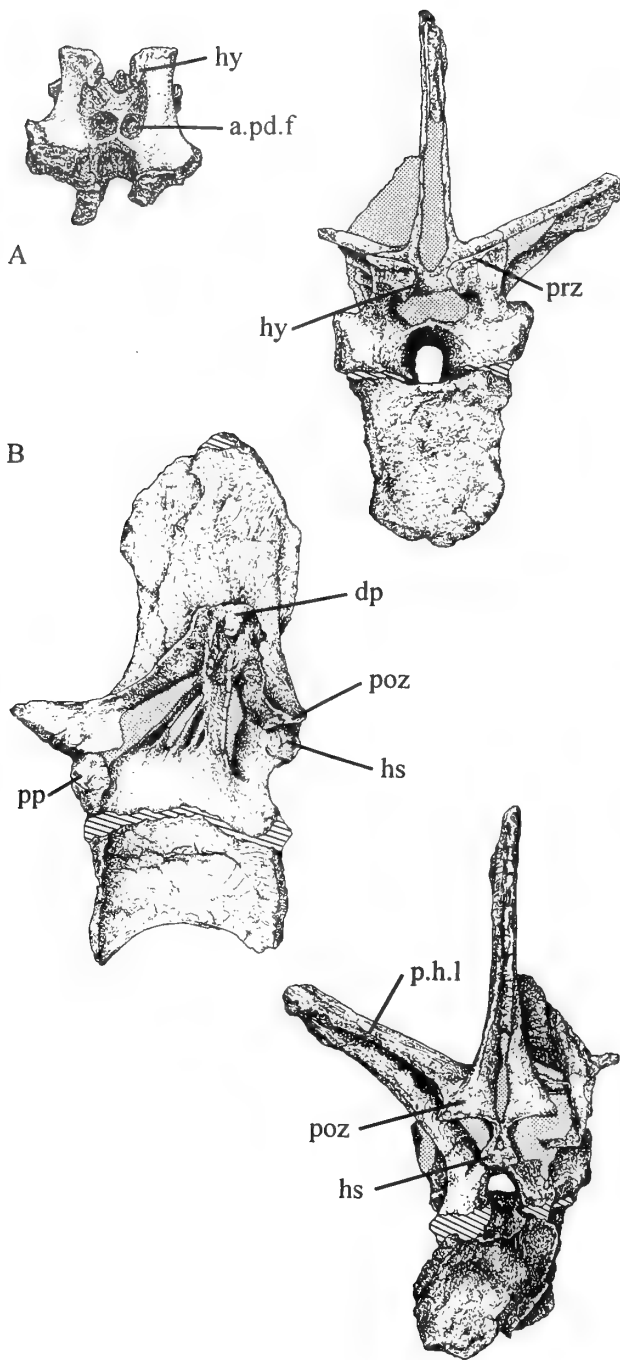


Fig. 25 *Baryonyx walkeri*, holotype, BMNH R9951; 10th-11th dorsal vertebrae. A, D10 neural arch fragment in anterior view; B, D11 in (from top downwards) anterior, left lateral, and posterior views. $\times 0.25$.

of its flat dorsal surface (i.e. at the base of the neural spine) there is what we might call a dorsal fenestration. Underneath the transverse process there are three ventral fenestrations, one at the apex of each fossa – an anterior, a middle, and a posterior – making four fenestrations altogether on each side of the vertebra.

In D4 and D5 the three ventral fenestrations only are present. In D6 and D7 there is also a dorsal fenestration, more pronounced in the

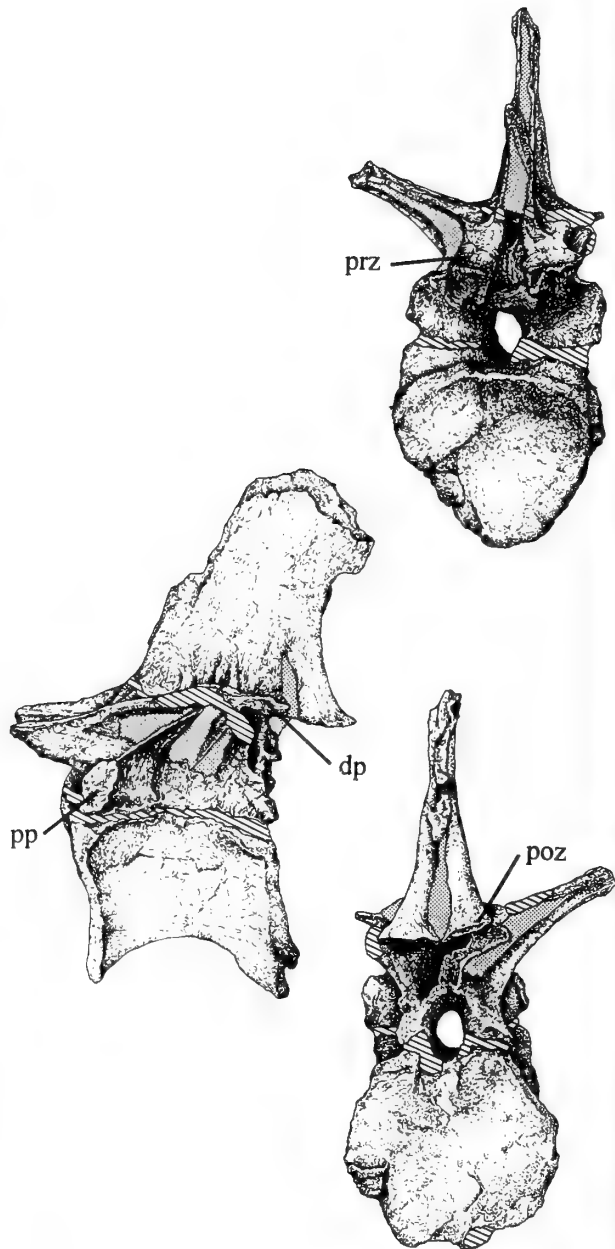


Fig. 26 *Baryonyx walkeri*, holotype, BMNH R9951; 14th dorsal vertebra in (from top downwards) anterior, left lateral, and posterior views. $\times 0.25$.

latter. In D10 the dorsal fenestration appears to penetrate the bone but the three ventral ones do not, for each corresponding fossa contains supplementary buttresses (see above). In D11 the dorsal fenestration is still present but the ventral fossae have not been fully prepared. In D14 the posterior (infrapostzygapophysial) fossa is a deep pocket.

It is evident throughout the series that, in this specimen at least, the vertebral centra and the neural arches had not co-ossified. In some vertebrae centra and arches had remained together in their proper positions, in others they were still together but relatively

displaced to varying extents, and in yet others they were found completely separate. Their rugose sutural surfaces on either side were unmistakable and generally complete. This lack of co-ossification in the vertebral column confirms our observations on the skull and our suggestion that this particular individual might well be – despite its great size – a juvenile.

The neurocentral suture itself is invariably straight. In D1 the centrum and neural arch were found in their natural relative position. In D2 they are more or less in their proper position but have come slightly adrift. In D3 the neural arch has been tipped forwards by about 45° so that, though still in articulation anteriorly, posteriorly it is separated from the centrum by a wide gap. In D5, D6, D11 and D14 the two components had parted completely but have been re-assembled in the laboratory.

The neural spines increase steadily in height (see Table 1, p. 30) from 87 mm in D1 to 197 mm in D11 and 201 mm incomplete in D14. (There is one exception to this in the case of D5, which at 96 mm complete is shorter than either D2 or D3.) D1 is very slender in lateral view, and D2 and D3 are successively more slender still, all three measuring considerably less in an axial direction than their transverse thickness. D5, however, reverses this trend, and from there on, while the transverse thickness remains much the same, the axial length increases steadily. Thus, in D14 the axial length is four and a half times the transverse thickness. To summarize, the neural spines change from a short stout rod at the front of the series to a tall broad plate at the back.

There are prominent rugosities on the neural spines of D1-D5, projecting in front of and behind the spine itself and of more or less uniform width along its height. They represent the ossified portions of the interspinous ligaments. These have the effect of giving the spine a cruciform cross-section in D1, an appearance which is accentuated in D2. In D3 the cross is transversely wider but not so deep anteroposteriorly; each rugosity projects dorsally above the top of the neural spine proper so as to give a pronounced saddle-shaped appearance in lateral view. In D5 there are still slight rugosities, the anterior being better developed than the posterior; the anterior margin of the spine slopes obliquely posterodorsally, the posterior margin is more or less vertical, and the short dorsal margin is transversely narrow, horizontal, and almost flat. Behind this point there are no more rugosities.

In D6 the anterior margin of the neural spine curves forwards towards the top; the posterior margin is again vertical, in the same plane as the posterior face of the centrum. The top of the spine, however, is much wider than in D5, and in lateral view is pitched like a roof, its apex being appreciably behind its mid-point. D7 is very similar, a little wider still, but with the apex of the roof-like dorsal margin exactly central. The neural spine of D11 is again very similar but a great deal wider, with a more steeply pitched 'roof' and with a median flange-like projection on its posterior margin; its widest point is therefore at about half height. In D14 the anterior edge of the neural spine is badly damaged but the base of a forward projection remains; more dorsally there is a very pronounced posterior projection overhanging the postzygapophyses and high above them. This last dorsal vertebra is the only one in which the full height of the neural spine is not preserved, but, even so, it is higher than any of the others. There are no spine tables anywhere in the series.

Another variable character is the angle of inclination (to the horizontal) of the zygapophysial facets (see Table 2), which are usually tilted so as to face dorsomedially (prezygapophyses) or ventrolaterally (postzygapophyses). Again, it is not possible to make precise measurements, but our somewhat crude figures give a good indication of general trends. The inclination tends to decrease as we pass backwards down the series. Note that there can be large

variations between different parts of the column (7°–32°), between adjacent vertebrae (20°–27°), and even between the pre- and postzygapophyses of the same vertebra (7°–18.5°). Nevertheless, it might be supposed that the postzygapophysial angle of a given vertebra should match the prezygapophysial angle of the vertebra behind, with which it articulated. In four of the six cases where there are two adjacent vertebrae with measurable facets there is indeed a close correspondence, with discrepancies of 0.5°, 1°, 1.5° and 2°; another is not too big, at 4.5°; but the worst case is a discrepancy of 13.5°, between the axis and the supposed third cervical, which leads us to suspect that the latter may be badly distorted.

Table 2 Inclination of the zygapophysial facets.

	A	B
Ce2 (axis)	—	18.5°
Ce3	32°	26.5°
Ce5	24°	19.5°
Ce6	20°	15°
Ce8	21°	25.5°
D1	—	20°
D2	24.5°	27°
D3	28°	30°
D5	14°	12°
D6	10.5°	17.5°
D7	15.5°	12°
D10	12°	—
D11	17.5°	7°
D14	7°	18.5°
unnumbered caudal	—	21°

A, angle of inclination of prezygapophysial facets (facing dorsomedially); B, angle of inclination of postzygapophysial facets (facing ventrolaterally).

The angle given is the angle between the zygapophysial facet and the horizontal plane, rounded off to the nearest half-degree. Where measurements can be made on both members of a pair of facets the figure quoted is the mean of the two.

In all but the most anterior dorsals of *Baryonyx* a hypophene and a hypantrum are well developed. The hypophene is a large solid median projection between and below the postzygapophyses. Seen from behind it is triangular, with the apex pointing upwards, and on either side a large semilunar facet is directed dorsolaterally. The hypophene as a whole fitted neatly into the gap between the prezygapophyses of the succeeding vertebra, where its facets articulated with the hypantrum; this latter comprises a pair of similar semilunar facets on the medial sides of the prezygapophysial peduncles, directed ventromedially.

In D1 the prezygapophyses are not preserved, in D2 they are very widely separated, and in D3 slightly less so. It is obvious, therefore, that hypantra were absent. In all three of those vertebrae the hypophene, if present at all, is the merest rudiment and could not have been functional. In contrast to this, both hypophene and hypantrum are well developed in D5 and – as far as the state of preservation will permit us to determine – from there on throughout the rest of the dorsal series to D14. Although the hypophene of D14 is broken off, enough of it remains to indicate unequivocally that there must have been a hypantrum on the first sacral vertebra.

In vertebrae D6-D10 (and perhaps D11) there is a pair of conical pits (peduncular fossae) on the anterior face of the neural arch, immediately above the opening of the neural canal and medial to the bases of the prezygapophyses. In D6 they are fairly widely spaced, circular and shallow. In D7 they are closer together and deeper. In D10 they are very close together, larger and deeper still. Similar pits are present in *Allosaurus* in vertebrae D9-D14, D12 excepted; they are developed best in D9.

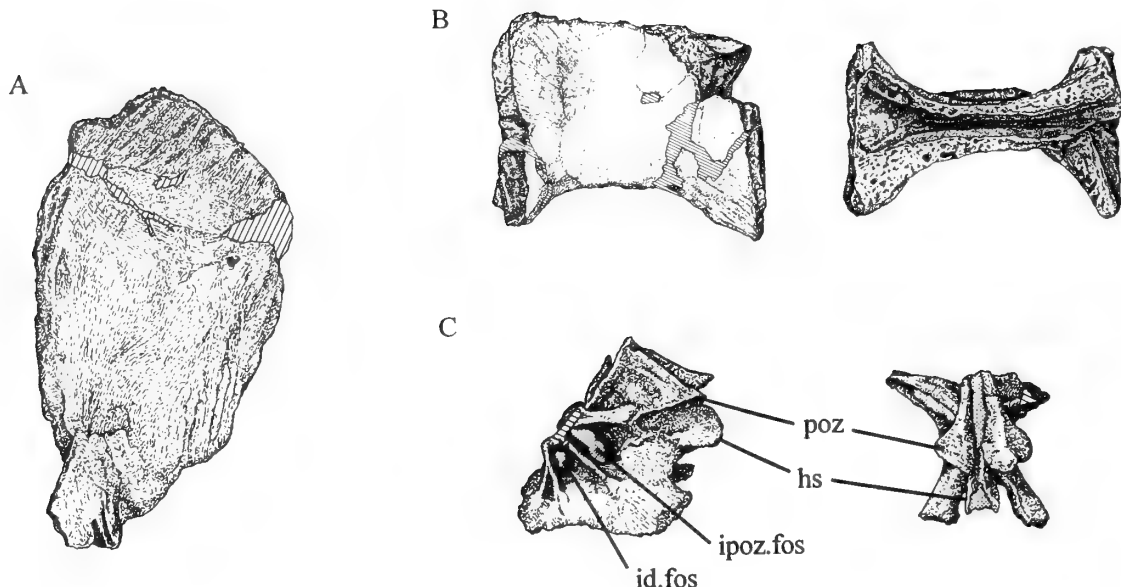


Fig. 27 *Baryonyx walkeri*, holotype, BMNH R9951; sacral/proximal caudal vertebrae. A, neural spine in left lateral view; B, proximal caudal centrum (aB) in left lateral and dorsal views; C, fragment of neural arch of proximal caudal vertebra, in left lateral and posterior views. $\times 0.25$.

CAUDAL REGION (Fig. 27). This region is represented only by the remains of six centra and one neural arch, together with two incomplete neural spines that almost certainly pertain to proximal caudals (or possibly sacrals).

Three isolated centra, though large, show no signs of any parapophyses, diapophyses, buttressing laminae, sacral ribs or pleurocoels. Further, the neural canal running along the dorsal surface of each is very narrow. Taken together, these characteristics suggest that the centra represent proximal caudals. On one of them (referred to below as CaB) the ventral rim of the posterior face is not curved but flattened, as is characteristic of proximal caudals.

There is no way in which the order of these three proximal caudal centra could be determined; indeed, there were probably more than three altogether. We refer to them here simply as Caudal A (CaA), Caudal B (CaB) and the partial Caudal C (CaC), the lettering having no significance as to their place in the vertebral succession.

These centra are of similar diameter to that of the last dorsal, D14, but are much longer; indeed, they are very much longer (134, 144 and 140 mm respectively) than any of the presacral centra (longest preserved is the eighth cervical at 120 mm). Their available measurements are listed in Table 1 (p. 30). They are very strongly 'waisted', with moderately amphicoelous ends; the anterior face is vertically oval (contrast the dorsal centra) and the posterior face is more or less circular. Two of them are reasonably complete up to the virtually straight neurocentral suture and still possess much of the rugose sutural surfaces for the neural arch; the third is only partial, lacking most of the posterior end.

Fragments of three other caudal centra are preserved. The largest consists of the posterior part of a centrum, showing an almost complete articular face measuring 65 mm transversely and an estimated 76 mm vertically. The middle of the face is somewhat hollowed out and its ventral portion bears a large and slightly eroded haemapophysial facet. Enough of the body of the centrum remains to show that it was hollow and strongly waisted and had a somewhat flattened ventral surface.

The other two fragments are too poorly preserved to merit description, but are recognisable as caudals by their small size and flattened ventral surfaces.

An isolated, incomplete, but well-preserved neural arch (Fig. 27C) was found, which can only represent a proximal caudal vertebra, but it does not fit on to any of the proximal caudal centra described above. The posterior edge of its transverse process is well separated from the anterior end of the postzygapophysial facet; in this it resembles the anterior dorsals (for example, D3) and is quite unlike the posterior dorsals, in which those two structures are contiguous. On the other hand, in other characters it is not unlike the posterior dorsals. These are the length of the fragment, which, at approximately 100 mm, is much longer than the total length of the centrum in D3-D8; the infradiapophysial laminae, which are well developed and enclose a deep infradiapophysial fossa; and the powerful hypophene, which projects farther posteriorly than the postzygapophyses themselves. In any case, the total width across the postzygapophysial facets is only 52 mm, much less than in any dorsal vertebra and they lie in a more or less horizontal plane. Also to be noted is the fact that the ventral margin of the arch, which appears to be complete and to represent the neurocentral suture, curls upwards at the back like the prow of a boat. (For nearest comparison see Welles on the proximal caudals of *Dilophosaurus*, 1984: 124 ff.).

A very large, flattened plate of bone, undoubtedly a neural spine, was found (Fig. 27A). It is much larger than any of the neural spines of the dorsal vertebrae as preserved. Another, smaller and less complete fragment of similar form was also found. The anteroposterior length of the larger spine is 142 mm, which is much the same length as the two longer proximal caudal centra (CaB 144 mm, CaC 140 mm) and is therefore very much longer than any other centrum preserved. Both spines were found in Block 43, from the pelvic region of the skeleton, and both possess a characteristic projection (see below) from the posterior or posterodorsal border, not unlike that described above for vertebra D14 (the last dorsal). These

characters, taken together, suggest that the spines in question are from the proximal caudal region of the *Baryonyx* vertebral column or from the otherwise unknown sacral region.

The larger spine is transversely very thin and has blade-like edges; it widens towards its distal end, which may not be quite complete. In lateral view its dorsal profile slopes upwards from either end towards an apex that is situated somewhat behind its middle. From the centre of the posterior part of that profile a symmetrically rounded swelling projects to a distance of about 13 mm. Towards the ventral break of the spine, on its posterior margin, there remains the base of the ridge that ran down towards the right postzygapophysis. Only the dorsal portion remains of the smaller spine; it is about two-thirds the linear dimensions of the larger, is thicker and has a more rectangular distal end. The posterior swelling lies more ventrally than in the larger spine, on what we presume to be the posterior profile.

Ribs

There are numerous rib fragments, mostly of the vertebral ribs but some abdominals too. Many are simply broken pieces of shaft and do not merit description.

VERTEBRAL. These we have arbitrarily classified, for purposes of description, into four groups:

1. Cervical ribs (the left rib of the axis, plus three others, all from the left side, of which only one is complete).
2. Slender uncinate ribs (two) that we tentatively assign to the anteriormost part of the dorsal series (probably D1 and D2).
3. Large, stout non-uncinate ribs (many) that clearly formed the greater part of the dorsal series (probably D3-D11).
4. Significantly smaller, slightly twisted ribs that we assign to the posteriormost part of the dorsal series (probably D12-D14).

CERVICAL RIBS (Fig. 28). The complete cervical rib is of typical 'crocodiloid' form and is tetraradiate in dorsal aspect. The body of the element is canoe-shaped; a short anterior process tapers forwards and curves medially, a longer posterior process tapers backwards and is virtually straight. The capitulum and tuberculum are short and stout, with a deep pneumatic pocket between their bases. This is not at all like the cervical ribs of *Allosaurus*, which are typified by a long, ventrally directed spine.

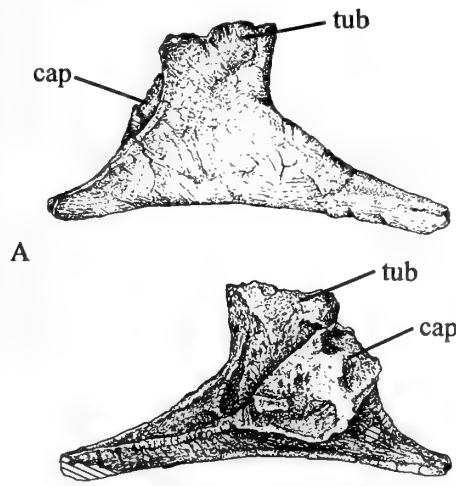


Fig. 28 *Baryonyx walkeri*, holotype, BMNH R9951; left cervical rib. A, lateral view; B, medial. $\times 0.25$.

A fragment of a more posterior cervical rib bears a laterally directed uncinate process, with a pneumatic pocket medial to it as well as the pocket on the medial side of the element. The posterior process is broken off but appears to have been more or less straight.

DORSAL RIBS (Fig. 29). We consider the 'Group 2' ribs to belong to the right side of D1 (first dorsal vertebra) and to the left side of D2 (second dorsal). Each possesses a prominent, keel-like uncinate process on its lateral surface, just below the junction of capitulum and tuberculum (the first dorsal rib of *Sinraptor* also has a vestigial uncinate process). On the medial surface, a short way proximal to this, is a deep circular pit with sloping sides; it lies closer to the posterior margin than to the anterior margin.

The best-preserved, typical ('Group 3') dorsal rib is of the right side and probably belongs to D3 (third dorsal). This robust element comprises a lightly curved shaft, 205 mm as preserved, that terminates dorsally in a short tuberculum; just below the tuberculum a relatively long capitulum diverges medially from the shaft at almost a right angle. (Unfortunately none of the three processes of this triradiate bone is complete right to its end.) The ventral profile of the capitulum and the medial profile of the shaft do not form a single smooth curve; the change in direction occurs mainly around the junction. The shaft tapers distally and its distal region is distinctly twisted so that the surface that faces anterolaterally above faces directly anteriorly below. The posteromedial surface of the shaft bears a deep, wide groove that confers an L-shaped cross-section upon the proximal region of the shaft but peters out distally. The capitulum is subtriangular in section, with a sharp dorsal margin and a stout, rounded ventral margin; its anterolateral surface has a shallow depression running centrally along its length. The medial surface of the tuberculum bears a prominent vertical buttress that disappears ventrally at the junction.

We tried to assign the other ribs in this arbitrary grouping (D4-D11?) to articulation with particular vertebrae but they are too incomplete to be ordered reliably.

The more posterior rib-heads ('Group 4', probably referable to D12 and D13) resemble those of other theropods in that they bear a long capitulum and a very short tuberculum. The tuberculum is reduced to a mere stub less than 20 mm long. There is no intercostal web of bone between the two heads. The presumed last dorsal rib, D14, is short (shaft length 194 mm from a point in the axil between the two rib-heads); its shaft is slender, flattened, convex, almost spatulate distally, with thin edges and a laterally directed tip.

ABDOMINAL (GASTRALIA). Several fragments are preserved. In general, they are pieces of slender, gently curved, tapering shafts, longitudinally grooved on the dorsal surface for articulation with the succeeding element. A few fragments, the two longest being 230 mm and 190 mm, have flattened, spoon-shaped, slightly twisted ends; these are similar to the medial ends of the same elements of *Sinraptor* (Currie & Zhao 1993), which articulate with the gastralia from the opposite side of the body. There are not enough gastralia fragments to determine the number of segments per side (*Sinraptor* has three; tyrannosaurids, *fide* Lambe 1917, have only two).

Chevrons (haemapophyses) (Fig. 30)

Five haemapophyses were found, four of them of very similar size and the fifth somewhat larger. All save one have lost varying amounts of their distal ends.

The one complete haemapophysis is 190 mm long and of fairly typical form. The paired facets which articulated with a caudal

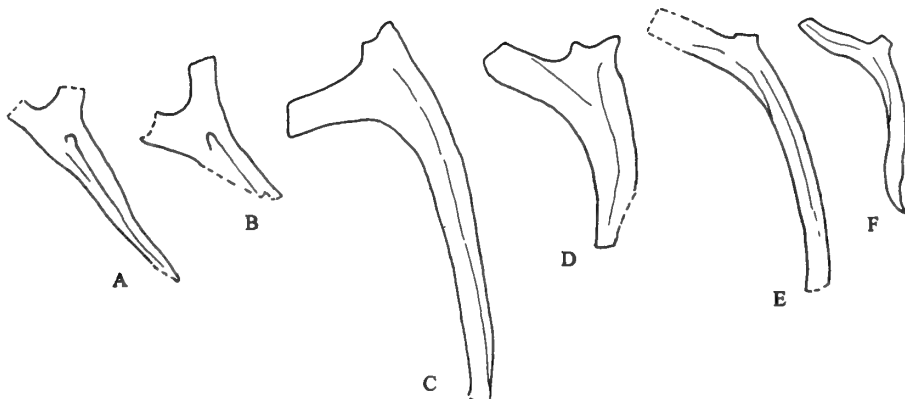


Fig. 29 *Baryonyx walkeri*, holotype, BMNH R9951; isolated dorsal ribs: A, B, anterior; C, D, mid-dorsals; E, F, posterior. $\times 0.17$.

vertebrae are united by a bridge, producing a saddle-shaped proximal end. The paired anterior processes found in *Dilophosaurus* and *Allosaurus* are altogether absent here, in which respect *Baryonyx* resembles *Ceratosaurus*. The distal portion of the bone, beyond the point of union of the two sides, is transversely flattened and expanded into a blade-like structure with a straight anteroventral margin and a concave posterodorsal margin.

Sternum (Fig. 31C)

A fragile plate of bone, in some places no more than 1 mm thick, has broken edges nearly everywhere. However, it is strongly ridged like a tile from the ridge of a pitched roof, with two smooth surfaces lying at an angle of some 40° to one another, suggesting that the fragment is a single median element with a median angulation. At what appears to be its anterior end the bone is considerably thickened; each half has a convexly curved anterior termination, and between the two is a median embayment. Part of the right-hand edge is a true margin which runs diagonally to the midline, thereby indicating that the bone originally widened rapidly towards its thickened posterior end.

Sternal elements have seldom been reported in theropods. In *Sinraptor* (Currie & Zhao 1993) a fragment of a broad plate with a median ventral ridge was found. Some other theropods, e.g. *Carnotaurus* (Bonaparte *et al.* 1990) and *Albertosaurus* (Lambe 1917), have paired, unfused sternals; this could be related to immaturity. The fusion of paired plates into a single median element in *Baryonyx* (despite the lack of co-ossification of the various components of the skull and vertebrae) might suggest the contrary, that the animal was fairly mature.

Pectoral girdle

SCAPULA (Fig. 31A). Both scapulae are preserved incomplete. Whereas the base of the left scapula lacks only part of the acromion process, the base of the right scapula is missing entirely, being broken off transversely a short distance above the glenoid. Both scapulae also lack the dorsal end of the blade, the right seeming to be almost complete distally but its partner rather less so. The following description is based on both.

The scapula is typically theropod in most respects, somewhat curved in anterior or posterior view to fit the shape of the body. The blade is long and strap-like with subparallel sides, although its distal (i.e. dorsal) end is slightly expanded. It is robustly constructed, with rounded edges; the anterior edge is a little thicker than the posterior. The blade thins somewhat dorsally and the edges become sharper, more truly blade-like.

Ventrally the blade expands greatly; it expands anteriorly into the thin (and broken off) acromion process, while the posterior edge thickens gradually in a mediolateral direction. At the same time it expands posteriorly, terminating in the backwardly directed scapular portion of the glenoid fossa and, adjacent thereto, in the ventrally directed facet for the coracoid. The glenoid facet is shaped like a deep inverted U, while the coracoid facet is broad and robust beneath the glenoid but tapers anteriorly towards the acromion process. A straight, distinct ridge is formed where these two facets meet at an angle of about 45° .

In lateral view the ventral margin of the scapula, where it fuses with the coracoid, forms a shallow single zigzag which is reflected exactly in the corresponding dorsal margin of the coracoid (see below).

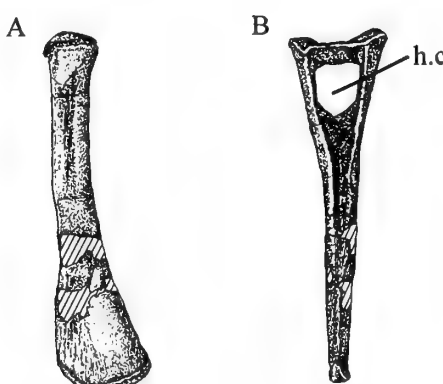


Fig. 30 *Baryonyx walkeri*, holotype, BMNH R9951; isolated haemapophyses. A, left lateral; B, posterior. $\times 0.25$.

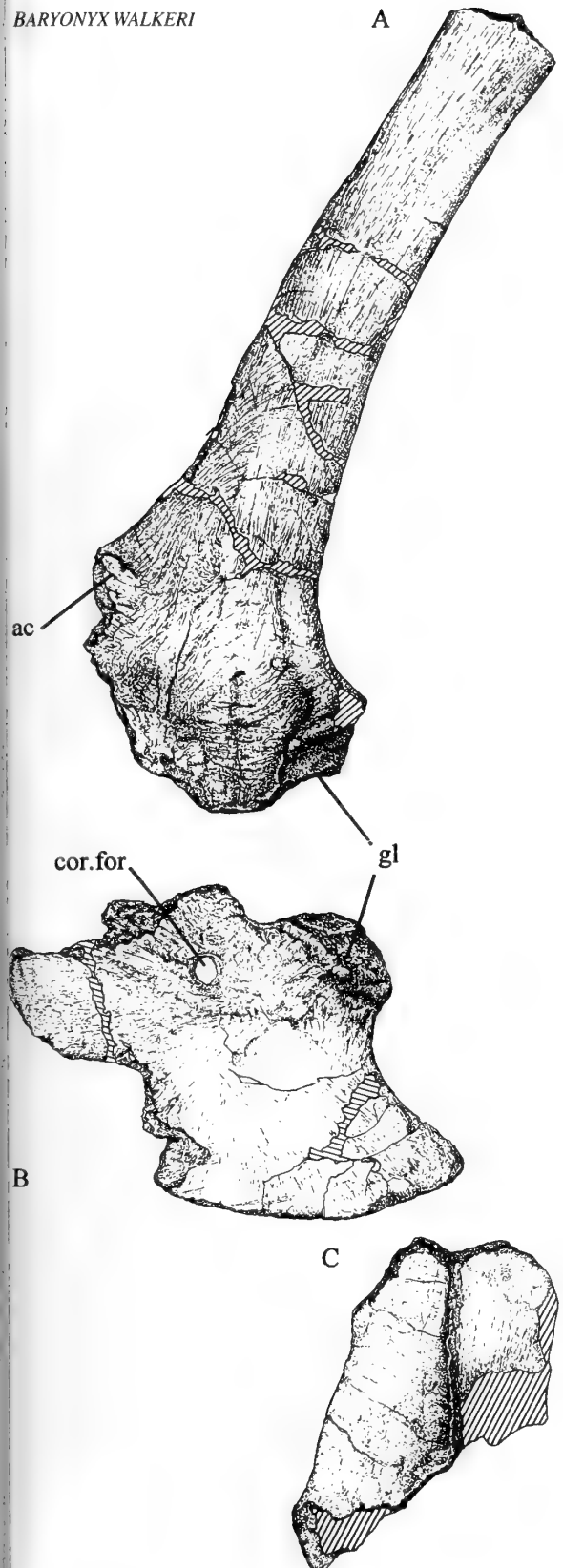


Fig. 31 *Baryonyx walkeri*, holotype, BMNH R9951; elements of pectoral girdle, including sternum. **A**, left scapula in lateral view; **B**, left coracoid in lateral view; **C**, sternum in ventral view. $\times 0.25$.

The thickened posterior edge of the lower part of the scapula, as it approaches the glenoid, bears a low but distinct muscle ridge running parallel to its lateral margin (Welles' 'slight rugosity', 1984: 127).

CORACOID (Fig. 31B). Both coracoids are preserved, but in neither has the anterior region escaped damage. The whole of this region is missing in the right coracoid; in the left, however, sufficient remains to determine its anterior extent but not the shape of the margin.

As usual in theropods, the plate-like coracoid is medially concave and laterally convex, continuing the line of curvature of the adjacent scapula. The perfectly preserved posterior region is shaped like a hatchet and projects directly backwards, not at all towards the midline as in some other theropods. The robust articular region bares dorsally the semicircular glenoid facet and the pear-shaped sutural surface for the scapula, its junction with the medial surface being marked by a prominent rugose ridge. As mentioned above, the line of articulation between scapula and coracoid is zigzag-shaped in lateral view. Ventral to this articulation the coracoid plate is perforated by the coracoid foramen, circular in lateral exposure, pear-shaped in medial exposure and approximately 25 mm in diameter.

Fore-limb

As is typical of theropods, all three major bones are short, relative to the general size of the animal; but they are also remarkably robust and wide, relative to their shortness, with stout shafts and broadly expanded ends.

HUMERUS (Fig. 32). The left humerus is essentially complete, although the medial side of the shaft is somewhat crushed. The right humerus shows a similar state of preservation, but lacks almost the whole of the ectepicondyle (ulnar condyle). The element is 463 mm long (Charig & Milner 1990).

The first impression is of a stout and stubby bone, with two broadly expanded ends connected by a straight and relatively short shaft; the maximal width of the proximal end is 242 mm and of the distal end 183 mm. The two ends, however, are flattened to a significant degree; the distal expansion, in particular, appears very thin in end view. The plane of the distal expansion is offset with respect to that of the proximal expansion by some 30°. At the proximal end there is considerable expansion of the deltopectoral crest on the anterior side, and a greater expansion of the internal tuberosity (the entotuberosity of Welles 1984) on the posterior side. Although the deltopectoral crest projects from the anterior side of the bone, its apical portion is bent round anteromedially so that the lateral surface of the proximal expansion is distinctly convex and its medial surface correspondingly concave.

The distance between the upper end of the humerus and the apex of the deltopectoral crest is approximately 43% of the entire length of the element, while the deltopectoral crest as a whole constitutes 51% of that length. Between the deltopectoral crest and the internal tuberosity lies the head of the humerus, a thickened region that articulated with the glenoid. On the medial surface of the proximal expansion, about half-way between the head and the apex of the deltopectoral crest, is a distinct ridge some 35 mm in length running along a line that is directed towards the centre point of the shaft. This ridge, which is clearly present on both humeri, is a rounded hump distally and tapers proximally to become lower and narrower as it approaches the edge of the bone. To the best of our knowledge, no similar structure has been found elsewhere; it may be a prominent insertion for the pectoralis muscle.

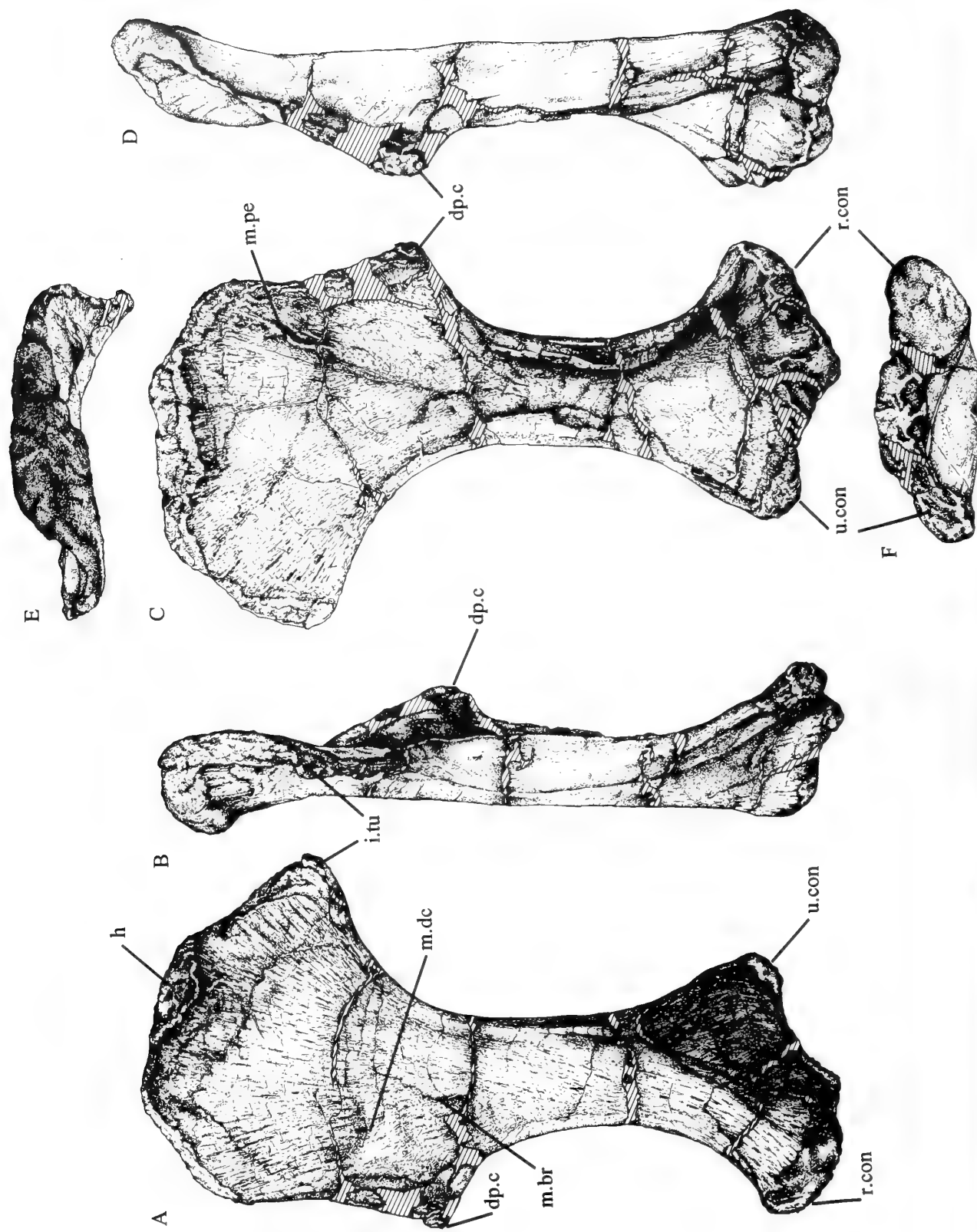


Fig. 32 *Baryonyx walkeri*, holotype, BMNH R9951: left humerus. A, lateral view; B, anterior view; C, posterior view; D, medial view; E, proximal; F, distal. $\times 0.25$.

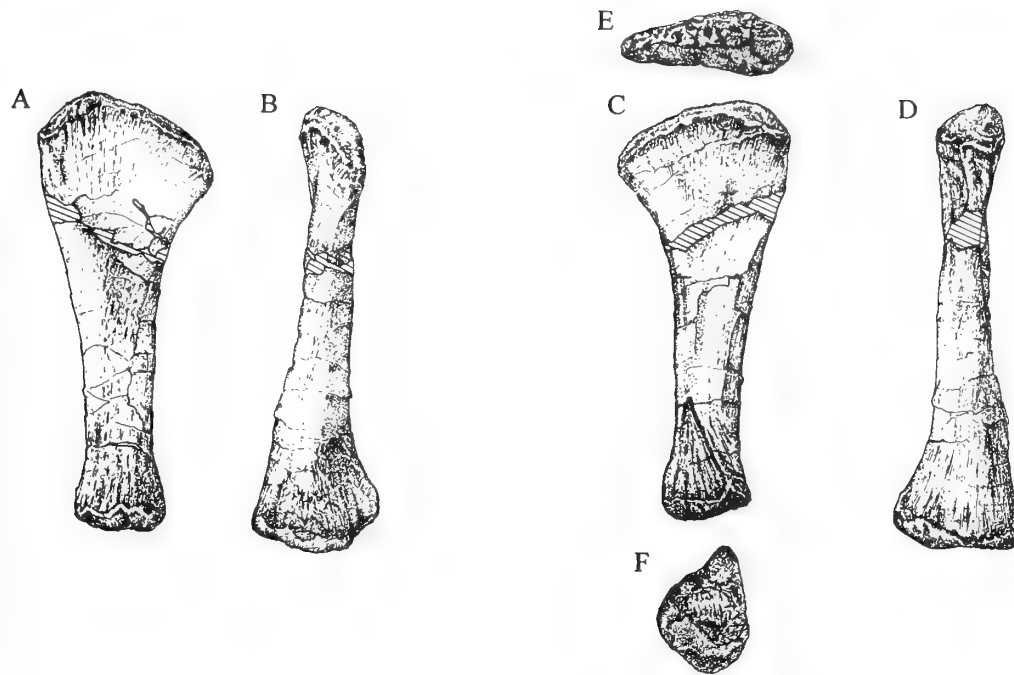


Fig. 33 *Baryonyx walkeri*, holotype, BMNH R9951; left radius. A, lateral view; B, posterior; C, medial; D, anterior; E, proximal; F, distal. $\times 0.25$.

On the lateral side of the proximal expansion, where it begins to narrow into the shaft, are two obvious areas of muscle attachment. Immediately posterior to the apex of the deltopectoral crest is a low, slightly rugose hump; this is presumed to have been the point of insertion of the deltoides clavicularis muscle (cf. Norman 1986: 338). A little lower down and more posterior in position, indeed almost in the centre of the lateral surface, is a large shallow depression with a distinct raised border below and on either side; this probably served as the point of origin of the brachialis muscle (cf. Norman 1986, *loc. cit.*).

At the distal end of the humerus the ectepicondyle is well expanded. The lower margins of the entepicondyle and the ectepicondyle form an angle of approximately 45° with each other, and their facets for articulation with the radius and ulna respectively are subequal in length (the ectepicondylar facet being just a little longer). In *Dilophosaurus* the humeral shaft is less straight than in *Baryonyx*, and in *Allosaurus* it is even more curved. The two ends are more offset in *Dilophosaurus* than in *Baryonyx*.

RADIUS (Fig. 33). Both radii are preserved, the left complete but the right lacking a section of the shaft so that the two ends are no longer connected. The radius is a short, straight, stout bone, not distinguished by any remarkable features. It is 225 mm long and therefore only 49% of the length of the humerus. The proximal end is flattened and expanded, its profile being convex in side view; it tapers smoothly into the roughly cylindrical shaft, which continues to taper slightly until it reaches the less expanded distal end. The latter differs from the proximal end in that it is narrower and not flattened; in end view it appears triangular with one corner extended, the longest side (in the plane of expansion) being almost perpendicular to the plane of flattening and expansion of the proximal end. The distal end-surface is perpendicular to the axis of the bone and has a shallow convexity at its centre.

ULNA (Fig. 34). Only the left ulna is preserved, almost complete and 283 mm long; thus it is considerably longer (61% of the length of the humerus) than is the radius. The ulna, unlike the radius, is distinctly bowed. The proximal end bears an unusually powerful olecranon, projecting posteromedially beyond the head of the bone. The articulating surface for the humerus projects anteriorly (making an angle of about 130° with the olecranon projection when viewed from the proximal end) and has a concavely curved anterior profile distal to its apex. The lateral surface of the proximal end actually consists of two surfaces, one facing obliquely forwards and the other obliquely backwards so that they together make a right angle. This angle forms a powerful projection which, unfortunately, has been severely damaged.

The most unusual feature of the ulna is the broad expansion of the distal end. This is essentially in the transverse plane, but the greatest part of the expansion is on the medial side where the bone has been extended anteromedially and, at the same time, somewhat dorsally. Although this medial expansion is distinctly more slender than the central part of the ulna, the bone thickens again towards the medial margin so that the articulating surface is of almost constant width. There is also a rather less prominent anterolateral expansion of the lateral side, but here the bone becomes appreciably thicker, so that this part of the articulating surface is virtually semilunate. The distal profile of the ulna, in anterior or posterior view, is markedly convex.

CARPUS. No recognisable remains of the carpal bones are preserved.

MANUS (Figs 35, 36). The metacarpals too have all been lost, but a few phalanges are preserved (including three unguals), and some are in excellent condition. They include the original and famous 'Claw', i.e. a huge ungual, together with what is probably the phalanx with which it articulated; three phalanges found in articulation

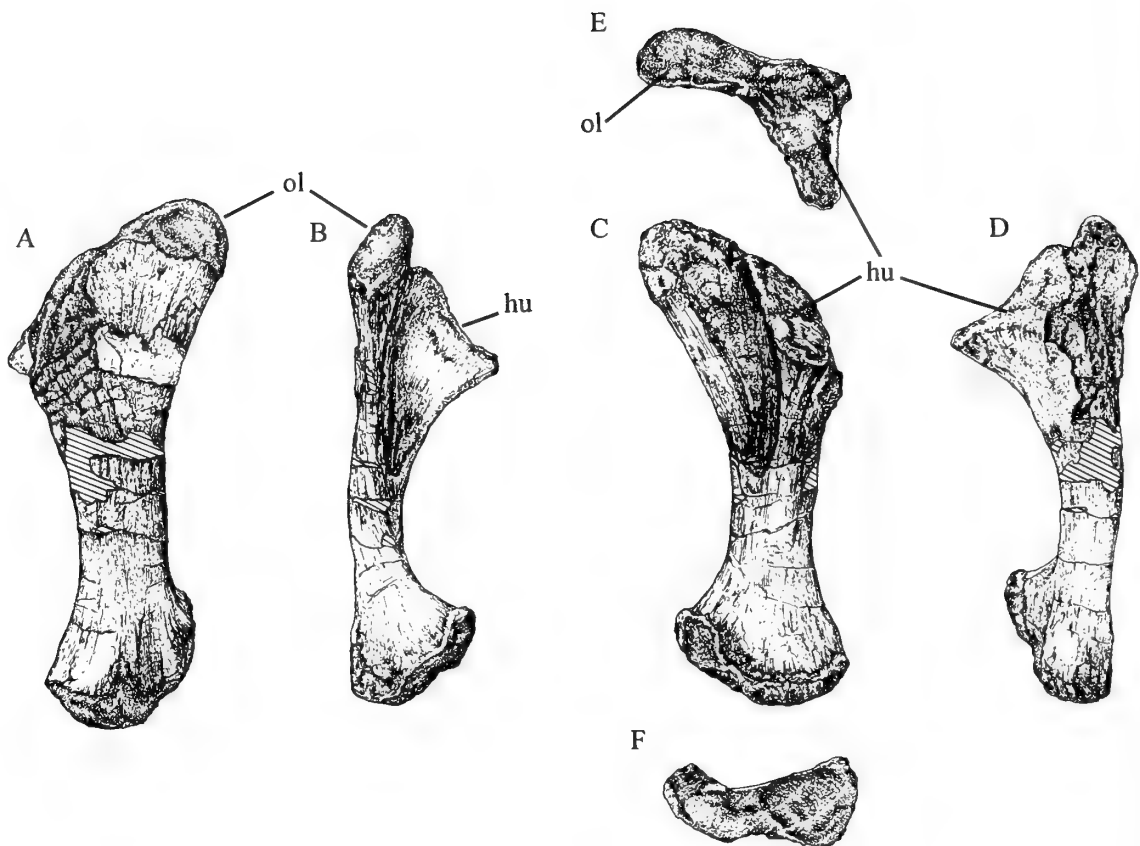


Fig. 34 *Baryonyx walkeri*, holotype, BMNH R9951; left ulna. **A**, lateral view; **B**, posterior; **C**, medial; **D**, anterior; **E**, proximal; **F**, distal. $\times 0.25$.

with each other, of which the most distal is a much smaller ungual; and another four, less complete phalanges. Also preserved are a few more small phalanges which are too incomplete and indeterminate to merit description.

We assume that *Baryonyx* possessed the typical theropod phalangeal formula of 2 : 3 : 4 : (1 vestigial or 0) : 0.

Before describing these phalanges it was desirable to determine:

1. Whether they belonged to the manus or the pes. Non-ungual phalanges from the theropod manus are generally smaller than those of the pes; this comparison, however, requires manual and pedal phalanges from the same individual. Unguals from the manus are more strongly curved than those on the pes. When non-unguals and unguis are found together in articulation, these two indicators should reinforce each other. The precise location of the phalanges within the excavation is another source of helpful information; for example, the only articulated digit found was in Block 27b, which, lying at the head end of the 'dig' (see Fig. 49) and containing also part of the left scapula, was more likely to contain parts of the manus than the pes.
2. Which side they belonged to, left or right. Recognition of which side of the phalanx is medial and which is lateral enables us to determine whether the element in question is from the left side or the right. A study of theropod phalanges illustrated in the literature (e.g. *Allosaurus* figured by Madsen 1976, pls 43 and 44) shows that the lateral profile of each non-ungual phalanx is almost parallel to the sagittal plane but the medial profile is

inclined obliquely, in such a way that the distal breadth is significantly broader than the proximal. Further, a longitudinal groove divides the distal end into two condyles in such a way that the lateral condyle is slightly wider than the medial. As for the unguis, the articulation for the adjacent phalanx is divided into two subequal facets, inclined obliquely to each other and separated by a ridge which begins in a dorsal swelling and then runs ventrally; the swelling and the ridge are a little closer to the lateral margin than to the medial. There is also a slight tendency for the distal tip, in dorsal or ventral view, to be very slightly curved towards the lateral side.

3. Which digit they belonged to and their position within the digit.

Evidence of this nature suggests that all the well-preserved phalanges are of the left manus.

LEFT DIGIT I (POLLEX) (Fig. 35). The attribution of the huge unguis to digit I is no more than a common-sense presumption based on its large size. Indeed, the large size is the only unusual feature of this claw-bone, which measures 310 mm in length around the curved dorsal margin. (The keratin sheath of the claw itself would have been considerably longer.) The slightly eccentric position of the dorsal swelling between the twin facets of the phalangeal articulation suggests that this unguis may be attributed to the left side. The arc of curvature is larger than in an *Allosaurus* of comparable size, i.e. it is less strongly curved. Otherwise this element is a fairly typical theropod unguis of average proportions, almost perfectly bilaterally

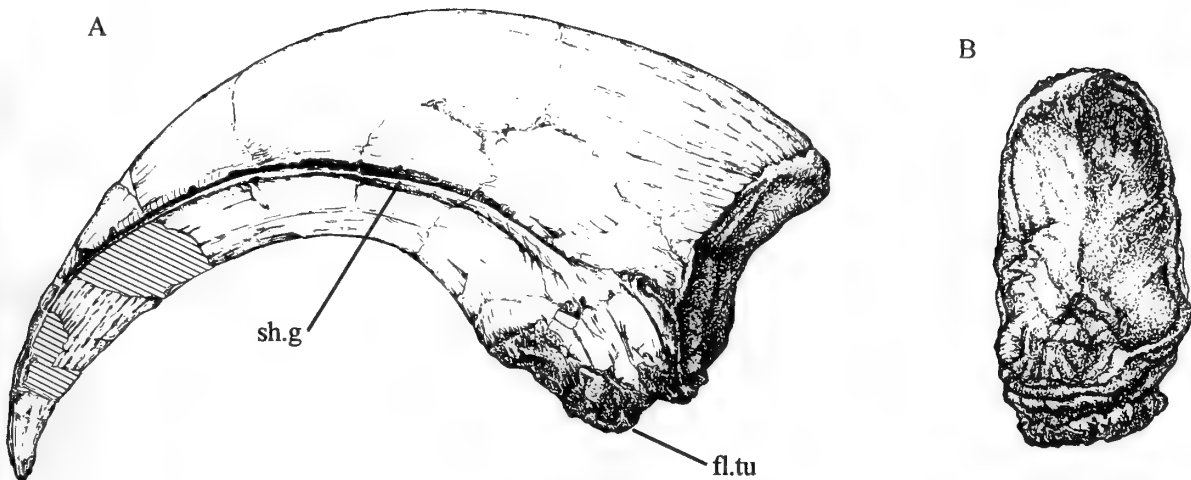


Fig. 35 *Baryonyx walkeri*, holotype, BMNH R9951; unguis attributed to left digit I (pollex). A, lateral view; B, proximal. $\times 0.5$.

symmetrical, very little compressed, smoothly rounded along its length, and sharply pointed. Grooves for the horny sheath run right to the tip, and the flexor tubercle is pinched off more sharply on the medial side than on the lateral.

A distal end of another large phalanx, broken on one side, is probably part of the first phalanx of the same digit. If so, it is with his element that the large ungual articulated. It appears to be a left phalanx, and it compares well with the articulated phalanx described immediately below as the first phalanx of left digit II or the second of left digit III. It has a deep groove between the two condyles, the medial condyle projects obliquely and has a very distinct ligament pit, and the lateral condyle is broken off almost entirely.

LEFT DIGIT II OR III (Fig. 36). The three phalanges that make up his digit were found in articulation; they might be either an entire digit II, or a digit III lacking its basal phalanx. We can try to resolve his dilemma by comparing the bones with the corresponding elements of *Allosaurus* and other theropods. The greater length of the phalanges suggests digit II. On the other hand, the proximal end-surface of the most proximal phalanx of the three (II_1 or III_2 ?) does not have the somewhat irregular, single-facetted form characteristic of a basal phalanx (which would articulate with the distal end of metacarpal II) but has instead the double-facetted form typical of a non-basal phalanx (which would articulate with the pulley-like distal end of phalanx III_1). These elements, in most respects, are standard for a theropod; the ungual, unlike its neighbour on digit I, is not enlarged, its length being estimated (it lacks its tip) at 165 mm. The middle phalanx of the three is appreciably shorter (91 mm) than the most proximal (132 mm). This contrasts with the condition in digit II of *Allosaurus*, where the second phalanx is very slightly longer than the first (Madsen 1976, pl. 45), and in *Deinonychus*, where it is considerably longer (Ostrom 1969: 104). Again, the elements are almost perfectly symmetrical, but a few minor asymmetries indicate that we are here dealing with a finger of the left hand. The most pronounced asymmetry is seen in distal view, where the lateral profile is almost parallel to the sagittal plane but the medial profile is inclined obliquely.

RIGHT UNGUAL II OR III. This element is poorly preserved, it lacks distal half and its proximal end is badly damaged. Nevertheless, it is apparent that it is a damaged mirror-image of the ungual

attributed to left digit II or III, and is therefore identified as the corresponding right ungual.

RIGHT DIGIT III OR IV. One of the smaller phalanges (length 65 mm) is presumably from a digit III or IV, and the obliquity of its medial profile in dorsal aspect indicates that it comes from the right side.

Pelvic girdle

ILIUM (Figs 37, 38). Only the right ilium is preserved. The remains consist of four substantial unconnected fragments of bone and one natural mould:

1. The pubic peduncle, with the anterior third of the acetabulum.
2. The ischiadic peduncle, with the posterior two-thirds of the acetabulum (there can be no more than a narrow gap between this and fragment no. 1).
3. A large part of the anterior portion of the iliac blade, albeit with no natural edges.
4. Part of the posterior process, with the brevis shelf and brevis fossa, and a large part of the iliac blade dorsal to it.
5. A mould of the medial surface of a large part of the iliac blade, lacking the anterior end; the original natural mould, formed on the rock which underlay the blade in the field, has been reproduced in plaster of Paris via a silicone pull.

The broken end of fragment no. 4 certainly joins on to fragment no. 2, but the loss of what appears to be a few millimetres of material prevents a firm connexion between them. The information afforded by all of the above permits us to describe the ilium as a whole.

The estimated length of the ilium, as preserved, is 835 mm. The material available suggests that the dorsal outline of the blade was a smooth convex curve. The length and precise form of both the anterior and posterior processes are unclear, but the posterior process seems to have tapered posteriad to a slightly pointed, spatulate termination. This process bears three diverging ridges separated by three concavities, i.e. it is triradiate in posterior view. Thus, we have a concave lateral surface, a concave medial surface, and a deeply

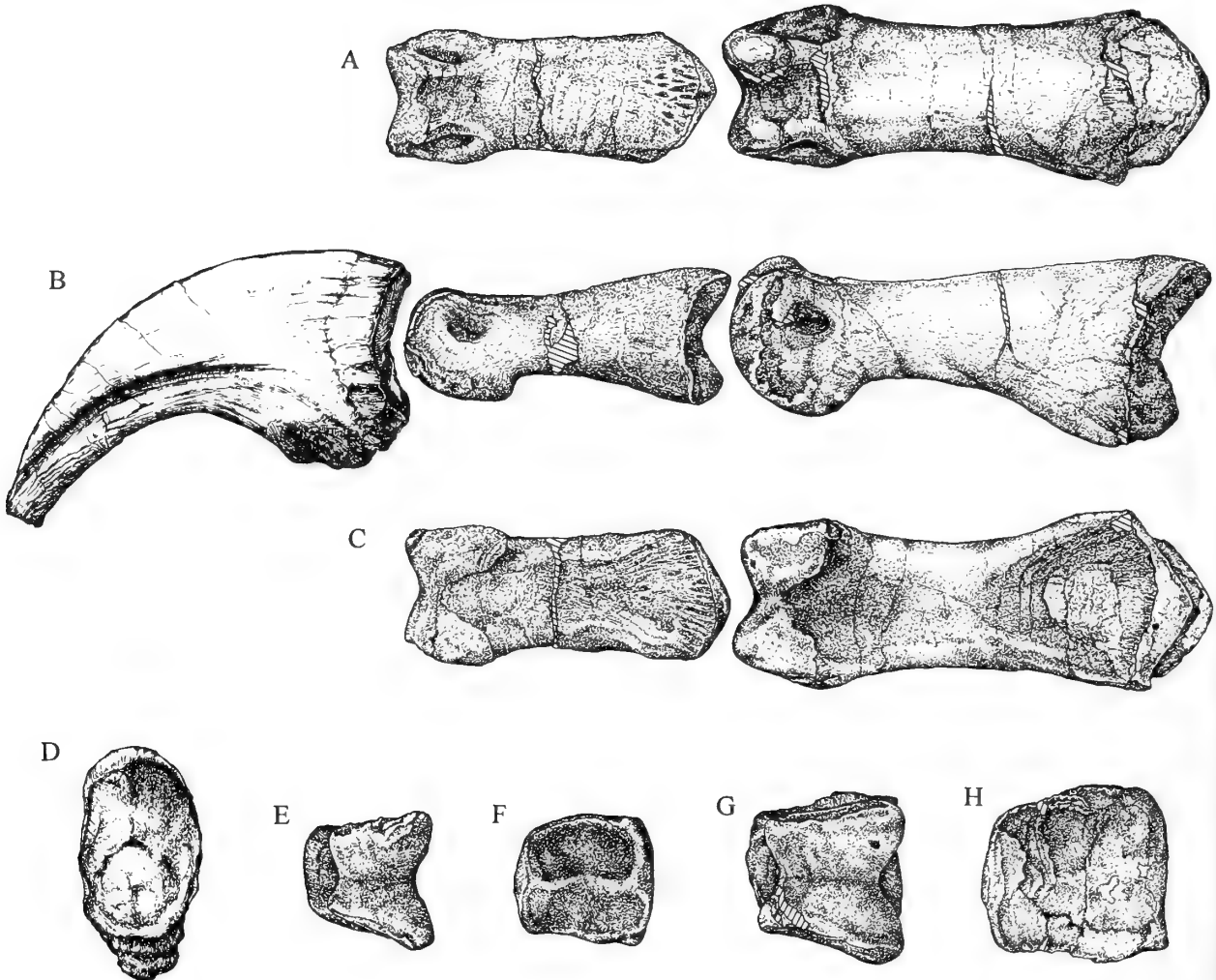


Fig. 36 *Baryonyx walkeri*, holotype, BMNH R9951; three articulated phalanges from digit II or III of left manus. **A**, proximal and middle phalanges in dorsal view; **B**, digit with ungual phalanx, left lateral; **C**, proximal and middle phalanges, ventral; **D**, proximal end of ungual; **E**, distal end of middle phalanx; **F**, proximal end of middle phalanx; **G**, distal end of proximal phalanx; **H**, proximal end of proximal phalanx. $\times 0.5$.

excavated ventral surface. This deep excavation is the brevis fossa, and the ventromedially directed ridge which partly encloses it is the brevis shelf. The ventral part of the otherwise concave medial surface is broadly convex, with faint subparallel ridges, and it appears to terminate posteriorly in a pronounced thickening; the rest of the ventromedial blade is very slender. The brevis shelf and the iliac blade are of uniform and approximately equal thickness along their length; the brevis shelf thins towards its ventral edges. The ventrolateral ridge, by contrast, is much stouter and smoothly rounded, and it thickens anteriorly in the direction of the acetabulum.

The iliac blade as a whole is of almost uniform thickness, and its lateral surface is strongly dished anteroventrally where it thickens towards the (missing) anteroventral termination. Further, its medial surface bears two scars for the direct attachment of the truncated diapophyses of the sacral vertebrae: one lies more or less dorsal to the pubic peduncle and is broadly U-shaped, the other lies dorsal to the ischiadic peduncle and is narrow and curved. (The distance between these two scars suggests that there must have been another scar midway between them, where the bone of the blade is missing

and the mould of its medial surface is not well enough preserved to indicate its presence.) These scars have no distinct border, but are characterized by their finely rugose surface, easily distinguishable from the smooth surface of the rest of the blade. It would be expected that the most ventral portion of the blade would bear another row of scars, marking the distal attachment of what are usually called 'sacral ribs' but which generally consist of no more than the capitulum of each rib; each capitulum is attached proximally to the intervertebrally placed parapophysis of its corresponding sacral vertebra and is truncated distally to attach directly to the medial surface of the ilium. In this specimen the most ventral portion of the blade is missing, but the mould of its medial surface shows two prominent and well-defined scars which presumably mark the attachment of the last two sacral ribs.

The pubic peduncle is very robust; its articular surface forms a narrow triangle, the short side being the acetabular edge. The surface of the acetabulum itself, just above this edge, shows a large, deep concavity. The anterior edge of the peduncle, though rounded, is unusually narrow, especially towards the pubic articulation.

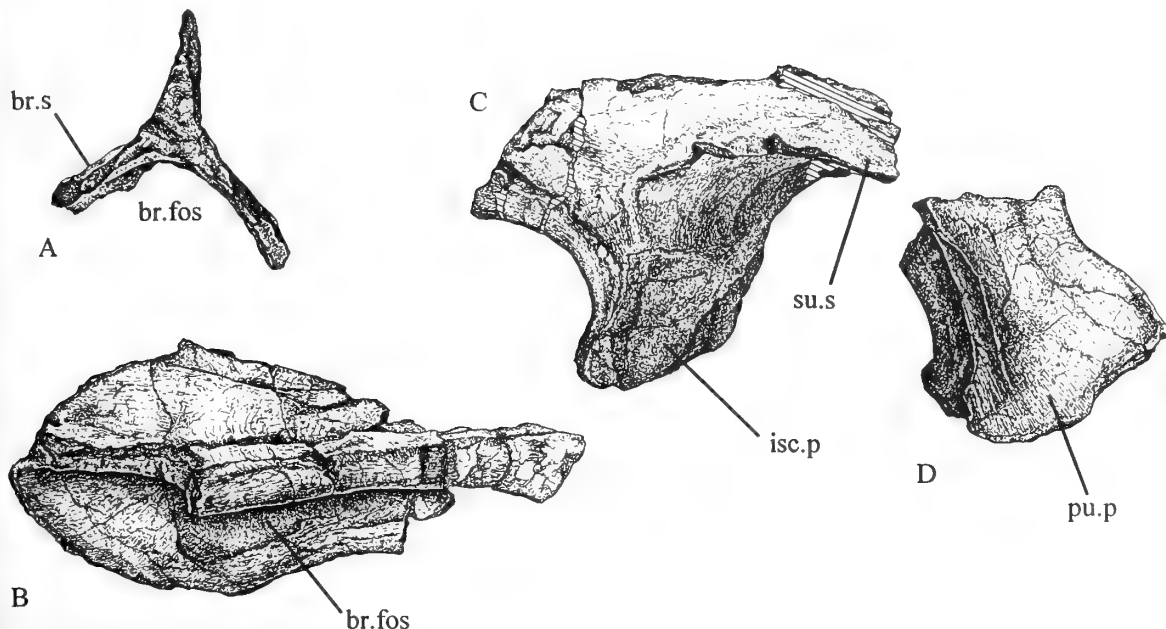


Fig. 37 *Baryonyx walkeri*, holotype, BMNH R9951; right ilium. A, posterior process in posterior view; B, same, ventrolateral; C, ischiadic peduncle, lateral; D, pubic peduncle, lateral. $\times 0.25$.

The ischiadic peduncle is shorter and much more slender. Its articular surface is much smaller, semicircular with its medial corner extended to a point (marking the sharp medial edge of the acetabulum) and extremely rugose. The supra-acetabular crest is well developed and has a sharp lateral edge.

PUBIS (Fig. 39A). One large elongated fragment, 277 mm long, is broken at one end and another fragment, 248 mm long, at both ends; one broken end on each resembles the other so much in size and shape that they are almost certainly parts of the same element, not immediately adjacent to each other but separated by a gap of indeterminate width. Both are stout shafts produced on one side into broad flange that could well represent part of one half of the 'pubic apron', concave on one side and flat on the other. The fragment with complete end is probably the distal part of the left pubis, the other fragment is probably the central part of the shaft of the same bone. A third fragment, 251 mm long, has the shape of one end (presumed distal) very like that of the proximal end of the central portion and is likely to be a more proximal piece of the same element. The lengths of the three pieces added together total 776 mm, and we estimate the length of the entire pubis to have been about 1000 mm; this is not unreasonable when compared with the overall length of the entire ilium (about 820 mm). The position of all three pieces on the block plan (Fig. 48) is fully in accord with this identification.

The acetabular portion of the left pubis is missing entirely. The proximal fragment of the shaft has a thick, rounded lateral edge; the medial border of this proximal part is a true edge, slightly downturned. The medial half of the dorsal surface is distinctly convex, bulging dorsally, and the lateral half is distinctly concave. The bone itself tapers considerably from its proximal end (from 105 mm at the break to a minimum of 71 mm), with its medial and lateral profiles symmetrical and slightly concave. The distal 100 mm or so of this fragment shows, on its medial side, the proximal beginnings of a medial flange, also with a true medial edge; lower down, on the proximal part of the central fragment, this could well have united

with its right counterpart to form a pubic apron (see next paragraph).

The central part of the left pubis is fairly straight and compressed in an oblique transverse plane. Its anterodorsal surface is more or less flat and has a thick rounded lateral edge which widens regularly towards the proximal end of the bone. Its posteroventral surface, by contrast, is strongly concave in transverse section, for it tapers medially into a thin flange. In the more proximal part of the preserved fragment this flange is thicker and is broken off on the medial side, suggesting that it might well have extended farther in that direction to join its fellow in a median symphysis as part of a pubic apron. The more distal part of the flange, however, is extremely slender and has a blade-like medial edge of finished bone, making it less likely that it extended to the midline. This means that a complete apron would have been formed only in the middle section of the pubis.

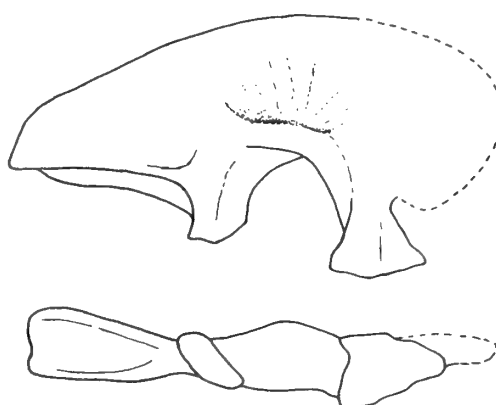


Fig. 38 *Baryonyx walkeri*, holotype, BMNH R9951; reconstruction of right ilium in lateral and ventral views. $\times 0.125$.

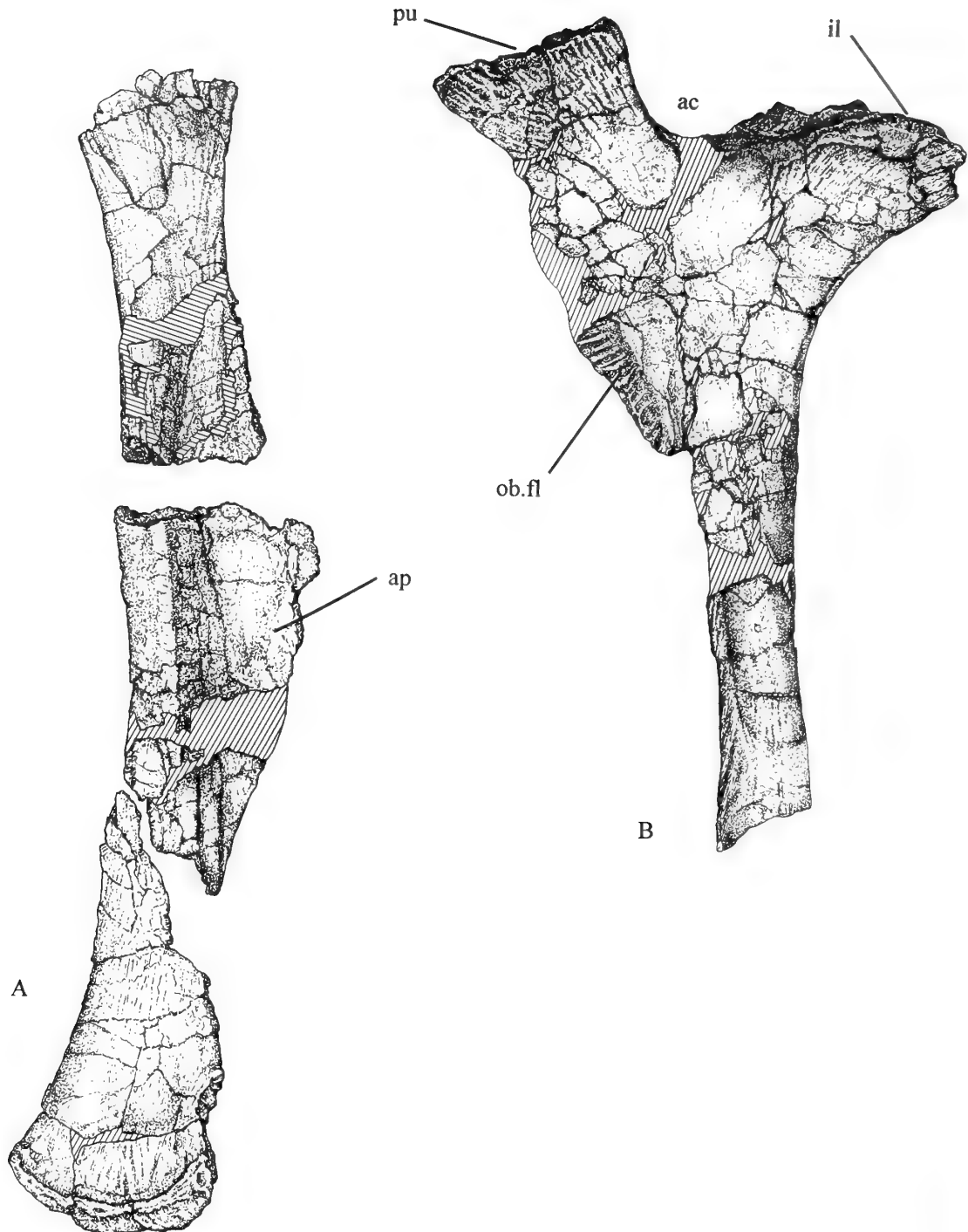


Fig. 39 *Baryonyx walkeri*, holotype, BMNH R9951; ventral elements of pelvis. **A**, left pubis lacking proximal end, posterior view; **B**, left ischium lacking distal end, lateral. $\times 0.25$.

The distal part of the left pubis is also flattened, with fairly thick, rounded edges; but it seems likely that the plane of flattening was somewhat different from that of the central fragment, parasagittal rather than transverse, from which we infer that there must have been some degree of torsion between the two pieces. This means that

the two surfaces would have faced medially and laterally respectively, and the positions of the two edges would have been anterodorsal and posteroventral; meanwhile the blade shows a distinct curvature towards the midline as it approaches its distal end. The anterodorsal edge thickens towards the distal end, its medial and lateral margins

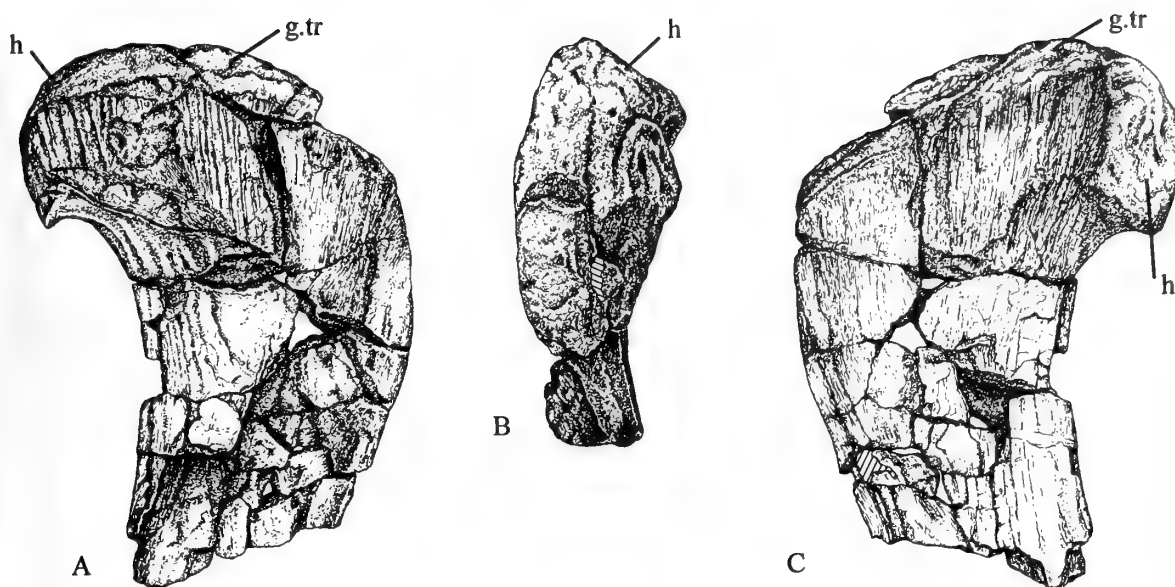


Fig. 40 *Baryonyx walkeri*, holotype, BMNH R9951; proximal part of left femur. A, lateral view; B, proximal; C, medial. $\times 0.25$.

diverging as gentle concave curves; the lateral margin develops a distinct lip, protruding laterally. The profile of the posteroventral edge is weakly concave, so that the pubis expands a little posteroventrally towards the distal end. However, the end itself does not expand extensively either anteriorly or posteriorly to form a 'pubic boot', as it does in many other theropods; indeed the distal profile of the medial or lateral surface forms a smooth convex curve. The medial surface is perceptibly concave towards its distal end.

ISCHIUM (Fig. 39B). A large part of the left ischium is preserved, including most of the shaft (total length of the element as preserved 470 mm). It lacks only the distal end of the shaft and a small part of the anterior edge of the pubic peduncle. Of the right ischium there remain only four fragments of the proximal end, none of which can be fitted together directly; one of them includes the pubic articulation with a small part of the acetabulum, another includes the obturator flange (see below), a third small piece is a further length of the acetabular margin, and a fourth piece is a length of the upper part of the shaft.

The element as preserved is a fairly typical ischium, shaped somewhat like a Y. Between the two peduncles is the most ventral portion of the acetabular ring, narrower in the centre and widening in either direction towards the articulating surfaces for the pubis and ilium respectively; the iliac surface is the larger of the two. Both peduncles (and of course the margins of their articulating surfaces) are convex on their lateral sides and concave medially. Ventral to this region the ischium forms a broad plate which has a stout posterior margin; just below the iliac peduncle this plate is weakly concave between two longitudinal ridges. Towards its anterior margin, below the pubic peduncle, the plate tapers to a slender flange. The ventral part of this flange with its distinctive fluted margin might be interpreted as the equivalent of an obturator process, but the evident absence of any notch or embayment proximal thereto suggests that here was no process projecting anteroventrally, such as is found in *Allosaurus*. There is, however, a slight notch in the anterior edge of the ischium distal to this region; we therefore propose to call this part

of the bone the obturator flange. This condition is very similar to that found in ceratosaurs, in particular *Dilophosaurus* (Welles 1984) and *Carnotaurus* (Bonaparte, Novas & Coria 1990).

The posterior surface of the shaft is broad and flat, but anteriorly it is produced into a thin flange that widens towards the broken distal end. The medial surface of this flange is more or less planar, but the lateral surface is weakly concave.

Hind limb

FEMUR (Figs 40, 41). Both femora suffered extreme damage from clay-winning operations before the presence of the dinosaur skeleton was recognized. The only fragments rescued were (from the left femur) the proximal end with the uppermost part of the shaft, together with the tibial condyle, and (from the right femur) the distal 40% or so of the bone. There was no overlap between the two sides, and it is therefore impossible to make an accurate estimate of the length of the entire element; 1,200 mm is probably a reasonable approximation.

Unfortunately, in this limited material many of the external features had either been destroyed without trace or would have been on regions of the bone that were not preserved; these include the internal and fourth trochanters.

The proximal end of the femur appears not to have been crushed but is nevertheless somewhat flattened anteroposteriorly. The inturned head is oval in outline and its articulating surface is directed, not medially, but rather posteromedially; it is separated from the much larger greater trochanter by a broad U-shaped vertical channel on the posterior side. The greater trochanter is elongated in a mediolateral direction and tapers towards the lateral side, with its anterior surface lightly convex and its posterior surface concave. The lateral edge, narrow proximally, swells out more distally into a distinct protuberance with a convex anterior margin and a straight posterior margin.

The shaft of the femur is more or less circular in cross-section. The distal end shows the usual two condyles, both well preserved;

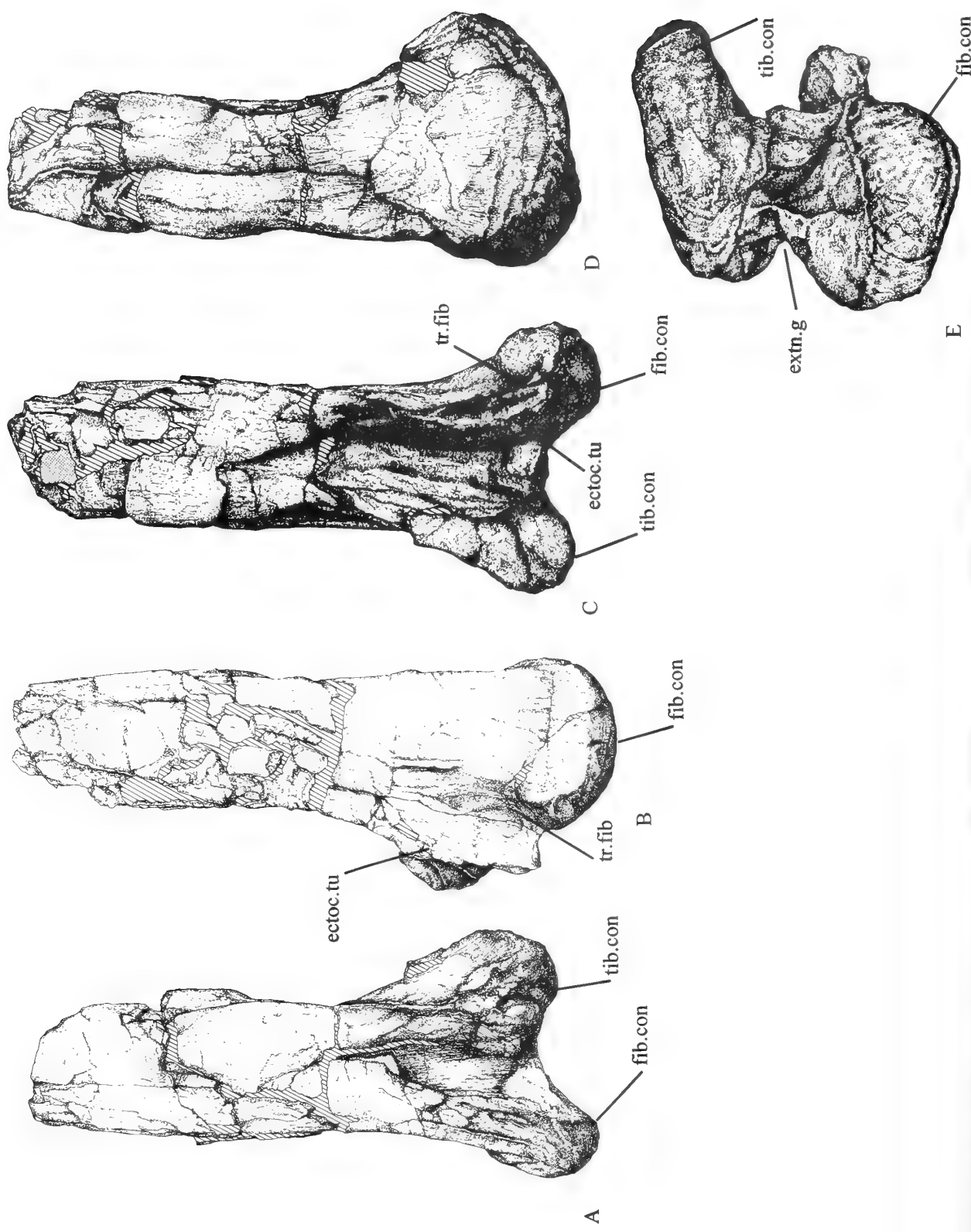


Fig. 41 *Baryonyx walkeri*, holotype, BMNH R9951; distal part of right femur. A, anterior view; B, lateral; C, posterior; D, medial; E, proximal. $\times 0.25$.

the lateral (fibular) extends about 15 mm below the medial (tibial). They are separated by deep intercondylar grooves on both anterior and posterior surfaces; the anterior groove is V-shaped, while the posterior is broader and U-shaped. The tibial condyle, seen in anterior or posterior view, appears to be displaced medially from the line of the shaft; it is greatly expanded anteroposteriorly (though somewhat obliquely) but is relatively narrow from side to side. The fibular condyle, by contrast, lies more or less on the line of the shaft and is less expanded anteroposteriorly. On its posteromedial surface arises a prominent longitudinal flange; this is equivalent to the 'blocky protuberance' described in *Allosaurus* by Madsen (1976: 43) and the 'ectocondylar tuber' described in *Dilophosaurus* by Welles (1984: 137). The deep concavity between this flange and the fibular condyle itself is the trochlea fibularis of Currie & Zhao (1993). A longitudinal groove, deep and V-shaped, runs up the medial surface of the distal part of the shaft; apart from this, the preserved portion of the shaft is in too poor a condition to merit description.

TIBIA. One fragment is recognisable as a distal part of a tibia, but it is too badly crushed to be described.

FIBULA (Fig. 42). The right fibula is in good condition and lacks only its extreme distal end; it is 510 mm long as preserved. The proximal end is broad and flat and expanded anteroposteriorly; the expansion is mostly towards the rear, so that the posterior profile is weakly concave. The lateral surface is weakly convex and the medial surface weakly concave (the latter would have faced the tibia). The elongated, weakly crescentic end-surface is just a little thicker anteriorly than posteriorly. The anteromedial edge of the shaft, just below the head, is slightly thickened for the attachment of the tibiofibular ligaments, but this thickening is less well developed in *Baryonyx* than in *Allosaurus*, *Dilophosaurus* and certain other theropods. Seen in lateral or medial view, the proximal end tapers rapidly distad (with a very weakly concave profile both anteriorly and posteriorly) into a straight, slender, rod-like shaft; the shaft continues to taper more gently, and its anterior and posterior margins eventually run parallel to each other, after which the fragment is terminated by the distal break.

The weak concavity of the medial surface of the proximal end, i.e. the medial sulcus, is continued distad into the medial surface of the shaft, eventually becoming a relatively deep V-shaped trough that terminates suddenly about half-way down the bone (as preserved). Below this the shaft is almost circular in cross-section for a short way but then becomes concave again on the medial side, so that the broken end-surface is clearly crescentic. This medial sulcus is better developed in *Allosaurus*, *Torvosaurus*, troodonts and dromaeosaurs; in *Allosaurus* it is continuous all the way down the shaft.

ASTRAGALUS. A flattened piece of bone compares well with the ascending process of the left astragalus of *Allosaurus*, but is too broken and irregular in outline to merit description.

CALCANEUM (Fig. 43). The right calcaneum is virtually complete. In lateral or medial view it is semilunate, with a weakly concave proximal profile and a strongly convex distal profile. In proximal view, the proximal surface is thick and rounded at the anterior end but tapers to a sharp point posteriorly; the surface itself is weakly concave to receive the distal end of the fibula. The lateral margin of this proximal surface is not higher than the medial margin, in which respect *Baryonyx* is like *Torvosaurus*, but unlike *Allosaurus* and *Sinraptor*.

The lateral surface is almost flat and very slightly dished. The medial surface is convex and bears, at its anterior end, two deep rounded hollows, with a slight protuberance between them. One of

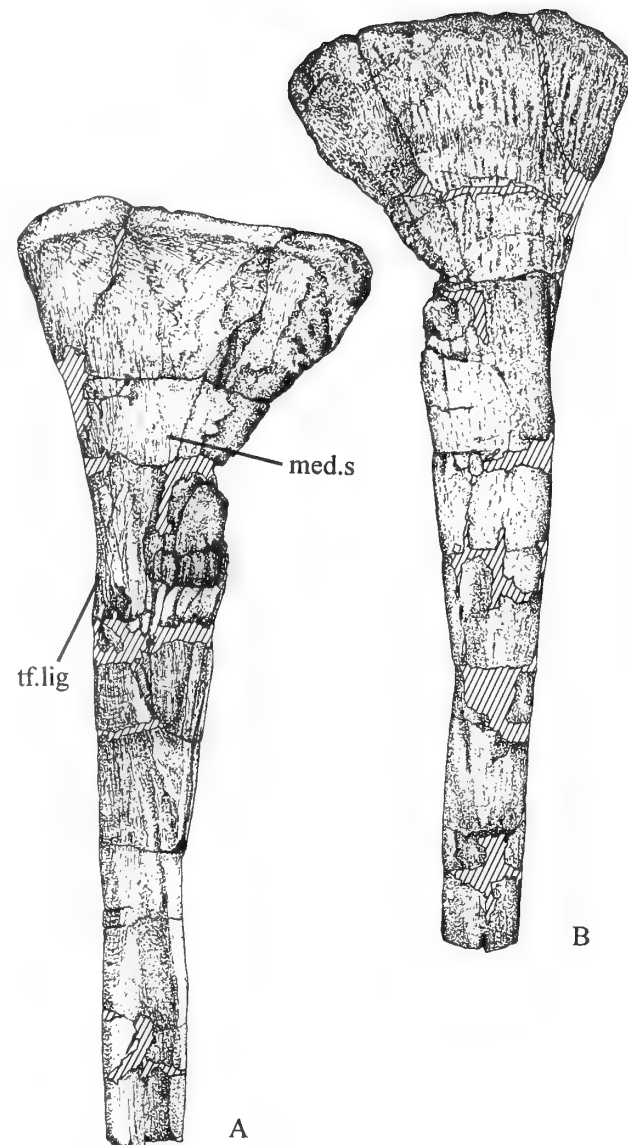


Fig. 42 *Baryonyx walkeri*, holotype, BMNH R9951; right fibula. A, medial view; B, lateral. $\times 0.25$.

these is above and slightly anterior to the other; they are the facets for the two lateral tuberosities of the astragalus, the proximal facet being the larger of the two. The remaining part of the medial surface forms a shallow facet for the reception of the tibia; this facet is much deeper and more cup-shaped in *Allosaurus*.

PES. The collection includes two damaged distal ends of metatarsals, with typical broad, rounded articular surfaces and with fairly well-developed ligament pits. They could be metatarsals II, III or IV of either foot.

Another fragment is the basal part of an ungual from the foot, as indicated by its large radius of curvature and flattened ventral (internal) surface.

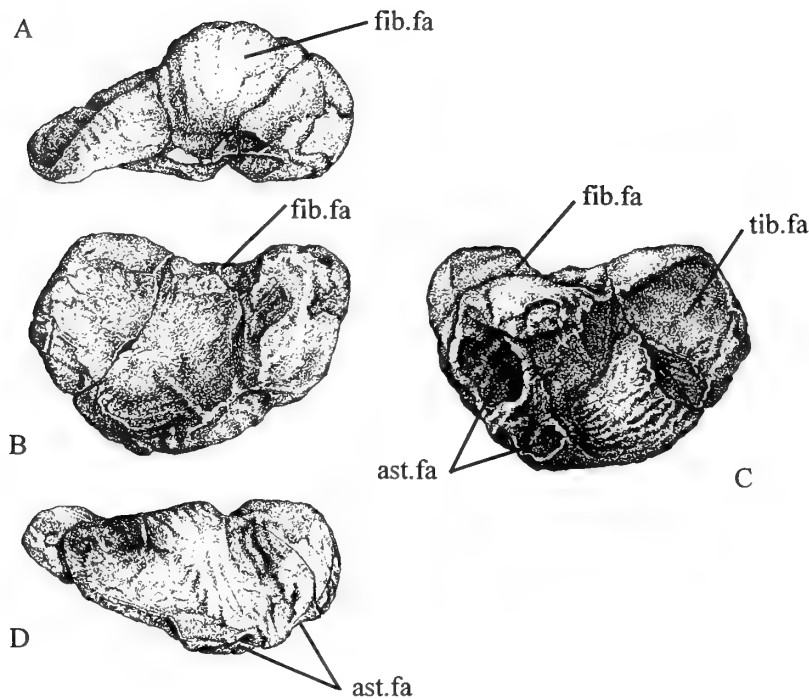


Fig. 43 *Baryonyx walkeri*, holotype, BMNH R9951; right calcaneum. **A**, proximal view; **B**, lateral; **C**, medial; **D**, distal. $\times 0.5$.

OTHER MATERIAL REFERRED TO THE SAME FAMILY

Taquet (1984) described two fragments from the Elrhaz Formation (Aptian) of Gadoufaoua, Niger, as mandibular symphyses of a spinosaurid (Musée National d'Histoire Naturelle, Paris, MNHN GDF 365 and 366); they were refigured more clearly in Kellner & Campos 1996 (fig. 7). Each is virtually identical to the conjoined premaxillae of the holotype of *Baryonyx* (Charig & Milner 1986; 1990: 139) except in that they possess seven alveoli on each side, not six on the left and seven on the right as in R9951. We consider that these snouts, despite their much younger age, are referable to *Baryonyx* sp. indet.

More recently, Viera & Torres (1995: figs 1–2) referred a left maxilla fragment (Museo de San Telmo, San Sebastian, GA-2065) from the Enciso Group, Barremian of Igea, La Rioja, Spain, to *Baryonyx walkeri*. It is less complete and about 75% of the size of the holotype maxilla but otherwise indistinguishable. The tip, anterior to the 3rd alveolus is missing but complete 8th, 9th and partial 10th alveoli are present confirming that the pattern of evenly spaced subcircular alveoli, gradually decreasing in size, continues further posteriorly than is preserved on the holotype maxilla.

The following isolated tooth crowns are referred to cf. *Baryonyx*; their fragmentary nature and the consequent lack of further information precludes a more precise identification.

Wessex Formation (=Wealden Shales, Barremian), Isle of Wight (Isle of Wight County Museum, Sandown IWCMS 3642 and 5120 from Hanover Point; IWCMS 5122, IWCMS 1995 207–209, University of Portsmouth, UOP.97, all unlocalised) described as possible baryonychid by Martill & Hutt (1996). All these crowns are virtually identical with the teeth of the holotype R9951 in their shape, ornamental

pattern, enamel texture, and possession of finely serrated anterior and posterior carinae with seven or eight denticles per millimetre.

Upper Weald Clay (Barremian), former Ewhurst Brickworks, Surrey (National Grid Reference TQ 108379), a single crown (Maidstone Museum MNEMG 1996.133) collected by Dr E A Jarzemowski in the mid 1980's and reported recently from just below BGS Bed 5c, equivalent to the top of the Smokejacks beds.

Ashdown Sand, (Hauterivian) at Redlands Bricks, Ashdown Works, Scallets Wood, Turkey Road, Bexhill-on-Sea, East Sussex, National Grid reference TQ60/70 721097, a single crown (Bexhill Museum BEXHM:1993.485), collected by Mr D. Brockhurst in 1993. This crown differs from the Barremian material only in that the carinae do not extend the full distance to the base of the crown.

PHYLOGENETIC RELATIONSHIPS AND SYSTEMATIC POSITION

Our first publication on *Baryonyx* (Charig & Milner 1986) made no suggestions as to the relationships of the genus, beyond the claim that it 'was a typical large theropod in certain respects, resembling, for example, *Allosaurus*'. We nevertheless considered it to be sufficiently distinctive to merit designation as the type-genus of a new family, Baryonychidae. Our second, more detailed publication (1990) confirmed our view of its separate family status; our only other conclusions were that it was not a spinosaurid and that it could not be fitted into Gauthier's (1984, 1986) cladistic classification of the theropods.

Other workers have referred to *Baryonyx* in various contexts. Their assessments of its phylogenetic position were made in the light of one or both of our preliminary descriptions, which were incomplete and contained some errors. Some of those assessments, because

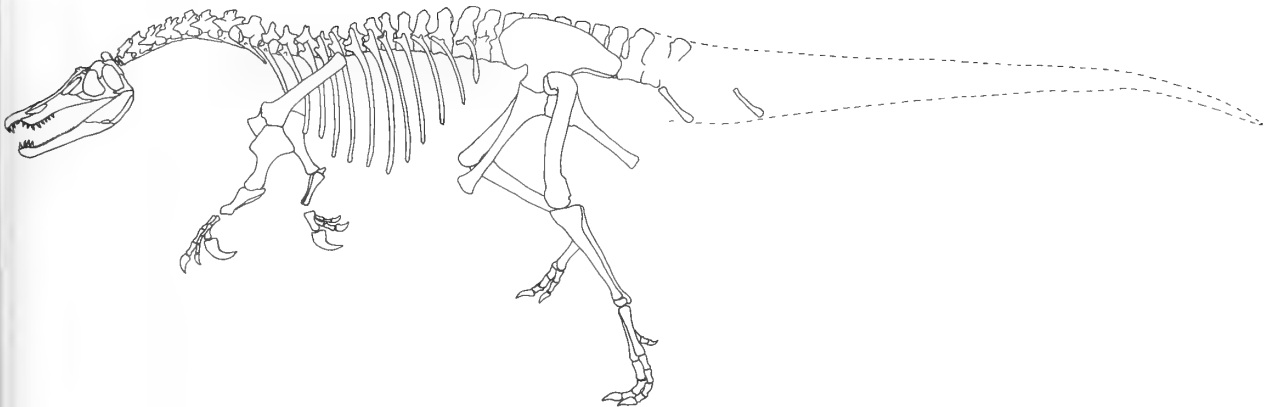


Fig. 44 *Baryonyx walkeri*, holotype, BMNH R9951; reconstruction of entire skeleton, $\times 0.020$.

of this inadequate basis and because of their brevity, scarcely merit discussion. Nevertheless the authors concerned (including ourselves) have generally considered *Baryonyx* to be a close or not-so-close relative of *Spinosaurus*, so that the two genera have often been placed together as a single family (Spinosauridae Stromer, 1915). This has led certain authors (notably Sereno *et al.* 1994) to employ that family as a single unit for the purpose of character distribution analysis.

Bonaparte (1991: 18) suggested a relationship between the Spinosauridae, later fragmentary theropods from Africa (*Carcharodontosaurus* and *Bahariasaurus*), and the South American Abelisauridae; he claimed that the femur of all these forms possessed an anteromedially directed head and a plesiomorphically low lesser trochanter and, if this were true, then they would together represent a major diverse clade (named Neoceratosauria by Novas in 1991), distributed mainly in Gondwana. Holtz (1994a: 1105) cited Bonaparte's work, but misleadingly stated that the Spinosauridae comprised *Spinosaurus* and *Baryonyx*; the latter genus, in fact, was never mentioned by Bonaparte. Holtz also questioned Bonaparte's suggestion, quoting our claim (1990) that *Baryonyx* possessed the tetanuran synapomorphy of an obturator process on the ischium; we now know that to be incorrect – the structure is only a flange. Nevertheless, we agree with Holtz because *Baryonyx* has the femoral head directed medially, not anteromedially, and its other characters are tetanuran rather than neoceratosaurian (see below). Meanwhile Sereno *et al.* (1996), on the basis of new material from the Cenomanian of Morocco, have interpreted *Carcharodontosaurus* as a member of the Allosauroidea.

Elzanowski & Wellnhofer (1992, 1993) proposed a monophyletic group of theropods consisting of *Baryonyx*, *Spinosaurus*, the Troodontidae, *Lisboasaurus* (tentatively identified as a maniraptoran by Milner & Evans in 1991 but reidentified more recently as a crocodylomorph by Buscalioni *et al.* 1996), and *Archaeornithoides* (a tiny fragmentary skull from the Late Cretaceous of Mongolia, described by Elzanowski & Wellnhofer in 1992). This suggestion was based on the following shared characters:

1. Interdental plates absent.
2. Paradental groove present (separating interdental septa from lingual wall of dentary).
3. Lingual wall of dentary lower than labial wall (*Baryonyx*, *Spinosaurus* and *Archaeornithoides* only).

4. Details of articulation between premaxilla and maxilla (*Baryonyx* and *Archaeornithoides* only).

5. Ridge in midline of anterior part of palate (*Baryonyx* and *Archaeornithoides* only).

Elzanowski & Wellnhofer suggested that *Archaeornithoides* was the closest known theropod relative of birds, and that its consistent similarities to *Baryonyx*, *Spinosaurus* and the troodontids narrowed down the ancestry of birds to those theropods that lacked interdental plates and possessed paradental grooves. However, interdental plates are unequivocally present in the dentary of *Baryonyx* (Figs 13, 14), forming a barrier between the alveoli and the paradental groove. Further, since *Baryonyx* does not possess any apomorphic characters of the Maniraptora¹ (in which taxon is placed the Troodontidae), both it and *Spinosaurus* must be far removed from the origin of birds. Another argument against the hypothesis of Elzanowski & Wellnhofer is that *Archaeopteryx* too had interdental plates (as shown by the dentary of the seventh specimen in lingual view, Elzanowski & Wellnhofer 1995). The same is true (Currie 1995) of *Dromaeosaurus*, type-genus of the family Dromaeosauridae, which many authors (most recently Holtz 1994a) regard as the sister-group of *Archaeopteryx*.

Claims of relationship at family level

A minor misunderstanding has arisen over the systematic relationship between (a) *Baryonyx*, (b) *Spinosaurus*, and (c) a partial maxilla from the Upper Cretaceous of Morocco, described and figured by Buffetaut (1989) as *Spinosaurus*. The maxilla of the *Spinosaurus* holotype is known only from a poorly preserved fragment now lost (see below p. 56). Buffetaut was therefore obliged to refer the Moroccan maxilla to *Spinosaurus* on the basis of the only structures common to both specimens, namely the teeth and their alveoli (using, for *Spinosaurus*, dentary teeth and alveoli and isolated teeth). Buffetaut claimed also that *Baryonyx* must be closely related to *Spinosaurus* (basing his evidence both on the original *Spinosaurus*

¹The name 'Maniraptora', proposed by Gauthier (1986: 30) and used by several workers since then, is etymologically wrong. *Manus* (which is Latin, not Greek as stated by Gauthier), meaning 'hand', is a fourth-declension feminine noun with the root *manu-* (see International Code of Zoological Nomenclature, 3rd edition, 1985: 215), not *man-* as Gauthier obviously supposed. His replacement of the English adjective *manual* with '*manal*', *op. cit.*, is presumably based on the same incorrect supposition.

and on the referred Moroccan fossil). He believed that both genera might be in the same family, but concluded that, for the time being, the Spinosauridae and the Baryonychidae should be regarded as separate but closely related. We subsequently argued (Charig & Milner 1990: 131–133, 139) that the Moroccan maxilla resembled *Baryonyx* more closely than it did *Spinosaurus*, and we stated unequivocally that it should be referred to the Baryonychidae as ‘baryonychid gen. et sp. indet.’.

Buffetaut (1992), however, listed certain objections to our arguments:

1. We had claimed that his 1989 illustrations of the Moroccan maxilla showed a ‘peg-like anterior extremity’ and noted also that the posterodorsal rim of the fragment was the ‘anteroventral portion of the rim of the external naris’, despite the fact that neither of those structures was mentioned in the legend or in his description. Buffetaut subsequently stated (1992) that no evidence of either structure could be seen on the specimen; it seems that we had misinterpreted as true edges the broken edges of the fragment (as seen in the illustrations).
2. We had wrongly accused Buffetaut of misinterpreting the broken posterodorsal rim of the fragment as evidence of an antorbital fenestra, failing to note his comment (1989: 82) that ‘no evidence of an antorbital fenestra is visible’.
3. We stated (1990: 32) that the characters common to the Moroccan specimen and to *Spinosaurus* ‘can hardly be considered on their own as diagnostic of a particular genus or even a particular family’, but we nevertheless included most of them in our list of the important characters which, in combination, typify *Baryonyx*. These statements, however, do not really contradict each other; characters that are insufficiently diagnostic on their own might yet be helpful in combination with others.

Moreover, further preparation and research have shown that our interim accounts of the partly developed *Baryonyx* contained some errors, e.g. we had stated wrongly (1990) that the animal possessed at least one elongated neural spine.

The matter was broken down by Buffetaut into two separate problems. Should *Spinosaurus* and *Baryonyx* be included in the same family? (If the answer is yes, then the family would have to be called by the older family name, viz. Spinosauridae.) The resolution of this problem depends only on material that may be included with near-certainty in one genus or the other, i.e. only on the two holotypes; the Moroccan maxilla is wholly irrelevant. Secondly, is it possible to tell whether the Moroccan maxilla is more similar to *Baryonyx* or to *Spinosaurus*, and if so, which?

Buffetaut (1992) was right in pointing out the incorrectness of the similarities that had caused us to ally the Moroccan maxilla with *Baryonyx* rather than with *Spinosaurus* (Charig & Milner 1990); without those alleged similarities the only structures on which the Moroccan maxilla may be compared with either *Baryonyx* or *Spinosaurus* are the teeth. Table 3 summarizes all relevant comparisons between the teeth of those three forms (as far as is possible with the extremely limited material at our disposal).

On teeth alone it can be seen that the Moroccan maxilla resembles *Spinosaurus* more closely than it does *Baryonyx*, which is what Buffetaut (1989) had originally claimed.

Sereno *et al.* (1994: 270) also proposed a unique family relationship between *Baryonyx* and *Spinosaurus*, based on a cladogram containing 44 characters in 9 terminal taxa, including the Spinosauridae (specifying *Baryonyx* and *Spinosaurus*) and *Afrovenator*, a new theropod of Early Cretaceous age. This relationship was based on the following proposed synapomorphies:

Table 3 Comparisons of teeth of *Spinosaurus* with those of related forms.

	<i>Baryonyx</i>	Moroccan maxilla	<i>Spinosaurus</i>
All teeth:			
curvature	recurved, slightly but consistently	?	hardly recurved at all
serrations	7 to the mm	none	none
fluting	lingual sides of crowns fluted	sometimes very faint, fine vertical striping on enamel towards base	
Upper teeth only:			
spacing	widely spaced	widely spaced	?
interdental plates	on both pmx and mx	none	?
labial edge of maxilla	wavy in ventral view	wavy in ventral view	?
Lower teeth only:			
number	32	?	not more than 15
spacing	close together	?	well separated
interdental plates	present	?	absent (<i>fide</i> Stromer and Buffetaut)

1. Elongate premaxillary snout. In *Baryonyx* the whole of the snout is elongate; in *Spinosaurus* it is unknown.
2. Specialized anterior dentition, manifested by increase in number of premaxillary teeth. *Baryonyx* has 6/7 premaxillary teeth, which is 1/2 more than the 5 usual in theropods; but, in any case, their number is unknown in *Spinosaurus*.
3. Specialized anterior dentition manifested also by terminal rosette. We coined that term for the horizontally expanded tip to the upper jaw in *Baryonyx*, almost completely surrounded by dental alveoli. The upper jaw of *Spinosaurus* is unknown except for a small fragment of maxilla.
4. Increase in height of dorsal neural spines. This was mistakenly reported in our 1990 publication and is incorrect. In contrast, the dorsal neural spines of *Spinosaurus* are greatly elongated (hence the generic name).

Thus, of the four allegedly synapomorphic character-states, three are unknown in *Spinosaurus* and may therefore be discounted. The last is present in *Spinosaurus* but absent in *Baryonyx*. This means that the synapomorphies of Sereno *et al.* (1994), considered on their own, provide no justification for placing the two genera concerned in the same family.

Consequently, we are now in agreement with Buffetaut in so far as we accept a particular relationship between Spinosauridae and Baryonychidae. However, in the absence of decisive evidence in either direction, the following factors predispose us against synonymising the two families:

1. The material of *Baryonyx* is far more complete than that of *Spinosaurus*, and *Baryonyx* would therefore make a much more informative type-genus for the family in which it is included. More importantly, all of Stromer's (1915) *Spinosaurus* material, housed in Munich Museum, was destroyed in an Allied bombing raid in 1944, and is therefore no longer available for comparisons; nor is there any other material that could be designated as a neotype.
2. The most important distinguishing feature of the Spinosauridae, as suggested by the name, is the elongation of the neural spines on the vertebrae. *Baryonyx* has no such elongated spines. The presence or absence of such spines may have little or no

phylogenetic significance, and it would not be against the International Code of Zoological Nomenclature to call *Baryonyx* a spinosaurid; nevertheless it could be very misleading.

3. The similarities between the two genera, as known at present, are not (in our opinion) sufficiently close to justify their treatment, for cladistic analysis, as a single O.T.U. (operational taxonomic unit).

Also of importance in this connexion are two recently discovered theropods from the Romualdo Member of the Santana Formation (Albian) of the Araripe Basin of north-eastern Brazil. Kellner & Campos (1996) described a fragmentary snout as a new member of the Spinosauridae and named it *Angaturama*. *Angaturama* is especially useful in that it shares certain apomorphic characters with *Spinosaurus*, yet, at the same time, possesses other apomorphic characters that it shares with *Baryonyx* but which could not be demonstrated in *Spinosaurus* itself because of the latter's incompleteness. We therefore believe that, using *Angaturama* as a link, we can justify a closer relationship between the Spinosauridae (*Spinosaurus*, *Angaturama* and the Moroccan maxilla) and the Baryonychidae (*Baryonyx*) than between either of those two families and any other. We further believe that this relationship might be reflected in the classification by placing those two families together in the same superfamily Spinoauroidea¹ Stromer, 1915, excluding the other genera previously placed there by Sereno *et al.* in 1994 (*Torvosaurus*, *Eustreptospondylus*).

The Spinoauroidea as defined here is characterized by the following apomorphic characters, unique among the Theropoda:

1. The elongation of the jaws, especially in the premaxillary region.
2. A greater or lesser tendency to develop a terminal rosette (greater in the upper jaw than in the lower).
3. The shape of the front of the lower jaw, turned upwards at the extreme anterior end and constricted transversely just behind that.
4. An increase in the number of premaxillary teeth to seven.
5. Teeth that show a reduction in:
 - (a) the compression of the whole tooth in a labio-lingual direction;
 - (b) the recurvature of the crown (only slight in *Baryonyx*, practically non-existent in *Spinosaurus*);
 - (c) the size of the denticles on the anterior and posterior carinae of the crown (very fine in *Baryonyx*, absent altogether in *Spinosaurus* and *Angaturama*).

The other Albian theropod from Brazil, *Irritator* Martill, Cruickshank, Frey, Small & Clarke 1996, is a partial skull lacking the end of the snout; this makes it difficult to compare with *Angaturama*, except in so far as both genera obviously had elongated jaws, external nares set far back, and teeth that share all the unique tooth characters of Spinosauridae (5. above). It seems very likely that *Irritator* too is a spinosaurid, and even possible that it is a senior synonym (by one month!) of *Angaturama*. Its authors, however, assigned it to the Bullatosauria Holtz, 1994a, a new taxon of maniraptorans that includes the Troodontidae and the Ornithomimosauria.

These characters could, of course, represent independent adaptations to similar diets. On the other hand, it is more parsimonious to

interpret the unique distribution of all seven in the Spinosauridae and the Baryonychidae as indicating a sister-group relationship between those two families. This latter interpretation is consistent with the fact that the degree of reduction shown in the tooth characters (b) and (c) above is significantly less in Baryonychidae than in the much later Spinosauridae, i.e. the characters reflect a trend which seems to have increased greatly during the time interval between the Barremian and the Cenomanian.

The systematic position of *Baryonyx* and its allies within the Theropoda

By far the most detailed analysis of theropod relationships published to date is Holtz's work of 1994a. His computer analysis of the data, based on a matrix of 19 O.T.U.s and 126 characters, produced a single most-parsimonious cladogram (his fig. 4), and a strict consensus cladogram of the six equally parsimonious 'runners-up' (his fig. 5).

Holtz's cladogram agrees in many respects with the cladograms of earlier workers, notably Gauthier's. In some details, however, it differs greatly. The most important difference lies in the positions assigned to the Tyrannosauridae and the Troodontidae, among the most highly derived Coelurosauria (within the Maniraptora and close to the Ornithomimosauria).

We assessed the phylogenetic relationships of *Baryonyx* by incorporating it as an additional, twentieth taxonomic unit into Holtz's data-matrix. It seemed to us, however, that a few of the characters that Holtz had used in his analysis were unsatisfactory and that others were scored wrongly. This opinion has been confirmed independently through the recent publication of criticisms by Clark, Perle & Norell (1994) of several of Holtz's characters (see Appendix C) leading to scepticism of his main conclusion, that the Tyrannosauridae should be placed within the Maniraptora. Our relatively minor modifications of Holtz's analysis have not affected that conclusion.

We deleted 8 characters from Holtz's data-matrix and re-scored a few others, thereby producing a modified data-matrix (Appendix C). All available information on *Baryonyx* (on 57 characters, information on the 61 others being unavailable or too uncertain to be of any value) was added and the analysis run with both the same computer programme (PAUP Version 3.0, Swofford 1990) and with Hennig86 (Farris 1988) and the results compared. PAUP was run under Heuristic and Branch & Bound algorithms and produced six equally parsimonious trees of 228 steps, with a consistency index (C.I.) of 51% and a retention index (R.I.) of 70%. Hennig86, using mh* and Branch & Bound options, gave similar results: six equally parsimonious trees of 234 steps, with a C.I. of 50% and an R.I. of 70%. These figures resemble Holtz's (51% and 71% respectively). Holtz's best cladogram had 244 steps, a few more, but it should be remembered that he used 126 characters as against our 118. All trees were rooted to a hypothetical ancestor on unordered characters.

All these trees (and the corresponding consensus trees) produced by both programmes display topologies that are generally similar to each other and which, in their broad outlines, resemble Holtz's single most-parsimonious cladogram. In all of them there is a monophyletic Ceratosauria arising from the basal node, and, much farther away from the root, a monophyletic Neotetanuriae. Between them are three other nodes that give rise to a polyphyletic assemblage that might be referred to collectively and informally as 'basal Tetanuriae' (among which *Baryonyx* is placed). The more detailed arrangement of the O.T.U.s was constant within the Ceratosauria but varied from tree to tree within the Neotetanuriae; those clades, however, do not concern us here, and discussion of such problems is beyond the scope of the present work.

¹Some confusion surrounds the superfamilial name Spinoauroidea (which, according to the Principle of Coordination laid down in Article 36(a) of the International Code of Zoological Nomenclature, must retain the same author and date as existing family-group names based upon the same type-genus). Sereno *et al.* (1994) proposed a taxon including *Baryonyx*, *Spinosaurus*, *Torvosaurus* and *Eustreptospondylus*, naming it Torvoauroidea. However, Sereno *et al.* (1996) changed the name of that nominal taxon to Spinoauroidea, presumably because the family name Spinosauridae Stromer, 1915 is senior to Torvoauroidea.

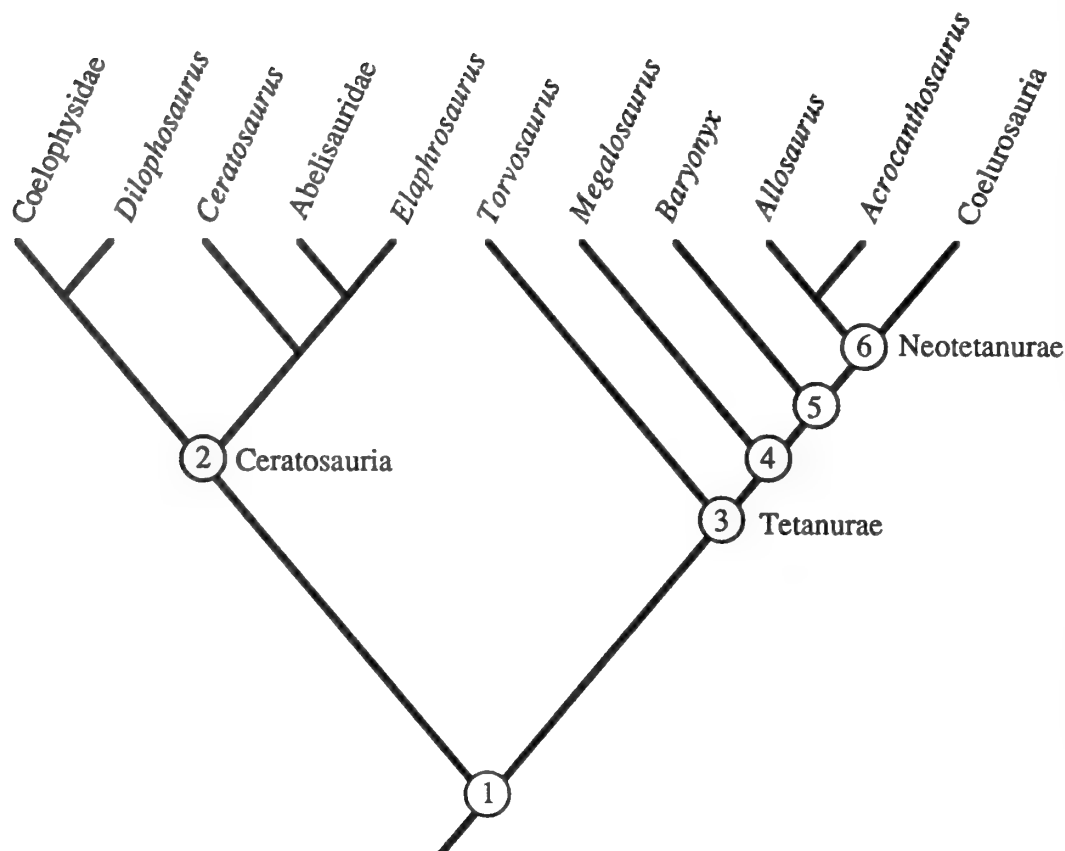


Fig. 45 Cladogram of the Theropoda, based on our modified version of Holtz's data-matrix and including also *Baryonyx*.

In all our cladograms (summarized in Fig. 45) *Baryonyx* is placed as the sister-group of the Neotetanuriae Sereno *et al.*, 1994 (=Avetheropoda Paul, 1988), arising from node 5 (numbering of nodes and characters are as used in this work, not Holtz 1994a; for details see Appendix C). The nearest outgroup of the combined clade is *Megalosaurus*, arising from node 4, and the second nearest *Torvosaurus*, arising from node 3. All these taxa (i.e., *Torvosaurus*, *Megalosaurus*, *Baryonyx* and Neotetanuriae) together comprise the Tetanurae Gauthier, 1986. If *Baryonyx* were inserted into Holtz's cladogram (his fig. 4) it would split off from the main stem of his Hennigian comb, leading to the Coelurosauria *sensu* Gauthier, between his nodes 6 and 7.

The specific evidence for the position of *Baryonyx* on our cladogram (Fig. 45) is assessed critically below.

At node 3 (*Torvosaurus* dichotomy, Holtz's node 5, Tetanurae) there are fourteen synapomorphies. *Baryonyx* provides positive evidence of only three of those, namely:

50. Dorsal vertebrae pleurocoelous ('unambiguous synapomorphy' of Tetanurae, *fide* Holtz *loc. cit.*).
4. Dorsal vertebrae with transverse processes that are not strongly backturned or triangular in dorsal view (supposedly reversed character).
110. All three pelvic elements not fused together in adults (supposedly reversed character).

At node 4 (*Megalosaurus* dichotomy, Holtz's node 6, unnamed)

there are eight synapomorphies, but unfortunately *Baryonyx* affords evidence of none of them.

At node 5 (*Baryonyx* dichotomy, new node, unnamed) there are five synapomorphies, on only one of which does *Baryonyx* provide data, namely:

96. Coracoid tapers posteriorly ('unambiguous synapomorphy' of Holtz). We thought it unwise to propose a new name for the taxon based on this node; the phylogeny is not yet sufficiently well established.

This evidence is not very convincing. More helpful is the list of synapomorphies for node 6 (dichotomy between *Allosaurus*/*Acrocanthosaurus* and Coelurosauria *sensu* Gauthier; Holtz's node 7; Neotetanuriae or Avetheropoda); there are four of them upon which diagnosis of the Neotetanuriae is based. In this case, fortunately, *Baryonyx* provides clear evidence to show that it has none of them:

105. Axis with spine table.
117. Manual digit I reduced in length.
88. Obturator process present.
92. Pubic boot pronounced ('unambiguous synapomorphy' of Neotetanuriae, *fide* Holtz *loc. cit.*).

Certain characters of *Baryonyx*, though used in Holtz's and our analyses and seeming to be apomorphous for that O.T.U., also occur elsewhere in the cladogram. If our suggested phylogeny is correct,

this means that they must have evolved independently in *Baryonyx* and in the other forms concerned. Examples are:

5. Pronounced subnarial gap, indicating a possibly mobile premaxillary-maxillary joint. This gap (renamed the *subrostral notch* in *Baryonyx*, see p. 14) occurs also in certain ceratosaurs, namely Coelophysidae and *Dilophosaurus*, and was therefore considered by Holtz (1994a: 1104) to be an unambiguous synapomorphy for the Coelphysoidae. Rowe & Gauthier (1990: 154) claimed that articulated material shows the premaxillary-maxillary joint of ceratosaurs to be a firm junction, as is also the case in *Baryonyx*.
77. Nasals narrow. This occurs also in *Dromaeosaurus*, *Archaeopteryx*, *Tyrannosaurus*, *Troodon* and *Ornithomimus*.
13. Parietals projected dorsally. This occurs also in *Ceratosaurus* and *Abelisaurus*.

We considered also the partial analysis of Sereno *et al.* 1994 (in which the synapomorphies are listed only under 'References and Notes'). Those authors did consider *Baryonyx*, though not as a separate O.T.U. but as part of the taxon Spinosauridae (see above, p. 56). Their cladogram (Fig. 46) shows the Spinosauridae as the sister-group of Torvosauridae, arising from node 4 (unnamed, our numbering); those two O.T.U.s together as the sister-group of *Afrovenator*, arising from node 3 (Torvosauroidea); and the Torvosauroidea as the sister-group of the Neotetanuriae. The Torvosauroidea and the Neotetanuriae together constitute the Tetanuriae. We replaced Spinosauridae as an O.T.U. by the genus *Baryonyx* on its own, in an otherwise unmodified data-matrix, then ran the programme as described above (p. 57). This produced a single most-parsimonious tree of 58 steps, C.I. 93%, R.I. 90%, identical to the tree figured by Sereno *et al.* except in that *Baryonyx* occupies the position that was previously occupied by Spinosauridae.

This cladogram requires critical scrutiny. Sereno *et al.*'s (1994) linking of the Spinosauridae (which included *Baryonyx*; Spinosauroides *sensu* this work) with the Torvosauridae (*Torvosaurus* + *Eustreptospondylus*) to form an unnamed taxon is supported by only two synapomorphies:

1. Radius less than 50% of humeral length. This is true of *Baryonyx* (49%), but in *Spinosaurus* neither humerus nor radius is known.

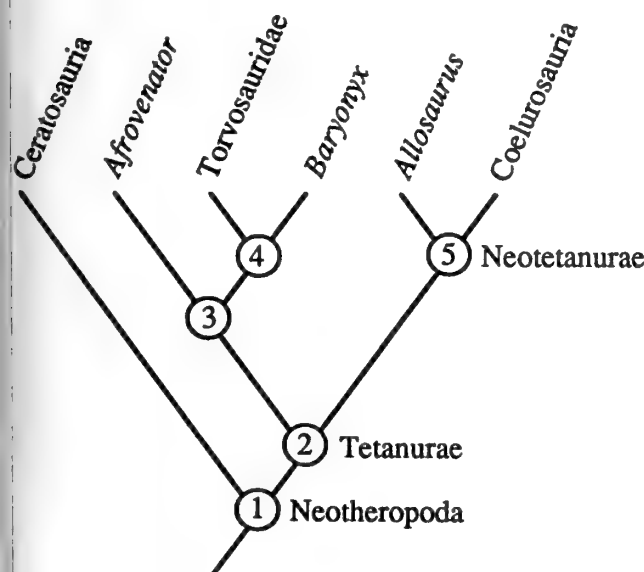


Fig. 46 Cladogram of the Theropoda, according to Sereno *et al.* (1994).

2. Manual digit I ungual elongate (three times height of proximal articular end). This is essentially true of *Baryonyx*, where the length of the ungual is more than four times the height of the proximal end: length of ungual measured around the outside of the curve 310 mm, height of end 73 mm. Again, the manus is unknown in *Spinosaurus*.

Thus, while there is no evidence either way for the condition in *Spinosaurus*, it seems that *Baryonyx* and *Torvosaurus* do share two characters. However, such similarities in relative proportions could easily have developed homoplastically and therefore lack phylogenetic significance. Further, while the reduction or absence of a quadrate foramen links *Torvosaurus* with *Afrovenator* (see below), that same foramen is prominent in *Baryonyx*; indeed, it is more of a fenestra than a foramen. Thus there does not seem to be an adequate demonstration of a close phylogenetic link between *Baryonyx* and the Torvosauridae.

Sereno *et al.* (1994) also claimed that this unnamed Torvosauridae + Spinosauridae taxon was the sister-group of their new Saharan theropod *Afrovenator*, ranking the combined taxon as a superfamily and naming it Torvosauroidea (though those same authors, in their 1996 publication, called it Spinosauroides). This was based on five synapomorphies, all characters of the skull:

1. Anterior ramus of maxilla as long anteroposteriorly as tall. In *Baryonyx* the whole of the maxilla as preserved is anterior to the antorbital fenestra and may therefore be presumed to be part of the 'anterior ramus' of Sereno *et al.*; in which case it is several times longer than tall. In *Spinosaurus* practically nothing of the maxilla is preserved and this character-state is therefore unknown.
2. Anterior ramus of lacrimal dorsoventrally narrow. In *Baryonyx* this structure, more usually referred to as the nasal or dorsal ramus, shows a condition intermediate between those of *Torvosaurus* and *Allosaurus*. Nothing is known of the condition in *Spinosaurus*.
3. Lacrimal foramen small and positioned at mid-length along the jugal ramus. This is confusing in so far as there are three lacrimal foramina in *Torvosaurus* (Britt 1991: 17–19); Britt's photograph of the lacrimal in medial view clearly shows that the large one, which he called the posterior lacrimal foramen, lies one-third of the way down the orbital side of the jugal ramus. In *Baryonyx* also there are three foramina, one large and, close together, two very small ones; the large one lies beneath the junction of the two rami, i.e. at the dorsal extremity of the jugal ramus. The corresponding character-state is unknown in *Spinosaurus*. This proposed synapomorphy is altogether unclear.
4. Ventral process of postorbital broader transversely than anteroposteriorly. This character-state is not found in *Baryonyx* and is unknown in *Spinosaurus*.
5. Quadrate foramen reduced or absent. *Baryonyx* has a large, prominent quadrate foramen between the quadrate and the quadratojugal. The condition is again unknown in *Spinosaurus*.

In summary, two of the relevant character-states (nos 1 and 2) may be present in *Baryonyx* but it is difficult to have much confidence in them. For the other three (nos 3, 4 and 5) the character is either unclear or in the opposite state. All five characters are unknown in *Spinosaurus*; and none appears in the abbreviated description and diagnosis of *Afrovenator abakensis* published by Sereno *et al.* (1994: 270). We can find no justification for the placing together of these alleged sister-groups.

The net result of our re-working of the analysis of Sereno *et al.*

(1994), with *Baryonyx* replacing Spinosauridae as an O.T.U., is to confirm the systematic position of *Baryonyx* as a 'basal tetanuran', and, at the same time, to cast serious doubts upon any particularly close connexion with *Torvosaurus* and/or *Afrovenator*.

Another cladistic analysis of the Theropoda that deserves brief consideration is that of Russell & Dong (1993: 2122–2125). Many of the O.T.U.s (mostly at family level, but including also *Baryonyx*) were novel, as were many of the synapomorphies proposed, and this resulted in a cladogram that was unusual in several respects. One group, including *Baryonyx*, *Yangchuanosaurus*, *Allosaurus*, dromaeosaurids and tyrannosaurids appeared to be defined 'by the acquisition of horn-like tuberosities along the dorsolateral edge of the skull and relatively large teeth which are few in number' (Russell & Dong, 1993: 2121). In fact, all that appears to pertain to *Baryonyx* in the former connexion is one small tuberosity on the lacrimal. Its teeth (in the lower jaw at any rate) are more numerous than in any other theropod except *Troodon* (Osmólska & Barsbold 1990) and *Pelecanimimus* (Pérez-Moreno *et al.* 1994), both of which are systematically remote from *Baryonyx*. Russell & Dong's analysis does not seem to shed any additional light upon the systematic position of the latter.

Finally, Holtz (1995) published a new phylogeny of the Theropoda in which he proposed a weakly supported monophyletic Megalosauroidea comprising *Afrovenator* + (*Megalosaurus* + *Baryonyx* + *Torvosaurus*).

Conclusions

Our final conclusions on the systematic position of *Baryonyx* are that it should remain as the type-genus of the family Baryonychidae; that its nearest relatives (to be placed in the same superfamily Spinosauroidea) are the poorly known *Spinosaurus*, *Angaturama* and perhaps *Irritator*; that this group lies within the Tetanurae, close to the base of that taxon, with the Neotetanurae as its sister-group; and that *Megalosaurus* and *Torvosaurus* respectively are progressively more distant outgroups to the combined Spinosauroidea+Neotetanurae clade.

This is the best that we can do in our present state of knowledge. Our conclusions are subject to the usual caveats:

1. Lists of characters for the same group, drawn up by different authors, are often very different¹ (Charig 1993) and are bound to be far from complete (Panchen 1982).
2. The itemisation of the characters and the scoring of the character-states for the data-matrix require a great number of difficult subjective decisions.
3. Small changes in selection of characters, itemisation and scoring can produce drastic changes in the results of the analysis.
4. Our knowledge of those same character-states in *Baryonyx* is very incomplete, and in certain cases the scoring was likewise difficult.
5. Other authors, generally using very different lists of characters and different O.T.U.s, have produced different cladograms for the Theropoda.
6. The most parsimonious cladogram does not necessarily represent the actual course of evolution (Charig 1982: 414).

At the same time we must point out that, when two or more analyses based on very different lists of characters produce remarkably

similar cladograms, the fact that the shared topology is supported by different rafts of evidence greatly enhances our confidence in its correctness.

PALAEOECOLOGY

In Early Cretaceous times the Weald of Surrey, Sussex and Kent was partly occupied by the Wealden Lake, a large lake of fresh to brackish water that extended westwards into Hampshire. To the north lay dry land in the region of what is now the London conurbation; to the south lay the Anglo-Paris Basin and the open sea. Two large rivers flowed down from the north and north-east to discharge their waters into the lake through a common delta, with shallow creeks and oxbows. The climate was, in modern terms, sub-tropical.

Ross & Cook (1995) have recently reported on the stratigraphy and sedimentology of the Smokejack's locality in particular. The exposure at that site consists of 23 m of Upper Weald Clay, all of it of early Barremian age (estimate of absolute age approximately 130 million years). The *Baryonyx* remains were in fine silty clays of non-marine origin, light olive-grey in colour and containing large irregular nodules of bioturbated sideritic siltstone. The sediments give indications of shallow-water facies (e.g. ripple-marks at the base of the dinosaur level) but show no signs of complete drying out (mud-cracks, erosion etc.), nor is there evidence of braided river deposition; they had obviously settled out of still water (a "low energy" environment). This lithology, both at the *Baryonyx* horizon and in the beds immediately below, has been interpreted by Ross & Cook as indicating a fluvial and/or mudplain environment with areas of shallow water, lagoons and marsh.

The fossil flora and fauna of the Smokejack's locality as a whole give some idea of the environment in which *Baryonyx* lived (Frontispiece), although it should be remembered that the flora, fauna and total environment all varied significantly at different levels in the sequence. Common plant remains include the fern *Weichselia reticulata* (Stokes & Webb), concentrated locally in layers within the clay and in sideritic lenses, and an aquatic or marsh-dwelling herbaceous plant that grew in monotypic stands, *Bevalstia pebjia* (Hill 1996). Also present were filicopsid ferns, horsetails, club mosses and conifers. Of great importance to the environmental interpretation are the abundance and variety of fossil insects at Smokejack's, 10 orders of which were recorded by Jarzembski (1984). The exact stratigraphical positions of many of the older finds are not known, but some insects have now been recovered *in situ* from sideritic siltstone lenses at a number of horizons below *Baryonyx* (Ross & Cook 1995). Other elements of the invertebrate fauna were ostracods, isopods, conchostraceans and bivalves.

The vertebrate fauna includes sharks, bony fishes (notably *Lepidotes mantelli* Agassiz), crocodiles, pterosaurs, and dinosaurs. Apart from *Baryonyx walkeri*, the only other dinosaur remains yielded by this locality consist of a considerable quantity of material referred to the relatively common ornithopod *Iguanodon atherfieldensis* Hooley, 1925, and a very few isolated bones of small saurropods. In 1982 we excavated the hind portion of an articulated *Iguanodon atherfieldensis* skeleton at a distance of only about 100 m from the *Baryonyx* site and at approximately the same stratigraphic level. Fragmentary remains of a large *Iguanodon bernissartensis* Boulenger, 1881, were collected in 1988 from a higher level in the sequence.

¹Holtz (1994a) used 126 characters in his analysis of the Theropoda; Sereno *et al.* (1994) used 80 (excluding the Ceratosauria). Even the most generous interpretation could find no more than 17 characters common to both, of which only 4 pertained to the skull and vertebral column.

FUNCTIONAL MORPHOLOGY AND MODE OF LIFE

We (Charig & Milner 1986) have suggested for *Baryonyx*:

- (a) ichthyophagy (a diet consisting mainly of fish) but with the further possibility of a scavenging habit;
- (b) a terrestrial existence; and
- (c) quadrupedality, facultative at least.

DIET AND METHODS OF FEEDING. Kitchener (1987) noted that 'The alternative lifestyle of a scavenger [had] received very little attention' in our paper; he followed this with the full details of our case for a scavenging habit (as presented by us at meetings in Drumheller and Belfast in 1986 but omitted from our publication because of lack of space). Kitchener then went on to state his preference for the idea of a scavenging habit over that of ichthyophagy, a preference which we do not share.

The characters suggesting a scavenging habit, as published by Kitchener, may be summed up as follows:

1. Stance facultatively quadrupedal.
2. Neck long (both 1 & 2 suitable for feeding at ground level).
3. Fore-limbs massively developed, with huge claws (ideal for breaking into a carcass).
4. Snout narrow (well suited to investigating the body cavity of the carcass).
5. External nares placed far back from tip of snout (permitting simultaneous feeding and breathing).
6. Premaxilla and maxilla connected by flexible hinge (allowing freer movement in the restricted space in the body cavity).
7. Teeth slender and finely serrated (for processing the soft viscera).

However, we now know that there is no evidence for characters nos 1, 2 and 6.

Kitchener also put forward one character as evidence against a typical macropredacious habit:

8. Mandible and teeth weakly developed (particularly unsuitable for killing and feeding on large herbivorous dinosaurs). Even crocodilians, after the birds the nearest living relatives of *Baryonyx*, have great difficulty in breaking through the skin of large prey.

He also made two arguments against ichthyophagy:

9. It is unlikely that such a heavy creature 'could have been sufficiently manouverable [sic] to catch fast-moving fish'.
10. *Baryonyx* has too many adaptations for fish feeding, viz. fore-limbs for hooking fish and teeth and jaws similar to the fish-eating gavial's; 'one adaptation would suffice'.

In a critical reply to Kitchener, Reid (1987) cited three counter-arguments:

To 3 above: Most available carcases would probably already have been broken into by the primary predator.

To 8 above: The teeth of modern crocodilians are more or less conical, not adapted to slicing, and are in no way comparable to the bilaterally compressed "steak-knife" teeth of typical theropod dinosaurs. (In fact, the condition in *Baryonyx* is intermediate between the two.)

To 9 above: Large animals, e.g. grizzly bears, are capable of

catching fast-moving fish, at least in shallow water. Techniques analogous to 'gaffing' or trout-tickling could also have been employed.

We add two further comments:

To 7 above: The crowns of the teeth were not slender; in fact, they were less compressed laterally than those of other, more 'typical' theropods.

To 10 above: There is no logic in the argument that, because an animal has two different adaptations that appear to have served the same purpose, neither of them can in fact have served that purpose.

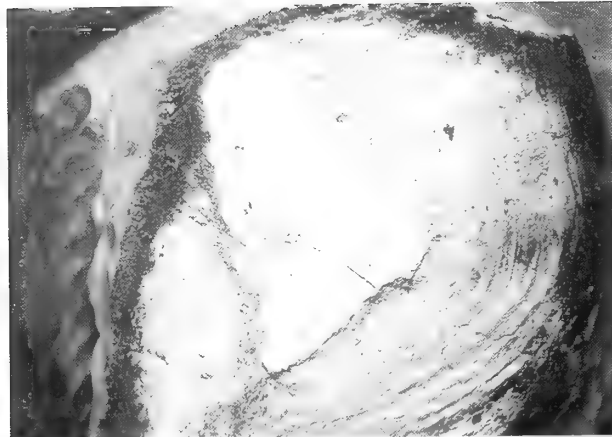
The information that may help us assess the diet and feeding methods of *Baryonyx* is as follows:

1. There is direct evidence of what the animal had been eating. Within its smashed-up rib-cage, in its stomach region, were found:
 - a. Acid-etched scales and teeth of the common Mesozoic fish *Lepidotes* (Fig. 47). These are of especially great significance.
 - b. The disarticulated skeletal remains of a young *Iguanodon* [See Appendix B] showing some evidence of abrasion (and/or etching).
2. There is also circumstantial evidence of the ichthyophagous habits of *Baryonyx*. Modern crocodilians have certain adaptations which are clearly effective in catching and swallowing fishes; analogous characters are found in *Baryonyx*:
 - a. The jaws are long and very narrow from side to side; they are expanded horizontally at the anterior end, with enlarged teeth around the margins of the expansions (Fig. 2). In the upper jaw this spatulate expansion forms a 'terminal rosette', not unlike the corresponding region of the skull of a modern gavial.
 - b. Seen from the side, both upper and lower jaws have sigmoid dentigerous margins (Fig. 1); the upper jaw has a downturned tip and a 'subrostral notch'. Altogether this particular aspect of the animal has an appearance that is distinctly crocodile-like, albeit only superficially so.

These similarities support the idea that *Baryonyx* caught small and moderate-sized fishes in a crocodilian manner, i.e., it seized them with the end of its pincer-like jaws and gripped them transversely in its subrostral notch and lateral teeth; the shape of the jaws and the nature of the teeth accord well with the suggestion that they somehow helped the grasping and manoeuvring of slippery prey. The animal might then have tilted its head back and manoeuvred the fish around so that the fish slid head-first down the gullet into its stomach, as do modern crocodilians. We believe that *Baryonyx* ate fish habitually, though not necessarily exclusively.

Whatever the nature of *Baryonyx*'s preferred diet, the animal seems ill-equipped to have been a typical theropod macropredator of the type that relied largely on short, powerful jaws and blade-like teeth with serrated edges to capture, kill and dismember its prey. This is because:

1. The middle part of each bony ramus of the mandible is wafer-thin.
2. The teeth are only slightly compressed from side to side, thus differing from those of typical macropredacious dinosaurs like *Allosaurus*.
3. The denticles on the carinae of the teeth are remarkably fine (about 7 per millimetre).



A



B

Fig. 47 *Lepidotes* scales, scanning electron micrographs. **A**, from rib-cage region (Block 44) of the *Baryonyx* skeleton, showing acid-etching of the enamel, $\times 8$; **B**, from the same horizon and locality but not associated with the *Baryonyx*, showing smooth unetched enamel, $\times 11$.

Conversely, *Baryonyx* possesses characters that suggest different methods of acquiring its food:

1. The jaws are long and narrow, not unlike a pair of forceps. They could have been dipped, either into water to seize relatively small fish, or into the body cavity of a large dead animal to seize the entrails.
2. The external nostrils were lateral and far posterior in position. This would have enabled the animal to continue breathing comfortably even while its snout was still deep in the water or in the body cavity of a carcass.
3. The large and presumably heavy head would have limited the mobility of the neck.
4. The ends of the cervical centra are not "offset"; it is therefore unlikely that the neck would have been held in a sigmoid curve.
5. The cervical vertebrae have well developed epiphyses, but their neural spines are low and lack spine tables. This suggests that the intervertebral muscles were strong and the neck highly mobile, which again would have helped its feeding activities.
6. The humerus is very robust, with both ends broadly expanded. The proximal end in particular is expanded anteriorly into an unusually long and high deltopectoral crest and posteriorly into a well-developed internal tuberosity (compare with other theropods, including *Torvosaurus*). The pectoral girdle too is well developed and there was also an ossified sternum. All this would have facilitated the powerful adduction, abduction (and perhaps rotation?) of the fore-limb as a whole.
7. The radius is relatively short and that too is robust and powerful. The same applies to the ulna without the olecranon, but the olecranon itself is remarkably long; thus the ratio 'length of olecranon/length of ulnar shaft' is exceptionally high. This produced a mechanical advantage (i.e., leverage) when the fore-arm was extended.
8. One manual ungual is enormous; it is of typical theropod form, though somewhat more slender than in *Allosaurus*, and it is not modified into a "sickle" like the enlarged pedal ungual of *Deinonychus* (Ostrom 1969). This was clearly an extremely powerful offensive weapon.

The characters of the fore-limb and manus suggest that the fore-limbs of *Baryonyx* were exceptionally powerful, the fore-arm being capable of exerting great force at the wrist when extended. By activating the enormous claw on the thumb, this would have enabled the animal not only to catch and kill its prey (if necessary), but also to rip and tear it to pieces. In short, the active predation of larger animals and the breaking up of its food were probably performed by the fore-limbs and claws rather than by the jaws and teeth. The enlarged claws could also have been used for 'gaffing', i.e. hooking or flipping fishes out of the water as is done today by grizzly bears.

The fine tooth denticles of *Baryonyx* do not seem to be suitable for the 'rip and grip' cutting action demonstrated by Abler (1992) for more coarsely serrate theropod teeth. Farlow, Brinkman, Abler & Currie (1991) suggested that theropod lateral teeth with very fine denticles might function in a manner indistinguishable from that of smooth-bladed teeth; this might be true of *Baryonyx*. Farlow *et al.* also showed that the lateral blade-like teeth of most theropods displayed a consistent relationship between tooth size and denticle size. They reasoned that a serrated blade might inflict as much damage as a smooth-edged thinner blade but would be less likely to break. Since the blade-like teeth of *Baryonyx* are less compressed than those of most other theropods, the reduction in the size of their denticles might be correlated with their greater robustness.

If we consider the function of the dentition as a whole, all the teeth seem suitable for piercing prey and cutting it smoothly. The long, comparatively straight teeth in the terminal rosette and expanded tip of the dentary also possessed a stabbing function.

Those teeth on the lower jaw that lie below the preserved portion of the maxilla were (on the evidence of the alveoli) smaller, more crowded together, and more than twice as numerous per unit length of jaw as the maxillary teeth that opposed them. A somewhat similar discrepancy is known not only in *Troodon*, which has 15–20 maxillary teeth opposed by 35 in the dentary (Currie *et al.* 1990), but has also been observed in the strange new ornithomimid *Pelecanimimus* (Pérez-Moreno *et al.* 1994). This discordance between the number of teeth in the upper jaw and the corresponding number in the lower is very unusual and, as far as we know, has no analogue among living

reptiles. One might speculate that its functional significance in *Baryonyx* might be somehow connected with the gripping and manipulation of food, the lower teeth forming a closely spaced series of piercing and holding points that opposed the more widely spaced upper teeth.

In connexion with the animal's feeding habits, it should also be mentioned that an apparent gastrolith was found within the rib-cage of the *Baryonyx*.

On balance, we still envisage *Baryonyx* as mainly a fish-eater. It probably crouched on the banks of lakes, creeks and rivers or waded in the shallows (Frontispiece), and it secured its prey by direct seizure with the jaws and perhaps also by 'gaffing'. Small fishes would have been swallowed whole, larger ones broken up by the powerful fore-limbs with their huge claws. Fishing, however, was not the only source of food; there is also:

1. Circumstantial evidence that it may well have been both an active predator (using its powerful fore-limbs and claws rather than its jaws and teeth) and/or an opportunistic scavenger.
2. Positive evidence (i.e. recognisable bony remains within its rib-cage) that it had eaten a small *Iguanodon*, though whether this was the result of active predation or scavenging cannot be determined.

TERRESTRIALITY. If we accept that fish formed a significant part of the diet of *Baryonyx*, then we must consider the possibility that the animal led an aquatic or semi-aquatic existence. Nevertheless, its anatomy gives no indication of any modifications towards that mode of life. For example, it certainly had no flipper-like modifications of the limbs and it lacked the dorso-ventrally flattened skull with dorsally situated external nares typical of crocodiles. Indeed, the position of the nostrils on the side of the skull would be disadvantageous to an animal spending much of its time in the water. However, *Baryonyx* could probably swim, as can most land vertebrates, despite their lack of any special adaptations.

STANCE AND GAIT. Despite our previous suggestions of quadrupedality (Charig & Milner 1986), the anatomy of *Baryonyx* affords no evidence of a gait any different from that of any other theropod. The length of the humerus of *Stegosaurus*, which is most certainly a quadruped, varies between 43% and 55% of the length of its femur; the corresponding ratio for *Baryonyx* is only 39% (based on an unprejudiced estimate of the femoral length). On the other hand, if *Baryonyx* really was a fish-eater, then it would have been obliged to capture its aquatic prey from a crouching or quadrupedal position, either on the edge of the water or actually in it; and its massive fore-limbs certainly possessed sufficient mechanical strength and adequate musculature for the quadrupedal posture.

TAPHONOMY

The details of the fossilisation of the *Baryonyx walkeri* holotype (some of which have already been published in Charig & Milner, 1986) are as follows:

MANNER OF OCCURRENCE. Most of the bones were encased in sideritic siltstone nodules of irregular shape and were directly surrounded by uneven accumulations of extremely fine sand and ilts; such accumulations are not found anywhere else. The rest of the bones lay unprotected in clay.

DEGREE OF ARTICULATION. The bones were largely disarticulated and somewhat scattered.

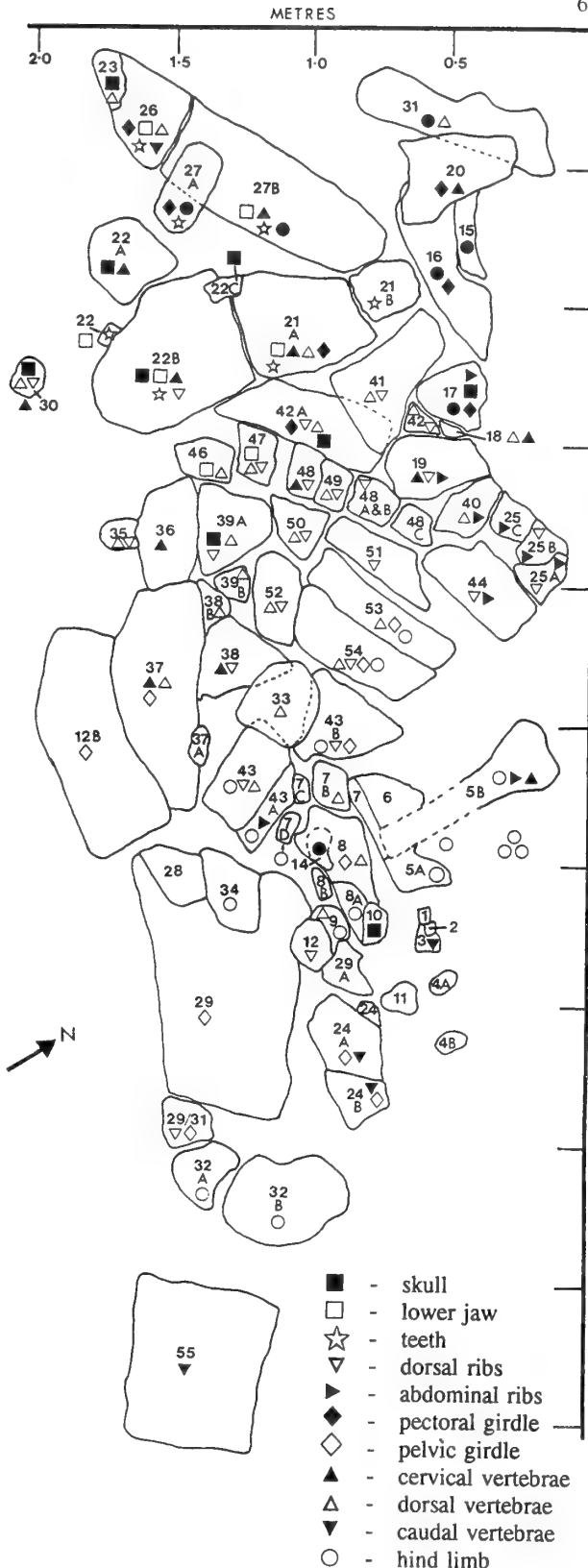


Fig. 48 Plan of the excavation at Smokejack's Brickworks, Ockley, May-June 1983, indicating the *in situ* positions of the numbered blocks and the distribution of skeletal elements.

AREA OF SCATTER. All the bones were found within an area measuring 5m × 2m (Fig. 48).

RELATIVE ORIENTATION OF ELEMENTS. The various elements were generally not far from their natural positions (except for a few that had previously been disturbed by the earth-moving operations). Thus most of the pieces of the skull, pectoral girdle and fore-limbs were at one end of the excavation and most of the pelvic girdle and hind-limbs at the other. (See Appendix B.)

WEATHERING. The degree of weathering of the bones was variable and some were unweathered. The most heavily weathered bones, in particular fragments of rib-shafts and gastralia, show pre-fossilisation splintering, flaking and splitting (stages 2–3 of Behrensmeyer 1978). It should be remembered that the climate of the region was warmer than it is today (more like that of the present-day Mediterranean area) and that the bones lay in a very exposed situation.

DISTORTION AND CRUSHING. Most of the bones were not crushed or distorted to any significant degree, but a few (e.g. the distal end of the tibia) did suffer severe post-mortem distortion.

BREAKAGE. Many of the bones were broken; the skull was in pieces and much of it was missing. However, bones that had lain undisturbed in the clay or in the nodules since fossilisation generally displayed only clean transverse breaks across their shafts, the broken ends showing few signs of weathering or erosion; some were effectively undamaged. In several cases adjacent parts of the same bone, separated by a clean unweathered break, were found in different nodules (for example, both scapulae); after preparation they fitted together precisely. The left dentary had been snapped in half, with the unweathered broken surfaces still in contact with each other at an acute angle. A weathered rib-shaft had been split longitudinally and was preserved with a fragment of another rib wedged at right angles in the gap.

INDICATIONS OF PREDATION OR SCAVENGING. There are no gnaw-marks or punctures produced by the teeth of predators or scavengers.

TEETH. All the lower teeth of *Baryonyx* had fallen out of their sockets, but some of the upper teeth remained in place.

TAIL. The tail was missing almost entirely; all that was found were a few fragmentary vertebrae and haemopophyses, mostly from its base.

Unrelated to all this is the regrettable fact that some of the bones had clearly been broken or severely crushed by mechanical equipment shortly before we collected them.

The deposition of fine-grained sediments around the bones of *Baryonyx* indicates the quiet, low-energy nature of the Smokejack's environment at that particular time; likewise the close association of large and small skeletal elements within a restricted area implies a lack of sorting by currents (Shipman 1981: 31 *et seq.*). These factors suggest that the carcase of the dinosaur was unlikely to have been carried any significant distance by the water, which, in any case, was probably too shallow to float and transport such a huge animal. Indeed, the immediate area of the burial was well suited to be the home territory of a large terrestrial piscivore, catching fish and perhaps scavenging on the mudplain; it might then have become mired in the soft silts, died, and been buried more or less *in situ*.

The excellent preservation of most of the skeletal elements, without evidence of predation or scavenging, suggests that the carcase must have been covered with sediment fairly rapidly. Total decomposition of soft tissues resulted in the disarticulation of the bones, including partial and total separation of centra and neural



Fig. 49 *Baryonyx walkeri*, holotype, BMNH R9951; model of carcase lying on mudbank or in shallow water. Model made by John Holmes.

arches. The differential weathering patterns suggest intermittent surface exposure of parts of the skeleton, either by receding water-level or by shifting of fine sediment. The girdle- and limb-bones, adjacent fragments of which were sometimes encapsulated into separate nodules, had evidently been broken before fossilisation. In particular, the unusual nature of the break in the left dentary suggests trampling by large animals while the bone was buried in shallow sediment (P.J. Andrews, pers. comm.), as does the condition of the split rib-shaft. This interpretation is in accord with the suggested shallowness of the water and sediment, for animals of any size, even the largest, are buoyed up and effectively weightless if the water is deep enough to support them; further, the surrounding sediments would hold the ends of the trampled bones close together and the disarticulated remains would be less liable to wide scattering than they would be at the surface or in clear water. In this context it is interesting to note the observation by Ross & Cook (1995) that the irregular nodules containing swirls of silt and sand at the *Baryonyx* horizon are reminiscent of the red clay, now exposed on the foreshore near Hanover Point on the Isle of Wight, that had clearly been trampled by dinosaurs. Indeed, many of the siltstone nodules found there are casts of large *Iguanodon* footprints, although none of the nodules at Smokejack's resembles footprints.

The total orientation of the bones, disarticulated though they were, suggests that the carcase lay on its back – maybe turned somewhat towards the left (i.e. with its right side uppermost; see Fig. 49). An upside-down position accords with the fact that all the lower teeth have dropped out of their sockets while some of the upper teeth have remained in theirs.

ACKNOWLEDGEMENTS. Our especial thanks are due to Mr William Walker for finding the original claw-bone and for so kindly donating it to the Museum. We are likewise grateful to the Chairman and Directors of the Ockley Brick Company Limited (now Ockley Building Products Limited, Blue Circle Industries plc) for giving the rest of the dinosaur to the Museum, for providing a large shotblasting machine to expedite its preparation, and for making us a grant to pay for the illustrations to this paper. We thank in

particular Mr Frank Datson, Mr Derek Sturt and their staff for the assistance they gave us in collecting the specimen and for their cheerful sufferance of the inconvenience we must have caused them. We should like to express our gratitude to the dozens of people, both Museum staff and others, who helped us to collect the skeleton; to the Museum photographers who recorded the excavation, in particular Colin Keates and Phil Crabb, who also prepared the photographs for drawing and for publication; to Chris Jones of the SEM unit, who helped produce the scanning electron micrographs used in this paper; and to Alison Longbottom, for general assistance in our research. John Holmes made the model of a *Baryonyx* carcase (Fig. 49) and Ms Jess Wallace made the drawings for this paper. We also thank Mr John Sibbick for generously permitting the reproduction of his painting of *Baryonyx* (Frontispiece). Our greatest debt of gratitude, however, is to Ron Croucher, formerly of the Museum's Palaeontology Laboratory, who, together with William Lindsay, Lorraine Cornish, Adrian Doyle, David Gray and other members of staff, devoted years of patient, skilful work to the development of the skeleton. For information and discussion on the taphonomy we are especially obliged to Dr Peter Andrews, and our stratigraphical advisers (both specialists on the Smokejack's succession) were Philip Palmer and Andrew Ross. Dr David Norman (Sedgwick Museum, Cambridge) kindly confirmed the identity of associated *Iguanodon* remains. Dr Ed Jarzembski (Maidstone Museum and Art Gallery) and Mr Julian Porter (Bexhill Museum) provided details of tooth crowns from other Wealden localities. Finally, we should like to acknowledge the generous help given us by Dr Philip Currie (Royal Tyrrell Museum, Drumheller, Alberta), Drs Gene Gaffney and Mark Norell (American Museum of Natural History, New York), Dr Jack Horner (Museum of the Rockies, Bozeman, Montana), Dr Nicholas Hotton III and Mr Michael Brett-Surman (United States National Museum, Washington D.C.), Dr Christopher McGowan (Royal Ontario Museum, Toronto), Dr James Madsen (Dinolab, Salt Lake City, Utah), Dr Wade Miller and Mr Kenneth Stadtman (Brigham Young University Museum of Earth Sciences, Provo, Utah), Drs Kevin Padian and Samuel Welles (Museum of Paleontology, Berkeley, California) and Mr Glen Unger (University of Utah Museum, Salt Lake City) in making comparative studies in their respective institutions.

REFERENCES

- Abler, W.L.** 1992. The serrated teeth of tyrannosaurid dinosaurs, and biting structures in other animals. *Paleobiology*, Menlo Park (California), **18**: 161–183.
- Bakker, R.T., Williams, M. & Currie, P.J.** 1988. *Nanotyrannus*, a new genus of pygmy tyrannosaur, from the latest Cretaceous of Montana. *Hunteria*, Boulder (Colorado), **1**: 1–30.
- Barsbold, R.** 1974. Saurornithoididae, a new family of small theropod dinosaurs from central Asia and North America. *Palaeontologia Polonica*, Warsaw, **30**: 5–22.
- 1983. [Carnivorous dinosaurs from the Cretaceous of Mongolia.] *Trudy Sovmestnoi Sovetskovo-Mongolskoj Paleontologicheskoi Ekspeditsii*, Moscow, **19**: 1–117. [In Russian, with English summary.]
- Behrensmeyer, A.K.** 1978. Taphonomic and ecologic information on some weathering. *Paleobiology*, Menlo Park (California), **4**: 150–162.
- Bonaparte, J.F.** 1991. The Gondwanian [*sic?*] theropod families Abelisauridae and Noasauridae. *Historical Biology*, London, **5**: 1–25.
- , **Novas, F. & Coria, R.A.** 1990. *Carnotaurus sastrei* Bonaparte, the horned, lightly built carnosaur from the Middle Cretaceous of Patagonia. *Contributions in Science, Natural History Museum of Los Angeles County*, Los Angeles, no. 416: 1–41.
- Britt, B.B.** 1991. Theropods of Dry Mesa Quarry (Morrison Formation, Late Jurassic), Colorado, with emphasis on the osteology of *Torvosaurus tanneri*. *Brigham Young University Geology Studies*, Provo (Utah), **37**: 1–72.
- 1993. Pneumatic postcranial bones in dinosaurs and other archosaurs. *Ph.D. dissertation, University of Calgary*.
- Buffetaut, E.** 1989. New remains of the enigmatic dinosaur *Spinosaurus* from the Cretaceous of Morocco and the affinities between *Spinosaurus* and *Baryonyx*. *Neues Jahrbuch für Geologie und Paläontologie, Monatshefte*, Stuttgart, **1989** (2): 79–87.
- 1992. Remarks on the Cretaceous theropod dinosaurs *Spinosaurus* and *Baryonyx*. *Neues Jahrbuch für Geologie und Paläontologie, Monatshefte*, Stuttgart, **1992** (2): 88–96.
- Buscalioni, A.D., Ortega, F., Pérez-Moreno & Evans, S.E.** 1996. The Upper Jurassic maniraptoran theropod *Lisboaasaurus estesi* (Guimarota, Portugal) reinterpreted as a crocodylomorph. *Journal of Vertebrate Paleontology*, **16**: 358–362.
- Charig, A.J.** 1956. New Triassic archosaurs from Tanganyika, including *Mandasuchus* and *Teleocrater*. *Ph.D. dissertation, University of Cambridge*, 503 pp.
- 1982. Systematics in biology: a fundamental comparison of some major schools of thought. In, Joysey, K.A. & Friday, A.E. (eds), *Problems of phylogenetic reconstruction (Systematics Association Special Volume 21)*, 363–440. Academic Press, London & New York.
- 1993. Recently proposed phylogenetic analyses of the Triassic Archosauria: a critical comparison and evaluation, facilitated by a simple technique for the modification of conflicting dendograms. In, Mazin, J.M. & Pinna, G. (eds), *Evolution, ecology and biogeography of the Triassic reptiles. Paleontologia Lombarda della Società Italiana di Scienze Naturali e del Museo Civico di Storia Naturale di Milano (n.s.) 2*: 45–62.
- & Milner, A.C. 1986. *Baryonyx*, a remarkable new theropod dinosaur. *Nature*, London, **324**: 359–361.
- & — 1990. The systematic position of *Baryonyx walkeri*, in the light of Gauthier's reclassification of the Theropoda. In, Carpenter, K. & Currie, P.J. (eds), *Dinosaur systematics: approaches and perspectives*: 127–140. Cambridge University Press.
- Clark, J.M., Perle, A. & Norell, M.A.** 1994. The skull of *Erlikosaurus andrewsi*, a Late Cretaceous 'segnosaur' (Theropoda: Therizinosauridae) from Mongolia. *American Museum Novitates*, New York, **3115**: 1–39.
- Colbert, E.H.** 1989. The Triassic dinosaur *Coelophysos*. *Museum of Northern Arizona Bulletin*, Flagstaff, **57**: 1–160.
- Currie, P.J.** 1987. Theropods of the Judith River Formation of Dinosaur Provincial Park, Alberta. In, Currie, P.J. & Koster, E.H. (eds), *Fourth Symposium on Mesozoic Terrestrial Ecosystems, Short Papers*, 52–60. Tyrrell Museum of Palaeontology, Drumheller (Alberta): Occasional Paper 3.
- 1995. New information on the anatomy and relationships of *Dromaeosaurus albertensis* (Dinosauria: Theropoda). *Journal of Vertebrate Paleontology*, Chicago, **15**: 576–591.
- , **Rigby, J.K. jr & Sloan, R.E.** 1990. Theropod teeth from the Judith River Formation of southern Alberta, Canada. In, Carpenter, K. & Currie, P.J. (eds), *Dinosaur systematics: approaches and perspectives*: 107–125. Cambridge University Press.
- & **Russell, D.A.** 1988. Osteology and relationships of *Chirostenotes pergracilis* (Saurischia, Theropoda) from the Judith River (Oldman) Formation of Alberta, Canada. *Canadian Journal of Earth Sciences*, Ottawa, **25**: 972–986.
- & **Zhao, X.-J.** 1993. A new carnivorous (Dinosauria, Theropoda) from the Jurassic of Xinjiang, People's Republic of China. *Canadian Journal of Earth Sciences*, Ottawa, **30** (10–11): 2037–2081.
- Elzanowski, A. & Wellnhofer, P.** 1992. A new link between theropods and birds from the Cretaceous of Mongolia. *Nature*, London, **359**: 821–823.
- & — 1993. Skull of *Archaeornithoides* from the Upper Cretaceous of Mongolia. *American Journal of Science*, New Haven, **293-A**: 235–252.
- & — 1995. The skull of *Archaeopteryx* and the origin of birds. *Archaeopteryx*, Munich, **13**: 41–46.
- Farlow, J.O., Brinkman, D.L., Abler, W.L. & Currie, P.J.** 1991. Size, shape, and serration density of theropod dinosaur lateral teeth. *Modern Geology*, London, **16**: 161–198.
- Farris, J.S.** 1988. *Hennig86 version 1.5*. Software and MSDOS programme.
- Gatesy, S.M.** 1990. Caudofemoral musculature and the evolution of theropod locomotion. *Paleobiology*, Menlo Park (California), **16**: 170–186.
- Gauthier, J.A.** 1984. A cladistic analysis of the higher systematic categories of the Diapsida. *Ph.D. dissertation, University of California*; published 1986 by University Microfilms International, Ann Arbor, Michigan, vii + 564 pp.
- 1986. Saurischian monophyly and the origin of birds. In, Padian, K. (ed.), *The origin of birds and the evolution of flight. Memoir of the California Academy of Sciences*, San Francisco, **8**: 1–55.
- Gilmore, C.W.** 1920. Osteology of the Carnivorous Dinosaurs in the United States National Museum, with reference to the genera *Antrodemus* (*Allosaurus*) and *Ceratosaurus*. *Bulletin of the United States National Museum*, Washington, **110**: 1–154.
- Hill, C.R.** 1996. A plant with flower-like organs from the Wealden of the Weald (Lower Cretaceous), southern England. *Cretaceous Research*, London, **7**: 27–38.
- Holtz, T.R. jr.** 1994a. The phylogenetic position of the Tyrannosauridae: implications for theropod systematics. *Journal of Paleontology*, Lawrence (Kansas), **68**: 1100–1117.
- 1994b. The arctometatarsalian pes, an unusual structure of the metatarsus of Cretaceous Theropoda (Dinosauria: Saurischia). *Journal of Vertebrate Paleontology*, Chicago, **14**: 480–519.
- 1995. A new phylogeny of the Theropoda. *Journal of Vertebrate Paleontology*, Chicago, **15** (Supplement to part 3): 35A.
- Hopson, J.A.** 1980. Relative brain size in dinosaurs – implications for dinosaurian endothermy. In, Thomas, R.D.K. & Olson, E.C. (eds), *A cold look at the warm-blooded dinosaurs*: 287–310. Westview Press, Boulder (Colorado).
- Hutt, S., Martill, D.M. & Barker, M.J.** 1996. The first European allosaurid dinosaur (Lower Cretaceous, Wealden Group, England). *Neues Jahrbuch für Geologie und Palaontologie, Monatshefte*, Stuttgart, **1996**: 635–644.

- Iordansky, N.N. 1973. The skull of the Crocodylia. In, Gans, C. & Parsons, T.S. (eds), *Biology of the Reptilia*, **4** (2): 201–262. Academic Press, London & New York.
- Jarzembski, E.A. 1984. Early Cretaceous insects from southern England. *Modern Geology*, Philadelphia, **9**: 71–93.
- Kellner, A.W.A. & Campos, D. de A. 1996. First Early Cretaceous theropod dinosaur from Brazil with comments on Spinosauridae. *Neues Jahrbuch für Geologie und Paläontologie, Abhandlungen*, Stuttgart, **199** (2): 151–166.
- Kitchener, A. 1987. Function of Claws' claws. *Nature*, London, **325**: 114.
- Kurzanov, S.M. 1976a. [A new Late Cretaceous carnivorous from Nogon-Tsav, Mongolia.] *Trudy Sovmestnoi Sovetskogo-Mongolskoi Paleontologicheskoi Ekspeditsii*, Moscow, **3**: 93–104. [In Russian, with English summary.]
- Lambe, L.M. 1917. The Cretaceous theropodous dinosaur *Gorgosaurus*. *Memoirs of the Geological Survey of Canada*, Ottawa, **100**: 1–84.
- Mader, B.J. & Bradley, R.L. 1989. A redescription and revised diagnosis of the syntypes of the Mongolian tyrannosaur *Alectrosaurus olseni*. *Journal of Vertebrate Paleontology*, Pittsburgh, **9**: 41–55.
- Madsen, J.H. Jr 1976. *Allosaurus fragilis*: a revised osteology. *Utah Geological and Mineral Survey Bulletin*, Salt Lake City, **109**: 1–163.
- Marsh, O.C. 1881. Classification of the Dinosauria. *American Journal of Science*, New Haven, (3) **23**: 81–86.
- Martill, D.M. & Hutt, S. 1996. Possible baryonychid dinosaur teeth from the Wessex Formation (Lower Cretaceous, Barremian) of the Isle of Wight, England. *Proceedings of the Geologists' Association*, Bath, **107**: 81–84.
- , Cruckshank, A.R.I., Frey, E., Small, P.G. & Clarke, M. 1996. A new crested maniraptoran dinosaur from the Santana Formation (Lower Cretaceous) of Brazil. *Journal of the Geological Society*, London, **153** (1): 5–8.
- Milner, A.C. & Croucher, R. 1987. 'Claws'. *The story (so far) of a Great British dinosaur, Baryonyx walkeri*. British Museum (Natural History), London, 16 pp.
- Milner, A.R. & Evans, S.E. 1991. The Upper Jurassic diapsid *Lisboaasaurus estesi* – a maniraptoran theropod. *Palaeontology*, London, **34**: 503–513.
- Molnar, R.E. 1990. Problematic Theropoda: 'Carnosaurs'. In, Weishampel, D.B., Dodson, P. & Osmólska, H. (eds), *The Dinosauria*, 306–317. University of California Press, Berkeley/Los Angeles/Oxford.
- Norman, D.B. 1986. On the anatomy of *Iguanodon atherfieldensis* (Ornithischia: Ornithopoda). *Bulletin de l'Institut Royal des Sciences Naturelles de Belgique*, Brussels, **56**: 281–372.
- Nolas, F.E. 1991. La evolución de los dinosaurios carnívoros. In, Sanz, J.L. & Buscalioni, A. (eds), *Los dinosaurios y su entorno biótico*, 123–163. Actas II Curso de Paleontología en Cuenca, Instituto 'Juan de Valdés', Ayuntamiento de Cuenca.
- Osborn, H.F. 1912. Crania of *Tyrannosaurus* and *Allosaurus*. *Memoirs of the American Museum of Natural History* (n.s.), New York, **1**: 1–30.
- Osmólska, H. 1981. Coossified tarsometatarsi in theropod dinosaurs and their bearing on the problem of bird origins. *Palaentologia Polonica*, Warsaw, **42**: 79–85.
- & Barsbold, R. 1990. Troodontidae. In, Weishampel, D.B., Dodson, P. & Osmólska, H. (eds), *The Dinosauria*, 259–268. University of California Press, Berkeley/Los Angeles/Oxford.
- , Roniewicz, E. & Barsbold, R. 1972. A new dinosaur, *Gallimimus bullatus* n. gen., n. sp. (Ornithomimidae) from the Upper Cretaceous of Mongolia. *Palaentologia Polonica*, Warsaw, **27**: 103–143.
- Ostrom, J.H. 1969. Osteology of *Deinonychus antirrhopus*, an unusual theropod from the Lower Cretaceous of Montana. *Bulletin of the Peabody Museum of Natural History*, Yale, **30**: 1–165.
- Panchen, A.L. 1982. The use of parsimony in testing phylogenetic hypotheses. *Zoological Journal of the Linnean Society*, **74** (3): 305–328.
- Paul, G.S. 1988. *Predatory dinosaurs of the world: a complete illustrated guide*. Simon & Schuster, New York. 464 pp.
- Pérez-Moreno, B.P., Sanz, J.L., Buscalioni, A.D., Moratalla, J.J., Ortega, F. & Rasskin-Gutman, D. 1994. A unique multitoothed ornithomimosaur dinosaur from the Lower Cretaceous of Spain. *Nature*, London, **370**: 363–367.
- Plot, R. 1677. *The natural history of Oxfordshire: being an essay toward the natural history of England*. Oxford, 358 pp.
- Raath, M.A. 1977. The anatomy of the Triassic theropod *Syntarsus rhodesiensis* (Saurischia: Podokesauridae) and a consideration of its biology. *Ph.D. dissertation, Rhodes University*, Grahamstown, South Africa.
- Reid, R.E.H. 1987. Claws' claws. *Nature*, London, **325**: 487.
- Romer, A.S. 1956. *Osteology of the reptiles*. University of Chicago Press, Chicago, pp. 772.
- Ross, A.J. & Cook, E. 1995. The stratigraphy and palaeontology of the Upper Weald Clay (Barremian) at Smokejacks Brickworks, Ockley, Surrey, England. *Cretaceous Research*, London, **16**: 705–716.
- Rowe, T. 1989. A new species of the theropod dinosaur *Syntarsus* from the Early Jurassic Kayenta Formation of Arizona. *Journal of Vertebrate Paleontology*, Pittsburgh, **9** (2): 125–136.
- & Gauthier, J.A. 1990. Ceratosauria. In, Weishampel, D.B., Dodson, P. & Osmólska, H. (eds), *The Dinosauria*, 151–168. University of California Press, Berkeley/Los Angeles/Oxford.
- Russell, D.A. 1969. A new specimen of *Stenonychosaurus inequalis* from the Oldman Formation (Cretaceous) of Alberta. *Canadian Journal of Earth Sciences*, Ottawa, **6**: 595–612.
- 1972. Ostrich dinosaurs from the Late Cretaceous of western Canada. *Canadian Journal of Earth Sciences*, Ottawa, **9**: 375–402.
- & Dong, Zh. 1993. The affinities of a new theropod from the Alxa Desert, Inner Mongolia, People's Republic of China. *Canadian Journal of Earth Sciences*, Ottawa, **30**: 2107–2127.
- Sereno, P.C., Dutheil, D.B., Iarochene, M., Larsson, H.C.E., Lyon, G.H., Magwene, P.M., Sidor, C.A., Varricchio, D.J. & Wilson, J.A. 1996. Predatory dinosaurs from the Sahara and Late Cretaceous faunal differentiation. *Science*, Washington D.C., **272**: 986–991.
- , Wilson, J.A., Larsson, H.C.E., Dutheil, D.B. & Sues, H.-D. 1994. Early Cretaceous dinosaurs from the Sahara. *Science*, Washington D.C., **265**: 267–271.
- Shipman, P. 1981. *Life history of a fossil: an introduction to taphonomy and paleoecology*. Harvard University Press, Cambridge (Mass.) & London, 222 pp.
- Stromer, E. 1915. Ergebnisse der Forschungsreisen Prof. E. Stromers in den Wüsten Ägyptens. II. Wirbeltier-Reste der Bahariye-Stufe (unterstes Cenoman). 3. Das Original des Theropoden *Spinosaurus aegyptiacus* nov. gen., nov. spec. *Abhandlungen der Königlich Bayerischen Akademie der Wissenschaften Mathematisch-physische Klasse*, Munich, **28** (Band 3): 1–28.
- Sues, H.-D. 1978. A new small theropod dinosaur from the Judith River Formation (Campanian) of Alberta, Canada. *Zoological Journal of the Linnean Society*, **62**: 381–400.
- Swofford, D.L. 1990. *PAUP: phylogenetic analysis using parsimony version 3.0*. Illinois Natural History Survey, Champaign, Illinois.
- Taquet, P. 1984. Une curieuse spécialisation du crâne de certains Dinosaures carnivores du Crétacé: le museau long et étroit des Spinosauridés. *Comptes Rendus Hebdomadaires des Séances de l'Academie des Sciences*, Paris, **299**(2) (5): 217–222.
- Viera, L.I. & Torres, J.A. 1995. Presencia de *Baryonyx walkeri* (Saurischia: Theropoda) en el Weald de La Rioja (España). Nota previa. *Munibe. Ciencias Naturales*, San Sebastian, no. 47: 57–61.
- Welles, S.P. 1984. *Dilophosaurus wetherilli* (Dinosauria, Theropoda): osteology and comparisons. *Palaentigraphica, Abt. A*, Stuttgart, **185**: 85–180.
- & Long, R.A. 1974. The tarsus of theropod dinosaurs. *Annals of the South African Museum*, Cape Town, **64**: 191–218.
- Wilson, M.C. & Currie, P.J. 1985. *Stenonychosaurus inequalis* (Saurischia: Theropoda) from the Judith River Formation of Alberta: new findings on metatarsal structure. *Canadian Journal of Earth Sciences*, Ottawa, **22**: 1813–1817.

APPENDIX A. ABBREVIATIONS USED IN THE ILLUSTRATIONS

On all figures stippling denotes matrix; cross-hatching denotes restoration.

III – XI	cranial nerves	gl	glenoid	ot.ca	otic capsule
a.h.l	anterior horizontal lamina	h	head	P	parietal
a.pd.f	anterior peduncular fossa	h.c	haemal canal	pd.g	paradental groove
a.li	anterior ligament scar	hs	hypophene	p.h.l	posterior horizontal lamina
a.peg	anterior peg	hy	hypotrum	p.li	posterior ligament scar
ac	acromion process	i.m.f	internal mandibular fenestra	pit.fos	pituitary fossa
acet	acetabulum	id.fos	infradiaphysial fossa	pl	pleurocoel
ad.fos	adductor fossa	id.p	interdental plate	pn.f	postnasal fenestra
alv.s	alveolar septum	in.s	internasal septum	po	postorbital articulation
ANG	angular	ipod.l	infradiaphysial lamina	poz	postzygapophysis
ang	angular articulation	ipoz.fos	infrapostzygapophysial fossa	pp	parapophysis
ao.f	antorbital fenestra	iprd.l	infraprezygapophysial lamina	pra	prearticular articulation
ap	pubic apron	iprz.fos	infraprezygapophysial fossa	PRF	prefrontal
ast.fa	facet for lateral tuber of astragalus	is.ped	ischiatric peduncle	prf	prefrontal articulation
at.in	atlantal intercentrum	J	jugal	PRO	prootic
ax.prz	axial prezygapophysis	j	jugal articulation	pro	prootic articulation
BO	basiooccipital	k	keel	prz	prezygapophysis
bpt	basipterygoid process	L	lacrimal	pt.fl	pterygoid flange
br.fos	brevis fossa	l.d	lacrimal duct	pu.p	pubic peduncle
br.s	brevis shelf	l.for	lacrimal foramen	Q	quadrate
BS	basisphenoid	l.h	lacrimal horn	q.for	quadrate foramen
cap	capitulum	LS	latersphenoid	QJ	quadratojugal
con	condyle	m.dc	deltpectoralis muscle	qj	quadratojugal articulation
cor.for	coracoid foramen	m.pe	pectoralis muscle	r.con	radial condyle
cot	cotyle	m.br	brachialis muscle	SA	surangular
CR	coronoid	Mk.g	Meckelian groove	sa	surangular articulation
d	dentary articulation	med.r	median ridge	sh.g	sheath groove
d.sell	dorsum sellae	med.s	median sulcus	SO	supraoccipital
dp	diapophysis	MX	maxilla	so.b	suborbital bar
dp.c	deltopectoral crest	mx	maxilla articulation	SPL	splenial
e.m.f	external mandibular fenestra	mx.no	maxillary notch	spl	splenial articulation
ect	ectopterygoid articulation	mx.s	maxillary sinus	spl.for	splenial foramen
ectoc.t	ectocondylar tuber	mx.t	maxillary trough	spl.g	splenial groove
ep	epiphysis	N	nasal	SQ	squamosal
EX	exoccipital	n.c	neural canal	sq	squamosal articulation
ext.n	external nasal opening	n	nasal articulation	sr.c	subrostral canal
extn.g	extensor groove	nu.g	nutrient groove	sr.f	subrostral foramen
F	frontal	nu.for	nutrient foramen	su.a	supra-acetabular crest
f	frontal articulation	o	orbit	tf.lig	tibiofibular ligaments
f.ov	fenestra ovalis	ob.fl	obturator flange	tib.fa	tibial facet
fib.con	fibular condyle	o.c	occipital condyle	tub	tuberculum
fib.fa	fibular facet	od	odontoid	u.con	ulnar condyle
fl.tu	flexor tubercle	ol	olecranon	V	vomer
g.tr	greater trochanter	OP	opisthotic		

APPENDIX B. LIST OF CONTENTS OF EACH BLOCK

List of elements by field block number.

3	caudal centrum fragment	20	I. cervical rib, l. & r. coracoids	29	ilium fragment, ?l. pubis fragment
5A	<i>Iguanodon</i> humerus, <i>Iguanodon</i> phalanx	21	r. dentary fragment, D1, D2	30	nasal fragments (2), l. quadrate, Ce5, dorsal rib fragments
5B	haemapophysis, gastralia, femur head, astragalus fragment	21A	teeth, l. scapula blade (distal)	31	D3, l. humerus
7A	sacral centrum fragment	22A	I. maxilla, nasals, l. lacrimal, l. prefrontal, occiput, teeth, l. cervical rib	32A	l. femur (distal), r. calcaneum
7B	D5 neural arch (part)	22B	I. jugal, r. neurapophysis, Ce8, D6 neural arch, l. cervical rib, posterior dorsal rib, gastralia	32B	r. fibula
8	l. ischium, r. ischium head		<i>Iguanodon</i> neural spine	34	l. femur head
9	D5 neural arch, D7 neural arch, r. femur (distal)	22C	r. frontal/latersphenoid fragment	36	Ce3
10	r. quadrate	23	premaxillae, dorsal rib fragment	37	axis (Ce2), D12–13 (?) neural arch fragment, r. pubic peduncle, r. ischiadic peduncle
11	<i>Iguanodon</i> , r. femur (distal)	24A	r. pubis foot	38	dorsal rib fragments
12	r. ilium blade		<i>Iguanodon</i> proximal caudal centrum	38B	dorsal rib fragments
13*	haemapophysis, ungual phalanx fragment	24B	haemapophyses (2)	39A	l. postorbital, D11 neural arch
14	two teeth, l. radius, l. ulna	25	dorsal rib fragments	39B	posterior dorsal rib heads (3)
15	r. humerus	26	I. dental tip, teeth, dorsal centrum fragment, proximal caudal neural arch, sternum	40	gastralia
16	l. scapula blade, r. radius (proximal)	27A	I. dentary, l. & r. splenial, Ce6 centrum, l. manus digit II/III	41	D4 transverse process, dorsal rib heads (4), rib fragments
17	gastralia, r. scapula blade, r. radius (distal)	27B	I. dentary, teeth, l. scapula (proximal)	42	D6 centrum
18	D10 neural arch, l. cervical rib			42A	D4 centrum, D5 centrum, D6 transverse
19	neural spine, dorsal rib fragments (6), gastralia (5), haemapophysis				

process, D7 neural arch, anterior dorsal rib head, rib fragments, r.scapula (proximal)	47	r. surangular, dorsal rib heads (2) and shaft fragments	54	indeterminate limb fragments, r. femur (distal)
D14 neural arch, proximal caudal neural spines (3), dorsal rib fragments	48	C6 neural arch, dorsal rib head fragments	54	D14 centrum, basal caudal centra (2), l. pubis, tibia (crushed), astragalus, distal metatarsal fragments
Agastralia, l. fibula proximal fragment	49	D6 centrum, D8 centrum, dorsal rib fragments	54	<i>Iguanodon</i> left metatarsals II, III, IV, phalanges (3)
dorsal rib fragment, l. distalmost rib, l. pubis (distal)	50	<i>Iguanodon</i> dorsal vertebra	55	caudal centrum fragments (2), haemapophyses (2)
dorsal rib fragments, gastralia	51	D11 centrum and other centra fragments		
<i>Lepidotes</i> teeth & scales	52	<i>Iguanodon</i> dorsal vertebrae		
<i>Iguanodon</i> manual phalanges	53	basal caudal centrum, dorsal rib fragments		
r. angular, dorsal rib heads (4) and shaft fragments		dorsal rib fragments, gastralia, l. pubis		
		fragment, r. femur (distal)		
		<i>Lepidotes</i> scales		
		<i>Iguanodon</i> supraoccipital, cervical vertebrae,		

* Block not marked on plan

APPENDIX C: LIST OF CHARACTERS AND DATA-MATRIX, MODIFIED FROM HOLTZ (1994a)

List of characters employed (the numbers in parentheses at end of each line are Holtz's original character numbers; the publications that follow are those in which these characters were first proposed as synapomorphies).

1. Pubic plate perforated by pubic fenestra below obturator foramen (1; Rowe 1989, Rowe & Gauthier 1990)
2. Distal end of fibula flares to overlap ascending process of astragalus (2; Rowe & Gauthier 1990)
3. Sacral ribs fused to centra in adults (3; Rowe & Gauthier 1990)
4. Cervical vertebrae with transverse processes strongly backturned and triangular in dorsal view (5; Rowe 1989)
5. Pronounced subnarial gap, indicating a possibly mobile premaxillary-maxillary joint (6; Welles 1984, Rowe 1989)
6. Metatarsals proximally co-ossified (7; Osmólska 1981, Rowe & Gauthier 1990)
7. Crista tibiofibularis with sulcus along medial side of base (8; Rowe 1989, Rowe & Gauthier 1990)
8. Axial parapophysis reduced (9; Gauthier 1986)
9. Axial diapophysis lost (10; Gauthier 1986)
10. Axial pleurocoels lost (11; Gauthier 1986)
11. Femoral head directed anteromedially (12; Bonaparte 1991)
12. Premaxilla very deep subnarily (13; Bonaparte 1991)
13. Parietal projected dorsally (14; Bonaparte 1991)
14. Lower temporal fenestra very large (15; Bonaparte 1991)
15. Manual digit III lost (16)
16. Manual unguals with pronounced lip on dorsal edge of proximal articulation (17; Currie & Russell 1988)
17. Parietals fused with laterosphenoids (18; Barsbold 1983)
18. Sternal plates fused (19)
19. Pubic boot longer anteriorly than posteriorly (20)
20. Pubic boot triangular (apex posterior) in ventral view (21)
21. Ilium with preacetabular portion expanded dorsoventrally (22; Gauthier 1986)
22. Astragalar condyle with pronounced horizontal groove across anterior face (23; Welles & Long 1974)
23. Supraoccipital crest pronounced (24; Gauthier 1986)
24. Premaxillary-maxillary fenestra (25; Osborn 1912)
25. Insertion area for pterygoideus muscle below mandibular condyle enlarged (26; Gauthier 1986)
26. Lacrimal fenestra present (27; Molnar 1990)
27. Orbit key-shaped (28; Gauthier 1986)
28. Mandibular fenestra reduced (29; Gauthier 1986)
29. Pubic foot projects only posteriorly (30; Gauthier 1986)
30. Pelvis opisthopubic (31; Gauthier 1986)
31. Pedal digit II longer than IV, closer in length to III (32; Gauthier 1986)
32. Obturator process placed distally (33; Gauthier 1986)
33. Ischium not more than two-thirds length of pubis (34; Gauthier 1986)
34. Fourth trochanter lost (35; Gauthier 1986)
35. Proximal caudal vertebrae highly modified (neural spine only in 1–9, box-like centra in 1–5, zygapophysial facets vertical) (36; Gauthier 1986)
36. Prefrontals extremely reduced or lost (37; Gauthier 1986)
37. Frontals separated by an anterior process of parietals (38; Currie 1987)
38. Pedal digit II hyperextensible (39)
39. Ulna bowed posteriorly (40; Gauthier 1986)
40. Furcula present (41)
41. Semilunate carpal present (42; Gauthier 1986)
42. Ischial foot lost (43)
43. Metacarpal III long and slender (44; Gauthier 1986)
44. Ilium with posterodorsal margin curving ventrally in lateral view (45; Gauthier 1986)
45. Coracoid subrectangular (46; Gauthier 1986)
46. Chevrons longer than deep (47; Gauthier 1986)
47. Sacral vertebrae pleurocoelous (48)
48. Quadrate articulation projecting deeply in posteroventral direction (49)
49. Quadrate-quadratojugal articulation mobile (50; Gilmore 1920, Ostrom 1969)
50. Dorsal vertebrae procoelous (51)
51. Humerus sigmoid in anterior view (52)
52. Ilium with preacetabular portion significantly longer than postacetabular portion (53; Currie & Russell 1988)
53. Metatarsals deeper anteroposteriorly than anterolaterally (55; Holtz 1994b)
54. Maxillary teeth lost (56)
55. Fibula with anterior protuberance below expansion (57; Mader & Bradley 1989)
56. Greater trochanter cleft from head (58; Russell 1969)

57. Carpals reduced to disc-like structures lacking distinct articular surfaces (59; Gauthier 1986)
 58. Paraphenoid capsule bulbous (60; Barsbold 1974, Osmólska *et al.* 1972)
 59. Pterygoid canal present (61; Kurzanov 1976a)
 60. Metatarsals II and IV contact each other distally on plantar surface (62; Wilson & Currie 1985)
 61. Frontals long and triangular (65; Currie 1987)
 62. Arctometatarsus present (66; Holtz 1994b)
 63. Metatarsus gracile (67; Holtz 1994b)
 64. Paroccipital process very deep top-to-bottom at root (68; Bakker *et al.* 1988)
 65. Iliac blades contact along most of dorsal surface (70)
 66. Ischium bears semicircular scar anteriorly (71)
 67. Orbit circular and expanded (73)
 68. Occipital region deflected ventrally (74)
 69. Endocranum enlarged (75; Russell 1972, Hopson 1980)
 70. Orbit with pronounced rim (76)
 71. Lesser trochanter extended by lamella of bone, separate from main body of femur (77; Currie & Russell 1988)
 72. Cervical zygapophyses flexed (78; Gauthier 1986)
 73. Subsidiary fenestra between palatine and pterygoid (79; Gauthier 1986)
 74. Obturator process triangular (80)
 75. Astragalar ascending process more than one-fourth length of epipodium (81)
 76. Anterior cervicals broader than deep on anterior surface, with kidney-shaped articular surfaces that are taller laterally than on midline (82; Gauthier 1986)
 77. Nasals narrow (83; Bakker *et al.* 1988)
 78. Tertiary antorbital fenestra present (84)
 79. Anterior cervical zygapophyses elongate (85; Gauthier 1986)
 80. Jugal expressed on rim of antorbital fenestra (86)
 81. Number of caudal vertebrae with transverse processes not more than 15 (87; Gatesy 1990)
 82. Ectopterygoid flange with deeply excavated pocket on ventral surface (88; Gauthier 1986)
 83. Surangular foramen large (89)
 84. Cervical vertebrae pleurocoelous (90)
 85. Obturator foramen lost (91)
 86. Lesser trochanter placed proximally (92)
 87. Presacral vertebral column reduced anteroposteriorly relative to femur length (93; Bakker *et al.* 1988)
 88. Obturator process present (94; Gauthier 1986)
 89. Basal half of metacarpal I closely appressed to metacarpal II (95; Gauthier 1986)
 90. Manual digit IV lost (96; Gauthier 1986)
 91. Tibial shaft with cnemial process arising out of lateral surface (97; Mader & Bradley 1989)
 92. Pubic boot pronounced (98)
 93. Astragalar ascending process more than one-sixth length of epipodium (99)
 94. Tibia with sharp anterolateral ridge for clasping fibula (100; Welles & Long 1974)
 95. Distal end of fibula reduced (101)
 96. Coracoid tapers posteriorly (102; Gauthier 1986)
 97. Occiput, in posterior view, deeper above foramen magnum (103; Bakker *et al.* 1988)
 98. Surangular with anterior portion deep (105; Gauthier 1986)
 99. Distal caudals strongly interlocked (106)
 100. Transition point in tail begins closer to proximal half (107; Gauthier 1986)
 101. Accessory antorbital fenestra pronounced and round (108; Bakker *et al.* 1988)
 102. Chevrons attenuated distally (109; Gauthier 1986)
 103. Last maxillary tooth lies anterior to orbit (110; Gauthier 1986)
 104. Anterior prong of angular penetrates dentary-splenial cavity (111; Bakker *et al.* 1988)
 105. Axis with spine table (112; Gauthier 1986)
 106. Scapula with narrow strap-like blade (113; Bakker *et al.* 1988)
 107. Interdental plates lost (114)
 108. Paroccipital root pneumaticised (116; Bakker *et al.* 1988)
 109. Lesser trochanter aliform (117; Gauthier 1986)
 110. All three pelvic elements fused together in adults (118; Rowe & Gauthier 1990)
 111. Premaxillary teeth lost (119)
 112. Dentary teeth lost (120)
 113. Number of sacral vertebrae more than five (121)
 114. Metatarsal IV longer than metatarsal II and closer in length to metatarsal III (122; Holtz 1994b)
 115. Astragalar ascending process with round external fossa at its base (123; Mader & Bradley 1989)
 116. Metacarpal I not more than one-third length of metacarpal II (124)
 117. Manual digit I reduced in length (125; Gauthier 1986)
 118. Premaxillary tooth crowns asymmetrical in cross-section (126; Bakker *et al.* 1988)

The following characters were used by Holtz (1994) in his data-matrix, but are considered by us to be unsatisfactory:

1. Cervical vertebrae with two pairs of pleurocoels (4; Gauthier 1986)
2. Tibia and metatarsus elongate (54; Holtz 1994b)
3. Occiput deeper above supraoccipital wedge (63; Bakker *et al.* 1988)
4. Periotic region with large depression (64; Bakker *et al.* 1988)
5. Fenestra ovalis surrounded by large excavation (69; Bakker *et al.* 1988)
6. Humerus straight (72)
7. Combined premaxillae at symphysis U-shaped (104; Bakker *et al.* 1988)
8. Periotic region highly pneumaticised (115; Bakker *et al.* 1988)

O.T.U.s	Character numbers (as listed above)													
	5	10	15	20	25	30	35	40	45	50	55	60		
	65	70	75	80	85	90	95	100	105	110	115	118		
<i>Coelophysis</i>	11111	11111	00000	000??	00000	000?0	00000	00000	00000	01000	00100	00000		
	00000	00000	00000	00000	00010	00000	00000	00000	00000	00001	00000	000		
<i>Dilophosaurus</i>	01111	01111	00000	000??	00101	011??	00000	00000	00000	01000	00000	00000		
	00000	00000	000??	00001	00010	00000	00000	00100	00000	10001	00000	000		
<i>Ceratosaurus</i>	11110	11000	11110	??0??	10111	10000	00000	00000	00000	00100	10000	02000		
	00000	00000	00200	00000	00010	00000	00000	00000	00010	00001	00000	000		
<i>Abelisaurus</i>	11010	??200	11110	20000	00101	01000	00000	10000	00000	00101	00200	0000?		
	02??0	00000	00200	00000	02010	000?0	11000	01000	00000	10011	001?0	0??0		
<i>Elaphrosaurus</i>	1??1?	01000	1????	?????	00???	??2??	20??0	??0??	20200	0??1?	001?0	0??0?		
	201?0	0????	00200	0???	??11	000??	1101?	??111	0???	??11	??100	??1??		
<i>Torvosaurus</i>	00??0	02000	20??0	02000	01???	10??0	20000	??0??	0000?	0?001	00000	0??20		
	200?0	00??0	20??0	??0??	??10	210??	02010	2000?	001??	20??0	000?0	0??0		
<i>Megalosaurus</i>	02000	0????	000??	0?00?	11???	??200	2000?	??0??	??200	21??1	00000	0??20		
	000?0	20??0	12???	??2??	??200	01?0?	0011?	0??2?	12???	10?10	00000	??20		
<i>Baryonyx</i>	??201	??000	001?0	00000	??10?	??200	200??	??2???	??200	0??21	00200	0??2??		
	??2??0	00?0?	??0???	??0???	??1???	??2???	??0???	??2???	??2???	??00?	002???	000?		
<i>Allosaurus</i>	00000	00000	00000	00011	11111	11100	00000	00001	00000	01111	10000	00000		
	00000	00000	10000	00000	00011	11111	11111	11111	11111	10010	00000	011		
<i>Acrocanthosaurus</i>	00?00	00???	0000?	?0111	??1??	12?00	??000	?10??	20???	??11	20020	0??0?		
	001??	00000	10??0	0???	01111	111??	11111	?1?11	?????	??110	??0???	??1??		
<i>Compsognathus</i>	00000	00000	00000	00000	000?0	00100	00010	00000	01000	021?0	00000	0??20		
	000?0	01000	201??	??200	121??	11111	?1111	121??	101?1	10?10	00000	01?		
<i>Ornitholestes</i>	00000	00???	00000	00?0?	0200?	00100	10100	??0???	211??	00000	10000	000?0		
	00000	01000	11?1?	10001	11?11	11111	1???	??111	121??	20010	00000	1??		
<i>Dromaeosaurus</i>	00000	00000	00000	00000	00000	00011	11111	11111	11111	11111	10000	00000		
	00000	00000	01111	11111	11111	11111	11111	11111	11111	100?0	00000	110		
<i>Archaeopteryx</i>	00000	00000	00000	00100	00000	00011	11111	1??11	11111	12?1?	10000	00??0		
	000?0	01000	01?11	11111	11011	11111	11111	121??	111?1	10?20	00000	110		
<i>Oviraptor</i>	00000	00000	00000	10100	00000	10000	21100	10011	11111	01001	10010	10000		
	00010	01000	11111	?0111	11011	11111	11111	11011	11??1	11110	11110	11?		
<i>Elmisaurus</i>	00000	00???	0??2?	1?000	00???	??2??0	011??	??0???	211??	11111	??1??	??1??	??1???	
	??1???	2????	10211	1???	??111	11111	11111	1???	??1???	??110	??100	11?		
<i>Avimimus</i>	00000	10000	00000	11200	000???	20200	0000?	??201?	2120?	20001	001?0	11001		
	??110	01000	00?01	1???	??011	11111	11111	11???	??2??1	??111	11100	21?		
<i>Tyrannosaurus</i>	00000	00000	00001	01000	00111	10100	00000	01000	01100	01001	00101	11000		
	01111	10000	10011	11111	11111	11111	11111	11111	11111	10110	00000	111		
<i>Troodon</i>	00000	00???	00000	11?00	00000	00100	00000	00111	111??	??000	??100	00111		
	1111?	??111	10111	11111	11?11	11111	11111	11111	11111	11110	00110	110		
<i>Ornithomimus</i>	00000	00000	00000	00000	00000	00000	00000	00000	00000	00000	00111	11111		
	11111	11111	11111	11111	11111	11111	11111	11111	11111	11110	00000	00?		

The Cretaceous-Miocene genus *Lichenopora* (Bryozoa), with a description of a new species from New Zealand

DENNIS P. GORDON

National Institute of Water & Atmospheric Research, P.O. Box 14–901, Kilbirnie, Wellington, New Zealand

PAUL D. TAYLOR

Department of Palaeontology, The Natural History Museum, Cromwell Road, London SW7 5BD, UK

SYNOPSIS. The type species of the cyclostome bryozoan *Lichenopora* Defrance, *L. turbinata* from the Eocene of France, is redescribed, allowing the concept of the genus to be revised. Colonies of *L. turbinata* consist of small, acute cones, unlike the majority of fossil and Recent species which have been since assigned to *Lichenopora*. Similar conical-pedunculate species of *Lichenopora sensu stricto* range from the Lower Cenomanian to the Lower Miocene. The youngest is a species from the Parnell Grit (Burdigalian) of Auckland, New Zealand, described here as *L. parva* sp. nov.

INTRODUCTION

The bryozoan genus *Lichenopora* is well-known to bryozoologists (e.g. Alvarez 1993) and, indeed, to ecologists and natural historians in parts of the world where encrusting lichenoporid bryozoans may be commonly associated with intertidal and shallow subtidal algae and rocky substrata (e.g. Sinel 1906; Rogick & Croasdale 1949; Morton & Miller 1968; Hayward 1988). About 40 nominal species of extant *Lichenopora* and over 100 fossil species have been described. As will be shown in this paper, however, *Lichenopora* should be restricted to a small suite of Cretaceous to Miocene species characterised, *inter alia*, by conical/pedunculate colonies.

The genus was proposed by Defrance (1823) for three bryozoan species having autozooids clustered in short radiating crests not fused centrally to form a star. Two, one conical the other adnate, were Middle Eocene in age; the other, apparently also adnate, was Maastrichtian. Only the conical form, *L. turbinata*, was illustrated, and this was chosen by d'Orbigny (1853: 963), who discovered additional conical/pedunculate forms, as type species and representative of the genus: "Pour conserver cette coupe générique, nous prenons pour type la première espèce de [Defrance], son *L. turbinata*, la seule qui présente plusieurs rangées de cellules aux lignées en cycles de la partie supérieure". Although d'Orbigny (1853) cited the genus as being characterised by the particular arrangement of autozooids in the colony, he did not include Recent adnate forms in it and, indeed, had previously diagnosed the genus as comprising "Bryozoaires coniques, fixées par le point du cone" (d'Orbigny 1852: 110), a viewpoint endorsed by Gregory (1909), who noted that even Busk (1859, 1875) did not attribute a single living species to *Lichenopora*. Instead, Busk (1859, 1875) used "*Disporella*, Gray" (error for *Disporella* Gray, 1848) for the living, adnate forms, as did Smitt (1867) when proposing the family Lichenoporidae.

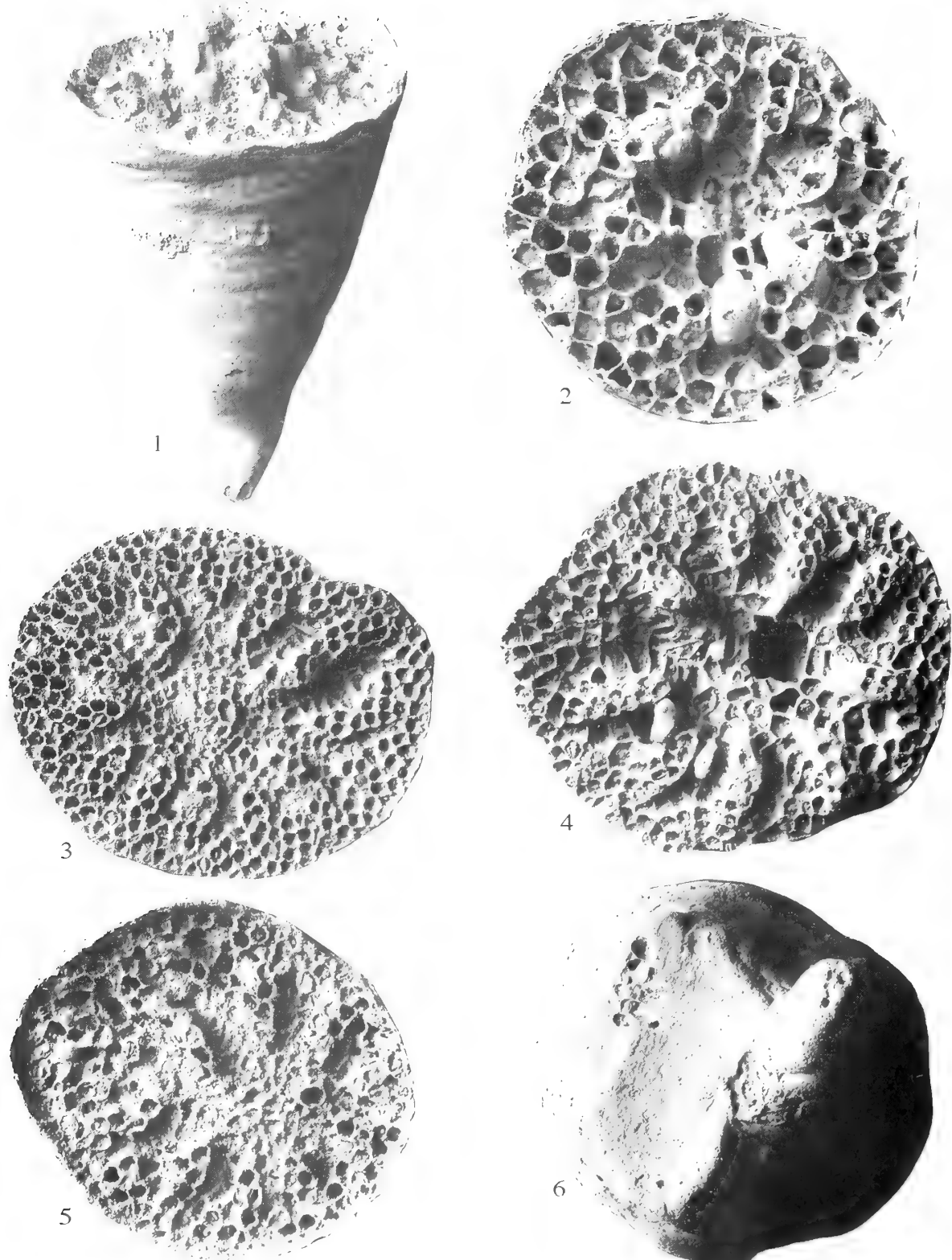
Prior to Gray's (1848) introduction of *Disporella*, some earlier authors (e.g., Milne Edwards 1838; Johnston 1847) had included living adnate lichenoporids in *Tubulipora*, a branching adnate genus with calcified frontal walls and which is not closely related to

lichenoporids. However, the French palaeontologist Michelin (1841–48), evidently following Defrance's (1823) wider view of the genus, included adnate forms in *Lichenopora*. So too did Reuss (1846). Whereas Smitt still used the combination *Disporella verrucaria* up to 1868, he later changed his view of generic relationships, attributing *D. verrucaria* to *Lichenopora* without explanation (Smitt 1878a,b). This appears to have persuaded Thomas Hincks, for, in his very influential work *British Marine Polyzoa* (Hincks 1880), he used the genus *Lichenopora* for *D. verrucaria* (and other living adnate species including *D. hispida*), citing Smitt (1878a) in his synonymy as the only previous author to use this combination. The use of *Lichenopora* for all living adnate forms continued until Borg (1933) reintroduced *Disporella* Gray, 1848 as a subgenus of *Lichenopora*, then as a full genus (Borg 1944) to accommodate the type species (*D. hispida* Fleming) and some other species, while continuing to use *Lichenopora* for *Madrepora verrucaria* Linnaeus and related species. Sabri (1988) pointed out that Brood (1972) was the first palaeontologist to use *Disporella* for fossil species.

SYSTEMATIC PALAEONTOLOGY

Specimen repositories and abbreviations: BMNH, The Natural History Museum, London; IGNS, Institute of Geological & Nuclear Sciences, Hutt City (formerly New Zealand Geological Survey, NZGS); MNHN, Muséum National d'Histoire Naturelle, Paris.

The species described were all studied by scanning electron microscopy (SEM), using type and/or topotypic specimens. Most SEM was carried out on uncoated specimens in an environmental chamber attached to an ISI ABT-55 scanning electron microscope. This generated back-scattered electron images in contrast to the secondary electron images which are used in conventional SEM of coated specimens. All figures are uncoated scanning electron micrographs. Morphometric determinations were made using an eyepiece micrometer affixed to a Wild M7 binocular microscope, or from SEM micrographs where necessary.



Figs 1–6 *Lichenopora turbinata* Defrance, 1823, Eocene, Manche, France. 1, MNHN, Canu Collection, R. 53447, M. Lutetian, Orglandes, profile of conical colony, $\times 18$. 2, BMNH BZ 3163, Hauteville, disc surface of small infertile colony, $\times 26$. 3–6, MNHN, d'Orbigny Collection, B.50246, 'Parisien', Orglandes; 3, disc of colony with well-developed autozooidal rays, $\times 13$; 4, disc of fertile colony, $\times 15$; 5, disc of another colony with raised edges, $\times 15$; 6, underside of colony with an extensive basal attachment to an unpreserved substratum represented by a mould bioimmuration, $\times 16$.

Order **CYCLOSTOMATIDA** Busk, 1852

Suborder **RECTANGULINA** Waters, 1887

Family **LICHENOPORIDAE** Smitt, 1867

Genus *LICHENOPORA* Defrance, 1823

TYPE SPECIES. *Lichenopora turbinata* Defrance, 1823, subsequently designated by d'Orbigny (1853: 963); Eocene (Lutetian), France.

DIAGNOSIS. Colony an even, acute cone, tapering basally, or with the cone expanded outward laterally and supported by a short peduncle; cone sides comprising a basal exterior wall with or without accessory kenozooidal prop-like processes. Zoids free-walled, tubular and straight in longitudinal section, opening on subcircular frontal disc; both autozooids and kenozooids arranged quincuncially near the edge of the disc, with older autozooids tending to become grouped in several elevated radial series that converge at or near the centre of the disc. Brood chamber located centrally, but may have lobes extending into interradial areas between autozooidal rows; roof comprising an interior wall typically overgrown by the walls of shallow kenozooids that develop on its surface. Ooeciopore relatively large, situated near the centre of the disc.

DISTRIBUTION. Cretaceous (Lower Cenomanian) – Eocene (Lutetian) of Europe; Lower Miocene (Burdigalian) of New Zealand.

Lichenopora turbinata Defrance, 1823

Figs 1–10

- 1823 *Lichenopora turbinata* Defrance: 257, pl. 46, figs 4, 4a.
- 1852 *Lichenopora turbinata* Defrance; d'Orbigny: 963.
- 1909 *Lichenopora turbinata* Defrance; Canu: 138, pl. 17, figs 13–15.
- 1953 *Lichenopora turbinata* Defrance; Bassler: 73, fig. 38, 1.
- 1956 *Lichenopora turbinata* Defrance; Balavoine: 321.
- 1970 *Lichenopora turbinata* Defrance; Labracherie: 37, pl. 6, figs 8–9.
- 1988 *Lichenopora turbinata* Defrance; Sabri: 141.

MATERIAL. MNHN, d'Orbigny Collection, B.50246 (a–f), Eocene, 'Parisien', Orglandes, Manche, France; MNHN, Canu Collection, R. 53447, Eocene, M. Lutetian, Orglandes, Manche, France; BMNH BZ 3163, Eocene, Hauteville, Manche, France, C. Lyell Collection, presented by T. R. Jones, 1896.

The type material of this species is thought to be lost: none of the MNHN specimens seem to represent that figured by Defrance.

DESCRIPTION. Colony an inverted cone (Fig. 1), up to 4.7 mm high and 3.3 mm diameter, the cone diverging at an angle of about 45°. Apical end of cone evenly tapered and straight, or the apex somewhat deflected at an angle from the axis; frequently broken, showing a dozen or so zooidal tubes in transverse section, each tube 0.09–0.13 mm diameter. Sides of cone formed of exterior wall (the upturned basal wall of the colony), more or less smooth textured; in profile, the sides of the cone may be nearly straight or very gently undulose; light concentric or subconcentric growth banding is typical. Supportive kenozooidal props have not been observed, but some colonies bear grooves or planar areas down one side of the cone or transversely near the apex, representing bioimmurations of a substratum to which the cone was attached laterally (Fig. 6). Disc circular or elliptical (Figs 2–5) and slightly depressed beneath the level of the rim in well-preserved specimens.

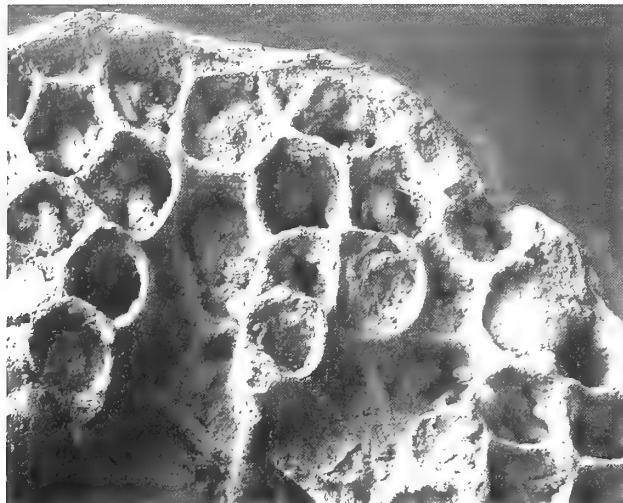
Zooidal apertures near the outer (distal) margin of disc are arranged quincuncially (Fig. 7), have more or less equal diameter (0.14–0.17 mm centre-to-centre spacing), and are polygonal in shape; there is no obvious distinction between autozooidal and kenozooidal apertures in these submarginal areas, but the outermost apertures beyond autozooidal rays are presumed to have been autozooids. In mature colonies with brood chambers, autozooids are arranged in elevated biserial rays with apertures alternating (Figs 3–5, 8), each aperture elliptical, up to 0.19 mm in diameter and elongated along the axis of the ray; there are up to 10 such rays, each with 4–6 pairs of autozooids, terminating abruptly near the concave centre of the disc. Between the rays are at least two rows of kenozooidal apertures. In immature colonies (i.e., smaller colonies without a visible brood chamber), the autozooidal rays are less distinct and shorter (Fig. 2), comprising 2–4 pairs of autozooids only, with some of the autozooids unpaired.

The disc centre is composed of kenozooids which may become covered by a brood chamber with lobes extending between the autozooidal rays (Fig. 4). The roof of the brood chamber appears to be sparsely porous and is overgrown by a network of ridges that define shallow kenozooidal chambers (alveoli). The prominent ooeciostome (Fig. 9), located at or near the centre of the disc, comprises a short broad tube with an oval ooeciopore (Fig. 10), 0.11–0.17 mm × 0.23 mm in diameter, roughly twice the width of an autozooidal aperture.

REMARKS. Canu (1909) illustrated *L. turbinata* using several light micrographs, of which plate 17, fig. 14 was reproduced as a mirror-image line drawing in Bassler's (1953: fig. 38.1) bryozoan *Treatise*. It is unfortunate that Bassler did not also illustrate *L. turbinata* in profile, for it has not generally been appreciated that the type species of *Lichenopora* is conical. According to Canu, the elongate conical form is rare, and shorter colonies are more commonly found; however, the only colony he figured in profile is steeply conical. Similarly, the colony shown in profile by Labracherie (1970: pl. 6, fig. 9) is also a high cone, and all of the material available to us had the same form. Kenozooidal props have not been described in the literature and were not encountered in our material.

A few remarks on the ecology of *L. turbinata* are possible. Although Defrance (1823) illustrated a slight expansion at the apex of the cone and a flattened base, indicating a direct and limited attachment to a substratum, the groove-like or planar bioimmurations (Fig. 6) on the sides of a few colonies are evidence of a more extensive lateral attachment in some instances. Inasmuch as the molluscan fauna associated with *L. turbinata* at the localities where it is found in the Paris Basin is characteristic of seagrass beds (Jon Todd & Didier Merle, pers. comms, December 1994), it is possible that colonies lived attached to seagrass. Associations between bryozoans and sea-grasses date back to the Maastrichtian (Voigt 1981), and are well-known from the Mediterranean at the present-day. For example, Hayward (1975) noted more than 30 bryozoan species, including one obligate epiphyte, living on *Posidonia oceanica* from Chios, Greece. However, none of these species have conical colonies like those of the Eocene *L. turbinata*, and fossil examples of seagrass associations from the Maastrichtian (Voigt 1981) and Eocene (Ivany *et al.* 1990) similarly lack conical colonies, although they do include lichenoporids.

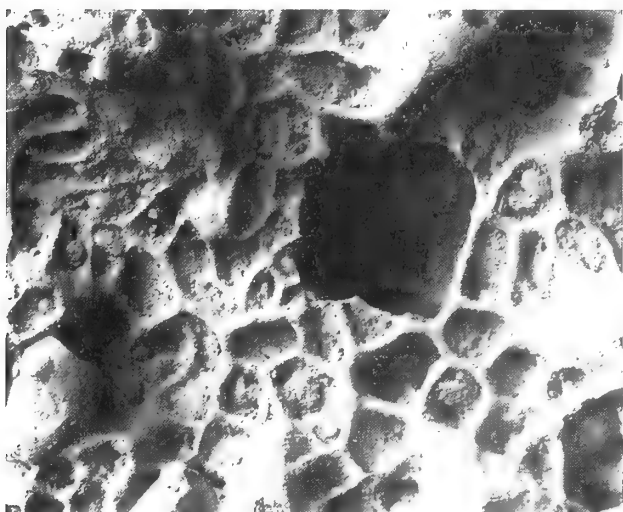
DISTRIBUTION. Eocene of France: Lutetian of the Paris Basin (Canu 1909), Middle-Upper Eocene of northern Aquitaine (Labracherie 1970).



7



8



9



10

Figs 7–10 *Lichenopora turbinata* Defrance, 1823, Eocene, Manche, France. **7**, BMNH BZ 3163, Hauteville, edge of disc showing initial quincuncial arrangement of zooids, $\times 73$; **8–10**, MNHN, d'Orbigny Collection, B.50246, 'Parisien', Orglandes; **8**, autozooidal rays separated by grooves containing kenozooids, $\times 43$; **9**, centre of a fertile colony with broken brood chamber roof to the left of which is an oocciostome, $\times 60$; **10**, oocciopore from the colony depicted in Fig. 5, $\times 150$.

Lichenopora parva sp. nov.

Figs 11–15, 17–20

HOLOTYPE. IGNS BZ 181, Miocene, Otaian (= Burdigalian), Waitemata Group, East Coast Bays Formation, Parnell Grit, Faulkner Bay, Manukau Harbour, Auckland, New Zealand (Grid Reference R11/654728), collected by D. P. Gordon & P. D. Taylor, March 1996. New Zealand Fossil Record Number R11/f197.

PARATYPES. IGNS BZ 182–3; BMNH BZ 3505–7; details as for holotype.

DIAGNOSIS. A small *Lichenopora*, not more than 2.5 mm high, the cone angle 45–85°; kenozooidal props present or absent; tubercle-like thickenings of zooidal walls near the disc centre.

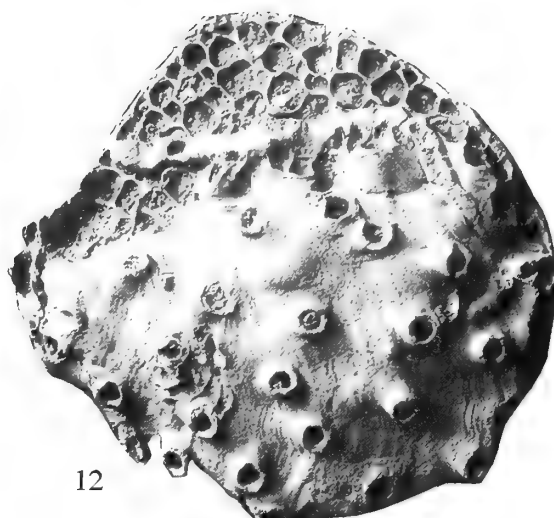
DESCRIPTION. Colony conical (Figs 11, 13–15, 17), tiny, about as

wide as high, preserved size not exceeding 2.5 mm high and 3.4 mm in diameter, the angle of the cone 45–85°. Outer (basal) surface of cone textured with faint concentric growth banding; cone apex symmetrical, rounded, or slightly irregular according to the substratum. Short, hollow kenozooidal props (Fig. 15) occur on some specimens, as many as 3 on one side, or these may be entirely absent. Disc nearly circular in outline, surface significantly depressed below the rim in well-preserved material (Fig. 14). Disc surface convex, rising to short prominences near the centre.

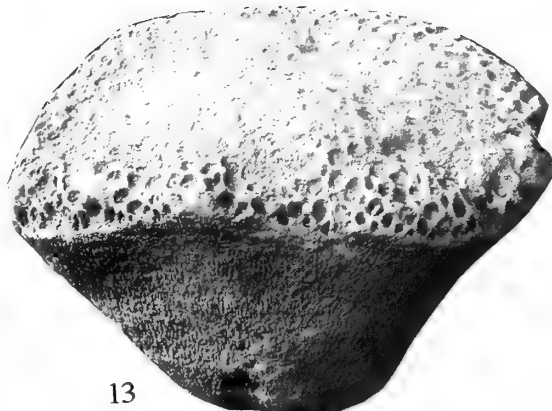
Zooids arranged in irregular quincunx, with considerable variation in apertural diameter, size generally increasing centripetally; the largest apertures (up to 0.20 mm in diameter) are assumed to be autozooidal, the smallest kenozooidal (i.e. alveoli) or new buds (Figs 19–20). Autozooids not clearly arranged in rays (Fig. 18).



11



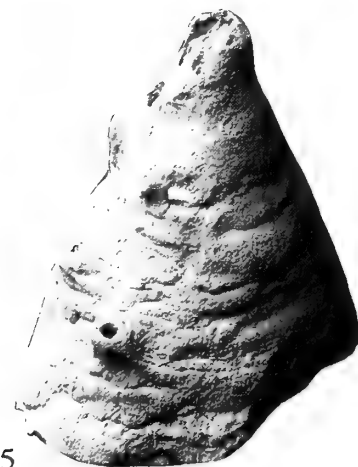
12



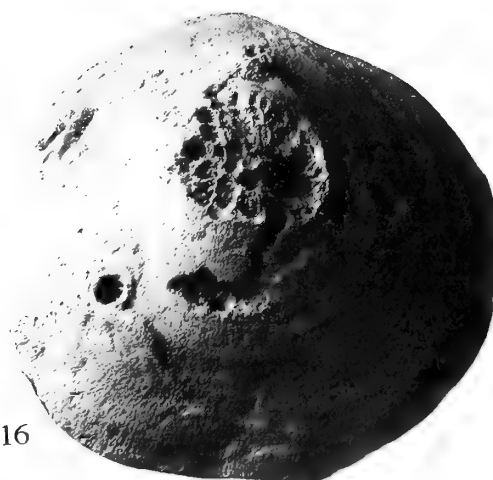
13



14



15



16

Figs 11–16 *Lichenopora parva* sp. nov., Miocene, Otaian, Parnell Grit, Faulkner Bay, Auckland, New Zealand. 11–12, BMNH BZ 3505; 11, profile of conical colony, $\times 38$; 12, surface of disc overgrown by a sheet-like and a uniserial tubuliporine cyclostome, $\times 40$. 13, BMNH BZ 3506, large conical colony with poorly-preserved surface, $\times 22$. 14, IGNS BZ 183, tiny cone with disc surface strongly depressed, $\times 40$. 15, BMNH BZ 3507, conical colony with the broken base of a prop (depicted upside-down because of constraints in SEM stage tilt), $\times 32$. 16, *Lichenopora pedunculata* Voigt, 1989, Cretaceous, Lower Cenomanian, Mülheim, Westfalia, Germany, BMNH D58007, underside of conical colony with broken stalk and the base of a prop, $\times 27$.

Broken apertural spines present on the proximal sides of autozooidal apertures in the least abraded specimen (Fig. 20). Centre-to-centre-spacing of the largest-diameter zooids is 0.12–0.20 mm. Stout tubercle-like thickenings of the zooidal walls are commonly developed near disc centre (Fig. 19), sometimes attaining the diameter of an autozooidal aperture.

Brood chamber not seen at disc surface; however, a questionable brood chamber was visible in a sectioned specimen below the disc surface.

REMARKS. *Lichenopora parva* differs from *L. turbinata* Defrance in its consistently smaller size, tubercle-like thickenings of the zooidal walls and lack of arrangement of autozooids into radial rays, and from other related conical/pedunculate species (see below) in the asymmetrical placement of the kenozooidal props and smaller cone angle, apart from differences in geographical distribution and stratigraphic age. In colonial morphology, the species that most closely resembles *L. parva* is *L. pedunculata* Voigt, 1989 from the Lower Cenomanian of Westfalia, Germany. This Cretaceous species has small conical colonies of almost the same form, not exceeding 3 mm height and diameter. Most strikingly, it also has kenozooidal props (Fig. 16) which appear to occur on all specimens, with 2–6 props distributed around the sides of the cone. However, autozooids are arranged in uniserial rays in *L. pedunculata*.

None of the six species of ‘*Lichenopora*’ recorded by Waters (1887) from the Cenozoic of New Zealand have conical colonies.

The mode of attachment during life of this tiny species is not known as the proximal cone apex is always missing, although evidence of supportive props suggests that secondary attachments to the substratum were developed. More intact props have been figured in *L. pedunculata* by Voigt (1989, pl. 7, figs 3, 4, 7, 8). One colony of *L. parva* is partly overgrown by a sheet-like tubuliporine cyclostome that started life on the side of a cone and then grew over the rim to cover virtually the entire disc surface (Fig. 12), and a uniserial tubuliporine.

The new species has been recorded only from the Parnell Grit. The Parnell Grit comprises several beds of Early Miocene (Otaian = Burdigalian) volcanoclastics interbedded with bathyal flysch, and each bed is interpreted as a deposit formed by a subaqueous gravity flow (submarine lahar) which picked up bryozoans as it passed over the shallow shelf (Ballance & Gregory 1991). Consequently, the colonies of *L. parva* are allochthonous and their original habitat is unclear.

DISTRIBUTION. Miocene: Otaian (= Burdigalian), Auckland, New Zealand.

DISCUSSION

Several pedunculate Cretaceous species superficially resembling the type and other conical species of *Lichenopora* were described and illustrated by d’Orbigny (1853). Using the nomenclature in d’Orbigny’s atlas of plates (pls 645, 646), they include: *Lichenopora compressa*, *L. elatior*, *L. irregularis*, *L. organisans*, *L. pocillum*, and *L. tuberculata*. Of these, *L. tuberculata* appears to be a tubuliporine; *L. organisans* was removed by Pergens (1890) to *Apsendesia* Lamouroux, another tubuliporine, and Pergens synonymised *L. compressa* with *L. pocillum*. We have not examined type or reliably determined material of *L. pocillum*, *L. elatior*, or *L. irregularis*, but have been able to study using SEM a possibly related species, *Defrancia cariosa* von Hagenow, 1851, which d’Orbigny (1853) included in *Lichenopora*. This is a robust pedunculate form that

superficially resembles *Lichenopora*, but has vertically stacked brood chambers. Without further revision of all of these forms, which require the brood chamber for taxonomic certainty, we cannot suggest an alternative genus. *Lichenopora defranciana* Michelin, 1845, also mentioned by d’Orbigny, is pedunculate and very like *Lichenopora* as here defined in the characters of the disc, but we have not encountered brood chambers in museum specimens and cannot comment further on its affinities. (It should be noted that, in his text, d’Orbigny (1853) used *Discocavea* (type species *L. irregularis*) for several species attributed to *Lichenopora* in his plates.) *Lichenopora convexa* Canu, 1909 from the Lutetian of the Paris Basin is a true *Lichenopora*. It forms small conical colonies ca. 2 mm high and up to 3.8 mm diameter, with an apparent cone angle of 100° based on the single colony illustrated in profile by Canu (1909). In addition to the cone apex by which the species appears to have been attached in life, Canu described a prop on one side of some colonies, giving the appearance of two basal supports. Autozooids are arranged in uniserial rows, unlike the biserial arrangement found in *L. turbinata*.

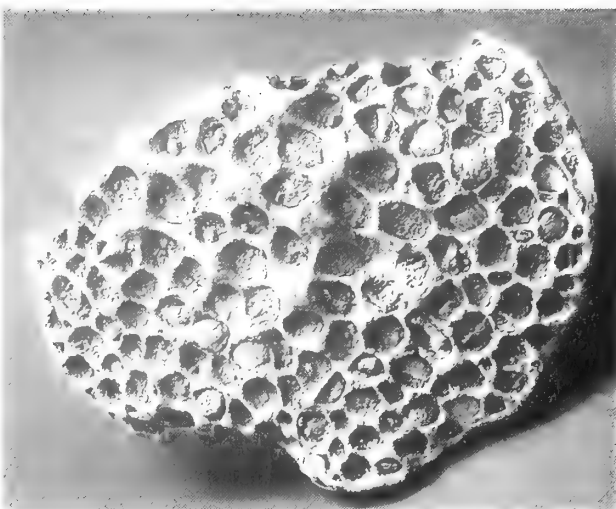
From all the material that we have seen, and from the literature, we conservatively interpret *Lichenopora* to include only conical and some conical-pedunculate species, e.g. Lower Cenomanian *L. pedunculata* Voigt, Lutetian *L. convexa* Canu and *L. turbinata* Defrance, Burdigalian *L. parva* sp. nov., and probably Danian-Lutetian *L. defranciana* (plus others of similar form that require restudy). All of these species are characterised by the possession of an erect, conical or conical-pedunculate colony form. This colony-form is regarded as an apomorphy relative to the more normal adnate discoidal colony forms found in other lichenoporid rectangulates and some closely-related cerioporines (e.g. *Favosipora*). Additionally, although not yet known in the type species, most species have supportive kenozooidal props. These props are not present in every colony of the species that can produce them, implying some phenotypic plasticity. Importantly, such props are not known in any modern species – there are instances in which some modern lichenoporids (e.g., expansive colonies of some *Disporella* species) are unable to be entirely adnate to a highly irregular substratum. In such cases, concentric ridges of calcification from the basal wall, representing earlier growth bands, “bend” into a concavity of the substratum while the general trend of the basal wall continues at right angles to the bend. These structures are solid, however, and do not contain kenozooidal chambers. Thus kenozooidal props would also appear to be an apomorphy characterising *Lichenopora sensu stricto*.

Recent species attributed to *Lichenopora* are strictly adnate (e.g. Alvarez 1993). Within 1–3 zooidal generations from the ancestrula, the proximal colony margin folds back over the protoecium to adhere immediately to the substratum, establishing evenly circumferential colony expansion. In some adnate species previously attributed to *Lichenopora*, especially when attached to erect bryozoans where space is lacking for lateral expansion, the so-called basal lamina or colony margin can curve upwards considerably, resulting in a calyciform colony. In longitudinal section, however, such colonies are still centrally adnate and broader-based and do not resemble the strictly conical forms with their narrower points of attachment to the substratum. A priori, it would seem logical to derive pedunculate and conical colonies from adnate forms by diminishing the area of attachment centrally.

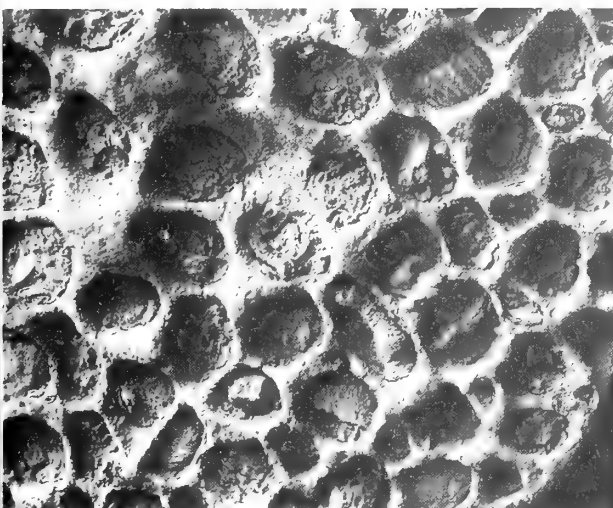
The question arises as to the generic placing of the numerous Cenozoic and Recent adnate species previously attributed to *Lichenopora*. For these, the genus *Patinella* Gray, 1848 (type species *Madrepora verrucaria* Linnaeus) is available, assuming that brood-chamber construction is indeed different from that of *Disporella* Gray, 1848 (see Schäfer 1991).



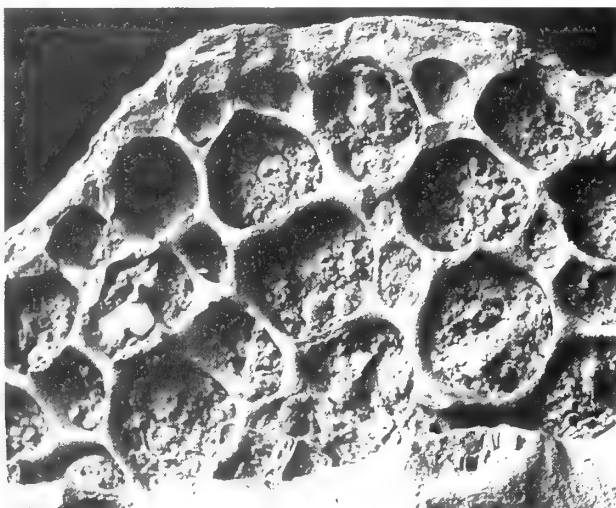
17



18



19



20

Figs 17–20 *Lichenopora parva* sp. nov., Miocene, Otaian, Parnell Grit, Faulkner Bay, Auckland, New Zealand. **17–19**, IGNS BZ 181, holotype; **17**, longitudinally fractured colony showing tubular zooids, $\times 35$; **18**, disc surface, $\times 35$; **19**, variably-sized zooidal apertures and tubercle-like wall thickenings, $\times 85$. **20**, BMNH BZ 3505, well-preserved disc surface showing apertural spines, $\times 145$.

ACKNOWLEDGEMENTS. We are grateful to The British Council for funding travel associated with this research through an academic link scheme, Professor E. Voigt for discussion and material, and Didier Merle for arranging and conveying a loan of specimens from the MNHN, Paris.

REFERENCES

- Alvarez, J. A. 1993. Sobre algunas especies de la familia Lichenoporidae Smitt, 1866 (Bryozoa, Cyclostomida) en la región Atlántico-Mediterránea. Parte II: estudio preliminar del género *Lichenopora* Defrance, 1823. *Cahiers de Biologie Marine*, **34**: 261–288.
Balavoine, P. 1956. Quelques Bryozoaires Eocénes du Bassin de Paris et du Cotentin de la collection Gustave-F. Dollfus. *Bulletin du Muséum National d'Histoire Naturelle, série 2*, **28**: 319–325.

- Ballance, P. F. & Gregory, M. R. 1991. Parnell Grits – large subaqueous volcaniclastic gravity flows with multiple particle-support mechanisms. *SEPM Special Publication*, **45**: 189–200.
Bassler, R. S. 1953. Bryozoa. In, Moore, R. C. (ed.), *Treatise on Invertebrate Paleontology*, Part G, xiv + 253 pp. New York & Lawrence.
Borg, F. 1933. Die Bryozoen. III. Teil: Die marinen Bryozoen (Stenolaemata und Gymnolaemata) des artischen Gebietes. *Fauna Arctica*, **6**: 515–551.
— 1944. *The stenolaematos Bryozoa. Further Zoological Results of the Swedish Antarctic Expedition 1901–1903*. 276 pp., 16 pls. Stockholm.
Brood, K. 1972. Cyclostomatous Bryozoa from the Upper Cretaceous and Danian in Scandinavia. *Stockholm Contributions in Geology*, **26**: 1–464, 78 pls.
Busk, G. 1852. An account of the Polyzoa, and sertrarian zoophytes, the Louisiade Archipelago, &c. In, MacGillivray, J., *Narrative of the voyage of H.M.S. Rattlesnake, commanded by the late Captain Owen Stanley... 1846–1850*. I: 342–402. London.
— 1859. A Monograph of the Fossil Polyzoa of the Crag. *Palaeontographical Society Monographs*, 1–136.
— 1875. *Catalogue of Marine Polyzoa in the Collection of the British Museum. Part III. Cyclostomata*. 39 pp., 34 pls. London.

- Canu, F.** 1909. Bryozoaires des terrains tertiaires des environs de Paris. *Annales de Paléontologie*, **4**: 133–140, pls 16–18.
- Defrance, J. L. M.** 1823. Polypiers. In, *Dictionnaire des sciences naturelles*. Vol. 26. Paris.
- Gray, J. E.** 1848. *List of the specimens of British animals in the collection of the British Museum. Part I, Centroniae or radiated animals [Polyzoa pp. 91–151]*. 173 pp. London.
- Gregory, J. W.** 1909. *Catalogue of the fossil Bryozoa in the Department of Geology, British Museum (Natural History). The Cretaceous Bryozoa. Volume II*. 346 pp., 9 pls. London.
- Hagenow, F. von** 1851. *Die Bryozoen der maastrichter Kreidebildung*. xv + 111 pp., 12 pls. Cassel.
- Hayward, P. J.** 1975. Observations on the bryozoan epiphytes of *Posidonia oceanica* from the island of Chios (Aegean Sea). *Documents des Laboratoires de Géologie de la Faculté des Sciences de Lyon*, (H.S.) 3 (2): 347–356.
- 1988. *Animals on seaweed*. v + 108 pp. Richmond.
- Hincks, T.** 1880. *A History of the British Marine Polyzoa*. cxli + 601 pp. (Vol. 1), 83 pls (Vol. 2). London.
- Ivany, L. C., Portell, R. W. & Jones, D. S.** 1990. Animal-plant relationships and paleobiogeography of an Eocene seagrass community from Florida. *Palaios*, **5**: 244–258.
- Johnston, G.** 1847. *A History of British Zoophytes*. 2nd edition. 488 pp. (Vol. 1), 74 pls (Vol. 2). London.
- Labracherie, M.** 1970. *Les Bryozoaires dans l'Eocène nord-aquitain. Signification biostratigraphique et paléocologique*. Thèse, Doctorat des Sciences Naturelles, Université de Bordeaux, no. 316. 314 + 34 pp., 61 tables, 3 + 21 pls. Bordeaux.
- Michelin, H.** 1841–8. *Iconographie Zoophytologie, description par localités et terrains des polypiers fossile de France et pays environnans*. viii + 348 pp., 79 pls. Paris.
- Milne Edwards, H.** 1838. Mémoire sur les Polypes du genre des Tubulipores. *Annales des Sciences naturelles (Zoologie)*, **8**: 321–338, pls 12–14.
- Morton, J. E. & Miller, M. C.** 1968. *The New Zealand sea shore*. 638 pp., 32 pls. London & Auckland.
- Orbigny, A. D. d'** 1852. *Cours élémentaire de paléontologie et de géologie stratigraphique*. Paris. [Tableau 10, Bryozoa].
- 1851–54. *Paléontologie Française. Description des Mollusques et rayonnés fossiles. Terrains crétacés. V. Bryozaires*. [Pp. 1–188 (1851); 185 bis–472 (1852); 473–984 (1853); 985–1192 (1854); pls 600–800, fide Sherborn 1899]. Paris.
- Pergens, E.** 1890. Revision des Bryozoaires du Crétacé figurées par d'Orbigny. Première partie. Cyclostomata. *Bulletin de la Société Belge de Géologie, de Paléontologie et d'Hydrologie*, **3**: 305–400, pls 11–13.
- Reuss, A. E. von** 1846. *Die Versteinerungen der bohmischen Kreideformation*, Vol. 2. 148 pp., 51 pls [Bryozoa pp. 63–70, pls 15–16]. Stuttgart.
- Rogick, M. D. & Croasdale, H.** 1949. Studies on marine Bryozoa. III. Woods Hole region Bryozoa associated with algae. *Biological Bulletin*, **96**: 32–69.
- Sabri, Z.** 1988. *Révision systématique du genre Lichenopora Defrance, 1823 (Bryozoa, Cyclostomata)*. Thèse, Doctorat de Troisième Cycle, Université Claude Bernard. 181 pp., 8 pls.
- Schäfer, P.** 1991. Brutkammern der Stenolaemata (Bryozoa): Konstruktionsmorphologie und phylogenetische Bedeutung. *Courier Forschungsinstitut Senckenberg*, **136**: 1–263.
- Sherborn, C. D.** 1899. On the dates of the "Paléontologie Française" of D'Orbigny. *Geological Magazine, series 4*, **6**: 223–225.
- Sinel, J.** 1906. *An outline of the natural history of our shores*. xvi + 347 pp. London.
- Smitt, F. A.** 1867. Kritisk forteckning öfver Skandinaviens Hafs-Bryozoor. *Öfversigt af Kongliga Vetenskaps-Akademiens Förhandlingar*, **23**: 395–533, pls 3–13.
- 1868. Bryozoa marina in regionibus arcticis et borealibus viventia recensuit. *Öfversigt af Kongliga Vetenskaps-Akademiens Förhandlingar*, **1867** (6): 443–487.
- 1878a. Recensio systematica animalium Bryozorum, quae in itineribus, annis 1875 et 1876, ad insulas Novaja Semlja et ad ostium fluminis Jenisei, duce Professore A.E. Nordenskiöld, invenerunt Doctores A. Stuxberg et H. Theel. *Öfversigt af Kongliga Vetenskaps-Akademiens Förhandlingar*, **1878** (3): 11–26.
- 1878b. Recensio animalium Bryozorum e mari arctico, quae ad paeninsulam Kola, in itinere anno 1877, duce H. Sandberg, inventit F. Trybom. *Öfversigt af Kongliga Vetenskaps-Akademiens Förhandlingar*, **1878** (7): 19–32.
- Voigt, E.** 1981. Upper Cretaceous bryozoan-seagrass association in the Maastrichtian of the Netherlands. In, Larwood, G. P. & Nielsen, C. (eds), *Recent and fossil Bryozoa*, pp. 281–298. Fredensborg.
- 1989. Neue cyclostome Bryozoen aus dem Untercenomanium von Mülheim-Broich (Westfalen). *Münstersche Forschungen zur Geologie und Paläontologie*, **69**: 87–113.
- Waters, A. W.** 1887. On Tertiary cyclostomatous Bryozoa from New Zealand. *Quarterly Journal of the Geological Society of London*, **43**: 337–350.

Bulletin of The Natural History Museum Geology Series

Earlier Geology *Bulletins* are still in print. The following can be ordered from Intercept (address on inside front cover). Where the complete backlist is not shown, this may also be obtained from the same address.

Volume 34

No. 1	Relative dating of the fossil hominids of Europe. K.P. Oakley. 1980. Pp. 1–63, 6 figs, 17 tables.	£8.00
No. 2	Origin, evolution and systematics of the dwarf Acanthoceratid <i>Protacanthoceras</i> Spath, 1923 (Cretaceous Ammonoidea). C.W. Wright & W.J. Kennedy. 1980. Pp. 65–107, 61 figs.	£6.25
No. 3	Ashgill Brachiopoda from the Glyn Ceiriog District, north Wales. N. Hiller. 1980. Pp. 109–216, 408 figs.	£14.75
No. 4	Miscellanea	
	Type specimens of some Upper Palaeozoic Athyridide brachiopods. C.H.C. Brunton. 31 figs.	
	Two new British Cretaceous Epitonidae (Gastropoda): evidence for evolution of shell morphology. R.J. Cleevely. 14 figs, 1 table.	
	Revision of the microproblematicum <i>Prethocoprolithus</i> Elliott, 1962. G.F. Elliott. 4 figs.	
	<i>Basilicus tyrannus</i> (Murchison) and the glabellar structure of asaphid trilobites. R.A. Fortey. 12 figs.	
	A new Lower Ordovician bivalve family, the Thoraliidae (?) Nuculoidea), interpreted as actinodont deposit feeders. N.J. Morris. 7 figs.	
	Cretaceous brachiopods from northern Zululand. E.F. Owen. 13 figs.	
	<i>Tupus diluculum</i> sp. nov. (Protodonata), a giant dragonfly from the Upper Carboniferous of Britain. P.E.S. Whalley. 1 fig.	
	Revision of <i>Plummerita</i> Brönniman (Foraminifera) and a new Maastrichtian species from Ecuador. J.E. Whittaker. 34 figs. 1980. Pp. 217–297.	£11.00

Volume 35

No. 1	Lower Ordovician Brachiopoda from mid and south-west Wales. M.G. Lockley & A. Williams. 1981. Pp. 1–78, 263 figs, 3 tables.	£10.80
No. 2	The fossil alga <i>Girvanella</i> Nicholson & Etheridge. H.M.C. Danielli. 1981. Pp. 79–107, 8 figs, 3 tables.	£4.20
No. 3	Centenary miscellanea	
	Reassessment of the Ordovician brachiopods from the Budleigh Salterton Pebble Bed, Devon. L.R.M. Cocks & M.G. Lockley. 35 figs.	
	Felix Oswald's Turkish Algae. G.F. Elliott. 3 figs.	
	J.A. Moy-Thomas and his association with the British Museum (Natural History). P.L. Forey & B.G. Gardiner. 3 figs.	
	Burials, bodies and beheadings in Romano-British and Anglo-Saxon cemeteries. M. Harman, T.I. Molleson & J.L. Price. 5 figs, 7 tables, VI appendices.	
	The Jurassic irregular echinoid <i>Nucleolites clunicularis</i> (Smith). D.N. Lewis & H.G. Owen. 4 figs.	
	<i>Phanerotinus cristatus</i> (Phillips) and the nature of euomphalacean gastropods. N.J. Morris & R.J. Cleevely. 12 figs.	
	Agassiz, Darwin, Huxley, and the fossil record of teleost fishes. C. Patterson. 1 fig.	

The Neanderthal problem and the prospects for direct dating of Neanderthal remains. C.B. Stringer & R. Burleigh. 2 figs, 1 table.

Hippoporidra edax (Busk 1859) and a revision of some fossil and living *Hippoporidra* (Bryozoa). P.D. Taylor & P.L. Cook. 6 figs. 1981. Pp. 109–252.

£20.00

No. 4 The English Upper Jurassic Plesiosauroidea (reptilia) and a review of the phylogeny and classification of the Plesiosauria. D.S. Brown. 1981. Pp. 253–347, 44 figs.

£13.00

Volume 36

No. 1	Middle Cambrian trilobites from the Sosink Formation, Derik-Mardin district, south-eastern Turkey. W.T. Dean. 1982. Pp. 1–41, 68 figs.	£5.80
No. 2	Miscellanea	
	British Dinantian (Lower Carboniferous) terebratulid brachiopods. C.H.C. Brunton. 20 figs.	
	New microfossil records in time and space. G.F. Elliott. 6 figs.	
	The Ordovician trilobite <i>Nesuretus</i> from Saudi Arabia, and the palaeogeography of the <i>Nesuretus</i> fauna related to Gondwanaland in the earlier Ordovician. R.A. Fortey & S.F. Morris. 10 figs.	
	<i>Archaeocidaris whatleyensis</i> sp. nov. (Echinoidea) from the Carboniferous Limestone of Somerset and notes on echinoid phylogeny. D.N. Lewis & P.C. Ensom. 23 figs.	
	A possible non-calcified dasycladalean alga from the Carboniferous of England. G.F. Elliott. 1 fig.	
	<i>Nanjinoporella</i> , a new Permian dasyclad (calcareous alga) from Nanjing, China. X. Mu & G.F. Elliott. 6 figs, 1 table.	
	Toarcian bryozoans from Belchite in north-east Spain. P.D. Taylor & L. Sequeiros. 10 figs, 2 tables.	
	Additional fossil plants from the Drybrook Sandstone, Forest of Dean, Gloucestershire. B.A. Thomas & H.M. Purdy. 14 figs, 1 table.	
	<i>Bintoniella brodiei</i> Handlirsch (Orthoptera) from the Lower Lias of the English Channel, with a review of British bintoniellid fossils. P.E.S. Whalley. 7 figs.	
	<i>Uraloporella</i> Korde from the Lower Carboniferous of South Wales. V.P. Wright. 3 figs. 1982. Pp. 43–155.	£19.80
No. 3	The Ordovician Graptolites of Spitsbergen. R.A. Cooper & R.A. Fortey. 1982. Pp. 157–302, 6 plates, 83 figs, 2 tables.	£20.50
No. 4	Campanian and Maastrichtian sphenodiscid ammonites from southern Nigeria. P.M.P. Zaborski. 1982. Pp. 303–332, 36 figs.	£4.00

Volume 37

No. 1	Taxonomy of the arthrodire <i>Phlyctaenius</i> from the Lower or Middle Devonian of Campbellton, New Brunswick, Canada. V.T. Young. 1983. Pp. 1–35, 18 figs.	£5.00
No. 2	<i>Ailsacrinus</i> gen. nov., an aberrant millericrinid from the Middle Jurassic of Britain. P.D. Taylor. 1983. Pp. 37–77, 48 figs, 1 table.	£5.90
No. 3	Miscellanea	

Glossopteris anatolica Sp. nov. from uppermost Permian strata in south-east Turkey. S. Archangelsky & R.H. Wagner. 14 figs.

The crocodilian *Theriosuchus* Owen, 1879 in the Wealden of England. E. Buffetaut. 1 fig.

A new conifer species from the Wealden beds of Féron-Glagon, France. H.L. Fisher & J. Watson. 10 figs.

Late Permian plants including Charophytes from the Khuff formation of Saudi Arabia. C.R. Hill & A.A. El-Khayal. 18 figs.

British Carboniferous Edrioasteroidea (Echinodermata). A.B. Smith. 52 figs.

A survey of recent and fossil Cicadas (Insecta, Hemiptera-Homoptera) in Britain. P.E.S. Whalley. 11 figs.

The Cephalaspids from the Dittonian section at Cwm Mill, near Abergavenny, Gwent. E.I. White & H.A. Toombs. 20 figs. 1983. Pp. 79-171. £13.50

No. 4 The relationships of the palaeoniscid fishes, a review based on new specimens of *Mimia* and *Moythomasia* from the Upper Devonian of Western Australia. B.G. Gardiner. 1984. Pp. 173-428. 145 figs. 4 plates. 0 565 00967 2. £39.00

Volume 38

No. 1 New Tertiary pycnodonts from the Tilemsi valley, Republic of Mali. A.E. Longbottom. 1984. Pp. #1-26. 29 figs. 3 tables. 0 565 07000 2. £3.90

No. 2 Silicified brachiopods from the Viséan of County Fermanagh, Ireland. (III) Rhynchonellids. Spiriferids and Terebratulids. C.H.C. Brunton. 1984. Pp. 27-130. 213 figs. 0 565 07001 0. £16.20

No. 3 The Llandovery Series of the Type Area. L.R.M. Cocks, N.H. Woodcock, R.B. Rickards, J.T. Temple & P.D. Lane. 1984. Pp. 131-182. 70 figs. 0 565 07004 5. £7.80

No. 4 Lower Ordovician Brachiopoda from the Tourmakeady Limestone, Co. Mayo, Ireland. A. Williams & G.B. Curry. 1985. Pp. 183-269. 214 figs. 0 565 07003 7. £14.50

Miscellanea

Growth and shell shape in Productacean Brachiopods. C.H.C. Brunton.

Palaeosiphonium a problematic Jurassic alga. G.F. Elliott.

Upper Ordovician brachiopods and trilobites from the Clashford House Formation, near Herbertstown, Co. Meath, Ireland. D.A.T. Harper, W.I. Mitchell, A.W. Owen & M. Romano.

Preliminary description of Lower Devonian Osteostraci from Podolia (Ukrainian S.S.R.). P. Janvier.

Hippurion sp. (Equidae, Perissodactyla) from Diavata (Thessaloniki, northern Greece). G.D. Koufos.

Preparation and further study of the Singa skull from Sudan. C.B. Stringer, L. Cornish & P. Stuart-Macadam.

Carboniferous and Permian species of the cyclostome bryozoan *Corynotrypa* Bassler, 1911. P.D. Taylor.

Redescription of *Eurycephalochelys*, a trionychid turtle from the Lower Eocene of England. C.A. Walker & R.T.J. Moody.

Fossil insects from the Lithographic Limestone of Montsech (late Jurassic-early Cretaceous), Lérida Province, Spain. P.E.S. Whalley & E.A. Jarzembski. 1985. Pp. 271-412, 162 figs. 0 565 07004 5. £24.00

Volume 39

No. 1 Upper Cretaceous ammonites from the Calabar region, south-east Nigeria. P.M.P. Zaborski. 1985. Pp. 1-72. 66 figs.

0 565 07006 1. £11.00

No. 2 Cenomanian and Turonian ammonites from the Novo Redondo area, Angola. M.K. Howarth. 1985. Pp. 73-105. 33 figs.

0 565 07006 1. £5.60

No. 3 The systematics and palaeogeography of the Lower Jurassic insects of Dorset, England. P.E.S. Whalley. 1985. Pp. 107-189. 87 figs. 2 tables. 0 565 07008 8. £14.00

No. 4 Mammals from the Bartonian (middle/late Eocene) of the Hampshire Basin, southern England. J.J. Hooker. 1986. Pp. 191-478. 71 figs. 39 tables. 0 565 07009 6. £49.50

Volume 40

No. 1 The Ordovician graptolites of the Shelve District, Shropshire. I. Strachan. 1986. Pp. 1-58. 38 figs. 0 565 07010 X. £9.00

No. 2 The Cretaceous echinoid *Boletechinus*, with notes on the phylogeny of the Glyptocyphidae and Temnopleuridae. D.N. Lewis.

1986. Pp. 59-90. 11 figs. 7 tables. 0 565 07011 8. £5.60

No. 3 The trilobite fauna of the Raheen Formation (upper Caradoc), Co. Waterford, Ireland. A.W. Owen, R.P. Tripp & S.F. Morris.

1986. Pp. 91-122. 88 figs. 0 565 07012 6. £5.60

No. 4 Miscellanea I: Lower Turonian cirripede—Indian coleoid *Naefia*—Cretaceous—Recent Craniidae—Lectotypes of Girvan trilobites—Brachiopods from Provence—Lower Cretaceous cheiostomes. 1986. Pp. 125-222. 0 565 07013 4. £19.00

No. 5 Miscellanea II: New material of *Kimmerosaurus*—Edgehill Sandstone plants—Lithogeochemistry of Mendip rocks—Specimens previously recorded as teuthids—Carboniferous lycopsid *Anabathra*—*Meyenodendron*, new Alaskan lepidodendrid. 1986. Pp. 225-297. 0 565 07014 2. £13.00

Volume 41

No. 1 The Downtonian ostracoderm *Sclerodus* Agassiz (Osteostraci: Tremataspidae). P.L. Forey. 1987. Pp. 1-30. 11 figs. 0 565 07015 0. £5.50

No. 2 Lower Turonian (Cretaceous) ammonites from south-east Nigeria. P.M.P. Zaborski. 1987. Pp. 31-66. 46 figs. 0 565 07016 9. £6.50

No. 3 The Arenig Series in South Wales: Stratigraphy and Palaeontology. I. The Arenig Series in South Wales. R.A. Fortey & R.M. Owens. II. Appendix. Acritharchs and Chitinozoa from the Arenig Series of South-west Wales. S.G. Molyneux. 1987. Pp. 67-364.

289 figs. 0 565 07017 7. £59.00

No. 4 Miocene geology and palaeontology of Ad Dabtiyah, Saudi Arabia. Compiled by P.J. Whybrow. 1987. Pp. 365-457. 54 figs.

0 565 07019 3. £18.00

Volume 42

No. 1 Cenomanian and Lower Turonian Echinoderms from Wilmington, south-east Devon. A.B. SMith, C.R.C. Paul, A.S. Gale & S.K. Donovan. 1988. 244 pp. 80 figs. 50 pls. 0 565 07018 5. £46.50

Volume 43

- No. 1 A Global Analysis of the Ordovician–Silurian boundary. Edited by L.R.M. Cocks & R.B. Rickards. 1988. 394 pp., figs. 0 565 07020 7. £70.00

Volume 44

- No. 1 Miscellanea: Palaeocene wood from Mali—Chapelcorner fish bed—*Heterotheca* coprolites—Mesozoic Neuroptera and Raphidioptera. 1988. Pp. 1–63. 0 565 07021 5. £12.00

- No. 2 Cenomanian brachiopods from the Lower Chalk of Britain and northern Europe. E.F. Owen. 1988. Pp. 65–175. 0565 07022 3. £21.00

- No. 3 The ammonite zonal sequence and ammonite taxonomy in the *Douvilleiceras mammillatum* Superzone (Lower Albian) in Europe. H.G. Owen. 1988. Pp. 177–231. 0 565 07023 1. £10.30

- No. 4 Cassiopidae (Cretaceous Mesogastropoda): taxonomy and ecology. R.J. Cleevely & N.J. Morris. 1988. Pp. 233–291. 0565 07024 X. £11.00

Volume 45

- No. 1 Arenig trilobites—Devonian brachiopods—Triassic demosponges—Larval shells of Jurassic bivalves—Carboniferous marattialean fern—Classification of Plectambonitacea. 1989. Pp. 1–163. 0 565 07025 8. £40.00

- No. 2 A review of the Tertiary non-marine molluscan faunas of the Pebasian and other inland basins of north-western South America. C.P. Nuttall. 1990. Pp. 165–371. 456 figs. 0 565 07026 6. £52.00

Volume 46

- No. 1 Mid-Cretaceous Ammonites of Nigeria—new amphisbaenians from Kenya—English Wealden Equisetales—Faringdon Sponge Gravel Bryozoa. 1990. Pp. 1–152. 0 565 07027 4. £45.00

- No. 2 Carboniferous pteridosperm frond *Neuropteris heterophylla*—Tertiary Ostracoda from Tanzania. 1991. Pp. 153–270. 0565 07028 2. £30.00

Volume 47

- No. 1 Neogene crabs from Brunei, Sabah & Sarawak—New pseudosciurids from the English Late Eocene—Upper Palaeozoic Anomalodesmata Bivalvia. 1991. Pp. 1–100. 0 565 07029 0. £37.50

- No. 2 Mesozoic Chrysalidinidae of the Middle East—Bryozoans from north Wales—*Alveolinella praequoyi* sp. nov. from Papua New Guinea. 1991. Pp. 101–175. 0 565 070304. £37.50

Volume 48

- No. 1 '*Placopsilina*' *cenomana* d'Orbigny from France and England—Revision of Middle Devonian uncinulid brachiopod—Cheiostome bryozoans from Upper Cretaceous, Alberta. 1992. Pp. 1–24. £37.50

- No. 2 Lower Devonian fishes from Saudi Arabia—W.K. Parker's collection of foraminifera in the British Museum (Natural History). 1992. Pp. 25–43. £37.50

Volume 49

- No. 1 Barremian—Aptian Praehedbergellidae of the North Sea area: a reconnaissance—Late Llandovery and early Wenlock Stratigraphy and ecology in the Oslo Region, Norway—Catalogue of the type and figured specimens of fossil Asteroidea and Ophiuroidea in The Natural History Museum. 1993. Pp. 1–80. £37.50

- No. 2 Mobility and fixation of a variety of elements, in particular, during the metasomatic development of adinoles at Dinas Head, Cornwall—Productellid and Plicatiferid (Productoid) Brachiopods from the Lower Carboniferous of the Craven Reef Belt, North Yorkshire—The spores of *Leclercqia* and the dispersed spore morphon *Acinosporites lindlarensis* Riegel: a case of gradualistic evolution. 1993. Pp. 81–155. £37.50

Volume 50

- No. 1 Systematics of the meliceritid cyclostome bryozoans: introduction and the genera *Elea*, *Semielea* and *Reptiomultilea*. 1994. Pp. 1–104. £37.50

- No. 2 The brachiopods of the Duncannon Group (Middle-Upper Ordovician) of southeast Ireland. 1994. Pp. 105–175. £37.50

Volume 51

- No. 1 A synopsis of neuropteroid foliage from the Carboniferous and Lower Permian of Europe—The Upper Cretaceous ammonite *Pseudaspidoceras* Hyatt, 1903, in north-eastern Nigeria—The pterodactyloids from the Purbeck Limestone Formation of Dorset. 1995. Pp. 1–88. £37.50

- No. 2 Palaeontology on the Qahlah and Simsima Formations (Cretaceous, Late Campanian-Maastrichtian) of the United Arab Emirates-Oman Border Region—Preface—Late Cretaceous carbonate platform faunas of the United Arab Emirates-Oman border region—Late Campanian-Maastrichtian echinoids from the United Arab Emirates-Oman border region—Maastrichtian ammonites from the United Arab Emirates-Oman border region—Maastrichtian nautioids from the United Arab Emirates-Oman border region—Maastrichtian Inoceramidae from the United Arab Emirates-Oman border region—Late Campanian-Maastrichtian Bryozoa from the United Arab Emirates-Oman border region—Maastrichtian brachiopods from the United Arab Emirates-Oman border region—Late Campanian-Maastrichtian rudists from the United Arab Emirates-Oman border region. 1995. Pp. 89–305. £37.50

Volume 52

- No. 1 Zirconite: a review of localities worldwide, and a compilation of its chemical compositions—A review of the stratigraphy of Eastern Paratethys (Oligocene–Holocene)—A new protorichthofenoid brachiopod (Productida) from the Upper Carboniferous of the Urals, Russia—The Upper Cretaceous ammonite *Vascoceras* Choffat, 1898 in north-eastern Nigeria. 1996. Pp. 1–89. £37.50

- No. 2 Jurassic bryozoans from Baltów, Holy Cross Mountains, Poland—A new deep-water spatangoid echinoid from the Cretaceous of British Columbia, Canada—The cranial anatomy of *Rhomaleosaurus thorntoni* Andrews (Reptilia, Plesiosauria)—The first known femur of *Hylaeosaurus armatus* and re-identification of ornithopod material in The Natural History Museum, London—Bryozoa from the Lower Carboniferous (Viséan) of County Fermanagh, Ireland. 1996. Pp. 91–171. £37.50

CONTENTS

- 1 The status of '*Plesictis*' *croizeti*, '*Plesictis*' *gracilis* and '*Lutra*' *minor*: synonyms of the early Miocene viverrid *Herpestides antiquus* (Mammalia, Carnivora)
M. Wolsan and M. Morlo
- 11 *Baryonyx walkeri*, a fish-eating dinosaur from the Wealden of Surrey
A.J. Charig and A.C. Milner
- 71 The Cretaceous-Miocene genus *Lichenopora* (Bryozoa), with a description of a new species from New Zealand
D.P. Gordon and P.D. Taylor

Bulletin of The Natural History Museum

GEOLOGY SERIES

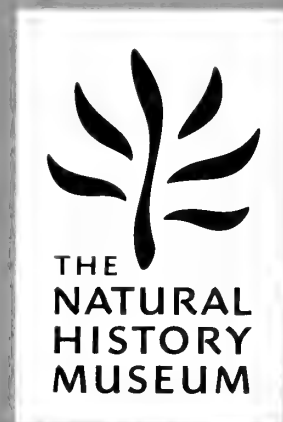
Vol. 53, No. 1, June 1997

PS.186.A

Bulletin of The Natural History Museum

THE NATURAL HISTORY MUSEUM
LONDON
27 NOVEMBER 1997
PALaeontological Society

Geology Series



VOLUME 53 NUMBER 2 27 NOVEMBER 1997

The *Bulletin of The Natural History Museum* (formerly: *Bulletin of the British Museum (Natural History)*), instituted in 1949, is issued in four scientific series, Botany, Entomology, Geology (incorporating Mineralogy) and Zoology.

The Geology Series is edited in the Museum's Department of Palaeontology
Keeper of Palaeontology: Dr L.R.M. Cocks
Editor of Bulletin: Dr M.K. Howarth
Assistant Editor: Mr C. Jones

Papers in the *Bulletin* are primarily the results of research carried out on the unique and ever-growing collections of the Museum, both by the scientific staff and by specialists from elsewhere who make use of the Museum's resources. Many of the papers are works of reference that will remain indispensable for years to come. All papers submitted for publication are subjected to external peer review for acceptance.

A volume contains about 160 pages, made up by two numbers, published in the Spring and Autumn. Subscriptions may be placed for one or more of the series on an annual basis. Individual numbers and back numbers can be purchased and a *Bulletin* catalogue, by series, is available. Orders and enquiries should be sent to:

Intercept Ltd.
P.O. Box 716
Andover
Hampshire SP10 1YG
Telephone: (01264) 334748
Fax: (01264) 334058

Claims for non-receipt of issues of the *Bulletin* will be met free of charge if received by the Publisher within 6 months for the UK, and 9 months for the rest of the world.

World List abbreviation: *Bull. nat. Hist. Mus. Lond. (Geol.)*

© The Natural History Museum, 1997

ISSN 0968-0462

Geology Series
Vol. 53, No. 2, pp. 79-139

The Natural History Museum
Cromwell Road
London SW7 5BD

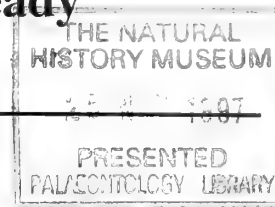
Issued 27 November 1997

Typeset by Ann Buchan (Typesetters), Middlesex
Printed in Great Britain by Henry Ling Ltd, at the Dorset Press, Dorchester, Dorset

Ordovician trilobites from the Tourmakeady Limestone, western Ireland

JONATHAN M. ADRAIN AND RICHARD A. FORTEY

Department of Palaeontology, Natural History Museum, Cromwell Road, London SW7 5BD



SYNOPSIS. Trilobites of the Tourmakeady Limestone, County Mayo, western Ireland, comprise 23 species and genera. This fauna is an early example of the Illaenid-Cheirurid biofacies, being dominated by a few species of the families Illaenidae, Cheiruridae and Celmidae. It is basal Whiterockian (upper Arenig) in age. Several of the trilobites are early representatives of clades which achieved subsequent prominence. All but one of the species are represented by silicified material, and many are supplemented by crackout specimens. Four trilobite species have been previously named: *Kawina divergens*, *Niobe ornata*, *Ooopsites hibernicus* and *Illaenus weaveri*, and are revised herein. One genus, *Mayopyge* (type species *M. zapata* sp. nov.), is new, as are the species *Phaseolops ceryx*, *Protostygina coronula*, *Glaphurus crinitus*, *Dimeropyge? ericina*, *Celmus michaelius*, *Agerina palabunda*, *Proscharyia platylimbata* and *Ceratocephalina ramskoeldi*. The remaining species are described in open nomenclature.

INTRODUCTION

The occurrence of trilobites in the upper Arenig Tourmakeady Limestone was recognized at the time Gardiner & Reynolds (1909, 1910) undertook the initial geological description of the Ordovician inliers of the Tourmakeady and Glensaul districts. Reed illustrated a few sclerites (*in* Gardiner & Reynolds 1909), and named two species. He later (1945) proposed a further two species, based on the illustrations of the 1909 work, but the scope and quality of the Tourmakeady faunas were not fully appreciated until the discovery by Williams in the 1960s that much of the material was silicified. Williams & Curry (1985) have subsequently described the rich brachiopod faunas of the unit, but the trilobites have only seen limited treatment. The trilobites described here were derived from the residues sorted by Williams & Curry (1985). Fortey (1975a, 1980) has illustrated some specimens for comparison with conspecific or closely related taxa from Spitsbergen. Fortey & Owens (1975) figured some sclerites to illustrate concepts within their new Proetida, and Fortey (1975b: 345) gave a preliminary sclerite count in a discussion of Early Ordovician trilobite communities.

The aim of the present work is the systematic description of the entire Tourmakeady trilobite fauna, based on all available material. The fauna is of interest particularly because of its stratigraphic position near the base of the Middle Ordovician. This was a time of significant phylogenetic turnover of trilobites, and the Tourmakeady assemblage contains several forms important to an understanding of this change.

AGE, PRESERVATION, AND COMPOSITION OF THE FAUNA

The Tourmakeady Limestone occurs as blocks within bedded tuffs and grits of the 'Shangort and Tourmakeady Beds' of Gardiner & Reynolds (1909, 1910). This was mapped by Williams & Curry (1985: fig. 1) as part of the Glensaul Group. Evidence of the age of the Tourmakeady Limestone is derived from graptolite collections reported from beds above and below the limestone blocks, and from the trilobites and brachiopods themselves.

The trilobites from the white crackout limestones are invariably

undistorted. Those from the blocks yielding silicified trilobites often show a modest degree of distortion (as do most of the brachiopods figured by Williams & Curry (1985)). At least one silicified sample yielding the type material of *Glaphurus crinitus* is without distortion. We do not understand the reasons for these differences. Possibly they are related to silification having occurred near faults. Whatever the cause, there appears to be no important difference in faunal composition between crackout and silicified collections. Relative abundances of particular taxa vary significantly between the crackout and silicified samples, but this is certainly due to the ease with which smoother, larger, and less convex specimens crack out.

Graptolites were reported by Dewey *et al.* (1970) from several localities on the western margin of Lough Mask. Three collections indicate that the underlying Mount Partry Group belongs to what they termed the '*Didymograptus protobifidus* Zone of North America'. Williams & Stevens (1988) doubted that the '*protobifidus* Zone' could be reliably distinguished from the North American *Didymograptus bifidus* Zone, which had been claimed to overlie it. This interval (*bifidus* + *protobifidus*) equates with the Chewtonian Stage of the Australian graptolitic standard, and with the mid-part of the Arenig Series of the Anglo-Welsh succession. Graptolitic rocks of the *D. bifidus* Zone are associated with the shelly Zone J faunas in the western USA (Braithwaite 1976), and hence with the upper part of the Ibexian Series of the North American stratigraphic standard in Utah (Ross *et al.*, 1993).

Within the Glensaul Group Dewey *et al.* (1970) listed a graptolite (fauna 4 on their fig. 2) from below the Tourmakeady Limestone which they state is 'intermediate between *Isograptus caduceus* var *victoriae* Harris and *I. caduceus* var *lunatus* Harris'. These varieties are usually regarded as subspecies of *I. victoriae* in current usage (e.g. Cooper & Lindholm 1991) and their intergradation occurs within the Castlemainian Stage at the junction of Ca1 and Ca2. A graptolite fauna from above the Tourmakeady limestone (Fauna 7 of Dewey *et al.* 1970: 29–30) yielded biserial graptoloids including *Undulograptus austrodentatus*; also listed is a didymograptid described as *Didymograptus* sp. 2, which seems to belong to the genus *Xiphograptus* Cooper & Fortey, 1982. The combination of *austrodentatus* group biserial graptoloids with *Xiphograptus* embraces a short interval at the top of the Arenig series (Mitchell & Maletz 1995), and at the base of the Darriwillian Stage of the Australian scheme.

Thus the time of Tourmakeady Limestone deposition is bracketed by graptolite faunas, which indicate it must be upper Castlemainian to Yapeenian, and late Arenig in terms of the Anglo-Welsh standard. This is consistent with the trilobite evidence cited below.

Williams & Curry (1985) stated that the Tourmakeady brachiopod fauna was 'equivalent to Zone K' of the North American shelly standard zonation. Zone K is a thin brachiopod coquina composed entirely of *Hesperonomiella minor* Cooper which is exposed in several sections in Utah and Nevada. Ross *et al.* (1993) no longer recognised it biostratigraphically, but incorporated it within the terminal Ibexian. Nonetheless, its position above Zone J does seem to be consistent with the occurrence of the Tourmakeady Limestone above Zone J equivalents in western Ireland.

Trilobite faunas described below are dominated numerically by Illaenidae, Cheiruridae and celtmids. As Fortey (1975b) originally pointed out, it is an illaenid-cheirurid biofacies fauna, associated with a limestone mound. The biogeographic affinities of the fauna are overwhelmingly Laurentian. Comparison is made first with two faunas previously known from Laurentia: the white limestone boulder at Lower Head, western Newfoundland (Whittington 1963) and the Meiklejohn bioherm in the western USA (Ross 1972). The latter lies above the Nine-mile Formation which yielded a Zone J trilobite and graptolite fauna; the Lower Head Boulder (James & Stevens 1986: fig. 40) lies above a sparse Cal graptolite fauna. Hence, both occupy stratigraphically comparable positions to the Tourmakeady Limestone. The Lower Head fauna is most similar. A species of *Geragnostus* is in common, while close comparisons are made with species of *Nileus*, *Illaenus*, *Glaphurus*, *Kawina*, *Isocolus*, *Celmus*, and *Phaseolops*. The first four genera named are present also in the Meiklejohn Peak, known from sparser material. The fact that the species are almost all different in points of fine detail allows for some difference in age between the Tourmakeady and Cow Head, but the difference cannot be great. Both these previously described faunas have been regarded as equivalent to Zone L (*Psephosthenaspis* Zone) of the Utah/Nevada stratigraphic standard, lying at the base of the Middle Ordovician (i.e., base of the Whiterockian) in North American terms. In its type section, this is developed in bathyurid biofacies (Fortey & Droser 1996) and hence has a different suite of taxa from the Tourmakeady Limestone. Note that younger (Zone M) Whiterockian faunas, similar to those of the Table Head Formation, western Newfoundland, are known in the Tourmakeady area from the base of the younger Glendavock Formation (Pudsey 1984). There are a few similarities at species level between the Tourmakeady and faunas of generally deeper-water biofacies described from the Valhallfonna Formation, Spitsbergen. The pelagic trilobites *Opipeteer inconnivus* Fortey, 1974 and *Oopsis hibernicus* (Reed in Gardiner & Reynolds, 1909) are both known from the Olenidsletta Member, where their ranges extend to just below the first occurrence of *Isograptus victoriae victoriae* (Fortey 1980; Cooper & Fortey 1982). Fortey (1975a: 31) suggested that *Niobe occulta* was virtually indistinguishable from the extremely fragmentary species from the Tourmakeady Limestone described by Reed (1945) as *Niobe ornata*. The species has a short range through the upper mid-part of the Olenidsletta Member, where it occurs immediately below beds with *Isograptus victoriae*, and immediately above the interval carrying *Oopsis hibernicus* and *Opipeteer inconnivus*, which was equated by Fortey (1980) with Zone J. Hence the Tourmakeady fauna is rather tightly constrained by species comparisons as lying within a short interval of the late Arenig between latest Chewtonian and early Castlemainian in graptolite terms.

In the platform sections of Utah and Nevada there is a sequence boundary just above the 'Zone K' brachiopod coquina and below the first trilobite fauna of the *Psephosthenaspis* (L) Zone. If this regres-

sive event were global, it is possible that this is the time at which illaenid-cheirurid 'mounds' developed in the volcanic setting of the South Mayo trough, since lowstands on the platform equate with enhanced deposition of fringing carbonates on offshore island sites. The Tourmakeady fauna might 'fit in' to the hiatus at the base of the North American Middle Ordovician. In the Meiklejohn 'reef' there is a 2 m interval of birdseye limestone without macrofossils above Zone J and below the bioherm itself, which occupies a comparable stratigraphical position.

Numbers of trilobite individuals for each species recovered from the entire silicified collection are given in Table 1.

Table 1 Number of cranidia (cr.), pygidia (pyg.), and individuals (ind.)

for all species recovered from silicified residues of the Tourmakeady Limestone, together with relative proportion of total number (% tot) of individuals (894) recovered. The single known pygidium of *Niobe ornata* (Reed, 1945), is a calcareous crackout specimen and is listed for completeness; no other species are known exclusively from non-silicified material.

	cr.	pyg.	ind.	% tot
<i>Celmus michaelmus</i>	276	4	276	30.9
<i>Mayopyge zapata</i>	265	50	265	29.6
<i>Illaenus weaveri</i>	109	99	109	12.2
<i>Geragnostus clusus</i>	31	14	31	3.5
<i>Oopsis hibernicus</i>	28	7	28	3.1
<i>Dimeropyge? ericina</i>	27	0	27	3.0
<i>Proscharaya platylimbata</i>	25	5	25	2.8
<i>Glaphurus crinitus</i>	23	0	23	2.6
<i>Agerina palabunda</i>	22	0	22	2.5
<i>Phaseolops ceryx</i>	20	6	20	2.2
<i>Opipeteer aff. O. inconnivus</i>	12	0	12	1.3
<i>Nileus</i> sp.	7	12	12	1.3
<i>Benthamaspis</i> aff. <i>B. diminutiva</i>	5	10	10	1.1
<i>Catilicephalid</i> gen. nov.	7	0	7	0.8
<i>Isocolus</i> sp. nov. A	6	2	6	0.7
<i>Kawina divergens</i>	6	1	6	0.7
<i>Ceraurinella</i> sp.	5	4	5	0.6
<i>Ceratocephalina ramskoeldi</i>	4	1	4	0.4
<i>Protostygina coronula</i>	2	2	2	0.2
<i>Ampyx cf. toxotis</i>	1	1	1	0.1
<i>Dividugnostus</i> sp. indet.	1	0	1	0.1
<i>Cybeline</i> sp.	1	0	1	0.1
<i>Niobe ornata</i>	0	1	1	0.1

ORDOVICIAN INSULAR FAUNAS, BIOGEOGRAPHY AND TAXONOMIC NOVELTY

Neuman (1984) has discussed how Ordovician brachiopod faunas from ancient island sites include a mixture of endemic genera, often with alleged first occurrences of 'ancestors' of forms known from younger rocks in platform successions. The implication is that such islands may have been sources of speciation leading to subsequent clades. The Ordovician South Mayo trough included a number of volcanic centres, possibly as part of a marginal basin resembling the Gulf of California (Ryan & Archer 1978). The fact that Williams & Curry (1985) reported some twelve new genera from the Tourmakeady brachiopods invites the question whether the trilobites show a similar 'insular' trend.

There is one endemic catilicephalid genus which we are unable to name formally. The fauna includes what may be the oldest known proetidean, *Phaseolops*, a group which became progressively more important through the Ordovician and later. The other typical repre-

sentatives of the illaenid-cheirurid biofacies (*Illaenus*, *Glaphurus*, *Ischyrotoma*, *Kawina*, etc.) are represented quite widely in contemporary deposits (e.g., Ingham *et al.*, 1986). The pelagic trilobites *Opipeuter* and *Ooopsites* are globally distributed at low palaeolatitudes (Cocks & Fortey 1990: fig. 2).

The recognition of phylogenetic affinities of some of these taxa with much older forms, for example, the glaphurids with the Cambrian raymondinids and the isocolids with the catillicephalids, serves to remove any notion of novelty from these faunal elements. This leaves *Phaseolops* as the sole example of a precocious genus of higher taxa, and we can match such single examples in several other faunas at the base of the Middle Ordovician, which was an important watershed for Laurentian faunas in general (Droser *et al.*, 1996). Thus, when considered critically, the trilobites of the Tourmakeady do not provide support for the notion of a special generative role for this particular insular fauna. However, such islands may have provided important refugia during times of global regression.

The closest biogeographic comparisons of the whole fauna are with illaenid-cheirurid biofacies faunas on the Laurentian palaeocontinent, and there is no reason to doubt that the South Mayo trough lay on the equatorial side of the Iapetus Ocean (Williams & Curry 1985). Similar conclusions were reached for the contemporary Dounans Limestone fauna (bathyurid biofacies) on the northern edge of the Midland Valley of Scotland (Ingham *et al.*, 1986). Amongst the Tourmakeady fauna there are several genera which are not confined to Laurentia, particularly those extending into Baltica: *Agerina*, *Celmus*, *Niobe*, *Illaenus*, *Nileus* and *Geragnostus*. Only two genera, *Protostygina* and *Geragnostus*, have Middle Ordovician Gondwanan records. The Baltic connections are of interest because the brachiopods (Williams & Curry 1985: 188) are stated to be quite different from those of that palaeocontinent.

SYSTEMATIC DESCRIPTIONS

REPOSITORY. Figured specimens are housed in the Sedgwick Museum, Cambridge (prefix SM) and the Natural History Museum, London (prefix It.).

Family METAGNOSTIDAE Jaekel, 1909
Genus GERAGNOSTUS Howell, 1935

TYPE SPECIES. *Agnostus Sidenbladhi* Linnarsson, 1869, from the Tremadoc of Sweden; by original designation.

Geragnostus clonus Whittington, 1963
 Pl. 1, figs 10, 13–16; Pl. 2, fig. 9

MATERIAL. Assigned specimens It. 25944–25948, 25961.

1963 *Geragnostus clonus* Whittington: 28–30, pl. 1, figs 1–17, text-fig. 3.

DISCUSSION. Whittington (1963) fully described this species from undistorted material from the Lower Head boulder. Because the terminal piece of the pygidium is longer than the postaxial field this species conforms to *Geragnostus* as opposed to *Arthrorhachis* in the revision of Fortey (1980). Cephalic shields of *Geragnostus* are all somewhat similar. Another closely similar form was figured by Ahlberg (1992) as *Geragnostus* sp. B, from the Lanna Limestone (Volkov Stage) of Sweden. The pygidium is the more distinctive part of the exoskeleton. The best Irish pygidium (Pl. 1, fig. 16)

compares closely with that of the holotype (Whittington 1963: pl. 1, figs 1–6) in having the axis two-thirds the total pygidial length, while the terminal piece occupies two-thirds of the axial length. On the holotype, the terminal piece tapers backwards from the preceding part of the axis; however, on another of Whittington's specimens (1963: pl. 1, fig. 14) the terminal piece is slightly wider (tr.) than the second axial ring, as it is on the Tourmakeady specimen. Whittington (1965) commented on how closely similar *G. clonus* was to *G. longicollis* (Raymond, 1925) from the middle Table Head Formation. Possibly the only convincing difference was a more pronounced angulation in the cephalic outline of the former; this is not visible on the specimen of Pl. 1, fig. 15, which has been tectonically elongated, but is apparent on a less distorted specimen (Pl. 1, fig. 13). *Geragnostus clonus* seems to be the best name to apply to the Irish specimens.

Genus **DIVIDUAGNOSTUS** Koroleva, 1982

TYPE SPECIES. *Dividuagnostus minus* Koroleva, 1982; by original designation.

***Dividuagnostus* sp indet.**

Pl. 1, fig. 17

MATERIAL. Incomplete cephalic shield, It 25951.

DISCUSSION. A small headshield shows a transglabellar furrow with the form of a shallow inverted 'v'. This is typical of *Dividuagnostus* according to the revision of Zhou Zhi-yi (1987). The unusually large, triangular occipital lobes are also typical of this genus. Of species of Arenig age, the Irish specimen differs from *D. whitlandensis* (Fortey & Owens, 1987) in its wide cephalic border, but appears to be like *D. scoltonensis* (Whittard, 1966; see also Fortey & Owens 1987, fig. 17b–c) in the same feature. *Dividuagnostus scoltonensis* ranges through the Fennian Stage in South Wales. Without an associated pygidium the determination must be tentative.

Family NILEIDAE Angelin, 1854
Genus NILEUS Dalman, 1827

TYPE SPECIES. *Asaphus (Nileus) armadillo* Dalman, 1827, from the Arenig of Husbyfjöld, Skarpasen, Sweden; by monotypy.

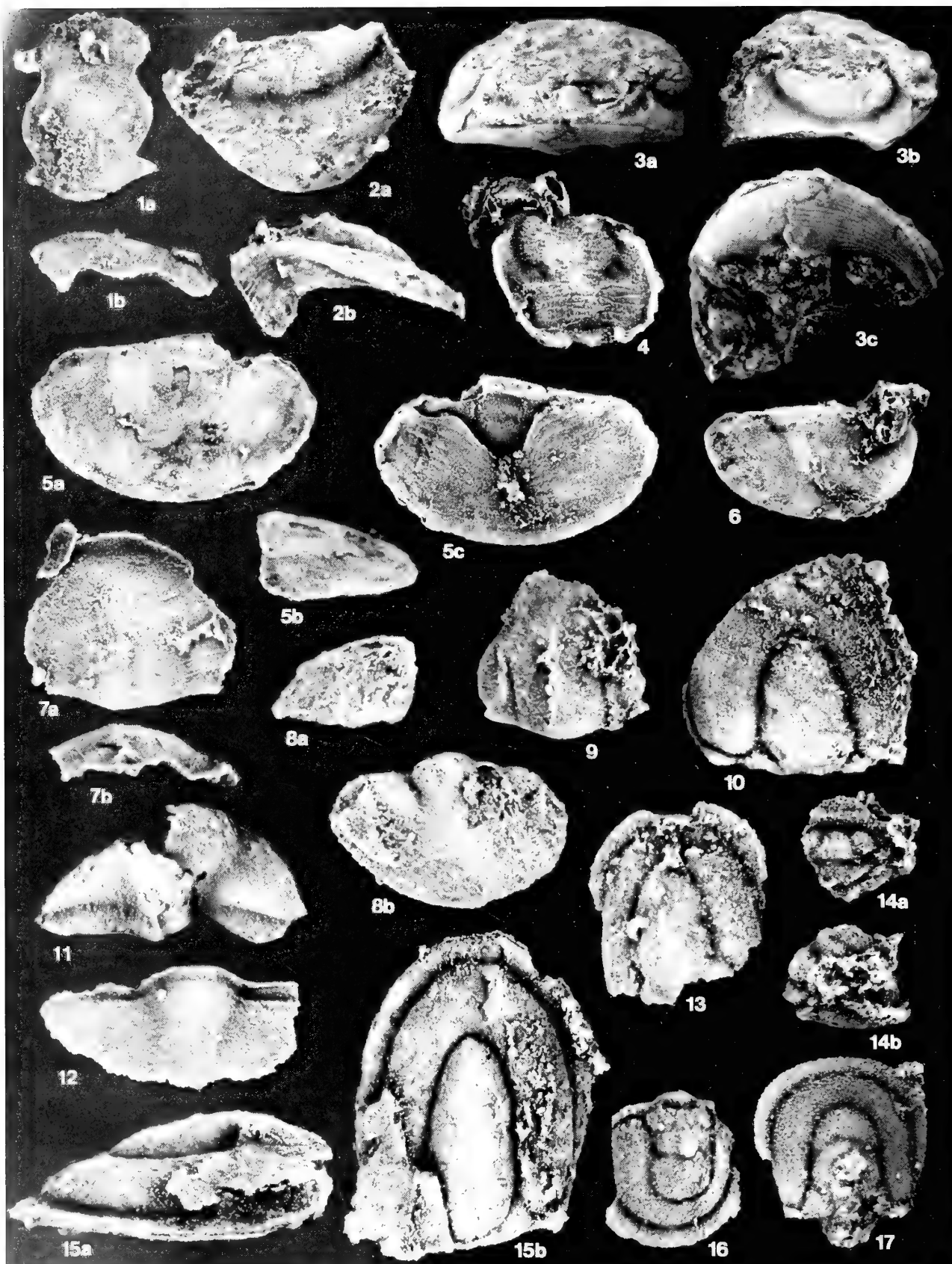
***Nileus* sp.**

Pl. 1, figs 1–6

MATERIAL. Assigned specimens It. 25935–25940, SM A10417.

DISCUSSION. The Tourmakeady species is similar to *Nileus affinis* from western Newfoundland (Whittington 1963, 1965). The specimens share similar posterior dimensions of the cephalic doublure (compare Pl. 1, fig. 3c with Whittington 1965: pl. 30, fig. 5); eyes of the same relative size and oblique inclination; hypostomes with narrow lateral rims (cf. Pl. 1, fig. 4 with Whittington 1965: pl. 31, fig. 6); pygidia with nearly identical shape and restriction of subdued dorsal terrace lines to the lateral margins; and pygidial doublure of nearly equal size with similar median embayment (cf. Pl. 1, fig. 5c with Whittington 1965: pl. 31, fig. 10).

The question of conspecificity cannot be evaluated with confidence given the few Irish specimens. The single cranidium recovered (Pl. 1, fig. 1a) is very narrow, but the specimen is a juvenile. Similarly, the Tourmakeady hypostome (Pl. 1, fig. 4) is nearly subquadrate, in contrast with the wider form known in *N. affinis*. The Irish specimen is small however, and lateral expansion with maturity can be observed in the ontogeny of various nileid hypostomes (e.g.,



Sympysurus arcticus Fortey, 1975a: pl. 21). On present evidence, the only feature that might indicate that the Irish material is distinct is a librigenal field that is smaller in area, particularly posteriorly, with the posterior section of the facial suture concomitantly shorter (Pl. 1, fig. 2a).

Family RAPHIOPHORIDAE Angelin, 1854
Genus *AMPYX* Dalman, 1827

Ampyx cf. *toxotis* Fortey, 1975a Pl. 1, figs 11, 12

MATERIAL. Assigned specimens It. 25949, 25950.

DISCUSSION. The Irish species, represented by only two specimens, shows strong similarity to *Ampyx toxotis* in its unusually long cranidial posterior border, relatively small and sub-rounded glabella, effaced pygidial axis, and relatively deep furrow along the pygidial anterior margin. The species differ in that the cranidial posterior border of the Irish species is not as exsagittally elongate, and the border furrow is better impressed, particularly proximally.

Family STYGINIDAE Vogdes, 1890
Genus *PROTOSTYGINA* Prantl & Pribyl, 1949

TYPE SPECIES. *Illaenus bohemicus* Barrande, 1872, Sarka Formation (Llanvirn), Czech Republic; by monotypy.

Protostygina coronula sp. nov. Pl. 2, figs 1–6, 8

ETYMOLOGY. Latin, small crown.

DIAGNOSIS. Anterior border furrow long and relatively deep; axial furrows strongly impressed posteriorly; S0 well impressed; pygidial axis elevated sharply from pleurae; pygidium with sagittal length about 60% of maximum width.

HOLOTYPE. Cranidium, It. 25952 (Pl. 2, fig. 1); paratypes It. 25953–25958.

DESCRIPTION. This is based primarily on the largest adult specimens.

Cranidium with sagittal length subequal to, to very slightly longer than, the width (tr.) across midlength of palpebral lobes; maximum cranidial width achieved across rear of posterior border; anterior sections of facial sutures subparallel immediately in front of palpebral lobes, then diverging slightly anteriorly; posterior sections of facial suture with strong (ca. 45 degrees from exsagittal plane) posterior divergence; anterior margin with strong anterior convexity; anterior border nearly flat, separated from front of glabella by

abrupt change in slope across trough-like anterior border furrow; border and border furrow of even length (sag.; exsag.) medially and laterally; axial furrows well impressed posteriorly, subparallel from S0 to opposite front of palpebral lobe, then diverging anteriorly; axial furrows effaced anteriorly opposite anterolateral corner of cranidium; preglabellar furrow absent, extent or presence of preglabellar field unknown; interocular fixigena large, with only weak dorsal convexity; palpebral furrow absent, palpebral lobe flat and grading directly into interocular fixigena; palpebral lobe narrow (tr.), elongate (exsag.); anterior glabellar furrows effaced; S0 shallow but well impressed, of similar length sagittally and exsagittally; L0 elongate (esp. sag.) and shelf-like, posterior margin with significant posterior convexity; L0 and rear of glabella with strong, arcuate dorsal convexity; posterior border narrow (tr.), only protruding laterally slightly past palpebral lobe; posterior border furrow very shallow; entire cranidium with very subdued dorsal sculpture of fine pits and small, low, anastomosing ridges.

Librigena, rostral plate, hypostome, and thorax unknown. Pygidium with sagittal length about 60% of maximum width; axis with maximum width about 75% of sagittal length; axis occupying about 60% of sagittal length of pygidium; anterior margin transversely straight within fulcra, turned sharply posteriorly at fulcrum to run distally at about 45 degrees to transverse plane; posterior margin subcircular in outline; first pleural furrow defined adaxially to fulcrum, shallow but deepest adaxially; all other pleural and interpleural furrows completely effaced; articulating half ring very short (sag., exsag.); axial furrows extremely shallow, defined mainly as a sharp break in slope between pleura and axis, converging gently posteriorly, nearly transverse at rear to fully circumscribe somewhat blunt posterior of axis; five or six axial rings discernible on internal mold, but difficult to discern dorsally; ring furrows transverse and shallow on internal mold; entire pleural region lacking dorsal sculpture; doublure broad, of even width medially and laterally, reaching sagittally to rear of axis; relatively strong subparallel doublural terrace lines developed and progressively closer spaced on anterior half of doublure.

DISCUSSION. Fortey (1980: 56, 57) described an isolated cranidium from what is now recognized as the uppermost Ibexian (V₂a) of Spitsbergen as *?Protostygina* sp. ind. This taxon is very similar to and definitely congeneric with *P. coronula* sp. nov. The species are distinguished mainly by the significantly deeper axial, anterior border, and occipital furrows of *P. coronula*. Fortey's suggestion that the Spitsbergen species (and hence the new Irish material) is related to *P. bohemica* (see Horny & Bastl (1970: pl. 8, fig. 3) remains the most tenable, despite the distorted internal mold preservation of the unique type specimen of that taxon. To the extent that evaluation is possible, *P. coronula* is distinguished from *P. bohemica* particularly by its longer pygidium with much more prominent axis. These features distinguish it also from the single exfoliated pygidium assigned to *Protostygina* sp. by Dean (1973;

PLATE 1

Figs 1–6 *Nileus* sp. 1a–b, It. 25935, cranidium, dorsal and right lateral views, ×10. 2a–b, It. 25936, left librigena, external and ventrolateral views, ×10. 3a–c, It. 25937, yolked librigenae-rostrum, anterior, right lateral, and ventral views, ×5. 4, It. 25938, hypostome, ventral view, ×10. 5a–c, It. 25939, dorsal, ventral, and left lateral views, ×10. 6, It. 25940, pygidium, dorsal view, ×7.5.

Figs 7–9 *Benthamaspis* sp. 7a–b, It. 25941, cranidium, dorsal and right lateral views, ×15. 8a–b, It. 25943, pygidium, right lateral and dorsal views, ×15. 9, It. 25942, cranidium, dorsal view, ×15.

Figs 10, 13–16 *Geragnostus clusus* Whittington, 1963 10, It. 25944, cephalic shield, dorsal view, ×10. 13, It. 25945, cephalic shield, dorsal view, ×15. 14a–b, It. 25946, enrolled specimen, thoracic and right lateral views, ×15. 15a–b, It. 25947, cephalic shield, left lateral and dorsal views, ×10. 16, It. 25948, pygidium, dorsal view, ×15.

Figs 11, 12 *Ampyx* cf. *toxotis* Fortey, 1975 11, It. 25949, cranidium, dorsal view, ×8.5. 12, It. 25950, pygidium, dorsal view, ×15.

Fig. 17 *Dividuagnostus* sp. indet., It. 25951, cranidium, dorsal view, ×15.

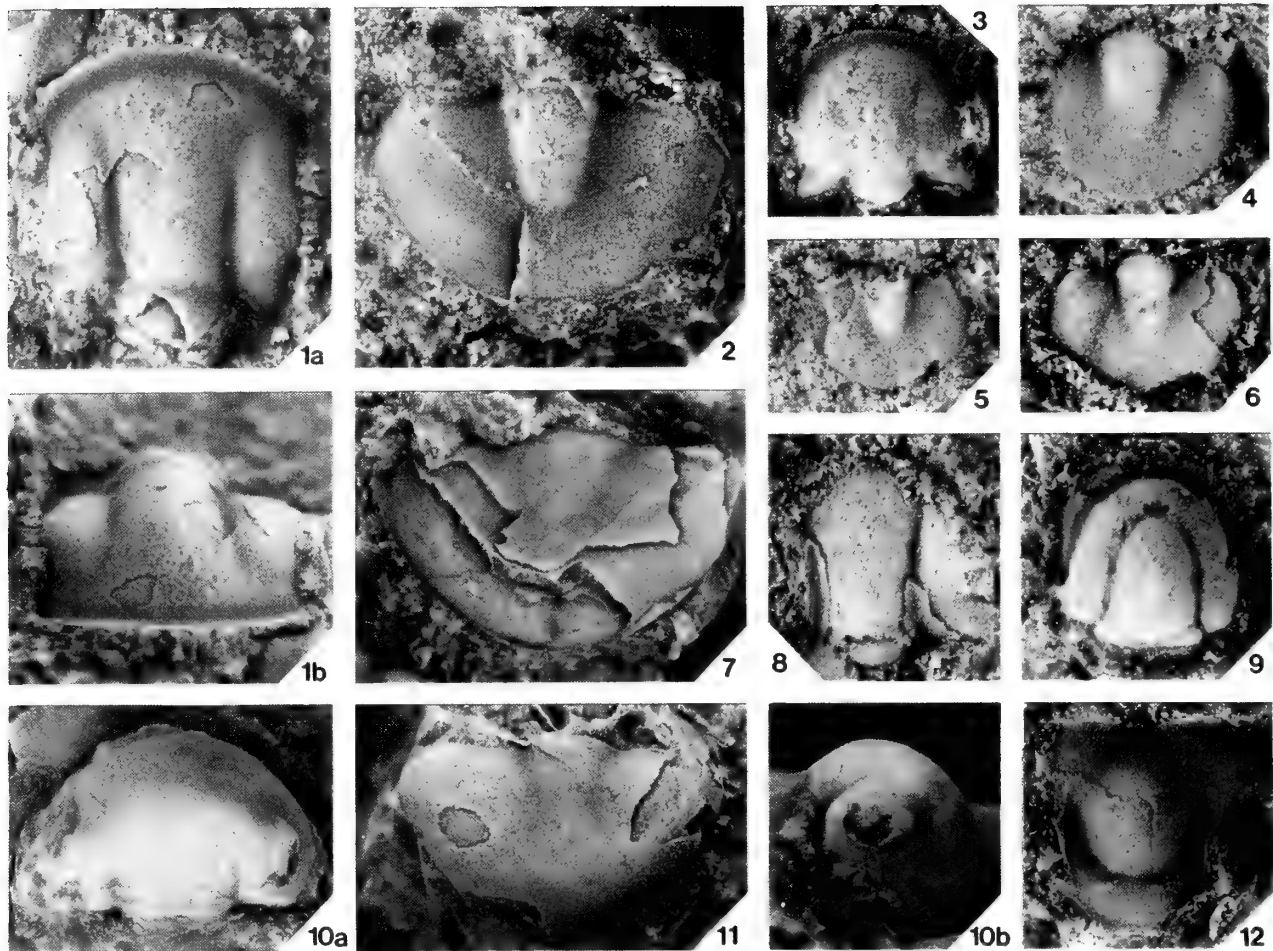


PLATE 2

Figs 1–6, 8 *Protostygina coronula* sp. nov. 1a–b, It. 25952, holotype, cranidium, dorsal and anterior views, ×15. 2, It. 25953, pygidium, dorsal view, ×15. 3, It. 25954, cranidium, dorsal view, ×15. 4, It. 25955, pygidium, dorsal view, ×15. 5, It. 25956, pygidium, dorsal view, ×15. 6, It. 25957, pygidium, dorsal view, ×15. 8, It. 25958, cranidium, dorsal view, ×15.

Figs 7, 10–12 *Illaenus weaveri* Reed in Gardiner & Reynolds, 1909 7, SM A10387, lectotype, pygidium, dorsal view, ×3.5. 10a–b, SM A10316, paralectotype, cranidium and right librigena, dorsal and right lateral views, ×5. 11, It. 25959, pygidium, dorsal view, ×5. 12, It. 25960, hypostome, ventral view, ×10.

Fig. 9 *Geragnostus clusus* Whittington, 1963, It. 25961, cephalic shield, dorsal view, ×15.

Sobova Formation, Upper Arenig, Turkey), although that specimen may well prove to be congeneric. *Protostygina adumbrata* Lisogor, 1995, is known from a single fragmentary cranidium. The species, from the Llanvirn of Kazakhstan, is certainly congeneric with *P. coronula*, but detailed comparison will require more complete material.

Family ODONTOPLEURIDAE Burmeister, 1843

Subfamily SELENOPELTINAE Hawle & Corda, 1847

Genus *CERATOCEPHALINA* Whittington, 1956

TYPE SPECIES. *Ceratocephala* (*Ceratocephalina*) *tridens* Whittington, 1956, Edinburg Formation, lower Mohawkian, Virginia; by original designation.

Ceratocephalina ramskoeldi sp. nov.

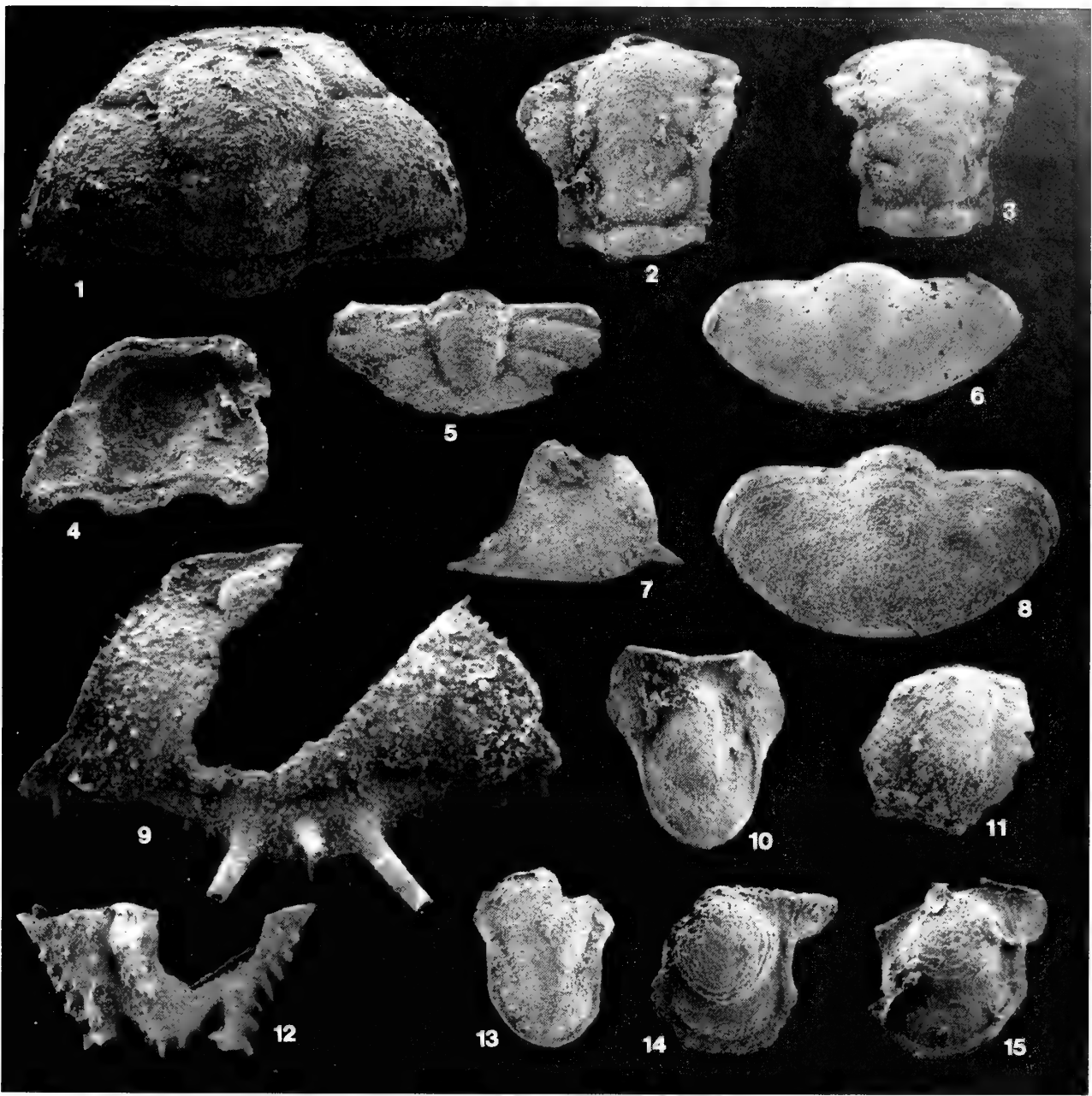
Pl. 3, figs 9, 12; Pl. 4, figs 9, 12–15

ETYMOLOGY. After Lars Ramsköld, University of Uppsala.

DIAGNOSIS. Cephalon with dense sculpture of fine tubercles; primary ontogenetic tubercles subdued and difficult to discern in holaspides; median occipital spine short; anterior border very short (sag; exsag.); slender genal spine continued on to librigenal field as interior border; border spines not distinct; epiborder furrow broad; epiborder spines small; pygidium with two marginal border spines and medial triangular projection.

HOLOTYPE. Cranidium, It. 25987 (Pl. 4, fig. 9); paratypes It. 25972, 25973, 25988–25990.

DISCUSSION. The morphology and relationships of this species have been commented upon by Ramsköld (1991: 163), although material has not previously been illustrated. The taxon ranks among the oldest odontopleurids for which relatively good morphological information is available (see Ramsköld 1991 for a review of Arenig species). It appears to display a mixture of features of two

**PLATE 3**

Figs 1–3, 5 *Isocolus* sp. nov. A. **1**, It. 25962, cranidium, dorsal view, $\times 60$. **2**, It. 25963, cranidium, dorsal view, $\times 33$. **3**, It. 25964, cranidium, dorsal view, $\times 27$. **5**, It. 25965, pygidium, dorsal view, $\times 27$.

Fig. 4 Catillicephalid gen. et. sp. nov., It. 25966, cranidium, ventral view, $\times 23$.

Figs 6–8, 10, 11 *Illaenus weaveri* Reed in Gardiner & Reynolds, 1909. **6**, It. 25967, pygidium, dorsal view, $\times 23$. **7**, It. 25968, left librigena, external view, $\times 23$. **8**, It. 25969, transitory pygidium, dorsal view, $\times 35$. **10**, It. 25970, hypostome, ventral view, $\times 23$. **11**, It. 25971, cranidium, dorsal view, $\times 33$.

Figs 9, 12 *Ceratocephalina ramskoeldi* sp. nov. **9**, It. 25972, cranidium, dorsal view, $\times 30$. **12**, It. 25973, pygidium, dorsal view, $\times 17$ (see also Pl. 4, fig. 15).

Fig. 13 Unassigned hypostome A, It. 25974, ventral view, $\times 33$.

Figs 14, 15 Unassigned hypostome B. **14**, It. 25975, ventral view, $\times 23$. **15**, It. 25976, ventral view, $\times 23$.

odontopleurid subfamilies, resembling Ceratocephalinae Richter & Richter, 1925, in pygidial details and Selenopeltinae in cephalic morphology. If Ramsköld's (1991: 166–168) character analysis is correct, however (and it is followed herein), *Ceratocephalina ramskoeldi* can be assigned with confidence as possibly the most primitive representative of Selenopeltinae. The following discussion is based primarily on Ramsköld's work.

The pygidium of *Ceratocephalina ramskoeldi* differs from those of all other assigned selenopeltines in the marginal position of its lateral border spines. In typical selenopeltines, these spines are supramarginal. The median area of the posterior margin is also distinctly triangular and drawn posteriorly, nearly into a median spine. In these features, the sclerite agrees with the pattern of three marginal spines characteristic of Ceratocephalinae. Ramsköld (1991) interpreted this pattern as plesiomorphic and probably general to a clade encompassing both subfamilies. Hence, the median area of the *C. ramskoeldi* pygidium possibly reflects a transition from a primitive median-spined condition to the arcuate condition with a fringe of small accessory spines seen in Selenopeltinae. The lateral spines are similarly in a plesiomorphic marginal position, and have not yet begun to migrate dorsally to the position apomorphic for the bulk of Selenopeltinae. The cephalic morphology of *C. ramskoeldi* is much less ambiguous. The presence of a very short (sag., exsag.) anterior border lacking spines or tubercles and of a slender genal spine base that overhangs and is not confluent with the posterior and exterior borders, but rather which runs onto the interior border on the field, are both basal selenopeltine apomorphies. In addition, the species bears none of the apomorphies of Ceratocephalinae (e.g., the third glabellar spine pair is not set atop an independently inflated swelling of the glabella).

Ceratocephalina ramskoeldi is most similar to *C. trispineus* (Young, 1973) from the Ibexian (Zone H) of Utah. *C. ramskoeldi* differs from the Utah species in the possession of denser, finer tuberculate sculpture; a shorter (sag., exsag.) anterior border; more prominently inflated L1 and L2; more deeply incised S0; a relatively shorter median occipital spine; broader librigenal field; and genal spine with a narrower base. As noted by Ramsköld (1991), the pygidia assigned by Young (1973) to *C. trispineus* are not those of an odontopleurid; they belong in fact to a pilekiid.

The single fragmentary cranium described by Fortey & Drosler (1996: 98, fig. 7.8) as *Diacanthaspis* sp. is also a primitive Ceratocephalina. It is more similar to *C. trispineus* than to *C. ramskoeldi* in the prominence of its anterior cranial border, but is distinguished from both by its much more robust dorsal tuberculation.

Family ISOCOLIDAE Angelin, 1854

DISCUSSION. As presently conceived, Isocolidae is restricted to the Middle and Upper Ordovician, and the Tourmakeady species, described below, is the oldest known member of the family. However, Fortey (1983) and Ingham (*in* Ingham *et al.* 1986) have

established the Ibexian presence of a group of genera similar to Sunwaptan forms currently assigned to the family Catillicephalidae. This latter record is herein extended to the basal Whiterockian (see below). These catillicephalids have so much in common with the isocolids that there is a strong likelihood they are phylogenetically related. The familial distinction between them may prove artificial. However, Catillicephalidae is itself in need of phylogenetic revision, and it remains to be established whether the Sunwaptan/Ibexian genera are related to several pre-Sunwaptan genera, including *Catillicephalia* itself. Pending a comprehensive cladistic review of the problems, we follow traditional usage and retain separate families.

Genus *ISOCOLUS* Angelin, 1854

TYPE SPECIES. *Isocolus Sjögreni* Angelin, 1854, from the Boda Limestone (Ashgill) of Dalarna, Sweden; by monotypy.

Isocolus sp. nov. A

Pl. 3, figs 1–3, 5; Pl. 4, figs 7, 8, 10, 11

MATERIAL. Assigned specimens It. 25962–25965, 25983–25986. **DESCRIPTION.** Craniidium with sagittal length about 75% of maximum width across posterior border and subequal to width across palpebral lobes; anterior margin of anterior border with gentle, even anterior convexity; anterior border very short (sag., exsag.), anterior border furrow sharply incised but extremely short (sag., exsag.); glabella widest anteriorly, maximum width about 80% of sagittal length excluding L0; preglabellar field very short, expanded laterally into narrow frontal area with considerable dorsal convexity; glabella laterally concave, axial furrows bowed inwards; S1 and S2 deeply incised and slot-like, deeper and longer (exsag.) proximally than distally near contact with axial furrow, lengthened into pitlike form at proximal end, declined posteriorly at about 30 degrees from transverse plane; S3 faint and transversely aligned, contacting axial furrow just behind eye ridge; anteromedian lobe of glabella slightly swollen and anteriorly expanded; L1 and L2 trapezoidal in outline; dorsal glabellar sculpture lacking; S0 much shorter (exsag.) than S1 and S2, evenly incised both medially and laterally, with very shallow 'W' shape, anteriorly convex medially; L0 longest medially, shortened significantly behind L1, transversely convex, but sagittally nearly flat-topped, median node very faint; narrow area of fixigena present opposite contact of axial and preglabellar furrow and in front of eye ridge; eye ridge faint, slightly declined posteriorly, relatively broad (tr.); palpebral lobe tiny; anterior sections of facial sutures very short (exsag.), subparallel in front of palpebral lobes, converging anteriorly; posterior sections of facial sutures with strong initial posterior divergence behind palpebral lobes, then more gentle divergence posteriorly; posterior fixigena with considerable area, moderate dorsal inflation, and lacking dorsal sculpture; posterior border furrow nearly straight, length (exsag.) similar along most of width, lengthening slightly abaxially; posterior border very short proximally, lengthening greatly distal to fulcrum. Pygidium incompletely

PLATE 4

Figs 1–6 Catillicephalid gen. et sp. nov. **1a–c**, It. 25977, craniidium and right librigena, oblique, right lateral, and left lateral views, $\times 15$. **2a–d**, It. 25978, craniidium, dorsal, posterodorsal, oblique, and ventral views, $\times 15$. **3a–b**, It. 25979, craniidium, dorsolateral and oblique views, $\times 15$. **4a–b**, It. 25980, craniidium, anterodorsal, left lateral, and dorsal views, $\times 15$. **5a–b**, It. 25981, craniidium, dorsal and right lateral views, $\times 15$. **6a–b**, It. 25982, craniidium, dorsal and anterior views, $\times 15$.

Figs 7, 8, 10, 11 *Isocolus* sp. nov. A. **7a–c**, It. 25983, pygidium, dorsal, ventral, and left lateral views, $\times 15$. **8**, It. 25984, craniidium, dorsal view, $\times 15$. **10**, It. 25985, craniidium, dorsal view, $\times 15$. **11**, It. 25986, articulated exoskeleton (destroyed after photography), dorsal view of cephalon, $\times 15$.

Figs 9, 12–15 *Ceratocephalina ramskoeldi* sp. nov. **9a–b**, It. 25987, holotype, craniidium, dorsal and oblique views, $\times 15$. **12a–c**, It. 25988, craniidium, dorsal, ventral, and anterior views, $\times 15$. **13a–c**, It. 25989, craniidium, left lateral, anterior, and dorsal views, $\times 15$. **14**, It. 25990, left librigena, external view, $\times 12$. **15**, It. 25973, pygidium, dorsal view, $\times 15$ (see also Pl. 3, fig. 12).



known; sagittal length approximately 60% of maximum width; axis with width about 70% of sagittal length; first three pleural furrows deeply incised; interpleural furrows nearly obscure; articulating half-ring set off from axis by prominent ring furrow; posterior axial rings and ring furrows difficult to discern; subdued but definite pygidial border developed around margin; posterior margin evenly arcuate; lateral and posterior aspects of cranium defined as subvertical wall (Pl. 4, fig. 7b), which is turned out again in a second, ventral, marginal rim; doublure relatively broad.

DISCUSSION. We have not formally named this species because the two best cranidia (Pl. 4, figs 8, 11) were lost or broken following photography, and there are no replacement specimens suitable to serve as types.

The Tourmakeady species is obviously related to previously described species of *Isocolus*, indicated particularly by the slot-like glabellar furrows that are greatly shallowed adaxial to the contact with the axial furrow. However, the laterally concave glabella of the Irish form is unique in the entire group. Other autapomorphic features include the apparently lacking dorsal sculpture, versus prominent raised lines in other species, the significantly broader posterior fixigena, and the posterolaterally directed, versus subtransverse, glabellar furrows.

The ventral morphology of the *Isocolus* pygidium has not previously been described. The Irish material reveals the unexpected presence of a vertically oriented wall beneath what appears dorsally to be the pygidial margin. This 'wall' is flared ventrally into a second, ventral rim (Pl. 4, fig. 7b). Reference to articulated material (Whittington 1956, 1963) indicates the larger, dorsally placed rim is almost certainly the true pygidial margin, and not analogous to the fulcral processes, rim, or spines often seen in groups like Entomaspidae Ulrich in Bridge, 1931 (e.g., Ludvigsen & Westrop in Ludvigsen *et al.*, 1989). The ventral wall and rim may therefore be doublural in origin.

Family CATILICEPHALIDAE Raymond, 1937

DISCUSSION. See remarks under discussion of Isocolidae above.

Catilicephalid gen. et sp. nov. Pl. 3, fig. 4; Pl. 4, figs 1–6

MATERIAL. Assigned specimens It. 25966, 25977–25982.

DISCUSSION. The forward-expanding glabella, very short preglabellar field, tiny palpebral lobe set near to the axial furrow, anterior eye position, broad posterior fixigena, and distally elongated (exsag.) posterior cranidial border all indicate relationship of this unusual Irish species to Sunwaptan-Ibexian forms presently assigned to Catilicephalidae. The size and attitude of the posterior border as well as the position and inclination of S1, position and size of the palpebral lobe, and size of the cephalic border are further similarities to the stratigraphically nearest species, ie. *Distazeris adoceta* Ingham (*in* Ingham *et al.*, 1986), from the Highland Border Complex of Scotland (Pratt 1992: 73 has criticized the generic assignment of this species).

PLATE 5

Figs 1–11 *Illaenus weaveri* Reed in Gardiner & Reynolds, 1909 **1a–b**, It. 25992, cranidium and left librigena, anterior and left lateral views, $\times 10$. **2a–b**, It. 25993, cranidium and right librigena oblique and anterior views, $\times 4.5$. **3a–c**, It. 25994, cranidium, dorsal, anterior, and left lateral views, $\times 7.5$. **4a–c**, It. 25995, cranidium, dorsal, anterior, and right lateral views, $\times 10$. **5a–c**, It. 25996, cranidium, dorsal, anterior, and left lateral views, $\times 15$. **6**, It. 25998, rostral plate, ventral view, $\times 10$. **7a–b**, It. 25997, rostral plate, ventral and dorsal views, $\times 7.5$. **8a–b**, It. 25999, rostral plate, posterior and ventral views, $\times 10$. **9a–b**, It. 26000, cranidium, dorsal and anterior views, $\times 15$. **10a–c**, It. 26001, cranidium, dorsal, anterior, and left lateral views, $\times 15$. **11**, It. 26002, cranidium, ventral view, $\times 10$.

The Irish species possesses a feature that distinguishes it from all related taxa, and apparently from all other trilobites: the development at the junction of the axial, posterior border, and occipital furrows of an exoskeletal hood that encloses a cone-shaped space opening laterally. The homology of this structure is very difficult to determine. The posterior border furrow runs directly into it, and appears to terminate beneath the hood (Pl. 4, fig. 2d). The occipital furrow meets the axial furrow on the adaxial side of the hood, and the junction of these furrows continues to circumscribe the hood posteriorly (Pl. 4, fig. 2b).

Family ILLAENIDAE Hawle & Corda, 1847

Genus *ILLAENUS* Dalman, 1827

TYPE SPECIES. *Entomostracites crassicauda* Wahlenberg, 1818, p. 27, from the Llandeilo of Fjäcka, Dalarna, Sweden; by subsequent designation of Pictet (1854: 515).

Illaenus weaveri Reed in Gardiner & Reynolds, 1909

Pl. 2, figs 7, 10–12; Pl. 3, figs 6–8, 10, 11;
Pl. 5, figs 1–11; Pl. 6, figs 1–12

- 1909 *Illaenus weaveri* Reed in Gardiner & Reynolds: 142, pl. 6, figs 1–3.
1910 *Illaenus weaveri* Reed in Gardiner & Reynolds: 272.
1945 *Illaenus weaveri* Reed: 63.
1968 *Illaenus weaveri* Reed; Whittington: 56.
1988 *Illaenus weaveri* Reed; Morris: 115.

DIAGNOSIS. Terrace lines on rear of cranium, restricted to anterior part of librigenal field; librigenal flange only moderately developed; vincular furrow only impressed posteriorly on librigenal doublure; pygidium with sagittal length 55–60% of maximum width.

MATERIAL. Lectotype, selected here, SM A10387, pygidium (Pl. 2, fig. 7), original of Reed in Gardiner & Reynolds (1909, pl. 6, fig. 2); paralectotype SM A10316, cranidium and right librigena (Pl. 2, fig. 10); topotypes It. 25959, 25960, 25967–25971, 25992–26014.

DESCRIPTION. Due to the varying amounts and vectors of distortion of much of the available material, measured ratios are approximate at best. The large pygidium of Pl. 6, fig. 7, is considered to be nearly undistorted, and pygidial ratios are based upon this specimen.

Cranidium with length (sag., measured in sagittal profile) 75–88% of maximum width across midlength (exsag.) of palpebral lobes; maximum anterior width about 90% of width across palpebral lobes; posterior sections of facial sutures declined nearly vertically when palpebral lobe is oriented in horizontal plane, diverging sharply posteriorly, nearly transverse; anterior sections of facial suture declined at about 30 degrees from horizontal when palpebral lobe is oriented in horizontal plane, slightly anteriorly divergent immediately in front of palpebral lobe, then forming even, laterally convex arc to converge near anterior margin; palpebral lobes relatively large and elongate; axial furrow strongly effaced, impressed only posteriorly, behind midlength of palpebral lobe; entire cranidium



vaulted, maximum sagittal curvature achieved slightly posterior to slightly anterior of palpebral lobes; anterior border and border furrow not evident; prominent terrace lines running subparallel to anterior margin, finer and more closely spaced near margin, coarser and more widely spaced dorsally; fine subparallel, transverse terrace lines developed across rear of glabella, occipital region, and rear of palpebral lobes, originating with close spacing laterally, spacing greater sagittally, forming ellipsoid pattern (Pl. 5, fig. 3a); occipital and posterior border doublure very short (sag., exsag.).

Librigena with prominent, closely spaced terrace lines on anterolateral aspect; coarser lines matching those on cranium only expressed on anterior part of field; posterolateral librigenal corner broadly lobate, ventrolateral margin bowed in, single prominent terrace line forming sharp posterolateral rim; field with moderate dorsal convexity, sculpture excluding anterior terraced lines smooth; posterior margin with strong posterior convexity; eye relatively large, exsagittal length slightly more than twice the width (tr.), doublure broad and robust; vincular furrow strong posteriorly beneath posterolateral corner, becoming effaced anteriorly.

Rostral plate subtrapezoidal; length (sag.) 40% of width; anterior margin with gentle, even anterior convexity; posterior margin nearly transverse, with slight sagittal posterior bulge; connective sutures obliquely inclined at about 45 degrees, laterally concave; ventral aspect with prominent, coarse, terraced lines, larger and more widely spaced (sag., exsag.) anteriorly; reentrant dorsal flange incompletely known, but robust.

Hypostome with sagittal length about 80% of maximum width across anterior wings; anterior margin (hypostomal suture) with lobate 'M' shape; anterior wings broad and nearly spatulate; wings grading into middle body posteriorly, but separated anteriorly by trough-like furrow delineating anterior part of body; lateral border narrow, sharply defined and ridge-like; lateral border furrow narrow and deeply incised; middle furrow deep, deepest laterally, fully impressed medially, with strong posterior curvature; middle body moderately inflated, lacking sculpture; maculae small but prominent, set just behind middle furrow; lateral border furrow grading without interruption into posterior border furrow; lateral border grading without interruption into posterior border; posterior border with posterior convexity nearly identical to that of middle furrow.

Thoracic segments poorly known; articulating half ring and ring furrows not discernible; axial furrow defined only as break in slope from pleura; axis with broad transverse convexity; prominent fulcrum on pleural lobe, 70–80% distance abaxially.

Pygidium with length (sag.) 55–60% of maximum width; axis with anterior width just under 40% of pygidial width; anterior margin transversely straight between fulcra; fulcrum set at 75% of distance between sagittal plane and lateral margin; prominent, subtriangular articulating facet forming obliquely inclined, anterolaterally directed plane distal to fulcrum; posterior margin nearly semicircular in plan view, subelliptical in posterodorsal view; pygidium with sagittal profile nearly flat anteriorly, prominently vaulted posteriorly, set at nearly 90 degrees to anterior part posteriorly near margin; plane of margin declined about 10 degrees from that of

anterior flat part of sagittal profile; axis only slightly raised from pleura, becoming increasingly less differentiated posteriorly; doublure broad, extended forward to rear of axis (about 60% of sagittal length from front of pygidium); doublure notched medially around termination of axis, protruding forward on either side of axis, then evenly arcuate distally.

DISCUSSION. *Illaenus weaveri* belongs to Jaanusson's (1957: 110) *I. sarsi* group, which includes the taxa *I. consimilis* Billings, 1865, *I. fraternus* Billings, 1865 (see Whittington 1965 for both), *I. auriculatus* Ross, 1967, and *I. oscitatus* Fortey, 1980 (see also Nielsen 1995). The group is characterized particularly by the form of the pygidial doublure, with its median notch flanked by anterior projections (e.g., Pl. 6, fig. 12), and all species show to greater or lesser extent the development of posterolateral 'flanges' on the librigena.

Illaenus weaveri is perhaps most similar to *I. auriculatus*, from the basal Whiterockian (Zone L) of the Antelope Valley Limestone, Pyramid Peak, California. However, the species differ in that *I. weaveri* has a relatively longer pygidium, much less pronounced medial pygidial doublural notching, a rostral plate that is much longer medially, and librigena with a less pronounced lateral flange. The vincular furrow of *I. weaveri* is restricted to the posterior part of the librigenal doublure (Pl. 6, figs 3b, 4b), whereas that of *I. auriculatus* is continued anteriorly (Ross 1967: pl. 5, fig. 29).

Illaenus weaveri differs from *I. oscitatus*, from the Whiterockian of Spitsbergen, in the lack of that species' prominently pitted sculpture and fully defined cranidial anterior border. Additionally, the cranidial sagittal profile of *I. oscitatus* is much more evenly convex than that of *I. weaveri* (compare Fortey 1980: pl. 10, figs 2, 6, with Pl. 5, figs 3c, 4c, 5c).

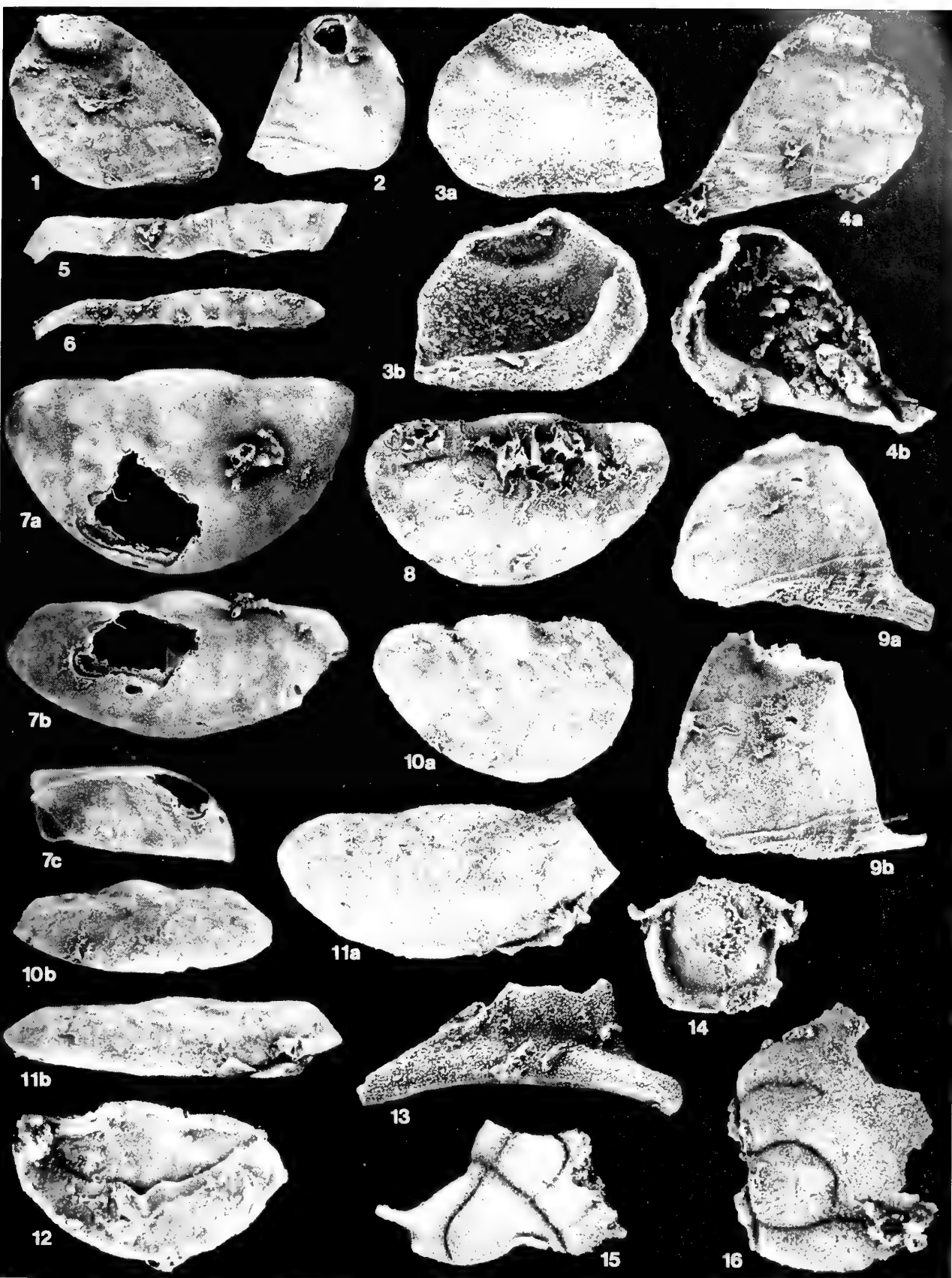
Both *I. consimilis* and *I. fraternus*, from the Whiterockian of Newfoundland, are distinguished from *I. weaveri* in the possession of prominent terrace lines over the entirety of their dorsal surface, including medially on the cranium, on the librigenal field, and on all of the pygidial axial and pleural region. The size and shape of the librigenal flange of *I. fraternus*, however, is similar to that of *I. weaveri* (e.g., Whittington 1965: pl. 45, fig. 17).

Family CHEIRURIDAE Hawle & Corda, 1847 Subfamily uncertain

DISCUSSION. Cheirurid subfamilial classification is in a state of flux. Several subfamilies (including Cheirurinae, Acanthoparyphinae, Heliomerinae, and Deiphoninae) are undoubtedly monophyletic. Others (e.g., Ectoptochilinae, Sphaerexochinae, Cyrtometopinae, Areinae) are more problematic, and their status as natural groups has yet to be convincingly established. Two of the genera dealt with herein (*Kawina* Barton, and *Mayopyge* gen. nov.) would be assigned, by current convention, to the subfamily Sphaerexochinae. This taxon, however, is particularly problematic because *Sphaerexochus* itself is a highly autapomorphic genus, the sister

PLATE 6

- Figs 1–12** *Illaenus weaveri* Reed in Gardiner & Reynolds, 1909 **1**, It. 26003, right librigena, external view, $\times 7.5$. **2**, It. 26004, left librigena, external view, $\times 5$. **3a–b**, It. 26005, right librigena, external and internal views, $\times 10$. **4a–b**, It. 26006, left librigena, external and internal views, $\times 7.5$. **5**, It. 26007, thoracic segment, dorsal view, $\times 5$. **6**, It. 26008, thoracic segment, dorsal view, $\times 5$. **7a–c**, It. 26009, pygidium, dorsal, posterior, and left lateral views, $\times 3.5$. **8**, It. 26010, pygidium, dorsal view, $\times 5$. **9a–b**, It. 26011, right librigena, ventrolateral and external views, $\times 10$. **10a–b**, It. 26012, pygidium, dorsal and posterior views, $\times 7.5$. **11a–b**, It. 26013, pygidium, dorsal and posterior views, $\times 5$. **12**, It. 26014, pygidium, ventral view, $\times 10$. **13**, It. 26015, left librigena, external view, $\times 6.5$. **14**, It. 26016, hypostome, ventral view, $\times 10$. **15**, It. 26017, cranium, oblique view, $\times 10$. **16**, It. 26018, cranium, dorsal view, $\times 10$.



taxon of which is unknown. Until such time as we are able to base the subfamilial classification of such genera on explicit and well-supported hypotheses of cladistic relationship, we prefer to regard their subfamilial affinities as uncertain.

Genus *KAWINA* Barton, 1916

Cydonecephalus Whittington, 1963: 97.

TYPE SPECIES. *Cheirurus vulcanus* Billings, 1865, from the Cow Head Group (lower Whiterockian), western Newfoundland; by original designation.

DISCUSSION. Whittington (1963: 97) distinguished his new *Cydonecephalus* (type species *C. grifus* Whittington, 1963, lower Whiterockian, western Newfoundland) from *Kawina* Barton, 1916, on the assertion that the 'glabella' is most convex anteriorly (not posteromedially) and juts forward, lobe 1p, and in some species 2p and 3p, are gently inflated, and occipital furrow curves forward (not back) medially.' Of these features, only the glabellar convexity holds for all six of the western Newfoundland species assigned to *Cydonecephalus*. The glabellar lobes of large specimens of *C. torulus* Whittington, 1963, are not markedly more inflated than those of *Kawina vulcanus* (Billings, 1865) (compare Whittington 1963: pl. 28, figs 5, 16), and the occipital furrows of both *C. torulus* and *C. grifus* both clearly curve backward (Whittington 1963: pl. 27, figs 3, 10, 13, 16; pl. 28, figs 1, 5; pl. 29, figs 1, 4).

All of the pygidia (Whittington 1963: pl. 31) which likely belong to species assigned by Whittington to *Cydonecephalus* have their pleural ribs fused along almost their entire length. *Kawina arnoldi* Whittington, 1963, however, has ribs with distally free tips (Whittington 1963: pl. 26, fig. 14). This is similar to the Irish species (Pl. 7, fig. 2), the pygidium of which differs from that of *K. arnoldi* only in proportions. However, the sagittal profile of the Irish cranidia is obviously like that of *Cydonecephalus*, with the point of maximum convexity anterior, not posterior. *Kawina arnoldi*, however, lacks the strong posterior convexity of the type species, and has a nearly evenly arcuate sagittal cranidial profile (Whittington 1963: pl. 26, fig. 8).

Considering all the species it is not possible to specify synapomorphic characters that would distinguish the two genera as separate monophyletic groups. Rather, species presently assigned to one or the other show overlapping variation in characters considered by Whittington to be diagnostic of *Cydonecephalus*, as well as in pygidial morphology. For these reasons, *Cydonecephalus* is placed in subjective junior synonymy of *Kawina* herein.

Kawina divergens (Reed, 1945)

Pl. 6, figs 13–16; Pl. 7, figs 1–5, 7

- 1909 *Pliomera* aff. *fischeri* (Eichwald); Reed in Gardiner & Reynolds: 144; pl. 6, fig. 4.
- 1925 *Kawina* sp., Raymond: 144.
- 1945 *Kawina divergens* Reed: 59.
- 1971 *Kawina?* *divergens* Reed; Lane: 56; text-fig. 9a.
- 1988 *Kawina?* *divergens* Reed; Morris: 119.

DIAGNOSIS. Dorsal sculpture of very fine, densely spaced granules; short, thorn-like genal spine retained in large holaspides; glabella with nearly even sagittal convexity, point of maximum convexity anterior; pygidium wide, with splayed, subquadrate ribs bearing free tips.

HOLOTYPE. Pygidium, SM A10396 (Pl. 7, fig. 2); topotypes It. 26015–26022, 26200.

DESCRIPTION. Cranidium with sagittal length 70–75% of maximum width across posterior border; glabella with width across midlength (exsag.) of L2 subequal to or slightly narrower than width across midlength of L1; maximum glabellar width subequal to length (measured in sagittal profile) excluding L0; anterior border short but complete medially; preglabellar furrow deeply incised, grading abaxially into axial furrow of similar depth; anterior fixigena a narrow, laterally convex strip, widest opposite midlength (exsag.) of L3, narrowing posteriorly in front of palpebral lobe; palpebral lobe narrow, entirely set off from interocular fixigena by very sharply incised palpebral furrow; interocular fixigena broadening posteriorly, smooth, with moderate dorsal convexity; interocular fixigena grading smoothly into broad posterior fixigena, held in plane declined about 60 degrees from horizontal; anterior sections of facial sutures short (exsag.), parentheses-shaped, with strong anterior convergence from midlength of L3 to front of glabella; glabella strongly inflated, sagittal profile with nearly even dorsal convexity, slightly more pronounced anteriorly; S1 nearly transverse distally, curved in nearly subcircular arc proximally, similar in depth to axial furrow but shallowing abruptly in front of S0 so that L1 is not quite fully isolated; L1 with only slight independent inflation, length (exsag.) subequal to width (tr.); S2 similar distally to S1, proximal part shorter and less posteriorly inclined; L2 with no independent inflation, length (exsag.) 80–85% of that of L1; S3 as deeply incised as S1 and S2, but not reaching as far adaxially, with less posterior curvature, and shallowed slightly near contact with axial furrow; L3 with slight anterolateral inflation, length about 80% of that of L2; frontal glabellar lobe with slight lateral inflation immediately anterior to S3, anterior margin with blunt anterior convexity; S0 composed of three distinct posteriorly bowed regions, two lateral ones behind L1, and a medial one between the L1 lobes, depth similar to axial furrow, medial region slightly longer (sag., exsag.) than lateral parts (exsag.); L0 similar in length to distal parts of posterior border, with nearly flat top in sagittal profile; posterior border sharply incised, very short (exsag.), and running nearly transversely to genal angle, where it is bowed anteriorly; posterior border very short proximally, but lengthening greatly distal to fulcrum to form lobate genal angle; short, thornlike, subtriangular genal spine retained on even largest specimens; entire dorsal cranidial surface with very fine, unimodal granular sculpture.

Librigena poorly known; field and lateral border both with fine granular sculpture similar to that of cranidium; lateral border well defined posteriorly, but grading into field anteriorly; lateral border furrow with concomitant shallowing anteriorly; field apparently quite narrow (tr.); eye unknown.

Rostral plate unknown. Hypostome with sagittal length 75% of maximum width across anterior wings; width across shoulders 80% of width across anterior wings; width across posterolateral corners two thirds that across anterior wings; anterior margin (hypostomal suture) with strong anterior convexity; sharp marginal rim and furrow developed laterally, middle body extended to margin medially; strong antennular notch between shoulder and anterior wing; lateral border broad and inflated, with fine granular sculpture; lateral border furrow shallow and broad (tr.); posterior margin with only slight posterior convexity; posterior border and posterior border furrow similar in dimensions to lateral border and furrow; middle body with sagittal length slightly greater than maximum width, moderate ventral inflation, strongest anteriorly; sculpture of fine granules somewhat more subdued than that of lateral border; middle furrow impressed only laterally, strongly declined posteriorly.

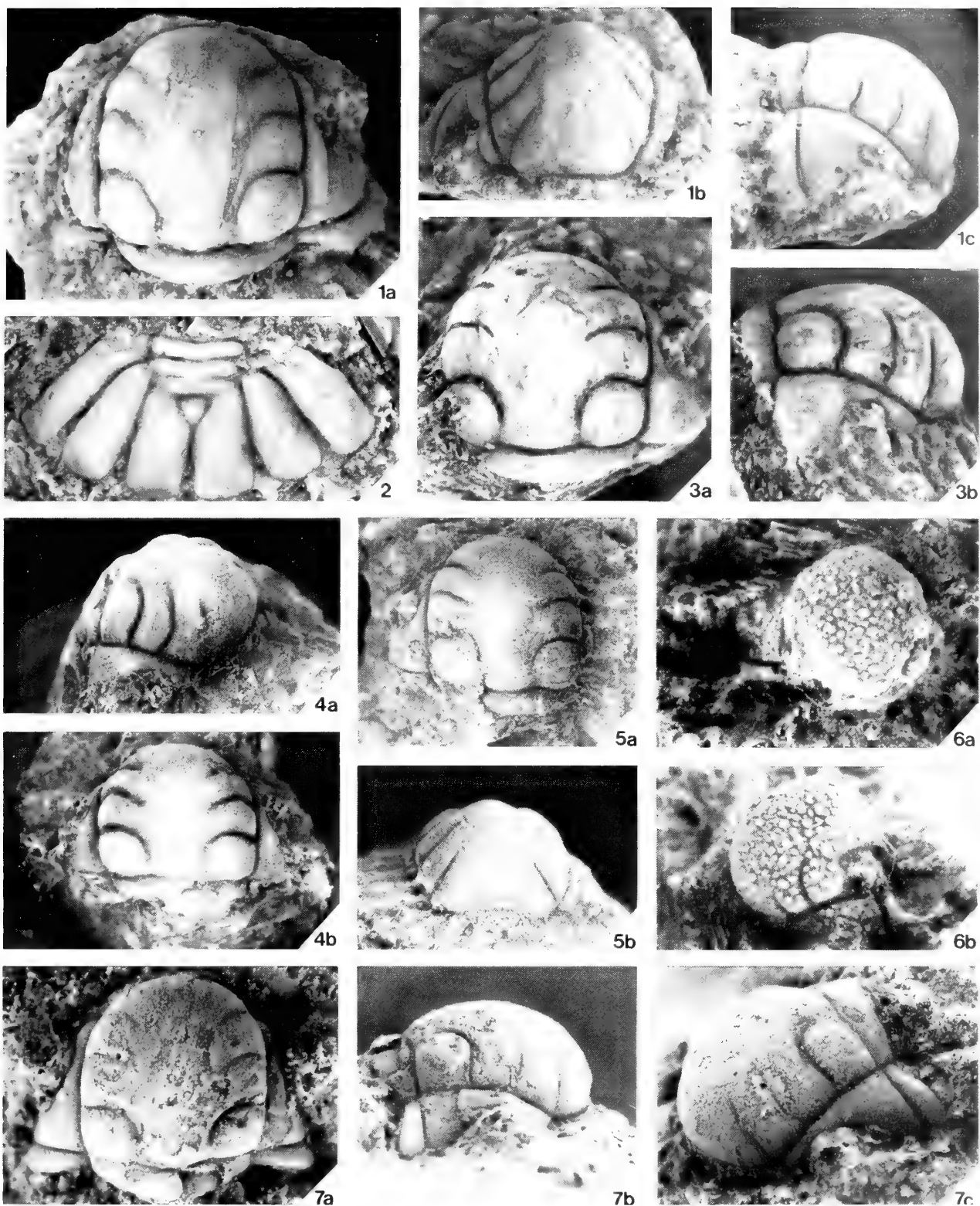
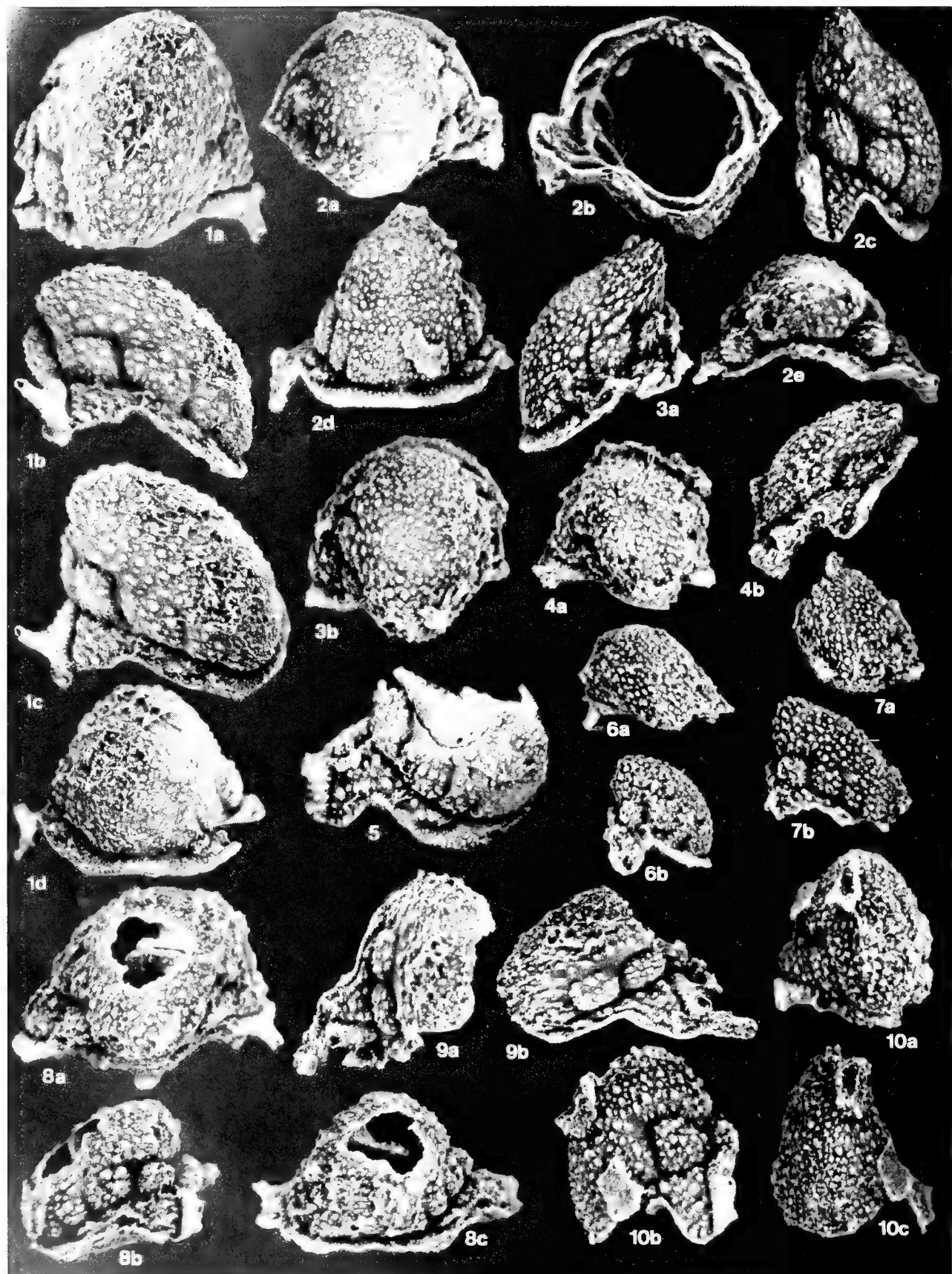


PLATE 7

Figs 1-5, 7 *Kawina divergens* (Reed, 1945). 1a-c, It. 26019, cranidium, dorsal, anterior, and right lateral views. $\times 5$, $\times 4$, $\times 4$. 2, SM A10396, pygidium, holotype, dorsal view, $\times 4$. 3a-b, It. 26020, cranidium, dorsal and right lateral views, $\times 4$. 4a-b, It. 26021, cranidium, oblique and dorsal views, $\times 4$. 5a-b, It. 26022, cranidium, dorsal and anterior views, $\times 4$. 7a-c, It. 26200, cranidium, dorsal, right lateral, and oblique views, $\times 7.5$.

Figs 6a-b *Mayopyge zapata* gen. et sp. nov. It. 26023, cranidium, dorsal and left dorsolateral views, $\times 15$.



Thorax unknown. Pygidium (see also Lane 1971: 56) with sagittal distance from articulating half ring furrow to rear of medial spines 44% of maximum width; pygidium composed of three distinct rings, pleural segments, and a small subtriangular terminal piece; interpleural furrows deeply incised, but first and second ribs fused to just over half distance abaxially, second and third ribs fused to about two thirds distance abaxially; pleural furrow shallow but incised on proximal part of first rib, very faint furrow visible on corresponding part of second rib; axial furrow moderately deep opposite first ring, progressively shallower posterior, but deepened around small terminal piece; first axial ring with significant sagittal convexity and bowed posteriorly in plan view; second ring less convex and more transverse; third ring not inflated and nearly transversely oriented; ring furrows shallowed medially; ribs with spatulate, subquadrate free tips.

DISCUSSION. *Kawina divergens* has previously been known only from its holotype pygidium (Pl. 7, fig. 2). The species is distinguished from *K. scrobiculus* (Whittington, 1963) and *K. prolificus* (Billings, 1865) in its less inflated lateral glabellar lobes and posteriorly versus anteriorly bowed occipital furrow. It differs from *K. mercurius* (Billings, 1865) in the lack of the autapomorphic tranversely impressed S1 of that species. *Kawina divergens* is quite similar to both *K. griffiths* and *K. torulus* (see generic discussion above), but differs from both in the presence of a much finer cephalic sculpture and an S1 that is much better impressed proximally to more fully isolate L1. The closest comparison among described species is with *K. arnoldi*. Pygidia of the two species are discussed above. Shared cephalic features include a similar sagittal convexity, similarly subdued dorsal sculpture (although that of *K. arnoldi* is slightly more robust), and similar posterior curvature of S0. The species differ particularly in the presence in *K. arnoldi* of an S1 that is strongly sigmoidal in lateral view.

Genus *MAYOPYGE* gen. nov.

TYPE SPECIES. *Mayopyge zapata* sp. nov., from the Tourmakeady Limestone, Co. Mayo, western Ireland.

OTHER SPECIES. ?*Pseudosphaerexochus tuberculatus* Warburg, 1925, Leptaena Limestones, Ashgill, Dalarne, Sweden, and the Chair of Kildare Limestone, Ashgill, eastern Ireland (Dean 1971).

ETYMOLOGY. After Co. Mayo, in which the type locality is situated, and the Greek noun *pyge*, tail.

DIAGNOSIS. Prominent eye ridge and relatively wide interocular fixigena; strong sutural ridge along anterior section of facial suture of librigena; swollen knob-like structure proximally on thoracic pleura; pygidium with three segments, anterior of which is similar to posterior thoracic segment; shallow, 'v'-shaped anterior pygidial doublural margin, with arcuate posterior embayment; densely and coarsely tuberculate dorsal sculpture.

DISCUSSION. The subfamilial affinities of *Mayopyge* gen. nov. are exceptionally difficult to judge. The densely tuberculate dorsal

exoskeleton is most similar to that developed in many acanthoparyphine clades. The prominent peak in convexity at the rear of the glabella, seen in many specimens, has obvious comparisons with the hypertrophied structure present in the same topological position in species of the primitive acanthoparyphine *Nieskowskia* Schmidt, 1881. Most species of *Nieskowskia* also have prominent tuberculate sculpture. However, *Mayopyge* lacks any of the acanthoparyphine apomorphies. Most importantly, *M. zapata* displays the primitive three-segmented pygidial condition, in contrast to the reduction to two segments characteristic of Acanthoparyphinae. In addition, the maximum glabellar width in the Irish species is achieved across L2, rather than across L1 as in acanthoparyphines.

Mayopyge does show some similarities to early species of *Sphaerexochus*. The hypostome of *M. zapata*, for example (Pl. 9, figs 17–20), is nearly identical to that of the upper Whiterockian *S. arenosus* (Chatterton & Ludvigsen, 1976, pl. 13, figs 32, 33, 37, 41, 42). *Mayopyge* also shares with *Sphaerexochus* fully isolated L1 with strong independent inflation.

In addition to several plesiomorphic features, including its relatively elongate anterior border and very prominent eye ridge, *Mayopyge zapata* displays several seemingly autapomorphic morphologies. The strong inflation of L2 and its near isolation from the median glabellar lobe in many specimens (Pl. 8, figs 1b, 2c, 9b) is not seen in any other species with a strongly inflated glabella. The thoracic pleural structure is also apparently unique. In contrast to the transverse furrow or row of pits common to most non-cheirurine cheirurids, *Mayopyge* shows only a faint, obliquely inclined furrow (Pl. 10, figs 1a, 2a, 4a), with the anterior pleural band swollen into a hemispherical knob and the posterior band greatly reduced. The structures seem analogous to those present in Cheirurinae, but in that taxon both the anterior and posterior pleural bands are swollen and the pleural furrow, though obliquely inclined, runs in a direction opposite to that seen in *Mayopyge*. In cheirurines, the pleural furrow contacts the axial furrow anteriorly, and runs posterolaterally. In *Mayopyge*, the contact is posterior and the furrow runs anterolaterally.

In summary, it does not seem possible at present to relate *Mayopyge* with confidence to other cheirurids. Potentially synapomorphic comparisons can be made with acanthoparyphines and with *Sphaerexochus*, but additional relevant diversity will probably be necessary to resolve the systematic position of the genus.

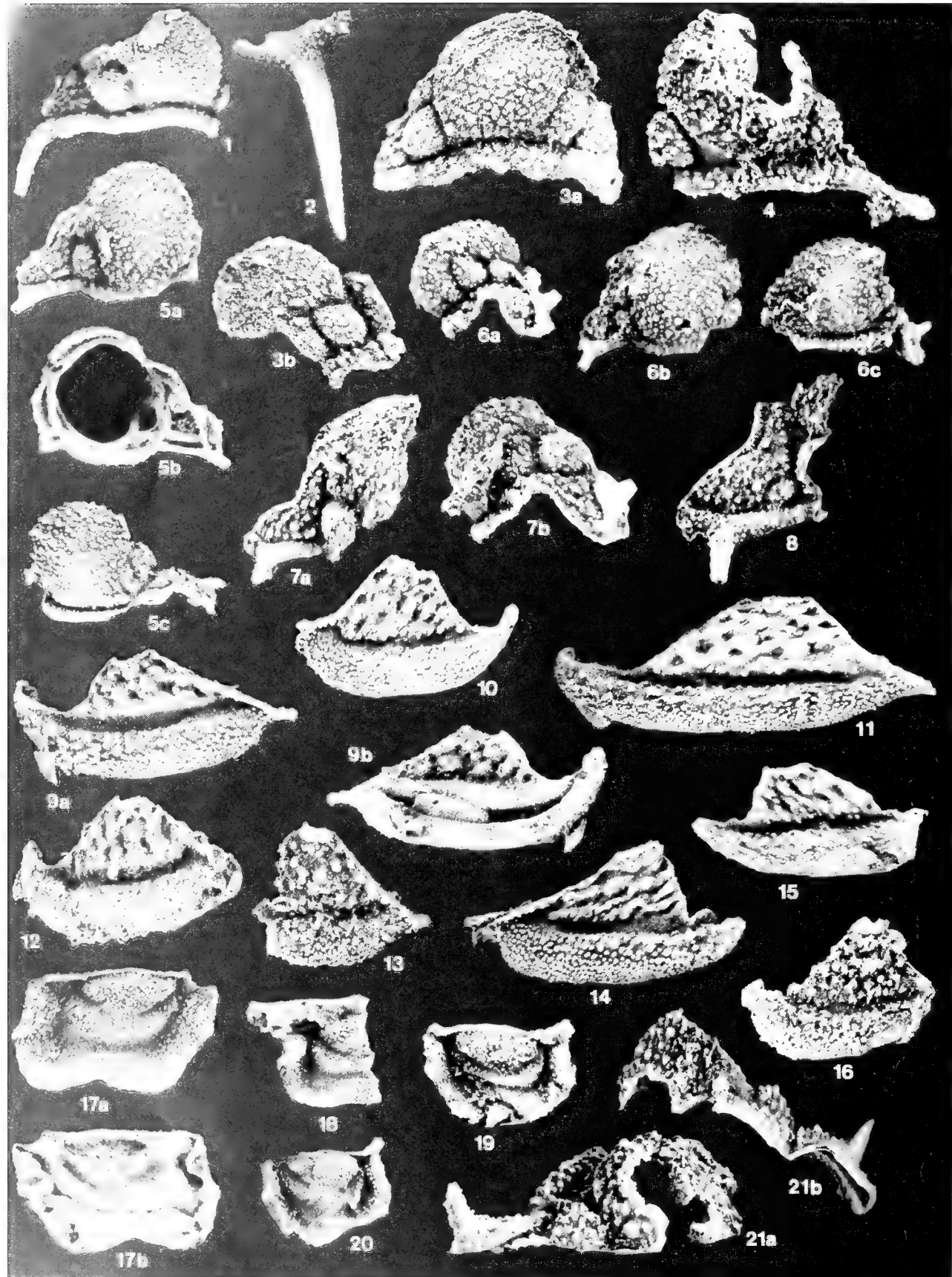
Two cranidia from the Ashgill Chair of Kildare limestone, eastern Ireland, figured by Dean (1971: pl. 11, figs 1–3, 9, 10) as *Pseudosphaerexochus?* *tuberculatus* Warburg, 1925, have coarse, dense, bimodal tuberculate sculpture. The species also agrees with *Mayopyge zapata* in its unusually well-impressed S2 and S3. Swedish type material of *P. tuberculatus* has never been photographically illustrated, but Warburg's (1925: pl. 10) cranidia are densely tuberculate. *Pseudosphaerexochus tuberculatus* possibly represents a species of *Mayopyge*, to which it is assigned with reservation herein, but it could equally prove to be an acanthoparyphine and confirmation will require more complete material.

Mayopyge zapata sp. nov.

Pl. 7, fig. 6; Pl. 8, figs 1–10;
Pl. 9, figs 1–21; Pl. 10, figs 1–17

PLATE 8

Figs 1–10 *Mayopyge zapata* gen. et sp. nov. **1a–d**, It. 26024, cranidium, dorsal, right lateral, oblique, and anterior views, $\times 7.5$. **2a–e**, It. 26025, cranidium, dorsal, ventral, right lateral, anterior, and posterodorsal views, $\times 10$. **3a–b**, It. 26026, cranidium, left lateral and dorsal views, $\times 10$. **4a–b**, It. 26027, cranidium, left lateral and dorsal views, $\times 10$. **5**, It. 26028, cranidium, oblique view, $\times 7.5$. **6a–b**, It. 26029, cranidium, dorsal and right lateral views, $\times 10$. **7a–b**, It. 26030, cranidium, dorsal and right lateral views, $\times 10$. **8a–c**, It. 26031, cranidium, dorsal, left lateral, and anterior views, $\times 10$. **9a–b**, It. 26032, cranidium, dorsal and oblique views, $\times 7.5$. **10a–c**, It. 26033, cranidium, dorsal, left lateral, and anterior views, $\times 10$.



ETYMOLOGY. The pygidial spines droop in the style of a moustache.

DIAGNOSIS. Occipital spine absent; L1 swollen and fully circumscribed by deep S1; S2 deep and L2 with prominent inflation; librigenal field with large, coarse pitting; first pair of pygidial spines longest.

HOLOTYPE. Pygidium It. 26059 (Pl. 10, fig. 6); paratypes It. 26023–26058, 26060–26071.

DESCRIPTION. Specimens of this taxon are so subject to varying amounts and vectors of distortion that relative cranidial dimensions are not meaningful. Anterior border relatively long (for subfamily), sculpture of numerous densely distributed fine tubercles; anterior margin with median part shaped like shallow inverted 'v' in plan view, with second distinct change in course in front of junction of axial and preglabellar furrow; anterior sections of facial sutures nearly straight, with considerable anterior convergence; axial furrows subparallel from S0 to opposite S2, anteriorly convergent in front of L2 to grade smoothly into preglabellar furrow; axial and preglabellar furrows deep; small trapezoidal frontal area with sculpture similar to anterior border; eye ridge prominent, running obliquely from opposite L3 to front of palpebral lobe, subparallel with lateral margin, defined by furrows, anterior of which is deepest, seen best ventrally (Pl. 8, fig. 2b); palpebral lobe very narrow, posteriorly contiguous with small sutural ridge; posterior furrow of eye ridge grading into incised palpebral furrow, continued posteriorly alongside posterior sutural ridge; interocular fixigena broad (tr.) for subfamily, with tuberculate sculpture somewhat coarser than that of frontal area; posterior fixigena with significant area and lateral development, subtriangular, sculpture of moderate sized tubercles; posterior border furrow similar in depth to axial furrow, of same length (exsag.) adaxially and abaxially; posterior border with strong dorsal convexity, adaxial length similar to adjoining L0, becoming longer abaxially, sculpture of fine, evenly spaced tubercles similar to that of anterior border; prominent tubular spine running posterolaterally from fulcrum of posterior border; glabella strongly inflated, prominent sculpture of fine to coarse tubercles, coarse, closely spaced tubercles becoming predominant posteriorly; sagittal convexity of most specimens showing strong peak posteriorly in cone-shaped dorsal projection in front of L0; L1 fully isolated by deep S1; L2 slightly smaller than L1; S2 well impressed, but shallower than S1; smooth band present on many specimens around anterior edge of S1 and S2; L3 strongly defined; S3 short (exsag.) and with reduced transverse course, but still quite strongly incised; S0 deep, of even length sagittally and exsagittally; L0 quite short (sag., exsag.), dorsally convex (sag., tr.), and with dense tuberculate sculpture similar to rear of pre-occipital glabella; tiny fossula present in axial furrow opposite midlength of eye ridge (Pl. 9, fig. 5b).

Librigenal lateral margin with strong, even lateral convexity; lateral border about 40% of width (tr.) of librigena, broadly inflated, with sculpture of dense tubercles, finer anteriorly and laterally, becoming coarse posteriorly along lateral border furrow; lateral

border furrow broad and deep, shallowing abruptly both posteriorly and anteriorly, terminated anteriorly by very pronounced sutural ridge along anterior section of facial suture; field with large, irregularly distributed pits and mixture of large, coarse tubercles and greater number of fine tubercles; single exsagittal row of very fine tubercles beneath eye; eye small (Pl. 9, figs 14, 16); doublure slightly narrower than lateral border, essentially flat and smooth, narrowing slightly posteriorly.

Rostral plate unknown. Hypostome with sagittal length about 55% of maximum width (excluding anterior wings) across shoulders; moderately strong sutural ridge along hypostomal suture; anterior margin anteriorly convex with more abrupt change in slope sagittally, bowed anteriorly around anterior wings; middle body separated from sutural ridge by very short (sag., exsag.) furrow, sagittal length about 60% of maximum width, sculpture of very fine tubercles, slightly coarser anteromedially; middle furrow deep laterally, running posteromedially, in some specimens shallowing but meeting sagittally to fully circumscribe anterior and posterior lobes; lateral border broad, with tuberculate sculpture slightly coarser than that of middle body; anterior wing tab-shaped, set at slightly oblique (30–45 degrees) angle; shoulder small but sharply protruded; lateral and posterior border furrows broad and very shallow; posterior border long (sag., exsag.), sculpture smooth, posterolateral corners lobate, embayed sagittally; doublure forming sharp dorsal fold and ridge around shoulder, lacking sculpture.

Thoracic segments with large articulating half-ring, set off posteriorly by sharp break in slope; axial ring longer (exsag.) laterally, shortened sagittally, sculpture of dense, fine to moderate sized tubercles; axial ring separated from articulating half-ring by broad, long preannular lobe, always developed as a depressed area, never with independent inflation; axial furrow very shallow, ring nearly contiguous with pleura; pleura proximal to fulcrum composed of subrectangular base topped by semicylindrical rib; rib with prominent knob-like swelling on anteroproximal part, with shallow, oblique furrow set posterior to swelling (Pl. 10, fig. 4a); pleura distal to fulcrum composed of free, tubular spine, lengthening and more posteriorly inclined on more posterior segments, with dorsal sculpture of moderately sized tubercles.

Pygidium composed of three segments, anterior segment with morphology essentially identical to that of posterior thoracic segment; articulating half-ring separated from first axial ring by narrow furrow, preannular lobe absent; axial furrows subparallel and deep on first segment, very shallow on second, entirely effaced on third; first axial ring with robust tuberculate sculpture; second ring very short (sag., exsag.), with four or five tubercles of same size as those on first ring; ring furrow between first and second rings broad and deep, forming pit laterally; second ring furrow slot-like (Pl. 10, figs 11a, 14a), in many specimens reduced to lateral pits (Pl. 10, figs 7, 9); third segment expressed as pair of median spines united by small, tuberculate terminal piece; first spine pair elongate, posteriorly recurved; second and third pairs progressively shorter; all spines with dorsal and dorsolateral tuberculate sculpture similar in size and

PLATE 9

Figs 1–21 *Mayopyge zapata* gen. et sp. nov. **1**, It. 26034, cranidium, dorsal view, $\times 6$. **2**, It. 26035, cranidial fragment, dorsal view, $\times 10$. **3a–b**, It. 26036, cranidium, dorsal and left lateral views, $\times 7.5$. **4**, It. 26037, cranidium, dorsal view, $\times 7.5$. **5a–c**, It. 26038, cranidium, dorsal, ventral, and anterior views, $\times 10$. **6a–c**, It. 26039, cranidium, left lateral, dorsal, and anterior views, $\times 10$. **7a–b**, It. 26040, cranidium, dorsal and left lateral views, $\times 7.5$. **8**, It. 26041, cranidium, dorsal view, $\times 7.5$. **9a–b**, It. 26042, right librigena, external and internal views, $\times 10$. **10**, It. 26043, left librigena, external view, $\times 7.5$. **11**, It. 26044, right librigena, external view, $\times 7.5$. **12**, It. 26045, right librigena, external and internal views, $\times 10$. **13**, It. 26046, left librigena, external view, $\times 7.5$. **14**, It. 26047, left librigena, external view, $\times 10$. **15**, It. 26048, right librigena, external view, $\times 7.5$. **16**, It. 26052, right librigena, external view, $\times 7.5$. **17a–b**, It. 26049, hypostome, ventral and dorsal views, $\times 7.5$. **18**, It. 26050, hypostome, ventral view, $\times 10$. **19**, It. 26051, hypostome, ventral view, $\times 7.5$. **20**, It. 26053, hypostome, ventral view, $\times 7.5$. **21a–b**, It. 26054, cranidium, oblique and posterior views, $\times 7.5$.



density to that of first axial ring; doublure forming narrow, convex ventral rim, with fine tuberculate sculpture; anterior doublural margin 'v'-shaped, with median posterior embayment.

DISCUSSION. This species is the second most common in our collections and, like other common taxa, displays several morphotypes due to tectonic distortion. In *Mayopyge zapata* the distortion seems to be nearly bimodal. Overwhelmingly common among the cranidia is the type illustrated on Pl. 8, which displays a conical dorsal swelling of the glabella in front of the occipital ring. Whether this is a biological structure or a result of distortion and enhancement of an original convexity peak is not known. The structure is so pervasive that it seems likely that at least some original inflation was present. The second cranidial type is that illustrated on Pl. 9, figs 1, 3a, 4, 5a, in which this projection is entirely absent and the glabella roundly and evenly inflated. An undistorted calcareous crackout cranidium (Pl. 7, fig. 6) shows an inflated convexity peak at the rear of the glabella. It is conceivable that different vectors and amounts of distortion could produce either of the silicified morphotypes from such an original morphology.

Pygidial types do not show as strong a disjunct occurrence as do the cranidia, but are even more morphologically discrete. The slightly more common form (Pl. 10, figs 6–10, 12, 13, 17) includes the holotype. It is relatively long versus wide (sagittal length 45–50% of anterior width), has long, posteriorly directed spines, a second ring furrow that is typically reduced to two lateral pits, and a rather sharp doublural embayment (Pl. 10, figs 6b, 8b). The second, slightly less common, form (Pl. 10, figs 11, 14–16) is much shorter (sagittal length 27–33% of anterior width), has more laterally splayed spines, with the median pairs apparently shorter, a second ring furrow that is a medially continuous slot (Pl. 10, figs 11a, 14a, 15a), and a relatively shallow doublural embayment (Pl. 10, figs 11b, 15b).

Given the apparent presence of two cranidial and pygidial morphotypes, there are three possibilities. First, the variation may be genuine and reflect sexual dimorphism. Second, the variation may be genuine and reflect the presence of two closely related species. And third, the dimorphism may be artefactual, and a result of the tectonic distortion affecting the entire fauna. Sexual dimorphism is improbable; it remains unproven in the trilobites as a whole (Adrain & Kloc 1997; Hughes & Fortey 1996; Ramsköld & Chatterton 1991; Ramsköld & Werdelin 1991). If sexual dimorphism were the case it might be expected that other acathoparyphines would also exhibit it, which species known from abundant silicified material manifestly do not. It cannot be entirely disproved that there are two, closely related species: since cheirurid pygidia are distinctive the name is attached to the best specimen of the commonest morph. Overall, we consider that bimodal tectonic distortion is responsible for the variation, since 'long' and 'short' forms have also been recognised in *Illaenus weaveri* and *Celmus michaelmus*, where the cause is demonstrably tectonic. However, the pygidial differences remain a cause for concern, as the different ring furrows are not readily accounted for by distortion alone.

Subfamily CHEIRURINAE Hawle & Corda, 1847

Genus *CERAURINELLA* Cooper, 1953

TYPE SPECIES. *Ceraurinella typa* Cooper, 1953, from the Edinburg Formation (Mohawkian), Virginia, U.S.A.; by original designation.

Ceraurinella sp.

Pl. 11, figs 1–9

MATERIAL. Assigned specimens It. 26072–26080.

DISCUSSION. The fragmentary nature of the available material does not allow a determination of the species, and several important morphological differentia (e.g., eye position) are not fully preserved. Nevertheless, the Tourmakeady species is clearly a primitive member of the *Ceraurinella* group (including *Sycophantia* Fortey, 1980). The Irish species differs from the Spitsbergen plesiomorph *S. seminosa* Fortey, 1980, in its much shorter anterior cranidial border (in which it resembles later and presumably more advanced species) and in the complete loss of the small median pygidial spine retained in *S. seminosa*. Both the available librigenae and fixigenal fragments, however, indicate that the Irish species retained very wide posterior fixigenae, similar to *S. seminosa*. Of other early species, the Tourmakeady taxon resembles *C. polydorus* (Billings, 1865) (see Whittington 1965: pl. 60) in the length of the anterior cranidial border, but differs in possessing less inflated lateral glabellar lobes (compare Pl. 11, fig. 1 with Whittington 1965: pl. 60, fig. 4), a broader posterior fixigena, and a narrower pygidium lacking an independently defined median spine.

Family ENCRINURIDAE Angelin, 1854

Subfamily CYBELINAE Holliday, 1942

Cybeline indet. (not figured)

MATERIAL. Assigned specimen It. 26201.

DISCUSSION. A single very poorly preserved cybeline cranidium has been recovered from the silicified residues. It is obscured by silicified debris, and identifiable only to subfamily level. It is noted here for completeness.

Family LECANOPYGIDAE Lochman, 1953

Genus *BENTHAMASPIS* Poulsen, 1946

TYPE SPECIES. *Benthamaspis problematica* Poulsen, 1946, Ibexian, Ellesmere Island, Canadian Arctic; by monotypy.

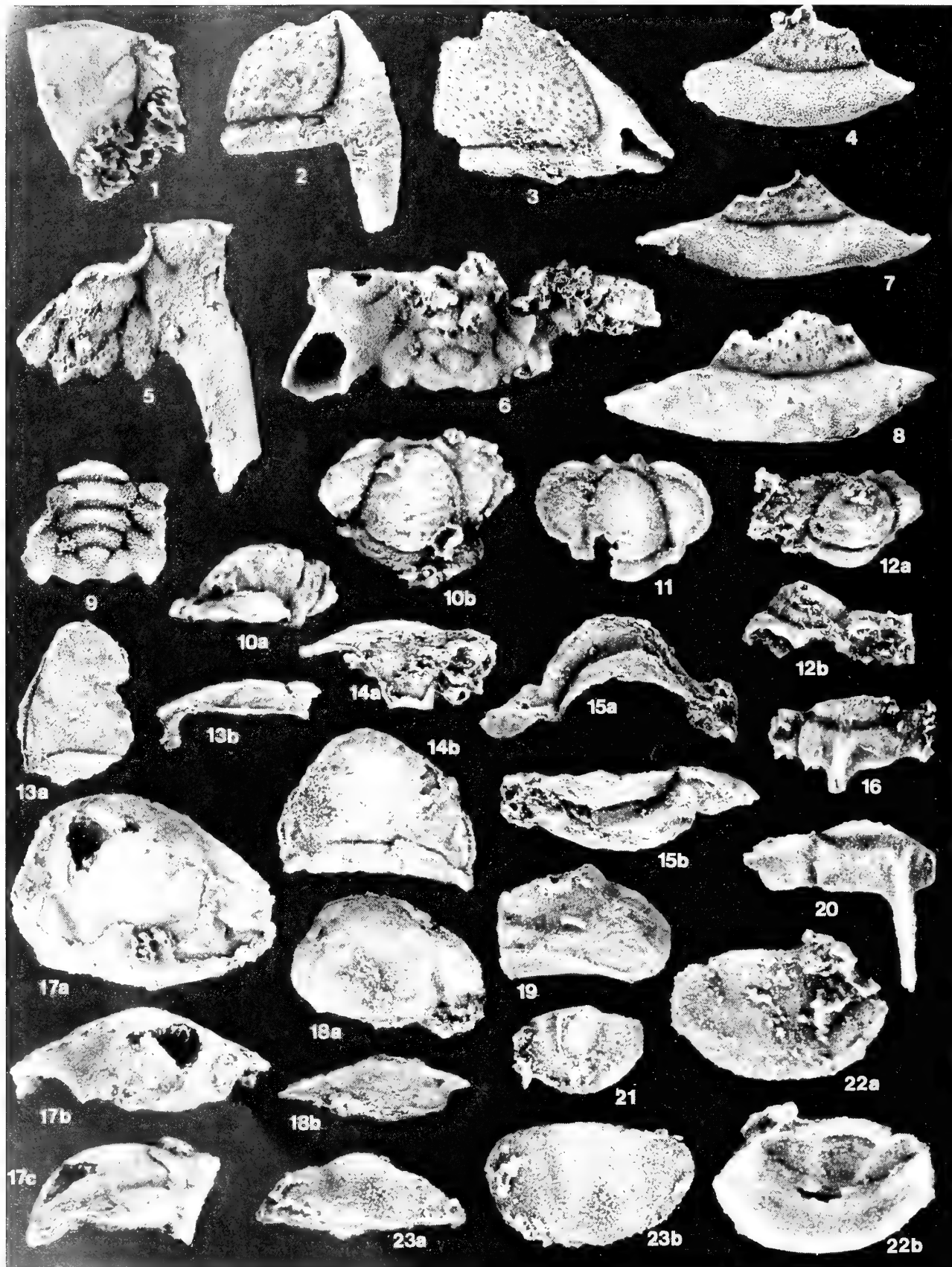
Benthamaspis aff. *B. diminutiva* Hintze, 1953

Pl. 11, figs 17–19, 21–23

MATERIAL. Assigned specimens It. 26089–26094.

PLATE 10

Figs 1–17 *Mayopyge zapata* gen. et sp. nov. **1a–b**, It. 26055, thoracic segment, dorsal and anterior views, $\times 7.5$. **2a–b**, It. 26056, thoracic segment, dorsal and anterior views, $\times 7.5$. **3a–b**, It. 26057, thoracic segment, dorsal and anterior views, $\times 7.5$. **4a–b**, It. 26058, thoracic segment, dorsal and anterior views, $\times 7.5$. **5a–b**, It. 26060, thoracic segment, oblique and dorsal views, $\times 7.5$. **6a–c**, It. 26059, holotype, pygidium, right lateral, dorsal, and ventral views, $\times 7.5$. **7**, It. 26061, pygidium, dorsal view, $\times 10$. **8a–b**, It. 26064, pygidium, dorsal and ventral views, $\times 7.5$. **9**, It. 26062, pygidium, dorsal view, $\times 7.5$. **10**, It. 26063, pygidium, dorsal view, $\times 10$. **11a–b**, It. 26066, pygidium, dorsal and ventral views, $\times 7.5$. **12**, It. 26065, pygidium, dorsal view, $\times 10$. **13**, It. 26067, pygidium, dorsal view, $\times 10$. **14a–b**, It. 26068, pygidium, dorsal and posterior views, $\times 7.5$. **15a–b**, It. 26069, pygidium, dorsal and ventral views, $\times 7.5$. **16**, It. 26070, pygidium, dorsal view, $\times 7.5$. **17**, It. 26071, pygidium, dorsal view, $\times 10$.



DISCUSSION. Fortey (1979: 100) has discussed the evolutionary trends evident in *Benthamaspis*, culminating in the considerably effaced species *B. diminutiva* Hintze, 1953. A species from the Tourmakeady Limestone is of interest in that it is the youngest known member of the genus and confirms the stratigraphically correlated pattern of progressive effacement. The species is very similar to the slightly older (Zone J) *B. diminutiva*, from Ibex, Utah, but differs in the possession of narrower palpebral lobes, more well impressed axial furrows, and retention of a complete, if very shallow, preglabellar furrow. The preglabellar furrow of *B. diminutiva* is effaced, so that the glabella grades anteriorly toward the anterior border furrow (Hintze 1953: pl. 13, figs 9b, 10c). In addition to effacement, the species are united by their nearly identical pygidia (compare Pl. 11, fig. 23, with Hintze 1953: pl. 13, figs 11a, 11b), and by the laterally concave glabellar margins. Most older Ibexian species have the axial furrows anteriorly convergent, but there is some indication of the beginnings of the axially bowed form with an anteriorly expanding glabella in certain specimens of *B. conica* Fortey, 1979, from the Catoche Formation of western Newfoundland (see particularly Fortey 1979: pl. 35, fig. 7). The librigena of *B. diminutiva* is not known, but that of the Irish taxon (Pl. 11, fig. 19) agrees well with those assigned to earlier species (Fortey 1979: pl. 34, fig. 3; pl. 35, fig. 4). We also figure as *Benthamaspis* sp. two cranidia with distinct borders (It 25941, 25942; Pl. 1, figs 7, 9) which are probably not conspecific with *B. aff. diminutiva*; a pygidium (It 25943; Pl. 1, fig. 8) may belong with these cranidia.

Family TELEPHINIDAE Marek, 1952

Subfamily TELEPHININAE Marek, 1952

Genus *OOPSITES* Fortey, 1975a

TYPE SPECIES. *Telephus hibernicus* Reed in Gardiner & Reynolds, 1909, from the Tourmakeady Limestone, upper Arenig, Ireland; by original designation.

DISCUSSION. *Oopsites* was erected (Fortey 1975a: 95) as an explicit 'morphological and stratigraphic intermediate' between the genera *Goniophrys* Ross, 1951, and *Telephina* Marek, 1952. As such, it may well prove paraphyletic. The situation, however, would be better understood in light of a comprehensive phylogenetic review of the telephinids, a task beyond the scope of the present work, and the original classification is retained herein.

Oopsites hibernicus (Reed in Gardiner & Reynolds, 1909)

Pl. 11, figs 10–12, 15; Pl. 13, figs 1–3; Pl. 16, fig. 24

- 1909 *Telephus hibernicus* Reed in Gardiner & Reynolds: 149; pl. 6, figs 10, 11.
 1930 *Telephus hibernicus* Reed; Ulrich: 17; pl. 2, figs 18, 19.
 1968 *Telephina hibernica* (Reed); Whittington: 56.

PLATE 11

Figs 1–9 *Ceraurinella* sp. 1, It. 26072, cranidium, dorsal view, $\times 8$. 2, It. 26073, cranidial fragment, dorsal view, $\times 6.5$. 3, It. 26074, cranidial fragment, dorsal view, $\times 6.5$. 4, It. 26075, right librigena, external view, $\times 10$. 5, It. 26076, pygidium, dorsal view, $\times 8$. 6, It. 26077, pygidium, dorsal view, $\times 6.5$. 7, It. 26078, left librigena, external view, $\times 10$. 8, It. 26079, right librigena, external view, $\times 3.5$. 9, It. 26080, pygidium, dorsal view, $\times 10$.

Figs 10–12, 15 *Oopsites hibernicus* (Reed in Gardiner & Reynolds, 1909). 10a–b, It. 26081, cranidium, left lateral and dorsal views, $\times 10$. 11, It. 26082, cranidium, dorsal view, $\times 15$. 12a–b, It. 26083, cranidium, dorsal and anterior views, $\times 10$. 15a–b, It. 26086, thoracic segment, anterior and dorsal views, $\times 7.5$.

Figs 13, 14, 16, 20 *Opipeuter* aff. *O. inconnivus* Fortey, 1974. 13a–b, It. 26108, cranidium, dorsal and left lateral views, $\times 10$. 14a–b, It. 26109, cranidium, anterior view, $\times 10$. 16, It. 26087, thoracic segment, dorsal view, $\times 15$. 20, It. 26088, thoracic segment, dorsal view, $\times 10$.

Figs 17–19, 21–23 *Benthamaspis* aff. *B. diminutiva* Hintze, 1953. 17a–c, It. 26089, cranidium, dorsal, anterior, and left lateral views, $\times 10$. 18a–b, It. 26090, cranidium, dorsal and anterior views, $\times 10$. 19, It. 26091, left librigena, external view, $\times 10$. 21, It. 26092, pygidium, dorsal view, $\times 15$. 22a–b, It. 26093, pygidium, dorsal and ventral views, $\times 15$. 23a–b, It. 26094, pygidium, posterior and dorsal views, $\times 15$.

1975a *Oopsites hibernicus* (Reed); Fortey: 97; pl. 33, figs 9–19; pl. 34, figs 1–7.

1988 *Oopsites hibernicus* (Reed); Morris: 156.

MATERIAL. Topotypes It. 26081–26083, 26086–26088, 26111–26113, 26176.

DISCUSSION. Fortey (1975a: 97, pl. 33, fig. 8) designated and illustrated a lectotype from Reed's (*in* Gardiner & Reynolds 1909) syntypes. This has been the only photographic illustration of a type specimen to date, although Fortey (1975a) figured well preserved Spitsbergen material assigned to the species. The additional Irish material figured herein confirms the specific identity with the Spitsbergen taxon beyond any doubt. The only possible difference between the two lots of specimens is that the palpebral furrow of the Spitsbergen cranidia is slightly deeper anteriorly than that of the Irish specimens (compare Fortey 1975a: pl. 33, fig. 12; pl. 34, fig. 6, with Pl. 13, fig. 1b).

Subfamily OPIPEUTERINAE Fortey, 1974

DISCUSSION. Opipeuteridae was originally proposed as a monogeneric family by Fortey (1974), who considered that this specialised pelagic form might be closest to remopleuridoids. Shergold (*in* Laurie & Shergold 1996) demonstrated that it is instead closely related to *Carolinites*, and hence a member of the Telephinidae. It is not yet clear how the *Carolinites* + *Opipeuter* group, which is very likely monophyletic, relates to other telephinids. Dean (1971) introduced the subfamily Carrickiinae to accommodate *Carrickia*, and the relationship of this genus to *Telephina* and *Goniophrys*, and all of these to *Carolinites* and *Opipeuter*, is as yet unclear. For the time being Opipeuterinae is retained as a subfamily of telephinids, to include *Opipeuter* and *Carolinites*, pending the clarification of their relationships to other pelagic taxa.

Genus *OPPIPEUTER* Fortey, 1974

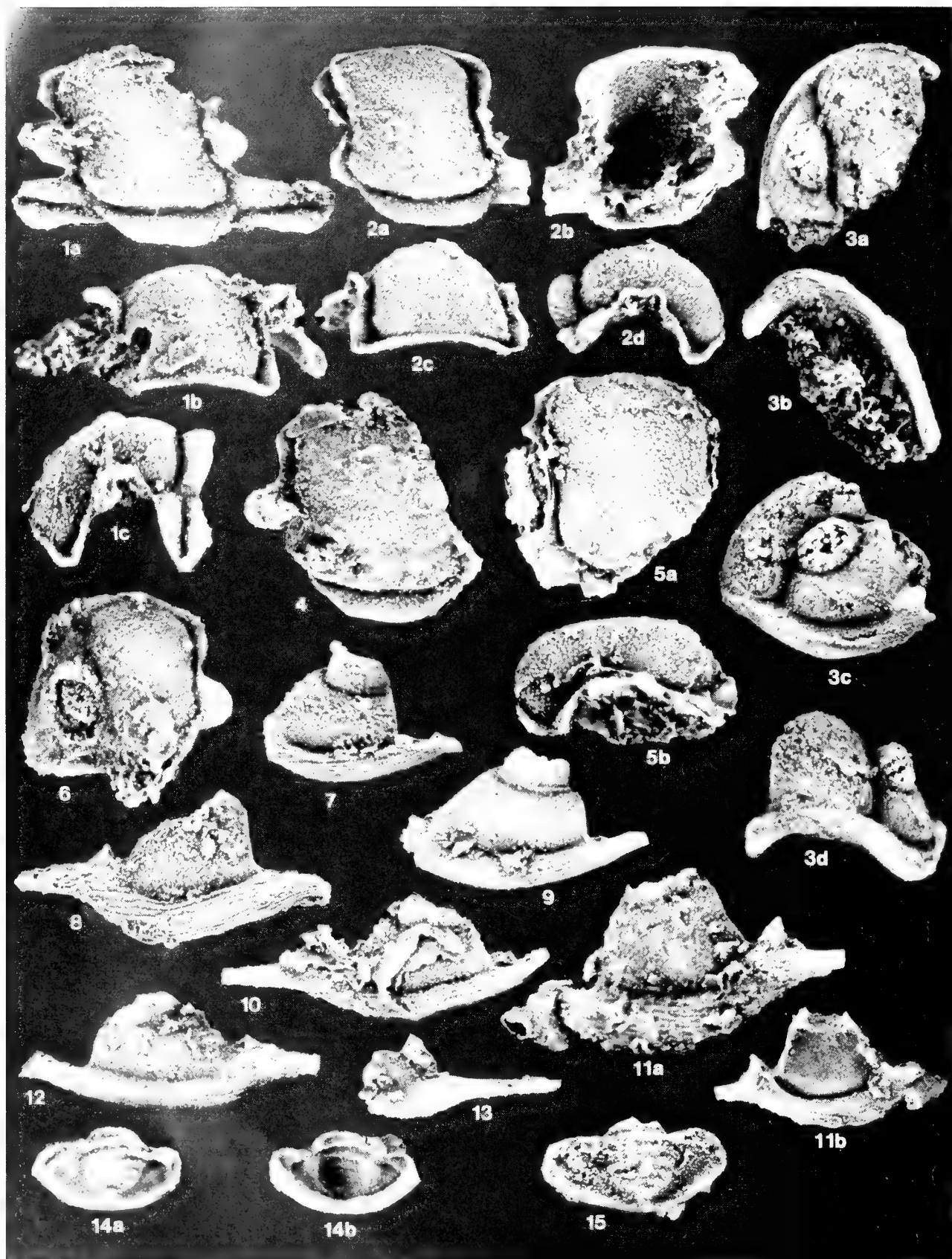
TYPE SPECIES. *Opipeuter inconnivus* Fortey, 1974, from the Valfallonna Formation (Arenig) of Spitsbergen; by original designation.

Opipeuter aff. *inconnivus* Fortey, 1974

Pl. 11, figs 13, 14, 16, 20; Pl. 13, figs 4, 5

MATERIAL. Assigned specimens It. 26087, 26088, 26108, 26109, 26114, 26115.

DISCUSSION. *Opipeuter inconnivus* was fully described by Fortey (1974) who included within that species a cranidium from the Tourmakeady Limestone. There are three species in stratigraphical succession through the Arenig, each with progressively narrower anterior glabellar tongues: *O. angularis* (Young, 1973), *O. inconnivus*, and *Opipeuter* sp. A of Fortey (1974), the last-named also having a



relatively wide genal field. New silicified material (Pl. 11, fig. 14a) shows a slightly narrower (tr.) glabellar tongue than is typical of *O. inconnivus*, and the librigena (Fortey 1974, pl. 14, fig. 13) has a relatively wide genal field. The population seems to be intermediate between *O. inconnivus* and *O. pipeute*, sp. A, and it is considered preferable to term it *O. aff. inconnivus*. Henderson (1983) described *O. insignis* from Queensland, Australia, based upon rather fragmentary material. The genal field is like that of *O. aff. O. inconnivus*. Henderson also stated that one thoracic segment carried a long, median spine. Fortey's (1974) reconstruction of *O. inconnivus* did not show such a spine, but was based upon an entire specimen in which the thoracic axis was poorly preserved. It seems likely that the thoracic segments figured here on Pl. 11, figs 16, 20 are this spinose segment.

Family LEIOSTEGIIDAE Bradley, 1925
Genus *AGERINA* Tjernvik, 1956

TYPE SPECIES. *Agerina erratica* Tjernvik, 1956, from the 'grey marly Upper Planilimbata limestone,' Lanne, Närke, Sweden; by original designation.

Agerina palabunda sp. nov.

Pl. 12, figs 1–15

ETYMOLOGY. Latin, wandering, referring to the widespread occurrence of the genus.

HOLOTYPE. Craniidium, It. 26095 (Pl. 12, fig. 1); paratypes It. 26096–26107, 26084, 26085.

DIAGNOSIS. Glabellar furrows almost entirely effaced, except for smooth patch at S1; glabella with clavate form, axial furrows strongly bowed inwards; dorsal cephalic sculpture of fine tubercles.

DESCRIPTION. Craniidium with sagittal length about 60% of maximum width across posterior border furrows; width across midlength (exsag.) of palpebral lobes two thirds that across posterior border furrows; anterior sections of facial sutures strongly divergent anteriorly in front of palpebral lobes, reaching maximum divergence opposite anterior border furrow, then strongly convergent opposite anterior border; posterior sections of facial sutures curving sharply immediately behind palpebral lobe to run nearly transversely, curving posteriorly around distal extremity of posterior fixigena; anterior border short (sag., exsag.), upturned, nearly flat, almost completely overhung by glabella medially, with sculpture of two or three linear terrace lines running parallel to margin; border lengthening abaxially, separated from anterior fixigena by weakly impressed border furrow; glabella moderately inflated, hourglass-shaped, anterior margin with gentle anterior convexity, lateral margins with strong lateral concavity; glabellar sculpture of dense, evenly distributed fine tubercles, all of similar size; S1 not incised, reflected as a smooth patch free of tuberculate sculpture (Pl. 12, figs 4, 5); anterior glabellar furrows indiscernible; anterior fixigena confined to narrow, subtriangular strip; axial furrow very deeply incised, bowed

strongly adaxially beside palpebral lobe; palpebral lobe large, similar in length (exsag.) to posterolateral projection of craniidium, held in horizontal plane, with dorsal sculpture of dense granules; posterior fixigena forming relatively long (exsag.) transverse strip, sculpture of fine tubercles similar to that of glabella; posterior border furrow similar in depth to axial furrow, of similar length medially and laterally, running nearly exactly transversely; posterior border relatively short proximally, lengthening and becoming slightly lobate laterally, with considerable exsagittal dorsal convexity; S0 with gentle posterior curvature, similar in depth and incision to axial furrow and posterior border furrow; L0 with posterior margin describing very shallow 'W' shape so that sagittal length is slightly shorter than nearby exsagittal length, then shortening considerably behind L1; L0 with tuberculate sculpture similar to that of anterior part of glabella, no distinct median node discernible, with moderate sagittal convexity.

Librigenal field with anterior width (tr.) 60–65% of maximum width just behind eye; maximum width about 55% of maximum length (exsag.); lateral border broad, slightly wider posteriorly than anteriorly, with prominent, rounded, dorsal inflation, sculpture of about nine coarse terrace lines, arranged subparallel to lateral margin anteriorly, running back to intersect margin posteriorly, more closely spaced near lateral margin, slightly anastomosing with some merging and disappearance of individual lines; lateral border furrow deep, narrow, shallowing abruptly posteriorly in front of genal spine; lateral border furrow and lateral margin with strong lateral curvature; genal spine long and tapering, terrace lines of lateral border continued along length without interruption; only small portion of posterior border developed on librigena, beside strong sutural embayment for posterolateral part of craniidium; field with gentle dorsal convexity, sculpture of fine tubercles, slightly coarser adaxially and beneath eye; prominent eye socle of single continuous, narrow band; eye large, with length (exsag.) slightly more than double width at midlength; doublure nearly flat, with subdued terrace lines developed mainly near lateral margin, much finer than those on dorsal aspect of lateral border.

Rostral plate subrectangular in anterior aspect, connective sutures longer than rostral suture; terrace lines of anterior librigenal projections continued across plate without interruption; connective sutures converging ventrally, nearly meeting posteriorly on strongly curved ventral part of plate.

Thorax unknown. Pygidium with sagittal length 50–55% of maximum width; wide, gently tapering and obtusely rounded axis slightly less than half pygidial width (as shown on best silicified specimen, Pl. 12, fig. 14a); axis extends close to border, in contact via narrow postaxial ridge; five narrow (tr.) axial rings extending to postaxial ridge; posteriormost ring may be obscure; gently convex pleural fields show two defined segments, only the anterior pleural furrows are at all deep; border is narrow and distinctly convex, and carries a sculpture of a few raised lines like those on the genal border; doublure recurved ventrally and wider than border, showing an anterolateral articular tooth (cf. *Annamitella* Fortey & Shergold 1984, pl. 38, fig. 15).

PLATE 12

Figs 1–15 *Agerina palabunda* sp. nov. **1a–c**, It. 26095, holotype, craniidium, dorsal, anterior, and left lateral views, $\times 15$. **2a–d**, It. 26096, craniidium, dorsal, ventral, anterior, and right lateral views, $\times 15$. **3a–d**, It. 26097, cephalon, dorsal, ventral, left lateral, and anterior views, $\times 15$. **4**, It. 26098, craniidium, dorsal view, $\times 15$. **5a–b**, It. 26099, craniidium, dorsal and left lateral views, $\times 15$. **6**, It. 26100, craniidium and left librigena, dorsal view, $\times 15$. **7**, It. 26101, right librigena, external view, $\times 15$. **8**, It. 26102, right librigena, external view, $\times 15$. **9**, It. 26103, right librigena, external view, $\times 15$. **10**, It. 26104, right librigena, external view, $\times 15$. **11a–b**, It. 26107, left librigena, external and internal views, $\times 15$ and $\times 10$. **12**, It. 26105, left librigena, external view, $\times 15$. **13**, It. 26106, left librigena, external view, $\times 15$. **14a–b**, It. 26084, pygidium, dorsal and ventral views, $\times 10$. **15**, It. 26085, pygidium, dorsal view, $\times 10$.

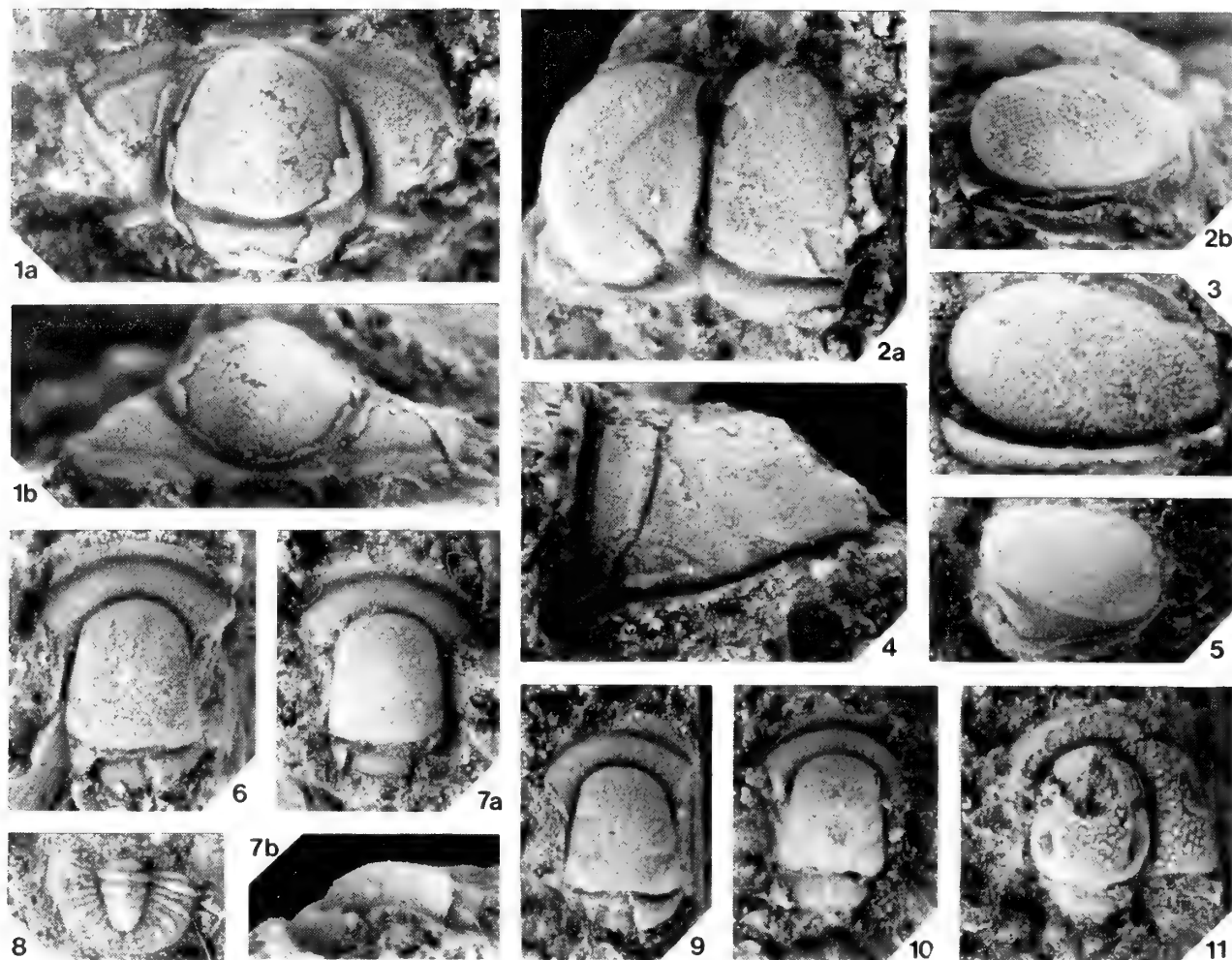


PLATE 13

Figs 1–3 *Oopsites hibemicus* (Reed in Gardiner and Reynolds, 1909). 1a–b, It. 26111, cranidium, dorsal and anterior views, $\times 15$. 2a–b, It. 26112, cranidium and left librigena, dorsal and left lateral views, $\times 15$. 3, It. 26113, left librigena, left lateral view, $\times 15$.

Figs 4, 5 *Opiputeer aff. O. inconnivus* Fortey, 1974 4, It. 26114, cranidium, right dorsolateral view, $\times 15$. 5, It. 26115, right librigena, external view, $\times 15$.

Figs 6, 7, 9, 10 *Phaseolops ceryx* sp. nov. 6, It. 12856, cranidium, dorsal view, $\times 15$. 7a–b, It. 12857, cranidium, dorsal and left lateral views, $\times 15$. 9, It. 26116, cranidium, dorsal view, $\times 15$; 10, It. 26117, cranidium, dorsal view, $\times 15$.

Fig. 8 *Proscharaya platyimbata* sp. nov. It. 26118, pygidium, dorsal view, $\times 15$.

Fig. 11 *Glaphurus crinitus* sp. nov. It. 26119, cranidium, dorsal view, $\times 10$.

DISCUSSION. Ludvigsen (1980: 99) has fully discussed this genus, assigning it to the Bathyuridae. Fortey & Shergold (1984: 322) considered that it was related to *Annamitella* Mansuy, 1920, on the basis of glabellar characters, and assigned both to Leiostegidae. Within the genus as conceived by these workers there is a group of similar species, including *A. acheila* (Harrington & Leanza, 1957), *A. norrisi* Ludvigsen, 1980, and *A. praematura* Tjernvik, 1956. It is these species that most resemble *Annamitella*, and all have a relatively elongate anterior border, incised glabellar furrows, a concave-sided glabella, and a pygidium with a subdued border lacking raised lines. The Sunwaptan species described as *Bellaspidella parallela* Ludvigsen & Westrop in Ludvigsen *et al.* 1989, appears to share all of these morphological features, and may prove to belong there. All are seemingly related to the Chinese taxon *Hexianella* Zhang, 1983, to which they are transferred herein. The pygidia assigned to *H. hexianensis* and *H. exigusulcata* by Zhang

(1983: pl. 75, figs 6, 8) do not belong, but appear to be nileid transitory pygidia.

A second group includes the type species of *Agerina* and *A. pamphylica* Dean, 1973. These species have the glabellar furrows considerably effaced, the glabella more nearly parallel sided, and the pygidium with a border carrying prominent subparallel raised lines. Of described species, *A. palabunda* is closer to this second, Arenig, group, and is perhaps most similar to *A. pamphylica*. Dean's species does show some lateral concavity of the glabella (Dean 1973: pl. 4, fig. 1), although it is less well developed and anterior than in *A. palabunda*.

Family CELMIDAE Jaanusson, 1956
Genus CELMUS Angelin, 1854

Ischyrophyma Whittington, 1963: 48.

TYPE SPECIES. *Celmus granulatus* Angelin, 1854, Skarpasen, Östergötland, Sweden; by monotypy.

OTHER SPECIES. *Glaphurina? insolita* Tjernvik, 1956; *Celmus? longifrons* Poulsen, 1965; *Ischyrophyma tuberculata* Whittington, 1963; *Ischyrophyma tumida* Whittington, 1965; *Ischyrophyma?* sp. indet. of Whittington (1963); the specimen figured by Whittington (1965: pl. 19, figs 16, 19, 20) as *Ischyrophyma?* sp. indet. is a calymenid related to or conspecific with his 'aff. *Calymenidius* sp. ind.' (Whittington 1965: pl. 59, figs 10, 12–15); work in progress on silicified Newfoundland faunas indicate this taxon is a species of *Sthenarocalymene* Siveter, 1977.

Celmus michaelmus sp. nov.

Pl. 14, figs 1–17; Pl. 15, figs 1, 2, 5–9; Pl. 16, figs 11, 20

1975 *Celmus* sp. Fortey & Owens Fig. 1A,B

ETYMOLOGY. Latin, a mouse called Michael (see Pl. 15, fig. 6a).

DIAGNOSIS. Dorsal sculpture densely tuberculate; several exsagittal rows of tubercles on anterior fixigena; posterolateral part of librigenal lateral border with sparse or absent tubercles, but prominent raised lines subparallel with margin; pygidium with nearly elliptical outline in plan view; pygidial flanges circular and prominent.

HOLOTYPE. Pygidium, It. 26123 (Pl. 14, fig. 4); paratypes It. 12853, 12854, 26120–26122, 26124–26141, 26168, 26169.

DESCRIPTION. Some of the silicified material upon which this species is based has suffered distortion; for example, the original of Pl. 14, fig. 6 has been foreshortened, and that of Pl. 14, fig. 3, elongated sagittally. The holotype, and such specimens as that figured on Pl. 14, fig. 2, are considered close to the undistorted state, and it is upon these that descriptions of proportions are based.

Cranidium as wide (tr.) at the posterior margin as long (sag.), this being three-quarters the width across the palpebral lobes; glabella about 1.5 times longer than wide, the maximum width being at L1 where the glabella bulges outwards before tapering gently anteriorly; S1 deep and distinct, the outer part slightly wider and almost transverse, the inner part geniculated backwards and on most specimens just falling short of reaching the occipital furrow (Pl. 14, fig. 7, in which it does, is also distorted); S2 is short, transverse, close to the anterior end of the palpebral lobe; glabella encroaches on the border, but at least some part of the border is visible in dorsal view; fixigenal and eye position are as in all other species of the genus; the palpebral lobes carry three or four prominent tubercles.

Librigena retains a knob at the genal angle, which is a remnant genal spine; on a small example (Pl. 14, fig. 12) it is much more prominent; bevelled border bears three or four very prominent raised lines which extend as far as the knob; a few scattered tubercles may be present between the lines; the elevated eye has a smooth eye socle beneath it, at its anterior end, a small, inflated lobe (see Pl. 15, fig. 1); doublure extends beneath border (Pl. 14, fig. 17), and carries an exterior groove on its posterolateral edge, which may have accommodated pleural tips upon enrollment (see Bruton 1983, pl. 28, fig. 2).

Thoracic segment shows general convexity of body (Pl. 15, fig. 2b); anterior ridge terminates in an articulatory notch; posterior band continues distally as a spine.

Minute pygidium is known from good isolated material; it comprises a single segment, with an articulating half-ring; posterior margin densely covered with raised lines subparallel to margin, and narrow doublure (Pl. 15, fig. 6c) with fine terrace lines; pygidium bears a pair of flat, rounded flanges which project backwards; the surface of the flanges is smooth.

The rest of the axial part of the exoskeleton, and the genal fields, is densely tuberculate; in some specimens the librigenal tubercles are of two sizes (Pl. 15, fig. 1), but this is less clearly so in others (Pl. 14, fig. 11).

DISCUSSION. This species is very similar indeed to the type species, *Celmus granulatus* (see Jaanusson 1956, Bruton 1983) from the Kundan stage of Sweden. Cephalic differences are trivial. The distinctive lobe at the anterior end of the eye socle of *C. michaelmus* is not mentioned in a detailed description by Bruton (1983, p. 216), but is visible on his figures (*ibid.* pl. 28, fig. 14). The sculpture on the Irish species is denser; for example the anterior fixed cheek of *C. granulatus* shows a single row of tubercles except at the anteriormost end, while several rows are present along its whole length in the new species (Pl. 14, figs 1c, 2c, 6b). The raised lines which extend to the genal spine remnant on the librigenal border of *C. michaelmus* stop well short of it in *C. granulatus*, and the portion of the border in front of the genal angle is far more densely tuberculate in the latter species. Finally, the prominent pygidial flanges of the Tourmakeady species are much better developed than a homologous pair of low ridges in *C. granulatus* (Bruton 1983: pl. 28, figs 10, 12), and the pygidium of the Irish species has an elliptical, versus trapezoidal, outline in plan view.

Genus *DIMEROPYGE* Öpik, 1937

TYPE SPECIES. *Sphaerexochus minutus* Nieszkowski, 1857, Middle Ordovician, Kukruse beds, Estonia; by monotypy.

Dimeropyge? *ericina* sp. nov.

Pl. 15, figs 15–17; Pl. 16, figs 17–19, 21–23

ETYMOLOGY. Latin, of a hedgehog.

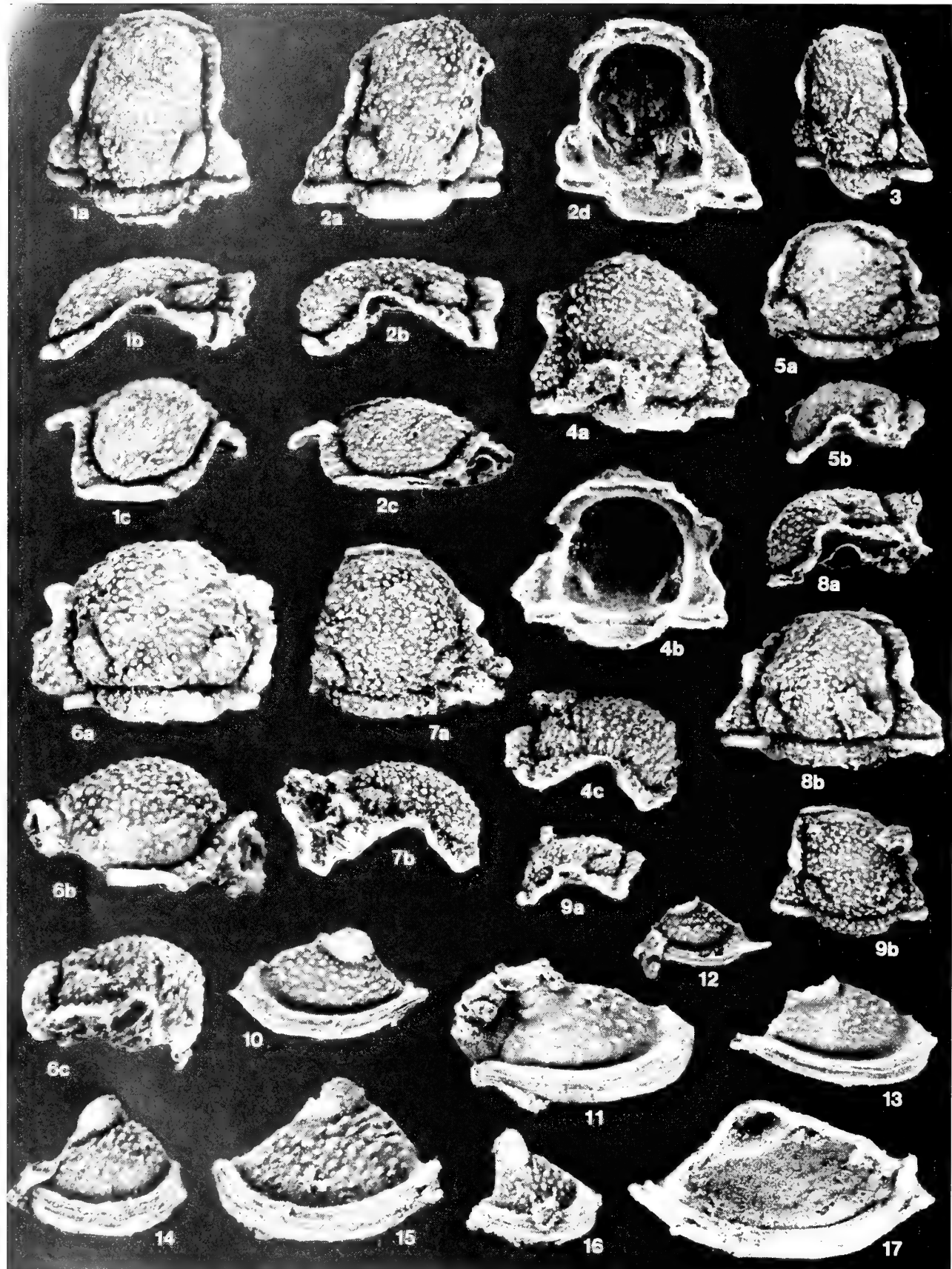
DIAGNOSIS. Elongate glabellar spines retained in holaspis; two pairs of glabellar spines, four pairs of fixigenal spines; librigena carries two spines on genal field and a few on border.

HOLOTYPE. Cranidium, It. 26150 (Pl. 15, fig. 15); paratypes It. 26151, 26152, 26170–26175.

DESCRIPTION. We have not discovered a pygidium of this unusual species, but the cephalic parts are so distinctive that it can be named as new.

Glabellar outline is best seen on the inner surface of the cranidium (Pl. 15, fig. 15b), which shows it extending to two-thirds cephalic length, convex (tr.), defined by deep axial furrows; width at L0 wider (tr.) than in front, thereafter expanding gently in width anteriorly to rounded front; L0 carries a pair of long, stout spines; two equally stout pairs are present on the glabella; fixigena are wider than glabella at posterior margin; they, too, carry spines, which can be matched with the glabellar ones, since one pair on the rather poorly defined posterior border matches the occipital segment, and there are two pairs anterior to this matching those on the glabella. In addition, there are prominent spines on the posterolateral cranidial corners; the anterior border, however (Pl. 15, fig. 16b) is without spines; the palpebral lobe is inconspicuous at cephalic mid-length.

Librigena has a prominent, and somewhat elevated eye lobe; on the genal field there are two spines; the lateral border is well defined, rounded, and carries only two or three comparatively subdued spines at its mid part; a thoracic segment can be confidently associated because it shows paired axial spines, and also two pleural spines, the inner one at the point of downward geniculation of the segment; the tips of the spines appear to be perforated.



DISCUSSION. The morphology of *Dimeropyge?* *ericina* is very unusual, and in fact has no direct comparison among mature or nearly mature material of any other dimeropygid. It may be understood, however, by reference to the very early developmental morphology of *Dimeropyge*. It is well established that the protaspis protocranidium of members of this genus, as well as cranidia probably assignable to meraspid degree 0 or 1, have only two pairs of glabellar spines and four pairs of fixigenal tubercles (Tripp & Evitt 1983: pl. 31, figs 6, 7, 10, 11, 16, 17, 23, pl. 32, fig. 6; Chatterton 1994: figs 4.3, 4.6, 4.8, 4.22, 4.23, 5.1). These tubercles are in identical positions to the cranidial spines of *D.? ericina*. In addition, early (M3) meraspid transitory pygidia of *Dimeropyge* show unreleased thoracic segments with paired axial and fulcral spines similar in position to those seen in a thoracic segment of the Irish species (compare Chatterton 1994: fig. 4.4 with Pl. 16, fig. 19). Finally, *D.? ericina* has a fine, transverse row of rounded tubercles aligned along the rear of its anterior border (Pl. 16, fig. 18) identical to that seen in juvenile *Dimeropyge* (e.g., Chatterton 1994: figs 4.9, 5.1, 6.2). From this it may be hypothesized that *D.? ericina* is a paedomorph, derived through neoteny from an earlier dimeropygid. Much more information would be required, both on the morphology of the Tourmakeady species and on relevant contemporaneous and earlier diversity, to form an opinion about the close affinity of the species. Its lack of genal spines, for example, indicates it may not be derived from ingroup *Dimeropyge*, which as far as is known maintains elongate genal spines from the earliest ontogenetic stages. For this reason, we have assigned it only provisionally to the genus.

Family SCHARYIIDAE Osmólska, 1957

Genus *PROSCHARYIA* Peng, 1990

TYPE SPECIES. *Proscharyia sinensis* Peng, 1990, Madaoyu Formation (Upper Tremadoc), northwest Hunan, south China; by original designation.

DISCUSSION. *Protarchaeconus sanduensis* Zhou, 1981, from the lower Tremadoc Guotang Formation, Guizhou, is very similar to the type species and definitely belongs to *Proscharyia*.

Proscharyia platylimbata sp. nov.

Pl. 15, figs 23, 24; Pl. 16, figs 7–10, 12–16

ETYMOLOGY. Greek *platys*, broad, and Latin *limbatus*, bordered.

DIAGNOSIS. *Proscharyia* having eyes distant from glabella and preocular sutures divergent at low angle; glabella tapers forward gently and glabellar furrows effaced; preglabellar field comparatively short (sag.); pygidial axis gently tapering.

PLATE 14

Figs 1–17 *Celmus michaelius* sp. nov. **1a–c**, It. 12853, cranidium, dorsal, left lateral, and anterior views, ×10 (figured Fortey & Owens 1975: fig. 1A).

2a–d, It. 26120, cranidium, dorsal, ventral, left lateral, and anterior views, ×10. **3**, It. 26121, cranidium, dorsal view, ×10. **4a–c**, It. 26123, **holotype**, cranidium, dorsal, ventral, and right lateral views, ×10. **5a–b**, It. 26122, cranidium, dorsal and left lateral views, ×10. **6a–c**, It. 26124, cranidium, dorsal, anterior, and right lateral views, ×7.5. **7a–b**, It. 26125, cranidium, dorsal and right lateral views, ×7.5. **8a–b**, It. 26126, cranidium, left lateral and dorsal views, ×10. **9a–b**, It. 26127, cranidium, left lateral and dorsal views, ×10. **10**, It. 26128, right librigena, external view, ×10. **11**, It. 26129, left librigena, external view, ×10. **12**, It. 26130, left librigena, external view, ×10. **13**, It. 26131, left librigena, external view, ×10. **14**, It. 26132, left librigena, external view, ×10. **15**, It. 26133, left librigena, external view, ×10. **16**, It. 26134, left librigena, external view, ×10. **17**, It. 26135, right librigena, internal view, ×10. view, ×15.

Figs 6, 7, 9, 10 *Phaseolops ceryx* sp. nov. **6**, It. 12856, cranidium, dorsal view, ×15. **7a–b**, It. 12857, cranidium, dorsal and left lateral views, ×15. **9**, It. 26116, cranidium, dorsal view, ×15; **10**, It. 26117, cranidium, dorsal view, ×15.

Fig. 8 *Proscharyia platylimbata* sp. nov. It. 26118, pygidium, dorsal view, ×15.

Fig. 11 *Glaphurus crinitus* sp. nov. It. 26119, cranidium, dorsal view, ×10.

HOLOTYPE. Cranidium, It. 26161 (Pl. 16, fig. 9); paratypes It. 26118, 26159, 26160, 26162–26167; questionably assigned specimens It. 26142, 26143.

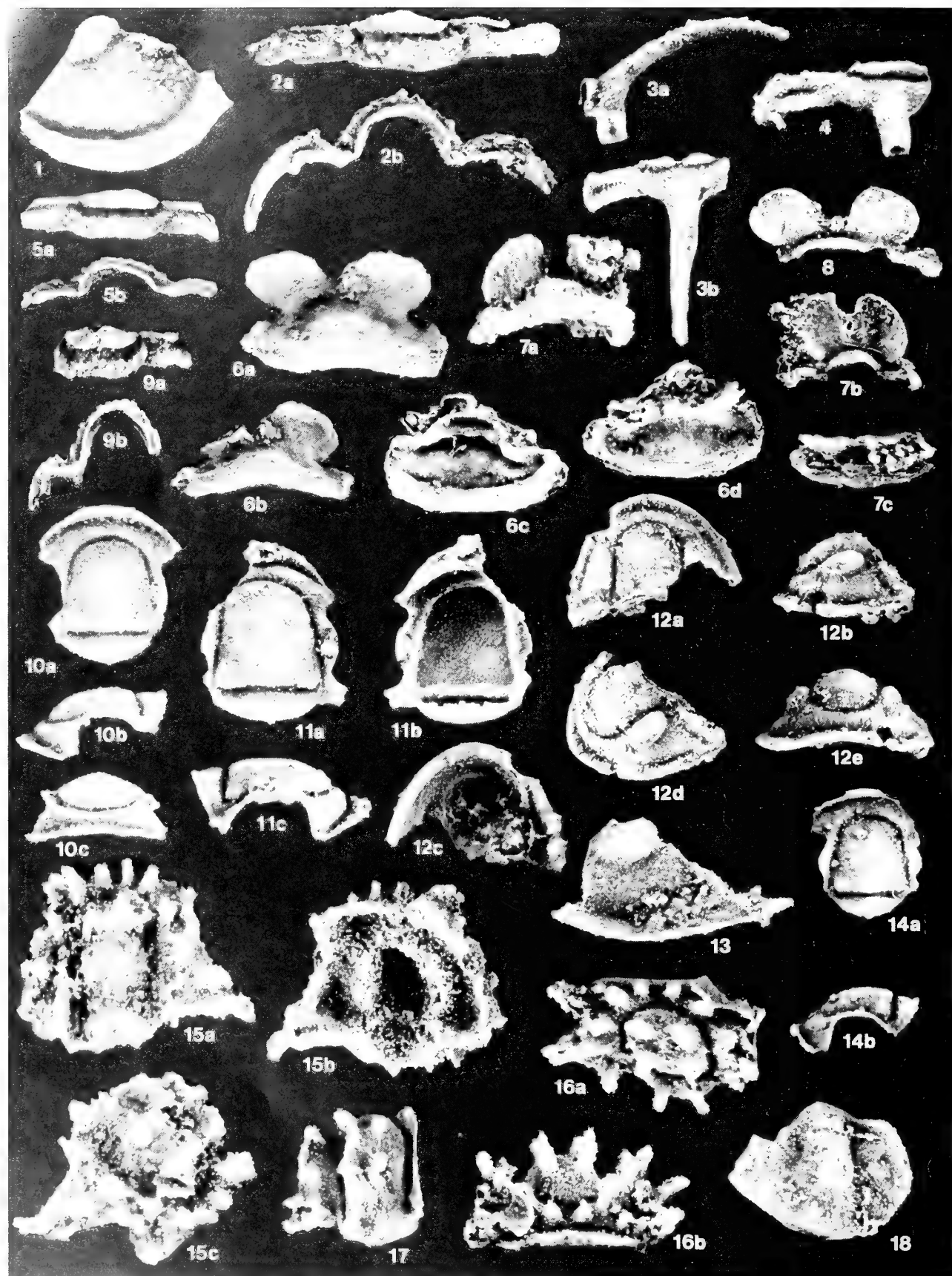
DISCUSSION. Peng (1990) gave a full description of the type species, *Proscharyia sinensis*, which is very like the new species in most features. Only points of difference require discussion here. The glabella of the type species tapers more strongly forwards (the closest specimen is that figured by Peng 1990: pl. 19, fig. 8) and the glabellar furrows are more strongly incised. On the Irish specimens only the posterior glabellar furrow is visible, whereas two or three pairs are seen on the Chinese species; however, the latter are known from internal moulds, on which glabellar furrows are usually clearer. The palpebral lobes of the Tourmakeady species are further from the glabella, such that the width of the interocular cheek is well over half that of the adjacent glabella (tr.), while it is under half in the Chinese species. The divergence of the anterior branches of the facial sutures is concomitantly less, and on some specimens (Pl. 16, fig. 8) they hardly diverge at all. However, on *P. platylimbata* the preglabellar field is much shorter (sag.) relative to the length of the anterior border. On *P. sinensis* the length of the preglabellar field exceeds that of the border as measured along the sagittal line, whereas on *P. platylimbata* the border is the longer. Pygidia of *P. platylimbata* are very similar to those of *P. sinensis* and both are unusual among post-Cambrian trilobites in having well-defined segments which extend all the way to the pygidial margin. The better definition of the pleural and interpleural furrows on the Chinese species is probably a consequence of the internal mold preservation on which the species was based.

Family RAYMONDINIDAE Clark, 1924

Glaphuridae Hupé, 1953.

DISCUSSION. As outlined by Ludvigsen and Westrop (*in* Ludvigsen et al., 1989: 61), Lochman-Balk's (*in* Moore, 1959) *Treatise* classification of Raymondinidae included ten Marjuman genera together with the late Sunwaptan *Raymondina*. Palmer (1962) and Rasetti (1965) transferred most of these taxa to Cedariidae, and Ludvigsen and Westrop considered the family Raymondinidae to be monotypic. As such, it contained only three species, known only from cranidial (in one case cephalic) material. Ludvigsen and Westrop's illustrations, however, reveal essential correspondence in most cephalic features between *Raymondina* and the Ordovician *Glaphurus*.

Most striking is the shared modification of the basal glabellar area, in which S1 is isolated from the axial furrow and aligned exsagittally, L1 and L2 are merged, and L2 is gently swollen. A second prominent similarity is the occurrence in either taxon of medially yolked librigenae. This was established for *Glaphurus* by



Whittington (1963: 52, pl. 8, fig. 14) and is confirmed by the Tourmakeady material (Pl. 17, fig. 1c, 1e). The same condition in *Raymondina immarginata* has been illustrated by Ludvigsen and Westrop (in Ludvigsen *et al.*, 1989, pl. 50, figs 13, 14). Finally, the genera are almost identical in overall cephalic/cranidial dimensions and distribution of features (e.g., forward eye position, median occipital node on anterior edge of L0). There is every reason to consider these shared character-states synapomorphic, and the genera closely related.

As a consequence, separation at the familial level is artificial. Retention of Glaphuridae would result in taxonomic pseudoextinction of Raymondinidae across the Cambrian-Ordovician boundary. Hence, Glaphuridae is placed in subjective junior synonymy of Raymondinidae, which is recognized as a clade with a stratigraphic range from uppermost Cambrian to Upper Ordovician.

Genus *GLAPHURUS* Raymond, 1905

TYPE SPECIES. *Arionellus pustulatus* Walcott, 1877, Lower Ordovician, New York State; by original designation (see Shaw 1968 for complete documentation of the species).

OTHER SPECIES. *Glaphurus alimbeiticus* Balashova, 1961, Tremadoc, Kazakhstan; *G. coronatus* Maksimova in Nikiforova, 1955, Tremadoc (Uskut Stage), Siberia; *G. divisus* Whittington, 1963, Whiterockian, western Newfoundland; *G. latior* Ulrich, 1930, Alabama and Virginia; *Glaphurus* sp. of Ross (1972: 31).

***Glaphurus crinitus* sp. nov.** Pl. 17, figs 1–17

1975 *Glaphurus* sp., Fortey & Owens : 230, fig. 1C.

ETYMOLOGY. Latin for hairy.

DIAGNOSIS. *Glaphurus* with densely tuberculate exoskeletal surface and tubercles of two sizes; glabella subrectangular; S2 not pit-like.

HOLOTYPE. Cephalon, It 26177 (Pl. 17, fig. 1); paratypes It 12855, 26119, 26178–26192.

DESCRIPTION. Cranidium trapezoidal in outline, with maximum width at posterior border, being 1.5–1.6 times the sagittal length (excluding anterior spines) in dorsal view in mature cranidia, and somewhat less in immature ones; entire silicified cephalon shows broad anterior arch (Pl. 17, fig. 1c) and that the free cheeks in life position were steeply declined, with the genal spines directed outwards; glabella occupies three-quarters cranidial length, and less than half its width, its outline rounded-subrectangular, widest at midlength circumscribed by deep furrows; S0 is of similar depth; L0 with median tubercle positioned immediately behind the furrow;

glabellar furrows emphasized as smooth patches of the exoskeleton; S1 shows a deepened, exsagittally aligned inner portion, whereas the shallow outer part runs approximately transversely towards the axial furrow; the deepened part amounts to 20% of glabellar length; S2 is short, slightly backward-directed; the short eyes are positioned anterior to S2, and the transverse distance between them is twice that of the intervening glabella; preglabellar field with length (sag.) as seen in dorsal view) similar to that of L0, down-sloping and bulging-convex; deep cranidial border furrow; the anterior border carries long, stout, anteriorly splayed spines; no border is perfectly preserved, but the bases of four such spines are seen separated by shorter spines; the anterior cranidial margin lies beneath these spines.

Librigenae without connective sutures along narrow doublure, which apparently lacks terrace lines; facial suture cuts posterior border very close to genal spine (Pl. 17, fig. 13), and runs inwards-forwards from there, arching outwards gently at middle of postocular section; at the genal angle there is a very deep pit in the doublure (Pl. 17, fig. 11b); eye elevated on a socle, which is deeper anteriorly; the structure of the lateral border is complex: dorsally it carries an array of alternating stout and small spines like those on the cranidial border; beneath this there is another row of tiny spines which run all the way around the cephalic margin and finish under the genal spine (Pl. 17, figs 1c, 15b); below this again, at the edge of the doublure, there is a minutely scalloped edge (Pl. 17, figs 11b, 15b); genal spine short and stout, carrying many smaller spines.

Sculpture of densely packed tubercles of two sizes; a thoracic segment (Pl. 17, fig. 16) carries similar tubercles on the axis and posterior part of the pleurae; it resembles the anterior segment of *G. pustulatus*, as figured by Shaw (1968, pl. 8, fig. 9).

Small cranidia (Pl. 17, figs 8–10) have narrower glabellae than larger ones, and posterior glabellar furrow is of more usual form, curving inwards and backwards; the smallest cranidium (Pl. 17, fig. 10) has a median occipital spine.

Hypostome and pygidium unknown.

DISCUSSION. This stratigraphically early *Glaphurus* species retains several plesiomorphic characters: the glabella is subrectangular, while the anterior glabellar furrow is not pit-like, and the posterior furrow shorter (exsag.) than is the case in the type species, *G. pustulatus*, which has a rounded glabella. The Tremadocian species *G. alimbeiticus* Balashova, 1961, from Kazakhstan, has an even more transverse anterior glabellar margin. The sculpture on this species, and on *G. pustulatus*, is much coarser than on the Irish species. The closest species is probably *G. divisus* Whittington, 1963, from western Newfoundland, which, however, has a rounded glabella like the type species, and lacks the anterior cephalic arch of *G. crinitus*. Whittington (1963: pl. 9, fig. 3) also illustrated three pairs of conspicuously large tubercles on the pre-occipital glabella which are more prominent than their counterparts in *G. crinitus*.

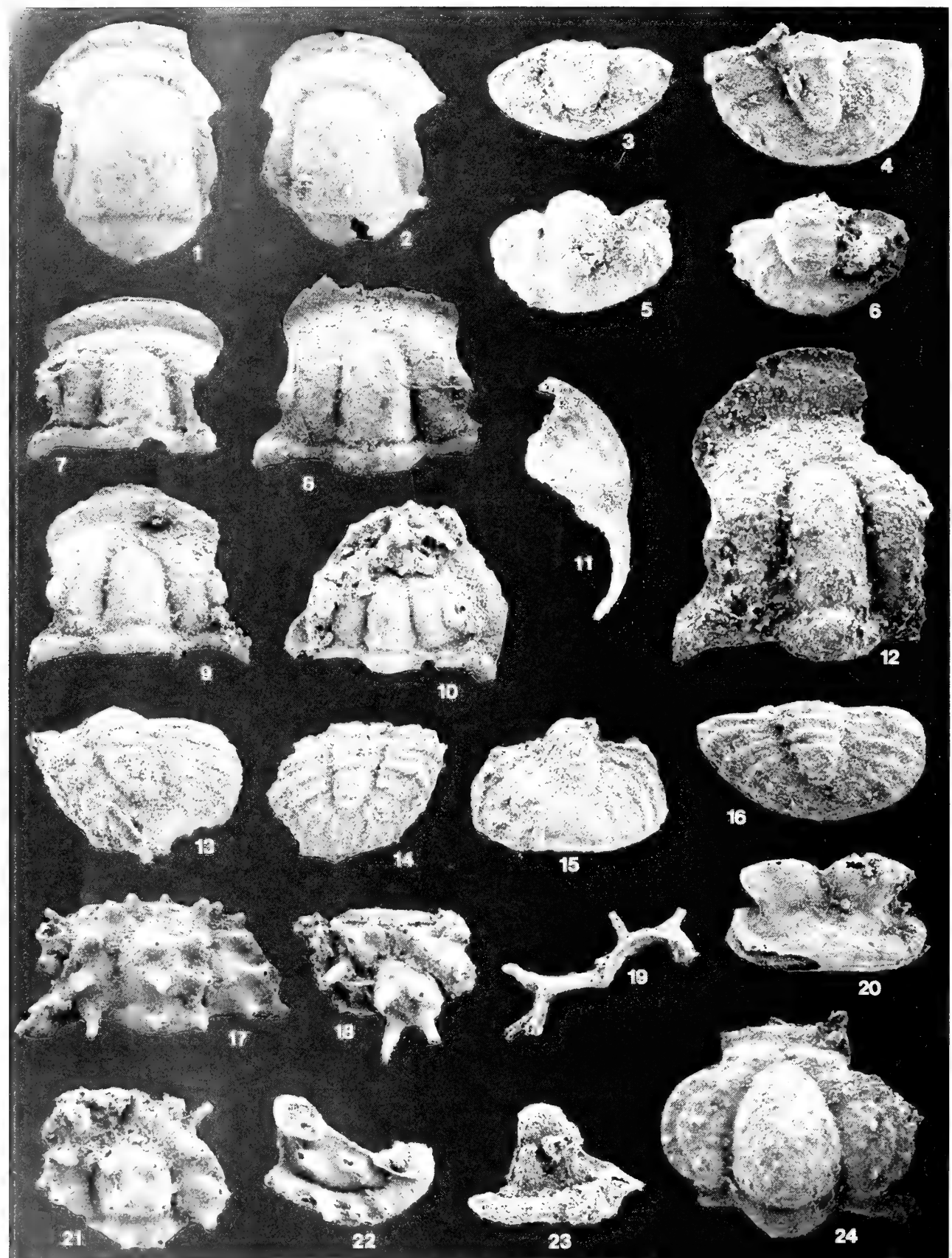
PLATE 15

Figs 1, 2–9 *Celmus michaelmus* sp. nov. 1, It. 26136, left librigena, external view, $\times 7.5$. 2a–b, It. 26137, thoracic segment, dorsal and anterior views, $\times 10$. 5a–b, It. 26138, thoracic segment, dorsal and anterior views, $\times 10$. 6a–d, It. 26139, pygidium (specimen broken slightly during photography), posterodorsal, posterior, ventral, and dorsal views, $\times 12$ and $\times 10$. 7a–c, It. 26140, pygidium, posterior, anterior, and dorsal views, $\times 12$, $\times 10$, $\times 10$. 8, It. 12854, pygidium, anterior view, $\times 10$ (figured Fortey & Owens 1975: fig. 1B). 9a–b, It. 26141, thoracic segment, dorsal and anterior views, $\times 10$.

Figs 3, 4 ?*Proscharvia platylimbata* sp. nov. 3a–b, It. 26142, thoracic segment, left lateral and dorsal views, $\times 15$. 4, It. 26143, thoracic segment, dorsal view, $\times 15$.

Figs 10–14, 18 *Phaseolops ceryx* sp. nov. 10a–c, It. 26144, cranidium, dorsal, left lateral, and anterior views, $\times 15$. 11a–c, It. 26145, holotype, cranidium, dorsal, ventral, and right lateral views, $\times 15$. 12a–e, It. 26146, cephalon, dorsal, left lateral, ventral, oblique, and anterior views, $\times 10$. 13, It. 26147, left librigena, external view, $\times 15$. 14a–b, It. 26148, cranidium, dorsal and left lateral views, $\times 15$. 18, It. 26149, pygidium, dorsal view, $\times 15$.

Figs 15–17 *Dimeropyge? ericina* sp. nov. 15a–c, It. 26150, holotype, cranidium, dorsal, ventral, and oblique views, $\times 15$. 16a–b, It. 26151, cranidium, dorsal and anterior views, $\times 15$. 17, It. 26152, cranidium, dorsal view, $\times 15$.



Family **TROPIDOCORYPHIDAE** Pribyl, 1946
 Genus **PHASEOLOPS** Whittington, 1963

TYPE SPECIES. *Phaseolops sepositus* Whittington, 1963, from the Cow Head Group (Whiterockian), western Newfoundland, Canada; by monotypy.

DISCUSSION. Whittington (1963) described *Phaseolops sepositus* as the oldest known proetid species, assigning it to the subfamily Phacopidellinae Hupé, 1953 (now generally regarded as a synonym of Tropidocoryphinae Pribyl, 1946). Hu subsequently (1971) erected *P. conus*, a species based upon mis-associated aulacopleurid cranidia and tropidocoryphid librigenae and pygidia (see Adrain & Chatterton 1995: 310). The taxon is not related to *P. sepositus*, but rather is an aulacopleurid, and will be revised in a forthcoming work by J.M.A. The only species subsequently assigned to the genus are *P. krafti* Šnajdr, 1983, and *Proetus? primulus* Barrande, 1872 (see Šnajdr 1983), from the Czech Republic. Neither is adequately known, but it is possible that they belong here.

Owens (1973a: 80, text-fig. 11) considered *Phaseolops ceryx* to represent the oldest and most primitive known proetid, and derived *P. sepositus* from it with question. He subsequently (in Owens & Hammann 1990) transferred *P. sepositus* to the aulacopleuroidean family Rorringoniidae. For reasons given below, we consider *P. ceryx* and *P. sepositus* to be closely related, and to represent the base of the radiation of at least the tropidocoryphid proetoids.

Phaseolops ceryx differs from the Newfoundland type species in several obvious respects, but all seem related to effacement. *Phaseolops ceryx* is more similar to younger tropidocoryphids in the lack of prominent tuberculate sculpture and the expression of the glabellar furrows mainly as shallow, smooth depressions on the exoskeleton. *Phaseolops sepositus* differs from virtually all younger taxa in the possession of deep, slot-like glabellar furrows and a robust tuberculate sculpture on the preglabellar area and librigenal field. The species, however, are almost identical in relative cephalic proportions. Particularly striking is the abrupt lateral deflection of the anterior section of the facial suture, so that it is held almost vertically when the cranidium is oriented with the palpebral lobe horizontal (Pl. 15, figs 10b, 11c; cf. Whittington 1963: pl. 5, figs 2, 5). Also compelling is the size and position of the median occipital tubercle. In most subsequent tropidocoryphids, this structure is set at more or less half the sagittal length of the occipital ring. In both *P. ceryx* (Pl. 15, figs 10a, 11a, 14a) and *P. sepositus* (Whittington 1963: pl. 5, fig. 4), it is set directly at the posterior margin, and actually protrudes backward from the margin. We regard these conspicuous shared features as synapomorphic, and consider the species, which are essentially contemporaneous, to be congeneric.

Beyond the conventional proetoid morphology of *P. ceryx*, possibly a key indicator of the affinities of *Phaseolops* lies in the thoracic structure of *P. sepositus*. Early tropidocoryphids possess thoracic

pleural tips in which the pleural furrow shallows abruptly adaxial to the tip, and the tip itself is produced laterally as a small, sinuous, posterolaterally directed spine. The morphology is perhaps best observed in *Stenoblepharum* (e.g., *S. warburgae* (Pribyl, 1946), see Owens 1973b, fig. 9C), but is present also in species presently assigned to *Decoroproetus* (e.g., *D. asellus* (Esmark, 1833), see Owens 1973b, fig. 4F) and species of *Aschetoptelis* (e.g., *A. bockelie* Owens, 1973b, fig. 2A). Exactly the same morphology is seen in *P. sepositus* (Whittington 1963: pl. 5, fig. 1), but not in *Rorringonia*, which has pointed but not spinose pleural tips (Owens 1981: pl. 1, fig. a). In addition, *P. sepositus* has the general proetoidian thoracic segment number of 10, in agreement with all tropidocoryphids, but in contrast to the 9 segments seen in *Rorringonia*. For these reasons, *Phaseolops* is herein regarded as a tropidocoryphid.

The genus may prove to be of significance in determining the affinities of Proetidea. The sister taxon of the group is at present entirely obscure. If the proposed relationship between *Phaseolops ceryx* and *P. sepositus* is correct, it is conceivable that the tuberculate morphology of the latter, with glabellar furrows deeply incised, is a clue to the nature of the sister taxon. Effaced, 'generalized' trilobites are not unknown in the Ibexian. They are generally assigned to the 'hystricurines,' a group which is at present little more than a polyphyletic catchall, and none described thus far share convincing apomorphies with the proetoids. The reason for this may be that following from the morphology of *P. sepositus*, the Lower Ordovician or Upper Cambrian precursor to the group was a non-effaced, tuberculate taxon. Such taxa, including most of the 'hystricurines,' are common in the Sunwaptan and Ibexian. Support for this scenario lies in the sporadic retention of at least tuberculate librigenae in otherwise advanced Ordovician tropidocoryphids (e.g., *Decoroproetus bodai* Owens, 1973b: fig. 4K).

***Phaseolops ceryx* sp. nov.**

Pl. 13, figs 6, 7, 9, 10; Pl. 15,
 figs 10–14, 18; Pl. 16, figs 1–6

1973a 'Tourmakeady cranidium', Owens: 80, text-fig. 11.

1975 *Decoroproetus?* sp., Fortey & Owens: 229, fig. 1d-1f.

ETYMOLOGY. From the Greek noun *keryx*, a herald.

DIAGNOSIS. Glabellar furrows very shallow, nearly effaced; eye socle simple and librigenal field lacking sculpture.

HOLOTYPE. It. 26145 (Pl. 15, fig. 11); paratypes It. 12856, 12857, 26116, 26117, 26144, 26146–26149, 26153–26158.

DESCRIPTION. Cranidium with width across midlength of palpebral lobes approx. 75% of length (sag.); glabella and L0 occupying 75–77% of sagittal length of cranidium; glabella with maximum width across posterior, approx. equal to length (excluding L0); anterior

PLATE 16

Figs 1–6 *Phaseolops ceryx* sp. nov. **1**, It. 26153, cranidium, dorsal view, $\times 27$. **2**, It. 26154, cranidium, dorsal view, $\times 33$. **3**, It. 26155, pygidium, dorsal view, $\times 27$. **4**, It. 26156, transitory pygidium, dorsal view, $\times 40$. **5**, It. 26157, pygidium, dorsal view, $\times 27$. **6**, It. 26158, pygidium, dorsal view, $\times 27$.

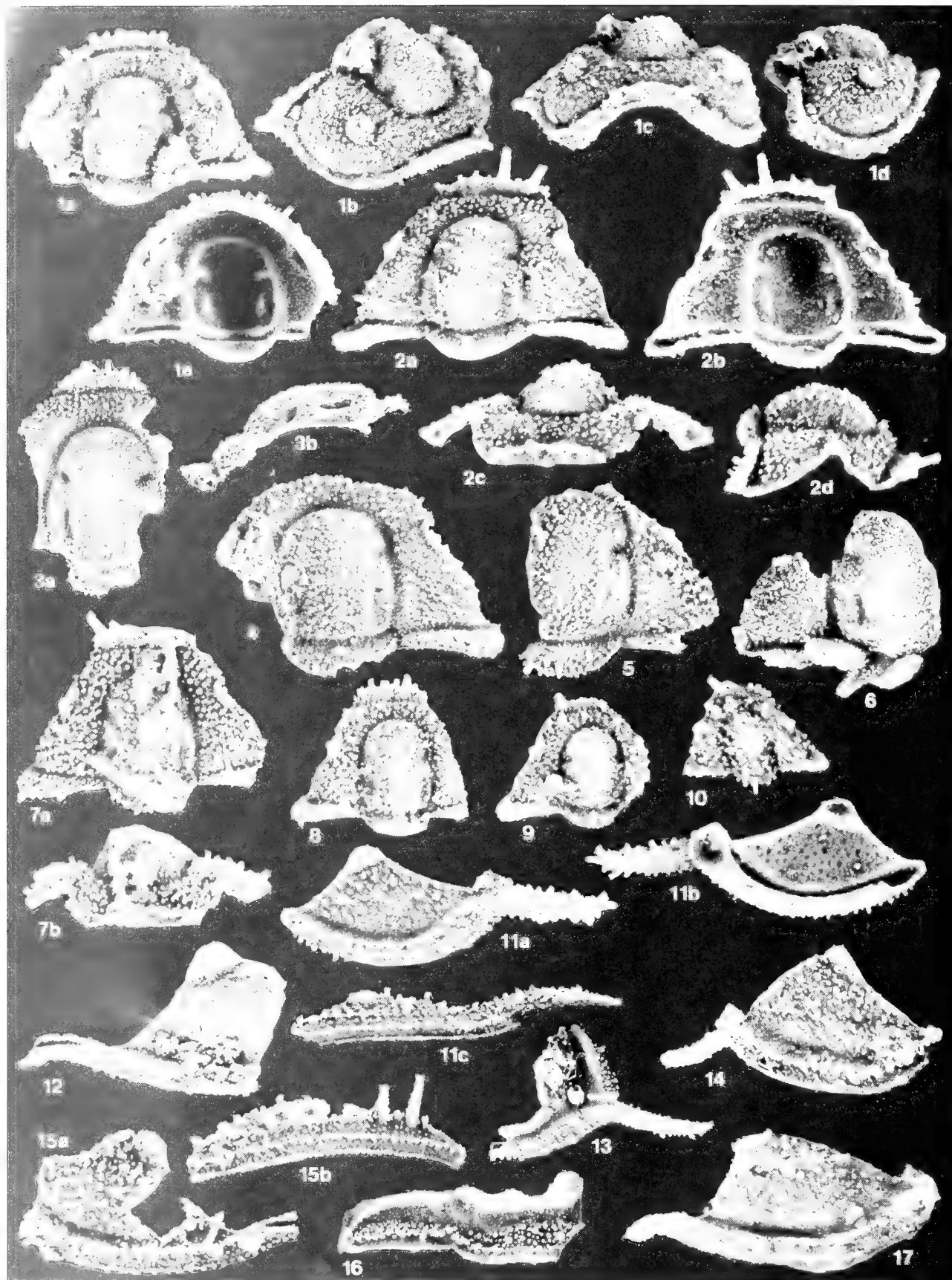
Figs 7–10, 12–16 *Proscarya platylimbata* **7**, It. 26159, cranidium, dorsal view, $\times 33$. **8**, It. 26160, cranidium, dorsal view, $\times 33$. **9**, It. 26161, holotype, cranidium, dorsal view, $\times 33$. **10**, It. 26162, cephalon, dorsal view, $\times 27$. **12**, It. 26163, cranidium, dorsal view, $\times 60$. **13**, It. 26164, pygidium, dorsal view, $\times 27$. **14**, It. 26165, pygidium, dorsal view, $\times 33$. **15**, It. 26166, pygidium, dorsal view, $\times 40$. **16**, It. 26167, pygidium, dorsal view, $\times 33$.

Figs 11, 20 *Celmus michaelmus* sp. nov. **11**, It. 26168, right librigena, external view, $\times 27$. **20**, It. 26169, pygidium, posterodorsal view, $\times 33$.

Figs 17–19, 21–23 *Dimeropyge?* *ericina* sp. nov. **17**, It. 26170, cranidium, dorsal view, $\times 23$. **18**, It. 26171, cranidium, dorsal view, $\times 33$. **19**, It. 26172, thoracic segment, anterior view, $\times 27$. **21**, It. 26173, cranidium, dorsal view, $\times 27$. **22**, It. 26174, left librigena, external view, $\times 27$. **23**, It. 26175, left librigena, external view, $\times 33$.

Fig. 24 *Oopsites hibernicus* (Reed in Gardiner & Reynolds, 1909) It. 26176, cranidium, dorsal view, $\times 40$.

All figures are scanning electron micrographs.



sections of facial suture with sharp anterior divergence in front of palpebral lobes; cranium moderately vaulted, anterior section of facial suture running subparallel to rear of L0 in lateral profile; cephalic border of continuous even width; cranidial anterior border longer medially than laterally due to oblique course of connective sutures; anterior border with considerable dorsal convexity, length (sag.) about two thirds L0, sculpture smooth; anterior border furrow short (sag., exsag.), posterior slope vertical and incised, anterior part with gentler slope leading onto border; preglabellar field slightly longer (sag.) than anterior border, with gentle dorsal convexity and smooth sculpture; axial furrows moderately convergent anteriorly, bowed out slightly around L1, running without interruption into anteriorly convex preglabellar furrow; axial and preglabellar furrows deeply incised, preglabellar furrow with very slight lengthening (sag.) medially; interocular fixigena reduced to narrow, smooth, slope from palpebral lobe to axial furrow; palpebral furrow absent; palpebral lobe elongate but very narrow, lacking obvious sculpture; posterior fixigena reduced to small, narrow triangle; glabella subtrapezoidal, with smooth dorsal sculpture; glabellar furrows very shallow but discernible; L1 with slight independent inflation; S1 relatively elongate (exsag.) and directed posteromedially in distal part, bifurcate proximally, posterior branch nearly reaching S0; S2 originating laterally opposite the anterior third of the palpebral lobe, much shorter than L1, directed posteromedially, not running proximally as far as S1; S3 similar in shape to S2, originating opposite the anterior section of the facial suture in front of the palpebral lobe, anteromedially directed; S0 slightly longer (sag., exsag.) than preglabellar furrow, deep, not as incised as axial furrows, slightly longer behind L1; L0 elongate and shelflike, longest medially, with smooth dorsal sculpture; median occipital node small, protruded posteriorly from posterior margin; axial furrow shallowed greatly opposite L0; posterior border furrow relatively shallow; posterior border short (exsag.), dorsally convex; occipital doublure underlying three quarters the length of L0; fossula not obvious.

Librigenal field with width at midlength of eye 35–40% of exsagittal length, sculpture smooth; eye socle not evident; eye large, width about 60% of exsagittal length; lateral border furrow and posterior border furrow of similar moderate depth; lateral border furrow shallowing abruptly in front of base of genal spine; lateral border not inflated, low dorsal convexity, with single terrace line set laterally and running subparallel to margin; genal spine relatively short and subtriangular, tapering distally to sharp tip; doublure with four or five linear, parallel, and evenly spaced terrace lines.

Rostral plate small and subtriangular, librigenal terrace lines continuous, with slight offset across connective sutures.

Hypostome and thorax unknown.

Pygidium with sagittal length 62–68% of anterior width; axis 68–69% of sagittal length of pygidium; three axial rings present, becoming increasingly less well defined posteriorly; first ring furrow well impressed, second very shallow; axial furrows gently convergent, forming broad arc posteriorly to completely define rear of axis; three pleural and two interpleural furrows defined, posteriormost almost completely effaced; furrows stop short of pygidial margin, but no true border developed.

DISCUSSION. *Phaseolops ceryx* is distinguished from *P. sepositus* in the effacement of its glabellar furrows, lack of tuberculate sculpture on preglabellar and librigenal fields, lack of eye socle, and possession of pygidium with a smooth versus broken margin.

ACKNOWLEDGEMENTS Preparation of this study was funded by NERC grant GR3/09654. We are grateful to D. J. Siveter (University Museum, Oxford) for review of the manuscript.

REFERENCES

- Adrain, J. M. & Chatterton, B. D. E. 1995. The otarianine trilobites *Harpidella* and *Maurotarian*, with species from northwestern Canada, the United States, and Australia. *Journal of Paleontology*, Lawrence, **69**: 307–326.
- & Kloc, G. J. 1997. Lower Devonian aulacoplateuroidean trilobites from Oklahoma. *Journal of Paleontology*, **71** (3).
- Ahlberg, P. 1992. Agnostid trilobites from the Lower Ordovician of southern Sweden. *Transactions of the Royal Society of Edinburgh: Earth Sciences*, **83**: 539–70.
- Angelin, N. P. 1854. *Palaeontologica Scandinavica. I: Crustacea formationis transitionis*. Fascicule 2: 21–92, 41 pls. Lipsiae.
- Balashova, E. A. 1961. Some Tremadoc trilobites of the Aktyubinsk Region. *Trudy Geologicheskii Instituta SSSR*, Moscow, **18**: 102–145, pls 1–4. [in Russian]
- Barrande, J. 1872. *Système silurien du centre de la Bohême. Ière Partie; Recherches paléontologiques. I. Supplément*, 647 pp, pls 1–35. Prague & Paris.
- Barton, D. C. 1916. A revision of the Cheirurinae, with notes on their evolution. *Washington University Studies, Scientific Series*, St. Louis, **3**: 101–152.
- Billings, E. 1865. *Palaeozoic fossils*. Vol. I (4): 169–344. Geological Survey of Canada, Montreal.
- Bradley, J. H. 1925. Trilobites of the Beckmantown in the Phillipsburg region of Quebec. *Canadian Field Naturalist*, Ottawa, **39**: 5–9.
- Brathwaite, L. F. 1976. Graptolites from the Lower Ordovician Pogonip of western Utah. *Geological Society of America Special Papers*, New York, **166**: 1–106, pls 1–21.
- Bridge, J. 1931. Geology of the Eminence and Cardareva quadrangles. *Missouri Bureau of Geology and Mines*, St. Louis, 2nd Series, **24**: 1–228.
- Bruton, D. L. 1983. The morphology of *Celmus* (Trilobita) and its classification. *Special Papers in Palaeontology*, London, **30**: 213–219.
- Burmeister, H. 1843. Die Organisation der Trilobiten. Georg Reimer, Berlin, 147 p.
- Chatterton, B. D. E. 1994. Ordovician proetid trilobite *Dimeropyge*, with a new species from northwestern Canada. *Journal of Paleontology*, Lawrence, **68**: 541–556.
- & Ludvigsen, R. 1976. Silicified Middle Ordovician trilobites from the South Nahanni River area, District of Mackenzie, Canada. *Palaeontographica, Abteilung A*, Stuttgart, **154**: 1–106.
- Clark, T. H. 1924. The paleontology of the Beckmantown Series at Lévis, Quebec. *Bulletins of American Paleontology*, Ithaca, **10**: 1–134, pls 1–9.
- Cocks, L. R. M. & Fortey, R. A. 1990. Biogeography of Ordovician and Silurian faunas. In: Scotese, C.R. and McKerrow, W.S. (eds), *Palaeozoic palaeogeography and biogeography. Memoir of the Geological Society of London*, **12**: 97–104.
- Cooper, B. N. 1953. Trilobites from the Lower Champlainian formations of the Appalachian Valley. *Geological Society of America Memoir*, Baltimore, **55**: 1–69, pls 1–19.
- Cooper, R. A. & Fortey, R. A. 1982. The Ordovician graptolites of Spitsbergen. *Bulletin of the British Museum (Natural History)*, London, *Geology*, **36**: 157–302.
- & Lindholm, K. 1991. A precise worldwide correlation of early Ordovician graptolite sequences. *Geological Magazine*, Cambridge, **127**: 497–525.
- Dalman, J. W. 1827. Om Palaeaderna eller de så kallade Trilobiterna. *Kungliga Svenska Vetenskapsakademien Handlingar*, Stockholm, **1826**: 113–152, 226–294, pls 1–6.
- Dean, W. T. 1971. The trilobites of the Chair of Kildare Limestone (Upper Ordovician) of eastern Ireland. Part 1. *Palaeontographical Society Monograph*, London, **531**: 1–60.

PLATE 17

- Figs 1–17** *Glaphurus crinitus* sp. nov. **1a–e**, It. 26177, holotype, cephalon, dorsal, oblique, anterior, right lateral, and ventral views, $\times 10$. **2a–d**, It. 26178, cranium, dorsal, ventral, anterior, and right lateral views, $\times 15$. **3a–b**, It. 26179, cranium, dorsal and left lateral views, $\times 15$. **4**, It. 26180, cranium, dorsal view, $\times 15$. **5**, It. 26181, cranium, dorsal view, $\times 10$. **6**, It. 26182, cranium, dorsal view, $\times 10$. **7a–b**, It. 26183, cranium, dorsal and anterior views, $\times 15$. **8**, It. 26184, cranium, dorsal view, $\times 15$. **9**, It. 12855, cranium, dorsal view, $\times 15$ (figured Fortey & Owens 1975: fig. 1C). **10**, It. 26185, cranium, dorsal view, $\times 15$. **11a–c**, It. 26186, left librigena, external, internal, and ventrolateral views, $\times 15$. **12**, It. 26187, left librigena, external view, $\times 15$. **13**, It. 26189, cranidial fragment and left librigena, external view, $\times 10$. **14**, It. 26190, right librigena, external view, $\times 10$. **15a–b**, It. 26188, right librigena, external and ventrolateral views, $\times 15$. **16**, It. 26191, thoracic segment, dorsal view, $\times 10$. **17**, It. 26192, left librigena, external view, $\times 10$.

- 1973. The Lower Palaeozoic stratigraphy and faunas of the Taurus Mountains near Beysehir, Turkey. III. The trilobites of the Sobova Formation (Lower Ordovician). *Bulletin of the British Museum (Natural History), London, Geology*, **24**: 279–348.
- Dewey, J. F., Rickards, R. B. & Skevington, D. 1970. New light on the age of Dalradian deformation and metamorphism in western Ireland. *Norsk Geologisk Tidsskrift*, Oslo, **50**: 19–44.
- Droser, M. L., Fortey, R. A. & Xing Li. 1996. The Ordovician radiation. *American Scientist*, New Haven, **84**: 122–131.
- Esmark, M. T. 1833. Om nogle nye Arter af Trilobiter. *Magazin Naturvidensk Christiania*, **11**: 268–270, pl. 7.
- Fortey, R. A. 1974. A new pelagic trilobite from the Ordovician of Spitsbergen, Ireland, and Utah. *Palaeontology*, London, **17**: 111–124.
- 1975a. The Ordovician trilobites of Spitsbergen. II. Asaphidae, Nileidae, Raphiophoridae and Telephinidae of the Valhallfonna Formation. *Norsk Polarinstitut Skrifter*, Oslo, **162**: 1–207.
- 1975b. Early Ordovician trilobite communities. *Fossils and Strata*, Oslo, **4**: 339–360.
- 1979. Early Ordovician trilobites from the Catoche Formation (St. George Group), western Newfoundland. *Geological Survey of Canada Bulletin*, Ottawa, **321**: 61–114.
- 1980. The Ordovician trilobites of Spitsbergen. III. Remaining trilobites of the Valhallfonna Formation. *Norsk Polarinstitut Skrifter*, Oslo, **171**: 1–163.
- 1983. Cambrian-Ordovician trilobites from the boundary beds in western Newfoundland and their phylogenetic significance. *Special Papers in Palaeontology*, London, **30**: 179–211.
- & Droser, M. L. 1996. Trilobites at the base of the Middle Ordovician, western United States. *Journal of Paleontology*, Lawrence, **70**: 73–99.
- & Owens, R. M. 1975. Proetida – a new order of trilobites. *Fossils and Strata*, Oslo, **4**: 227–239.
- & — 1987. The Arenig Series in South Wales. *Bulletin of the British Museum (Natural History), London, Geology*, **41**: 69–307.
- & Shergold, J. H. 1984. Early Ordovician trilobites of the Nora Formation, central Australia. *Palaeontology*, London, **27**: 315–366, pls 38–46.
- Gardiner, C. I. & Reynolds, S. H. 1909. On the igneous and associated sedimentary rocks of the Tournakedy district (Co. Mayo), with a palaeontological appendix by F. R. C. Reed. *Quarterly Journal of the Geological Society, London*, **65**: 104–156.
- & — 1910. The igneous and associated sedimentary rocks of the Glensaul district (Co. Galway), with a palaeontological appendix by F. R. C. Reed. *Quarterly Journal of the Geological Society, London*, **66**: 253–279.
- Harrington, H. J. & Leanza, A. F. 1957. Ordovician trilobites of Argentina. *Special Publication of the University of Kansas, Department of Geology*, Lawrence, **1**: 1–276.
- Hawle, I. & Corda, A. J. C. 1847. *Prodrom einer Monographie der böhmischen Trilobiten*. 176 pp. Prague.
- Henderson, R. A. 1983. Early Ordovician faunas from the Mount Windsor Subprovince, northeastern Queensland. *Memoirs of the Australasian Association of Palaeontologists*, Brisbane, **1**: 145–175.
- Hintze, L. F. 1953. Lower Ordovician trilobites from western Utah and eastern Nevada. *Utah Geological and Mineralogical Survey Bulletin*, Salt Lake City, **48**: 1–249.
- Holliday, S. 1942. Ordovician trilobites from Nevada. *Journal of Paleontology*, Menasha, **16**: 471–478, pls 73, 74.
- Horny, R. & Bastl, F. 1970. *Type specimens of fossils in the National Museum, Prague*. Volume 1. Trilobita. 354 pp, pls 1–20. Museum of Natural History, Prague.
- Howell, B. F. 1935. Cambrian and Ordovician trilobites from Hérault, southern France. *Journal of Paleontology*, Menasha, **9**: 218–221.
- Hu, C.-H. 1971. Ontogeny and sexual dimorphism of Lower Paleozoic Trilobita. *Palaeontographica Americana*, Ithaca, **7**: 31–155, pls 7–26.
- Hughes, N. C., & Fortey, R. A. 1996. Sexual dimorphism in trilobites, with an Ordovician case study. In, Cooper, J.D., Droser, M.L., & Finney, S.C. (eds.), *Ordovician odyssey: short papers for the Seventh International Symposium on the Ordovician System. Pacific Section, Society for Sedimentary Geology*, Fullerton, Book **77**: 419–421.
- Hupé, P. 1953. Classe des Trilobites. In, Piveteau, J. (ed.), *Traité de Paléontologie*, **3**: 44–246. Paris.
- Ingham, J. K., Curry, G. B. & Williams, A. 1986. Early Ordovician Dounans Limestone fauna, Highland Border Complex, Scotland. *Transactions of the Royal Society of Edinburgh*, **76** (for 1985): 481–513.
- Jaanusson, V. 1956. On the trilobite genus *Celmus* Angelin, 1854. *Bulletin of the Geological Institutions of Uppsala*, Uppsala, **36**: 35–49.
- 1957. Unterordovizische Illaeniden aus Skandinavien. *Bulletin of the geological Institutions of the University of Uppsala*, Uppsala, **37**: 79–165.
- Jaekel, O. 1909. Über die Agnostiden. *Ztschrift der Deutschen Geologischen Gesellschaft*, **61**: 380–400.
- James, N. P. & Stevens, R. K. 1986. Stratigraphy and correlation of the Cambro-Ordovician Cow Head Group, western Newfoundland. *Geological Survey of Canada Bulletin*, Ottawa, **366**: 1–99.
- Koroleva, M. N. 1982. Ordovician trilobites of South-central Kazakhstan. Nedra, Moscow. 192 pp.
- Lane, P. D. 1971. British Cheiruridae (Trilobita). *Palaeontographical Society Monograph*, London, **530**: 1–95.
- Laurie, J. R., & Shergold, J. H. 1996. Early Ordovician trilobite taxonomy and biostratigraphy of the Emanuel Formation, Canning Basin, western Australia. *Palaeontographica, Abteilung A*, Stuttgart, **240**: 65–103.
- Linnarsson, J. G. O. 1869. Om Västergötlands Cambrika och Siluriska aflagringar. *Kungliga Svenska Vetenskapsakademien Handlingar*, Stockholm **8**: 1–89, pls 1, 2.
- Lisogor, K. A. 1995. Llanvirn trilobites from the Orovician of Betpak-Dali (southern Kazakhstan). *Vestnik kazakhskogo Natsional'nogo Tekhnicheskogo universiteta Geolo-Mineralogicheskie nauki, Alma-ata*, **4**: 110–115, pl. 1. [In Russian].
- Lochman, C. 1953. Notes on Cambrian trilobites – homonyms and synonyms. *Journal of Paleontology*, Menasha, **27**: 886–896.
- Ludvigsen, R. 1980. An unusual trilobite faunule from Llandeilio or lowest Caradoc strata (Middle Ordovician) of northern Yukon Territory. In, *Current Research, Part B. Geological Survey of Canada, Paper*, Ottawa, **80-1B**: 97–106.
- Westrop, S. R. & Kindle, C. H. 1989. Sunwaption (Upper Cambrian) trilobites of the Cow Head Group, western Newfoundland, Canada. *Palaeontographica Canadiana*, Toronto, **6**: 1–175.
- Mansuy, H. 1920. Nouvelle contribution à l'étude des faunas palaeozoiques et mesozoïques. *Mémoires du Service Géologique de l'Indochine*, Hanoi-Haiphong, **7**: 1–22, pls 1–3.
- Marek, L. 1952. Contribution to the stratigraphy and fauna of the uppermost part of the Králov Dvůr Shales (Ashgillian). *Sborník Ústředního Ústavu Geologického (Paleontology)*, Prague, **19**: 429–455.
- Mitchell C. E. & Maletz, J. 1995. Proposal for adoption of the base of the *Undulograptus austrodentatus* Biozone as a global Ordovician stage and series boundary level. *Lethaia*, Oslo, **28**: 317–331.
- Moore, R. C. 1959. *Treatise on Invertebrate Paleontology. Part O. Arthropoda I*. 560pp. Lawrence & Meriden.
- Morris, S. F. 1988. A review of British trilobites, including a synoptic revision of Salter's monograph. *Monograph of the Palaeontographical Society*, London, **574**: 1–316.
- Neuman, R. B. 1984. Geology and paleobiology of islands in the Ordovician Iapetus Ocean: review and implications. *Bulletin of the Geological Society of America*, Boulder, **95**: 1188–1201.
- Nielsen, A. T. 1995. Trilobite systematics, biostratigraphy and palaeoecology of the Lower Ordovician Komstad Limestone and Huk Formations, southern Scandinavia. *Fossils and Strata*, Oslo, **38**: 1–374.
- Nieszkowski, J. 1857. Versuch einer Monographie der in den silurischen Schichten der Ostseeprövinzen vorkommenden Trilobiten. *Archiv für die Naturkunde Liv, Ehst- und Kurlands*, Dorpat, **1**: 57–626, pls 1–3.
- Nikiforova, O. I. 1955. *Field atlas of the Ordovician and Silurian fauna of the Siberian Platform*. Moscow, 266 pp., 62 pls. [In Russian].
- Öpik, A. 1937. Trilobites aus Estland. *Acta et Commentationes Universitatis Tartuensis*, Tartu, **32**: 1–163.
- Osmólska, H. 1957. Trilobites from the Couvinian of Wydryszów (Holy Cross Mountains, Poland). *Acta Palaeontographica Polonica*, Warsaw, **2**: 53–77, pls 1–3.
- Owens, R. M. 1973a. British Ordovician and Silurian Proetidae (Trilobita). *Palaeontographical Society Monograph*, London, **535**: 1–98.
- 1973b. Ordovician Proetidae (Trilobita) from Scandinavia. *Norsk Geologisk Tidsskrift*, Oslo, **53**: 117–181.
- 1981. The Ordovician proetacean trilobite *Rorringtonia*. *Geological Magazine*, Cambridge, **118**: 89–94, pl. 1.
- Owens, R. M. & Hammann, W. 1990. Proetidae trilobites from the Cystoid Limestone (Ashgill) of NW Spain, and the suprageneric classification of related forms. *Paläontologische Zeitschrift*, Berlin, **64**: 221–244.
- Palmer, A. S. 1962. *Glyptagnostus* and associated trilobites in the United States. *United States Geological Survey Professional Paper*, Washington, **374-F**: 1–49.
- Peng, S. 1990. Tremadoc stratigraphy and trilobite faunas of northwestern Hunan. 2. Trilobites from the Panjiazhu Formation and the Maodaoyu Formation in Jiangnan Slope Belt. *Beringeria*, Würzburg, **2**: 55–171, pls 1–23.
- Pictet, F.-J. 1854. *Traité de Paléontologie*. 2nd edition. Vol. 2, 727 pp., pls 31–56.
- Poulson, C. 1946. Notes on Cambro-Ordovician fossils collected by the Oxford University Ellesmere Land Expedition, 1934–5. *Quarterly Journal of the Geological Society of London*, **102**: 299–337.
- Poulson, V. 1965. An early Ordovician trilobite fauna from Bornholm. *Meddelelser fra Dansk Geologisk Forening*, Copenhagen, **16**: 49–113, pls 1–9.
- Prantl, F. & Pribyl, A. 1949. A study of the superfamily Odontopleuracea nov. superfam. (Trilobites). *Rozpravy Ustředního Ústavu Geologického*, Prague, **12**: 1–221, pls 1–11.
- Pratt, B. R. 1992. Trilobites of the Marjuman and Steptoean stages (Upper Cambrian), Rabbitkettle Formation, southern Mackenzie Mountains, northwest Canada. *Palaeontographica Canadiana*, Toronto, **9**: 1–179.
- Pribyl, A. 1946. Příspěvek k poznání českých Proetid. *Rozpravy České Akademie Věd a Umení*, Prague, **55**: 1–37. [In Czech].
- Pudsey, C. J. 1984. Ordovician stratigraphy and sedimentology of the South Mayo Inlier. *Irish Journal of Earth Sciences*, Dublin, **6**: 15–45.
- Ramsköld, L. 1991. Pattern and process in the evolution of the Odontopleuridae

- (Trilobita). The Selenopeltinae and Ceratocephalinae. *Transactions of the Royal Society of Edinburgh: Earth Sciences*, **82**: 143–181.
- & Chatterton, B. D. E. 1991. Revision and subdivision of the polyphyletic 'Leonaspis' (Trilobita). *Transactions of the Royal Society of Edinburgh: Earth Sciences*, **82**: 333–371.
- & Werdelin, L. 1991. The phylogeny and evolution of some phacopid trilobites. *Cladistics*, Westport, **7**: 29–74.
- Rasseti, F. 1965. Upper Cambrian trilobite faunas of northeastern Tennessee. *Smithsonian Miscellaneous Collections*, Washington, **148**: 1–128.
- Raymond, P. E. 1905. The trilobites of the Chazy Limestone. *Annals of the Carnegie Museum*, Pittsburgh, **3**: 328–386, pls 10–14.
- 1925. Some trilobites of the lower Middle Ordovician of eastern North America. *Bulletin of the Museum of Comparative Zoology*, Harvard, Cambridge, **67**: 1–180, pls 1–10.
- 1937. Upper Cambrian and Lower Ordovician Trilobita and Ostracoda from Vermont. *Bulletin of the Geological Society of America*, Baltimore, **48**: 1079–1146, pls 1–3.
- Reed, F. R. C. 1945. Revision of certain Lower Ordovician faunas from Ireland. I. Trilobites. *Geological Magazine*, Cambridge, **82**: 55–66.
- Richter, R., & Richter, E. 1925. Unterlagen zum Fossilium Catalogus, Trilobita. II. Senckenbergiana, **7**: 126.
- Ross, R. J., Jr. 1951. Stratigraphy of the Garden City Formation in northeastern Utah, and its trilobite faunas. *Peabody Museum of Natural History Bulletin*, New Haven, **6**: 1–161.
- 1967. Some Middle Ordovician brachiopods and trilobites from the Basin Ranges, western United States. *United States Geological Survey Professional Paper*, Washington, **523-D**: 1–43.
- 1972. Fossils from the Ordovician bioherm at Meiklejohn Peak, Nevada. *United States Geological Survey Professional Paper*, Washington, **685**: 1–47.
- , Hintze, L. F., Ethington, R. E., Miller, J. F., Taylor, M. E., & Repetski, J. 1993. The Ibexian Series (lower Ordovician) a replacement for the 'Canadian Series' in North American Chronostratigraphy. *United States Geological Survey Open File Report*, Washington, **93-598**: 75pp.
- Ryan P. & Archer J. B. 1978. The South Mayo Trough: a possible Ordovician Gulf of California-type marginal basin in W Ireland. *Canadian Journal of Earth Sciences*, Ottawa, **14**: 2453–2461.
- Schmidt, F. 1881. Revision der ostbaltischen Silurischen Trilobiten nebst geognostischer Übersicht der ostbaltischen Silurgebiets, Abth. I. Phacopiden, Cheiruriden und Encrinuriden. *Mémoires de l' Académie Impériale des Sciences de St. Pétersbourg*, **30**: 1–237, pls 1–16.
- Shaw, F. C. 1968. Early Middle Ordovician Chazy trilobites of New York. *New York State Museum and Science Service Memoir*, Albany, **17**: 1–163.
- Siveter, D. J. 1977. The Middle Ordovician of the Oslo region, Norway, 27. Trilobites of the family Calymenidae. *Norsk Geologisk Tidsskrift*, Oslo, **56**: 334–396. [for 1976]
- Snajdr, M. 1983. Bohemian Ordovician Proetidae (Trilobita). *Vestník Ustředního ústavu geologického*, Prague, **58**: 23–29.
- Tjernvik, T. E. 1956. On the Early Ordovician of Sweden. *Bulletin of the Geological Institutions of Uppsala*, Uppsala, **36**: 107–284, pls 1–11.
- Tripp, R. P. & Evitt, W. R. 1983. Silicified trilobites of the genus *Dimeropyge* from the Middle Ordovician of Virginia. *Special Papers in Palaeontology*, London, **30**: 229–240, pls 31–33.
- Ulrich, E. O. 1930. Ordovician trilobites of the family Telephidae and concerned stratigraphic correlations. *Proceedings of the United States National Museum*, Washington, **76**: 1–101, pls 1–8.
- Vogdes, A. W. 1890. A bibliography of Paleozoic Crustacea from 1698 to 1890 including a list of North American species and a systematic arrangement of genera. *Bulletin of the United States Geological Survey*, Washington, **63**: 1–177.
- Wahlenberg, G. 1818. Petrificata Telluris Svecanae. *Nova Acta Regiae Societatis Scientiarum Upsaliensis*, Uppsala, **8**: 1–116, pls 1–4.
- Walcott, C. 1877. Advance sheets. *31st Annual Report of the New York State Museum of Natural History*, Albany, p. 15.
- Warburg, E. 1925. The trilobites of the Leptaena Limestone in Dalarna with a discussion of the zoological position and the classification of the Trilobita. *Bulletin of the Geological Institution of the University of Uppsala*, Uppsala, **17**: 1–446, pls 1–11.
- Whittard, W. F. 1966. Ordovician trilobites of the Shelve Inlier west Shropshire. Part 8. *Palaeontographical Society Monographs*, London: 265–306, pls 46–50.
- Whittington, H. B. 1956. Silicified Middle Ordovician trilobites: the Odontopleuridae. *Bulletin of the Museum of Comparative Zoology*, Harvard, Cambridge, **114**: 155–288, pls 1–24.
- 1963. Middle Ordovician trilobites from Lower Head, western Newfoundland. *Bulletin of the Museum of Comparative Zoology*, Harvard, Cambridge, **129**: 1–118, pls 1–36.
- 1965. Trilobites of the Ordovician Table Head Formation, western Newfoundland. *Bulletin of the Museum of Comparative Zoology*, Harvard, Cambridge, **132**: 275–442, pls 1–68.
- 1968. Zonation and correlation of early Mohawkian series. In: Zen, E., White, W. S., Hadley, J. B., and Thompson, J. B. (eds), *Studies of Appalachian Geology: Northern and Maritime*: 49–60. Interscience, New York.
- Williams, A. & Curry, G. B. 1985. Lower Ordovician Brachiopoda from the Tourmakeady Limestone, Co. Mayo, Ireland. *Bulletin of the British Museum (Natural History)*, London, **Geology**, **38**: 183–269.
- Williams, S. H. & Stevens, R. K. 1988. Early Ordovician graptolites of the Cow Head Group, western Newfoundland. *Palaeontographica Canadana*, Toronto, **5**: 1–167.
- Young, G. E. 1973. An Ordovician (Arenigian) trilobite fauna of great diversity from the Ibex area, western Utah. *Brigham Young University Geology Studies*, Provo, **20**: 91–115.
- Zhang 1983. Trilobita. In, Nanjing Institute of Geology and Mineralogy (ed.), *Palaeontological atlas of east China*, **1**, Early Paleozoic: 28–254, pls 11–88. Beijing.
- Zhou Tian-rong. 1981. New materials of early Tremadocian trilobites from Sandu and Pu'an, Guizhou. *Acta Palaeontologica Sinica*, Beijing, **20**: 241–246.
- Zhou Zhi-ji. 1987. Notes on Chinese Ordovician agnostids. *Acta Palaeontologica Sinica*, Beijing, **26**: 639–661.



Ordovician Bryozoa from the Llandeilo Limestone, Clog-y-fran, near Whitland, South Wales

CAROLINE BUTTLER

Department of Geology, National Museums and Galleries of Wales, Cathays Park, Cardiff, CF1 3NP

SYNOPSIS. A diverse bryozoan fauna is described from the Llandeilo Limestone (from the upper part of the classical Llandeilo Series), Clog-y-fran, between Whitland and St. Clears, Carmarthenshire, Wales. The fauna is dominated by trepostomes (17 species) but one cryptostome and two fenestrate species are present. Two new trepostome species, *Dittopora sanclerensis* and *Batostoma clogyfranensis*, are described.

INTRODUCTION

Ordovician bryozoans from Britain have been neglected. This neglect can be attributed to poor preservation, the need to prepare oriented thin sections for identification, and also to the lack of a strong tradition of bryozoan research in Britain. Bryozoans are commonly preserved in Ordovician rocks as decalcified moulds which are easy to recognise but are very difficult to identify to genus and species level. Calcified specimens are often only noticed when a rock is cut and thin sections or peels are prepared.

The bryozoan fauna from Clog-y-fran is particularly important because it is the most diverse of those described from the Ordovician of the British Isles. In the only previous study of a Welsh mid-Ordovician bryozoan fauna, Spjeldnaes (1963) described upper Llanvirn/lower Llandeilo silicified material from south Wales. This included abundant bryozoans: six trepostome species, two bifoliate cryptostomes and arthrostylid fragments. Due to the silicified preservation identification is particularly difficult and only two species were named: *Orbignyella favulosa*? (Phillips) and *Mesotrypa* aff. *lens* (M'Coy).

MATERIAL

The Llandeilo limestone crops out in Carmarthenshire, near Clog-y-fran Farm (SN 239161) (Strahan *et al.* 1909) between Whitland and St. Clears and to the south of Pont-y-fenni (Fig. 1). Collection *in situ* is no longer possible but blocks from a previously dug trench are available for study. The fauna is very rich; bryozoans dominate but there are also brachiopods, trilobites, echinoderms, molluscs and conularids. All material described in this study is from the *Marrollmentus favus* Biozone, upper 'Llandeilo Series' (lower Caradoc Series, upper Ordovician, see Fortey *et al.*, 1995: 16), Llandeilo Limestone, Clog-y-fran.

The bryozoan fauna is extremely diverse; 20 species are described. Trepostomes dominate with seventeen species but one cryptostome and two fenestrate species are also present. Four of the 20 species from Clog-y-fran have been recognised as known species and two new species are also present. The other 14 could not be identified precisely to species level due to poor preservation or lack of material. These species are left in open nomenclature and are

referred to as 'cf.', 'aff.' and 'sp.' based on the recommendations of Bengtson (1988).

All the bryozoans from this locality are abraded and incomplete. Fragments are observed in acetate peels which may be from species not described in this study but they are too small to attempt any kind of identification.

The dominant morphological form of the fauna is erect. All but two of the 17 trepostome species are erect and some are branching, but others are impossible to tell because only incomplete colonies are present. The other two trepostomes have a massive hemispherical form. This may not be a true reflection of the living bryozoan community, but the result of taphonomic processes.

BIOGEOGRAPHICAL COMPARISONS

A total of 15 genera are recognised from Clog-y-fran. All are cosmopolitan and have been previously described from outside south Wales. Ordovician bryozoans from Wales are known to have broad geographical ranges (Buttler 1991a). A long-lived planktotrophic larval stage may explain this wide dispersal (Taylor & Cope, 1987). Living cyclostomes have non-planktotrophic larvae but Taylor & Cope considered that early stenolaemates may have inherited planktotrophic larvae from their inferred ctenostome ancestors.

During the Ordovician south Wales formed part of Avalonia, along with the Ardennes of Belgium and northern France, England, southeast Ireland, the Avalon Peninsula of eastern Newfoundland, parts of Nova Scotia, southern New Brunswick and coastal areas of New England (Scotese & McKerrow, 1990). Avalonia was separated from Laurentia (North America) by the Iapetus Ocean and from the Baltica by Tournquist's Sea, both of which began to narrow in the early Ordovician. By the late Caradoc Avalonian faunas were similar to those of Baltica (Scotese & McKerrow, 1990).

As 16 of the 20 species from Clog-y-fran cannot be precisely related to known taxa it is difficult to make biogeographical comparisons, although Welsh bryozoans generally show the greatest affinity to Baltica. The four species that have been previously described are known from Baltica, North America and Wales. *Hemiphragma pygmaeum* is known from Sweden, *Graptodictya bonnemai* from Estonia and Russia, *Hallopore peculiaris* from Latvia and south Wales, and *Eridotrypa simulatrix* from Russia and North America

Species	ZOW	EXW	MXZD	MNZD	MXMD	ZWT	ZMM	DEX	DEN	DMEX	DMEN	CMM	AD	AZ	AMM
<i>Ditopora sanctoerensis</i>	5.8 (9) 4-10	1.1 (9) 0.57-1.62	0.26 (7) 0.17-0.32	0.22 (7) 0.13-0.29	0.11 (6) 0.04-0.21	0.075 (8) 0.02-0.13	8.25 (7) 6-8	0.13 (9) 0.06-0.29	-	0.083 (9) 0.04-0.17	-	-	0.041 (7) 0.023-0.054	4.1 (3) 1-7	18 (2) 14-23
<i>Hemiphragma pygmaeum</i>	4.5 (2) 4-5	1.24 (2) 1.14-1.33	0.23 (2) 0.17-0.29	0.19 (2) 0.15-0.25	0.1 (2) 0.06-0.13	0.07 (2) 0.02-0.11	12.7 (2) 10-15	0.15 (2) 0.08-0.23	0.17 (1) 0.11-0.27	0.08 (2) 0.04-0.11	-	-	0.051 (2) 0.045-0.077	4.67 (2) 4-5	23 (1) 23
<i>Hemiphragma sp.</i>	2.5 (1) 2.5	-	0.47 (1) 0.38-0.57	0.39 (1) 0.32-0.46	-	0.02 (1) 0.02	4.3 (1) 4-5	0.36 (1) 0.29-0.49	0.62 (1) 0.16-0.87	-	-	-	-	-	-
<i>Heterotrypa sp.</i>	4 (1) 4	0.57 (1) 0.57	0.19 (1) 0.13-0.23	-	0.12 (1) 0.1-0.15	0.055 (1) 0.04-0.08	9 (1) 9	-	-	0.09 (1) 0.06-0.11	0.14 (1) 0.11-0.19	-	0.052 (1) 0.045-0.059	-	-
<i>Leiocleema sp. A</i>	8 (2) 8	1.9 (2) 1.8-2	0.26 (2) 0.21-0.34	0.18 (2) 0.13-0.23	0.093 (2) 0.06-0.11	0.13 (2) 0.1-0.17	8.1 (2) 6-9	-	-	0.1 (2) 0.06-0.17	0.15 (2) 0.11-0.19	-	0.03 (2) 0.02-0.04	5.1 (2) 4-6	29 (2) 25-34
<i>Leiocleema sp. B</i>	1.5 (1) 1.5	0.67 (1) 0.67	0.11 (1) 0.08-0.13	0.993 (1) 0.08-0.11	0.04 (1) 0.02-0.06	0.08 (1) 0.04-0.1	47 (1) 39-55	-	-	0.04 (1) 0.02-0.06	-	-	0.027 (1) 0.023-0.32	1.2 (1) 1-2	29.5 (1) 26-33
<i>Leiocleema ? sp.</i>	12 (1) 12	2.28 (1) 2.28	0.45 (3) 0.32-0.55	0.37 (3) 0.3-0.49	0.14 (3) 0.04-0.1	0.06 (3) 0.04-0.1	3.67 (3) 2-5	-	-	0.11 (3) 0.06-0.15	0.13 (2) 0.08-0.21	-	0.09 (3) 0.05-0.12	7.7 (3) 5.9	12.5 (3) 10-17
<i>Hallopore peculiaris</i>	5.6 (1) 5.6	-	0.29 (5) 0.26-0.3	-	-	0.1 (4) 0.09-0.1	-	0.17 (6) 0.07-0.19	-	0.07 (7) 0.05-0.08	0.1 (7) 0.08-0.11	-	-	-	-
<i>Hallopore aff. wesenbergiana</i>	11 (3) 10-12	1.81 (3) 1.81	0.27 (2) 0.23-0.34	0.21 (2) 0.17-0.27	0.1 (2) 0.04-0.13	0.03 (2) 0.02-0.04	10.2 (2) 9-12	0.11 (3) 0.06-0.21	0.26 (2) 0.1-0.57	0.07 (3) 0.04-0.11	0.08 (2) 0.06-0.13	-	-	-	-
<i>Batostoma clogynense</i>	3.9 (23) 2-5	0.8 (22) 0.48-1.43	0.18 (23) 0.1-0.34	0.15 (23) 0.11-0.23	0.09 (21) 0.04-0.17	0.08 (21) 0.02-0.13	13.6 (19) 10-20	0.15 (22) 0.02-0.46	0.28 (23) 0.1-0.67	0.07 (23) 0.04-0.13	-	-	0.03 (21) 0.014-0.06	12.6 (12) 10-16	67.3 (5) 50-77
<i>Batostoma cf. polare</i>	4.5 (1) 4.5	1.14 (1) 1.14	0.2 (1) 0.13-0.29	0.16 (1) 0.11-0.23	0.1 (1) 0.08-0.13	0.11 (1) 0.1-0.13	10.7 (1) 10-12	0.06 (1) 0.02-0.11	0.38 (1) 0.13-0.78	0.05 (1) 0.02-0.1	-	-	0.018 (1) 0.014-0.06	14 (1) 10-16	30 (1) 30
<i>Eridotrypa simulatrix</i>	3.3 (4) 3-4	0.64 (4) 0.38-0.95	0.18 (4) 0.13-0.3	0.13 (4) 0.1-0.19	0.09 (4) 0.04-0.11	0.06 (4) 0.04-0.1	15 (4) 12-19	0.13 (4) 0.06-0.29	0.35 (4) 0.19-0.99	0.07 (2) 0.04-0.1	-	-	0.02 (4) 0.014-0.032	-	-
<i>Monticulipora aff. compacta</i>	4 (1) 4	1.05 (1) 1.05	0.16 (1) 0.13-0.21	0.13 (1) 0.1-0.17	0.08 (1) 0.06-0.13	0.05 (1) 0.02-0.06	28 (1) 25-30	0.07 (1) 0.04-0.13	0.15 (1) 0.08-0.23	0.06 (1) 0.04-0.08	-	-	0.24 (1) 0.15-0.38	0.028 (1) 0.023-0.032	4.3 (1) 4.5
<i>Homotrypa cf. similis</i>	8 (1) 8	1.62 (1) 1.62	0.23 (1) 0.17-0.29	-	0.08 (1) 0.06-0.1	0.04 (1) 0.02-0.04	-	0.1 (1) 0.08-0.15	0.26 (1) 0.15-0.4	0.04 (1) 0.02-0.08	-	10 (1) 8-12	-	-	-
<i>Monotrypa sp.</i>	13.5 (2) 12-15	-	0.32 (2) 0.25-0.4	0.29 (2) 0.21-0.4	-	0.02 (2) 0.02-0.04	9.2 (2) 6-15	-	1.8 (2) 0.57-2.9	-	-	-	-	-	-
<i>Amplexopora sp.</i>	8 (2) 7-9	1.9 (2) 1.7-2.1	0.3 (2) 0.21-0.38	0.24 (2) 0.15-0.32	0.12 (2) 0.04-0.15	0.08 (2) 0.04-0.11	11 (2) 9-13	0.09 (2) 0.04-0.19	0.23 (2) 0.1-0.38	0.05 (2) 0.02-0.1	-	-	0.05 (2) 0.03-0.07	3.9 (2) 2-5	14 (2) 12-17
<i>Halloporma cf. crenulata</i>	4.5 (1) 4.5	0.76 (1) 0.76	0.22 (1) 0.21-0.23	0.18 (1) 0.15-0.21	0.08 (1) 0.04-0.11	0.05 (1) 0.04-0.08	14 (1) 12-15	-	-	-	-	-	-	-	-

Table 1 Summary of the biometric details of all trepostome species from the Llandeilo Limestone, Clog-y-fran. In each case, upper figures are mean values, followed by the number of specimens in brackets. Lower figures are ranges. All measurements are in millimetres except for ZMM, CMM, AZ and AMM. ZOW = zoarial diameter, EXW = exozonal width, MXZD = maximum autozoocial diameter, MNZD = minimum autozoocial diameter, MXMD = maximum mesozoocial diameter, ZWT = autozoocial wall thickness, ZMM = autozooceria per mm, DEX = distance between exozonal autozoocial diaphragms, DMEN = distance between endozonal mesozoocial diaphragms, DMEX = distance between endozonal autozoocial diaphragms, DMEN = distance between endozonal mesozoocial diaphragms, DMEX = distance between endozonal autozoocial diaphragms, DMEN = number of acanthostyles per autozooceria, AMM = number of cystostyles per square mm.

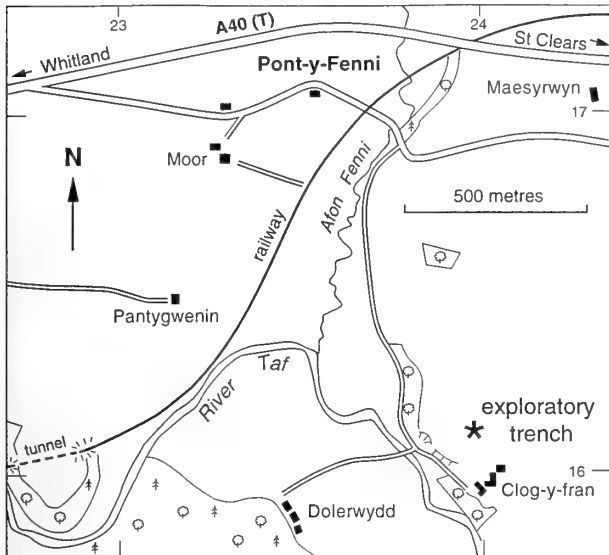


Fig. 1 Locality map showing position of exploratory trench where the limestone blocks containing the fauna were collected.

SYSTEMATIC PALAEONTOLOGY

The terminology in all descriptions is that of Boardman *et al.* (1983). All genera are placed in families based on the following sources: Trepostomata – Astrova (1978); Cystoporata – Utgaard (*in* Boardman *et al.*, 1983). Family level classification is generally unsatisfactory in Palaeozoic trepostomes and is currently being revised for the *Treatise on Invertebrate Paleontology* by R.S. Boardman.

Biometric details for all trepostome species are tabulated (Table 1). Each measurement was made up to seven times per specimen, and the means and ranges calculated for each parameter. Raw data can be found in an unpublished Ph.D. thesis (Buttler 1988). All specimens are represented by thin sections or acetate peels. Measurements given in the systematic descriptions are all mean values unless otherwise stated. All material is deposited in The Natural History Museum, London.

Phylum **BRYOZOA** Ehrenberg, 1831
 Class **STENOLOAEMATA** Borg, 1926
 Order **TREPOSTOMATA** Ulrich, 1882
 Suborder **HALLOPOROIDEA** Astrova, 1965
 Family **HETEROTRYPIDAE** Ulrich, 1890
 Genus **DITTOPORA** Dybowski, 1877

Dittopora sanclerensis sp. nov.

Figs 2–3

HOLOTYPE. NHM PD 8338.

PARATYPES. NHM PD 8333–8337, 8339–8341.

NAME. The species is named after St. Clears (Sancler in Welsh), the nearest town to the type locality.

DIAGNOSIS. Colony large, ramosa. Autozoocia, with very thin, slightly wavy walls in endozone, which curve out from branch axis to intersect zoarial surface; polygonal in zoarial transverse section, rounded-circular in shallow zoarial tangential sections. Circular

mesozooecia present, originating in outer endozone/inner exozone. Partial and complete diaphragms in exozonal autozoocia; numerous diaphragms in mesozooecia. Acanthostyles large and abundant in exozone.

DESCRIPTION. Zoaria erect with thick cylindrical branches, on average 5.8 mm in diameter.

Autozoocia curve out gently from the branch axis in the endozone to meet the zoarial surface at 90°. Autozoocia within the endozone have very thin, slightly wavy walls.

The exozone has an average diameter of 1.1 mm (although the range is large: 0.57–1.62 mm) and is recognised by a thickening of the zoocelial walls. Autozoocia all originate in the endozone where they are polygonal in transverse section, becoming rounded-circular in the exozone, as seen in tangential sections of branches. Autozoocia in the exozone contain abundant partial diaphragms and complete diaphragms (spaced on average 0.13 mm apart) which increase in thickness distally along the autozoocia. All diaphragms are basal and are deflected orally at their junctions with zoocelial walls. Their laminae are continuous with the autozoocial linings.

Mesozooecia are common and originate in the outer parts of the endozone and inner parts of the exozone. They are circular in shallow tangential sections and contain numerous thick, orally deflected basal diaphragms, spaced on average 0.83 mm apart and generally increasing in thickness distally along the mesozooecia.

Acanthostyles are abundant and large, with an average diameter of 0.04 mm and density of four per mm². They originate deep within the exozone and can on rare occasions indent the zoocelial apertures. A hyaline core is surrounded by steeply dipping conical laminae.

Autozoocial wall thickness averages 0.08 mm in the exozone. Wall microstructure is composed of steeply inclined, U-shaped laminae. Zooecial boundaries are indistinct due to the presence of large acanthostyles which disrupt the wall structure. Frequently the autozoocia, and virtually all of the mesozooecia, are infilled with laminar calcite close to the zoarial surface. In longitudinal section this infilling consists of broad U-shaped laminae. Often large areas of adjacent zoocelia are infilled.

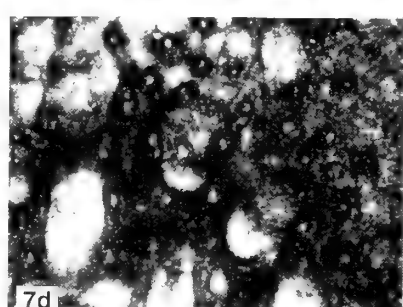
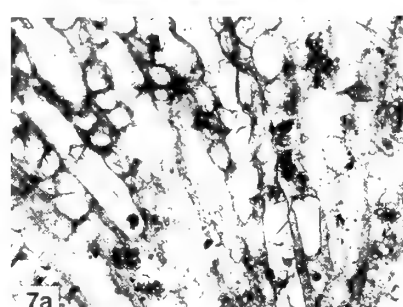
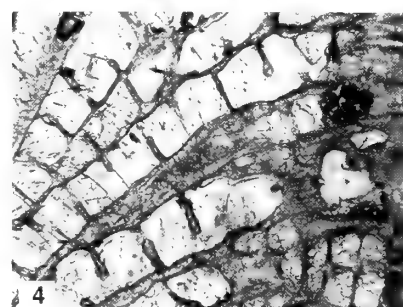
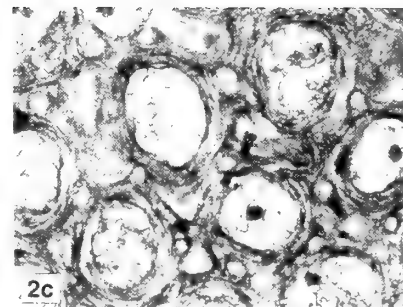
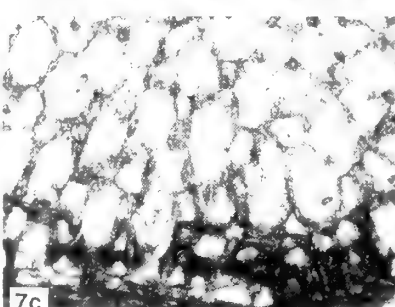
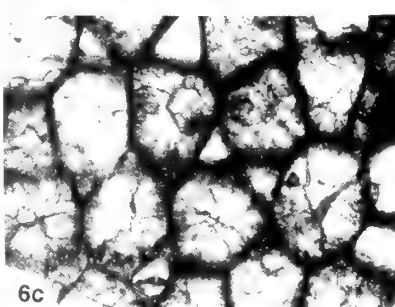
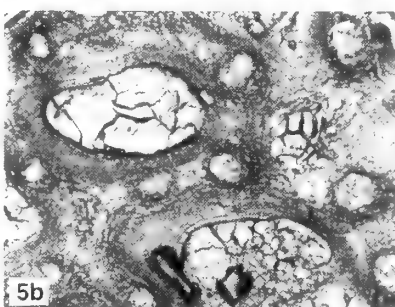
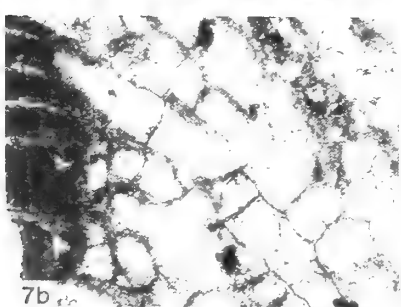
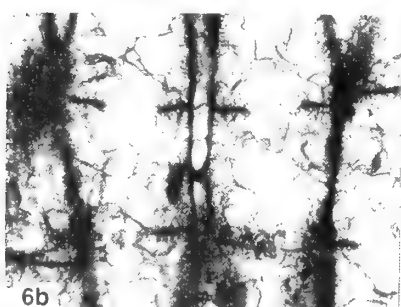
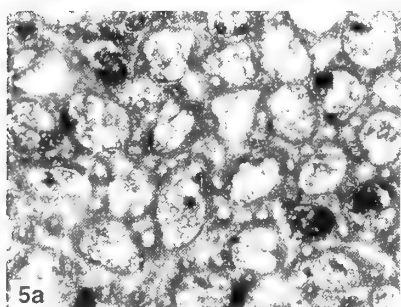
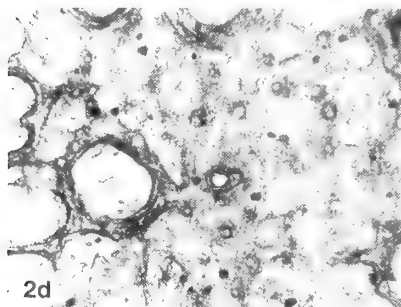
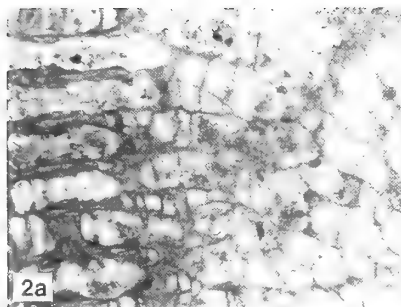
An intrazoarial overgrowth is recognised in one specimen (PD 8334). It is continuous with the exozone and has endozonal and exozonal components.

REMARKS. *Dittopora sanclerensis* sp. nov. is characterised by extremely thin endozonal walls which thicken markedly in the exozone. Partial and complete diaphragms are present in the exozonal autozoocia. Circular mesozooecia with numerous diaphragms are present. Acanthostyles are large and abundant in the exozone.

Dittopora annulata (Eichwald, 1860), from the Orthoceras Limestone (Llanvirn) in Estonia and the Glauconite Limestone in Russia, is similar internally to *Dittopora sanclerensis*. However, *D. annulata* has alternating bands of autozoocia and mesozooecia, whereas in *D. sanclerensis* they are not arranged in bands.

Modzalevskaya (1953) described two new species of *Dittopora*, *D. sokolon* and *D. ramosa*, from the western Russian Platform: *D. sokolon* has similar autozoocia, diaphragms and acanthostyles to *D. sanclerensis* but thicker endozonal walls; *D. ramosa* has similar diaphragms but smaller and more abundant acanthostyles.

A common feature of *D. sanclerensis* is that zoocelia close to the zoarial surface are filled with U-shaped laminar calcite (Fig. 2). This may be because the studied material consists mainly of the basal parts of colonies with ontogenetically older zooids.



Genus ***HEMIPHRAGMA*** Ulrich 1893

Hemiphragma pygmaeum Bassler, 1911 Figs 4–5

- 1911 *Hemiphragma pygmaeum* Bassler: 289, fig. 176.
non 1970 *Hemiphragma pygmaeum* Bassler; Nekhorosheva: 84; pl. vii, figs 5–6.

SYNTYPES. NHM D 22829, D 22536; Chasmops Limestone (upper Caradoc), Oland, Sweden.

MATERIAL. NHM PD 8331a, b.

DESCRIPTION. Zoaria erect with quite thick cylindrical branches, on average 4.5 mm in diameter.

Autozoocia curve out gradually from the branch axis to meet the zoarial surface at 90°. The autozoocia within the endozone have thick straight walls.

The exozone has an average diameter of 1.24 mm. It is recognised by a thickening of the zooecial walls. Autozoocia all originate in the endozone, where they are rounded and occasionally petaloid in transverse section, becoming rounded to circular as seen in tangential sections of branches. Autozoocia diameters average 0.19 mm by 0.23 mm within the exozone. Diaphragms are found throughout the colony but are not common. Partial diaphragms are, however, very abundant everywhere. They are spaced on average 0.17 mm apart in the endozone and 0.15 mm apart in the exozone, and tend to occur on alternating sides of the autozoocia. The direction of deflection of the laminae of the diaphragms at their junctions with zooecial walls cannot be distinguished.

Mesozoocia are present, although not common, and originate in the outer parts of the endozone. They are rounded in tangential section and have an average maximum diameter of 0.1 mm. Mesozoocia contain orally deflected basal diaphragms, spaced on average 0.08 mm apart.

Acanthostyles are large and abundant with an average diameter of 0.05 mm and density of 23 per mm². They originate throughout the colony and can indent the autozoocia apertures to produce a petaloid shape. In the outer exozone they are normally found in the centre of the thick walls. A large hyaline core is surrounded by steeply dipping conical laminae.

Autozoocia wall thickness averages 0.07 mm in the exozone. Wall microstructure is composed of steeply inclined, U-shaped laminae. Adjacent zooecial wall boundaries are occupied by wide granular areas. The wall structure is hard to distinguish because it is greatly disrupted by the large acanthostyles. Frequently zooecia are infilled with laminar calcite close to the zoarial surface. In longitudinal section this infilling consists of broad U-shaped laminae.

REMARKS. *Hemiphragma pygmaeum* was originally described by Bassler (1911) from the Chasmops Limestone (upper Caradoc) of Oland, Sweden but has not hitherto been recognised elsewhere. Bassler characterised the species by its ‘mushroom’-shaped colonies, thick zooecial walls, large acanthostyles throughout the colony and the abundant partial diaphragms.

The specimens from Clog-y-fran are known only in section. They differ from the Swedish *H. pygmaeum* in having a straight-sided,

more erect colony form and slightly smaller acanthostyles. Also the mesozoocia do not appear to originate as deeply in the colony. At present the Welsh material is placed within *H. pygmaeum* and the differences with the Swedish material are considered to represent intraspecific variability until more material can be examined.

The genus *Hemiphragma* has not be previously described from Great Britain. A second species from Clog-y-fran, *Hemiphragma* sp., is also described here. The two species are very different, *H. pygmaeum* being ramose in form, with thick walls and large acanthostyles, and *Hemiphragma* sp. being hemispherical, with thin walls and ring-diaphragms.

H. pygmaeum was described from the middle Ordovician of Pai-Khoi and Vaigach Island, Russia (Nekhorosheva 1970). The illustrations, however, show thin-walled specimens with abundant diaphragms and small acanthostyles; these are considered not to be *H. pygmaeum*.

***Hemiphragma* sp.**

Fig. 6

MATERIAL. NHM PD 8327.

DESCRIPTION. Zoaria large and hemispherical, on average 2.5 mm in diameter. Autozoocia all originate from the basal lamina and curve outwards towards the zoarial surface. Autozoocia walls are straight throughout the colony; there is no differentiation between endozone and exozone. Autozoocia are large with an average diameter of 0.39 mm × 0.47 mm and are polygonal/rounded to rounded in transverse section throughout the colony. Thin diaphragms and ring diaphragms are present in all zooecia, spaced 0.62 mm apart in the endozone and 0.36 mm in the exozone. These are basal diaphragms which are orally-deflected at their junctions with the zooecial walls and have laminae continuous with the autozoocia linings.

Possible acanthostyles occur in the outer parts of the colony, but are rare. Autozoocia wall thickness averages 0.02 mm at the periphery of the colony. It is not possible to identify the microstructure from available peels and thin sections.

REMARKS. The specimen described herein is characterised by a hemispherical colony shape. Autozoocia have straight, thin walls throughout the zoarium, and the autozoocia apertures are polygonal-rounded to rounded in transverse section. Diaphragms and ring diaphragms are present in all autozoocia.

Bassler (1911: 282, fig. 170) described and illustrated specimens of *H. tenuimurale* Ulrich, 1893 from the type locality, the *Clitambonites* and *Nematopora* Beds, Lower Trenton, Minnesota and Iowa; and from the Wassalem Beds (Caradoc), Uxnorm, Estonia. The Welsh specimen is similar to the Estonian material: it has thin walls and mesozoocia are lacking, but differs in having a hemispherical rather than ramose colony, diaphragms within the endozone, and by the presence of ring diaphragms rather than partial diaphragms. *H. tenuimurale* described by Ulrich (1893) from Minnesota (see Bassler, 1911: fig. 171) has fewer diaphragms in the endozone compared to the Estonian material. Brown (1965) described specimens of *H. tenuimurale* from the Logana and Jessamine

Figs 2–3 *Dittopora sanclerensis* sp. nov. 2, NHM PD 8338 (holotype); 2a, longitudinal section, x22; 2b, transverse section, x22; 2c, tangential section, x53; 2d, tangential section, showing infilled zooecia, x53. 3, NHM PD 8333 (paratype); longitudinal section, showing infilled autozoocia, x37.

Figs 4–5 *Hemiphragma pygmaeum* Bassler, 1911. 4, NHM PD 8331a; longitudinal section, showing partial diaphragms, x35. 5, NHM PD 8331b; 5a, tangential section, x35; 5b, tangential section, x94.

Fig. 6 *Hemiphragma* sp., NHM PD 8327; 6a, longitudinal section, x23; 6b, longitudinal section, showing ring diaphragms, x37; 6c, tangential section, x30.

Fig. 7 *Heterotrypa* sp., NHM PD 8314; 7a, longitudinal section, x26; 7b, longitudinal section, x47; 7c, transverse section, showing infilled zooecia in the exozone, x37; 7d, tangential section, x70.

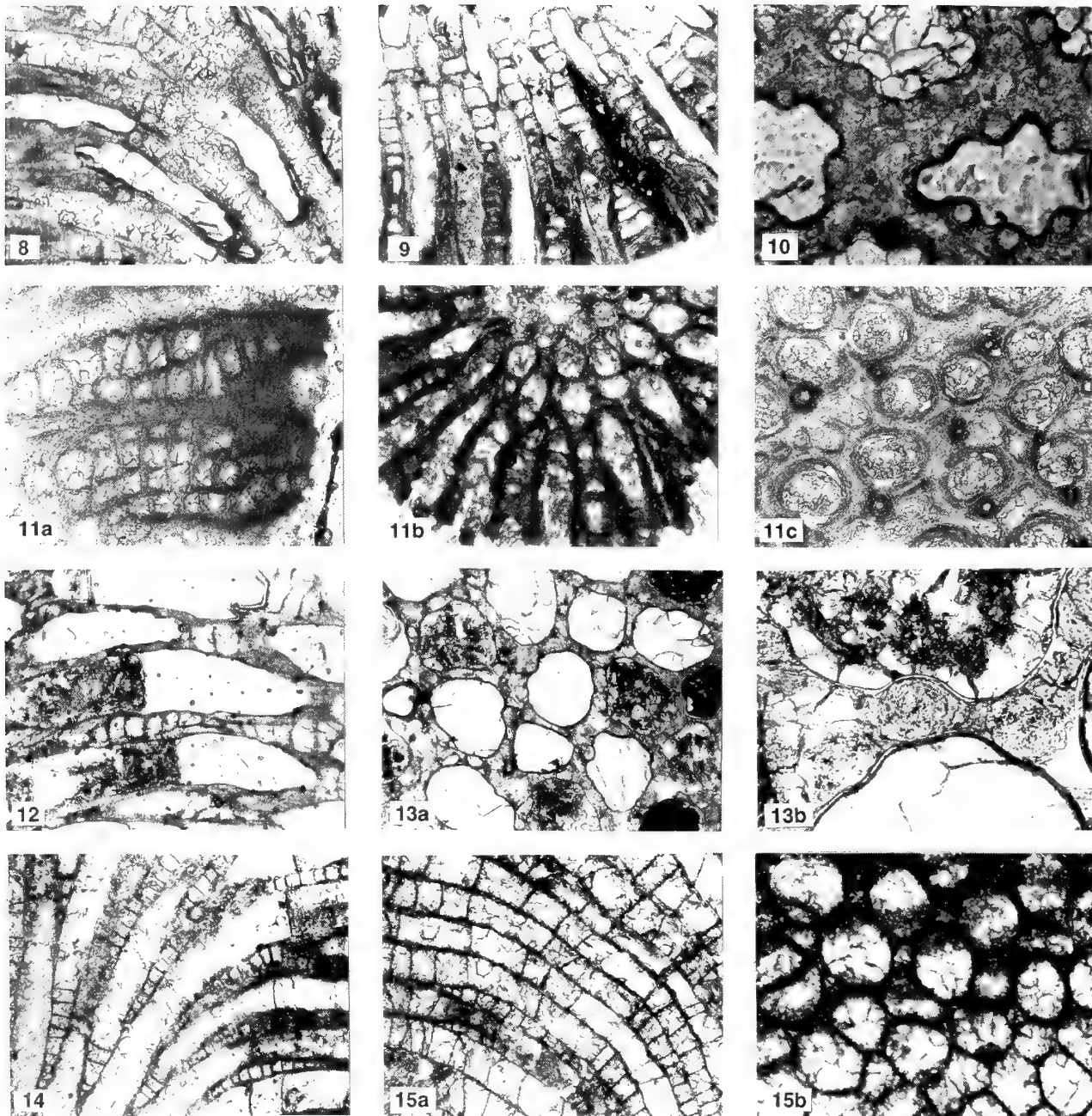


Fig. 8 *Leioclema* sp. A. NHM PD 8307; longitudinal section, x22.

Figs 9–10 *Leioclema* sp. A. **9**, NHM PD 8308; transverse section, x22. **10**, NHM PD 8307; tangential section, showing petaloid autozooecia, x101.

Fig. 11 *Leioclema* sp. B., NHM PD 8306; **11a**, longitudinal section, x86; **11b**, transverse section, x55; **11c**, tangential section, x86.

Figs 12, 13 *Leioclema?* sp. **12**, NHM PD 8138; longitudinal section, x22. **13**, NHM PD 8137; **13a**, tangential section, x30; **13b**, tangential section, showing large acanthostyles indenting autozooecial walls, x112.

Fig. 14 *Hallopora peculiaris* Pushkin (in Ropon & Pushkin, 1987). NHM PD 8396; longitudinal section, x22.

Fig. 15 *Hallopora* aff. *wesenbergiana* (Dybowski, 1877), NHM PD 8312; **15a**, longitudinal section, x22; **15b**, tangential section, x37.

Limestones (middle Ordovician) of Kentucky which are very similar to those from Minnesota and Iowa. Restudy is needed to assess the variability within the species, and it is possible that the Estonian and American forms are different species.

Until further material can be examined, this one incomplete specimen is left in open nomenclature.

Genus *HETEROTRYPA* Nicholson, 1879

Heterotrypa sp.

Fig. 7

MATERIAL. NHM PD 8314.

DESCRIPTION. Zoarium erect with thin cylindrical branches, on average 4 mm in diameter.

Autozoocia curve outwards gradually from the branch axis to meet the zoarial surface at 90°. Autozoocia within the endozone have thin, slightly wavy walls.

The exozone is narrow with an average width of 0.57 mm. It is recognised by a thickening of the zooecial walls. Autozoocia all originate in the endozone where they are rounded-polygonal in transverse section, becoming rounded to slightly petaloid in the exozone as seen in tangential sections of branches. Autozoocia diameters average 0.19 mm in the exozone. Diaphragms are rare in the autozoocia, and when present only one or two are found in the outer endozone and exozone. These basal diaphragms are all orally-deflected at their junctions with the zooecial walls.

Mesozooecia are common and originate throughout the endozone; their shape in shallow tangential section has not been observed. Orally deflected basal diaphragms are found along the entire length of the mesozooecia. Vertical walls are extensively constricted at the positions of the diaphragms, producing a pronounced beaded (in some cases vesicular) appearance.

Acanthostyles are large and abundant, with an average diameter of 0.05 mm. They originate throughout the colony and commonly indent the autozoocia. Acanthostyle microstructure is difficult to distinguish, but seems to consist of a hyaline core surrounded by steeply dipping conical laminae.

Autozoocia wall thickness averages 0.06 mm. Wall microstructure is composed of inclined laminae, but is hard to distinguish because the walls are greatly disrupted by acanthostyles. Frequently, the zooecia are infilled with laminar calcite close to the zoarial surface. The zooecia in large parts of the colony have been found to be all infilled. In shallow tangential sections of these areas, all that is seen is the laminar calcite wall pierced by acanthostyles.

REMARKS. Only one poorly preserved specimen of this species has been found. It is characterised by the ramosc colony form and meandering endozonal walls. Autozoocia are rounded to slightly petaloid in shallow tangential sections, and beaded mesozooecia are common throughout the colony. Diaphragms are rare in autozoocia but abundant in mesozooecia throughout the colony. The irregularly shaped, beaded zooecia make this a particularly characteristic species and distinguish it from *H. sladei* described by Buttler (1991b). Identification is, however, left in open nomenclature until better preserved material can be examined.

Heterotrypa sp. is similar to the Russian species *H. ovata* Astrova, 1957, but has more weakly beaded zooecia and less prominent acanthostyles.

Genus *LEIOCLEMA* Ulrich, 1882

Leioclema sp. A

Figs 8–10

MATERIAL. NHM PD 8307–8308.

DESCRIPTION. Zoaria erect with cylindrical branches on average 8 mm in diameter.

Autozoocia curve outwards gradually from the branch axis to meet the zoarial surface at 80°–90° and have moderately thick, slightly wavy walls within the endozone.

The exozone is quite large with an average diameter of 1.9 mm. It is recognised by an extensive thickening of the zooecial walls. Autozoocia all originate in the endozone, where they are rounded-petaloid in transverse section becoming extensively petaloid in the exozone as seen in tangential sections of branches. Autozoocia diameter averages 0.18 mm by 0.26 mm within the exozone. Diaphragms are rare and frequently wholly absent in autozoocia.

Mesozooecia are very common and originate in the outer parts of the endozone and inner parts of the exozone. They are rounded and have a maximum diameter averaging 0.09 mm. The mesozooecia contain abundant orally-deflected basal diaphragms, spaced on average 0.15 mm apart in the endozone and 0.1 mm apart in the exozone, with successive diaphragms often increasing in thickness distally along the mesozooecia.

Acanthostyles are large and very abundant with an average diameter of 0.03 mm and density of 29.5 per mm². They originate throughout the colony and are very abundant in the exozone, where they indent the autozoocia apertures, producing a petaloid shape. Acanthostyles are larger in size in the outer exozone than in the rest of the colony. In longitudinal section acanthostyles can be identified protruding into the zooecial chambers. Acanthostyles are composed of a broad hyaline core surrounded by steeply dipping conical laminae.

Autozoocia wall thickness averages 0.13 mm in the exozone. Wall microstructure is composed of steeply inclined, U-shaped laminae. In tangential sections a thick granular layer can be identified between adjacent zooecia. Virtually all mesozooecia, and some autozoocia, are infilled with laminar calcite close to the zoarial surface. In longitudinal section this infilling consists of broad U-shaped laminae. The infilling of the mesozooecia commences in the middle exozone, whereas the autozoocia are infilled in the outer exozone.

REMARKS. Only two poorly preserved specimens of this species have been found at Clog-y-fran. The colonies are primarily recognised by the erect form, and by autozoocia walls that are thick throughout the colony. Autozoocia apertures are rounded-petaloid in transverse section and markedly petaloid in shallow tangential section. Rounded mesozooecia are common with abundant diaphragms; diaphragms are rare in the autozoocia. Acanthostyles are present throughout the colony; they are large and abundant in the exozone.

The identification of this species is difficult because of the poor quality of the two known specimens. *Leioclema* sp. A is placed in open nomenclature until better preserved material can be obtained and a complete description of this possibly new species can be made.

Leioclema sp. B

Fig. 11

MATERIAL. NHM PD 8306.

DESCRIPTION. Zoaria erect with very thin cylindrical branches, on average 1.5 mm in diameter.

Autozoocia curve away gradually from the branch axis in the endozone and then more abruptly in the exozone to meet the zoarial surface at 90°. Autozoocia within the endozone all have straight thin walls.

The exozone is extremely broad with an average width of 0.67 mm. It is recognised by a simultaneous thickening of zooecial walls and a change in zooecial orientation. Autozoocia all originate in the endozone where they are rounded in transverse section. They retain this shape in the exozone, as seen in tangential sections of branches. Autozoocia diameters average 0.09 mm by 0.11 mm within the exozone. Diaphragms are absent in the autozoocia. Occasional cystiphragms can, however, be found in the outer exozone.

Mesozooecia are common and originate in the inner parts of the exozone. They are rounded in shape in tangential sections and have a maximum diameter averaging 0.04 mm. The mesozooecia contain abundant orally deflected, thick, basal diaphragms, spaced on average 0.04 mm apart, and generally increasing in thickness distally along the mesozooecia.

Acanthostyles are common and have an average diameter of 0.03 mm and density of 29.5 per mm². They originate deep in the exozone, extend the length of the exozone, and are composed of a hyaline calcite core surrounded by steeply dipping conical laminae.

Autozoocelial wall thickness averages 0.08 mm in the exozone. Wall microstructure is composed of steeply inclined, V-shaped laminae. The zoocelial boundaries are, however, indistinct. Zooecia are frequently infilled with laminar calcite close to the zoarial surface. In longitudinal section this infilling consists of broad U-shaped laminae.

REMARKS. *Leioclema* sp. B is primarily characterised by: the small size of the erect branches; autozoocelial apertures rounded in transverse section throughout the colony; an exozone which is very wide in comparison with the endozone; common rounded mesozoecia containing abundant diaphragms; and small but long acanthostyles. Only one specimen is known from Clog-y-fran. *Leioclema* sp. B can be distinguished from *Leioclema* sp. A by the smaller colony size.

Owen (1962, 1965, 1969) described numerous species of *Leioclema* and the related *Asperopora* from the Silurian of the Welsh Borderland and Shropshire. *L. halloporoides* Owen, 1962 was described from the Ludlow Aymestry Limestone of Shropshire. This also has very small colony branches (2 mm diameter) and mesozoecia containing diaphragms. *Leioclema* sp. B, however, has more abundant diaphragms within the mesozoecia and larger acanthostyles.

Leioclema sp. B is possibly a new species but, as it is represented only by one poorly preserved specimen, no specific name will be assigned until further material is obtained.

Leioclema? sp.

Figs 12–13

MATERIAL. NHM PD 8316–8318.

DESCRIPTION. Zoaria erect with thick cylindrical branches, on average 12 mm in diameter.

Autozoocelia curve outwards gradually from the branch axis to meet the zoarial surface at 90°. The autozoocelia within the endozone have very thick walls.

The exozone has an average diameter of 2.28 mm. It is recognised by a slight thickening of the zoocelial walls. Autozoocelia all originate in the endozone where they are rounded-polygonal in transverse section; they become irregular-rounded in the exozone, as seen in tangential sections of branches. Autozoocelial diameters average 0.37 mm × 0.45 mm within the exozone. Thin basal diaphragms, which are orally-deflected at their junctions with the zoocelial walls, are rare.

Mesozoecia occur in the exozone, on shallow tangential sections. They are rounded with a maximum diameter averaging 0.14 mm, and contain abundant, thick, orally-deflected, basal diaphragms, which are spaced on average 0.13 mm apart in the endozone and 0.1 mm in the exozone.

Acanthostyles are large and abundant with an average diameter of 0.09 mm and density of 12.5 per mm². They vary greatly in size, ranging in diameter from 0.05 mm to 0.12 mm, and originate throughout the colony. They are often wider than the zoocelial walls. The acanthostyles are composed of a broad hyaline core; no sheathing laminae can be identified.

Autozoocelial wall thickness averages 0.06 mm in the exozone. Wall microstructure is composed of inclined, V-shaped laminae, but is exceedingly poorly preserved.

REMARKS. Only three fragmentary specimens of this species have

been found. The colonies are erect with thick autozoocelial walls. The autozoocelia are rounded-polygonal to slightly petaloid in shallow tangential section. Rounded mesozoecia are present and have abundant diaphragms. Diaphragms are rare in autozoocelia. Acanthostyles are large and abundant throughout the colony, occasionally inflecting autozoocelial walls.

Identification of the species is difficult because of the poor preservation of the material. The abundance of diaphragms in the mesozoecia and the lack of them in the autozoocelia fit within the generic concept of *Leioclema* followed here. However, the acanthostyles are large (often wider than the zoocelial walls), abundant and originate throughout the colony. A thick hyaline core is identifiable but no surrounding laminae are present, as found in the acanthostyles of other species of *Leioclema*. The acanthostyles are similar to those observed in the early Ordovician genus *Orbipora* Eichwald, 1856, illustrated in Astrova (1978: pl. ii, fig.i) and Taylor & Cope (1987: fig.1). *Orbipora* is, however, characterised by its massive form and absence of mesozoecia.

The precise taxonomic placing of the species is uncertain because of the poor quality of the material available. The specimens are therefore tentatively designated *Leioclema?* sp.

Family HALLOPOROIDAE Bassler, 1911

Genus *HALLOPORA* Bassler, 1911

Hallopora peculiaris Pushkin, 1987

Fig. 14

1987 *Hallopora wesenbergiana peculiaris* Pushkin in Ropot & Pushkin: 153; pl. 8, fig. 5, pl. 9, fig. 1.

1991b *Hallopora peculiaris* Pushkin; Buttler: 86; pl. 3, figs 3–8.

MATERIAL. NHM PD 8396.

OTHER OCCURRENCES. Piriguskii Stage (Lower Ashgill, upper Ordovician), Shikipi, Latvia (see Pushkin in Ropot & Pushkin, 1987), Slade and Redhill Beds (upper Rawtheyan, Ashgill), A40 Pengawse Hill diversion, W. of Whitland, Dyfed, Wales (SN 164170) (see Buttler 1991b).

DESCRIPTION. Zoarium erect with cylindrical branches on average 5.7 mm in diameter.

Autozoocelia curve gradually away from the branch axis in the endozone and meet the zoarial surface at approximately 80–90°. In the endozone the zoocelial walls are very thin.

The exozone, recognised by a thickening of the zoocelial walls, has an average width of 1.52 mm. Autozoocelia are circular in transverse section throughout the colony and average 0.29 mm in diameter in the exozone. Diaphragms are rare within the autozoocelia and when present, usually occur closely spaced in the distal exozone. These basal diaphragms are orally-deflected at their junctions with the zoocelial walls and their laminae are generally continuous with the zoocelial linings. The average spacing between diaphragms is 0.17 mm in the exozone.

Mesozoecia are common throughout the whole zoarium, often originating in the inner parts of the endozone. Mesozoecial walls are thin in the endozone and thicken in the exozone. They are polygonal to polygonal-rounded in shallow tangential sections. Basal diaphragms are present throughout their length, spaced on average 0.1 mm apart in the endozone and 0.07 mm in the exozone. Diaphragms tend to increase in thickness distally along the mesozoecia. In some colonies mesozoecial walls are constricted at the position of the diaphragms, producing a slightly beaded appearance.

Autozoocial wall thickness averages 0.1 mm in the exozone. Wall microstructure is composed of steeply inclined, V-shaped laminae. The precise contact between the zoocia is indistinct. The thickened exozonal diaphragms in the mesozoocia are also laminar and are continuous with the wall laminae.

Maculae composed of a concentration of mesozoocia can be recognised in thin sections.

REMARKS. *Hallopore peculiaris* is primarily characterised by the extensive beaded mesozoocia which originate in the inner endozone. The autozoocia are circular throughout the colony, and diaphragms are rare in the endozone, becoming more abundant in the outermost regions.

H. peculiaris has also been described from the Slade and Redhill Beds (Ashgill) of South Wales (Buttler, 1991b).

***Hallopore aff. wesenbergiana* (Dybowski, 1877). Fig. 15**

MATERIAL. NHM PD 8310–8313.

DESCRIPTION. Zoaria erect with thick cylindrical branches, on average 11 mm in diameter.

Autozoocia are parallel to the branch axis in the inner endozone and then curve outwards gradually to meet the zoarial surface at 80°–90°. Within the endozone autozoocial walls are thin and straight.

The exozone is difficult to distinguish; it can be recognised by a slight thickening of the zoocial walls. Autozoocia all originate in the endozone where they are polygonal-rounded in transverse section, becoming circular in the exozone as seen in tangential sections of branches. Autozoocial diameters average 0.21 mm by 0.27 mm within the exozone. Diaphragms are very abundant throughout the autozoocia. In the endozone there are periodic concentrations of diaphragms which occur throughout the colony at the same level. Within the concentrations, diaphragms are spaced on average 0.1 mm apart; elsewhere they are spaced on average 0.6 mm apart. In the exozone, diaphragms are very abundant and on average spaced 0.11 mm apart. All the diaphragms are basal and orally-deflected at their junctions with the zoocial walls.

Mesozoocia are present, originating in the outer parts of the endozone and inner parts of the exozone. They are rounded in shallow tangential sections and have a maximum diameter averaging 0.1 mm. They contain abundant orally deflected basal diaphragms spaced on average 0.07 mm apart in the exozone.

Autozoocial wall thickness averages 0.03 mm in the exozone. The wall microstructure is poorly preserved but vague laminations can be recognised in one tangential section.

REMARKS. *Hallopore aff. wesenbergiana* (Dybowski, 1877) is characterised by the ramos colony form with thick branches. Thin-walled zoocia have rounded apertures in shallow tangential sections. Diaphragms are abundant throughout the whole colony and are periodically concentrated in bands, which possibly indicate periods of slow growth. Bassler (1911) illustrated *H. wesenbergiana* from the Wesenberg Limestone and Wassalen Beds (Caradoc) in Estonia. This material is similar to the Welsh; it has thin-walled autozoocia with abundant diaphragms, although these do not occur in bands. The banding, or lack of it, may not be a specific feature but may relate to an environmental influence acting on the colonies. The poor quality of the Welsh material does not allow a more precise specific identification.

Genus *BATOSTOMA* Ulrich, 1882

***Batostoma clogyfranense* sp. nov.**

Figs 16–18

HOLOTYPE. NHM PD 8362.

PARATYPES. NHM PD 8353–8361, 8363–8375.

NAME. After the type locality.

DIAGNOSIS. Colony small, ramos. Autozoocia curve out gradually from branch axis to zoarial surface. Autozoocial walls thin in endozone. Autozoocia polygonal-rounded in transverse section, circular in shallow tangential sections. Small polygonal-rounded mesozoocia present, originating in outer endozone. Diaphragms present in all zoocia. Acanthostyles small, abundant in exozone.

DESCRIPTION. Zoaria erect with narrow cylindrical branches, on average 3.9 mm in diameter.

Autozoocia curve out gradually from the branch axis to meet the zoarial surface at an angle of 70°–80°. The autozoocia within the endozone have thin walls.

The exozone is narrow with an average diameter of 0.8 mm; it is characterised by a thickening of the zoocial walls. Autozoocia originate in the endozone where they are polygonal-rounded in transverse section, becoming circular in the exozone as seen in tangential sections of branches. Autozoocial diameters average 0.15 mm by 0.18 mm in the exozone. Diaphragms are found throughout the autozoocia, although they are less common in the inner exozone. They are spaced on average 0.28 mm apart in the endozone, and 0.15 mm apart in the exozone. These basal diaphragms are all orally-deflected at their junctions with the zoocial walls and their laminae are continuous with the zoocial linings.

Mesozoocia are present and originate in the outer parts of the endozone. They are polygonal-rounded in shallow tangential sections with a maximum diameter which averages 0.09 mm. Orally-deflected basal diaphragms are found along the length of the mesozoocia, spaced on average 0.07 mm apart.

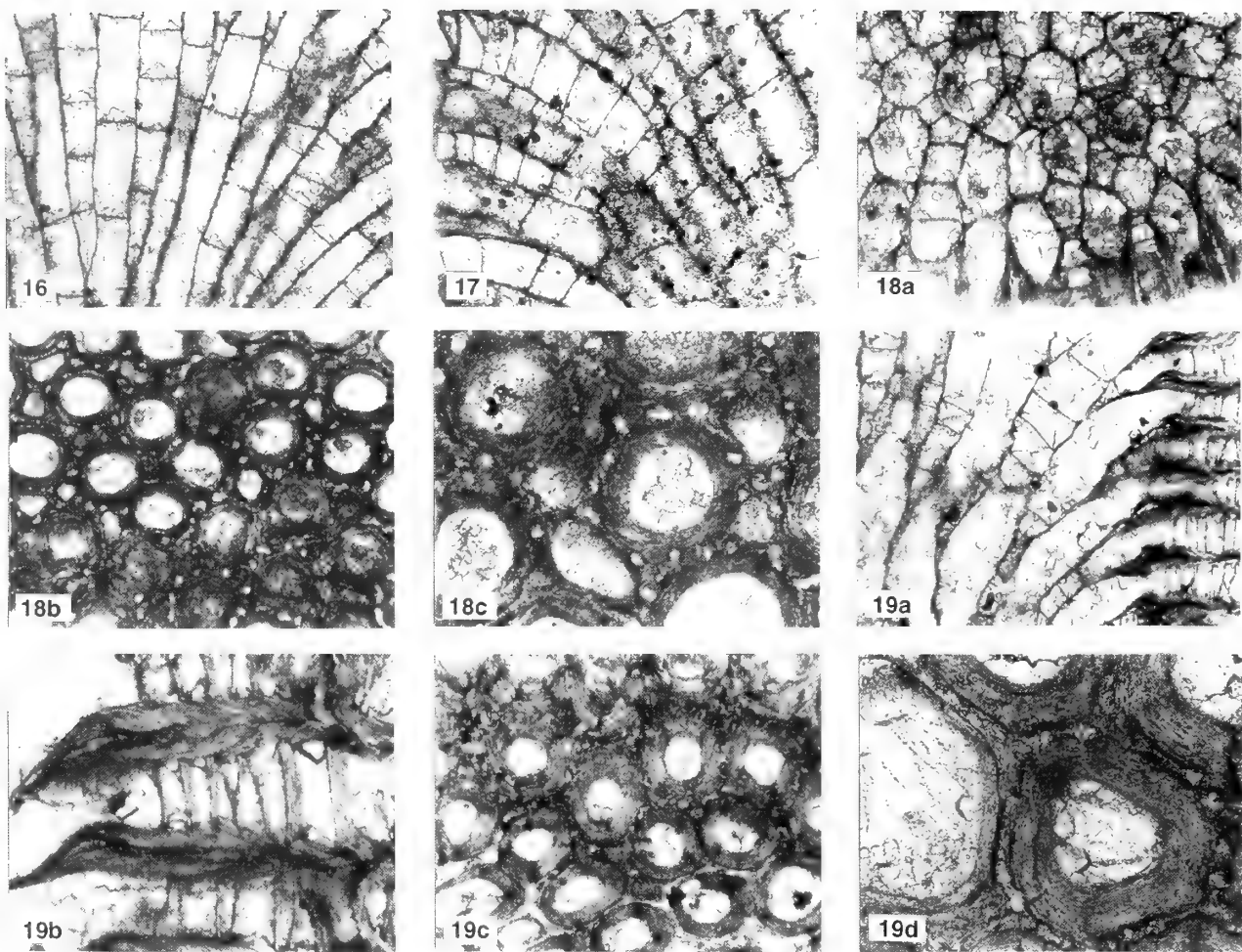
Acanthostyles are small, often irregularly shaped and highly abundant, with an average diameter of 0.03 mm and density of 67 per mm². They originate in the exozone and usually form a ring around the autozoocia, consisting of approximately ten acanthostyles. The acanthostyles are composed of a circular, or sometimes irregular hyaline core surrounded by indistinct dipping conical laminae.

Autozoocial wall thickness averages 0.08 mm in the exozone. Wall microstructure is composed of inclined, U-shaped laminae; however, it is poorly preserved. Frequently, zoocia are infilled with laminar calcite close to the colony surface; in longitudinal section this infilling consists of broad U-shaped laminae; large sections of zoaria often have all the zoocia infilled in this way.

REMARKS. *Batostoma clogyfranense* sp. nov. is primarily characterised by thin, straight zoocial walls, a narrow exozone, and diaphragms regularly spaced throughout the colony. Autozoocial apertures are rounded in shallow tangential section, and polygonal-rounded mesozoocia occur. Acanthostyles are abundant and occasionally irregular in shape.

Another species of *Batostoma*, *B. cf. polare* Astrova, 1965, that is described here can be distinguished from *B. clogyfranense* by the thicker exozonal walls and the less abundant diaphragms in the exozone.

The middle Ordovician species *B. subtile* Astrova (1965: pl. 50, fig. 2, pl. 51, fig. 1), from Vaigach Island, Novaya Zemlya, Russia, has a similar pattern of diaphragms within the endozone to *B. clogyfranense*. Diaphragms are, however, more abundant in the



Figs 16–18 *Batostoma clogyfranense* sp. nov. **16**, NHM PD 8362 (holotype), longitudinal section, x22. **17**, NHM PD 8374 (paratype), longitudinal section, x30. **18**, NHM PD 8362 (holotype); **18a**, transverse section, x30; **18b**, tangential section, showing infilled zooecia, x37; **18c**, tangential section, x86.

Fig. 19 *Batostoma* cf. *polare* Astrova 1965, NHM PD 8324; **19a**, longitudinal section, x22; **19b**, longitudinal section, x70; **19c**, tangential section, x41; **19d**, tangential section, x96.

exozone, and mesozoecia are less common in the Russian species.

Two species of *Batostoma* have been previously described from the Lower Palaeozoic of the Welsh Basin. *B. murchisoni* was described by Spjeldnaes (1957) from 'Horderley' in Shropshire. This species has few diaphragms and mesozoecia, and acanthostyles are absent, suggesting that the species may not belong to *Batostoma*. A re-examination of the type material is required. Owen (1962) described *Batostoma* sp., from the Aymestry Limestone (Ludlow Series, Silurian), Wenlock. This species has a very small exozone and mesozoecia are absent.

Batostoma cf. *polare* Astrova, 1965

Fig. 19

MATERIAL. NHM PD 8324.

DESCRIPTION. Zoarium erect with narrow cylindrical branches, on average 4.5 mm in diameter.

Autozoecia are parallel to the branch axis within the endozone and curve abruptly outwards in the exozone to meet the zoarial surface at 90°. The autozoecia within the endozone have thin, slightly wavy walls.

The exozone is thick with an average diameter of 1.1 mm. It is recognised by an extensive thickening of the zoocial walls and a simultaneous change in zoocial orientation. Autozoecia all originate in the endozone, where they are polygonal-rounded in transverse section. They become circular in the exozone, as seen in tangential sections of branches. Autozoecial diameters average 0.16 mm by 0.2 mm within the exozone. Diaphragms are present throughout the autozoecia, spaced on average 0.06 mm apart in the endozone and increasing greatly to 0.38 mm apart in the exozone. The majority of these are basal diaphragms, which are deflected orally at their junctions with the zoocial walls. Successive diaphragms increase in thickness distally along the autozoecia. Several subterminal, aborally deflected diaphragms have been recognised at the distal end of the colony.

Mesozoecia are present, although not abundant, and originate in the inner parts of the exozone. They have a maximum diameter averaging 0.1 mm. In shallow tangential sections they are rounded. The mesozoecia contain abundant, thick, orally deflected, basal diaphragms, which are spaced on average 0.05 mm apart.

Acanthostyles are small and abundant with an average diameter of 0.02 mm and density of 30 per mm². They originate in the exozone

and usually form a ring around the autozoocia, approximately 14 acanthostyles surrounding one autozoocium. The acanthostyles have a hyaline core surrounded by steeply dipping conical laminae.

Autozoocial wall thickness averages 0.11 mm in the exozone. Wall microstructure is composed of steeply inclined, V-shaped laminae. Zooecial boundaries are dark, crenulated and granular. Some zoocia are infilled with laminar calcite close to the colony surface. In longitudinal section this infilling consists of broad U-shaped laminae.

An intrazoarial overgrowth has been recognised which is continuous with the underlying branch and is composed of outer endozonal/inner exozonal components.

REMARKS. Only one specimen of *Batostoma cf. polare* Astrova, 1965, has been found during this study. It is characterised by the ramos colony form and particularly thin autozoocial walls in the endozone, which thicken extensively in the exozone. Autozoocial apertures are circular in shallow tangential sections, and rounded mesozoocia, which originate in the outer endozone, are present. Thick diaphragms are abundant in the exozone and thin diaphragms occur in the endozone. Acanthostyles are small and numerous in the exozone.

B. polare Astrova, 1965, described from the Varnek Stage, Vaigach and Novaya Zemlya, Russia, is very similar to the specimen from Clog-y-fran. They both have thin zooecial walls in the endozone which thicken in the exozone, abundant basal exozonal diaphragms, small mesozoocia and acanthostyles. Measurements for the Soviet and Welsh specimens are similar. The major difference between the Welsh specimen and type *B. polare* is the presence of the diaphragms within the endozone of the former.

Genus *ERIDOTRYPA* Ulrich, 1893

Eridotrypa simulatrix (Ulrich, 1890)

Fig. 20

- 1890 *Batostoma simulatrix* Ulrich; 432, pl. 35, fig. 1.
- 1893 *Monticulopora simulatrix* (Ulrich); James: 194.
- 1908 *Eridotrypa simulatrix* (Ulrich); Cummings: 828, pl. 16, fig. 4.
- 1928 *Eridotrypa simulatrix* (Ulrich); Bassler: 152
- 1987 *Eridotrypa simulatrix* (Ulrich); Ropot & Pushkin: 171, pl. 15, fig. 2.

MATERIAL. NHM PD 8342–8352.

OTHER OCCURRENCES. Cincinnati Group, Savanna, Illinois, USA; English Head and Vaureal Formations, Anticosti Island, Quebec, Canada; Waynesville Formation, Harmons Station, Indiana, USA; Purguski Stage (Caradoc), Yuzhnoi, Pribaltiki, Russia.

DESCRIPTION. Zoaria erect with narrow cylindrical branches, on average 3.3 mm in diameter.

Autozoocia meander roughly parallel to the branch axis within the endozone and then curve slightly in the exozone to meet the zoarial surface at 50°. Within the endozone they have thin walls.

The exozone is narrow with an average diameter of 0.64 mm. It is recognised by an extensive thickening of the zooecial walls. Autozoocia all originate in the endozone and are rounded-polygonal in transverse section, becoming oval-rounded in the exozone as seen in tangential sections of branches. In branch transverse section the autozoocia are larger in diameter in the inner endozone than in the outer endozone. Autozoocial diameters average 0.13 mm by 0.18 mm within the exozone. Diaphragms are occasionally present in the endozone and exozone, spaced on average 0.35 mm apart in

the endozone and 0.13 mm in the exozone. In some specimens they are very abundant (PD 8348). These basal diaphragms are all deflected orally at their junctions with zooecial walls and their laminae are continuous with the zooecial linings.

Mesozoocia are present and originate in the endozone. They are rounded in shallow tangential section, with a maximum diameter averaging 0.09 mm. Abundant orally deflected diaphragms are found along the length of the mesozoocia, spaced on average 0.07 mm apart.

Acanthostyles are small, occasionally irregular, abundant, with an average diameter of 0.02 mm. They are composed of a hyaline calcite core surrounded by indistinct dipping conical laminae.

Autozoocial wall thickness averages 0.06 mm in the exozone. Wall microstructure is rather indistinct (only peels of these specimens are available) and is composed of steeply inclined, V-shaped laminae. Zooecial boundaries have not been distinguished. Autozoocia, and more especially mesozoocia, are frequently infilled with laminar calcite close to the zoarial surface. In longitudinal section this infilling consists of broad V-shaped laminae; large areas of the colony can be infilled.

REMARKS. *Eridotrypa simulatrix* is characterised by the ramos colony with narrow branches. Autozoocial walls are thin and meandering in the endozone and thicken in the exozone. Autozoocial apertures are large and rounded/polygonal in transverse section, and small and oval in shallow tangential section. Diaphragms are present and abundant small acanthostyles occur in the exozone.

It is not easy to compare the Russian and American specimens of *E. simulatrix* because those from North America are only illustrated by line drawings. The Welsh and Russian specimens appear to be identical but together may prove to represent a distinct species from the American specimens when direct comparisons have been made using the actual material.

Genus *MONTICULIPORA* d'Orbigny, 1850

Monticulipora aff. compacta Coryell, 1921.

Fig. 21

MATERIAL. NHM PD 8328, 8331c.

DESCRIPTION. Zoaria erect with narrow cylindrical branches, on average 4 mm in diameter.

Autozoocia curve out gradually from the branch axis in the endozone and meet the zoarial surface at 90°. The autozoocia within the endozone have thin, slightly wavy walls.

The exozone is moderately broad with an average width of 1.05 mm. It is recognised by a thickening of the zooecial walls. Autozoocia all originate in the endozone, where they are circular in transverse section. They become rounded in the exozone as seen in tangential sections of branches. Autozoocial diameters average 0.16 mm by 0.13 mm within the exozone. Diaphragms are present throughout the autozoocia. They are spaced on average 0.15 mm apart in the endozone and increase to 0.07 mm apart in the exozone. The majority of the diaphragms are basal, deflected orally at their junctions with the autozoocial walls. Some diaphragms are possibly subterminal, but the poor preservation of the specimen does not allow this to be confirmed. Cystiphragms are numerous along the whole length of the autozoocia, especially in the exozone. The cystiphragms are normally restricted to one side of an autozoocium.

Mesozoocia are uncommon, and originate in the outer parts of the endozone and inner parts of the exozone. They have an average maximum diameter of 0.08 mm, are rounded in shallow tangential section and contain abundant, orally deflected basal diaphragms.

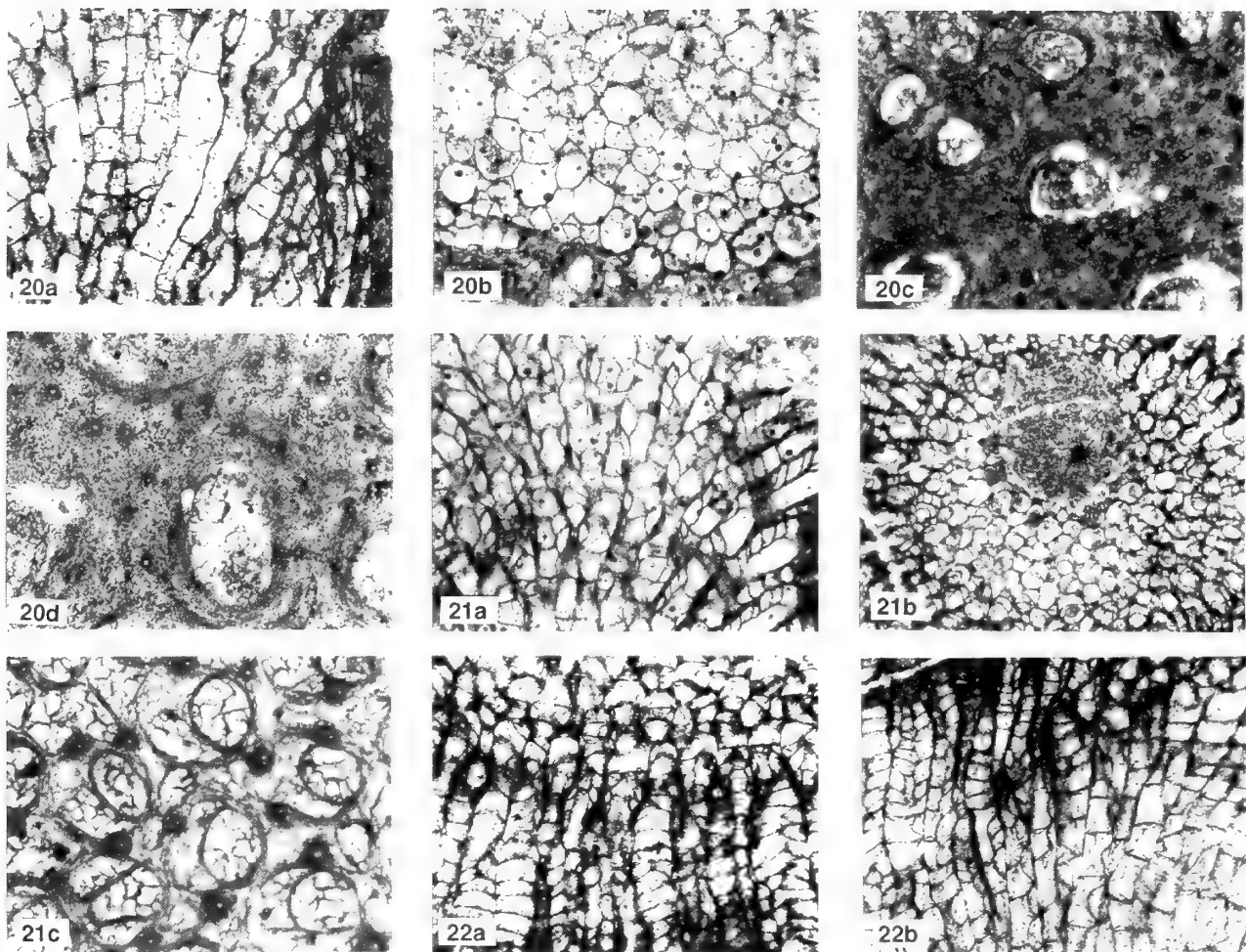


Fig. 20 *Eridotrypa simulatrix* (Ulrich, 1890), NHM PD 8343; **20a**, longitudinal section, x25; **20b**, transverse section, x25; **20c**, tangential section, x53; **20d**, tangential section, x103.

Fig. 21 *Monticulipora* aff. *compacta* Coryell, 1921, NHM PD 8328; **21a**, longitudinal section, x30; **21b**, transverse section, x22; **21c**, tangential section, x86.

Fig. 22 *Homotrypa* cf. *similis* Foord 1883, NHM PD 8323; **22a**, longitudinal section, x30; **22b**, transverse section, x30.

Acanthostyles are abundant with an average diameter of 0.03 mm and density of 47 per mm². They originate throughout the whole colony and occasionally indent autozoocial apertures. The acanthostyles are composed of a hyaline calcite core surrounded by steeply dipping conical laminae.

Autozoocial wall thickness averages 0.05 mm in the exozone. Wall microstructure is composed of steeply inclined, V-shaped laminae. It is, however, indistinct due to the presence of the acanthostyles. Occasional zoocia are infilled with laminar calcite close to the zoarial surface. In longitudinal section this infilling consists of broad U-shaped laminae.

REMARKS. This species is characterised by the ramosc colony form and autozoocial apertures which are rounded in shallow tangential section. Zooecial walls are thin in the endozone, thickening in the exozone. Diaphragms and/or cystiphragms occur in the autozoocia, while the mesozoocia contain only diaphragms. Acanthostyles are abundant throughout the colony. This is the only species of *Monticulipora* encountered in the present study and the material is poorly preserved and visible only in section.

Monticulipora compacta Coryell, 1921, described from the Pierce

Limestone (Caradoc), Tennessee, USA (Coryell 1921: 283), Novaya Zemlya, Vaigach, and Stodolbskgo (middle Ordovician), Zapadno-Arkticheska Province, Russia (Astrova 1965: 197), has a pattern of diaphragms and cystiphragms, and rare mesozoocia similar to the Welsh specimens. In tangential section (Coryell, 1921: pl. iv, fig. 6) the autozoocial apertures are polygonal-rounded. This figured section is, however, quite deep and so cannot be accurately compared with the shallow Welsh sections. In *M. compacta* acanthostyles are reported from within the axial region, but they are not identified from the exozone, in contrast to the Welsh material. The specimens described herein are therefore assigned to *M. aff. compacta* until better preserved material can be examined.

Genus **HOMOTRYPA** Ulrich, 1882

Homotrypa* cf. *similis Foord, 1883

MATERIAL. NHM PD 8323.

DESCRIPTION. Zoarium erect with cylindrical branches, on average 8 mm in diameter.

Fig. 22

Autozoooecia are roughly parallel to the branch axis within the endozone, and gradually curve outwards to meet the zoarial surface at approximately 70°. Walls are thin and slightly wavy within the endozone.

The exozone has an average diameter of 1.6 mm, and is recognised by a slight thickening of the zoocial walls. The autozoooecia originate within the endozone, where they are polygonal in transverse section. No tangential sections are available. Diaphragms are present throughout the autozoooecia. They are spaced on average 0.26 mm apart in the endozone and 0.1 mm apart in the exozone. The diaphragms are basal and are orally deflected at their junctions with the zoocial walls. Many diaphragms in the endozone are inclined and some are sigmoidal. Cystiphragms are numerous in the exozone where there are, on average, ten present per mm. The cystiphragms are normally restricted to one side of the autozoooecia.

Mesozoocia are rare and originate in the exozone when present, with an average maximum diameter of 0.08 mm. They contain abundant orally deflected basal diaphragms, spaced on average 0.04 mm apart.

Small inconspicuous acanthostyle-like structures have been observed in the exozone; tangential sections are needed for their precise identification.

Autozoocia wall thickness averages 0.04 mm in the exozone. Wall microstructure is composed of inclined V-shaped laminae. The zoocial boundaries are dark and crenulated. Some zoocia are infilled close to the zoarial surface. In longitudinal section this infilling consists of broad U-shaped laminae.

REMARKS. Only one incomplete specimen of *Homotrypa* has been found in this present study; this has made identification difficult, especially as no tangential section could be obtained. The specimen is characterised by thin autozoocia walls in the exozone and rare mesozoocia. The autozoocia contain abundant diaphragms, especially in the exozone, often sigmoidal in shape in the endozone. Cystiphragms are extremely numerous in the exozone.

Ross (1963, 1965) described three Ordovician species; *Homotrypa* sp. A, *Homotrypa* sp. B and *H. oweni* from the Hoar Edge Group (Caradoc Series), Shropshire. *Homotrypa* sp. A of Ross (1963) has widely spaced diaphragms and cystiphragms; mesozoocia and dense acanthostyles are present but not always easy to observe in tangential section. The autozoocia apertures are polygonal to subpolygonal in shallow tangential sections. *Homotrypa* sp. B of Ross (1963) has thin autozoocia walls within the endozone and subpolygonal zoocial apertures. Diaphragms are present throughout the colony and acanthostyles are long and thin. The specimen from Clog-y-fran differs from *Homotrypa* sp. A in having more abundant diaphragms and cystiphragms; and from *Homotrypa* sp. B by the absence of long thin acanthostyles. *Homotrypa oweni* Ross, 1965 differs from the Clog-y-fran specimen in having a cone-shaped or encrusting colony form, mesozoocia and rare diaphragms.

The arrangement of the cystiphragms and diaphragms in the Welsh specimen is similar to that found in *Homotrypa similis* Foord, 1883 (e.g. Karklins 1984: pl. 5, figs 2, 3). This species is well known in North America and Eastern Europe. *H. similis* has acanthostyles in the exozone but in the specimen from Clog-y-fran their presence is questionable. Bork & Perry (1968: 1053) recognised *H. similis* (from the Guttenberg and Ion Formations, middle Ordovician, Iowa, USA) in longitudinal section 'by extremely gradual curvature of the zoocia towards the zoarial surface, diaphragms throughout most of the axial region and well-developed cystiphragms and diaphragms in the mature zone'; the Welsh specimen fits this description.

Karklins (1984: 29) noted a difference between specimens of *H. similis* from the Trenton Beds (middle Ordovician), Ottawa, Canada,

and the Lexington Limestone (middle/upper Ordovician), Kentucky, USA, and those from the Wassalen Beds (Caradoc) of Estonia (described by Bassler 1911). Specimens from Estonia have relatively broadly serrated autozoocia boundaries and well-defined acanthostyles which commonly indent the autozoocia apertures. North American specimens have narrower serrated boundaries and poorly-defined acanthostyles. The cystiphragms in the Estonian specimens are more closely spaced in the exozone than those of North America. Middle Ordovician specimens from Vaigach Island in Russia, illustrated by Astrova (1965: pl. 35), do not, however, have large acanthostyles, and their cystiphragms first occur in the outer endozone and become closely-spaced in the exozone. Thus, there appears to be a wide range of variation within the species *H. similis*.

The Clog-y-fran specimen is compared herein with *H. similis* rather than positively identified as this species because the incomplete specimen does not provide sufficient information.

Genus *MONOTRYPA* Nicholson, 1879

Monotrypa sp.

Figs 23–24

MATERIAL. NHM PD 8329, 8330.

DESCRIPTION. Zoaria hemispherical, on average 13.5 mm in diameter.

The majority of autozoocia originate from the basal lamina and curve gently outwards to meet the zoarial surface. Autozoocia walls are straight throughout the colony. No differentiation between endozone and exozone can be recognised. The autozoocia are polygonal-rounded in transverse section, with an average diameter of 0.29 mm by 0.32 mm. Diaphragms are rare, usually only one per autozoocium. In one specimen (PD 8329), however, there is a small area of the colony with relatively numerous diaphragms which are thin, basal and orally deflected at their junctions with the zoocial walls.

Autozoocia wall thickness averages 0.02 mm at the periphery of the colony. Wall microstructure is composed of inclined U-shaped laminae; the zoocial boundaries are indistinct. Occasionally zoocia are infilled with laminar calcite close to the zoarial surface. In longitudinal section this infilling consists of broad U-shaped laminae.

REMARKS. The specimens described herein are characterised by the hemispherical colony form and polygonal-rounded autozoocia. Autozoocia walls are thin and straight, with no differentiation between endozone and exozone. Diaphragms are generally uncommon. Only two specimens are known, both in peels.

Several species of *Monotrypa* with thin straight walls and sparse diaphragms have previously been described, e.g. *M. testudiformis* and *M. cantareloidea* described by Dreyfuss (1948: pl. 2, figs 4, 5, 8–10) from the upper Ordovician of the Montagne Noire.

The poor quality of the Welsh specimens prevents detailed comparisons with other species, so their identification is left in open nomenclature.

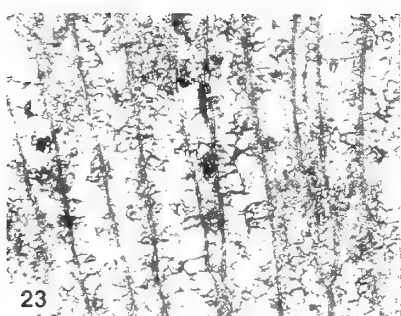
Genus *AMPLEXOPORA* Ulrich, 1882

Amplexopora sp.

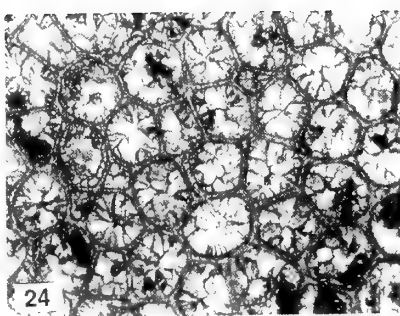
Figs 25–26

MATERIAL. NHM PD 8325, 8326.

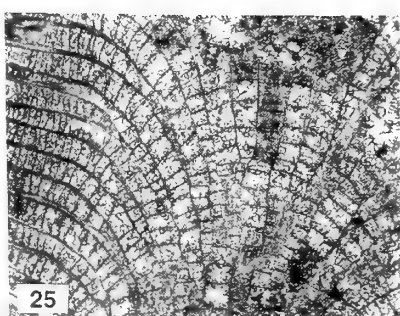
DESCRIPTION. Zoaria erect with thick cylindrical branches, on average 8 mm in diameter.



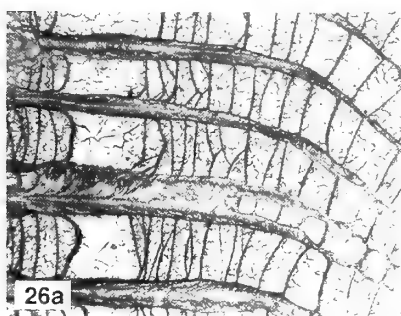
23



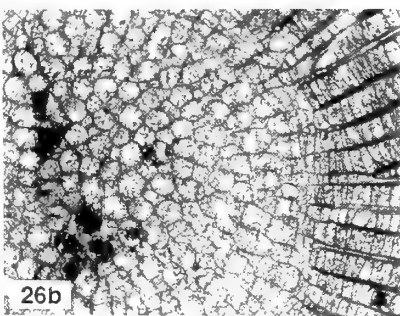
24



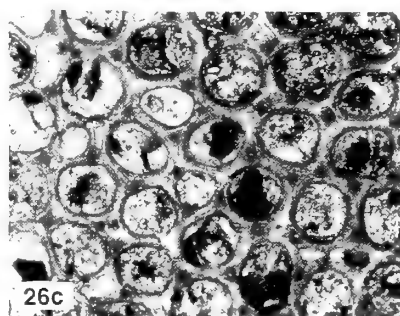
25



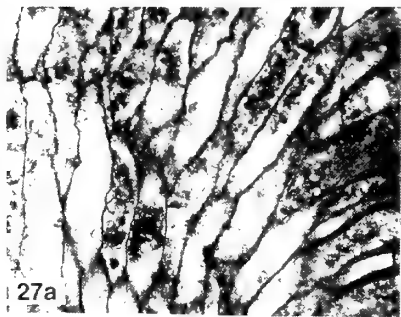
26a



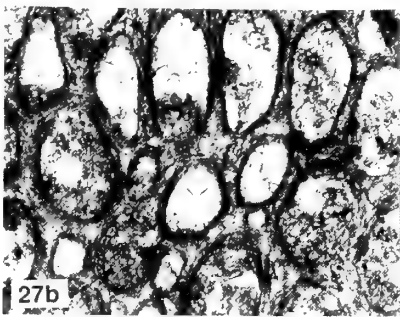
26b



26c



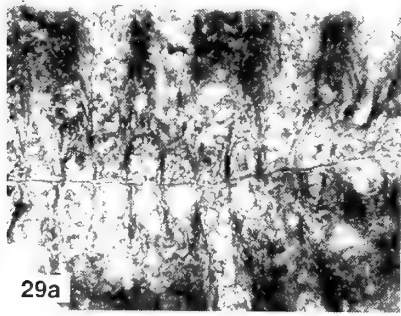
27a



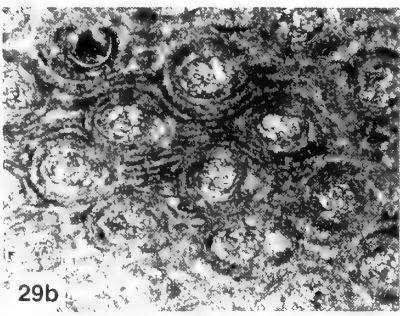
27b



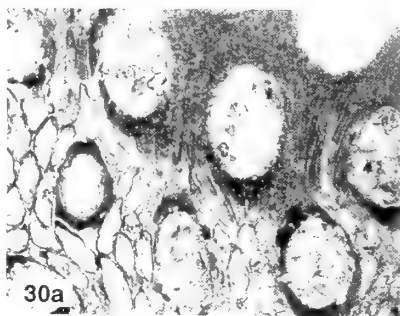
28



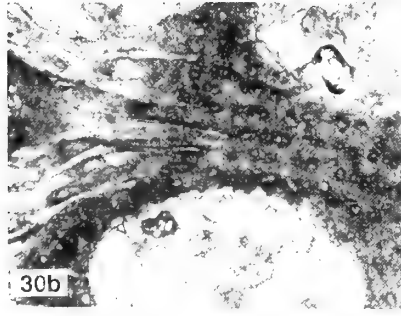
29a



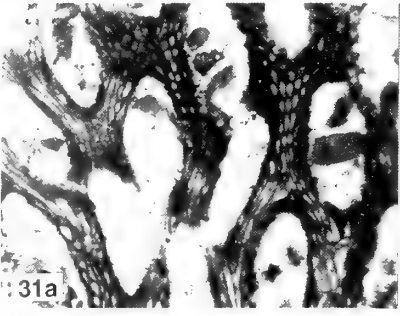
29b



30a



30b



31a



31b

Autozoocia curve out gradually from the branch axis in the endozone and change direction abruptly in the exozone to meet the colony surface at 90°. Autozoocia within the endozone all have very thin walls.

The exozone is wide, with an average diameter of 1.9 mm. It is recognised by a thickening of the zooecial walls and a simultaneous change in zooecial orientation. Autozoocia all originate in the endozone where they are rounded in transverse section, becoming irregularly rounded in the exozone as seen in tangential sections of the branches. Autozoocia diameters average 0.24 mm by 0.3 mm within the exozone.

Diaphragms are very abundant and closely spaced along the whole length of the autozoocia. They are spaced on average 0.23 mm apart in the endozone, decreasing to 0.09 mm apart within the exozone. All diaphragms are basal and are orally deflected at their junctions with the zooecial walls. In the mid exozone of specimen PD 8325 there is a large interval (0.34 mm) between two adjacent diaphragms, which is found in the same position throughout the colony. The first diaphragms on the distal side of this interval are greatly deflected orally. In the majority of the colony, growth resumes as normal after the interval; however, in some small sections the thickened exozonal wall terminates and is replaced by one much thinner.

Mesozoocia are present, although not abundant, and have a maximum diameter averaging 0.12 mm. They originate in the exozone, are oval in shape in shallow tangential sections, and contain abundant orally deflected basal diaphragms, spaced on average 0.05 mm apart.

Acanthostyles are large and abundant, with an average diameter of 0.05 mm and density of 14 per mm². They originate throughout the exozone, commonly extending the entire length of the exozone, and can slightly indent the zooecial apertures. The acanthostyles are composed of a hyaline core surrounded by steeply dipping conical laminae.

Autozoocia wall thickness averages 0.08 mm in the exozone. Wall microstructure is composed of inclined U-shaped laminae. Zooecial boundaries are indistinct. Some zooecia (especially mesozoocia) are infilled with laminar calcite close to the zoarial surface; in longitudinal section this infilling consists of broad U-shaped laminae.

REMARKS. This species is characterised by the ramosc colony form, thin autozoocia walls and rounded apertures in shallow tangential section. Oval mesozoocia are present and originate in the outer endozone/inner exozone. Basal diaphragms are abundant throughout the colony, and large acanthostyles are abundant in the exozone.

Three species of *Amplexopora* have been previously described from the Welsh Basin. All were described by Ross (1963, 1965) from the Hoar Edge Limestone, Hoar Edge Group (Caradoc), Evenwood Quarry, Shropshire, and all vary markedly from the species described herein. *A. thomasi* Ross, 1963 is a bifoliate species with

small acanthostyles and lacking diaphragms in the endozone. *A? evenensis* Ross, 1965 and *Amplexopora?* sp. A of Ross, 1965 both have crenulate walls, diaphragms confined to the exozone and small acanthostyles.

The specimens of *Amplexopora* from Clog-y-fran are similar to *A. septosa* (Ulrich, 1879) (redescribed by Boardman 1960) from the Fairview Formation (Ashgill), Covington, Kentucky. The major differences in *A. septosa* are the absence of diaphragms in the endozone and the presence of numerous short, off-set acanthostyles, as well as the long acanthostyles which occur throughout the exozone. Off-set acanthostyles can be identified in specimen PD 8326, but have not been recognised in PD 8325.

Other examples of *Amplexopora* containing abundant diaphragms in the endozone have been described by Brown & Daly (1985) from the Dillsboro Formation (Cincinnatian Series) of SE Indiana; they were identified as *A. cf. septosa*. Numerous specimens (over 150) of *A. septosa* were collected from this formation, including a few atypical specimens with abundantly spaced diaphragms in the endozone. Brown & Daly (1985: 24) suggested that because the specimens were similar in all other respects to *A. septosa* the differences may be due to environmental factors. The specimens from Clog-y-fran are very similar to those from the Dillsboro Formation, except that the short acanthostyles are less common and the diaphragms more abundant.

Genus *HALLOPORINA* Bassler, 1911

Halloporma cf. crenulata (Ulrich, 1893)

Fig. 27

MATERIAL. NHM PD 8315, 8394.

DESCRIPTION. Zoaria erect with cylindrical branches, on average 4.5 mm in diameter.

Autozoocia are parallel to the branch axis within the endozone and then curve outwards gradually in the exozone to meet the zoarial surface at 70°. The autozoocia within the endozone have very thin wavy walls.

The exozone is narrow with an average diameter of 0.76 mm. It is recognisable by a thickening of the zooecial walls and a simultaneous change in zooecial orientation. Autozoocia all originate in the endozone where they are polygonal-rounded in transverse section, becoming oval-rounded in the exozone, as seen in tangential sections of branches. Autozoocia diameter averages 0.18 mm by 0.22 mm within the exozone. Basal diaphragms are rare or even wholly absent in the autozoocia and, if present, only one or two are found in the exozone. They are all deflected orally at their junctions with the zooecial walls and their laminae are continuous with the autozoocia linings.

Exilazooecia are present and originate in the exozone. They are rounded in shape in shallow tangential sections, with a maximum diameter averaging 0.08 mm. They occasionally contain orally

Figs 23, 24 *Monotrypa* sp. 23, NHM PD 8330; longitudinal section, x30. 24, NHM PD 8329; tangential section, x30.

Fig. 25 *Amplexopora* sp., NHM PD 8325; longitudinal section, x12.

Fig. 26 *Amplexopora* sp., NHM PD 8325; 26a, longitudinal section, showing large interval between adjacent diaphragms, x35; 26b, transverse section, x12; 26c, tangential section, x30.

Fig. 27 *Halloporma cf. crenulata* (Ulrich 1893), NHM PD 8315; 27a, longitudinal section, x22; 27b, tangential section, x61.

Figs 28, 29 *Graptodictya bonnemai* Bassler 1911. 28, NHM PD 8392b, longitudinal section, x30. 29, NHM PD 8389; 29a, transverse section, x55; 29b, tangential section, x55.

Fig. 30 *Pushkinella* sp., NHM PD 8376; 30a, tangential section, x22; 30b, tangential section, x53.

Fig. 31 *Phylloporina* sp., NHM PD 8384; 31a, tangential section, x12; 31b, tangential section, x22.

deflected basal diaphragms, and are therefore mesozoocia (*sensu stricto*), but the term exilazoocia is retained for consistency with the genus description.

Autozoocia wall thickness averages 0.05 mm in the exozone. Wall microstructure is composed of steeply inclined, V-shaped laminae; the zoocia wall boundaries are dark and granular. Some exilazoocia are infilled with laminar calcite close to the zoarial surface. In longitudinal section this infilling consists of broad U-shaped laminae.

REMARKS. *Halloporella crenulata*, the type species of the genus, has been described from the Black River and Trenton Formations (middle Ordovician) of the U.S. mid-west but has not been recognised elsewhere. Only one other species of *Halloporella* has hitherto been identified: *H. parva* (Ulrich & Bassler, 1904), also from the Black River and Trenton Formations of the U.S. mid-west. *H. crenulata* is distinguished from *H. parva* in having a larger zoarium, larger rounded zoocia apertures (*H. parva* has polygonal zoocia apertures) and more abundant exilazoocia. Nothing is known about the range of variation within either species of *Halloporella*. Ulrich & Bassler (1904: pl. xiv) illustrated the two species. Colony size appears to be the only major difference between them as shown in the illustrations. The drawings indicate little difference in zoocia aperture shape; the tangential section of *H. crenulata* is, however, deeper than in *H. parva*. A re-examination of the species and further material, is needed for a greater understanding of these species.

The specimens from Clog-y-fran are identified only as *H. cf. crenulata*. The identification is tentative due to the presence of occasional diaphragms within the outer exozone. The rounded zoocia and relatively abundant exilazoocia suggest similarity to *H. crenulata* rather than *H. parva*.

Order CRYPTOSTOMATA Vine, 1884

Suborder PTILODICTYINA Astrova & Morozova, 1956
Family ESHAROPORIDAE Karklins, 1983
Genus *GRAPTOGLOSSA* Ulrich, 1882

Graptodictya bonnemai Bassler, 1911

Figs 28–29

- 1911 *Graptodictya bonnemai* Bassler: 122, pl. 8, fig. 3, text-fig. 48.
- 1921 *Graptodictya bonnemai jaervensis* Bekker: 58, pl. 8, figs 1–4.
- 1952 *Graptodictya bonnemai* Bassler; Toots: 126, pl. 7, figs 5, 8, pl. 8, fig. 3, pl. 9, figs 1, 2, pl. 10, fig. 1.
- 1965 *Graptodictya bonnemai* Bassler; Astrova: 2252, pl. ix, fig. 2, pl. lxi, fig. 1.
- 1970 *Graptodictya bonnemai* Bassler; Nekhorosheva: 86, pl. viii, fig. 1.

MATERIAL. NHM PD 8389–8391, 8392b, 9393.

OTHER OCCURRENCES. Kuckers Shale (Kukruse Stage, Llandeilo), Baron Toll's Estate, Estonia; Jarve, Kukersite Quarry, Wesenberg Limestone (Kukruse Stage, Llandeilo), Wesenberg, Estonia; Vaigach Island and Pai-khoi (Yugorskiy Stage, Llandeilo/Caradoc), Urals, Russia.

DESCRIPTION. Zoaria erect with thin branches, on average 1.85 mm wide by 0.69 mm deep. The margins of the branches are striated.

Mesothecae are thin and sinuous. In the exozone the autozoocia form 90° angles with the mesothecae. Autozoocia apertures are oval in shallow tangential sections and average 0.48 mm by 0.3 mm

in the exozone. Short superior hemisepta are commonly present. Autozoocia boundaries are slightly serrated. Zooacial wall microstructure is composed of broadly U-shaped laminae. Exilazoocia and diaphragms are absent.

REMARKS. *Graptodictya bonnemai* was first described by Bassler (1911: 122) from Estonia, as being very similar to the type species of *Graptodictya* (*G. perelegans*). The two species were distinguished by *G. bonnemai* branching less frequently and having more elongate autozoocia apertures.

Order FENESTRATA Elias & Condra, 1957
Suborder PHYLLOPORININA Lavrentjeva, 1979
Family ENALLOPOROIDAE Miller, 1889
Genus *PUSHKINELLA* Lavrentjeva, 1979

Pushkinella sp.

Fig. 30

MATERIAL. NHM PD 8376–8378, 8380–8383.

DESCRIPTION. Zoaria are reticulate and anastomosing; only fragmentary specimens have been found at Clog-y-fran. No exterior frontal views of the colonies are available because frontal surfaces are all embedded in sediment.

Fenestrules are oval-rounded, with diameters averaging 0.58 mm by 0.42 mm. Branches are rounded and average 0.38 mm diameter.

The exozone is distinguished by a change in the orientation of the autozoocia and considerable thickening of the zoocia walls. Autozoocia are rounded in the endozone, becoming rounded-slightly petaloid in the exozone, where they average 0.16 mm in diameter. Across one branch one to three autozoocia are present.

Wall microstructure is hard to distinguish. In one specimen (PD 8378) longitudinal laminar microstructure can be identified. Short, narrow acanthostyles are abundant throughout the colony; in the exozone they occasionally indent the autozoocia apertures. The acanthostyles are composed of a hyaline core surrounded by conical laminae, and are on average 0.1 mm in diameter.

REMARKS. The genus *Pushkinella* was previously known only from the Baltic region of the former Soviet Union. Two Ordovician species have been recognised: *P. mirabilis* Lavrentjeva 1979, and *P. robusta* Lavrentjeva 1979, from Estonia, and one Silurian, *P. acanthroporoides* Pushkin 1976, from Byelorussia.

The Welsh specimens of *Pushkinella* are characterised by the anastomosing colony form, the small oval-rounded fenestrules and rounded branches. Autozoocia walls are extensively thickened in the exozone and autozoocia apertures are rounded to slightly petaloid. Short and narrow acanthostyles are abundant.

The Welsh specimens differ from *P. robusta* in having more zoocia apertures per branch, and from *P. acanthroporoides* in having a greater number of acanthostyles. *P. mirabilis* has similar-sized apertures and acanthostyles to the Welsh material, but differs in having occasional basal diaphragms, which are absent in the Welsh specimens.

Family PHYLLOPORINIDAE Ulrich, 1890
Genus *PHYLLOPORINA* Foerste, 1887

Phylloporina sp.

Fig. 31

MATERIAL. NHM PD 8384.

DESCRIPTION. Zoaria are reticulate and anastomosing, only fragmentary specimens have been found at Clog-y-fran. No exterior frontal views of the colonies are available because frontal surfaces are all embedded in sediment.

Fenestrales are oval, with diameters averaging 0.78 mm by 1.67 mm. Branches are rounded and average 0.48 mm diameter. The reverse side of the colony is striated.

The exozone is distinguished by a change in the orientation of the autozoocia and a thickening of the zooecial walls. Rounded zooecial apertures are present on the frontal side of the colony. The apertures average 0.09 mm by 0.12 mm in diameter in the exozone. Three to four zooecial rows occur on each branch.

Zooecial walls are thin and straight. Occasional basal diaphragms have been observed which are deflected orally at their junction with the zooecial walls and in some cases have laminae continuous with the zooecial linings.

The microstructure is laminar, although hard to distinguish. Possible acanthostyle-like structures are present.

REMARKS. The specimen from Clog-y-fran is fragmentary and embedded in sediment, which makes identification difficult. It is characterised by rounded branches and oval fenestrales. Zooecial walls are straight in the endozone, becoming thickened in the exozone. Zooecial apertures are rounded and three to four rows occur on each branch. Occasional diaphragms are present and acanthostyle-like structures have been recognised.

Phylloporina hillistensis, described from Estonia by Lavrentjeva (1985: pl. iii, fig. 2), has similar thick straight endozonal walls and occasional diaphragms but differs from the Clog-y-fran specimen in having more abundant zooecia per branch and lacking striae on the reverse of the colony.

ACKNOWLEDGEMENTS. I would like to thank Dr. P.D. Taylor and Dr. J.C.W. Cope for supervising this project, which was carried out under the tenure of a Natural Environment Research Council Studentship. I am grateful to Dr. D.H. Evans and Mr. F. Cross for assistance in the field. I would also like to thank Mrs D.G. Evans for drafting Table 1 and Fig. 1, and Mrs L. Weaver for re-typing the manuscript.

REFERENCES

- Astrova, G.G. 1965. Morfologiya, istoriya razvitiya i sistema ordovikskikh i siluriiskikh mshanok. *Trudy Paleontologicheskogo Instituta Akademii Nauk SSSR*, Moscow, **106**: 432 pp, 84 pls (In Russian).
- 1978. Istorya razvitiya, sistema i filogeniya mshanok, Otryad Trepostomata. *Trudy Paleontologicheskogo Instituta Akademii Nauk SSSR*, Moscow, **169**: 240 pp., 46 pls (In Russian: Engl. transl. by D.A. Brown, 307 pp, no pls.).
- & Morozova, I.P. 1956. K sistematike mshanok otryada Cryptostomata. *Doklady Akademii Nauk SSSR*, Sovetskikh Sotsialisticheskikh Republik. St Petersburg, **110**: 661–664 (In Russian).
- Bassler, R.S. 1911. The Early Paleozoic Bryozoa of the Baltic Provinces, *Bulletin of the United States National Museum*, Washington, **77**: 11–137.
- 1928. Bryozoa. In, Twenhofel, W.H., Geology of Anticosti Island, *Memoirs of the Geological Survey of Canada*, Ottawa, **154**: 143–168.
- Bekker, H. 1921. The kukers stage of the Ordovician rocks of N.E. Estonia. *Acta et Commentationes Universitatis Tartuensis*, Dorpat, A2: 92 pp.
- Bengston, P. 1988. Open nomenclature. *Palaontology*, London, **31**: 223–227.
- Boardman, R.S. 1960. A revision of the Ordovician bryozoan genera *Batostoma*, *Anaphragma* and *Amplexopora*. *Smithsonian Miscellaneous Collections*, Washington, **140**: 28 pp.
- , Cheetham, A.H., Blake, D.B., Utgaard, J., Karklins, O.L., Cook, P.L., Sandberg, P.A., Lutaud, G. & Wood, T.S. 1983. Bryozoa (revised). In, Robison, R.A. (ed), *Treatise on Invertebrate Paleontology*, G (1): 625 pp. Boulder, Colorado and Lawrence, Kansas.
- Borg, F. 1926. Studies on recent Cyclostomous Bryozoa. *Zoologiska Bidrag fran Uppsala*, **10**: 181–507.
- Bork, K.B. & Perry, T.G. 1968. Bryozoa (Ectoprocta) of Champlainian age (Middle Ordovician) from northwestern Illinois and adjacent parts of Iowa and Wisconsin. Part III, *Homotrypa*, *Orbignyella*, *Prasopora*, *Monticulipora* and *Cyphotrypa*. *Journal of Paleontology*, Menasha, **42**: 1042–1065, pls 133–138.
- Brown, G.D. 1965. Trepostomatous Bryozoa from the Logana and Jessamine Limestone (Middle Ordovician) of the Kentucky Bluegrass region. *Journal of Palaeontology*, Tulsa, **39**: 974–1006.
- & Daly, E.J. 1985. Trepostome Bryozoa from the Dillsboro Formation (Cincinnatian Series) of south-eastern Indiana. *Special report of the Geological Survey of Indiana*. Bloomington, **33**: 1–95.
- Buttler, C.J. 1988. Studies on Ordovician bryozoans from Wales and the Welsh Borderland. Ph.D. thesis. University of Wales (unpublished).
- 1991a. Bryozoans from the Llanbedrog Mudstones (Caradoc), north Wales. *Bulletin of British Museum of Natural History (Geology Series)*, London, **47**: 153–168.
- 1991b. Studies on Ordovician bryozoan fauna from the Slade and Redhill Beds, South Wales. *Palaontology*, London, **34**: 77–108.
- Coryell, H.N. 1921. Bryozoan faunas of the Stones River Group of central Tennessee. *Proceedings of the Indiana Academy of Sciences*, Brookville, **1919**: 261–340, 14 pls.
- Cummings, E.R. 1908. The Stratigraphy and Palaeontology of the Cincinnati Series of Indiana. *Annual Report, Indiana Department of Geology and Natural Resources*, Indianapolis, **32** (for 1907): 605–1188, 55 pls.
- Dreyfuss, M. 1948. Contribution à l'étude géologique et paléontologique de l'Ordovicien supérieur de la Montagne Noir. *Mémoires de la Société Géologique de France. Paléontologie*, Paris, **58**: 63 pp.
- Dybowski, W. 1877. Die Chaetetiden der ostbaltischen Silurformation. *Verhandlungen der Russisch-Kaiserlichen Mineralogischen Gesellschaft zu St. Petersburg*, St. Petersburg, **14**: 1–134.
- Ehrenberg, C.G. 1831. In, Hemprich, F.G. & Ehrenberg, C.G., *Symbolae physicae, seu icones et descriptiones animalium evertebratorum*. **4** (Evertebrates 1). 126 pp., 10 pls. (1828), Stockholm.
- Eichwald, E. 1856. Beitrag zur geographischen Verbreitung der fossilen Thiere Russland. *Bulletin de la Société Impériale de Naturalistes de Moscou*. Moscow, **29**: 91–96.
- 1860. *Lethaea russica ou Paleontologie de la Russie. Ancienne Periode*. Stuttgart, I: 355–419, 434–435, 450–452, 475–495.
- Elias, R.J. & Condra, G.E. 1957. *Fenestella* from the Permian of West Texas. *Memoirs of the Geological Society of America*, Washington, **70**: 158 pp.
- Foerste, A.F. 1887. The Clinton Group of Ohio, Pt.III. *Bulletin of the Scientific Laboratories of Denison University*, Granville, Ohio, **2**: 140–176.
- Foord, A.N. 1883. Contribution to the micropalaeontology of the Cambro-Silurian rocks of Canada. *Geological and Natural History Survey*, Canada, Ottawa, 26 pp.
- Fortey, R.A., Harper, D.A.T., Ingham, J.K., Owen, A.W. & Rushton, A.W.A. 1995. A revision of the Ordovician series and stages from the historical type area. *Geological Magazine*, **132**: 15–30.
- James, J.F. 1893. Manual of the palaeontology of the Cincinnati Group. *Journal of the Cincinnati Society of Natural History*, Cincinnati, **15**: 144–159.
- Karklins, O. 1983. Ptilodichyoid Cryptostomata Bryozoa from the Middle and Upper Ordovician rocks of Central Kentucky. *Journal of Paleontology*, Tulsa, **57**: (Memoir 14): 1–31.
- 1984. Trepostomate and cystoporite bryozoans from the Lexington Limestone and Clays Ferry Formation (Middle and Upper Ordovician) of Kentucky. *Professional Paper, United States Geological Survey*, Washington, **1066-1**: 105 pp.
- Lavrentjeva, V.D. 1979. Novii portirad paleozoicheskikh mshanok. *Paleontologicheskiy Zhurnal*, Moscow, 9–68. (In Russian).
- 1985. Mshanki Podotriada Phylloporinina. *Trudy Paleontologicheskogo Instituta Akademii Nauk SSSR*. Moscow, **214**: 102 pp.
- Miller, S.A. 1889. *North American Geology and Palaeontology*. Western Methodist Book Concern, Cincinnati, 664 pp.
- Modzalevskaya, E.A. 1953. Trepostomaty Ordovika Pribaltiki i ikh stratigraphicheskoe znachenie. *Trudy Vsesouznogo Neftyanogo Nauchno-Issledovatel'skogo Geologo-Razvedochnogo Instituta (VNIGRI)*, Leningrad & Moscow, **Y 78**: 91–167, 14 pls (In Russian).
- Nekhorosheva, L.V. 1970. Ordovician bryozoans from the north of Pai-khoi, Vaigach, and the south of Novaya Zemlya. In, Bondarev, V.I. (ed.), *Opornyiy razrez Ordovika Pai-khoya, Vaigacha i yugo Novoi Zemli*: 63–95, 9 pls. Leningrad, Izd-vo NIIGA, (In Russian).
- Nicholson, H.A. 1879. *On the Structure and Affinities of the 'Tabulate Corals' of the Palaeozoic Period with Critical Descriptions of Illustrative Species*. 342 pp. Edinburgh.
- Orbigny, A. d' 1850. *Prodrome de paleontologie stratigraphique universelle*. **1**: 394 pp., Paris.
- Owen, D.E. 1962. Ludlovian Bryozoa from the Ludlow District. *Palaontology*, London, **5**: 195–212.
- 1965. Silurian Polyzoa from Benthall Edge, Shropshire. *Bulletin of the British Museum of Natural History (Geology)*, London, **10**: 95–117.
- 1969. Wenlockian Bryozoa from Dudley, Niagara and Gotland and their palaeogeographic implications. *Palaontology*, London, **12**: 621–636.
- Pushkin, V.I. 1976. Novye vidy mshank iz Ordovika i Silura brestskoi vpadiny. V Kn.:

- Novye vidy iskopaemykh zhivotnykh i rastenii Belorussii. *Nauka i tekhnika*, Minsk, 40 pp. (In Russian).
- Ropot, I.V. & Pushkin, V.I.** 1987. *Ordovik Beloruskiy*. 234 pp., 23 pls. Minsk, Institut Geochemimii i Geofiziki Akademii Nauk Beloruskoj S.S.R. & Beloruskiy Nauchno-Issledovatel'skiy Geologorazvedochnyy Institut. (In Russian).
- Ross, J.R.P.** 1963. Trepostome Bryozoa from the Caradoc Series, Shropshire. *Palaeontology*, London, **6**: 1–11.
- 1965. *Homotrypa* and *Amplexopora*? from the Caradoc series, Shropshire. *Palaeontology*, London, **8**: 5–10.
- Scotese, C.R. & McKerrow, W.S.** 1990. Revised world maps and introduction. In, McKerrow, W.S. & Scotese, C.R. (eds), Palaeozoic palaeogeography and biogeography. *Memoir of the Geological Society of London*, **12**: 1–12.
- Spjeldnaes, N.** 1957. A redescription of some type specimens of British Ordovician Bryozoa. *Geological Magazine*, Hertford, **94**: 364–376, pls. 12–13.
- 1963. Some silicified Ordovician fossils from south Wales. *Palaeontology*, London, **6**: 254–263, pls. 36–37.
- Strahan, A., Cantrill, T.C., Dixon, E.E.L. & Thomas, H.H.** 1909. The geology of the South Wales coal-field, Part X, The county around Carmarthen. *Memoirs of the Geological Survey*, London, **229**: 177 pp.
- Taylor, P.D. & Cope, J.C.W.** 1987. A trepostome bryozoan from the Lower Arenig of South Wales: implications of the oldest described bryozoan. *Geological Magazine*, Cambridge, **124**: 367–371.
- Toots, H.** 1952. Bryozoan des estruschen Kukersits. *Mitteilungen aus dem geologischen Staatsinstitut in Hanburg*, **21**: 113–137.
- Ulrich, E.O.** 1879. Descriptions of a new genus and some new species of Bryozoa from the Cincinnati Group. *Cincinnati Society of Natural History Journal*, **2**: 119–131, pl. xii.
- 1882. American Palaeozoic Bryozoa. *Cincinnati Society of Natural History Journal*, **5**: 121–175, 232–257.
- 1890. Palaeontology of Illinois. Section VI. Palaeozoic Bryozoa, *Geological Survey of Illinois, Geology and Palaeontology*, Chicago, **8**: 283–688, pls. 29–78.
- 1893. On Lower Silurian Bryozoa of Minnesota. *Minnesota Geological and Natural History Survey, Final Report*, **3**: 96–332.
- & Bassler, R.S. 1904. A revision of the Palaeozoic Bryozoa, Pt. II – on genera and species of Trepostomata, *Smithsonian Miscellaneous Collections*, Washington, **47**: 15–55.
- Vine, G.R.** 1884. Fourth report of the Committee appointed for the purpose of reporting on fossil Polyzoa. *Report of the British Association for the Advancement of Science 1883*, London, 161–209.

TREPOSTOME IDENTIFICATION KEY

In order to identify trepostome bryozoans from Clog-y-fran thin sections are needed. Ideally at least two oriented sections (longitudinal and tangential) are required. However, specimens can sometimes be identified from randomly oriented sections. Identification can be hindered when specimens are fragmented and abraded. The key aims to aid identification, but results should be carefully checked against the complete descriptions and the illustrations of the species.

1. Zoaria massive and hemispherical 2
- Zoaria erect 3

2. Ring diaphragms present *Hemiphragma* sp
Ring diaphragms and mesozoecia absent *Monotrypa* sp
3. Hemiphragms present 4
Hemiphragms absent 5
4. Mesozoecia abundant with numerous diaphragms along their length *Dittopora sancterenensis*
Mesozoecia present, but not common *Hemiphragma pygmaeum*
5. Cystiphragms present 6
Cystiphragms absent 7
6. Abundant acanthostyles present *Monticulipora* aff. *compacta*
Small indistinct acanthostyles present *Homotrypa* cf. *similis*
7. Acanthostyles present 8
Acanthostyles absent 15
8. Diaphragms rare in autozoecia 9
Diaphragms abundant in autozoecia 12
9. Mesozoecial walls constricted at the position of the diaphragms producing a beaded appearance *Hetrotrypa* sp
Mesozoecial walls straight in appearance 10
10. Branches >3 mm in diameter 11
Branches <3 mm in diameter *Leioclema* sp. B
11. Acanthostyles composed of broad hyaline core with no sheathing laminae *Leioclema*? sp.
Acanthostyles composed of broad hyaline core surrounded by steeply dipping conical laminae *Leioclema* sp. A
12. Autozoecial basal diaphragms very abundant and regularly spaced throughout colony *Amplexopora* sp.
Autozoecial basal diaphragms present throughout colony but more abundant in the exozone 13
13. Meandering autozoecia roughly parallel to branch axis in endozone then curving very slightly to meet zoarial surface *Eridotrypa simulatrix*
Straight autozoecia roughly parallel to branch axis in endozone curve to meet zoarial surface 14
14. Thick exozonal walls with abundant diaphragms *Batostoma* cf. *polare*
Otherwise *Batostoma clogyfranense*
15. Mesozoecia present 16
Mesozoecia absent, exilazooecia present. *Halloporeta* cf. *crenulata*
16. Mesozoecia beaded in appearance *Halloporeta peculiaris*
Mesozoecia straight-walled *Halloporeta* aff. *wesenbergiana*

New information on Cretaceous crabs

C.W. WRIGHT

The Old Rectory, Seaborough, Beaminster, Dorset DT8 3QY

SYNOPSIS. Re-examination of the supposedly Jurassic, Tithonian crab fauna from Klement in Austria shows that it is Cretaceous, Cenomanian, thus removing the puzzling record of *Diaulax* from the Jurassic. A new species of *Paranecrocarcinus* is described from the Lower Cretaceous, Barremian of Zululand, South Africa. New material from the English Lower Cretaceous is described, including a new species of *Rathbunopon* from the Lower Aptian and important new information about *Withersella*.

THE KLEMENT ‘TITHONIAN’ CRAB FAUNA

In 1931 Glaessner listed a small fauna of Crustacea from a block of presumed Tithonian limestone in a conglomerate at Klement in Lower Austria. It is of importance because it included a species of *Diaulax*, a relatively advanced genus otherwise known only from the Cretaceous, Lower Albian to Cenomanian. Shortly before his death Glaessner entrusted me with his Klement specimens with a view to joint description, since he had doubts about their Jurassic date. These doubts were fully justified, since revised identifications indicate that the fauna is almost certainly of Cenomanian date.

The original (Glaessner, 1931) and the new identifications are:

Original:	Revised:
<i>Prosopon verrucosum</i> Reuss	<i>Rathbunopon obesum</i> (Van Straelen)
<i>Pithonotus marginatum</i> Meyer	<i>Pithonotus cenomanense</i> Wright & Collins
<i>Cyphonotus oxythyreiformis</i> (Gemmellaro)	<i>Palaeodromites incertus</i> (Bell)
<i>Diaulax</i> sp.	<i>Diaulax oweni</i> (Bell)

The ‘*Prosopon verrucosum*’ (BMNH IC 6, Fig. 1) resembles very closely the fragmentary English Cenomanian specimen identified by Wright & Collins (1972: 23, pl. 1, fig. 8) as *Rathbunopon obesum* (Van Straelen), a species originally described from the Cenomanian of Navarre, Spain. A second, minute, specimen (BMNH IC 14, Fig. 2) probably belongs to the same species but is too juvenile for certain attribution.

The ‘*Pithonotus marginatum*’ (BMNH IC 17, Fig. 3) conforms well with *P. cenomanense* Wright & Collins in the outline of the cephalothorax, the course of the cervical and branchiocardiac grooves, and the disposition of the granules. Differences between species of *Pithonotus* are generally fine, but identity with *P. cenomanense* seems highly probable.

The ‘*Cyphonotus oxythyreiformis*’ (BMNH IC 8, Fig. 4), though incomplete, is beautifully preserved and is undoubtedly identical with *Palaeodromites incertus*, of which an English specimen of the same size is figured for comparison (Fig. 5). Species of *Palaeodromites* were shown by Wright & Collins to have a short range in the Cretaceous and this Klement specimen alone is sufficient to demonstrate the Cenomanian age of the fauna.

The ‘*Diaulax* sp.’ (BMNH IC 7, Fig. 6) is certainly a *Diaulax* and differs in no way from the abundant English material of *D. oweni* from the Lower Albian to the Cenomanian. The immediate ancestor of *D. oweni* has not been identified but Wright & Collins (1972: 55) referred to the origin of *Diaulax* in ‘broad flat species of *Pithonotus*’;

they commented (p. 56) on the supposed Upper Jurassic occurrence from Klement as representing ‘a very early development of a relatively advanced carapace form’, an anomaly now removed by the revised dating of the Klement fauna.

A NEW SPECIES OF PARANECROCARCINUS FROM THE BARREMIAN OF ZULULAND

Genus *Paranecrocarcinus* Van Straelen, 1936

TYPE SPECIES. *Paranecrocarcinus hexagonalis* Van Straelen, 1936 (p. 36, pl. 4, figs. 6, 7) from the Hauterivian of Auxerre, France, by monotypy.

DISCUSSION. Wright & Collins (1972) differentiated *Paranecrocarcinus* from *Necrocarcinus* by the bifid rostrum of the former and the trifid rostrum of the latter. They then united Förster’s (1968) *Protocarcinus*, as a synonym, and *Pseudonecrocarcinus* as a subgenus of *Paranecrocarcinus*, separating the two subgenera partly on the basis that *P. (Paranecrocarcinus)* did not have and *P. (Pseudonecrocarcinus)* did have post-rostral slits in the carapace. This distinction was false, since the type species *P. hexagonalis* does have post-rostral slits. The remaining diagnostic character of *Pseudonecrocarcinus*, the many small rounded tubercles on the surface of the carapace, as seen both in the Maastrichtian type species *P. (Pseudonecrocarcinus) quadriscissus* (Noetling) and in the Cenomanian *P. (P.) biscissus* Wright & Collins, might be thought sufficient to justify the two subgenera. However, some doubt is cast on this idea by the juvenile specimen of *P. biscissus* discussed in the last section of this paper below. Provisionally I am inclined to abandon the distinction of two subgenera.

Paranecrocarcinus kennedyi sp. nov.

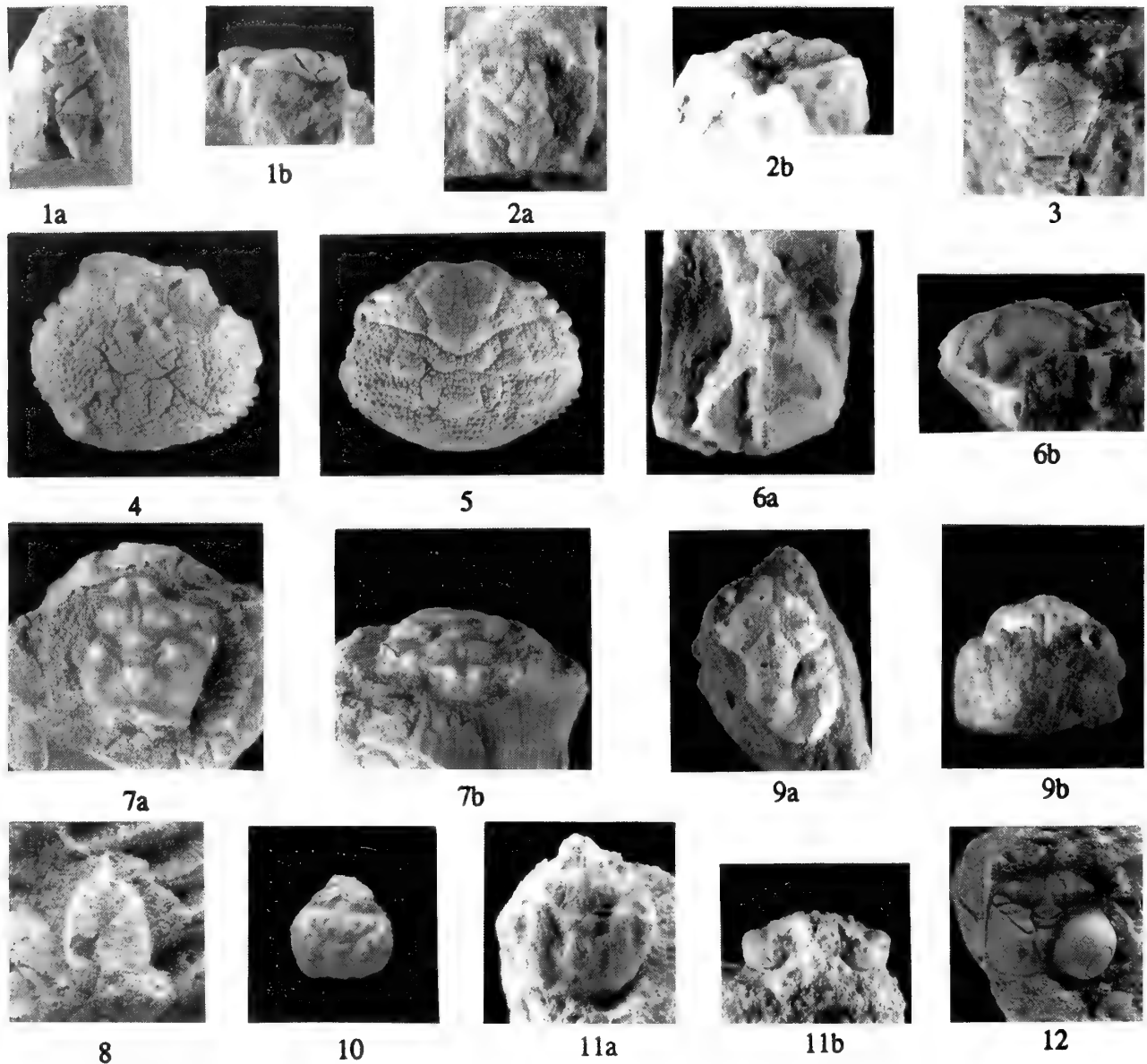
Figs 7, 13

NAME. For Professor W J Kennedy who found the specimen.

HOLOTYPE. BMNH IC 16, from the Barremian Makatini Formation, Mlambongwenya Spruit, Zululand, South Africa.

DIAGNOSIS. A *Paranecrocarcinus* with a transverse row of nine tubercles across the gastric regions and a single one on each metabranchial lobe and with two prominent spines on the anterolateral border; apparently without post-rostral slits.

DESCRIPTION. The holotype consists of an internal mould with the rostrum and margins only partially preserved, together with the counterpart showing the central area of the cephalothorax in hard



Figs 1, 2 *Rathbunopon obesum* (Van Straelen). Limestone boulder in conglomerate, Klement, Lower Austria, Cenomanian. **1.** BMNH IC6; **1a**, upper, **1b**, right side, $\times 2$; **2.** BMNH IC 14, **2a**, upper, **2b**, right side, $\times 4$.

Fig. 3 *Pithonotus cenomanense* Wright & Collins. As for Figs. 1, 2. BMNH IC 17. $\times 2$.

Figs 4, 5 *Palaeodromites incertus* (Bell). **4.** as for Figs. 1, 2. BMNH IC 8, $\times 2$. **5.** Cenomanian Sands, Lower Cenomanian, *Mantelliceras dixoni* Zone, White Hart Pit, Wilmington, Devon. BMNH IC 9, $\times 2$.

Fig. 6 *Diaulax oweni* (Bell). As for Figs. 1, 2. BMNH IC 7; **6a**, upper, **6b**, right side, $\times 2$.

Fig. 7 *Paranecrocarcinus kennedyi* sp.nov. Holotype. Makatini Formation, Barremian, Mlambongwenya Spruit, Zululand, South Africa. BMNH IC 16; **7a**, upper, **7b**, front, $\times 2$.

Fig. 8 *Galathea* sp. Lower Greensand, Crackers Bed, *Deshayesites forbesi* Zone, Atherfield, Isle of Wight. BMNH IC 13, $\times 4$.

Fig. 9 *Rathbunopon ?atherfieldense* sp.nov. Holotype. As for Fig. 8. BMNH IC 11; **9a**, upper, **9b**, front, $\times 4$.

Fig. 10 *Paranecrocarcinus biscissus* Wright & Collins. Cenomanian Limestone, Bed A or B, Whitecliff, Seaton, Devon. BMNH IC 10, $\times 2$.

Fig. 11 *Paranecrocarcinus digitatus* Wright & Collins. As for Fig. 5. BMNH IC 5; **11a**, upper, **11b**, front, $\times 2$.

Fig. 12 *Withersella crepitans* Wright & Collins. As for Fig. 8. BMNH IC 15, upper, $\times 2$.

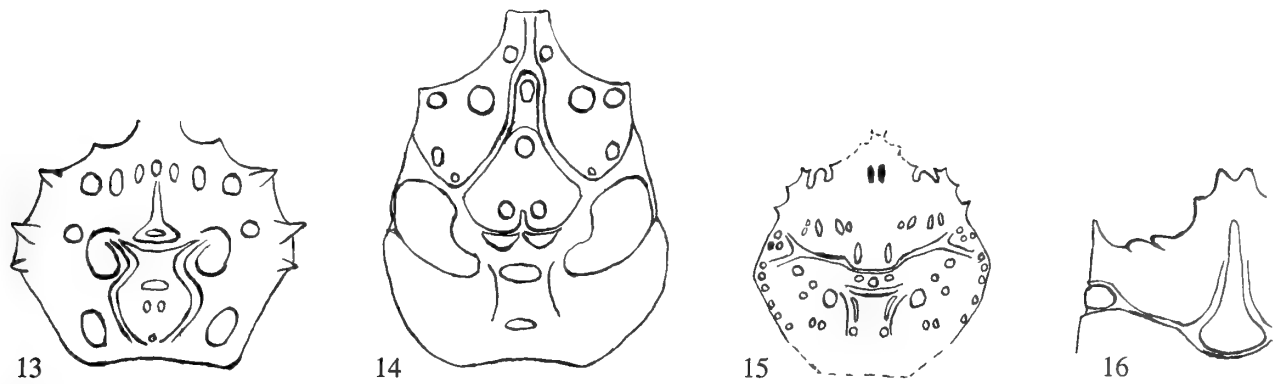


Fig. 13 *Paranecrocarcinus kennedyi* sp.nov. Makatini Formation, Barremian, Zululand, South Africa. Reconstruction, based on the holotype. Fig. 7. \times ca. 3.

Fig. 14 *Rathbunopon? atherfieldense* sp.nov. Lower Greensand, Crackers Bed, Lower Aptian, Atherfield, Isle of Wight. Reconstruction, omitting the granulation, based on the holotype, Fig. 9, and paratype. The orbito-frontal margins are diagrammatic, since details of fissures and teeth are not preserved. \times ca. 8.

Fig. 15 *Paranecrocarcinus biscissus* Wright & Collins. Cenomanian Limestone, Whitecliff, Seaton, Devon. Diagrammatic reconstruction, based on specimen in Fig. 10. \times ca. 4.

Fig. 16 *Withersella crepitans* Wright & Collins. Lower Greensand, Crackers Bed, Lower Aptian, Atherfield, Isle of Wight. Diagram of left frontal margin, based on specimen in Fig. 12. \times ca. 5.

matrix and visible only from underneath. The cephalothorax is roughly pentagonal in outline with slightly convex anterolateral, straight posterolateral and slightly concave posterior margins. It is weakly arched in transverse and longitudinal sections, with apparently deeply undercut sides. The front is produced into a broad sulcate rostrum, incompletely preserved but showing upwardly directed rostral spines. The orbital margins are not well-preserved but the orbits appear to have been moderately wide with a fissured upper rim and an outer orbital spine; the orbito-frontal width was about half that of the carapace.

The anterolateral margin ends in a spine at the lateral angle, and there is one between this and the outer orbital spine. The long posterolateral margins are almost straight and converge towards the slightly concave posterior margin.

The cervical sulcus is bent strongly round the rear of the mesogastric lobe and then takes a sinuous oblique course to the margins. Distinct epibranchial sulci branch obliquely to the rear and define small triangular epibranchial lobes. The branchiocardiac sulci are weaker than the cervical and are more or less parallel to it in their outer part; they run back between the small triangular cardiac lobe and a small parallel ridge on either side.

DISCUSSION. The Hauterivian *P. hexagonalis* has two large tubercles on the mesogastric lobe but no others forward of the cervical sulcus and has a pair of post-rostral slits. The Cenomanian *P. mozambiquensis* Förster, 1970, has a single large tubercle on each protogastric lobe. *P. libanicus* Förster, 1968, from the Cenomanian of Lebanon has a single small tubercle on the mesogastric lobe, two large ones on each protogastric and two smaller ones on each anterior branchial lobe; it also has two post-rostral slits. The Turonian *P. ovalis* Stenzel from Texas has an aligned row of large tubercles across the hepatic and protogastric lobes as in *P. kennedyi*, but the cephalothorax is much broader than long and has a less pentagonal outline, as does the Upper Albian *P. graysonensis* Rathbun, 1935, with weaker tuberculation. *P. digitatus* Wright & Collins, 1972, from the English Cenomanian has a pair of post-rostral slits (Collins et al., 1995: 198), and is characterised by its elongated radiating ridges on the protogastric lobes. *P. foesteri* Wright & Collins, 1972,

differs in having strongly granulated posterolateral margins and posterior edges of the branchiocardiac furrows. However, none of these species is known by more than a very few specimens and the extent of intraspecific variation is unknown.

SOME NEW ENGLISH CRETACEOUS CRABS

Galathea sp. nov.?

Fig. 8

A poorly preserved *Galathea* has been found in Lower Aptian Crackers material from Atherfield, supplied by Prof. W.J. Kennedy. It is inadequate for proper description, but it is worth recording since, with a specimen from the Aptian of Spain (Via Boada, oral communication), it is probably the oldest known species of the genus.

Rathbunopon? atherfieldense sp. nov.

Figs 9, 14

TYPES. The holotype is BMNH IC 11 and paratype IC 12, both from Lower Greensand, Crackers Bed, Lower Aptian, *D. callidiscus* Zone, Atherfield Point, Isle of Wight.

DIAGNOSIS. A presumed primitive *Rathbunopon*, longer than wide, with the paired bosses at the rear of the mesogastric lobe small and close together; the urogastric lobe feebly developed, divided by a shallow longitudinal groove.

DESCRIPTION. Small, 7 mm long, about 25% longer than wide, narrowed in front and with slightly convex margins; strongly arched in transverse section, less so in longitudinal; front turned down and deeply furrowed; orbitofrontal margins oblique at about 45°. The furrows delimiting the mesogastric lobe are shallow in front but deepen as they approach the cervical furrow, which is wide and deep laterally. The branchiocardiac furrows are shallower than the cervical. There is a strong circular epigastric boss on either side of the medial furrow, a feeble longitudinal oval one on the anterior process

of the mesogastric lobe, a large round one on the middle of the lobe and a transverse pair of small ones to the rear; there is a large round boss on the middle of each hepatic lobe and an outer small one, all forming a transverse line with the anterior mesogastric boss. All the raised areas of the cephalothorax have well-separated small granules between the bosses.

DISCUSSION. The holotype is incomplete, lacking nearly all of the frontal and lateral margins. The arrangement of the lobes, except for the urogastric which is weakly bilobed longitudinally rather than divided transversely into two bars, is close to that of *R. polyakron* Stenzel and *R. woodsi* Withers. The epigastric, mesogastric and hepatic bosses also are similar in disposition. It is highly probable that the present species is a primitive *Rathbunopon* but in the absence of evidence of the characteristic orbits attribution must remain uncertain. There is some resemblance to the fragmentary holotype of the Hauterivian *Homolopsis tuberculata* Van Straelen, 1936, which may also be a *Rathbunopon*.

***Paranecrocacinus biscissus?* Wright & Collins, 1972**
Figs 10, 15

An incompletely preserved internal mould from the Cenomanian of Whitcliff, Seaton, Devon (BMNH IC 10) has the same arrangement of outer orbital spines and fissures as *P. biscissus* Wright & Collins (1972: text-fig. 10b) and a multiplicity of small tubercles, including three on the urogastric lobe. However the number and arrangement of the other tubercles is not exactly as in the holotype of *P. biscissus*. The present specimen has an estimated breadth of 9 mm, against 12 mm of the holotype, and is probably an earlier moult of the same species.

***Paranecrocarinus digitatus* Wright & Collins, 1972**
Fig. 11

A further specimen from Wilmington (BMNH IC 5) confirms the restoration given by Wright & Collins (1972: text-fig. 10a).

***Hemioon elongatum* (Milne-Edwards, 1862)**

A poorly preserved specimen has been found in Bed C of the Devon Cenomanian Limestone, thus extending the range of this species to the *Calycoceras guerangeri* Zone of the Upper Cenomanian.

***Withersella crepitans* Wright & Collins, 1972 Figs 12, 16**

Wright & Collins (1972: 91) established *W. crepitans* on the basis of 14 specimens of a delicate crab from the Crackers Bed at Atherfield. They gave a restored diagrammatic view of the cephalothorax showing the frontal margin with broad rectangular indentations and teeth. Subsequently a specimen was found (BMNH IC 15) with the left frontal margin almost perfectly preserved indicating that the diagram in Wright & Collins was based on a broken edge of the thin carapace.

The actual frontal margin (Figs 12, 16), is bounded by large outer orbital spines and is rather concave, interrupted only by paired oblique supraorbital fissures and a marked inner orbital spine on either side of a bifid rostrum. In effect the front of *Withersella* is extremely close to that of *Carcineretes walcotti* Withers, except for the greater projection of the rostrum in *Withersella*, thus confirming the attribution to Carcineretidae by Wright & Collins, which Glaessner (1980: 180) had regarded as unconvincing. Also, the front of *Withersella* more closely resembles that of *Binkhorstia* than was apparent in 1972, although there are significant differences in the latter's peculiar spatulate rostrum, third supraorbital fissure and less oblique fissures (Collins, Fraaye & Jagt, 1995: figs 12a-c).

REFERENCES

- Bell, T. 1863. A monograph of the fossil malacostraceous Crustacea of Great Britain. Part II. Crustacea of the Gault and Greensand. *Monograph of the Palaeontographical Society of London*. viii + 40 pp., 11 pls.
 Collins, J.S.H., Fraaye, R.H.B. & Jagt, J.W.M. 1995. Late Cretaceous anomurans and brachyurans from the Maastrichtian type area. *Acta Palaeontologica Polonica*, **40**: 165–210, 12 figs.
 Glaessner, M.F. 1931. Geologisches Studien in des äusseren Klippenzone. *Jahrbuch der geologischen Bundesanstalt*, Wein, **81**: 1–23.
 Förster, R. 1968. *Paranecrocacinus libanicus* n. sp. (Decapoda) und die Entwicklung der Calappidae in der Kreide. *Mitteilungen der Bayerischen Staatssammlung für Paläontologie und historische Geologie*, **8**: 167–195, pl. 13.
 — 1970. Neue Decapoden Reste aus der Oberkreide von Moçambique, Norddeutschland und den bayerischen Alpen. *Paläontologische Zeitschrift*, **44**: 134–144, pl. 17.
 Stenzel, H.B. 1945. Decapod crustaceans from the Cretaceous of Texas. *Bulletin of the University of Texas Bureau of Economic Geology and Technology*, **4401**: 401–476, pls. 34–45.
 Withers, T.H. 1928. New Cretaceous crabs from England and Syria. *Annals and Magazine of Natural History*, (10) **2**: 456–462, pl. 13.
 Wright C.W. & J.S.H. Collins, 1972. British Cretaceous Crabs. *Monograph of the Palaeontographical Society of London*. 114pp., 22 pls.

CORRIGENDUM

Correction to: Barrett, P.M. 1996. The first known femur of *Hylaeosaurus armatus* and re-identification of ornithopod material in the Natural History Museum, London. *Bull. nat. Hist. Mus. Lond. (Geol.)* **52** (2): 115–118.

In the Synopsis (p. 115), line 1, the words ‘ornithopod dinosaur’ should be replaced by ‘nodosaurid ankylosaur’.



Bulletin of The Natural History Museum Geology Series

Earlier Geology *Bulletins* are still in print. The following can be ordered from Intercept (address on inside front cover). Where the complete backlist is not shown, this may also be obtained from the same address.

Volume 34

- No. 1 Relative dating of the fossil hominids of Europe. K.P. Oakley. 1980. Pp. 1-63, 6 figs, 17 tables. £8.00

- No. 2 Origin, evolution and systematics of the dwarf Acanthoceratid *Protacanthoceras* Spath, 1923 (Cretaceous Ammonoidea). C.W. Wright & W.J. Kennedy. 1980. Pp. 65-107, 61 figs. £6.25

- No. 3 Ashgill Brachiopoda from the Glyn Ceiriog District, north Wales. N. Hiller. 1980. Pp. 109-216, 408 figs. £14.75

- No. 4 Miscellanea

Type specimens of some Upper Palaeozoic Athyridide brachiopods. C.H.C. Brunton. 31 figs.

Two new British Cretaceous Epitonidae (Gastropoda): evidence for evolution of shell morphology. R.J. Cleevely. 14 figs, 1 table.

Revision of the microproblematicum *Prethocoproolithus* Elliott, 1962. G.F. Elliott. 4 figs.

Basilicus tyrannus (Murchison) and the glabellar structure of asaphid trilobites. R.A. Fortey. 12 figs.

A new Lower Ordovician bivalve family, the Thoraliidae (? Nuculoidea), interpreted as actinodont deposit feeders. N.J. Morris. 7 figs.

Cretaceous brachiopods from northern Zululand. E.F. Owen. 13 figs.

Tupus diluculum sp. nov. (Protodonata), a giant dragonfly from the Upper Carboniferous of Britain. P.E.S. Whalley. 1 fig.

Revision of *Plummerita* Brönniman (Foraminifera) and a new Maastrichtian species from Ecuador. J.E. Whittaker. 34 figs. 1980. Pp. 217-297. £11.00

Volume 35

- No. 1 Lower Ordovician Brachiopoda from mid and south-west Wales. M.G. Lockley & A. Williams. 1981. Pp. 1-78, 263 figs, 3 tables. £10.80

- No. 2 The fossil alga *Girvanella* Nicholson & Etheridge. H.M.C. Danielli. 1981. Pp. 79-107, 8 figs, 3 tables. £4.20

- No. 3 Centenary miscellanea

Reassessment of the Ordovician brachiopods from the Budleigh Salterton Pebble Bed, Devon. L.R.M. Cocks & M.G. Lockley. 35 figs.

Felix Oswald's Turkish Algae. G.F. Elliott. 3 figs.

J.A. Moy-Thomas and his association with the British Museum (Natural History). P.L. Forey & B.G. Gardiner. 3 figs.

Burials, bodies and beheadings in Romano-British and Anglo-Saxon cemeteries. M. Harman, T.I. Molleson & J.L. Price. 5 figs, 7 tables, VI appendices.

The Jurassic irregular echinoid *Nucleolites clunicularis* (Smith). D.N. Lewis & H.G. Owen. 4 figs.

Phanerotinus cristatus (Phillips) and the nature of euomphalacean gastropods. N.J. Morris & R.J. Cleevely. 12 figs.

Agassiz, Darwin, Huxley, and the fossil record of teleost fishes. C. Patterson. 1 fig.

The Neanderthal problem and the prospects for direct dating of Neanderthal remains. C.B. Stringer & R. Burleigh. 2 figs, 1 table.

Hippoporidra edax (Busk 1859) and a revision of some fossil and living *Hippoporidra* (Bryozoa). P.D. Taylor & P.L. Cook. 6 figs. 1981. Pp. 109-252. £20.00

- No. 4 The English Upper Jurassic Plesiosauroidea (reptilia) and a review of the phylogeny and classification of the Plesiosauria. D.S. Brown. 1981. Pp. 253-347, 44 figs. £13.00

Volume 36

- No. 1 Middle Cambrian trilobites from the Sosink Formation, Derik-Mardin district, south-eastern Turkey. W.T. Dean. 1982. Pp. 1-41, 68 figs. £5.80

- No. 2 Miscellanea
- British Dinantian (Lower Carboniferous) terebratulid brachiopods. C.H.C. Brunton. 20 figs.

New microfossil records in time and space. G.F. Elliott. 6 figs.

The Ordovician trilobite *Neseuretus* from Saudi Arabia, and the palaeogeography of the *Neseuretus* fauna related to Gondwanaland in the earlier Ordovician. R.A. Fortey & S.F. Morris. 10 figs.

Archaeocidaris whatleyensis sp. nov. (Echinoidea) from the Carboniferous Limestone of Somerset and notes on echinoid phylogeny. D.N. Lewis & P.C. Ensom. 23 figs.

A possible non-calcified dasycladalean alga from the Carboniferous of England. G.F. Elliott. 1 fig.

Nanjinoporella, a new Permian dasyclad (calcareous alga) from Nanjing, China. X. Mu & G.F. Elliott. 6 figs, 1 table.

Toarcian bryozoans from Belchite in north-east Spain. P.D. Taylor & L. Sequeiros. 10 figs, 2 tables.

Additional fossil plants from the Drybrook Sandstone, Forest of Dean, Gloucestershire. B.A. Thomas & H.M. Purdy. 14 figs, 1 table.

Bintoniella brodiei Handlirsch (Orthoptera) from the Lower Lias of the English Channel, with a review of British bintoniellid fossils. P.E.S. Whalley. 7 figs.

Uraloporella Korde from the Lower Carboniferous of South Wales. V.P. Wright. 3 figs. 1982. Pp. 43-155. £19.80

- No. 3 The Ordovician Graptolites of Spitsbergen. R.A. Cooper & R.A. Fortey. 1982. Pp. 157-302, 6 plates, 83 figs, 2 tables. £20.50

- No. 4 Campanian and Maastrichtian sphenodiscid ammonites from southern Nigeria. P.M.P. Zaborski. 1982. Pp. 303-332, 36 figs. £4.00

Volume 37

- No. 1 Taxonomy of the arthrodire *Phlyctaenius* from the Lower or Middle Devonian of Campbellton, New Brunswick, Canada. V.T. Young. 1983. Pp. 1-35, 18 figs. £5.00

- No. 2 *Ailsacrinus* gen. nov., an aberrant millerigocrinid from the Middle Jurassic of Britain. P.D. Taylor. 1983. Pp. 37-77, 48 figs, 1 table. £5.90

- No. 3 Miscellanea

Glossopteris anatolica Sp. nov. from uppermost Permian strata in south-east Turkey. S. Archangelsky & R.H. Wagner. 14 figs.

The crocodilian *Theriosuchus* Owen, 1879 in the Wealden of England. E. Buffetaut. 1 fig.

A new conifer species from the Wealden beds of Féron-Glagon, France. H.L. Fisher & J. Watson. 10 figs.

Late Permian plants including Charophytes from the Khuff formation of Saudi Arabia. C.R. Hill & A.A. El-Khayal. 18 figs.

British Carboniferous Edrioasteroidea (Echinodermata). A.B. Smith. 52 figs.

A survey of recent and fossil Cicadas (Insecta, Hemiptera-Homoptera) in Britain. P.E.S. Whalley. 11 figs.

The Cephalaspidids from the Dittonian section at Cwm Mill, near Abergavenny, Gwent. E.I. White & H.A. Toombs. 20 figs. 1983. Pp. 79-171. £13.50

No. 4 The relationships of the palaeoniscid fishes, a review based on new specimens of *Mimia* and *Moythomasia* from the Upper Devonian of Western Australia. B.G. Gardiner. 1984. Pp. 173-428. 145 figs. 4 plates. 0 565 00967 2. £39.00

Volume 38

No. 1 New Tertiary pycnodonts from the Tilemsi valley, Republic of Mali. A.E. Longbottom. 1984. Pp. #1-26. 29 figs. 3 tables. 0 565 07000 2. £3.90

No. 2 Silicified brachiopods from the Viséan of County Fermanagh, Ireland. (II) Rhynchonellids. Spiriferids and Terebratulids. C.H.C. Brunton. 1984. Pp. 27-130. 213 figs. 0 565 07001 0. £16.20

No. 3 The Llandovery Series of the Type Area. L.R.M. Cocks. N.H. Woodcock, R.B. Rickards, J.T. Temple & P.D. Lane. 1984. Pp. 131-182. 70 figs. 0 565 07004 5. £7.80

No. 4 Lower Ordovician Brachiopoda from the Tourmakeady Limestone, Co. Mayo, Ireland. A. Williams & G.B. Curry. 1985.

Pp. 183-269. 214 figs. 0 565 07003 7. £14.50

No. 5 Miscellanea
Growth and shell shape in Productacean Brachiopods. C.H.C. Brunton.

Palaeosiphonium a problematic Jurassic alga. G.F. Elliott.

Upper Ordovician brachiopods and trilobites from the Clashford House Formation, near Herbertstown, Co. Meath, Ireland. D.A.T. Harper, W.I. Mitchell, A.W. Owen & M. Romano.

Preliminary description of Lower Devonian Osteostraci from Podolia (Ukrainian S.S.R.). P. Janvier.

Hipparium sp. (Equidae, Perissodactyla) from Diavata (Thessaloniki, northern Greece). G.D. Koufos.

Preparation and further study of the Singa skull from Sudan. C.B. Stringer, L. Cornish & P. Stuart-Macadam.

Carboniferous and Permian species of the cyclostome bryozoan *Corynotrypa* Bassler, 1911. P.D. Taylor.

Redescription of *Eurycephalochelys*, a trionychid turtle from the Lower Eocene of England. C.A. Walker & R.T.J. Moody.

Fossil insects from the Lithographic Limestone of Montsech (late Jurassic-early Cretaceous), Lérida Province, Spain. P.E.S. Whalley & E.A. Jarzemowski. 1985. Pp. 271-412, 162 figs. 0 565 07004 5. £24.00

Volume 39

No. 1	Upper Cretaceous ammonites from the Calabar region, south-east Nigeria. P.M.P. Zaborski. 1985. Pp. 1-72. 66 figs.	£11.00
No. 2	Cenomanian and Turonian ammonites from the Novo Redondo area, Angola. M.K. Howarth. 1985. Pp. 73-105. 33 figs.	£5.60
No. 3	The systematics and palaeogeography of the Lower Jurassic insects of Dorset, England. P.E.S. Whalley. 1985. Pp. 107-189. 87 figs. 2 tables. 0 565 07008 8.	£14.00
No. 4	Mammals from the Bartonian (middle/late Eocene) of the Hampshire Basin, southern England. J.J. Hooker. 1986. Pp. 191-478. 71 figs. 39 tables. 0 565 07009 6.	£49.50

Volume 40

No. 1	The Ordovician graptolites of the Shelve District, Shropshire. I. Strachan. 1986. Pp. 1-58. 38 figs. 0 565 07010 X.	£9.00
No. 2	The Cretaceous echinoid <i>Boletechinus</i> , with notes on the phylogeny of the Glyptocyphidae and Temnopleuridae. D.N. Lewis.	
	1986. Pp. 59-90. 11 figs. 7 tables. 0 565 07011 8.	£5.60
No. 3	The trilobite fauna of the Raheen Formation (upper Caradoc), Co. Waterford, Ireland. A.W. Owen, R.P. Tripp & S.F. Morris.	
	1986. Pp. 91-122. 88 figs. 0 565 07012 6.	£5.60
No. 4	Miscellanea I: Lower Turonian cirripede—Indian coleoid <i>Naefia</i> —Cretaceous—Recent Craniidae—Lectotypes of Girvan trilobites—Brachiopods from Provence—Lower Cretaceous cheiostomes. 1986. Pp. 125-222. 0 565 07013 4.	£19.00
No. 5	Miscellanea II: New material of <i>Kimmererosaurus</i> —Edgehill Sandstone plants—Lithogeochemistry of Mendip rocks—Specimens previously recorded as teuthids—Carboniferous lycopsid <i>Anabathra</i> — <i>Meyenodendron</i> , new Alaskan lepidodendrid. 1986. Pp. 225-297. 0 565 07014 2.	£13.00

Volume 41

No. 1	The Downtonian ostracoderm <i>Sclerodus</i> Agassiz (Osteostraci: Tremataspididae). P.L. Forey. 1987. Pp. 1-30. 11 figs. 0 565 07015 0.	£5.50
No. 2	Lower Turonian (Cretaceous) ammonites from south-east Nigeria. P.M.P. Zaborski. 1987. Pp. 31-66. 46 figs. 0 565 07016 9.	£6.50
No. 3	The Arenig Series in South Wales: Stratigraphy and Palaeontology. I. The Arenig Series in South Wales. R.A. Fortey & R.M. Owens. II. Appendix. Acritarchs and Chitinozoa from the Arenig Series of South-west Wales. S.G. Molyneux. 1987. Pp. 67-364. 289 figs. 0 565 07017 7.	£59.00
No. 4	Miocene geology and palaeontology of Ad Dabtiyah, Saudi Arabia. Compiled by P.J. Whybrow. 1987. Pp. 365-457. 54 figs.	
	0 565 07019 3.	£18.00

Volume 42

No. 1	Cenomanian and Lower Turonian Echinoderms from Wilmington, south-east Devon. A.B. SMith, C.R.C. Paul, A.S. Gale & S.K. Donovan. 1988. 244 pp. 80 figs. 50 pls. 0 565 07018 5.	£46.50
-------	---	--------

Volume 43

- No. 1 A Global Analysis of the Ordovician–Silurian boundary. Edited by L.R.M. Cocks & R.B. Rickards. 1988. 394 pp., figs. 0 565 07020 7. £70.00

Volume 44

- No. 1 Miscellanea: Palaeocene wood from Mali—Chapelcorner fish bed—*Heterotheca* coprolites—Mesozoic Neuroptera and Raphidioptera. 1988. Pp. 1–63. 0 565 07021 5. £12.00

- No. 2 Cenomanian brachiopods from the Lower Chalk of Britain and northern Europe. E.F. Owen. 1988. Pp. 65–175. 0 565 07022 3. £21.00

- No. 3 The ammonite zonal sequence and ammonite taxonomy in the *Douvilleiceras mammillatum* Superzone (Lower Albian) in Europe. H.G. Owen. 1988. Pp. 177–231. 0 565 07023 1. £10.30

- No. 4 Cassiopidae (Cretaceous Mesogastropoda): taxonomy and ecology. R.J. Cleevley & N.J. Morris. 1988. Pp. 233–291. 0 565 07024 X. £11.00

Volume 45

- No. 1 Arenig trilobites—Devonian brachiopods—Triassic demosponges—Larval shells of Jurassic bivalves—Carboniferous marattialean fern—Classification of Plectambonitacea. 1989. Pp. 1–163. 0 565 07025 8. £40.00

- No. 2 A review of the Tertiary non-marine molluscan faunas of the Pebesian and other inland basins of north-western South America. C.P. Nuttall. 1990. Pp. 165–371. 456 figs. 0 565 07026 6. £52.00

Volume 46

- No. 1 Mid-Cretaceous Ammonites of Nigeria—new amphisbaenians from Kenya—English Wealden Equisetales—Faringdon Sponge Gravel Bryozoa. 1990. Pp. 1–152. 0 565 07027 4. £45.00

- No. 2 Carboniferous pteridosperm frond *Neuropteris heterophylla*—Tertiary Ostracoda from Tanzania. 1991. Pp. 153–270. 0 565 07028 2. £30.00

Volume 47

- No. 1 Neogene crabs from Brunei, Sabah & Sarawak—New pseudosciurids from the English Late Eocene—Upper Palaeozoic Anomalodesmata Bivalvia. 1991. Pp. 1–100. 0 565 07029 0. £37.50

- No. 2 Mesozoic Chrysalidinidae of the Middle East—Bryozoans from north Wales—*Alveolinella praequoyi* sp. nov. from Papua New Guinea. 1991. Pp. 101–175. 0 565 070304. £37.50

Volume 48

- No. 1 ‘*Placopsisilina*’ *cenomana* d’Orbigny from France and England—Revision of Middle Devonian uncinulid brachiopod—Cheilostome bryozoans from Upper Cretaceous, Alberta. 1992. Pp. 1–24. £37.50

- No. 2 Lower Devonian fishes from Saudi Arabia—W.K. Parker’s collection of foraminifera in the British Museum (Natural History). 1992. Pp. 25–43. £37.50

Volume 49

- No. 1 Barremian—Aptian Praehedbergellidae of the North Sea area: a reconnaissance—Late Llandovery and early Wenlock Stratigraphy and ecology in the Oslo Region, Norway—Catalogue of the type and figured specimens of fossil Asteroidea and Ophiuroidea in The Natural History Museum. 1993. Pp. 1–80. £37.50

No. 2

- Mobility and fixation of a variety of elements, in particular, during the metasomatic development of adinoles at Dinas Head, Cornwall—Productellid and Plicatiferid (Productoid) Brachiopods from the Lower Carboniferous of the Craven Reef Belt, North Yorkshire—The spores of *Leclercqia* and the dispersed spore morphon *Acinosporites lindlarensis* Riegel: a case of gradualistic evolution. 1993. Pp. 81–155. £37.50

Volume 50

- No. 1 Systematics of the meliceritid cyclostome bryozoans: introduction and the genera *Elea*, *Semielea* and *Reptomultelea*. 1994. Pp. 1–104. £37.50

- No. 2 The brachiopods of the Duncannon Group (Middle–Upper Ordovician) of southeast Ireland. 1994. Pp. 105–175. £37.50

Volume 51

- No. 1 A synopsis of neuropteroid foliage from the Carboniferous and Lower Permian of Europe—The Upper Cretaceous ammonite *Pseudaspidooceras* Hyatt, 1903, in north-eastern Nigeria—The pterodactyloids from the Purbeck Limestone Formation of Dorset. 1995. Pp. 1–88. £37.50

No. 2

- Palaeontology on the Qahlah and Simsima Formations (Cretaceous, Late Campanian–Maastrichtian) of the United Arab Emirates–Oman Border Region—Preface—Late Cretaceous carbonate platform faunas of the United Arab Emirates–Oman border region—Late Campanian–Maastrichtian echinoids from the United Arab Emirates–Oman border region—Maastrichtian ammonites from the United Arab Emirates–Oman border region—Maastrichtian nautioids from the United Arab Emirates–Oman border region—Maastrichtian Inoceramidae from the United Arab Emirates–Oman border region—Late Campanian–Maastrichtian Bryozoa from the United Arab Emirates–Oman border region—Maastrichtian brachiopods from the United Arab Emirates–Oman border region—Late Campanian–Maastrichtian rudists from the United Arab Emirates–Oman border region. 1995. Pp. 89–305. £37.50

Volume 52

- No. 1 Zirconlite: a review of localities worldwide, and a compilation of its chemical compositions—A review of the stratigraphy of Eastern Paratethys (Oligocene–Holocene)—A new protorichthofenoid brachiopod (Productida) from the Upper Carboniferous of the Urals, Russia—The Upper Cretaceous ammonite *Vascoceras* Choffat. 1898 in north-eastern Nigeria. 1996. Pp. 1–89. £43.40

No. 2

- Jurassic bryozoans from Baltów, Holy Cross Mountains, Poland—A new deep-water spatangoid echinoid from the Cretaceous of British Columbia, Canada—The cranial anatomy of *Rhomaleosaurus thortoni* Andrews (Reptilia, Plesiosauria)—The first known femur of *Hylaeosaurus armatus* and re-identification of ornithopod material in The Natural History Museum, London—Bryozoa from the Lower Carboniferous (Viséan) of County Fermanagh, Ireland. 1996. Pp. 91–171. £43.40

Volume 53

- No. 1 The status of ‘*Plestictis*’ *croizeti*, ‘*Plestictis*’ *gracilis* and ‘*Lutra*’ *minor*: synonyms of the early Miocene viverrid *Herpestides antiquus* (Mammalia, Carnivora)—*Baryonyx walkeri*, a fish-eating dinosaur from the Wealden of Surrey—The Cretaceous–Miocene genus *Lichenopora* (Bryozoa), with a description of a new species from New Zealand. 1997. Pp. 1–78. £43.40

CONTENTS

- 79 **Ordovician trilobites from the Tourmakeady Limestone, western Ireland**
J.M. Adrain and R.A. Fortey
- 117 **Ordovician Bryozoa from the Llandeilo Limestone, Clog-y-fran, near Whitland, South Wales**
C. Buttler
- 135 **New Information on Cretaceous crabs**
C.W. Wright

Bulletin of The Natural History Museum

GEOLOGY SERIES

Vol. 53, No. 2, November 1997







